Indexed
ENGINEERING-TRANSPORTATION
LIBRARY

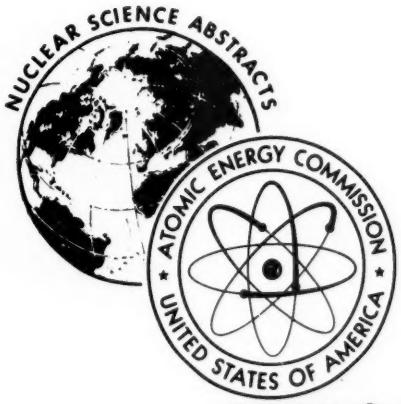

THE UNIVERSITY OF MICHIGAN
MAY 31 1966
ENGINEERING LIBRARY

NUCLEAR SCIENCE ABSTRACTS

Volume 20 Number 8

Abstracts 12563–14230

April 30, 1966

UNITED STATES ATOMIC ENERGY COMMISSION
Division of Technical Information

DEPOSITED BY THE
UNITED STATES OF AMERICA

USAEC DEPOSITORY LIBRARIES

Collections of USAEC reports are maintained in the libraries of the organizations listed below for reference use by the general public. Facilities for making photocopies are available. The USAEC also makes available through these libraries atomic energy reports of countries other than the U. S. that are abstracted in *Nuclear Science Abstracts*.

ALABAMA
Auburn, Auburn University
ALASKA
College, University of Alaska
ARIZONA
Tucson, University of Arizona
ARKANSAS
Fayetteville, University of Arkansas
CALIFORNIA
Berkeley, University of California
Davis, University of California
Los Angeles, University of California
San Diego, Public Library
Stanford, Stanford University
COLORADO
Boulder, University of Colorado
Denver, Public Library
CONNECTICUT
New Haven, Yale University
DELAWARE
Newark, University of Delaware
DISTRICT OF COLUMBIA
Washington, Library of Congress
FLORIDA
Coral Gables, University of Miami
Gainesville, University of Florida
Tallahassee, The Florida State University
GEORGIA
Atlanta, Georgia Institute of Technology
HAWAII
Honolulu, University of Hawaii
ILLINOIS
Chicago, John Crerar Library
Chicago, University of Chicago
Evanston, Northwestern University
Urbana, University of Illinois
INDIANA
Bloomington, Indiana University
Lafayette, Purdue University
IOWA
Ames, Iowa State University
KANSAS
Manhattan, Kansas State University
KENTUCKY
Lexington, University of Kentucky
Louisville, University of Louisville
LOUISIANA
Baton Rouge, Louisiana State University
New Orleans, Tulane University
MARYLAND
Baltimore, Johns Hopkins University
College Park, University of Maryland
MASSACHUSETTS
Cambridge, Harvard University
Cambridge, Massachusetts Institute of Technology
MICHIGAN
Ann Arbor, University of Michigan
Detroit, Public Library
East Lansing, Michigan State University
MINNESOTA
Minneapolis, University of Minnesota
MISSISSIPPI
State College, Mississippi State University
MISSOURI
Kansas City, Linda Hall Library
Rolla, University of Missouri School of Mines and Metallurgy
St. Louis, Washington University
MONTANA
Bozeman, Montana State College
NEVADA
Las Vegas, Nevada Southern University
Reno, University of Nevada
NEW JERSEY
Princeton, Princeton University
Teaneck, Fairleigh Dickinson University
NEW MEXICO
Albuquerque, University of New Mexico
NEW YORK
Albany, The University of the State of New York
Buffalo, State University of New York at Buffalo
Ithaca, Cornell University
New York, Atomic Industrial Forum, Inc.
New York, Columbia University
New York, New York University
Rochester, University of Rochester
Schenectady, Union College
Syracuse, Syracuse University
Troy, Rensselaer Polytechnic Institute
NORTH CAROLINA
Charlotte, Public Library of Charlotte and Mecklenburg County
Durham, Duke University
Raleigh, North Carolina State College
NORTH DAKOTA
Grand Forks, University of North Dakota
OHIO
Cincinnati, University of Cincinnati
Cleveland, Public Library
OHIO (CONT.)
Columbus, Ohio State University
Toledo, University of Toledo
Youngstown, Youngstown University
OKLAHOMA
Norman, University of Oklahoma
Stillwater, Oklahoma State University
OREGON
Corvallis, Oregon State University
Portland, Reed College
PENNSYLVANIA
Philadelphia, University of Pennsylvania
Pittsburgh, Carnegie Library
University Park, Pennsylvania State University
PUERTO RICO
Rio Piedras, University of Puerto Rico
RHODE ISLAND
Providence, Brown University
SOUTH CAROLINA
Columbia, University of South Carolina
TENNESSEE
Knoxville, University of Tennessee
Memphis, Public Library
Nashville, Joint University Libraries
Oak Ridge, Oak Ridge Associated Universities
TEXAS
Austin, University of Texas
College Station, Texas A & M University
Dallas, Southern Methodist University
Houston, Rice University
Lubbock, Texas Technological College
San Antonio, Public Library
UTAH
Salt Lake City, University of Utah
VIRGINIA
Blacksburg, Virginia Polytechnic Institute
Charlottesville, University of Virginia
Norfolk, Old Dominion College
WASHINGTON
Pullman, Washington State University
Seattle, University of Washington
WEST VIRGINIA
Morgantown, West Virginia University
WISCONSIN
Madison, University of Wisconsin
Milwaukee, Public Library
WYOMING
Laramie, University of Wyoming

DEPOSITED BY THE
TED STATES OF AMERICA

Volume 20, Number 8, April 30, 1966

NUCLEAR SCIENCE ABSTRACTS

A semimonthly publication of the USAEC Division of Technical Information, Edward J. Brunenkant, Director. Published by the USAEC Division of Technical Information Extension, Robert L. Shannon, Extension Manager.

Nuclear Science Abstracts covers the international literature on nuclear science and technology and provides the only comprehensive abstracting and indexing of this body of information. Published twice each month since 1947, *NSA* covers technical reports of the U. S. Atomic Energy Commission and its contractors, technical reports of U. S. Government agencies and other governments, universities, industrial and research organizations, as well as patents, books, and journal literature on a world-wide basis. Nearly 350,000 abstracts have appeared in *NSA* through Volume 19. The subject matter covered in *NSA* is described in issue Number 1 and in TID-4552, *Subject Scope of Nuclear Science Abstracts*, available free from the U. S. Atomic Energy Commission, Division of Technical Information Extension, P. O. Box 62, Oak Ridge, Tennessee 37830.

Abstracts are arranged according to a number of subject categories and subcategories. Definitions of categories appear in issues Number 1 and 13. If the language of the original item is not English, the language will be indicated. Translations are not abstracted where an abstract of the original item has appeared in *NSA*.

INDEXES TO NSA

Corporate author, personal author, subject, and report number indexes appear in each issue and are cumulated quarterly, semiannually, and annually. Multi-volume cumulations have been issued as indicated on the following page. Report number indexes for all volumes (1–18) were issued at the end of Vol. 18. At the end of Vol. 19, the indexes for Vols. 1–15 were reissued to include additional public availability information. This cumulation will be a permanent shelf item and will not be reissued. Report number indexes for Vol. 19 are included as a cumulation beginning with Vol. 16.

AVAILABILITY OF PUBLICATIONS ABSTRACTED

The public availability of all U. S. Atomic Energy Commission reports is indicated in the report number indexes. The availability of other reports, when known, is also indicated. The availability of some unnumbered reports is given in the abstract.

Dissertations abstracted in *Dissertation Abstracts* and included in *NSA* are available from University Microfilms, Inc., 315 N. First Street, Ann Arbor, Michigan 48103.

Most of the published literature abstracted in *NSA* is on deposit at the Library, Oak Ridge Associated Universities, Oak Ridge, Tennessee, (a USAEC depository library) and is available through interlibrary loan. When requesting papers from this source, it is important that *NSA* volume and abstract number be cited.

HOW TO OBTAIN NUCLEAR SCIENCE ABSTRACTS

NSA is available on an exchange basis to universities, research institutions, industrial firms, and publishers of scientific information. Inquiries should be directed to the U. S. Atomic Energy Commission, Division of Technical Information Extension, P. O. Box 62, Oak Ridge, Tennessee 37830.

Government agencies may obtain *NSA* free of charge.

NSA is available to the general public on a subscription basis from the Superintendent of Documents, U. S. Government Printing Office, Washington, D. C. 20402, as follows:

For the 24 regular issues, $30.00 domestic, $37.00 foreign. A single issue costs $1.75, plus 25 per cent for foreign mailing. Domestic rates apply to the United States, Canada, Mexico, and Central and South American countries except Argentina, Brazil, British and French Guiana, Surinam, and British Honduras. Foreign rates apply to the countries excepted above and to all other countries throughout the world.

For the quarterly, semiannual, and annual indexes, $22.00 domestic, $25.00 foreign.

Multivolume subject and author indexes are available as follows:

Vols. 1–4 (1948–1950) Johnson Reprint Corporation, 111 Fifth Avenue, New York, N. Y. 10003, $30.00.

Vols. 5–10 (1951–1956) Superintendent of Documents, U. S. Government Printing Office, Washington, D. C. 20402, $5.25.

Vols. 11–15, Subjects, Superintendent of Documents, U. S. Government Printing Office, Washington, D. C. 20402, $19.00.

Vols. 11–15, Personal Authors, Superintendent of Documents, U. S. Government Printing Office, Washington, D. C. 20402, $14.25.

Vols. 11–15, Corporate Authors, Superintendent of Documents, U. S. Government Printing Office, Washington, D. C. 20402, $2.50.

Cumulative Report Number Index, Vols. 1–15, Revised, is available from the Superintendent of Documents, U. S. Government Printing Office, Washington, D. C. 20402, $4.00.

Cumulative Report Number Index, Vols. 16–19, is available from the Superintendent of Documents, U. S. Government Printing Office, Washington, D. C. 20402, $2.50.

Annual Indexes are available separately from the U. S. Government Printing Office as follows:

Vol. 16, Subject and Authors, $9.75.
Vol. 17, Subject and Authors, $12.25.
Vol. 18, Subject and Authors, $12.50.
Vol. 19, Subject and Authors, $12.50.

ACKNOWLEDGMENTS

Agreements between the United States Atomic Energy Commission and the following organizations with regard to providing continuing services and specific literature coverage for *Nuclear Science Abstracts* are gratefully acknowledged:

American Institute of Physics; Atomic Energy of Canada Limited; Atomic Energy Research Establishment, United Kingdom; European Atomic Energy Community (EURATOM); Gmelin Institute; International Atomic Energy Agency; Japan Atomic Energy Bureau — Japan Atomic Energy Research Institute; Netherlands Patent Office; Reactor Centrum Nederland.

TABLE OF CONTENTS

Volume 20, Number 8, April 30, 1966

Category	Page
BIOLOGY AND MEDICINE	1537
General	1537
Ecology	1537
Metabolism, Tissue Distribution, and Toxicology	1540
Radiation Effects on Biochemicals	1544
Radiation Effects on Tissues	1546
Radiation Effects Therapy and Countermeasures	1559
Radiation Hazards and Protection	1561
Radiotherapy and Radiodiagnosis	1561
CHEMISTRY	1566
General	1566
Analytical Procedures	1566
Inorganic and Physical Chemistry	1572
Organic Chemistry	1580
Radiation Chemistry	1581
Radiochemistry	1584
Separation Processes and Procedures	1585
ENGINEERING	1589
General	1589
Facilities and Equipment	1589
Heat Transfer and Fluid Flow	1591
Materials Testing	1592
Space Propulsion	1593
GEOLOGY, METEOROLOGY, AND MINERALOGY	1594
General	1594
Meteorology	1594
Natural Radioactivity and Fallout	1594
Techniques and Equipment	1595
Thorium and Uranium Minerals	1596
HEALTH AND SAFETY	1598
INSTRUMENTATION	1602
General	1602
Radiation Detection	1605
Radiation Effects	1613
ISOTOPE TECHNOLOGY	1615
Industrial Applications	1615
Power Application	1617
Separation and Production	1617
MATHEMATICS AND COMPUTERS	1619
METALS, CERAMICS, AND OTHER MATERIALS	1620
General	1620
Corrosion	1622
Fabrication	1624
Properties and Structure	1627
Radiation Effects	1640
PHYSICS	1644
General	1644
Accelerators	1645
Astrophysics and Cosmology	1650
Atomic Physics	1651
Cosmic Radiation	1653
Direct Energy Conversion	1653
Elementary Particles and Radiations	1656
Field Theory, Scattering Theory, and Symmetries	1665
Fluid Physics and Thermodynamics	1675
Geophysics	1677
Gravitation, Quantum Mechanics, and Relativity Theory	1677
Low Temperature Physics	1679
Neutron Physics	1683
Nuclear Properties and Reactions	1689
Plasma Physics and Thermonuclear Processes	1706
Shielding	1714
Solid State Physics	1715
REACTOR TECHNOLOGY	1720
General	1720
Auxiliaries and Components	1721
Criticality Studies	1725
Design and Feasibility	1731
Fuels	1732
Power and Power-Breeder Reactors	1733
Process Heat Reactors	1739
Production Reactors	1739
Propulsion and Space	1740
Research and Test Reactors	1741
WASTE DISPOSAL AND PROCESSING	1746
GENERAL AND MISCELLANEOUS	1747
CORPORATE AUTHOR INDEX	INDEX-1
PERSONAL AUTHOR INDEX	INDEX-11
SUBJECT INDEX	INDEX-47
REPORT NUMBER INDEX	INDEX-116

STAFF OF NUCLEAR SCIENCE ABSTRACTS

MANAGING EDITOR

John W. Norris

ASSISTANT MANAGING EDITOR

Donald D. Davis

ASSOCIATE EDITORS

Lawrence T. Whitehead
David E. Bost
Robert C. Kelly
Lee M. Thompson

SUBJECT INDEX EDITOR

Everett J. Hoffman

EVALUATORS

William D. Matheny
John H. Mitchell
Mary H. Newman

ABSTRACTORS

F. S. Armstrong (AECL)
Jane G. Buchanan
D. Lamar Cason
Helen G. Donald
James R. Dulaney
Wells L. Green
Mary Catherine Grissom
Fernando J. Hamilton
Phyllis C. Hansen
Thomas F. Heagerty
Carolyn D. Houston
Rose V. Jermain
Betty L. McDowell
Jean F. Peckham
Mona H. Raridon
Julia Redford
Lila B. Smith
Charles E. Stuber
Martha J. Thomas
Anne G. Ward
David C. West
Milton O. Whitson
Gabriel O. Ycaza

SUBJECT HEADING SPECIALIST

Robert E. Upchurch

CORPORATE AUTHOR SPECIALIST

Clara L. Fox

DESCRIPTIVE CATALOGING SPECIALIST

J. Paul Meredith

SCHEDULING AND PUBLISHING COORDINATOR

Brainard L. Patton

Communication concerning the editorial policy and content of *NSA* should be addressed to the Managing Editor, *Nuclear Science Abstracts*, AEC Division of Technical Information Extension, P. O. Box 62, Oak Ridge, Tennessee 37830.

Use of funds for printing this publication approved by the Director of the Bureau of the Budget, May 20, 1963

OR

to the
nsion,

, 1963

Volume 20, Number 8 April 30, 1966

NUCLEAR SCIENCE ABSTRACTS

BIOLOGY AND MEDICINE

General

12563 AUTORADIOGRAPHY: TECHNIQUE FOR DRASTIC REDUCTION OF EXPOSURE TIME TO ALPHA PARTICLES. Hsieh, Jack J. C.; Hungate, F. P.; Wilson, S. A. (Battelle Memorial Inst., Richland, Wash.). Science, 150: 1821-2(Dec. 31, 1965).

High-speed, gross, alpha autoradiographs can be made if silver-activated zinc sulfide is used as an intensifier in conjunction with high-speed film. The intensifier is interposed between the sample and film. This technique requires about $1/1000$ of the exposure time required with NTB plates. The gross autoradiographs have greater contrast but slightly less resolution than conventional plates. (auth)

12564 GENETICS TODAY. Proceedings of the XI International Congress of Genetics, The Hague, The Netherlands, September 1963. Volume 2. Reports, Records and Plenary Sessions. Symposia 1–13. Geerts, S. J. (ed.). New York, Pergamon Press, 1965. 596p. (CONF-241(Vol. 2)).

Forty-one papers discuss various aspects of genetics, including gene structure, the genetic code, genetic control, developmental genetics, radiation genetics, chemical mutagenesis, chromosome structure and function, cytotaxonomy, experimental taxonomy, and ecological genetics. (C.H.)

12565 GENETICS TODAY. Proceedings of the XI International Congress of Genetics, The Hague, The Netherlands, September 1963. Volume 3. Symposia 14–25. List of Members. Index of Authors. Geerts, S. J. New York, Pergamon Press, 1965. 580p. (CONF-241(Vol. 3)).

Thirty-seven papers discuss various aspects of population genetics, plasmatic inheritance, the genetics of incompatibility, applications of genetics in animal and plant breeding studies, immunogenetics, behavioral genetics, and human genetics and dermatoglyphics. (C.H.)

Ecology

12566 (COO-1006-4) RATES AND PATTERN OF RADIOISOTOPE RELEASE FROM FRESH TREE LITTER AT THREE LEVELS OF MESIC FOREST DEVELOPMENT. Petty, R. O.; Williams, E. C. Jr. (Wabash Coll., Crawfordsville, Ind. Dept. of Biology). 1965. Contract AT (11-1)-1006. 104p. Dep. mn. CFSTI $4.00 cy, $0.75 mn.

Findings are summarized from a 4-year study of the rates and pattern of release of certain radioactive elements from fresh tree litter at three stages of mesophytic forest development. Young saplings of various tree species were inoculated with tracer amounts of ^{137}Cs, ^{32}P, ^{86}Rb, or ^{89}Sr and the activities in leaves, twigs, adjacent soil, and leaf litter were determined after various time intervals. The ecosystems studied included an old field, an oak forest, and a beech-maple climax forest. Records of precipitation and temperature were maintained and a number of related studies were carried out, including a study of secondary uptake of radionuclides by proximal vegetation, a survey of microbal populations in the leaf litter, and the uptake of ^{32}P by insects inhabiting the forests. Ecological implications of the findings are discussed. (C.H.)

12567 (ORNL-TM-1232) OAK RIDGE, TENNESSEE, FLORA: 1. PRELIMINARY ALPHABETIC INVENTORY OF VASCULAR PLANTS. Olson, J. S.; Cristofolini, G.; Cristofolini, S. (eds.) (Oak Ridge National Lab., Tenn.). Feb. 1966. Contract W-7405-eng-26. 27p. Dep. mn. CFSTI $2.00 cy, $0.50 mn.

Over 1500 higher plant taxa contribute to the genetic diversity of woodland and herbaceous ecosystems in Oak Ridge and surrounding Morgan, Roane, Anderson, Knox, and Loudon counties in Eastern Tennessee. This is an initial working checklist, so the number of species and the knowledge of their distributions will presumably be increased in future editions. Notations in the appended list (by county) include representation in: the ORNL Ecology Herbarium; the University of Tennessee Herbarium county maps; and additional records, mostly sight records. The Appendix represents an experiment in composition by a Friden Justowriter, from punched paper tape generated by IBM-1401 computer from input of IBM punched cards. These cards furnish a flexible file for continuous revision, for computer listings as needed, and for future rearrangements by sorting in taxonomic order, by ecological role, or by life forms. Numerical codes for order and family in the plant kingdom are adopted from the Internal Plant Index without implying judgment on the validity of the nomenclature which it accepts for operating categories. The speed with which additions and corrections have been (or can be) made furnishes an encouraging aid to an orderly progress in compiling regional floras, ecosystem inventories, and international studies such as those on terrestrial productivity and conservation for the International Biological Program. (auth)

12568 (TID-22639) EFFECTS OF RADIATION ON MIGRATORY ORIENTATION OF SALAMANDERS. Progress Report, May 1, 1965–February 1, 1966. Shoop, C. Robert (Wellesley Coll., Mass. Dept. of Biological Sciences). Contract AT(30-1)-3554. 5p. Dep. mn. CFSTI $1.00 cy, $0.50 mn.

Preliminary data on migratory orienting abilities of Ambystoma maculatum are reported. Population ecology studies were continued. Studies of population dynamics indicated that portions of the populations fail to return to the breeding ponds each year. Publications during the report period are listed. (H.G.D.)

12569 PROCEEDINGS OF THE HANFORD SYMPOSIUM ON RADIATION AND TERRESTRIAL ECOSYSTEMS, RICHLAND, WASHINGTON, 3–5 MAY 1965. Health Phys., 11: 1255-1675(Dec. 1965). (CONF–650523).

Separate abstracts are provided for each of the forty-three papers presented.

For abstracts of individual papers see: 12570–12587, 12607–12611, 12666–12675, 12915, and 12981–12988.

12570 FEEDBACK BETWEEN RADIATION ECOLOGY AND GENERAL ECOLOGY. Odum, Eugene P. (Univ. of Georgia, Athens). Health Phys., 11: 1257-62(Dec. 1965).

In an analogy with a feedback system, it is suggested that symposia should function as error detectors as well as serve as sources of information for researchers. It is further suggested that the interdisciplinary field of radiation ecology is now ready to move from a primary preoccupation with techniques and description to a position of making major contributions to the theory of ecosystems. Radiation procedures offer powerful means for solving the twofold problem of ecosystems, that of relating the one-way flow of energy to the cycling of materials and of discovering how physical and biological factors interact to control the functioning ecosystem. Only by understanding these matters in depth can man act as his own error detector and correct for the perturbations caused by his own technology which increasingly tend to disrupt the organization of nature. (auth)

12571 COSMIC-RAY PRODUCED RADIONUCLIDES IN THE ENVIRONMENT. Perkins, R. W.; Nielsen, J. M. (Battelle Memorial Inst., Richland, Wash.). Health Phys., 11: 1297-1304(Dec. 1965). (BNWL–SA-120).

The production rates of radionuclides in the atmosphere are strongly dependent on both altitude and geomagnetic latitude. The uses of the radionuclides ^{14}C and tritium in radioactive dating, atmospheric and ocean transport, and other studies are well known. While the radionuclides ^{14}C, ^{7}Be, ^{10}Be, and tritium are produced from the light element constituents of the atmosphere, numerous radionuclides are produced by spallation reactions on atmospheric argon. To date the radionuclides ^{22}Na, ^{24}Na, ^{32}Si, ^{32}P, ^{33}P, ^{35}S, ^{38}S, ^{36}Cl, ^{38}Cl, and ^{39}Cl have been reported. The meteoritic dust which is continually showered into the atmosphere contains spallation products of iron and other cosmic ray induced radionuclides. The concentrations of most of the radionuclides are extremely low and in some cases their artificial production by weapons testing has greatly exceeded their natural production. The biosphere is continually exposed to the wide spectrum of cosmic-ray produced radionuclides and some of these can serve as tracers in studies of the biological processes in nature. (auth)

12572 INTERCEPTION AND RETENTION OF FALLOUT BY DESERT SHRUBS. Martin, William E. (Univ. of California, Los Angeles). Health Phys., 11: 1341-54(Dec. 1965).

Concentrations of ^{131}I and ^{89}Sr on plants contaminated by fallout from Project Sedan tended to decrease with increasing distance from ground zero and increasing time after the detonation. Microscopic and radiometric examinations of foliage indicated that most of the activity deposited on leaves was probably due to particles <5 μ in diameter, and virtually none of it was due to particles >44 μ in diameter. A comparison between the theoretical and observed interrelations of gamma dose rates, ^{131}I and ^{89}Sr deposition rates, and ^{131}I and ^{89}Sr interception by desert shrubs indicated a deficiency of ^{131}I relative to ^{89}Sr in areas more than 40 miles from ground zero and an excess of both ^{131}I and ^{89}Sr relative to dose rates in areas about 100 miles from ground zero. The effective half lives of ^{131}I and ^{89}Sr on plants were shorter than their radioactive half lives, and a comparison of environmental half lives suggested that ^{131}I may have been lost from plants by some process, such as vaporization, which had no effect on the retention of ^{89}Sr. Statistical analyses indicated that the frequency distributions of variates representing maximum concentrations of ^{131}I and ^{89}Sr on plants, and in the tissues of rabbits collected at the same times and locations in the fallout field, were not normal but lognormal. Similar analyses indicated that the frequency distributions of effective half life estimates could be treated as either normal or lognormal. (auth)

12573 RADIONUCLIDE CYCLING: CURRENT STATUS AND FUTURE NEEDS. Auerbach, S. I. (Oak Ridge National Lab., Tenn.). Health Phys., 11: 1355-61(Dec. 1965). (ORNL-P-1305).

Because of increased recognition of the importance of cycling, there has been a considerable increase in biogeochemical studies of terrestrial environments. That the ecologic processes of biogeochemical cycling govern the movement of and are the determinants affecting long-term behavior of long-lived radionuclides, were not recognized sufficiently to merit serious research attention until the late 1950's. Since then, radionuclide cycling has become a recognized facet of radioecological research. The concept currently appears to include four categories of investigation. They are: deductive analyses derived from studies of fallout nuclides in different trophic levels of varying ecosystems; tracer experiments to elucidate links in a food chain and develop data on rate of movement in the chain; studies of rates of turnover of particular radionuclides within a single trophic level; and experiments employing tracers to measure the complete cycle in an ecosystem. Current problems such as interpretation of the significance of ^{90}Sr and ^{137}Cs levels in selected compartments of arctic ecosystems reinforce the need for more experiments of the fourth category emphasizing simple ecosystems. (auth)

12574 MINERAL CYCLING IN A DOUGLAS FIR FOREST STAND. Riekerk, Hans; Gessel, Stanley P. (Univ. of Washington, Seattle). Health Phys., 11: 1363-9(Dec. 1965).

The movement of mineral elements through the forest soil was studied. The early fall rains cause a flushing of decay products accumulated during the summer. Movement of the various mineral elements depends very much on their chemical characteristics, and on the fixation properties of the soil system. Phosphorus-32 release from the forest floor ranged from 2 to 14 percent, ^{86}Rb release was 0.01 to 1.88 percent and ^{45}Ca release was 0.06 to 0.86 percent for similar periods of leaching. Calcium-45 release over periods of leaching two to three times longer amounted to 0.1 to 4.1 percent. Release of ^{32}P from the surface soil was about 2800 times less than that from the forest floor. Rubidium-86 was 2200 times less and ^{45}Ca was about 160 times less than the release from the forest floor. Release patterns of ^{45}Ca indicated a slow movement as compared to ^{32}P and ^{86}Rb. Uptake of ^{32}P by the trees was evident within a week after application. Phosphorus-32 uptake was about ten times more during spring than during fall. Uptake of ^{86}Rb was evident after about a month during the spring season, but was not observed during fall. Uptake of ^{45}Ca was not significant. (auth)

12575 MINERAL TRANSFER IN A GREASEWOOD COMMUNITY AND ION UPTAKE BY GRASSES. Rickard, W. H.; Cline, J. F. (Battelle Memorial Inst., Richland, Wash.). Health Phys., 11: 1371-4(Dec. 1965). (BNWL–SA-157).

Greasewood, Sarcobatus vermiculatus (Hook.) Torr., has altered soil chemistry beneath its canopy by accumulating sodium in leaves. Leaf decay has increased concentrations of exchangeable sodium in the surface soil beneath the canopy spread. Cheatgrass, Bromus tectorum L., growing beneath the greasewood canopies had higher concentrations of sodium than did cheatgrass growing in the spaces between the shrubs. This indicates a transfer of sodium from greasewood to cheatgrass. Laboratory-grown barley seedlings also accumulated more sodium when grown in soil taken from beneath greasewood, but the uptake of added ^{45}Ca and ^{86}Sr was reduced. (auth)

12576 RADIOCESIUM DISPERSION IN A CRYPTOZOAN FOOD WEB. Reichle, David E.; Crossley, D. A. Jr.

(Oak Ridge National Lab., Tenn.). Health Phys., 11: 1375-84(Dec. 1965). (ORNL-P-1327).

Radiocesium dispersal in a forest floor food web is being studied in a Liriodendron stand previously tagged with ^{137}Cs. Initial studies traced the movement and equilibration of ^{137}Cs in the forest floor stratum. Subsequently, weekly samples are revealing seasonal shifts in concentration of ^{137}Cs in available food materials (leaf litter, wood, roots, and mosses). Pitfall trap collections form the basis for estimates of ^{137}Cs equilibrium concentrations in arthropods. Laboratory measurements of biological half-lives are being made for radiocesium in the major arthropod species. A preliminary synthesis of these data suggests that radiocesium techniques can be used to provide much detail on structure and function in this food web, but some relationships between animal species remain obscure. (auth)

12577 EQUATIONS FOR CESIUM TRANSFER IN A LIRIODENDRON FOREST. Olson, Jerry S. (Oak Ridge National Lab., Tenn.). Health Phys., 11: 1385-92(Dec. 1965). (ORNL-P-1470).

Simple compartment models can simulate the rapid net transfers of cesium from tree boles to foliage and roots, and to the forest environment. Only 2 to 4 weeks after inoculating 467 mCi into the dominant tulip poplar trees in a 500-m^2 plot, the upward flux of ^{137}Cs to foliage via transpiration was exceeded by losses due to rain leaching and downward translocation via phloem to roots. Fairly high root-soil turnover of cesium (0.003 $days^{-1}$) must explain the build-up in soil radioactivity, which is greater than rainout or autumn leaf fall can account for. A model with a matrix of constant fractional coefficients of transfer simulated the observable changes during early months. However, periodically varying coefficients are needed to allow for seasonal rhythms of the forest nuclide cycling and dispersal over a period of years. (auth)

12578 THE TRANSPORT OF ^{137}Cs FROM LICHEN TO ANIMAL AND MAN. Svensson, Goeran K.; Liden, Kurt (Univ. of Lund). Health Phys., 11: 1393-1400(Dec. 1965).

Lichen samples from the reindeer breeding areas of Sweden were analyzed. Large groups of Lapps in northern Sweden were measured once a year since 1961. The grazing habits of the reindeer and the fallout pattern imply that there is a delay of 7 to 10 months in the transfer of ^{137}Cs from lichen to man. From September 1962 to September 1964, the ^{137}Cs content in lichen per unit area was increased by a factor varying from 1.5 to 2.7 (average 2.0). The corresponding ^{137}Cs level in male Lapps has increased by a factor 1.5 to 2.0 (average 1.8) from April 1963 to March 1965. (auth)

12579 PRELIMINARY STUDIES OF THE PERSISTENCE OF TRITIUM AND ^{14}C IN THE PACIFIC PROVING GROUND. Koranda, John J. (Univ. of California, Livermore). Health Phys., 11: 1445-57(Dec. 1965). (UCRL-12302-T).

The results of a preliminary survey of detonation environments in the Pacific Proving Grounds indicate that residual tritium and ^{14}C are present in relatively high concentrations in soil materials of the detonation sites at times up to 12 years after the event. Exchange of soil-bound tritium with the available soil water takes place at a slow but significant rate and tritium is detectable in plants growing in the detonation environments. Carbon-14 is also elevated in the terrestrial plants. The basis for the elevated ^{14}C is not implicit in these preliminary data. Tritium and ^{14}C are also present in elevated concentrations in marine organisms. However, due to the high rate of exchange of the lagoon waters with the open sea, these elevated concentrations are highly localized in the vicinity of the detonation site (Mike Crater). (auth)

12580 APPLICATION OF SOME OPERATIONS RESEARCH TECHNIQUES TO FOOD CHAIN ANALYSIS PROBLEMS. van Dyne, George M. (Oak Ridge National Lab., Tenn.). Health Phys., 11: 1511-19(Dec. 1965). (ORNL-P-1290).

Attributes of species in mixed samples may be predicted from the attributes of the entire sample and from the species composition by weight of the sample. Thus, the relation between the composition of a given chemical as a proportion of the total sample in the ith mixed sample (C_i), the chemical content as a percent of the jth species, plant part, or plant group in the sample (P_j), and the percent weight of the jth species, plant part or plant group in the ith sample (W_{ij}) is: $C_i = \Sigma_j (P_j W_{ij})$ where $j = 1, 2 \ldots m$ species, parts or groups in the sample. Least squares and nonlinear programming routines were compared for solving for the P_j by minimizing a function Q as follows: $Q = \Sigma_i [C_i - \Sigma_j (P_j W_{ij})]^2$ subject to $0 \leq P_j \leq 100$ and $i = 1, 2 \ldots n$ samples. Known P_j and W_{ij} were used to generate C_i to test these techniques. Variability of P_j and W_{ij} was obtained with random number generators, and known bias was included in some W_{ij} values in thirty computer experiments. $\hat{P}_j$, predicted by the above methods from the generated C_i and W_{ij}, were compared to P_j, the true values which were used in generating the data. Both least squares and nonlinear programming gave acceptable $\hat{P}_j$ in most instances. These techniques were applied successfully to data from range nutrition experiments with cattle and sheep to predict the crude protein content of five groups of species in the diets from the botanical composition and the crude protein in the mixed sample. (auth)

12581 A FIELD METHOD FOR STUDYING ROOT SYSTEMS. Price, Keith R. (Univ. of Nevada, Reno). Health Phys., 11: 1521-5(Dec. 1965).

A field method using a radioisotope of iodine for the study of root systems is described. Limitations and precautions for the method and interpretation of data are discussed. Aluminum tubing, special plastic bottles, and a modified lead-shielded syringe are used to inject the radionuclide into the soil at predetermined positions. The distribution of the radioactivity within the soil profile is determined by autoradiography. Plant shoots determined radioactive by treatment are assumed to have roots in the contaminated soil. If the same area is contaminated at different times and results are correlated with phenological, physiological, and environmental factors, the dynamic as well as the static aspects of natural plant communities and ecosystems can be studied. (auth)

12582 DECAY CHARACTERISTICS OF NEUTRON INDUCED RADIOACTIVITY IN SOILS. Nishita, H. (Univ. of California, West Los Angeles). Health Phys., 11: 1527-41(Dec. 1965).

Radioactive decay characteristics were studied in several different soils and clay minerals irradiated in the UCLA Engineering Nuclear Reactor. Decay characteristics of simulated soils of specified elemental composition also were predicted by computer calculations. Although the neutron activated soils differed widely in physical and chemical properties from an agronomic point of view, the general trends in their decay curves were quite similar up to 10,000 hrs suggesting that the elemental composition of these soils was similar. The differences in the absolute amounts of each element in the soils were manifest by the differences in the activity levels per unit weight of the soils and the slopes of the decay curves at a specified time. The radioactive decay rates were relatively rapid up to about 200 hrs after irradiation and then changed to noticeably slower rates. Depending on the time after irradiation, the beta and gamma decay constants of the experimental soils varied between $T^{-0.2}$ and $T^{-5.0}$. Although many radionuclides were formed, relatively few determined the shapes of the decay curves. (auth)

12583 ^{45}Ca LABELING OF MAMMALS FOR USE IN POPULATION STUDIES. Rongstad, Orrin J. (Univ. of Wisconsin, Madison). Health Phys., 11: 1543-56(Dec. 1965).

Techniques are described for labeling young thirteen-lined ground squirrels, cottontail rabbits, and snowshoe hares with ^{45}Ca. The isotope was implanted subcutaneously into adult females during the breeding season and subsequently passed to their offspring. The labeled young were used to make spring population estimates by means

of the Lincoln Index and to determine movements. This technique gave increased numbers of marked animals per marking effort and reduced the trap bias that is common in trap-retrap census methods. Thirty microcuries of ^{45}Ca implanted in a female thirteen-lined ground squirrel labeled her offspring for a year or more after birth. Sixty microcuries of ^{45}Ca labeled all four litters of snowshoe hares and could be detected until the September following birth. Sixty microcuries of ^{45}Ca were in most cases sufficient to label all cottontail litters, but 175 μCi insured labeling fifth and sixth litters and prolonged the time of detection. The petrosal bone of the inner ear had the slowest turnover of ^{45}Ca and was thus the best bone for detecting the presence of radioactivity. By varying strengths of implanted capsules or times of implant in relation to parturition, littermates among thirteen-lined ground squirrels could often be identified by amounts of radioactivity present. Spring population estimates were obtained on study areas for snowshoe hares and ground squirrels by means of ^{45}Ca labeling. (auth)

12584 RADIATION AND ANIMAL POPULATIONS: PROBLEMS, PROGRESS AND PROJECTIONS. French, Norman R. (Univ. of California, Los Angeles). Health Phys., 11: 1557-68(Dec. 1965).

A review of recent literature suggests the importance of measuring the functional efficiency of irradiated populations. Population ecology provides methods suitable for evaluating the performance of populations. Dosimetry in radiation studies is simplified by new microthermoluminescent dosimeters. A population can be irradiated by administration of a single acute exposure of each individual animal, by chronic exposure of a large study area with an established population, or by administration of an isotope for internal exposure of the animals. Irradiation may impair a population primarily through reduction in fertility, and to some extent by reduction of life-span. In mammalian populations, reduced fertility would not under ordinary conditions be hazardous to survival, except when other environmental stress causes a shift in the age structure of the population to the point where reproduction by older individuals is important to maintenance of the population. (auth)

12585 EFFECTS OF RADIATION ON THE NATALITY, DENSITY AND BREEDING STRUCTURE OF A NATURAL POPULATION OF LIZARDS, UTA STANSBURIANA. Tinkle, Donald W. (Texas Technological Coll., Lubbock). Health Phys., 11: 1595-9(Dec. 1965).

Two 2-acre study areas designated as experimental and control areas were established in western Texas in 1960 and 1961. Adult lizards on one area were given 450 R of gonadal radiation in 1962 just prior to the breeding season. After 2 yrs of intensive study, a switchback experiment was performed in which animals on the former control area were given the same single radiation dose. The irradiation resulted in a nearly 50 percent decline in natality that resulted in a striking decrease in density the year after irradiation. The breeding structure of the population was affected through interference by irradiation with the normal selective processes in a natural population. The results were apparently duplicated in the switchback experiment. (auth)

12586 RADIATION EFFECTS ON PLANT POPULATIONS AND COMMUNITIES: RESEARCH STATUS AND POTENTIAL. Platt, Robert B. (Emory Univ., Atlanta). Health Phys., 11: 1601-6(Dec. 1965).

The research status and future potential for studies concerned with the effects of ionizing radiation on plants at the organism, population, community and ecosystem levels are reviewed. Opportunities for future development in this field are considered; including experimental techniques and methods for irradiation, dosimetry data retrieval and analysis systems, organisms, homeostatic mechanisms, prediction of radiation effects, physiological stimulation, catastrophic effects of ionizing radiation, and effects of continuous low-level irradiation. (auth)

12587 REASSESSING THE BIOLOGICAL ROLE OF BACKGROUND TERRESTRIAL RADIATION AS A CONSTITUENT OF THE NATURAL ENVIRONMENT. Mericle, L. W.; Mericle, R. P. (Michigan State Univ., East Lansing). Health Phys., 11: 1607-20(Dec. 1965). (COO-1400-5).

Experimental evidence clearly establishes that exposure levels from natural terrestrial radiation can be of potential genetic and ecological importance to highly radiosensitive plant populations. Other facets of the physical environment are capable of strong synergistic interactions, or attenuation of the radiation responses to the point of near cancellation. Changes in the rate of development, inherent with age or developmental stage or induced by the environment, can also influence the intensity of the radiation response and the degree to which an organism can discriminate between radiation levels. For plant populations indigenous to regions of high radioactivity, dosages may be materially altered by meteorological conditions, developmental rates and the absorption of radionuclides by the plant roots. (auth)

Metabolism, Tissue Distribution, and Toxicology

Refer also to abstract 12984.

12588 (AD-626320) METABOLISM OF SELECTED RADIONUCLIDES FED IN VARIOUS PHYSICAL FORMS TO ANIMALS. Final Report, June 4, 1964-June 30, 1965. Comar, C. L.; Wentworth, R. A.; Lengemann, F. W. (New York State Veterinary Coll., Ithaca, N. Y. Dept. of Physical Biology). Contract OCD-PS-64-117. 41p. CFSTI $2.00 cy, $0.50 mn.

Body retention and secretion into milk were determined for ^{85}Sr and ^{134}Cs from the following sources: simulants of local fallout, $^{85}Sr(NO_3)_2$, $^{85}SrCl_2$, and $^{134}CsCl$. Four cows, 15 goats, and 16 hogs were used. The Whole-Body Counter was employed to measure retention in the goats and hogs. The biological availability of radiocesium and strontium was found to be dependent upon the solubility characteristics of the fallout simulant and appears to be predictable from in vitro tests under some conditions. Interspecies differences in biological availability were not large. (auth)

12589 (AECL-2507) THE FATE OF TERPHENYL IN THE RAT. Petkau, A.; Rayner, H. L. (Atomic Energy of Canada Ltd., Pinawa (Manitoba). Whiteshell Div.). Nov. 1965. 12p. Dep. AECL $0.50.

Rats, exposed orally to the mixture of polyphenyls known as Santowax OM, developed hematuria, glucosuria, polyuria, and hypoalbuminuria. They excreted unmetabolized terphenyl and significantly increased amounts of glucuronic and galacturonic acids in the urine. Additional, but as yet unidentified, phenolic components were also excreted in the urine. (auth)

12590 (CEA-R-2825) RYTHMES DE VEGETATION DE QUELQUES ESPECES LIGNEUSES. ABSORPTION RADICULAIRE ET TRANSPORT DE SELS ALCALINO-TERREUX (^{45}Ca,^{140}Ba) AU COURS D'UN CYCLE VEGETATIF COMPLET, MARS 1963-AVRIL 1964. (Vegetative Rhythms of Some Woody Species. Radicular Absorption and Transport of Alkaline Earth (^{45}Ca,^{140}Ba) Salts During a Complete Vegetative Cycle, March 1963-April 1964). Gagnaire, Janine (Commissariat a l'Energie Atomique, Grenoble (France). Centre d'Etudes Nucleaires). Oct. 1965. 50p. Dep. mn.

Variations of calcium absorption by roots and translocation speed towards aerial parts of young Norway spruce (Picea excelsa) growing in hydroponic media were studied during a 12-mo period. From early April until the end of May a rapid rise of minerals from roots to young parts of the tree, associated with a redistribution of calcium formerly fixed in tissues was observed. In June and July, an equilibrium in mineral exchanges between the different parts of the tree was observed. From early August to the end of October, a pre-dormancy phase, marked by a slowing of translocation was noted, and in November and De-

cember an absolute dormancy period existed. From January to March, a post-dormancy phase was noted in which root absorption and translocation to aerial parts recovered. (auth)

12591 (EUR–2475.f) ETUDE DE L'ABSORPTION SELECTIVE DU STRONTIUM PAR LES ACANTHAIRES. (Study of the Selective Absorption of Strontium by Acantharia). Annual Report, February 1963–March 1964. Delrio, G.; Merinfeld, G. (Brussels Univ. (Belgium). Laboratoire de Zoologie et Biologie). 1965. Contract 015-62-2 BIOB. 80p. Dep. mn.

Preliminary biological and ecological studies were undertaken in an attempt to study the problem of the metabolism of strontium sulphate in Acantharia in the best possible conditions. In the course of this work extensive tests on methods of collecting and cultivating Acantharia were conducted, together with physical and chemical measurements of the habitat of these protozoa. In order to obtain more accurate biochemical data, cytochemical and cytological research was carried out on various types of Acantharia, as well as observations on their ultrastructure under the electron-microscope. Various observations under the optical and electron-microscope show that certain changes should be made in the classification and phylogenesis of Acantharia. With regard to actual biochemical research, the dry weight and the percentage of organic nitrogen in Acantharia were determined and their amino acid content studied by chromatography. In an attempt to determine the nature of the salts which make up their skeleton, a qualitative and quantitative ion analysis of Acantharia was carried out by emission-spectrophotography. In order to study the metabolism of the SO_4^{2-} ion and to elucidate the part, whether organic or inorganic, it plays in the formation of the $SrSO_4$ skeleton, incorporation experiments were performed with the radiosulphate Na_2SO_4, cystine-^{35}S and methionine-^{35}S using autoradiography. At the same time, identical methods were employed to examine the uptake of ^{90}Sr. (tr-auth)

12592 (NP–15671) COORDINATED PROGRAM ON THE APPLICATION OF ISOTOPES AND RADIATION IN RICE CULTIVATION. Progress Report No. 1. (Taiwan Provincial Chung-hsing Univ., Taichung (China). Dept. of Agronomy). Mar. 1965. Contract 257/OB. 8p. Dep. mn.

Progress is reported on experiments carried out to determine the efficiency of fertilizer nitrogen and fertilizer phosphorus applied to lowland rice as affected by time and rate of application. Nitrogen-15-labeled and unlabeled ammonium sulfate and ^{32}P-labeled and unlabeled superphosphate were used. Data on number of tillers, average plant height per hill from yield sub-plots, and yields from plots to which fertilizer applications were made at various times and in various amounts are tabulated. Four illustrations are included. (H.G.D.)

12593 (NP–15672) COORDINATED PROGRAM ON THE APPLICATION OF ISOTOPES AND RADIATION IN RICE CULTIVATION. Final Report No. 2. Ouang, T. Y. (Taiwan Provincial Chung-hsing Univ., Taichung (China). Dept. of Agronomy). Aug. 1965. Contract 257/OB. 18p. Dep. mn.

Progress is reported on tracer studies of the efficiency of nitrogen fertilizer applied to lowland rice as affected by time and rate of application. Taichung No. 65 rice was grown on slightly acid soils and under conditions of irrigation because of the sparse rainfall during the growing season. No significant differences were found between the amount and time of nitrogen fertilizer application and ear weight or 1000 grain weight, nor between the time of application and numbers of tillers, ears, or grain yield. However, the amount of nitrogen fertilizer applied significantly affected numbers of tillers and ears and grain yield. Dry matter was produced proportionally to the amount of fertilizer used. (H.G.D.)

12594 (NP–15679) SOME FACTORS INFLUENCING MAMMALIAN RETENTION OF RADIOACTIVE STRONTIUM. Progress Report, October 1, 1961–March 31, 1962. Vouk, V. B. (Yugoslav Academy of Sciences and Arts, Zagreb. Inst. for Medical Research). Apr. 1, 1962. Contract 113/RB. 34p. Dep. mn.

Developments in studies on: influence of negative Sr balance on the retention of radioactive Sr and Ca in rat skeleton; influence of dietary P on Ca and Sr metabolism in rats; toxicity of new chelating agents for radiostrontium removal; and synthesis of chelating agents for use in radiostrontium removal from the body are reported. (P.C.H.)

12595 (NP–15680) SOME FACTORS INFLUENCING MAMMALIAN RETENTION OF RADIOACTIVE STRONTIUM. Progress Report, March 31, 1962–October 1, 1962. Vouk, V. B. (Yugoslav Academy of Sciences and Arts, Zagreb. Inst. for Medical Research). Oct. 1, 1962. Contract 113/RB. 24p. Dep. mn.

Developments are reported for studies on: influence of negative strontium balance on retention of radioactive Sr and Ca in the skeleton; influence of negative and positive P balance on retention of radioactive Sr and Ca in the skeleton; effects of dietary P on Ca and Sr metabolism in rats after oral and intraperitoneal entry of ^{85}Sr and ^{47}Ca; and synthesis and study of chelating agents of possible use for removal of radiostrontium from the body. (P.C.H.)

12596 (NP–15681) SOME FACTORS INFLUENCING MAMMALIAN RETENTION OF RADIOACTIVE STRONTIUM. Progress Report, October 1, 1962–March 31, 1963. Vouk, V. B. (Yugoslav Academy of Sciences and Arts, Zagreb. Inst. for Medical Research). Apr. 1, 1963. Contract 113/RB. 39p. Dep. mn.

Developments are reported for studies on: effects of dietary phosphate changes on Sr and Ca metabolism; mechanism of action of phosphate ions on Sr and Ca metabolism; efficiency of new chelating agents for radiostrontium removal; stability constants of 1,2-diamino-cyclopentane-N,N,N′,N′-tetraacetic acid; and synthesis of new chelating agents. (P.C.H.)

12597 (NP–15682) SOME FACTORS INFLUENCING MAMMALIAN RETENTION OF RADIOACTIVE STRONTIUM. Progress Report, March 31, 1963–June 30, 1963. Vouk, V. B. (Yugoslav Academy of Sciences and Arts, Zagreb. Inst. for Medical Research). June 21, 1963. Contract 113/RB. 25p. Dep. mn.

Rats were fed diets containing different amounts of phosphates (from 0.5 to 1.2% P). This was found to influence the subsequent Sr and Ca metabolism as indicated by the skeletal retention of ^{85}Sr and ^{47}Ca after oral and intravenous application. The dominant effect of the increased dietary phosphorus on Ca and Sr metabolism in the rat was a decrease in the GI absorption of both ions; the absorption of Sr was preferentially affected. It was concluded that decreasing the absorption from the GI tract may be the most effective protection against deposition of radiostrontium in the skeleton. (P.C.H.)

12598 (NP–15683) SOME FACTORS INFLUENCING MAMMALIAN RETENTION OF RADIOACTIVE STRONTIUM. Progress Report, June 30, 1963–March 31, 1964. Vouk, V. B. (Yugoslav Academy of Sciences and Arts, Zagreb. Inst. for Medical Research). Mar. 31, 1964. Contract 113/RB. 20p. Dep. mn.

Developments are reported for studies on: turnover of radioactive strontium in new born rats; influence of dietary calcium and phosphate changes on calcium and strontium metabolism; and efficiency of chelating agents on radioactive strontium removal. (P.C.H.)

12599 (NP–15684) SOME FACTORS INFLUENCING MAMMALIAN RETENTION OF RADIOACTIVE STRONTIUM. Progress Report, March 31, 1964–June 30, 1964. Vouk, V. B. (Yugoslav Academy of Sciences and Arts, Zagreb. Inst. for Medical Research). June 30, 1964. Contract 113/RB. 22p. Dep. mn.

Developments are reported for studies on turnover of Sr in newborn rats and influence of dietary calcium and phosphate changes on Ca and Sr metabolism. (P.C.H.)

12600 (NP–15685) SOME FACTORS INFLUENCING MAMMALIAN RETENTION OF RADIOACTIVE STRONTIUM. Final Report, October 1, 1961–September 30, 1964. (Yugoslav Academy of Sciences and Arts, Zagreb. Inst. for Medical Research). Sept. 30, 1964. Contract 113/RB. 82p. Dep. mn.

Studies were made primarily on the way in which changes in the dietary phosphorus within the physiological range influence the comparative metabolism of Ca and Sr and on the use of chelating agents as a means for enhancing radioactive Sr elimination from the body. It was found that the phosphate level of the diet has a pronounced effect on the skeletal retention of radioactive Sr. The phosphate level of the diet at the time of the entry of radioactive Sr into the body seems to be the factor that influences the absorption and elimination of Sr and Ca and not the previous diet or any late application of the diet. Studies on the mechanism of the phosphate action in the body revealed that phosphate ions act at two sites in the body; the gastrointestinal tract and the kidneys. Experiments on newborn rats indicated that the phosphate intake of nursing mothers could also provide an effective means of decreasing the uptake of radioactive Sr in the newborn. The toxicity of the chelating agents used was found to be of the same order of magnitude as the toxicity of EDTA. The chelating agents applied as strontium disodium salts caused a slight decrease in the skeletal deposition of radioactive Sr, the best effect being obtained by application of $SrNa_2$ CPDTA. (P.C.H.)

12601 (TID–22526) A STUDY OF FACTORS CONCERNED IN THE UPTAKE, PHYSIOLOGY AND RETENTION OF ^{65}Zn IN THE MALE REPRODUCTIVE SYSTEM OF THE RAT. Final Report. Gunn, Samuel A. (Miami Univ., Fla. Dept. of Pathology). Dec. 1965. Contract AT(40-1)-2023. 13p. ORAU.

Research accomplishments during a 10-yr study of factors concerned in the uptake and retention of Zn in the male reproductive organs of rats are summarized. Studies, using ^{65}Zn as a tracer, demonstrated that this element localized in specific lobes of the rat prostate. The role of Zn in the physiology of the male reproductive system was investigated. A list is included of 30 publications during the period. (C.H.)

12602 (JPRS–33958) RECENT DEVEOPMENTS IN STUDIES OF RADIOACTIVE SUBSTANCES. Translation of Med. Radiol., 10: No. 10, 15-19; 75-80; 89-93(1965). 30p. (TT–66-30401). CFSTI $2.00 cy, $0.50 mn.

Three papers are included: separate abstracts were prepared for two. The remaining paper on the first scientific session of the Institute of Radiology of the Academy of Sciences, USSR was not abstracted for NSA. (H.G.D.)

For abstracts of individual papers see: 12603 and 12604.

12603 (JPRS–33958, pp 1-7) TOXICITY OF MODERN RADIOACTIVE LUMINOUS COMPOUNDS. Halik, J. Translated from Med. Radiol., 10: No. 10, 15-19(1965).

Radium absorption in animals was studied in white male rats that had ingested aqueous radium dyes or that had received radium chloride in gastric implants. Urinary and fecal excretion and tissue distribution were determined. Results indicated distribution of the aqueous compound and the radium chloride were qualitatively the same. Radium excretion was detected in urine before fecal excretion. Retention within the organisms decreased rapidly up to the 5th day, but was greater at the 10th day in the group receiving the radium dye. It is concluded that toxicity of radium compounds containing radium salt is similar to that of the radium salt. (H.G.D.)

12604 (JPRS–33958, pp 8-19) DISTRIBUTION OF CERTAIN RADIOACTIVE SUBSTANCES UPON THEIR INHALATION. Korolev, G. K. Translated from Med. Radiol., 10: No. 10, 75-80(1965).

Clinical and experimental data on absorption of radioactive particles by respiratory tissues are reviewed. Upon inhalation, entry into the tissues may be via the gastrointestinal tract or respiratory organs. Evidence indicates that a significantly higher entry-rate occurs in respiratory organs, particularly in the case of the rare earth elements. (H.G.D.)

12605 DISTRIBUTION OF STRONTIUM AND CALCIUM IN PISUM SATIVUM IN RELATION TO THE STRONTIUM/CALCIUM RATIO OF THE CULTURE FLUID. Myttenaere, C.; Masset, M. (EURATOM, Ispra, Italy). Ann. Physiol. Veg., 7: 97-104(1965). (In French).

Pea (P. sativum, var. Espoir de Grembloux) seedlings were grown in nutrient fluid containing Sr and Ca in three different proportions, along with tracer amounts of ^{85}Sr and ^{45}Ca, and analyses for the two elements were made in various plant parts after different growth intervals. Thus, the absorption and distribution of Sr and Ca were investigated for three Sr/Ca ratios of the nutrient solution: 0/5, 0.5/4.5, and 2.5/2.5 meq/l. The stable Sr content of the aerial parts and the roots increased with the Sr/Ca ratio of the nutritive solution. Examination of the variation of the ratio of Sr content in the aerial parts and the roots (mg/g dry matter) revealed a greater retention of Sr at root level for a low Sr/Ca ratio; a similar investigation carried out for Ca showed a different behavior for the two ions. The major part of Sr and Ca in the tissues can be extracted by hydrochloric and perchloric acids. The lipid, nucleic acids, and residual components contain little of these elements. The fraction containing the pectates varied in content according to the Sr/Ca ratio of the nutrient solution and with the element assayed. The results illustrate the caution needed in examining the metabolism and tissue distribution of Ca and Sr; they show that the two elements are not handled physiologically by the plant in an identical way. (BBB)

12606 EFFECT OF PHOSPHATES, CARBONATES, AND MAGNESIUM OXIDE UPON THE INTESTINAL ABSORPTION OF ^{85}Sr IN RATS. Volf, V. (Inst. of Radiation Hygiene, Prague). Experientia, 21: 571-2(1965).

The effects of various phosphates, carbonates, and magnesium oxide on the metabolism of orally administered ^{85}Sr in rats were studied. The substances were administered to 93 starved male Wistar albino rats by stomach tube 10 min. after an oral dose of carrier-free ^{85}Sr chloride solution. The animals were sacrificed 48 hr later. In the skeleton of rats treated with phosphates, 40 to 65% less ^{85}Sr was retained in comparison with controls. In the group receiving tricalcium phosphates with disodium phosphates the average skeletal retention was reduced by nearly 90%. Only calcium carbonate among the carbonates tested proved effective. It reduced whole-body retention of ^{85}Sr by 40% in comparison with controls. In rats receiving MgO, 50% less ^{85}Sr was retained. (M.C.G.)

12607 INTERCEPTION AND RETENTION OF AIRBORNE MATERIAL ON PLANTS. Russell, R. Scott (Agricultural Research Council Radiobiological Lab., Wantage, Eng.). Health Phys., 11: 1305-15(Dec. 1965).

The uptake and retention of airborne materials by plants is discussed in respect to the extent to which these factors may influence the total radiation dose received by members of ecosystems, particularly those ecosystems created or modified by man. Radiation dose and radioisotopes serving as major sources of internal contamination are considered quantitatively. Evidence is presented suggesting that the direct contamination of vegetation is responsible for a larger fraction of the ^{90}Sr in the food chain than formerly supposed is presented. (H.G.D.)

12608 SOIL-PLANT RELATIONSHIPS OF RADIOACTIVE ELEMENTS. Menzel, R. G. (Department of Agriculture, Beltsville, Md.). Health Phys., 11: 1325-32 (Dec. 1965).

The plant concentration of various radioactive elements, after they have been added to soils in water-soluble forms, may be several orders of magnitude higher or lower than

the concentration in the soil. Those that are most readily absorbed are soluble in the soil or are isotopic with elements that have metabolic functions in the plant. Those that are least absorbed are quite insoluble in the soil. The gamma radiation doses to plants would come predominantly from the soil, as would the beta radiation doses except for the beta radiation from those few elements which may be highly concentrated in certain plant tissues. The role of plants in movement of radionuclides in soil is minor except over very long periods of time. (auth)

12609 THE COMPARATIVE METABOLISM OF STRONTIUM, CALCIUM AND CESIUM IN DEER AND SHEEP. Goldman, Marvin; Longhurst, W. M.; Della Rosa, R. J.; Baker, N. F.; Barnes, R. D. (Univ. of California, Davis). Health Phys., 11: 1415-22(Dec. 1965).

Six deer and six sheep were fed either alfalfa (calcium 0.97 percent, calcium/phosphorus = 5.1) or a pelleted ration (calcium 0.68 percent, calcium/phosphorus = 0.9) for 2 weeks prior to and 30 days following a single intraruminal injection of $^{85}Sr + {}^{47}Ca + {}^{137}Cs$. Weekly whole-body gamma spectrometry and post-sacrifice measurements on portions of skeleton, gastrointestinal tract, viscera, skin, and muscle mass were performed. The observed ratio (OR) ($^{85}Sr/^{47}Ca$) total body or bone was 0.5 in sheep and deer fed pellets, while on alfalfa the OR was 0.4 for sheep and 0.3 for deer. The dietary calcium level was approximately inversely related to the percent radionuclide uptake while the difference in OR appeared to be phosphate-dependent in both species. Cesium-137 was retained with an average biologic half-period of 17 days in all animals. (auth)

12610 RADIOTRACER, GRAVIMETRIC AND CALORIMETRIC STUDIES OF INGESTION AND ASSIMILATION RATES OF AN ISOPOD. Hubbell, Stephen P.; Sikora, Anne; Paris, Oscar H. (Univ. of California, Berkeley). Health Phys., 11: 1485-1501(Dec. 1965).

A direct comparison was made of radiotracer and gravimetric measurements of ingestion and assimilation rates, and of assimilation fraction, in Armadillidium vulgare under laboratory and field conditions. The elimination ^{85}Sr was also measured in the laboratory and field. Radiostrontium was excreted more rapidly in the field. The radiotracer and gravimetric measurements gave similar estimates of ingestion and assimilation rates, and of assimilation fraction. Assimilation fraction varied, ranging from 0.06 to 0.13 in the laboratory to 0.53 to 0.75 in the field. Assimilation fraction appears to be inversely related to rate of ingestion, resulting in a relatively constant assimilation rate over a wide range of ingestion rates. Conversion of radiotracer and gravimetric estimates to caloric estimates, using bomb calorimetry, revealed a greater caloric value of assimilated material than of the food ingested. (auth)

12611 A TROPHIC LEVEL EFFECT ON ^{137}Cs CONCENTRATION. Pendleton, Robert C.; Mays, Charles W.; Lloyd, Ray D.; Church, Bruce W. (Univ. of Utah, Salt Lake City). Health Phys., 11: 1503-10(Dec. 1965).

In many animal species, the cesium/potassium ratio in the body is about two to three times higher than the cesium/potassium ratio in their normal diets. Data indicate that this increased ratio is greater with increased potassium intake and is larger in adult humans than in children. (auth)

12612 USE OF ^{51}Cr-LABELLED HAEMOGLOBIN AND ^{47}Sc AS INERT FAECAL MARKERS. Pearson, J. D. (Guy's Hospital Medical School, London). Int. J. Appl. Radiat. Isotop., 17: 13-16(Jan. 1966).

Fecal recoveries of ^{51}Cr (administered as labeled hemoglobin) and ^{47}Sc were measured following their oral administration. Both these substances were found to be unabsorbed and furthermore there was no significant difference in their gastrointestinal transit time. There was no significant fecal excretion of ^{47}Sc following its intravenous administration. Because of these properties and also because of its favorable radiation characteristics it is suggested that ^{47}Sc is a suitable isotope to use as a fecal marker in metabolic work, in particular it is useful when the excretion of ^{51}Cr is being studied, making it necessary to use another isotope as the inert marker. (auth)

12613 INVESTIGATION OF THE SALURETIC AND KALIURETIC PROPERTIES OF A DIURETIC AGENT IN SWINE BY IN VIVO WHOLE BODY COUNTING. Shaw, Stanley M.; Kessler, Wayne V.; Christian, John E. (Purdue Univ., Lafayette, Ind.). J. Pharm. Sci., 54: 1208-10 (Aug. 1965).

An investigation was made of the utilization of a large-animal whole-body liquid scintillation counter for the determining the saluretic and kaliuretic properties of a diuretic compound in large animals. Small pigs were chosen as subjects because of the biological similarity of swine to man. A simple analytical technique developed for evaluation of diuretic agents. Whole-body liquid scintillation counting, in conjunction with ^{24}Na and ^{42}K, was utilized to determine directly the retention of the isotopes during control and diuretic treatment. A radioactive tracer was orally administered and allowed to equilibrate in the animals, and control or drug treatment was initiated. Animals were counted at selected time intervals. The percent retention of the radioisotope was calculated for each whole-body tracer determination. Control and treated data were compared for the loss of sodium and potassium due to diuretic action. The diuretic agent, furosemide, was found to exhibit a marked saluretic activity in swine, while causing a small loss of potassium. The short half-lives of ^{24}Na (15.05 hr) and ^{42}K (12.47 hr) allow the utilization of the same animals for control and drug studies. Utilizing this assay procedure, the difficulties found in flame photometric analysis are eliminated. (BBB)

12614 A RADIOLOGICAL METHOD FOR THE DETERMINATION OF CAMBIAL ACTIVITY. Waisel, Yoav; Fahn, Abraham (Tel-Aviv Univ., Israel). Physiol. Plant., 18: 44-7(1965).

A new radioisotope method, utilizing ^{14}C, is described for evaluating the activity of cambium. The two usual methods (nonradioisotopic) for determining whether cambium is dormant or active have several drawbacks, which are discussed. These objections called for a search for a better method by which both the rate of cell division and the rate of cell differentiation could be precisely determined. In exploratory studies, active and dormant potted plants of Acacia tortilis, Pistacia lentiscus, Zygophyllum dumosum, and Eucalyptus camaldulensis were exposed to labeled $^{14}CO_2$ in light for 48 hr. By this time the applied $^{14}CO_2$ (5 μC/10 mg $BaCO_3$) had been fully assimilated. To ascertain distribution of the labeled assimilates, the plants were left untouched for another week. Samples of the axis below the labelled branch were taken and microsome sections 10 μ thick were prepared. The sections were repeatedly rinsed in water and in oxidizing agent to destroy the protoplast, and remove the labeled soluble compounds. The sections were then examined by autoradiography. As only the most recently deposited cell wall materials would be labeled with ^{14}C, the newly divided and differentiated cells of the active tissues could be easily distinguished. In dormant plants no labeling could be observed. Moreover, it is seen that in the xylem elements, located inward of the cambial zone, which histologically appear as fully differentiated, newly formed substances are still deposited. (TCO)

12615 THE EFFECT OF A CARRIER ON THE PULMONARY RETENTION OF THE RADIOCERIUM. Pleskova, A.; Beno, M.; Trnovec, T.; Vladar, M. Prac. Lek., 17: 350-3(1965). (In Czech).

The effect of a Ce^{3+} carrier on the retention and organ deposition of ^{144}Ce after the intratracheal administration to rats was investigated. The decrease of ^{144}Ce in the lungs is described by a power function. The maximum change of the rate constant of the radiocerium retention in the lungs was caused by addition of the carrier up to 160 μg Ce^{3+}. The radiocerium retention in the lungs was significantly increased by the carrier. (tr-auth)

12616 QUANTITATIVE AUTORADIOGRAPHY. Perry, Robert P. (Inst. for Cancer Research, Philadelphia). pp 304-26 of Methods in Cell Physiology, Vol. 1. Prescott, D. (ed.). New York, Academic Press, 1964.

This review considers factors involved in making a quantitative autoradiographic measurement: (1) specimen geometry and its relation to the photographic emulsion, (2) density of the specimen, (3) energy spectrum of the β rays which are emitted from the particular radioactive atom, and (4) thickness and sensitivity characteristics of the emulsion. Grain number must be adjusted to an optimum which is high enough relative to background for statistical accuracy and yet low enough so that coincidence events are at a negligible level. The interplay of these factors is illustrated by examples. Electrons from emitters such as ^{32}P (max energy, 1.7 Mev; average range in water, 1250 μ), ^{35}S (0.167 Mev; 50 μ), and ^{14}C (0.155 Mev; 40 μ) are ejected in all directions and suffer little or no attenuation in passing through comparatively thin specimens. Consequently, electrons emitted from a certain region of the specimen are likely to give rise to grains at points which do not lie directly over the region. This gives rise to image spread (hence poor resolution) and to loss of contrast due to crossfire. The situation with an emitter such as ^{3}H (0.018 Mev; 1 μ) is different. The electrons emitted by tritium have an average range in fixed biological material of a few microns at most. Problems of image spread and crossfire are considered in detail, with calculations of the effects for ^{3}H in particular. Practical considerations and techniques are also reviewed, with data allowing determination of parameters for self-absorption corrections. The method for determining the densities of the different cell compartments by microinterferometry is outlined, as are three different methods for the quantitative assessment of an autoradiograph: (1) measurement with a microdensitometer or similar instrument of the degree of blackening in a given area, (2) visual counting of individual grains, and (3) track counting. (BBB)

Radiation Effects on Biochemicals

See also CHEMISTRY — Radiation Chemistry

Refer also to abstract 12782.

12617 (NP–15863) THE ROLE OF PROTECTIVE SUBSTANCES DURING IRRADIATION AND A FURTHER STUDY OF THE DAMAGE TO THE BACTERIOPHAGE AND OF THE REPARATION AFTER THE EFFECT OF RADIATION AND RADIOMIMETICS. Final Report. (Czechoslovak Academy of Sciences, Brno. Inst. of Biophysics). Contract No. 142/R 1, R2/RB. 23p. Dep. mn.

Progress is reported on: the effect of protective substances on the increase of radioresistance in bacteriophages; radiation damage to adsorption and injection in phages; repair of radiation damage; and comparison of the effects of hydroxylamine, uv, and x radiation on bacteriophages. Protective substances increased phage resistance to x irradiation, although they did not influence the damage to adsorption and injection. It was shown that x ray causes different types of lesions and that 20% of all lethal lesions go to the adsorption and injection processes. The only marked reactivation phenomenon observed with x-inactivated lambda phages was a certain marker rescue, undamaged parts of the irradiated genome being incorporated to a measurable extent into simultaneously infecting, non-irradiated phages. Hydroxylamine produced damage in the phage DNA, but did not affect adsorption and injection. (H.G.D.)

12618 (TID–22399) STABILITY OF FOOD LIPIDS TO IONIZING RADIATION. Progress Report, February 1, 1965–August 31, 1965. Nawar, Wassef W. (Massachusetts Univ., Amherst. Dept. of Food Science and Technology). Contract AT(30-1)-3499. 9p. Dep. mn. CFSTI $1.00 cy, $0.50 mn.

Radioinduced changes in fish oils were studied. Total lipids were extracted from Canadian Mackerel within 24 hr before ^{60}Co gamma irradiation. Using gas chromatography, at least 42 components were detected in the irradiated samples. A literature survey was made on the effects of ionizing radiation lipids, and 53 references are cited. (P.C.H.)

12619 ALTERATIONS IN THE TRANSFER RIBONUCLEIC ACID METHYLASES AFTER BACTERIOPHAGE INFECTION OR INDUCTION. Wainfan, Elsie; Srinivasan, P. R.; Borek, Ernest (Columbia Univ., New York). Biochemistry, 4: 2845-8 (Dec. 1965).

The relative levels of base-specific transfer ribonucleic acid (t-RNA) methylases are constant in a given species. In E. coli B, grown on different nutrient media or after ultraviolet irradiation, the relative activities of enzymes which methylate adenine, guanine, and uracil in t-RNA remain constant within experimental error. On the other hand, after T2 infection major shifts in the relative levels of base-specific t-RNA methylases occur. For example, the methylations of uracil and adenine were enhanced 100% relative to the methylation of guanine. The methods employed detect only changes in the total number of methyl groups introduced, not changes in sites. With these methods no changes were detected upon infection with T1 bacteriophage. However, after induction of λ in E. coli K_{12} extensive changes were found both in the absolute and relative levels of the t-RNA methylases. The shifts in enzyme activities are not simply the sequels of uv irradiation but appear to be a result of the induction since irradiation of nonlysogenic organisms produced no measurable changes in the enzymes. (auth)

12620 STUDIES ON THE RELATIONSHIP BETWEEN THE TRANSFORMING ACTIVITY AND THE INTEGRITY OF DNA AS REVEALED BY ULTRAVIOLET FLOW DICHROISM. Moriguchi, E. (National Inst. of Radiological Sciences, Chiba City, Japan); Suzuki, K.; Wada, A. Biochim. Biophys. Acta, 109: 578-84 (Nov. 29, 1965).

Aqueous solutions of the transforming DNA of Diplococcus pneumoniae were irradiated with ultraviolet light, x rays, and sonic waves or treated with pancreatic deoxyribonuclease. The treated as well as the untreated solutions were submitted for measurements of ultraviolet flow dichroism, sedimentation coefficient at a definite concentration and temperature, and transforming assay. The rotary diffusion coefficient was also obtained from the measurement of dichroic effect. The relationships between inactivation and the changes in these physical properties, which indicate the macromolecular state of DNA, showed that inactivation by ultraviolet light did not produce any large modification in the secondary structure or in the molecular size of DNA, whereas inactivation by sonic irradiation was accompanied by a large reduction in molecular size and flow dichroism. The inactivation by x rays resulted in an intermediary state and was similar to inactivation by pancreatic deoxyribonuclease. These results, as well as the sedimentation data, supported the current view that the single-strand break accounts for the inactivation of transforming DNA by x irradiation. (auth)

12621 THE BIOLOGICAL IMPORTANCE OF ULTRAVIOLET LIGHT INDUCED DNA-PROTEIN CROSSLINKS IN ESCHERICHIA COLI 15 TAU. Smith, K. C.; Hodgkins, B.; O'Leary, M. E. (Stanford Univ., Palo Alto, Calif.). Biochim. Biophys. Acta, 114: 1-15 (Jan. 18, 1966).

The sensitivity of Escherichia coli 15 TAU to killing by ultraviolet light (2537 Å) when grown for various times under several nutritionally restricted conditions (+T – AU; –T + AU; –T – AU) was measured. Concurrent measurements were made on the amount of DNA crosslinked to protein by these same doses of ultraviolet light. There appears to be a direct correlation between the amount of DNA crosslinked to protein by a given dose of ultraviolet light and the intrinsic sensitivity of the cells to killing by ultraviolet light under the several growth conditions studied. These results strongly suggest that the crosslinking of DNA and protein by physiological doses of ultraviolet light must play an important

role in the loss of viability of ultraviolet light irradiated cells. (auth)

12622 THE REACTION OF RADICALS INDUCED IN ESCHERICHIA COLI B/r BY γ-RAYS WITH CYSTEAMINE AND WITH OXYGEN. Baker, A. (Royal Military Coll. of Science, Shrivenham, Eng.); Ormerod, M. G.; Dean, C.; Alexander, P. Biochim. Biophys. Acta, 114: 169-81 (Jan. 18, 1966).

In dry Escherichia coli B/r irradiated with γ-rays at -196° the electron spin resonance spectrum changes as the cells are warmed. There is a rapid decay in the number of radicals and the spectrum of those that remain, changes slowly from a singlet ($R_1^{\cdot}$ type) to a doublet ($R_2^{\cdot}$ type). In the presence of oxygen the decay is accelerated because of the formation of an unstable peroxide radical that can be studied at -77°. In the presence of cysteamine the change from $R_1^{\cdot}$ to $R_2^{\cdot}$ is accelerated because of the formation of the sulphur radical $NH_2 \cdot C_2H_4S^{\cdot}$ which acts as a catalyst. In the presence of oxygen the catalytic action is prevented by the formation of a sulphoxy radical ($PSO_2^{\cdot}$) that does not react with bacteria. In systems where $PS^{\cdot}$ cannot abstract hydrogen (such as nucleic acid) cysteamine protects in the absence of oxygen. In bacteria $PS^{\cdot}$ causes damage and its formation is therefore not protective, while in the presence of oxygen the conversion to $PSO_2^{\cdot}$ renders the reaction of cysteamine with the primary radicals ($R_1^{\cdot}$ type) one of protection. (TCO)

12623 ENZYMIC PROCESSES AND VASCULAR CHANGES IN THE SKIN RADIATION REACTION. Jolles, B.; Harrison, R. G. (General Hospital, Northampton, Eng.). Brit. J. Radiol., 39: 12-18(Jan. 1966).

Factors influencing the early phase of the inflammatory reaction occurring within minutes after irradiation were studied. The capillary permeability changes were estimated by measurement of the leakage of a vital dye injected into the experimental animals immediately after irradiation. The effect of different enzyme systems and their inhibitors on this phase of the radiation-induced inflammatory reaction were studied. While histamine and 5-hydroxytryptamine do not play a significant role, the participation of a protease system was established. The action of the latter indicates the participation of lysosomal derivatives in the sequence of events leading to increased permeability. The degree of diminution of capillary permeability or its abolition by these inhibitors was tabulated and compared with the effects of compounds with a desludging or vasodilating effect on vessels (meso-inositol-hexanicotinate-Hexopal) and a substance which reduces capillary fragility (tri-hydroxyethyl-rutoside—Factor P Zyma). The mechanism of action of these compounds and the interrelationship between the early impact of ionizing radiations on the tissue catalytic systems and extracellular tissue events following irradiation are discussed. (auth)

12624 BEHAVIOR OF SULFHYDRYL GROUPS OF SEA URCHIN EGGS UNDER THE BLOCKAGE OF CELL DIVISION BY UV AND HEAT SHOCK. Ikeda, Mariko (Tokyo Metropolitan Univ.). Exp. Cell Res., 40: 282-91 (Nov. 1965).

In the sea urchins Hemicentrotus pulcherrimus, Anthocidaris crassispina, and Clypeaster japonicus, cleavage of the eggs can be suppressed by short treatment with higher temperature (34°C) or by uv irradiation. While the division of the cell body is blocked in the heat treatment, nuclear division is not affected by uv irradiation, but it is suppressed. During heat treatment, usual cyclic change in SH amounts of 0.6 M KCl-soluble protein stops while in uv treatment, it persists. There are two cycles present in the cell that are independent from each other: one is the nuclear cycle and the other is the cytoplasmic SH cycle. Since cleavage does not take place if one of the two cycles is blocked or they are pushed out of pace, synchronization of the two cycles is a necessary condition for a cleavage to occur. From the fact that the time of micromere formation in uv irradiated eggs always occurs simultaneously with the fourth cleavage of the untreated controls and at the fourth peak of SH, a possibility is considered that the cyclic change of SH may be a pacemaker for differentiation. (auth)

12625 CARCINOSTATIC EFFECT OF EXTRACTS FROM HUMAN GASTRIC CANCER. Funaoka, Hiroaki (Hiroshima Univ.); Ezaki, Haruo; Araki, Fumio; Sugihara, Yoshio. J. Radiat. Res. (Jap.), 5: 159-65(Sept.-Dec. 1964).

Saline extracts from human gastric cancer divided into two parts, one of which was irradiated by x-ray of 2000 R before homogenization, were fractionated with ethanol, in which S_1 was 30% vol. ppt., S_2 was 30-70% vol. ppt., and S_3 was supernatant. Further, S_1 and S_2 were fractionated with $(NH_4)_2SO_4$ into P_1 (30% sat. ppt.), P_2 (30-50% sat. ppt.), P_3 (50-70% sat. ppt.), and P_4 (supernatant). The non-irradiated S_2P_1 and S_2P_2 fractions inhibited the growth of subcutaneous solid Ehrlich ascites tumor in mice, which were respectively significant at the level of 10% and 5%, but the same fractions irradiated lost the growth inhibitory activity. The irradiated S_2P_3 fraction inhibited the growth of solid tumor at the level of 20%, and was different from the equivalent non-irradiated fraction having mitosis promoting activity at the significance of 0.5% level. These data may show that malignant tumor contains the growth inhibiting substance that is not species specific, and the carcinostatic effect of x irradiation is due to the destruction of balance between growth promoting and inhibiting substances inside of the tumor tissue. (auth)

12626 THE PROGNOSTIC SIGNIFICANCE OF THYROID ANTIBODIES IN THE MANAGEMENT OF THYROTOXICOSIS. Irvine, W. J.; Macgregor, A. G.; Stuart, A. E. (Univ. of Edinburg). Lancet, 2: 843-7(Oct. 27, 1962).

The effect of ^{131}I treatment for hyperthyroidism on changes in thyroglobulin and complement-fixing antibody titers was determined in 34 patients and compared with results in comparable cases treated with antithyroid drugs or submitted to partial thyroidectomy. The possibility of using antibody titers to determine whether ^{131}I therapy should be used and, if so, at what dose was also explored. Early postoperative hypothyroidism was common where the precipitin test was positive and, more particularly, where there was a high titer of complement-fixing antibody; but hypothyroidism after radioiodine therapy could not be predicted from the titer of thyroid antibodies present. There was no evidence that the response to treatment with antithyroid drugs could be predicted from the presence of raised titers of thyroid autoantibodies. (TCO)

12627 GAMMA RAY DEGRADATION OF CHLOROPLAST STRUCTURE AND PHOTOREDUCTION [Thesis]. Rubenstein, Daniel. Davis, Calif., Univ. of California, 1965. 116p.

Chloroplasts exposed to ^{60}Co gamma radiation were observed by electron microscopy and were used for four photochemical assays. A comparison was made of the physical damage observed and inactivation of the photochemical mechanism. The related radiosensitivities of four types of photochemical activity were assayed with a view of separating loci of photosynthetic electron transport. Electron micrographs of Chlorella cells, Tetragonia leaves, and tobacco chloroplasts all indicate serious disruption and dissolution of the chloroplast lamellae by an order of radiation (1 krad) that hardly affected their capacity for photoreduction. This function does not seem to reside in the gross membrane structure. Chloroplasts and chloroplast fragments were isolated from the leaves of Tetragonia expansa in various buffers. A new one developed to give the highest photochemical activity and presumably superior retention of the physical structure contains 2mM ATP, 0.6M mannitol, and 0.05M phosphate at pH 7.4. The preparations were stored in and irradiated in liquid nitrogen for high stability and low sensitivity to radiation. The abilities of irradiated chloroplast fragments to photoreduce dichloroindophenol, tetranitro blue tetrazolium, and ferricyanide ion, and to evolve oxygen were tested. The doses of gamma radiation required to cause 50% inactivation were 8 Mrad for indophenol and tetrazolium reduction, 3.5 Mrad for ferricyanide reduction, and 5 Mrad for oxygen evolution. A striking reac-

tivation of photochemical activity occurred in fragments irradiated with large gamma doses. For the three photoreductions – indophenol, tetrazolium, and ferricyanide activity declined with increasing dose until 3 Mrad, increased to approximately control levels at 6 Mrad, and declined again to 10 Mrad. Oxygen evolution showed no reactivation response. The existence of at least two separate sites of action or sensitive steps is indicated. (Dissertation Abstr.)

Radiation Effects on Tissues

12628 (AD–626997) LONGEVITY IN NEUTRON-EXPOSED GUINEA PIGS. Kimeldorf, D. J.; Phillips, R. D.; Jones, D. C. (Naval Radiological Defense Lab., San Francisco, Calif.). Dec. 3, 1965. 16p. (USNRDL-TR–941). CFSTI $1.00 cy, $0.50 mn.

Life span data were accumulated for male guinea pigs from a specific pathogen free Hartley strain colony, maintained on a vitamin C supplemented diet. Observations were made on 25 sham-irradiated controls and 78 animals exposed as young adults to a simulated fission energy spectrum of neutrons obtained by the bombardment of a thick beryllium target with 12 Mev protons. The neutron-exposed groups included 18 animals subjected to a high sublethal dose (100 rads, first collision dose), and 60 animals which were the 30-day survivors of 120–160 rad doses. Approximately 11 to 72% of the animals died during the first 30 days after 120–160 rads. The median age at death for the sham-exposed controls was 828 days, 730 days for animals exposed to the sublethal dose, and 698 days for survivors of the 30-day lethal dose range. Both median life span values were significantly ($p < 0.01$, analysis of variance) smaller than that for controls. Observations in the guinea pig regarding a reduction in life span after a single whole-body exposure to neutrons, corroborate in an additional species, conclusions previously based solely on studies of rats and mice. (auth)

12629 (AED-C–04-22) RADIATION EFFECTS ON LIVING TISSUES AND ORGANISMS. Series C: Bibliographies. Stahlhofen, W. (comp.) (Max-Planck-Institut fuer Biophysik, Frankfurt am Main (West Germany)). July 1965. 98p. Dep. mn.

References (302) are given to reports and journals published from 1963 through 1965. Separate author, subject, and report number indexes are included. (P.C.H.)

12630 (BNL–8383) THE EFFECT OF X-IRRADIATION AND THERMAL TRAUMA ON THE INTESTINAL MUCOSA. Baker, D. G.; Valeriote, F. A. (Brookhaven National Lab., Upton, N. Y. Toronto Univ. (Ontario). Banting and Best Dept. of Medical Research). [1963]. Contract AT-30-2-GEN-16. 15p. Dep. mn. CFSTI $1.00 cy, $0.50 mn.

The administration of a 1-minute thermal trauma to rats decreased the mucosal total nitrogen only in the duodenal segment at the second day after trauma. At day 4 and 6 after trauma, an elevation occurred in the nitrogen content over the control value in this segment. When x irradiation was administered to the animals at a dose which did not produce deaths from gastrointestinal dysfunction, a minimal mucosal total nitrogen was found in all segments by the second day after x irradiation with recovery by day 4. When thermal trauma was administered with a dose of x-irradiation which in itself lead to a 6% mortality from gastrointestinal dysfunction, the combined injuries produced a 55% mortality. The increase in intestinal death resulting from combined thermal burn and x irradiation was due to a rate of recovery in the intestinal mucosa, probably mediated by some toxin(s) liberated from the burned region. (auth)

12631 (CEA-R–2776) RESTAURATION ET RADIO-RESISTANCE CHEZ LA SOURIS APRES IRRADIATION EXTERNE. (Recovery and Radio-Resistance in Mice After External Irradiation). Le Guillou, Sylvain (Commissariat a l'Energie Atomique, Fontenay-Aux-Roses (France). Centre d'Etudes Nucleaires). Oct. 1965. 80p. Dep. mn.

A review is presented on recovery from external irradiation and experimental data that suggest the idea of a radioresistance in animals, as well as the hypotheses put forward for explaining this phenomenon. An experiment was carried out on mice whose $LD_{50/30}$ days increased from 1005 to 1380 rads. It was found that an increase occurred in the number of certain anti-bodies circulating after a low dose of γ irradiation. 128 references are cited. (auth)

12632 (EUR–2546.f) COMPARAISON DES EFFETS DE DIFFERENTS AGENTS MUTAGENES PAR L'ETUDE DE LA MUTAGENESE DE QUELQUES PLANTES TYPES. Rapport Annuel, 1964. (Comparison of the Effects of Various Mutagenic Substances by Studying the Mutagenesis of Some Typical Plants. Annual Report, 1964). Dommergues, P.; Gillot, J.; Touvin, H.; Bodergat, R.; Le Couviour, M. (Institut National de Recherche Agronomique, Dijon (France). Station d'Amelioration des Plantes). Aug. 25, 1965. 20p. Dep. mn.

The stability of chimeras isolated from different varieties of fruit-trees was analyzed and their genetic structure was studied by re-treating with gamma radiation. The stability and genetic homogeneity of certain chimeras were confirmed. Experiments with rose-trees show that during the first three years after treatment, 90% of the chimeras are found on the treated clone. A study of the stability of the red chimeras obtained by irradiating the White-Sim variety of carnation showed that two successive clonings were needed for uniform isolation of deep tissues. A classification was devised for wheat chlorophyll mutants, based on the evolution versus time of the mutant phenotype and on a number of pigment analyses. Studies of correlations between mutagenesis, organogenesis and precocity were carried out on wheats of different ploidies. The experiments show that sterility is increasingly pronounced as the ploidy level drops, and chlorophyll mutations increase in number with the drop in the ploidy level. This experiment furthermore demonstrates that a correlation exists between the mutation rates and precocity. The study of agronomic mutations isolated from different varieties of wheat continued with an investigation of characteristics in relation to yield. (auth)

12633 (NP–15348) ACTIVITIES OF THE MED FLY INVESTIGATION SECTION DURING JULY 10, 1963–JUNE 30, 1964 ON INSECT CONTROL BY RADIATION OIRSA, SAN SALVADOR, EL SALVADOR. Morales, E. (Organismo Internacional Regional de Sanidad Agropecuaria, San Salvador (El Salvador)). 19p. Dep. mn.

Procedures used for the rearing and radiation exposure of massive numbers of mediterranean fruit flies are discussed. Adult flies were exposed to 10,000 R γ radiation and pupae were exposed to 2,500 R. Several hundred thousand adult flies were released in a test area to study the effects of sterile adults on population control. Preliminary results are reported. Studies were also conducted on the biological control of the mediterranean fruit fly by parasites and the behavior of the flies, in which flies marked with radioisotopes or color points were released. (C.H.)

12634 (NP–15349) SUMMARY OF THE MEDFLY INVESTIGATION SECTION'S ACTIVITIES DURING THE PERIOD JUNE 1964–MARCH 1965 ON INSECT CONTROL BY RADIATION. Morales, E. (Organismo Internacional Regional de Sanidad Agropecuaria, San Salvador (El Salvador)). 13p. Dep. mn.

Procedures for the rearing of mass numbers of mediterranean fruit flies, exposed to ^{60}Co γ radiation during various developmental stages, and the marking of irradiated flies with fluorescent powders are described. Preliminary results are reported from studies on the effects of the release of radiation sterilized flies on populations of the insects in Nicaragua and Panama. (C.H.)

12635 (NYO–2786-1) CYTOCHEMICAL AND ELECTRON MICROSCOPIC STUDIES OF RADIATION DAMAGE.

Final Report. Novikoff, Alex B. (Albert Einstein Coll. of Medicine, Yeshiva Univ., Bronx, N. Y.). [1964]. Contract AT(30-1)-2786. 5p. Dep. mn. CFSTI $1.00 cy, $0.50 mn.

Techniques of enzyme cytochemistry were combined with electron microscopy in studies of the effects of radiation on the cytoplasmic organelles. Results are reported for studies of the effects of radiation from ^{131}I on the thyroid epithelium of rats; morphological changes in cells of rat intestinal mucosa, thymus, lymph node, and spleen induced by whole-body x irradiation; and changes in cultured cells derived from a human oral carcinoma induced by exposure to high doses of uv or x radiation. (C.H.)

12636 (TID-21459) RATES OF VISIBLE MUTATIONS AS RELATED TO THE MATURITY OF MALE GERM CELLS OF DROSOPHILA MELANOGASTER AT THE TIME OF RADIATION. Hannah-Alava, Aloha (Turku Univ. (Finland). Dept. of Genetics). [1961]. Contract AT(30-1)-2690. 18p. Dep. mn. CFSTI $1.00 cy, $0.50 mn.

An investigation was made on the effects of x-radiation damage—as measured by mutation rates at nine loci in the third-chromosome, and dominants and minutes in all chromosomes—upon the male germ cells of Drosophila melanogaster in different stages of maturity at the time of irradiation. The results are based on seven replicate experiments testing a total of 31 control males and 368 irradiated (3000 R) males mated sequentially at two or three day intervals for eight broods or until the male died. The lowest fertility, the lowest fecundity, and the highest mutation rates except for the minutes was in brood-3 (6–8 days after irradiation and the initial mating of the parental male). The average mutation rate for nine third-chromosome loci was: 0.19 per cent (7.02×10^{-8}/R/locus) in brood-1, 0.41 (16.06) in brood-2, 1.17 (43.40) in brood-3, 0.08 (3.13) in brood-4, and 0.01 (0.26) in broods-5–8. A number of factors that could influence the brood pattern were also tested. With the possible exception of number of females, the only detectable effect on the mutation rates appeared to be an increase in the variance. The results suggest that mutation rates at specific loci may be a more precise way, than other criteria, of measuring the curve of response of germ cells in different stages of maturity to radiation damage, but if so, the number of males tested in each replicate experiment should be increased considerably (four- to five-fold) for detecting significant differences between broods. (P.C.H.)

12637 (TID-21466) TEMPORAL PATTERN OF THE EARLY STAGES OF SPERMATOGENESIS OF ADULT DROSOPHILA MELANOGASTER MALES AFTER TREATMENT WITH X-RAYS. Puro, Jaakko A. (Turku Univ. (Finland). Dept. of Genetics). [1961]. Contract AT(30-1)-2690. 16p. Dep. mn. CFSTI $1.00 cy, $0.50 mn.

Radiation effects as measured by rates of 3rd chromosome recessive lethal and visible mutations of Drosophila melanogaster in different stages of spermatogenesis at the time of exposure are reported. Adult males were irradiated with 3000 R x rays and mated sequentially with virgin females at two or three day intervals for seven broods or until the male died. Mutation studies were made in brood-1 (1–3 days after treatment) and in broods -4, -5, -6, and -7 (days 8–10, 11–12, 13–14, 15–17, after treatment respectively). The results from mutation clusters suggest that mutations occurring in predefinitive gonia are available from brood-5 on. In replicate experiments there was considerable variance in later broods but analysis showed this to be related, with all probability, to the few number of predefinitive cells. Mutation rates in predefinitive gonia were compared to the rates in mature sperm. (auth)

12638 (TID-21474) A STUDY OF DNA LABELED CELLS AT DIFFERENT TIMES AFTER HIGH DOSES OF RADIATION. Looney, W. B. (Virginia Univ., Charlottesville. Radiobiology and Biophysics Lab.). [1963]. Contract AT(40-1)-2889. 17p. Dep. mn. CFSTI $1.00 cy, $0.50 mn.

Radiation effects on somatic cells were studied as a function of time (9 hr.) in rats after radiation. The method used is described. The depression of DNA synthesis following 750, 3000, and 12,000 R is described by a modified exponential equation. The most significant result was a decreasing number of labeled cells with increasing doses of radiation. Mechanisms for the depression of DNA synthesis are discussed. (P.C.H.)

12639 (TID-21517) ACTIVE TUBERCULOSIS IN LEUKEMIA, MALIGNANT LYMPHOMA AND MYELOFIBROSIS. Morrow, Lewis B.; Anderson, Robert E. (Atomic Bomb Casualty Commission, Hiroshima (Japan)). [1964]. Contract AT(49-1)-Gen-72. 29p. Dep. mn. CFSTI $2.00 cy, $0.50 mn.

The prevalence of active tuberculosis in 213 cases of leukemia, myelofibrosis, and malignant lymphoma autopsied at the Atomic Bomb Casualty Commission (ABCC) during the period 1949–62 inclusive was studied. An increased prevalence of disseminated tuberculosis was found in 43 cases of chronic myelogenous leukemia and 12 cases of myelofibrosis; the prevalence of this type of tuberculosis in the acute leukemias and malignant lymphomas was less than the prevalence in the remainder of the ABCC autopsy population. The increased prevalence of disseminated tuberculosis in chronic myelogenous leukemias and myelofibrosis was directly proportional to the estimated duration of the hematologic course and was little influenced by antileukemic therapy although there may have been a slight increase in association with therapeutic x-ray. Cases of chronic myelogenous leukemia arising in proximally exposed survivors of the atomic explosion showed a statistically significant increase in the prevalence of disseminated tuberculosis in comparison with comparable distally exposed cases; no similar difference existed in the remainder of the ABCC autopsies. These data are discussed and related to other evidence suggestive of basic differences between radioinduced leukemia and the naturally occurring variety. (auth)

12640 (TID-22378) THE EFFECTS OF PRE- AND POSTNATAL GAMMA IRRADIATION ON REPRODUCTION IN THE ALBINO RAT. Final Report. Krise, George M. (Texas Engineering Experiment Station, College Station). Sept. 7, 1965. Contract AT(40-1)-2849. 106p. Dep. mn. CFSTI $4.00 cy, $0.75 mn.

A study was made to determine the effects of chronic low level radiation on the developing testes at specific intervals during pre- and postnatal development in two strains of albino rats. The investigation was divided into four phases to produce the required data necessary to locate stages of extreme sensitivity. Animals receiving 1 and 2 R per day were found to be different histologically from the controls. When 5 R was administered, only the rats irradiated from day 15 prenatal to day 3 of postnatal life showed histological damage to the testes. This damage was not evidenced at 170 days, indicating that regeneration of germinal epithelium had taken place by this time. A total dose of 100 R at the rate of 10 R per day caused damage which was still apparent at 170 days of age. Though animals exposed to this level of irradiation thus showed permanent histological damage, they were not found to be sterile when tested at 143 days of age. Administration of 20 R per day for a total dose of 200 R caused permanent sterility in the Sprague-Dawley rats, but Wistar rats exposed to the same dose were able to produce some litters. A dose of 40 R per day for a total dose of 400 R caused complete destruction of the germinal epithelium in both strains. Wistar rats throughout the study were found to be more radioresistant than Sprague-Dawley rats in almost all cases. The results suggest that the damage to animals in the continuous prenatal and postnatal irradiation study was received during the prenatal and early postnatal period of irradiation. (P.C.H.)

12641 (TID-22582) INVESTIGATIONS ON MUTABILITY OF POLYGENES AND ON UTILIZATION OF INDUCED GENETIC VARIABILITY. Scossiroli, R. E. (Pavia Univ. (Italy). Istituto di Genetica. Catania Univ. (Italy). Istituto di Genetica). Jan. 1, 1966. Contract AT(30-1)-2466-11. 33p. Dep. mn. CFSTI $2.00 cy, $0.50 mn.

Genetic studies on irradiated maize and wheat are reported. Reasons underlying the appearance of the luxuriance phenomenon were investigated in maize. Three luxuriant lines from a single plant partly irradiated with 3000 R were selfed. Part of the progeny from such selfing was again selfed and part used for reciprocal back crossings to the normal (non luxuriant) parent. The results suggest that the maternal effect as detected through the reciprocal crosses may be underestimated as a consequence of nucleocytoplasmic interaction. A depression effect was found in irradiated dormant wheat seeds. Also in wheat, it was found that phenotypic differences contain a genetic component in early generations. (P.C.H.)

12642 (Y-IA-17) FABRICATION OF MINIATURIZED HARDWARE FOR SPACE EQUIPMENT. Oliphant, G. W. (Union Carbide Corp., Oak Ridge, Tenn. Y-12 Plant). Jan. 20, 1966. Contract W-7405-eng-26. 16p. Dep. mn. CFSTI $1.00 cy, $0.50 mn.

Fabrication and testing of equipment for use in investigations concerning synergistic effects of zero gravity and radiation on human white blood cells are described. (J.R.D.)

12643 (ANL-Trans-264) THE RADIOSENSITIVITY OF GUINEA PIGS WITH HYPOCATALASIA WITH SPECIAL ATTENTION TO THE SIGNIFICANCE OF HYDROGEN PEROXIDE IN THE PATHOGENESIS OF ACUTE RADIATION SICKNESS. Rusev, G.; Radev, T.; Belokonski, I.; Petkov, B. Translated by Carol-Joyce Howell (Argonne National Lab., Ill.), from Izv. Inst. Sravnitelna Patol. Domashnite Zhivotni, Bulg. Akad. Nauk, 8: 119-29(1960). 17p. Dep. mn. JCL $1.60 fs, $0.80 mf.

Studies were made on the significance of catalase reactions with water-soluble peroxides in the pathogenesis of acute radiation sickness (ARS). Hypocatalasic guinea pigs served as the experimental material. These animals, like the control (normal) guinea pigs, were x irradiated at 500 R. Clinical and biochemical studies showed that the hypocatalasic guinea pigs were no more radiosensitive than the normal animals. On the contrary, comparison of a number of metabolic and physiologic indexes showed that ARS evolved in a milder form in the hypocatalasic guinea pigs — which rules out the role of hydrogen peroxide as a toxic factor. The hypocatalasic guinea pigs differ constitutionally from normal animals in that their tissues contain a larger amount of dehydrases and their glycolytic capacity is greater. Thus, the milder course of ARS in hypocatalasic guinea pigs at the beginning was attributed to these features of tissue respiration. However, even these features did not prevent the onset of death on the ninth day. (P.C.H.)

12644 THE HEXOSAMINE: COLLAGEN RATIO AS A MEASURE OF BIOCHEMICAL AGE IN HIROSHIMA ATOMIC BOMB SURVIVORS. Anderson, Robert E. (Univ. of New Mexico School of Medicine, Albuquerque). Amer. Heart J., 70: 283-4(Aug. 1965).

Determinations were performed on samples of skin and aorta obtained from men autopsied at the Atomic Bomb Casualty Commission during the period 1962 to 1964. Tissue from a proximally exposed individual (less than 1400 m from the hypocenter at the time of the explosion) was paired with tissue from an individual not in Hiroshima at the time of the bomb. Chemical determinations were performed in 14 experimental pairs on dried, defatted, acid-hydrolyzed skin and aorta for hexosamine and collagen content. In 11 of the pairs, aorta ratios were lower and skin ratios were smaller in the exposed member than in the nonexposed one. Demonstration of these biochemical alterations in persons with no other known morphologic, clinical, or chemical indication of previous exposure to significant amounts of ionizing radiation suggests the possibility of accelerated aging among proximally exposed survivors of the atomic bomb. (TCO)

12645 THE FEASIBILITY OF SURGERY AFTER WHOLE-BODY X IRRADIATION AND ADMINISTRATION OF A RADIOPROTECTIVE AGENT. Schweikert, C. H.; Ladner, H. A. (Univ., Freiburg i. B.). Arch. Klin. Chir., 308: 65-70(Nov. 17, 1964).

To prevent immune reactions to tissue transplants and thus facilitate the transplantation of organs or organ parts, very large doses of irradiation must be administered. Bone marrow transplantation is often required to permit survival after such high irradiation doses. In order to find a substance which would be suitable to reduce the irradiation effects, pyridoxal-5-phosphate was administered to dogs that were given 400 or 700 R of whole-body x irradiation. All of the treated animals survived the irradiations, although untreated control animals who received 400 R died on the average within 21 days after irradiation, and those untreated animals that received 700 R died after about 12 days. Additional studies on 75 dogs indicate that surgical operations can be performed within 24 hr after sublethal whole-body x irradiation if the radioprotective material is given. Survival of homologous transplants in the tracheobronchial tree was lengthened, although stenoses developed if the wounds were not implanted with an alloplastic material. (BBB)

12646 SURGICAL COMPLICATIONS IN IRRADIATED PATIENTS. Habel, Dan William (Univ. of Michigan Medical Center, Ann Arbor). Arch. Otolaryngol., 82: 382-6(Oct. 1965).

The problem of preoperative irradiation and its effect on postoperative complications and wound healing were studied in patients who had undergone a surgical resection for tumors about the head and neck. Of the 463 cases studied, 172 patients received preoperative irradiation therapy to the area to be resected. Sixty-five % of those irradiated were treated with ^{60}Co therapy, and the average tumor dose was 6200 R. Thirty-five % received orthovoltage therapy, with an average tumor dose of 5800 R. The surgical procedures included: radical neck dissection, parotidectomy or thyroidectomy, with radical neck dissection, and supraomohyoid node dissection. When the times required to heal the wounds postoperatively were determined and averaged for each operative group, little difference was seen in healing time between the irradiated and nonirradiated patients, if no complications occurred. However, in the healing times of those patients who developed postoperative wound complications, a significant difference between the irradiated and nonirradiated patients was found. The study suggests that irradiated tissue is less likely to heal a complication if it develops. Complications occurring in the irradiated group tended to be of a greater magnitude and, hence would require a longer time to heal. In all three operative groups the overall postoperative complication rate was substantially increased if preoperative irradiation was given. (TCO)

12647 THYMIC, LYMPHOID AND MARROW INOCULA IN CYTOGENETIC REPOPULATION STUDIES OF IRRADIATED MICE. Ilbery, P. L. T. (Univ. of Sydney). Austral. J. Exp. Biol. Med. Sci., 43: 579-92(Oct. 1965).

The ability of transplanted hematopoietic cells to lower the incidence of radioinduced leukemia was investigated in two experiments. The first study was made using a subacute leukemogenic schedule of irradiation, and the second using an acute irradiation dose to deplete the hemopoietic and lymphopoietic organs. $(C57 \times CBA/H)F_1$ mice one month old received four fractions of 200 rad of ^{60}Co γ irradiation at weekly intervals. Within one hour of the last irradiation the mice were given intravenous inocula from the tissues of $(C57 \times CBA.T6T6)F_1$ mice also one month old. One group received 4×10^6 bone marrow cells, another 10^7 fetal liver cells, and a third group 6×10^6 lymphocytes. The second experiment concerned acute lethal 1050 R irradiation of CBA/H or CBA.T6T6 mice. The incidence of lymphoma was lowered from 62% to 27% by postirradiation bone marrow grafting. The concept that inhibition of lymphoma is due to colonization of the host's tissues by unirradiated graft cells appears only partly true. The inability of lymphocytes to protect against the supervention of lymphoma was reflected in their inability, observed cytogenetically, to penetrate the thymus. Combination of

the cytogenetic data and the information from mitotic rates in bone marrow and thymus showed that a cell derived from the recolonized hemopoietic tissue gained entry to the thymus. After failure of lymphoid material to colonize the thymus the circulating lymphocytes were derived from the grafted hemopoietic elements and they were immunologically competent. (BBB)

12648 ON THE ORIGIN OF URINARY EXCRETION OF TAURINE BY THE RAT IRRADIATED WITH ^{60}Co. [PART] I. Boquet, P. L.; Fromageot, P. (CEA, Saclay, France). Biochim. Biophys. Acta, 111: 40-50(Nov. 15, 1965). (In French).

Rats exposed to γ radiation increase their urinary secretion of taurine. By using rats whose taurine pools are in isotopic equilibrium, it has been shown that the taurine excreted after irradiation originates from a pre-existing pool, whose specific radioactivity is equal or very close to that of the pools with a rapid turnover rate. This pool of taurine exists in animals deficient in pyridoxal phosphate. When endogenous taurine biosynthesis is sufficiently lowered by pyridoxal phosphate deficiency, the excess urinary secretion following irradiation is either abolished or greatly reduced. This reduction is attributed to the preferential utilization of taurine by extra renal tissues in such pyridoxine deficient animals. The competition between kidney reabsorption of other reactions extracting taurine from the plasma is the reason for the peculiar behavior of such deficient rats. (auth)

12649 CHANGES IN THE CONTENT OF ASCORBIC ACID IN THE CROWN-GALL TUMOR TISSUE OF NICOTIANA TABACUM UNDER THE INFLUENCE OF ^{60}Co γ RAYS. Antoszewska, L.; Rennert, A.; Kroh, J. (Univ. of Lodz, Poland). Biol. Plant. Acad. Sci. Bohemoslov., 7: 387-90(1965).

Experiments were designed to produce permanent radiation changes in ascorbic acid content in the culture in vitro of Nicotiana tabacum (var. White Burley) crown-gall tumor tissue. The tissue cultivated on the standard medium and on the medium supplemented with honeycomb extract was irradiated with 500, 1000, 2000, and 5000 rad doses of ^{60}Co γ rays. The dose rate was 0.2 Mrad/hr. After irradiation the tissue was transferred to a new culture medium. Part of the colonies died in the course of several first passages. Even at low doses (1000 rad), partial atrophy of the tissue was observed in the course of several first passages. The tissue irradiated with a dose of 5000 rad could not be cultivated on a standard medium, whereas on a complete medium this dose appears to be beneath the lethal level and the tissue continues to grow. Thus, it is possible to lessen or even eliminate the negative effects of irradiation by the suitable choice of culture medium. A distinct increase in the ascorbic acid content was found both for standard and completed medium. For the dose of 2000 rad the ascorbic acid content in comparison with the control increases by more than 30%. The data suggest that the complete medium favors the radiation-induced increase of ascorbic acid content in the tissue. It is concluded that ^{60}Co γ rays cause a marked increase of the content of ascorbic acid in crown-gall tumor tissue of N. tabacum cultivated in vitro. This effect seems to have a fairly permanent character and maintains itself for at least one year. The addition of honeycomb extract to the medium increases the resistance of the tissue against the action of ^{60}Co γ rays and simultaneously accelerates the increase of the ascorbic acid content in irradiated material. (BBB)

12650 EFFECT OF IONIZING RADIATIONS, INCLUDING RADIOISOTOPES, ON THE PLACENTA AND EMBRYO. Rugh, Roberts (Coll. of Physicians and Surgeons, New York). Birth Defects, Orig. Article Ser., 1: 64-73(Apr. 1965).

Data relating to radiation injury of the embryo and fetus are discussed. Injury to the placenta and its relation to radioinduced fetal abnormalities are also considered. It is technically difficult to irradiate the placenta or the fetus without exposing the other. In an experiment designed to establish the lethal dose of x rays for the mouse embryo at various stages of development, it was found that the most radiosensitive periods occurred prior to the full development of the placenta. Acute exposures of the formed placenta to 400 R of x rays caused no demonstrable damage to the chorionic epithelium or to vascular endothelium of the placenta. With the increased vascularity of the placenta as it develops there is no evidence of any correlated increases in radiosensitivity, and the evidence is rather to the contrary. The better radiotolerance of late fetal mice is due in part to the completion of organogenesis, but a 17-day mouse fetus cannot be killed in utero by exposures to x rays at levels much higher than the $LD_{50/30}$ for the mother. Even 800 R was insufficient to damage the placenta and cause death of the fetus. This fact, plus the absence of histopathologic changes in the placenta following high levels of exposure to x rays, suggests that this organ is unusually radioresistant. (TCO)

12651 OBSERVATIONS ON BONE-MARROW TRANSFUSION IN THE WHOLE-BODY IRRADIATED, TUMOR-BEARING RAT. Witte, S.; Barth, G.; Graebner, H.; Schricker, K. Th. (Univ., Erlangen-Nuernberg, Ger.). Blut, 11: 257-67(Aug. 1965). (In German).

Attempts were made to eliminate tumor cells from rats bearing a rapidly growing tumor (Guerin) by a single lethal dose of radiation, while preventing hematopoietic failure by bone marrow grafting. The male Sprague-Dawley rats were given subcutaneous injections of the readily metastasizing tumor and two to three weeks later exposed to 1000 R of ^{60}Co γ rays. Isologous bone marrow injections were given 6 to 24 hours later. In the tumor-bearing animals, prior to ^{60}Co treatment, there were anemia, leucocytosis, and thrombopenia proportional to the extent of the tumor growth. After irradiation and transfusion of marrow cells, anemia and thrombocytopenia became more severe, probably due to bleeding from the necrotic tumor tissue. The enhanced leucopoiesis in the tumor-bearing animals was radio-resistant; the white cells in the blood fell to a lesser degree and for a shorter time than in tumor-free animals given the same treatment. No differences were noted in results between fresh bone marrow and bone marrow preserved at 70° in dimethylsulfoxide. The usually lethal outcome of a hematological radiation syndrome in the tumor-bearing animals was prevented by transfusion of bone marrow. No definite effect on the course of the tumor growth could be observed from a single large dose of whole-body irradiation; both controls and irradiated rats survived as long as four weeks. The tumor grew slowly but progressively in both groups and autopsy revealed no difference between them. Evidently, higher radiation doses are required to control the tumor. (BBB)

12652 THE ULTRASTRUCTURE OF EXPERIMENTAL ADENOHYPOPHYSIAL THYROTROPIC TUMORS AFTER RADIOTHYROIDECTOMY. Theret, Claude; Renault, Henri (Ecole Pratique des Hautes Etudes, Paris). Bull. Ass. Franc. Etude Cancer, 51: 505-34(Oct.-Dec. 1964). (In French).

Eighty C57 black male mice received 100 μC of ^{131}I in two doses. Animals were systematically sacrificed from the sixth week up to a year after injection or at 18 months. Reactions of the adenohypophysis and progressive tumor development were studied. Pathological changes in hypophyseal tissue appearing up to 18 mos post-irradiation are described histologically. (H.G.D.)

12653 CICATRIZATION AFTER TELECOBALT THERAPY IN SURGERY OF THE NECK AND BUCCAL CAVITY. Rodier, D.; Herdly, J. Bull. Ass. Franc. Etude Cancer, 52: 63-8(Jan.-Mar. 1965). (In French).

Problems encountered in surgical manipulation of an irradiated field are exemplified in a study of 68 patients with cancer of the mouth, oropharynx, hypopharynx, or larynx, that had received surgery after telecobalt therapy. It is concluded that if later surgery is contemplated, the radiation dose to the affected area should be limited to 3500 to 4000 R, otherwise failure of healing and fistula formation may develop as serious late sequelae. (H.G.D.)

12654 EFFECTS OF X-IRRADIATED FEEDER LAYERS ON MITOTIC ACTIVITY AND DEVELOPMENT OF ANEUPLOIDY IN MOUSE-EMBRYO CELLS IN VITRO. Rothfels, Klaus H.; Kupelwieser, Elisabeth B.; Parker, Raymond C. (Univ. of Toronto). Can. Cancer Conf., 5, 191-223(1963).

Two changes were studied that develop frequently in cells in vitro: changes in karyotype and changes toward malignancy. Investigation of karyotype changes in CR1 mouse cell lines during in vitro culture showed that cumulative changes over a number of years may lead to the L cell chromosome pattern. Attempts were also made to delay or prevent the in vitro chromosomal changes by the use of x-irradiated feeder layers both in short-term and long-term cultures. In long-term experiements the use of x-irradiated feeder cells eliminated the refractory period and delayed the appearance and ascendance of aneuploid cells. Young cell lines derived from kidney and lung of an adult CF1 mouse were characterized by chromosome numbers in the subtetraploid range and chromosomes of acrocentric morphology. Fifteen C3H mouse lines were tested for malignancy by injection into isologous baby mice. Most, if not all, of these lines produced tumors, whereas primary cell suspensions and short-term cultures did not. (TCO)

12655 THE GENETIC INTEGRITY OF UPGRADED AND DOWNGRADED ALLELES OF THE MELEZITOSE LOCUS IN SACCHAROMYCES. Hwang, Donna S.; Lindegren, Carl C.; Bhattacharjee, Jnanendra K.; Roshanmanesh, Al (Southern Illinois Univ., Carbondale). Can. J. Genet. Cytol., 6: 414-18(Dec. 1964).

The fermentation of melezitose by Saccharomyces is controlled by a single gene (MZ), which generates the adaptive enzyme, melezitase, capable of hydrolyzing the six α-glucosides, turanose, maltose, sucrose, palatinose, α-methyl-glucoside, and melezitose. The totipotent allele responds to six α-glucosides and is designated TMSGZ. A series of multiple alleles which differ from one another by their ability to react adaptively to the five specified α-glucosidic inductors are designated TMSGZ, TMSGz, TMSgz, TMsgz, Tmsgz, and tmsgz. (The small letters indicate the inabilities of a culture to respond adaptively to the corresponding substrates.) When cells of a haploid, totipotent TMSGZ culture (#D1008Z) were irradiated with different doses of uv light, TMSGz, TMSgz, TMsgz, and Tmsgz (but no tmsgz) mutants were obtained. Cells of a mutant TMsgz culture were plated on melezitose, and totipotent backmutant colonies capable of fermenting melezitose appeared after 6 days incubation. Three of these upgraded totipotent backmutants, #H, #X, and #Y, were a analyzed genetically. Since the MZ locus, with different allelic manifestations, produces one enzyme, and since no reciprocal recombinations have been found involving the five elements (T, M, S, G, and Z), the locus is a single gene and the radiation damage or substrate repair is an intragenic phenomenon. (TCO)

12656 NEW METHODS OF INDUCTION OF A TOLERANCE TO ALLOGENIC GRAFTS. Sekiguchi, Morimasa; Vaubel, Ekkehard; Mathe, Georges; Amiel, Jean-Louis (Hopital Paul Brousse, Villejuif, France). Compt. Rend., 261: 2969-71(Oct. 11, 1965). (In French).

Tolerance to allogenic skin grafts was induced in lethally x irradiated mice by a graft of isogenic medullary cells maintained for 2 hr at 37°C in Tyrode solution. Immune reactions involved are discussed. (C.H.)

12657 SUPERSTRUCTURE OF ADENOHYPOPHYSIAL TUMORS OF THE GONADOTROPE TYPE RESULTING FROM THE COMBINED EFFECTS OF RADIOIODINE (^{131}I) AND OF CHLORPROMAZINE. Theret, Claude; Lalegerie, Pierre; Tamboise, Edmond (Ecole Pratique des Hautes Etudes, Paris). Compt. Rend., 261: 2993-5(Oct. 11, 1965). (In French).

The radiothyroidectomy performed with moderate doses of ^{131}I in the mouse C 57/Bl was modified by chronic administration of chlorpromazine. Instead of a systematic tumoral transformation of the adenohypophysis of the mouse, 40% of the animal carriers of hypophysial tumors had tumors much smaller than those of typical thyrotropic tumors. The other animals showed only a slight increase of the volume of the adenohypophysis without deformation or necrosis. An electron microscopic examination of the tumors showed that they were composed entirely of newly formed cellule roots and of mature cellules repeating the granulation mode of the ICSH and FSH types of gonadotrophic cellules. The electron microscopic representations obtained are discussed in some detail. (J.S.R.)

12658 ABNORMALITIES OF HUMAN CHROMOSOMES FOLLOWING THERAPEUTIC IRRADIATION. Millard, Rosemary E. (Royal Marsden Hospital, London). Cytogenetics, 4: 277-94(1965).

Blood leukocytes were cultured from six men before and at intervals after therapeutic irradiation of the abdomen and pelvis. There was no evidence of increased aneuploidy after exposure. By the end of radiotherapy, 32% of metaphases showed chromosome structural aberrations (control 2%); these declined to 8% by the end of the follow-up (17 to 19 months after treatment). Cells with unstable aberrations declined faster than stable cells. No clones of cells were observed. Many polyploid metaphases were seen in the cultures after irradiation. There was no evidence that they were derived from circulating tumor cells or other large cells. The irradiated bone marrow was aplastic. Cells from unirradiated bone marrow had normal chromosomes. Thus, there was no evidence for the propagation of small lymphocytes (or other cells) with radioinduced chromosome markers in the bone marrow. (auth)

12659 CYTOLOGICAL TEST FOR DIAGNOSIS OF RADIORESISTANT CARCINOMA OF THE CERVIX UTERI. Slawov, L. (Pavlov Higher Medical Inst., Plovdiv, Bulgaria). Folia Med. (Plovdiv), 6: 204-8(1964). (in German).

The effect of various dosages of irradiation on morphological changes produced in surface biopsy samples of cervical carcinoma tissue, prepared according to the method of Ayre, was studied. The samples were obtained from patients with inoperable cervical cancer who received focal doses of from 675 to 6400 R of telecobalt or x irradiation. Examinations of the biopsy samples indicated major changes in the malignant cells within 3 weeks of irradiation. These included reduction in number of cells, fragmentation, pyknosis, nuclear swelling, appearance of chromatin, and lysis. These histological changes were found in all tumors that were favorably affected by the irradiations. Cytological study of changes that occur in carcinomas of the cervix after telecobalt or x irradiation may have value as a test for the destruction or inhibition of growth of radioresistant forms of these tumors. (BBB)

12660 THE EFFECT OF IONIZING RADIATION ON THE FLAVOR OF WHOLE-EGG MAGMA. Grim, Alfred C.; Goldblith, Samuel A. (Massachusetts Inst. of Tech., Cambridge). Food Technol., 19, 138-40(Oct. 1965).

The effect of temperature during ^{60}Co irradiation and dose level on the production of off-flavor compounds in whole-egg magma was investigated by a trained taste panel. No significant differences in flavor difference threshold doses were observed in egg magma held at 32, 60, 80, 100, and 130°F during irradiation. The dose-response curve for off-flavor production was nonlinear. Off-flavors could seldom be detected below a dose level of 9000 rad. Between 9000 and up to 30,000 rad there was a sharp increase in the rate of formation of off-flavor compounds. Taste panel tests using the dilution technique were used to study the dose-response effect, between 25,000 and 400,000 rad, on off-flavor production. The intensity of off-flavor increased with increased radiation dose but not at a linear rate. The finding of identical values for the flavor-difference threshold doses at the different temperatures may be explained by either the fact that the rate of free radical recombination also increased at the higher temperatures, or the oxidizing radicals such as the hydroxyl and hydroperoxyl radicals suffered increased recombination, or these oxidative radicals reacted at greater rates at the higher temperatures with compounds

present in the eggs, forming nonflavorful or nonodoriferous reaction products. (BBB)

12661 VIABILITY OF HETEROZYGOTES FOR INDUCED MUTATIONS IN DROSOPHILA MELANOGASTER. II. MEAN EFFECTS IN IRRADIATED AUTOSOMES. Falk, Raphael; Ben-Zeev, Nehama (Hebrew Univ., Jerusalem). Genetics, 53: 65-77(Jan. 1966).

The viability of flies heterozygous for unselected samples of irradiated second chromosomes was studied in repeated tests in different genotypic combinations. A dose of 2000R caused no significantly detectable reduction in the viability of heterozygotes for irradiated chromosomes. The slight effect suggested by the results could be due to induced lethals. Severe detrimental mutations were rare, and only 10 to 20% of the deleterious effect in homozygotes was due to nonlethals. It could not be decided whether their effect in heterozygous condition was too small or whether they had no effect at all. (auth)

12662 CHROMOSOMAL POLYMORPHISM IN IRRADIATED NATURAL POPULATIONS OF CHIRONOMUS. Blaylock, B. Gordon (Oak Ridge National Lab., Tenn.). Genetics, 53: 131-6(Jan. 1966). (ORNL-P-1560).

Chromosomal polymorphism in a natural population of Chironomus tentans inhabiting a stream contaminated by radioactive waste was compared with a nonirradiated population. Ten inversions and one deletion were found in the irradiated population but not in the control population. The frequencies of three endemic inversions which were found in both populations were not significantly different in the irradiated and nonirradiated populations. It was concluded that in the irradiated population, where an increased frequency of new chromosome aberrations was detected, the frequencies of the endemic inversions were unchanged by the chronic radiation. (auth)

12663 MUTATION FREQUENCIES DETECTED FOLLOWING IRRADIATION OF VIRGIN AND INSEMINATED DROSOPHILA MELANOGASTER FEMALES. Lefevre, G. Jr. (Harvard Univ., Cambridge, Mass.). Genetics, 53: 137-43(Jan. 1966).

Sex-linked recessive lethal mutation frequencies were detected at successive intervals after irradiation with 4,000R of 3-day-old females, which were then mated with nonirradiated males. The mutation frequencies detected were compared with those obtained in parallel experiments in which irradiated females were mated with males that were separately exposed to the same dose of radiation, and with those detected following the irradiation of inseminated females. The irradiation of both paternal and maternal genomes, rather than only the maternal genome, results in a highly significant reduction in the frequency of mutations detected among eggs laid during the first four days after irradiation. Among eggs laid later, a small, but insignificant, reduction in frequency of mutations is detected when both genomes are irradiated. The suggestion is made that interaction between the two genomes, when both have been irradiated, leads to the elimination of a proportion of mutants induced in relatively mature germ cells. Since a similar loss of mutants does not occur following the irradiation of immature female germ cells, it is further suggested that mutants associated with chromosomal aberrations are preferentially eliminated by interaction of the two irradiated genomes. (auth)

12664 CYTOGENETIC STUDIES ON THE WHITE LOCUS IN DROSOPHILA MELANOGASTER. Lefevre, G. Jr.; Wilkins, M. D. (Harvard Univ., Cambridge, Mass.). Genetics, 53: 175-87(Jan. 1966).

It was concluded that the white locus is contained within salivary chromosome band 3C2. Deficiency for this band in the male does not give rise to a lethal effect; rather, males lacking only 3C2 are viable, fertile, and white-eyed. The survival of flies homozygous deficient for the white locus may be correlated with the apparent homology between white and zeste. Mutants that are described as male-lethal white deficiencies lack, in reality, not only band 3C2, but also adjacent bands as well. Analysis of a new white-mottled inversion, w^{mJ}, indicates that typical white variegation can be expressed when heterochromatin is inverted so as to lie immediately adjacent to the white locus. It is not necessary for the expression of white variegation that the white locus be inverted so as to lie immediately adjacent to proximal heterochromatin, as in the case of w^{m4}. The scarcity of white-mottled inversions, as compared with white-mottled translocations, can be explained by a sharply restricted spread of position effect from the point of chromosome breakage in x-chromosome inversions. (auth)

12665 INTEGRATION EFFICIENCY AND GENETIC RECOMBINATION IN PNEUMOCOCCAL TRANSFORMATION. Lacks, Sanford (Brookhaven National Lab., Upton, N. Y.). Genetics, 53: 207-35(Jan. 1966).

Seventy-six mutations at the amylomaltase locus of pneumococcus were analyzed with respect to mutagenic origin, reversion to wild type, integration of both positive and negative markers in transformation, and frequencies of recombination between pairs of markers. Overlapping multi-site mutations established the linear order of sites in the locus. Single-site mutations gave efficiencies of integration of the wild-type marker. Different mutations at a single site gave different efficiencies. Integration efficiencies of negative markers correlated with the reciprocal efficiencies. It was concluded that particular base changes are responsible for the observed integration efficiencies. Tentative assignments of base changes corresponding to the various classes were made. By the use of doubly marked DNA, it was shown that incompatible base changes responsible for low integration efficiency also exclude adjacent donor markers. The relationship between exclusion and linkage is such that the recombination index is an approximately valid measure of genetic distance, as deduced from the order of sites in the locus. A model, based on synapsis of a donor single strand with the host cell DNA followed by a dynamic equilibrium between segments of donor and host strands in the resultant three-stranded structure, is proposed to account in molecular terms for the phenomena of exclusion and genetic recombination. (auth)

12666 THE EFFECT OF RADIOACTIVE FALLOUT AT THE NEVADA TEST SITE ON THE CHROMOSOMES OF THE POCKET MOUSE. Towner, Joseph W. (Northrop Space Labs., Hawthorne, Calif.). Health Phys., 11: 1569-71(Dec. 1965).

Native Populations of the Long-Tailed Pocket Mouse, Perognathus formosus, were trapped at the Nevada Test Site from an area with a history of heavy contamination by radioactive fallout, but uncontaminated for 3 yrs previous to trapping; and from an unexposed control area. With one possible exception, no unequivocal evidence was obtained for the presence of a persistent, inherited chromosome aberration in either population. (auth)

12667 EFFECT OF ACUTE GAMMA RADIATION ON WILD OPOSSUM, GRAY FOX, RACCOON AND BOBCAT. Golley, Frank B.; Rauber, Ernest L.; Morgan, Eric L.; Jenkins, James H. (Univ. of Georgia, Athens). Health Phys., 11: 1573-6(Dec. 1965).

The radiation response to acute ^{137}Cs radiation was tested in wild-trapped opossums, raccoons, gray foxes, and bobcats collected on the AEC Savannah River Plant, Aiken, South Carolina. The $LD_{50/30}$ for the raccoons and gray foxes was 580 and 710 R respectively. Data were insufficient to determine the $LD_{50/30}$ for the opossums and bobcats; however, the relationship between average survival and dose indicated that the opossum appeared to be the least sensitive species tested and the bobcat the least resistant. In general, decedent wild mammals did not exhibit symptoms of radiation sickness, other than anorexia, until several days before death. Lethality in these wild species was within reported limits for domesticated or laboratory mammals of approximately the same body weight. (auth)

12668 LONG-TERM EFFECTS OF ACUTE LOW-LEVEL X-RAYS ON THE POPULATION DYNAMICS OF THE YELLOW FEVER MOSQUITO, AEDES AEGYPTI.

Willard, William K. (Univ. of Tennessee, Knoxville). Health Phys., 11: 1577-83(Dec. 1965).

Populations of four life-history stages (eggs, first instar larvae, pupae, and adults) of the yellow fever mosquito were subjected to acute low-level x-rays and followed through three generations. Fecundity, egg viability, larval growth rate, and mean longevity were population parameters utilized in evaluating the long term effects. Effects were most strongly exerted in the first generation and gradually subsided in subsequent generations. Doses of 50 to 400 R were found to be stimulatory in some cases, while doses of 800 R and above were detrimental. The egg stage was found to be most sensitive followed by the larval, pupal, and adult stages. Effects on egg viability were most drastic and persisted through three generations. (auth)

12669 GROWTH OF LIZARDS IN NATURAL POPULATIONS EXPOSED TO GAMMA IRRADIATION. Turner, F. B.; Hoddenbach, G. A.; Lannom, J. R. Jr. (Univ. of California, Los Angeles). Health Phys., 11: 1585-93 (Dec. 1965).

Growth of the iguanid lizard, Uta stansburiana, was analyzed in four 20-acre areas in Nevada between July and November 1964. One plot was irradiated continuously during this interval (except for sampling time). Growth of lizards in all areas appeared the same until October and November, when growth in the irradiated plot fell behind that occurring in the control areas. Analyses of variance involving both body lengths and weights showed highly significant differences between areas which are primarily attributable to the retardation of growth in the irradiated plot. The difference between plots is not, at this time, attributed to irradiation. Some alternative interpretations of the situation are discussed. (auth)

12670 EFFECTS OF RADIOACTIVE AND NON-RADIOACTIVE DUST UPON LARREA DIVARICATA CAV., NEVADA TEST SITE. Beatley, Janice C. (Univ. of California, Los Angeles). Health Phys., 11: 1621-5(Dec. 1965).

Among populations of Larrea divaricata Cav., monitored for ionizing radiation exposure following nuclear detonations that occurred in July 1962 at the Nevada Test Site, two sustained heavy coatings of fine-particle dust. All dust-covered plants eventually became defoliated during the following year; in those irradiated but not dust-coated, there was no defoliation. One of the dusted populations was exposed to 3000 to 6000 roentgens during this year, and the other to negligible dosages; defoliation and subsequent death of stems in the irradiated population was evidently the result, therefore, of dust effects and not the ionizing radiation. Defoliated plants have recovered or are recovering by basal and/or stem sprouts. (auth)

12671 SIMULATED FALLOUT STUDIES IN CONIFERS—A PRELIMINARY REPORT. Clark, G. M.; Roy, R. M.; Baker, D. G.; Bunting, W. R. (Univ. of Toronto). Health Phys., 11: 1627-36(Dec. 1965).

Dry seed and 1-year old dormant seedlings for the following species: black spruce, jack pine, red pine, Scotch pine, white spruce, and white pine were exposed to irradiation to simulate the gamma component in an early fallout field over a period of 96 hrs ($t_{10}-t_{106}$). Seven total dosages ranging from 452 to 8640 R were employed and the dose-rate (R_t) was made to vary as a power function of time where $R_t = R_{10}t^{-1.2}$. A comparable group received the same total dosages over 96 hrs but at a constant rate. Germination was higher for all species under laboratory conditions than in the field where survival of seedlings from irradiated seed was scored 4 months after irradiation (Sg). The $LD_{100/30}$ for seeds ranged from 3260 R for white pine to 8640 R for black spruce with the exception of jack pine where germination occurred at all dosages employed. Constant and fallout dose regimes gave comparable results with the exception of Scotch pine and red pine. The $LD_{100/120}$ for field-grown seeds varied from 1720 R for white pine to 4730 R for jack pine. Fallout and constant rate regimes gave comparable results with the exception of Scotch pine and white pine. One-year-old seedlings survived higher dosages than did irradiated seed scored at 4 months after irradiation. The $LD_{100/120}$ for the constant rate regime varied from 3260 R for white spruce to 8640 R for jack pine. Comparable results were obtained under the fallout regime for white pine and white spruce, however with jack pine, red pine and Scotch pine lower total dosages produced an $LD_{100/120}$ under fallout than under the constant-rate regime. In the case of Scotch pine and jack pine other parameters of radiation injury, e.g., fresh and dry weights, seedling lengths, root and stem caliper measurements, supported the aforementioned findings. (auth)

12672 RADIATION DAMAGE TO FOREST SURROUNDING AN UNSHIELDED FAST REACTOR. Witherspoon, John P. (Oak Ridge National Lab., Tenn.). Health Phys., 11: 1637-42(Dec. 1965). (ORNL-P-1230).

In May 1964, radiation effects were observed in conifer and hardwood tree species growing within 20 m of the Health Physics Research Reactor. Cumulated fast neutron doses ranged from 265 to 996 rad (tissue dose in air), delivered sporadically over the previous year. During the summer, vegetation damage patterns extended out to 40 m from the reactor. Conifers within this distance exhibited severe growth retardation and needle mortality in areas receiving total cumulated fast neutron doses of between 100 and 250 rad. Site factors such as soil disturbance, moisture stress, and poor nutrient status contributed to observed radiation effects. (auth)

12673 INTERACTIONS OF GAMMA RADIATION AND OTHER ENVIRONMENTAL STRESSES UPON PINE SEEDS AND SEEDLINGS. McCormick, J. Frank; McJunkin, Robert E. (Univ. of North Carolina, Chapel Hill. Univ. of Georgia, Athens). Health Phys., 11: 1643-52(Dec. 1965).

A pilot study was conducted to determine the effects of ionizing radiation upon slash (Pinus elliottii) and longleaf (Pinus palustris) pine seeds and seedlings, and to identify environmental factors that modify species radiation sensitivities. Seeds and seedlings were exposed to several radiation doses and then grown in a variety of post-irradiation environments, some of which included high temperature, low moisture and low light. Percent germination, growth, physiological tolerances, and survival usually varied inversely with the radiation dose received. Germination rates, drought tolerances, and growth under low light intensities were increased by doses in the range of 100 to 500 R. Slash seeds were more sensitive than longleaf seeds, but the order of seedling sensitivity was reversed. Results of the study indicate that the condition of the organism and the nature of the environment prior to and following irradiation must be rigorously defined in order to evaluate radiation effects. (auth)

12674 CHANGES IN RADIOSENSITIVITY OF PINE SEEDLINGS SUBJECTED TO WATER STRESS DURING CHRONIC GAMMA IRRADIATION. Miller, Lee N. (Duke Univ., Durham, N. C.). Health Phys., 11: 1653-62(Dec. 1965). (CONF-650523-4).

To test the hypothesis that water stress during irradiation may cause increased radiation damage, Pinus taeda seedlings were subjected to several levels of water stress during 30 days of gamma irradiation. Internal water stresses in the plants were measured with thermocouple psychrometers. A highly significant interaction was observed in effects of simultaneous water stress and 50 R/day radiation on needle growth (cells dividing during treatment). The interaction was weak at 20 or 30 R/day. No interaction was noted between effects of radiation and water stress on the elongation of stems whose apical cells were dormant during treatment with 20 R/day. These results suggest that radiosensitivities of plants in natural ecosystems may be underestimated by greenhouse or garden experiments in which environmental stresses are reduced and cells divide rapidly. (auth)

12675 RECOVERY OF HARDWOOD STANDS 3–5 YEARS FOLLOWING ACUTE IRRADIATION. Cotter, David J.; McGinnis, John T. (Alabama Coll., Montevallo. Univ. of Georgia, Athens). Health Phys., 11: 1663-73(Dec. 1965).

An analysis was made of the degree and type of vegetation recovery exhibited by an upland mixed pine-hardwood forest exposed to 13,000 to 47,000 rad from an unshielded nuclear reactor in north Georgia. Stem growth was measured in August 1963 following two acute exposures to radiation which occurred in the summers of 1959 and 1960. The major form of recovery of the irradiated forest was by sprouting from protected under-ground tissues. Yearly growth of sprouts decreased with time so that 3 years after irradiation the amount of yearly growth no longer reflected the damage received. As a measure of cumulative growth, the height of the tallest stem was found to be the most significant factor expressing the recovery of plants and was related to dose if age was considered. Age was inversely proportional to radiation, and plants near the reactor showed a delay of up to 3 years in initiating a recovery response. The five understory species demonstrated two to four times as much resiliency (recovery potential) as the five overstory species. Radiation eliminated seed reproduction. The character of the early recovery forest will be controlled largely by the rate of sprout growth, and future development will be dependent on the time it takes for different species to resume normal reproduction or on the rate of emigration from adjacent undisturbed areas. By the elimination of pines and the reversal of the normal overstory-understory relation, the radiation-disturbed community is not in the normal successional pattern and could be called a radiation subclimax. (auth)

12676 DISTURBANCES IN MICROSPOROGENESIS CAUSED BY X RAYS IN SUGAR BEET DI- AND TETRAPLOIDS. Kuzdowicz, A. (Inst. for Plant Breeding and Acclimatization, Bydgoszcz, Poland). Hodowla Roslin, Aklim. Nasienn., 8: 249-54(1964). (In Polish).

The morphology and fertility of spores was examined after x irradiation of diploid and tetraploid sugar beet plants to doses of 1, 5, 10, 20, or 30 kR. These observations on the effect of the x rays on the inflorescence of the sugar beet before blooming showed that a dose of 5 to 30 kR causes in diploids the formation of large pollen grains with a large number of pores and in tetraploids a larger amount of such pollen than in diploids. In the progeny of X_2 plants tetraploids appeared while in X_2 tetraploids neither diploids nor aneuploids were observed, although the seed plants produced a large amount of small pollen grains. Obviously, this abnormal pollen of tetraploids is sterile. Some diploid seed plants of X_2 also produced, besides the normal haploid pollen, tetraploid pollen as well. (BBB)

12677 RESISTANCE TO THE BACTERICIDAL EFFECT OF ULTRAVIOLET RADIATION CONFERRED ON ENTEROBACTERIA BY THE COLICINE FACTOR COL I. Howart, Sheila (Univ. of Otago Medical School, Dunedin, N. Z.). J. Gen. Microbiol., 40: 43-55(July 1965).

Strains of Salmonella typhimurium and Escherichia coli which have acquired the colicine factor, col I, are less sensitive to the lethal effects of uv radiation than the non-colicinogenic parent strain. The dose of uv radiation required to kill 50% of the population of S. typhimurium strain LT2 colicinogenic for colicine I was greater by a factor of three than that required to kill 50% of the noncolicinogenic parents. The number of survivors of the noncolicinogenic strain decreased exponentially with dose; the survival curve of the colicinogenic strain had a pronounced shoulder. Experiments with a strain of E. coli K 12 carrying lambda prophage indicated that the presence of col I decreased the incidence of phage induction following uv irradiation. It is proposed that the effect of col I in protecting apparently nonlysogenic and noncolicinogenic strains against the lethal effects of uv irradiation results from its ability to suppress the lethal induction of a defective plasmid in these strains without itself being induced. Nevertheless, col I is inducible in sublines of Escherichia coli K 12. Experiments showed that uv induction of the production of colicine E2 in S. typhimurium is partly prevented by col I, but this effect cannot account for the increased survival of bacteria carrying col I as well as col E2; because, though col E2 is inducible, its presence does not increase the susceptibility of S. typhimurium LT2 to the lethal effects of irradiation. The hypothesis that col I protects by suppressing induction of defective plasmids in the strains concerned predicts that, unlike photoreactivation, it will decrease the lethal but not the mutagenic effect of irradiation. Preliminary experiments showed that the presence of col I in some auxoautotrophic mutants of S. typhimurium strain LT2 did not result in a decrease of the number of revertants for a given dose of uv radiation, but an actual increase. (BBB)

12678 EFFECTS OF X-RADIATION ON INTRACISTRON RECOMBINATION AT THE WAXY LOCUS IN MAIZE. Briggs, Robert W.; Smith, Harold H. (Brookhaven National Lab., Upton, N. Y.). J. Heredity, 56: 157-62(July-Aug. 1965). (BNL-9044).

Experiments were conducted to determine if x radiation would influence the rate of intracistron recombination in the waxy locus in maize. Waxy alleles, wx^c, wx^{90} and wx^{H21}, available in the homozygous condition and all possible hybrid combinations, were used. An acute dose of 200 R of x radiation (250 kv) was applied to each maize plant during meiosis. Any significant difference in frequency of wx pollen grains between a treated and untreated heteroallelic cross, after subtraction of back mutation frequencies of homoallelic parents, was considered to be due to an effect induced in genetic recombination. Data on individual plants in two of the three heteroallelic crosses showed significant effects of x radiation on intragenic recombination. One increase and several decreases were found. Also, when the data from the treated heteroallelic plants were bulked and compared to the bulked untreated heteroallelic plants the $wx_c \times wx^{90}$ group was significant at the 0.1% level. The $wx^{90} \times wx^{H21}$ heteroallelic group was significant at the 10% level. The apparent effect of irradiation on recombination could be due to an elimination of recombinant or nonrecombinant gametes. That is, where a decrease in recombination is found an elimination of wx pollen grains could have taken place. It is suggested that irradiation may be interfering with the genetic recombination mechanism to bring about reduced recombination. However, one increase in recombination was noted that indicates this is certainly not always true. Therefore, irradiation may also be enhancing the recombination mechanism. The mechanism involved in intergenic recombination does not appear to be affected by irradiation. The stage of meiosis as related to an effect on intragenic recombination by irradiation is discussed. (BBB)

12679 RADIOSENSITIVITY STUDIES ON AN INTERSPECIFIC GRASS HYBRID. Bottino, Paul J. (Utah State Univ., Logan). J. Heredity, 56: 225-8(Sept.-Oct. 1965).

An investigation was made to determine whether average interphase chromosome volume could be used as a valid index of the radiosensitivity of native forage grasses. The primary criteria used to determine radiosensitivity were lethal level and severe growth inhibition. Other criteria included effects on pollen mother cell and root tip divisions, and anatomical modification of the apical meristem. A naturally occurring sterile hybrid between Agropyron subsecundum and Agropyron cristatum was used. The hybrid has 21 chromosomes, 14 from A. subsecundum and 7 from A. cristatum. Seven acute radiation levels of ^{60}Co γ radiation were employed: 200, 500, 1000, 2000, 3500, 5000, and 8000 R. When lethality and severe growth inhibition were used as criteria for radiosensitivity, the observed lethal level was about 4000 R. Additional evidence from analysis of pollen mother cells and root tip divisions substantiated 4000 R as an approximately lethal level. Bridges, acentric fragments, stickiness, and micronuclei were the most commonly observed chromosome aberrations. As expected, the frequency of aberrations increased as the dose increased, while the frequency of divisions was inversely proportional to dose. The percentage of cells showing aberrations increased from 2.5% in the 200 R level plants to 100% in the 8000 R level. A marked decrease in the mitotic activity was noted in plants receiving 5000 and 8000 R. Shoot meristems were profoundly affected by the higher radiation levels, including absence of young pri-

mordia at 3500 R, partial collapse of the apical meristem at 5000 R, and complete collapse of the apical meristem at 8000 R. The observed lethal level is in good agreement with the predicted lethal level on the basis of average interphase chromosome volume. (BBB)

12680 PROTECTION MECHANISMS OF NON-MALIGNANT AND MALIGNANT CELLS AGAINST IONIZING RADIATION. I. THE CYTOLOGICAL EFFECTS OF 2-MERCAPTOETHYLAMINE ON THE RAT AND MOUSE ASCITES TUMORS. Kawamura, Fumio; Kobayashi, Jindo (Tokushima Univ., Japan). J. Radiat. Res. (Jap.), 5: 166-71(Sept.-Dec. 1964).

Cytological effects of 2-mercaptoethylamine were investigated on the Yoshida-sarcoma, the MTK-sarcoma III and Ehrlich ascites tumor with emphasis on tumor cell growth. Mercaptoethylamine exerts influence upon tumor cells in process of mitosis, especially on an increase of mitotic cells, leading to increase of prophasic cells at first and metaphasic cells secondarily. The protection mechanism against radiation exerted by 2-mercaptoethylamine indicated that this drug induced an increase of mitotic activity. The increase of mitotic activity might be interpreted as a protecting effect against radiation injury. (auth)

12681 ELECTRON MICROSCOPIC STUDIES ON THE NORMAL MOUSE SPLEEN AND ITS MORPHOLOGICAL CHANGES AFTER TOTAL-BODY IRRADIATION. Seki, Masatoshi; Sekiyama, Shigetaka; Yoneyama, Tatsuo (National Inst. of Radiological Sciences, Chiba, Japan). J. Radiat. Res. (Jap.), 5: 183-205(Sept.-Dec. 1964).

Electron microscopic observations of the normal mouse spleen confirm the role of reticular cells in erythropoiesis and lymphocytopoiesis. The possibility of DNA reutilization is discussed in connection with phagocytic bodies (phagosomes) that are derived from phagocytized nuclear substance. A special lock-gate-like structure of the sinus wall was observed and it is suggested that this makes blood channel formation possible between the pulp cord and sinus by an open-and-close mechanism. Changes in mouse spleen after whole-body irradiation of 1,000 R were studied. Half an hour after the irradiation, the formation of clear foci was prominent in the nucleus, cytoplasm and mitochondrial matrix of the lymphocytes. Later the clear foci in the cytoplasm disappeared and focal aggregation of chromonema with increasing intensity occurred. The changes were concluded to be due to radioinduced alteration of molecular structure of the constituents. Two hours after irradiation, the reticular cells adhered to the lymphocytes, which were dehydrated and condensed. The condensed lymphocytes were then phagocytized and digested by the reticular cells. (TCO)

12682 STUDIES ON LYMPH NODE AND THYMUS TISSUE CULTURE. PART I. INFLUENCE OF THE RADIOACTIVE ISOTOPE ^{32}P AND THYMUS EXTRACT ON THE LYMPH NODE AND THYMUS SUSPENSION CULTURES. Imamura, Yoshinori (Hiroshima Univ.). Med. J. Hiroshima Univ., 13: 43-51(Jan.-Feb. 1965). (In Japanese).

The possibility that the function of thymus and lymph node cells may be different was investigated. Radiophosphorus was added to the medium of tissue cultures of thymus and lymph node cells to observe its influence on the cells. The thymus and mesenteric lymph nodes of one-month-old DD-K male mice were used for the tissue cultures. At a high concentration of ^{32}P, the growth of both thymus and lymph node cells was retarded. However, at low concentrations of ^{32}P (0.45 $\mu C/2$ ml) both types of cells showed improved growth as compared with the controls. Effects of addition of trypsin and of increasing ^{32}P concentrations were more pronounced in the lymph node cells than thymus cells. With the addition of thymus extracts and ^{32}P, both cells showed increased longevity and increased sensitivity to ^{32}P in the lymphoid cells. Although lymph node and thymus are both composed of lymphoid tissues they probably have the basic differences in their nature. In vitro, the sensitivity to ^{32}P is less than in vivo. Beyond a certain intensity, radioactivity will destroy the cell directly. The addition of the thymus extracts prolongs the life of the cell in the presence of ^{32}P; this may be due to the fact it can promote the production of lymphocytes. (BBB)

12683 EXPERIMENTAL STUDIES ON EFFECTS DUE TO IRRADIATION LOW DOSE IN UTERO (PRELIMINARY REPORT). Nakagawa, Shigeru; Hirata, Masashi; Hori, Ippei; Matsuda, Michinori (Hiroshima Univ.). Med. J. Hiroshima Univ., 13: 93-100(Jan.-Feb. 1965). (In Japanese).

Phenotypic damage of the irradiated fetus may be largely due to low dose irradiation rather than large dose irradiation, as previously reported. X rays (50 rad) and neutrons (15 rad) were used to irradiate pregnant ddN strain mice. With 50-rad x irradiation during pregnancy, no significant difference was seen in number of viable offspring or the gestation time between the experimental and control group, but the sex ratio was decreased and growth retardation slightly more frequent in the experimental group. Incidence of pregnancy was increased in the mice irradiated as fetuses by the 16th week of age as compared with that of the control group. Irradiated males and irradiated females produced more frequent stillborn fetuses, offspring with a higher sex ratio and more growth-retarded offspring; irradiated females and normal males produced fetuses with an abnormally high incidence of retarded growth and stillbirths as well as increased sex ratio; the newborn of the normal mother and the irradiated father were likely to be born dead and to have an elevated sex ratio. There was no evidence for increased incidence of malformations in the experimental group but the gestation period was increased as compared with the control group. The 15-rad neutron irradiated group showed a decreased total number of the newborn and the number of the newborn per female mouse as well as increased incidence of the perinatal deaths and increased sex ratio, as compared with the x-irradiated group. (BBB)

12684 ON THE PROBLEM OF COMBINED RADIOLOGIC AND SURGICAL INJURIES. Messerschmidt, O.; Melching, H. J.; Dinkloh, H. (Univ., Freiburg i. B.). Med. Klin. (Munich), 60: 877-82(May 28, 1965). (In German).

The author reviews several aspects of the combined effect of ionizing radiation and surgical injury. Usually this combination leads to a disease picture that differs significantly from the separate types of injury. A limited number of studies have been reported on combinations of irradiation injuries with burns, wounds or fractures, environmental injuries such as heat and cold, hunger, thirst, or fatigue. The effect of the time interval between whole-body x irradiation and production of open wounds on survival of mice was studied. It was found that mortality was markedly increased if the interval amounted to from 2 to 9 days. If the animals were wounded before irradiation, the mortality was relatively decreased. Several possible reasons for these differences are discussed. (BBB)

12685 RESPONSE TO WHOLE-BODY IRRADIATION OF MICE PRETREATED WITH DRUGS HAVING A STIMULATING EFFECT ON THE CENTRAL NERVOUS SYSTEM. Stuart, C.; Cittadini, G.; Tomiselli, G. (Univ., Siena, Italy). Minerva Radiol., Fisioterap. Radiobiol., 10: 445-8 (Oct. 1965). (In Italian).

The differences in the survival of whole-body irradiated mice treated with drugs having a general stimulating effect on the central nervous system (pentamethylenetetrazol and dimefline) are reported. Dimefline has a radiosensitizing effect for a subsequent exposure to x radiation at 800 R. (tr-auth)

12686 DELAYED EFFECTS OF IONIZING RADIATION: CHANGES IN THE SEMINAL TISSUE. Bosio, F.; Monateri, P. C. (Univ., Turin). Minerva Radiol., Fisioterap. Radiobiol., 10: 449-53(Oct. 1965). (In Italian).

In a series of experimental histological studies, the delayed effect of ionizing radiations on the seminal tissue of the testicle was studied. It was shown that impairment of

spermatogenesis is apparent 5 days after whole-body irradiation at 75R with protection of the testis. This impairment is more marked after 10 days in animals exposed to 150 R. The most probable theories suggested to explain the delayed effect of ionizing radiations are briefly discussed. The present studies were made principally to confirm the existence of the phenomenon in the seminal tissue as it was previously shown in other tissues with similar morphofunctional features, such as the lymphatic and hematopoietic tissues. (tr-auth)

12687 REPAIR MECHANISMS AND VARIATIONS IN UV SENSITIVITY WITHIN THE CELL CYCLE. Davies, D. Roy (Wantage Research Lab., Eng.). Mutat. Res., 2: 477-86(Dec. 1965).

Studies were made of the uv sensitivity of a series of stages in the cell cycle of synchronous populations of diploid meiotic spores of Chlamydomonas reinhardi. Early stages had sigmoid survival curves, but at successively later stages of development, D_Q values were continuously reduced, and the latest stages had exponential survival curves. D_0 values, though changing only to a minor extent, were at a maximum in mid-cycle. From studies of the effects of various post-irradiation treatments and in particular of the effect of inhibitors of dark-repair processes, it was concluded that much of the variation in stage sensitivity was attributable to different repair activities. Those stages farthest from division had the longest period in which to repair uv lesions, whereas successively later stages had less time and thus exhibited an enhanced sensitivity. (auth)

12688 THE EFFECT OF DOSE DURATION IN THE INFLUENCE OF IRRADIATION ON RECOMBINATION IN CHLAMYDOMONAS. Lawrence, C. W. (Wantage Research Lab., Eng.). Mutat. Res., 2: 487-93(Dec. 1965).

The effect on meiotic recombination of acute irradiation treatments, lasting 2 min or less, were compared with the effect of protracted treatments lasting 24 min. Doses from 2 to 8 krad were used in both cases. The results support the previous finding that non-lethal doses of radiation change recombination only if administered during two short stages, one in preleptotene and the other in prophase. The differences between the acute and protracted dose-response curves at the preleptotene stage are dependent on the duration of the sensitive stage, estimated to be about 12 min, in relation to the degree of synchrony in the cell population. At the prophase stage, the difference between the results from the two kinds of treatment arise from a true dose-rate effect, low dose rates failing to produce any change in recombination frequency. The targets at both the preleptotene and the prophase stage are thought to be concerned with DNA synthesis. (auth)

12689 EFFECTS OF X-RAYS ON FEMALE GERM CELLS OF DROSOPHILA MELANOGASTER. II. CROSSING-OVER IN THE X-CHROMOSOME. Bateman, A. J.; Chandley, A. C. (Christie Hospital and Holt Radium Inst., Manchester, Eng.). Mutat. Res., 2: 506-22(Dec. 1965).

Distal segments of the X-chromosome show reduced recombination after x-irradiation. This reduction is confined to eggs laid 6 days and more after irradiation and persists at least until the 14th day. It is roughly proportional to dose over the range 1 krad to 8 krad. Proximal segments of the X (between *f* and the centromere) show increased recombination after x irradiation. The increase is first evident in eggs laid 4 days after irradiation and persists at least until the 11th day. The maximum effect follows 4 krad. Intermediate segments show increased recombination at doses up to 4 krad and reduced recombination at higher doses. It is concluded that the increases and decreases in recombination following x irradiation are independent effects with different dose dependences. The increased recombination is attributed to the direct induction of crossing-over in early oocytes or oogonia in synapsed regions. It is postulated that the reduction in recombination is due to the disruption of synapsis, beginning at the telomere and extending towards the centromere as the dose is increased. It is supposed that when the pairing of oogonial chromosomes is disrupted the disruption persists through to the oocyte. The sensitivities of the various stages of oogenesis to induced crossing-over, reduced crossing-over, non-disjunction, and dominant lethals are compared. (auth)

12690 CHROMOSOME PAIRING AND INDUCED EXCHANGE IN DROSOPHILA. Parker, D. R. (Univ. of California, Riverside). Mutat. Res., 2: 523-9(Dec. 1965).

Fragments of Y chromosomes were induced by irradiating attached-X Drosophila melanogaster females carrying a doubly marked Y chromosome, and detected by loss of one of the Y markers. Slightly more than half of the 55 fragments recovered showed linkage of fourth chromosome markers, implying a high frequency of association of Y and fourth chromosomes in oocytes. Where such fragments were shown to have Y centromeres, a high incidence of non-disjunction from the attached X was found, suggesting that exchange between heterologues leads to their separation at anaphase I, and frequent non-disjunction from their regular pairing partners. It is suggested that non-reciprocal exchanges induced between the two Y arms may account for other fragments, these likewise being pairing-dependent. There is as yet no evidence that any exchange process occurs with appreciable frequency in oocytes in stage 7 or earlier that is not dependent on regular, frequent associations of the chromosomes involved. (auth)

12691 RADIOSENSITIVITY OF FEMALE GERM CELL STAGES OF DAHLBOMINUS. Baldwin, W. F. (Atomic Energy of Canada Ltd., Chalk River, Ont.). Mutat. Res., 2: 530-3(Dec. 1965).

Male progeny from females irradiated as adults showed approximately 5 times as many eye-color mutations as those irradiated in the larval stage. Also, the frequency of mutants increased with age of the adult, being approximately twice as high at 108 hrs of age as at 12 hrs. This phenomenon was attributed to a larger number of radiosensitive oocytes in the ovarioles of the older adults. (auth)

12692 COMPARATIVE STUDIES OF MUTATION FREQUENCIES INDUCED BY ^{32}P TREATMENT AND γ-IRRADIATION IN THE MALE SILKWORM. Ikenaga, Mituo; Kondo, Sohei (National Inst. of Genetics, Misima, Jap.). Mut. at Res., 2: 534-43(Dec. 1965).

The frequency of mutations induced in the male silkworm fed with ^{32}P on the third day of the fourth instar (shortly before meiosis) was compared with that induced by γ-irradiation. The daily dose of γ rays was carefully adjusted day by day so as to fit the daily change in the absorbed dose delivered to the gonad by the ingested ^{32}P. The gonad dose for the ^{32}P treated group was estimated by applying Loevinger's equation; the parameters involved in the equation were experimentally determined with special care for biological factors. Using the ^{32}P dose estimates thus determined, it was found that the mutation frequency was equal for the ^{32}P and γ-ray groups at the same absorbed dose. It was concluded that there could be no chance for the mutation induced by ^{32}P transmutation to show up under the present conditions and that the proposed ^{32}P dosimetry is satisfactory. (auth)

12693 THE EFFECT OF HYPOTHERMIA ON THE INDUCTION OF CHROMOSOMAL MUTATIONS BY ACUTE X-IRRADIATION OF MICE. Ashwood-Smith, M. J.; Evans, E. P.; Searle, A. G. (Medical Research Council Radiobiological Research Unit, Harwell, Eng.). Mutat. Res., 2: 544-51(Dec. 1965).

Male mice were given 600 rad acute x-irradiation when hypothermic or at normal body temperature. In mice irradiated when hypothermic the yield of dominant lethal mutations from treated spermatozoa was slightly but not significantly reduced, while the incidence of cytologically identifiable reciprocal translocation configurations in primary spermatocytes derived from irradiated A type spermatogonia was halved (8.3% instead of 17.1%). The

usual post-radiation sterile period after 600 rad was abolished in the males made hypothermic and the testis weights showed less reduction than in those given x rays alone. Evidence for the protection of spermatogonia from somatic and genetic radiation injury by hypothermia shows that oxygen tension differences are important in determining the extent of both types of damage in the immature germ cells. With mature germ cells, however, hypothermia or other methods of oxygen deprivation provide little if any protection from genetic radiation damage to spermatozoa, presumably because they are normally hypoxic. (TCO)

12694 RADIATION SENSITIVE MUTANTS OF USTILAGO MAYDIS. Holliday, Robin (John Innes Inst., Hertford, Eng.). Mutat. Res., 2: 557-9(Dec. 1965).

Isolation and phenotypic description of several radiosensitive strains of the smut fungus Ustilago maydis are reported. Log phase wild-type haploid cells of Ustilago were irradiated with a uv dose giving 15% survival, prior to plating on complete medium. Colonies were replicated to minimal medium and the replicas irradiated for 15 sec before incubation. Examination of approximately 20,000 colonies yielded 46 mutants that were classified as being markedly more sensitive than the wild-type. Phenotypes of three of the mutants are briefly described. (H.G.D.)

12695 DETECTION OF ULTRAVIOLET ABSORBING SUBSTANCES IN LIVING MYCELIUM OF FUNGI. Leach, Charles M. (Oregon State Univ., Corvallis). Mycologia, 57: 291-300(Mar.-Apr. 1965).

Further information on the nature of the photochemical processes involved in light-induced sporogenesis in fungi was sought on the basis of the fact that uv radiation is most effective in inducing sporulation. The similarity of the monochromatic light requirements of some fungi suggests that a common photochemical mechanism may be involved. Thus, the uv absorption by living, uninjured mycelium of Ascochyta pisi, Pleospora herbarum, and Pyronema omphalodes was studied spectrophotometrically, using two specially devised methods. Differences between sporulating colonies exposed to near-uv radiation and nonsporulating colonies grown in darkness were evident, particularly in P. omphalodes. Exposed colonies showed increased absorption mainly in the region 300-350 mμ. Substances causing this increased absorption were located in irradiated vegetative mycelium of P. omphalodes and possibly in the spores of A. pisi. Absorption of 300 to 350 mμ radiation by mycelium corresponds to one waveband of radiation (310 mμ) previously found to be very effective in inducing sporulation in A. pisi, P. herbarum, and Alternaria chrysanthemi. If photosporogenesis in fungi involves a photoreceptor pigment, it is probable that this pigment is present in small amounts in darkness. It is not possible at present to define the role of the 300 to 350 mμ absorbing substances occurring in irradiated sporulating mycelium; however, the absorption of these substances does correspond to the waveband of radiation found to be very effective in inducing sporulation. The isolation and characterization of uv-absorbing substances associated with photosporogenesis are being undertaken. (BBB)

12696 EVALUATION OF RECTAL COMPLICATIONS FOLLOWING RADIUM TREATMENT OF CARCINOMA OF THE UTERUS ACCORDING TO MODIFIED MANCHESTER METHOD. Wozniakowska, Z.; Hliniakowa, I. Nowotwory, 15: 359-64(1965). (In Polish).

The relation of postradiation reaction in the rectum to the dose measured in the course of radium treatment is discussed. Measurements in the rectum were made immediately after radium application using Siemens Gammameter. Reaction was observed in 221 patients with stage I and II carcinoma of the uterine cervix treated according to Manchester method. Maximum tolerance dose to the rectal wall was arbitrarily set at 7000 R. Observations proved that there is no relationship between the intensity and frequency of reaction in the rectum and the rectal dose or between the size and amount of radium in ovoids, within the limits accepted as tolerance doses. Routine measurements of doses in the rectum and radiological checking of position of applicators seems to be necessary for proper course of treatment. (TCO)

12697 THERMOSTABILITY OF RAT ERYTHROCYTES IRRADIATED IN VITRO WITH LARGE DOSES OF IONIZING RADIATION. Sebestik, V. (Inst. of Haematology and Blood Transfusion, Prague). Physiol. Bohemoslov., 14: 343-8(1965).

The degree of erythrocyte hemolysis in rat blood irradiated with x rays in vitro (200 kv, 15 ma, 0.5 mm Cu + 1 mm Al, focal distance 16.5 cm, output 300 R/min), using doses of 5,000 and 30,000 R, was tested. The irradiated erythrocytes were exposed to a temperature of 53°C, and the degree of hemolysis was determined by spectrophotometry. A dose of 5,000 R did not significantly affect thermal hemolysis. A dose of 30,000 R caused slight, but statistically significant, acceleration of hemolysis. The experiments confirmed the high resistance of mammalian erythrocytes to the effects of ionizing radiation. (auth)

12698 EFFECT OF LARGE DOSES OF IONIZING RADIATION ON THE PHAGOCYTIC ACTIVITY OF LEUKOCYTES IN PRESERVED BLOOD. Fiala, J.; Sebestik, V. (Inst. of Haematology and Blood Transfusion, Prague). Physiol. Bohemoslov., 14: 349-53(1965).

Blood collected in acid glucose-citrate solution was x-irradiated in one series with a dose of 5,000 R and in another with a dose of 30,000 R. The blood was then stored and the phagocytic activity of the leukocytes was tested on the first, fourth, and seventh (and after a dose of 30,000 R on the tenth) days after irradiation. No significant differences were found between the phagocytic activity of the leukocytes in either of the irradiated groups and the non-irradiated control specimens. (auth)

12699 RECENT OPINIONS ON THE EFFECTS OF IONIZING RADIATION ON HUMAN POPULATION. Majle, Tadeusz. Rocz. Panstw. Zakladu Hig., 16: 509-16(1965). (In Polish).

Seventy years ago artificial sources of radioactivity were added to natural sources of ionizing radiation as a part of the human environment. The knowledge that doses of artificial and natural radiation were cumulative was both interesting and alarming. A force had come into existence that threatened the human population genetically. Current theory on the effects of ionizing radiation on human populations is discussed. (H.G.D.)

12700 THE HISTOLOGICAL AND HISTOCHEMICAL CHANGES OF THE SMALL BOWEL MUCOSA IN THE SEGMENTS OUTSIDE THE RADIATION BEAM IN PATIENTS IRRADIATED OVER THE ABDOMEN. De Dominicis, Raffaella; Grechi, G. (Univ., Florence). Sperimentale, 115: 82-103(Mar.-Apr. 1965). (In Italian).

Histologic studies of duodenal mucosa were made in 22 women subjected to telecobalt therapy for uterine cancer. The pelvic radiation field varied from 240 to 290 cm^2 and the specimens were taken outside this field at various stages of therapy, at which time total doses of 180 to 5200 rad had been given (in weekly fractions of 600 to 1000 rad). It is concluded that the duodenal mucosa is very radiosensitive and is altered morphologically by relatively low doses, such as those received outside the radiation field. However, no close correlation between the severity of histologic changes and dose could be detected. Submucosal connective tissue was affected as well as glandular mucosa. (TCO)

12701 CHANGES IN RADIOSENSITIVITY BY PRE-IRRADIATION. Taenzer, Volker; Krokowski, Ernst (Univ., Berlin). Strahlentherapie, 129: 1-9(Jan. 1966). (In German).

The increase in resistance by pre-irradiation with x rays was investigated in rats, since previous results in the literature are partly contradictory. In order to obtain a critical evaluation, results obtained with very small doses and high doses as well have to be compared. The dose-time-effect-relation, obtained in the different experiments, per-

mits conclusions on the mechanism of the radiogenic radiation resistance. Pre-irradiation with smallest doses resulted in an effect corresponding to the adaption syndrome; while in case of sublethal pre-irradiation a temporary immunization is responsible for the increase in radiation tolerance. (tr-auth)

12702 INVESTIGATIONS ON INFLUENCING OF THE RESPIRATORY CENTER BY X-RADIATION. Becker, Hans-Wolfgang; Becker, Christa (Martin-Luther-Univ., Halle-Wittenberg, Ger.). Strahlentherapie, 129: 51-63 (Jan. 1966). (In German).

The effect of low x-ray intensities (50 and 150 R SD) on the respiratory center was investigated using depth therapy conditions. The excitability and the excitation value of the respiratory center was determined in persons by registering the linear portion of the excitation curve using the O_2-rebreathing experiment with continuous CO_2-accumulation. The linear portion of the excitation curve was calculated as a regression line using the experimental results (pCO_2 alv. with corresponding RMV); the slope of this curve (excitability) as well as its extrapolated intersection with the x-axis (apnea point) are of interest. Three excitation curves were determined for each person: the first one on the first day, the second one on the second day, and the third one on the fourth day. The irradiations of the respiratory center with 50 R and 150 R were done 2 hours prior to the determination of the second excitation curve. Using 14 persons, a total of 42 excitation curves of the respiratory center were determined. From the results it can be concluded that low x-ray doses (≦150 R SD) have no influence on the excitation of the respiratory center. The excitation value of the respiratory center does not seem to be influenced either. However, a slight displacement of the apnea point to lower pCO_2 alv.-values, indicating an increase in excitation value of the respiratory center, is obtained in $^2/_3$ of all persons whose respiratory center was irradiated with x-ray doses exceeding the excitation threshold. (tr-auth)

12703 INFLUENCE OF BODY BURDEN ON RADIATION SENSITIVITY OF RATS. Braun, Heribert; Hornung, Guenter (Medizinische Universitaetsklinik, Wuerzburg, Ger.). Strahlentherapie, 129: 95-103(Jan. 1966). (In German).

The influence of the metabolism upon the survival time, changed by physical stress at different time intervals prior to or after total-body or partial-body irradiation with x rays, was investigated in rats. Mortality of the animals was distinctly increased when the stress occurred immediately, before or after irradiation. An extended interval between irradiation and stress resulted in an almost complete recovery by the organism from the radiation insult. Severe irreparable damages were obtained when metabolism was increased during irradiation. A fractionated total-body irradiation followed by stress was considerably more compatible than a single dose. The compatibility was increased with smaller single doses. Furthermore, there was a lower mortality in animals which received partial-body irradiation before the stress than in those which received total-body irradiation before the stress. (tr-auth)

12704 INVESTIGATIONS ON COMBINATION INJURIES. PART IV. ON THE QUESTION OF GENERAL INFECTIONS IN CASE OF A COMBINATION OF WHOLE-BODY IRRADIATION AND SKIN WOUNDS IN MICE. Messerschmidt, Otfried; Petersen, Kurt-Friedrich; Melching, Hans-Joachim (Univ., Freiburg i. B.). Strahlentherapie, 129: 104-11(Jan. 1966). (In German).

Bacteriological controls of the blood, as well as comparative studies in open and closed skin wounds, lead to the assumption that the rapid rise in mortality observed in mice during a combination of total-body x irradiation with skin wound inflicted 2 days later cannot be clearly interpreted as a result of microbial invasion via the skin wound. The observed increase of E. coli in the blood can be interpreted as a result of an increased invasion of bacteria through the intestinal wall due to an additional decrease in resistence of the irradiated animal after inflicting a skin wound. It might be possible that disturbances in biochemical processes could be responsible for the fatal course of the combination damages. (tr-auth)

12705 EFFECTS OF WHOLE-BODY IRRADIATION AS WELL AS BONE MARROW IRRADIATION ON THE OSMOTIC RESISTANCE OF THE RESERVE LEUKOCYTES. Ormai, Sandor; Krasznai, Istvan; Pal, Imre; Zadori, Ernoe (Research Inst. for Experimental Medicine, Hungarian Academy of Sciences, Budapest). Strahlentherapie, 129: 118-22(Jan. 1966). (In German).

The changes of osmotic resistance in circulating and reserve leukocytes of rats was assessed, following whole-body irradiation with 300 R x ray and the bone marrow irradiation with 300 rad ^{90}Y. Following whole-body irradiation the osmotic resistance values decreased. After irradiation of bone marrow they remained unchanged. (tr-auth)

12706 INVESTIGATIONS ON THE REACTIONS OF EMBRYOS TO IRRADIATION OF THE EXTRAEMBRYONAL REGION OF THE HENS (DISTANCE EFFECT). Zoeller, Wolfgang W. (Univ. Bonn. Kernforschungsanlage, Juelich, Ger.). Strahlentherapie, 129: 123-38 (Jan. 1966). (In German).

Chicken embryos x irradiated with 1200 R die in the egg within a few hours as a result of toxic products circulating in the blood. Selective irradiation of the extraembryonal blood vessels with 1200 R causes an early death of the embryo after the same time period. This indirect effect is the result of a radiation induced poisoning of the embryonal blood. (tr-auth)

12707 GENERAL PATHOGENESIS OF LEUKEMIA. Georgii, Axel (Univ., Munich). Strahlentherapie, Sonderbaende, 57: 9-29(1964). (In German).

There are several different causes of leukemia. In general, these are carcinogens, viruses, and ionizing radiation. All known types of leukemia can be induced by any one of these factors. The explosion of atomic bombs did not induce any new or particular forms of leukemia, but only an absolute increase in the numbers in the same pattern that prevailed up to that time. This is also true for other radiations. These facts indicate that there is probably no single reaction of the blood-forming organs that depends on a single one of the leukemia-inducing factors. Probably the factor that induces leukemia acts on the still undifferentiated bone marrow cells. Other, unknown conditions are necessary for the development of a distinct, morphologically definite cell type. According to findings of chromosomal abnormalities, the new cell types appear to possess a genetically determined substance which is characteristic of the leukemia cells formed. These results show that leukemia does not present a single unitary disease picture, but a group of changes whose causal heterogeneity contrasts with a spectrum of systematized reaction of the blood forming tissues. References cited, 120. (BBB)

12708 THE GORDON WILSON LECTURE: IONIZING RADIATION AND THE DEVELOPMENT AND SURVIVAL OF LIFE. Ross, Joseph F. (Univ. of California, Los Angeles). Trans. Amer. Clin. Climatol. Ass., 76: 80-98 (1964). (UCLA-12-545).

Levels and effects of artificial natural background radiation to which man is exposed were surveyed. Implications of these levels on development of leukemia, cancer, and genetically determined disorders are considered. It is concluded that exposure to ionizing radiation may result in neoplastic disease in various organs. The susceptibility to radiation induced neoplasia appears to be greater in the younger age groups, and the evidence indicates that a linear relation exists between the dose and incidence of the tumor. However, evidence is not available to establish or deny the existence of such a linear relation at low doses, but it is reasonable to assume that all ionizing radiation, even in very small doses, is capable of producing some biological effect. (TCO)

12709 BEAN MUTANT INDUCED BY IONIZING RADIATION. I. DWARF MUTANT. Moh, C. C.; Alan, J. J.

(Inter-American Inst. of Agricultural Sciences, Turrialba, Costa Rica). Turrialba, 14: 82-4(Apr.-June 1964).

Attempts were made to develop economically useful mutants of the common bean (Phaseolus vulgaris), a major food crop in Central America and serving as a main source of protein in the daily diet of various local populations. In connection with the bean improvement program, cytogenetic studies of beans were also carried out. In studying the relation between the radiation dose and mutation rate, seed progenies from a single plant of a line of the common bean (Mexico 80-R), selfed for two generations, were irradiated with a series of γ radiation doses from a ^{137}Cs source. The dose rate was 1000 R/min. A dwarf mutant was isolated from the R_2 population irradiated with 2000 R. Morphological characteristics of this dwarf mutant are described. The germination rate of its seeds and those of normal plants showed no difference. When the primary leaves appeared, the dwarf character became apparent, the growth rate of the hypocotyl and epicotyl being extremely slow. In a fully developed mutant plant, the stem portion from soil surface to the primary leaf node (part hypocotyl and epicotyl) was about half that of the normal plant. Even more drastic was the reduction in growth in the length of internodes of the stem. The average length of internodes in the mutant was 1 cm or less, as compared with 3 to 5 cm in the normal. Therefore, the compound leaves grew in a congested cluster on the top of the plant. The average height of a fully developed dwarf mutant was 8.2 cm as compared to a height of 72.6 cm for a normal plant. A genetic study was conducted with the selfed progenies of the R_6 and R_7 generations. Among 146 plant progenies tested, there were 38 homozygous normal, 80 heterozygous, and 28 homozygous for the dwarf. These data did not deviate from a 1:2:1 ratio. Further study on the 80 heterozygous plants showed that they produced 1238 phenotypically normal progenies and 400 dwarfs which closely associate with a 3:1 ratio. These results indicate that the dwarf character is recessive to normal with single gene control. (BBB)

12710 BEAN MUTANT INDUCED BY IONIZING RADIATION. II. YELLOW MOSAIC MUTANT. Moh, C. C.; Alan, J. J. (Inter-American Inst. of Agricultural Sciences, Turrialba, Costa Rica). Turrialba, 14: 199-201(July-Sept. 1965).

A bean (Phaseolus vulgaris) mutant isolated from an irradiation experiment is described. This mutant has an appearance similar to that induced by the disease caused by yellow mosaic virus. Therefore, this mutant has been tentatively called yellow mosaic. The mutation frequency and mutation spectrum induced by a semi-lethal dose of acute irradiation on seeds of a bean variety, S182N were examined. The seeds were from a single plant selection, selfed for three generations. In a pilot experiment to determine the LD_{50}, seed samples were placed in a humidity-controlled chamber (55% relative humidity) for three weeks, and then irradiated with a series of γ doses from a ^{60}Co source. The dose-rate was 1500 R/min. After four weeks, the number of survivals at each radiation dose was determined; the LD_{50} was found to be about 12 kR. Forty 100-seed samples taken from the same seed lot were irradiated with 12 kR and directly sown in the field. Genetic data are presented for the progeny tests in the R_4 and R_5 generations. A morphological description of the mutant is given. As the primary leaves grow to medium size, yellow chlorotic spots begin to develop at random on the leaves. The spots increase in size rapidly, and fuse with each other forming an irregular yellow mosaic area in the leaf. The development of compound leaves in the mutant was generally later than in the normal plant. The shape of the true leaves of the mutant was narrower and more elongated than those of the normal plant. The mutant did not produce flowers. The mutant line was maintained by keeping the seeds of the heterozygous plants. Genetic data indicate that the yellow mosaic mutant is of a recessive character with single gene control. (BBB)

12711 THE EFFECT OF UV-RADIATION ON HeLa CELLS INFECTED WITH ADENOVIRUS. Wassermann, Felix E. (New York Medical Coll., N. Y.). Virology, 27: 193-8(Oct. 1965).

The Luria-Latarjet experiment was performed on adenovirus-infected HeLa cells. The singly infected cells were irradiated with uv light at various times during the viral latent period. The results showed that extracellular virus is more resistant to irradiation than the infective centers. The rate of inactivation of the capacity of the cells to become infective centers was the same as that of the infective centers. There was no change in the rate of the inactivation of the infective centers during the entire viral latent period. Increased resistance to irradiation was accompanied by the appearance of newly synthesized virus. It was also found that multiple infected cells yield different data, apparently because they contain, at all times during the latent period, uneclipsed virus that is infectious when released from the disrupted cells. The results indicate that the uv-sensitive event in the cells must occur late in the viral development, since irradiation of cells 14 hr after infection is as effective as irradiation 1 hr after infection, and that the effect must be on a cellular function rather than on the virus since it is immaterial whether the cell is irradiated prior to or after infection. Because no evidence of significant virus maturation was evident at 14 hr, it may be that the uv-sensitive step involves the final assembly of the mature virus particles. It appears that intracytoplasmic virus can neither contribute to the plaque formation of the cell nor to its radioresistance. Once released by disruption of the cell, it is infectious and as radioresistant as free virus. The single burst experiment showed that all irradiated cells that make virus also score as infective centers. (BBB)

12712 A DIFFERENCE IN UV-SENSITIVITY BETWEEN GENES IN THE REPRESSED AND GENES IN THE DE-REPRESSED STATE. Koelsch, Eckehart; Starlinger, Peter (Univ., Cologne). Z. Verebungsl., 96: 297-303 (1965).

In experiments on the inactivation of genes by irradiation with uv light, a comparison was made of different strains of E. coli under various conditions of growth. It was found that the kinetics of inactivation differed in a characteristic manner which could be interpreted most easily as a difference in uv sensitivity between genes in the repressed and genes in the de-repressed state. (TCO)

12713 A DIFFERENCE IN THE PHOTOREACTIVATION OF UV-DAMAGE BETWEEN GENES IN THE REPRESSED AND GENES IN THE DE-REPRESSED STATE. Koelsch, Eckehart; Starlinger, Peter (Univ., Cologne). Z. Verebungsl., 96: 304-6(1965).

Differences between functioning and nonfunctioning genes in the photoreactivation of uv damage in Escherichia coli strains W-8 and Hfr-7 (λ), irradiated and incubated under conditions differing with respect to illumination and to the presence and absence of inducer, are discussed. Photoreactivation of the galactokinase-forming capacity was studied. With both strains photoreactivation of the galactokinase-forming capacity could only be carried out in the absence of inducer. Similar results were obtained with strain Hfr-7 (λ). In control experiments, prolonged incubation of irradiated cells in the presence of inducer led to a proportional increase in enzyme. The photoreactivation curves obtained in the light and in the dark were identical. Inducer therefore prevented photoreactivation for at least 90 min. The presence or absence of inducer had no influence on the photoreactivation of bacterial survival. (BBB)

12714 THE EFFECT OF AN X IRRADIATION ON CROSSING POPULATIONS OF BARLEY IN THE M1 AND M2 GENERATION. Keppler, E.; Siegert, W. (Univ., Jena, Ger.). Zuechter, 35: 50-6(1965). (In German).

Studies were conducted to ascertain whether the radiosensitivity and mutation frequency of hybrid populations were the same as their homozygotic parents. The parents consisted of five types of barley with an average kernel size was between 2.3 and 2.5 mm. They were equilibrated to an average water content of 12.8% before exposure to x

irradiation. The barley was irradiated at a dose rate of 200 R/min with total dosages of 12, 15, or 18 R. From 1000 to 4000 kernels were irradiated in each group. The degree of sterility of the M1 plants was used to measure chromosomal mutations, and the frequency of factor mutations greater than the chlorophyll mutation rate was measured in the M2 generation. In the M1 generation the populations were less radiosensitive than their parents as far as germination damage, growth depression, and death rate were concerned. However, the number of chromosomal mutations, as measured by the sterility of the M1 ears, was the same as in the parents. In the M2 generation the heterozygotes with the same survival rates showed a higher frequency of chlorophyll mutations. The mutation spectrum was not altered. The smaller physiological damage to the populations of the M1 generation could be explained by the presumably greater stability of their protoplasm and their strong mutability may signify a greater lability of their gene loci. Both results stand in causal connection with the greater heterozygotism of the F_2 populations. (TCO)

12715 CYTOGENETIC STUDIES FOLLOWING HIGH DOSAGE PATERNAL IRRADIATION IN THE MEALY BUG, PLANOCOCCUS CITRI (RISSO) [Thesis]. Chandra, Hombe Gowda Sharat. Berkeley, Calif., Univ. of California, 1962. 103p.

When females of the mealy bug P. citri are mated to heavily irradiated males (60,000–90,000 rep), the progeny is largely female and few or no sons survive. The daughters that develop after heavy paternal irradiation all have unbroken chromosomes and they are therefore gynogenetic. The origin, development, chromosome constitution, and breeding behavior of these gynogenetic females were studied. The majority of these females are triploid (3N = 15), some are diploids, and a few are 3n–2n and 2n–n mosaics. These triploid females have been shown to arise through a fusion nucleus of the I and II polar bodies (polar body I with 10 and polar body II with 5 chromosomes). The triploid polar body derivatives carry on a successful embryogeny when the zygote nucleus is unable to do so because of the heavily damaged paternal set. The chromosomes of mealy bug are holokinetic, and consequently the paternal set is not eliminated easily. It manages to divide with the undamaged maternal chromosomes but does not always segregate as successfully. Restitution, fragment loss, and sticky bridges were some of the mitotic abnormalities observed in these embryos. Most of the gynogenetic diploids probably arise through a doubling of the maternal contribution to the zygote during early cleavage division. A study of meiosis in triploid females demonstrated the inverted nature of the meiotic sequence in this species. There was always a 15 : 15 separation of the chromatids at Anaphase I, irrespective of the nature and frequency of the prior associations. Among embryos produced by 3N♀ × 2N♂ matings aneuploid embryos showed the typical lecanoid heterochromatization of the paternal complement. A search for adults with 10 euchromatic + 5 heterochromatic chromosomes was unsuccessful. The bearing of these results on the general problem of heterochromatization and sex determination is discussed. (Dissertation Abstr.)

Radiation Effects Therapy and Countermeasures

12716 (AD–626682) BONE MARROW AS THE MAJOR SOURCE OF POTENTIAL IMMUNOLOGICALLY COMPETENT CELLS IN THE ADULT MOUSE. Tyan, M. L.; Cole, L. J. (Naval Radiological Defense Lab., San Francisco, Calif.). Dec. 8, 1965. 16p. (USNRDL-TR–946).

Groups of F_1 hybrid mice (A × B) were sublethally irradiated and injected with cells from various lymphoid tissues of adult parental strain (A) mice. Spleen and lymph node cells and cells from the thymus of the survivors were then injected into an F_1 hybrid of another type (A × C). A significant number of deaths occurred among the secondary hosts only when they had received spleen cells from mice which had been injected with adult bone-marrow cells. (auth)

12717 (NP–15666) SELECTIVE PROTECTION OF DAMAGES INDUCED BY X-IRRADIATION AND RADIOMIMETIC DRUGS. Progress Report, November 1, 1964–January 31, 1965. Garattini, S.; Palma, V.; Reyers-Degli Innocenti, I.; Guaitani, A. (Istituto di Ricerche Farmacologiche Mario Negri, Milan (Italy)). Contract 204/RB. 8p. Dep. mn.

Studies were made to determine in a clear and reproducible way the conditions in which radioprotector drugs interact with alkylating agents in tumor-bearing mice. However, only negative data are reported. The drugs tested were: serotonin creatinine sulfate; L-cysteine; cysteamine-HCL; thiourea; AET; 2-methyl-piperazine-dithioformic acid; morpholine salt of morpholino-dithioformic acid. Cyclophosphamide and DL-sarcolysine were used as radiomimetic agents. Data are tabulated. (P.C.H.)

12718 (NP–15667) SELECTIVE PROTECTION OF DAMAGES INDUCED BY X-IRRADIATION AND RADIOMIMETIC DRUGS. Annual Report. Garattini, S.; Palma, V.; Reyers-Degli Innocenti, I.; Guaitani, A. (Istituto di Recerche Farmacologiche Mario Negri, Milan (Italy)). Sept. 15, 1964. Contract 204/RB. 19p. Dep. mn.

The specificity of action of radioprotective drugs given in combination with radiomimetic agents (DL-sarcolysine and cyclophosphamide) in mice was evaluated. The radioprotective drugs used were: serotonin creatinine sulfate; L-cysteine; cysteamine/HCl; thiourea; AET; 2-methyl-piperazine-dithioformic acid; and morpholine salt of morpholino-dithioformic acid. The animals were treated 6 days after tumor transplantation and drugs were given daily for 6 days. The results indicated that indiscriminate use of radioprotective drugs in combination with radiomimetic drugs, and, possibly, with irradiation, may prove unuseful in achieving better antitumoral effect and even antagonize the antitumoral activity of radiomimetic drugs. (P.C.H.)

12719 (NP–15668) SELECTIVE PROTECTION OF DAMAGES INDUCED BY X-IRRADIATION AND RADIOMIMETIC DRUGS. Report No. 4 (Final). Garattini, S.; Palma, V.; Reyers-Degli Innocenti, I.; Guaitani, A. (Istituto di Ricerche Farmacologiche Mario Negri, Milan (Italy)). Sept. 30, 1965. Contract 204/RB. 23p. Dep. mn.

Studies were made on the interaction of several radioprotectors with different antitumoral agents in two experimental tumors, namely, sarcoma 180 and Ehrlich carcinoma transplanted in mice in the solid form. The radioprotectors used were: serotonin creatinine sulfate; L-cysteine; cysteamine; thiourea; AET; 2-methylpiperazinedithioformic acid; and morpholine salt of morpholinodithioformic acid. The antitumoral drugs were: DL-sarcolysine; 2,4,6-tris (1-aziridinyl)-, s-triazine; 2,2′-dichloro-N-methyl-diethylamine; N,N-bis(2-chloroethyl)alanine; 5-fluorouracil; Mitomycin C; Vinkaleucoblastine sulfate; and cyclophosphamide. It was concluded that indiscriminate use of radioprotectors in combination with radiomimetic drugs and, possibly, with irradiation, are not useful to achieve better antitumoral effect and even disadvantageous because of the antagonism toward the antitumoral activity of radiomimetic drugs. 58 references are cited. (P.C.H.)

12720 (TID–22466) BIOCHEMICAL AND IMMUNOLOGICAL STUDIES OF X-IRRADIATED MICE FOLLOWING BONE MARROW INJECTIONS. Final Report. Royal, George C. Jr.; Royal, Gladys W. (Agricultural and Technical Coll. of North Carolina, Greensboro). Oct. 1965. Contract AT(40-1)-2399. 7p. Dep. mn. CFSTI $1.00 cy, $0.50 mn.

Body weight, proteins, viscosity, and serotonin decreased in mouse organs following LD_{100} x-irradiation. Isologous bone marrow therapy acted as a control mecha-

nism, while heterologous (rat) bone marrow therapy reflected inherent biological variation which was detectable in larger standard deviations of relevant parameters. Some rat bone marrow samples offered immediate injection mortality. Thirty percent survival among x-irradiated hosts was usual for rat marrow treated mice. Tibia bovine bone marrow contains some agent or agents apparently capable of circumventing the normal x-irradiation response through an unspecified, altered glycolipid metabolism. Details of glycolipid metabolism are desirable to explain the specifics of this hypothesis. The effective agent in bovine marrow therapy for x-irradiated mice appears to be glycolipid generally, and galactolipid specifically; with an implied interrelationship between brain and spleen metabolism during the response to irradiation injury. (auth)

12721 (BNWL-tr-11) COMPARATIVE INVESTIGATIONS ON THE DEFENSE MECHANISM OF CYSTEAMINE AND AET FOR "INTESTINAL RADIATION DEATH." Zseboek, Zoltan B.; Petranyi, Gyoezoe Jr. Translated by Judy M. Lankard (Battelle-Northwest, Richland, Wash. Pacific Northwest Lab.), from Strahlentherapie, 127: 452-62(1965). 18p. Dep. mn. JCL $1.60 fs, $0.80 mf.

The radiation protective mechanisms of AET and cysteamine for intestinal radiation death were investigated in rats. Sodium absorption in the small intestine and extracellular, exchangeable, or total sodium content, as well as the inulin volume and the serum sodium concentration were used as indicators for changes in the sodium- and liquid metabolism. Results obtained with AET and cysteamine were compared. The results showed that lethal disturbances in sodium- and liquid metabolism can be inhibited indirectly by cysteamine by means of mobilization of sodium-liquid reserves within the organism. AET did not protect significantly, however, in the small intestine; with the loss in sodium and liquid only slight protection was observed. (auth)

12722 (JPRS-33766) POLYGLUCINE USED IN BLOOD TRANSFUSION AND RADIATION SICKNESS. Translation of Probl. Gemitol. Pereliv. Krovi, 10: No. 10, 23-34(1965). 17p. (TT-66-30209). CFSTI $1.00 cy, $0.50 mn.

Three papers are included: a separate abstract was prepared for one. The remaining papers on use of polyglucin in the treatment of traumatic shock by a specialized first-aid team and selection of the optimal molecular weight for polyglucine were not abstracted for NSA. (H.G.D.)

For an abstract of the individual paper see: 12723.

12723 (JPRS-33766, pp 3-7) COMPARATIVE STUDY OF THE ACTION OF POLYGLUCINE OF VARIOUS MOLECULAR WEIGHTS ON ACUTE RADIATION SICKNESS IN DOGS. Shitikova, M. G. (and others). Translated from Probl. Gemitol. Pereliv. Krovi, 10: No. 10, 23-34(1965).

The effect of plethoric transfusions of polyglucin of different molecular weights on the course of acute radiation sickness was studied in dogs given 600 or 800 rad x-ray doses. Polyglucin was administered on the day of irradiation and on the 1st, 2nd, 5th, 7th, 9th, 11th, and 13th days post-irradiation. No reactions to the polyglucin preparations were observed. Morphological composition of peripheral blood and spinal punctuates, blood coagulation time, bleeding time, and free heparin content were determined in experimental animals. Polyglucine concentrations in plasma and urine were also measured. All polyglucin preparations protected against leukopenia in the 400 rad group, but only preparations having a molecular weight of 84,000 completely prevented the hemorrhagic syndrome. A therapeutic effect was apparent in those animals given the 600 rad x-ray doses only when polyglucine transfusions of molecular weight 84,000 were given. (H.G.D.)

12724 NEWER THERAPEUTIC POSSIBILITIES FOR THERMONUCLEAR INJURIES. **Zimmermann, W. E. (Univ., Freiburg i. B.). Arch. Klin. Chir., 308: 60-5 (Nov. 17, 1964). (In German).**

Disturbances of oxidative processes either by injuries to enzymes caused by whole-body irradiation or anoxia in shock and severe burn injuries impair energy production and phosphorylation reactions. Concentrations of lactate, pyruvate, lactic dehydrogenase, diphospho-pyridine nucleotide, and bicarbonate in blood were studied in cats given 1000 R of whole-body x irradiation. From 6 to 8 hr after irradiation, lactate and lactic dehydrogenase concentrations rose markedly, while the diphosphopyridine nucleotide concentration fell. The animals exhibited a metabolic acidosis that usually was fatal. In animals that were treated with tris(hydroxymethyl)aminomethane (Tris) within 6 or 8 hr after irradiation did not show such severe symptoms of metabolic acidosis and survived. This substance is believed to exert an effect both intracellularly and extracellularly, favoring the oxidation of diphosphopyridine nucleotide and stabilizing intracellular enzyme systems. The most favorable effects were observed when the Tris was administered as a 0.3M isotonic solution in low mol wt dextran (Rheomacrodex). (BBB)

12725 THE EFFECT ON CELL SURVIVAL OF INHALATION OF OXYGEN UNDER HIGH PRESSURE DURING IRRADIATION IN VIVO OF A SOLID MOUSE SARCOMA. **Hewitt, Harold B. (Mount Vernon Hospital, Middlesex, Eng.). Brit. J. Radiol., 39: 19-24(Jan. 1966).**

Solid transplanted sarcomas of CBA mice that are known to contain a high proportion of anoxic cells were irradiated in vivo in mice breathing either oxygen at 45 lb/sq.in. or air at atmospheric pressure before and during irradiation. The effects of irradiation under the two conditions were compared in terms of the size of the fraction of reproductively intact cells surviving irradiation, as measured by in vivo transplantation assay. In the single-dose range 2,040 to 3,280 R 250 kv x rays, the surviving fraction after irradiation in air was greater than that in HPO by a factor ranging between 0.73 and 4.8. It is suggested that the enhancement of radiosensitivity indicated by these experiments would represent only a meager therapeutic advantage in clinical terms. (auth)

12726 PRESERVATION BY PHYTOHEMAGGLUTININ (PHA) OF THE MEDULLO-RESTORING AND HEMATOPOIETIC PROPERTIES OF MEDULLARY CELLS CULTIVATED IN VITRO. **Halpern, Bernard; Liacopoulos-Briot, Monique (College de France, Paris. Hopital Broussais, Paris). Compt. Rend., 261: 3217-22(Oct. 18, 1965). (In French).**

Bone marrow cells cultivated in vitro lose, for the most part in 48 hours, their transplantation potential and remain incapable of producing a radioprotective effect when injected in lethally x irradiated animals. Phytohemagglutinin added at low concentrations to the culture medium exercises a remarkable preserving action both on the blood-restoring properties of the cultivated cells and on their radioprotective effects. (tr-auth)

12727 PROTECTION OF LETHALLY IRRADIATED GUINEA PIGS WITH FRESH AND FROZEN HOMOLOGOUS PERIPHERAL BLOOD LEUKOCYTES. **Perry, Vernon P.; Malinin, Theodore I.; Kerby, Carey C.; Doland, Michael F. (National Naval Medical Center, Bethesda, Md.). Cryobiology, 1: 233-9(Jan.-Feb. 1965).**

Lethally irradiated (550 R of ^{60}Co γ rays) Princeton guinea pigs survive beyond a 30-day period following the early postirradiation infusion of adequate numbers of either fresh (1×10^8) or frozen (1×10^9) homologous peripheral blood leukocytes. The $LD_{50/30}$ in controls is 500 R. The 500 R dose is equivalent to $LD_{100/17}$ in controls. Animals infused with larger numbers of fresh homologous cells 24 hr following irradiation died, as did all control animals. Animals surviving the lethal period failed to demonstrate any gross evidence of homologous disease as late as 272 days following irradiation. It is suggested that leukocytes have an immediate detoxification role in providing for the recovery of animals following irradiation. Any detoxification that might have occurred was probably secondary to a therapeutic effect which prevented lethal bacterial infection. It was also observed that platelets

may have contributed to the survival of these animals. (TCO)

12728 REDUCTION OF RADIATION DAMAGE TO TRADESCANTIA CHROMOSOMES BY ADENOSINE TRIPHOSPHATE, PROLINE, AND HISTIDINE. Beatty, Alvin V.; Beatty, Jeanne W. (Emory Univ., Atlanta). Genetics, 53: 47-54(Jan. 1966).

The effects of ATP, histidine, and proline on radiation recovery were studied in Tradescantia using both aberration yield and the luciferin-luciferinase assay for ATP as experimental procedures. ATP, proline, and histidine had no effect on the rate of progress of the developing Tradescantia microspore through its successive stages, nor did they have any radiomimetic properties. ATP showed a linear relationship between both duration of treatment and concentration and the reduction of damage; while proline and histidine, after an initial reduction, exhibited thresholds during which limited or no effect was shown. Pretreatment with any of the three remained effective in reducing aberrations well into the recovery period following irradiation. ATP reduced radiation damage in all gas atmospheres used while histidine and proline were effective only in the absence of oxygen. Treatments in ATP solutions resulted in increased ATP in the periplasmodium within the anther, the greatest increase being in those also irradiated. Treatment in histidine and proline did not affect the ATP content in the periplasmodium. (H.G.D.)

12729 INFLUENCE OF RADIOPROTECTIVE SUBSTANCES ON DAMAGES TO BONE GROWTH IN RATS. Irie, Hideo; Yoshihara, Hidetosi; Osiumi, Yosihiko (Univ. Fukuoka, Japan). Strahlentherapie, 129: 112-17 (Jan. 1966). (In German).

The influence of a radioprotective substance upon bone growth was investigated in rats. Growth inhibition caused by x irradiation was decreased by administration of MEG prior to irradiation. (tr-auth)

12730 MEASURING TECHNIQUES SERVING RADIATION PROTECTION. Jaeger, Robert G. (Univ., Mainz). VDI (Ver. Deut. Ing.) Z., 107: 1590-4(Nov. 1965). (In German).

Peaceful uses of nuclear energy have accentuated the hazards to man both from external exposure and internal contamination. Therefore, development of instruments and methodology for radiation monitoring achieved impetus, and prevention of radiation injuries became a significant endeavor. (H.G.D.)

12731 TRANSPLANTATSIONNYI IMMUNITET I RADIATSIONNYE KHIMERY. (Transplantation Immunity and Radiative Chimeras). Petrov, R.; Zaretskaya, Yu. Moscow, Atomizdat, 1965. 232p.

Problems connected with the transplantation of hematopoietic tissues after radiation injury are considered. Transplantation immunity—the incompatibility of transplanted tissues—and methods for overcoming it are discussed. The effect of radiation on immunological tolerance is described. The medical effectiveness of transplanting bone marrow to an irradiated recipient is discussed. A detailed description is given of the biology of radiation chimeras—organisms arising as a result of the acclimatization of cells transplanted after irradiation. Possibilities of using radiation chimeras in irradiated animals for solving radiobiological questions are considered. An immunogenetic concept of the consequences of radiation damage is expounded. (M.J.T.)

Radiation Hazards and Protection

See also HEALTH AND SAFETY

12732 (AERE-R-5084) THE ADVANCED COURSE IN THE PRINCIPLES OF RADIATION PROTECTION. PART I. Whitehouse, W. J.; Dyson, E. D. (Atomic Energy Research Establishment, Harwell (England)). Nov. 1965. 23p. Dep. BIS $0.70. HMSO 3s. 6d.

Nine advanced courses in the principles of radiation protection were held at Harwell from 1959 to 1964. Each course lasted approximately three months. The background, history, and initial organization of the courses are reviewed, and their subject matter, including lectures, practical work, visits, and films are summarized. The reasons for arranging and presenting the courses, in the way that was adopted, are discussed. (auth)

Radiotherapy and Radiodiagnosis

Refer also to abstracts 12696, 12918, 13010, and 13013.

12733 (AED-C-10-04) NUCLEAR MEDICINE. Series C: Bibliographies. Oeff, K. (comp.) (Zentralstelle fuer Atomkernenergie-Dokumentation, Gmelin-Institut fuer Anorganische Chemie und Grezgebiete, Frankfurt am Main (West Germany)). Sept. 1965. 110p. Dep. mn.

Approximately 800 references to literature on nuclear medicine are presented. Titles listed are in English, French, German, and Italian. References appear under the following categories: diagnostic nuclear medicine; therapeutic nuclear medicine; blood balance; resorption-water and electrolyte; resorption-amino acids; resorption-lipids; resorption-carbohydrates; resorption-vitamins; resorption-others; excretion-proteins and other macromolecules; excretion and secretion-other; cell metabolism and kinetics; and radiobiology. A separate author index is included. (H.G.D.)

12734 (BNL-9911) POSITRON SCANNER FOR BRAIN TUMORS. Robertson, J. S.; Bozzo, S. R. (Brookhaven National Lab., Upton, N. Y.). [1962]. Contract AT(30-2)-Gen-16. 15p. (CONF-754-6). Dep. mn. CFSTI $1.00 cy, $0.50 mn.

From International Business Machines Medical Symposium, Poughkeepsie and Upton, N. Y., Oct. 1964.

Design features of a multi-detector positron scanner for the localization of brain tumors after the administration of preferentially localizing positron-emitting radioisotopes are described. Thirty-two one-inch NaI crystals are arranged in a ring and, although several sets of counts are needed to scan the entire head, the procedure is made shorter than when only two detectors are used. In order to analyze the data, a mathematical model was developed, upon which a computer program for solution and display of the results is based. Use is made of a master library that contains individual distributions for 384 symmetrically distributed point sources across a horizontal cut of a model head. The mathematical results are translated into a display that is meaningful to the surgeon. Clinical results are reported on scans made on a series of patients with symptoms of intracranial lesions. Results using the multi-detector scanner are compared with those using the standard two-detector method. (C.H.)

12735 EXTERNAL COUNTING OF ^{85}Sr AND ^{47}Ca IN LOCALIZED BONE INFECTIONS. Dymling, John-Fredrik; Wendeberg, Bo (Univ. of Lund, Sweden). Acta Orthop. Scand., 36: 8-20(1965).

External counting of ^{85}Sr and ^{47}Ca over localized bone infections in the extremities was explored as a possible supplementary clinical diagnostic test. Carrier-free ^{47}Ca (half life 4.9 days) or ^{85}Sr (half life 65 days) were used. The isotope was given as a single, rapid, intravenous injection, and external counting was performed, usually 168 and 336 hr after injection over the diseased part of the skeleton, over contralateral side, and over the knees and thighs. A 12° wide-angle collimator placed in contact with the skin over the area to be counted was routinely used. A cylindric collimator with an opening of 24 mm was used in children, and for specific purposes a 10-mm slot collimator was used. The maximum dose administered was 1 μC/kg of body weight or 50 μC. Among the 17 cases of active and 8 cases of nonactive

bone or joint infections studied, increased uptake of these bone-seeking radioisotopes were regularly found in areas of active bone infection, when the symptoms had lasted for ~14 days. Active and nonactive bone infections could be completely separated by this method. External counting gave reliable information earlier than roentgenologic investigation in acute cases, and was particularly useful as a complement to roentgenograms in evaluating recurrence of the infectious process in chronic cases. (TCO)

12736 RADIOACTIVE IODINE TREATMENT OF GRAVES' DISEASE: RESULTS IN 32 CHILDREN UNDER 16 YEARS OF AGE. Crile, George Jr.; Schumacher, O. Peter (Cleveland Clinic Foundation). Amer. J. Dis. Children, 110: 501-4(Nov. 1965).

Between 1949 and 1961, 32 children with Graves' disease, in the age range of 7 years through 15 years, were treated with ^{131}I. Their average age was 12 yr. The dose of ^{131}I employed in the 30 fully treated patients ranged from a single treatment of 2.0 mC to three treatments totaling 39.0 mC. The average dose was 9.9 mC; 10 patients received doses of more than 10.0 mC. The average dose was 0.095 mC/g of thyroid. Radioiodine uptakes were measured with ^{131}I usually at 24 hr after a dose of from 3.0 to 10.0 mC of radioiodine was given. In 18 patients only one treatment was required to control hyperthyroidism, in 8 patients two treatments, and in 4 patients three treatments. In the 30 fully treated and followed patients, out of the 32 original patients, hyperthyroidism was controlled and did not recur. (TCO)

12737 HYPERPIGMENTATION AND PITUITARY TUMOR AS SEQUELAE OF THE SURGICAL TREATMENT OF CUSHING'S SYNDROME. McKenzie, A. D.; McIntosh, H. W. (Univ. of British Columbia, Vancouver, Can.). Amer. J. Surg., 110: 135-41(Aug. 1965).

Among 17 patients with Cushing's syndrome studied, two received ^{60}Co γ radiation directed to the pituitary with successful results. Results of radiotherapy in other reported series are reviewed. Radiation offers a variable degree of success and appears to be effective in preventing the progression of the disease in 50% or less of cases of Cushing's syndrome. Criteria for selective treatment of Cushing's syndrome due to adrenal hyperplasia are proposed. (H.G.D.)

12738 TREATMENT OF INOPERABLE PRIMARY PANCREATIC AND LIVER CANCER BY THE INTRA-ARTERIAL ADMINISTRATION OF RADIOACTIVE ISOTOPES (^{90}Y RADIATING MICROSPHERES). Ariel, Irving M. (Pack Medical Foundation, New York). Ann. Surg., 162: 267-78(Aug. 1965).

Experience with patients, suffering from inoperable primary pancreatic and liver cancer, who were treated by the intra-arterial administration of ^{90}Y radiating microspheres is described. Photoscans of the abdomen were obtained using ^{169}Yb as a suitable γ emitter attached to the microspheres and scanning. The distribution of the administered radioactive microspheres throughout the abdominal cavity is shown. Intra-arterial administration of the ^{90}Y microspheres was used successfully in 4 patients with primary cancer of the liver and in six patients with primary cancer of the pancreas. Effects on the blood elements of intra-arterial ^{90}Y microspheres are described. It is concluded that administration of intra-arterial isotopes into the hepatic artery may be well tolerated by the liver and, in some instances, may partially control the cancer to some degree. (H.G.D.)

12739 THE EFFECTS OF RADIATION INJURY ON INTESTINE AND URETER. Reme, H. (Univ., Luebeck, Ger.). Arch. Klin. Chir., 308: 172-7(Nov. 17, 1964). (In German).

Effects of radiation in the intestine are often delayed for several years after exposure before they become evident. They appear most often as stenoses, perforations, or ulcers. These are characterized histologically by avascularity, fibrosis, edema, and atrophy. Diagnosis is made difficult by the chronic nature of these changes, and it is frequently difficult to determine differences between recurrence of a tumor and irradiation injury. If these symptoms appear in a tumor patient who has been irradiated, the conclusion too frequently drawn is that they are due to tumor recurrence. However, in 90% of almost 200 cases studied the symptoms were due to delayed irradiation injury. Treatment frequently used consists of primary resection without ileostomy for the small intestine, and colostomy for the large intestine. Similar considerations should be kept in mind for the prognosis of irradiation injuries to the ureter. If the tissue injuries are the result of tumor formation, palliative measures are the best approach. If the injury has resulted from prior irradiation, procedures should be carried out to improve functional efficiency of the patient. (BBB)

12740 HISTOLOGICAL CHANGES IN IRRADIATED MALIGNANT INTRAOCULAR TUMORS. Lommatzsch, P.; Goder, G. (Humboldt-Univ., Berlin). Arch. Ophthalmol., 168: 198-219(Apr. 23, 1965). (In German).

Radiotherapy of intraocular tumors is discussed. Histological effects of irradiation on intraocular tumors of enucleated human bulbi were studied. The tumors consisted of retinoblastomas, melanoblastomas, and uveal mammary metastases, and were irradiated with x ray, ^{60}Co, or Ra. The doses of irradiation administered were about 6000–9000 R. The most frequently observed histological change was tumor necrosis of various extent and characteristics. The differences observed between the necroses were largely quantitative. Generally, the results indicated that irradiation treatment of intraocular tumors has some limited value which is modified by the size of the tumor and its cellular structure. Long-term studies indicate that regression of retinoblastomas cannot be produced by radiotherapy if it extends over more than one third of the fundus. When radioisotope applicators are used, the active border of the application should extend at least 1 mm beyond the edge of the ophthalmologically detectable tumor. (BBB)

12741 RADIATION THERAPY IN LUNG CANCER. Stevens, Walton E. (Ohio State Univ., Columbus). Geratrics, 20: 816-34(Oct. 1965).

Modern concepts in applying various types of radiation in the treatment of lung cancer are reviewed with emphasis on tendency to increase the dose and volume irradiated. Radiation therapy has played a minor role in the treatment of lung cancer heretofore. One reason for this is that orthovoltage equipment has caused high morbidity, for example, skin reaction, radiation sickness, or prolonged treatment to achieve adequate dosage. This dosage often was inadequate, when compared with present concepts. Attempts to make use of various brachytherapy devices and cytotherapeutic injectable materials are described. The most promising brachytherapy device has been the ^{198}Au seed gun. This should be used as a supplement to surgical pneumonectomy and mediastinal node dissection. Tumor deposits that cannot be easily removed or questionable areas of involvement could then be implanted and irradiated at the time of surgery. Additional teletherapy may then be directed either to the marked area or to adjacent areas of nonproved spread, if necessary. The use of ^{198}Au seed implant techniques requires careful calculation of the needed dose. The greatest indication, perhaps, for this type of therapy is in late stage II and early stage III lesions. The disadvantages to brachytherapy are several: nonhomogeneous dose, nonavailability of sources, need to use intense short-lived sources, or radiation not reaching areas of possible spread. In the author's opinion, its advantages do not outweigh those of supervoltage teletherapy. (TCO)

12742 MACROAUTORADIOGRAPHY WITH RADIOPHOSPHORUS IN CANCER OF THE STOMACH. Gregor, O.; Andrysek, O.; Bednar, B.; Hanik, L.; Vaneckova, O.; Sistek, L. (Charles Univ., Prague). Gut, 6: 234-9(June 1965).

A new technique for using ^{32}P in the diagnosis of cancer of the stomach is described. Investigations were made on 50 patients examined clinically, radiologically, and by gastroscopy. Twenty-four hr before operation each patient

was given 500 μC ^{32}P, in the form of sodium hydrophosphate, intravenously. The resected stomachs were evaluated by their immediate macroscopic appearance, by measuring radioactivity, and histologically. Two groups of patients, 24 with cancer of the stomach and a control group of 19 with peptic ulceration were studied. In addition, macroautoradiography was carried out in 13 stomachs resected for malignant proliferation, in three resected for gastric polyps, and, for comparison, in 10 stomachs resected for peptic ulceration. There was complete agreement between autoradiography and histological findings, showing that under conditions ^{32}P could be used for the differential diagnosis of cancer of the stomach. Other studies involved introduction of a miniature Geiger-Mueller tube fixed to a flexible rubber catheter under radiological control, and introducing a miniature Geiger-Mueller tube mounted on a gastroscope under visual control. It was shown that radiophosphorus can be used to diagnose cancer of the stomach, and the early results of pre-operative measurements using a radiotube and a radiogastroscope indicate that these methods may be suitable for clinical diagnosis. (BBB)

12743 THE TREATMENT OF POLYCYTHEMIA VERA AND THROMBOCYTHEMIA WITH MYLERAN (BUSULPHAN). **Epstein, I. S. (Prince Henry's Hospital, Melbourne). Israel J. Med. Sci., 1: 797-9(July 1965).**

Use of ^{32}P and a cytostatic drug for the treatment of polycythemia vera is discussed. Although radiophosphorus has become established as an effective treatment of polycythemia vera, occasional cases are relatively resistant to it. The experience with two radiophosphorus-resistant cases which responded to Myleran prompted this study. The first case, a 52-year-old male was given 5 μC of ^{32}P, but his hemoglobin level was not controlled and four months later a further 4 μC of ^{32}P was administered. As the polycythemic state was not controlled, Myleran was commenced, a total of 364 mg being given over 19 weeks, with a subsequent complete remission which lasted 16 months. All subsequent cases of polycythemia vera have been treated with Myleran initially, and a therapeutic response has been observed in all. However, one case, a 78-yr-old man who had had six doses of radiophosphorus over the preceding 12 years, was given a course of 224 mg of Myleran over an 8-week period and then developed bone marrow depression with pancytopenia. This patient who developed pancytopenia received only 224 mg and it appears that the long history of the disease, and the fact that he had received a relatively large amount of ^{32}P previously, combined to make his marrow extremely sensitive to Myleran. (BBB)

12744 THE CLINICAL SIGNIFICANCE OF THE COMPLEMENT-FIXATION TEST IN THYROTOXICOSIS. **Buchanan, W. Watson; Koutras, D. A.; Crooks, J.; Alexander, W. D.; Brass, W.; Anderson, J. R.; Goudie, R. B.; Gray, K. G. (Western Infirmary, Glasgow). J. Endocrinol., 24: 115-25(Mar. 1962).**

The effect of ^{131}I treatment on the level of autoantibodies to thyroglobulin in 468 patients with thyrotoxicosis was examined, and the significance of a positive thyroid complement-fixation (CF) test in thyrotoxicosis was investigated by studying the correlation between various features of the disease. A significant correlation was found between the positivity of the CF test and the degree of lymphocytic infiltration in the gland; incidence of postoperative hypothyroidism; size of the goiter; previous treatment with radioiodine, and a family history of thyroid disease. No correlation was found between the results of the test and the incidence of reactions to antithyroid drugs. A much higher incidence of positive CF tests was seen in patients who had received treatment with ^{131}I. The increased positivity of the CF test after ^{131}I therapy may be related to the histological lesions resembling Hashimoto's thyroiditis which have been found in the thyroid gland after ^{131}I therapy. It is therefore suggested that destructive forms of antithyroid therapy might predispose the thyroid to the development of autoimmunity. (TCO)

12745 THERAPY OF ANGIOMAS. **Pflegers, L. (Univ.-Hautklinik, Vienna). Klin. Med. (Vienna), 20: 236-9(May 1965). (In German).**

Since angiomas frequently disappear or regress considerably with age there is some question as to whether they should be treated. If treatment is decided on for cavernous angiomas, it should be started at an early age since the radiosensitivity of angiomas to Ra decreases rapidly even as early as 18 to 24 months of age. Irradiation treatments should be given at 14-day intervals and be stopped at the first signs of regression. Healing usually starts at the center of the lesion after the first or second treatment. In almost all patients observed 13 to 15 yr after treatment with x irradiation, severe late injuries such as thickening of the skin, pigmentation, atrophy, teleangiectases, and ulcerations were observed, even though only small amounts of x irradiation were administered. An additional disadvantage of x irradiation as compared to Ra treatment is the difficulty of holding small children quiet under the x-ray equipment. With Ra used in the form of plaques or tubes this difficulty does not arise. (BBB)

12746 A NEW FAST RADIOIODINE TEST FOR TESTING THYROID FUNCTION WITH SIMULTANEOUS ESTIMATION OF PERIPHERAL HORMONAL IODIDE SUPPLY. **Boerner, Wilhelm (Univ., Wurzburg, Ger.). Klin. Wochensch., 39: 990-8(Oct. 1, 1961). (In German).**

Extrathyroidal activity in the neck was continuously recorded and used to correct the radioiodine uptake of the thyroid. The amount of radioactivity recorded over the femur was used for estimation of radioiodine in the tissues. The values obtained were used to estimate the hormonal I concentrations in the peripheral tissues. The more severe the thyroidal hypofunction is and the longer it has remained untreated, the higher are the tissue values measured over the femur. Treatment with thyroid hormone brings the values measured down to normal. In order to ascertain the reproducibility of test results, studies were repeated over periods of 5 days or less. The average relative variation amounted to ±15%, which is in agreement with results reported in similar studies. The test developed has been carried out in over 500 patients. The results obtained indicate that the test requires only 20 min. For this reason the use of the short-lived radioisotope ^{132}I is justified, permitting the radiation burden to be considerably reduced, as compared with the use of ^{131}I. The time required for the test is so short that it can be repeatedly performed. This is a distinct advantage for follow up studies of treatment results. The test is particularly useful for rapid diagnosis of hypothyroidism. (40 references cited.) (BBB)

12747 STUDIES ON THE DOSE DISTRIBUTION OF ROTATION THERAPY WITH THE 15 Mev BETATRON FOR CERVICAL CANCER. **Takayama, Kazuo (Kyushu Univ., Fukuoka, Japan). Kyushu J. Med. Sci., 15: 189-200(Dec. 1964).**

Dose distributions in bodylike water phantoms were measured with 15 Mv x ray from the betatron by means of ionization chambers and compared with cobalt-60 γ dose distribution. With 15 Mv x rays the build-up region is from 0 to 3.5 cm and depth dose is very high, while the surface dose is only about 40% with steep dosage gradients along the geometrical edge of the beam. Using directly opposing portal for cervical cancer with supervoltage machines, the tissue doses are very homogeneous, but risk to normal tissues is increased. Here rotational therapy is needed with supervoltage therapy. Rotation therapy with x rays of the betatron permits homogeneous irradiation of a tumor region with high dosage, while the volume dose to normal tissues remains smaller than cobalt-60 γ radiation. Supervoltage rotation therapy permits delivery of large doses of radiation to a well defined predetermined volumes of tissue, with minimal effects on normal tissues. The tumor doses were much greater than could be safely administered by conventional techniques. (auth)

12748 PLASMA-GROWTH-HORMONE LEVELS IN UNTREATED ACROMEGALY AND AFTER RADIOACTIVE IMPLANTS INTO THE PITUITARY. Greenwood, F. C. (Imperial Cancer Research Fund, London); Stewart, Helen J.; Forrest, A. P. M.; Wood, R. G. Lancet, 2: 555-8 (Sept. 18, 1965).

Estimations of growth hormones were carried out in 15 patients with acromegaly and in 8 of these patients estimations were carried out before and at intervals up to 15 months after the implantation of ^{198}Au by transnasal cannulation. Two seeds of ^{198}Au were placed near the floor of the fossa to give an estimated dose of radiation to the diaphragma sellae of 10,000 rad. The total activity thus depended on the size of the fossa and varied from 26 to 60 mC. In each patient the actual dose delivered was calculated from subsequent x rays. In one of the 8 patients twin sources of ^{90}Y (total amount 6.6 mC) had previously been implanted into the pituitary. Five other patients were studied five to nine years after the implantation of ^{90}Y alone (3 patients) or ^{90}Y with a small dose of ^{198}Au (2 patients). In these 5 patients the total activity of ^{90}Y was large and varied from 14 to 36 mC. In the 8 acromegalic patients studied before and one to 15 months after treatment by pituitary implant of ^{90}Y or ^{198}Au seeds, treatment was found to have variable effects on growth hormone levels and on the clinical course of the disease. (TCO)

12749 THYROID SCINTIGRAPHY WITH ^{99m}Tc. Boerner, W.; Moll, E.; Bayer, H. (Univ., Wurzburg, Ger.). Med. Welt., 21: 1151-5(May 22, 1965). (In German).

Technetium-99m (half life, 6 hr), obtained by separation from ^{99}Mo, is particularly suitable for scanning of the thyroid gland. Its main advantages are that it is more easily detected than ^{131}I; the irradiation dose received from it is less than with either ^{131}I or ^{125}I, thus making it more feasible for use in children; scanning can be started within one hr after administration; it can be used in combination with ^{132}I to study thyroid function and localization within a single day; and scanning with a second dose of ^{99m}Tc can be repeated within 1 day. Compared to these, the disadvantages of ^{99m}Tc are that alone it cannot be used for simultaneous studies of function and localization like ^{131}I can be; it is less suited for detection of dystrophic thyroid tissue; it is concentrated poorly by thyroid metastases; and its cost is greater than the cost of ^{131}I. (BBB)

12750 HEMANGIOMA ASSOCIATED WITH THROMBOCYTOPENIA: REPORT OF TWO CASES AND REVIEW OF THE LITERATURE WITH EMPHASIS ON METHODS OF THERAPY. Thompson, Leonard R.; Umlauf, Harry J. Jr. (Fitzsimons General Hospital, Denver). Mil. Med., 129: 652-8(July 1964).

Radiotherapy of hemangioma associated with thrombocytopenia in children is considered, with reference to two cases and a review of the literature concerning 37 other cases. Evidence is presented that x-ray therapy is superior to all other methods of treatment for this syndrome, and precautions to be observed in irradiating these lesions in children are stated. It is pointed out that x-ray therapy should not be used for benign diseases in children. However, small doses of x-ray are sufficient to cure the thrombocytopenia and shrink the hemangioma. In most cases the platelet count returns to normal within a few months following successful x-ray therapy. With small doses and proper protection of the epiphyseal centers when indicated, injury to the skin and underlying structures is unlikely. Doses as small as 300 to 500 R to hemangioma are usually sufficient to obtain the desired effects. (TCO)

12751 INTRA-OPERATIVE DETECTION OF THE PELVIC LYMPH NODES BY RADIOACTIVE ISOTOPES. Marchesi, F.; Laconi, A.; Maneschi, M.; Ragonese, P.; Cittadini, E.; Quartararo, P. (Univ., Palermo, Italy). Minerva Radiol., Fisioterap. Radiobiol., 10: 395-401(Oct. 1965). (In Italian).

The methods available for impregnation of the pelvic lymphatic vessels with radioisotopes for the localization of lymph nodes affected by metastatic neoplasma of genital cancers are considered. These are the direct endolymphatic method and indirect injection into the tissues. Some criteria for the choice of the radioactive substance to be used are presented and the comparative value of radiographic and tracer techniques are considered. The favorable results obtained in the localization of pelvic lymph nodes using ^{131}I, ^{198}Pu, or ^{32}P and external counting are described. (tr-auth)

12752 RADIATION HAZARDS: AN EXERCISE IN VALUE JUDGMENT. Chamberlain, Richard H. (Univ. of Pennsylvania School of Medicine, Philadelphia). Postgrad. Med., 38: 591-2(Nov. 1965).

The tendency toward excessive public concern for radiation hazards is discussed, and the problems faced by radiologists and other physicians in realistically assessing hazards of various radiodiagnostic and therapeutic technics are examined. Two elements of value judgment are involved in the wise use of radiation in medicine. One relates to how much radiation is used; it is determined by experts in the field of radiology and yet involves weighing of general values. The other relates to benefits expected or achieved and calls for the cooperative exercise of informed judgment by all physicians. Legislative or fixed-rule control methods are applicable only to a part of the first element. The risk versus the benefit should be evaluated for each individual situation. (TCO)

12753 PITUITARY IMPLANTATION FOR PITUITARY TUMOURS. Forrest, A. P. M.; Greenwood, F. C.; Stewart, H. J.; Thomas, J. P.; Wood, R. G.; Thomas, W. R. G.; Bligh, A. S.; Mitchell, G. M. (Welsh National School of Medicine, Cardiff, Wales). Proc. Roy. Soc. Med., 58: 475-80(July 1965).

Technics, doses, clinical results, and complications are described with reference to radioisotope implantation of the pituitary by the transnasal route to treat 361 patients, most of whom had advanced cancer of the breast. In most, two sources of ^{90}Y were implanted in an attempt to achieve complete pituitary ablation. A rod of ^{90}Y, encased in Nylon and fixed into a small stainless steel screw-threaded base, is screwed into a drillhole in the anterior wall of the fossa and holds the source in the desired position. The precision with which the ^{90}Y sources can be placed by this technic resulted in low mortality and morbidity. In the last 100 patients only 1 has developed a defect of vision and 1 persistent rhinorrhea. Pituitary implantation was also used to treat 19 patients with pituitary tumors, 14 associated with acromegaly, 3 with hyperadrenalcorticism (2 Cushing's disease; 1 excess oxosteroid excretion) and two with hypopituitarism. Yttrium-90 was the isotope of choice initially and this was used alone in 8 patients. Recently, however, radiogold (^{198}Au) was preferred, and was the only source implanted in 7 patients and was combined with ^{90}Y (either simultaneously or sequentially) in 4. Acromegalics were also treated by the implantation of ^{90}Y by the screw technique. The dose of ^{90}Y in 8 patients varied from 6.6 to 31.0 mC, two or four sources being used. In one patient a small amount of ^{198}Au (3.5 mC) was included in the implant and in two a second implant, one with ^{90}Y (26.4 mC) plus ^{198}Au (3.4 mC) and one with ^{198}Au alone (26.2 mC) were performed. Four patients had an unsatisfactory operative course, with severe headache, photophobia, visual disturbance, and polyuria. These were temporary and presumed due to swelling or hemorrhage into the tumor. One patient had severe but temporary epistaxis and another has had occasional running nose. (BBB)

12754 CRITICAL STUDY OF THE RADIOIMMUNOLOGIC METHOD OF DETERMINATION OF INSULIN (METHOD OF HALES AND RANDLE). Moody, A. J.; Felber, J.-P. (Clinique Medicale Univ., Lausanne, Switzerland). Schweiz. Med. Wochschr., 95: 766-72 (June 5, 1965). (In French).

Use of radioisotope methods (mainly with ^{131}I-labeled hormones) to measure circulating levels of protein hormones is discussed. In particular, the use of ^{131}I-insulin in a radioassay technic is critically examined. Questions examined included: (1) whether the antigenicity of ^{131}I-

labeled insulin is identical to that of native insulin; (2) whether antibody is saturated at all concentrations of insulin used in the assay; (3) whether the concentration of antibody is such that in the absence of unlabeled insulin it will fix 40 to 55% of ^{131}I-labeled insulin; if the concentration of ^{131}I-insulin is 2.5 μg/ml, the assay will measure between 1 and 200 μU/ml of insulin; and (4) whether the presence of a control substance (e.g., serum) will not change the reciprocal concentrations of the different elements in the system, in particular that of the antiserum. Accuracy of the radioimmunological method of Hales and Randle (Biochem. J., 84: 79P(1962)) in determining circulating insulin depends on a number of factors: the concentration of anti-insulin antiserum, the concentration of precipitating antiserum, and the purity and origin of the tagged insulin used. The method can be validly employed to measure the concentration of circulating insulin in human serum only under well-defined conditions. The insulin response to glucose loading serves to differentiate two principal types of diabetes: cases where an elevated blood sugar level is accompanied by an increase in blood insulin, and those where the rise in blood sugar is not followed by a similar response and where a low fasting insulin level rises little or not at all in response to glucose. (BBB)

12755 DEVELOPMENT OF A RADIOIMMUNOLOGIC METHOD FOR THE DETERMINATION OF THYROID-STIMULATING HORMONE: PRELIMINARY RESULTS. Lemarchang-Beraud, Th.; Felber, J.-P.; Vannotti, A. (Clinique Medicale Univ., Lausanne, Switzerland). Schweiz. Med. Wochschr., 95: 772-6(June 5, 1965). (In French).

A radioisotope method for estimation of thyrotropin (TSH) was developed; the technic and results obtained with it in clinical studies on 37 patients with various thyroid disorders are also reported. TSH labeled with ^{131}I binds antibody to form a ^{131}I-TSH-antibody complex. An isotope dilution principle is involved. Thus, if antibody to TSH is present in limited amount, it binds indiscriminantly unlabeled TSH and added labeled TSH. Thus the radioactivity of the antigen-antibody complex will depend on the amount of unlabeled TSH diluting the known amount of added ^{131}I-TSH. Preparation of TSH labeled with ^{131}I of high sp act. enabled development of this radioimmunologic test. With this extremely sensitive method it is possible to measure as little as 5 μU of unlabeled TSH. The optimum conditions for the measurement of endogenous TSH in man were studied. The concentration of antiserum appears to be an important factor in eliminating the nonspecific inhibitors in the blood. The preliminary results obtained with this radioimmunologic method in man show the following mean values: 0.38 mU/ml in euthyroid patients, 0.26 mU/ml in hyperthyroid patients, 0.43 mU/ml in hyperthyroid patients treated with ^{131}I, and 2.3 mU/ml in hypothyroid patients. (BBB)

12756 IMPORTANCE OF BIOCHEMICAL INVESTIGATIONS OF CONNECTIVE TISSUE COMPONENTS DURING RADIOTHERAPY. I. ELECTROPHORETIC PREPARATION OF ACID MUCOPOLYSACCHARIDES IN SERUM, URINE, AND TISSUE. Kaercher, Karl Heinz (Univ. Strahlenklinik, Heidelberg). Strahlentherapie, 129: 80-94(Jan. 1966). (In German).

Data are reviewed from studies on the changes of components of connective tissue under the influence of ionizing radiation. The method of extraction of acid mucopolysaccharides from tissue, serum, and urine, as well as the electrophoretic isolation and staining was described. The electrophoretic changes of acid mucopolysaccharides in a patient with bronchial carcinoma and radiation fibrosis following cobalt-60 γ radiation and similar changes in a patient with multiple myeloma after radiation therapy using ^{32}P are cited as examples of the effects of radiation on acid mucopolysaccharides. (tr-auth)

12757 RADIATION EXPOSURE OF PATIENTS AND RADIOLOGICAL EMPLOYEES IN HEART PROBES AS WELL AS CONTRAST MEDIUM REPRESENTATION OF THE HEART AND THE LARGE BLOOD VESSELS. PART I. INTRODUCTION—METHODS—MEASUREMENTS ON A APPARATUS FOR IMAGE INTENSIFIER TELEVISION TRANSILLUMINATION AND IMAGE INTENSIFIER KINEMATOGRAPHY. Schulte-Brinkmann, Wolfgang (Univ. Duesseldorf). Strahlentherapie, 129: 139-55(Jan. 1966). (In German).

Radiation protection measurements done during special angiocardiographic examinations were reported. The literature is surveyed, methods reported, and results obtained using image intensifier-television transillumination and image intensifier-kinematography are presented. The SD-rate which was measured at a phantom under different conditions was used for calculation of the skin dose in 100 heart soundings and the surface dose received by patients during the sounding procedure of the heart was determined. The dose to the male gonads was measured during heart soundings in 100 patients. An inverse correlation between age and body size of the patients and the amount of the gonadal dose was found. Measurements of scattered radiation intensity were done at many places in the examination room; the results were used for calculating the exposure dose for the examiner and his assistants during an average sounding procedure. Moreover, the scattered radiation exposure of the personnel was measured at the lower leg and back of the hand during numerous heart soundings. (tr-auth)

12758 UNILATERAL INSERTION OF ^{60}Co IMPLANTS IN THYROID CARTILAGE FOR LARYNGEAL CARCINOMA: EXTENSION OF CURRENT PROGNOSTIC STATUS. Minnigerode, B. (Univ., Goettingen, Ger.). Z. Laryngol., Rhinol. Otol., 44: 334-9(May 1965). (In German).

The advantages of contact irradiation of early vocal cord carcinoma with ^{60}Co compared to percutaneous x or telegamma irradiation include reduction in radiation dose to the surrounding soft tissues and large blood vessels; greater flexibility in the size of the source; thus making for improved adaptation to the size and location of the particular tumor treated; constant, fixed geometry between irradiation source and tumor so that irradiation dose can be calculated more accurately; uninterrupted duration of irradiation; and relative decrease in time required for irradiation. The use of metallic ^{60}Co implants permits exact isodose calculations to be made. This is not possible if radioactive plastics, such as plastobalt or macrobalt are used. In addition, the metal carrier containing the ^{60}Co implant is very resistant to corrosion, and thus prevents damage to the Ni or Au covering of the ^{60}Co. This protects the patient and medical personnel against danger from corrosion of the ^{60}Co irradiation source. Out of 21 cases treated with ^{60}Co inserts, 19 were symptom free 3 to 5 yr after treatment. (BBB)

12759 RADIO-ISOTOPES ET AFFECTIONS DU SYSTEME NERVEUX CENTRAL (DIAGNOSTIC ET BASES BIOLOGIQUES). (Radioisotopes and Afflictions of the Central Nervous System (Diagnostics and Biological Bases). Planiol, Therese. Paris, Masson et Cie, 1965. 110p.

The six papers presented at the Session of September 24, 1963, at Strasbourg under the auspices of the World Federation of Neurology are compiled. Positro-cephalography, based on the use of positron emitters, is discussed and its use, in conjunction with the electroencephalogram, to detect or exclude the presence of an intracranial tumor is described. The use of γ encephalography for the diagnosis of intracranial lesions; the use of angiography in the diagnosis of extra-tensorial lesions; and the value of scanning in the localization of lateral and frontal planes are described. The biological bases of gamma encephalography are defined. The technique of myeloscintigraphy to reveal partial or total obstructions of the spinal subarachnoid space is discussed. (J.S.R.)

CHEMISTRY

General

Refer also to abstracts 14008 and 14016.

12760 (AD–611432) PROCEEDINGS OF THE 1964 ARMY SCIENCE CONFERENCE, UNITED STATES MILITARY ACADEMY, WEST POINT, N. Y., 17–19 JUNE 1964. VOLUME I. (PRINCIPAL AUTHORS A THRU H). (Office, Chief of Research and Development (Army), Washington, D. C.). 506p. (CONF-640630(Vol.I)). CFSTI $8.25 cy, $2.25 mn.

Separate abstracts were written for 2 of the 36 included papers. Four of the papers appeared previously in NSA as 17: 30406, 19: 12655, 46475, and 47214. The remaining papers deal mainly with various chemical and astrophysical studies. (M.O.W.)

For abstracts of individual papers see: 13970 and 14023.

Analytical Procedures

See also Separation Processes and Procedures

Refer also to abstracts 12914, 12976, 13372, and 14168.

12761 (AERE-R–4911) THE DETERMINATION OF ^{231}Pa IN URINE. Sandalls, F. J. (Atomic Energy Research Establishment, Harwell (England)). Dec. 1965. 16p. Dep. BIS $0.80, HMSO 4s.

A sensitive method for the determination of protactinium-231 in urine is described. The urine is wet-ashed with nitric acid and dissolved in a solution of hydrochloric and hydrofluoric acids. After saturating the solution with aluminum chloride, the protactinium is extracted into di-isobutyl ketone. A solution of hydrochloric and hydrofluoric acid is then used to extract the protactinium from the ketone. The hydrochloric-hydrofluoric acid solution is evaporated to dryness, the residue taken up in hydrochloric acid and the protactinium electrodeposited onto platinum from a solution of ammonium chloride. An overall recovery of 82 ± 5 percent was obtained and decontamination from other alpha emitters was high. The electrodeposited protactinium could be counted with conventional or solid-state detectors but is also in a suitable form for autoradiographic counting techniques. The limit of detection is about 0.03 pC. (auth)

12762 (BNWL–173) CONTINUOUS SEPARATION OF CERIUM FROM TRIVALENT RARE EARTHS BY PERSULFATE OXIDATION AND D2EHPA SOLVENT EXTRACTION: PILOT PLANT STUDIES. Richardson, G. L. (Battelle-Northwest, Richland, Wash. Pacific Northwest Lab.). Nov. 1965. Contract AT(45-1)-1830. 21p. Dep. mn. CFSTI $1.00 cy, $0.50 mn.

A process proposed for continuously separating cerium from other rare earths was successfully demonstrated in a dual-purpose IC column. Satisfactory separation was achieved with 2M HNO_3 strip solutions (ICX) containing either 0.2M persulfate with 0.02 to 0.03M silver catalyst or 0.3M persulfate with 0.0012 to 0.012M silver. The latter composition was preferred because of the lower chemical cost and a lesser sensitivity to the reducing normality of the solvent. Typical cerium contamination in the rare earth product (ICP) was less than 0.3% of that entering the column with ICX flows ranging from 10 to 20% of the solvent feed (ICF) flow. Operating conditions contributing to high cerium separation and low rare earth losses are described. An adverse effect of HEDTA-complexing on rare earth extraction kinetics at pH 3.8 was overcome by operating the IA column at 50°C with the aqueous phase continuous to maximize the aqueous phase residence time. (P.C.H.)

12763 (CNEA–162) SEPARACION DE ROSA DE BENGALA ^{131}I POR CROMATOGRAFIA EN CAPA DELGADA. (Separation of ^{131}I-Rose Bengal by Thin-Layer Chromatography). Mitta, Aldo E. A.; Camin, Leopoldo (Comision Nacional de Energia Atomica, Buenos Aires (Argentina)). 1965. 3p. (CONF-641123–2). Dep. mn.

From 11th Argentina Chemical Conference, Bahia Blanca, Argentina.

A chromatographic method for the separation of ^{131}I-labeled Rose Bengal with a specific activity of 5 to 7 mC/mg is presented. The method can be used for quantities of 1 mg. (J.S.R.)

12764 (CONF-660305–8) CHEMICAL SEPARATION OF REACTOR PRODUCED ^{171}Tm. Perkins, W. C. (Du Pont de Nemours (E. I.) and Co., Aiken, S. C. Savannah River Lab.). Jan. 1966. Contract AT(07-2)-1. 5p. Dep. mn. CFSTI $1.00 cy, $0.50 mn.

From American Nuclear Society Topical Meeting, Augusta, Ga.

The development of a recovery process for the separation of Er and Tm is reported. Erbium oxide and erbium metal were irradiated at the Savannah River Plant to produce ^{171}Tm. Erbium oxide was then used to test the ion exchange separation technique. Approximately 8 mg of the ^{171}Tm was separated from the dissolved Er_2O_3 targets by chromatographic elution from cation exchange resin with hydroxyethylethylenediaminetriacetate (HEDTA). The ^{171}Tm was recovered from the product solution by precipitation as the oxalate, which was decomposed to Tm_2O_3, an acceptable form for encapsulation. (J.B.)

12765 (DP–1004) DETERMINATION OF FLUORIDE BY PYROHYDROLYSIS AND AUTOMATED COLORIMETRY. Harrington, David E.; Dorsett, Robert S. (Du Pont de Nemours (E. I.) and Co., Aiken, S. C. Savannah River Lab.). Dec. 1965. Contract AT(07-2)-1. 14p. Dep. mn. CFSTI $1.00 cy, $0.50 mn.

A pyrohydrolytic-colorimetric method was developed for the determination of fluoride in the presence of high concentrations of interfering elements. Adaption of the colorimetric reaction of fluoride with the lanthanum chelate of alizarin complexone to an automated system gave a minimum detectable limit of 0.050 μg/ml of fluoride in pure solutions and 25 μg of total fluoride in samples that required the pyrohydrolytic separation from interferences. The relative standard deviation of the method is better than 1% at twenty times the limit of detection. (auth)

12766 (GEAP–4178) SODIUM MASS TRANSFER. VII. METHODS FOR DETERMINING IMPURITIES IN SODIUM SAMPLES. Sabol, W. W.; Lockhart, R. W. (General Electric Co., San Jose, Calif. Atomic Power Equipment Dept.). Sept. 1963. Contract AT(04-3)-189. 54p. Dep. mn. CFSTI $3.00 cy, $0.50 mn.

A compilation and updating of analytical procedures, sampling methods, and special techniques that have been applied to sodium samples submitted for chemical analysis in connection with the Sodium Mass Transfer program is presented. By application of these procedures, data have been generated to assist in the evaluation of mass transfer and corrosion mechanisms that are associated with loop operations described previously. (auth)

12767 (GEAP–4833) SODIUM MASS TRANSFER. XVII. THE DETERMINATION OF HYDROGEN IN LOOP SODIUM AND COVER GASES. Dutina, D.; Simpson, J. L. (General Electric Co., San Jose, Calif. Atomic Power Equipment Dept.). June 1965. Contract AT(04-3)-189. 18p. Dep. mn. CFSTI $1.00 cy, $0.50 mn.

A modified version of the diffusion gasometric technique was set up for the measurement of hydrogen in sodium sampled from the mass transfer loops. A major innovation was the use of gas chromatography, a specific method for

the determination of hydrogen in place of the non-specific manometric techniques used previously. The sensitivity of the technique is about 1 ppM when a 5 gram sample of sodium is used and the precision at this level is approximately ±0.7 ppM at 1σ. The method was applied to the analysis of sodium sampled from the mass transfer loops. Hydrogen was found in the loop sodium at concentrations of about 5 ppM but no correlation was found with the multi-break phenomena observed in plugging indicator runs performed on the loops. The method for sampling and analyzing the argon cover gas protecting the sodium in the loops for impurities is presented. Hydrogen, nitrogen, and an occasional trace of carbon-containing gases were observed in the cover gas. (auth)

12768 (IEA–97) DETERMINATION OF CHLORINE AND COPPER IN HIGH PURITY WATER BY RADIOACTIVATION ANALYSIS. Giambastiani, Romolo; da Silva Filho, Joaquim G.; Lima, Fausto W. (Instituto de Energia Atomica, Sao Paulo (Brazil)). Aug. 1965. 14p. Dep. mn.

A radioactivation procedure for quantitative determination of chlorine and copper in parts per billion (ppB) level, in high purity water is described. Water samples (100 ml) in polyethylene containers were irradiated for 35 minutes in a 10^{13}n/sec cm^2 thermal neutron flux. After a 10 min cooling time, carriers for iron, chlorine, and copper were added and the hydroxides precipitated by addition of sodium hydroxide. Chlorine was precipitated in the filtrate as silver chloride, the precipitate separated on a sintered glass plate and the induced Cl-38 (37.3 minutes half life, beta of 4.8 Mev) is beta counted with a G-M tube using an aluminum absorber to cut eventually extraneous beta contamination. The iron and copper hydroxides were dissolved with hydrochloric acid and the iron was precipitated again with NH_3 gas. The iron hydroxide was centrifuged and discarded. The supernatant was acidified and the copper precipitated as sulfide. The precipitate was mounted and gamma-counted, its activity measured by the height of the Cu-64 (0.510 Mev, 12.8 hours half life) photo-peak, using a single pulse height analyzer. (auth)

12769 (IEA–98) ACTIVATION ANALYSIS OF GOLD IN ORES SAMPLES. da Silva Filho, Joaquim G.; Abrao, Alcidio; Lima, Fausto W. (Instituto de Energia Atomica, Sao Paulo (Brazil)). Aug. 1965. 20p. Dep. mn.

The determination of gold in ores by neutron activation is described. In order to overcome inhomogeneity, the samples were chemically processed before irradiation. The ore was digested in aqua regia, the gold retained on an anionic ion exchanger, and the resin irradiated in a neutron flux of 5×10^{12}n/cm^2 sec. The gold content was calculated using gold standards fixed on anionic resins, which were irradiated simultaneously with the samples and in the same geometry and counted with a single channel pulse height analyzer. The gold content of the ores was in the range 0.05–70.0 ppM, and the chemical yield, in terms of gold recovery, was over 97%. (P.C.H.)

12770 (IFA/CO/28) BIBLIOGRAPHY OF ^{14}C MEASUREMENTS. PART 2. (1961–1963). Genunche, Ana (Institutul de Fizica Atomica, Academia R. P. R., Bucharest (Romania)). 1964. 32p. Dep. mn.

References (167) on chemical, medical, engineering, technological, and economic aspects of ^{14}C measurements are given to reports and journals published from 1961 through 1964. An author index is included. (P.C.H.)

12771 (NLCO–967) THE EFFECTS OF VARIOUS GRADES OF GRAPHITE ELECTRODES ON THE CARRIER DISTILLATION OF IMPURITIES IN U_3O_8. SUPPLEMENTAL REPORT—POCO EP-192, EP-192C, AND EP-1924 AND GENERAL GRAPHITES. Pepper, C. E.; Pardi, A. J.; Dingeldein, W. H. (National Lead Co. of Ohio, Cincinnati). Dec. 1965. Contract AT(30-1)-1156. 15p. Dep. mn. CFSTI $1.00 cy, $0.50 mn.

Graphite grades EP-192, EP-192C, and EP-1924 and a graphite designated General, were evaluated as anode electrodes to determine the graphite effect upon the carrier distillation excitation of impurities in U_3O_8. The carrier material was 10% AgCl–LiF (11:1 by weight). National SPK and Ultra U-7 graphite electrodes were included as reference electrodes. Quantometric time-resolved spectra were made to determine the relative spectral sensitivities of nine impurities in U_3O_8 with each graphite. The analytical precisions for eight impurities were also determined with each graphite. The POCO graphites did not show any significant advantages when compared with the U-7 and SPK graphites. In most comparisons they were excelled by the U-7 electrodes. (P.C.H.)

12772 (ORNL–3840) LARGE SCALE PREPARATION OF HIGH PURITY ^{131}I AND ^{133}Xe BY SORPTION TECHNIQUES. Case, F. N.; Acree, E. H. (Oak Ridge National Lab., Tenn.). Jan. 1966. Contract W-7405-eng-26. 15p. Dep. mn. CFSTI $1.00 cy, $0.50 mn.

Isolation of ^{131}I and ^{133}Xe from fission product mixtures was accomplished by sorbing the ^{131}I on platinum and the ^{133}Xe on charcoal or on a molecular sieve. Very high radiochemical purity is obtained by this method. The process is easily controlled to minimize the loss of ^{131}I to waste gas streams and compact equipment allows manipulator cell operation. (auth)

12773 (PEL–80) DETERMINATION OF CARBON IN URANIUM MONOCARBIDE. Lovell, G. H. B.; Britz, E. J. (Atomic Energy Board, Pelindaba (South Africa)). June 1965. 6p. Dep. mn.

A method is described for the determination of the carbon content of uranium monocarbide by combustion of a carbon tetrachloride slurry. The method obviates the use of inert atmosphere glove-boxes, and affords considerable accuracy. (auth)

12774 (PG-Report–685) ANALYTICAL METHOD FOR THE DETERMINATION OF ^{144}Ce IN REACTOR FUEL SOLUTIONS (DI-2-ETHYL HEXYL PHOSPHORIC ACID EXTRACTION). (Production Group, United Kingdom Atomic Energy Authority, Sellafield (England)). 1965. 8p. Dep. BIS $0.30. HMSO 1s. 9d.

A method for the determination of radiocerium in nitric acid solutions of mixed fission products is described. It was developed specifically for the analysis of irradiated uranium dioxide specimens and irradiated uranium–aluminum and plutonium–aluminum foils. Radiocerium, together with added carrier, were extracted into bis-2-ethyl hexyl phosphate. The cerium was back extracted into a mixture of nitric acid and hydrogen peroxide. Traces of ruthenium were removed by fuming with sodium bismuthate and a portion of the treated sample was mounted on a stainless steel tray. The β-activity of the praseodymium-144 daughter of the cerium-144 was measured with a plastic phosphor scintillation counter which was adjusted so that it did not count the particles from cerium-141 or its daughter. (J.B.)

12775 (RFP–601) THE PYROHYDROLYSIS OF PLUTONIUM TETRAFLUORIDE. Vejvoda, E. (Rocky Flats Div., Dow Chemical Co., Golden, Colo.). Dec. 17, 1965. Contract AT(29-1)-1106. 24p. Dep. mn. CFSTI $2.00 cy, $0.50 mn.

A procedure was developed for the determination of fluorine and plutonium in plutonium tetrafluoride based on the pyrohydrolytic decomposition of the plutonium tetrafluoride. (auth)

12776 (RT/PROT(65)33) CHROMATOGRAFIA DI PARTIZIONE A FASI INVERTITE E SUE APPLICAZIONI. (Reversed-Phase Partition Chromatography and Its Application). Testa, C. (Comitato Nazionale per l'Energia Nucleare, Rome (Italy)). Oct. 1965. 28p. Dep. mn.

The advantages and the application of reversed-phase partition chromatography are described both for paper and column separations, and the relations between this new technique and liquid-liquid extraction are emphasized. The results obtained with paper treated with tri-n-octylamine (TNOA), tri-n-octylphosphine oxide (TOPO), and di-(2-ethylhexyl) orthophosphate (HDEHP) are reported, par-

ticularly for rare earth separation. As regards column chromatography, several methods are mentioned which make use of both cellulose powder and Kel-F (polytrifluorochloroethylene) impregnated with TNOA, TOPO, HDEHP, tri-n-butyl phosphate, Aliquat-336, dipicrylamine, tetraphenyl borate, and tetrachlorohydroquinone. The possibility of preparing electron-exchange columns by supporting tetrachlorohydroquinone on Kel-F is emphasized: by such redox columns it is possible to oxidize or reduce metal ions and molecules without adding any reagent, and, moreover, to make indirect redox titrations. Some Italian and foreign polymers were also tried, which can successfully substitute Kel-F as the supporting agent. The advantages of reversed-phase partition chromatography in respect to traditional chromatography and solvent extraction are pointed out, particularly for rare earth separation. (auth)

12777 (UJV–1431/65) POUZITI VYSOCE CITLIVEHO INTERGRATORU V PLYNOVE CHROMATOGRAFII. (Application of a Highly Sensitive Integrator in Gas Chromatography). Feist, I.; Sojka, B. (Ustav Jaderneho Vyzkumu, Ceskoslovenska Akademie Ved, Rez). 1965. 10p. Dep. mn.

An integrator type with a blocking oscillator in which condenser charge is compensated was used in a gas chromatograph with a flame ionization detector. Simple registration in gas chromatography is discussed, and the results of measurements in a mixture of three organic substances are reported. The possibility of other applications is also discussed. (P.C.H.)

12778 (UJV–1434/65) STUDY OF SOME CONCENTRATION-DEPENDENT DISTRIBUTION METHODS FOR THE DETERMINATION OF ZIRCONIUM IN SUBMICROGRAM AMOUNTS. Kyrs, M.; Rais, J.; Pistek, P.; Selucky, P. (Ustav Jaderneho Vyzkumu, Ceskoslovenska Akademie Ved, Rez). 1965. 19p. Dep. mn.

Several heterogenous systems were used to test the possibility of determining Zr in concentrations of 5×10^{-6} M and higher, and to allow a decision on the experimental arrangement most suitable for the needed sensitivity of the determination. In these systems Zr underwent distribution with no masking reagent present and another distribution was accomplished in the presence of EDTA and oxalic acid in concentrations of 2.5×10^{-7} M. From the results, it was concluded that the method of concentration-dependent distribution, a method based on the radial distribution on a paper disc, into which about 0.06 ml of the solution are transferred, appears to be best suited for a practical application. (P.C.H.)

12779 (USNRDL-TR-924) QUANTITATIVE RADIOCHEMICAL DETERMINATION OF ^{63}Ni IN SEAWATER. Lai, M. G.; Goya, H. A. (Naval Radiological Defense Lab., San Francisco, Calif.). Nov. 3, 1965. Contract AT(49-5)-2084. 17p. Dep. mn. CFSTI $1.60 cy, $0.80 mn.

A liquid scintillation method for the quantitative determination of ^{63}Ni in seawater is described. The method consists of complexing the nickel in seawater with dimethylglyoxime, extracting it into chloroform, and then back-extracting the nickel into an aqueous phase using dilute sulfuric acid. An aliquot of this sample is added to a scintillation solvent and counted in a liquid scintillation counter. (auth)

12780 (ORNL-tr-931) DETERMINATION OF OXYGEN IN SODIUM BY LIQUID AMMONIA. Attas, V.; Boudier, C. (Commissariat a l'Energie Atomique, Fontenay-Aux-Roses (France). Centre d'Etudes Nucleaires). Translated by Gregory L. Boisvert (Oak Ridge National Lab., Tenn.), from report DRP/ML/FAR-R.–160. Mar. 1965. 14p. Dep. mn. JCL $1.60 fs, $0.80 mf.

A method of determining the oxygen content in sodium by dissolving the sodium in liquid ammonia is presented. The apparatus and its mode of operation are described. The method consists in treating the sodium sample with liquid ammonia until all of it has been dissolved. The oxide is then collected and measured. The sodium found in the ammonia is also measured; from these two measurements the oxide to sodium ratio is found and from there the oxygen content. Only a few rough analyses have been carried out; but the results are encouraging. (J.B.)

12781 THE REGRESSION AND CORRELATION IN SCINTILLATION GAMMA-RAY SPECTROMETRY OF SHORT-LIVED RADIOISOTOPES. Sterlinski, Slawomir (Inst. of Nuclear Research, Warsaw). Acta Phys. Pol., 28: 533-43(Oct. 1965).

Formulas are derived for the correlation coefficient and the regression line for counts of the gamma scintillation spectrum of a short-lived radioisotope in two neighboring (nonoverlapping) channels. The relations derived can be applied in activation analysis for simultaneous measurements involved in the determination of limiting trace amounts in samples. (auth)

12782 AUTOMATIC DETERMINATION OF THE DECARBOXYLASE FOR AROMATIC AMINO ACIDS IN MOUSE LIVER. Scheuerbrandt, Guenter (Univ., Freiburg i. B.). Anal. Biochem., 13: 475-82(Dec. 1965).

An automated simultaneous determination of the total protein content and of the activity of the decarboxylase for aromatic amino acids in mouse liver is described. (auth)

12783 MODULATION TECHNIQUE FOR NEUTRON CAPTURE GAMMA RAY MEASUREMENTS IN ACTIVATION ANALYSIS. Isenhour, T. L.; Morrison, G. H. (Cornell Univ., Ithaca, N. Y.). Anal. Chem., 38: 162-7(Feb. 1966).

Neutron-capture-gamma activation analysis offers a number of reactions not available to delayed gamma activation analysis. The development of a system for using a modulated neutron beam allows cancellation of the half-life-dependent delayed gamma reactions producing a pure capture gamma spectrum. Neutron-capture-gamma activation analysis has greater inherent sensitivity than conventional activation analysis for most elements, but is presently limited by the difference in obtainable flux. (auth)

12784 DETERMINATION OF BORON BY THERMAL NEUTRON ACTIVATION ANALYSIS USING A MODULATION TECHNIQUE. Isenhour, T. L.; Morrison, G. H. (Cornell Univ., Ithaca, N. Y.). Anal. Chem., 38: 167-9 (Feb. 1966).

An activation method is provided for the quantitative determination of boron using the $^{10}B(n,\alpha)^{7m}Li$ ($T_{\frac{1}{2}} = 5 \times 10^{-14}$ sec) reaction. Gamma spectrometric measurements of the samples irradiated by a modulated neutron beam permit determination of the short-lived product. Use of an internal standard overcomes the problem of variations in reactor flux as well as the asymptotic relation between concentration and count rate for materials of high cross section. The approach is applicable to many short-lived reactions. (auth)

12785 RAPID DETERMINATION OF ^{210}Pb AND ^{210}Po IN ENVIRONMENTAL SAMPLES BY DEPOSITION ON NICKEL. Blanchard, Richard L. (Robert A. Taft Sanitary Engineering Center, Cincinnati). Anal. Chem., 38: 189-92(Feb. 1966).

A procedure for determining ^{210}Po and ^{210}Pb simultaneously in environmental samples was developed by finding the optimum conditions for the spontaneous deposition of ^{210}Po and ^{210}Bi on nickel from an HCl solution. The effects of HCl concentration, hydrazine concentration, temperature, time of deposition, surface area of the planchet, and the presence of the $HClO_4$ used to ensure oxidation of environmental samples were studied. Recoveries of ^{210}Po, ^{210}Bi, and ^{210}Pb were determined for various environmental samples spiked with a ^{210}Pb–^{210}Bi–^{210}Po standard. The average efficiencies for the deposition of ^{210}Po and ^{210}Bi were 96 ± 4 and 94 ± 3%. The average efficiency for the deposition of ^{210}Pb, determined by decay measurement, was 13 ± 2%. The ^{210}Po concentrations were determined by alpha counting. The ^{210}Pb concentrations were determined by beta counting the ^{210}Bi daughter. An

aluminum absorber was used to eliminate the ^{210}Po alpha and ^{210}Pb beta particles. (auth)

12786 MASS SPECTROMETRIC ANALYSIS OF BORON TRIFLUORIDE. Horton, J. C. (Oak Ridge Gaseous Diffusion Plant, Tenn.). Anal. Chem., 38: 198-9(Feb. 1966). (K-L-6057).

A mass spectrometer and an analytical method for measuring the abundance of the boron isotopes in boron trifluoride to a standard deviation of 0.0014 are described. Heretofore, memory prevented rapid measurements of isotopically different samples; a system was devised that reduced memory to an acceptable level at which a correction factor could be accurately determined and applied. (auth)

12787 SPECTROFLUOROMETRIC TRACE DETERMINATION OF TRIVALENT SAMARIUM, EUROPIUM, TERBIUM, AND DYSPROSIUM IN SODIUM TUNGSTATE SOLUTIONS. Alberti, Giulio; Massucci, Maria A. (CNEN, Rome. Univ., Rome). Anal. Chem., 38: 214-16(Feb. 1966).

Sodium tungstate acts as a specific reagent for enhancing the fluorescence intensity of samarium, europium, terbium, and dysprosium in aqueous solutions. Maximum fluorescence intensity is obtained by irradiating at 265 to 270 mμ, lanthanides dissolved in 0.6M sodium tungstate solution with a final pH of 9 and a temperature of 20°C. All measurements were related to the fluorescence intensity of a quinine sulfate solution. Correction for quenching by inorganic ions and conditions for decreasing positive interferences are given. The sensitivity was 10^{-1} to 10^{-3} μg/ml. (auth)

12788 SPECTROPHOTOMETRIC DETERMINATION OF RUTHENIUM WITH 1-NITROSO-2-NAPHTHOL. Kesser, Gwendolyn; Meyer, R. J.; Larsen, R. P. (Argonne National Lab., Ill.). Anal. Chem., 38: 221-4(Feb. 1966).

A spectrophotometric method was devised for determination of microgram amounts of ruthenium utilizing the reaction between 1-nitroso-2-naphthol and ruthenium tetroxide in carbon tetrachloride solution. Ruthenium was determined by measurement of the absorbance of its 1-nitroso-2-naphthol complex at 645 mμ. The molar absorptivity was 18,300. Separation from other sample constituents was accomplished by distilling ruthenium tetroxide and trapping the tetroxide in carbon tetrachloride at 0°C. The method was successfully applied to the determination of 0.005 to 0.1% ruthenium in zinc–magnesium alloys. (auth)

12789 GAS CHROMATOGRAPHIC ANALYSIS OF SOLVENT USED IN REACTOR FUEL REPROCESSING AND FISSION PRODUCT RECOVERY. Campbell, Milton H. (General Electric Co., Richland, Wash.). Anal. Chem., 38: 237-40(Feb. 1966).

Gas chromatography is a valuable technique for measuring the solvent quality of organic extractants used in reactor fuel reprocessing. Retention data and column characteristics are presented for tributyl phosphate, dibutyl butyl phosphonate, di(2-ethyl hexyl) phosphate, trioctyl phosphine oxide, tertiary amines from C_8 to C_{12}, and straight chain hydrocarbons from C_8 to C_{12}. Quantitative calibrations for each of the extractants in hydrocarbon or carbon tetrachloride diluents are discussed. Standard deviations for the calibrations are ±0.2 to ±0.3 vol% of the extractant. Detection levels of one extractant as a contaminant in another are determined. (auth)

12790 A COMPACT 1900 deg F. RESISTANCE-WOUND COMBUSTION FURNACE FOR REMOTE OPERATION. Farmelo, Donald R. (Pratt and Whitney Aircraft, Middletown, Conn.). Anal. Chem., 38: 365-6(Feb. 1966).

The furnace design is discussed and a diagram is shown. The combustion of 8 to 10 samples can be carried out without changing crucibles or interrupting the gas flow. It also has a continuous heat source. The resistor has a room temperature resistance of 0.28 ohm and requires about 20 amperes at 20 volts to maintain 1950°F. The results of several remote analyses on a niobium alloy are given. Standard steel samples were also analyzed and the average value was within 3% of the reported value. Normally, in bench-top operation, a sample can be analyzed in ~5 to 6 min. The errors can be reduced by burning larger samples and minimizing the length of the gas line between the furnace and analyzer. (F.J.H.)

12791 A METHOD FOR DETERMINING OPTIMAL LAYER THICKNESS FOR C/H-ANALYSIS BY MEANS OF NEUTRONS. Netz, V. (VEB Vakutronik WIB, Dresden). Atompraxis, 11: 670-5(Nov.-Dec. 1965). (In German).

In hydrogen determination with neutrons, measurement sensitivity is affected by the layer thickness of the substance to be measured. C/H-analysis of pure carbohydrates is taken as an example to show that the use of an optimal instead of an "infinite" layer thickness leads to a significant increase in sensitivity, and thus to a marked decrease in the margin of error. The neutron method, with its inherent advantages, can thus be used successfully for higher hydrogen concentrations as well. A procedure for determining the optimal layer thickness is proposed. (auth)

12792 POSSIBILITIES OF CAPILLARY CHROMATOGRAPHY IN THE ANALYSIS OF ISOMERS AND ISOTOPES OF HYDROGEN. Cercy, Colette; Botter, Fernande (CEN, Saclay, France). Bull. Soc. Chim. France, No. 11, 3383-90(Nov. 1965). (In French).

Studies of the analysis of isotopes of hydrogen in helium carrier in a capillary column of alumina were completed with an improvement of the detection limits and analysis of tritiated isotopic species. Two new separations were realized; an isotopic one in hydrogen carrier in a capillary column of 5 Å molecular screen and the other of the ortho and para isomers of hydrogen in a capillary column of 13 X molecular screen in helium carrier. A comparison of the theoretical and applied order was made with noncapillary chromatography and experimental data on the physical absorption and the isotopic separation factor are reported. (tr-auth)

12793 DETERMINATION OF SULFUR IN COPPER BY NEUTRON ACTIVATION. Cuypers, Marc; Le Hericy, Jacques; Cuypers, Jacqueline; Albert, Philippe (Centre National de la Recherche Scientifique, Vitry, France). Compt. Rend., 261: 5494-6(Dec. 20, 1965). (In French).

Two methods are described for determination of sulfur in copper, one by thermal-neutron activation for concentration above 10^{-6} and the other by fast-neutron activation for concentrations below 10^{-6}. These concentrations make it possible to control the elimination of sulfur from copper of various origins purified by the zone melting method. (tr-auth)

12794 NEUTRON ACTIVATION: RELATIONSHIP OF SAMPLE MASS TO SELF-SHIELDING FACTOR. Kenna, B. T.; Van Domelen, B. H. (Sandia Lab., Albuquerque, N. Mex.). Int. J. Appl. Radiat. Isotop., 17: 47-50(Jan. 1966).

The sample mass corresponding to any self-shielding factor and sample geometry can be calculated by means of a method adopted from the analytical approximation of Nisle. The validity of the method is demonstrated by its agreement with experimental data of various investigators. (auth)

12795 SAMPLE HANDLING CONVENIENCES FOR ACTIVATION ANALYSIS. Battistone, G. C.; Feldman, M. H. (Walter Reed Army Inst. of Research, Washington, D. C.). Int. J. Appl. Radiat. Isotop., 17: 74-5(Jan. 1966).

Two experimental devices used for sample handling in the activation analysis studies are described. A quick-opening rabbit that can be handled rapidly by one individual was developed. The rabbit is constructed to contain either two 0.3-ml polyethylene tubes or one ½ × 1 in. polyethylene vial. A "cartridge belt" arrangement made of worn cotton cloth, was used to index sample tubes, to keep them together, and to protect and keep intact fragile sample tubes with slip fit caps. (F.J.H.)

12796 ELECTROMETRIC STUDIES ON THE COMPOSITIONS OF URANYL VANADATES. Mittal, M. L.; Saxena, R. S. (Government Coll., Rajasthan, India). J. Inorg. Nucl. Chem., 27: 2553-9(Dec. 1965).

The stoichiometry of the compounds formed by the interaction of uranyl nitrate and different sodium vanadates (ortho-, pyro-, meta-, and poly-) were investigated by means of amperometric, pH, and potentiometric titrations. The breaks and inflections in the titration curves provided evidence for the formation of $(2.5UO_2 \cdot Na)V_2O_8$, $(1.5UO_2 \cdot Na)V_2O_7$, and $(0.5UO_2 \cdot Na)V_2O_6$ at pH ranges of 5.6 to 6.5, 4.7 to 5.5, and 4.0 to 4.6, respectively. The precipitation of $(2.5UO_2 \cdot Na)V_2O_8$ was quantitative; amperometric titrations yielded more precise results than other techniques and offer a simple, rapid, and accurate method for the determination of UO_2^{2+} ions in solutions at suitable concentrations and pH ranges. (auth)

12797 CHEMICAL ANALYSIS OF BROMINE TRIFLUORIDE. Sakurai, Tsutomu; Kobayashi, Yasuko; Iwasaki, Matae (Japan Atomic Energy Research Inst., Tokyo). J. Nucl. Sci. Technol. (Tokyo), 3: 10-13(Jan. 1966).

The chemical analysis of bromine trifluoride (BrF_3) was studied with the view to establishing a method for determining the purity of this substance, as attained by vacuum distillation. A sample was hydrolyzed in NaOH solution. The fluorine in the bromine trifluoride was converted to fluoride (F^-) by hydrolysis, and could thus be determined by thorium nitrate titration. The bromine in the bromine trifluoride was converted to bromide (Br^-), hypobromite (BrO^-), and bromate (BrO_3^-), and was determined by the Mohr method, after reducing the BrO^- and BrO_3^- to Br^- with hydrazine hydrate ($H_2NNH_2 \cdot H_2O$) A value of 2.97 ± 0.03 was obtained as ratio of fluorine to bromine for purified bromine trifluoride, and 2.84 for unpurified bromine trifluoride. Prior to analyzing the sample the conditions for reducing BrO_3^- to Br^- by hydrazine hydrate were studied, using $KBrO_3$. It was found that the alkalinity of the sample solution and the reduction temperature had considerable influence on the reduction. (auth)

12798 PHOTOPOLAROGRAPHIC BEHAVIOR OF INORGANIC DEPOLARIZERS. Durst, R. A. (Boston Coll.); Taylor, J. K. J. Res. Nat. Bur. Stand., 69A: 517-22(Nov.-Dec. 1965).

Nickel(II), cobalt(II), and uranium(VI) were studied polarographically to determine the effects of uv-visible radiation on their reduction characteristics. Photoeffects were observed in all cases. Two mechanisms are proposed for the nickel photokinetic prewave, and the complex photoeffects observed with cobalt and uranium are described. (auth)

12799 SOME PROBLEMS IN THE DETERMINATION OF URANIUM WITH ARSENAZO III. Mohai, Miklos; Upor, Endre; Jurcsik, Istvan (Mecsek Ore Mining Enterprise, Pecs, Hungary). Magyar Kem. Foly., 71: 334-8(Aug. 1965). (In Hungarian).

Determination of uranium in ores containing low concentrations of uranium by a method based on the photometry of the uranium(IV)–Arsenazo-III complex is reported. Experience gained in the use of this method is described. A method suitable for utilizing liquid-phase reduction and reduction with titanium(III) was developed. Elements interfering with the determination are titanium, thorium, iron, and phosphorus. Their removal is discussed. (20 references) (CFSTI)

12800 DETERMINATION OF THE ^{18}O CONTENT IN SMALL SAMPLES OF WATER BY MASS SPECTROMETRY UTILIZING THE EQUILIBRIUM REACTION BETWEEN WATER AND CARBON DIOXIDE. Tamas, Jozsef; Opauszky, Istvan (Eotvos Lorand Univ., Budapest). Magyar Kem. Foly., 71: 352-6(Aug. 1965). (In Hungarian).

The method used for ^{18}O determination in H_2O is based essentially on the Brodskii technique modified to make it suitable for small samples (10 to 15 mg) and substituting the room-temperature equilibrium reaction between water and carbon dioxide for the high-temperature isotope-exchange reaction. While this method takes longer (a determination takes up to 24 hr), it is more reproducible and simpler than the original technique. (CFSTI)

12801 MEASUREMENT OF ISOTOPES EMITTING SOFT β RADIATION WITH THE AID OF A LIQUID SCINTILLATOR IN A SINGLE-CHANNEL MEASURING INSTRUMENT. PART 3. MEASUREMENT OF THE ^{14}C ISOTOPE WITH THE AID OF AN OPTICAL FILTER. Levay, Bela; Csanyi, Piroska (Eotvos Lorand Univ., Budapest). Magyar Kem. Foly., 71: 356-60(Aug. 1965). (In Hungarian).

The optimum parameters for the measurement of ^{14}C with the aid of a mass spectrometer equipped with an optical filter were determined. Detection sensitivity under optimum conditions was 0.5×10^{-6} μC/ml using a 16-ml sample and a measuring time of 300 sec. (CFSTI)

12802 COLORIMETRIC DETERMINATION OF VANADIUM IN URANIUM COMPOUNDS USING p-METHOXYBENZOTHIOHYDROXAMIC ACID. Skorko-Trybula, Zofia (Katedra Chemii Analitycznej Politechniki, Warsaw). Nukleonika, 10: 559-65(1965). (In Polish).

The extraction and colorimetric determination of vanadium in uranium compounds are described. Vanadium with p-methoxybenzothiohydroxamic acid forms, in 6N hydrochloric acid, the green compound that is extractable into chloroform and higher alcohols. The sensitivity of the reaction is equal to 0,002 μg V/cm^2 and the molar absorption coefficient equals to 20040 (λ = 372 mμ). Ti, Fe, Mo, and Nb ions interfere with the determination of vanadium. A rapid method of eliminating the influence of these ions is described. This method was used successfully for the analysis of uranyl acetate and nitrate and U_3O_8 containing 10^{-3} to 10^{-4}% vanadium. (auth)

12803 A SEPARATION PROCESS FOR GENERAL USE IN ACTIVATION ANALYSIS. PART I. Gebauhr, W. (Siemens Schuckert Werke AG, Erlangen, Ger.). Radiochim. Acta, 4: 191-7(Dec. 1965). (In German).

Activation analysis of impurities in very pure materials nearly always necessitates their chemical separation. Because samples are often small, and costly, as many components as possible have to be determined in one run. A system of chemical separations is proposed, which applies to several matrices (main substances) and more than 30 elements along with the rare earth group. The separation reactions used were tested with the aid of radionuclides. The behavior of the elements is described. The final analytic method was checked on two test mixtures. (auth)

12804 MEASUREMENT OF LOW-ENERGY β EMITTERS IN HETEROGENEOUS PHASES WITH LIQUID SCINTILLATORS. Hoffmann, W. (Farbwerke Hoechst AG, Frankfurt am Main). Radiochim. Acta, 4: 222-4(Dec. 1965). (In German).

Examples of determining radioactive materials in heterogeneous phases by liquid scintillators are given, one with a suspension of polymer scintillator in ^3H- and ^{14}C-containing water and another with a sample suspension in the scintillator solution ($BaCo_3$-^{14}C, ^3H-labeled polymers after dispersion in toluene/Aerosil). Measuring activities in heterogeneous phases may have certain advantages over the determination in the liquid phase: insoluble compounds and substances with high fluorescence quenching can often be determined with sufficient counting rate. (auth)

12805 NEUTRON ACTIVATION ANALYSIS OF DIVALENT IONS IN ALKALI HALIDE CRYSTALS. Okada, Touichi (Osaka Univ.); Ikeya, Motoji; Suita, Tokuo; Kawai, Keiji. Radioisotopes (Tokyo), 15: 14-18(1966).

A quantitative analysis of impurities in the alkali halide single crystals was carried out using neutron activation methods for both the nominal pure and doped crystals. Barium and manganese ion impurities could be determined up to 2.3×10^{-4} and 1.5×10^{-5} mol percent in KCl crystals, and 9.6×10^{-4} and 3.9×10^{-5} mol percent in NaCl crystals with chemical separation and 4.6×10^{-2} mol percent in NaCl crystals with nondestructive analysis. Results of the analyses showed that the impurity content

varies with a position of a single crystal obtained by Kyropoulos method and is less than amount of impurity added to the melt. The distribution of the impurities in the zone refined ingot was also determined. The results were used to investigate impurity effect on the hardening and the coloration phenomena. (auth)

12806 SPECTROMETRIC DETERMINATION OF RARE EARTHS WITH 2-(p-SULPHOPHENYL-AZO)-1,8-DIHYDROXYNAPHTHALENE-3,6-DISULPHONIC ACID (SPADNS). Spacu, P.; Antonescu, E.; Plostinaru, S. (Inorganic Chemistry Research Center, Bucharest). Rev. Roum. Chim., 10: 843-8(Sept. 1965).

Rare earths compounds with SPADNS were studied. By applying Job's method it was found that, in solution, compounds having the ratio 1 : 2, $[Me(SPADNS)_2]^-$, are formed. (auth)

12807 EXPERIENCE WITH SPECTROSCOPIC ^{15}N DETERMINATION WITH USE OF A STEP FILTER FOR A Q24 ZEISS SPECTOGRAPH. Sommer, K.; Kick, H. (Univ., Bonn). Z. Anal. Chem., 214: 415-22(1965). (In German).

The selection of step-filters and possible systematic errors in spectrographic determination of 0.38 to 15.00% ^{15}N in gases are discussed. For this range of concentration a 6 step-filter is recommended with optical transmissions of 100.00, 39.00, 14.00, 5.00, 1.80, and 0.70%. In discussion of possible errors emphasis was placed on the superimposed bands at high concentrations of ^{15}N when spectrographs with relatively small resolving power are used. (auth)

12808 SOME ANALYTICAL ASPECTS OF THE CHEMISTRY OF TECHNETIUM [Thesis]. Hirsch, Roland Felix. Ann Arbor, Mich., Univ. of Michigan, 1965. 108p.

Two important aspects of technetium chemistry have been investigated: the acid-base behavior of the plus seven oxidation state and the reactivity of several oxidation levels with 8-quinolinol. Technetium(VII) is the highest oxidation state of this element. The acid $HTcO_4$, pertechnic acid, is a strong acid, completely dissociated in dilute solutions. The dissociation constant is shown to be large by the potentiometric method, and at least five by the spectrophotometric method of determining dissociation constants. The peracid of rhenium was also investigated. The perrhenate ion appears to be more stable in strong sulfuric or perchloric acid solutions than is the pertechnetate ion. Also, perrhenic acid is as efficient a catalyst for the hydrolysis of sucrose as is hydrobromic acid, and a better catalyst than is hydrochloric acid. Chelates of technetium(IV) and rhenium(IV) with 8-quinolinol (oxine) were prepared, and several methods are described for obtaining them. They are stable over a wide pH range. The complexes have interesting infrared spectra, with a very strong band at 1030 cm^{-1} that does not appear in the spectra of the other oxinates investigated. The properties of the Tc(IV) and Re(IV) oxinates suggest that these complexes contain oxygen atoms other than those in the ligand. The non-reactivity of technetium(VII) with oxine under all normal, and some rather extreme, conditions was established. The existence of an extractable, but oxidation-sensitive, compound of a lower state (II or III) of technetium with oxine is indicated. The analytical applications of these oxinates are discussed, and schemes for the rapid isolation of technetium from complicated mixtures, such as the fission products, are suggested. (Dissertation Abstr.)

12809 INVESTIGATION OF THE ANALYTICAL CHEMISTRY OF TECHNETIUM [Thesis]. Pacer, Richard Arnold. Ann Arbor, Mich., Univ. of Michigan, 1965. 139p.

Possible structural changes in the Tc(VII) species considered include a tetrahedral to octahedral change in coordination, polymer formation, mesopertechnetate formation, formation of a cationic Tc(VII) species, and formation of undissociated $HTcO_4$. Evidence indicating that the only significant Tc(VII) species is the tetrahedral pertechnetate ion includes the conformity of Tc(VII) to Beer's Law, constancy of the uv absorption spectrum of Tc(VII) over a wide pH range, and relative constancy of the distribution coefficient in a liquid-liquid extraction study. The features of pertechnetyl chloride are studied in rejecting the possibility of cationic Tc(VII) species. The reported red species of Tc occurring in concentrated $HTcO_4$ solutions is explained in terms of the occurrence of some reduction where the red coloration does not characterize a (VII) species. The coulometric reduction of Tc is undertaken in an attempt to prepare a Tc(III) oxide; all attempts to isolate an oxide from the products failed. Technetium dioxide was the sole oxide obtained. Titration curves are given for a number of potentiometric titrations of Tc(VII), all based on prereduction to Tc(IV) followed by oxidation with ceric sulfate. No direct titration was found to be practical. Zinc metal, stannous chloride, and sodium sulfite gave the most promising results of the reagents tested. The proposed technetate(VI) state is supported by spectrophotometric studies and the isolation of a barium salt. Aqueous phosphate solutions of Tc(III) were prepared and the species further characterized. The electrodeposition of Tc into Hg resulted in a finely dispersed deposit of metal rather than a true solution. (A.G.W.)

12810 L'ANALYSE SPECTROGRAPHIQUE D'EMISSION. INFLUENCE DES ATMOSPHERES GAZEUSES. APPLICATIONS AUX TERRES RARES. (Emission Spectrographic Analysis. Effect of Gaseous Atmospheres. Applications to the Rare Earths). Vilnat, Jacqueline. Supplement au Bulletin de la Societe Francaise Ceramique No. 67, Avril–Juin 1965. Memoires de la Societe Francaise de Ceramique, Centre National d'Etudes et Recherches Ceramiques. Paris, Societe Francaise de Ceramique, 1965. 140p.

The value of certain quantitative spectrographic analysis methods for high and low concentrations was investigated in several nonconducting samples. The effects of various atmospheres on the results were also studied. After a review of various devices and methods used, a statistical study for the quantitative analysis of silica and aluminum is given. The results obtained chemically and spectrographically are compared. The distribution of the individual results seemed to indicate the existence of a systematic error. The imprecision of the results came from the emission conditions more than from the calibration. It is emphasized that spectrographic analysis is not a method for the determination of high concentrations but a technique for determination of trace amounts. Different devices used to obtain a controlled atmosphere in the electrode gap are described. The blower electrode and the double injector furnish the best results. They allow the suppression of cyanogen bands. In a helium atmosphere it was possible to excite, in the continuous arc, the halogens, sulfur, and selenium. Tests made with a plasma jet confirmed observations made with continuous arc for the various gases used. A method is given for the determination of rare earths in glasses. It is based on the use of solutions containing internal standards and using fused graphite electrodes. The determination of 100 to 50,000 ppM Y, La, Ce, Pr, and Sm and of 500 to 50,000 ppM Nd was accomplished. The precision was acceptable, especially for Ce, La, and Y. In order to suppress the cyanogen bands and to regulate the emission, the blower electrode or the double ejector was used in the Ar atmosphere. (tr-auth)

12811 DETERMINATION OF PLUTONIUM BY DOUBLE-TRACER ISOTOPIC DILUTION: APPLICATION TO BURN-UP MEASUREMENTS. Chenouard, J.; Lucas, Monique (CEN, Saclay, France). pp 63-74 of STI/PUB/105(Vol. II). (In French).

The plutonium content of irradiated fuels can be determined by isotopic dilution using a solution containing both uranium-233 and plutonium-242. The measurement method, its calibration, the solution preparation techniques, and analysis by mass spectrometry are described. The chemical treatment involves a valence cycle which should give homogeneous distribution of the isotopes in the tracer-sample mixtures and a suitable U/Pu separation. The

presence of excess uranium greatly changes the plutonium redox kintics. The stability of the thermo-ionic emission of Pu in relation to the amount of residual uranium is improved, resulting in more accurate analyses. Isotopic contamination is eliminated to the maximum extent. The tracer is calibrated using a standard solution prepared from weighed quantities of plutonium and uranium of known chemical purity. The use of an electronic computer shortens the calculations and simplifies the checking of results. The uranium-235 burnup in the fuel is measured by isotopic analysis of the metal converted into uranium hexafluoride. The plutonium content is determined with an accuracy of 2%. The ^{235}U depletion is measured to within $\pm 5 \times 10^{-4}$. (auth)

12812 THE NON-DESTRUCTIVE DETERMINATION OF BURN-UP BY MEANS OF THE ^{144}Pr 2.18 Mev GAMMA-ACTIVITY. Forsyth, R. S.; Blackadder, W. H. (Aktiebolaget Atomenergi, Studsvik, Sweden). pp 399-411 of STI/PUB/105(Vol. II).

Experiments carried out to calibrate a gamma scanner for quantitative measurements by counting the 2.18-Mev gamma activity due to ^{144}Pr, the short-lived daughter of ^{144}Ce($T_{\frac{1}{2}}$ 285 d) from selected pellets in several UO_2 fuel specimens are described. Accurate burnup values were determined by dissolution and application of the isotopic dilution method using stable molybdenum fission products. The elements, which were rotated about their longitudinal axes to minimize asymmetry effects, were viewed by a sodium iodide crystal and a multichannel analyzer through a suitable collimator. Correction for attenuation of the gamma activity (much less than for 0.75 Mev) in the fuel elements which were of different diameters (12.6 to 15.04 mm) was made by applying relative attenuation factors, and the effective geometry factor of the instrument was determined. In order to check the corrections applied, the counter factor was also calculated for the 0.75-Mev activity from $^{95}Zr/^{95}Nb$, and in certain cases for the 0.66-Mev activity from ^{137}Cs. The results obtained demonstrate that, at least over the range of diameters and cooling times used, the method is suitable for quantitative determinations. Preliminary experiments to explore the possibility of using the high energy gammas (2.35, 2.65 Mev) from ^{106}Rh as a method for estimating the fraction of fission events which have taken place in the ^{239}Pu formed during irradiation were also carried out. Determination of the relative intensities of the gammas suggests that the method is of only limited application. (auth)

12813 IMPROVEMENTS IN INSTALLATIONS FOR THE SPECTROPHOTOMETRIC QUANTITATIVE ANALYSIS OF RADIOACTIVE SOLUTIONS. Chazot, Henri; Garcia, Gilbert; Maria, Alain; Vacher, Robert (to Commissariat a l'Energie Atomique). British Patent 1,015,777. Jan. 5, 1966. Priority date July 6, 1962, France.

An installation for the spectrophotometric analysis of radioactive solutions includes three shielded enclosures, two adjacent to each other and connected by an air lock and a pivotal gate arrangement and the third above and in communication with one of the other two through a hole in the roof. One of the enclosures includes remote handling equipment such as pipets for sampling the materials and any other sample preparation. The unmodified spectrophotometer is located in the enclosure with a third enclosure above it. Samples are transferred through the gate and air lock into a funnel arrangement in the upper enclosure and there into an analysis tank. This tank is lowered by a hoist into a sealed casing communicating with the shielded enclosure. The sealed casing has optical ports centered on the optical path of the spectrophotometric light beam and is made to fit exactly into the volume of the spectrophotometer designed to receive the samples. With this arrangement the spectrophotometer is located in its own enclosure for shielding purposes but is completely isolated from the contamination and may be removed at any time for repairs or other uses. (B.L.M.)

12814 METHOD AND APPARATUS FOR MEASURING FISSIONABLE ISOTOPE CONCENTRATION. Einfeld, Klaus (to Interatom). U. S. Patent 3,222,521. Dec. 7, 1965. Priority date Oct. 17, 1959, Germany.

A non-destructive method is described for measuring the concentration of at least two fissionable isotopes of elements selected from the group consisting of Th, U, and Pu in a sample. The sample is sequentially irradiated with a number of neutron spectrums, the number of spectrums being equal to the number of isotopes to be measured and each spectrum having a different energy. After each irradiation, the number of fissions resulting from each radiation are sequentially counted, and each of the counts is compared as a function of the fission cross section of the isotope for the particular average energy of each neutron spectrum. (B.L.M.)

Inorganic and Physical Chemistry

Refer also to abstract 14169.

12815 (ANL–7025) CRITICAL TEMPERATURES AND DENSITIES OF THE ALKALI METALS. Dillon, Ira G.; Nelson, P. A.; Swanson, B. S. (Argonne National Lab., Ill.). Aug. 1965. Contract W-31-109-eng-38. 67p. Dep. mn. CFSTI $3.00 cy, $0.75 mn.

The results showed that the alkali metals deviate somewhat from the "law of corresponding states" based on nonmetallic substances. Also, the behavior of alkali metals was found to be somewhat different from that of mercury in that the shape of the density vs temperature curves is different and the entropy of vaporization is lower than that of mercury at reduced temperatures above 0.5. (131 references). (P.C.H.)

12816 (BNWL–158) ELECTROCHEMISTRY OF PLUTONIUM(III) IN MOLTEN ALKALI CHLORIDES. Nissen, D. A. (Battelle-Northwest, Richland, Wash. Pacific Northwest Lab.). Nov. 1965. Contract AT(45-1)-1830. 8p. Dep. mn. CFSTI $1.00 cy, $0.50 mn.

Chronopotentiometric and cyclic voltametric techniques were used to study the electrochemical reduction of Pu(III) to the metal in molten chloride solutions, in particular, the eutectic LiCl/KCl system. A postulated mechanism for the cathodic reduction of Pu(III) in this melt system as well as information on its diffusion properties are presented. The results showed that Pu(III) exhibits dissimilar behavior as the temperature of the melt is changed. At 400°C a characteristic function, the $i_0\tau^{\frac{1}{2}}$ product, is invariant with current density. At higher temperatures this function changes as the current density changes. It would appear on this basis that at 400°C plutonium, possibly in the form of a complex molecule, undergoes direct reduction to the metal. At temperatures in excess of 400°C, an equilibrium apparently exists between two complex species of plutonium; and the rate of transformation from one form to another is the rate controlling step. (P.C.H.)

12817 (IS–1311) THE STABILITY CONSTANTS OF RARE EARTHS WITH SOME CARBOXYLIC ACIDS. Schoeb, Virginia R.; Powell, Jack E. (Ames Lab., Iowa State Univ. of Science and Tech.). Jan. 1966. Contract W-7405-eng-82. 83p. Dep. mn. CFSTI $3.00 cy, $0.75 mn.

The stepwise formation constants for complexes between yttrium, lanthanum, and the rare earths, except promethium, and the ligands quinate, mandelate, and dilactate were measured at 25°C and the ionic strength of 0.1M ($NaClO_4$). They were determined potentiometrically using a Beckman Research pH meter. Optimum values of the successive equilibrium constants were computed via a least squares technique using an IBM-7074 computer. The presence of hydroxyl groups enhanced the stability of rare-earth quinates over rare-earth 1-hydroxycyclohexanecarboxylates. The mandelates in solution could be nine-coordinated in the case of the light rare earths and either eight- or nine-coordinated in the case of the heavy rare earths, with mandelate acting bidentately throughout. Dilactic acid seemed to be at least a tridentate ligand if not a pentadentate ligand. 92 references are cited. (auth)

12818 (IS-T-52) PARTIAL MOLAL HEAT CAPACITIES OF SOME AQUEOUS RARE-EARTH CHLORIDE SOLUTIONS AT 25 deg C [Thesis]. Jones, Kenneth Cecil (Ames Lab., Iowa State Univ. of Science and Tech.). Nov. 1965. Contract W-7405-eng-82. 86p. Dep. mn. CFSTI $3.00 cy, $0.75 mn.

An adiabatic calorimeter was designed and built to measure the specific heats of aqueous solutions at 25°C with a precision of at least 0.05%. Specific heats were determined for a number of aqueous solutions of lanthanum, neodymium, dysprosium, erbium, and ytterbium chlorides at 25°C. The concentration range covered was from 0.1 molal to saturation (approximately 4.0 molal). From the specific heat data, apparent molal heat capacities were calculated for each of the rare-earth chloride solutions. Partial molal heat capacities of the solute and solvent were calculated for each rare-earth salt from these polynomial equations. The apparent molal heat capacity data obtained indicate the rare earths may be divided into two subgroups at moderate concentrations, with the heavy rare earths belonging to one group and the light rare earths to another. This behavior was qualitatively explained by assuming that the heavy rare-earth ions have a lower coordination number for water than the light ones, and evidence to support this assumption was presented. The partial molal heat capacities showed possible evidence for complex-ion formation near saturation. (J.B.)

12819 (IS-T-53) THE STRUCTURES OF THE ETHYL GRIGNARD REAGENT IN DIETHYL ETHER AND A TROPONOID PHOTO-OXIDATION PRODUCT [Thesis]. Guggenberger, Lloyd Joseph (Ames Lab., Iowa State Univ. of Science and Tech.). Nov. 1965. Contract W-7405-eng-82. 103p. Dep. mn. CFSTI $4.00 cy, $0.75 mn.

The structure of the ethyl Grignard reagent in ethyl ether, $EtMgBr \cdot 2Et_2O$, was determined by x-ray diffraction techniques. This compound crystallizes in the monoclinic space group $P2_1/c$ with cell parameters $a = 13.18 \pm 0.03$, $b = 10.27 \pm 0.03$, $c = 11.42 \pm 0.03$Å, and $\beta = 103.3 \pm 0.3$Å. A single crystal was grown from the liquid and the data recorded at about −75°C. The structure consists of ethylmagnesium bromide monomers with the ethyl group, a bromine atom, and two ether molecules forming a somewhat distorted tetrahedron about a single magnesium atom. Pertinent structural features are short Mg−O bonds (2.04Å), trigonal bonding about the oxygen atoms, and the configuration of the ether methyl groups where the methyl groups are rotated out of the ether planes with one methyl carbon forward and the other back. The troponoid photooxidation product $C_{16}H_{11}O_3Cl$, was prepared from 2-(p-chlorophenoxy)-4,5-benztropone ($C_{17}H_{11}O_2Cl$). This compound crystallizes in the orthorhombic space group $P2_12_12_1$ with cell parameters $a = 13.21 \pm 0.02$, $b = 13.80 \pm 0.02$, and $c = 7.33 \pm 0.02$Å. The structure of $C_{16}H_{11}O_3Cl$ was solved using image-seeking methods. (P.C.H.)

12820 (IS-T-57) THE TRANS-EFFECT IN HYDROLYSIS REACTIONS OF TRICHLOROAMMINEPLATINATE(II) ION [Thesis]. Tucker, Mary Ann (Ames Lab., Iowa State Univ. of Science and Tech.). Aug. 1965. Contract W-7405-eng-82. 79p. Dep. mn. CFSTI $3.00 cy, $0.75 mn.

The acid and base hydrolyses for trichloroammineplatinate(II) ion were followed spectrophotometrically. Both reactions are reversible in high chloride solution at pH <4. The six rate constants characterizing the three reactions were evaluated for both 20 and 25°C. $(PtNH_3) + H_2O \underset{k_{-t}}{\overset{k_t}{\rightleftharpoons}} \underline{trans}\text{-}[Pt(NH_3)Cl_2(H_2O)] + Cl^-$, $[Pt(NH_3)Cl_3]^- + H_2O \underset{k_{-c}}{\overset{k_c}{\rightleftharpoons}} \underline{cis}\text{-}[Pt(NH_3)Cl_2(H_2O)] + Cl^-$, and $\underline{trans}\text{-}[Pt(NH_3)Cl_2(H_2O)] \underset{k_{ct}}{\overset{k_{tc}}{\rightleftharpoons}} \underline{cis}\text{-}[Pt(NH_3)Cl_2(H_2O)]$. At 20°C $k_t = 0.40 \times 10^{-5}$ sec^{-1}, $k_{-t} = 30.55 \times 10^{-5}$ sec^{-1}, $k_c = 3.06 \times 10^{-5}$ sec^{-1}, $k_{-c} = 2690 \times 10^{-5}$ sec^{-1}, $k_{tc} = 0.43 \times 10^{-5}$ sec^{-1}, and $k_{ct} = 5.56 \times 10^{-5}$ sec^{-1}. At 25°C $k_t = 0.63 \times 10^{-5}$ sec^{-1}, $k_{-t} = 48.0 \times 10^{-5}$ sec^{-1}, $k_c = 5.6 \times 10^{-5}$ sec^{-1}, $k_{-c} = 4300 \times 10^{-5}$ sec^{-1}, $k_{tc} = 0.75 \times 10^{-5}$ sec^{-1}, and $k_{ct} = 7.5 \times 10^{-5}$ sec^{-1}. The last reaction is considered to occur via the acid hydrolysis of each isomer to $\underline{cis}\text{-}[Pt(NH_3)Cl(H_2O)_2]^+$. The assigned rate constants account for the chloride-exchange rates. The significance of the results to the quantitative expression of the cis and trans effects is discussed. (auth)

12821 (IS-T-62) A PHASE STUDY OF THE DYSPROSIUM–DYSPROSIUM(III) CHLORIDE SYSTEM [Thesis]. McCollum, Bill Crews (Ames Lab., Iowa State Univ. of Science and Tech.). Nov. 1965. Contract W-7405-eng-82. 41p. Dep. mn. CFSTI $2.00 cy, $0.50 mn.

Phase studies on the salt rich portion of the dysprosium-dysprosium(III) chloride system indicated the formation of two new subchlorides which may be formulated $DyCl_{2.1\pm0.03}$ and $DyCl_2$. Both subchlorides are black and are salt-like in that crude conductivity measurements showed high resistance values, thus eliminating possible formulations involving free electrons such as $Dy^{+3}(e^-)(Cl^-)_2$. Cryoscopic data are consistent with the dissolution of Dy in $DyCl_3$ as monomeric Dy^{+2} ions. Powder patterns indicated that the structures are closely related and the structure of $DyCl_2$ is isostructural with that of $YbCl_2$. (57 references). (auth)

12822 (IS-T-68) ISOTOPIC EXCHANGE STUDY OF TUNGSTEN IN A SODIUM METATUNGSTATE–SODIUM ORTHOTUNGSTATE AQUEOUS SYSTEM [Thesis]. Jones, Yvonne Marie (Ames Lab., Iowa State Univ. of Science and Tech.). Aug. 1965. Contract W-7405-eng-82. 58p. Dep. mn. CFSTI $3.00 cy, $0.50 mn.

Isotopic exchange was studied for ^{185}W between the orthotungstate ion, WO_4^{-2}, and the metatungstate polymeric ion, $[H_2W_{12}O_{40}]^{-6}$ in unbuffered solutions of their sodium salt. Under these conditions, pH > 6.5 at 25°C, the metatungstate ion was slowly decomposed into the WO_4^-. No isotopic exchange was detectable in a period of 720 hours, and an upper limit to a second order exchange rate constant can be set as 1.3×10^{-7} M^{-1} sec^{-1}. (auth)

12823 (LA-3391) MOLECULAR AND PRINCIPAL SERIES ABSORPTION IN CESIUM–ARGON MIXTURES. Sollid, J. E. (Los Alamos Scientific Lab., Univ. of California, N. Mex.). Sept. 17, 1965. Contract W-7405-eng-36. 24p. Dep. mn. CFSTI $2.00 cy, $0.50 mn.

An experimental study of the absorption spectrum of cesium-argon gaseous mixtures was made. Cesium pressures ranged from 1 to 5 torr and argon pressures from 5 to 1520 torr. The absorption intensities of the cesium principal-series resonance lines were observed to decrease with increasing argon pressure, but cesium molecular absorption remained unchanged. It was concluded that the change in line intensities is not due to an argon-induced change in the cesium vapor pressure. Quantitative results are given for molecular absorption. Line broadening effects in cesium are discussed. A bibliography with 55 references to works on molecular structure, line broadening, and foreign gas effects is presented. (auth)

12824 (LA-DC-6749) SPECTRA OF ION EXCHANGERS CONTAINING ABSORBED COBALT(II) CHLORIDE; TRANSITIONS BETWEEN OCTAHEDRAL AND TETRAHEDRAL SPECIES. Coleman, James S. (Los Alamos Scientific Lab., Univ. of California, N. Mex.). [1964]. Contract W-7405-eng-36. 17p. Dep. mn. CFSTI $1.00 cy, $0.50 mn.

The spectrum of chloride-form anion exchanger containing absorbed cobalt established that the Co(II) is octahedrally coordinated when the resin is equilibrated over water. Equilibration over concentrated HCl solutions or air-drying transforms the Co(II) to the tetrahedrally coordinated species, $CoCl_3^-$. The spectrum of cation exchanger containing Co(II) changes from that of $Co(H_2O)_6^{2+}$ to that of a tetrahedral species, probably $Co(H_2O)Cl_3^-$, when equilibrated with vapors from M HCl. Spectra were obtained using discs cut from single beads of the ion exchangers. (auth)

12825 (NYO-2082-1) DENSITIES, VOLUMES, EXPANSION, COMPRESSIBILITY AND PRESSURE COEFFICIENTS AND DERIVED FUNCTIONS OF METALLIC MERCURY FOR ITS ENTIRE LIQUID RANGE, i.e., FROM ITS MELTING POINT TO ITS CRITICAL POINT. Grosse, Aristid V. (Temple Univ., Philadelphia, Pa. Research Inst.). May 3,

1965. Contract AT(30-1)-2082. 124p. Dep. mn. CFSTI $4.00 cy, $1.00 mn.

The volumetric behavior of mercury is described over its entire liquid range, from its melting point to its critical point, along the saturation line, as a function of temperature and pressure for both liquid and saturated vapor. Partial derivatives and the coefficients of expansion, compressibility, and pressure are given, both for liquid and saturated vapor, over the entire liquid range for the first time. Various derived properties of liquid mercury, such as kinetic pressure, C_p-C_v, C_p and C_v, $\beta_{(adiab.)}$, the sound velocity, and the Gruneisen constant were estimated over the entire liquid range. Numerical data of various functions are collated. (auth)

12826 (SC-RR-65-569) THE COMBUSTION AND EXPLOSION OF ZIRCONIUM DROPLETS IGNITED BY FLASH HEATING. Nelson, L. S. (Sandia Corp., Albuquerque, N. Mex.). Jan. 1966. Contract AT(29-1)-789. 58p. Dep. mn. CFSTI $3.00 cy, $0.75 mn.

The method of flash heating was applied to single zirconium droplets (diameters between 49 and 525 microns) in air, oxygen, and various mixtures of oxygen with argon and nitrogen. The brightly burning droplets were studied during free fall by still and high-speed photography, transmission grating spectroscopy, and pyrometry. Droplets were also quenched in liquid argon at various stages in the combustion and studied by photomicrography, ultramicro weighings, and x-ray diffraction. Durations of incandescence in liquid argon were also measured. The chemical and physical changes of the droplets were determined at various stages in the combustions. Particular emphasis was placed on understanding the curious explosions of some droplets a few hundred milliseconds after ignition. It was concluded that the overall burning reaction is Zr (liquid) + O_2 (gas) → ZrO_2 (liquid). However, if nitrogen is present in the oxidizer (as in air or other oxygen-nitrogen mixtures) or in the metal (as an impurity or intentionally alloyed), the reaction has intermediate stages. An analogous set of reactions may hold for carbonaceous contaminants in the combustion, where CO instead of N_2 is the driving gas. Explosions occur also with hydrogen, but only as a result of thermal overpressure in the metal as it ignites. No appreciable oxidation is necessary as in the nitrogen situation. The experiments described rule out previously proposed mechanisms for explosion of zirconium droplets—those that rely solely upon the interaction of condensed phases or upon boiling of either the metal or its oxide. Other metallic materials that explode during combustion as droplets are discussed. (74 references). (P.C.H.)

12827 (TID-21583) THE SOLUBILITY OF HELIUM IN LIQUID LITHIUM AND POTASSIUM. Slotnick, H.; Cleary, R. E.; Kapelner, S. M. (Pratt and Whitney Aircraft, Middletown, Conn. Connecticut Advanced Nuclear Engineering Lab.). Jan. 25, 1965. Contract AT(30-1)-2789. 22p. Dep. mn. CFSTI $1.00 cy, $0.50 mn.

The solubility of helium in lithium and potassium was determined to 871 and 704°C, respectively and pressures to 3 atmospheres. Solubilities of the noble gas in both liquid metals are presented as functions of temperature and pressure. A hole model of the solution process is presented and compared with experimental results in terms of the total enthalpy of the gas in solution. A thermodynamic treatment of the system is also given in an effort to predict actual solubilities. (auth)

12828 (TID-21587) TRENDS IN TRANSITION METAL ION-LIGAND COVALENCY FROM NMR CONTACT SHIFTS. Wayland, Bradford B.; Drago, Russell S. (Noyes Lab. of Chemistry, Univ. of Illinois, Urbana). [1964]. Contract AT(11-1)-758. 24p. Dep. mn. CFSTI $1.00 cy, $0.50 mn.

NMR contact shifts are reported for a series of transition metal ion complexes of hexamethylphosphoramide. Evidence is reported to indicate that several of these complexes exist as tetrahedral complexes in the solvent nitrobenzene. The effect of excess ligand on the species in solution is investigated. The contact shifts also indicate that pronounced changes occur when several of the complexes are dissolved in some acidic and basic solvents. The NMR contact shifts of the tetrahedral complexes are interpreted as indicating an increase in covalent bonding ability for the series Mn(II) < Fe(II) < Co(II) < Ni(II) < Cu(II). The electron spin-nuclear spin coupling constants were found to correlate with the respective metal ion ionization potentials and with the first formation constant for some oxygen donors with the respective metal ions. (auth)

12829 (TID-22502) THE DISSOCIATION PRESSURE OF THE SYSTEM YTTERBIUM-YTTERBIUM DIHYDRIDE [Thesis]. Cho, Tong Y.; Gibb, T. R. P. Jr.; Messer, C. E. (Tufts Univ., Medford, Mass. Dept. of Chemistry). [1964]. Contract AT(30-1)-1355. 13p. Dep. mn. CFSTI $1.00 cy, $0.50 mn.

Submitted by Tong Y. Cho.

The equilibrium hydrogen dissociation pressure of the system $Yb-YbH_n$, n ranging from 0 to 1.82, was measured from 600 to 750°C and from 0.1 to 760 mm pressure, by a modified Sieverts technique. The standard type of metal-hydride behavior was found. One phase regions of composition were found for $n < 0.10-0.28$ and for $n > 1.80$. The intermediate plateau pressure may be represented by the equation: $\log P_{atm} = -9656/T°K + 7.396$. This gives plateau pressures identical with those of the $Ca-CaH_2$ system to ±2% over the temperature range. (auth)

12830 (UCRL-7802) VAPOR PRESSURE AND EVAPORATION COEFFICIENT STUDIES OF THE BERYLLIUM NITRIDE DECOMPOSITION REACTION. Hoenig, Clarence L.; Searcy, Alan W. (Lawrence Radiation Lab., Univ. of California, Livermore). Oct. 1, 1964. Contract W-7405-eng-48. 20p. Dep. mn. CFSTI $1.00 cy, $0.50 mn.

Beryllium nitride vaporizes congruently in the temperature region 1640-1950°K according to the reaction $Be_3N_{2(c)} = Be_{(g)} + N_{2(g)}$, where the equilibrium nitrogen pressure, in atmospheres of nitrogen, is given by the expression $\log P_{N_2} = -1.898 \times 10^4\ T^{-1} + 6.213$. The measured enthalpy of decomposition yields an enthalpy of information for $Be_3N_{2(c)}$ of −136 ± 5 kcal/mole. Beryllium nitride has an evaporation coefficient upper limit of 0.001. The Langmuir enthalpy of activation (430.2 ± 6.8 kcal/mole) of a porous (~18% porosity) specimen was about 17% greater than the equilibrium enthalpy. The second law entropy for Langmuir evaporation (ΔS°_{298} = 122.0 ± 4 cal/mole-°K) was slightly less than the calculated equilibrium entropy (ΔS°_{298} = 131.4 ± 2 cal/mole-°K). (auth)

12831 (UCRL-16516) THE ABSORPTION SPECTRUM OF Cf^{+3} AND CRYSTALLOGRAPHY OF CALIFORNIUM SESQUIOXIDE AND CALIFORNIUM TRICHLORIDE [Thesis]. Green, J. L. (Lawrence Radiation Lab., Univ. of California, Berkeley). Nov. 1965. Contract W-7405-eng-48. 95p. Dep. mn. CFSTI $3.00 cy, $0.75 mn.

Procedures used for the purification of approximately 6 μg of ^{249}Cf are described in detail as are the analytical techniques used for purity evaluations. A detailed discussion is given of the techniques that were developed for obtaining the absorption spectrum of microsamples of Cf^{3+}. Absorption spectrum data from 400 to 800 mμ are presented for Cf^{3+} absorbed in cation exchange resin beads and for solid hydrated californium trichloride. The spectrum of these materials is expected to be very similar to the spectrum of Cf^{3+} in solution. A sample of anhydrous $CfCl_3$ was prepared that apparently is a single crystal. Room temperature absorption spectra from 4000 to 9000 A were taken of this material. Tentative calculations are presented which fit these data to a theoretical energy level scheme. Several polycrystalline samples of californium sesquioxide were prepared and studied using x-ray-diffraction techniques. The structure exhibited by these samples was the monoclinic Sm_2O_3 structure having a = 14.124 ± 0.020, b = 3.591 ± 0.003, c = 8.809 ± 0.013 Å, and β = 100.31 ± 0.02 deg. Similarly, prepara-

tions of $CfCl_3$ were found to exhibit the hexagonal UCl_3 structure having a = 7.393 ± 0.040 and c = 4.090 ± 0.060 Å. The ionic radius for californium computed from the trichloride data is 0.98 A. (P.C.H.)

12832 (UCRL-Trans-1244(L)) PHYSICAL CHEMISTRY OF PROTACTINIUM. Guillaumont, Robert. Translated for Univ. of California Lawrence Radiation Lab., Livermore, from Colloq. Int. Centre Nat. Rech. Sci., No. 154, 1-14(1965). 30p. Dep. mn; JCL $2.60 fs, $1.10 mf.

The distribution of penta- and tetravalent protactinium between various aqueous solutions complexing and or not complexing and benzene solutions of thenoyltrifluoroacetone was studied. The distribution coefficient was measured as a function of the concentration of chelating agent in the organic phase, as a function of the acidity and concentration of complexing anions in the aqueous phase and also as a function of protactinium. At tracer levels, Pa(V) is present as two ionic species in equilibrium $PaPOH)_3^{3+}$ (or $PaO(OH)^{2}$) and $Pa(OH)_4^{+}$ (or $PaO(OH)^{2+}$ or PaO_2^{+}) in the medium $[H^+]$ = x N $[Li^+]$ = (3-x)N $[ClO_4^-]$ = 3N. In 3N $HClO_4$ solution, the monomeric ion corresponding to the tetravalent state is Pa^{4+}. When $[H^+]$ decreases the species $Pa(OH)_n^{(4-n)+}$ with n = 1, 2, and 3, appear successively. When the protactinium concentration increases $Pa(OH)_3^{3+}$ is not polymerized in contrast to $Pa(OH)_4^{+}$. In 3N $HClO_4$ medium tetravalent protactinium is present as dimer or trimer species when Pa concentration reaches 10^{-5} M. The hydrolysis constants of the cations $Pa(OH)_3^{3+}$ and Pa^{4+} were calculated as well as the partial constant polymerization of the $Pa(OH)_4^{+}$ ion. The formulas and formation constants of the first complexes of Pa(V) and Pa(IV) which appear in solution of carrier free ^{233}Pa at ionic strength 3 in presence of Cl^-, SO_4^{2-}, $C_2O_4^{2-}$, and F^- were determined. (auth)

12833 SYSTEMS BETWEEN NIOBIUM OXIDE AND THE OXIDES OF ALUMINUM AND CHROMIUM. Burdese, Aurelio; Borlera, Maria Lucco; Rolando, Piero. Atti Accad. Sci. Torino: I. Cl. Sci. Fis., Mat. Natur., 99: 1079-87(1964-65). (In Italian).

The constitution diagram of the systems $Nb_2O_5-Al_2O_3$ and $Nb_2O_5-Cr_2O_3$ were studied. In the zone richest in niobium oxide, three niobates appear in both systems analogous to the Magnelli phases of the type $NbO_{2.48}-NbO_{2.46}-NbO_{2.40}$, and all with incongruent fusion. In the system $Nb_2O_5-Al_2O_3$, the phase type $AlNbO_4$ has a composition range which is extended at the maximum from 45 to 70 mol% of Al_2O_3. It has a eutectic with $Al_2O_3 \cdot 9Nb_2O_5$ at 1410°C and decomposes in a peritectic fashion at 1640°C to liquid aluminum and aluminum sesquioxide. The rhombic lattice has the lattice constants a = 6.17, b = 7.38, and c = 8.61 Å. In the system $Nb_2O_5-Cr_2O_3$ the $CrNbO_4$ phase has a composition range which extends at the maximum from 35 to 66 mol.% Cr_2O_3. This melts at 1700°C and yields two eutectics, one with $Cr_2O_3.9Nb_2O_5$ at 1470°C and one with Cr_2O_3 at 1670°C. It was a tetragonal lattice of the rutile type. The stoichiometric composition has the lattice constants a = 4.644 and c = 3.009 Å. (tr-auth)

12834 REFINEMENT OF THE CRYSTAL STRUCTURE OF Li_2BeF_4. Burns, John H.; Gordon, E. Kent (Oak Ridge National Lab., Tenn.). Acta Crystallogr., 20: 135-8(1966). (ORNL-P-1294).

Single crystals of Li_2BeF_4 were grown by slow cooling of a melt of composition 66.7 mole % LiF and 33.3 mole % BeF_2 in a furnace. Intensities were measured with a single-crystal orienter and scintillation detector employing zirconium-filtered Mo radiation. Positional parameters from least-squares refinement are given along with observed and calculated structure factors. The structure of Li_2BeF_4 is isotypic with that of Be_2SiO_4. Both the Be^{2+} and Li^+ ions are tetrahedrally coordinated by fluoride ions, and these tetrahedra share all their corners to form a three-dimensional network. Continuous channels through the crystal, ~2Å in diameter, parallel to C were observed. (M.C.G.)

12835 THE CRYSTAL STRUCTURE OF DICAESIUM TETRACHLORODIOXOURANIUM (VI). Hall, D.; Rae, A. D.; Waters, T. N. (Univ. of Auckland, N. Z.). Acta Crystallogr., 20: 160-2(Feb. 10, 1966).

Dicesium tetrachlorodioxouranium(VI), $Cs_2UO_2Cl_4$, crystallizes in space group C2/m with 2 molecules in the cell of dimensions a = 11.92, b = 7.71, and c = 5.83 Å and β = 99° 40′. The structure contains octahedral $[UO_2Cl_4]^{2-}$ ions, with cesium ions in elevenfold coordination. (auth)

12836 A NEUTRON DIFFRACTION STUDY OF ORTHOBORIC ACID $D_3{}^{11}BO_3$. Craven, B. M. (Univ. of Sydney); Sabine, T. M. Acta Crystallogr., 20: 214-19(Feb. 10, 1966).

A neutron-diffraction study of orthoboric acid $D_3{}^{11}BO_3$ showed that the O–D ... O hydrogen bonds joining the D_3BO_3 molecules are essentially straight, confirming the result obtained by Zachariasen from an x-ray diffraction study of H_3BO_3. The coherent neutron scattering length for ^{11}B was determined (0.61 ± 0.01 cm^{-12}). (auth)

12837 THE VATERITE-TYPE ABO_3 RARE-EARTH BORATES. Bradley, W. F. (Univ. of Texas, Austin); Graf, D. L.; Roth, R. S. Acta Crystallogr., 20: 283-7 (Feb. 10, 1966).

Approximate models are proposed for the room-temperature modifications of the vaterite-type rare earth borates. A low temperature model based on three-membered rings of borate tetrahedra was found to be reconcilable with the x-ray powder diffraction data, the optical properties, and the infrared absorption character. A high-temperature model containing triangular borate ions was relatable to the $CaCO_3$ vaterite modification. (auth)

12838 COMPOSITION AND CRYSTALLOGRAPHIC DATA FOR THE HIGHEST BORIDE OF TUNGSTEN. Romans, P. A.; Krug, M. P. (Bureau of Mines, Albany, Oreg.). Acta Crystallogr., 20: 313-15(Feb. 10, 1966).

The composition of the highest boride of tungsten was studied and the unit cell was found to be hexagonal with A_0 = 5.200 and C_0 = 6.340 Å. In x-ray spectrographic analysis for tungsten the results generally fell between the theoretical values of WB_4 and WB_5 but were not consistent enough to indicate definitely one or the other. The samples studied were prepared by sintering, then arc melting a mixture of high purity boron and tungsten. A density of 5.25 was measured for a solid sample with a 12:1 atomic ratio of boron to tungsten. The proposed structure is closely related to the AlB_2 structure, which consists of closely packed layers of metal atoms located directly above one another with boron atoms in the interstices. (F.J.H.)

12839 REORIENTATION TIMES, TRANSITION TIMES, AND QUADRUPOLE COUPLING CONSTANTS IN SOME ORGANIC FLUIDS FROM NUCLEAR MAGNETIC RELAXATION TIME MEASUREMENTS. Zeidler, M. D. (Univ., Muenster, Ger.). Ber. Bunsenges. Physik. Chem., 69: 659-69(1965). (In German).

The nmr spin-lattice relaxation time T_1 of protons and deuterons was measured by pulse methods for ten organic liquids, which were present in the normal proton-containing form or were completely deuterated. From measurements of the proton relaxation time in mixtures of proton-containing and deuterated molecules the intramolecular as well as the intermolecular contributions to the relaxation rate were determined. Furthermore, using the normal proton-containing substances, self-diffusion coefficients were measured by nmr pulse methods. The measurements permitted conclusions concerning molecular-kinetic processes in these solutions. Thus reorientation times, jumping times, and mean jumping distances could be calculated. By comparison with viscosity data, values of the microviscosity coefficients for rotation and translation were deduced. Finally the deuteron relaxation times were used to calculate quadrupole coupling constants of the deuteron. (auth)

12840 REACTION RATE AND SEPARATION FACTOR ISOTOPE EFFECTS IN THE HYDROGEN EVOLUTION REACTION. Salomon, M. (Princeton Univ., N. J.); Conway, B. E. Ber. Bunsenges. Physik. Chem., 69: 669-74(1965).

Calculations are presented for the isotope effects, which arise in H_2, HD, D_2 evolution at Pt and Pd cathodes. It is shown that the quantities S_D (separation factor) and R (exchange current density ratio) characterizing the kinetic isotope effects are related in a manner that can be a useful diagnostic indication of reaction mechanism. The method avoids a priori calculation of transition state force constants and hence the associated uncertainties of such calculations. (auth)

12841 NORMAL COORDINATE ANALYSIS OF $XeOF_4$ IN THE UREY-BRADLEY FIELD. Yeranos, W. A. (Northern Illinois Univ., DeKalb). Bull. Soc. Chim. Belges, 74: 407-13(Sept.-Oct. 1965).

Using published infrared and Raman data, the Urey-Bradley force constants of $XeOF_4$ were determined. The analysis was carried out within Wilson's G-F matrix method and the constants evaluated by the use of a computer program, which refined the differences of the experimental and calculated frequencies in the least-squares sense. The G and F matrix elements, in both the GVFF and UBFF, of any molecule of the type MYX_4 and of C_{4v} symmetry are reported ($\alpha = \gamma = 90°$). The normal coordinates, as well as the potential energy distribution matrix, of $XeOF_4$ in the field force determined are given. (auth)

12842 VIBRATIONAL ANALYSIS OF IO_4^- AND XeO_4. Yeranos, W. A. (Northern Illinois Univ., DeKalb). Bull. Soc. Chim. Belges, 74: 414-17(Sept.-Oct. 1965).

The vibrational spectrum and the potential constants of IO_4^- and XeO_4 were studied. The following data are presented: observed and calculated frequencies; Urey–Bradley force constants; normal coordinates; and the potential energy distribution. (F.J.H.)

12843 THE HYDRATES AND THE THERMAL DECOMPOSITION OF URANIUM SULFATE. Leroy, Jean-Marie; Tridot, Gabriel (Faculte des Sciences, Lille). Compt. Rend., 261: 5505-8(Dec. 20, 1965). (In French).

Uranium(IV) sulfate possesses only two hydrates, with four and one molecules of water, respectively. They are characterized by x-ray diffraction. The preparation and the x-ray spectrum of the anhydrous salt are described. Its thermal decomposition leads at 665°C to uranyl sulfate, and the activation energy of the reaction, deduced from the kinetic study, is 33 ± 1 kcal/mole. (tr-auth)

12844 XENON HEXAFLUORIDE: CRYSTALLOGRAPHIC DATA AND PHASE TRANSITIONS. Agron, Paul A.; Johnson, Carroll K.; Levy, Henri A. (Oak Ridge National Lab., Tenn.). Inorg. Nucl. Chem. Lett., 1: 145-8 (Dec. 1965). (ORNL-P-1874).

The crystal structure of XeF_6 is being studied by x-ray and neutron diffraction. The structure of one modification of XeF_6, crystallographic data on a second modification and possible identification of the phase regions observed in the thermal study are reported. For the first modification, the following unit cell dimensions were obtained: a = 9.33, b = 10.96, and c = 8.95 Å (standard errors, 0.03 Å), $\beta = 91.9 \pm 0.2°$; probable space group $P2_1/m$ or $P2_1$. The theoretical density is 3.56 g cm^{-3}. Positions of the 8 Xe atoms in the unit cell were determined. The second modification was found to be fcc with a = 25.34 ± 0.05 Å and a probable space group $F\bar{4}3c$ or Fm3c. (M.C.G.)

12845 INVESTIGATIONS OF INTERACTIONS IN Nb–N–C AND Ta–N–C SYSTEMS. Levinskii, Yu. V. Izv. Akad. Nauk SSSR, Metal., No. 3, 151-7(May-June 1965). (In Russian).

The reactions at temperatures of 1150 to 2370°C of the carbides of Nb and Ta with N, of Nb and Ta with N and C, and of solid solutions $NbN_{0.7}C_{0.3}$ with carbon were investigated. It is shown that the reactions $NbN + C \rightleftharpoons NbC + \frac{1}{2}Nb_2$ and $TaN + C \rightleftharpoons TaC + \frac{1}{2}N_2$ at nitrogen pressures of 1 atm and temperatures above 1150°C are completely displaced to the right. The absence of reactions of Nb and Ta carbides with N at temperatures above 1150°C makes it possible to sinter these carbides and to perform any other form of thermal processing in a nitrogen atmosphere. (tr-auth)

12846 X-RAY EMISSION SPECTRA OF NIOBIUM AND ZIRCONIUM AND THE CHARACTER OF THEIR INTERATOMIC BOND. Korsunskii, M. I.; Genkin, Ya. E. (Inst. of Nuclear Physics, Alma-Ata, USSR). Izv. Akad. Nauk SSSR, Neorg. Mater., 1: 1701-9(Oct. 1965). (In Russian).

Investigation of the emission spectra of niobium and zirconium showed that the external energetic energy bands of these elements contain electrons of at least two types. The electrons have the appurtenance of all crystals and answers to the metallic part of the bond. The second group of electrons participate in the formation of strong covalent bonds. That part of the valence electrons can maintain an atomic character is not excluded. However, such electrons were not observed in significant quantity in either niobium or zirconium. The investigation showed that in the transition metals and approximation of almost-free electrons can be used. The use of this approximation is necessary not only with all valence electrons but also in the case of completely coordinated electrons. In this case the states of collective electrons in the lattice of the indicated elements differ substantially from gases of free electrons by the presence of parts of p and d states, which leads to the presence in these electrons of appropiate orbital and magnetic moments developed in the magnetic properties of the solid materials. (tr-auth)

12847 CHEMICAL BOND IN TRANSITION METAL HYDRIDES. Antonova, M. M. (Inst. of Problems in Studies of Materials, Kiev). Izv. Akad. Nauk SSSR, Neorg. Mater., 1: 1758-63(Oct. 1965). (In Russian).

On the basis of published data on interatomic distances in hydrides of the transition metals, it is impossible to draw conclusions on the predominance in the hydrides of ionic or covalent bonds. Analysis of data on the physical properties, paramagnetic resonance, and x-ray spectral investigations confirmed the conclusion, based on theoretical considerations, that the bonds in hydrides of the transition metals are ionic-covalent nonlocalized. (tr-auth)

12848 NATURE OF THE CHEMICAL BOND IN TITANIUM AND ZIRCONIUM SUBOXIDES. Kornilov, I. I.; Glazova, V. V. (Baikov Inst. of Metallurgy, USSR). Izv. Akad. Nauk SSSR, Neorg. Mater., 1: 1778-86(Oct. 1965). (In Russian).

Investigation of titanium–oxygen systems by physical and chemical analysis methods showed that the suboxide compounds Ti_6O and Ti_3O, with metallic-type bonds, are formed. The compound Ti_6O of the Kurnakov type was formed from α-solid solutions and was stable up to temperatures of 820 to 830°C. The compound Ti_3O was formed by crystallization from melts at a temperature of 1940°C. Both compounds possessed singular points on the composition-property diagram (microhardness–composition, electric resistance–composition, and thermoelectromotive force–composition). By investigation of the zirconium–oxygen system, compounds with the composition Zr_6O and Zr_3O were also detected. On the composition–electric resistance diagram of the zirconium–oxygen system, two sharply expressed signal maxima, correlating with the compounds Zr_6O and Zr_3O, were detected. This confirmed the semiconductor nature of the compounds detected. Investigation of the temperature dependence of the electric conductivity of the compounds Ti_6O and Ti_3O and also Zr_6O and Zr_3O confirmed the hypothesis on the metallic-type bonds of the Ti_6O and Ti_3O compounds and the semiconductor-type bonds in Zr_6O and Zr_3O. The possibility of the existence of the compounds Hf_6O and Hf_3O in the hafnium–oxygen system can be assumed. (tr-auth)

12849 PHYSICAL PROPERTIES AND CHEMICAL BOND IN RARE EARTH CHALCOGENIDES. Lashkarev, G. V.; Paderno, Yu. B. (Inst. of Problems in Studies of Materials, Kiev). Izv. Akad. Nauk SSSR, Neorg. Mater., 1: 1791-1802(Oct. 1965). (In Russian).

Data available in the literature on the crystal structure and magnetic, electric, thermal, and galvanic magnetic

properties of the rare earth chalcogenides were reviewed. The widths of the forbidden zone of sesquiselenides from La to Sm and of Sm_2S_3 were determined. The coefficients of thermal expansion of the oxytellurides of Pr, Nd, and Sm, and the coefficients of thermal conductivity of the sesquiselenides of La, Ce, and Nd were measured. Calculations of the interatomic distances M – M, M – X, and X – X in the mono- and sesquichalcogenides and ditellurides of the rare earths are reported. From a comparison of experimental and calculated data on the ionic crystal radius of the interatomic distances and from an analysis of the physical properties, conclusions were drawn on the character of the chemical bonds in rare earth chalcogenides. Tests showed that the zones of conductivity in the rare earth chalcogenides are the 5d band. Changes in the physical properties of the chalcogenides during passage along the rare earth series and during transition from the sulfide to the selenide and telluride are reported. The possibility of determining the energy difference between $4f^6$, $4f^7$, and $4f^{14}$ levels of rare earth ions by means of the investigation of the low-lying levels of Sm, Eu, and Yb monochalcogenides was suggested. It was shown that the change in the composition of the sesquiselenide of La from $LaSe_{1.5}$ to $LaSe_{1.43}$ reduces its electric resistance. The semiconductive character of the conductivity of the sesquichalcogenides of Sm, Eu, and Yb of the composition $M_2X_3 - M_3X_4$ was predicted. The semiconductor character of the conductivity of the oxychalcogenide M_2O_2Te was predicted and experimentally detected. (tr-auth)

12850 TEMPERATURE DEPENDENCE OF ELECTROCONDUCTIVITY OF TITANIUM AND ZIRCONIUM SUBOXIDES. Glazov, V. V.; Kornilov, I. I. (Baikov Inst. of Metallurgy, USSR). Izv. Akad. Nauk SSSR, Neorg. Mater., 1: 1834-7(Oct. 1965). (In Russian).

The temperature dependence of the electric conductivity of the suboxides Ti_6O, Ti_3O, Zr_6O, and Zr_3O was investigated. It was established that the compounds Ti_6O and Ti_3O have metallic-type bonds and the compounds Zr_6O and Zr_3O are characterized by covalent-ionic type bonds. Calculations showed that the width of the forbidden zones for the suboxides Zr_6O and Zr_3O are 0.18 and 0.20 ev, respectively. (tr-auth)

12851 REACTIONS OF ZIRCONIA WITH RUBIDIUM CARBONATE AND SILICATE. Chukhlantsev, V. G.; Alyamovskaya, K. V. (Ural Polytechnic Inst., Sverdlovsk, USSR). Izv. Akad. Nauk SSSR, Neorg. Mater., 1: 1994-9 (Nov. 1965). (In Russian).

The reactions of zirconia with rubidium carbonates or silicates were investigated at 870 to 950°C. The composition and properties of the products formed during sintering were investigated. The previously unknown $Rb_2ZrSi_2O_7$ was detected, and some of its properties were determined. (tr-auth)

12852 PREPARATION OF ELEMENTAL ^{13}C IN HIGH YIELD FROM $^{13}CO_2$. Rutherford, William M. (Mound Lab., Miamisburg, Ohio). J. Amer. Chem. Soc., 88: 179-80(Jan. 5, 1966). (MLM-1306J).

The method for preparing elemental ^{13}C from carbon dioxide in high purity and yield is described. The method is based on two reactions; the reduction of CO_2 to CO by zinc and the reduction of CO over an iron catalyst in the presence of hydrogen. In a test run with 4.5% of $^{13}CO_2$, 96% of the carbon content of the CO_2 charge was recovered as purified elemental carbon. (F.J.H.)

12853 CHELATE CHEMISTRY. IV. TEN-COORDINATE THORIUM AND URANIUM(IV). Muetterties, E. L. (E. I. du Pont de Nemours and Co., Wilmington, Del.). J. Amer. Chem. Soc., 88: 305-6(Jan. 20, 1966).

Pentakis(tropolono)thorium(IV), pentakis(tropolono) uranium(IV), and pentakis(γ-isopropyltropolono)thorium (IV) anions were prepared by reaction of the neutral tetrakis chelates of thorium or uranium with the sodium salt of the corresponding tropolone anion. (auth)

12854 THERMAL CONDUCTIVITIES OF MgO, Al_2O_3, AND ZrO_2 POWDERS TO 850 deg C. I. EXPERIMENTAL. Godbee, Herschel W. (Oak Ridge National Lab., Tenn.); Ziegler, Waldemar T. J. Appl. Phys., 37: 40-55(Jan. 1966). (ORNL-P-933).

Thermal conductivities were measured for extensively characterized magnesia, alumina, and zirconia powders. Thermal conductivities of the powders in dry air at atmospheric pressure were determined at volume fractions solid varying from 0.49 to 0.70 as a function of temperature from about 100 to about 850°C. Particle-size distribution, chemical composition, x-ray diffraction pattern, weight loss on heating, pore-free density, and surface area of each powder were measured. Thermal conductivities were determined by a steady-state method employing radial heat flow in a hollow cylinder and by an unsteady-state method based on the model of heating a cylinder of a perfect conductor surrounded by an infinite amount of the material whose thermal conductivity is being measured. (auth)

12855 THERMAL CONDUCTIVITIES OF MgO, Al_2O_3, AND ZrO_2 POWDERS TO 850 deg C. II. THEORETICAL. Godbee, Herschel W. (Oak Ridge National Lab., Tenn.); Ziegler, Waldemar T. J. Appl. Phys., 37: 56-65(Jan. 1966).

A theoretical expression is presented to relate the effective thermal conductivity of statistically describable two-phase systems to the conductivities of the pure phases, the volume concentrations of the phases, and a shape factor. Auxiliary equations to relate bulk gas conductivity and small interparticle distance and to predict a radiation heat transfer contribution to effective thermal conductivity are also presented. The shape factor is a property of the discontinuous phase and is related to the two-phase system only through the volume balance of the phases. In the derivation of the expression no assumptions are made concerning particle shape, size, or spatial arrangement. However, the derivation is based on a simplified model in that the isotherms in the model are assumed to be planes perpendicular to the heat flow. In exact solutions of the heat flow equation, no assumptions are made regarding the heat flow or temperature pattern. On the other hand, exact solutions are carried out only for simple shapes in fixed arrangements that seem to fall short of describing actual powder-gas systems. (auth)

12856 PREPARATION OF URANIUM SULFIDE SINGLE CRYSTALS. Van Lierde, W.; Bressers, J. (SCK-CEN, Mol, Belg.). J. Appl. Phys., 37: 444(Jan. 1966).

A method for preparing US monocrystals using solid-state techniques is presented. Powdered U is reacted with an excess of H_2S at 500°C according to $U + H_2S \rightarrow \frac{1}{2} US_2 + \frac{1}{2} U$. This mixture is reacted in a vacuum enclosure for 4 hr, at a temperature increasing slowly from 1700 to 1900°C; this procedure allows US monocrystals to be formed, according to $\frac{1}{2} US_2 + \frac{1}{2} U \rightarrow US$. (M.J.T.)

12857 VIBRATION-ROTATION SPECTRA OF MONOMERIC HCl, DCl, HBr, DBr, AND HI IN THE RARE-GAS LATTICES AND N_2-DOPING EXPERIMENTS IN THE RARE-GAS LATTICES. Bowers, M. T.; Flygare, W. H. (Univ. of Illinois, Urbana). J. Chem. Phys., 44: 1389-1404(Feb. 15, 1966).

Extensive experiments are performed on the trapping of HCl, DCl, HBr, DBr, and HI molecules in rare gas lattices. Concentration, deposition rate, and temperature-dependent studies yield the monomer spectra of the molecules. The HCl and DCl monomers in Ar, Kr, and Xe showed hindered rotational spectra that is interpreted on the basis of 0_h site symmetry. HCl in Ne also appeared to rotate. HBr and DBr in Ar showed additional splitting, which was attributed to either site splitting due to loss of one of the near-neighbor atoms or site distortion toward D_{3h} symmetry. HBr and DBr in the larger Kr lattice gave spectra similar to the HCl spectra. The spectra indicated that the predominant local symmetry is 0_h. The barriers to rotation in the lattices are given from an interpretation of the spectra. The barriers to rotation were interpreted

by extension of an electrostatic model. Calculations of rotational energy levels were performed for the linear molecule in a lattice site of D_{3h} symmetry. The perturbed rigid-rotor levels are given as a function of lattice-molecule coupling constants. No experimental evidence was found for D_{3h} site symmetry. N_2-doping experiments were performed with HCl in the argon lattice. N_2 doping (1 to 4%) was found to give predominately two sites for the HCl molecule; one site similar to the case of pure HCl in Ar and another site in which the rotation is frozen out giving a single transition for HCl. The frozen site was attributed to the nearest-neighbor presence of N_2. The spectra are interpreted in terms of a hindered rotor or a librator. Most of the spectra is interpreted on the basis of a hindered rotor but some spectra such as the N_2-doping experiments required the librator analogy similar to CO in Ar and CN^- in KCl. The vibrational shifts of the monomers in the rare gas lattices are given for all cases studied where the predominant shift is to lower energy. These shifts are also qualitatively explained by localized nonbonded dispersion and overlap repulsion effects. (auth)

12858 SIGNIFICANT-STRUCTURE THEORY APPLIED TO WATER AND HEAVY WATER. Jhon, Mu Shik; Grosh, Joe; Ree, Taikyue; Eyring, Henry (Univ. of Utah, Salt Lake City). J. Chem. Phys., 44: 1465-72(Feb. 15, 1966).

Significant-structure theory was successfully applied to water and heavy water. The thermodynamic and transport properties were calculated and the theory gave maximum density at ~4°C for H_2O and at 11.23°C for D_2O. The calculated results for entropy of vaporization, vapor pressure, molar volume, heat capacity, and the critical values were in good agreement with the observed values. The calculated curve for viscosity under pressure above 1 atm showed the observed minimum and was in satisfactory numerical agreement with the experimental values. According to the model, clusters of Ice-I-like molecules were in equilibrium with Ice-III-like molecules. The lifetime of the Ice-I-like cage structures was long compared to the relaxation time in viscous flow but short compared to the relaxations observed in NMR. (auth)

12859 LOW-FREQUENCY MOTIONS AND BARRIER TO ROTATION IN PHOSPHONIUM IODIDE. Rush, J. J. (Argonne National Lab., Ill. National Bureau of Standards, Washington, D. C.). J. Chem. Phys., 44: 1722-3(Feb. 15, 1966).

The vibrational spectrum of PH_4I phosphonium iodide was investigated by the energy-gain scattering of cold neutrons. The neutron spectrum for a thin sample of PH_4I at 292°K is shown. Three distinct inelastic-scattering maxima were observed at energy gains corresponding to 110,335, and 614 cm^{-1}. The intense band peak at 335 cm^{-1} was assigned to the $1 \rightarrow 0$ transitions ($h\nu_t$) of the torsional oscillations of the PH_4^+ ions in the lattice. The less intense maximum around 614 cm^{-1} was attributed to the $2 \rightarrow 0$ transitions of the torsional modes. The peak at 110 cm^{-1} was tentatively assigned to the translational optic vibrations of the PH_4^+ ions. The problem of the barrier to rotation of tetrahedral PH_4^+ ions in a CsCl-type lattice was considered by Gutowsky et al. (J. Chem. Phys., 22: 643(1954). A high barrier was found using their formula. For pseudocubic PH_4I with ν equal to 1.42 A and d assumed to be 4.6 Å, the electrostatic calculation yields a barrier of 7.5 kcal/mole, in good agreement ν with the experimental value of 7.1. (F.J.H.)

12860 ON THE STRUCTURE OF GASEOUS XeF_6. Hedberg, Kenneth (Oregon State Univ., Corvallis); Peterson, Steven H.; Ryan, Robert R.; Weinstock, Bernard. J. Chem. Phys., 44: 1726(Feb. 15, 1966).

A comparative study was made of XeF_6 and TeF_6 molecular structures by electron diffraction. The XeF_6 sample (>99% pure) was prepared by direct fluorination of xenon at high pressures. The diffraction experiments were made at nozzle temperatures of about 22°C at a camera distance of 25 cm using 0.06 Å wavelength electrons and a ν^3 rotating sector. Exposure times were 1 to 4 min. Microphotometric data from photographic plates for each compound are presented. The differences in shapes of the two curves proved that the two molecules are of different structure. The preliminary results strongly supported the conclusion that XeF_6 is not a regular octahedron. (F.J.H.)

12861 THE INFRA-RED ABSORPTION OF 75 percent ^{18}O-BARIUM PHOSPHATE. Petreanu, E.; Pinchas, S.; Samuel, D. (Weizmann Inst. of Science, Rehovoth, Israel). J. Inorg. Nucl. Chem., 27: 2519-23(Dec. 1965).

The infrared absorption of Nujol mulls of normal and 75 at.% ^{18}O-barium phosphate was measured in the 3700 to 360 cm^{-1} region. The assignment of all the observed bands is discussed and confirmed on basis of the valence forces assumption. The agreement between the observed and calculated frequencies of the labeled sample bands is satisfactory. (auth)

12862 THERMOGRAVIMETRIC ANALYSIS OF La, Ce, Pr AND Nd OXALATES IN AIR AND IN CARBON DIOXIDE ATMOSPHERE. Subba Rao, V. V.; Rao, R. V. G.; Biswas, A. B. (National Chemical Lab., Poona). J. Inorg. Nucl. Chem., 27: 2525-31(Dec. 1965).

Thermogravimetric analysis of lanthanum, cerium, praseodymium, and neodymium oxalates was made in the temperature range from 30 to 1100°C in air and in carbon dioxide. The results indicated that all except cerous oxalate decompose through formation of an intermediate oxycarbonate of the type $M_2O_3 \cdot CO_2$. The decomposition was delayed and sluggish in carbon dioxide, which might be due to delayed nucleation and slow growth rate. Rate parameters were calculated for dehydration and decomposition. (auth)

12863 THE KINETICS AND MECHANISM OF THE DISSOLUTION OF URANOUS–URANIC OXIDE IN SULPHURIC ACID IN PRESENCE OF FERRIC ION. Celeda, J.; Lara, J. Gomez (Inst. of Chemical Tech., Prague. Univ. Nacional Autonoma, Mexico City). J. Inorg. Nucl. Chem., 27: 2561-72(Dec. 1965).

Measurements of the dissolution rate of U_3O_8 in sulfuric acid under oxidation by ferric ions was carried out in order to obtain information on the influence of all variables. The results indicated that the rate-controlling step is the transformation of activated surface centers to oxidized products accessible to dissolution. These centers are created as the result of the establishing a redox-equilibrium between the oxidizing solution and the surface of the solid, probably by adsorption of free OH^- radicals. Each one of these single-electron transfers results in the formation of two activated centers, thus leading to a square-root dependence between the reaction rate and the Fe^{3+}/Fe^{2+} ratio. (auth)

12864 THE DONOR-ACCEPTOR INTERACTION OF ALUMINUM TRIIODIDE WITH ORGANIC MOLECULES; EFFECT OF ADDITION OF VARIOUS ORGANIC COMPOUNDS ON THE ISOTOPIC EXCHANGE OF IODINE IN THE ALUMINUM IODIDE–ETHYL IODIDE LIQUID SYSTEM. Polaczek, A.; Kaminski, A. (Warsaw Univ.). J. Inorg. Nucl. Chem., 27: 2585-8(Dec. 1965).

It is shown, that organic molecules for which a strong donor-acceptor interaction with aluminum triiodide can be expected, with formation of a molecular complex, cause a strong exchange blocking effect in the $AlI_3-C_2H_5I$ liquid system. Independently of the amount of the added foreign compound, however, a significant part (about 20 to 30%) of the radioiodine atoms primarily present in the metal iodide is transferred to the ethyl iodide in the first rapid period of the exchange. This suggests a significant role for intermediate compounds and/or solid-liquid surface exchange. Aromatic hydrocarbons and olefines, which are supposed to form π-complexes with aluminum trihalides, cause no effect on the iodine exchange in the system investigated. (auth)

12865 NEW COMPOSITIONS WITH K_2NiF_4 STRUCTURE. Blasse, G. (Philips' Gloeilampenfabrieken, Eindhoven, Netherlands). J. Inorg. Nucl. Chem., 27: 2683-4(Dec. 1965).

Mixed metal oxides with the K_2NiF_4 structure are reported and the lattice parameters given. For nearly all compounds with the K_2NiF_4 structure a c/a ratio of 3.30 ± 0.05 was obtained. $La_2Li_{0.5}Ni_{0.5}O_4$ (c/a = 3.44) is an exception. Data from x-ray diffraction studies are given for $SrLaCrO_4$, $SrLaMnO_4$, $SrLaFeO_4$, $SrLaCoO_4$, $SrLaNiO_4$, $SrLaGaO_4$, $SrLaRhO_4$, $La_2Li_{0.5}Co_{0.5}O_4$, $La_2Li_{0.5}Ni_{0.5}O_4$, $Sr_{1.5}La_{0.5}Co_{0.5}Ti_{0.5}O_4$, and $Sr_{0.5}La_{1.5}Mg_{0.5}Co_{0.5}O_4$. (F.J.H.)

12866 THE NEPHELAUXETIC EFFECT IN RARE EARTH COMPLEXES ILLUSTRATED FOR PRASEODYMIUM(III). Sinha, S. P.; Schmidtke, H.-H. (Cyanamid European Research Inst., Cologny, Geneva). Mol. Phys., 10: 7-11(1965).

With the availability of the free ion spectrum of trivalent praseodymium a closer analysis of the nephelauxetic effect in praseodymium complexes was made. An explanation for the greater decrease of F_2 parameter compared to F_4 and F_6 is presented. A theoretical explanation of the two slopes resulting for the plot of the term scheme of praseodymium complexes against the free ion is also given. (auth)

12867 THE ELECTROLYTIC PREPARATION OF LEAD TARGETS FROM STABLE ISOTOPES ^{206}Pb AND ^{207}Pb IN SULPHATES FORM. Mikulski, Jan; Szeglowski, Zdzislaw (Inst. of Nuclear Physics, Krakow). Nukleonika, 10: 517-18(1965).

Preparation of high-purity lead by electrochemical methods is described. Double electrolysis was used since lead deposited in the electrolysis of lead complex salt solutions is not suitable for forming targets. The lead deposited in this electrolysis is therefore dissolved in perchloric acid and electrolyzed once more. As the result of the second electrolysis metallic lead of a fine-grained structure and good adherence to a platinum electrode was obtained. (M.C.G.)

12868 THE PRODUCTION OF URANIUM DIOXIDE BY THE ELECTROCHEMICAL REDUCTION OF U (VI) IN SODIUM CARBONATE SOLUTIONS AT A MERCURY CATHODE. I. THE REDUCTION OF U (VI) AT A MERCURY CATHODE IN SODIUM CARBONATE SOLUTIONS. Perec, Miecyslaw (Instytut Badan Jadrowych, Warsaw). Nukleonika, 10: 575-83(1965). (In Polish).

Investigations were made on the process of U(VI) reduction in the sodium carbonate solutions at a mercury cathode. The composition used was similar to that of the solutions resulting from the alkaline leaching of uranium-bearing raw materials. Polarographic studies, the character of current-time curves, determination of the influence of $[N(CH_3)_4]^+$ on the double layer differential capacity, and the reduction overpotential led to the conclusion that the cathodic reduction occurs without any preliminary dissociation of the carbonate-uranyl ion. The polarographic waves observed during the reduction process are of the one-electron type and do not represent the two-stage reduction of U[VI] producing UO_2 as the final product. The polarographic wave occurring at a more negative potential results from the reduction of the hydrolysis products of the $[UO_2(CO_3)_3]^{4-}$ ion. (auth)

12869 THE RATE OF HETEROGENEOUS ISOTOPIC EXCHANGE ON THE SURFACES OF IONIC CRYSTALS. Lieser, K. H.; Guetlich, Ph.; Rosenbaum, I. (Technische Hochschule, Darmstadt, Ger.). Radiochim. Acta, 4: 216-22(Dec. 1965). (In German).

The following equations were derived for the rate of heterogeneous isotopic exchange reactions: when the surface reaction is rate-determining, $\ln(1-\lambda) = -k(n_O + n_L)t$, and when the diffusion in the solution is rate-determining, $\ln(1-\lambda) = -k_D(n_O + n_L/n_O)t$, with λ the fraction exchange, n_O the number of moles of exchangeable ions at the surface, n_L their number in the solution, and t the time. Using these equations, the rate constants for the systems $BaSO_4/Ba^{2+}$, $BaSO_4/SO_4^{2-}$, $SrSO_4/Sr^{2+}$, and $AgCl/Cl^-$ were determined for the ratio n_O/n_L and varied in the widest range possible. In all these systems the surface reaction was rate-determining. (auth)

12870 COMPLEXES OF CARMINIC ACID WITH TER- AND TETRAVALENT METALS. I. THE COMPLEX OF CARMINIC ACID WITH THORIUM. Dragulescu, C.; Simonescu, T.; Policec, Septimia (Scientific Research Station, Timisoara, Rumania). Rev. Roum. Chim., 10: 821-6(Sept. 1965).

A spectrophotometric study was made on the thorium-carminic acid complex in absolute ethanol medium. After establishing optimum working conditions, the 1:1 composition of the complex was proved by continuous-variation and slope-ratio methods. The formation constant of the complex computed by means of Job's curves at different concentrations, has the value $K = 1.2 \times 10^6$ moles/l. (auth)

12871 FORMATION OF COMPLEX ERBIUM HALIDES BY REFRACTOMETRY IN AQUEOUS SOLUTIONS. Spacu, P.; Ivan, Eugenia (Inorganic Chemistry Center, Bucharest). Rev. Roum. Chim., 10: 837-42(Sept. 1965).

In concentrated aqueous solutions, the refractometric method showed, for the systems $ErCl_3-Me^ICl$(Me^I = Na, and Rb), the formation of the stable combination $Me^I[ErCl_4]$. For the systems $ErBr_3-Me^IBr$(Me^I = Na and K), no evidence for the formation of any combination could be found. (auth)

12872 ON THE STRUCTURE OF THE A-FORM OF THE SESQUIOXIDES OF THE RARE EARTHS. STRUCTURE INVESTIGATIONS ON La_2O_3. Mueller-Buschbaum, Hk.; v[on] Schnering, H. G. (Univ., Muenster, Ger.). Z. Anorg. Allg. Chem., 340: 232-45(1965). (In German).

Well-developed crystals of A-type La_2O_3, prepared by heating pellets at about 2200°C, gave good single-crystal photographs. These showed symmetry elements and systematic absences hitherto undescribed and disagreed with the structures formerly proposed for A-type sesquioxides. The high-temperature form of La_2O_3 crystallized in the space group $P6_3/mmm-D^4_{3h}$. Some microtwinning, not detectable by optical methods, caused a set of intensities that could only be well interpreted in that space group by assuming a statistic distribution. The results are discussed in comparison with earlier x-ray and neutron diffraction investigations. The special geometric arrangement of atomic positions (c/a, parameters) is explained by discussing the Madelung constants for La_2O_3-type substances. (auth)

12873 A STUDY OF SORPTION OF CESIUM BY MONTMORILLONITE [Thesis]. Metzger, Charles Frederick. Urbana, Ill., Univ. of Illinois, 1965. 68p.

In the study of sorption of cesium by montmorillonites, four samples with interlayer cation percentages of Ca_{100}, $Ca_{56}Na_{44}$, $Na_{56}Ca_{44}$, Na_{100} were used in order to determine the effect of the interlayer cation on the sorption of cesium. The sorption studies were carried on by contacting 0.25 grams of each sample with 100 ml of cesium nitrate plus cesium-137 as contacting solution. Master and sample aliquots were then compared at various time intervals by counting the cesium-137 present, to determine the amount of sorption of cesium. One-dimensional Fourier syntheses and electron density projections were made of the untreated and cesium-treated samples, and the interlayer positions compared to see if cesium had replaced the exchangeable interlayer cations of the montmorillonite samples. Results of the sorption analyses indicate the exchangeable cations of the montmorillonites have no appreciable effect on the amount of cesium sorbed. Studies of one sample that had extremely low sorption and a high K_2O content led to the conclusion that the K_2O is present on the edges of the clay platelets and results in a blocking of the cesium causing a decrease in sorption. In comparing the one-dimensional Fourier syntheses and electron density projections of the untreated and cesium-treated montmorillonites, it was seen that no cesium had entered the interlayer position of the clay minerals. Therefore, it is concluded that the cesium fixation is of the edge type rather than interlayer type fixation. A "core-rind" model of the clay platelets is proposed to explain the sorption properties of the montmorillonites. The inner "core" is thought to be a well-crystallized montmorillonite which shows good diffraction and

gives data that produced a Fourier projection of a normal well-crystallized montmorillonite, whereas the "rind" is the less ordered portion surrounding the "core," which produces few diffraction data and in which sorption of cesium takes place. This "core-rind" model also accounts for the decrease in sorption when potassium is present. Potassium on the edges of the montmorillonite platelets would cause a collapse of this area, making it difficult for the larger cesium atom to enter, thus causing lower sorption. (Dissertation Abstr.)

12874 A STUDY OF PRASEODYMIUM DIOXIDE PREPARED BY ACETIC ACID LEACHING [Thesis]. Hughes, Kenneth John. Lafayette, Ind., Purdue Univ., 1964. 186p.

PrO_2 was produced at 25°C by the solvolytic disproportionation of $PrO_{1.83}$ using a range of 90–110 mole % acetic acid solutions. The resulting dark brown, finely divided crystalline substance yielded an average composition of $PrO_{1.991}$ as determined iodometrically and a cell edge of 5.394 ± .001 Å for the face-centered cubic structure. Infrared, elemental, and thermogravimetric analyses show that the acetic acid-leached PrO_2 contains an average of 1.52 weight percent acetate. Surface-area and particle-size measurements indicate that a monomolecular layer of acetate is chemisorbed on the surface of the dioxide. Simultaneous differential and thermogravimetric analyses show that the acetate decomposes exothermically between 225 and 275°C with the subsequent decomposition of the remaining PrO_2 commencing around 300°C. The results of attempts to study the chemical composition of the acetate impurity by ultraviolet and visible spectrophotometry were inconclusive, although a mathematical interpretation of the data favors a basic praseodymium(IV) acetate. Iodometric and x-ray-diffraction analyses indicate a corresponding loss of oxidizing power in PrO_x after removal of the acetate thermally, revealing the presence of both the PrO_2 and $PrO_{1.83}$ phases. On the average two gram-atoms of Pr(IV) are reduced to $PrO_{1.83}$ for every gram-ion of acetate oxidized. Reproducible thermogravimetric data indicate metastable compositions for PrO_x ($1.83 < x < 2.0$) at the x values of 1.86–1.87 and 1.88–1.90 when the PrO_2 remaining after oxidative removal of the acetate is further thermally reduced in vacuo. A temperature range of 400 to 420°C is needed for decomposition of the higher metastable composition; the lower metastable composition reduces between 480 and 500°C to $PrO_{1.83}$. (Dissertation Abstr.)

12875 PROCESS FOR COATING POWDER REACTOR FUELS WITH CARBON. (to United Kingdom Atomic Energy Authority). British Patent 1,017,089. Jan. 12, 1966. Priority date Nov. 29, 1961, Austria.

A fluidized bed process is described for coating particulate reactor fuels with carbon by heating the fuel particles at a high temperature in a hydrocarbon-beaming atmosphere in which the hydrocarbon decomposes and builds up a carbon layer around each particle. The apparatus for carrying out the process consists of a reaction chamber, an inlet at the base of the reaction chamber consisting of an inlet tube for the hydrocarbon gas, a supply of hydrocarbon gas connected to the inlet tube, a concentric tube disposed around the inlet tube connected to a supply for the introduction of carrier gas into the chamber, and a heater for raising the temperature of the hydrocarbon gas above its decomposition temperature. Water cooling tubes are disposed around the concentric tube to ensure that the hydrocarbon gas is maintained below its decomposition temperature prior to entering the chamber. (B.L.M.)

12876 CELL FOR THE PRODUCTION OF URANIUM. Allen, Donald R.; Anneke, S. (to Dow Chemical Co.). Canadian Patent 720,107. Oct. 19, 1965.

Uranium metal is produced by the electrolysis of a uranium salt in a fused salt bath. A carbon anode of a special shape also serves as the container for the cell. The central cathode may be any metal of high melting point such as steel. The electrolyte is a fused salt mixture of an alkali metal uranous fluoride and sodium chloride. Fusion occurs at 800–850°C when a burner flame plays on the carbon anode. Suitable vents are provided for removing the chlorine gas while the uranium collects on the cathode and then falls on bottom of carbon anode container. The method of removing the metallic uranium is not stated but a current efficiency of 80% is claimed. (F.S.A.)

Organic Chemistry

Refer also to abstracts 12595 and 12819.

12877 (BNL–955) LIQUID FUEL SYNTHESIS USING NUCLEAR POWER IN A MOBILE ENERGY DEPOT SYSTEM. Beller, M.; Steinberg, M. (Brookhaven National Lab., Upton, N. Y.). Nov. 1965. Contract AT-30-2-GEN-16. 11p. Dep. mn. CFSTI $1.00 cy, $0.50 mn.

The problem of providing large masses of liquid fuels for modern armies, which are dependent upon internal combustion engine-driven vehicles, is discussed. The choice of fuel is mainly dictated by the consideration of raw material availability in the field. The advantages of methanol over ammonia as a fuel are listed, and requirements for the production of 1000 gal per day of methanol from carbon dioxide and moisture in air are given. (P.C.H.)

12878 WILZBACH TRITIATION STUDIES. II. STEREOSPECIFICITY IN THE TRITIATION OF ALCOHOLS. Crawford, B. R.; Garnett, J. L. (Univ. of New South Wales, Kensington). Austral. J. Chem., 18: 1951-8(Dec. 1965).

The mechanism of tritium labeling by the Wilzbach gas exposure method was examined in terms of stereochemical effects on solid and liquid alcohols. Predominant retention of configuration was observed with (+)- and (–)-oct-2-yl hydrogen phthalate while octan-2-ol racemized to the extent of 80%. Theories were developed to explain the effect of phase on the extent of inversion and on the relatively fast rate of tritiation of the hydrogen attached to the asymmetric carbon of octan-2-ol. Aryl hydrogens of the esters tritiated ten times faster than alkyl hydrogens. (auth)

12879 HYDROGEN BONDING AND VAPOR PRESSURE ISOTOPE EFFECTS IN N-DEUTERATED METHYL AND ETHYL AMINES. Wolff, H.; Hoepfner, A. (Univ., Heidelberg). Ber. Bunsenges. Physik. Chem., 69: 710-16(1965). (In German).

The vapor pressure isotherms of the systems CH_3ND_2–n-hexane, $C_2H_5ND_2$–n-butane, and $C_2H_5ND_2$–n-hexane were measured between +20 and –55°C. From the isotherms, the activity coefficients were evaluated and from these, by use of Prigogine's theory of associated liquids, heats of association, association constants, and heats of evaporation and solvation of D-substituted amines were calculated. The association constants were found to be slightly larger than for systems with the corresponding nondeuteriated amines; the association constants had the same values within the limits of experimental error. Although no marked influence of deuterium substitution in the amine groups on the association data could be recognized there was a distinct isotope effect on the vapor pressures. For the undiluted compounds it amounted to 3 to 10% over the temperature range investigated. Conditions that favor association of the amines (increase of the amine concentration or decrease of temperature) cause the vapor pressure of the deuteriated amine to become less than that of the nondeuteriated amine, whereas at first the vapor pressure of the D-substituted amine is greater, i.e., the initially inverse vapor pressure isotope effect change into a normal effect. This argues in favor of a causual connection between the transition from inverse to normal isotope effect and association. (auth)

12880 DEUTERIUM AND TRITIUM EXCHANGE REACTIONS OF PHENOLS AND THE SYNTHESIS OF LABELLED 3,4-DIHYDROXYPHENYLALANINES. Kirby, G. W.; Ogunkoya, L. (Imperial Coll. of Science and Tech., London). J. Chem. Soc., 6914-22(Dec. 1965).

Preparative procedures are outlined for the labeling of phenols with deuterium and tritium by exchange in alkaline

solution. The use of phenols, labeled with tritium at the ortho and para positions, in biosynthetic investigations is discussed. The methods developed are illustrated by the synthesis of (±)-3,4-dihydroxyphenylalanine labeled specifically at each of the nuclear and side-chain positions. (auth)

Radiation Chemistry

See also BIOLOGY AND MEDICINE — Radiation Effects on Biochemicals Radiation Effects on Tissues

Refer also to abstract 13982.

12881 (AD–626609) ^{60}Co GAMMA-RADIOLYSIS OF DEUTERIUM-OXYGEN MIXTURES. Kubose, D. A. (Naval Radiological Defense Lab., San Francisco, Calif.). Nov. 3, 1965. 19p. (USNRDL-TR-931).

The rates of formation of deuterium oxide in ^{60}Co gamma-irradiated gaseous mixtures of deuterium and oxygen were examined at initial deuterium concentrations, $[D_2]_0$, ranging from 3.7×10^{-4} to 3.7×10^{-4} to 3.7×10^{-3} mole l^{-1}. First- and zero-order reaction rates with respect to deuterium were observed for the low and high $[D_2]_0$, respectively. The corresponding rate constants found were 5.3×10^{-3} hr^{-1} and 4.5×10^{-6} mole l^{-1} hr^{-1} at a dose rate of 5.61×10^{16} ev cc^{-1} hr^{-1}. The initial G values for deuterium oxide formation, $G_0(D_2O)$, for the low and high $[D_2]_0$ were 2.9 and 7.3, respectively. A search for reaction products other than deuterium oxide, using ferrous sulfate and titanium sulfate reagents, established that no deuterium peroxide was formed as a stable reaction product and a wall-stabilized species, whose identity was not established, was observed; it oxidized the ferrous sulfate reagent but did not react with the titanium sulfate reagent. An 8-fold change in the surface-to-volume ratio of the irradiation vessel did not significantly affect the concentration of this species. (auth)

12882 (IA–1065) ON THE MECHANISM OF RADIOLYSIS OF CARBON DIOXIDE. Anbar, M.; Perlstein, P. (Israel Atomic Energy Commission, Yavne. Soreq Research Establishment). Oct. 1965. 31p. Dep. mn.

The radiolytic behavior of CO_2 was investigated following the $C^{16}O_2 - {}^{18}O_2 - C^{16}O$, $C^{18}O_2 - {}^{18}O_2 - C^{16}O$, $C^{18}O_2 - C^{16}O$, $C^{16}O_2 - {}^{18}O_2$, ${}^{13}CO - C^{16}O_2 - {}^{18}O_2$ as well as the $C^{18}O_2 - C^{16}O_2$ and ${}^{18}O_2 - {}^{18}O_2 + CO_2$ isotopic exchange reactions. CO is formed as primary product with a G value of approximately 11. O_2 was found to be a secondary product presumably formed by the decomposition of CO_3 molecules. The latter species was suggested to be liable for the oxidation of CO to CO_2, for the perpetuation of the $CO_2 - CO_2$ isotopic exchange as well as for the inhibition of the $O_2 - O_2$ exchange. (auth)

12883 (ORO–634) RADIATION-INDUCED OXIDATION OF HYDROCARBONS. Armstrong, Arthur A. Jr.; Walsh, William K. (North Carolina State Univ., Raleigh. Dept. of Textile Chemistry). July 15, 1965. Contract AT(40-1)-3210. 39p. Dep. mn. CFSTI $2.00 cy, $0.50 mn.

The radioinduced oxidation of ethane, propane, and isobutane was studied in a flow-type reactor using hydrogen bromide as a catalyst. A cobalt-60 source (Gammacell 220) was used for the irradiation. The exposure dose rate inside the reactor was approximately 1.8×10^5 R/hr. In the oxidation of ethane a G-value of 800 was obtained for the production of acetic acid. An increase in total flow rate of ethane to the reactor increased the production rate of acetic acid. The most pronounced effect was noted from an increase in pressure. An increase in the rate of production of acetic acid of 8 times was obtained by increasing the total pressure from 1 to 4 atmospheres. In the oxidation of propane a G-value of 10,000 was obtained for the production of acetone. Increases in total flow rate did not affect the rate of production. An increase in total pressure up to 3 atmospheres increased the rate of production of acetone but decreased the rate above that. At 4 atmospheres, corrosion products were deposited on the reactor surface which accounted for the decrease in the rate of production of acetone. In the oxidation of isobutane the products were t-butyl bromide, methyl bromide, and water. (P.C.H.)

12884 (RRL–2310-171) QUARTERLY REPORT, OCTOBER 1, 1965–DECEMBER 31, 1965. Fundamental Research No. 6041. (Radiation Research Labs., Mellon Inst., Pittsburgh, Pa.). Jan. 10, 1966. Contract AT(30-1)-2310. 10p. Dep. mn. CFSTI $1.00 cy, $0.50 mn.

Developments are reported for studies on: kinetics of ferrous-nitric oxide complex formation; rate of hydrogen atom abstraction reaction in liquid hexane; HI as a radical scavenger in the radiolysis of hydrocarbons; ESR spectra of fluorinated ethyl radicals; transient iron species in pulse irradiated ferric perchlorate solutions; radiolysis of liquid argon—hydrocarbon solutions; gas phase dosimetry; and mercury photosensitized decomposition of hydrocarbons. (P.C.H.)

12885 (UCD–34P80-3, pp 59-68) GAMMA RAY RADIOSYNTHESIS OF OZONE FROM AIR. Shah, J.; Maxie, E. C. (California Univ., Davis. Dept. of Pomology).

The formation of ozone was studied in a flowing air system by passing 6,500 ml air/min through a radiation chamber and also in a static system. Ozone concentration in a static system varied from 7.4 ppM at 59 krad to 58.1 ppM at 1000 krad. Values of G attained a maximum of 6.2 at the lowest dose, and then gradually fell to 2.5 at 1000 krad. It was concluded that the relation between formation of ozone and dose is nonlinear. In the flowing system, the G values were relatively constant (11.0 to 11.3) over the entire dose range; the concentration of ozone varied from 1.68 to 1.74 ppM. The results confirmed that maximum formation of ozone occurs in a flowing system. (P.C.H.)

12886 (SC-T–66-0706) MASS-SPECTROMETRIC DETECTION OF REACTIONS BETWEEN HIGHLY EXCITED HYDROGEN ATOMS AND ETHYLENE MOLECULES. Kuprianov, S. E. Translated by Marcel I. Weinreich (Sandia Corp., Albuquerque, N. Mex.), from Dokl. Akad. Nauk SSSR, 162: 865-8(1965). 10p. Dep. mn. CFSTI $1.00 cy, $0.50 mn. JCL $1.10 fs, $0.80 mf.

The results of studies made concerning reactions in ethylene with the participation of highly excited hydrogen atoms are reported. The number of highly excited carbon atoms formed was considerably smaller than the number of hydrogen atoms; therefore their importance in the processes involved is apparently not great. During a rise in pressure on the ethylene, the ion source generates other ions, including $C_2H_4^+$, $C_2H_3^+$, and $C_2H_2^+$. Mechanisms for the formation of these ions are discussed. (P.C.H.)

12887 MEAN LIFETIME OF FREE RADICAL CHAINS IN ^{60}Co γ-IRRADIATED CHLORAL HYDRATE AND BROMAL HYDRATE SOLUTIONS. McIntosh, R. G.; Eager, R. L.; Spinks, J. W. T. (Univ. of Saskatchewan, Can.). Can. J. Chem., 43: 3490-5(Dec. 1965).

The radiation chemistry of aqueous solutions of chloral hydrate and of bromal hydrate was studied by using a rotating sector to obtain intermittent irradiation. ^{60}Co gamma radiation was used for the irradiation. The mean free radical chain lifetime, τ, was determined for each of a series of solutions of different concentration and pH. Values for τ from 0.62 to 1.3 were obtained for chloral hydrate and values of 1.4 and 1.6 for bromal hydrate, depending on the concentration and dose rate. (M.C.G.)

12888 STUDY BY ELECTRON PARAMAGNETIC RESONANCE OF POTASSIUM CHLORATE IRRADIATED WITH X RAYS. Fayet, Jean-Claude; Thieblemont, Bernard (Faculte des Sciences, Orsay, France). Compt. Rend., 261: 5420-3(Dec. 20, 1965). (In French).

By irradiation at room temperature of potassium chlorate with x rays, at least three paramagnetic centers are obtained. One of these is constituted by the radical ClO_2. (tr-auth)

12889 GAMMA IRRADIATION OF SOLID-STATE N AND C TERMINALLY PROTECTED OLIGOPEPTIDES AND AMINO ACIDS. CARBOBENZOXY DERIVATIVES AND ESTERS OF AMINO ACIDS. Badiello, R.; Breccia, A.; Budini, R. (Univ., Bologna). Int. J. Appl. Radiat. Isotop., 17: 61-7(Jan. 1966).

The effects of γ radiation on various solid-state N-carbobenzoxy derivatives and esters of amino acids were studied by chemical and physicochemical methods. Data on decarboxylation and destruction of these derivatives and on the formation of stable radicals are presented and a comparison was made with corresponding data for free amino acids, emphasizing the differences in radiosensitivity between the two kinds of derivatives. In the protected compounds there was a very low production of stable radicals [G(radicals) = 10^{-5} to 10^{-6}] while the total transformation by irradiation was of the same magnitude as in the free compounds [G(transformation) = 2 to 15]. On the basis of these data the contribution of stable free radicals in the chemical transformation occurring during radiolysis of protected amino acids in the solid state is very small. (auth)

12890 ELECTRON SPIN RESONANCE STUDY OF X-IRRADIATED BINARY MIXTURES OF BENZENE AND ALCOHOLS. Leone, J. A.; Koski, W. S. (John Hopkins Univ., Baltimore). J. Amer. Chem. Soc., 88: 224-7 (Jan. 20, 1966).

Binary mixtures of benzene with methanol and ethanol were irradiated with x rays at 77°K and studied by ESR and mass spectral methods. Using isotopic labeling of the benzene and the various positions in the alcohols, it was found that on irradiation the hydroxyl hydrogen was liberated. It then added to the benzene molecule to form $C_6H_7\cdot$ or abstracted an α hydrogen from the alcohol to form the corresponding alcohol radical. A mechanism is discussed for the process. (auth)

12891 LUMINESCENCE PROCESSES GENERATED BY IONIZING RADIATION IN KI AND KI:Tl. Kaufman, R. Gilbert, Hadley, Wayne B. (Zenith Radio Corp., Chicago). J. Chem. Phys., 44: 1311-17(Feb. 15, 1966).

Undoped KI and thallium-doped KI were irradiated with x rays at 78°K. Luminescence and energy storage, in the form of trapped electrons and holes, were produced during irradiation. After irradiation phosphorescence was observed at 425 mμ and stimulation with light gave an emission quite similar to that during irradiation with bands at 302, 370, and 425 mμ. It is suggested that the luminescence produced during irradiation is predominantly from recombination. In stimulation the 425-mμ band characteristic of thallium grows and decays slower than the 302- and 370-mμ bands characteristic of the KI host. It is suggested that the phosphorescence is the result of the direct recombination of I_2^- and Tl^0, and that the same process occurs during stimulation and irradiation. In addition it was observed that 370-mμ emission produced during irradiation decreased in intensity with increasing temperature and that the 425-mμ emission intensity increased. It is suggested that 370-mμ emission decreased because of a radiationless transition and that 425-mμ emission increased because of the increase of recombinations at thallium sites. (auth)

12892 INFLUENCE OF TEMPERATURE ON THE F-CENTER ABSORPTION IN SODIUM FLUORIDE. Amenu-Kpodo, Kwasi; Neubert, Theodore J.; Youngblade, Walter (Illinois Inst. of Tech., Chicago). J. Chem. Phys., 44: 1324-6(Feb. 15, 1966). (COO-1044-18).

The F-center absorption in NaF, x-irradiated at CO_2 temperature, was studied as a function of temperature after a preanneal at 100°C. Three absorptions occur in such crystals: an unnamed band at 5.70 ev (218 mμ); the K band at 4.35 ev (285 mμ), whose peak position and half-width (1.0 ev) are not temperature sensitive; and the F band, which has its peak at 2.71 ev (334 mμ) at 80°K after correction for K-band overlap. The data for half-width of the F band as a function of temperature when fitted to the well-known hyperbolic-cotangent relation, indicated a value of $H_0 = 0.358 \pm 0.002$ ev for the half-width at 0°K and a value of $\nu_g = (7.7 \pm 0.2) \times 10^{12}$ sec^{-1} for the effective frequency of the phonons, which interact with the F-center electron in its ground state. That frequency (ν_g) appeared to be approximately one-half the frequency (ν_0) of the longitudinal optical modes, for NaF and for the five other alkali halides for which data are published. (auth)

12893 DETECTION OF RADIATION DAMAGE IN ANTHRACENE CRYSTALS BY SPACE-CHARGE-LIMITED CURRENT MEASUREMENTS. Weisz, S. Z.; Cobas, Amador; Richardson, Paul E.; Szmant, H. Harry; Trester, Seymour (Univ. of Puerto Rico). J. Chem. Phys., 44: 1364-8(Feb. 15, 1966).

It is shown that hole traps are induced in anthracene crystals by irradiating the crystals with either gamma or x rays. These traps are detected by measuring the steady-state current-voltage characteristic of the crystal in the space-charge-limited current region. A modified type of Kallmann-Pope cell employing a sodium sulfate solution as one electrode and a sodium iodide–iodine solution as the hole injecting electrode was used. After irradiating the crystals with gamma rays or x rays, part of the current-voltage curve showed a square-law dependence and current saturation occurred at higher voltages than in the nonirradiated crystals. By applying space-charge-limited current theory and interpreting the voltage at which the departure from the square law occurs as the trap-filled-limit voltage for induced deep traps, the density of these traps could be estimated. Using this calculated density it was found that one deep trap is created for every 45 kev of incident energy absorbed in the crystal. (auth)

12894 GAS-PHASE RADIOLYSIS OF CYCLOBUTANE. Doepker, R. D.; Ausloos, P. (National Bureau of Standards, Washington, D. C.). J. Chem. Phys., 44: 1641-7 (Feb. 15, 1966).

The gas-phase radiolysis of cyclo-C_4H_8 and cyclo-C_4D_8 was investigated in the presence of O_2, NO, H_2S, NH_3, and several organic compounds. From the products formed, it could be inferred that the following fragmentation processes occur: $C_4H_8^+ \rightarrow C_3H_5^+ + CH_3$, $C_4H_8^+ \rightarrow C_2H_5^+ + C_2H_4$, $C_4H_8^+ \rightarrow C_2H_5^+ + C_2H_3$, and $C_4H_8^+ \rightarrow C_3H_4^+ + CH_4$. At 20 Torr, the ion-pair yields, which can be ascribed to some of these processes, were lower than the corresponding ion-pair yields observed in the mass spectrometer at a pressure of 10^{-5} Torr. When compounds such as NO(IP = 9.25 ev) or $(CH_3)_3N$(IP = 7.8 ev) were added to cyclobutane, butene (IP = 9.13 to 9.58 ev) was a major product. On the other hand, when organic or inorganic compounds with ionization energies higher than that of butene were added to cyclobutane, the yield of butene was in most cases, negligibly small. The formation of butene could be tentatively accounted for by a ring opening of the parent ion followed by charge transfer. On the basis of this mechanism, a minimum value of 0.42 ± 0.02 can be ascribed to $M(C_4H_8^+)/N$. When an electric field was applied in the saturation current region, during radiolysis of cyclobutane–NO mixtures, the yields of methane, ethane, and butene, which have the parent ion or fragments thereof as precursors, remain unchanged. On the other hand, the yields of products such as ethylene, allene, acetylene, and 1,3-butadiene increased due to increased excitation by electron impact. In the absence of an electrical field, the number of neutral excited molecule decompositions per ion pair was estimated to be $\leq 0.65 \pm 0.05$. (auth)

12895 Ag I AND Ag III FROM SOLVATED Ag II BY RADIATION-CHEMICAL CONVERSION IN γ-IRRADIATED SOLUTIONS AT 77°K. Shields, L. (The University, Leeds, Eng.). J. Chem. Phys., 44: 1685-9(Feb. 15, 1966).

EPR evidence is advanced for the radiation-chemical production of silver I and silver III complexes from silver II salt solutions frozen in liquid nitrogen. The complexes are distorted from cubic symmetry by an extension along one polar axis. (auth)

12896 APPLICATION OF PRIMAK'S METHOD FOR THE DETERMINATION OF ACTIVATION ENERGY SPECTRUM IN ANNEALING PROCESSES AFTER NUCLEAR

RECOIL IN METAL COMPLEXES. Shankar, J.; Lal, M. (Atomic Energy Establishment, Trombay, India). J. Inorg. Nucl. Chem., 27: 2507-11(Dec. 1965).

The Primak treatment was applied to kinetic data on the annealing of chemical recoil damage in trisacetylacetone Co(III). A frequency factor of $4.5 \times 10^{11} sec^{-1}$ and a spread of activation energies from 1.09 ev to 1.22 ev were obtained. (auth)

12897 DYNAMIC EXTRACTION OF RECOIL PRODUCTS FROM COMPLEX-IONS ADSORBED ON AN ION-EXCHANGER. APPLICATION TO THE HEXAMMINE- AND TRISETHYLENEDIAMINE-COBALT IONS. Matsuura, T. (Rikkyo Univ., Yokosuka, Jap.). J. Inorg. Nucl. Chem., 27: 2669-73(Dec. 1965).

A continuous extraction of recoil products from the Szilard–Chalmers reaction on a complex ion adsorbed on an ion-exchange resin was proposed for obtaining a high yield and specific activity. The method was tested using hexamminecobalt and trisethylenediaminecobalt ions. The recoiling radioactive aquocobaltous ion was continuously eluted with a 0.5% ammonium citrate solution (pH 5.0). When the concomitant ionizing radiation dose rate was high the method gave a lower retention. (auth)

12898 PREPARATION OF XENON COMPOUND BY ACTIVATION PROCESSES FOR FLUORIDE SYSTEM. Kamemoto, Y. (Japan Atomic Energy Research Inst., Tokyo). J. Inorg. Nucl. Chem., 27: 2678-9(Dec. 1965).

Xenon compounds was prepared by using nuclear fission recoil. A lithium fluoride and uranium dioxide powder mixture in a weight ratio of 4:1 was irradiated at a neutron flux of about $3 \times 10^{11} n/cm^2/sec$ for 1 day. The irradiated mixture was sealed in an evacuated glass tube and then heated at 450°C for 5 hr. The count rates from ^{133}Xe obtained at different position on the glass tube are shown. The results showed that the xenon compounds formed were not produced by the action of the decay energy of iodine, but were produced by some action of either the nuclear recoil energy, in-pile gamma rays, or heat of the alpha particles of lithium, or of a combination of them all. (F.J.H.)

12899 RESPONSE OF NaI, ANTHRACENE AND PLASTIC SCINTILLATORS TO ELECTRONS AND THE PROBLEMS OF DETECTING LOW ENERGY ELECTRONS WITH SCINTILLATION COUNTERS. Porter, F. T.; Freedman, M. S.; Wagner, F. Jr.; Sherman, I. S. (Argonne National Lab., Ill.). Nucl. Instrum. Methods, 39: 35-44(Jan. 1966).

The electron response of NaI(Tl) is measured with magnetic-spectrometer-energy-selected electrons incident on cleaved crystal surfaces, in the energy range 5 to 1000 kev. The light output/kev (≡ response) shows a maximum in the neighborhood of 15 to 20 kev, which is some 20% larger than that at 1 Mev; below 15 kev the response falls sharply, reaching 80% of the peak value at ~5 kev. The electron response of anthracene and a plastic scintillator (Pilot B) is measured under the same experimental conditions for comparison. Both anthracene and Pilot B show nonproportional response in the low energy region. At 500 kev the ratio of the responses NaI(Tl)/anthracene/Pilot B are 1.6/1.0/0.38; at 20 kev the ratios are 2.5/1.0/0.41. Decay curve analysis yields for some of the long lived states (excited by incident electrons) in NaI(Tl), lifetimes of 200 to 300 μsec, 7 to 9 msec, 40 to 80 msec, 4 sec, 1 min, and 12 min; and for anthracene 36 μsec, 120 μsec, and 570 μsec. Relatively intense long lived states and more backscattering make NaI(Tl) not generally useful as a low energy electron detector. Uncovered anthracene mounted directly on a photomultiplier and the combination cooled to prevent sublimation of the phosphor in the high vacuum of the beta spectrometer provides a counter which has efficiencies measurable from the pulse height distributions down to ~6 kev. At backgrounds of 300 to 500 cpm it has usable efficiencies down to 1 kev. (auth)

12900 NOTE ON FORMATION AND THERMAL BLEACHING OF COLOR CENTERS IN SODIUM CHLORATE CRYSTALS IRRADIATED BY γ-RAYS. Czerwonko, Anna; Damm, Jozef Zbigniew (Inst. of Chemical Physics, Wroclaw). Nukleonika, 10: 531-4(1965).

The properties of $NaClO_3$ crystals that condition their application in radiation dosimetry were studied. $NaClO_3$ crystals were prepared and irradiated in dry air by gamma rays at room temperature. The color of the crystals changed with radiation dose from yellow to brownish. Thermal bleaching experiments were performed at 100, 150, and 200°C. Two bands appeared in irradiated crystals at 420 and 305 nm. The optical density increased linearly with radiation dose. Within the first minutes of bleaching an abrupt loss of absorption took place after which the process proceeded very slowly down to a plateau. (M.C.G.)

12901 PRIMARY PROCESSES IN RADIATION CHEMISTRY AS STUDIED BY MASS SPECTROMETRY. IV. ION-MOLECULE REACTIONS IN TETRAHYDRONAPHTHALENE. Wincel, Henryk; Kecki, Zbigniew (Inst. of Nuclear Research, Warsaw). Nukleonika, 10: 567-73(1965).

Ion-molecule reactions in which neutral and ionized molecules of tetrahydronaphthalene take part were investigated with a mass spectrometer. Relative cross-section values of individual reactions were determined and the reactions occurring in the radiolysis process of tetrahydronaphthalene in the liquid phase are discussed. (auth)

12902 COMPLEX POLYPHOSPHATES IN IRRADIATED PHOSPHORUS OXY-ANIONS. Anselmo, Vincent C. (New Mexico Highlands Univ., Las Vegas). Radiochim. Acta, 4: 203-6(Dec. 1965).

Several salts of phosphorus oxy-anions were investigated by anion exchange chromatography with a view toward resolving whether complex polyphosphates were formed following neutron capture. For the sodium monohydrogen and dihydrogen orthophosphates a significant fraction of the activity was found on elution with a strong acid solution indicating the presence of such complex material. Trisodium orthophosphate gave anomalous results while the reduced state showed negligible concentrations. (auth)

12903 THERMAL ANNEALING AND ROLE OF THE WATER OF CRYSTALLIZATION IN POTASSIUM TRIOXALATOFERRATE IRRADIATED WITH NEUTRONS. Rusi, A.; Calusaru, A. (Inst. of Atomic Physics, Bucharest). Radiochim. Acta, 4: 206-11(Dec. 1965). (In French).

The thermal annealing of neutron irradiated potassium trioxalatoferrate corresponded to isotherms with different pseudo-plateaus. The annealing curves, taken for the crystalline product with light, heavy, and without water, showed a distributed spectrum of activation energies, from which the following characteristic values were derived: 0.50 to 0.57 ev for the lattice with light water, 0.63 to 0.67 ev for that with heavy, and 0.52 ev for that without water. The Fe^{3+}/Fe^{2+} ratio in the recoil was notably affected by water of crystallization. In the water-containing lattices it was 1.18 to 1.35; without water it was about 0.6. The complete oxidation of Fe^{2+}, at temperatures below the recovery limit, showed that only Fe^{3+} participates in the reaction mechanism. (auth)

12904 THERMAL ANNEALING IN POTASSIUM CHROMATE: A COMPARISON OF ^{51}Cr ANNEALING KINETICS IN NEUTRON-IRRADIATED AND IN ^{51}Cr(III)-DOPED POTASSIUM CHROMATE. Collins, C. H.; Collins, K. E.; Ghoos, Y. F.; Apers, D. J. (Univ., Louvain, Belg. Institut Interuniversitaire des Sciences Nucleaires, Brussels). Radiochim. Acta, 4: 211-16(Dec. 1965).

Close quantitative similarity was observed between the kinetics of thermal annealing of ^{51}Cr in neutron-irradiated, inactive-Cr(III)-doped potassium chromate and in ^{51}Cr(III)-doped potassium chromate when both types of crystals received similar levels of radiation damage. This similarity suggested that the same annealing mechanism might be operating in both kinds of crystals. Several possible oxidative annealing mechanisms for potassium chromate are discussed. (auth)

12905 NEW PRODUCTS OF IRRADIATED POLYETHYLENE. Hakamada, Koichi. Sumitomo Elec. Tech. Rev., No. 1, 122-8(Jan. 1963).

Development of irradiated polyethylene into practical materials is discussed. The properties of irradiated polyethylene and products made from irradiated polyethylene are described. (auth)

12906 APPLICATION OF A LARGE ACCELERATOR TO PRODUCE IRRADIATED POLYETHYLENE PRODUCTS. Tsuji, Yoshio; Kawashima, Maumi. Sumitomo Elec. Tech. Rev., No. 4, 104-6(July 1964).

One method of reducing the price of irradiated products is to develop larger accelerators. The NS electron beam accelerator is described and engineering problems are discussed. The operating efficiency of the acceralator is 90%, with a maximum period of continuous operation of ten hr. (auth)

12907 STUDIES ON IRRADIATION EFFECTS OF POLYVINYL CHLORIDE AND SOME APPLICATIONS FOR WIRE INSULATION. Izumi, M.; Suzuki, F.; Yuri, T. Sumitomo Elec. Rev., No. 90, 44-52(Oct. 1965). (In Japanese).

The proper irradiation conditions for improving the properties of PVC by irradiation were studied. Several experiments concerning the cross-linking effects of atmosphere, radiation source, and PVC compositions (cross-linking agent, polymer, stabilizer, plasticizer, fillers, etc.) are discussed. Electric wires insulated with irradiated cross-linked PVC were produced and tested. Improved properties of the wires were as follows: heat resistance property (especially nonsoftening property to about 300°C); nonsolvent property for chemical agents; and excellent electrical properties. Irradiated cross-linked PVC showed many interesting properties and can be applied for other uses also. (auth)

12908 RADIATION INDUCED CRACKING OF PENTANES AND DIMETHYLBUTANES [Thesis]. Carnahan, Brice. Ann Arbor, Mich., Univ. of Michigan, 1965. 471p.

The promotion of the cracking reactions of four simple straight-chain and methyl-substituted paraffins (n-pentane, isopentane, 2,3-dimethylbutane, 2,2-dimethylbutane) by ionizing radiation produced in a nuclear reactor was investigated. Pilot scale flow equipment suitable for carrying out irradiation experiments was built. The pilot plant consists of a beamport assembly containing a small pressure vessel with attendant heaters, thermocouples, and access tubing, and an external assembly containing the feeding, controlling, and product-recovery equipment. The beamport assembly is inserted into a beamport of a swimming pool reactor while the external assembly is wholly outside the reactor shield. Over 140 irradiation experiments were done at elevated pressures (250–1000 psig) and incipient thermal cracking temperatures for the selected paraffins (650–850°F). The absorbed radiation dose rate was 2.0×10^5 rad/min; the maximum total absorbed dose was $\cong 6$ megarad. Under incipient thermal cracking conditions, ionizing radiation (principally gamma radiation) at the radiation dose rate level employed induces substantial decomposition rates for all the paraffin hydrocarbons investigated, the G values being typically in the range 30–1200. The decomposition rate and overall G value show no significant pressure dependence in the range investigated. Both decomposition rate and overall G value decrease exponentially with increasing total radiation dose. A first order kinetic model adequately describes the rate data for all compounds, once the data are normalized to a standard radiation dose. The radiation-thermal first order reaction rate constants exhibit a temperature dependence described by the Arrhenius equation. While radiation induced cracking contributes by far the major portion of the cracked product under incipient thermal cracking conditions, strictly thermal cracking contributes by far the major portion of cracked product at normal thermal cracking temperatures. The product distributions for radiation and thermally induced cracking are virtually the same. These conclusions point to the use of ionizing radiation as a new tool for investigating thermally initiated free radical chain reactions. A by-product of the dosimetry work was the development of a simple calorimetric technique for the measurement of radiation dose rates in chemical equipment near intense sources having multi-energy gamma spectra. (A.G.W.)

12909 CROSS-LINKING OF POLYVINYLIDENE FLUORIDE AND WIRE COATED WITH THE CROSS-LINKED RESIN. Timmerman, Robert (to Radiation Dynamics, Inc.). U. S. Patent Re. 25,904. Nov. 16, 1965. Filed Feb. 24, 1965.

A composition comprising a resinous polymer of vinylidene fluoride crosslinked by high energy ionizing radiation in the range of approximately 8 megarads and higher is described. The crosslinked polymer provides a measurable improvement in thermal resistance, deformation-under-load characteristics, and tensile strength as compared with unirradiated polymers of the same material. A length of wire may be coated with the resin polymer and exposed to ionizing radiation to crosslink the polymer in situ. (B.L.M.)

Radiochemistry

See also Separation Processes and Procedures

Refer also to abstract 12770.

12910 (AECD/CH/3) CALIBRATION OF ^{60}Co GAMMA CELL. Rahman, Abdur; Shamsuddin, A. K.; Bashiruzzaman, Mohammad (Atomic Energy Centre, Dacca (Pakistan). Chemistry Div.). June 1965. 8p. Dep. mn.

A calibration procedure for ^{60}Co gamma sources using ferrous iron in sulfuric acid solutions is discussed. Dosimetry data are presented for distances ranging from 10 to 100 cm. (M.O.W.)

12911 (AECD/HP/3) A 500 CURIES IRRADIATION FACILITY AT THE ATOMIC ENERGY CENTRE, DACCA. Lustinec, Jiri; Siddiqi, Aziz Ahmad, Abdullah, S. Abu; Habibullah, A. K. M.; Mia, M. Mohtazuddin; Haq, A. M. Sirajul (Atomic Energy Centre, Dacca (Pakistan)). Aug. 1965. 21p. Dep. mn.

A gamma irradiation facility with about 500 Curies of ^{60}Co was installed at the Atomic Energy Center, Dacca, in December, 1964. Some details of design and construction of the facility are described. The modified Fricke dosimeter was used for calibration of the source. In order to increase the sensitivity of ferrous sulfate dosimetry for small gamma doses, the spectrophotometric determination of residual ferrous ions instead of the ferric ions formed was carried out using the ferrous orthophenanthroline method. The procedure was modified by utilization of sensitizers to increase the G-value (Fe^{2+} and Fe^{3+}). (auth)

12912 (CNEA–161) PREPARACION DE ALIL-INULINA ^{131}I. (Preparation of ^{131}I-Allyl-Inulin). Mitta, Aldo E. A.; Camin, Leopoldo L. (Comision Nacional de Energia Atomica, Buenos Aires (Argentina)). 1965. 5p. (CONF-641126–2). Dep. mn.

From 1st Symposium on Nuclear Medicine, Mendoza, Argentina.

A method is presented for the preparation of ^{131}I-labeled-allylinulin in which the pure radioactive iodine is replaced by ^{131}ICl. The labeled ICl is obtained by isotopic exchange between Na^{131}I and iodine chloride. A radiochemical yield of 70% is obtained in only one hour. (J.S.R.)

12913 (EUR–2446.f) SYNTHESE DU LINOLENATE ET DE L'ARACHIDONATE DE CHOLESTERYLE DOUBLEMENT MARQUES. (Synthesis of Double Labelled Cholesteryl Linolenate and Arachidonate). Crastes de Paulet, A.; Bardou, L. (Montpellier Univ. (France). Faculte de Medecine). 1965. 15p. Dep. mn.

The transesterification method used previously for cholesteryl ester synthesis, following the scheme cholesteryl acetate + fatty acid methyl ester → cholesteryl ester + methyl acetate, was adapted to the microscale

(1 to 10 μM) imposed by the use of labeled molecules of high specific activity. This method is particularly suitable for the synthesis of polyethylenic fatty acid cholesteryl esters. The following esters: 4 ^{14}C and 7 $\alpha^{3}H$ cholesteryl linolenate and arachidonate, cholesteryl linolenate U ^{14}C, and arachidonate (5-6, 8-9, 11-12, 14-15)^{3}H were obtained; the mixture of these two types of esters of high specific activity give rise to series of doubly labeled esters, at the user's convenience. (auth)

12914 (IEA–100) DEVELOPMENT OF RADIOCHEMISTRY ACTIVITIES IN NEW RESEARCH REACTOR CENTERS. Lima, Fausto W. (Instituto de Energia Atomica, Sao Paulo (Brazil)). Aug. 1965. 28p. (CONF-631104–8). Dep. mn.

From the Meeting on the Utilization of Research Reactors, Sao Paulo, Brazil.

The types of research in radiochemistry and chemistry that are liable to be found, and have to be solved, in new institutions centralizing their activities around a research reactor of the swimming-pool type are described. The three main types of research to be developed include: tracer studies, production and processing of radioisotopes, and radiochemical and classical chemical analysis. (P.C.H.)

12915 SOIL CHEMISTRY OF RADIONUCLIDES. Schulz, R. K. (Univ. of California, Berkeley). Health Phys., 11: 1317–24(Dec. 1965).

Biological importance of radionuclides found in the soil is determined by half-life and by mobility of the nuclides in soil. Further, the amount and species of complementary ions in a soil mass strongly influence the redistribution of nuclides in the soil profile and will affect their uptake. (H.G.D.)

12916 RECOVERY OF TELLURIC ACID FROM ^{131}I PRODUCTION WASTE. Lin, Chien-Chang (National Tsing, Hua Univ., Hsinchu, Taiwan). Ho Tsu K'o Hsueh, 4: No. 3-4, 81-3(Aug. 1965).

Telluric acid may be recovered from ^{131}I production waste by precipitation with concentrated HNO_3. A recovery yield of 85% was obtained. Spectrophotomeric and chemical analysis of telluric acid showed that the purity of the recovered telluric acid is satisfactory. (auth)

12917 PRODUCTION OF ^{87}Y AND A ^{87m}Sr GENERATOR. Hillman, M.; Greene, M. W.; Bishop, W. N.; Richards, P. (Brookhaven National Lab., Upton, N. Y.). Int. J. Appl. Radiat. Isotop., 17: 9-12(Jan. 1966). (BNL-9152).

Methods are described for the production of ^{87}Y by the Rb(α,xn)Y reaction and for the preparation of a generator from which ^{87m}Sr of high purity may be repeatedly milked. The ^{87}Y was prepared by the reaction of 35-Mev α particles with a thick target of RbCl, and the generator was prepared by absorbing the yttrium on Dowex-1 in the carbonate form. Elution of the ^{87m}Sr is accomplished by means of a dilute solution of citric acid at pH 5. (auth)

12918 CONTROL OF THE RADIOCHEMICAL PURITY OF SOME ORGANIC RADIOPHARMACEUTICALS LABELED WITH ^{131}I. Gopal, N. G. S. (Centre d'Etudes Nucleaires, Saclay, France). Int. J. Appl. Radiat. Isotop., 17: 75-7 (Jan. 1966).

The radiochemical purity of organic radiopharmaceuticals labeled with iodine-131 was studied. The possibility of using two ion-exchange cellulose papers for control of some organic radiopharmaceuticals was determined. The products were prepared and separated by chromatography and electrophoresis on cellulose paper. Chromatography was carried out by the ascending technique with 0.25M sodium citrate at pH 8.2. Paper electrophoretic analysis was carried out at 7v/cm for 1 hr on paper strips moistened with 0.025M sodium citrate. Results are presented in autoradiograms. It was found that chromatography is preferable for Rose Bengal–^{131}I and erythrosin–^{131}I, that chromatography and electrophoresis are both satisfactory for thyroxine–^{131}I, and that for hypaque–^{131}I and diodone–^{131}I electrophoresis is preferable. (F.J.H.)

12919 PREPARATION OF SULPHIDES AND ELEMENTAL SULPHUR LABELLED WITH ^{35}S FROM NEUTRON IRRADIATED POTASSIUM CHLORIDE. Suarez, C. (Junta de Energia Nuclear, Madrid). Int. J. Appl. Radiat. Isotop., 17: 77-9(Jan. 1966).

Neutron-irradiated KCl is dissolved in 0.05N HCl containing a small amount of H_2SO_4 as isotopic carrier. After the ^{35}S is carried down with $BaSO_4$, the washed precipitate is transferred into a flask where H_3PO_4 and powered Cr are added. The mixture is heated and H_2S obtained. The activity recovered as H_2S is higher than 99%. (M.C.G.)

12920 25 YEARS OF NUCLEAR FISSION. METHODS AND RESULTS OF CHEMICAL STUDIES. 2. METHODS. Hermann, Guenter (Univ., Mainz). Radiochim. Acta, 4: 173-88(Dec. 1965). (In German).

Methods and results of chemical studies on low-energy fission of heavy nuclei are reviewed. Topics covered include: detection of fission products by direct and indirect measurements, fission yields, radiometric and mass spectrometric methods for determining fission yields, procedures for studying nuclear charge distribution by independent yields of shielded fission products and fractional yields of fission-chain members, and studies of mass and charge distributions by physical methods. (auth)

12921 IMPROVEMENTS IN OR RELATING TO LUMINESCENT MATERIALS. Ault, John Douglas (to Saunders Roe and Nuclear Enterprises Ltd.). British Patent 1,016,902. Jan. 12, 1966. Filed July 4, 1961.

A self-luminous substance of generally granular structure is characterized in that the first and second principal constitutents of the substance, each in granular form, are separated from the third constitutent. In an example of the substance, the first constitutent may be either Ti or Zr powder compounded with tritium and then coated with the second constitutent that is a metal such as Cu, Ag, or Ni to prevent the escape of tritium. The coated particles are then intimately mixed with a suitable sulfide phosphor powder to form a luminescent paint powder. (B.L.M.)

12922 PROCESS FOR MAKING HIGH PURITY RADIOACTIVE ^{131}I. Gemmill, Wayne J. (to Union Carbide Corp.). U. S. Patent 3,226,298. Dec. 28, 1965. Filed Oct. 24, 1963.

A method of producing radioactive ^{131}I comprises the steps of heating finely ground TeO_2 at a temperature of from 550 to 600°C for at least one hour, irradiating the dioxide with thermal neutrons, and separating the radioactive ^{131}I formed from the residual TeO_2 by dry distillation at a temperature of 600 to 700°C under vacuum. (B.L.M.)

Separation Processes and Procedures

See also Analytical Procedures
ISOTOPE TECHNOLOGY — Separation and Production

Refer also to abstracts 12997, 13018, 13780, and 14193.

12923 (ANL–6898) ENGINEERING DEVELOPMENT OF FLUID-BED FLUORIDE VOLATILITY PROCESSES. PART 3. FLUID-BED FLUORINATION OF URANIUM DIOXIDE FUEL PELLETS. Anastasia, L. J.; Gabor, J. D.; Mecham, W. J. (Argonne National Lab., Ill.). Aug. 1965. Contract W-31-109-eng-38. 81p. Dep. mn. CFSTI $3.00 cy, $0.75 mn.

The fluorination of nonirradiated UO_2 pellets in a 3-in.-dia fluidized-packed bed reactor system was carried out to demonstrate the fluorination step on a pilot-plant scale. The packed bed was formed by a batch of cylindrical pellets which were too large to fluidize directly. An inert fluidized medium was provided in the voids of the pellet bed and in

the space above the bed to aid in heat removal for the highly exothermic reactions involved. Additional cooling capacity was provided by passing a stream of air past external fins attached to the reactor. The experimental effects of most interest were the production rates for UF_6, the efficiency of fluorine utilization, and control of the reaction temperature. The fluorination proceeds through an induction period of UO_2F_2 formation followed by a reaction period of high UF_6 production and high fluorine utilization. The presence of oxygen enhanced the fluorination by formation of U_3O_8 fines of high specific surface area and high reactivity. The temperature coefficient (E′) for reaction with fluorine diluted with either oxygen or nitrogen was 14 kcal/g-mole UO_2. Application of fluidized-bed techniques to the dejacketing of clad, simulated fuel elements was also investigated and found to be effective for Zircaloy-2 and stainless steel claddings. (P.C.H.)

12924 (ANL–6973) ENGINEERING DEVELOPMENT OF FLUID-BED FLUORIDE VOLATILITY PROCESSES. PART 8. PILOT-PLANT DEVELOPMENT OF A PROCESS FOR URANIUM ALLOY FUELS. Holmes, John T.; Stethers, Howard; Barghusen, John J. (Argonne National Lab., Ill.). Aug. 1965. Contract W-31-109-eng-38. 63p. Dep. mn. CFSTI $3.00 cy, $0.75 mn.

A fluid-bed fluoride volatility (FBV) process for the recovery of uranium from highly enriched uranium-Zircaloy–2 (U-Zr) and uranium-aluminum (U-Al) alloy fuels was developed on a pilot-plant scale. The conceptual operation of the process consists of three major steps: a hydrochlorination step, in which alloying materials are separated by virtue of the volatility of their chlorides; a fluorination step, in which the uranium is volatilized and recovered as the hexafluoride; and a final product-decontamination step. The first two reactions are conducted in a single vessel (halogenation reactor) in which a bed of inert alumina particulate material is fluidized by the reagent gases. The use of a fluid bed facilitates dissipation of the reaction heat. An important feature of this process is the use of a packed bed of alumina particulate materials as a high-temperature filter. (auth)

12925 (EURAEC–1446) REPROCESSING OF IRRADIATED FUELS. Quarterly Report No. 20, January 1–March 31, 1965. (Centre d'Etude de l'Energie Nucleaire, Mol (Belgium)). Contract 004-64-4-RCIB(RD). 55p. (EUR–2380; R–2347). Dep. mn; CFSTI $3.00 cy, $0.75 mn.

Work Performed under United States–Euratom Joint Research and Development Program.

Investigations of the reactions of dioxides with ClF_3 were continued for separation of U and Pu, and for decontamination. The reaction of ClF_3 with sintered dioxide containing 10% of PuO_2 removed the greater part of the U present. Research with regard to the same reaction on sintered UO_2 revealed that between 75 and 165°C, with a 25% concentration of ClF_3, the reaction rate is not very sensitive to temperature. With ClF_3 concentrations lower than 25% the reaction rate is proportional to the linear velocity of the gases, calculated at the reaction temperature. At 100°C the reaction rate is approximately proportional to the ClF_3 concentration. UF_6 produced under these conditions may be fixed on NaF. The tests resulted in a UO_2-to-UF_6 conversion rate of the order of 3.8 kg. h^{-1} dm^{-2} higher than what is generally expected, in the industrial stage, for the F_2 cycle. Extrapolation of the data indicates that production several times greater could be attained with F_2 yields exceeding 80% and a quantitative yield of UF_6. Investigations of fission products under the action of ClF_3 confirmed the sublimation of I_2, Zr–Nb, Ru, Te, and Np. It was also found that treatment of UO_2 irradiated by a mixture of O_2 and HF at 600°C induced disposal of the I_2 and part of the Zr–Nb. Reactions between high-density UC and O_2, water vapor, $H_2I–O_2$ mixtures, HF and HF–O_2 mixtures were investigated. The reactions are slow and result in bad spray yields in nearly all instances. (J.R.D.)

12926 (IDO–14669) URANIUM RECOVERY FROM ALUMINUM ALLOYED FUEL ICPP RUN NO. 21. Wheeler, B. R.; Offutt, G. F.; Commander, R. E. (Phillips Petroleum Co., Idaho Falls, Idaho. Atomic Energy Div.). Jan. 1966. Contract AT(10-1)-205. 35p. Dep. mn. CFSTI $2.00 cy, $0.50 mn.

About 505 kg of high-enriched uranium were recovered from aluminum alloyed fuels during Run No. 21 at the Idaho Chemical Processing Plant. Overall product recovery exceeded 99.85 percent, and product log decontamination factors exceeded 7.0. This processing campaign was unique in that 66 of the 505 kg of uranium were recovered on a part-time basis with spare manpower not needed for operation of the Waste Calcining Facility. The feasibility of recovering neptunium at ICPP was demonstrated during the run by recovering over 90 percent of the neptunium in the second cycle raffinate generated during the campaign. Pre-run modifications to the extraction systems simplified the processing campaign and as a result of the experience gained on the run other modifications and processing schemes are actively being considered at ICPP. (auth)

12927 (NP–15756) ELECTRODELESS CONDUCTIVITY METER FOR ON-STREAM MEASUREMENTS. De Carolis, M.; Mongon, A. (European Company for the Chemical Processing of Irradiated Fuels, Mol (Belgium)). Aug. 1965. 22p. (ETR–175). Dep. mn. CFSTI $1.00 cy, $0.50 mn.

An instrument developed for the measurement of the conductivity of the feed solutions of the first extraction cycle of the Eurochemic Reprocessing Plant is described. The instrument can be used to measure conductivities in the range from 0.15 to 0.80 mho-cm^{-1} at temperatures from 20 to 38°C. (D.C.W.)

12928 (ORNL–3868) UNIT OPERATIONS SECTION QUARTERLY PROGRESS REPORT, APRIL–JUNE 1965. Whatley, M. E.; Haas, P. A.; Horton, R. W.; Ryon, A. D.; Suddath, J. C.; Watson, C. D. (Oak Ridge National Lab., Tenn.). Dec. 1965. Contract W-7405-eng-26. 105p. Dep. mn; CFSTI $4.00 cy, $0.75 mn.

The stacked-clone contactor was tested for transfer of U between HNO_3- and sodium nitrate-salted solutions and TBP-Amsco, transfer of nitric acid with aluminum nitrate salting, and transfer of acetic acid into hexone. A conceptual flowsheet for close-coupled processing of the fuel and fertile streams of a molten-salt breeder reactor is presented. Both an intact, unirradiated, Dresden Type-IV fuel assembly (Zy-2-clad UO_2) and a loose bundle of fuel rods were successfully sheared by the ORNL 250-ton shear. The effective thermal conductivity of sheared ss-clad UO_2 pieces in air ranges from 0.41 Btu hr^{-1} deg^{-1} at 474°F, to 3.42 at 1474°F. Fine grinding of graphite fuel containing abrasive carbides in a high-speed mill caused excessive wear of the discharge screen. Solid–liquid separation still is a problem in leaching of finely ground U–graphite fuel. Crushed HTGR "A" compacts were successfully burned with O_2 in a fluid bed containing 60 to 90 mesh alumina, and 99.7% of the U and Th was subsequently leached from the bed material. Mechanical-handling tests of equipment in the cell mockup of the Transuranium Processing Facility are virtually complete. A test (R-89) of the rising-level glass method of fixing radioactive waste was terminated after 43 hours operation because a hole was corroded through the stainless steel vessel. (J.R.D.)

12929 SELECTIVE ELUTION OF SCINTILLATION PHOSPHORS FROM CHROMATOGRAPHY PAPER FOLLOWING RADIOACTIVITY MEASUREMENTS. Mercer, Nina J. H.; Henderson, J. Frank (Univ. of Alberta, Can.). Anal. Biochem., 13: 559-61(Dec. 1965).

A procedure for the selective elution of POPOP and PPO from paper strips without removal of water-soluble compounds is described. Acetone was used for elution of the paper strips. The efficiency of the method is shown in graphs. (M.C.G.)

12930 GAS CHROMATOGRAPHY OF ISOTOPIC MOLECULES ON OPEN TUBULAR COLUMNS. Bruner, Fabrizio; Cartoni, Gian Paolo; Liberti Arnaldo (Univ., Naples). Anal. Chem., 38: 298-303(Feb. 1966).

Glass capillary columns either with modified internal area or coated with a layer of liquid phase exhibit a very high resolution and may be used to separate isotopic molecules. Optimum working conditions were established in terms of peak resolution and analysis time. The following systems were studied by operating at temperatures up to 77°K: CH_4-CD_4, $C_2H_6-C_2D_6$, $C_2H_4-C_2D_4$, $C_7H_8-C_7D_8$, and $^{16}O_2-^{18}O_2$. The gas chromatographic behavior is discussed and the changes of the relative retention volumes ratio and of the vapor pressure ratio with the temperature are compared. At very low temperature the mass difference is the determining factor, and a normal effect is observed, as the lighter species is eluted first. In most cases, however, a reverse effect is exhibited, with the heavier isotopic species being less retained by the chromatographic column. (auth)

12931 EXTRACTION OF URANIUM(VI) AND THORIUM FROM NITRIC ACID SOLUTIONS BY TRI-n-BUTYL PHOSPHATE. Sato, Taichi (Shizuoka Univ., Hamamatsu, Japan). J. Appl. Chem., 15: 489-95(Nov. 1965).

The partitions of uranium(VI) and thorium between nitric acid solutions and kerosene solutions of tri-n-butyl phosphate (TBP) were investigated at different concentrations of nitric acid and solvent and at different temperatures. An infrared spectral study was also made of the organic solutions obtained. (auth)

12932 ION EXCHANGE PROPERTIES OF VANADIUM FERROCYANIDE. II. DYNAMIC EXPERIMENTS. Krtil, J. (Nuclear Research Inst., Czechoslovak Academy of Sciences, Rez). J. Chromatog., 21: 85-91(Jan. 1966).

The use of vanadium ferrocyanide for the separation and isolation of heavy alkali metals under dynamic conditions was studied. The capacity of this sorbent for Cs, Rb, Sr, and Ce was determined, and the conditions for maximum sorption and elution of these elements were also determined. The application of vanadium ferrocyanide to the isolation of ^{137}Cs from a solution of fission products was tested. (auth)

12933 A NEW SEPARATION OF NIOBIUM AND MOLYBDENUM BY SOLVENT EXTRACTION WITH QUATERNARY AMMONIUM HALIDES. Abecasis, S. M.; Scott, B. B. (Univ. Nacional, La Plata). J. Inorg. Nucl. Chem., 27: 2665-8(Dec. 1965).

A fast efficient separation of niobium and molybdenum, even in unfavorable proportions, is described. It makes use of the extraction of the niobium–pyrogallol complex, in the presence of tetra-n-butylammonium bromide, into ethyl acetate. The radiochemical purity of the separated molybdenum and niobium fractions was checked by measuring the γ-spectra. The decontamination of niobium from molybdenum was better than 10^5. (auth)

12934 CHEMICAL DEGRADATION OF KEROSENE DILUENT WITH NITRIC ACID. Ishihara, Takehiko; Ohwada, Ken (Japan Atomic Energy Research Inst., Tokyo). J. Nucl. Sci. Technol. (Tokyo), 3: 20-6(Jan. 1966).

Chemical degradation of kerosene diluent with nitric acid was studied to clarify its effect on the uranium distribution ratio and fission product retention in the presence of degradation products. The decontamination of fission products retained in degraded kerosene was also investigated. From the results of infrared spectrometry, it was recognized that nitro compounds, carboxylic acids, nitrate esters and nitroso compounds were formed as the main degradation products. The uranium distribution ratio in the extraction with TBP/degraded kerosene decreased with increasing concentration of nitric acid above 5N, with rising temperature, and with increasing concentration of olefinic and aromatic hydrocarbons in the kerosene. It is suggested that the decrease of uranium distribution ratio may be due to the formation of carboxylic acids caused by kerosene degradation. Some fission products, in particular $^{95}Zr-^{95}Nb$ and ^{131}I, were retained in the organic phase, but $^{106}Ru-^{106}Rh$ did not remain after scrubbing with 3N HNO_3. Fission product retention caused a decrease of the uranium distribution ratio. The usual acid-alkali washing could not remove $^{95}Zr-^{95}Nb$ and ^{131}I into the aqueous phase, but $^{95}Zr-^{95}Nb$ was eliminated by oxalic acid washing. (auth)

12935 RAPID METHOD OF OBTAINING CERIUM PREPARATION OF VERY HIGH PURITY. II. Borkowski, Boguslaw; Borkowska, Aleksandra; Banczykowna, Krystyna. Przem. Chem., 44: 667-70(Dec. 1965). (In Czech).

Experiments were carried out to improve previously described methods for obtaining cerium of spectral purity by purification of $(NH_4)_2\,Ce(NO_3)_6$. The presence of neutral, cationic, and anionic forms of cerium complexes was found in aqueous solutions of this compound. The relative concentration of the neutral form of cerium increased with the increase of dilution and reached a maximum after aging the solution. Additional complexing by acetic acid caused 80% of cerium present in the solution to occur in the neutral form. Under these conditions, other trivalent lanthanides gave cationic complexes with acetic acid. By pouring the solution thus prepared through a cationic column in the hydrogen form, cerium free from other lanthanides was obtained. The yield of the process depended on the solution pouring rate through the column. This is explained by the fact that hydrogen ions, set free during the purification process, destroy acetate cerium complexes. An ion exchanger in the ammonium form can be used, which also permits employing higher concentrations of $(NH_4)_2Ce(NO_3)_6$ (up to 50 g/l) in the process of obtaining pure Ce. Pure Ce with a yield of over 90% could be obtained at a Ce : CH_3COOH ratio = 1 : 8. (auth)

12936 RAPID RADIOCHEMICAL SEPARATION. I. SEPARATION OF Cd AND In FROM FISSION PRODUCT MIXTURES. Muenzel, H.; Koch, L. (Kernforschungszentrum, Karlsruhe, Ger.). Radiochim. Acta, 4: 188-91 (Dec. 1965). (In German).

Dithizone extraction was studied as a means of separating Cd and In from a mixture of fission products. Separation procedures for both elements are suggested. The time required to complete the procedures and the separation factors achieved are given. (auth)

12937 A NEW RAPID SEPARATION OF ^{231}Pa FROM ITS DAUGHTERS Ra, Th, Bi, Rn, AND Po BY TRICAPRYLMETHYLAMMONIUM CHLORIDE LIQUID-LIQUID EXTRACTION. Gerontopulos, P. Th. (SNAM-LRSR, Milan); Rigali, L.; Barbano, P. G. Radiochim. Acta, 4: 224-5 (Dec. 1965).

Some preliminary experiments were carried out to evaluate the possibility of rising xylene solutions of tricaprylmethylammonium chloride for separation of protactinium from its daughters Ra, Th, Bi, Rn, and Po. It was concluded that excellent purification of protactinium can be obtained in a single extraction cycle. Activity measurements showed that 99.76% of the protactinium passed into the organic phase. (M.C.G.)

12938 REMOVAL OF FISSION PRODUCTS BY DIATOMACEOUS EARTH OF ISHIKAWA PREFECTURE. Itakura, Tadashi (Public Health Lab., Ishikawa, Japan). Radioisotopes (Tokyo), 15: 4-13(1966). (In Japanese).

Long-lived nuclides could be preferentially separated from fission products by use of refined diatomaceous earth. Raw materials from the Ishikawa Prefecture were treated with an acid mixture of HCl and H_2SO_4 and then calcined at 500°C. These refined materials are commercially employed as a filter-aid material for industrial use, but it was also found that the material behaves as a good adsorbent for radioactive nuclides in water. ^{137}Cs, ^{89}Sr, ^{90}Sr, ^{91}Y, ^{95}Zr, ^{144}Ce, ^{147}Pm, ^{103}Ru, and ^{106}Ru, as well as mixed fission products, were used for the examination. For various concentrations of nuclides, pH, and presence or absence of other salts, the adsorptivity of the earth material was examined. The refined diatomaceous earth (100 mg) was put into 50 ml of an aqueous solution containing a definite amount of radionuclide (less than 1×10^{-3} μCi/ml) and shaken for three minutes. After centrifuging the mixture for five minutes, the radioactivity of the supernatant was measured. The difference of activities between the original

solution and the supernatant showed the amount of nuclide removed and the percentage removal was calculated. The nuclides treated may be classified in the following four groups from a point of the adsorptivity of the diatomaceous earth: cationic ^{137}Cs, ^{89}Sr, and ^{90}Sr (in neutral solutions, more than 98% ^{137}Cs could be removed and 90% of the ^{89}Sr or ^{90}Sr was removed when it was carrier free and 20% removed in the presence of other salts, but in alkaline medium the removal percentage increased up to 99%, especially in the presence of iron (III) ion); anionic ^{103}Ru and ^{106}Ru (as much as 95% of these were removed when iron (III) ion was present); hydrolytic ^{91}Y, ^{95}Zr, ^{144}Ce, and ^{147}Pm (these were removed well even when the pH of the solution was about 4 to 5); the fission products (the solution including the above three group nuclides) lost 99% of its activity after treatment with the diatomaceous earth in alkaline medium. (auth)

12939 THE PAPER CHROMATOGRAPHY OF INORGANIC SUBSTANCES. III. THE R_F-VALUES OF INORGANIC IONS IN ETHANOL-MINERAL ACIDS. Nascutiu, T. (Inst. for Atomic Physics, Bucharest). Rev. Roum. Chim., 10: 989-94(Oct. 1965).

The R_F values of inorganic ions were determined by ascending chromatography using (2:1) ethanol with 2, 4, 6, 8, and 10N HCl and ethanol with 2, 4, and 6N HNO_3. The R_F values are listed according to the atomic numbers and migration rates of the ions. Conclusions on the effectiveness of the mixtures were drawn. (auth)

12940 IRRADIATED FUEL REPROCESSING. Anderson, Cleve R.; Alter, Henry Ward (to General Electric Co.). U. S. Patent 3,222,124. Dec. 7, 1965. Filed Dec. 26, 1962.

In a method for treating an aqueous solution of irradiated nuclear reactor fuel, the solution is first contacted with an anion exchange resin to retain Pu and produce an aqueous feed effluent stream containing U and substantially all the fission products. The anion exchange resin is eluted to transfer the Pu and trace amounts of fission products to a first elution effluent that is contacted with a second anion exchange resin to retain the Pu leaving a second aqueous feed effluent containing traces of fission products. The Pu is then eluted from the second exchange resin. The first aqueous Pu-free feed effluent stream is dehydrated, and the solids are then directly fluorinated to convert the U and fission products to the corresponding fluorides. The relatively high boiling fission product fluorides are separated from the low boiling UF_6 to achieve separate recovery of U, Pu, and the fission products from the irradiated fuel. (B.L.M.)

12941 EXTRACTION OF METAL VALUES FROM ACID SOLUTIONS. Hart, James L. (to Phillips Petroleum Co.). U. S. Patent 3,223,476. Dec. 14, 1965. Filed July 27, 1962.

A process is described for extracting metal values from aqueous acidic solutions containing Mo or Mo associated with either V or U by extracting the acidic solution with kerosene solution of a long chain aliphatic amine plus an ether. The aqueous Mo containing phase is maintained at a pH below 3.0 by the addition of mineral acid if necessary. After the metal values are extracted into the kerosene phase, the metal loaded kerosene phase is separated from the remaining acidic solution. The extracted metal values are recovered from the kerosene phase. (B.L.M.)

12942 RADIOACTIVE FALLOUT TREATMENT KIT. Calmon, Calvin; Gilwood, Martin E.; Termini, John P. (to Pfaudler Permutit Inc.). U. S. Patent 3,223,619. Dec. 14, 1965. Filed Feb. 21, 1962.

A device for rendering potable, water contaminated with radioactive fission products and toxic chemical agents comprises a pliable water tight container with inlets and outlets that may be closed off and containing a treatment composition. The composition includes an anion exchange resin, a cation exchange resin, a filter aid, and a clarifying agent. If bacteria may be present in the water, a bactericide comprising an insoluble Ag salt is added to the composition. The container filled with water need only be shaken to bring the water into contact with the composition to render the water potable when withdrawn through a filter from the container. (B.L.M.)

ENGINEERING

General

Refer also to abstract 12642.

12943 (ANL–7097) THREE-DIMENSIONAL STRESS CONCENTRATION AROUND A CYLINDRICAL HOLE IN A SEMI-INFINITE ELASTIC BODY. Youngdahl, Carl K.; Sternberg, Eli (Argonne National Lab., Ill.). Sept. 1965. Contract W-31-109-eng-38. 159p. Dep. mn. CFSTI $5.00 cy, $1.00 mn.

Included is a three-dimensional solution, exact within classical elastostatics, for the stresses and deformations arising in a half-space with a semi-infinite transverse cylindrical hole; if the body—at infinite distances from its cylindrical boundary—is subjected to an arbitrary, uniform plane field of stress that is parallel to the bounding plane. The solution in integral form was deduced with the aid of the Papkovich stress functions by means of an especially adapted, unconventional, integral-transform technique. Numerical results for the nonvanishing stresses along the boundary of the hole and for the normal displacement at the plane boundary, corresponding to several values of Poisson's ratio, are also included. These results exhibit in detail the three-dimensional stress boundary layer that emerges near the edges of the hole in the analogous problem for a plate of finite thickness, as the ratio of the plate thickness to the diameter of the hole grows beyond bounds. The results obtained illustrate the limitations inherent in the two-dimensional plane-strain treatment of the spatial plane problems; in addition, they are relevant to failure considerations and are of interest in connection with experimental stress analysis. (auth)

12944 MATERIAL REQUIREMENTS FOR THE ELASTIC ORTHOGONALLY REINFORCED MAXWELL BODIES WITH SMALL REINFORCING MEMBERS (FOR EXAMPLE STEEL CONCRETE). PART II. Hilliges, Dieter (Technische Univ., Berlin). Nucl. Struct. Eng., 2: 449-63(Nov.-Dec. 1965). (In German).

The displacement equation for bound bodies was derived. The equations derived are illustrated by the example of hollow spheres with external pressure. (J.S.R.)

Facilities and Equipment

Refer also to abstracts 13032 and 13714.

12945 (ORNL-TM–1383) MACHINE TO REMOTELY FILL AND COMPACT NUCLEAR FUEL TUBES BY VIBRATION. Cannon, D. D.; Davis, F. C. (Oak Ridge National Lab., Tenn.). Jan. 20, 1966. Contract W-7405-eng-26. 20p. Dep. mn. CFSTI $1.00 cy, $0.50 mn.

The fill-compact machine was designed as one of a series of machines that constitute the Oxide Fabrication Process planned for the Thorium-Uranium Fuel Cycle Development Facility. The fill-compact machine loads a fuel tube with thorium-uranium oxide powder and compacts this powder by using vibrational energy. The requirements, design problems, solution of these problems, and the proposed test program for the machine are discussed. (auth)

12946 (UCRL–11674) LOW-BACKGROUND CONCRETE. Wollenberg, Harold A.; Smith, Alan R. (Lawrence Radiation Lab., Univ. of California, Berkeley). Sept. 18, 1964. Contract W-7405-eng-48. 38p. Dep. mn. CFSTI $2.00 cy, $0.50 mn.

An examination of possible sources of low-radioactivity aggregate and portland cement was conducted in anticipation of construction of a concrete low-background structure. Samples were analyzed for total radioactivity and concentrations of the elements K, Th, and V by means of a 100-channel gamma-ray spectrometer. The spectrometer analysis and economic considerations indicated serpentinized ultramafic rock to be the most suitable source of low-background aggregate. Radiometric testing of raw materials from the operating portland cement plants in California, and finished products from over 80 cement plants in the United States and Canada led to the choice of a cement from Vancouver Island, British Columbia, as the lowest radioactivity cement product commercially available. Besides the aggregate and cement, the radioactivities of sources of water, reinforcing steel, and concrete additives must be considered. Radioactive contamination from mining and handling of concrete ingredients and placing of the concrete is also an important consideration. In addition to the Lawrence Radiation Laboratory facility, low-background facilities incorporating concrete in the shielding structure are constructed, under construction, or being planned at the Franklin Institute, Brookhaven National Laboratory, San Francisco General Hospital, and the Oak Ridge Institute of Nuclear Studies. With respect to shielding and low radioactivity, it was found that concrete can successfully compete with steel; also, concrete is about one fourth as expensive as low-radioactivity steel on an installed-cost-per-unit-area basis. (auth)

12947 STATEMENT OF THE MAIN CIVIL ENGINEERING PROBLEMS RAISED BY BUILDING THE CADARACHE NUCLEAR STUDIES CENTRE. Labbe, J. Ann. Inst. Tech., Trav. Publics, No. 209, 643-68(May 1965). (In French).

After listing the objectives of the guiding plan governing the erection of the Cadarache Nuclear Studies Centre, the following are examined in detail: the general infrastructure of the Centre (thoroughfares, water supply, electricity supply, etc.); the design of the plant; and erection of the main structural shell. (auth)

12948 DEVELOPMENT OF A HIGH-TEMPERATURE MOLTEN LITHIUM PUMP. Kelly, R. W.; Wood, G. M.; Milich, J. J.; Ferguson, C.; Manfredi, D. V. (Pratt and Whitney Aircraft, Middletown, Conn.). New York, American Society of Mechanical Engineers, 1965, Preprint No. 65-WA/FE-18, 9p. (CONF-651110–7). ORINS.

From American Society of Mechanical Engineers, Annual Winter Meeting, Chicago.

The circulation of the liquid-metal heat-transport fluids used in high-performance, mobile, nuclear power plants requires high-temperature pumps. These pumps must be capable of moderately high efficiency over a very long lifetime and have small size, low weight, and high reliability. As an initial phase of a lithium pump development program and to provide pumps for companion development programs, a 195-gpm pump was designed and successfully developed. Extensive testing of pump components, as well as water and liquid-metal tests of complete pump assemblies, was accomplished to meet the program objectives of high performance and high reliability for the required long operating lifetime. Several successful lithium tests of 10,000-hr duration were accomplished with the lithium development pumps and a pump used in a companion heat-exchanger development program. (auth)

12949 IMPROVEMENTS IN OR RELATING TO SEALING MEANS FOR PROVIDING A SEAL BETWEEN TWO RELATIVELY MOVABLE PARTS. Wills, Stanley Charles Frederick (to Strachan and Henshaw Ltd.). British Patent 1,013,683. Dec. 15, 1965. Filed Mar. 15, 1961.

A sealing means is provided for use between two relatively movable parts that are subjected to pressurized fluid tending to escape between the parts, e.g., the assembly of elements on a reactor standpipe. The sealing means includes a piston and cylinder assembly with mutually opposed steps in their cylindrical surfaces. A sealing ring groove is located on one of the cylindrical surfaces so that a ring located in the groove makes a face seal when brought into contact with the opposed mutual

step by relative movement of the piston and cylinder and a piston seal with the surface of the cylinder when not in contact with the step on the cylinder. (B.L.M.)

12950 IMPROVEMENTS IN OR RELATING TO IRRADIATION PLANT. Rogers, Frank (to United Kingdom Atomic Energy Authority). British Patent 1,015,342. Dec. 31, 1965. Filed July 29, 1963.

An entrance or exit door to an irradiation cell has a central portion in the form of a right vertical cylinder of shielding material rotatable about its vertical axis. A number of detachable projecting leaves or vanes project radially from this central portion. Means are provided for moving containers of irradiation material into a recess between the vanes and for rotating the door to bring the recess into register with the interior or exterior of the cell. A push rod type device extends diametrically between the recesses for moving a container from a recess, and the entrance of a carrier into one recess will eject a carrier from the other. (B.L.M.)

12951 IMPROVEMENTS IN OR RELATING TO TUBE JOINTS. Boocock, Peter Munro; Milne, George Angus (to United Kingdom Atomic Energy Authority). British Patent 1,015,653. Jan. 5, 1966. Filed Nov. 20, 1963.

A joint between a larger tube and a smaller tube having different coefficients of thermal expansion comprises an internal flange on the larger tube, an external flange on the smaller tube within the larger tube, and a gasket between the flanges. A thrust reaction member is mounted on one of the tubes, and a series of thermal compensating struts act between the thrust reaction member and the flange on the other tube. When the joint is in use in a hot environment, the differential in linear thermal expansion between the tubes is compensated by the expansion of the struts, and relaxation of bolt load due to yield and creep of the flanges is compensated by the inherent resilience of the struts. (B.L.M.)

12952 METHOD OF, AND APPARATUS FOR, ACCELERATING IONIZED GAS. Consoli, Terenzio; Hall, Richard B. (to Commissariat a l'Energie Atomique). British Patent 1,015,734. Jan. 5, 1966. Priority date Apr. 29, 1963, France.

The proposed particle acceleration process and apparatus utilize both magnetic fields and electromagnetic radiation and is suitable for use in space propulsion systems, vacuum creating systems, and high temperature fusion systems. The particles are simultaneously subjected to an electric field of frequency f transverse to the direction of particle acceleration and having a gradient in that direction and to a magnetic field having its axis parallel to the direction of acceleration. The magnetic field has an intensity which maintains the ratio f_c/f greater than 1 where the electric field gradient and magnetic field have the same sense and less than 1 where they have opposite senses. f_c is the cyclotron frequency established by the magnetic field for the particles to be accelerated. (B.L.M.)

12953 IMPROVEMENTS IN HOT CELLS. Cazalis, Jean Pierre; Lebeaupini, Denis; Lefort, Guy; Vertut, Jean (to Commissariat a l'Energie Atomique). British Patent 1,016,029. Jan. 5, 1966. Priority date Nov. 2, 1962, France.

A device is described that allows passage through the wall of a hot cell of a mechanical part such as a tool while giving protection against radiation. An annular member supports, by means of two interior pins, a protective sphere formed of at least two separable elements. The annular member itself rests, by means of two exterior pins disposed on an axis at right angles to that connecting the two interior pins, upon a fixed supporting member located in the thickness of the wall to be passed through. The fixed supporting member is hollow on the inside to allow the respective clearances of the annular member and the protective sphere. (B.L.M.)

12954 NEUTRON IRRADIATION APPARATUS. Haram, Sevrin Andrew (to Nuclear Materials and Equipment Corp.). British Patent 1,016,329. Jan. 12, 1966. Filed Sept. 21, 1964.

An apparatus for irradiating specimens of material for study and investigation of neutron phenomena and/or for producing isotopes of elements includes a mass of neutron moderating and/or absorbing material or a tank of such material. A well having one or more removable plugs of neutron moderating material is provided in the mass or tank of material. The plugs have coaxial longitudinal holes for the insertion of neutron sources or material to be bombarded. Preferably, a central hole is surrounded by peripheral holes; the source(s) and materials to be bombarded may be interchangeably mounted in the central and peripheral holes; and the effects of neutrons on the bombardment material may be observed. (B.L.M.)

12955 IMPROVEMENTS IN OR RELATING TO INTERLOCKS. Jefferson, Sidney (to United Kingdom Atomic Energy Authority). British Patent 1,016,733. Jan. 12, 1966. Filed March 25, 1963.

An interlock system for use between a source of radiation and an access door to the cell in which the source is located includes first and second electrical circuits and a transformer. A primary winding on the transformer is connected to the first circuit, while the secondary winding is connected to the second circuit. A solenoid operated detent on the door prevents the withdrawal of a latch bar from a keeper unless the source is in a shielded position and is releasable by a current in the second circuit. Means are associated with the transformer core so that the windings are magnetically coupled only when the source is in a shielded position. The source is movable vertically between the shielded and operating positions, and a portion of the transformer core moves with the core to magnetically couple or uncouple the transformer windings. (B.L.M.)

12956 APPARATUS FOR MOVING A RADIATION SOURCE. Hashimoto, Kenjiro (to Tokyo Shibaura Electric Co., Ltd.). Japanese Patent 1964-27178. Nov. 27, 1964. Filed July 9, 1963.

An apparatus for moving a radiation source includes a base rail on which a cart with the radiation source runs and a guide rail above the base rail. The rails run in the shielding water tank, first horizontally on the bottom, then in the form of an arc, and then vertically to the surface of the water tank. A set of radiation source holding plates and an arm are attached to the cart. The plates are always held at a suitable angle at the pivot, and a wheel that rolls on the guide rail is installed at the end of the arm. The wheel serves to lead the radiation source, and the source is always held in the same posture and is not tilted in the course of movement. (TCO)

12957 DEVICE FOR IRRADIATING VERTICALLY WITH ACCELERATED CHARGED PARTICLES AT EXTREMELY LOW TEMPERATURES. Fujizaki, Tatsuo (to Agency of Ind. Sci. and Tech.). Japanese Patent 1964-29020. Dec. 14, 1964. Filed Apr. 10, 1963.

A device is provided for use with an accelerator for irradiating vertically at extremely low temperature. The device consists of at least two concentric tubes with thermal shields. The sample material is fixed on the bottom of the inner tubes. A coolant container with a coolant entrance and exit surrounds the inner tube. Another coolant container also with an entrance and exit surrounds most of the outer surface of the inner container. Between the two containers is an evacuated spatial thermal shield, and another spatial thermal shield surrounds the other container. The outer shield space is either evacuated, independently or with the inner space, or maintained under vacuum. On the top end of the tube a part is installed for fixing the irradiation window, or for connecting the accelerating tube or its extension. The tubular body (with an irradiation material) is provided with either the entrance or exit of a gas, or both, and the accelerated-particle beam runs vertically through the tubular body to the sample material. (TCO)

12958 MANIPULATOR ARM. Hermann, Horst (to European Atomic Energy Community). U. S. Patent 3,217,908. Nov. 16, 1965. Priority date Jan. 23, 1963, France.

A manipulator system includes a pair of chain-like assemblies, each having a series of interpivotal link members. Both assemblies can be concurrently fed out over respective paths converging towards a common line along which the assemblies are substantially coincident and can be retracted in the opposite direction away from the line. Disengageably interengageable means on link members of the respective assemblies interengage on coincidence of the assemblies along the line to interlock both assemblies into a rigid undeformable manipulator arm and disengage on separation of the assemblies as they are retracted in the opposite direction. (B.L.M.)

12959 CONTROL OF PLASMA. Richards, Keith C. (to Owens-Illinois Glass Co.). U. S. Patent 3,222,568. Dec. 7, 1965. Filed Sept. 18, 1963.

A control device is provided for a plasma generator in which a plasma jet is formed and maintained between a cathode and an anode by the application of electric power to the electrodes. A pair of oppositely disposed electrodes are placed in a relatively cool portion of the plasma jet, variations in conductivity across the electrodes are measured when they are in position. The current flow between the cathode and anode of the generator is controlled in response to variations in conductivity between the electrodes to maintain the current between the electrodes substantially constant and in turn the ionization level and heat content of the plasma jet constant. (B.L.M.)

Heat Transfer and Fluid Flow

See also PHYSICS — Fluid Physics and Thermodynamics

Refer also to abstracts 13696, 14015, 14027, 14035, 14041, 14116, and 14131.

12960 (EURAEC–1515) SWIRL FLOWS IN BOILING WATER. HYDRODYNAMIC STUDY OF TWO-PHASE TWISTED FLOW REGIME IN A TUBE. Special Report No. 20. Rosue, A.; Tournier, G. (Societe Nationale d'Etude et de Construction de Moteurs d'Aviation, Suresnes (France). Division Atomique). July 15, 1965. Contract 061-64-7-TEEF. 47p. (EUR–2667). Dep. mn. CFSTI $2.00 cy, $0.50 mn.

Work Performed under United States–Euratom Joint Research and Development Program.

Hydrodynamic tests with air and water at atmospheric pressure have enabled some aspects of twisted flow regime in a tube to be defined. The experimental tests are made in the range of velocities 0.75 m/s < Vl_0 < 4m/s. Pressure drop and void fraction measurements are in good agreement with those obtained in previous studies. Liquid velocity has a little influence on void fraction. Visualization, void fraction and electrical probe measurements were used to define the different flow patterns and water and air distribution in a channel cross section. In the range of very low qualities $x \leq 2.10^{-3}$ centrifugation of water becomes efficient at liquid velocity above 1 m/s. For qualities above $x \simeq 2.10^{-3}$ observed flow regimes with efficient centrifugation. Three flow patterns are defined: bubble flow, annular flow, mist annular flow. These flow patterns are different from those observed in straight flow, because the distribution of the two phases is not the same. A liquid film exists near the wall of the tube while air is more concentrated near the axis of the tube. A liquid film along the twisted tape was observed, but it is very thin and the liquid mass flow rate in this film is negligible compared to the liquid mass flow rate in the total cross section. The thickness of this liquid film is a function of the velocity and the quality. (auth)

12961 (GEAP–4786) SINGLE-ROD, FORCED FLOW, TRANSITION BOILING HEAT TRANSFER FROM SMOOTH AND FINNED SURFACES. Quinn, E. P. (General Electric Co., San Jose, Calif. Atomic Power Equipment Dept.). Aug. 1965. Contract AT(04-3)-189. 45p. (EURAEC–1560). Dep. mn. CFSTI $2.00 cy, $0.50 mn.

Work Performed under United States–Euratom Joint Research and Development Program.

The results of transition-boiling and film-boiling heat-transfer measurements are presented for a single-rod annular geometry. Tests were performed at 1000 psia and mass velocities of 0.5 and 1.0M lb/h-ft^2 over the quality range from 17 to 55%. The transition-boiling region was found to exist over a heat-flux range at constant quality of only 6% for steady flow. The size of the transition-boiling region and the magnitude of temperature fluctuations were found to be very dependent on the intensity of two-phase flow variations. Heat-transfer coefficients for steady film boiling were found to exhibit thermal entrance length behavior. Fully developed coefficients were reached after a sufficiently long, dry surface length was established. A special, finned, heated surface was developed and was tested. The finned surface reduced transition-temperature fluctuations to 20% of smooth-surface values and indicated a significant increase in film-boiling coefficients. (auth)

12962 (GEAP–4959) A PROGRAM OF TWO-PHASE FLOW INVESTIGATION. Tenth Quarterly Report, July–September 1965. Bijwaard, G.; Staub, F. W.; Zuber, N. (General Electric Co., San Jose, Calif. Atomic Power Equipment Dept.). Oct. 1, 1965. Contract AT(04-3)-189. 54p. (EURAEC–1526). Dep. mn; CFSTI $3.00 cy, $0.50 mn.

Work Performed under United States–Euratom Joint Research and Development Program.

Instrumentation items were recalibrated and installed in the test loop at the conclusion of loop-modification for 500 psi operation. The loop metal test section was leak and pressure tested. An earlier test run was repeated at a reduced pressure (ratio of local static-to-critical pressure) of 0.22. Data from the run agreed with those obtained originally. The empirical correlations of the boiling heat transfer coefficients obtained at reduced pressures of 0.12, 0.22, and 0.39 are summarized. Two analyses were carried out to evaluate effects of heat addition on flow regimes. An analysis of the constitutive equation for predicting vapor formation rates was initiated. Mechanisms of thermo-hydraulic oscillations in two-phase flow systems with heat additions are being investigated. (J.R.D.)

12963 (WANL-TME–1108) MODIFIED TRANSIENT AND/OR STEADY STATE (TOSS) DIGITAL HEAT TRANSFER CODE. Pierce, B. L. (Westinghouse Electric Corp., Pittsburgh, Pa. Astronuclear Lab.). Apr. 1964. Contract SNP-1. 53p. Dep. mn. CFSTI $3.00 cy, $0.50 mn.

The TOSS program, modified to include temperature-dependent specific heat and thermal conductivity and time-dependent forced film convection coefficients, is described. The other modifications to the program are also outlined. (D.C.W.)

12964 MEASUREMENT OF VOID FRACTION WITH IMPEDANCE GAUGE TECHNIQUE. Cimorelli, L.; Premoli, A. (CEN, Rome. Centro Studi Nucleari della Casaccia, Rome). Energia Nucl. (Milan), 13: 12-23(1966).

The application of electrical impedance to void measurement is discussed. A method was developed and first results obtained at atmospheric pressure under subcooled boiling conditions are presented. (auth)

12965 CRITICAL HEAT FLUX ON SUBMERGED SURFACES DURING BOILING OF ORGANIC COOLANTS. Sterman, L. S.; Vilemas, Yu. V. (Moscow Inst. of Power Engineering). Teplofiz. Vysok. Temp., 3: 609-16(July-Aug. 1965). (In Russian).

Critical heat flux on heat-transfer surfaces made of various materials was studied in a wide range of pressure variations with respect to the geometry and roughness of the surface during boiling of organic coolants (biphenyl, monoisopropylbiphenyl, biphenyl oxide, Dowtherm, and

benzene). The surface to be studied was placed in a carbon steel high pressure chamber. Vapors of the liquid being studied were condensed in an air-cooled condenser. The liquid was heated by a submerged tubular electric heater. Heat losses were compensated by a nichrome coil connected to a voltage regulator. Heat flux was created by passing an alternating current through the surface being studied. Calculation of this flux was based on the amount of electric power fed to the surface. Transition from nucleate boiling to film boiling was determined by a sharp change in the resistance of the submerged surface at the critical point, using an oscillograph connected across the diagonal of a balanced bridge with the submerged surface making up the two arms. A thermocouple welded to the surface being studied was also used in determining the transition to film boiling. Heat fluxes determined by both methods were identical. Experimental and theoretical data are compared with respect to formulas derived previously, and a formula is given for calculating the average deviation of the experimental data from the values calculated by the various formulas. (ATD)

12966 RADIATIVE HEAT-TRANSFER THROUGH AN ABSORBING BOUNDARY LAYER. Fritsch, C. A. (Bell Telephone Labs., Inc., Whippany, N. J.); Grosh, R. J.; Wildin, M. W. New York, American Society of Mechanical Engineers, 1965, Preprint No. 65-WA/HT-21, 8p. (CONF-651110-10). ORINS.

From American Society of Mechanical Engineers, Annual Winter Meeting, Chicago.

An analytical investigation is made of a method of shielding a surface from parallel beams of thermal radiation by distributed injection of a fluid containing absorbing particles into the boundary-layer flow over the surface near the stagnation point. Superposition of various solutions is used to obtain results for a wide range of parameter values from a relatively small number of functions. Three optical conditions of the surface are considered: Specular reflection, diffuse reflection, and black. It is found that injection of absorbing particles helps to shield the surface if the injection rate is relatively high. (auth)

12967 HEAT TRANSFER IN PARALLEL ROD ARRAYS. Sutherland, W. A. (General Electric Co., San Jose, Calif.); Kays, W. M. New York, American Society of Mechanical Engineers, 1965, Preprint No. 65-WA/HT-7, 8p. (CONF-651110-8). ORINS.

From American Society of Mechanical Engineers, Annual Winter Meeting, Chicago.

The general problem of turbulent flow heat transfer in parallel rod arrays is considered. To accommodate the complexity introduced by this configuration, a method of analysis is developed using the technique of superposition of fundamental solutions. Fundamental solutions are determined experimentally which may be used to predict heat transfer in parallel rod arrays of various spacings and with arbitrary power distribution from rod to rod and around the periphery of the rods. The experimental investigation was conducted with airflow (Pr = 0.70) past electrically heated rods. Rod center-to-center spacing to rod diameter ratios of 1.15 and 1.25 were investigated for fully developed turbulent flow. Experimentally determined fundamental solutions are presented for Reynolds numbers from 7000 to 200,000. (auth)

12968 EMPIRICAL CORRELATION OF FACTORS INFLUENCING DEPARTURE FROM NUCLEATE BOILING IN STEAM-WATER MIXTURES FLOWING IN VERTICAL ROUND TUBES. Pasint, D.; Pai, R. H. (Foster Wheeler Corp., Livingston, N. J.). New York, American Society of Mechanical Engineers, 1965, Preprint No. 65-WA/HT-24, 7p. (CONF-651110-12). ORINS.

From American Society of Mechanical Engineers, Annual Winter Meeting, Chicago.

An empirical correlation of forced convection, DNB for steam-water mixtures between 500 and 3000 psia in uniformly heated vertical tubes is proposed. DNB quality is expressed in terms of pressure, mass flow, inlet enthalpy, heated length from inlet to DNB point, and tube diameter. The experimental data at 2000–3000 psia, 250,000–1,000,000 lb/hr sq ft mass flow, and 40,000–180,000 Btu/hr sq ft heat flux, obtained from a 6 ft long, $\frac{3}{4}$-in.-ID electrically heated vertical tube, are correlated with other results ranging from 500 to 2000 psia. (auth)

12969 SIMULTANEOUS RADIATION, CONDUCTION, AND CONVECTION IN A SPECTRALLY SELECTIVE, EMITTING, AND SCATTERING POROUS BED. Leung, A. T.; Edwards, D. K. (Univ. of California, Los Angeles). New York, American Society of Mechanical Engineers, 1965, Preprint No. 65-WA/HT-23, 8p. (CONF-651110-11). ORINS.

From American Society of Mechanical Engineers, Annual Winter Meeting, Chicago.

An exact formulation of simultaneous radiation, conduction, and convection heat transfer for steady-state conditions in a one-dimensional, semi-infinite, isotropic, homogeneous, absorbing, and scattering porous bed is presented. Both diffuse and collimated radiant fluxes are incident on the bed causing absorption, scattering, emission, and heating of the bed which in turn heats a transparent, constant-property fluid flowing normal to the surface. Spectral selectivity is allowed for when the source energy is of shorter wavelength than the emitted energy. Exact and approximate numerical solutions and a linearized closed-form solution are given for inflow, as in a solar heat collector, and outflow, as with a heat shield. (auth)

12970 IMPROVEMENTS IN AND RELATING TO SHELL AND TUBE HEAT EXCHANGERS. Bell, Alan (to Foster Wheeler Ltd.). British Patent 1,014,855. Dec. 31, 1965. Filed Sept. 7, 1961.

One or more heat exchange units are disposed within the shell of the proposed tube and shell heat exchanger. Each exchange unit comprises inlet and outlet headers joined by a bank of tubes defining circuits of substantially identical length and disposition between the headers. Each bank of tubes includes a number of clusters of tubes of hexagonal cross section, and each cluster forms a circuit and comprises a tube having in it a succession of U-bends so that it provides a number of tube lengths running generally lengthwise of the shell. The clusters are disposed side by side and are so formed that their juxaposition gives substantially uniform distribution of the tube length over the cross section of the shell available for tubes. (B.L.M.)

12971 HEAT EXCHANGE SYSTEM. Brill, Edward F. (to Allis-Chalmers Mfg. Co.). U. S. Patent 3,223,860. Dec. 14, 1965. Filed Feb. 16, 1962.

A high temperature heat exchange system using liquid slag as a heat exchange medium is described for particular use with a MHD electrical power generating plant. The system includes a first heat exchanger into which the molten slag and the exhaust gas from a combustion chamber are directed and a second heat exchanger in which the heated molten slag gives up its excess heat to preheat the combustion gases before their introduction into the combustion chamber to combine with the burning fuel. The combustion air and the heat exchange medium in the second exchanger have a temperature relationship that the slag always remains in the liquid state and is pumped from the second exchanger back to its source for recirculation through the first exchanger. (B.L.M.)

Materials Testing

Refer also to abstracts 13154, 13318, 13343, 14017, 14032, 14160, 14194, 14195, and 14197.

12972 (BNWL-168) A DOUBLE CANTILEVER BEAM SPECIMEN FOR DETERMINING THE PLANE STRAIN FRACTURE TOUGHNESS OF METALS. Hoagland, R. G. (Battelle-Northwest, Richland, Wash. Pacific Northwest Lab.). Dec. 1965. Contract AT(45-1)-1830. 29p. Dep. mn. CFSTI $2.00 cy, $0.50 mn.

The feasibility of the testing method for obtaining data

under conditions of limited space is demonstrated. Two favorable features are the amount of fracture toughness data that can be obtained from one specimen and the restraint against excessive deformation near the crack tip provided by the sharp grooves in the specimen. (W.L.G.)

12973 (EURAEC–1519) NON-DESTRUCTIVE WELD STUDIES. Quarterly Report No. 17, July 1–September 30, 1965. (Roentgen Technische Dienst N. V., Rotterdam (Netherlands)). Nov. 18, 1965. Contract 045/61/5 RDH. 53p. (EUR–2671). Dep. mn. CFSTI $3.00 cy, $0.50 mn.

Work Performed under United States–Euratom Joint Research and Development Program.

A recording system for ultrasonic data was evaluated. Dynamic screen images were used that contained the Z-axis as an added dimension. Movement of the probe perpendicular to the weld produced motion in the Y-axis of the oscilloscope. In addition, a flaw echo recording pen was used whereby the same probe movement controlled the position of a moving gate, which limited the path length to cover the weld only. The effects of the composition and thickness of screens on the image quality of radiographs produced by a ^{60}Co source and a 5 Mev linear accelerator was studied. Screens of Cu, Pb, Ag, Sn, and Ta with thickness of 0.25 to 2.5 mm were evaluated. For the radiographs made with the 5 Mev linear accelerator, neither the screen thickness nor composition had an appreciable influence on the image quality. Radiographs made with the ^{60}Co source and Cu screens had the best image quality. The image quality was not controlled by the thickness of the Cu screens. The thickness of Pb or Ta screens did influence the image quality; a thickness of 1.5 mm gave the best results. (W.L.G.)

12974 ON THE STUDY OF INTENSIFICATION OF FRONT LEAD SCREEN FOR γ-RAY RADIOGRAPHY. Ohno, Akira; Nojiri, Toshiaki (Industrial Research Inst. of Kanagawa Prefecture, Japan). Radioisotopes (Tokyo), 15: 33-9(1966). (In Japanese).

The effects of lead screens for gamma radiography are the intensified action by the secondary electrons and the shielded one in the low-energy scattering of γ rays by surrounding materials. Intensification of front lead screens with several thicknesses for the ^{60}Co, ^{137}Cs, and ^{192}Ir γ radiography was studied. The exposure doses to obtain 1.75 photographic density for x-ray films were determined by experiments for several thick foils of lead using a standard developing method. Angular distributions of photoelectric electrons and Compton electrons by interaction of γ photons with lead atoms were calculated. For the photographic emulsion itself, calculations were made on the assumption that the content of AgBr in the emulsion is 50 wt %, the density is 2.0g/cm^3, and the thickness is 20μ. Some of these secondary electrons are absorbed in the film emulsion and the blackening due to γ rays is proportional to the energy loss under electron ionization in the emulsion. It is important to know how much the electron beams are absorbed in the lead foils and the film emulsions. Agreement with experiments and calculations was sufficient except for thin-layer lead screens for ^{60}Co in the reduction of intensification. The maximum intensification factors of front lead screens were about 2.5 for ^{60}Co γ sources with 0.3 mm-thick lead screens, 2.3 for a ^{137}Cs source with 0.1 mm screen, and 3.3 for an ^{192}Ir source with 0.07 mm screen. (auth)

Space Propulsion

See also ISOTOPE TECHNOLOGY — Power Application
REACTOR TECHNOLOGY — Propulsion and Space

12975 A STATUS REPORT ON AN ION ENGINE DEVELOPMENT PROGRAM. Zimmerman, R. L.; King, H. J. (Hughes Aircraft Co., Malibu, Calif.). New York, American Inst. of Aeronautics and Astronautics, 1965, Preprint No. AIAA 65-374, 34p., $1.00. (CONF-650711–53). ORINS.

From AIAA 2nd Annual Meeting and Technical Demonstration, San Francisco.

Progress on the development of a multistrip Cs contact ion engine is reported. Two engine configurations — a four- and a 13-strip integral focus engine — were studied. The engine design and the results of engine-life testing are described. The performance of Re- and Ir-coated W ionizers is discussed. The status of the Hg electron-bombardment thrustor program is summarized. Operation and testing of a liquid-Hg cathode and of an oxide cathode are described. (M.J.T.)

GEOLOGY, METEOROLOGY, AND MINERALOGY

General

12976 MANGANESE NODULES: THEIR EVOLUTION. Bender, Michael L.; Ku, Teh-Lung; Broecker, Wallace S. (Columbia Univ., Palisades, N. Y.). Science, 151: 325-8(Jan. 21, 1966).

That manganese nodules and adjacent deep-sea sediments accumulate manganese at almost the same rate was established by ^{230}Th dating of both sediments and nodules of known manganese content. The rate of manganese deposition is nearly constant over the world oceans. A relatively simple model of nodule evolution explains the distribution of manganese nodules between sediment column and sediment-water interface; the model appears to apply to other trace elements such as copper, nickel, and cobalt. (auth)

Meteorology

See also Site Survey and Selection

12977 DETERMINATION OF SOME PARAMETERS OF NATURAL RADIOACTIVE AEROSOL REMOVAL FROM AIR. Styra, B. J.; Vebra, E. Yu.; Shopauskas, K. K. Izv. Akad. Nauk SSSR, Fiz. Atmos. Okeana, 1: 1299-1309(1965). (In Russian).

A technique of measurements of radioactivity in the free atmosphere and inside cloud systems is described. A theory of the measurements is provided. Formulas were obtained for calculation of the parameter, Λ, for nonradioactive removal of radioactive aerosols into cloud droplets. Two methods of Λ determination are proposed: use of radioactive aerosol concentration profiles within the cloud and outside of it and consideration of breakdown of radioactive equilibrium between radon decay products within the cloud. Using the values found for Λ and other data on cloud droplet concentration the value of the coefficient K for radioactive aerosol coagulation on droplets was calculated. The mean value of which was 3×10^{-6} cm^3/sec^{-1}. (auth)

Natural Radioactivity and Fallout

See also HEALTH AND SAFETY

Refer also to abstracts 12572, 12573, 12578, and 12946.

12978 (AD-627077) DASA FALLOUT AND TRANSIT DOSE RATE MEASUREMENT SYSTEM. Brown, J. E.; Webb, R. I. A. (Edgerton, Germeshausen and Grier, Inc., Santa Barbara, Calif.). Dec. 1965. Contract DA-49-146-XZ-292. 114p. (DASA-1688; NDL-TR-71). CFSTI $4.00 cy, $0.75 mn.

The results of a study and design effort that demonstrates the feasibility of an improved system for the measurement and collection of residual radiation dose rate information are presented. The improved system consists of as many as 100 data collection points at which up to 200 detectors may be located. Data are telemetered to a centrally located on-line computer for real time computation. Suitable performance characteristics and system compatibility were demonstrated by an experimental detector station fabricated for test and evaluation. Other system components were selected from available off-the-shelf commercial items. Included in the system is a provision for differentiation between the dose rate contributed by the deposited fallout and the transit dose rate. (auth)

12979 (EUR-2287.d) UNTERSUCHUNG UEBER DIE RADIOAKTIVE KONTAMINATION DER VON TIEREN STAMMENDEN LEBENSMITTEL. (Investigation on Radioactive Contamination of Foodstuffs Stemming From Animals). Leistner, L. (European Atomic Energy Community. Commissariat a l'Energie Atomique, Paris (France)). Jan. 4, 1965. 60p. Dep. mn.

Data relating to the transfer of the most important radionuclides from the environment through animal products to man are presented. As these are not directly utilized for the countries of the European Community, further studies are proposed on the changing ecological conditions. (auth)

12980 ISOTOPIC COMPOSITION OF STRONTIUM IN FOUR CARBONATE VEIN-DIKES. Powell, J. L. (Oberlin Coll., Ohio). Amer. Mineral., 50: 1921-8(Nov.-Dec. 1965).

The $^{87}Sr/^{86}Sr$ ratios of 8 specimens from the carbonate veins or vein-dikes at Ravalli Co., Montana; the Rocky Boy Stock, Montana; Lemhi Co., Idaho; and Cardiff Uranium Mines, Haliburton Co., Ontario, varied from about 0.704 to 0.706 and averaged 0.7051. Their $^{87}Sr/^{86}Sr$ ratios were in general significantly higher than those of accepted carbonatites, lower than those of most limestones, and similar to those of mafic igneous rocks. Neither isotopic fractionation nor contamination of carbonatitic fluids or magmas with crustal radiogenic strontium appeared to be an adequate general explanation for the higher $^{87}Sr/^{86}Sr$ ratios of the four vein-dikes. This may indicate that the vein-dikes studied are not genetically related to massive carbonatite. (auth)

12981 RADIOACTIVE FALLOUT PHENOMENA AND MECHANISMS. Klement, Alfred W. Jr. (Atomic Energy Commission, Washington, D. C.). Health Phys., 11: 1265-74(Dec. 1965).

In this review nuclear detonations are briefly described. The characteristics of fallout material and its behavior in the atmosphere are discussed with particular regard to recent findings and theories. An indication of the current fallout situation is given. Reference is made to other reviews as well as to specific research papers and documentations of fallout data. (auth)

12982 PRIMORDIAL RADIONUCLIDES: THEIR DISTRIBUTION, MOVEMENT, AND POSSIBLE EFFECT WITHIN TERRESTRIAL ECOSYSTEMS. Osburn, W. S. (Colorado State Univ., Fort Collins). Health Phys., 11: 1275-95(Dec. 1965).

The world-wide distribution of naturally occurring radioactive materials is summarized and a more detailed account of their occurrence and movement within specific ecosystems is provided. General pathways of nuclide distribution and sites of concentration are pictured by tracing radioactive substances from the long-lived primary materials to the inactive end product. This tracing includes major environmental and biological transport mechanisms to which radionuclides are subjected during the course of their life span. Thus, the biology of these naturally occurring nuclides is reviewed. The ecological life history of various plants and animals are outlined, and the radiosensitivity of the various stages are considered. Where stages of high radiosensitivity are coincidental with exposure to relatively high levels of background radiation, possible biological effects are discussed. Special attention is given to the interaction of ionizing radiation with other environmental stresses. (auth)

12983 SEASONAL CYCLE OF ^{137}Cs IN SOME ALASKAN NATIVES AND ANIMALS. Hanson, W. C.; Palmer, H. E. (Battelle Memorial Inst., Richland, Wash.). Health Phys., 11: 1401-6(Dec. 1965). (BNWL-SA-222).

Cesium-137 concentrations were measured in lichens, caribou, and Eskimos at Anaktuvuk Pass, Alaska, during summers of 1962 and 1963 and at approximately 2-month intervals during the period January 1964, through April 1965. Maximum ^{137}Cs body burdens in Eskimos occurred during summer months and then decreased steadily until

the following spring. This seasonal cycle resulted from the Eskimo practice of killing and storing caribou at times of seasonal highs and lows of ^{137}Cs concentrations in caribou flesh, which formed the food base for the village. Maximum body burdens in Eskimos occurred 1 to 2 months after maximum concentrations in caribou flesh. Eskimo ^{137}Cs body burdens in the summer of 1963 were about 50% greater than during 1962, and during 1964 were about twice those of 1963. Average whole-body radiation dose received during 1964 from ^{137}Cs body burdens in Anaktuvuk Pass adults was estimated at 150 mrem. Maximum exposure was estimated at 300 mrem. Cesium-137 concentrations in wolverines, wolves, and foxes were highest during winter months and were greater than in caribou flesh. Cesium-137 body burdens in native groups which utilized caribou meat predominantly during winter and spring months were 50 to 70% greater during spring than during summer months when fish was the main protein source. (auth)

12984 FACTORS INFLUENCING THE ACCUMULATION OF FALLOUT ^{137}Cs IN COLORADO MULE DEER. Whicker, F. W.; Farris, G. C.; Remmenga, E. E.; Dahl, A. H. (Colorado State Univ., Fort Collins). Health Phys., 11: 1407-14 (Dec. 1965).

Concentrations of ^{137}Cs were measured by gamma-ray spectrometry in mule deer muscle tissues, air, precipitation, soils, and twelve forage species that were sampled over a 3 yr period in north-central Colorado. Maximum levels of ^{137}Cs in air, vegetation, and deer occurred in 1963. Spring peaks were noted for both air concentrations and deposition of ^{137}Cs. Maximal deposition of ^{137}Cs occurred when both precipitation and air concentrations were high, and fallout levels in soil generally increased with elevation and precipitation averages. Vegetation collected above 8500 ft was generally higher in ^{137}Cs than vegetation collected at lower elevations. Plant species varied significantly in radiocesium burdens. Leaves were generally higher than stems in ^{137}Cs content. Deer collected above 8500 ft were significantly higher in muscle ^{137}Cs concentrations than deer collected at lower elevations. Levels of ^{137}Cs in deer were highly correlated with the mean levels in vegetation collected during common time periods. Neither age nor sex produced statistically significant variations in muscle ^{137}Cs concentrations. Inhalation, the drinking of surface waters, and the ingestion of snow were minor sources of ^{137}Cs intake by deer in comparison to the ingestion of forage. (auth)

12985 MOVEMENT AND DISTRIBUTION OF RADIONUCLIDES ON GRANITIC OUTCROPS WITHIN THE GEORGIA PIEDMONT. Plummer, Gayther L.; Helseth, Frank (Univ. of Georgia, Athens). Health Phys., 11: 1423-8(Dec. 1965).

Parmelia conspersa, an upland lichen, had higher concentrations of ^{137}Cs (up to 300 pCi/g dry wt.) than any other plant in 1964. Viguiera porteri, an aster, held the largest concentrations of ^{90}Sr (up to 125 pCi/g). Concentrations of fallout were higher in upland Juniperus virginiana than in lowland populations, although the spectrum of isotopes at both sites was similar. Even though each granitic outcrop as a whole is a relatively simple ecological system, it consists of smaller systems wherein the dynamics of radioisotope movements and bioaccumulation can be understood only in terms of intimate familiarity with each little system contributing to the whole. Maximum concentration levels for any component were not ascertained; nevertheless, accumulation of isotopes within Parmelia and Viguiera may well indicate the extent to which fallout has become an environmental contaminant in the Southeast. (auth)

12986 MOVEMENT OF FALLOUT RADIONUCLIDES IN IRRIGATED ECOSYSTEMS OF THE PO VALLEY, ITALY. Bourdeau, Philippe; Cavalloro, Raffaele; Myttenaere, Constant; Verfaillie, Georges (Joint Research Center, Ispra, Italy). Health Phys., 11: 1429-44(Dec. 1965).

In 1963 and 1964 in the Po Valley, ^{137}Cs, ^{90}Sr, ^{106}Ru, ^{144}Ce, and ^{54}Mn increased in rice until harvest. In grains, most of the ^{144}Ce and ^{90}Sr was in the hull; ^{137}Cs was the most active nuclide in the endosperm. Activities were higher in perennial meadows. Covering flooded rice reduced ^{144}Ce in shoots by 72%, ^{90}Sr and ^{137}Cs by 23 to 26%, and ^{54}Mn by 4%. Draining reduced ^{137}Cs by 19%, but increased ^{54}Mn by 62%. Panicles were similarly affected. Covering reduced all nuclides to a greater extent in meadow than in rice. ^{137}Cs appears to be quite available to rice from flooded soils. Levels in animals seemed to reflect habitat and diet. (auth)

12987 ON THE RADIOACTIVITY OF PLANTS FROM THE HIGH RADIATION AREAS OF THE KERALA COAST AND ADJOINING REGIONS. II. STUDIES ON THE UPTAKE OF ALPHA AND GAMMA EMITTERS. Mistry, K. B.; Gopal-Ayengar, A. R.; Bharathan, K. G. (Atomic Energy Establishment Trombay, Bombay). Health Phys., 11: 1459-70(Dec. 1965).

Gamma and alpha activity measurements were carried out on samples from thirty plant species covering eighteen families and including both monocotyledons and dicotyledons, during the course of a radioecological survey of high background radiation areas of the Kerala and Madras States. Data are discussed from the stand point of the extent of accumulation of the radionuclides of the thorium series by various plant species. The distribution of radioelements in different tissues of some perennial species was also examined. Since the present study includes several edible species, an attempt was made to estimate the daily intake of alpha activity through dietary items of plant origin. (auth)

12988 SURVEY OF RADIOACTIVE CONTENT OF FOOD GROWN ON BRAZILIAN AREAS OF HIGH NATURAL RADIOACTIVITY. Franca, E. Penna; Ribeiro, C. Costa; Teitakowski, M.; Londres, H.; Santos, P. L.; Albuquerque, H. A. (Univ. do Brazil, Rio de Janeiro). Health Phys., 11: 1471-84(Dec. 1965).

The monazite sand region along the Atlantic coast of Brazil and the zone of volcanic intrusives in the inland state of Minas Gerais were studied. In both regions, there are groups of people living on variable fields of radiation ranging from 0.03 to 1.0 mR/hr. The most representative towns and villages in these areas are being intensively investigated in order to investigate possible long-term consequences to human beings exposed to continuous levels of radiation. Food produced in the areas was extensively sampled and assayed for its radioactive content. Total alpha counting, fast alpha pair coincidence counting, radiochemical analysis of ^{226}Ra, ^{228}Ra, and ^{228}Th as well as gamma and alpha spectrometry were employed. The total alpha activities found in foods of the monazite sand areas ranged from 4 to 260 pC/kg of fresh weight. Since the per cent of these foods in the local diet is quite small, present work centers on the effects of external radiation. In the volcanic intrusive region around Araxá, radioactive minerals are associated with apatite, a natural fertilizer. Levels of total alpha activities found in local foods present wide ranges: beans 71 to 800 pC/g, vegetables 3 to 1990 pC/g, and citrus fruits 2 to 2000 pC/kg fresh weight. Ratios of $^{226}Ra/^{228}Ra$ are quite variable. A systematic sampling is being conducted there to determine the range of levels in the most important crops cultivated in different areas, the differences in values found in various foods grown on the same soils, and the importance of highly contaminated food on the total local crops. Attempts are being made to estimate daily intakes of Ra in some of the isolated and highly contaminated farms. Indirect measurements of intake were also made by analysis of urine and feces. (TCO)

Techniques and Equipment

12989 (NVO-1312-1(Vol.1)) CAVITY STABILITY INSTRUMENTATION AND OBSERVATION. Final Report, Phase I. Volume I, Sections 1-4. Brandt, R. J. (United ElectroDynamics, Inc., Pasadena, Calif.). June 1963. Contract AT(29-2)-1312. 175p. Dep. mn. CFSTI $5.00 cy, $1.00 mn.

The over-all purpose of the Dribble project is briefly reviewed. A review of mine safety instrumentation applications is presented. A detailed theoretical analysis of the stability of underground cavities is presented in terms of stress concentration factors in an elastic medium, depth of plastic zone, state of stress around an underground cavity, and the deformational response of an infinite medium with growing cavity. The performance of signal cables, displacement gages, strain gages, and stress evaluation systems is discussed. (M.O.W.)

12990 (NVO-1312-1(Vol.2)) CAVITY STABILITY INSTRUMENTATION AND OBSERVATION. Final Report, Phase I. Volume 2, Sections 5-7. Brandt, R. J. (United ElectroDynamics, Inc., Pasadena, Calif.). June 1963. Contract AT(29-2)-1312. 158p. Dep. mn. CFSTI $5.00 cy, $1.00 mn.

The development and testing of displacement, strain, and stress gages for Project Dribble are discussed in detail. The basic instrumentation system, dynamic recording system, and the data processing and evaluation systems are discussed. (M.O.W.)

12991 LEAD ISOTOPES AND THE AGE OF THE EARTH. Tilton, G. R.; Steiger, R. H. (Carnegie Inst. of Washington, D. C.). Science, 150: 1805-8(Dec. 31, 1965).

Calculations based on comparison of the isotopic composition of lead from iron meteorites with that of various modern terrestrial leads placed the age of the earth at around 4550 million years. However, data from young volcanic rocks revealed that modern terrestrial lead can have a wide range of isotopic composition. The variations in its composition mean that one or more of the assumptions used in age calculation were violated. Meteorite lead was compared with lead from rocks 2700 million years old, from the Canadian Shield. Using this method and the same constants and assumptions utilized in earlier calculations an age of 4750 ± 50 million years was calculated for the earth. The earth may be approximately 200 million years older than previously thought; alternatively, primordial terrestrial lead may not have had the same isotopic composition as lead in iron meteorites. (auth)

12992 STRONTIUM–RUBIDIUM AGE OF AN IRON METEORITE. Wasserburg, G. J. (California Inst. of Tech., Pasadena); Burnett, D. S.; Frondel, C. Science, 150: 1814-18(Dec. 31, 1965).

The isotopic compositions and concentrations of rubidium and strontium were determined in silicate nodules contained in Weekeroo Station meteorite, a brecciated coarse octahedrite. The strontium had a $^{87}Sr:^{86}Sr$ range from 0.729 to 0.768, showing considerable enrichment in ^{87}Sr in comparison with achondrites. Data for six samples of nodules lay on a straight line on the Sr–Rb evolution diagram, with an initial $^{87}Sr:^{86}Sr$ ratio of 0.696 to 0.702; the slope was 0.0674, corresponding to an age of 4.7×10^9 years for $\lambda = 1.39 \times 10^{-11}$ year^{-1}. These data agreed with previously assigned ages for the formation of stony meteorites and the earth; they supported the conclusion that the major period of chemical and physical differentiation in the solar system occurred in a narrow interval at about this time. This result disagreed with the $^{40}Ar-^{40}K$ ages of 5 to 13×10^9 years determined from other iron meteorites. (auth)

12993 PHYSICAL POSSIBILITIES OF GAMMA-GAMMA LOGGING. Czubek, J. A. (Inst. of Nuclear Research, Krakow). Vienna, International Atomic Energy Agency, 1965, Preprint No. SM-68/34, 45p. (CONF-651023-26). ORINS.

From Symposium on Radioisotope Instruments in Industry and Geophysics, Warsaw.

Gamma-gamma logging is applied in two modifications: as a formation density logging or as a selective gamma-gamma logging which permits the obtaining of the average concentration of heavy elements in rocks. The physical principles for both methods are given, as well as a new method for obtaining from these principles the optimum parameters for the construction of the logging tools. The physical considerations of the gamma spectra scattered in the mono-element media in connection with the principle of similitude provide for the conception of the equivalent atomic number (Z_{eq}) of multicomponent media, e.g., the rocks. One can obtain the physico-chemical limitations for the existence of Z_{eq} as well as the energetic limitation for the spectra which are independent of the chemical composition of rocks. Thus the scattered gamma radiation which depends only on the density of rocks is obtained. The special filters for such energy limitation in logging probes are recommended. These filters are necessary for the GM detectors and are desirable also for the scintillation detectors with the spectrometric discrimination. The special method for the determination of the influence of the chemical composition on the response of the gamma-gamma probe is proposed. The relation between source-detector spacing, rock density, chemical composition effect and the response of the gamma-gamma probe is discussed. After such considerations one can obtain the analytical, semiempirical shape of the response curve for the formation-density logging probes. The standard deviation of the measured density is presented as a function of the construction factors of different logging tools. From such considerations the optimum parameters for the density logging probes are obtained. The second modification of the gamma-gamma method is applied for the determination of heavy element concentration in rocks and ores. In this method the soft part of the registered scattered gamma spectrum is utilized. The influence of rock density on such measurements is discussed. The new method for obtaining the measurement results independent of the rock density is presented. This method is based on the consideration of the scattered gamma spectrum in two regions: soft and hard. One can obtain from these a parameter which is dependent only on the heavy element concentration. The theoretical results are compared with the experiment. (auth)

12994 SOLVING NUCLEAR GEOPHYSICS PROBLEMS BY THE MONTE CARLO METHOD. Denisik, S. A.; Lebedev, V. E.; Lukhminskii, B. E.; Rezvanov, R. A. (All-Union Research Inst. for Nuclear Geophysics and Geochemistry, Moscow). Vienna, International Atomic Energy Agency, 1965, Preprint No. SM-68/36, 25p. (In Russian). (CONF-651023-27). ORINS.

From Symposium on Radioisotope Instruments in Industry and Geophysics, Warsaw.

The perfecting of pulsed neutron methods and equipment provided a stimulus to the carrying out of non-stationary neutron-field calculations in rocks. The basic relations between results yielded by the methods and the composition and properties of the rock and the filling of the borehole at normal and high temperatures are considered. The requirements in respect of certain parameters of the equipment, including minimum source strength, measuring procedures over a period of time and optimum probe length, are determined. Calculations are performed for the photo-neutron field generated in rocks by a beam of gamma rays. Requirements regarding the parameters of the apparatus, including source strength and probe dimensions, are laid down. (auth)

12995 NUCLEAR BLAST AND OVERPRESSURE DETECTION AND RECORDING SYSTEM. Furman, Daniel W. (to Dunlap and Associates, Inc.). U. S. Patent 3,226,546. Dec. 28, 1965. Filed Dec. 3, 1962.

A method and apparatus are described for determining the location and magnitude of nuclear detonations. A system employing a number of these devices is described for accurately determining the weapon yield, burst height, and location of ground zero of the detonation. (B.L.M.)

Thorium and Uranium Minerals

Refer also to abstract 14105.

12996 (JEN-155-SIG/I-4) CONSIDERACIONES SOBRE LA GENESIS DE LOS YACIMIENTOS URANIFEROS. II. ALGUNOS PROBLEMAS DEL ESTADO TERMODINAMICO DE LOS SISTEMAS METALOGENICOS. (Considerations on the Genesis of Uraniferous Deposits. II. Some Problems of the Thermodynamic State of Metallogenic Systems).

Mingarro, E. (Junta de Energia Nuclear, Madrid (Spain). Seccion de Investigacion Geologica). 1965. 29p. Dep. mn.

In order to get a classification of the uranium deposits, the geological processes were ordered in thermodynamic systems according to the independent parameters that define their equilibrium state. Also, to apply the phase rule, it is assumed that the ore forming elements are always ideally mobile components; that is, in the geological systems, these components are defined by their chemical potentials. It is shown that in random conditions i.e., for any possible value of the factors of equilibrium or state, the stable mineralizations are formed only in metasomatic regimes; so that the mineralogical sequence is a function both of the Helmholtz's free energy and the crystallization pressure of the minerals. (auth)

HEALTH AND SAFETY

See *also* BIOLOGY AND MEDICINE — Radiation Hazards and Protection
GEOLOGY, METEOROLOGY, AND MINERALOGY — Natural Radioactivity and Fallout

Refer also to abstracts 12942, 13077, 14077, and 14093.

12997 (AD-626210) ADVANCED STUDY OF MILK DECONTAMINATION BY ELECTRODIALYSIS. Greatorex, John L.; Glass, Werner (Ionics, Inc., Watertown, Mass. Research Div.). Oct. 1965. Contract OCD-PS-64-281. 27p. CFSTI $2.00 cy, $0.50 mn.

A five gph electrodialytic milk decontamination test plant was built and operated. Previous research had established that radioactive contamination can be removed by flushing cations through a layer of milk. The cations leaving the milk include the radioactive species such as ^{90}Sr and ^{137}Cs. The milk itself flows in a constrained path between a pair of cation-selective membranes. The cation motion from a salt make-up solution, through the milk, and into a waste solution is induced by a DC electric field. It had been shown that the cation composition of the treated milk could be controlled by suitable selection of the composition of the salt make-up stream. The membrane life, effect of time on current efficiency, and cleaning technique were studied. Approximately 8,000 lbs of milk were treated. Decontamination averaged 90%. The ion-selective membranes showed no decrement in performance following an initial drop from 90% current efficiency to 82% during the first 60 hours of operation. A suitable in situ method of cleaning the membrane stack was developed. It consisted of consecutive rinses of water, 5% NaOH, warm (150°F) water, 5% HCl and water. The chemical costs of this cleaning method come to about 0.03¢/gallon milk. Bacteria counts always remained below the 50,000 per ml USPHS standard. The appearance and taste of the treated milk was very similar to that of the raw milk. Rat-feeding and vitamin-analysis tests conducted by independent laboratories showed that the electrodialytically decontaminated milk was nutritionally indistinguishable from untreated milk. (auth)

12998 (ANL-7104) ENVIRONMENTAL RADIOACTIVITY AT ARGONNE NATIONAL LABORATORY. Report for 1964. Sedlet, J.; Iwami, F. S. (Argonne National Lab., Ill.). Oct. 1965. Contract W-31-109-eng-38. 45p. Dep. mn. CFSTI $2.00 cy, $0.50 mn.

Results of the environmental monitoring program at Argonne National Laboratory during 1964 are presented. The purposes of the program are to measure the natural radioactive content of the ANL site and its surroundings, and to determine the origin, identity, and magnitude of any radioactivity not naturally present. Of primary interest is the detection of radioactive materials released to the environment as a result of Argonne operations. The radioactive content of the environment was determined by radiochemical analyses, total activity measurements, and gamma-ray spectrometric measurements performed on several types of natural materials collected on the ANL site and from locations up to 100 miles from the site. The frequency of sampling decreased with increasing distance from the Laboratory. The sampling locations are described in Part II of this report. Since air and water are the most probable media for spreading radioactive contamination, the sampling program concentrated on these materials. Argonne waste water is discharged into Sawmill Creek, which in turn flows into the Des Plaines River, and special emphasis was placed on these streams. (auth)

12999 (CEA-R-2746) SURVEILLANCE DU PERSONNEL EXPOSE PROFESSIONNELLEMENT AUX RADIATIONS IONISANTES (RAYONS X) [Theses]. (Inspection of Professional Personnel Exposed to Ionizing Radiation (X-Rays) [Thesis]). Chalabreysse, Jacques (Commissariat a l'Energie Atomique, Pierrelatte (France)). 1965. 71p. Dep. mn.

Submitted to Lyon Univ., France.

After a short introduction giving the physical characteristics and the possible interactions of x rays, this report considers in more detail the basis of the dosimetry and the units used. Taking into account the dangers of irradiation and the professional norms applicable, the report reviews the physical methods (collective and individual dosimetry) and the biological method (based on the systematic study of the hemogram) which are used to ensure that these professional norms are respected. Data are included from studies on the influence of repeated doses of x rays on the hemogram of x-ray technicians, when the individual radiation levels are known through dosimetric films. Two processes are used: one considers the mean values (irradiation and average hemogram for each person), the other requires the use of an electronic computer and uses each hemotological variable as a function of the monthly or cumulative doses, and gives correlation coefficients for the different variables. The results obtained are compared to those conventionally accepted, and the validity of the hemogram is evaluated as a criterion for the radiation protection of medical personnel. (tr-auth)

13000 (EUR-2520.f) NIVEAUX DE CONTAMINATION RADIOACTIVE DU MILIEU AMBIANT ET DE LA CHAINE ALIMENTAIRE. Rapport Annuel, 1964. (Radioactive Contamination Levels in the Environment and in the Food Chain. Annual Report, 1964). (Commissariat a l'Energie Atomique, Fontenay-aux-Roses (France). Centre d'Etudes Nucleaires). 1965. 31p. Dep. mn.

Data are presented on radioactive contamination levels in the environment and in food chains in EURATOM countries during 1964. Emphasis was placed on the content of ^{137}Cs, ^{89}Sr, and ^{90}Sr in samples of air, soil, and water. Data are included from a study of iodine metabolism in children and from a study of the gastrointestinal transit time of ingested materials. A mathematical model of gastrointestinal transit time was developed for adults and infants, based on dietary habits of 9,000 families. The model was used for a study of the transfer of radioactive contamination from the source to foodstuffs and hence to man. (C.H.)

13001 (GAT-T-1222) RADIATION ALARM INSTRUMENT INSTRUCTION MANUAL. Mustard, G. L. (Goodyear Atomic Corp., Piketon, Ohio). Oct. 13, 1965. Contract AT(33-2)-1. 36p. Dep. mn. CFSTI $2.00 cy, $0.50 mn.

The theory of operation and the specifications are presented for the integrating-type criticality alarm instrument used at the Portsmouth Gaseous Diffusion Plant. The advantages of the gamma and neutron-sensitive ion chamber with short-term integration are discussed. The major design features are described in detail. (auth)

13002 (JAERI-4034) BIBLIOGRAPHY ON "ACCIDENTS IN NUCLEAR FACILITIES". Kobayashi, Yukichi; Kobayashi, Hiroo; Akaishi, Jun; Iijima, Toshitetsu (Japan Atomic Energy Research Inst., Tokyo). May 1965. 36p. Dep.mn.

Abstracted references to 120 items on personnel radiation exposure and accidents at nuclear facilities are presented. Author and subject indexes are included. The subject index is divided into two categories: accidents and emergency planning. (H.G.D.)

13003 (JAERI-4035) COMPARISON OF THE METHODS OF PERSONNEL-MONITORING DOSIMETRY PRAC-

TISED IN NUCLEAR ESTABLISHMENTS OF DIFFERENT COUNTRIES. Miyanaga, Ichiro; Tanooka, Hiroshi; Yamamoto, Hozumu; Bingo, Kazuyoshi; Nishi, Tatsuo (Japan Atomic Energy Research Inst., Tokyo). July 1965. 25p. (In Japanese). Dep. mn.

Methods of personnel monitoring dosimetry, used in nuclear establishments of different countries, are described, with emphasis on film badges. These methods used in other countries are compared with those developed and used in JAERI. Design of film-badges, methods of dose evaluation, monitoring systems, etc., are also discussed. The comparison revealed many advantages possessed by the JAERI methods. (auth)

13004 (LA–1981(Rev.)) PLUTONIUM DISPERSAL BY ACCIDENTAL OR EXPERIMENTAL LOW-ORDER DETONATION OF ATOMIC WEAPONS. Langham, W. H.; Harris, P. S.; Shipman, T. L. (Los Alamos Scientific Lab., Univ. of California, N. Mex.). Dec. 1955. Revised Feb. 1966. Contract W-7405-eng-36. 40p. Dep. mn. CFSTI $2.00 cy, $0.50 mn.

Accidental or experimental detonation of atomic weapons that contain Pu under conditions such that the degree of criticality produced is insignificant may create an immediate and a residual or delayed Pu health hazard. The immediate hazard is associated with the inhalation of Pu during cloud passage and on the basis of theoretical considerations appears to be relatively insignificant. The delayed hazard results from residual Pu deposited in the fall-out pattern, which may produce chronic contamination over a long period of time. Theoretical curves for maximum allowable air concentrations as a function of time of exposure, based on the assumption of a maximum permissible level of 0.008 μc of Pu in the lung and a maximum permissible total body level of 0.5 μg, were developed. These curves may be quite useful in assessing the magnitude of the immediate and residual hazards. Suggestions are made as to the course of action that should be followed in the event of an accidental detonation of the type under consideration. (auth)

13005 (LA–3366) CRITICALITY CONTROL IN OPERATIONS WITH FISSILE MATERIAL. Paxton, H. C. (Los Alamos Scientific Lab., Univ. of California, N. Mex.). Dec. 1964. Contract W-7405-eng-36. 48p. Dep. mn. CFSTI $3.00 cy, $0.50 mn.

A discussion of criticality control is presented to encourage a working knowledge on the part of those who design and perform operations with fissile material. Responsibilities of the AEC and of operating organizations and an outline of nuclear-safety experience lead to reasonable principles of nuclear safety. Next, empirical criticality information is presented to help develop a feel for conditions to be avoided during operations. The final portion covers criticality-control methods that are consistent with the stated principles and available criticality data. (auth)

13006 (ORNL-TM–1384) DESCRIPTION OF THE CELL VENTILATION MONITOR FOR THE FISSION PRODUCTS DEVELOPMENT LABORATORY BUILDING 3517. Knowles, D. J.; Danforth, H. P.; Chase, L. H. (Oak Ridge National Lab., Tenn.). Dec. 15, 1965. Contract W-7405-eng-26. 7p. Dep. mn. CFSTI $1.00 cy, $0.50 mn.

The exhaust ventilation air from the Fission Products Development Laboratory (FPDL) Building 3517 is filtered before it flows to the 3039 stack. The air is monitored for radioactive particulates after being filtered at Building 3517 and again at the 3039 stack. The intended function and details of the components in the FPDL Duct Monitor at Building 3517 are described. A checkout procedure is attached. (auth)

13007 (NP-tr–1336) NOTES ON THE RADIOACTIVITY OF THE WATERS OF THE PACIFIC OCEAN. Sysoyev, N. N.; Kirilyok, Yu. I. Translated from Okeanologiya, 2: 734-5(1962). 5p. Dep. mn. CFSTI $1.00 cy, $0.50 mn. JCL $1.10 fs, $0.80 mf.

Data on the contents of ^{137}Cs, ^{90}Sr, Th, and ^{230}Th, in the off-shore waters of California and Japan (Pacific Ocean) are reported. The results showed that it took 1½ years from the time of atomic explosions on the Marshall Islands for a significant reduction to take place in the ^{137}Cs and ^{90}Sr mean in Japanese waters. (P.C.H.)

13008 THE PHOTOGRAPHIC REPRESENTATION OF ISODOSE PATTERNS BY THE APPLICATION OF THE SABATTIER EFFECT. Tsien, K. C.; Robbins, Robert (Temple Univ. Medical Center, Philadelphia). Brit. J. Radiol., 39: 1-6(Jan. 1966).

The method of showing isodose patterns utilizing the Sabattier effect with photographic film was investigated, and the technique is described. Four examples of dose distributions obtained by this method are presented including ^{60}Co beam rotation, wedge-filtered beams, electron beam, and a radium volume implant. The advantages and limitations of this method are discussed. (auth)

13009 MEASUREMENT OF TISSUE-AIR RATIOS AND SCATTER FUNCTIONS FOR LARGE FIELD SIZES, FOR ^{60}Co GAMMA RADIATION. Gupta, S. K.; Cunningham, J. R. (Univ. of Toronto. Ontario Cancer Inst., Toronto). Brit. J. Radiol., 39: 7-11(Jan. 1966).

Currently available data for tissue-air ratios and scatter functions for ^{60}Co radiation were extended to large field sizes and depths of 30 cm following ionization chamber measurements in a water phantom. The measurements were made using circular fields of radii up to 22.5 cm. A small systematic error in currently published data was noted and the results are presented first in the form of a table of scatter functions for field radii of 2 to 25 cm and a source-to-surface distance of 80 cm. A more versatile form for scatter data, independent of source-to-surface distance, is suggested and a corresponding table of values is presented. Finally, tissue-air ratios for square fields ranging from 4 × 4 to 35 × 35 cm were prepared using the Clarkson method. The data for field sizes larger than 20 × 20 cm and depths greater than 20 cm are new, while the remainder represent previously published data slightly amended. (auth)

13010 GRID FIELD DOSIMETRY FOR ^{60}Co BEAMS. Bryant, T. H. E. (Middlesex Hospital Medical School, London). Brit. J. Radiol., 39: 75-7(Jan. 1966).

Design of a grid suitable for use with a ^{60}Co unit is described, and results of dose distribution measurements made with an ionization chamber are presented. Basic advantages of ^{60}Co radiation in giving reduced skin reaction, increased depth dose, and lower differential bone absorption were retained when using the grid. However, physical thickness of the grid produces a γ isodose chart that has a large penumbra, making it inferior to that of a 250 kv x-ray beam. Further the grid technique for ^{60}Co γ therapy when tested clinically did not offer any advantages over the more usual four oblique field technique. It is concluded that the use of grids with kilocurie isotope sources has limited application. (H.G.D.)

13011 GROWTH STATUS OF CHILDREN EXPOSED TO FALLOUT RADIATION ON MARSHALL ISLANDS. Sutow, W. W. (Univ. of Texas M. D. Anderson Hospital and Tumor Inst., Houston); Conard, R. A.; Griffith, K. M. Pediatrics, 36: 721-31(Nov. 1965). (BNL–8656).

Follow-up studies are reported on the inhabitants of three atolls (Rongelap, Ailingnae, and Utirik) of the Marshall Islands who were accidentally exposed to fallout radiation from the experimental detonation of a large thermonuclear device over Bikini Atoll in 1954. This report summarizes the findings of growth and development studies, for 1958 through 1963, of those who were in the pediatric age group (less than 20 yr of age) at the time of exposure. Longitudinal studies on 38 children revealed retardation in both statural growth and skeletal maturation among the exposed boys as compared to nonexposed comparison children. The retardation was noted among boys who were under 5 yr of age when exposed to the fallout, being most prominent among those who were 12 to 18

months old at time of exposure. No significant differences were noted in the growth patterns between the exposed and the nonexposed group of girls and between 39 children born to exposed parents subsequent to fallout and 53 children born to nonexposed parents. It is believed that in these Marshall Islands children any radiation effect on bone growth must have resulted from penetrating γ radiation at the time of original exposure. The accumulated dose to the bones from absorbed radionuclides, such as ^{90}Sr, is believed to be negligible compared with the dose of γ radiation originally received. However, the dose of penetrating radiation received was much lower than that expected to produce retardation by direct effect on osseous growth. In 25 of 31 exposed Rongelap children, in whom weights were documented, a weight loss of several pounds each occurred during the first 6- to 8-week period following exposure. This may have been a reflection of radiation effect on metabolism. (BBB)

13012 A COMPARISON OF ^{90}Sr COMPONENT OF HUMAN AND COWS' MILK. Straub, Conrad P.; Murthy, Gopala K. (Robert A. Taft Sanitary Engineering Center, Cincinnati). Pediatrics, 36: 732-5(Nov. 1965).

To obtain data on radionuclide concentrations in human milk, samples of human milk were obtained from Denver, Colorado (July 9, 1959, through February, 1961), and Chicago, Illinois (December 21, 1959, through August, 1961). The Denver samples represented pooled human milk collected postpartum, while those from Chicago represented human milk from individual donors contributing to a milk bank. For comparison, samples of cows' milk corresponding to that consumed by the donors in Chicago were also collected. Samples were analyzed for Ca, K, ^{90}Sr, and ^{137}Cs, and the results are summarized in tables. Data are reported to show that in the metabolism of cows' milk and production of human milk, the mother discriminates in favor of Ca over Sr by a factor of about 2.5 which accounts for the lower levels of both radiostrontium and stable Ca. In terms of the ^{90}Sr and Ca concentrations, the differences between human and cows' milk were equivalent to a factor of about 11 to 4.5, respectively. Since ^{90}Sr concentrations in human milk are smaller than those in cows' milk by an order of magnitude, the consumption of human milk should result in a lower intake of this radionuclide by infants, which should reduce potential radiation exposure, unless there is a difference in metabolism of the two sources of milk. The concentrations of ^{137}Cs in the human milk samples were very small and did not exceed 20 pC/l, and in most cases were close to the min detectable amount for this radionuclide under the conditions of measurement. Cesium-137 concentrations in cows' milk were also small, 5 to 25 pC/l, during this period. The observed ratio for the discrimination of ^{137}Cs in relation to K was found to be 1.0 and 0.81 for March and April, 1961, respectively. (BBB)

13013 GONAD DOSE OF PATIENTS IN THE X-RAY TREATMENT OF BENIGN TUMORS AND SOME PROBLEMS IN THE GONADAL EXPOSURE OF ATTENDANTS IN RADIOTHERAPY OF THE INFANTS. Iba, Shozo; Arimizu, Noboru; Kakehi, Hirotake (Chiba Univ. Hospital, Japan). J. Radiat. Res. (Jap.), 5: 139-46(Sept.-Dec. 1964).

Many patients given radiotherapy for benign tumors and chronic inflammatory diseases are among the younger age groups and their child expectancy is usually high. If the patients are few in number, but the amount of gonadal exposure is considerably high in radiation treatment, attention should be paid to reduce the gonad dose. Gonadal exposure in radiation treatment should be considered for the attendant who watches an infantile patient to prevent movement during the treatment. Gonad dose in conventional x-ray treatment was measured in fifty patients with benign tumors and tuberculous cervical lymphadenitis and in eighteen persons attending infantile patients with malignant tumors. Total gonad dose in one session of x-ray treatments was 300 mR or less in most cases but more than 500 mR in a few cases. Fundamental experiments were performed concerning the gonad dose. The scattered dose inside and outside the phantom was measured on various field sizes, filtration and kilovoltages. Measurements were made on phantoms using usual commercial pocket chambers and dosemeters. Several procedures are discussed for reducing the gonadal exposure of the attendants of infantile patients. (TCO)

13014 X RAYS FROM COLOR TELEVISION RECEIVERS. Hayashi, Satori (Osaka Public Health Inst.); Kitao, Takaya; Hayashi, Miyoko; Oki, Iwashiro; Oshino, Akira. J. Radiat. Res. (Jap.), 5: 147-58(Sept.-Dec. 1964).

Sources of x-ray leakage from color television receivers manufactured in Japan were determined. Observations were made of the energy distribution, the geometrical distribution, and the dose level and its correlation to beam current or applied voltage. Radiations from completed television receivers were also investigated. The radiation levels from both sources showed a significant difference among individual products. A method was proposed to estimate the percentage of television receivers that leak radiation beyond a certain dose level. It was found that the shunt regulator valve gives a high level of leakage radiation. It is suggested the regulator be shielded more cautiously than the cathode-ray tube. The dose level may be reduced below the maximum permissible limit by means of a simple shielding. (TCO)

13015 BIOMETEOROLOGY—MEDICAL METEOROLOGY—ANTHROPOMETEOROLOGY. Kiel, K. Meterol. Rundsch., 18: 114-17(July-Aug. 1965). (In German).

The radioactivity contained in air plays an important role in human health and survival. Through all previous ages man has been subjected to irradiation from radioactive materials and cosmic radiation. Atomic tests have altered the base level of this irradiation and have imposed the necessity for strict monitoring of these levels. For many years the German weather services have performed these services. Although the genetic and somatic effects of radioactivity have been the concern chiefly in biology they also interest the anthropometeorologists. One instance of this is the possible stimulatory effect of Rn and its daughters on the central nervous system in certain weather conditions that might possibly cause disorganization of the autonomic equilibrium. This is only one of the questions with which anthropometeorology is concerned. Weather, man, and climate are factors which are interrelated. How to protect people from elements of the weather, such as increased radioactivity and weather complexes is a matter for the anthropometeorologists. Physicians should recognize that there are problems here that will require close, sincere cooperation between themselves and meteorologists before they can be solved. (BBB)

13016 BERYLLIUM POISONING—LESSONS IN CONTROL OF MAN-MADE DISEASE. Hardy, Harriet L. (Massachusetts General Hospital, Boston). New Engl. J. Med., 273: 1188-99(Nov. 25, 1965).

The history of occupational hazards and development of measures for their control are reviewed. From medical literature and clinical data of the author, facts are presented that indicate criteria for control of beryllium poisoning and other man-made diseases. (H.G.D.)

13017 PROGRESS AND PROBLEMS IN RADIATION STANDARDS AND RADIOACTIVE WASTE DISPOSAL. Ramey, James T. Nucl. Energy, 333-41(Nov.-Dec. 1965).

The development and application of radiation standards are reviewed and the specific application of standards in the field of radioactive waste disposal are discussed. Concepts of radiation standards, the role of ICRP and NCRP, the role of the Federal Radiation Council, the role of the Public Health Service, the role of the AEC, the responsibilities of the states, and problems of standards setting are considered. Radiation protection in the AEC radioactive waste disposal program is described. The concepts of concentrate and contain and dilute and disperse for waste disposal are considered. Estimates of wastes from the civilian power program are presented. (M.C.G.)

13018 EXPERIENCE IN THE DEVELOPMENT AND ADMINISTRATION OF THE CRITICALITY CONTROL PROGRAM IN A COMMERCIAL PLUTONIUM PROCESSING

AND FABRICATION PLANT. Puechl, K. H. (Nuclear Materials and Equipment Corp., Apollo, Pa.). Vienna, International Atomic Energy Agency, 1965, Preprint No. SM-70/45, 23p. (CONF-651103-24). ORINS.

From IAEA Symposium on Criticality Control of Fissile Materials, Stockholm.

The technical, administrative, and economic considerations that are used to set criticality control policies at the NUMEC Plutonium Laboratory are discussed in this paper. Also presented is the insight gained through administration of these policies over the past five years. The nature of the operations, since they involve both research and development and fuel materials production, dictates a criticality control program that permits flexibility of operations, yet one that is amenable to administration through simple, precise controls without the necessity for elaborate reviews and paperwork. This is particularly true since the production operations are not determined from within but rather are dependent upon contracts received and therefore such operations cannot be precisely defined and/or scheduled prior to receipt of contract. Generally, it has been found that simple criticality controls that can be uniformly applied throughout the plant and hence that can be easily administered are in the overall the most economic procedures. Further, such broadly applicable procedures can be expected to be safely carried out by employees who have a minimum of training in the sciences and who have essentially no experience in working in a nuclear plant. Also, through the use of such broadly applicable procedures, agencies that are responsible for licensing of nuclear facilities need not be informed and convinced every time a process is modified even in the slightest fashion. At the NUMEC Plutonium Laboratory, except for rare instances dictated by peculiarities of the process and/or the particular geometry of equipment, a set of nine simple rules are in force throughout the plant and have been adhered to with a minimum of exceptions, and it is under these procedures that approximately 300 kilograms of plutonium were processed economically during the past year. (auth)

13019 BORON POISONING OF PLUTONIUM SOLUTIONS. Chalmers, J. H. (United Kingdom Atomic Energy Authority, Risley, Eng.). Vienna, International Atomic Energy Agency, 1965, Preprint No. SM-70/10, 13p. (CONF-651103-20). ORINS.

From IAEA Symposium on Criticality Control of Fissile Materials, Stockholm.

The results of a theoretical investigation into the possible relaxation of criticality concentration limits in wet chemical reprocessing plants, due to the introduction of boron poisoning, are reported. The following systems were considered: 1" N.B. stainless steel tubes filled with boron carbide at various pitches in homogeneous mixtures of $^{239}Pu(NO_3)_4$ $5H_2O$ and water, 1" and 2" borosilicate glass raschig rings in homogeneous mixtures of $^{239}Pu(NO_3)_4$ $5H_2O$ and water, the concentration of natural boron required for $k_\infty = 1$ in homogeneous mixtures of $^{239}Pu-B-H_2O$. The method of calculation was Monte Carlo using the GEM code with Nuclear Data File cross-sections. The core model consisted of a cubic arrangement of unit cubes of solution within each of which a raschig ring was centrally placed. The arrangement was such that the rings were regularly stacked with axes parallel, but the side of the unit cube was fixed to preserve the random packing density. Comparison is made with other reported results on boron poisoning. (auth)

13020 MANAGEMENT AND OPERATIONAL CONTROL OF CRITICALITY. Daniels, J. T. (United Kingdom Atomic Energy Authority, Risley, Eng.). Vienna, International Atomic Energy Agency, 1965, Preprint No. SM-70/11, 14p. (CONF-651103-21). ORINS.

From IAEA Symposium on Criticality Control of Fissile Materials, Stockholm.

Six process criticality accidents have been reported to date and without exception they were due to the failure of operational controls. In no instance was a criticality accident in processing due to the use of wrong data or inaccurate calculation. Important as correct criticality calculations are, there are many other considerations which require the exercise of judgement in establishing the conditions that can readily exist in an operational environment. The evidence of process criticality accidents supports the view that accidents are least likely to occur in the production stream but are more likely to be associated with ancillary equipment and operations. In any particular set of circumstances there are a number of different ways of achieving safe operation. A higher assurance of safety can be given when control can be exercised independently of the human element. The exercise of judgement required in making a criticality assessment is not the prerogative of any particular discipline; it requires a background of operational experience coupled with a thorough understanding of the basic principles of criticality. The economic optimization of criticality controls leads eventually to some control of the environment in which fissile materials are handled so that conditions of limited reflection and/or moderation may be achieved. The environment is much more difficult to assess and control than the fissile material itself and satisfactory procedures must be established to enforce such control. No operation involving fissile material should be permitted without a formal review resulting in a documented statement of the environmental assessment, the nuclear safety arguments which demonstrate safety under that environment, and the operational requirements which will ensure the validity of under the conditions of the environmental assessment. To ensure the continued viability of the environmental assessment and the continued reliability of clearance conditions there should be close supervision by operating management, and periodic checks made by site nuclear safety staff. Additionally, there should be periodic and systematic examinations by competent persons who are not responsible to the over-all management of the site. (auth)

13021 COMPUTERS AND SIMULATORS OF ATOMIC RADIATION. Falk, Fred W.; Edwards, George C. (to U. S. Army). U. S. Patent 3,226,847. Jan. 4, 1966. Filed July 11, 1962.

A computer system for solving equations having the form $y = bx^k$ is described that is particularly applicable for simulating radioactive fallout data. The system includes a voltage sensitive meter having a logarithmic scale for indicating radiation data in response to voltages supplied to the meter and two voltage supply means. A first voltage supply means supplies a first voltage predetermined as a function of maximum radiation dose rate, and the second voltage supply means supplies a second voltage that varies unidirectionally as a function of time and as a function of a decay rate for the radiation dose rate. The two voltage supply means are connected in series with the meter in such a way that the voltage supplied to the meter represents the sum of voltage supplied by the two supply means. The second voltage supply means comprises a clock driven variable resistor means coupled with the voltage source for controlling the output of the second supply means. (B.L.M.)

INSTRUMENTATION

General

Refer also to abstract 12818.

13022 (AFCRL-65-859) PLASMA-COVERED SLOT ANTENNAS. Final Report, November 1, 1962–September 30, 1965. Galejs, J.; Mentzoni, M.; Seshadri, S. (Sylvania Electronic Systems, Waltham, Mass. Applied Research Lab.). Oct. 1965. Contract AF19(628)-2410. 57p. CFSTI $3.00 cy, $0.75 mn.

Theoretical studies have led to several formulations of antenna impedances in a plasma environment, the accuracy of which was verified experimentally. Analytical work is also reported on finite temperature effects on plasma-covered antennas and on antennas in a generally stratified dielectric. An initial study on nonlinear and breakdown effects of signals was reported. The results of microwave diagnostic studies of electron removal and energy relaxation rates in atmospheric gases are also summarized. (auth)

13023 (CONF-660206-1) ON THE MEASUREMENT OF CHARACTERISTIC KERNELS OF A CLASS OF NONLINEAR SYSTEMS. Hooper, Richard J. (Knolls Atomic Power Lab., Schenectady, N. Y.); Gyftopoulos, Elias P. (Massachusetts Inst. of Tech., Cambridge). [1966]. Contract W-31-109-eng-52. 23p. Dep. mn. CFSTI $1.00 cy, $0.50 mn.

From Symposium on Neutron Noise, Waves, and Pulse Propagation, Gainesville, Fla.

The results of some simulated experiments in which the dynamic response characteristics of several nonlinear systems were measured by means of input-output cross correlation techniques are presented. Periodic discrete level input signals were used, and the cross correlation time was taken equal to the period of the test signal. (auth)

13024 (EUR-2544.d) ENTWICKLUNG EINES KALK-STAUBMENGENMESSGERAETES. (Development of a Chalk Dust Measuring Device). Schmidt, K.; Naseband, A. (Internationale Atomreaktorbau G.m.b.H., (West Germany)). 1965. 54p. Dep. mn.

It was found that ionizing radiations can be used for fine chalk density determination. Suitable sources are the bremsstrahlung for Sr/Y-90 backscattered from a silver target, the beta-radiation from Sr/Y-90, and the gamma-radiation from Am-241. The first measuring rig is based on a zero compensation involving constant comparison of the measuring radiation intensity with that of a standard radiation. In the second rig detector amplification is stabilized by means of a standard radiation. The measuring radiation intensity recorded indicates the fine chalk density. The use of bremsstrahlung involved a margin of error of as much as 10% at an acceptable radiation source activity and an adequate recording speed. With beta radiation, the measuring values are reproducible within 1% margin of error. With Am-241 gamma radiation, the second rig gave a margin of error of 1% with a long-time stability within 1-2%. Costs for the construction of the device amounted to about 18,000 to 20,000 DM. (P.C.H.)

13025 (IPP-2/37) MESSUNG DER KENNGROESSEN EINER FELDEMISSIONSSTRECKE MIT EINER WECHSELSTROMMETHODE: GENAUIGKEIT UND PRAKTISCHE DURCHFUEHRUNG. (An A.C. Method for Measuring the Characteristic Data of a Field Emission Point: Accuracy and Experimental Realization). Vernickel, H. (Institut fuer Plasmaphysik, G.m.b.H. Garching (West Germany)). May 1965. 25p. Dep. mn.

An a-c method for continuous measurement of a change in work function of a field emission point was reported earlier. The method was improved by phase-sensitive detection of the a-c signal. Changes in work function can be measured with an accuracy of ±1 to 2% of the reference value. In its present form the method may be used down to field emission currents of some 10^{-9} amp. It is compared with the conventional method of measuring Fowler-Nordheim plots. (auth)

13026 (IPP-2/39) EIN ZWEIKAMMER-IONISATIONS-MANOMETER. (A Two-Chamber Ionization Gage). Blauth, E. W.; Venus, G. (Institut fuer Plasmaphysik, G.m.b.H. Garching (West Germany)). June 1965. 43p. Dep. mn.

In order to avoid perturbations of the pressure measurement with an ionization gauge caused by the interaction of the electron gun with the gas in the volume to be measured, a two-chamber ionization gauge was constructed. Electron beam propagation and ionization take place in two spaces separated almost completely as regards vacuum technique. The two-chamber gauge was calibrated for the range from 10^{-1} to 10^{-10} torr and its behavior studied by investigations connected with Blears effect. (auth)

13027 (IPP-4/24) ZUENDEN VON HOECHSTSPANNUNGS-FUNKENSTRECKEN MITTELS LICHTTRIGGERUNG. (Lighting of Very High Voltage Spark Gaps by Means of Light Triggering). Baeumler, J. G. (Institut fuer Plasmaphysik, G.m.b.H. Garching (West Germany)). Aug. 1965. 11p. Dep. mn.

In order to avoid the insulation problem when triggering spark gaps in the very high voltage region a light trigger system was developed. A spark gap as light source, mounted in sufficient distance to the main gap, radiates its negative electrode with uv-light. There the high-energetic light liberates photoelectrons which start the ignition. Measurements of delay and jitter were made on the main spark gap at working voltages of 95 to 98, 172.5 to 177.5, and 240 to 247.5 kv. (auth)

13028 (KAPL-M-6498) REFERENCE TABLE: THERMOCOUPLE EMF VS. TEMPERATURE FOR TUNGSTEN-3 PERCENT RHENIUM VS. TUNGSTEN-25 PERCENT RHENIUM THERMOCOUPLES. Schoenig, F. C.; Kadlecek, J. A. (Knolls Atomic Power Lab., Schenectady, N. Y.). [1965]. Contract W-31-109-eng-52. 9p. Dep. mn. CFSTI $1.00 cy, $0.50 mn.

A tabulation of thermocouple emf vs temperature is presented for W-3%Re/W-25%Re thermocouples over the range of temperatures from 0 to 2390°C. (D.C.W.)

13029 (LA-3423) AN ULTRA-HIGH VACUUM THERMOBALANCE FOR LANGMUIR VAPORIZATION STUDIES; VAPOR PRESSURE OF MOLYBDENUM. Fries, R. Jay (Los Alamos Scientific Lab., Univ. of California, N. Mex.). Nov. 1965. Contract W-7405-eng-36. 22p. Dep. mn. CFSTI $1.00 cy, $0.50 mn.

An ultrahigh vacuum thermobalance suitable for Langmuir evaporation rate studies at temperatures from 1200 to 3000°K in background pressures of the order of 5×10^{-9} torr is described. The performance of the system was evaluated by measuring the vapor pressure of molybdenum. A heat of vaporization of 157.3 kcal/mole and a pressure-temperature relation of $\log_{10} P(atm) = 7.118 - 3.320\ (10^4/T)$ is recommended. (auth)

13030 (LA-3443) FABRICATION OF PRECISION LEAD COLLIMATORS. Ruess, Hermann M. (Los Alamos Scientific Lab., Univ. of California, N. Mex.). Sept. 1965. Contract W-7405-eng-36. 16p. Dep. mn. CFSTI $1.00 cy, $0.50 mn.

A fabrication technique was developed for the manufacture of precision lead collimators with slits or round holes. A precision casting process is used to obtain collimators of such quality that no subsequent machining is necessary. Mold design specifications, casting procedure, and recommendations based on test results are included. (auth)

13031 (NYO-2910-13) APPLICATIONS OF ULTRASONIC ENERGY: ULTRASONIC INSTRUMENTATION FOR

NUCLEAR APPLICATIONS. Bimonthly Progress Report No. 25, October 1–November 30, 1965. (Aeroprojects Inc., West Chester, Pa.). Dec. 1965. Contract AT(30-1)-2910. 8p. Dep. mn. CFSTI $1.00 cy, $0.50 mn.

Tests on an incipient boiling detection instrument used in molten metal indicate that difficulties experienced in its use result from a change in the metallurgical properties of the alloy used in its construction at high temperature. This change produces variations in the acoustic properties, causing a significant shift in the resonant frequency and transmission losses. Equipment modifications are made. (auth)

13032 (ORNL-TM-1352) THE INTERACTION OF MULTIPLE COILS ON A CYLINDRICAL INDUCTION HEATING LOAD. Jury, S. H. (Oak Ridge National Lab., Tenn.). Dec. 28, 1965. Contract W-7405-eng-26. 68p. Dep. mn. CFSTI $3.00 cy, $0.75 mn.

The problem of interaction of multiple coils on a cylindrical induction heating load is identified in relation to induction heating of waste calciners and the tendency of adjacent active coils to "take over" the load of an inactive one. The problem is subjected to rigorous mathematical analysis based on the basic equations of electromagnetic theory, the purpose being to develop equations for computing the power supplied to the load via active coils adjacent to an active versus inactive one. The difference is a measure of the "take over effect." The results involve rather complicated quantities, the real and imaginary portions of which were identified. In so doing, a number of different forms of the results were presented to facilitate machine programming and evaluation by anyone interested in pursuing the matter to this point. Various special cases of the more general theory are derived to demonstrate the restrictions on, and the limitations of, classical induction heating equations frequently publicized in textbooks on the subject. (auth)

13033 (TLW-1110) PROTOTYPE RADIOISOTOPE INSPECTION SYSTEM TO MEASURE RESIDUAL FLUX ON AUTOMATICALLY PROCESSED ELECTRONIC CIRCUIT BOARDS. Final Report. Sturman, I.; Wright, I. J. (Tracerlab/West, Richmond, Calif.). July 1965. Contract AT(04-3)-548. 114p. Dep. mn. CFSTI $4.00 cy, $0.75 mn.

The quantitative measurement of residual solder flux on automatically processed electronic circuit boards is successfully performed by the addition of a radioisotope tracer to the flux. The automatic solder process is briefly described. A large-area plastic scintillator beta detector designed and fabricated for this purpose is described, as well as calibration techniques. Health and safety techniques and procedures required because the study was performed in a production area with production personnel are shown to be economically reasonable so that the technique of radioisotope tracing may be considered as a production control tool. Data show that less than one percent of the flux remained after processing to the applicable specification. (auth)

13034 A PULSED ELECTRON BEAM SYSTEM. Forst, H. C.; Knapton, J. D.; Comer, R. H. (Aberdeen Proving Ground, Md.). IEEE (Inst. Elec. Electron. Eng.) Trans. Instr. Meas., IM-14: 69-71(Mar.-June 1965).

A versatile and simplified electron beam system for producing variable duration pulses is described. The electron beam is swept over a narrow slit; the electrons passing through the slit form the variable duration pulse. A minimum pulse duration of 3 nsec is theoretically possible with the present maximum sweep frequency of 1 Mc. However, the system should be adaptable with modification to accommodate higher sweep frequencies with a corresponding decrease in the pulse duration. Longer duration pulses, manually controlled single pulses, and repetitive pulses can be readily obtained. The electron beam is accelerated up to ground potential by a max accelerating potential of 60 kv. Beam currents up to 125 μa were measured; however, beam currents considerably higher should be possible. The system demonstrated the feasibility of a comparatively simplified electron beam system, which affords a high-energy, short-duration pulse of electrons in which the exit end, adjacent to the experimental chamber, is at ground potential. A drawback of the electron beam system encountered earlier, a 60-cps ripple in the beam intensity, was reduced by simply phasing the beam-gate pulse to 60 cps. (BBB)

13035 A μ SEC-PULSE GENERATOR WITH 10Mw PULSE POWER AT 200 kv PULSE VOLTAGE. Fronia, J.; Heinz, W. (Freie Univ., Berlin). Nucl. Instrum. Methods, 39: 58-60(Jan. 1966). (In German).

A pulse generator for 200 kv pulse voltage, 10 Mw pulse power and 1 to 2.5 μsec pulse duration is developed and built. The generator drives the electron gun for electron accelerators. An essential part is a pulse transformer with high transformation ratio (n = 20). Principal design calculations are shown, and a relation for the maximum value of n is derived. Directions for construction are given. (auth)

13036 A PULSED INJECTOR FOR LARGE CURRENT AND VOLTAGE. Heinz, W. (Freie Univ., Berlin). Nucl. Instrum. Methods, 39: 61-7(Jan. 1966). (In German).

Design, construction, and performance of a pulsed high-current electron injector is described. The current is space-charge limited. The focusing system is determined according to the procedure of Pierce. The injector yields a current up to 10 A at a pulse voltage of 200 kv for a duration of up to 2 μsec and can be used for injection into a FFAG-electron-synchrotron or a linac. (auth)

13037 A RANDOM PULSE GENERATOR. Divon, B.; Rozen, S. (Israel Atomic Energy Commission, Tel Aviv). Nucl. Instrum. Methods, 39: 77-87(Jan. 1966).

A random pulse generator is described, the output pulses of which are randomly distributed in time, with mean rates in the range of 10 to 10^5 sec^{-1}. The advantages of this generator are: linear relationship between the output mean rate and the control voltage; and provision for excursion over a wide range by means of an external voltage waveform applied instead of the control voltage. These features are obtained by close control through an overall negative feedback loop. The stability is ±0.3% of the maximum rate in each range for ±10% line variations and ±1% for ±10°C temperature changes. The stability during 8 hr of operation is better than ±0.2%. The response of the unit to an increasing exponential excursion having a period of 3 sec is analyzed. (auth)

13038 ON UNFOLDING AN APPARATUS FUNCTION FROM DATA OF LOW STATISTICAL ACCURACY. Emmerson, J. McL. (Oxford Univ.). Nucl. Instrum. Methods, 39: 163-8(Jan. 1966).

A numerical method is presented for unfolding an apparatus function from an experimental histogram when the experimental data has low accuracy but the form of the results is known approximately. It is shown that it is possible to overcome the effects that cause normal unfolding procedures to lead to wildly oscillating functions. Sample analyses show that the method introduces only a slight additional uncertainty, which is small compared with that inherent in the data. The case in which the quantity being measured is significant beyond the limits of the experimental range is included. (auth)

13039 A SIMPLE CURRENT GENERATOR. Whittaker, J. K. (National Bureau of Standards, Washington, D. C.). Nucl. Instrum. Methods, 39: 183-4(Jan. 1966).

Two current generators having outputs of ±40 and ±400 ma respectively are described. The generators incorporate high-resolution, stable controls, and allow current control in both directions without switching. (T.F.H.)

13040 ON ERROR PROPAGATION IN THE RESOLUTION CORRECTION. Quittner, G. (Oesterreichische Studiengesellschaft fuer Atomenergie, Seibersdorf, Austria). Nucl. Instrum. Methods, 39: 271-7(Jan. 11, 1966).

If experimental functions subject to random fluctuations are replaced by appropriate smoothed versions, the appearance of spurious oscillations in the results of resolu-

tion correction can be avoided. The truncation of series expansions of the experimental functions with respect to a suitable system of orthogonal functions is a smoothing operation of this kind. Three of such smoothing operations, for the input, for the resolution- and for the output-function respectively, are introduced and some comments on their use are given. An analysis, by means of Fourier transforms, of a simplified resolution equation is used to give insight into the respective roles of the frequency spectrum of the true function, of the uncertainties of the input function and of the resolution function, and of the resolution width in determining the amount of true details in the results of measurement. Implications for the proper number of equations to be used in the solution of the resolution equation and for the choice of the resolution width of an experimental arrangement are considered. (auth)

13041 PILE-UP EFFECTS IN TIME MEASUREMENTS. De Lotto, J. (CNR-CISE, Milan); Dotti, D. Nucl. Instrum. Methods, 39: 281-92(Jan. 11, 1966).

The pile-up amplitude distribution of pulses having the most common shape is studied (single and double RC differentiation, single and double delay line differentiation). The pile-up effects on timing circuits are then analyzed, and experimental results are discussed. Finally the efficiency of pile-up rejection circuits is examined in order to design the most suitable ones. (auth)

13042 ANALOG-TO-DIGITAL CONVERTER NONLINEARITY DUE TO THE LOSS CURRENT. Szavits, O. (Inst. Rudjer Boskovic, Zagreb). Nucl. Instrum. Methods, 39: 293-6(Jan. 11, 1966).

A pulse amplitude error, which occurs in pulse stretchers due to the RC-shaped input pulses when the loss current cannot be neglected is analyzed. An expression is derived showing the dependence of this error on pulse amplitude, loss current, and pulse shape. (auth)

13043 SENSITIVE, 100 MHz PULSE DISCRIMINATOR AND SHAPING CIRCUIT. Coli, M. (Laboratori Nazionali di Frascati, Rome). Nucl. Instrum. Methods, 39: 297-302(Jan. 11, 1966).

A discriminator and pulse shaper is described with the following characteristics: 1 mamp minimum threshold ranging up to 30 mamp, maximum input repetition rate of 100 megapulses/s for threshold variation within 5%; delay 4 ns at 1% overdrive, time slewing (for input pulse risetime 0.5 ns) is 2 ns for 80% and 4 ns for factor of 100 overdrive. At minimum threshold (0.5 mamp) the circuit can be overdriven by at least a factor of 10, more for higher threshold settings. This was obtained by input limitation and complete isolation of the output tunnel shaper during all the input pulse width. (auth)

13044 AN IMPULSE GENERATOR FOR ADJUSTMENT AND TESTING OF COINCIDENCE SYSTEMS WITH CROSSOVER CIRCUITS. Seyfried, P.; Deike, S. (Physikalisch-Technische Bundesanstalt, Brunswick). Nucl. Instrum. Methods, 39: 313-20(Jan. 11, 1966). (In German).

A pulse generator was developed for quick and accurate adjusting and testing of coincidence systems with crossover circuits. It has two separate outputs, which deliver exponentially rising and falling pulses. By means of a modulation circuit the amplitudes may be changed periodically and linearly over a range of 10:1. The modulating signals of the two channels are opposite in sign. Therefore the amplitude is increasing in time in one channel and decreasing in the other one. The output signals are generated either simultaneously, with a delay of less than 1 ns with regard to a trigger pulse, or with a fixed delay of 100 ns in channel I and a continuously adjustable or automatically changing delay from 0 to 200 ns in channel II. A voltage proportional to this delay is derived. In connection with an oscilloscope a very sensitive adjustment of cross-over circuits can be made by looking for minimum time-jitter of the output pulses. Using a ratemeter and x-y recorder a plot of coincidence counting rate vs delay is obtained. (auth)

13045 RADIOACTIVE SOURCE MANOMETER. Boiziau, C. Vide, No. 116, 100-8(Mar.-Apr. 1965). (In French).

The Applied Physics Service of the Saclay Nuclear Studies Centre (French Atomic Energy Authority) has designed and built a manometer with a radioactive source, known as the "Pluton." As radioactive source, this instrument employs plutonium-240. It enables linear and continuous measurements to be made with a single measuring head. It is safer than manometers with radium radioactive sources and can be used on a ultra-vacuum system. All parts are metal, and can be heated up to 300°C. (auth)

13046 HIGH-SENSITIVITY HELIUM MAGNETOMETER FOR USE AT LOW TEMPERATURES. Doll, R.; Graf, P. (Bayerische Akademie der Wissenschaften, Herrsching, Ger.). Z. Angew. Phys., 20: 97-102(Dec. 1965). (In German).

A metastable helium magnetometer for use at low temperatures is described. The device measures magnetic fields from 10 to 100 Oe with equal accuracy of 5×10^{-6} Oe in the whole temperature range from 300°K to 1.5°K and may be used in holes with a diameter of 15 mm and a depth of 800 mm. The additional field produced by the sensing head is less than 0.5 m Oe. (auth)

13047 AN ION CONVERTER DETECTOR WITH GATE CONNECTIONS FOR MASS SPECTROMETRIC INVESTIGATIONS. Herold, D.; Schoenheit, E. (Freie Univ., Berlin). Z. Angew. Phys., 20: 102-12(Dec. 1965). (In German).

After a survey of the known ion converters and their applications, a detector arrangement for positive ions is described which is mainly meant for the integrating measurement of ion currents appearing in photoionization. A simple electric changeover makes possible the measurement of larger ion currents by the collector method and thus the calibration of the detector by determining the relative secondary emission factors. The ions are postaccelerated to 25 kev and strike oblique a copper-beryllium target. Mass discrimination is slight at this energy. The fluorescent screen consists of ZnS(Ag) or $CaWO_4$. In connection with a photomultiplier of the type RCA 931 A a gain (anode current/ion current) of 10^9 is obtained. The detector behaves linearly for a range of at least six orders of magnitude. To reduce noise the electron multiplier can be gated in the case of pulsing ion currents. The mean fluctuations of the zero current are about 4×10^{-21} amp, relating to the ion current, the time constant being 1 second, the repetition frequency 40 c/sec and the mark-to-space ratio at the optimum value. Under normal conditions (open multiplier) the stability of zero is of the order of 3×10^{-20} amp. Thus extreme small ion currents can be measured with an accuracy limited only by statistical fluctuations. (auth)

13048 SWITCHING CHARACTERISTICS OF SMALL GEOMETRY THIN FILM SUPERCONDUCTORS. Slay, B. G.; Pritchard, J. P. Jr.; Pierce, J. T. (Texas Instruments Inc., Dallas). 17p. (CONF-650953-1). ORINS.

From Technical Conference on Materials Science and Technology in Integrated Electronics, San Francisco.

A short discussion is given of the cryotron as a superconducting switch. The parameters of interest such as gain, critical gate current, critical control current, and critical surface current density are described. The photomask-photoresist process makes possible the study of much narrower dimensioned cryotrons than previously possible using mask stencils. Data are given for the above parameters as a function of width, thickness, temperature and crossing ratio. Photographs of the various circuits used are shown. The techniques involved in making connection to the circuits and the precautions taken to avoid side effects in the measurements are discussed. In particular data are given for critical currents of superconducting lines down to 2×10^{-4} inches. A rise in critical surface current density is observed for the smaller lines in both lead and tin. A discussion of the impact of these measurements in the design of future cryotron circuitry is given. In addition to the improvement in device density achieved by simple

scale reduction, additional gains in density may result through improved device form factor. (auth)

13049 RADIOMETRIC DETERMINATION OF THE SPATIAL CONCENTRATION OF INHOMOGENEOUS FLUID IN PIPE LINES. Jurkiewicz, L. (Inst. for Nuclear Research, Krakow); Korbel, K.; Przewlocki, K.; Umiastowski, K. Vienna, International Atomic Energy Agency, 1965, Preprint No. SM-68/49, 21p. (CONF-651023-32). ORINS.

From Symposium on Radioisotope Instruments in Industry and Geophysics, Warsaw.

One of the most important parameters of the flow of non-homogeneous fluids is a spatial concentration distribution in a cross-section of the pipeline. It represents the resultant of all forces appearing by the flow, acting on a solid component. This parameter has not been measured up to now, due to the lack of an appropriate measuring method. Existing suggestions about the distribution of concentration as a function of the depth in the rill can be applied only when concentration is small. They tell nothing however about the physical phenomena describing the hydrotransportation on an industrial scale, when the concentration is high. The method of measurement of the distribution of concentration presented assumes that the mean density of a hydromixture can be maintained constant for a time interval of several minutes, and that in this time a quasi-static distribution of concentration occurs inside a pipeline. The method itself is based on the passage of a narrow beam of ^{60}Co-gamma rays through the pipeline using a special instrument to perform spiral scanning in a certain cross section of a pipeline. This way the information about the distribution of material concentration is gathered. One run takes about two minutes. In the same time, on the inlet of the pipeline, the stability of the ratio of solids to fluid is controlled by means of the radioisotope density gauge. From the recorder tape, on which the results of measurements are registered automatically, the mean density across the chosen (40) chords can be determined. The method of interpretation is based on the assumption that the distribution of concentration can be approximated by the polynomial of a four degree $q(x,y) = f(x,y)$. Having the value of the mean density for 40 chords it is possible to find the coefficients of a polynomial and determine the density or concentration distribution for the whole cross section. Using the described method the measurement of the distribution of concentration on a horizontal section of a mining filling-up pipeline was done. Sand was the solid component, water was used as the fluid, in the hydromixture investigated. The experimental data given in the paper show that in actual mining practice the filling of pipelines produces a non-homogeneous concentration distribution which depends on the density and flow velocity of the fluidized solids. Examples of the distributions are given. (auth)

13050 RADIOISOTOPE X-RAY BACKSCATTER GAGE FOR SYNTHETIC FIBRE THICKNESS MEASUREMENT. Berry, P. F.; Tolmie, R. W. (Atomic Energy of Canada Ltd., Ottawa). Vienna, International Atomic Energy Agency, 1965, Preprint No. SM-68/47, 26p. (CONF-651023-22). ORINS.

From Symposium on Radioisotope Instruments in Industry and Geophysics, Warsaw.

An instrument for measuring the thickness of synthetic fibre bundles is described. The technique used is that of backscattering low energy x or γ radiation from a short length of fibre and measuring the intensity of the backscattered radiation. (auth)

13051 ION SOURCE FOR USE IN A MASS SPECTROMETER. Kazato, Kenji (to Japan Electron Optics Lab. Co., Ltd.). Japanese Patent 1964-28699. Dec. 11, 1964. Filed Mar. 26, 1962.

An improved ion source is provided for use in a mass spectrometer and can be inclined, as required, to the axis of the spectrometer. The ion required is produced by the ionization by a spark discharge. By inclination of the source, the most intense beam produced by the source is detected to increase the efficiency of the spectrometer and to reduce the measuring time. (TCO)

13052 VANADIUM WINDOW FOR AN ATOMIC PARTICLE AND RADIATION EMITTING DEVICE. Hueschen, Robert E. (to General Electric Co.). U. S. Patent 3,222,558. Dec. 7, 1965. Filed May 22, 1961.

An electron discharge device comprises an evacuated chamber terminating in a lateral flange that is integrally formed with the chamber and that defines an oblong opening to be transversed by high speed electrons. A window assembly including an electron permeable V foil is arranged transverse to the direction of electron flight across the opening. The outside edge of a first oblong ring is welded directly to the oblong opening. The V foil is engaged between second and third rings with the second bearing on the first ring. All of the rings and foil are brazed together as a unit with either Ag or Cu or their alloys as brazing metal. (B.L.M.)

13053 MASS SPECTROMETER WITH PARTICULAR ION SOURCE FOR ANALYSIS OF SOLID BODIES. Haenlein, Walter; Guenther, Karl-Georg (to Siemens-Schuckertwerke Aktiengesellschaft). U. S. Patent 3,223,836. Dec. 14, 1965. Priority date Apr. 29, 1961, Germany.

A mass spectrometer with a novel ion source is described for the analysis of "solid bodies," substances such as glasses, ceramics, and alloys, by subjecting the material under investigation to cathode sputtering, ionization, and analysis in the spectrometer proper. The electron collision ion source comprises a cathode structure having an extraction channel through which the ions may pass into the space where they are utilized and anode means coaxially disposed with respect to the extraction channel. The cathode structure includes electric-field concentrating means having its maximum field density near the extraction channel at the anode side. A hollow rod cathode extends toward the extraction channel, and magnetic means are provided that have a magnetic pole end at the same location. Thus, the magnetic and electric fields spatially and temporarily fix the discharge plasma near the extraction channel. The material under investigation is disposed in the hollow rod cathode and is released at that end of the cathode that is directed toward the analyzer part of the apparatus. (B.L.M.)

13054 METHOD AND APPARATUS FOR MEASURING THE PROPERTY OF A MAGNETIZABLE WORKPIECE USING NUCLEAR RADIATION. Varner, Donald E. (to Industrial Nucleonics Corp.). U. S. Patent 3,223,840. Dec. 14, 1965. Filed Apr. 27, 1961.

A method and apparatus are described for continuously, non-contactingly, and non-destructively testing the hardness of a fast-traveling metallic workpiece using a penetrative radiation reflection technique. The workpiece is guided along a fixed path with a nuclear radiation reflection gage mounted alongside the path for continuously measuring the hardness of the material. A source of nuclear energy is mounted in the gage and has an energy characteristic such that the material presents an infinite absorber to the radiation. The reflected radiation returned backwardly from the surface is detected to provide an electrical signal proportional to the intensity of the reflected radiation and, an indicator calibrated in hardness units registers the hardness of the material response of the electrical signal. Provision is made alongside the path and upstream of the gage for continuously demagnetizing the material before it passes the gage. (B.L.M.)

Radiation Detection

Refer also to abstracts 12899, 12978, 13001, 13006, 13163, 13367, 13713, 13714, 13805, and 14012.

13055 (AD-626998) CALCULATED RESPONSE OF AIR-WALL DOSIMETERS OR GEIGER-MUELLER TUBES TO MONOENERGETIC PHOTONS BETWEEN 1 AND 10 Mev. Redmond, A. (Naval Radiological Defense Lab., San Francisco, Calif.). Dec. 13, 1965. 24p. (USNRDL-TR-944). CFSTI $1.00 cy, $0.50 mn.

The question of registering dose from weapon and reactor photons of 2 to 10 Mev energy has led to a study of the capability of conventional dosimeters and Geiger-Mueller tubes to respond accurately to these energies. Calculations of the response of thin and thick air-wall dosimeters have been made. The results are given as "efficiencies", or the ratio of the chamber response in charge per cubic centimeter in the dosimeter per incident photon fluence, to the same quantity in an ideal air-wall chamber in electronic equilibrium. Stated in this way the results do not specifically refer to any type of chamber, but rather to interactions which result from normally incident photons. A very broad beam including scattered photons or an isotropic photon flux should give results approximately proportional to those computed. The cases are analyzed of $\frac{1}{16}$-in. and $\frac{1}{8}$-in. air-wall dosimeters under bombardment with these high energy photons, and also under bombardment with these photons plus the electron flux density coming from an air absorber of sufficient thickness to ensure primary to secondary radiation equilibrium. Finally dosimeters of two different wall thicknesses, 2.5 and 5 grams/cm^2, are studied, the latter of which can reach primary-to-secondary equilibrium under 10 Mev photons (and, of course, under all lower energies). The attenuation of the primary flux density is relatively small even at the larger thickness. The results given in tables and graphs show that the thin wall dosimeters will give a distorted indication of dose at higher energies. The chamber with 5 grams per square centimeter wall responds in constant ratio to the response of the ideal air wall chamber for photons from 1 to 10 Mev and can therefore be used under all conditions for a register of dose. (auth)

13056 (AD-627000) CHARACTERISTICS OF ^{40}K DISTRIBUTED SOURCES IN WATER. Wesley, E. J.; Nyberg, R. A. (Naval Radiological Defense Lab., San Francisco, Calif.). Nov. 23, 1965. 19p. (USNRDL-TR-937). CFSTI $1.00 cy, $0.50 mn.

Measurements on ^{40}K gamma rays from a distributed source in water are reported. The data are presented in terms of the pulse height spectra and count rates observed as the size of the source was increased from a small pool surrounding the detector to an "infinite" distributed source and then the infinite source was viewed through increasing thicknesses of water. This work was accomplished by using solutions of a potassium salt in graduated spherical balloons which encompassed the detector and were themselves completely surrounded by fresh water. The predominantly low-energy pulse height spectra observed from sources in water were obtained using large crystal detectors. A count rate build-up factor was calculated for the increasing thickness of absorber and compared to calculated values for dose-rate build-up factors at the same primary energy. (auth)

13057 (AD-627567) DOSE RATE AND SPECTRAL MEASUREMENTS FROM PULSED X-RAY GENERATORS. Tochilin, E.; Goldstein, N. (Naval Radiological Defense Lab., San Francisco, Calif.). Dec. 3, 1965. 28p. (DASA-1703; USNRDL-TR-939).

Typical x-ray spectra from high intensity pulsed x-ray sources were determined by means of an equivalent constant voltage accelerator. The photon energy spectrum for the forward x-ray beam was measured with various x-ray target thicknesses at accelerator voltages of 1.0, 1.5, and 2.0 Mv. Spectra were also obtained from a reflection x-ray target at angles of 7 and 45° with respect to the x-ray beam at applied potentials of 0.55, 1.0, and 2.0 Mv. The dose rate dependence of thermoluminescent LiF, silver-activated phosphate glass, and dosimetry film was investigated over a range of dose rates extending from 10^4 to 10^{11} rad/sec with three separate flash x-ray systems. (auth)

13058 (AD-627930) GERMANIUM (LITHIUM) DETECTOR FABRICATION. Mathiesen, J. M.; Hurley, J. P. (Naval Radiological Defense Lab., San Francisco, Calif.). Dec. 9, 1965. 29p. (USNRDL-TR-949). CFSTI $2.00 cy, $0.50 mn.

The techniques used in the fabrication of lithium-drifted germanium detectors at NRDL are described. Some examples of gamma pulse-height spectra were recorded with one of the detectors are included. (D.C.W.)

13059 (AEEW-R-411) AN EXPERIMENTAL SYSTEM FOR THERMOLUMINESCENT DOSIMETRY. Perry, K. E. G.; George, E. (Atomic Energy Establishment, Winfrith (England)). Aug. 1965. 23p. Dep. BIS $1.40. HMSO 7s.

A thermoluminescent dosimeter reader was developed for experimental investigations on the use of lithium fluoride for "finger tip" dosimetry. The design of the reader is based on the maximum use of standard electronic units in the A.E.R.E. Type 2000 series but some new unit development was necessary. The reader gives improved experimental facilities over present commercially available designs. The technique for "finger-tip" dosimetry is described and the initial experimental results are given. (auth)

13060 (CEA-R-2891) DOSIMETRIE DES NEUTRONS AU MOYEN DE COMPTEURS PROPORTIONNELS A PAROI EQUIVALENTE AUX TISSUS [Theses]. (Neutron Dosimetry by Means of Proportional Counters with Tissue-Equivalent Walls [Thesis]). de Kerviler, Herve (Commissariat a l'Energie Atomique, Saclay (France). Centre d'Etudes Nucleaires). 1965. 68p. Dep. mn.

Submitted to Paris Univ., Orsay (France). Faculte des Sciences.

Calculational methods for neutron dosimetry are briefly reviewed. Various proportional counters were tested with tissue equivalent materials. The multiplication factor and neutron energy response of these counters were investigated and compared with those obtained with ethylene lined polyethylene counters. The conditions for using such counters for neutron dosimetry in the energy range 10^{-2} to 15 Mev are outlined. (M.O.W.)

13061 (IDO-17134) COMPILATION OF RESOLUTIONS AND INTENSITIES OF SLOW NEUTRON, INELASTIC SCATTERING, TIME-OF-FLIGHT INSTRUMENTS. Brugger, R. M.; Harker, Y. D. (Phillips Petroleum Co., Idaho Falls, Idaho. Atomic Energy Div.). Jan. 1966. Contract AT(10-1)-205. 45p. Dep. mn. CFSTI $2.00 cy, $0.50 mn.

A compilation of the intensities and resolutions of slow-neutron time-of-flight instruments is presented. The data for the various instruments are compared. (D.C.W.)

13062 (IEA-96) ETUDE DES CASCADES GAMMA-GAMMA DANS LA DESINTEGRATION DU NOYAU COMPOSE, FORME PAR CAPTURE NEUTRONIQUE, A L'AIDE D'UN CIRCUIT DE HOOGENBOOM. (Study of Gamma-Gamma Cascades in Disintegration of Compound Nuclei Formed by Neutron Capture, With the Aid of a Hoogenboom Circuit). de Abreu, Manoel Americo Nogueira (Instituto de Energia Atomica, Sao Paulo (Brazil)). June 1965. 28p. Dep. mn.

The method proposed by Hoogenboom for studying gamma-gamma cascades in the excited nucleus disintegration is to subject the pulse height analysis of the gamma detector to two conditions: the coincidence with a pulse from another gamma detector and the addition of these two pulse heights corresponding to the full cascade energy. Theoretically this is possible only when the two pulses result from the full energy absorption of the cascade photons. A study of the method, its possibilities, and its applications is presented with an analysis of the gamma-gamma cascade from the ^{200}Hg formed from neutron capture. (auth)

13063 (JAERI-1092) CHARACTERISTICS OF A GAMMA-BLOCK STILBENE DETECTOR. Okano, Kotoyuki (Japan Atomic Energy Research Inst., Tokyo). June 1965. 12p. (In Japanese). Dep. mn.

A fast neutron detector of a gamma suppressed type was constructed, using a stilbene crystal 2" in diameter and 2" thick. The pulse-shape discrimination circuit used for the gamma suppression is similar to that of Daehnick and

Sherr. Minor modifications and changes were done to the circuit parameters in order to improve the discrimination characteristics. The performance characteristics such as gamma-rejection ratio and recoil-proton counting efficiency at the low-energy side were tested by using gamma sources, a RaD–Be neutron source, and the neutrons from the T–p, D–d and T–d reactions. The response of the discrimination circuit to the high-energy gamma rays was also tested by using the 6.14 and 17.6-Mev gamma rays from the $^{19}F(p,\alpha\gamma)^{16}O$ and $^{7}Li(p,\gamma)^{8}Be$ reactions, respectively. It is found that the lowest energy of recoil-protons which can be detected with almost 100% efficiency is about 0.6 Mev if the gamma-rejection ratio is maintained at 1000 : 1 and gamma rays with energies higher than several Mev are not present. If gamma rays of about 10- to 20-Mev energy are present, the characteristics at the low-energy side have to be sacrificed to suppress the high energy gamma rays, and the lowest energy of recoil protons which can be detected with almost 100% efficiency is 1 to 1.5 Mev. Examples of neutron spectra measured by using the gamma-block detector are illustrated. The neutron groups from (d,n) and (^{3}He,n) reactions leading to the low-lying levels of residual nuclei are clearly resolved and discriminated from large gamma backgrounds. (auth)

13064 (JINR-E-2494) MAGNETIC BETA-SPECTROMETER WITH TWO-FOLD FOCUSING AT THE ANGLE $\pi\sqrt{2}$. Adam, I.; Chumin, V. G.; Denisov, Yu. N.; Finger, M.; Gromov, K. Ya.; Kuznetsova, M. Ya.; Lu, Si-ting (Joint Inst. for Nuclear Research, Dubna (USSR). Lab. of Nuclear Problems). 1965. 15p. Dep. mn.

A betaspectrometer with two-fold double focusing at the angle $\pi\sqrt{2}$ is considered. The resolving power of the spectrometer is 0.21% when a 1×15 mm^2 source and a solid angle of about 0.1% of 4π is being used. The equilibrium orbit radius is 140 mm. The accidental coincidence background of three counters (the value of the magnetic field corresponds to the focusing of 4 Mev electrons) is smaller than 1 pulse per 15 hours for a ^{166}Tm source of about one millicurie. The proton resonance with running water method for measuring the magnetic fields is used, which allows to determine the energy of the conversion electrons to an accuracy better than 0.08%. All the processes on the betaspectrometer except the measurement of the magnetic field are automatized. (auth)

13065 (JUL-295-NP) EIN HOCHAUFLOESENDES SPEKTROMETER FUER SEHR LANGSAME NEUTRONEN ZUR VERWENDUNG AN DER KALTEN QUELLE EINES HOECHSTFLUSSREAKTORS. (A High-Resolution Spectrometer for Very Slow Neutrons for Use on Cold Sources of a Very High Flux Reactor). Scherm, R. (Kernforschungsanlage, Juelich (West Germany). Institut fuer Neutronenphysik). Aug. 1965. 24p. Dep. mn.

A spectrometer designed for neutrons with wavelengths of 4 to 25 Å is described. The energy resolution of the spectrometer is between 0.4 and 5.0%. (D.C.W.)

13066 (JUL-298-PC) VERGLEICHENDE UNTERSUCHUNGEN UEBER ZAEHLMETHODEN ZUR ABSOLUTBESTIMMUNG DER AKTIVITAET VON ALPHA-STRAHLERN. (Comparative Investigations on Counting Methods for the Absolute Determination of the Activity of Alpha Emitters). Ihle, H.; Karayannis, M.; Murrenhoff, A. (Kernforschungsanlage, Juelich (West Germany). Institut fuer Physikalische Chemie). Sept. 1965. 70p. Dep.mn.

In order to improve the accuracy in absolute counting of alpha emitters, a comparative investigation was made of 4π counting with liquid scintillators and with proportional counters. The sources of errors in these methods were studied, and conditions were found under which the results obtained by the two methods agree within a few tenths of a percent. A device for nondestructive testing of the electric conductivity of thin foils used on 4π source carriers is described. (D.C.W.)

13067 (JUL-308-RB) GAMMA-SPEKTROMETRIE MIT HALBLEITERDETEKTOREN. (Gamma Spectrometry With Semiconductor Detectors). Riepe, G.; Petri, H. (Kernforschungsanlage, Juelich (West Germany). Institut fuer Reaktorbauelemente). Oct. 1965. 16p. Dep. mn.

Two semiconductor counters, Ge(Li) and Si(Li), prepared by the Li-drift method, were compared with an NaI(Tl) scintillation counter in a multichannel spectrometer. The results showed that the Ge(Li) counter is superior to the NaI scintillation counter with respect to resolution, but the reverse is true with respect to the γ yield. The rise-time constant for the pulse in the Ge(Li) counter is about 30 nsec, almost 10 times smaller than in a NaI scintillation counter. (J.S.R.)

13068 (MLM-1263) DETERMINATION OF COINCIDENCE CORRECTIONS IN A PROPORTIONAL COUNTER. III. LEAST SQUARES ANALYSIS BY THE VARIATIONAL AND GENERAL METHODS. Kirby, H. W.; Braun, J. Z. (Mound Lab., Miamisburg, Ohio). Sept. 15, 1965. Contract AT(33-1)-Gen-53. 31p. Dep. mn. CFSTI $2.00 cy, $0.50 mn.

The half life of a short-lived radioisotope and the resolution time of a counting system can be simultaneously determined by either of two adaptations of the method of least squares. In the variational method, the equations are first linearized by assuming exact values for either of the two constants sought and then finding the pair of values which minimize the sums of the squares of the weighted residuals. In the general method, standard techniques are applied to determining the three constants of a non-linear equation. Both methods yield the same results. It is found that both the variational and the general methods yield more realistic estimates of the uncertainties in the half life and the resolution time than do the customary methods of computation. The FORTRAN programs used in making these computations are included. (auth)

13069 (NASA-CR-54468) ANALYTICAL STUDY OF THE FEASIBILITY OF A PNEUMATIC NEUTRON FLUX DETECTOR. Final Report. (Bendix Corp., Southfield, Mich. Research Labs. Div.). May 1965. Contract NAS3-6207. 110p. (BRLD-2933).

An analytical study to determine the feasibility of developing a pneumatic neutron flux detector was conducted. The concept examined consisted of an electrofluidynamic pump for converting thermal neutron flux to a pneumatic pressure signal which is amplified by a logarithmic vortex amplifier. At least five decades of neutron flux from 10^7 to 10^{12} neutrons/cm^2-sec can be detected. Response times (95 percent final value) approaching 0.06 sec can be achieved. Quantitative definition of accuracy requires additional experimental evaluation. Methods of gamma compensation, sensitivity to temperature changes, and capability of meeting operational modes were also considered in this feasibility analysis. A conceptual design of a feasible neutron flux detector is provided. (auth)

13070 (RCN-40) REVIEW OF ACTIVATION METHODS FOR THE DETERMINATION OF INTERMEDIATE NEUTRON SPECTRA. Zijp, W. L. (Reactor Centrum Nederland, Petten). Oct. 12, 1965. 107p. Dep. mn.

A review is given of the possibilities for determining flux densities, fluences, and spectra of intermediate neutrons from the counting results obtained with resonance detectors. After introductory sections in which several basic concepts and formalisms are mentioned, some resonance reactions of interest are considered. Following chapters are devoted to the concepts of cadmium ratio and cadmium cut-off, to the resonance integral concept and to the self-shielding effect. Procedures for determining intermediate flux densities are discussed for the case of a 1/E spectrum and for an unknown spectrum. Tables with nuclear data and an extensive bibliography are included. (auth)

13071 (RHEL/R-111) THE JOKING SYSTEM: JOINT KINEMATICAL AND GEOMETRICAL ANALYSIS OF BUBBLE CHAMBER EVENTS. Sedman, E. C. (National Inst. for Research in Nuclear Science, Chilton (England). Rutherford High Energy Lab.). Aug. 1965. 42p. Dep. mn.

The special features of the JOKING system for the analysis (geometry and kinematics) of bubble chamber events are described. (D.C.W.)

13072 (RT/EL(65)7) RIVELATORI A SEMICONDUTTORE DEL TIPO A BARRIERA SUPERFICIALE. (Semiconductor Detectors of the Surface Barrier Type). Coiante, D.; Michalowicz, J.; Parisi Presicce, L.; Spoglia, U. (Comitato Nazionale per l'Energia Nucleare, Rome (Italy)). Sept. 1965. 17p. Dep. mn.

A method of making semiconductor surface barrier particle detectors and their epoxy resin encapsulation is described. The electrical and radiation testing results of devices are presented. (auth)

13073 (SAN-549-1) RESEARCH AND DEVELOPMENT ON SINGLE-CRYSTAL HIGH RESISTIVITY CADMIUM TELLURIDE FOR USE AS A GAMMA RAY SPECTROMETER. Annual Report. Baily, N. A. (Hughes Research Labs., Malibu, Calif.). June 1965. Contract AT(04-3)-549. 43p. Dep. mn. CFSTI $2.00 cy, $0.50 mn.

Methods of preparing single crystals of CdTe were studied, as well as the properties of such crystals. Methods of preparing CdTe junctions were also investigated, and the characteristics of several diodes were measured. The response of the diodes to radiation was also studied. (D.C.W.)

13074 (SRRC-11/65) A SHADOW-SHIELDED WHOLE-BODY COUNTER OF HIGH SENSITIVITY. Boddy, Keith (Scottish Research Reactor Centre, East Kilbride (Scotland)). [1964]. 12p. Dep. mn.

Preliminary shielding studies were undertaken to find a suitable "lightweight" shield and a prototype shadow-shielded whole-body counter was constructed from materials and equipment originally acquired for other purposes. The detector is a 3- × 3-in. sodium iodide crystal located in a central shield. Scanning-bed geometry is used in which the subject passes beneath the detector. An estimate of the counter's sensitivity for isotopes of medical interest, was obtained using a crude phantom containing water and appropriate radioisotopes. Natural body levels of ^{40}K and ^{137}Cs can be detected and this information and that from a similar counter operated by Hanford Laboratories were used to predict the performance of the proposed mobile counter. The advantages of the "shadow-shield" and "mobile" concepts are outlined and the future plans for the prototype and mobile counters are briefly discussed. (M.O.W.)

13075 (UJV-1450/65) A TIME SELECTOR FOR TWO-DIMENSIONAL ANALYSIS. Kosina, Zdenek (Ustav Jaderneho Vyzkumu, Ceskoslovenska Akademie Ved, Rez). 1965. 14p. Dep. mn.

Auxiliary equipment is described which was built in the Fast-chopper laboratory of the UJV for use with the 2048 channel time-of-flight analyzer to measure gamma spectra from resonance-neutron capture in eight selected neutron energy intervals simultaneously. The position and width of the corresponding time channels may be chosen independently and entirely arbitrarily in steps of 1 us or 2 us within range of 2048 or 4096 us respectively. The same equipment also provides possibility of common time-of-flight measurements, realized by means of the same "time scale." (auth)

13076 (UR-875-117) CHARGED PARTICLE COUNTING SYSTEM, WITH PARTICLE SEPARATION BY dE/dx MEASUREMENT. Bahnsen, A.; West, R. W. (Rochester Univ., N. Y. Dept. of Physics and Astronomy). Jan. 1, 1966. Contract AT(30-1)-875. 18p. Dep. mn. CFSTI $1.00 cy, $0.50 mn.

A counter and electronic system designed for the purpose of identifying charged particles is described. It consists of a proportional dE/dx counter-solid state E counter telescope, a pulse multiplier and additional electronics to store the energy spectra of protons and deuterons in separate parts of a 400-channel analyzer. This system was used in an investigation of the $^{12}C(d,p)$ reaction near 4 Mev. The discussion is concerned with the problem of identifying protons and deuterons. But with minor changes, the system is applicable to other particles. The design and performance of the particle detector and the electronics system are considered, and the data reduction is also discussed. (J.F.P.)

13077 (Y-1503) HIGH-VOLUME, AIR-MONITOR CALIBRATION FACILITY. Sanders, Merwyn; McRee, P. C. (Union Carbide Corp., Oak Ridge, Tenn. Y-12 Plant). Feb. 9, 1966. Contract W-7405-eng-26. 9p. Dep. mn. CFSTI $1.00 cy, $0.50 mn.

A high-volume, air-monitor calibration facility was designed and built to accurately calibrate, simply and at a nominal cost, high-volume air samplers. The facility is described. (auth)

13078 RELATION BETWEEN THE LOWER LIMIT OF DETECTION OF A RADIOACTIVITY COUNTER AND THE TIME OF MEASUREMENT. Sterlinski, Slawomir (Inst. of Nuclear Research, Warsaw). Acta Phys. Pol., 28: 559-61(Oct. 1965).

Equations are derived for the minimum significant measured activity and the minimum detectable true activity for long-lived radioactivity as functions of the time of measurement and the background count rate. Results of a sample calculation are shown. (M.J.T.)

13079 THE ESSENTIAL SPECIFICATIONS OF THE HAMBURG 4π-LARGE VOLUME RADIOACTIVITY DETECTOR WITH LIQUID ORGANIC SCINTILLATOR. [PART] II. Heinrich, H. C.; Gabbe, E. E.; Whang, D. H. (Univ., Hamburg). Atompraxis, 11: 660-3(Nov.-Dec. 1965). (In German).

Basic considerations resulted in definitions for the amounts of radioactivity which can still be measured or detected with a large volume radioactivity detector. The still measurable lower limit of radioactivity (in nC) is measured within a counting period of 1000 seconds and with a ±10% standard error. The detectable lower limit of radioactivity is estimated with a ±33.3% standard error within a 1000 second counting time and discriminated from background with 99.9% probability. Depending on the γ-emission rate of the measured radionuclides measurable lower limits of radioactivity between 0.78 nC(^{60}Co) and 24 nC(^{51}Cr) and detectable lower limits of radioactivity between 0.23 nC (^{60}Co) and 7.2 nC(^{51}Cr) are characteristic specifications for the Hamburg 4π-large volume radioactivity detector with liquid organic scintillator. (auth)

13080 IMPROVEMENT IN THE DIRECT MEASUREMENT OF β-ACTIVITY IN LIQUID SCINTILLATION COUNTERS BY ADDITION OF A FLUORESCENT SUBSTANCE. Haberer, K.; Koelle, W. (Technische Hochschule, Karlsruhe, Ger.). Atompraxis, 11: 664-5(Nov.-Dec. 1965). (In German).

Direct measurement of β activity in liquid scintillation counters with the aid of the Cherenkov effect is possible only with a low degree of efficiency, if the β radiation energy is slight. Counting results can be considerably improved, especially for low-energy β sources, if a water-soluble fluorescent substance (sodium α-naphthylamine sulfonate) is added to the aqueous solution of the nuclide to be measured. The optimal concentration of the fluorescent substance was found to be between 10^{-1} and 10^{-2} mol per l of measurement solution. The procedure described makes possible a considerable extension of the direct measurement of β activity in aqueous solutions. (auth)

13081 DEVICE FOR THE DETECTION OF NEUTRONS AT ENERGIES UP TO 50 Mev. Costa, S.; Ferrero, F. Atti Accad. Sci. Torino: I. Cl. Sci. Fis., Mat. Natur., 99: 1103-9(1964-65). (In Italian).

A neutron detector is described whose efficiency remains almost constant in the interval from 1 to 50 Mev. The practical utilization of the device was illustrated in a study of the photoneutron emission of ^{6}Li. (tr-auth)

13082 PARTICIPATION OF AN EXCITONIC MECHANISM IN THE FORMATION OF THE LATENT IMAGE IN

AN IONOGRAPHIC EMULSION. Lory, Jacqueline (Lab. de Physique-Enseignement, Paris). Compt. Rend., 261: 5435-7(Dec. 20, 1965). (In French).

The value of the probability of the creation of an exciton by a charged particle in an ionographic emulsion to take into consideration the energy loss of the particle due to the formation of excitons. The study of the interactions of excitons with phonons and crystal imperfections leads to a mechanism of energy transport across this crystal by the formation and decomposition of excitons. (tr-auth)

13083 AFTER-PULSES OF THE GM COUNTER DEPENDENT UPON THE INTENSITY OF NUCLEAR RADIATION. Narita, Yuichi (Akita Univ., Japan); Narita, Masakuni; Ozawa, Yasutomo. Denki Gakkai Zasshi, 85: 1063-9(June 1965). (In Japanese).

The occurrence of pseudopulses dependent on radiation intensity was found in the measurement of high intensity nuclear radiation by a GM counter. This pseudopulse was induced from external stimulations and was designated as after-pulse. Occurrence of after-pulses of various GM counters and their dependence on the intensity of radiation were investigated. Different GM tubes filled with alcohol or halogenated gases were tested. The occurrence of after-pulses increased with the increase of radiation intensity and tube voltage, and was found to be proportional to $(\log I)^n$ of the radiation intensity and to m power of tube voltage, that is: $N_s = k(\log I)^n$ and $N_s = V^m$, where N_s = occurrence of after-pulses, I = intensity of radiation, N = a parameter depending on characteristics of different tubes (this value is about 1), k = coefficient determined for each tube, and V = tube voltage. The value of m is ~1. The occurrence of after-pulses in alcohol-quenched GM counters was found to be much higher than in halogen-quenched counters. (BBB)

13084 LASER-STIMULATED NUCLEATION IN A BUBBLE CHAMBER. Stamberg, R. C.; Gillespie, D. E. (Univ. of Michigan, Ann Arbor). J. Appl. Phys., 37: 459-61(Jan. 1966).

A 6-in. bubble chamber containing $CBrF_3$ at 30.7°C was found to be sensitive to nucleation stimulated by a pulsed ruby laser with output at 6943 Å. The chamber was more sensitive to laser-stimulated than gamma-stimulated nucleation, with the nucleation threshold for the laser beam below 0.2 mJ/cm^2. The nucleation was shown to be due to deposition of part of the energy of the laser beam onto small dust particles floating randomly in the freon; bubbles then formed in the freon surrounding the hot particles. (M.J.T.)

13085 ABSOLUTE DOSE RATE MEASUREMENTS OF VERY SOFT AND WEAK X RAYS BY MEANS OF A GM COUNTER. Hayashi, Miyoko; Hayashi, Satori (Osaka Public Health Inst.). J. Radiat. Res. (Jap.), 5: 172-82 (Sept.-Dec. 1964).

In order to determine the dose rate of x-rays having energies below 35 kev, a method was investigated in which counting rates determined with a GM-counter were converted to dose rate. A radiation field with near background intensity can be measured by this method. Conversion coefficients from counting rate to dose rate were calculated as a function of photon energy for some GM-tubes available in Japan. The characteristics of the conversion coefficient were examined and the nature of GM-tubes favorable for monitoring was discussed. By the proposed method a continuous x-ray field can be measured with a satisfactory accuracy and a precision of about 5%. The method can be applied to the determination of absorbed dose rate as well as exposure dose rate. (auth)

13086 CONTINUOUS RECORDING OF SPECTRA WITH A DRg-140 RECORDING INSTRUMENT AND A NZG-319 SINGLE-CRYSTAL GAMMA-II SCINTILLATION SPECTROMETER USING A NUG-216 HLASICA LEVEL OF RADIOACTIVITY. Banas, Julius; Zaduban, Milan (Inst. of Experimental Biology, Slovak Academy of Sciences, Kosice). Jad. Energ., 11: 428-9(Nov. 1965). (In Czech).

An instrument is described, which is simple, sufficiently sensitive, and can follow with great precision the course of the spectrum of a measured radiation source. Any integrator can be used as the integration circuit. The possibilities of application of the instrument in the laboratory with only a small financial outlay is pointed out. (auth)

13087 FIRST ORDER THEORY OF A HIGH-DISPERSION SPECTROMETER WITH WINDING MAGNETIC FIELD. Tauscher, L.; Daniel, H.; Schmutzler, F. (Max-Planck-Institut fuer Kernphysik, Heidelberg). Nucl. Instrum. Methods, 39: 1-7(Jan. 1966). (In German).

A winding magnetic field is proposed for a high-dispersion β-ray spectrometer. The focusing properties have been investigated with a first-order perturbation theory. It is shown that winding fields at focusing angles of more than 2π lead to a high dispersion. (auth)

13088 AN ASSOCIATED PARTICLE TIME OF FLIGHT SYSTEM FOR USE WITH D-D NEUTRONS. Hsu, T. H.; Robson, J. M. (Univ. of Ottawa). Nucl. Instrum. Methods, 39: 8-12(Jan. 1966).

An associated particle time of flight system is described which can be used with 2.4-Mev neutrons produced in the low energy $D(d,n)^3He$ reaction. The ^3He detector is a thin plastic scintillator and the neutrons are detected by a liquid scintillation counter provided with a neutron gamma discrimination system effective at low neutron energies. (auth)

13089 DESIGN OF A 180 deg ELECTRON SCATTERING FACILITY. Rand, R. E. (Stanford Univ., Calif.). Nucl. Instrum. Methods, 39: 45-57(Jan. 1966).

The study of elastic electron scattering from nuclei, at angles near 180°, permits an examination of nuclear magnetic multipole distributions as well as the testing of certain aspects of quantum electrodynamics. Apparatus is therefore designed to enable such experiments to be performed at the Stanford Mark III linear accelerator. The special problems connected with 180° elastic scattering are discussed. In general, it is necessary to subtract from the data, contributions from ordinary charge (Coulomb) scattering. This background is mainly due to electrons which scatter at angles other than 180° and yet enter the detector because of multiple scattering in the target, finite beam spread and finite solid angle. 180° scattering is achieved by passing the incident beam through a magnetic field before it strikes the target. Backward scattered electrons then pass through a field a second time, bending away from the incident beam, and enter a spectrometer. The momentum range restrictions of the magnet optics and the optimization of the solid angle are discussed. A novel method is presented of varying the scattering angle around 180° without causing significant phase space restrictions. Practical details of the apparatus are discussed and an outline of the data reduction methods used in such experiments is presented. (auth)

13090 NEUTRON RESONANCE SCATTERING MEASUREMENTS WITH ^6Li GLASS DETECTORS. Asghar, M.; Brooks, F. D. (Atomic Energy Research Establishment, Harwell, Eng.). Nucl. Instrum. Methods, 39: 68-76(Jan. 1966). (AERE-NP/GEN/40).

A detector for the measurement of neutron elastic scattering cross section in the resonance region is described. The detector consists of five lithium-loaded glass scintillators assembled into two groups, the scintillators in the first group having a ^6Li content 46 times greater than those in the second. The response of the two groups to gamma rays is matched as closely as possible, so that when the output of the second group is subtracted from that of the first, the effective sensitivity of the system to gamma rays is close to zero. Measurements of ^{169}Tm, ^{197}Au, and ^{232}Th demonstrate that scattering cross section data accurate enough to determine resonance spins may readily be obtained. (auth)

13091 A METHOD FOR CALCULATIONS OF THE REDUCTION OF THE RESOLUTION IN A UNIFORM-FIELD MAGNETIC ANALYZER SYSTEM DUE TO INHOMOGENEITY OF THE MAGNETIC FIELD. Yagi, K. (Tokyo Univ.). Nucl. Instrum. Methods, 39: 88-92(Jan. 1966).

A formula for calculations of image broadening owing to inhomogeneity of the magnetic field is derived for an ion focusing system of a uniform-field magnetic analyzer. (auth)

13092 A 1 percent PRECISION ABSOLUTE COUNTING OF X-RAYS OF LOW ENERGY. Bambynek, W.; Lerch, O.; Spernol, A. (EURATOM, Geel, Belg.). Nucl. Instrum. Methods, 39: 104-8(Jan. 1966). (In German).

A simple medium geometry solid angle counter for precision absolute counting of x rays of low energies is described. Accuracies of less than 1% can be reached without difficulties. (auth)

13093 FABRICATION AND STUDY OF THICK BASE FREE SURFACE BARRIER DETECTORS. Meyer, O.; Langmann, H. J. (Kernforschungszentrum, Karlsruhe, Ger.). Nucl. Instrum. Methods, 39: 119-24(Jan. 1966). (In German).

Surface barrier detectors are fabricated with depletion layers up to 3 mm. Some special construction details, necessary to produce fully depleted counters, are given. Fully depleted counters used in a stack diminish the pulse rise time and stop high energy particles. A reproducible measurement of the resistivity of the bulk material is described. The best energy resolution obtained with a 2-mm-thick liquid-air-cooled counter for 1 Mev electrons was 2.1 kev. The Fano factor for electrons is found to have a value of 0.13 ± 0.02. (auth)

13094 A γ-SPECTRUM STABILIZER WITH COMPENSATION FOR THE EFFECTS OF DETECTOR TEMPERATURE VARIATION. Williams, D.; Snelling, G. F.; Pickup, J. (Atomic Energy Research Establishment, Harwell, Eng.). Nucl. Instrum. Methods, 39: 141-9(Jan. 1966). (AERE-R-4923).

A compact system of spectrum stabilization is provided, for use principally with single channel systems, and including compensation for detector temperature variations. Various methods of reference provision are discussed and the development of an appropriate type described. Details are given of the electronic control circuit and the performance of the complete system. It is shown that a stabilization ratio of approximately 500 : 1 is obtained and the effective temperature coefficient of the detector reduced by an order of magnitude, to less than ±0.05%/°C. (auth)

13095 MEASUREMENT OF HIGH-ENERGY γ-RAYS WITH Ge(Li) DETECTORS. Berg, R. E.; Kashy, E. (Michigan State Univ., East Lansing). Nucl. Instrum. Methods, 39: 169-72(Jan. 1966).

A method of measuring the energy of high-energy gamma rays is described. Parallel capacitors are used as an effective energy multiplier of a pulser signal to compare unknown high-energy gamma rays to known low-energy standards. This method has also provided an effective tool for measuring the linearity of the energy response of Ge(Li) detectors. This response is found to be linear to better than ±0.03% in the range 662 to 2614 kev and better than ±0.1% up to 6 Mev. As an example of this capacitor multiplying method the energy of the gamma ray from the 3^- excited level of ^{16}O is measured to be 6127.8 ± 1.2 kev. (auth)

13096 A STATISTICAL MODEL FOR PHOTOMULTIPLIER SINGLE-ELECTRON STATISTICS. Prescott, J. R. (Univ. of Alberta, Calgary). Nucl. Instrum. Methods, 39: 173-9(Jan. 1966).

A statistical model is proposed to describe secondary electron emission in photomultipliers, based on the Polya or "negative binomial" distribution, which contains the exponential and Poisson distributions as special cases. Computations of the single-electron spectra have been carried out for a variety of stage-gains. Limited comparisons with available experimental data confirm that the effective statistical distribution of secondary emission in photomultipliers is broader than Poissonian, and an interpretation in terms of non-uniformity of the dynodes is discussed. (auth)

13097 MODIFICATION OF THE RCL 512-CHANNEL ANALYZER FOR TIME OF FLIGHT ANALYSIS. Gaitanis, N.; Kostikas, A. (Nuclear Research Center Democritus, Athens). Nucl. Instrum. Methods, 39: 180(Jan. 1966).

An external circuit is added to the RCL 512-channel pulse-height analyzer, thus making possible the use of the pulse-height analyzer for time-of-flight analysis without requiring a time-to-pulse-height converter. (T.F.H.)

13098 GAMMA SPECTROMETER SYSTEMS EMPLOYING AN ANTI-COMPTON ANNULUS. Kantele, J.; Marttila, O. J.; Hattula, J. (Univ. of Helsinki). Nucl. Instrum. Methods, 39: 194-216(Jan. 11, 1966).

The use of an annular anti-Compton mantle of NaI(Tl) in conjunction with the following scintillation spectrometer types was investigated: direct and total absorption gamma spectrometer, anti-Compton spectrometer, summing Compton spectrometer, pair spectrometer, coincidence spectrometer employing the pair spectrometer plus an additional detector, multiple coincidence spectrometer, ordinary and sum-peak coincidence spectrometers, sum-coincidence spectrometer and a spectrometer for the detection of gammas and gamma cascades in coincidence with positrons. In these spectrometer systems, the annulus functions as the principal detector or is used for coincidence or anti-coincidence gating. Suitable electronic and geometrical arrangements, shielding, collimators and antiscattering shields are described. Most of the spectrometer combinations feature high efficiency, low background and spectra with low Compton tails. Many of the results obtained are applicable also to systems containing semiconductor radiation detectors. The advantages and limitations of the various methods are discussed and a number of further application possibilities of coincidence spectrometers employing an anti-Compton mantle are suggested. (auth)

13099 OBSERVATION OF FISSION EVENTS IN MICA SANDWICHES. Cieslak, E. (Univ. of Warsaw); Piekarz, J.; Zakrzewski, J.; Dakowski, M.; Piekarz, H.; Sowinski, M. Nucl. Instrum. Methods, 39: 224-31(Jan. 11, 1966).

A method is described for preparation of mica sandwiches that could be used in experiments to study the cross section of heavy nuclei for the high-energy fission. Mica sandwiches with natural uranium, prepared by this method, were exposed to thermal neutrons from a reactor. After appropriate chemical treatment, fission fragment tracks were observed under an optical microscope. The average efficiency of observation of fission events in such sandwiches was estimated with the help of semiconductor detectors. (auth)

13100 PERFORMANCE STUDIES OF THE PHILLIPS 56 AVP AND XP 1020 PHOTOMULTIPLIER TUBES. Dolan, K. W.; Hurley, J. P.; Mathiesen, J. M. (Naval Radiological Defense Lab., San Francisco). Nucl. Instrum. Methods, 39: 232-48(Jan. 11, 1966).

Performance characteristics were measured for the Phillips type 56 AVP and type XP 1020 photomultiplier tubes using NaI(Tl) crystals as scintillators. The measurements consisted of recording coincidence-delay curves as a function of gamma-ray energy and photomultiplier high voltage, determining the linearity of pulse height distributions as a function of gamma-ray energy and high voltage, and measuring the gamma-ray energy equivalent of noise pulse as a function of high voltage. (auth)

13101 A SIMPLE METHOD FOR THE MEASUREMENTS OF TOTAL NEUTRON CROSS SECTIONS. Roessle, E.; Tauber, M. (Johann-Wolfgang-Goethe-Univ., Frankfurt am Main). Nucl. Instrum. Methods, 39: 261-4(Jan. 11, 1966).

The ground state transition of the reaction $^{28}Si(n,\alpha)^{25}Mg$ in solid state detectors is used for recording the neutron intensities in the transmission experiments for the evaluation of neutron total cross sections. The absorber is placed between two solid state detectors and the transmission determined in a single measurement. The method is

particularly suitable in the energy range of $6 < E_n < 9$ Mev. (auth)

13102 LOW BACKGROUND BETA DETECTOR FOR SOLID SAMPLE ASSAY. Noshkin, V. E. (Woods Hole Oceanographic Institution, Mass.); De Agazio, E. Nucl. Instrum. Methods, 39: 265-70(Jan. 11, 1966). (NYO-2174-31).

The construction and performance of four side-window gas-flow counters operated in the Geiger region used in the measurement of low levels of beta activity from solid sources are described. The average background with anticoincidence for the four counters over the period August 1963–September 1964 was 0.334 ± 0.005 cpm. A detailed discussion of the associated anticoincidence circuitry is also presented. (auth)

13103 EFFICIENCY OF SECONDARY ELECTRON EMISSION MONITORS FOR 70 Mev ELECTRONS. Blankenburg, S. A.; Cobb, J. K.; Muray, J. J. (Stanford Univ., Calif.). Nucl. Instrum. Methods, 39: 303-8(Jan. 11, 1966).

The secondary electron emission coefficient from several elements in the form of thin foils was measured using 70-Mev electrons as bombarding particles. Using foils with different atomic numbers, it was found that the secondary emission coefficient per target electron in the metal is noticeably larger for light elements, especially in cases of beryllium and aluminum. This indicates that metal oxide on the foil surface (Malter effect) is playing a dominant role in the secondary emission of these metals. For other metals, the experimental results seem to indicate a relatively small variation in the secondary emission coefficient per target electron, less than that predicted by Vanhuyse and Van de Vijver, but with the same general behavior. The lack of thickness dependence in the case of tantalum foils is in agreement with the extensive experimental work of Planskoy and with the theoretical treatment of the secondary emission by Aggson. The secondary electron emission coefficients will be given for the measured foils and the experimental values will be compared with the existing theories. (auth)

13104 SYNTHESIS OF AN OPTIMUM FILTER FOR TIMING SCINTILLATION PULSES. Gatti, E. (CISE, Milan); Svelto, V. Nucl. Instrum. Methods, 39: 309-12 (Jan. 11, 1966).

An optimization problem is solved for timing scintillation pulses. An optimum linear filter is calculated as a function of the "equivalent illumination." Limit values are obtained for the time resolution which can be achieved with a given "equivalent illumination." (auth)

13105 INVESTIGATION OF A TOTAL ABSORPTION LEAD-GLASS CHERENKOV γ-SPECTROMETER IN THE ENERGY RANGE 0.25–4.0 Gev. Azimov, M. A.; Pantujev, V. S.; Khachaturyan, M. N. (Joint Inst. for Nuclear Research, Dubna, USSR). Nucl. Instrum. Methods, 39: 325-8(Jan. 11, 1966).

The possibility is studied of using lead-glass Cherenkov spectrometers of relatively small size ($18 \times 18 \times 30$ cm^3), to measure the energy of gamma quanta above 1 Bev. The spectrometer was calibrated using monoenergetic electrons of energy 0.25, 0.5, 2.0, and 4.0 Bev. Within this range the γ spectrometer has a linear dependence of Cherenkov pulse amplitude with energy and a high-energy resolution (half-width at half-maximum) of ±5% for electrons with $E_e = 4$ Bev. (auth)

13106 A PROGRAMMED SPOT AUTOMATIC SCANNING SYSTEM FOR SPARK CHAMBERS. Saulys, A.; Meyer, D. I.; Allen, R. (Univ. of Michigan, Ann Arbor). Nucl. Instrum. Methods, 39: 335-8(Jan. 11, 1966).

A relatively simple system was built for automatically scanning any rectangular array of spark chamber views on film. It was successfully used to scan an experiment with 24 views at the rate of about one frame per second. The optics, electronics, programming and the principles of operation are discussed. (auth)

13107 THE LIQUID DIELECTRIC IONIZATION CHAMBER AS A MEANS TO STUDY MIXED RADIATION FIELDS. Ladu, M.; Pelliccioni, M. (CNEN, Frascati, Italy). Nucl. Instrum. Methods, 39: 339-42(Jan. 11, 1966).

Measurements made by a dielectric liquid ionization chamber are reported. Dielectric liquids n-pentane, n-hexane, n-heptane, and iso-octane were used. In particular the response of the chamber to a mixed radiation field of γ rays and neutrons was studied. It is shown that, after previous calibration, the instrument is able to measure the contribution of the two components of the radiation field. The results of the calibration for ^{60}Co γ rays and for Po–Be neutrons are given. (auth)

13108 A CIRCUIT FOR PULSE SHAPE DISCRIMINATION. Schweimer, W. (Kernforschungszentrum, Karlsruhe, Ger.). Nucl. Instrum. Methods, 39: 343-4(Jan. 11, 1966).

A simple circuit for a NE 213 scintillator based on the Alexander and Goulding principle was used. The circuit diagram of the pulse-shape discriminator is shown and described. The regions of the energy-pulse shape plane where electron cosmic meson (μ), and proton events fall in are also shown. The electron and proton events were obtained from a Po–Be source as well as from a neutron beam. (J.F.P.)

13109 INVESTIGATION OF Gev-NEUTRON REGISTRATION EFFICIENCY BY SCINTILLATION COUNTERS. Galaktionov, Yu. V.; Landsberg, L. G.; Lyubimov, V. A. (Inst. for Theoretical and Experimental Physics, Moscow). Nucl. Instrum. Methods, 39: 351-2(Jan. 11, 1966).

The efficiency of Bev neutron registration was investigated using scintillation counters. The installation with which these measurements were performed is diagramed. Two kinds of scintillation counters were tested. In the first a plastic block was used for neutron registration. In the second three thin (15 mm) scintillation counters were used. Schemes for each kind of scintillation counter and the neutron registration efficiency for various neutron momenta are given. (J.F.P.)

13110 IMPROVED PARTICLE SEPARATION WITH PULSE-SHAPE DISCRIMINATION IN THE CASE OF A CsI(Tl) SCINTILLATOR. Mathe, Gy. (Hungarian Academy of Sciences, Debrecen). Nucl. Instrum. Methods, 39: 356-8(Jan. 11, 1966).

Signals of the photomultiplier were amplified by a NE 5259 amplifier. Thus it is possible to integrate and to differentiate them. The pulses shaped in this way were analyzed by a base-line cross-over pulse-shape discriminator. An investigation was made to find the effects of a simultaneous differentiation on the process of particle identification, based on the assumption that the differentiation compensates in part for the deterioration of deadtime. This investigation showed a considerable improvement in particle separation as a result of pulse shaping. It was found that the separation efficiency can be increased by a factor of more than two as a result of integration. It is possible to separate the alpha particles from the gamma background with a wide safety margin above 300 kev. (J.F.P.)

13111 A TECHNIQUE OF n-γ DISCRIMINATION. Fabiani, F.; Longo, G.; Saporetti, F.; Venturini, G. (CNEN, Bologna). Nuovo Cimento, (1), 3: Suppl., 187-91 (1965).

A method of neutron-gamma discrimination is described, which uses the Owen pulse-formation technique and a time-to-pulse height converter for the zero crossing time determination. The operational block diagram for pulse-shape discrimination and time-of-flight spectrometer is shown. Results are presented of measurements of relative detection efficiencies in the neutron energy range 1.0 to 3.7 Mev and for ^{60}Co and ^{137}Cs sources. (L.B.S.)

13112 RESEARCH WORK ON CLOUD CHAMBERS FILLED WITH A DIELECTRIC LIQUID. Blanc, D.; Mathieu, J.; Torres, L.; Vermande, P. Onde Elec., No. 457: 466-71(Apr. 1965). (In French).

A general summary is presented of the work performed by the Nuclear Physics Centre since 1958: residual current, characteristic curves under alpha and gamma radiation, and response to rapid neutron fluxes (3 and 14 Mev). The present research work deals with a comparison of staged curves obtained for alpha, gamma or neutron radiations: for each type of radiation, the elongation of the stages corresponding to various flux values converge in a point lying on the abscissae axis. The characteristic points of the incident rays are distributed along the x-axis in an order which would appear to be that of the relative biological efficiencies. These results make such detectors of high interest in biological analysis. (auth)

13113 MEASUREMENT OF STANDARD ION DOSES IN SOLID AND FLUID MEDIA FOR X AND γ RADIATION WITH ENERGIES BETWEEN 50 kev AND 3 Mev. II. FIRST DISCUSSION OF A GENERAL EQUATION FOR DETERMINATION OF THE STANDARD ION DOSE IN SOLID AND FLUID MEDIA WITH IONIZATION CHAMBERS. Rakow, Adalbert; Will, Wolfram (Medizinisch-Biologische Forschungszentrum, Berlin). Strahlentherapie, 129: 72-9(Jan. 1966). (In German).

To explain the deviations in the measurements of the standard ion dose (exposure) in solid and liquid media obtained with different ionization chambers calibrated free in air, the chamber factor which gives the standard ion dose by multiplying this value with the dosimeter value, is divided into several factors. The different behavior of these factors in air and in dense media is discussed. (auth)

13114 CALORIMETRIC DETECTOR FOR MEASURING THE ENERGY OF AN IONIZED BEAM. Smetanina, L. I.; Matveeva, I. I.; Bruk, Z. V. Teplofiz. Vysok. Temp., 3: 623-6(July-Aug. 1965). (In Russian).

The operating principles and construction of a calorimeter based on heat transfer by thermal conductivity under steady state conditions are described. The instrument is applied as a detector for measuring the energy of an ionized beam in a deep vacuum. Choice of materials for the calorimeter must meet the following requirements: the heat conductor must assure the required sensitivity of the instrument and measurement of the energy over a sufficient range and the pickup must have a minimum capacity for secondary emission and a stable degree of blackness. Aluminum and molybdenum give good stability against secondary emission. (ATD)

13115 CRITICALITY DETECTION AND ALARM SYSTEMS—DESIGN PRINCIPLES. Aspinall, K.; Daniels, J. (United Kingdom Atomic Energy Authority, Risley, Eng.). Vienna, International Atomic Energy Agency, 1965, Preprint No. SM-70/13, 18p. (CONF-651103-22). ORINS.

From IAEA Symposium on Criticality Control of Fissile Materials, Stockholm.

A review is made of the criticality detection and alarm arrangements adopted at the different establishments of the U.K.A.E.A. and the principles which should underlie the future provision and design of criticality detection and alarm systems. The discussions are confined to gamma detection which is used throughout the U.K.A.E.A. The basic tenets are: The object is not the more rudimentary one of detecting any abnormal radiation, it is one of balancing the hazards from abnormal radiation against the hazards and costs associated with the instant evacuation of working plants. Therefore the alarm is not to be operated unless the radiation is of such a nature as could emanate from accidental criticality, but when the radiation is of such a nature then the alarm must be triggered reliably and quickly. Where an alarm system is provided it should be designed to be operated by the minimum foreseeable initial excursion regardless of whether or not the circumstances may be that such an initial excursion of itself could result in unacceptable doses to men. Arguments, resting largely on analyses of data from past incidents as reported by Stratton, are deployed to derive those detailed technical criteria needed by designers of detection and alarm systems, and to quantify them where appropriate. Recommendations are made for a detection threshold for general use, a detection threshold for special use in areas of high ambient gamma background, dose/fission ratios and system response time. Reliabilities of detection systems and of alarm noise generation, transmission and propagation are discussed. Lastly, evacuation principles and facilities are discussed and recommendations made concerning evacuation area boundaries and methods. (auth)

13116 IMPROVEMENTS RELATING TO RADIATION DETECTORS. Hunt, Stanley Ernest (to Associated Electrical Industries Ltd.). British Patent 1,014,682. Dec. 31, 1965. Filed June 4, 1961.

A radiation detector suitable for neutron detection includes a semi-conductor having formed in it a p-n junction with a thick depletion zone, means for applying a reverse voltage bias to the p-n junction, and an additional surface layer in the semi-conductor of a threshold detector material that does not respond to radiation below a predetermined energy level but responds to radiation above this threshold level releasing secondary particles into the depletion zone to cause pulse discharge through the p-n junction. A number of these semi-conductor p-n junction devices, each coated with a different threshold detector material having a different energy threshold level, may be combined to selectively determine neutron radiation of different energy levels. Means are provided for detecting the pulse discharge pulses produced in each detector. (B.L.M.)

13117 IMPROVEMENTS IN OR RELATING TO RADIATION SENSITIVE DEVICES. Bryer, Robert George (to R. A. Stephen and Co., Ltd.). British Patent 1,014,839. Dec. 31, 1965. Filed May 22, 1963.

A phosphate glass dosimeter reader is described. The glass can be quickly and easily inserted for comparison with a reference and for exposure to radiation from an ultra-violet source. The reader is designed to permit radiation to fall on the element from one direction and to allow radiation to emerge from the element in a different direction, both through suitable filters and shutters to limit the radiation detected by a photocell to that emitted at 6400 Å by the luminescent centers of neutral silver atoms formed by the penetrating radiation. (B.L.M.)

13118 IMPROVEMENTS RELATING TO SPECTROMETERS. (to Kabushiki Kaisha Hitachi Seisakusho). British Patent 1,017,094. Jan. 12, 1966. Priority date Dec. 25, 1961, Japan

A multi-channel charged-particle spectrometer is described that is of substantially simple construction and yet is capable of accurate measurement of a broad range of momenta in an extremely short time. The spectrometer includes a radiation source for emitting charged particles, a number of radiation detectors, and means for creating a magnetic field. The field is adapted to deflect the charged particles and selectively to project each deflected particle into a different one of the radiation detectors in accordance with different particle momenta. The outputs of the radiation detectors are mutually time delayed, and the time delayed signal outputs are selectively introducted into mutually different channels of a multi-channel time analyzer to be analyzed. (B.L.M.)

13119 SOLID PROBE CAPABLE OF BEING ACTIVATED FOR NUCLEAR REACTORS. Sauter, Eugen (to Siemens-Schuckertwerke AG). German Patent 1,204,757. Nov. 11, 1965. Filed July 11, 1964.

A solid radioactive indicator was designed for the measurement of neutron flux in nuclear reactors, which contains physically or chemically bound deuterium. (Gmelin Inst.)

13120 INSTRUMENT FOR THE MEASUREMENT OF THE DOSE RATE OF GAMMA RADIATION AND THE DETECTION OF BETA RADIATION. Bienek, Guenther; Loseries, Hans-Georg (to Reichert-Elektronik GmbH and Co. KG). German Patent 1,205,199. Nov. 18, 1965. Filed Feb. 28, 1963.

The instrument is provided with a meter switch and a multiple measuring range dial. A plurality of radially

directed, arc-shaped scales is equally distributed on the annular dial which is coupled to the meter switch for rotation about its axis. The pointer instrument is mounted excentrically within the annulus. (Gmelin Inst.)

13121 DEVICE FOR MEASURING BIOLOGICAL EFFECT OF RADIATION. Goodale, Edmund E.; Rochlin, Robert S.; Verbinski, Victor V. (to General Electric Co.). U. S. Patent 3,221,165. Nov. 30, 1965. Filed Mar. 6, 1961.

A radiation measuring device is provided for indicating the biological effect of radiation impinging on a linear detector element in the device. The device is responsive to ionizing radiation that may include simultaneously any combination of protons, electrons, alpha particles, neutrons, and high energy photons and is useful for measuring biological effect of the high intensity belts of ionizing radiation around the earth. The detector element generates output pulses having an alternating current component that is isolated and amplified. An oscillator is included that has output pulses of constant shape so that the output power of the oscillator is dependent upon the frequency of the oscillator. Means are provided for maintaining the output power of the oscillator equal to the output power of the amplifier, and the frequency of the oscillator is measured in terms of the biological dose of the radiation impinging upon the linear detector. (B.L.M.)

13122 LOW COUNT RATE RADIO-ACTIVITY ALARM SYSTEMS. Allenden, Dennis (to Associated Electrical Industries Limited). U. S. Patent 3,221,166. Nov. 30, 1965. Priority date, Feb. 12, 1962, Great Britian.

A radioactivity alarm system for use with a monitoring device includes a dust sampling device and a detector means responsive at the end of a sampling period to the radioactivity level of the sample collected in that period. The system includes a counter operable by the detector means to indicate the level after a certain period has elapsed, a reset device to reset the counter to zero at the end of each counting period, and an alarm actuated by the counter on exceeding a predetermined maximum count. Switching means actuated by the counter on reaching a predetermined lower level count in one of the counting periods temporarily inhibits the reset device so that the counter counts over a number of successive sampling periods and registers the total count for all the periods. The system is described for particular application to the monitoring of air borne particles of U or Pu. (B.L.M.)

13123 IONIZATION CHAMBER TYPE RADIATION DOSIMETER. Kowalski, Emil (to Landis and Gyr, AG). U. S. Patent 3,222,523. Dec. 7, 1965. Priority date May 19, 1961, Switzerland.

A small, portable, pocket type dosimeter of the type having an ionization chamber to which a voltage is applied and through which a current flows when irradiation occurs is described in which the usual disadvantages are avoided by providing separate capacitances for supplying the ionization chamber voltage and for integrating the ionization chamber current. The two capacitances may take the form of two spatially separated capacitances or two partial capacitances of the same capacitance. In either case, the two capacitances must be dielectrically separated. (B.L.M.)

13124 CIRCUIT ARRANGEMENT FOR RADIATION DOSE-MEASUREMENT. Westerkowsky, Kurt (to North American Philips Co., Inc.). U. S. Patent 3,223,843. Dec. 14, 1965. Priority date May 26, 1961, Germany.

X-ray measuring apparatus for measuring the energy supplied to a specimen irradiated by a source of x rays includes a radiation sensitive means for intercepting the radiation and converting it into a proportional amount of electrical energy. Capacitor means are provided for storing the electrical energy during a first time period, and timing means indicate the amount of energy supplied by the source during this first time period. Control means that actuate the timing means begin a timing operation at the end of the first time period and comprise further means that are responsive to the amount of energy stored during the first period to control the duration of the timing operation for a second period of time proportional to the first. (B.L.M.)

13125 RADIATION DOSIMETER WITH A RADIOCHROMIC COUPLE SUSPENDED IN AN ESSENTIALLY ANHYDROUS SOLID TRANSLUCENT MATRIX. Potsaid, Majic S. (to The Massachusetts General Hospital). U. S. Patent 3,226,545. Dec. 28, 1965. Filed May 29, 1962.

A radiation dosimeter is patented that comprises a solid optically translucent matrix in which a radiochromic couple is suspended that responds to radiation at doses in the range of 5 to 5000 R. The radiation dose may cause a color change or result in a precipitate that can be separated when the dosimeter is melted to yield an actual measure of the radiation dose. The dosimeter may take the form of an in-phantom dosimeter for radiotherapy or radiodiagnosis use. (B.L.M.)

13126 THERMAL NEUTRON FLUX MEASURING DEVICE USING TWO BORON THERMISTORS. Bloom, Justin L. (to Martin-Marietta Corp.). U. S. Patent 3,226,547. Dec. 28, 1965. Filed July 10, 1962.

A thermal neutron flux measuring device includes two boron thermistors enclosed in an encapsulating can either under vacuum or an inert atmosphere. The first thermistor is composed of a substantially greater (17 to 94% more) proportion of ^{10}B than is the second thermistor. The difference between the electrical resistances of the two thermistors is determined to yield a measure of the thermal neutron flux to which the pair of thermistors have been exposed. The device is applicable to thermal neutron flux measurements in a reactor core. (B.L.M.)

Radiation Effects

Refer also to abstracts 14170 and 14175.

13127 (CONF-651101–61) CRYOGENIC IRRADIATION OF RESISTANCE TEMPERATURE TRANSDUCERS FOR NERVA. Greenhow, W. A.; Schenz, R. F.; Gilchrist, E. J. (Aerojet-General Corp., Azusa, Calif.). Nov. 1965. Contract SNP-1. 25p. Dep. mn. CFSTI $1.00 cy, $0.50 mn.

From 13th Conference on Remote Systems Technology, Washington, D. C.

Eighteen platinum-wire resistance-temperature transducers (RTT) of six different design configurations, (wire diameter 0.3 to 2.0 mils) were irradiated in LH_2 at the Gound Test Reactor (GD/FW) while being maintained at −423°F. The integrated neutron exposure ranged from 3.1×10^{16} to 2.2×10^{17} nvt (E > 1.0 Mev). The resistance of the RTT sensing element was measured periodically and correlated to temperature-measurement error. The results of these tests followed closely the predicted temperature-measurement deviations (2 to 8°F). The calculations and analyses performed indicate that the change in platinum sensing element resistance is due to interstitials resulting from recoil-proton bombardment in the LH_2 which surrounds the platinum sensing elements. Since the recoil protons have a range of 10^{-4} cm in platinum, a surface defect results which has a greater influence on the resistance of the smaller diameter wire. Based on analytical and experimental data, the optimum design for RTT sensing element wire diameter is 1.0 mils. (auth)

13128 (NP–15835(Suppl.)) INVESTIGATION OF TRANSIENT RADIATION DAMAGE IN SEMICONDUCTOR MATERIALS. Supplement 9A, May 1–July 31, 1965. Lichtenstein, Roland M.; Willard, H. James Jr.; Corelli, John C.; Frederickson, A. Robb; Westhead, James W. (Rensselaer Polytechnic Inst., Troy, N. Y.). Contract DA-36-039-AMC-02165(E). 18p. CFSTI $1.00 cy, $0.50 mn.

Tests for electron-induced transient radiation damage in 27, 600, and 6300 ohm-cm p-type silicon were made using a photoconductivity method. Separate results are presented. A low-noise system is described for studying the transient radiation effects. (M.O.W.)

13129 (ORNL-P-1943) RECENT SOURCE DEVELOPMENTS WITH AEROSPACE UTILITY. Case, F. N. (Oak Ridge National Lab., Tenn.). [nd]. Contract W-7405-eng-26. 19p. (CONF-660207-3). Dep. mn. CFSTI $1.00 cy, $0.50 mn.

From Radioisotope Applications in Aerospace Symposium, Dayton, Ohio.

The use of radioisotope sources to simulate the electron energy distribution and flux in space is discussed, and the fabrication and properties of some specific sources are summarized. Sources for other aerospace applications, including radiographic inspection of aircraft components, are also considered. (D.C.W.)

13130 (SC-DC-65-1892) ATOMIC ORIGINS OF TRANSIENT NUCLEAR RADIATION EFFECTS IN ELECTRONICS. Snyder, A. William (Sandia Corp., Albuquerque, N. Mex.). Jan. 27, 1966. Contract AT(29-1)-789. 27p. (CONF-660301-2). Dep. mn. CFSTI $2.00 cy, $0.50 mn.

From IEEE International Convention, New York.

A survey is presented of the processes by which the effects of neutrons and gamma radiation arise. The neutrons and prompt gamma rays from the fission of ^{235}U and the neutrons from the d-t fusion reaction are considered. (D.C.W.)

13131 EFFECT OF THE ARTIFICIAL RADIATION BELT ON SOLAR POWER SYSTEMS. Fischell, R. E. (Johns Hopkins Univ., Silver Spring, Md.). APL Tech. Dig., 2: 8-13(Nov.-Dec. 1962).

The deterioration of the solar cells of the Transit 4B and TRAAC satellites up to and after the high-altitude nuclear test of July 1962 is described. Effects of trapped charged-particle fluxes and energy spectra are discussed. The variations of the performance of p-on-n solar cells during bombardment by 1-Mev electrons are illustrated. Possibilities for increasing the lifetime of satellite solar-cell power systems are discussed, including providing a large margin of initial over-design and using n-on-p cells and thick cover slides. (M.J.T.)

13132 CRYSTAL COUNTER INVESTIGATIONS OF CdS CLEAVAGE CELLS BY GAMMA EXCITATION. Schnuerer, E. (Physikalisch-Technisches Institut, Berlin). Phys. Status Solidi, 12: 181-9(1965). (In German).

Photocurrent noise and current pulse heights in CdS crystals counters with ohmic contacts that have been irradiated by gamma rays, have a dependence on applied voltage which is greater than linear. It is assumed that this effect is due to negative space charges arising from majority carrier injection. An estimate of possible pulse heights is made. (auth)

13133 DISPLACEMENT DAMAGE IN MOS TRANSISTORS. Messenger, G. C.; Steele, E. J.; Neustadt, M. (Northrop Corp., Newbury Park, Calif.). 8p. (CONF-650707-11). ORINS. Gmelin, AED-CONF-65-152-15.

From IEEE Annual Conference on Nuclear and Space Radiation Effects, Ann Arbor, Mich.

The changes in MOS device characteristics produced by neutron irradiation from the Northrop TRIGA reactor were observed. Three damage mechanisms were identified: an increase in net surface state density, a decrease in substrate resistivity, and a decrease in carrier mobility in the channel. The surface effect is usually dominant, although the bulk resistivity effect becomes increasingly important as the resistivity of the substrate is decreased. An exact closed form expression for the turn-on voltage was derived by obtaining a solution to Poisson's equation in the gate region. The open circuit gate to substrate capacitance as a function of gate to substrate voltage was obtained by numerical integration techniques in terms of the charge density and dielectric constants present in the SiO_2 layer and Si substrate. For both enhancement and depletion devices, an increase in positive charge density was apparent in the oxide region. It is postulated that the observed increase in positive charge density is due to creation of mobile positive ions, and that the decreasing net accumulation rate with increasing flux is due to a diffusion or recombination process competing with the creation process. On this basis, a rate effect is expected. (auth)

ISOTOPE TECHNOLOGY

Industrial Applications

Refer also to abstracts 12909 and 13033.

13134 (AD–625252) DETERMINATION OF EQUIVALENCE BETWEEN STERILIZATION PROCESS AND COMMERCIAL THERMAL PROCESS FOR CURED MEATS. Greenberg, R. A.; Bladel, B. O.; Zingelmann, W. J. (Swift and Co., Chicago, Ill.). Oct. 1965. Contract DA 19-129-QM-2008. 28p. (FD–28) CFSTI $2.00 cy, $0.50 mn.

Chopped ham, inoculated with spores of Clostridium botulinum strains 33A and 41B, was canned and subjected to an enzyme-inactivating heat pasteurization. The cans were then irradiated with 0.5, 1.5, 2.5, and 3.5 Mrads ^{60}Co γ radiation. A portion of the pack was not irradiated and received a commercial thermal process of $F_0 = 0.2$. Toxic spoilage occurred in inoculated product irradiated at 0 and 0.5, but not at 1.5, 2.5, or 3.5 Mrad. Inoculum survivors were isolated from all product variables before and after six mos incubation at 80 to 100°F. However, neither growth nor toxin was observed in unspoiled product. The injury phenomenon previously described in thermally processed cured meats (survival of botulinal spores without capacity of outgrowth and/or toxinogenesis) apparently occurs also in irradiated cured meats. (auth)

13135 (AD–625483) A STUDY OF THE RADIATION-INDUCED SOFTENING OF PLANT TISSUES. Kertesz, Z. I.; Massey, L. M. Jr. (New York State Agricultural Experiment Station, Geneva). Oct. 1965. Contract DA-19-129-QM-1584. 48p. (FD–27). CFSTI $2.00 cy, $0.50 mn.

Radioinduced changes in a large variety of fresh fruits and vegetables were investigated, and the physiology and biochemistry of some changes, particularly softening, were investigated in detail. Possible beneficial results with several commodities, particularly apples, were noted. (auth)

13136 (AED-C–02-06) RADIATION EFFECTS ON FOOD (INCL. RADIOACTIVE CONTAMINATION). Series C: Bibliographies. Lueck, Hanna (comp.) (Zentralstelle fuer Atomkernenergie-Dokumentation, Gmelin-Institut fuer Anorganische Chemie und Grezgebiete, Frankfurt am Main (West Germany)). June 1963. 274p. Dep. mn.

Approximately 1500 references to literature on radiation effects on food and radioactive contamination of food are presented. Titles listed are in English, French, German, and Italian. Report number, author, and subject indexes are included. (H.G.D.)

13137 (NP-15360) EFFECT OF CHEMICAL SENSITIZERS ON THE RADIATION RESISTANCE OF SOME FRUIT-SPOILAGE FUNGI. Georgopoulos, S. G.; Macris, B.; Georgiadou, E. ("Democritus" Nuclear Research Center, Athens (Greece)). [1964]. 14p. Dep. mn.

Iodoacetamide showed a dramatic radiosensitizing activity on 6 different species of fruit-spoilage molds and yeasts. The effects of vitamin k_5 and N-ethylmaleimide on radiolethality could not be studied due to high toxicity under the conditions of the tests. Of the naphthalene compounds, structurally related to vitamin k_3, 1-naphthol achieved a considerable increase of radiolethality in Aureobasidium pullulans and Candida-tropicalis but not in 4 species of typically filamentous fungi, except, perhaps, for lethality due to considerably high radiation doses. Maleic acid and p-aminophenol could not sensitize A. pullulans or Penicillium italicum. In no case was considerable increase of radiolethality observed under conditions of anoxia. In Botrytis cinerea increase of lethality by iodoacetamide was achieved rather by increasing the number of spores uncapable of germinating. (auth)

13138 (UCD–34P80-3) RADIATION TECHNOLOGY IN CONJUNCTION WITH POSTHARVEST PROCEDURES AS A MEANS OF EXTENDING THE SHELF LIFE OF FRUITS AND VEGETABLES. Period Covered: February 1, 1964–January 30, 1965. Maxie, E. C.; Sommer, N. F.; Brown, D. S. (California Univ., Davis. Dept. of Pomology). Contract AT(11-1)-34. 195p. Dep. mn; CFSTI $5.00 cy, $1.00 mn.

Thirteen articles are included; separate abstracts were prepared for 12. The remaining article not abstracted in NSA was on the effects of pulp temperature during irradiation on quality attributes of Shasta strawberries. (P.C.H.)

For abstracts of individual papers see: 12885, and 13139–13149.

13139 (UCD–34P80-3, pp 9-26) THE INTERACTION OF GAMMA IRRADIATION, SEALED PACKAGES, AND CONTROLLED ATMOSPHERE ON INCIDENCE OF BOTRYTIS ROT IN STRAWBERRIES. Chalutz, Edo; Maxie, E. C.; Sommer, N. F. (California Univ., Davis. Dept. of Pomology).

The comparative effectiveness of gamma irradiation and controlled atmospheres as protective measures against post-harvest decay in Shasta strawberries was studied. Irradiation treatments were found to be more effective than were modified atmospheres in controlling development of lesions of B. cinerea. Inhibition of rot development was greater when berries were subjected both to irradiation and to a modified atmosphere. Modified atmospheres inside sealed polyethylene bags had a marked effect on delaying rot development in unirradiated strawberries, but contributed little additional protection to fruit subjected to 200 krad of gamma irradiation. The results also indicated that irradiation treatments do not increase the susceptibility of strawberries to infection by B. cinerea. Therefore, there is no need for microbe-proof, air-tight packages to protect irradiated strawberries from reinfection during commercial storage, provided that berry temperatures are maintained at 32 to 41°F. (auth)

13140 (UCD–34P80-3, pp 27-47) GAS EXCHANGE IN 'BARTLETT' PEARS IN RELATION TO GAMMA IRRADIATION. Bussel, Joseph; Maxie, E. C. (California Univ., Davis. Dept. of Pomology).

A study was made on the rate of gas exchange in Bartlett pears. Movement of oxygen into or from the internal atmosphere was very rapid, and was not restricted severely as the fruits ripened. Irradiation with 300 krad of gamma rays, or a temperature of 86°F, stimulated production of ethylene. Flushing the fruit with nitrogen inhibited production of ethylene. Upon transfer of anoxic fruits to air, production was renewed, during the 42 minutes of the experiment, only in the irradiated pears. Production of ethylene by pears at different stages of the climateric was inhibited when the fruits were transferred to nitrogen, and was renewed upon their return to air. Because of the rapid movement of gases into or from the internal atmosphere of Bartlett pears, irradiation of the fruits in anaerobic conditions seems impractical. (auth)

13141 (UCD–34P80-3, pp 48-51) CHERRIES. Johnson, Carol F.; Boyd, Camilla; Maxie, E. C. (California Univ., Davis. Dept. of Pomology).

The results of a sensory evaluation on irradiated Bing cherries are reported. The cherries were exposed to 0, 200, 300, and 400 krad. Storage and irradiation temperature was 32°F throughout. Flavor, texture, and appearance were evaluated. Analyses of data showed a significant difference for all treatments except between 200 and 300 krad. There was a significant increase in the firmness of the cherries each week. This could probably be attributed to water loss. Data are tabulated. (P.C.H.)

13142 (UCD–34P80-3, pp 52-4) THIAMINE AND NIACIN ANALYSIS OF IRRADIATED STRAWBERRIES.

Rae, Henry; Boyd, Camilla; Maxie, E. C. (California Univ., Davis. Dept. of Pomology).

The thiochrome method of thiamine analysis and the cyanogen bromide method of niacin analysis were used to measure the effects of gamma rays on the content of these vitamins on strawberries analyzed immediately and 10 days after treatment to 200 krad. The results showed that irradiation did not cause a nutritionally significant reduction in thiamine. In the case of niacin, irradiated fruits contained somewhat higher amounts of the vitamin. (P.C.H.)

13143 (UCD-34P80-3, pp 55-7) Mn^{2+} IN ^{60}Co GAMMA-IRRADIATED STRAWBERRIES. Shah, J.; Landgraf, W. C.; Maxie, E. C. (California Univ., Davis. Dept. of Pomology).

Irradiated strawberries were analyzed for long-lived organic radicals. Greenhouse-grown Shasta strawberries were irradiated at 200 krad at 0°C and maintained at this temperature for 64 hrs. Only Mn^{2+} was detected in the samples. At the present, it is assumed that wholesomeness of irradiated strawberries is not affected by the presence of Mn^{2+} radicals. (P.C.H.)

13144 (UCD-34P80-3, pp 69-74) EFFECT OF GAMMA IRRADIATION ON FRESH PRUNES. Maxie, E. C.; Johnson, Carol F.; Boyd, Camilla (California Univ., Davis. Dept. of Pomology).

The effects of gamma radiation on the quality of dried prunes. Fresh, French prunes were irradiated to 0, 100, 200, 300, 400, and 600 krad, then dried to a moisture content of 20%. The dehydrated fruits were stored at 36°F for about 5 months, then evaluated. The results of tests showed that differences in flavor and aroma were significant. In most cases the irradiated prunes appeared to have a higher gain in weight. Also, following stewing, all irradiated samples were significantly softer than controls. (P.C.H.)

13145 (UCD-34P80-3, pp 75-83) EFFECT OF GAMMA IRRADIATION ON LEMON FRUITS HELD IN NON-REFRIGERATED STORAGE. Maxie, E. C.; Rae, Henry L.; Boyd, Camilla (California Univ., Davis. Dept. of Pomology).

Lemons were irradiated at 0, 100, 200, and 300 krad and then placed at 77°F in an atmosphere containing 93% relative humidity. The results showed that lemons would still contain nutritionally significant levels of ascorbic acid, even after 15 days, when subjected to 200 krad. (P.C.H.)

13146 (UCD-34P80-3, pp 84-91) EFFECT OF GAMMA IRRADIATION ON RIPENING OF GROS MICHEL BANANAS. Amezquita, Rafael; Maxie, E. C.; Johnson, Carol F. (California Univ., Davis. Dept. of Pomology).

Bananas with uniform green color and grade were irradiated at ambient temperature to 0, 35, and 50 krad and then ripened slowly or treated with ethylene to initiate ripening. However the results showed that differences in ripeness were too great to allow detection of differences between fast and slow ripened fruit. Apparently irradiation at these dose levels does not have an adverse effect on bananas, as no preference for any treatment occurred during 3 weeks of tasting. (P.C.H.)

13147 (UCD-34P80-3, pp 92-8) EFFECT OF GAMMA IRRADIATION ON PEACHES. Maxie, E. C.; Johnson, Carol F.; Boyd, Camilla; Rae, Henry L.; Stallman, R. F. (California Univ., Davis. Dept. of Pomology).

Studies were made to determine whether peaches irradiated green, then ripened, would be as acceptable to a taste panel as fruits irradiated ripe. However, there was some difficulty in ripening the irradiated fruit and unirradiated fruit to the same degree. There was a definite tendency for the peaches irradiated green to ripen more rapidly. The fruit irradiated green was chosen for its sweeter peach flavor. A tendency to rate control fruit as softer than fruits irradiated when ripe was found in the tasters. (P.C.H.)

13148 (UCD-34P80-3, pp 99-175) THE EFFECT OF GAMMA IRRADIATION ON THE POST-HARVEST BEHAVIOR OF TOMATO FRUITS. Abdel-Kader, Adel S.; Morris, L. L.; Maxie, E. C. (California Univ., Davis. Dept. of Pomology).

Tomatoes of comparable maturity, size, and ripeness were gamma irradiated and studies were made on rate of respiration, ethylene production, ripening, and shelf life. The results showed that adverse effects of irradiation were less in fruits irradiated at the pink or table-ripe stage. An extension of shelf life of 4-12 days was obtained by irradiation at doses between 200 and 350 krad. However, the magnitude of shelf life extension depends upon the condition of fruits at harvest, handling procedures, postirradiation attack by decay organisms, and storage temperature. Two factors which may limit the use of irradiation with tomatoes are: increased softening of fruits by irradiation may affect their susceptibility to transit injury; and effects on flavor. An immediate increase in the respiratory activity of tomatoes, with the magnitude of the increase directly proportional to dose was found. Retardation of ripening of mature-green fruits by doses of 300 krad or more can be reversed by using ethylene treatment. (P.C.H.)

13149 (UCD-34P80-3, pp 176-89) COMPARATIVE INACTIVATION OF CONIDIA, MYCELIA, AND SCLEROTIA OF BOTRYTIS CINEREA BY GAMMA RADIATION. Sommer, N. F.; Fortlage, R. J.; Buckley, Patricia M.; Maxie, E. C. (California Univ., Davis. Dept. of Pomology).

The radiosensitivity of conidia, mycelia, and sclerotia of Botrytis cinerea was compared using an end-point technique. Young mycelia were more resistant than either mature mycelia or sclerotia when populations of these structures were equated by dry weight, protein, or DNA content. Sclerotia were more resistant than mature mycelia and conidia on the basis of equivalent protein and more resistant than conidia on a dry weight basis. (auth)

13150 DENSITY MEASUREMENT WITH RADIOACTIVE BEAMS IN EXPLOSION-POSSIBLE ATMOSPHERES. Mengelkamp, Bernhard. A E G Mitt., 55: 499-502(1965). (In German).

The continuous measurement of the density of solids and loose materials with radiation beams is reviewed. The development of densitometers in explosion-protected models makes it possible to carry out measurements in places in which the earlier instruments could not be used. (tr-auth)

13151 THICKNESS MEASUREMENT WITH γ BEAMS. Burbach, Werner; Flormann, Paul. A E G Mitt., 55: 503-11(1965). (In German).

The application possibilities of γ beams to thickness measurements are shown. The measurement problems in rolling-mill operations are treated extensively. (tr-auth)

13152 STORAGE OF EVISCERATED HADDOCK IN REFRIGERATED SEA WATER TREATED WITH GAMMA RADIATION. Nickerson, J. T. R.; Licciardello, J. J. (Massachusetts Inst. of Tech., Cambridge). J. Milk Food Technol., 28: 223-6(July 1965).

The possibility of using ^{60}Co γ radiation to improve the storage of freshly caught fish aboard fishing boats was investigated in a system whereby irradiated cold brine was circulated around the eviscerated fish. Two different procedures were employed for irradiation of the sea water. In the first, sea water was continuously recirculated from the refrigerated bath to a reservoir flask in a ^{60}Co radiation field where the radiation intensity was 2250 rad/min. In the second method the sea water was irradiated by a batch process. Haddock kept in unirradiated refrigerated sea water up to a 7-day period was sampled for bacterial content and tasted. The fish was judged to be of good quality. After the 7th day the fish were of unacceptable quality. The irradiation treatment seemed to have extended the storage life of the fish a few extra days compared to the control method. When a higher irradiation dose was applied, a more significant extension of storage life resulted. (TCO)

13153 MEASUREMENT OF LEAKAGE TRITIUM FROM TRITIUM SELF-LUMINOUS PAINTS. Ikeda, Masamichi;

Yanagi, Takako; Shinozaki, Yoshiharu (Tokyo Metropolitan Isotope Research Center). Radioisotopes (Tokyo), 15: 19-22(1966).

Studies were made in order to establish the measurement of the leakage tritium from the tritium self-luminous paints made in England, U.S.A., Germany, and Japan. The amount of tritium contained in a paint sample was about 25 mC, the amount necessary for a clock or an alarm clock to have enough luminosity, and the measurements of tritium leakage were made by the flow method using a gas flow counter. The results showed that the amount of tritium leakage depends only on the initial amount of tritium applied, not the kind of paint nor on the specific activities of the tritium in the paint. The safety of commercial tritium self-luminous paints was examined in connection with the maximum permissible amounts of tritium. (auth)

13154 A DENSITY OPERATIONAL AMPLIFIER AND ITS APPLICATION TO γ-RAY DENSITY GAGE FOR INSPECTION OF FUEL ROD. Satomi, Yoshiyasu (Japan Radiation and Medical Electronics, Inc., Tokyo). Radioisotopes (Tokyo), 15: 27-32(1966). (In Japanese).

In the transmission-type γ density gage, the density of the material can be determined by measuring the intensity of radiation transmitted through the material. However, the intensity of radiation is an exponential function of density, so that it is necessary to make corrections. Therefore, a density-operational amplifier for a γ density gage was developed. This amplifier can compute the density from the intensity of radiation transmitted through the material so that its output shows directly the value of density. This is done by introducing the value of the mass absorption coefficient and the thickness of the sample. Its circuit is a type of analog operational circuit, which utilizes a log-diode as the computing element, and which gives excellent accuracy with a simple circuit. In the operation of the γ density gage for inspection of fuel rods utilizing this amplifier, evaluation and analysis of the result were considerably improved and the measuring range was expanded. The principles and the characteristics of the density-operational amplifier and the γ density gage for inspection of fuel rods with this amplifier are described. (auth)

13155 TRUDY VSESOYUZNOGO SEMINARA PO PRIMENENIYU IZOTOPOV V KHIMICHESKOI I NEFTEPERERABATYVAYUSHCHEI PROMYSHLENOSTI g. EREVAN, 1963 g. (Bulletin of the All-Union Seminar on the Isotope Applications in Chemistry and Petroleum Industry, Erevan, 1963). Moscow, Atomizdat, 1964. 134p.

Fifteen papers are included on measurement and control of levels in high-pressure scrubbers, automatization of technological processes using radioisotope sensing units, automatic control of the concentration of weak nitric acid, testing of the use of radioisotopic means for the automatization and technological control of industrial enterprises in the Lugansk district, the UR-8 level gage and the PZhR-5 density gage and prospects of their use, the level gage "Udar-3" and prospects of its use, measurement of flow rate of liquid metals using modulated radiation, ionization detector for gas chromatography, use of radioactive ^{36}Cl for determining the isomeric state of hexachloran, plastic and liquid scintillators, testing the exploitation of radioisotope devices in the petroleum industry, the effectiveness of using radioisotope devices and methods in the chemical industry, testing the exploitation of radioisotope level gages and gamma relays, the automatic analyzer of the AZhS-1 series in diesel fuel and tests of its use in the Kuibyshev petroleum factory, and decisions of the conference on the introduction of radioisotope methods and devices into the chemical and petroleum industry. (M.J.T.)

13156 MOISTURE CONTROL IN A MIXTURE FOR AGGLOMERATION, USING A NEUTRON PROBE. Kohn, A. (Institut de Recherches de la Siderurgie, St. Germain-en-Laye, France). Vienna, International Atomic Energy Agency, 1965, Preprint No. SM-68/40, 18p. (In French). (CONF-651023-33). ORINS.

From Symposium on Radioisotope Instruments in Industry and Geophysics, Warsaw.

The main tests carried out in research subsidized by the CECA to examine the possibilities of using a neutron probe for controlling the moisture of products to be used for agglomeration are described. During the first series of experiments a study was made of the factors affecting the number of slow neutrons received by a probe emitting fast neutrons. The product under study was distributed in casks within which the measuring probe was situated. The results obtained in these tests helped shed light on the nature of the various physical factors (chemical composition of the mixture, density, coke content, etc.) likely to affect the count rate. The second part of the work was devoted to practical tests on the agglomeration line. In these tests, the probe was arranged in a tube placed slightly above the mixture layer. These trials consisted in observing the instrument readings for several days and comparing them with the results of moisture determination in terms of loss of weight of samples taken during countings, after stove drying. The following results were obtained: In spite of some scatter of the measured values due to weight losses, statistical analysis of the results showed that there was in fact a linear relation between the counting results and the moisture content of the mixture; Under the trial conditions (50 mc Ra/Be source, measurement for 5 min), it was possible to detect a moisture variation of 0.5% in the mixture, provided that certain factors (density, probe-mixture distance) remained constant; Nevertheless, a prerequisite for the industrial use of this method is a certain degree of technological improvement designed to eliminate the disturbing effects of variations in the geometric conditions under which measurement is carried out. (auth)

Power Application

See also ENGINEERING — Space Propulsion

Refer also to abstract 13444.

13157 (ORNL-P-1945) HEAT TRANSFER IN THE DESIGN OF LARGE RADIOISOTOPIC HEAT SOURCES. Posey, J. C.; McHenry, R. E. (Oak Ridge National Lab., Tenn.). [nd]. Contract W-7405-eng-26. 8p. (CONF-660305-9). Dep. mn. CFSTI $1.00 cy, $0.50 mn.

From American Nuclear Society Topical Meeting, Augusta, Ga.

Methods are outlined by which temperatures in heat sources with simple geometric shapes can be calculated, and design techniques by which the temperatures can be held to reasonable levels are suggested. (D.C.W.)

13158 ADVANCED RADIOISOTOPE THERMOELECTRIC SPACE POWER SYSTEM. Elias, D.; Gray, I. L. (Martin-Marietta Corp., Baltimore). New York, Society of Automotive Engineers, Inc., 1965, Preprint No. 650792, 8p. (CONF-651034-2). ORINS.

From Society of Automotive Engineers, National Aeronuatic and Space Engineering and Mfg. Meeting, Los Angeles.

A radioisotope thermoelectric generator (RTG) using curium-242 as fuel, developed as an alternate power supply, was shown to be compatible with the Atlas-Centaur and Surveyor requirements. This power supply provides a relatively low weight and highly reliable system capable of producing 25 watts output under lunar conditions for a mission life of 120 days. The system is unique in that it utilizes a thermal control system that maintains a relatively constant thermal input to the energy conversion components. Major program effort was focused on nuclear safety, thermoelectric generator development, converter development, and system qualification tests. (auth)

Separation and Production

See also CHEMISTRY — Separation Processes and Procedures

Refer also to abstract 13752.

13159 SEPARATION OF RADIOCESIUM BY EFFECT OF THERMOIONIZATION. Nguyen-Long-Den (Institut du Radium, Orsay, France). Compt. Rend., 261: 5465-8 (Dec. 20, 1965). (In French).

A fast separation method, occurring at the interior of the ion source of an isotope electromagnetic separator and based on the differences in volatility and ionization potentials of the elements Ce, La, Ba, and Cs, was developed for the production of radiochemically and isotopically pure Cs. The method was applied to the determination of the cross sections for the formation of the isomeric states of ^{134}Cs and ^{135}Cs produced by the reaction La (p,3pxn)Cs. (tr-auth)

13160 EFFECT OF THE SURFACE DIFFUSION ON THE SEPARATION EFFICIENCY IN BRETON-MASSIGNON'S THEORY. Fiocchi, R. (CNEN, Milan. Univ., Milan). Energia Nucl. (Milan), 13: 24-31(1966).

Current theories of isotope separation by gaseous diffusion through porous barriers are almost all based on the model of strongly elongated cylindrical capillary pores. Recently Breton and Massignon have established a consistent separation theory based on the model of a disordered and isotropic pack of identical spheres, which describes more exactly most of the porous barriers. Since the surface migration of adsorbed molecules may play an important role in the separation process, the effect of the surface diffusion on the separation efficiency derived from Breton-Massignon's theory is investigated. This analysis is essentially devoted to the uranium isotope separation: the results are compared with those obtained from previous theories. (auth)

13161 MATERIAL EXCHANGE COLUMNS. (to Sulzer Brothers Ltd.). British Patent 1,013,776. Dec. 22, 1965. Priority date Mar. 22, 1963, Switzerland.

A material exchange column is proposed for the distillation, rectification, or extraction of a component from a gaseous mixture by means of an external separating liquid or for the separation of isotope elements from a substance by means of a chemical exchange reaction. The column contains a number of zones containing packing material of at least two different rates of pressure drop. The different zones are so distributed over the column length that a zig-zag direction of flow is superimposed on the longitudinal flow through the column of the gas or vapor of different rates of pressure drop. In a preferred construction, the column has contiguous parallel flow channels, which have boundary walls having apertures through them. The walls are provided by at least one element having rectangular cells. The channels have packing materials of different pressure drop but substantially the same number of theoretical plates, and at least some of the packing material is in the form of corrugated contacting lamellae with the corrugations of adjacent lamellae extending in different directions. The corrugations of at least one of each adjacent pair of lamellae are inclined to the vertical column axis. (B.L.M.)

13162 MATERIAL EXCHANGE COLUMNS. (to Sulzer Brothers Ltd.). British Patent 1,013,777. Dec. 22, 1965. Priority date Mar. 21, 1963, Switzerland.

A material exchange column is proposed for the simultaneous flow of a liquid and a gas or vapor that has contiguous vertical flow channels containing packing and means for distributing the liquid to the tops of the channels. The boundary walls between adjacent flow channels contain apertures permitting the gas or vapor to become distributed over the column but not permitting passage of the liquid. Each flow channel contains at least two packing elements one above the other and of the same cross section as the flow channel. Each element consists of or includes contacting vertical corrugated lamellae having their lamellae in vertical planes, which are displaced from one another. The corrugations of adjacent lamellae extend in different directions; the corrugations of at least one of each adjacent pair of lamellae extend at an angle to the vertical column axis; and the corrugated lamellae alternate with uncorrugated lamellae in a horizontal plane. (B.L.M.)

MATHEMATICS AND COMPUTERS

Refer also to abstract 13806.

13163 (ANL–7129) APPLIED MATHEMATICS DIVISION SUMMARY REPORT, JULY 1, 1964–JUNE 30, 1965. (Argonne National Lab., Ill.). Contract W-31-109-eng-38. 53p. Dep. mn. CFSTI $3.00 cy, $0.50 mn.

The computer programs that were prepared during the period are summarized, together with developments in programming and computer systems. Some applications of computers to specific problems are outlined. (D.C.W.)

13164 (COO–415-1028) A NOVEL FAMILY OF DIGITAL CIRCUITS [Thesis]. Report No. 169. Collins, Donnell Michael Jr. (Illinois Univ., Urbana. Digital Computer Lab.). Sept. 22, 1964. Contract AT(11-1)-1018. 86p. Dep. mn. CFSTI $3.00 cy, $0.75 mn.

Logic elements were described which offer a novel solution to the problem of compatibility of input and output levels. The basic design of an inverting NOR/NAND element was developed, together with that of a restoring OR/AND variant, available with minor component rearrangement. The existence was shown of workable circuits using identical components in either of the two available configurations. The resulting logic elements have several desirable features, including single power supply operation, absence of close tolerance requirement and simple control of switching thresholds. The OR/AND circuit, in addition to simplifying decoder design, was shown to be suited to the economic production of the composite logic functions required by storage and pulse forming elements. (M.O.W.)

13165 (JINR-E–2542) ON THE GENERAL STRUCTURE OF AN OPERATOR WHICH IS MULTIPLICATIVE WITH RESPECT TO A SYMMETRY GROUP. Ul'mann, A. (Joint Inst. for Nuclear Research, Dubna (USSR). Lab. of Theoretical Physics). 1966. 5p. Dep. mn.

An operator is said to be a multiplicative one with respect to a group, if $A(\omega_1 \times \omega_2) = A\omega_1 \times A\omega_2$ is valid for the Kronecker product. A theorem on the general structure of these operators was obtained. (auth)

13166 (KFK–371) MESPRO 64—DAS BETRIEBSSYSTEM FUER DIE INTEGRIERTE COMPUTERANLAGE MIDAS. (MESPRO 64—A Program for the On-Line Computer MIDAS). Krueger, G.; Zipf, G. (Kernforschungszentrum, Karlsruhe (West Germany). Institut fur Angewandte Kernphysik). Oct. 1965. 54p. Dep. mn.

The MIDAS installation is described and the principles of the program construction are given. The time schedules and programming schedules are discussed. The individual programs are described. (J.S.R.)

13167 (ORNL–3873) MINIMUM BIAS DESIGNS FOR AN EXPONENTIAL RESPONSE [Thesis]. Manson, A. R. (Oak Ridge National Lab., Tenn.). Feb. 1966. Contract W-7405-eng-26. 178p. Dep. mn. CFSTI $5.00 cy, $1.00 mn.

Submitted to Virginia Polytechnic Inst., Blacksburg.

For the exponential response $\eta_u = \alpha + \beta e^{\gamma Z_u}$ (u = 1, 2, ... ,N) where α and β lie on the real line $(-\infty, \infty)$, and γ is a positive integer; the designs are given which minimize the bias due to the inherent inability of the approximation function $\hat{y}_u = \sum_{j=0}^{d} b_j e^{jZ_u}$ to fit such a model. Transformation to $\eta_u = \alpha + \beta x_u^{\gamma}$ and $\hat{y}_u = \sum_{j=0}^{d} b_j x_u^j$ facilitates the solution for minimum bias designs. The minimum bias designs are obtained for specific values of N with a maximum protection level, $\gamma_d^*(N)$, for the parameter γ and an approximation function of degree d. These designs obtained possess several degrees of freedom in the choice of the design levels of the x_u or the Z_u, which may be used to satisfy additional design requirements. It is shown that for a given N, the same designs which minimize bias for approximation functions of degree one also minimize bias for general degree d, with a decrease in $\gamma_d^*(N)$ as d increases. In fact $\gamma_d^*(N) = \gamma_1^*(N) - d + 1$, but with the decrease in $\gamma_d^*(N)$ is a compensating decrease in the actual level of the minimum bias. Furthermore, $\gamma_d^*(N)$ increases monotonically with N, thereby allowing the maximum protection level on γ to be increased as desired by increasing N. In the course of obtaining solutions, some interesting techniques are developed for determining the nature of the roots of a polynomial equation which has several known coefficients and several variable coefficients. (auth)

13168 ON SERIES EXPANSION OF A DETERMINANT AND SOLUTION OF THE SECULAR EQUATION. Chan, Yau W. (Brookhaven National Lab., Upton, N. Y.). J. Math. Phys., 7: 27-34(Jan. 1966). (BNL–9126).

A determinant and its cofactors are expanded in terms of the cyclic products of its elements. With the aid of this expansion, an implicit equation for the eigenvalue and an explicit equation for amplitudes of the corresponding eigenfunction are obtained, respectively, in terms of a ratio of two simple series expansions. Comparisons with Feenberg's perturbation formula and with Sasakawa's perturbation method are also discussed. (auth)

13169 LEKTSII PO TEORII GRUPP LI. (Lectures on the Lie Group Theory). Zhelobenko, D. P. Dubna, USSR, Joint Inst. for Nuclear Research, 1965. 344p.

Basic considerations are presented on topological and Lie groups, problems of representation theory, and the difference between compact and noncompact Lie groups. Compact Lie groups and their representations are discussed, including the global theorem, analytic continuation, irreducible representations of the U(n) group, tensors and Young diagrams, the algebra of Z-multipliers and the character of irreducible representations, Casimir operators and the center of the ring group, and the tensor derivation of two irreducible representations. Elements of the theory of noncompact Lie groups are presented, with discussions of the adjoint representation, the classification of semisimple complex groups and Lie algebras, the connection between real and complex semisimple groups and Lie algebras, the theory of representations of semisimple Lie groups, and elements of general representation theory. (M.J.T.)

METALS, CERAMICS, AND OTHER MATERIALS

General

Refer also to abstract 14008.

13170 (BM-RI-6736) REACTION RATE OF URANIUM METAL WITH URANIUM TETRAFLUORIDE IN MOLTEN FLUORIDE SOLUTIONS. Porter, Bernard; Meaker, R. E.; Henrie, T. A. (Bureau of Mines, Reno, Nev. Reno Metallurgy Research Center). July 1965. 11p. Bureau of Mines Free.

The rate of the heterogeneous reaction between high-purity uranium metal and uranium tetrafluoride in molten lithium fluoride was measured. The apparent heat of activation for the reaction was 16.91 kilocalories per mole of UF_4. A surface controlled mechanism is suggested in which UF_4 is adsorbed on the uranium metal surface. Additional UF_4 reacts with the adsorbed species and the metal site to form an activated complex that decomposed to the product UF_3. The reaction is an important source of metal loss in the electrowinning of uranium metal. (auth)

13171 (BMI-1751) PROGRESS RELATING TO CIVILIAN APPLICATIONS DURING NOVEMBER 1965. Dayton, Russell W.; Paprocki, Stan J. (Battelle Memorial Inst., Columbus, Ohio). Dec. 1, 1965. Contract W-7405-eng-92. 25p. Dep. mn. CFSTI $2.00 cy, $0.50 mn.

Progress in studies on fuels, reactor materials and components, uranium–plutonium mononitride fuel materials, coated-particle fuel materials, and corrosion of structural materials used in the fluidized-bed fluoride-volatility process is reported. (W.L.G.)

13172 (CONF-170) CONFERENCE ON THE PHYSICAL METALLURGY OF BERYLLIUM HELD AT GATLINBURG, TENNESSEE, APRIL 30–MAY 1, 1963. (Oak Ridge National Lab., Tenn.). Contract W-7405-eng-26. 247p. Dep. mn. CFSTI $2.50 cy, $1.25 mn.

Abstracts were prepared for 12 of the 14 papers given at the conference. Two papers were previously abstracted for NSA, see: 17: 36299 and 18: 37703. (W.L.G.)

For abstracts of individual papers see: 13173–13175, 13237–13244, and 13323.

13173 (CONF-170, pp 1-5) THE PURIFICATION OF BERYLLIUM METAL BY A DISTILLATION PROCESS. A Summary Report. Hooper, E. W.; Keen, N. J. (Oak Ridge National Lab., Tenn.).

The process depends on two separation mechanisms: the fractional evaporation of Be from many of the less volatile impurities, and the fractional condensation on a heated surface at such a temperature that entrained impurity atoms of the more volatile elements are able to re-evaporate, leaving purer Be. (W.L.G.)

13174 (CONF-170, pp 184-213) THE AIR FORCE SPONSORED BERYLLIUM RESEARCH AND DEVELOPMENT PROGRAM. Gelles, S. H. (Ledgemont Lab., Kennecott Copper Corp., Lexington, Mass.).

A research and development program aimed at making Be more useful as an Air Force structural material is described. Three approaches were used: to improve the inherent mechanical properties of the metal by purification, to alter the properties by changing structural parameters such as grain size and the preferred orientation, and to increase the technology and understanding of commercial Be. In the field of purification, research is described on the preparation of pure Be by the decomposition of beryllium iodide and on the preparation and evaluation of high purity Be produced by distillation alone and by a combination of distillation and zone refining. In addition, other efforts designed at understanding the role of impurities in Be are treated. These include a study of aging and strain aging behavior of commercially pure Be, a study of the flow and fracture characteristics as a function of grain size, purity level, and heat treatment, a study of the dislocation structure, of recrystallization and grain growth, and of impurities and precipitates. In addition, a limited study of the basal slip characteristics of high purity Be single crystals grown from the melt is described. The programs aimed at altering the properties and increasing the technology of commercially pure Be include studies of joining by TIG welding, resistance welding, furnace brazing, and ultrasonic welding; a program on the effect of low temperature, low reduction rolling on the mechanical properties of Be and Be alloy sheet; and a program dealing with surface damage in Be. Recommendations for further work in Be research and development are made. (auth)

13175 (CONF-170, pp 214-20) A STATUS REPORT ON PURIFICATION OF BERYLLIUM AND ITS PROPERTIES. Bunshah, R. F. (Lawrence Radiation Lab., Univ. of California, Livermore).

Purification of Be was accomplished by crucible-free vacuum melting and distillation. The distillate is collected in the form of a sheet, which is then mechanically worked. The results of a limited number of bend tests on foil and sheet shows improved bend ductility over commercial material. At this stage it is not possible to state whether this improvement is a result of higher purity and/or less pronounced basal texture as compared to commercial material. (auth)

13176 (EURAEC-1503) USE OF PLUTONIUM AS A FUEL IN NUCLEAR REACTORS. Quarterly Report Nos. 1 and 2. (Societe Belge pour l'Industrie Nucleaire, Brussels. Centre d'Etude de l'Energie Nucleaire, Brussels (Belgium)). Nov. 1964. Contract 001-64-1-TRUB. 84p. (EUR-2661; BN-6411-02). Dep. mn. CFSTI $3.00 cy, $0.75 mn.

Experiments showed the importance of the drying and grinding stages in preparation of fine Pu-bearing powders used for the fabrication of vibratory compacted fuel elements. Tamped densities of the order of 64% of theoretical may be obtained after roasting at 1200°C. The conditions under which UO_2 and PuO_2 powders were mixed seemed to have an effect on the ultimate Pu distribution in the vibratory compacted elements. High-density mixed powders were prepared by pelletization, grinding the untreated pellet, screening, and sintering the powder of the desired particle size distribution. Fuel rods prepared from such powders showed a relative longitudinal variation in the Pu content of 5–6%. Elements with improved thermal performance were fabricated by vibrating powder (designed to be enriched with Pu) around natural UO_2 pellets. The assay of Pu and its valency states in a solution can be performed by coulometry at constant current as beneficially as by coulometry at controlled potential; the final point is determined more accurately by the first method, however. The longitudinal Pu content of the fuel rods is determined with a gamma spectrometer on the basis of ^{239}Pu 384 kev line. For this purpose, only the 340-430 kev window was counted; although this precaution limits the background count due to U, this count must be established experimentally in each particular case. Theoretical calculations show that the effect of radial Pu localization on the absorption of radiation in the material is relatively slight, except for Pu on the surface of the fuel; this phenomenon is a considerable safety factor. The filler gas has a strong effect on heat transfer inside vibration tamped fuel. Tests performed at atmospheric pressure on samples at about 85% of theoretical density show that this effect becomes less marked as the temperature and partial pressure rise. Studies on Pu reprocessing revealed that there is little variation in the capacity of Permutit SK resin for supply solution concentrations of between 5 and 111 g Pu/liter. The flow rate

of the supply solution can be increased if the Pu concentration is higher. Preliminary tests in the neutron study of the $UO_2-PuO_2-H_2O$ lattices using a Sames BSI accelerator on pulsed operation showed the effect of the various operating parameters; in particular, the detection chain was improved. To test that the installation was operating correctly, decay constant measurements were taken in water poisoned to varying degrees of impurity, and experimental determination of the $\alpha(B_g^2)$ relation in pure water is in progress. The important contribution of harmonics was shown by analysis of the experimental results; methods for evaluating and correcting their effects on alpha measurement are currently being developed. (auth)

13177 (EURAEC–1504) USE OF PLUTONIUM AS A FUEL IN NUCLEAR REACTORS. Quarterly Report Nos. 3 and 4. (Societe Belge pour l'Industrie Nucleaire, Brussels. Centre d'Etude de l'Energie Nucleaire, Brussels (Belgium)). Mar. 1965. Contract 001-64-1-TRUB. 78p. (EUR–2662; BN–6503-01). Dep. mn. CFSTI $3.00 cy, $0.75 mn.

Work Performed under United States–Euratom Joint Research and Development Program.

Study of the plutonium hydroxide drying and roasting conditions revealed the influence of the humidity of the precipitate on the density, porosity, and hardness of the dioxide obtained after roasting. The precipitation, drying, and roasting conditions developed for Pu were successfully applied to coprecipitates of $UO_2-40\%$ Pu. Some particle size distribution staggering of the mean grade of the powders scarcely affected the density and homogeneity of the fuel elements prepared by vibratory compaction. Densification of the fuel by vibration affects the weldability of type 304 stainless steel canning, when used in the work-hardened state. For 10% work-hardening, however, the production of sound welds is still possible by making some adjustments to welding parameters. The reproducibility and accuracy of electrochemical analyses for Pu by coulometry at controlled potentials vary from ±0.2% for a concentration of a few mg/ml, to ±1.5% for a concentration of a few μg/ml. The sensitivity of x-ray weld examination was improved by careful selection of operating conditions. The present resolution limit is a standard defect 50 μ deep for a can 500 μ thick. The influence of gas on actual thermal conductivity of fuels densified by vibration was experimentally confirmed by additional tests using nitrogen and argon. The nature and pressure of the filler gases have a negligible effect above 1100°C. At temperatures below 1000°C, PuO_2 has a higher real thermal conductivity than UO_2, for identical measurement conditions. The comparative study of the various ion-exchanger resins was continued with a view to the processing of diluted plutonium solutions containing large quantities of uranium as well. In the neutron study of the $UO_2-PuO_2-H_2O$ lattices the $\alpha = f(B_g^2)$ relation for light water at 20°C was determined by detecting the breakthrough flux. Analysis of the pulsed measurements with a single exponential reveals the importance of harmonics in the measurement geometry adopted. Space-time measurements made on two pure water geometries led to the conclusion that, to determine the characteristics of moderator media, it is necessary: to take the measurements after waiting long enough for the fundamental mode to assert itself within the mass; or to make an analysis with a multiple exponential; or to analyze and interpret the space-time measurements. (auth)

13178 (GEMP–55A) HIGH-TEMPERATURE MATERIALS PROGRAM PROGRESS REPORT NO. 55, PART A. (General Electric Co., Cincinnati, Ohio. Nuclear Materials and Propulsion Operation). Jan. 21, 1966. Contract AT(40-1)-2847. 80p. Dep. mn. CFSTI $3.00 cy, $0.75 mn.

Separate abstracts were prepared for the four sections of the report. (W.L.G.)

For abstracts of individual sections see: 13179 and 13249–13251.

13179 (GEMP–55A, pp 13-28) OXIDATION-RESISTANT FUEL ELEMENT MATERIALS RESEARCH. (General Electric Co., Cincinnati, Ohio. Nuclear Materials and Propulsion Operation).

Laboratory testing of Fe–Cr–Al–Y-clad fueled specimens containing either UO_2 or UN exceeded 10,000 hrs at 950°C in air with no detectable surface U concentration for Fe matrix core specimens; Cr matrix core specimens showed as much as 1100 ppm U on the cladding surface. Alpha counting techniques indicate that U diffusion through Fe–15Cr–4Al–1Y cladding is equivalent for all test temperatures from 750 to 1250°C after 500 hrs. An in-pile test of a Fe–15Cr–4Al–1Y-clad Fe–40UO_2 specimen operated in the LITR at 950°C in peak flux with coolant airflow of 1700 l/min. After 1100 hrs, the magnitude of the fractional release of fission products was lower than any previous test (R/B 2×10^{-7} for ^{133}Xe) and was attributed to recoil only. Improved impact properties and higher strength at 800°C were achieved in an Fe–5Cr–6Al–3Y alloy prepared by powder metallurgy techniques. The powder was prepared by atomizing of a melt. Tensile testing of irradiated Fe–15Cr–4Al–1Y alloy shows that the strength at 600°C is generally decreased but the ductility as measured by total elongation remains unaffected by irradiation at 700°C to a fast-neutron exposure of 3.5×10^{20} nvt. Resistivity measurements indicate that effects of irradiation are annealed out at 320°C. (auth)

13180 (IS-RD–4) REACTOR MATERIALS DEVELOPMENT QUARTERLY [REPORT], OCTOBER–DECEMBER 1965. Voigt, A. F. (ed.) (Ames Lab., Iowa State Univ. of Science and Tech.). Contract W-7405-eng-42. 32p. Dep. mn. CFSTI $2.00 cy, $0.50 mn.

Progress in studies on metal preparation and purification, phase diagrams, reactor materials development, and properties of materials at high temperatures is reported. (W.L.G.)

13181 (K-L–6076) ALLOY POWDER PREPARATION BY FLAME REDUCTION TECHNIQUES. Smiley, S. H.; Brater, D. C.; Kaufman, H. L. (Oak Ridge Gaseous Diffusion Plant, Tenn.). [1965]. Contract W-7405-eng-26. 26p. (CONF-660205–2). Dep. mn. CFSTI $2.00 cy, $0.50 mn.

From Metallurgical Society of the American Institute of Mining, Metallurgical, and Petroleum Engineers, New York.

The preparation of high purity W–Re powders by the H_2 reduction of the volatile fluorides using a unique flame process is described. The technological and economic potential of a fluoride volatility process for recovering valuable fabrication scrap, out-of-specification flame reduction powder, and other reject materials is discussed in detail. Preliminary estimates of reconversion costs of the hexafluorides to high purity alloy powders are included. (W.L.G.)

13182 (TID–4005(Pt.1, 9th Ed.)) SUMMARIES OF THE USAEC BASIC RESEARCH PROGRAMS IN METALLURGY, SOLID STATE PHYSICS AND CERAMICS (FISCAL YEAR 1965). (Division of Research (AEC), Washington, D. C.). Jan. 1966. 485p. Dep. mn. CFSTI $5.00 cy, $2.25 mn.

Indexes prepared by Division of Technical Information Extension (AEC), Oak Ridge, Tenn.

The summary covers the fiscal year 1965 and is divided into two parts according to research done in AEC laboratories and elsewhere. (W.L.G.)

13183 (TID–6506(Pt.2, 3rd Ed.)) SUMMARIES OF FUELS AND MATERIALS DEVELOPMENT PROGRAMS, MATERIALS RESEARCH UNDER REACTOR PROGRAMS. Rice, William L. R. (ed.) (Division of Reactor Development and Technology (AEC), Washington, D. C.). May 1965. 84p. Dep. mn. CFSTI $3.00 cy, $0.75 mn.

The research is identified by the reactor project. The contractors are listed alphabetically and a subject index is included. For those contracts having a number of tasks with separate objectives, each task is summarized separately. (W.L.G.)

13184 (TID-11295(Pt.1, 4th Ed.)) NUCLEAR FUELS AND MATERIALS DEVELOPMENT. Rice, William L. R. (ed.) (Division of Reactor Development and Technology (AEC), Washington, D. C.). June 1965. 146p. Dep. mn. CFSTI $5.00 cy, $1.00 mn.

Work performed under the Advanced Reactor Technology program of the Division of Reactor Development and Technology, materials projects authorized by the U. S.-Euratom Joint Research and Development Board, and other related materials developments during the calander year 1964 are summarized. Work is identified by site, rather than topic. (W.L.G.)

13185 (TID-22424) FEDERAL MATERIALS RESEARCH PROGRAM—OPPORTUNITIES, ROADBLOCKS, [AND] PROBLEMS. (Federal Council for Science and Technology, Washington, D. C. Coordinating Committee on Materials Research and Development). Nov. 1965. 33p. Dep. mn. CFSTI $2.00 cy, $0.50 mn.

Some of the areas of research in materials that the Coordinating Committee on Materials Research and Development believes should receive increased emphasis are identified. Only subjects of significant importance to more than one Federal agency are discussed. Because of this, problems and readblocks not recognized as of direct concern to any agency are not included, even though they may be of national importance. The major technical materials problems of most general concern to the Federal government are high temperature materials, high strength-light weight materials and the degradation of materials in use. (auth)

13186 (TRG-Report-840) STEELS DATA MANUAL. Properties of Interest in Reactor Design. Seddon, B. J. (comp.) (Reactor Group, United Kingdom Atomic Energy Authority, Risley (England)). Apr. 9, 1965. 218p. (R-1788). Dep. BIS $7.00. HMSO 35s.

A compilation of the physical, mechanical, chemical, and irradiation properties of several steels of interest in reactor technology, particularly for pressure vessels and canning materials, is presented. These steels include: low-carbon high-manganese steels, low-alloy Cr-Mo steels, 9 Cr-1 Mo steel, 12% Cr steels, and the austenitic stainless steels. (W.L.G.)

13187 ELECTROLYTIC SWAB ETCHING FOR THE METALLOGRAPHY OF PLUTONIUM. Greeson, R. L.; Johns, W. L.; Jackson, R. J. (Dow Chemical Co., Golden, Colo.). J. Nucl. Mater., 18: 247-51(1966).

A metallographic technique employing electrolytic swab etching for the structural delineation of plutonium and its alloys is described. Also presented is a discussion of the etching solutions and conditions along with photographic results which indicate the applicability of the method. (auth)

13188 CONTROLLED EXPANSION OF UC PELLETS BY SURFACE OXIDATION IN A CLADDING. Mustacchi, C.; Wahl, H.; Gautsch, O. (EURATOM, Ispra, Italy). J. Nucl. Mater., 18: 206-9(Feb. 1966).

An experiment was made to improve the heat transfer from a UC fuel element to the metallic cladding by controlled chemical swelling of the pellet surface. As a result, an improvement of the conductance by a factor of 2 was found. (auth)

13189 SOME SPECIAL CHARACTERISTICS OF PROCESSES FOR GROWING HIGH-MELTING CRYSTALS IN HIGH-FREQUENCY PLASMA BURNERS. Donskoi, A. V.; Dresvin, S. V.; Voronin, K. K.; Volynets, F. K. (Leningrad Polytechnic Inst.). Teplofiz. Vysok. Temp., 3: 627-31(July-Aug. 1965). (In Russian).

Construction details of a high frequency burner which assures long term operation at sufficiently high values of the discharge power are presented. The simplest type of induction plasma burner consists of an inductive discharge without electrodes in a quartz tube. By blowing gas through the tube, a plasma flame is formed at the end of the tube which resembles an ordinary chemical flame. Feed source for the burner is a lamp generator with a power of 5-30 kilowatts and a frequency of 1-60 megacycles. If no measures were taken for heat shielding the quartz walls of the tube against the high temperatures of the plasma (9000-10,500°K), the walls would melt within 20-30 sec. Three shielding methods are outlined: (1) burner with forced gas cooling of the tube, (2) burner with water cooling, and (3) burner with cooling coils. To obtain crystals of high melting materials in a high frequency plasma burner with a metal water-cooled chamber, the standard powder for a gas flame burner is used. Crystal growth is 13-15 mm/hour. A long focus lens is used for observation of the crystal growth. Addition of a small percent of air in the argon fed to the burner improves the heat characteristics of the burner. (ATD)

13190 PROCESS FOR THE PREPARATION OF URANIUM MONOCARBIDE POWDER. Blum, Pierre; Moreau, Claude (to Commissariat l'Energie Atomique). U. S. Patent 3,223,475. Dec. 14, 1965. Priority date Aug. 5, 1959, France.

A process comprising two successive stages, one for carbonizing and the other for diffusing, is described for the preparation of a sinterable powder of UC. The process consists of introducing U powder into a sealed reaction chamber and producing a vacuum or inert atmosphere during elevation of the temperature. A gaseous aliphatic hydrocarbon is introduced into the reaction chamber and sweeps out the inert atmosphere gas if it is present. The carbonization is carried out at temperatures between 700 and 900°C and is continued until a proportion of combined carbon of 4.8% is obtained. Diffusion of the carbon is effected after evacuation of the gaseous hydrocarbon either by evacuation or by sweeping out with the inert atmosphere gas. The heating stage is preferably conducted in from 3 to 5 hr. The powdered material is continuously stirred by tumbling during both the stages. (B.L.M.)

Corrosion

Refer also to abstracts 13320 and 14021.

13191 (NASA-CR-54476) STUDIES OF ALKALI METAL CORROSION ON MATERIALS FOR ADVANCED SPACE POWER SYSTEMS. Quarterly Progress Report 4, March 26, 1965-June 26, 1965. Harrison, R. W. (General Electric Co., Cincinnati, Ohio. Space Power and Propulsion Section). Contract NAS 3-6012. 46p.

A preliminary stress corrosion reflux capsule test was terminated as a result of excessive expansion in the reduced wall sections of the capsule during the heat-up cycle. In subsequent investigations, an instrumentation error was found in the thermocouple circuitry resulting in a positive temperature error of approximately 400°F. This instrumentation error has been corrected, and another capsule was placed on test. Two additional D-43 alloy stress corrosion reflux capsules were fabricated and heat treated for 1 hr at 2400°F. One capsule was filled with potassium and installed in the test facility. A split tantalum strip heater for the boiling nucleator was designed, constructed, and installed in the test facility. The capsule test was initiated. Creep rate measurements indicated a faster rate at 2250°F than calculated from pretest uniaxial creep data. After additional temperature adjustments and creep rate measurements, a temperature of 2100°F was selected to give the desired creep strain (5-10%) in the time duration specified (500-2000 hrs). (auth)

13192 (NASA-CR-54843) POTASSIUM CORROSION TEST LOOP DEVELOPMENT. Quarterly Progress Report 8, April 15, 1965-July 15, 1965. Hoffman, E. E. (ed.) (General Electric Co., Cincinnati, Ohio. Space Power and Propulsion Section). Nov. 23, 1965. Contract NAS 3-2547. 45p.

The fabrication of the Prototype Loop was completed and the assembled loop mounted on the test chamber spool piece was transferred to the test site. Purification of the alkali metals for the Prototype Loop was performed. Installation

and instrumentation of the Prototype Loop was completed and the loop and spool piece were mounted on the test chamber sump. Following sealing of the test chamber, the system was baked out under vacuum for 180 hrs. The filling, flushing and sampling of the transfer system and the primary and secondary circuits of the loop was performed. Samples of sodium and potassium taken after circulating through the loop for 1 hr at 500°F analyzed less than 10 ppm oxygen. Checkout tests of the Prototype Loop equipment and controls were conducted and calibration of system instrumentation was completed prior to increasing system temperatures and flows to the design conditions. The results of the 5000-hr, 2000°F refluxing potassium capsule test to determine the compatibility of Mo–TZM alloy in a Nb–1Zr container indicate that no significant corrosion problem exists in this system at temperatures equivalent to those planned for the Prototype Loop test. (auth)

13193 (NASA-CR-54845) ADVANCED REFRACTORY ALLOY CORROSION LOOP PROGRAM. Quarterly Progress Report 2, July 15, 1965–October 15, 1965. Harrison, R. W. (ed.) (General Electric Co., Cincinnati, Ohio. Space Power and Propulsion Section). Oct. 29, 1965. Contract NAS3-6474. 26p.

Progress in material procurement, alkali metal purification, loop design, and quality assurance efforts directed towards the fabrication, operation, and evaluation of a potassium corrosion test loop constructed of T-111 tantalum alloy is reported. (W.L.G.)

13194 CONTACT REACTION OF TITANIUM WITH NIOBIUM CARBIDE ON GRAPHITE. Sigalovich, V. V.; Volkova, G. A. Izv. Akad. Nauk SSSR, Neorg. Mater., 1: 1345-8(Aug. 1965). (In Russian).

During the reaction of fused titanium with niobium carbide, which was deposited as thin layers on graphite, a film between the melt and the carbide was formed with a 1- or a 2-phase structure, corresponding to the phase diagram of the Ti–Nb–C system. The thickness of the intermediary film increased with an increase in the temperature and duration of the annealing. (tr-auth)

13195 KINETICS OF MOLYBDENUM DISILICIDE OXIDATION AT 1500 TO 1800 deg C. Ivanov, V. E.; Nechiporenko, E. P.; Zmii, V. I.; Krivoruchko, V. M.; Verkhorobin, L. F.; Aleksandrov, O. M.; Mitrofanov, A. S.; Poltavtsev, N. S. (Inst. of Physics and Tech., Academy of Sciences, Ukrainian SSR). Izv. Akad. Nauk SSSR, Neorg. Mater., 1: 1354-9(Aug. 1965). (In Russian).

The oxidation kinetics of $MoSi_2$ were investigated from 1500 to 1800°C. It was established that the rate of oxidation of $MoSi_2$ depends on the temperature and the degree of its homogeneity. The increase of the oxide film follows a parabolic law, which indicates its protective properties up to 1800°C. The oxidation rate of $MoSi_2$ has a linear dependence on the orientation of its crystal. (tr-auth)

13196 OXIDATION OF TUNGSTEN DISILICIDE AT 1500 TO 1800 deg C. Ivanov, V. E.; Nechiporenko, E. P.; Krivoruchko, V. M.; Zmii, V. I.; Mitrofanov, A. S.; Aleksandrov, O. M. (Inst. of Physics and Tech., Academy of Sciences, Ukrainian SSR). Izv. Akad. Nauk SSSR, Neorg. Mater., 1: 1360-3(Aug. 1965). (In Russian).

The oxidation kinetics of WSi_2 were investigated from 1500 to 1800°C. The oxidation kinetic curves were parabolic. The effect of the preparation temperature and degree of homogeneity of the sample of WSi_2 on the oxidation rate was investigated. It was shown that the oxidation rate of WSi_2 at 1500 to 1700°C is approximately the same as that of $MoSi_2$, but is somewhat lower at 1800°C. (tr-auth)

13197 OXIDATION OF TANTALUM DISILICIDE IN TEMPERATURE RANGE FROM 1400 TO 1600 DEG C. Ivanov, V. E.; Nechiporenko, E. P.; Krivoruchko, V. M.; Zmii, V. I.; Mitrofanov, A. S.; Aleksandrov, O. M. (Inst. of Physics and Tech., Academy of Sciences, Ukrainian SSR). Izv. Akad. Nauk SSSR, Neorg. Mater., 1: 1364-7(Aug. 1965). (In Russian).

The oxidation kinetics of $TaSi_2$ were investigated from 1400 to 1600°C. The $TaSi_2$ was produced by the vacuum method. The effect of the temperature of preparation of the sample and the degree of homogeneity on its oxidation rate was established. The oxidation of $TaSi_2$ in the primary stages follows a linear dependence. After a given time interval, Ta_5Si_3 appears and an abrupt increase of the oxidation rate occurs that leads to its disintegration. The possibility of a thermal stabilization of $TaSi_2$ to 1600°C was shown. (tr-auth)

13198 OXIDATION OF LOWER TUNGSTEN AND MOLYBDENUM SILICIDES. Efimenko, L. N.; Verkhorobin, L. F.; Shbydchenko, A. G. (Inst. of Physics and Tech., Academy of Sciences, Ukrainian SSR). Izv. Akad. Nauk SSSR, Neorg. Mater., 1: 1911-16(Nov. 1965). (In Russian).

Monophase samples of the lower silicides of tungsten and molybdenum (W_5Si_3 and Mo_5Si_3) were prepared in a vacuum by exposure of the metal to silicon. The oxidation kinetics of W_5Si_3 and Mo_5Si_3 in the atmosphere were investigated in the temperature range from 500 to 1000°C. The phase structures of the oxides formed were determined and an oxidation mechanism proposed. It is shown that the lower oxides of W and Mo are less stable with respect to oxidation than the disilicides. (tr-auth)

13199 CONTRIBUTION TO THE STUDY OF THE SAFETY OF USE OF MAGNESIUM ALLOY CLADDING IN REACTORS COOLED BY CARBON DIOXIDE. Baque, P.; Darras, R. (CEN, Saclay, France). J. Nucl. Mater., 17: 283-93(Dec. 1965). (In French).

The effects of various factors on the safety of use of magnesium alloys in nuclear reactors in the presence of carbon dioxide were analyzed. While small metallic additions have little effect on the ignition temperature of magnesium in carbon dioxide, an increase in specific surface area of the samples may increase it considerably, and self-heating then becomes serious. The ignition temperature rises with increasing pressure of carbon dioxide, diminishes very rapidly when the water vapor content rises to 3000 vpm, and diminishes steadily as the partial pressure of air or oxygen increases. Nevertheless, in the presence of carbon dioxide, even if very impure, the ignition temperatures of magnesium or of its alloys in massive form, such as fuel cans for use in graphite/CO_2 reactors, never drop below a lower limit approximately equal to the melting point of magnesium. (auth)

13200 THE CORROSION AND IGNITION BEHAVIOUR OF SOME URANIUM/PLUTONIUM/IRON ALLOYS. Picton, G.; Sackman, J. F. (Atomic Weapons Research Establishment, Aldermaston, Eng.). J. Nucl. Mater., 18: 292-304(1966).

The corrosion, both atmospheric and accelerated, and ignition behavior of uranium–plutonium alloys containing iron at approximately 5, 7, 8, and 16 at. % was studied. All ignited in air at some temperature between 100 and 315°C and only chill-cast specimens showed good corrosion resistance when exposed to moist air. Under accelerated corrosion conditions the 16 at. % iron alloy can corrode more rapidly at approximately 0% than at 95% relative humidity, owing to cracking and disintegration. It is concluded that casting conditions are the most important parameters for good corrosion and ignition behavior. (auth)

13201 KINETICS AND MECHANISM OF HYDROGEN PERMEATION OF OXIDE FILMS ON ZIRCONIUM. Smith, Tennyson (North American Aviation Science Center, Thousand Oaks, Calif.). J. Nucl. Mater., 18: 323-36(1966).

The rate of hydrogen permeation of oxide films on crystal bar zirconium samples (cylindrical with hemispherical ends) was found to be inversely proportional to the film thickness (100–2500 Å), exponentially related to the temperature (200–700°C) and related to the hydrogen pressure (1–860 mm Hg) by the function $[bP/(1 + bP)]$. An empirical equation relating the hydrogen permeation rate r, with thickness δ, temperature T, and hydrogen pressure P is: $r = (1/\delta)[bP/(1 + bP)]\, k_{b,0} \exp(-Q_b/RT) + k_{L,0} \exp$

($-Q_1/RT$), where r is expressed in moles $H_2/cm^2 \cdot sec$, $b \approx 4.6 \times 10^{-3}$, $Q_b \approx 43$ kcal/mole, $Q_l \approx 9$ kcal/mole, $k_{b,0} \approx 4 \times 10^{-3}$ moles $H_2/cm \cdot sec$ and $k_{L,0} \approx 7 \times 10^{-3}$ $N_{s,L}$, where $N_{s,L}$ is the number of the surface atoms that begin a line defect (10^{-11} to $10^{-8}/cm^2$). A theoretical interpretation is given which states that hydrogen permeation occurs by two diffusion processes; lattice interstitial diffusion of hydrogen molecules in which anion vacancies are necessary to allow motion from interstice to interstice; and line defect diffusion along easy diffusion paths such as dislocation lines or grain boundaries. (auth)

13202 STUDY ON THE SYSTEM NIOBIUM–NITROGEN. III. KINETICS OF OUTGASSING OF NIOBIUM–NITROGEN MIXED CRYSTALS IN HIGH-VACUUM. Gebhardt, E.; Duerrschnabel, W.; Hoerz, G. (Institut fuer Sondermetalle, Stuttgart). J. Nucl. Mater., 18: 149-60(Feb. 1966). (In German).

The degassing kinetics of niobium–nitrogen solid solutions were determined by annealing in high vacuum between 1630 and 1970°C. Nitrogenated niobium wires of 0.5 mm dia, containing about 3 at. % N, were resistance-heated by d-c. Continuous resistance measurements during annealing served to follow the degassing process. In order to interpret the degassing experiments, the rate and degassing laws and also the expressions for the rate constants and half-times were computed for various rate-determining sub-processes. Detectable degassing begins above 1600°C; above 2000°C a few minutes sufficed to achieve complete degassing. The degassing can be described by a rate law of second order with an activation energy of 124 kcal/mole N_2. The rate-determining factor is taken to be the recombination of nitrogen atoms at the metal surface and their subsequent desorption. A relation is quoted for the temperature dependence of the degassing rate which is valid for nitrogenated niobium samples which are thin but otherwise of arbitrary shape. (auth)

13203 A STUDY OF THE LONG-TERM COMPATIBILITY OF THERMIONIC CONVERTER MATERIALS WITH CESIUM. Hargreaves, F.; Mayo, G. T. J.; Thomas, A. G. (Allen Clark Research Centre, Towcester, Eng.). J. Nucl. Mater., 18: 212-18(Feb. 1966).

The results of previous short-term cesium compatibility studies, designed to assess the suitability of materials for use in the construction of nuclear thermionic converter devices, are outlined and compared with those of other authors. A technique of sealing into stainless steel capsules, developed during this initial work, was employed to carry out 10,000 hr tests at 450 and 550°C on a number of metals and ceramics, which were unaffected during the earlier 100 hr tests. It is concluded that suitable materials are available for use at these temperatures in cesium. The selection of metals presents few problems, but it is shown that purity is not the sole criterion in the choice of suitable alumina ceramic. In addition, evidence is presented that irradiation may have an adverse effect on the properties of otherwise satisfactory alumina. (auth)

13204 PREANODIZATION OF TANTALUM ELECTRODES. Fuss, Fred N. (to Bell Telephone Labs., Inc.). U. S. Patent 3,222,751. Dec. 14, 1965. Filed May 23, 1960.

A method of fabricating a Ta solid electrolytic capacitor comprises the steps of anodizing a mechanically worked dense Ta body, coating the body with a semiconductive layer, and depositing a counter-electrode upon and in intimate contact with the semiconductive layer. A film of Ta_2O_5 of a thickness in the range of 1000 to 3000 Å is anodically deposited on the dense Ta body, and the coated body then is heated in a vacuum at a pressure of the order of 10^{-4} mm of Hg at a temperature of the order of 1700 to 2600°C for a period of time ranging from 30 to 60 min prior to anodizing. (B.L.M.)

Fabrication

Refer also to abstracts 12945, 13261, 14105, and 14122.

13205 (AD–626622) PILOT PRODUCTION AND EVALUATION OF TANTALUM ALLOY SHEET. PART III. Summary Phase Report, April 28, 1964 to October 30, 1965. Ammon, R. L.; Filippi, A. M.; Harrod, D. L. (Westinghouse Electric Corp., Pittsburgh, Pa. Astronuclear Lab.). Contract NOw-64-0394-d. 70p. (WANL-PR-M–014). CFSTI $3.00 cy, $0.75 mn.

Two 80-pound, 4-inch diameter double arc cast T-222 ingots were produced and converted to three wide sheets. Excellent primary (forging) and secondary (rolling) fabricability was displayed by the material, and an approximately ⅓ ingot-to-sheet conversion yield was obtained. The sheets displayed physical and mechanical properties comparable to those previously reported for T-222, as well as good product consistancy. Light microscopy, electron microscopy, and x-ray-diffraction techniques were employed to study the morphology and structure of precipitated phases in T-222. Second phases present after aging T-222 were found to be dependent upon mechanical-thermal history. Analysis of metallographic and mechanical property data on T-222 indicate that the interstitial strengthening effect may result from immobilization of dislocations by strain induced precipitation and/or precipitation during cooling from the solution annealing temperature. The results also indicated that the optimum metallurgical condition for T-222 alloy is that obtained by recrystallization and solution annealing. In general, a one hour anneal at 3000°F will provide this condition. (P.C.H.)

13206 (ANL–6417) THE FABRICATION AND TESTING OF DEPLETED URANIUM BLANKET SLUGS FOR EBR-II. Burt, W. R. Jr.; McGowan, R. D.; Bean, C. H. (Argonne National Lab., Ill.). Nov. 1965. Contract W-31-109-eng-38. 21p. Dep. mn. CFSTI $1.00 cy, $0.50 mn.

The production of depleted, unalloyed-uranium blanket slugs used in fabricating blanket elements for the Experimental Breeder Reactor II is described. Slug production included conversion of UF_4 to uranium metal, ingot casting, billet breakdown and rod rolling, beta heat treatment, machining, and inspection. Emphasis is placed on evaluation of the beta heat treatment via thermal cycling tests and on grain-size uniformity of machined slugs via ultrasonic, through-transmission testing. (auth)

13207 (ANL–6893) FABRICATION AND EVALUATION OF THORIA–URANIA FUEL MATERIAL. Lynch, E. D.; Handwerk, J. H. (Argonne National Lab., Ill.). Nov. 1965. Contract W-31-109-eng-38. 29p. Dep. mn. CFSTI $2.00 cy, $0.50 mn.

Various fabrication techniques for ThO_2-UO_2 compositions such as dry-pressing, hot-pressing, and slip-casting were studied. A procedure was established for large-scale fabrication of a $ThO_2-U_3O_8$ composition to be used in a fuel loading. The effects of variables in fabrication and materials on the sintering behavior of $ThO_2-U_3O_8$ compositions were evaluated. Various samples were prepared for the evaluation of the behavior of ThO_2-UO_2 compositions under irradiation. In addition to the irradiation specimens for material evaluation, samples differing in porosity were prepared for a study of the effect of voids on irradiation behavior, and other samples were prepared for use in determining the effects of dispersed metal fibers on the irradiation behavior of ThO_2-UO_2 fuels. (auth)

13208 (ANL–6969) PRODUCTION OF PLUTONIUM MONOCARBIDE BY REACTION OF ELEMENTAL PLUTONIUM AND CARBON. Tope, William G. (Argonne National Lab., Ill.). July 1965. Contract W-7405-eng-38. 27p. Dep. mn. CFSTI $2.00 cy, $0.50 mn.

A production process was developed for forming plutonium carbide by direct reaction of the elements. The process consists of charging plutonium into a graphite crucible liner, vacuum melting, and machining the remaining excess graphite from the produced button. Carbon is controlled by reaction temperature and holding time. A 350-g melt, when cycled between 1610 and 1660°C for 45 min, will analyze 4.3 ± 0.2 wt.% carbon. Metallographic examination showed a PuC matrix with 10 to 15%

Pu_2C_3 appearing as dendrites. An unidentified precipitate exists within the Pu_2C_3 phase. A 1-kg batch, when cycled for 75 min, will analyze near 4.6 wt.% carbon. The 1-kg-size batches exhibited the same microstructure as the 350-g-size batches but were less homogeneous. Reacting at a constant temperature gave a carbon-rich core in the carbide button. Typical product impurities were 225 ppM oxygen, 20 ppM nitrogen, and a total near 1000 ppM for other minor-element impurities. Carbon content can be adjusted. A carbon-rich product can be diluted by adding either plutonium or low-carbon stock and remelting in carburized tantalum components. A carbon-poor product can be recharged into a graphite liner and reacted again. Sound castings, 0.9 cm in diameter and greater than 6 cm in length, were made by melting in a tantalum crucible and casting into tantalum-coated graphite sleeve molds. (auth)

13209 (ANL–7062) GLASSY MATERIALS FOR NUCLEAR REACTOR APPLICATIONS. Lynch, E. D. (Argonne National Lab., Ill.). Nov. 1965. Contract W-31-109-eng-38. 26p. Dep. mn. CFSTI $2.00 cy, $0.50 mn.

Studies were made to determine the feasibility of preparing fuel-bearing glasses and glasses bearing neutron-absorbing materials. Devitrification-resistant glasses were prepared that contained sufficient urania or rare-earth oxide to be used for fuel or control purposes, respectively. Fabrication methods were devised to form crystalline-glass mixtures to usable densities. Shapes were formed by pressing and sintering, warm pressing at 600°C, vibratory compaction and sintering, and extrusion at 800°C. A control-rod loading was fabricated by vibratory compaction of B_4C-glass into the cladding. Induction heating was used to bond the materials in the cladding tube. Glass-bonded uranium dioxide samples were prepared for Doppler-coefficient measurements. (auth)

13210 (AWRE/LIB/BIB/13) ULTRASONIC WELDING (1960–1965). Woolley, F. M.; Corbett, L. (Atomic Weapons Research Establishment, Aldermaston (England)). Jan. 1966. 26p. Dep. mn. BIS $0.80. HMSO 4s. 0d.

One-hundred-sixteen references are given and are arranged according to source: articles in books and periodicals, patents, Russian literature, Russian patents, reports, and bibliographies covering the period prior to 1960. Except for the reports, which are in report number order, entries are alphabetical by author. (W.L.G.)

13211 (BNWL–124) NICKEL ELECTROPLATING ON URANIUM: SURFACE PREPARATION AND PLATING SOLUTION STUDIES. Lundquist, J. R.; Stromatt, R. W. (Battelle-Northwest, Richland, Wash. Pacific Northwest Lab.). Oct. 1965. Contract AT(45-1)-1830. 36p. Dep. mn. CFSTI $2.00 cy, $0.50 mn.

An improved method for nickel electroplating on uranium is described. It was found possible in the laboratory to prepare adherent 11-μ thick plates with porosities equivalent to the porosity of 18-μ plates prepared by the standard procedure. An improved anodic etch solution, 0.32M HCl in 6.0M H_2SO_4 is used. This treatment not only provides a uniform, finely etched surface, but does so with the dissolution of less uranium metal than with the H_3PO_4–HCl anodic etch treatment. Bromide is substituted for the chloride normally present in the conventional Watts nickel plating bath. An x-ray fluorescence technique for the determination of relative porosity of nickel plated uranium specimens was also developed. The specimen is briefly anodized in a $K_4Fe(CN)_6$–KNO_3 solution, and the resulting uranyl ferrocyanide precipitate at the pore sites is determined by measurement of the intensity of the x-ray fluorescence from the iron component of the precipitate. (P.C.H.)

13212 (CEA-R–2866) FUEL CYCLE OPTIMISATION: MARGINAL VALUES OF LOSSES. Gaussens, Jacques (Commissariat a l'Energie Atomique, Saclay (France). Centre d'Etudes Nucleaires); de Lasteyrie, Bernard; Doumerc, Jean (Compagnie pour l'Etude et la Realisation de Combustibles Atomiques, Bonneuil-sur-Marne (France)). Aug. 1965. 61p. (In English and French). Dep. mn.

An analysis of the costs of uranium losses in the production of fuel elements is presented, and a method of optimizing production costs with respect to these losses is outlined. (D.C.W.)

13213 (EUR–2447.f) RECHERCHE SUR LE MATERIAU ALUMINIUM–ALUMINE FRITTOXAL EN VUE DES APPLICATIONS NUCLEAIRES. (Research on the Aluminum–Alumina Material Frittoxal with a View to Nuclear Applications). Biais, R.; Moisan, J.; Jehenson, P.; Herenguel, J. (Societe TREFIMETAUX, Argenteuil (France)). Sept. 1, 1964. 24p. Dep. mn.

A comprehensive study was made on the improvement of the characteristics and technology of sintered aluminium-alumina material fabricated by the TREFIMETAUX company under the name of Frittoxal. The starting powders are prepared by TREFIMETAUX, which has developed a process for the manufacture of fine products of degassed quality (code-letter D), degassing of the material being effected before extrusion-sintering by phased heating under 10^{-2}/mm Hg vacuum. This treatment is essential to the compactness, stability of its properties under protracted heatings at high temperature and welding behavior of the material. The first phase of the work consisted in selection of the powder grades for fabrication of the fuel-element clads and the pressure tubes. Sinters obtained by extrusion-sintering were characterized by cold and hot mechanical tests and by creep tests. The results enabled certain data to be pinpointed on the annealing of Frittoxal and on the anisotropy of the mechanical properties. An outline is also given of the research being carried out with a view to improving the general characteristics of Frittoxal and bearing in particular on the following factors: fineness of the starting powder; and purity of the basic aluminium. (P.C.H.)

13214 (EURAEC–1484) FABRICATION OF A SECOND SET OF U–Pu FUEL ELEMENTS FOR SUBSTITUTION EXPERIMENTS. Special Report No. 29. Mercier, C. (Commissariat a l'Energie Atomique, Paris (France)). Aug. 1965. 42p. Dep. mn. CFSTI $2.00 cy, $0.50 mn.

Work Performed under United States–Euratom Joint Research and Development Program.

The fabrication and composition control of homogeneous U–0.30 wt % Pu fuel rods is described. The desired isotope content was measured and controlled by counting the spontaneous fission neutrons. (W.L.G.)

13215 (ORNL–3885, pp 3-86) FUELED-GRAPHITE DEVELOPMENT. Coobs, J. H.; Sisman, O.; McCurdy, H. C. (Oak Ridge National Lab., Tenn.).

Methods for coating pyrolytic carbon to UC_2 and ThC_2 fuel particles are discussed in some detail. The results of a phase study of the pseudobinary system UC_2–ThC_2 are presented. Tabulations of thermodynamic data for the UC and UC_2 systems are given. Techniques for converting sol-gel oxide particles to carbides are discussed. Heat and irradiation tests were performed on the pyrolytic carbon coated fuel particle. Results from these tests are presented. Fuel assemblies employing carbon coated fuels were tested. (M.O.W.)

13216 (ORNL–P–1899) PREPARATION OF ISOTOPIC METALLIC FOILS AND BULK ISOTOPIC METALS FROM OXIDES. Kobisk, E. H. (Oak Ridge National Lab., Tenn.). Dec. 28, 1965. Contract W-7405-eng-26. 7p. (CONF-651055–1). Dep. mn. CFSTI $1.00 cy, $0.50 mn.

From Preparation and Standardization of Isotopic Targets and Foils Conference, Harwell, Eng.

Methods for the preparation of metallic calcium and magnesium isotopes either in bulk quantity or in thin film form are described. Special attention was given to the resistance heating method. Rare earth metals of high isotopic purity were prepared and rolled into thin foils of <1 mg/cm^2 in areal density of ~50 μin. in thickness. Rare earth metals successfully prepared by reduction-condensation with <300 ppM of reductant as im-

purity were Eu, Gd, Ho, Er, Yb, and Lu. Other possible techniques to be used are discussed. (P.C.H.)

13217 (ORNL-TM-1377) FABRICATION OF ALUMINUM-BASE IRRADIATION TEST PLATES. Martin, M. M.; Werner, W. J.; Leitten, C. F. Jr. (Oak Ridge National Lab., Tenn.). Feb. 1966. Contract W-7405-eng-26. 44p. Dep. mn. CFSTI $2.00 cy, $0.50 mn.

The fabrication of the miniature aluminum-clad plates with cores of either U_3O_8 or Nb-coated UO_2-ZrO_2 dispersed in a matrix of X8001 aluminum is described, and the results of pre-irradiation examinations of the plates are presented. (D.C.W.)

13218 (ORNL-TM-1412) BALL-MILLING OF GRAPHITE-BASE REACTOR FUEL. Witte, H. O.; Ferris, L. M. (Oak Ridge National Lab., Tenn.). Feb. 3, 1966. Contract W-7405-eng-26. 8p. Dep. mn. CFSTI $1.00 cy, $0.50 mn.

The practicality of using ball milling for fine grinding of graphite reactor fuels was evaluated briefly. The results indicated that ball milling is not a feasible approach primarily because the grinding efficiency was low. Consequently, very long grinding times would probably be required to grind rough-crushed coated particle fuels fine enough to rupture the particle coatings (approximately to 100 mesh). (auth)

13219 (RL-SEP-710) PROGRAMMED TUBE TO TUBESHEET WELDING ON HANFORD HEAT EXCHANGERS USED IN NUCLEAR PROCESSING SERVICE. Bradley, L. B. (General Electric Co., Richland, Wash. Hanford Atomic Products Operation). Jan. 1966. Contract AT (45-1)-1851. 19p. Dep. mn. CFSTI $1.00 cy, $0.50 mn.

The welding sequence of a typical automated TIG weld of the type 304L stainless steel components is given. The wiring diagram of the variable program weld controller is included. (W.L.G.)

13220 (RMI-3) QUARTERLY PROCESS SUMMARY [ON EXTRUSION OF U], JULY-SEPTEMBER 1964. (Reactive Metals, Inc., Ashtabula, Ohio). Oct. 29, 1965. Contract AT(30-1)-1405. 87p. Dep. mn. CFSTI $3.00 cy, $0.75 mn.

A comparison of extrusion pressure and grain growth response was made at the reduction ratios of 14 : 1 and 19 : 1. A practical operating range was defined in terms of billet preheat temperature and press ram speed within which extrusion was readily accomplished without the formation of coarse grain at the tube ID (duplexing). The precision extrusion of normal U was investigated via the warm extrusion route. Three experiments were conducted to study the feasibility of ECM (electrochemical machining) for drilling U billets. A summary of the work is included and the practicability of ECM analyzed for drilling and cutting of U. Two areas of improved economics of tooling costs were evaluated. Cast Stellite die inserts were compared with production tool steel dies and methods of reclaiming out of specification production mandrels are presented. Eccentricity of the pierced billet ID's continues to be a major problem. Three possible contributing sources were evaluated. These are the effects of incomplete billet upset, back extrusion of the billet during piercing, as well as press and tool alignment. Misalignment was found to be a significant factor contributing to ID eccentricities at both the rear and front of pierced billets. The Dynapak high energy rate forming equipment was investigated as a possible production tool for the extrusion of I and E "O" type U fuel elements. A pilot run was concluded which was aimed at this objective and the feasibility of this production route is discussed. (auth)

13221 INFLUENCE OF THE PRESSURE FOR PREPARATION OF SAMPLES BY PRESSING OF POWDERS ON THE BACKSCATTERING COEFFICIENTS OF β RADIATION. Krivan, V. (Katedra Radiochemie a Radiacnej Chemie Slovenskej Vysokej Skoly Technickej, Bratislava). Chem. Zvesti, 19: 699-702(1965). (In Czech).

In isotropic and 60° detection geometry, in the interval from 810 to 12,230 kp/cm^2, the effect of pressure during sample preparation by powder compaction on the value of the backscattering coefficients was investigated. For atomic numbers of the target in the interval from 13 to 82 Mev and maximum energies in the interval from 0.223 to 2.27 Mev, the independence of the backscattering coefficients on the compression pressure was confirmed. These conclusions were valid for all cases in which there was not too large a volume change during the compression. (tr-auth)

13222 STUDY OF ZIRCALOY-2-STAINLESS STEEL DIFFUSION BONDS. Perona, G. (Centro Informazioni Studi Esperienze, Milan); Sesini, R.; Nicodemi, W.; Zoja, R. J. Nucl. Mater., 18: 278-91(1966).

The nature of the layer of intermetallic diffusion on Zircaloy-stainless steel joints was investigated. Bonds were obtained by hot spontaneous diffusion and hot plastic deformation. Attempts were made to single out intermetallic compounds and their distribution in the diffusion layer. By extrapolation, the conclusion was reached that only in the presence of diffusion thicknesses of the orders of 2 μm (practically 4-5 μm) the maximum strength can be obtained since then the intermetallic compounds formed are reduced to negligible amounts. (auth)

13223 STUDY OF U + C → UC REACTION IN THE SOLID STATE, IN MIXED URANIUM AND CARBON POWDERS. PART II. Gregoire, Pierre. Mem. Sci. Rev. Met., 62: 705-20(Oct. 1965). (In French).

The reaction U + C → UC takes place in two successive stages. The second stage corresponds to a very marked anisotropy of the dimensional changes, which is due to the texture imposed on the graphite matrix by the compression of the powders. Tests showed that there is no sintering of the uranium, but a dispersion of the particles in the graphite matrix. (auth)

13224 HIGH-REMELT-TEMPERATURE BRAZING OF TANTALUM USING A DIFFUSION SINK CONCEPT. Stone, L. H.; Freedman, A. H.; Mikus, E. B. (Northrop Corp., Hawthorne, Calif.). Metals Eng. Quart., 6: 35-42(Feb. 1966).

High-remelt temperatures for brazing of joints were achieved on Ta-10W honeycomb structures by brazing with pure Ti, using diffusion sink brazing. Optimum properties were produced by a combination braze-diffusion cycle of 10 min at 3200°F in vacuum. Honeycomb and lap-joint remelt temperatures exceeded 3800°F. Lap-shear strength at 3500°F was approximately 2350 psi and honeycomb specimens withstood 1-hr stress-rupture testing at 3500°F under a 1.2 psi flatwise tensile stress. Diffusion sink brazing with Ti permitted 800°F lower processing temperatures than required for brazing with Hf-40Ta. (auth)

13225 STUDY ON THE FABRICATION OF UO_2 FUEL ELEMENT BY VIBRATORY COMPACTION. Nishiyama, Atsushi; Kasamatsu, Toshio; Ishida, Ryuichi; Yata, Minoru; Konishi, Chugo; Hasegawa, Isao; Naritomi, Tatsuo. Sumitomo Elec. Tech. Rev., No. 3, 93-7(Jan. 1964).

The vibratory compaction of UO_2 fuel was performed and the basis for the fabrication of vibrationally compacted fuel was established. Subsequently a fuel element for SOCE experiments was fabricated. (auth)

13226 THE PARTICLE SIZE OF SUBMICRON TUNGSTEN AND TUNGSTEN CARBIDE POWDERS FOR WC-Co ALLOY. Miyoshi, Akiyoshi; Doi, Yoshihiko. Sumitomo Elec. Tech. Rev., No. 4, 80-6(July 1964).

In order to control the submicron grain in cemented tungsten carbides, the relation between the morphological properties of W powders and the properties of WO_3, H_2WO_4, and $3(NH_4)_2O \cdot 12WO_3 \cdot 5H_2O$ (ammonium paratungstate), and the transition of particle sizes after the reaction W + C → WC, were studied. The permeability, the apparent and tap density, and the color of submicron W powders depended on the secondary particle size (aggregated particle size). The size of the primary (or unit) particles could be determined better by using x-ray, gas absorption, and electron micrograph methods. The secondary particle size of fine

W powders depended on the size of WO_3 particles but it was supposed that the primary particle size is subject to the rate of the H_2 reduction. The particle size of WC powders depended on the primary particle size of W powders either when the secondary particles of the W powders were the weakly point-contact-sintered aggregates, or when they were strongly plane-contact-sintered aggregates. The WC grain size of WC–Co alloy depended on the size of WC powders, if the grain growth was restrained during sintering. (auth)

13227 FABRICATION STUDY OF URANIUM NITRIDE FUEL. Nishiyama, Atsushi; Kasamatsu, Toshio; Itani, Kaichi; Katsuya, Hiroo Sumitomo Elec. Tech. Rev., No. 5, 88-93(Jan. 1965).

The preparation and sintering of UN powder was studied for fabrication of high-density sintered UN pellets for use as a nuclear fuel. A method was developed in which metallic uranium was used as the raw material and the relation among the reacting temperature, time, atmosphere, and the quality of formed UN and its composition was studied. Then the relations among the sintering temperature, sintering atmosphere, density of the sintered UN pellet, its porosity, and its composition were studied by using UN powder made from metallic uranium. The sintered UN pellet had a 93% theoretical density when it was sintered in N_2. The density was higher in vacuum and lower in argon. This pellet was light grey in external appearance and UN monophase in composition. (auth)

13228 IMPROVEMENTS IN OR RELATING TO FUEL FOR NUCLEAR REACTORS. Steele, Bernard Robert (to United Kingdom Atomic Energy Authority). British Patent 1,015,004. Dec. 31, 1965. Filed Oct. 30, 1963.

A method is patented for the production of a nuclear fuel body of UO_2 that is highly retentive of gaseous fission products while having a high resistance to swelling under irradiation. The method consists of forming a mixture of UO_2 powder, of a form which after compaction sinters to a high density, with powder of a higher oxide of U, with UO_2 predominating; limiting the mixing of the powders to a degree such that agglomerates of the powder of the higher oxide exist in a continuous matrix of the UO_2 powder; compacting the mixed powders; and sintering the compact in a reducing atmosphere so that the higher oxide becomes reduced to UO_2 prior to the actual sintering and in so doing shrinks more than does the UO_2 originally present to produce a body of high density containing discrete regions of internal porosity. (B.L.M.)

13229 PROCESS OF FABRICATION OF SINTERED COMPOUNDS BASED ON URANIUM AND PLUTONIUM. Pascard, Roger (to Commissariat a l'Energie Atomique). Canadian Patent 723,583. Dec. 14, 1965.

A U–Pu alloy prepared in an arc furnace with a Pu content of 15–80% is ground in an inert atmosphere of argon. Metallic or non-metallic elements may be incorporated into the alloy possibly to form compounds. After compression and sintering under vacuum at about 1450°C useful high-density reactor fuels are obtained. (F.S.A.)

13230 HOT PRESSING ZIRCONIA. Robinson, Lawrence B.; Vahldiek, Fred W.; Lynch, Charles T. (to U. S. Air Force). U. S. Patent 3,218,673. Nov. 23, 1965. Filed Sept. 26, 1963.

A method and apparatus are described for producing hard and dense refractory inorganic materials, particularly zirconia, of uniform and fine-grained structure close to the theoretical density of the material. A specimen enclosing cell is removably inserted within a pressure cylinder. The cell comprises the following concentric tubes or sleeves: a platinum tube for enclosing the specimen, a first BN insulation sleeve, a C-SiC heater, a second BN insulation sleeve, and a lava insulation sleeve. A pair of lava plugs are disposed on the axially opposite sides of the Pt enclosed specimen, and a pair of C inserts are on the axially opposite sides of the pair of lava plugs. The specimen is placed in the holder and subjected to pressures of up to 18,000 atm. and temperatures of up to 1800°C. (B.L.M.)

13231 PROCESS FOR ASSEMBLING CONCENTRICALLY SPACED NUCLEAR FUEL ELEMENTS. Zambrow, John L.; Litt, Benjamin (to Sylvania Electric Products, Inc.). U. S. Patent 3,222,773. Dec. 14, 1965. Filed Aug. 29, 1960.

A method is described for assembling cylinders within tubes to close tolerances, to obtain uniform spacing along the entire common length of the cylinders and to provide spacers for use between cylinders and tubes which will not vibrate because of flow between the tube and cylinder. The method is particularly applicable to the fabrication of an outer tubular fuel element covered with cladding material and an inner cylindrical fuel element covered with cladding material. An intermediate tube is passed over the inner fuel element. The intermediate tube has a number of radially extending holes spaced apart from one another, and dowels having a length sufficient to engage the outer tube and the inner cylinder when they are in spaced relationship and having one metallic surface are placed in the holes. An outer sheath is slipped over the assembly, and then the dowels are metallurgically bonded to either the inner or outer elements by a hot pressing procedure. Then the outer tube is removed by dissolution in a suitable solvent. (B.L.M.)

Properties and Structure

See also CHEMISTRY — Inorganic and Physical Chemistry
PHYSICS — Solid State Physics

Refer also to abstracts 13029, 13205, and 13213.

13232 (AGN–8162) ALKALI METALS EVALUATION PROGRAM. FORCED CONVECTION CONDENSING HEAT TRANSFER FOR RUBIDIUM AND CESIUM. Fisher, C. R. (Aerojet-General Nucleonics, San Ramon, Calif.). Jan. 1966. Contract AT(04-3)-368. 73p. Dep. mn. CFSTI $3.00 cy, $0.75 mn.

Investigations were made of the heat transfer characteristics of rubidium and cesium under conditions of forced convection condensation in a round tube in both vertical and horizontal orientations. The experiments were performed in type 316 stainless steel loop, with a nickel test section. Data were obtained at temperatures up to 1360°F. Operating parameters were varied to obtain information useful for the design of condensers for space power systems. The data are presented in tabular form. Experimental uncertainties are discussed in detail. Useful data on thermophysical properties of the fluids studied are presented. (auth)

13233 (ANL–6943) A NEUTRON-DIFFRACTION STUDY OF URANYL NITRATE HEXAHYDRATE. Final Report, Program 4.1.29. Taylor, J. C.; Mueller, M. H. (Argonne National Lab., Ill.). Nov. 1965. Contract W-31-109-eng-38. 57p. Dep. mn. CFSTI $3.00 cy, $0.75 mn.

The crystal structure of uranyl nitrate hexahydrate, $UO_2(NO_3)_2 \cdot 6H_2O$, was determined by neutron diffraction. The crystals are orthorhombic with $a = 13.197 \pm 0.003$, $b = 8.035 \pm 0.002$, $c = 11.467 \pm 0.003$ Å, and belong to the space group $Cmc2_1$. Complete neutron-diffraction data to $2\theta = 105°$ were collected (1136 independent reflections, 25 unobservably small) with a neutron wavelength of 1.065 Å. The structure was solved from the three-dimensional neutron Patterson and Fourier syntheses and refined by full-matrix least squares. Separate refinements were carried out with the following three different weighting schemes: $w = 1$, $w = |F|$, and a scheme based on the counting statistics. The final weighted R-factors were 7.5, 4.5, and 3.9%, respectively, and the results were within experimental error of each other. Six oxygen atoms are bound to the uranyl grouping in its equatorial plane, forming an irregular hexa-

gon around it. Four of these oxygens are from the two non-equivalent, bidentate nitrate groups, and the other two are reflection-equivalent, water-oxygen atoms. In the nitrate groups, the N–O bonds involving oxygens covalently bound to the uranium are about 0.03 to 0.05 Å longer than the N–O bonds not involved in U–O bonding; also the O–N–O angles differ significantly from 120°. All the hydrogen atoms are involved in hydrogen bonding that can be divided into (a) O(water) ... O(water) hydrogen bonds of length 2.68–2.76 Å and (b) weaker O(water ... O(nitrate) hydrogen bonds of length 2.92 and 3.00 Å. The observed O–H distances in the water molecule, when corrected for the effects of thermal motion, lie between 0.92 and 1.14 Å. The water angles are 106.9, 106.8, and 114.6°. (auth)

13234 (ANL–7094) REVIEW OF STATUS OF SELF-DIFFUSION IN US, UN, UO_2, AND UC. Walter, C. M. (Argonne National Lab., Ill.). Nov. 1965. Contract W-31-109-eng-38. 25p. Dep. mn. CFSTI $2.00 cy, $0.50 mn.

The nature of imperfections and their contribution to the diffusion mechanism are of primary interest in a self-diffusion study. With this in mind, the literature on US, UN, UO_2, and UC was reviewed. The state of knowledge of UO_2 was found to be much more advanced than for the other materials considered. (49 references). (J.B.)

13235 (BMI–1755) PHASE EQUILIBRIA IN THE URANIUM–TUNGSTEN–OXYGEN SYSTEM. Smith, Roy A.; Kizer, Donald E.; Speidel, Edward O.; Keller, Donald L. (Battelle Memorial Inst., Columbus, Ohio). Jan. 17, 1966. Contract W-7405-eng-92. 22p. Dep. mn. CFSTI $0.50 cy, $0.50 mn.

A ternary eutectic, oxygen-8 at. % uranium-22 at. % tungsten, melting between 1300 and 1325°C was found to lie within a UO_2–U_xWO_3–tungsten three-phase region. This ternary-eutectic composition is near an apparent quasi-binary UO_2–U_xWO_3 eutectic. Fragmentary data suggest a low-melting (1300°C or below) ternary eutectic between UO_2, U_xWO_3, and UO_2WO_4 on the oxygen-rich side of the UO_2–U_xWO_3 quasi-binary. Between 1250 and 1300°C, the U_xWO_3–UO_2–tungsten region is split into UO_2–U_xWO_3–WO_2 and UO_2–WO_2–tungsten regions by a peritectoid reaction between U_xWO_3 and tungsten to form UO_2 and WO_2. At 1800°C, liquid-phase formation was observable in alloys on the oxygen-rich side of a $UO_{2.012}$–tungsten tie line. Negligible chemical interaction of molten UO_2 and tungsten at 2800°C indicates that UO_2 and tungsten form a eutectic or divorced peritectic near UO_2. (auth)

13236 (CEA–R–2797) METHODE D'ANALYSE CALOMETRIQUE EN REGIME VARIABLE. (Method for Calorimetric Analysis in Variable Conditions). Berthier, Guy (Commissariat a l'Energie Atomique, Saclay (France). Centre d'Etudes Nucleaires). Nov. 1965. 99p. Dep. mn.

It is reported that by analysis of the transitory thermal conditions given by the quenching of a sample in a furnace maintained at a high temperature, it is possible to study the thermal diffusivity of some materials, and that of solid state structure transformation on a qualitative as well as quantitative standpoint. As examples, the transformation energy of α-quartz into β-quartz and the Wigner energy stored within neutron irradiated beryllium oxide were measured. (auth)

13237 (CONF–170, pp 29-47) AGEING EFFECTS ON BERYLLIUM SINGLE CRYSTALS. Beasley, D.; Moore, A. (Oak Ridge National Lab., Tenn.).

A study was made of the effect of thermal treatment on both the flow stress and the occurrence of yield point phenomena of single crystals of Be. Vacuum-cast-and-extruded electrolytic flake metal of two grades, commercial Pechiney and S. R. Pechiney were refined by a vertical floating zone technique using between 1 and 6 passes. Crystals in the solutionized condition, i.e., 2 hrs at 800°C and oil quenched relative to the precipitation ageing process, were subsequently aged between 200 and 550°C. Over the range 350 to 550°C a progressive increase in flow stress was observed reaching a maximum after times of ~150 and ½ hrs respectively, and followed by a decrease. At 200 to 300°C the change in flow stress was erratic. After a total of 5 passes the effect was present at 350°C, but undetectable at 450°C. No such changes were detected in crystals initially conditioned by an overageing treatment of 500 hrs at 575°C and oil quenched, although a marked decrease (55%) in flow stress at 450°C relative to that of the solutionized condition was observed. Derivations of the activation energy for these low temperature ageing processes suggest that the reaction is two stage each associated with 16 and 48 kcals/g-mole, respectively. It is argued that an interstitial atom, possibly C, is associated with the initial part of the ageing process and subsequently a substitutional atom becomes involved: it may be that an interstitial impurity precipitates and forms a nucleus for a substitution impurity which was previously considered not too nucleate below 575°C. The present differences in flow stress between single crystals initially solutionized and overaged at temperatures ~575°C are in marked contrast to corresponding behavior in polycrystalline material where differences ~10% were observed. Strain ageing effects were observed in crystals tested in the solutionized condition over the range 300 to 390°C. The activation energy for yield point return was calculated to be ~19 kcals/g-mole, whereas yield point loss in the range 490 to 540°C was related to dislocation locking by an interstitial impurity, possibly C, and subsequent coalescence as a precipitate within the matrix. This latter observation was supported, though not proved conclusively by low angle X-ray diffraction studies. (auth)

13238 (CONF–170, pp 48-68) BASAL PLANE FRACTURE OF BERYLLIUM SINGLE CRYSTALS. Herman, M.; Spangler, G. E. (Oak Ridge National Lab., Tenn.).

Single crystals of Be prepared by zone melting were tensile tested at room temperature with orientations such that basal glide was the principal deformation system. Fracture occurred in most cases by cleavage on the basal plane where the extent of deformation prior to fracture was enhanced by the effect of purification. This improvement in ductility resulted from lowering the critical resolved shear stress and the work hardening characteristics and minimizing crack nucleating precipitates. The results were analyzed with respect to two theoretical treatments for the propagation of cleavage cracks in metals which can glide and cleave on the same crystallographic plane. The first considers the conditions for propagating a crack nucleated by the splitting of a wall of dislocations while the second considers the case where a dislocation pile-up is responsible for the crack. Both schemes evolve similar stress relations but differ in the dependence of fracture on crystal orientation. The results of the analysis indicate that the cleavage of beryllium on the basal plane during tensile testing is associated with the split bend plane mechanism of crack initiation and propagation. (auth)

13239 (CONF–170, pp 90-101) THE EFFECT OF PURIFICATION AND RECONTAMINATION ON (0001) AND ($10\bar{1}0$) SLIP IN BERYLLIUM SINGLE CRYSTALS. Tristem, C. E. R.; Moore, A. (Oak Ridge National Lab., Tenn.).

Be single crystals of greater than 99.95% purity were used for the determination of critical resolved shear stress of both (0001) and ($10\bar{1}0$) slip from 20 to 600°C. Compared with corresponding work on crystals of about 99.85% purity there was a decrease at 20°C from about 2000 to 400 psi in (0001) slip and a proportionally much smaller decrease in ($10\bar{1}0$) slip, from 11,000 to 7000 psi. At higher temperatures both these decreases are less marked. All tests were carried out on single crystals, oriented for slip on a single system, and grown from the melt using a vertical floating zone technique in an atmosphere of Ar 99.995% pure. Up to six zone passes were carried out; and preliminary analysis indicates that C, about 100 ppm, is the main impurity remaining after zone refining. Evidence was obtained that implies that the ultra-pure Be, obtained by zone refining metal of base purity 99.95% six times, may be readily contaminated by annealing in a dynamic vacuum (5×10^{-6} cm of Hg) at 1000°C for 18 hrs in such a way that the critical resolved shear stress at 20°C for (0001) slip

increases from 400 to 1200 psi. Up to about ⅓ of this increase can be attributed to an oxide coating; and it is concluded that an impurity from the dynamic vacuum, possibly C, diffuses into the Be crystal. It was not determined to what extent contamination of the crystal affects prismatic slip. Purification, however, clearly facilitates slip; but to evaluate the effect, recontamination during testing and annealing must be prevented. (auth)

13240 (CONF–170, pp 102-20) AN ACCOUNT OF DEFORMATION AND FRACTURE IN SINGLE AND POLYCRYSTALLINE BERYLLIUM BETWEEN 20 AND 450 deg C. Moore, A.; Ellis, G. C. (Oak Ridge National Lab., Tenn.).

Compression tests were made at 165 to 280°C on single crystals (99.85%) oriented such that the resolved shear component in ⟨hko⟩ was zero. Between 280 and 195°C these crystals appeared to slip on $(10\bar{1}1)$ and assuming slip occurred in the closest packed direction, ⟨1123⟩, the critical resolved shear stress for slip, neglecting friction, is ~42,000 psi. This resolved shear stress is high and comparable with the cohesive strength of polycrystalline Be. Pyramidal slip was not observed below 195°C, but strains ~3% were accommodated by twinning on $(10\bar{1}2)$ and basal slip within the twinned regions. The appearance of $(10\bar{1}2)$ twins in crystals compressed in the c-direction is not expected for this requires extension in the c-direction. However, Be can deform in three directions mutually at right angles above 195°C, but slip appears to be restricted to ⟨hko⟩ directions below 195°C. This restriction is believed to be the basis of the ductile-brittle transition that occurs in the region 150 to 200°C. These general conclusions were supported in studies using polycrystalline Be tested in tension at 150°C and examined both metallographically and by Laue asterism. The studies showed that although prolific (0001) and $(10\bar{1}0)$ slip occurs in ⟨1120⟩, slip on $(10\bar{1}1)$ also occurs in an unknown direction out of the basal plane. Although this latter work requires confirmation, it is believed that slip on $(10\bar{1}1)$ in ⟨hkl⟩ occurs to relieve strains induced in neighboring grains by slip in ⟨1120⟩ and on (0001) and $(10\bar{1}0)$. (W.L.G.)

13241 (CONF-170, pp 121-5) DISCUSSION OF "AN ACCOUNT OF DEFORMATION AND FRACTURE IN SINGLE AND POLYCRYSTALLINE BERYLLIUM BETWEEN 20 AND 450°C" BY A. MOORE AND G. C. ELLIS. Jacobson, Martin I. (Lockheed Missiles and Space Co., Palo Alto, Calif.).

Samples were cut from extruded rods with the specimen axes either parallel or at 45° to the extrusion direction. This produced samples favorably oriented for duplex prismatic slip and for basal slip, respectively. The duplex prismatic slip specimens exhibited an increase in tensile strength, a decrease in yield strength, and an increase in elongation as the temperature was varied from –200 to 100°C. The basal slip specimens showed a decrease in tensile strength, a lesser decrease in the yield strength, and a less rapid rate of decrease in elongation than the duplex prismatic slip specimens. At certain temperatures, the ductilities of the basal slip specimens were greater than the duplex prismatic slip specimens. The relation between the strengths and ductilities of the two types of specimens is explained on the basis of twinning. (W.L.G.)

13242 (CONF–170, pp 126-37) BURGER'S VECTORS IN BERYLLIUM AND THEIR EFFECT ON DUCTILITY. Walters, G. P.; Van Der Walt, C. M.; Makin, M. J. (Oak Ridge National Lab., Tenn.). (AERE-R–4287).

Thin film electron microscope and selected area diffraction techniques were used to determine the possible Burger's vectors in Be. Dislocation loops and dislocations having various vectors were observed and likely slip directions determined. Slip in directions out of the basal plane was observed at room temperature in thin foils. These slip directions may not operate in bulk material at room temperature if the critical resolved shear stress is high. Twinning may be the more favorable deformation mode. However, if the critical resolved shear stress for slip out of the basal plane is lowered by purification, then the slip modes observed in thin foil experiments might operate in bulk material at room temperature. (auth)

13243 (CONF–170, pp 160-83) THE RECRYSTALLISATION CHARACTERISTICS OF WROUGHT INGOT BERYLLIUM SHEET. Cheer, D. A.; Lowe, J. N. (Oak Ridge National Lab., Tenn.).

Extrapolation of previous results showed that reducing the grain size to approximately 10 μ would produce a decrease in the ductile to brittle transition temperature to room temperature. The complete range of subrecrystallization working temperatures and subsequent annealing treatments were covered systematically in an attempt to produce fine grained Be sheet. The gr..in size of wrought sheet could not be reduced below 30 μ by conventional warm working and recrystallization techniques. The limiting factor was the inability to produce homogeneous nucleation due to heterogeneous deformation resulting from the limited number of available slip systems. Recovery processes precede recrystallization and although connected with the kinetics of recrystallization, do not affect the final grain size. (W.L.G.)

13244 (CONF–170, pp 221-44) THE STRUCTURAL APPLICATION OF BERYLLIUM IN THE U. K. Worker, J. M.; Moore, A.; Ellis, G. C. (Oak Ridge National Lab., Tenn.).

The purity, texture, strength, grain size, and formability of both powder and ingot Be were measured and structural applications most beneficial to each form were suggested. The high rigidity of Be provided care is exercised to minimize machining and fitting damage, can be exploited for specialized structural aircraft components. Ductile crack propagation is possible in cross rolled ingot sheet and is comparable to Mg alloy sheet used structurally in aircraft. The material damping of Be is comparable to Al, but this is of no consequence as the required damping in a structure can be obtained from carefully designed joints. Dimensional stability involves the usual factors that effect internal stress and also the study of low temperature ageing. An incomplete survey of mechanical properties showed a fatigue limit at room temperature of >85% UTS in mean stress P, ±0.9P range loading cycle. This could be associated with limited slip modes below the brittle-ductile temperature, but it is anticipated that in the ductile temperature region conventional fatigue limits of 55% UTS are expected. (W.L.G.)

13245 (CONF-651017–7) YIELD POINT OCCURRENCE IN POLYCRYSTALLINE ALPHA-ZIRCONIUM. Weinstein, D. (IIT Research Inst., Chicago, Ill. Metals Research Div.). [1965]. Contract AT(11-1)-578. 32p. Dep. mn. CFSTI $2.00 cy, $0.50 mn.

From Electrochemical Society Meeting, Buffalo.

An abrupt yield point was found to exist during the tensile deformation of high-purity zirconium having grain diameters smaller than 0.0065 mm. Yield point occurrence was favored by air cooling from the recrystallization temperature as compared to water quenching. Specimens cut transverse to the rolling direction showed greater yield drops, and the discontinuity persisted to larger grain sizes. Existence of a yield point was favored at temperatures above –22°C, and disappearance of abrupt yield was noted at lower temperatures. It is shown that a Cottrell pinning/subsequent-unpinning mechanism does not account for the results; other mechanisms proposed for yield point occurrence in zirconium were examined in the light of these data. On the basis of supplementary microstraining experiments and in consideration of other known deformation characteristics of zirconium, the occurrence of a yield point is best explained by the dynamic dislocation model for yielding in body-centered cubic materials. (auth)

13246 (CONF-651017–13) SOME EFFECTS OF PRESTRAIN AT 77 DEG K ON THE MECHANICAL PROPERTIES OF ZIRCONIUM AT ROOM TEMPERATURE. Reed-Hill, R. E.; Dahlberg, E. P. (Florida Univ., Gainesville. Dept. of Metallurgical and Materials Engineering). Oct. 1965. Contract AT(40-1)-3262. 27p. Dep. mn. CFSTI $2.00 cy, $0.50 mn.

From Electrochemical Society Meeting, Buffalo.

The effects of twinning on the ductility of zirconium at room temperature and deformation at 77°K are discussed. Newly discovered effects of twinning by prestrain at 77°K on the mechanical properties of Zr at room temperature are reported and discussed. (P.C.H.)

13247 (GA–6831) ADVANCED GRAPHITE FUEL SYSTEMS. Quarterly Progress Report for the Period Ending November 14, 1965. Bokros, J. C.; Engle, G. B.; Goeddel, W. V.; Price, R. J.; White, J. L. (General Atomic, San Diego, Calif. John Jay Hopkins Lab. for Pure and Applied Science). Dec. 10, 1965. Contract AT(04-3)-167. 51p. Dep. mn. CFSTI $3.00 cy, $0.50 mn.

Developments in studies on the relation between binder-filler interactions and the microstructure, preferred orientation, selected physical properties, and irradiation behavior of molded graphite bodies are reported. Molded bodies containing natural flake graphite showed that the molding process causes extensive damage to the flakes by bending, twinning, and delamination; subsequent heat-treatment had little further effect. The calcined coke particles used in the molded bodies showed two types of structure: a lamellar structure suggestive of flow at some stage in coking; and a non-lamellar structure which includes relatively large non-graphitic regions. Investigations directed toward relating the preferred orientation and thermal expansion coefficient for non-graphitic carbons indicated a systematic dependence between the two variables similar to that observed for well-crystallized graphite. Final results of thermal conductivity measurements performed on seven pyrolytic carbon coatings, irradiated at 540 to 1060°C and to an exposure of $>10^{21}$ nvt (fast) in capsule G-9, confirmed that: low-density isotropic carbons show no change in conductivity; granular and medium-to-high density isotropic carbons decrease in conductivity; and laminar carbons increase in conductivity. Mechanical property measurements on the same pyrolytic carbon specimens indicated that the elastic modulus increased sharply for all structures, i.e., from 30 to 100%. The relationship between radio-induced length changes and preferred orientation in polycrystalline graphite was investigated by measuring the pre- and post-irradiation dimensions of samples which were cut from an extruded graphite tube and had different preferred orientations. (P.C.H.)

13248 (GEAP–4678) FRACTURE MECHANICS AND THE STABILITY OF ENGINEERING STRUCTURES. Reynolds, M. B. (General Electric Co., San Jose, Calif. Atomic Power Equipment Dept.). Sept. 1965. Contract AT(04-3)-189. 55p. Dep. mn. CFSTI $3.00 cy, $0.50 mn.

A review is presented on the stability of engineering structures. Catastrophic failures in structures are of two types: those resulting from the very rapid propagation of a brittle crack; and those of the ductile tearing type. The conditions for unstable deformation are developed by examining the deformation behavior of a solid cylinder under uniaxial tension. The effect of both the stress-strain characteristics of the material and the stiffness of the applied load are considered. It is shown that for stability the condition $(dP/d\lambda) \geq -k$ must be satisfied, where k is the stiffness of the applied load and $dP/d\lambda$ is the slope of the load-deformation curve for the structure. The Tresca and von Mises criteria for plastic yielding under multiaxial stresses are given, followed by review of several papers on the homogeneous plastic deformation of hollow spheres and cylinders under internal pressure. The Griffith and Irwin criteria for stability of a brittle crack are described, followed by development of the fracture toughness concept and discussion of the corrections necessary to apply the Griffith-Irwin fracture mechanics to relatively ductile materials. The brittle-ductile fracture transition is described in terms of the effect of temperature on the yield and fracture stresses of the material. Finally, the commonly used criteria for fracture-safe design in ferritic alloys are discussed. Two appendices are devoted to techniques for fracture toughness testing and to a brief summary of fatigue crack growth laws. (100 references). (auth)

13249 (GEMP–55A, pp 29-53) HIGH-TEMPERATURE REACTOR MATERIALS RESEARCH. (General Electric Co., Cincinnati, Ohio. Nuclear Materials and Propulsion Operation).

Creep-rupture tests of arc-cast W sheet and arc-cast W–25Re sheet at 2000°C and 0.703 kg/mm^2 in H_2 showed the W to be more creep resistant than W–25Re by approximately a factor of three in the range of 5 to 20% strain. The times to rupture for the W–25Re and the W were 964 and 1592 hrs, respectively. Creep-rupture tests of arc-cast W–25Re sheet in H_2 at 2000°C and various stresses after annealing at 2000 and 2400°C show a decrease in the creep resistance after annealing at the higher temperature. Following an anneal at 2400°C, the creep curve at 2000°C was found to approximate a parabolic form from 0.1% strain. No such form was observed at this same temperature following the 2000°C anneal, hence a structural change is indicated. Creep tests of arc-cast Mo sheet in H_2 at 1600°C and 1.41 kg/mm^2 after annealing at 1600, 2000, 2200, and 2400°C show a decrease in the creep resistance and the rupture life as the annealing temperature is increased. Also determined was the time required for the application of full load at a load travel rate of 0.30 cm/min. The specimen annealed at 1600°C required 7 sec to become fully loaded at which time the strain was 0.2%. The specimen annealed at 2400°C required 32 sec to become fully loaded at which time the strain was 2.5%. Two additional creep equations were investigated to determine their effectiveness in expressing transient creep behavior. The effectiveness of the expression involving a logarithmic term was rather poor as compared to the equation forms previously evaluated. The de Lacombe equation was comparable to the previously evaluated equation forms and appears to be very effective in representing transient creep behavior. Analysis of combined first- and second-stage creep data for arc-cast W at 2400°C using the de Lacombe equation indicates an effective representation which is more accurate than the Andrade, Garofalo, and Cottrell-Aytekin equations. Studies were initiated to investigate the ability of a single creep equation form to describe strain–time behavior for the entire creep curve. Further studies of the slip behavior and mode of deformation for the creep-rupture tests of arc-cast Mo rod at 2200°C show that the plane of fracture is $\{001\}$ with a $\langle 110 \rangle$ direction along the rod axis and $\langle \bar{1}10 \rangle$ along the fracture edge. Etch-pit studies of arc-cast Mo after annealing and after creep testing at 2200°C were performed. Annealed Mo shows no etch-pits on $\{111\}$ while after stressing these planes contain the greatest number. This is directly related to the slip mechanism known to operate in bcc metals. Etch-pit density is related to the angle at which the dislocation lines interesect the grain surfaces. The thermal conductivity of W–40UO_2 was determined for the temperature range from 900 to 2300°C. (auth)

13250 (GEMP–55A, pp 55-6) HIGH-TEMPERATURE THERMOCOUPLE AND ELECTRIC MATERIALS RESEARCH. (General Electric Co., Cincinnati, Ohio. Nuclear Materials and Propulsion Operation).

Evaluation of CaO as a possible thermocouple insulator inside a W–5Re sheath at high temperature in a carbonaceous hydrogen atmosphere at 2450°C indicated that pressure damage to the sheath could result. (auth)

13251 (GEMP–55A, pp 57-82) REFRACTORY-METAL ALLOY RESEARCH AND DEVELOPMENT. (General Electric Co., Cincinnati, Ohio. Nuclear Materials and Propulsion Operation).

The integrity and ductility of electron-beam welds in a series of W–Re–Mo alloys showed good ductility in the weld fused material. Porosity resulting during welding appears to be influenced more by oxygen than by carbon impurities. W–30Re alloy processed with high, intermediate, or normal thermal treatments was age-hardened by holding for 2, 10, and 100 hrs at 1000, 1200, 1400, 1600, and 1800°C following solution treatments of 1 hr at 1800, 2000, 2200, and 2400°C. Marked age-hardening developed at the 1400, 1600, and 1800°C aging temperatures

but the 1000 and 1200°C aging treatments did not result in hardness increases. Large quantities of W–Re sigma phase are available as a precipitant in the W–30Re alloy. Improving of unalloyed Mo through purification treatments resulted in hot-rolled sheet of 9 to 12 ppm C and less than 5 ppm O_2. No porosity was observed in simulated welds of the hot-rolled sheet. However, identical material after processing to cold-worked sheet developed microporosity in welding. A set of phase-versus-electron charts as evolved from the Brewer-Engel work are presented as a basis for alloy discussion. Sheet, plate, and tubing of W–30Re–30Mo alloy were produced; this marks the first trial production attempts for the W–30Re–30Mo alloy. (auth)

13252 (IS–1269) THE BISMUTH–ZIRCONIUM ALLOY SYSTEM. Hamilton, C. B.; Wilhelm, H. A. (Ames Lab., Iowa State Univ. of Science and Tech.). Apr. 1964. Contract W-7405-eng-82. 24p. Dep. mn. CFSTI $2.00 cy, $0.50 mn.

The bismuth–zirconium alloy system was investigated by thermal and metallographic examinations of alloys prepared by heating liquid bismuth with solid zirconium in tantalum and in graphite containers. Indications are that at least three intermetallic compounds exist in these alloys. The previously established compound $ZrBi_2$ formed peritectically on cooling at 714°C. A compound, assumed to be ZrBi, exhibited a peritectic at 1300°C, while a third compound, having the composition of Zr_3Bi_2, appeared to have a congruent melting point at 1495°C. There was evidence of a fourth compound which formed peritectically at 1340°C, near the composition of Zr_2Bi. A eutectic is reported to exist at 1290°C for 75 at.% zirconium. The maximum solid solubility of bismuth in zirconium, which occurs at this temperature, is approximately 15 at.%. No eutectic or solid solubility was observed for bismuth-rich alloys. (auth)

13253 (IS-T-65) DEFORMATION BEHAVIORS OF NIOBIUM AND TANTALUM AT LOW TEMPERATURES [Thesis]. Cowgill, Dale Stephen (Ames Lab., Iowa State Univ. of Science and Tech.). May 1964. Contract W-7405-eng-82. 211p. Dep. mn. CFSTI $6.00 cy, $1.25 mn.

The deformation behaviors of equivalent niobium and tantalum were investigated over the ductile-to-brittle transition range in niobium. For metals of equivalent composition and structure, tensile testing at equal temperatures and strain rates resulted in virtually the same yield strengths in both niobium and tantalum. Cleavage was observed on {110} and {100} planes in niobium specimens which fractured after more than 27 percent reduction in area, but none of the tantalum specimens exhibited cleavage. The niobium ductile-to-brittle (shear-to-cleavage) transition temperature was found to increase from −180 to −160°C with an increase in nitrogen content from 100 to 250 ppM. Twinning was observed in all tantalum specimens tested at low temperatures, but was observed in only those niobium specimens which subsequently failed by cleavage. In both materials the amount of twinning increased with increasing interstitial impurities and with decreasing temperatures. Slip behavior was more often observed in low temperature tantalum test specimens than in equivalent niobium specimens. It was concluded that the occurrence of cleavage in niobium is not solely dependent on composition, initial structure, temperature, and strain rate but is controlled by some mechanism operating during plastic deformation after yielding. (P.C.H.)

13254 (IS-T-70) THE CALCIUM–YTTERBIUM SYSTEM [Thesis]. Soderquist, Sven Dale (Ames Lab., Iowa State Univ. of Science and Tech.). Nov. 1965. Contract W-7405-eng-82. 49p. Dep. mn. CFSTI $2.00 cy, $0.50 mn.

The calcium–ytterbium phase diagram was determined by differential thermal analysis. It is characterized by two solid solutions, one fcc and the other bcc, in correspondence with the low and high temperature allotrope of each element. From low temperature resistivity measurements it was concluded that there is no long range ordering or immiscibility in the fcc solution. A Debye temperature of 260°K ± 12.5° for fcc calcium calculated from the resistivity data is in fair agreement with literature value (specific heat) of 235°K. Similarly, a Debye temperature for fcc ytterbium of 121.5°K ± 7.5 is in good agreement with the literature value (specific heat) of 118°K. (auth)

13255 (KAPL–3108) FATIGUE CHARACTERISTICS OF Ni–Cr–Fe ALLOYS WITH EMPHASIS ON PRESSURE-VESSEL CLADDING. Mowbray, D. F.; Sokol, G. J.; Savidge, R. E. (Knolls Atomic Power Lab., Schenectady, N. Y.). July 1, 1965. Contract W-31-109-eng-52. 88p. Dep. mn. CFSTI $3.00 cy, $0.75 mn.

An extensive fatigue-testing program was conducted to establish the fatigue characteristics of Ni–Cr–Fe alloys in various fabricated conditions, with special emphasis on cladding. Nineteen different materials were tested including Ni–Cr–Fe alloy in the clad, wrought, and cast form, and nuclear pressure vessel steel. Characteristic fatigue curves were established for each material at room temperature with zero mean strain superimposed. Less extensive investigations of the effects of elevated temperature, superimposed mean stress, and specimen size on the fatigue strength of Ni–Cr–Fe alloy, were included. The numerous tests conducted on Ni–Cr–Fe alloy cladding provided a good indication of variability in cladding fatigue strength due to variation in composition and welding practice. The tests conducted on other materials provided a basis for comparing the fatigue strengths of Ni–Cr–Fe alloy in its various fabricated conditions, and for comparing cladding fatigue strength with that of pressure vessel steel, for which cladding provides corrosion protection. Information on processing, mechanical properties, microstructure, and inspection results for each of the materials tested is appended. (auth)

13256 (NASA-TN-D-3222) ULTRAHIGH-VACUUM CREEP BEHAVIOR OF COLUMBIUM AND TANTALUM ALLOYS AT 2000 AND 2200 deg F FOR TIMES GREATER THAN 1000 HOURS. Titran, Robert H.; Hall, Robert W. (National Aeronautics and Space Administration, Cleveland, Ohio. Lewis Research Center). Jan. 1966. 26p. CFSTI $1.00 cy, $0.50 mn.

Creep tests of 1000 hours and greater were conducted at 2000 and 2200°F on six commercially available refractory alloys at pressures of 10^{-8} to 10^{-9} torr. The creep behavior of three niobium alloys, FS-85 (Nb + 28Ta + 10W + 1Zr), D-43 (Nb + 10W + 1Zr + 0.1C), and Nb-752 (Nb + 10W + 2.5Zr), and three tantalum alloys, T-222 (Ta + 9.6W + 2.4Hf + 0.01C), T-111 (Ta + 8W + 2Hf), and Ta-10W (90Ta + 10W) was determined at stress-to-density ratios of 2.6×10^4 and 1.3×10^4 inches, respectively, at 2000 and 2200°F. Comparison of creep behavior on the density-compensated basis showed that the tantalum alloy T-222 was the most creep resistant material evaluated. A total creep strain of only 0.1 percent resulted from testing this alloy for 5000 hours at 2000°F at a stress of 15,900 pounds per square inch; while at 2200°F and 8000 pounds per square inch, 0.65-percent strain occurred in 5000 hours. The relative order of creep resistance, on a density-compensated basis, was the same for the materials evaluated at 2000 and 2200°F: T-222, Ta-10W, D-43, FS-85, T-111, and Nb-752. (auth)

13257 (NASA-TN-D-3232) MECHANICAL PROPERTIES AND RECRYSTALLIZATION BEHAVIOR OF ELECTRON-BEAM-MELTED TUNGSTEN COMPARED WITH ARC-MELTED TUNGSTEN. Klopp, William D.; Witzke, Walter R. (National Aeronautics and Space Administration, Cleveland, Ohio. Lewis Research Center). Jan. 1966. 35p. CFSTI $2.00 cy, $0.50 mn.

A study was made on the properties of tungsten fabricated from three ingots consolidated by electron-beam melting. The study included purity as a function of number of melts, recrystallization and grain growth behavior, low-temperature ductility, and high-temperature tensile and creep strength. The level of most metallic impurities

in tungsten decreased with increasing number of electron-beam melts. The levels of interstitial impurities generally were not affected by remelting. The recrystallization rates for worked, electron-beam-melted (EB-melted) tungsten were significantly higher than those observed earlier for arc-melted tungsten. The grain growth rates of EB-melted tungsten were also higher than those reported previously for arc-melted tungsten. The ductile-brittle bend transition temperature for EB-melted tungsten was slightly higher in the worked condition than that reported for arc-melted tungsten. In the recrystallized conditions, the transition temperatures for EB- and arc-melted tungsten were similar. The tensile strength of EB-melted tungsten at 2500 to 4000°F was less than that of arc-melted tungsten. This is partly associated with the large grain size of EB-melted tungsten. The high-temperature creep strength of EB-melted tungsten was less than that of arc-melted tungsten, but this appears to be entirely the result of the larger grain size of EB-melted tungsten. Step-load creep tests at 2250 to 3630°F established that, at the stress levels studied (2130 to 6870 psi), EB-melted tungsten exhibited only transient creep behavior at 2250° to 2750°F. At 2875°F and higher, EB-melted tungsten exhibits transient creep initially, followed by steady creep, and finally a period of accelerating creep rate terminating in failure. The activation energies for transient and steady creep were 106,400 and 141,000 calories per gram-mole respectively. (P.C.H.)

13258 (NASA-TN-D-3238) INFLUENCE OF ORIENTATION OF GRAINS IN TUNGSTEN ON ITS FRICTION CHARACTERISTICS. Buckley, Donald H. (National Aeronautics and Space Administration, Cleveland, Ohio. Lewis Research Center). Jan. 1966. 22p. CFSTI $1.00 cy, $0.50 mn.

The influence of crystallographic orientation on the friction properties of tungsten was determined in both air and vacuum. Friction measurements were made with a 3/8-inch oriented sapphire ball sliding on a large grained tungsten disk, and the orientation of each grain (crystal) on the tungsten surface was determined. The two sapphire orientations examined were the (0001) plane, [10$\bar{1}$0] direction, and the (10$\bar{1}$0) plane, [0001] direction, sliding on the tungsten surface. The sapphire ball was loaded against the disk with a 500-gram load. The disk was then rotated to produce sliding velocities of 0.013 and 0.001 centimeter per second. The vacuum experiments were conducted with electron-cleaned surfaces at 10^{-10} millimeter of mercury. The results indicate that tungsten exhibits anisotropic friction properties. Friction characteristics on different crystal planes in a particular direction did not differ markedly; considerable differences in friction coefficient, however, existed in changing crystallographic directions on particular planes. Further, marked differences in friction were observed with changes in crystallographic orientation of the sapphire. Friction decreased considerably when vacuum measurements were repeated in air. (auth)

13259 (NLCO-968) A STUDY OF AS-CAST AND HEAT-TREATED URANIUM-URANIUM CARBIDE ALLOYS BY OPTICAL AND ELECTRON MICROSCOPY. Althaus, William A.; Cook, Marlin M.; Bieker, Richard J. (National Lead Co. of Ohio, Cincinnati). Feb. 1966. Contract AT(30-1)-1156. 41p. Dep. mn. CFSTI $2.00 cy, $0.50 mn.

Examinations of as-cast uranium-base dilute-carbon alloys revealed the growth characteristics of primary carbides in the liquid state, and as-cast and heat-treated samples showed the nature of the network phases. A tentative peritectic phase diagram is proposed to explain the structures seen in as-cast samples. Age-hardening treatments revealed that uranium-base dilute-carbon alloys were not suitable for dispersion hardening processes. A fine random dispersion of carbides was unobtainable with gamma heat treating followed by alpha annealing. (auth)

13260 (NP-15852) CRYSTAL CHEMISTRY STUDIES. First Quarterly Report, May 13, 1965-August 13, 1965. Roy, Rustum; Kachi, S.; McCarthy, G. J.; Muller, O.; White, W. B. (Pennsylvania State Univ., University Park. Materials Research Lab.). Aug. 24, 1965. Contract DA28-043-AMC-01304(E). 15p. CFSTI $1.00 cy, $0.50 mn.

Research has primarily been concerned with: the systematic crystal chemistry of rare earth and chromium systems in a search for new ferrimagnetic oxides; the vanadium-oxygen system; the samarium-oxygen and europium-cxygen systems; and site preferences in glass. Pyrochlore-like phases were found with the compositions near $Ho_2Re_2O_7$, $Y_2Re_2O_7$, and $Dy_2Re_2O_7$. The $MgO-Cr_2O_3-O$ and $CdO-Cr_2O_3-O$ systems were examined systematically to locate possible Cr^{4+} compounds stable at high oxygen pressures. New phases with the nominal compositions $MgCrO_x$, $CdCrO_x$, and Cd_2CrO_x were found. The phase diagram for the vanadium-oxygen system is nearly complete and a tentative diagram is included. Seven intermediate oxides occur in the composition interval between V_2O_3 and V_2O_5. SmO was prepared in a closed system as well as several samarium silicates. The whole matter of site population of Co^{2+} on reduction of cobalt glasses was re-examined, and it was concluded that the change in site population, observable in nickel glasses, is below the threshold of detectability in cobalt glasses. (auth)

13261 (ORNL-3885, pp 87-149) INVESTIGATIONS OF FUELED-GRAPHITE SYSTEMS. Sisman, O.; Savage, H. W.; Watson, G. M. (Oak Ridge National Lab., Tenn.).

Discussions are presented on instantaneous fission gas release experiments, fission product release from high-burnup coated UC_2, $(Th,U)C_2$, and UO_2 particles by post-irradiation annealing, sorption of fission product vapors on structural metals, compatibility of pyrolytic carbon-coated fuel particles with water vapor, and recoil of fission products in pyrolytic carbon. (M.O.W.)

13262 (ORNL-3885, pp 195-235) INVESTIGATIONS OF MODERATOR MATERIALS. Coobs, J. H.; Watson, G. M.; McCurdy, H. C.; Witt, F. J. (Oak Ridge National Lab., Tenn.).

The dimensional stability and thermal conductivity of AGOT graphite were investigated. Discussions and results are presented on the creep of graphite under irradiation, deposition of carbon on ATJ graphite, BeO-graphite compatibility, and failure characteristics of EGCR-Type AGOT graphite. (M.O.W.)

13263 (ORNL-TM-1355) EQUILIBRIUM SOLID SOLUTIONS OF NITROGEN IN Cb-1 percent Zr BETWEEN 1200-1800 deg C. Inouye, H. (Oak Ridge National Lab., Tenn.). Feb. 1966. Contract W-7405-eng-26. 16p. (CONF-651025-12). Dep. mn. CFSTI $1.00 cy, $0.50 mn.

From Symposium on Physical Metallurgy of Refractory Metals, French Lick, Ind.

An ultrahigh vacuum technique capable of measuring sorption rates as low as 4×10^{-3} ppM N/hr and pressures of 10^{-10} torr of nitrogen was used to measure the thermodynamic properties of solutions of nitrogen in Nb-1% Zr between 1200 and 1800°C. In the composition range 31 to 278 ppM N, the solutions obeyed Sievert's law. An anomalous solution behavior that was dependent on the amount of nitrogen in solution occurred between 1200 and 1400°C and was attributed to an oxygen-nitrogen interaction. The partial molar free energy expression for the equilibrium $\frac{1}{2}N_2 = \underline{N}$ in the temperature range 1400 to 1800°C was $\Delta\overline{F}^0 = -51{,}500 + 20.74T$, and $\Delta\overline{F}^0 = -34{,}200 + 9.52T$ for the temperature range 1200 to 1400°C. (auth)

13264 (WANL-PR(P)-008) DETERMINATION OF THE WELDABILITY AND ELEVATED TEMPERATURE STABILITY OF REFRACTORY METAL ALLOYS. Quarterly Report No. 8, March 21-June 20, 1965. Lessmann, G. G.; Stoner, D. R. (Westinghouse Electric Corp., Pittsburgh, Pa. Astronuclear Lab.). Contract NAS-3-2540. 93p. (NASA-CR-54723).

A weldability study of yttrium modified D-43 was completed. As with C-129Y and AS-55, yttrium additions to D-43 resulted in improved weld ductility. Weld parameters were varied over a broad range and welds were bend tested in both the longitudinal and transverse directions. In addi-

tion to the improved performance of yttrium modified D-43 (D-43Y), the post weld annealing response for 1 hr anneals at 1900, 2100, and 2400°F of D-43Y was considerably different than for D-43. Annealing resulted in moderately improved weld ductility for D-43 whereas D-43 responded to increased annealing temperature by displaying a severe loss and then recovery of ductility through an apparent age-overage reaction. D-43Y displayed a hot tearing tendency in TIG welding, the cause of which was not determined. A study to determine the causes and effects of weld porosity in refractory metal alloys was completed. Porosity appears to result from the degassing during welding of a pickling residue (or adsorbed hydrogen) from the surfaces of the joint interface. Hence, minimizing the joint surface area and eliminating crevices at the interface is desirable. In this respect, machined edges are better than sheared edges. Considerable variation in porosity sensitivity is observed between alloys. Overall alloy fabricability and porosity sensitivity appear to be closely related. The most fabricable alloys can be welded using sheared edges, whereas the less fabricable alloys require machined edges and vacuum degassing following pickling. No significant effects of weld porosity on weld ductility were observed. Nine alloys were included in a plate weldability evaluation. The alloys evaluated, in order of decreasing plate weld ductility, were: Ta-10W, T-111, T-222, SCb-291, FS-85, C-129Y, D-43, Cb-752, and B-66. The tantalum alloys, as a group, were considerably more ductile than the niobium alloys. All were readily weldable with the exception of B-66 which has a tendency to hot tear, making thick section welding difficult. The three alloys included in the study of the effect of oxygen contamination on weldability were doped to the first test level and evaluated. The first contamination level is 500 ppm in FS-85 and 350 ppm in T-111 and T-222, providing approximately equal contamination in atomic percent. Evaluation at this level was completed. The results tend to confirm preliminary data. T-111 was least sensitive. T-222 was most sensitive, significantly more so than T-111. The difference in T-111 and T-222 remains surprising in view of their close similarity in chemistry. (auth)

13265 (AD-623208) VAPORIZATION OF PURE-OXIDE CERAMICS AT HIGH TEMPERATURES. Lukin, E. S.; Poluboyarinov, D. N. Translated from Ogneupory, 29: 418-24(1964). 16p. (FTD-TT-65-934). CFSTI $1.00 cy, $0.50 mn.

The vaporization of pure oxide ceramics in a high temperature furnace at temperatures to 2300°C in a vacuum of 10^{-4} mm Hg and in helium at positive pressure of 0.2 atm was studied. It was found that the vaporization of the ceramics BeO, CaO, MgO, MgO · Al_2O_3, ZrO_2, Al_2O_3, and $3Al_2O_3$ · 2 SiO_2 was significantly less in helium than in vacuum. The most readily vaporized material considered was MgO. Additions of alumina to MgO decreased vaporization. The rate of vaporization of all oxides increased with an increase in temperature. The vaporization rate of ZrO_2 stabilized with CaO was somewhat higher than ZrO_2 stabilized with MgO. Specific gravity and porosity changes during the vaporization process were noted. Interaction of each oxide with molybdenum and tungsten wires (used for weighing samples) was observed. Vapor pressures for each sample were calculated. (J.B.)

13266 (AD-624905) PROPERTIES AND USES OF RHENIUM. Povarova, K. B.; Tylkina, M. A. Translated from Byull. Tekh.-Ekon. Inform., Gos. Nauch.-Issled. Inst. Nauch. Tekh. Inform., 16: No. 9, 7-11(1963). 8p. (FTD-TT-65-976). CFSTI.

Physico-chemical properties, processing, and uses of rhenium and its alloys are reviewed. Uses of rhenium coatings are also discussed. (P.C.H.)

13267 (AD-624909) RECRYSTALLIZATION OF HIGH-MELTING METALS IN WELDING AND SOLDERING. Grebtsev, N. V.; Klebanov, G. N. Translated from Izv. Akad. Nauk SSSR, Otd. Tekh. Nauk, Met. Toplivo. No. 5, 62-9(1961). 18p. (FTD-TT-65-1010). CFSTI.

Recrystallization processes in welding and soldering of Mo, W, Ta, and Nb, and the influence of these processes on the structure and mechanical properties of these metals in the zone around the seam were investigated. In the rapid heating encountered in welding, the initial recrystallization temperatures of Mo and W rose by 250 and 400°C, respectively, tending toward some limiting value. For Ta and Nb, this temperature rise amounted to 120–150 and 170–200°C. Under the conditions of rapid heating, considerable grain growth was observed in Mo at temperatures above 1600°C. Cumulative recrystallization proceeded most rapidly as the heating temperature was increased. In soldering with working temperatures below 1600°C, the duration of the process had little effect on the grain size of the base metal. Grain growth in Ta and Nb was influenced most by heating temperature, followed in order of importance by the holding times above the recrystallization temperature in heating and cooling. (P.C.H.)

13268 (JPRS-33605, pp 64-7) A STUDY OF THREE VALENCE RARE EARTH OXIDES–BERYLLIUM OXIDE SYSTEM. Han, Wen-lung. Translated from K'o Hsueh Tung Pao, No. 9, 831-2(1965).

Phase equilibria in the BeO–Gd_2O_3 system were studied. A new crystal phase with diffraction coefficients of n_p = 1.89 and n_g = 1.94 was discovered. Under the experimental conditions used, the new phase was slightly below maximum stability, and there was no stability phase area in the Gd_2O_3–BeO binary phase diagram. Specimens that went through the melting and rapid cooling process contained less stable Gd_2O_3–2BeO, which is the chemical composition, and the common melting point was about 4°C lower than that of BeO and Gd_2O_3. (P.C.H.)

13269 THE CRYSTAL STRUCTURE OF HIGH-PRESSURE UO_3. Siegel, S.; Hoekstra, H.; Sherry, E. (Argonne National Lab., Ill.). Acta Crystallogr., 20: 292-5 (Feb. 10, 1966).

The high-pressure modification of uranium trioxide is orthorhombic with a = 7.511 ± 0.009, b = 5.466 ± 0.008, and c = 5.224 ± 0.008 Å. The unit cell contains four formula weights and the space group is $P2_12_12_1$. Each uranium atom is bonded to seven oxygen atoms leading to shared $[UO_7]$ configurations. Two short bonds of 1.80 and 1.85 Å are nearly equal and collinear and are identified as uranyl bonds. The five secondary bonds form a puckered pentagonal coordination about the uranyl groups. The formula may thus be written as $(UO_2)O$. Bond distances vary considerably but are consistent with published bond strength–bond length values. (auth)

13270 METHODS OF MEASUREMENT OF LOW INTERMETALLIC DIFFUSION COEFFICIENTS. Gainotti, A.; Zecchina, L. (Univ., Parma, Italy). Energia Nucl. (Milan), 13: 32-8(1966).

The various methods used to measure intermetallic diffusion coefficients are reviewed. Particular emphasis is given to methods which allow measurements of diffusion coefficients down to 10^{-20} cm^2/sec. (auth)

13271 PHYSICAL AND MECHANICAL PROPERTIES OF Ti–Nb–Al ALLOYS. Kalinin, G. P.; Elyutin, O. P.; Mamontovskaya, L. V. Izv. Akad. Nauk SSSR, Metal., No. 3, 146-50(May-June 1965). (In Russian).

As a result of investigations of the thermal conductivity, electric resistance, dependence of electric resistance on temperature, thermal emf, and the mechanical properties of alloys of the ternary system Ti–Nb–Al, containing up to 10% Al and 50% Nb, composition-property diagrams were constructed. It is shown that the materials at the boundaries of the $(\alpha + \beta) - \beta$ phases of the areas of the equilibrium diagrams have satisfactory ductility and the best properties. (tr-auth)

13272 TERNARY SYSTEMS Hf–Nb–C, Zr–Nb–C, AND Ti–Nb–C. Fedorov, T. F.; Popova, N. M.; Gladyshevskii, E. I. Izv. Akad. Nauk SSSR, Metal., No. 3, 158-63(May-June 1965). (In Russian).

Phase equilibrium diagrams of the ternary systems Hf–Nb–C, Zr–Nb–C, and Ti–Nb–C were established by x-ray phase analysis and microscopic analysis. The existence of

a series of solid solutions between the monocarbides was established and the solubility of Hf, Zr, and Ti in Nb_2C was found. (tr-auth)

13273 INVESTIGATION OF EQUILIBRIUM DIAGRAM OF THE QUASI-TERNARY SYSTEM Ti_3Al–Ti_3Sn–Zr. Kornilov, I. I.; Nartova, T. T. Izv. Akad. Nauk SSSR, Metal., No. 3, 170-5(May-June 1965). (In Russian).

A systematic investigation was made of the system Ti–Zr–Al–Sn. The characteristics of the metallochemical bonds of these components are reflected in the character in the chemical reactions of the components of these alloys. The investigation of phase equilibrium was begun by preparation of rational triangulation profiles on the basis of assumed and actual existence in the Ti–Al and Ti–Sn systems of the compounds Ti_6Al, Ti_3Al, TiAl, and Ti_3Sn. The character of the phase equilibrium in the quasi-ternary system Ti_3Al–Ti_3Sn–Zr system was established at temperatures of 1200, 1000, and 800°C. At high temperatures the phase equilibrium is characterized by quasi-ternary constitution diagrams composed of three quasi-binary systems, two of which, Ti_3Al–Ti_3Sn and Ti_3Sn–Zr, have diagrams of the eutectic type. The other quasi-binary system, Ti_3Al–Zr, has a diagram with a continuous series of solid solutions. At low temperatures in all the concentration intervals investigated in the quasi-ternary system Ti_3Al–Ti_3Sn–Zr there was a continuous series of solid solutions. On the basis of studies of the isothermal cross section, the polythermal constitution diagram was constructed for the quasi-ternary system Ti_3Al–Ti_3Sn–Zr. The phase areas of the system where the crystallization at room temperature was initiated are described. (tr-auth)

13274 STRUCTURE AND PHYSICAL AND MECHANICAL PROPERTIES OF WC–NbC–Co SYSTEMS. Meerson, G. A.; Panov, V. S. Izv. Akad. Nauk SSSR, Metal., No. 3, 176-81(May-June 1965). (In Russian).

The dependence of the mechanical properties of WC–NbC–Co systems on the ratio WC/NbC and on the Co concentration was investigated. At the boundaries of the triphase regions (WC, NbC–WC, Co) the properties of the alloys changed linearly with the composition (with similar grain size of the carbide phase). At the boundaries of the two-phase area (NbC–WC, Co) alteration of the properties depended on the concentration of WC in the carbides of the solid solution, which led to a deviation from linear dependence. The introduction of 2 to 10 mole% NbC (with respect to the sum WC + NbC) in the system WC–Co increased the hardness at 20°C and the resistance during bending at 800°C with some reduction of the resistance to bending and shock strength at 20°C. With concentrations of NbC higher than 10 mole% (with respect to the sum WC + NbC) these mechanical properties decreased significantly. The greatest increase of the strength at 800°C as a result of the introduction of niobium carbide was observed for alloys with 5 mole% NbC and with 6 to 12 wt% Co. The effects of additions of NbC and TaC on the properties of WC–Co were compared and it was established that alloys containing 2 to 12 mole% niobium carbide with respect to the sum WC + NbC and 6 to 12 wt% Co have increased strength at 800°C and increased hardness at 20°C. (tr-auth)

13275 HETEROGENEOUS PHASES OF Nb_3(Al, Ge, AND Sn). Ageev, N. V.; Shamrai, V. F. (Baikov Inst. of Metallurgy, USSR). Izv. Akad. Nauk SSSR, Neorg. Mater., 1: 1277-84(Aug. 1965). (In Russian).

It was established that the range of homogeneous phases with the structure of β-W in the system Nd–Ge occurs at 18 to 20% Ge. This phase appears with a solid solution of Nd in the hypothetical compound Nb_3Ge and can be correlated with the berthollide type. In the Nb–Sn system, phases with the β-W exists near 23% Sn and appear with solid solutions of Nd in the compound Nb_3Sn, existing beyond the limits of the homogeneous phases. This phase also is correlated with the berthollide type. In the Nb–Al system, phases with the β-W structure exist at 25% Al, and the stoichiometric composition of the compound Nb_3Al exist in solid homogeneous phases and forms a range of solid solutions. This phase probably belongs to the daltonide type. It was shown that in the quaternary systems Nb–Al–Sn–Ge the compounds Nb_3Al, Nb_3Ge, and Nb_3Sn with the β-W structure form an unlimited series of solid solutions; the range of homogeneity of β-phases in the concentration tetrahedron was determined. (tr-auth)

13276 CONSTITUTION DIAGRAM OF ZrB_2–Cr. Kostikov, V. I. (Inst. of Steel and Alloys, USSR). Izv. Akad. Nauk SSSR, Neorg. Mater., 1: 1285-8(Aug. 1965). (In Russian).

The solidus line of alloys of the ZrB_2–Cr system was constructed. By means of metallographic investigation, measurement of the electric resistance, and x-ray analysis, the existence of the compound $CrZrB_2$ was established. The character of the constitution diagram of ZrB_2–Cr was made more precise. (tr-auth)

13277 MECHANICAL PROPERTIES OF URANIUM-ACTIVATED SODIUM FLUORIDE SINGLE CRYSTALS. Alybakov, A. A.; Builko, V. M.; Shamyrkanov, Y. (Inst. of Physics and Mathematics, Academy of Sciences, USSR). Izv. Akad. Nauk SSSR, Neorg. Mater., 1: 1326-7(Aug. 1965). (In Russian).

With an increase of the concentration of uranium admixtures, the mechanical properties of sodium fluoride single crystals improves. The length of the dislocation etch pattern is the more sensitive indication of the change of mechanical properties of the crystal in comparison with the microhardness. The improvement of the mechanical properties of the impure crystals is caused by the formation of point defects apparent in the absorption spectra. (tr-auth)

13278 INVESTIGATION OF THE OPTICAL PROPERTIES OF COMPOUNDS FORMED IN Ln_2O_3–SrO AND Ln_2O_3–BaO SYSTEMS. Lopato, L. M.; Yaremenko, Z. A.; Tresvyatskii, S. G. (Inst. of Problems in Metallography, Academy of Sciences, Ukrainian SSR). Izv. Akad. Nauk SSSR, Neorg. Mater., 1: 1368-71(Aug. 1965). (In Russian).

The characteristics of the optical properties of compounds of the types $SrLn_2O_4$ and $BaLn_2O_4$, where Ln is Sm, Eu, Gd, Tb, Dy, Y, Ho, Er, Tm, Yb, Lu, and Sc were given. It was found that the value of the refractive index of the compounds $SrLn_2O_4$, where Ln is the rare earth elements from Ho to Lu, and the compounds SrY_2O_4 and $BaSc_2O_4$ is higher than the refractive index of the original oxides. On the basis of the crystallo-optical characteristics, a hypothesis on the crystalline structure of the compounds is suggested. (tr-auth)

13279 PHASE COMPONENTS IN ZrO_2–$PrO_{1.83}$ SYSTEM. Strekalovskii, V. N.; Volchenkova, Z. S.; Samarina, V. A. (Inst. of Electrochemistry, Academy of Sciences, Ukrainian SSR). Izv. Akad. Nauk SSSR, Neorg. Mater., 1: 1372-5(Aug. 1965). (In Russian).

By investigation of the mixed oxides ZrO_2–$PrO_{1.83}$ annealed at 1200 and 1550°C, a wide range of solid solution with the fluoride structure and chemical compounds of equal molar composition were detected. (tr-auth)

13280 RARE EARTH ALLOYS AND COMPOUNDS. Savitskii, E. M.; Terekhova, V. F.; Burov, I. V.; Naumkin, O. P.; Markova, I. A. (Baikov Inst. of Metallurgy, USSR). Izv. Akad. Nauk SSSR, Neorg. Mater., 1: 1648-59(Oct. 1965). (In Russian).

Available experimental data on the formation of intermetallic compounds between rare earth elements of the yttrium and cerium subgroups (cerium to gadolinium and thulium to neodymium), which are characterized only by the number of electrons in the 4f shell and the orientation of the spin, indicate that the type of constitution diagram and the nature of the intermediate phase in systems of rare earth elements is determined not only by the valence electrons but also by the electron composition of the deep-lying inner shells, especially electrons of the 4f shell. The solution to the problem of working and fabricating is to learn the physical and chemical properties of the rare earth alloys and their intermediate phases. (tr-auth)

13281 X RAY INVESTIGATIONS OF BINARY OXIDES OF ZIRCONIUM AND NIOBIUM. Trunov, V. K. (Moscow

State Univ.). Izv. Akad. Nauk SSSR, Neorg. Mater., 1: 1949-51(Nov. 1965). (In Russian).

The lattice parameters of the binary oxides $ZrO_2 \cdot 5Nb_2O_5$ and $ZrO_2 \cdot 7Nb_2O_5$ were determined. It was shown that the compound $ZrNb_{14}O_{37}$ does not belong to the homologous series $Me_{3n}O_{8n-3}$. (tr-auth)

13282 STUDIES OF BaO–ZrO_2 SYSTEMS RICH IN BaO. Galkin, Yu. M.; Chukhlintsev, V. G. (Ural Polytechnic Inst., Sverdlovsk, USSR). Izv. Akad. Nauk SSSR, Neorg. Mater., 1: 1952-4(Nov. 1965). (In Russian).

The reactions of BaO and $BaCO_3$ with ZrO_2 at BaO : ZrO_2 ratios from 1 to 5 were studied. It is shown that at the ratio BaO : ZrO_2 = 2 and at temperatures from 1150 to 1350°C the orthozirconate Ba_2ZrO_4 is formed, which is stable with respect to BaO. The x-ray phase analysis of this compound is reported and some of its properties described. (tr-auth)

13283 STUDIES OF Nd_2O_3–ZrO_2 SYSTEMS RICH IN NEODYMIUM OXIDES. Glushkova, V. B.; Davtyan, I. A.; Keler, E. K. (Grebenshchikov Inst. of Chemistry of Silicates, Academy of Sciences, USSR). Izv. Akad. Nauk SSSR, Neorg. Mater., 1: 1955-64(Nov. 1965). (In Russian).

By means of chemical and x-ray phase analysis the Nd_2O_3–ZrO_2 system was investigated and the diagram of the phase conversion for the neodymium oxide-rich phase was constructed. The stability of the cubic solid solution based on Nd_2O_3 was determined and found to be stable only at temperatures above 1500°C. During preparation of the systems by coprecipitation into the amorphous state with subsequent crystallization from 400 to 800°C or by decomposition of mixtures of the nitric salts, cubic solid solutions were formed in the primary phases. During the continuous change of the composition of these metastable solid solutions, constant changes of their crystal structure occurred, from the Mn_2O_3 type characteristic of the low-temperature C-form of Nd_2O_3 through the pyrochlore type to the fluorite type in which the low-temperature form of ZrO_2 is crystallized. The effect of additions of ZrO_2 on the C–A transition of Nd_2O_5 was investigated. A small amount of ZrO_2 was found to impede the transition of the cubic solid solution (C-form) to the hexagonal (A) form. With large concentrations of ZrO_2 (10 to 20%) in the cubic solid solution, solid solutions of intermediate products were formed, crystallizing in the lower symmetry (B-type). After heating to 1350 to 1400°C mixtures of the solid solution with hexagonal and pyrochlore structures were transformed into equilibrium mixtures. (tr-auth)

13284 TRIANGULATION OF THE Na_2O–ZrO_2–SiO_2 SYSTEM. Polezhaev, Yu. M.; Chukhlantsev, V. G. (Ural Polytechnic Inst., Sverdlovsk, USSR). Izv. Akad. Nauk SSSR, Neorg. Mater., 1: 1990-3(Nov. 1965). (In Russian).

By the method of x-ray phase analysis and chemical analysis, the triangulation of the system Na_2O–ZrO_2–SiO_2 was constructed in the solid state. On the basis of experimental data obtained and literature data the stability diagram was constructed for the system along with 13 supplementary compatibility triangles. (tr-auth)

13285 PHASE STUDIES IN THE SYSTEM UP–UO_2. Baskin, Y. (Argonne National Lab., Ill.). J. Amer. Ceram. Soc., 48: 652-3(Dec. 1965).

Compositions in the UP–UO_2 system at 12.5 mol. % intervals were blended, milled, and pellets were pressed. Melting temperatures of the various compositions under helium were determined. Examination by x-ray diffraction analysis revealed no solid-state interaction between UP and UO_2. No evidence of an intermediate phase was detected, and the lattice constants of the two compounds did not vary with the composition of the sample. The phase diagram presented shows no intermediate compounds and no solubility between the phases. A eutectic occurred at 38 wt % UP–62 wt % UO_2 and 2390 ± 30°C. Weight losses at 2000°C in a vacuum were measured. (M.C.G.)

13286 SOME PHASE EQUILIBRIA IN THE URANIUM–NITROGEN SYSTEM. Benz, R.; Bowman, M. G. (Los Alamos Scientific Lab., N. Mex.). J. Amer. Chem. Soc., 88: 264-8(Jan. 20, 1966).

Portions of the U–N phase diagram were determined by x-ray, metallographic, chemical, and thermal analyses of phases equilibrated with N_2 (up to 5 atm) at temperatures up to 2850°C. The U–UN portion of the diagram is a eutectic with the eutectic composition near pure U. The UN phase region has a U-rich boundary with an N : U ratio equal to or less than 0.96 ± 0.02 at 1500 and 0.92 ± 0.02 at 1800°C. The N-rich boundary has a N : U ratio of 1.04 ± 0.02 at 1600°C. The mononitride melts congruently with the N : U ratio 0.96 ± 0.03 at 2835 ± 30°C. The bcc ⇌ hexagonal transition of the sesquinitride was found to occur at 1120°C, but the transition temperature may be dependent on composition. The composition of the hexagonal phase is $UN_{1.47\pm0.02}$ near the decomposition pressure at 1315°C. (auth)

13287 URANIUM–MOLYBDENUM ALLOY FOR USE IN A PROMPT-BURST REACTOR. Rienecker, F.; Moran, W. H. (Univ. of California, Livermore). J. Basic Eng., 87: 865-70(Dec. 1965). (UCRL-12397).

A large prompt-burst nuclear reactor, "Super Kukla," required a core of material that would withstand unusually high stress levels resulting from rapid thermal expansion and inertia loads. An experimental investigation was undertaken to determine the properties of cast uranium–10 wt % molybdenum alloy under static and dynamic conditions of loading at various temperatures for application in this reactor. Techniques were developed to cast, inspect by radiographic and ultrasonic means, machine, and nickel plate the material. Castings are in the form of rings, 30 in. OD, 18 in. ID, and 2 in. thick. Sound material with a carbon content of less than 250 ppM was found to have a static yield strength of approximately 130,000 psi, ultimate strength of 133,000 psi, and elongation of 10% at room temperature. Sustained static loads of more than 40,000 psi in a normal atmosphere were found to induce a brittle fracture attributed to stress corrosion. Test specimens subjected to strain rates on the order of 20 in/in/sec withstood stresses of 200,000 psi in the gage region, but usually failed in the threaded ends. (auth)

13288 HIGH-TEMPERATURE VAPOR-PRESSURE STUDIES OF UO_2 BY THE EFFUSION METHOD AND ITS THERMODYNAMIC INTERPRETATION. Ohse, Roland W. (EURATOM, Karlsruhe, Ger.). J. Chem. Phys., 44: 1375-8(Feb. 15, 1966).

A high-temperature effusion investigation under vacuum of the vapor pressure of UO_2 is presented over the temperature range from 2200 to 2800°K. A least-square analysis of the experimental results yielded the equation log p (mm) = 12.426 – 3.318 (10^4/T). The latent heat of sublimation ΔH^0_{298} = 148.6 kcal/mole was determined by applying the third-law method of thermodynamics. Blackbody hole readings, corrected for both the transmissivity of interposed windows and the cavity temperature, were checked by measuring the spectral emissivity of the optically smooth polished tungsten surface at 0.65 μ, which decreased from 0.44 at 2300°K to 0.416 at 2850°K. Compatibility tests at 2800°K revealed no signs of a noticeable reaction between UO_2 and the tungsten effusion cell. (auth)

13289 DIFFUSION STUDIES OF ^{95}Nb IN POLYCRYSTALLINE UO_2 BETWEEN 1100 AND 2100 deg C. Federer, J. I.; Padgett, R. A. Jr. (Oak Ridge National Lab., Tenn.). J. Nucl. Mater., 17: 294-304(Dec. 1965). (ORNL-TM-1018).

Diffusion of ^{95}Nb in polycrystalline UO_2, prepared by pressing and sintering powders and by fusing, was studied in the temperature range from 1100 to 2100°C. Precision-grinding sectioning methods allowed the penetration of ^{95}Nb to be determined accurately. Activity profiles given by ln A(x) vs x^2 for ^{95}Nb penetration in both types of UO_2 consisted of curved segments near the surface followed by linear portions extending to the limit of ^{95}Nb detection. The character of these profiles was attributed to the combined effects of lattice and grain boundary diffusion, with the latter being primarily responsible for the deeper penetration. Meaningful diffusion coefficients could

not be calculated from the near-surface region of the activity profiles. Coefficients calculated from the linear portions were considerably larger than any previously reported values for isotope diffusion in UO_2. The results of this study indicated that future studies of diffusion in UO_2 should utilize better quality specimens of coarse-grained or single-crystal material. (auth)

13290 IN-PILE FISSION-GAS RELEASE FROM FINE-GRAIN UO_2. Carroll, R. M.; Sisman, O. (Oak Ridge National Lab., Tenn.). J. Nucl. Mater., 17: 305-12(Dec. 1965). (ORNL-P-793).

According to the defect-trap theory for fission-gas release the rate of escape of gas from UO_2 is controlled by the number of defects in the UO_2 structure. Defects are created by fission and may also be inherent flaws, such as grain boundaries and pores. To test this theory the release rate of gas from single crystal UO_2 was compared to that from fine-grained UO_2. It was found that the single crystal did release much more gas (a factor of 17 at 1000°C) than the fine-grained material. Post-irradiation examination showed that the grain boundaries trapped fission products. The theory further states that the number of radioinduced traps at a given temperature will be roughly proportional to the fission rate, under the conditions of this experiment. At a high fission rate, therefore, there will be more fission-gas but also a higher probability of trapping the gas atoms, and a change in fission rate should not produce much change in the fission-gas release rate. In the fine-grained material, a change in fission rate by a factor of 4.5 did not produce a detectable change in the rate of gas release. These results confirmed the defect-trap model for fission-gas release, and are directly opposed to any gas release mechanism that is diffusion controlled. (auth)

13291 THE PLUTONIUM–CARBON–OXYGEN SYSTEM. Mulford, R. N. R.; Ellinger, F. H.; Johnson, K. A. (Los Alamos Scientific Lab., N. Mex.). J. Nucl. Mater., 17: 324-9(Dec. 1965). (LA-DC-6703).

A portion of the Pu–C–O condensed ternary phase diagram was examined. A single-phase field containing a Pu(C,O) phase was found. Lattice parameter data and the composition range for the Pu(C,O) phase are described. Adjoining the Pu(C,O) single-phase field, three two-phase fields containing Pu + Pu(C,O), Pu_2O_3 + Pu(C,O), and Pu_2C_3 + Pu(C,O) were found. A three-phase field containing Pu + Pu_2O_3 + Pu(C,O) was also delineated. (auth)

13292 THE EFFECTS OF HIGH PRESSURE AND TEMPERATURE ON THE MICROSTRUCTURE OF PLUTONIUM. Liptai, R. G.; Lloyd, L. T.; Friddle, R. J. (Argonne National Lab., Ill.). J. Nucl. Mater., 17: 330-5(Dec. 1965).

The effects of high pressures (to 35 kilobar) and temperatures on the microstructure of plutonium were studied. Metallographic and x-ray evidence showed that these parameters provide a method for accomplishing recrystallization and grain growth in alpha-plutonium. (auth)

13293 AN ELECTRON FRACTOGRAPHIC STUDY OF ALPHA PLUTONIUM. Bronisz, S. E.; Douglass, D. L. (Los Alamos Scientific Lab., N. Mex.). J. Nucl. Mater., 17: 336-40(Dec. 1965). (LA-DC-6418).

The fracture behavior of alpha plutonium, broken so that the stress immediately prior to fracture is tensile, is shown to be temperature dependent. At 191°K and below the fracture is transgranular and proceeds in a ductile manner. At 297°K and above the fracture is intergranular. At all fracture temperatures the total plastic deformation associated with the fracture is small. At those temperatures where fracture is intergranular, much of the deformation is localized at grain boundaries. (auth)

13294 CAUSES OF HIGH TEMPERATURE SUBSTOICHIOMETRY IN SINTERED URANIUM DIOXIDE. Rothwell, E. (Univ. of Sheffield, Eng.). J. Nucl. Mater., 17: 344-6(Dec. 1965).

High-temperature substoichiometry in uranium dioxide is discussed. Uranium inclusions segregated at grain boundaries after prolonged annealing of UO_2 compacts at 1950°C are considered. It is proposed that at a low oxygen potential UO_2 loses oxygen above 1800°C to give a substoichiometric UO_{2-y}, which on cooling reverts to $UO_{2.0}$ and free uranium. (F.J.H.)

13295 STRAIN INDUCED ACTIVITY IN THORIA AND ITS RELIEF WITH TEMPERATURE. Lewis, D.; Lindley, M. W. (Battersea Coll. of Tech., London). J. Nucl. Mater., 17: 347-9(Dec. 1965).

A study was made to assess the contribution of strain energy to the activity of thoria and to determine how this strain is removed on annealing at various temperatures. Strain was removed uniformly over the temperature range from 400 to 1300°C and all strain was removed by 1600°C. The mean strain induced by the deformation was 0.01. The stored energy was calculated. The mean strain energy contribution was 11 cal/g. (M.C.G.)

13296 THERMAL TRANSFORMATIONS OF ALUMINAS EXTRACTED FROM Al–Al_2O_3 COMPOSITES. Beghi, G.; Cazzaniga, E.; Piatti, G. (Centre Commun de Recherche Nucleaire, Ispra, Italy). J. Nucl. Mater., 18: 237-46 (1966). (In French).

The transformation of transition aluminas present in Al–Al_2O_3 composites in the form of α-Al_2O_3 in the presence of the liquid aluminum matrix, takes place at temperatures lower than normal. A better understanding of this transformation can give a useful insight into the behavior of the oxide and aluminum-alumina bonds in Al–Al_2O_3 composites. A study was made of the thermal transformations of the aluminas in question in the absence of aluminum with the aim of comparing their behavior and of clarifying the influence of aluminum. The transition aluminas were extracted from an Al–Al_2O_3 composite by dissolving the matrix and then thermally treated in air or under vacuum. It was confirmed that transition aluminas examined transform into the α-phase without detectable intermediate transformations, at temperatures in the ranges of 900–1000°C and 1100–1200°C in air and in vacuum respectively. Consequently, the presence of liquid aluminum seems to have an influence only in the sense of lowering the transformation temperature. It was found that the color of the aluminas varied with experimental conditions; this was probably related to the non-stoichiometry of the oxide. The influence of previous constraints acting on transition alumina was verified; experiments were made on hydration and dehydration. (auth)

13297 GRAIN GROWTH IN PURE AND TITANIA-DOPED URANIUM DIOXIDE. Amato, I.; Colombo, R. L.; Balzari, A. Petruccioli (Sezione Energia Nucleare, Turin, Italy). J. Nucl. Mater., 18: 252-60(1966).

Current literature data of grain growth of uranium dioxide sintered in reducing or neutral and in slightly oxidizing atmospheres are critically reviewed. It appears that the growth rate is higher in the latter case and that consequently the activation energy calculated by fitting the data to a rate equation is lower. Grain growth is followed in pure and titania-doped uranium dioxide bodies held for different times at temperatures from 1450 to 1630°C in a hydrogen atmosphere. It is found that the growth rate is higher in the specimens of the latter type, which would be consistent with the idea that titania promotes off-stoichiometry in uranium dioxide; however, the activation energy derived as above appears to be higher. The scant reliability of calculations of this kind is discussed and assessed. (auth)

13298 THE SOLUBILITY OF IRON IN SOLID URANIUM BETWEEN 0.003 wt percent AND 0.3 wt percent IRON. Swindells, N. (Univ., Liverpool). J. Nucl. Mater., 18: 261-71(1966).

The solubility of iron in solid uranium was redetermined up to a concentration of 0.3 wt % iron by metallographic methods. The eutectoid temperatures were found by a new application of quantitative metallography. At 660°C α-uranium can dissolve 0.003 wt % Fe (0.013 at. %) and the

eutectoid point for the β-phase is at 661°C and 0.027 wt % (0.12 at. %). Maximum solubility in the β-phase is 0.085 wt % (0.37 at. %) at 763°C and the γ eutectoid point is at 0.15 wt % (0.65 at. %). At 780°C the solubility in the γ phase is 0.223 wt % (0.97 at. %) and at 800°C is 0.305 wt % (1.33 at. %). (auth)

13299 A STUDY OF THE THERMOELECTRIC PROPERTIES OF Pt/Ru-ALLOYS. Israel, J. (Philips' Gloeilampenfabrieken, Eindhoven, Netherlands). J. Nucl. Mater., 18: 272-7(1966).

Pt–Ru alloys with up to 10 wt % Ru were studied for their thermoelectric force against Pt up to 1600°C. The Ru content of the wires was found by measuring the resistivity. For this purpose the resistivity of Pt–Ru alloys was determined as a function of Ru content, since the values found in the literature were contradicting. (auth)

13300 THE X-RAY THERMAL EXPANSION OF NEAR-STOICHIOMETRIC UO_2. Baldock, P. J.; Spindler, W. E.; Baker, T. W. (Atomic Energy Research Establishment, Harwell, Eng.). J. Nucl. Mater., 18: 305-13(1966). (AERE-R-5007).

The thermal expansion UO_2 samples having compositions between $UO_{1.98}$ and $UO_{2.00}$ was determined over the range 20 to 2300°C using a high temperature x-ray diffractometer. The expansion is linear above 400°C and the mean coefficient of thermal expansion over the range 20 to 2300°C was found to be $(10.8 \pm 0.1) \times 10^{-6}$/°C. Previous to this work, x-ray measurements have only been reported up to 900°C. The present work agrees with those results and gives a coefficient of thermal expansion of $(10.4 \pm 0.2) \times 10^{-6}$/°C over the range 20–900°C. The present work is also in agreement with bulk expansion measurements up to 1400°C. Above this temperature, the x-ray expansion is found to be significantly lower than the bulk expansion. (auth)

13301 A METALLOGRAPHIC AND X-RAY STUDY OF THE LIMITS OF OXYGEN SOLUBILITY IN THE UO_2–ThO_2 SYSTEM. Cohen, I.; Berman, R. M. (Bettis Atomic Power Lab., Pittsburgh). J. Nucl. Mater., 18: 77-107(Feb. 1966). (WAPD-T-1766).

Metallographic and x-ray diffraction techniques were used to explore the extent of oxygen solubility in UO_2-ThO_2 solid solutions as a function of temperature and composition. The value of x in $(Th,U)O_{2+x}$ increases continuously from 0, at ThO_2, to a value of 0.25 for $(U_{0.9}Th_{0.1})O_{2.25}$ at 1200°C. The entire portion of the UO_2-ThO_2-O ternary diagram bounded by this curve is the stability field of a single, continuous face-centered-cubic phase. This phase, for the most part, obeys Vegard's law; contours representing equal cell sizes are straight and uniformly spaced. High-urania solid solutions, between $(U_{0.9}Th_{0.1})O_{2+x}$ and $(U_{0.5}Th_{0.5})O_{2+x}$, are in equilibrium with U_3O_8. There is a 3-phase field, in which U_3O_8, O_2, and $U_{0.5}Th_{0.5}O_{2+x}$ are in equilibrium. High-thoria solid solutions, from $(U_{0.5}Th_{0.5})O_{2+x}$, are in equilibrium with oxygen. The limits of solubility at 1200°C in air can be calculated and accurately predicted if it is assumed that it is controlled by a structural requirement that limits interstitial oxygens to 1 per unit cell and by the availability of uranium ions among the nearest neighbors to compensate for the excess charge. Subject to this structural requirement, interstitial oxygens can fill vacancies bounded by two or more uranium ions. It can also fill 18% of the suitable vacancies bounded by only one uranium ion. In high-urania solid solutions, above $U_{0.9}Th_{0.1}O_{2+x}$, anomalies appear. Vegard's law is no longer followed. The limits of the continuous cubic phase become dependent on temperature, reaching the U–O binary at the point shown by previous work on that binary. A three-phase field, in which U_4O_9, U_3O_8 and the cubic phase are in equilibrium, appears. These anomalies are probably an expression of the tendency to form an ordered phase, found in the vicinity of U_4O_9. (auth)

13302 STUDY OF THE SYSTEM NIOBIUM–NITROGEN. I. PROPERTY CHANGES IN NIOBIUM BY DISSOLVED NITROGEN. Gebhardt, E.; Duerrschnabel, W.; Hoerz, G. (Institut fuer Sondermetalle, Stuttgart). J. Nucl. Mater., 18: 119-33(Feb. 1966). (In German).

The electric resistance, the lattice parameter, the hardness, and the internal friction of niobium–nitrogen solid solutions were determined as a function of nitrogen content in the range 0 to 1.5 at. % N. These properties largely vary in a linear manner with solute content. 1 at. % nitrogen in solid solution in previously degassed niobium raises the electric resistance at 10°C from 14.1 to 18.2 $\mu\Omega \cdot$ cm, the lattice parameter at 20°C from 3.300 to 3.304 Å and the microhardness under 50 g load at 20°C from 63 to 245 kg/mm^2. The nitrogen damping peak at 260°C (frequency 0.73/sec) for 0.5 at. % N reaches a level of $\vartheta = 560 \times 10^{-4}$. The activation energy of the simple relaxation process is 33.8 kcal/mole. The property changes induced in niobium by dissolved nitrogen were compared with the corresponding values for the solid solution systems niobium–oxygen, tantalum–oxygen, tantalum–nitrogen, vanadium–nitrogen, and vanadium–oxygen. (auth)

13303 STUDY ON THE SYSTEM NIOBIUM–NITROGEN. II. PRECIPITATION PROCESS IN NIOBIUM–NITROGEN MIXED CRYSTALS. Gebhardt, E.; Duerrschnabel, W.; Hoerz, G. (Institut fuer Sondermetalle, Stuttgart). J. Nucl. Mater., 18: 134-48(Feb. 1966). (In German).

The solubility limit of nitrogen in niobium between 450 and 1000°C was determined by measuring the lattice parameters of supersaturated, annealed and subsequently quenched solid solutions. A distinct temperature dependence of the solubility was found (0.55 at. % N at 1000°C and 0.07 at. % N at 450°C). The solubility increases rapidly above 800°C. The difference of partial enthalpy for the transition of 1 gram-atom of nitrogen from the nitride phase into the α solid solution is 15 kcal for temperatures between 1000 and 800°C and only 4 kcal for temperatures between 800 and 450°C. The precipitated phase is Nb_2N. There are no x-ray or micrographic indications for a change in precipitation mode at 800°C. The kinetics of precipitation from supersaturated niobium–nitrogen alloys with 0.8 at. % N were determined between 350 and 600°C by measurement of the lattice parameter and the microhardness of annealed and quenched samples. The isotherms could be subdivided into incubation, precipitation, and equilibrium stages. The activation energy of the precipitation reaction is 35 kcal/mole and corresponds approximately to that for diffusion of nitrogen in niobium. At 450°C the distribution of precipitates after short annealing times is very inhomogeneous; the number of particles is strongly time dependent. At 600°C the precipitates are distributed fairly uniformly and the number of particles virtually constant. At a mean particle separation of 10^4 to 10^5 Å no precipitation-hardening was observed. (auth)

13304 TEMPERED STRUCTURES OF A Zr–2.5 wt percent Nb ALLOY. Williams, C. D.; Gilbert, R. W. (Atomic Energy of Canada Ltd., Chalk River, Ont.). J. Nucl. Mater., 18: 161-6(Feb. 1966).

A transmission electron microscope study was carried out on specimens of a Zr–2.5 wt % Nb alloy tempered at 500°C after a water quench from 1000°C. The martensitic product of the $\beta \rightarrow \alpha'$ transformation is found to contain fine twins; niobium-rich precipitates are nucleated at the twin interfaces, the α' grain boundaries, and homogeneously within the matrix. On extended tempering the niobium content of the precipitates increases until the composition of the β-Nb phase is reached. It is suggested that changing matrix/precipitate coherency and niobium content of the homogeneously nucleated precipitates are mainly responsible for the change in hardness observed on tempering. A similar inference is drawn with respect to changes in oxidation resistance of the alloy with tempering at 500°C. (auth)

13305 DISLOCATION VECTORS RELATED TO THE DUCTILITY OF BERYLLIUM. Scott, V. D.; Lindsay, H. M. (Atomic Weapons Research Establishment, Aldermaston, Eng.). J. Nucl. Mater., 18: 176-86(Feb. 1966).

Specimens subjected to prescribed amounts of deformation by rolling were examined by thin foil electron microscopy and the observed dislocation structures related to the variation of ductility with temperature, particular attention being focused on the brittle-to-tough transition in beryl-

lium. A typical feature of the specimen examined was the heterogeneous high-density dislocation arrays which consisted of networks and of tangles with associated prismatic loops. The loops are elongated in the $\langle 10\bar{1}0\rangle$ direction with a Burgers vector $\frac{1}{3}\langle 11\bar{2}0\rangle$, the presence of more than one oriented set being indicative of their formation during simultaneous slip in more than one basal direction. Apart from the expected dependence of dislocation density upon strain, no obvious differences were found between the dislocation structures in beryllium rolled at 250, 450, and 650°C. A significant feature of the present work was, however, the identification of non-basal, $\frac{1}{3}\langle 11\bar{2}3\rangle$, slip vectors in these materials together with the observation that no such vectors could be located in metal deformed at room temperature. Some dislocations were observed to move in the electron microscope and where these were amenable to identification they were found to have a $\frac{1}{3}\langle 11\bar{2}0\rangle$ Burgers vector. The apparent absence of moving $\frac{1}{3}\langle 11\bar{2}3\rangle$ dislocations implies that non-basal dislocations may experience a higher Peierls-Nabarro force than basal dislocations. No evidence was found to suggest that impurities are the prime reason for the low-temperature brittleness of beryllium and it is proposed, therefore, that the ductility-temperature behavior may be more satisfactorily explained by consideration of the Peierls-Nabarro forces acting upon the different types of dislocation. (auth)

13306 EXPERIMENTAL INVESTIGATION ON THE THERMAL AND ELECTRICAL CONDUCTIVITY OF SAP. Nobili, D.; De Bacci, M. A. (CCR EURATOM, Ispra, Italy). J. Nucl. Mater., 18: 187-96(Feb. 1966).

The thermal conductivity of 99.99% aluminum and of different types of SAP, containing up to 14 wt % of alumina, was measured between 100 and 500°C utilizing a new, accurate transient flow method. Electrical conductivity determinations were carried out in parallel. It was noticed that SAP is anisotropic with respect to both transport properties, lower conductivities were measured in the direction normal to the extrusion axis. The Lorenz constant of SAP was found to lie in the range $(5.5 \pm 0.15) \times 10^{-9}$ cal · ohm/sec · °C^2. This value is, within the limits of error, the same as for pure aluminum, showing that above 100°C, for any given composition and flow direction, the heat conduction through the alumina is a small fraction, a few per cent at most, of the total. The anisotropy of resistivity and a large increase in the resistivity of SAP compared to aluminum are determined by the geometrical features of the dispersed phase. Plastic deformations can markedly reduce both anisotropy and resistivity, by decreasing the cross section of the oxide through orientation of the particles. (auth)

13307 THE MECHANISM AND TRANSFORMATION KINETICS OF THE $\beta \rightarrow \alpha$ PHASE CHANGE IN THE URANIUM/1 AT % PLATINUM ALLOY. Kitchingman, W. J.; Pickwick, K. M.; Brown, I. G.; Edwards, R. J. (Univ. of Manchester, Eng.). J. Nucl. Mater., 18: 219-25(Feb. 1966).

Electric resistivity investigations of the $\beta \rightarrow \alpha$ transformation in a U–1 at. % Pt alloy suggests three mechanisms of transformation in the temperature range 0 to 660°C. One at higher temperatures is consistent with a thermally activated diffusion controlled reaction, an intermediate mechanism is probably of a bainitic type, while the low temperature reaction is characterized by a shear mechanism. All mechanisms show time-dependent characteristics. Dilatometric measurements are unable to separate the two high-temperature mechanisms. (auth)

13308 HIGH TEMPERATURE LOW CYCLE FATIGUE OF AN EXTRUDED ALUMINUM–SILICON–MAGNESIUM–NICKEL ALLOY. Davies, V. De L.; Bakken, K. (Univ. of Norway, Trodheim). J. Nucl. Mater., 18: 226-30(Feb. 1966).

The frequency was varied from 1500 to 0.2 cycles/hr at test temperatures of 250, 300, and 350°C. Test results on the Al–12 Si–1 Ni–0.8 Mg alloy showed no correlation between frequency and number of cycles to failure. The stress was both frequency and temperature dependent. (W.L.G.)

13309 DIFFUSION CREEP DEFORMATION IN A MAGNESIUM REACTOR COMPONENT. Haddrell, V. J. (Berkeley Nuclear Labs., Eng.). J. Nucl. Mater., 18: 231-2(Feb. 1966).

An example of diffusion creep in a two-phase Mg–0.7 wt % Mn alloy, which was used as a reactor fuel element component, is presented. (W.L.G.)

13310 THE SPECIFIC HEAT OF ZIRCALOY-2 FROM 50 TO 700 DEG C. Brooks, C. R.; Stansbury, E. E. (Univ. of Tennessee, Knoxville). J. Nucl. Mater., 18: 233-4(Feb. 1966).

The specific heat was measured by dynamic adiabatic calorimetry. An abnormal rise in the specific heat occurred from 50 to 280°C in a sample in the as-received condition and is attributed to the solution of zirconium hydride. (W.L.G.)

13311 METALLOGRAPHIC OBSERVATIONS ON CREEP DEFORMATION OF MAGNOX AL 80. Nagasaki, Ryukichi; Shiraishi, Kensuke (Japan Atomic Energy Research Inst., Tokyo). J. Nucl. Sci. Technol. (Tokyo), 3: 32-40(Jan. 1966).

A study, with emphasis on metallographic observations, was made on the creep deformation of Magnox AL80 at 250, 300, 350, and 400°C. The creep deformation at 250°C was different from those at 300°C and above. In deformation at 250°C, grains broke down into cells that were marked and were smaller in size nearer the grain boundaries. This phenomenon was not observed in specimens subjected to creep at higher temperatures. Wavy grain boundaries, caused by uneven migration, were seen at 250°C, while projection of grain boundaries, caused by localized migration, often occurred at higher temperatures. It was concluded that creep cavities are nucleated at the tips of the ripples and projections of the grain boundary, which act like jogs and triple points. (auth)

13312 EFFECT OF PRESSURE ON THE MAGNETIC SUSCEPTIBILITY OF MANGANESE AND SCANDIUM. Svechkarev, I. V.; Panfilov, A. S. (Physico-technical Inst. of Low Temperatures, Academy of Sciences, Ukrainian SSR). JETP Lett. (USSR) (Engl. Transl.), 2: 313-4(Dec. 1, 1966).

Translated from Zh. Eksp. Teor. Fiz., Pis'ma Redakt., 2: 501-2(Dec. 1, 1965).

The magnetic susceptibility of manganese and scandium under hydrostatic pressures up to 2000 atm was measured. (D.C.W.)

13313 DIFFUSION IN THE PLUTONIUM–URANIUM SYSTEM. Dupuy, M.; Calais, D. (CEN, Fontenay-aux-Roses, France). Mem. Sci. Rev. Met., 62: 721-32(Oct. 1965). (In French).

Studies were made of chemical plutonium-uranium diffusion in couples of pure U and U–Pu alloy with 1.75% Pu. The interdiffusion coefficient and activation energy were determined for the temperature range from 400 to 550°C. (auth)

13314 SOME PROPERTIES OF BORON CARBIDE SINTERED UNDER PRESSURE. Rutkowski, W.; Szteke, W. (Instytut Baden Jadrowych, Swierk, Poland). Nukleonika, 10: 485-92(1965). (In Polish).

In connection with the manufacture of the boron carbide control and safety rods for the zero-power Anna reactor, tests were made of some properties of pressure-sintered boron carbide. Hardness, and its dependence on the pressing-piston distance, tensile strength, microstructure, and diffraction patterns were investigated. (auth)

13315 INVESTIGATIONS ON SELF-DIFFUSION OF INDIUM BY ABSORPTION METHOD, MAKING USE OF THE INTERNAL CONVERSION ELECTRONS OF ^{114}In. Jagielak, J.; Pawlicki, G.; Sobaszek, A. (Katedra Radiologii Politechniki Warszawskiej, Warsaw). Nukleonika, 10: 541-51 (1965). (In Polish).

Results of investigations on the self-diffusion of indium are presented. These investigations were carried out by making use of internal conversion electrons of ^{114}In. At

the absorbent thickness 1.6 to 11 mg/cm^2 Al, the absorption coefficient $\mu = 779$ cm^{-1} Al was obtained, with a relative average square error $\Delta\mu/\mu = 6.5\%$. Formula are given for determining diffusion coefficient in the case when the function of the radiation absorption in material is a straight line. The formulas were compared with those of Steigman, Shockley, and Nix deduced for exponential form of absorption function. The measurements were made by applying the methods of Steigman, Shockley, and Nix on polycrystalline samples 99.9999% pure In at 130 to 149°C and a value of 8.0 exp (–21.2 ± 0.6/RT) cm^2/sec was obtained for the self-diffusion coefficient. (auth)

13316 EFFECT OF VERY HIGH PRESSURE ON THE STRUCTURE OF SOME hcp METALS AND ALLOYS. Perez-Albuerne, E. A.; Clendenen, R. L.; Lynch, R. W.; Drickamer, H. G. (Univ. of Illinois, Urbana). Phys. Rev., 142: 392-9(Feb. 1966). (COO–1198-304).

The effect of pressure up to several hundred kilobars was measured on the lattice parameters of a number of hcp metals and alloys including magnesium and six dilute alloys, cadmium and two alloys, two alloys of silver with indium and two with antimony, and the rare-earth metals holmium, erbium, and thulium. For magnesium and its alloys the x-ray data combined with resistance data give rather clear evidence for a transition at high pressure from hcp to dhcp (ABABAB ... to ABACABAC ...). Electrical resistance measurements on pure cadmium indicate a similar event. No transition is noted for the cadmium alloys. All four silver alloys underwent a similar transition at high pressure. The rare earths show a high-pressure transition accompanied by an increase in the lattice parameter c with increasing pressure, which may be related to those appearing in the group II metals and the silver alloys. (auth)

13317 THE LATTICE PARAMETERS AND SOLUBILITY LIMITS OF ALPHA IRON AS AFFECTED BY SOME BINARY TRANSITION-ELEMENT ADDITIONS. Abrahamson II, E. P.; Lopata, S. L. (Army Materials Research Agency, Watertown, Mass.). Trans. Met. Soc. AIME, 76: 76-87(Jan. 1966).

The lattice parameters of α-iron with binary additions of all the transition metals, except technetium, were accurately determined on solid samples. No direct correlation with solute size was observed, but an effect of electron configuration was noted. The solubility limits of α-iron with Tl, Cu, Zr, Nb, Mo, Hf, Ta, and W were determined at 600, 700, 800, and 900°C. (auth)

13318 ULTRASONIC INSPECTION FOLLOWING HEAT TREATMENT OF URANIUM ALLOYS. Destribats, Marie-Therese; Cherpentier, C.; Papezik, F.; Pigeon, M. (CEN, Saclay, France). pp 3-21 of STI/PUB/105(Vol. II). (In French).

The inspection system adopted is based on the principle of absorption of ultrasonic waves by materials. This absorption depends on the structure of the medium. If λ is small in relation to grain size G, absorption is low; whereas if G is of the order of $\lambda/2$, absorption is very high. The tests were made first in air, using the multiple-echo system, then by measuring the height of the first echo, and finally by transmission in water, the height of the transmitted echo being compared with that of the initial signal. In industrial use, the amplitude of the echo transmitted by the material is compared with the echo obtained from a standard of the same characteristics and shape. Inspection takes place in a special machine in which the materials are rotated by rollers and adjustable transducers move over the element. The helicoidal scanning is carried out with a pitch of less than 5 mm. The ultrasonic generator includes a control system ensuring a constant reference echo. The results obtained with various alloys and in particular the faults observed in elements treated by induction upon linear displacement are discussed. The arrangement can detect faulty treatment zones of less than 1 cm^2. (auth)

13319 SOME NON-DESTRUCTIVE TESTING METHODS APPLICABLE TO SINTERED MATERIALS. Labusca, Elena; Mirion, L.; Andreescu, N.; Alecu, M.; Biscoveanu, I. (Inst. of Atomic Physics, Bucharest). pp 75-106 of STI/PUB/105(Vol. II). (In French).

Bearing in mind the specific granular structure of sintered materials produced from powders, whose compaction process is linked with the sintering treatment, the methods of checking the degree of sintering and certain other properties were investigated. The non-destructive methods used include: (1) Examination of the crystalline structure of solid sinters, using metallography and electron microscopy. These methods show the homogeneity of the structure, the grain size and orientation, the presence of various flaws such as inclusions and pores, and the actual course of the sintering process, including crystal formation, grain growth, etc. In certain cases the microscopic examination can be combined with micro-hardness tests. This examination of the microcrystalline structure is one of the principal methods of checking the quality of sintered materials, and is irreplaceable by any other method. (2) The degree of compaction, which is the main factor in determining the quality of sintered materials, can also be checked by measuring certain properties such as electric and thermal conductivity in relation to density, since for sintered materials conductivity is directly proportional to the degree of sintering. Experimental data on the application of these methods to certain sintered materials of importance in nuclear technology are presented. (auth)

13320 NON-DESTRUCTIVE EXAMINATION OF THE HEAT-AFFECTED ZONE OF WELDED Zr–Nb ALLOY. Hanstock, R. F.; Walker, D. C. B. (United Kingdom Atomic Energy Authority, Culcheth, Eng.). pp 277-84 of STI/PUB/105(Vol. II). (TRG-Report-950).

An alloy of zirconium, 2½% niobium has advantages for pressure containment in water-moderated reactors owing to the strength attainable by heat treatment. The corrosion resistance of the alloy under reactor operating conditions is also sensitively affected by heat treatment and zones of low corrosion resistance may be produced in the heat-affected zones of fusion welds. The zones susceptible to corrosion may be identified by autoclave treatment but this is not convenient when extensive pressure circuits are being assembled by welding. It was found that heat-affected zones susceptible to corrosion can be detected nondestructively by measuring the thermoelectric potential between a heated metallic point probe in contact with particular regions of the weld and adjacent metal. The construction of the thermoelectric probe is similar to one devised by the British Nonferrous Metals Research Association for measuring plating thickness on metal substrates and a commercially available instrument incorporating this type of probe is, with simple modification, suitable for testing welds in Zr–Nb alloys. An example is given of the variation of probe response across the heat-affected zones of a weld and is compared with an autoclave test for corrosion. (auth)

13321 MEASUREMENT OF INTERNAL FRICTION ON NUCLEAR MATERIALS. Hasiguti, R. R. (Tokyo Univ.); Igata, N.; Tonomae, R.; Nakamura, Y.; Sasao, N.; Domoto, K. pp 307-29 of STI/PUB/105(Vol. II).

The internal friction measurement is applicable to the inspection of metallic uranium, uranium dioxide pellets and zirconium alloys. This is because of its great sensitivity to the concentration of point defects and impurity atoms, to the density of dislocations and also to the microstructure of crystals. A relaxation peak at about 100°C was found from internal friction measurements of as-cast uranium, at various temperatures with free decaying method. The peak height increases by quenching and decreases by annealing after quenching. The peak temperature is almost the same in commerical and in high purity uranium, but it shifts a little to higher temperature by the addition of a small amount of aluminum, and much more by the addition of 1% molybdenum. The amplitude dependent internal friction of uranium was also measured. As the Granato-Lucke relation is satisfied in this case, the dislocation density and the dislocation loop length was calculated. These quantities were obtained, as the uranium

specimens were cold-rolled, annealed and quenched. The internal friction measurements of UO_2 pellets were performed using ultrasonic attenuation in the region of maximum concentration. From the temperature dependence of internal friction, a new relaxation peak was observed at low temperatures. In the measurements on zirconium alloys, the snoek peak of hydrogen was found. (auth)

Radiation Effects

See also CHEMISTRY — Radiation Chemistry

Refer also to abstracts 13247, 13425, 13973, and 14059.

13322 (BNWL–178) RADIATION-INDUCED DIMENSIONAL CHANGES OF RAW-COKE GRAPHITES. Helm, J. W. (Battelle-Northwest, Richland, Wash. Pacific Northwest Lab.). Dec. 1965. Contract AT(45-1)-1830. 15p. Dep. mn. CFSTI $1.00 cy, $0.50 mn.

Two series of irradiations were conducted to provide data on the comparative radioinduced dimensional changes of raw-coke graphites and a nuclear-grade conventional-coke graphite, CSF. The raw-coke graphites showed much less contraction than the CSF at 500 to 600°C and showed an expansion rather than a contraction at 700 to 800°C. The length changes for both the base stock and the impregnated graphite were very isotropic, particularly at the lower temperature. The CT graphites showed a much more anisotropic behavior, with the parallel samples contracting much more than the transverse samples. The length change for the raw-coke graphite in the transverse direction (550 to 650°C) was considerably less than for the other graphites. The results indicate the bonding between the coke and binder of graphite is of importance in dimensional behavior during irradiation. (P.C.H.)

13323 (CONF–170, pp 138–59) EFFECTS OF NEUTRON IRRADIATION ON THE MECHANICAL PROPERTIES OF HOT PRESSED AND EXTRUDED BERYLLIUM. Walters, G. P. (Oak Ridge National Lab., Tenn.).

Hot pressed and extruded Pechiney and Brush Be was examined after irradiation at 100, 350, and 600°C at doses to 6×10^{20} n/cm^2. No volume increases occurred during irradiation. Tensile tests were carried out at 20, 150, 350, 450, and 600°C. There was an increase in yield stress and a decrease in elongation during irradiation at 100 and 350°C. No changes in specimens irradiated at 600°C occurred. The yield stress dose dependence and thermal recovery are discussed in terms of thin film microstructure. Irradiated yield stress values can be calculated approximately if the He bubble configuration in the grains is known. (auth)

13324 (EURAEC–1529) INFLUENCE OF NITROGEN IN IRON AND STEEL UNDER FAST NEUTRON IRRADIATION. Quarterly Report No. 8, July 1–September 30, 1965. Rossin, F. (Societa Ricerche Impianti Nucleari, Sluggia (Italy). Centro Ricerche Nucleari). Nov. 1965. Contract 004-63-10-TEEI(RD). 9p. (EUR–267f). Dep. mn. CFSTI $1.00 cy, $0.50 mn.

Work Performed under United States–Euratom Joint Research and Development Program.

Tests were made on unirradiated, irradiated, and irradiated plus annealed materials. Tests on N_2 enriched Fe, before and after irradiation, gave a good agreement with literature results, while Fe–Ti alloys data do not seem to fit the Petch and Hall equation. (auth)

13325 (GEAP–4968) STAINLESS STEEL FAILURE INVESTIGATION PROGRAM. Second Quarterly Progress Report, July–September 1965. Pashos, T. J. (comp.) (General Electric Co., San Jose, Calif. Atomic Power Equipment Dept.). Oct. 1965. Contract AT(04-3)-189. 57p. (EURAEC–1541). Dep. mn. CFSTI $3.00 cy, $0.75 mn.

Work Performed under United States–Euratom Joint Research and Development Program.

Results of 24 hrs corrosion tests on irradiated and unirradiated type 304 stainless steel in boiling $HNO_3 - K_2Cr_2O_7$ indicate that irradiation exposure increases susceptibility to corrosion. The weight loss of irradiated cladding samples was consistently higher than that of unirradiated control specimens by a factor of two. Autoclave testing in high temperature $FeCl_3$ solutions was improved to reproducibly produce intergranular cracking of type 304 stainless steel. There was a marked difference in results of corrosion tests in $FeCl_3$ solution between unirradiated commercial type 304 stainless steel cladding and the cladding from co-extruded UO_2 in stainless steel fuel rod. Commercial tubing cracked intergranularly in from 1 to 2 days whereas the co-extruded specimen had not failed after 8 days exposure. Tensile tests at 650°F and at strain rates of 0.024 and 0.0024 in/in/min and at constant load were performed on irradiated cladding samples. The tensile fractures were all transgranular and ductile with no evidence of intergranular separation. Electron microscopy was performed on an incipient crack that extended one-third of the way through the cladding. The tips of the crack were observed to be rounded with no evidence of mechanical fracture. (auth)

13326 (GEAP–5100C) HIGH-PERFORMANCE UO_2 PROGRAM IRRADIATION OF 0.5 INCH DIAMETER, SOLID-PELLET UO_2 FUEL RODS AT 1,000,000 BTU/H-FT^2 PEAK HEAT FLUX. Lyons, M. F.; Nelson, R. C.; Pashos, T. J.; Wilson, C. R.; Weidenbaum, B. (General Electric Co., San Jose, Calif. Atomic Power Equipment Dept.). Oct. 1965. Contract AT(04-3)-189. 12p. (EURAEC–1537). Dep. mn. CFSTI $5.00 cy, $1.00 mn.

Work Performed under United States–Euratom Joint Research and Development Program.

The fabrication data, irradiation history, and the complete, correlated postirradiation examination results are described for a four-rod fuel assembly, designated EPT-10, that operated in the GETR-PWL with extensive central melting to a burnup of 1450 Mwd/te. The fuel rods were unsegmented, reactor-length rods containing 95% dense, solid, sintered UO_2 pellets in free-standing Zircaloy-2 cladding. This fuel assembly was the third of a series irradiated to investigate the feasibility and limitations in UO_2 fuel-rod operation with central melting. Postirradiation examination of this assembly revealed the most extreme examples of clad swelling observed with pellet fuel and confirmed that the swelling, expressed as a volume increase, is a function of the fuel rod thermal performance level. This severe, localized clad swelling proved to be the basic obstacle to achieving satisfactory operation with central melting in high density fuel. Later work proved that the clad swelling resulted from the UO_2 phase change volume expansion and could be corrected by proper fuel rod design. (auth)

13327 (ORNL–TM–1354) RECOMBINATION AND TRAPPING IN ^{60}Co GAMMA-IRRADIATED N-TYPE GERMANIUM [Thesis]. Streetman, B. G. (Oak Ridge National Lab., Tenn.). Feb. 1966. Contract W-7405-eng-26. 121p. Dep. mn. CFSTI $4.00 cy, $0.75 mn.

Submitted to Texas Univ., Austin.

Carrier recombination and trapping processes were studied in n-type germanium irradiated at 77°K with ^{60}Co gamma rays. The experiment involved measurement of the carrier lifetime from 110° to 330°K by the photoconductive decay method. Irradiations and isochronal annealing studies were made on both Sb- and As-doped samples over a range of carrier concentrations. The samples were maintained in a vacuum during the entire irradiation-measurement-annealing procedure to eliminate variations in the surface effect. The irradiation produced a recombination level 0.35 ev above the valence band in Sb-doped material, and a level 0.32 ev above the valence band for As doping. The irradiation formed a hole trap at 0.37 ev above the valence band in the Sb-doped material, and the annealing created an additional trap 0.21 ev above the valence band. Each of these trapping centers exhibited a multiple negative charge at low temperatures. The annealing created the 0.21-ev level in considerable concentration and this center exhibited multiple trapping. The irradiation created a trap in As-

doped material and a new trap during annealing. The energy level positions for these traps are uncertain, but both exhibited a multiple negative charge at low temperature. Most of the recombination centers annealed at 70°C in As-doped material, but a reverse anneal centered at about 180°C followed this stage. The annealing of recombination centers in Sb-doped material exhibited a reverse anneal at room temperature followed by two annealing stages centered at 70° and 130°C. The relative amount of annealing in these two stages was dependent upon the carrier concentration and the extent of the early reverse anneal. The carrier lifetime in the recombination region recovered essentially to its original value after annealing at about 250°C. (auth)

13328 (ORNL-TM-1359) EFFECT OF IRRADIATION ON THE STRESS-RUPTURE CHARACTERISTICS OF A 20 percent Cr-25 percent Ni NIOBIUM-STABILIZED STAINLESS STEEL. Venard, J. T.; Weir, J. R. (Oak Ridge National Lab., Tenn.). Feb. 1966. Contract W-7405-eng-26. 15p. Dep. mn. CFSTI $1.00 cy, $0.50 mn.

In-reactor and out-of-reactor stress-rupture tests were performed on a 20% Cr-25% Ni niobium-stabilized stainless steel that had been annealed at 800°C for 60 hr after cold drawing. The specimens were internally pressurized closed-end, thin-walled tubes. Average dose rates were 6×10^{13} neutrons cm^{-2} sec^{-1} thermal at the specimen midline and the experiment was exposed for approximately 1000 hr. No effect of irradiation on rupture strength was seen; however, comparison of the test results with earlier work demonstrated that the material given an 800°C, 60-hr anneal was weaker but more ductile than another heat given a 1050°C, ½-hr anneal. X-ray analysis indicated that this particular cast of material forms sigma phase. (auth)

13329 (RT/FI(65)46) A CONTRIBUTION TO THE STUDY OF THE BEHAVIOUR OF FISSION GAS BUBBLES. Segre, G. J. (Comitato Nazionale per l'Energia Nucleare, Rome (Italy)). Nov. 1965. 28p. Dep. mn.

The behavior of fission gases in uranium dioxide fuel elements irradiated at severe thermal conditions was studied. Causes and modalities of the movement of the gases were analyzed to determine more facts concerning their release. (P.C.H.)

13330 HOMOGENIZATION OF TWO-PHASE MIXTURES OF ZrO_2–UO_2 BY IRRADIATION. Berman, R. M. (Bettis Atomic Power Lab., West Mifflin, Pa.). J. Nucl. Mater., 17: 313-23(Dec. 1965).

Plates of ZrO_2 36.8 wt % UO_2 and ZrO_2 46 wt % UO_2, consisting initially of two phases, were clad in Zircaloy and irradiated to various burnups from 1 to 6×10^{20} fissions/cm^3. X-ray diffraction showed that the axial ratio of the zirconia-rich tetragonal phase decreased toward unity with irradiation and the cell volume of the tetragonal phase increased until it reached the value appropriate for a single homogeneous phase. These changes proceeded more rapidly ZrO_2 46 wt % UO_2 than in ZrO_2 36.8 wt % UO_2. The process of homogenization can be satisfactorily defined by a diffusion equation, if a value for the diffusion constant, D of 3.32×10^{-14} cm^2/sec is used. This D value indicates that a single fission homogenizes a volume containing 1.66×10^7 atoms. This number is two orders of magnitude too large to be explained by Brinkman's displacement spike hypothesis. Calculations based on Konobeevsky's hypothesis of a thermal pulse show that the liberation of 23 Mev of thermal energy at the center of such a volume is sufficient to cause homogenization. This seems well within the capabilities of a fission event. (auth)

13331 FURTHER REPLICA ELECTRON MICROSCOPY STUDIES OF IRRADIATED BeO. Rau, R. C. (General Electric Co., Cincinnati). J. Nucl. Mater., 17: 341-3(Dec. 1965).

The effects of radiation on BeO were studied in terms of changes in microstructure. Replica studies of the gas bubbles are described. Specimens irradiated to 3.5×10^{20} nvt (>1 Mev) at 830°C showed gas bubble formation while these irradiated only to 2.8×10^{20} nvt showed no indication of gas bubble formation. The effects of post-irradiation annealing on gas bubbles were also studied. Electron micrographs of an irradiated BeO rod before and after annealing are shown. The lack of grain boundary separation in the specimen irradiated at 915°C prevented the escape of the gas during annealing, and led to the growth of larger bubbles. (F.J.H.)

13332 ON THE FORMATION AND BEHAVIOR OF POINT DEFECT CLUSTERS IN NEUTRON IRRADIATED URANIUM CARBIDE. Eyre, B. L.; Sole, M. J. (Atomic Energy Research Establishment, Harwell, Eng.). J. Nucl. Mater., 18: 314-22(1966). (AERE-R-4956).

Hyperstoichiometric uranium carbide single crystals specimens were irradiated to doses of up to 5.4×10^{16} f/cm^3 at ~130°C. A transmission electron microscope examination of thin films showed that a dose of 1.4×10^{16} f/cm^3 results in the formation of observable clusters in the uranium carbide matrix, the size and number of which increase with dose. Observable point defect clusters are only formed in the uranium dicarbide platelets after the highest dose studied. On annealing, the point defect clusters in both phases start to disappear above 700°C. On annealing at 1200 and 1300°C, however, the clusters in the uranium carbide matrix grow and become resolvable as loops. The results are explained on the hypothesis that the point defect clusters in the irradiated material are interstitial in nature. It is suggested that the vacancies become mobile at 700°C and produce the observed annealing effects by recombining with the interstitial clusters. A model is proposed for the formation of interstitial loops that is consistent with the observed loop behavior. (auth)

13333 CHANGES OF MECHANICAL PROPERTIES OF CHROMIUM–NICKEL–STEEL AND NICKEL ALLOYS AFTER NEUTRON IRRADIATION. Boehm, H.; Dienst, W.; Hauck, H.; Laue, H. J. (Kernforschungszentrum, Karlsruhe, Ger.). J. Nucl. Mater., 18: 337-47(1966). (In German).

Austenitic Cr–Ni steels and Ni-alloys were irradiated at 70°C and the changes in the mechanical properties between room temperature and 750°C were studied. At room temperature the materials show the typical brittleness due to neutron irradiation. The yield strength and the tensile strength increase while the total elongation decreases. An exception are the values of the tensile strength of the precipitation hardened alloys which decrease when irradiated with small neutron doses. The changes in the mechanical properties seem to be saturated after a neutron dose of $3-5 \times 10^{20}$ n/cm^2 for the austenitic steels and after 1×10^{21} n/cm^2 for the Ni-alloys. Recovery of the mechanical properties set in above 500°C in all the alloys studied. Annealing at 550°C did not lead to a full recovery. The brittleness remaining increases with increasing irradiation dose. The original values of the mechanical properties were reached first after annealing at 700°C. High temperature embrittlement, which is indicated by the decrease in ductility, begins at 550°C in the Ni-alloys and above 600°C in austenitic steels. The mechanism of high temperature embrittlement is discussed. (auth)

13334 AN INVESTIGATION OF ATOMIC COLLISION SEQUENCES AND THERMAL SPIKES IN α-URANIUM. Nelson, R. S. (Atomic Energy Research Establishment, Harwell, Eng.). J. Nucl. Mater., 18: 348-56(1966). (AERE-R-5059).

The production of irradiation damage in α-uranium was investigated by observing the ejection of atoms from single crystal and polycrystalline specimens during irradiation with 80 kev Kr^+ ions. Ejection from the single crystals was found to occur preferentially near to the [100], [110], and [487] type directions. This is interpreted in terms of focused collision sequences traveling along these directions which, on intersecting the surface, cause ejection in the same direction. The possible focusing mechanisms are discussed for each sequence, and an estimate made of their focusing energies. Atomic ejection from the poly-

crystals was measured as a function of temperature. The sputtering ratio (the average number of atoms ejected per ion) remained effectively constant from room temperature up to about 400°C; however, between 400 and 600°C an approximately exponential increase was observed. The increase is explained in terms of evaporation from thermal spikes created by the individual bombarding ions, and analysis of the results has provided information as to the spike's size, life-time, and temperature. In the light of the present results the spatial distribution of interstitials and vacancies produced in α-uranium as a result of recoils from direct collisions with fast neutrons is discussed qualitatively. Some of the main conclusions are also appropriate to a better understanding of the damage produced by fission fragments. (auth)

13335 INFLUENCE OF GRAIN SIZE ON THE IRRADIATION EMBRITTLEMENT OF STAINLESS STEEL AT ELEVATED TEMPERATURES. Martin, W. R.; Weir, J. R. (Oak Ridge National Lab., Tenn.). J. Nucl. Mater., 18: 108-18(Feb. 1966). (ORNL-P-1044).

The influence of grain size in the range of ASTM 3 to 10 on the postirradiation ductility of stainless steels was studied. The strain at fracture for irradiated and unirradiated material was analyzed in terms of grain-boundary sliding, slip within the grain matrix, and the strain attributable to widening of cracks. The ductility of irradiated materials may be increased significantly by reducing the grain size. A stainless steel having a grain size of ASTM 8 to 10 is at least twice as ductile as a material having a grain size of ASTM 3. Irradiated materials fractured at strains for which no grain boundary sliding was detected. (auth)

13336 ON THE RELEASE OF FISSION GAS FROM AN EVAPORATING FUEL BODY. Chambre, P. L. (Univ. of California, Berkeley). J. Nucl. Mater., 18: 167-75 (Feb. 1966).

Isothermal postirradiation anneal experiments were extensively used to determine diffusion coefficients for fission gases in nuclear fuel bodies. Several of these experiments were carried out at temperatures sufficiently high for an appreciable evaporation rate of the fuel body, but the effect of this evaporation upon the release of the fission gas and upon the determination of diffusion coefficients has heretofore not been analyzed. In the following the time-dependent lattice diffusion of a radioactive gas contained in solids of simple shapes (sphere, slab, cylinder and certain partially unbounded media) is analyzed. The solid sublimes into a vacuum and as a result the boundary surface regresses. This regression is assumed to be a linear function of time. It is shown that the effect of the moving boundary increases the rate of diffusion of the gas through the boundary because the regression of the interface steepens the surface concentration gradient compared with a stationary interface. If surface evaporation is ignored, the predicted diffusion coefficient in a post-irradiation anneal experiment can be erroneously high by several orders of magnitude. (auth)

13337 THE EFFECT OF NEUTRON IRRADIATION ON ALUMINUM OXIDE. Hickman, B. S.; Walker, D. G. (Australian Atomic Energy Research Establishment, Sydney). J. Nucl. Mater., 18: 197-205(Feb. 1966).

Results are presented of studies of single crystal and polycrystalline aluminum oxide after neutron irradiation to doses up to 5×10^{20} nvt (>1 Mev). The macroscopic and x-ray growth were found to be equal both during irradiation and during post-irradiation annealing. On the basis of thin film electron microscopy, reciprocal lattice photography and the growth measurements, some conclusions are drawn as to the nature of the defect structure. It is shown that the postirradiation annealing and the effect of irradiation temperature can be described quantitatively by an annealing process with a spectrum of activation energies. Optical metallography and some limited mechanical property measurements showed no evidence for deterioration of the properties of polycrystalline material and it is concluded that irradiation damage should not place serious limitations on the use of aluminum oxide in a reactor environment. (auth)

13338 ELIMINATION OF DEFECTS IN ALUMINIUM IRRADIATED BY FAST NEUTRONS IN LIQUID NITROGEN. Frois, C.; Dimitrov, O. (Centre d'Etudes de Chimie Metallurgique, Vitry-sur-Seine, France). Mem. Sci. Rev. Met., 62: 697-704(Oct. 1965). (In French).

Experimental conditions for irradiation and measurement are described. The recovery of electric resistivity of irradiated aluminum was determined. The recovery appeared to occur in two stages: a complex stage in which the defects were healed, followed by the disappearance of vacancy defects. (auth)

13339 MODIFICATION OF THE ELECTRON STRUCTURE OF GOLD BY α IRRADIATION AND SUBSEQUENT RECOVERY. Gschaider, Siegfried; Stangler, Ferdinand (Univ., Vienna). Oesterr. Akad. Wiss., Math.-Naturwiss. Kl., Sitzungsber., Abt. II, 173: 141-55(1964). (In German)

The effects of α particles at 78°K and subsequent isothermal recovery on the electron structure of different thicknesses of gold foil were investigated. The parameters of the electron structure were calculated from experimentally established values of electric resistance, the Hall constant, and increases in magnetic resistance. The study showed, in agreement with the electron structure used, an irradiation behavior similar to that of copper. On the basis of the electron structure it was established that vacancies arising in the irradiation are Frenkel effects. From the differing recovery behavior of the different thicknesses of foils it was concluded that the α particles in the first part of their range in gold produce preponderantly Frenkel pairs widely separated from each other and that in the second part of their path the number of Frenkel pairs close to each other predominate. (tr-auth)

13340 DOSE DEPENDENCE OF THE ANNEALING STAGE II IN NEUTRON IRRADIATED ALUMINUM. Burger, C.; Isebeck, K.; Meissner, H.; Schilling, W.; Wenzl, H. (Technische Hochschule, Munich). Phys. Lett., 20: 124-5(Feb. 1, 1966).

The recovery of electric resistivity in aluminum following low temperature irradiation with reactor neutrons was studied in the temperature region 55–150°K. The temperatures of the main annealing peaks found are dose independent in a dose range 1:100. (auth)

13341 ON THE INFLUENCE OF NETWORK DEFECTS ON THE OPTICAL CHARACTERISTICS OF GLASSES. Knechtel, G.; Scharmann, A. (Univ., Giessen, Ger.). Z. Angew. Phys., 20: 141-4(Dec. 1965). (In German).

The application of the terminology of network defects after Stevels on the optical properties of silicate glasses enables a relation to be obtained between the short wave limit of transmission of uv-light and the optical resistivity against high-energetic radiation. In the case of Mg-phosphate glass two absorption bands are observed, one after a heating process and the other after irradiation. These absorption bands are attributed to Q-respectively Q_{2+}-centers. (auth)

13342 PROPERTIES OF GERMANIUM UNDER 9.6 Mev DEUTERON IRRADIATION [Thesis]. Kleitman, David. Lafayette, Ind., Purdue Univ., 1958. 113p.

Carrier concentration and Hall mobility changes resulting from 9.6-Mev deuteron irradiation were measured for a variety of n and p type germanium specimens at 85°, 205° and 300°K. Evidence for major bombardment defect levels introduced within 0.05 ev of both band edges was obtained. Deeper levels were introduced near E_{VB} + 0.2 ev (205°K). Levels between E_{CB} − 0.1 ev and E_{CB} − 0.3 ev were indicated as was a level near E_{VB} + 0.08 ev. Maximum carrier removal rates for p type specimens are lower than for n type and both are below theoretical estimates. The possible nature of a bombardment level model is discussed as is the fitting of the observed Hall mobility changes to a model. Complex effects were noted at 85°K such as a double minimum for the conductivity vs. flux curve. Unlike irradiated p type germanium where warming from 85°K to 300°K can

produce large changes, such warming of n type specimens results in smaller change, while annealing processes occur. Annealing after deuteron irradiation of a 30-cm p type specimen at 300°K was compared to related 5.3-Mev alpha and 4.5-Mev electron results. Photoconductivity was observed after bombardment at 85°K of initially high-resistivity n type specimens. Structure was seen at 2.2μ and 3.5μ both as a positive and negative photoconductivity, depending upon the stage of bombardment. Interpretations are discussed. The existence of low-temperature imperfection conduction due to lattice displacement produced defects alone was clearly demonstrated. Larger polished surfaces of Ge, InSb and GaSb were irradiated at 85°K and examined interferometrically. An unexpectedly large expansion was observed in GaSb specimens after warming to 300°K while a somewhat similar expansion was seen with InSb, but no expansion was detected with a Ge sample. The expansion observed in GaSb is near the upper limit that could be explained by point defect considerations. (Dissertation Abstr.)

13343 DIMENSIONAL MEASUREMENTS AND FLAW DETECTION. **Brebant, C.; Huillery, R.; Roussel, E. (CEN, Saclay, France).** pp 151-66 of STI/PUB/105 (Vol. II). **(In French).**

Nondestructive tests on irradiated fuels were carried out in concrete cells in the very high-activity laboratories at Saclay and Cadarache. The equipment in use can be used for all types of fuel. The cells used for these tests contain the following equipment: Radiographic equipment scanning either around or along the sample; leak-testing equipment; observation equipment; and standard metrological equipment. Radiography and leak testing are discussed. For the rotary scanning equipment, the slugs are x-rayed and the films are introduced into the x-ray beam via an aperture in the rear door. The film exposure time is regulated by a rocker. The slug is placed in the beam by heavy remote-handling equipment. Several emulsions are available, the one most suited to the specific activity of the fuel being selected. The results obtained to date are excellent, and it is hoped that they can be improved still further by the adoption of a new type of equipment scanning along the sample, whose operation is described. The leak test is carried out in a transparent vessel which may contain either ethylene glycol or white spirit. Leaks are detected by progressive evacuation. Surface bubbling is eliminated by various methods of treating the surface of the slugs. For detecting microleaks the fuel is previously pressurized in a bath of helium at 35 kg (cm^2). This equipment is satisfactory, and makes it possible to produce photographic record locating the leak. (auth)

PHYSICS

General

Refer also to abstracts 12760 and 13364.

13344 (AEEW-M-604) THE KDF9 PROGRAMME EDIT1. Doherty, G. (Atomic Energy Establishment, Winfrith (England)). July 1965. 6p. Dep. BIS $0.30. HMSO 1s. 9d.

EDIT1 is a KDF9 FORTRAN program for producing a nuclear data tape, either in binary records, or on the BCD low density mode satisfying the format requirements of the UKAEA nuclear data library. The program operates only on complete files which may be in binary or BCD mode for input, though the single IBM compatible tape unit cannot be used for both input and output in the same job. Programs using the data library on the KDF9 will operate in the binary mode but facilities for reading and writing BCD card image libraries are necessary for compatibility with other computer installations. (auth)

13345 (NP-15772) ANNUAL REPORT [ON NUCLEAR RESEARCH], 1964. (Institute for Nuclear Study, Tokyo Univ. (Japan)). 84p. Dep. mn.

Operation of the fixed frequency cyclotron during the report period is summarized. Information is included on development of apparatus and instruments, investigation of nuclear structure, and nuclear reactions. Design and operation of the electron synchrotron are also summarized. A general description of the air shower division is presented, and improvements in equipment are described. Collaboration with the Bolivian air shower experiment is discussed along with development of low-background counting techniques. Results of work on high-energy interactions are presented. An analysis of high-energy jet showers is presented, and balloon flights are described. Development of computer codes DWBA2 for scattering cross sections, and DWBA3 for knock on, stripping, and pick up reactions is reported. Studies of nuclear reactions, isotopic exchange kinetics, and long-term variation of cosmic ray intensity are reported. Activities in the mechanical shop, electronic shop, computer room, and health physics division are summarized. Institute publications are listed. (J.R.D.)

13346 (SC-RR-65-396) MIE SCATTERING FUNCTIONS (MSF) COMPUTER PROGRAM DESCRIPTION. Warnke, D. F. (Sandia Corp., Albuquerque, N. Mex.). Feb. 1966. Contract AT(29-1)-789. 55p. Dep. mn. CFSTI $3.00 cy, $0.50 mn.

The results of the Mie Scattering theory were programmed on Sandia's CDC-3600 computer. Data inputs are the particle size parameter, complex index of refraction, scattering angle, and wave length. Data outputs are the scattering and extinction coefficients, intensity functions, radar cross section, angular scattering cross section, and the 180-degree total scattering cross section for a given mass of monodispersed aerosol. (auth)

13347 (UCRL-16511) PHYSICS DIVISION SEMIANNUAL REPORT, MAY-OCTOBER 1965. (Lawrence Radiation Lab., Univ. of California, Berkeley). Nov. 10, 1965. Contract W-7405-eng-48. 62p. Dep. mn. CFSTI $3.00 cy, $0.75 mn.

Separate abstracts were prepared for the 2 included sections. (M.O.W.)

For abstracts of individual sections see: 13368 and 13463.

13348 A NEW METHOD FOR THE CALCULATION OF TEMPERATURE AVERAGES. Praveczki, E. (Central Research Inst. of Physics, Budapest). Acta Phys. Acad. Sci. Hung., 19: 315-19(1965).

A new method will be presented for the calculation of the temperature averages. The method is in close connection with the Green's function method, as it is based upon the so called projection relations, which can be regarded as the solutions of the Green's function problem. From the projection relations we get the exact formulas and series expansions with the help of the principle of perturbation and renormalization. (auth)

13349 THE THERMAL CONDUCTIVITY IN A ROTATING CYLINDER EXPOSED TO RADIATION. Goldoni, Gino. Atti Accad. Sci. Torino: I. Cl. Sci. Fis., Mat. Natur., 99: 917-37(1964-65). (In Italian).

The temperature distribution in a rotating homogeneous cylinder exposed to radiation is studied. The temperature at the profile is then studied as a periodic function of time. Although the case of the cylindrical artificial satellite in trajectory has been considered previously, the present study is devoted to more general conditions. (tr-auth)

13350 PARTICLE OPTICS INSIDE AN ABSORBER. Banaigs, J.; Citron, A.; Fronteau, J.; Goldzahl, L.; Hornsby, J. (CERN, Geneva). Nucl. Instrum. Methods, 39: 150-6(Jan. 1966).

The transmission of charged particles through an absorber is treated, including the case where the absorber is placed inside a magnetic focusing device. The energy loss in the absorber and multiple scattering are taken into account. The method is adapted to computer calculations. (auth)

13351 GENERALIZED VARIATIONAL PRINCIPLES IN CLASSICAL MECHANICS. Linder, A. (Royal Inst. of Tech., Stockholm). Nuovo Cimento, (1), 3: Suppl., 117-46(1965).

The problem of finding a variational principle in classical mechanics is investigated, which gives a canonical momentum for time as well as for the space coordinates. The parametrized principles are considered from a general point of view as invariant principles, i.e., principles which are invariant under arbitrary transformations of the parameter of integration u. The problem of modifying any given invariant variational principle so as to permit a regular canonical formalism which preserves the original extremal conditions, is investigated. The theory of the generalized principles is then applied to classical mechanics. Some examples are given of the class of generalized principles corresponding to Hamilton's principle for arbitrary mechanical systems with n degrees of freedom. The variational principles are then investigated for a particle in an electromagnetic field. (L.B.S.)

13352 TRANSITION RADIATION FROM RELATIVISTIC ELECTRONS CROSSING DIELECTRIC BOUNDARIES. Inman, Fred W. (Univ. of the Pacific, Stockton, Calif.); Muray, J. J. Phys. Rev., 142: 272-6(Feb. 1966).

A coincidence technique was used to observe transition radiation from fast electrons crossing the boundary between a vacuum and a dielectric. Gold, nickel, aluminum, and Mylar were the dielectrics used. A photomultiplier was used to count single photons in coincidence with the arrival of the electron at the boundary, as observed with a lithium-drifted germanium detector. The electrons were from a cesium-137 source. The relative photon yields for the three metals were: Al yield/Au yield = 1.03 ± 0.22, Ni yield/Au yield = 0.61 ± 0.09. The absolute yield for gold was $(10 \pm 3) \times 10^{-3}$ photons per electron, in agreement with theory. The results with Mylar are complicated by fluorescence effects, but there is evidence that the transition-radiation yield is of the same order of magnitude as the yield in gold. The yield was measured as a function of electron energy; it is a monotonically increasing function of the energy from 0.33 to 0.662 Mev, in qualitative agreement with theory. (auth)

13353 CONDITIONAL PROBABILITY IN PHYSICS. Watanabe, Satosi (Yale Univ., New Haven). [Progr. Theoret. Phys. (Kyoto), 34: Suppl., 135-60(1965)].

It is contended that the phenomenological one-way-ness of temporal developments in physics is due to irretrodictability, and not due to irreversibility. This irretrodictability is shown to originate from a simple property of the very notion of conditional probability, independent of the structure of dynamical theories. It is demonstrated how macroscopic irretrodictability can be reconciled with microscopic retrodictability in classical physics. Quantum physics is irretrodictable, microscopically as well as macroscopically, whether it is invariant for T, TC, TP, or TCP, or not invariant at all in any such sense. (auth)

13354 ATOMISM AND COSMOLOGY. Hayakawa, Satio (Nagoya Univ., Japan). [Progr. Theoret. Phys. (Kyoto), 34: Suppl., 532-41(1965)].

Under the postulate that the present form of matter is a consequence of the evolution and therefore the laws of physics are dictated by the structure of the universe, arguments for this idea are presented. A number of fundamental physical constants are correlated with cosmological constants. In particular, physical constants important in atomic physics, such as the unit electric charge, Planck's constant and the weak coupling constants, are expressed by combinations of the cosmic radius and the total numbers of particles in the universe. (auth)

Accelerators

Refer also to abstracts 12906, 12957, 13347, and 13715.

13355 (AD-626999) A GENERAL ORBIT PROGRAM FOR SECTOR-FOCUSED CYCLOTRONS. Shaw, L. (Naval Radiological Defense Lab., San Francisco, Calif.). Nov. 23, 1965. 40p. (USNRDL-TR-936). CFSTI $2.00 cy, $0.50 mn.

A program for computer studies of general ion orbits in sector focused cyclotrons is described. Several of the improvements to the original version of the code are discussed, including time dependent acceleration with four dee gaps in any harmonic mode. The general features of the code are described, such as tracing of orbits in the backward direction, simultaneous tracking of two orbits, and axial motion. A discussion of the input parameters and instructions for the operation of the program are included. (auth)

13356 (AECD/EP/6) A REPORT ON INSTALLATION OF A 3-Mev VAN DE GRAAFF AT DACCA. Hussain, Md. Emdad (Atomic Energy Centre, Dacca (Pakistan). Experimental Physics Div.). July 1965. 44p. Dep. mn.

Descriptions of the various components of the Dacca 3-Mev Van de Graaff are presented. (M.O.W.)

13357 (AED-C-18-06) ACCELERATORS. Series C: Bibliographies. Mausberg, W. (comp.) (Frankfurt Univ. (West Germany)). 1965. 92p. Dep. mn.

References (328) to literature on accelerators are given. Author, patent-number, and report-number indexes are included. (D.C.W.)

13358 (BNL-9944) APERTURE AND CELL SIZE EFFECTS ON SHUNT IMPEDANCE OF ALTERNATING PERIODIC STRUCTURES. Carter, D.; Nishikawa, T. (Brookhaven National Lab., Upton, N. Y.). Dec. 17, 1965. Contract AT-30-2-GEN-16. 14p. Dep. mn. CFSTI $1.00 cy, $0.50 mn.

To find the dependence of shunt impedance on both cell length ratio and coupling aperture size, it suffices to find an approximation for the field distribution along the axis. The field around the aperture was resolved into symmetric and antisymmetric parts. The shunt impedance was calculated. The technique for calculation is presented. (M.O.W.)

13359 (CERN-65-36) SEPTUM MAGNETS WITH 10 AND 20 KG FIELDS FOR SLOW AND FAST EJECTION FROM THE CPS. Umstaetter, H. H. (European Organization for Nuclear Research, Geneva (Switzerland)). Nov. 2, 1965. 71p. Dep. mn.

The following report summarizes the results of measurements and calculations on the new septum magnets designed for both fast and slow ejection (resonant extraction system) from the CERN Proton Synchrotron (CPS). A first pair of magnets was installed in the east ejection area, and two further pairs are completed. One magnet reaches 10 kG with 0.06% stray field in front of the septum, the other 20 kG with −0.25% stray field. (auth)

13360 (CERN-65-42) FOCUSING AND CHROMATIC ABERRATIONS IN A PERIODIC AG BEAM TRANSPORT SYSTEM. Regenstreif, E. (European Organization for Nuclear Research, Geneva (Switzerland)). Dec. 15, 1965. 44p. Dep. mn.

The focusing properties of a periodic beam transport system were examined in the light of its AG behavior, and the effect of chromatic aberrations in a channel of this type was considered with particular reference to optimum mode and minimum aberrations. The latter were compared to the aberrations under stigmatic conditions. The properties of the channel are first analyzed in terms of the thin lens approximation which reveals all important features of a system of this type. The thick lens approach then takes into account the fine structure of the system. The relevant characteristics are given in graphical form as a result of the calculations. The channel was considered as a system in itself, i.e., although its properties are examined in view of subsequent matching, no attempt was actually made to match to the channel the source emittance or the detector acceptance. (M.O.W.)

13361 (EGG-1183-2066) RADIATION CALIBRATION OF A 20 Mev LINAC. Sandifer, C. W.; George, W. D. (Edgerton, Germeshausen and Grier, Inc., Santa Barbara, Calif.). Nov. 1965. Contract AT(29-1)-1183. 26p. (CONF-651109-16). Dep. mn. CFSTI $2.00 cy, $0.50 mn.

From 1st Symposium on Accelerator Radiation Dosimetry and Experience, Upton, N. Y.

Data are presented on the calibration of a 20-Mev electron linear accelerator in the following areas: energy calibration of beam handling system, bremsstrahlung production and angular distribution, bremsstrahlung spectral distribution. A technique employing the ^{12}C (γ,γ) resonance for calibration of the beam handling system is discussed. Experimental results are presented, and a calibration factor is obtained. A fluor/photodiode detector calibrated against Victoreen thimble chambers was used to determine the bremsstrahlung production from a 0.2 radiation length gold-tungsten target as a function of electron beam energy and current. Angular distribution of the bremsstrahlung field was determined by ion chambers enclosed in lead caps and lucite blocks. Bremsstrahlung energy spectra were measured using a NaI gamma-ray spectrometer with pulse pile-up rejection. Spectra are reported from 5 to 21 Mev with pile-up limited to about 1 per cent. Variation of energy spectra with angle is also presented. (auth)

13362 (JINR-P-2503) DIAFRAGMIROVANNYI VOLNOVOD KAK OTKLONYAYUSHCHAYA SISTEMA VYSOKOCHASTOTNOGO SEPARATORA. (A Diaphragmed Waveguide as a Deflection System of a High Frequency Separator). Aleksandrov, I. A.; Vagin, V. A.; Kotov, V. I. (Joint Inst. for Nuclear Research, Dubna (USSR). Lab. of High Energy). 1965. 22p. Dep. mn.

Characteristics of the diaphragmed waveguide as a deflection system of a high energy particle separator were considered in detail in the one-wave approximation. A method is given for choosing the optimal parameters. The results obtained are compared with the rigorous theory and experimental data. (auth)

13363 (JINR-P-2507) VOLNY S KOMPLEKSNYMI POSTOYANNYMI RASPROSTRANENIYA V DIAFRAGMIROVANNOM VOLNOVODE. (Waves With Complex Propagation Constants in a Diaphragmed Waveguide). Aleksandrov, I. A.; Vagin, V. A.; Kotov, V. I. (Joint Inst. for Nuclear Research, Dubna (USSR). Lab. of High Energy). 1965. 12p. Dep. mn.

A theory is given of non-symmetrical waves with complex propagation constants in the diaphragmed waveguide without losses. The existence of different forms of com-

plex solutions corresponding to a different character of hybrid waves is shown. The evolution of dispersion characteristics of propagating, above limiting and complex waves is plotted graphically against the structure parameters. (auth)

13364 (LAL–1148) RAPPORT D'ACTIVITE, 15 AVRIL–15 OCTOBRE 1965. (Report of Activities, 15 April–15 October 1965). (Laboratoire de l'Accelerateur Lineaire, Univ. de Paris, Orsay (France)). Nov. 1965. 68p. Dep. mn.

The improvement and utilization in the accelerator is summarized, together with research progress on nuclear physics, nuclear spectroscopy, pion physics and storage rings. Development of associated experimental equipment and radiation control are also reported. A bibliography of the publications during this period is appended. (J.S.R.)

13365 (SLAC–39(Rev.)) MAGNETIC FIELD MEASUREMENT AND SPECTROSCOPY IN MULTIPOLE FIELDS. Cobb, J. K.; Muray, J. J. (Stanford Linear Accelerator Center, Stanford Univ., Calif.). Nov. 1965. Contract AT(04-3)-400. 83p. Dep. mn. CFSTI $3.00 cy, $0.75 mn.

The techniques used to measure magnetic field parameters in the strong-focusing lenses of the Stanford Linear Accelerator are reviewed. Specifically, the theory and techniques used to determine such parameters as the magnetic center in multipoles, the length of the gradient fields, and the harmonic content in strong-focusing lenses are described. The calculation of the optical properties of a magnet from the measured parameters is also outlined. (D.C.W.)

13366 (SLAC–53) TWO-MILE ACCELERATOR PROJECT. Quarterly Status Report, July 1–September 30, 1965. (Stanford Linear Accelerator Center, Stanford Univ., Calif.). Nov. 1965. Contracts AT(04-3)-400; AT(04-3)-515. 100p. Dep. mn. CFSTI $4.00 cy, $0.75 mn.

The status of the Stanford Linear Accelerator and associated facilities is summarized, together with support activities. (D.C.W.)

13367 (UCRL–16445(Rev.)) ACCELERATOR RADIATION MONITORING AND SHIELDING. Patterson, H. Wade (Lawrence Radiation Lab., Univ. of California, Berkeley). Nov. 17, 1965. Contract W-7405-eng-48. 18p. (CONF-651109–15). Dep. mn. CFSTI $1.00 cy, $0.50 mn.

From 1st Symposium on Accelerator Radiation Dosimetry and Experience, Upton, N. Y.

Radiation measurements and shielding studied were made on the 60-inch cyclotron, the 184-inch cyclotron, the electron synchrotron, the electron linear accelerator, the bevatron, the heavy-ion linear accelerator, the proton linear accelerator, and the 88-inch cyclotron. These measurements were mostly made with the purpose of identifying the various components of the radiation field and determining their energy distribution. A general rule that has emerged from these studies is that fast neutrons (0.1 to 10 Mev) dominate the biological hazard of the radiation field existing near a well-shielded particle accelerator by contributing more than half the total rem dose. Gamma rays and low-energy neutrons contribute 10 to 20%, and high-energy neutrons make up the balance. The development and use of neutron detectors that allow an estimation of the neutron spectrum are emphasized. (Measurements of accelerator radiation in rad or rem units are not generally made, since they give no information that can be used to recommend protective shielding.) Neutron detectors that are found most effective are moderated slow-neutron detectors, threshold reaction detectors, emulsion, and the polyethylene-lined proportional counter. The accelerator neutron spectrum that is inferred from the response of these detectors is nearly the same as the measured cosmic-ray neutron spectrum. Furthermore, the shape of the measured spectrum is consistent with that calculated by several independent groups and individuals. Also the detectors were used to successfully predict the effect of shielding with a wide variety of materials to both protect personnel and reduce radiation background around bubble chambers, NaI crystals, and plastic scintillators. Techniques of measurement, application of specific detectors to certain problems, and practical illustrative examples of monitoring problems and their solutions are given in some detail. (auth)

13368 (UCRL–16511, pp 54–8) ACCELERATOR OPERATION AND DEVELOPMENT. (Lawrence Radiation Lab., Univ. of California, Berkeley).

The operation and research carried out at LRL with the electron linear accelerator, the 88-inch, and the 184-inch cyclotrons during this period are briefly discussed. (M.O.W.)

13369 STUDY OF AN ELECTRON GROUPING SYSTEM AT THE INPUT OF A LINEAR ACCELERATOR AND STUDY OF THE COEFFICIENTS OF SPACE HARMONICS OF THE ACCELERATING STRUCTURE. Hirel, Renee (Ecole Normale Superieure, Orsay, France). Ann. Phys. (Paris) (13), 10: 623-40(Sept.-Oct. 1965). (In French).

A theoretical study was made of an electron bunching system at the input of an accelerator and of a deflecting system that makes it possible to eliminate the electrons that can not be bunched so that they do not disturb the operation of the machine. An experimental study was made of the measurement method used for the coefficients of spatial harmonics of the iris structures for the accelerator guide. The values of these coefficients are compared for different thicknesses of the disc. (J.S.R.)

13370 STUDY OF A CLASS OF GUIDED ELECTROMAGNETIC WAVES: THE EH WAVES. APPLICATION TO THE HIGH FREQUENCY DEFLECTORS OF FAST PARTICLES. Garault, Yves (Faculte des Sciences, Orsay, France). Ann. Phys. (Paris) (13), 10: 641-72 (Sept.-Oct. 1965). (In French).

Deflector waves for ultrarelativistic particles ($v \cong c$) and structures able to propagate them are studied. After showing that the deflection force is always proportional to the transverse gradient of the longitudinal component E_z of the electric field, a second type of solutions to the Maxwell equations linearly independent of TEM solutions or with E_z (H_z) = C^{te} is introduced when $v_p = c$. These solutions are called "EH waves" in order to recall the simultaneous existence of the E_z and H_z components. These waves are propagated, for example, in guides partially filled with dielectrics or periodic structures. After a study of the properties of the electromagnetic field of these waves and their general solutions in circular cylindrical coordinates, the particular solutions in the circular guide with metallic irises or in an iris guide are examined theoretically. The iris guide is studied with an infinitely thin iris model and with a zero step. The results of this study are compared with experimental studies made on the two types of irises. (tr-auth)

13371 NON LINEAR THEORY OF THE MOTION OF FAST CHARGED PARTICLES IN HELICAL TOROIDAL MAGNETIC FIELDS. Khapaev, M. M. (Moscow State Univ.). Dokl. Akad. Nauk SSSR, 163: 343-6(July 11, 1965). (In Russian).

Magnetic systems, suitable for the hard focusing of charged particles in accelerators and in devices used for channeling charged particles, were examined. The systems studied were based on helical toroidal fields, the average radius R of which was much larger than the radius σ_0 of the transverse cross section; the pitch L of the helical field was assumed to be larger than σ_0. The field was rotated along the trajectory of the fast particles, although in the currently employed hard-focusing systems the field possesses an alternating sign of the gradient. The equations describing the nonlinear equations of motion, similar to the betatron oscillations, were linearized for low amplitudes; the formulas describing their frequency indicated the fundamental linear resonances of the system. The motion of a given particle in the helical toroidal field was calculated with and without an additional applied field, yielding correlations between R, L, σ_0 and the intensities H and H_0 of the helical and auxiliary fields. A new design was proposed on the bases of the results, which was designated as the "magnetic hose" for the channeling of

charged particles. This will allow the transfer of fast particles in the helical field within a wide range of velocities while minimizing the particle losses. (TTT)

13372 ION BEAM ANALYSIS BY AN ELECTROSTATIC TECHNIQUE. Martin, D. H.; Wakefield, R. H. (North Carolina State Univ., Raleigh). J. Appl. Phys., 37: 398-401(Jan. 1966).

A method of spatially analyzing a positive ion beam by electrostatic means is presented. In this method, a small portion of a given ion beam passes through a low-density gas-filled chamber, where ionization and charge exchange products are collected and analyzed so as to reveal the original positive and neutral beam components. Results of a detailed spatial analysis of a 10-kev argon ion beam from a Von Ardenne duoplasmatron ion source are given and discussed. Comparison of integrated beam components with theoretical beam blowup indicates that microscopic and macroscopic neutralizations are the same within limits of the measurements. (auth)

13373 THE EXPERIMENTAL EVALUATION OF CHARACTERISTICS OF A LINEAR HIGH-FREQUENCY ELECTRON ACCELERATOR. Sochor, Vaclav; Hamal, Karel (Inst. of Nuclear Physics, Prague). Jad. Energ., 11: 415-18(Nov. 1965). (In Czech).

With the use of a sector magnet spectrometer, the characteristics of a linear high frequency electron accelerator were measured as follows: the mean total energy E, the spectrum width ΔE, the dependence of the spectrum shape on high frequency input power and on injection voltage, the frequency characteristic and the current characteristic. At nominal frequency, the maximum energy was found to be achievable at minimum spectrum width. The spectrum splitting was observed at higher input power than nominal. (auth)

13374 ELECTRON BUNCHING IN TRAVELING WAVE LINEAR ACCELERATORS. Haimson, J. (Varian Associates, Palo Alto, Calif.). Nucl. Instrum. Methods, 39: 13-34(Jan. 1966).

Several new concepts are presented including the presence of a standing wave domain in the terminal semicavity regions of the waveguide and launching of a traveling wave at the input coupler mid-plane. The influence of space harmonics on particle phase orbital behavior is discussed. Space harmonics are evaluated from traveling wave experiments and results are illustrated for several circuit configurations. Equations of motion using the space harmonic synthesized electric field instead of the fundamental component indicate a broadening of energy spectra and bunch width over the initial few wavelengths of trajectory after injection. Electron de-bunching longitudinal space charge effects are analyzed for the input coupler standing wave environment and for the traveling wave orbits. Simultaneous computation of the electron orbits enables the changing charge distribution and geometry of the bunch to be monitored, thereby permitting space charge fields and reactive distortion phase shifts to be taken into account. Some space charge corrected examples of high current transient bunching are discussed in a concluding section. (auth)

13375 POLARIZED-PROTON SCATTERING FACILITY AT THE OAK RIDGE ISOCHRONOUS CYCLOTRON. Blumberg, L. N.; Gross, E. E.; Van Der Woude, A.; Zucker, A. (Oak Ridge National Lab., Tenn.). Nucl. Instrum. Methods, 39: 125-32(Jan. 1966). (ORNL-P-1485).

In the facility described, polarized proton beams are produced either as recoil protons from a hydrogen-gas target bombarded by α particles or by elastically scattered protons from a solid ^{40}Ca target. At a polarized-proton energy of 40 Mev, the polarization is 89 ± 7% for the hydrogen polarizer and 35.5 ± 3% for the ^{40}Ca polarizer. A system of two quadrupole-doublet lenses transports the polarized proton beam about 18 ft and focuses the beam to a 1/4 by 1 in. spot at the center of a scattering chamber. Energy spectra of protons scattered from a secondary target are obtained at 32 angles simultaneously by using 32 NaI scintillation counters with a 20,000-channel multiparameter analyzer used as thirty-two 400-channel analyzers. (auth)

13376 NEGATIVE H AND Li IONS IN A DUOPLASMATRON. Bethge, K.; Rau, G. (Univ., Heidelberg). Nucl. Instrum. Methods, 39: 157-62(Jan. 1966). (In German).

Negative ions are extracted out of a duoplasmatron ion source. The conditions under which optimal current output is achieved are determined. The maximum output is, on H^-, 70 μA, and on Li^- 55 nA. On the basis of these results the possible mechanisms of negative ion production is discussed. (auth)

13377 A QUICK METHOD FOR CALIBRATING THE ELECTRON OF AN ELECTRON ACCELERATOR. Tang, M. D. (Westinghouse Electric Corp., Pittsburgh). Nucl. Instrum. Methods, 39: 181-2(Jan. 1966).

A method is described for calibrating the energy of an electron beam in the 0.6 to 1.8 Mev range. The method is based on beam-electron absorption by Al foils of varying thicknesses and has an accuracy of 5%. (T.F.H.)

13378 SYNCHROTRON RADIATION AND OBSERVATION OF BUNCHES IN STORAGE RINGS. Di Giugno, G. (Univ., Napoli, Italy); Haissinski, J.; Marin, P. Nucl. Instrum. Methods, 39: 217-23(Jan. 11, 1966). (In French).

Storage rings for electrons or positrons provide unique experimental conveniences to observe synchrotron radiation. Several experiments concerning this radiation were made on the AdA, storage ring. The first bears on the total power radiated as a function of the energy of the radiating particles, the second is a direct check of the spectral law, and the third is a measurement of the angular distribution of the radiation at three different energies. On the other hand, synchrotron radiation can be used to get valuable information on the structure of the stored beams; a measurement of the transverse particle density within the beams at various energies and a measurement of the length of the bunches are described. All experimental results are compared to theoretical predictions: the agreement is, on the whole, very satisfactory. (auth)

13379 A 5.5-Mev ION BUNCHER OF MOBLEY TYPE. Tsukada, K.; Tanaka, S.; Maruyama, M.; Tomita, Y. (Japan Atomic Energy Research Inst., Tokyo). Nucl. Instrum. Methods, 39: 249-55(Jan. 11, 1966).

An ion buncher of Mobley type, a system for producing ion bursts of high intensity and of nanosecond duration, was constructed for proton and deuteron beams from a 5.5-Mv Van de Graaff accelerator and was successfully used in fast-neutron time-of-flight experiments. In the system an r-f resonator is employed in order to obtain a high voltage (50 kv) of 24 Mc which is supplied to the deflector. The Mobley magnet has a mass-energy product of 17. Bunched pulses of 1.0–2.8 ns duration at the target for proton and deuteron beams with energies of 1.2–5.5 Mev were observed on a sampling oscilloscope. The bunching ratio larger than 10 was obtained for the proton pulses of energies higher than 3 Mev and for the deuterons higher than 4 Mev. It was found that the inherent beam spread was almost canceled out at the target by the linear-acceleration effect which was caused by the change in potential between the deflector plates. (auth)

13380 SOME EVIDENCE ON THE ELECTRIC DISSOCIATION OF THE NEGATIVE HYDROGEN ION NEAR 2.4 Mev/cm. Cahill, T. A.; Richardson, J. Reginald; Verba, J. W. (Univ. of California, Los Angeles). Nucl. Instrum. Methods, 39: 278-80(Jan. 11, 1966).

The dissociation of the negative hydrogen ion (H^-) by electric $v \times B$ stripping in a magnetic field was measured for electric fields near 2.4 Mev/cm. The ions were obtained from the sector-focused cyclotron and were stripped by the 24.86 kG hill field at energies up to 48 Mev. The experimental results are compared with the predictions of Khuri, Khoe, Darewych and Neamtam, and Hiskes are found to favor strongly the values predicted by Hiskes. Other observations of $v \times B$ stripping are compared with the present data. (auth)

13381 AUTOMATIC-CONTROL-SYSTEM DESIGN FOR THE BERKELEY 88-INCH CYCLOTRON. Struthers, D. R. (Univ. of California, Berkeley). Nucl. Instrum. Methods, 39: 321-4(Jan. 11, 1966). (UCRL-16210).

The automatic-control requirements of the 88-inch cyclotron are analogous to the requirements of many process controls in industry. The system being designed will reduce setup time from twenty to five minutes and will be capable of being overridden manually. Although the system is primarily analog, the input is on punched tape or IBM cards in order to make it compatible with eventual beam optimization when digital-computer techniques will be used. (auth)

13382 SECONDARY ELECTRON TRAJECTORIES IN A FARADAY CUP MAGNETIC FIELD. Pruitt, J. S. (National Bureau of Standards, Washington, D. C.). Nucl. Instrum. Methods, 39: 329-34(Jan. 11, 1966).

Trajectories of electrons with energies between 10 ev and 1 Mev were studied in inhomogeneous magnetic fields to choose a deflecting magnet for the capture of secondary electrons generated in the mouth of a Faraday cup. The results show that a solenoidal field abets their escape, but the field of two repelling bar magnets completely stops electrons with energies less than about 1 kev. Additional information relevant to Faraday cup design is also presented. (auth)

13383 MEASUREMENT OF ELECTRON BEAM CURRENT. Kawashima, M. Sumitomo Elec. Rev., No. 83, 93-101(Dec. 1963). (In Japanese).

Two methods were developed to measure the accelerated electron beam current from 1.0 to 2.0 Mev. One is an ionization chamber method; the other is a method using a Hall element to measure the magnetic field which is induced by the electron beam current. The results of tests showed that the electron beam current up to 1 mamp can be measured with an ionization chamber directly. The possibility of directly measuring electron beam current up to 30 μamp by a Hall element was proved. These methods are quite suitable for measuring the beam current of large accelerators. (auth)

13384 A PENNING ION SOURCE FOR INCREASED ION CURRENTS. Papkow, A. (Max-Planck-Institut fuer Kernphysik, Heidelberg). Z. Angew. Phys., 20: 81-5(Nov. 1965). (In German).

A continuously operated PIG ion source with an anode in form of several disks is described. The heat produced by the discharge is drawn off radially. This design makes it possible to obtain an ion beam up to 10 ma. (auth)

13385 ION SOURCE FOR THE GENERATION OF A CONCAVE ION BEAM. Wassermann, Marien (to Compagnie Generale de Telegraphie sans Fil). German Patent 1,204,754. Nov. 11, 1965. Priority date Feb. 2, 1959, France.

An ion source is given in which the electrons as well as the ions follow trochoidal trajectories in crossed electric and magnetic fields. An azimuthal magnetic field penetrating the whole ion source is produced by an elongated electric conductor located in the axis of symmetry of the ion source. A radial electric field is generated between the ion extracting electrode and the central electrical conductor, which is surrounded by the coaxially arranged extracting electrode. (Gmelin Inst.)

13386 ELECTRON-BOMBARDMENT ION SOURCE. Sano, Kikuo (to Kabushiki Kaisha Hitachi Seisakusho). German Patent 1,205,202. Nov. 18, 1965. Priority date Apr. 18, 1963, Japan.

The electron-bombardment ion source comprises an electron source composed of a straight cathode wire or strap which is surrounded by a focusing electrode. The focusing electrode consists of two plates parallel to each other and to the cathode, the front edges of which are provided with recesses arranged symmetrically in relation to the midpoints of the edges. (Gmelin Inst.)

13387 ARRANGEMENT FOR THE MEASUREMENT OF THE PHASING OF AN ION BUNCH IN AN ORBITAL PATH IN ISOCHRONOUS CYCLOTRON. Feldmann, Hans-Helmut (to Licentia Patent-Verwaltungsgesellschaft GmbH). German Patent 1,205,207. Nov. 18, 1965. Filed July 11, 1965.

The phasing is measured by means of induction probes located in the vicinity of the orbit. For noise suppression the probes are arranged in pairs on opposite sides of the orbit and are connected at the outlet side to transposing devices which are coupled in such a way that noise signals are in phase opposition and useful signals are in-phase in the output circuit. (Gmelin Inst.)

13388 PROTECTIVE DEVICE FOR THE ACCELERATING TUBE. Sugimoto, Shun (to Tokyo Shibaura Electric Co., Ltd.). Japanese Patent 1964-18489. Aug. 31, 1964. Filed Feb. 13, 1963.

If an accidental short circuit is produced between the poles of a particle accelerating tube such as in a betatron, the proposed protective device breaks the short circuit immediately and prevents the destruction of the equipment. The device consists of a part for forming the incident pulse voltage to impress the electron gun, and a part for extinguishing the incident pulse voltage for making the voltage forming part inactive. The saturating action of the core or the shielding action of the electric valve is effected by the voltage drop due to the discharge current at the accidental spark discharge. (NSA of Japan)

13389 LINEAR ACCELERATOR USING MULTI-CAVITY TYPE SPEED-MODULATION TUBE OSCILLATOR. Yoshida, Yoshinori (to Kobe Kogyo Corp.) Japanese Patent 1964-18491. Aug. 31, 1964. Filed Sept. 19, 1962.

The proposed linear accelerator with the multi-cavity type speed-modulation tube oscillator is characterized in that the high frequency energy originating in the output cavities is supplied to the accelerating tube through a suitable high frequency connector, and the high frequency feedback circuit for the oscillation is formed by connecting the front of the non-reflecting end in the particle accelerator to the input cavity of the speed-modulation tube through a phase shifter. The accelerating tube also serves as the oscillator with a filtrating effect due to the stabilized cavities in the high frequency feedback circuit. (NSA of Japan)

13390 CHARGED PARTICLE ACCELERATOR. Maekawa, Akitsugu (to Hitachi, Ltd.). Japanese Patent 1964-18492. Aug. 31, 1964. Filed Feb. 14, 1963.

A charged-particle accelerator is proposed in which a compensation is made for the discrepancy between the high frequency for accelerating the charged particles and the design frequency of the accelerating tube. The mutual reaction is produced between the electric field in the accelerating tube and the charged particles injected from the source in the space between the input and output of the high frequency. This mutual reaction is controlled by the detected difference in the phase between the input and output. (TCO)

13391 BETATRON. Tanaka, Osamu (to Mitsubishi Electric Mfg. Co., Ltd.). Japanese Patent 1964-18495. Aug. 31, 1964. Filed Apr. 3, 1963.

An electron gun for a betatron is so located as to be on the boundary or outside of the betatron accelerating magnetic field along with a number of accelerating and collecting electrodes. By means of these electrodes, the energy of the electrons injected into the stable orbit can be increased to 100–120 kev from the conventional several tens kev, and also the electrons are well focused. Thus, the intensity of the accelerated electron beam from the betatron window can be very high. With this arrangement of the electron gun outside the magnetic field, highly accelerated and focused electrons can be obtained, irrespective of the size of an electron gun. (NSA of Japan)

13392 IRON CORE, HAVING MANY LEGS, FOR A BETATRON. Mitsuhashi, Tadashi (to Tokyo Shibaura Electric Co., Ltd.). Japanese Patent 1964-18496. Aug. 31, 1964. Filed Sept. 12, 1963.

An improved iron core for a betatron with many legs

includes the central (or inner) magnetic poles and the outer hollow, cylindrical magnetic poles concentrically arranged. A number of yokes connect radially to the magnetic poles. The inner and outer magnetic poles are connected to each other by one engaging into the other, and although the inner pair and the outer pair of magnetic poles are actually separate members, they are magnetically one whole body. The ring-shaped accelerating tube is located between the upper and lower poles. Both the inner and outer magnetic poles are constructed by piling up narrow metal plates radially to the axis, and the yoke is constructed by piling up narrow metal plates parallel to the axis of the yoke. Provision is made for adjusting the diameter of a stable orbit for particle acceleration. (TCO)

13393 PARTICLE ACCELERATOR. Maruyama, Masuo (to Tokyo Shibaura Electric Co., Ltd.). Japanese Patent 1964-27175. Nov. 27, 1964. Filed June 24, 1963.

An improved particle accelerator, which can accelerate particles to 1–2 Mv, uses a container of 1m in diameter and 2–3m in height. The accelerating tube is mounted in an insulated cylindrical body, and the container is filled with a high-pressure insulating gas, while the insulated body is filled with an insulating oil. (TCO)

13394 ACCELERATING TUBE FOR A PARTICLE ACCELERATOR. Adachi, Takeshi (to Tokyo Shibaura Electric Co., Ltd.). Japanese Patent 1964-27176. Nov. 27, 1964. Filed Sept. 5, 1963.

An improved evacuation system and insulation structure are proposed for a particle accelerator, such as in a neutron generator. The evacuation system consists of the evacuation device, its piping on the axis of the accelerating tube, and the evacuated space formed by the cylinder and its end plates including the accelerating electrodes, etc. The particle accelerator itself consists of the ion source, the first focusing lens, the accelerating electrodes, and the target holder with a target material. The high voltages applied to the accelerator electrodes and the lens are insulated from the earth and the evacuation device by the cylinder and its end plates. The distance between the target material and the ion source is reduced, and a high vacuum is also maintained in the vicinity of the ion source and the focusing lens. (NSA of Japan)

13395 DEVICE FOR CONTROLLING A PARTICLE ACCELERATOR. Komai, Kenichiro (to Hitachi, Ltd.). Japanese Patent 1964-29018. Dec. 14, 1964. Filed Dec. 28, 1962.

A control device for a particle acclerator includes a light pulse generator. In testing a semiconductor element by a charged particle beam, it is necessary to use the pulsed beam. In the usual particle accelerator, a pulse oscillator is incorporated in the accelerator to obtain a pulsed beam; consequently, when a continuous pulsed beam is required, it is very inconvenient to control the pulse width and frequency, because the oscillator is at the same high voltage as the accelerator itself. In the proposed device the pulse oscillator can be installed separate from the accelerator, and the pulsed beam can be controlled by means of a push button. The neon light pulses control photoelectrically the high voltage circuit of the accelerator. (NSA of Japan)

13396 PARTICLE ACCELERATOR. Iwashita, Fumio (to Tokyo Shibaura Electric Co., Ltd.). Japanese Patent 1964-29019. Dec. 14, 1964. Filed Oct. 5, 1963.

A particle accelerator, such as one used in a neutron generator, with a simple and improved evacuating system is described. The accelerator is contained in an insulated cylindrical body that is divided in the middle by an end plate. This end plate with one end plate of the cylindrical body forms an air tight chamber, and the chamber is evacuated by means of a vacuum pump located outside the cylinder and communicating through the cylinder's outer end plate. The target and the accelerating electrodes are located in the air tight chamber. An inner cylinder is formed within the remaining part of the cylinder body with one of the end plates being the end plate of the air tight chamber and the other one being the other end plate of the body itself. A particle pulsation device is located in this inner cylinder. (TCO)

13397 DEFLECTOR FOR CHARGED PARTICLES. Seki, Yoshinaga (to Mitsubishi Electric Mfg. Co., Ltd.). Japanese Patent 1964-30365. Dec. 26, 1964. Filed May 18, 1962.

A charged-particle deflector is proposed by means of which particles having a wide range of momenta can be deflected and collected again into the orbit. (NSA of Japan)

13398 PARTICLE ACCELERATOR. Iwashita, Fumio (to Tokyo Shibaura Electric Co., Ltd.). Japanese Patent 1964-30366. Dec. 26, 1964. Filed Sept. 27, 1963.

In a particle accelerator, the air-tight room, containing the accelerating electrodes, and the compartment (before the room) containing the auxiliary power supply with cladding to shield the high potential part, are contained in an insulating cylindrical body with two end plates. The outside of the cylindrical body and the two ends are maintained at ground potential. The accelerator can be placed in either an upright or horizontal position. (TCO)

13399 PARTICLE ACCELERATOR WITH AN ELECTRIC-SHOCK PREVENTING DEVICE. Iwashita, Fumio (to Tokyo Shibaura Electric Co., Ltd.). Japanese Patent 1964-30367. Dec. 26, 1964. Filed Sept. 30, 1963.

An improved particle accelerator includes a high voltage power supply with an electric shock preventing device and is entirely enclosed in an insulated cylindrical body. The cylindrical body is divided halfway by an end plate. An air tight chamber formed by one of the cylinder end plates and the halfway end plate contains the accelerating electrodes. The end plate of the cylinder holds the target, and the halfway end plate includes an ion source. At the middle of the cylinder is a closed chamber formed by the end plate of the air tight chamber containing an auxiliary power supply. A third chamber next to the power supply chamber and formed by part of the cylindrical body and the other cylinder end plate is at atmospheric pressure and contains a high-voltage power supply and accelerating equipment. A deuterium bomb and a cooling fan are affixed to the end plate of this third chamber. The outer surface and the two end plates of the insulated cylindrical body are maintained at ground potential. (TCO)

13400 CHARGED-PARTICLE SOURCE, CONSISTING OF A PLURAL NUMBER OF SUB-SOURCES. Komai, Kenichiro (to Hitachi, Ltd.). Japanese Patent 1964-30368. Dec. 26, 1964. Filed Feb. 2, 1963.

An improved charged-particle source consists of a number of sub-sources of charged particles. The charged-particle current intensity and beam cross section of each sub-source can be controlled independently. Each of the sub-sources has an accelerating electrode, and all the electrodes are connected to each other and are maintained at the same potential. With this construction of the charged particle source, a desired cross-sectional shape of charged particle beam and a desired distribution of particle density on the beam cross section are possible. (TCO)

13401 PARTICLE ACCELERATOR. Iwashita, Fumio (to Tokyo Shibaura Electric Co., Ltd.). Japanese Patent 1964-30369. Dec. 26, 1964. Filed Sept. 30, 1963.

An improved tandem type, Van de Graaff accelerator is proposed. The accelerator consists of a negative ion source; a magnet for deflecting the negative ion beam and analyzing the energies of the particles; an accelerating and collecting tube; a charge conversion stripper; a pair of quadrupole lens, located between the magnet and the accelerator tube for focusing the negative ions on the stripper; and a window for the positive ion beam. The quadrupole lens, based on the principle of intense focusing, can easily and effectively collect the negative ion beam in a wide energy range on to the incident window of the charge conversion stripper. (NSA of Japan)

13402 LINEAR ACCELERATOR. Komai, Keniichiro (to Hitachi, Ltd.). Japanese Patent 1964-30375. Dec. 26, 1964. Filed Jan. 13, 1964.

In the proposed linear accelerator, the average output

electron current (or produced x-ray intensity) can be changed easily with the output electron energy maintained at the same value. The electron pulses are accelerated at the rate of one electron pulse per more than two integer modulated high-frequency pulses. (TCO)

13403 ACCELERATING TUBE FOR A LINEAR ACCELERATOR. Komai, Kenichiro (to Hitachi, Ltd.). Japanese Patent 1964-30376. Dec. 26, 1964. Filed Feb. 5, 1964.

A design of an accelerating tube for use in a linear accelerator is proposed that is simple and easy to construct. The inner members of an accelerating tube are contained in an outer cylindrical body of a non-magnetic material. A number of short tubes of a non-magnetic and electrically conductive material and a plural number of discs with holes for the passage of charged particles of the same kind of material, are connected in a series inside the outer cylindrical body. To obtain close contact between the tubes and discs, means are provided to press the members from both sides. Packings of a soft metal are provided between the ends of the tubular members and the inner surface of the outer body to insure the air-tightness of the entire unit. (TCO)

13404 BETATRON. Iwashita, Fumio (to Tokyo Shibaura Electric Co., Ltd.). Japanese Patent 1964-30377. Dec. 26, 1964. Filed Apr. 20, 1964.

A betatron is described in which the two iron cores can easily be separated or put together without additional equipment. The betatron include two separate iron cores with a number of magnetic poles and four legs. One of the two cores is held by the support, and two electric motors are installed on the other core. The iron core held by the support has screw holes in it which engage with the screw bars installed on the core having the motors. Thus, by operating the electric motors, and hence, rotating the screw bars, the upper and lower iron cores can be separated or put together. (TCO)

13405 DEFLECTOR FOR PULSED CHARGED PARTICLES. Iwashita, Fumio (to Tokyo Shibaura Electric Co., Ltd.). Japanese Patent 1964-30378. Dec. 26, 1964. Filed Oct. 16, 1963.

An improved electric and magnetic deflector for the pulsed charged particles is proposed for providing a larger irradiation field. It consists of a pair of coiled magnets, placed perpendicular to the beam axis, and a field limiting aperture. The coiled magnets are synchronously energized electrically by the out-put of the accelerator circuit. (NSA of Japan)

Astrophysics and Cosmology

13406 ON A UNIVERSE ADMITTING A FOUR PARAMETER GROUP OF MOTIONS. Datta, Bidyut Kumar (Surendra Nath Coll., Calcutta). Acta Phys. Pol., 28: 545-9(Oct. 1965).

The derivation of a universe admitting a four parameter group of motions is made on the assumption of positive pressure and positive density. Under these conditions the stress tensor does show an anisotropy in the pressure. (auth)

13407 MAGNETIC BREMSSTRAHLUNG IN A VARIABLE FIELD AS THE MECHANISM BEHIND THE CHANGING RADIANCE OF QUASISTELLAR RADIO SOURCES. Ozernoi, L. M. (Lebedev Inst. of Physics, Moscow). Dokl. Akad. Nauk SSSR, 163: 54-7(July 1, 1965). (In Russian).

Variations in the brilliance of quasar radio sources have been previously attributed to magnetic bremsstrahlung. The well investigated source 3C273 exhibits a systematic change of brilliance within a period of about 10 years and flash-type variations lasting up to several weeks. An attempt was made to explain the periodicity of the changes on the basis of the internal properties of the source. In analogy with the optical light emission of quasar 3C48, the continuous spectrum of the 3C273 source was also attributed to magnetic bremsstrahlung, rather than to f-f transitions. Thus, periodic changes in the radiance of quasars may be due to oscillations in the tension H of the magnetic field and the concentration N_e of the relativistic electrons; the first factor appears to be the most important one. The magnetic field changes may be due to geometric factors, such as rotation of the source, as a result of which the radiation intersects regions of varying tension of the quasiregular, nonhomogeneous field, or to physical factors, represented by the pulsations of the superstar. The magnetic field oscillation over a dynamic background is accompanied by a secular compression of the nucleus and of the superstar. The field modulations may also be due to circulatory movements within the nucleus. (TTT)

13408 THERMAL AND DYNAMICAL PROPERTIES OF A PROTOSTAR AND ITS CONTRACTION TO THE STAGE OF QUASI-STATIC EQUILIBRIUM. Hayashi, Chushiro; Nakano, Takenori (Kyoto Univ.). Progr. Theoret. Phys. (Kyoto), 34: 754-75(Nov. 1965).

The thermal and dynamical evolution of a protostar of one solar mass is investigated from the stage transparent to radiation to the state of the beginning of quasihydrostatic equilibrium. The evolution in the transparent stage is studied in the ρ-T diagram by comparing the time-scale of cooling or heating with the time-scale of free contraction or free expansion. The emission of radiation by H_2 molecules, grains, and ions (C^+, Si^+, and Fe^+) is taken into account as cooling processes, and interstellar star-light and cosmic ray particles are considered as heating sources. It is shown that, where $\rho \lesssim 2 \times 10^{-18}$ g/cm^3, the gas cloud of one solar mass expands and returns to the interstellar gas, while the cloud of $\rho \gtrsim 2 \times 10^{-18}$ g/cm^3 contracts to become a star. In the subsequent opaque stage the energy loss from the star is determined by the diffusion of photons, and the contraction becomes more and more adiabatic. When the contraction proceeds to a certain extent, the growth of a pressure gradient in the central region gives rise to a bounce of this region. The bouncing core and the contracting envelope build up a new density distribution, and the protostar contracts again as a whole. The protostar repeats this process a few times. When the release of gravitational energy becomes large enough to ionize hydrogen atoms completely, the bounce of the core gives rise to a strong shock wave. The arrival of the shock wave at the surface gives rise to a sudden increase in the luminosity accompanied probably by explosive phenomena such as the production of high energy particles and the light elements Li, Be, and B. Afterward the star is in quasi-hydrostatic equilibrium, and in a short period of about 10^3 years the star becomes wholly convective. The subsequent evolution is a quasistatic contraction toward the main sequence. (auth)

13409 CONTINUUM ELECTROMAGNETIC RADIATION FROM SOLAR FLARES AND OBSERVATIONS OF THE SOLAR CORONA FROM THE LIMB OF THE SUN TO THE ZODIACAL LIGHT, JULY 20, 1963 [Thesis]. Stein, Wayne Alfred. Minneapolis, Minn., Univ. of Minnesota, 1964. 127p.

Continuum electromagnetic radiation from solar flares is discussed in terms of the energy loss processes of electrons in the solar atmosphere. It is shown that it is possible to attribute the continuum radiation both at radio frequencies and at visible frequencies to synchrotron radiation by exponential rigidity distributions of electrons. Photographs of the solar corona and zodiacal light from cameras flown on balloons at an altitude of 110,000 feet were obtained on July 20, 1963. The absolute intensity of the light of the solar corona between the limb of the sun and 70 degrees elongation was determined from the photographs. The absolute brightness, polarization, and direction of polarization of the inner corona at effective wavelengths of 4750 Å and 8300 Å were measured from a station at The Forks, Maine. Finally, as a result of photographs taken from the ground, from a jet aircraft at 40,000 feet over Canada, and from balloons at 110,000 feet, it was possible to determine the sky brightness during the eclipse as a function of atmospheric pressure in order to plan for future observations. (Dissertation Abstr.)

13410 BETA-DECAY INHIBITION AND STELLAR ABUNDANCE RATIOS IN NUCLEOSYNTHESIS [Thesis]. Peterson, Vern LeRoy. Bloomington, Ind., Indiana Univ., 1963. 97p.

Neutron-capture on a slow time scale (the s-process) is thought to synthesize the elements sodium through bismuth in the interiors of highly evolved stars. Since the abundances established during the s-process are dependent upon the beta-decay rates of the isotopes involved as well as the mean neutron-capture times, it is important to know under what conditions the beta-decay rate will be altered. One of a number of possible mechanisms for altering the decay rate is considered. If the electron density is very high near the center of a star, the exclusion principle must be considered when calculating beta-decay rates. When the electron gas is highly degenerate, most of the low-energy states will be occupied. A low-energy beta decay will therefore be greatly inhibited. Tables are given showing the dependence of the beta-decay rate upon the local temperature and density, maximum beta-decay energy, and type of decay involved. Abundance ratios for adjacent elements for material removed from the neutron flux long enough for the short-lived isotopes to have decayed but not yet mixed with other material is calculated for eight cases. The abundance ratios calculated are those that may be altered in a stellar interior due to exclusion principle inhibition of the beta-decay rate. The ratios are calculated for equilibrium conditions and as a function of the mean neutron-capture time and change in beta-decay rate. It is found that the abundance ratios are more critically dependent upon the mean neutron-capture time than on the change in the decay rate. The neutron-capture rate will have to be known to within a factor of two before knowledge of the change in the beta-decay rate can be used. Changes produced in these abundance ratios when the material is transported from the core of the star to the surface are considered. (Dissertation Abstr.)

Atomic Physics

Refer also to abstracts 13505 and 13855.

13411 (CEA-R-2855) ETUDE DE L'ETAT 2^1S DE L'HELIUM PAR LA METHODE DE HARTREE-FOCK. (Study of the 2^1S State of Helium Using the Hartree-Fock Method). Masse, Jean-Leon (Commissariat a l'Energie Atomique, Saclay (France). Centre d'Etudes Nucleaires). Oct. 1965. 18p. Dep. mn.

The Hartree-Fock method has been widely applied to atoms and molecules. However, it raises special objections as regards excited states which generally include incompletely filled orbital groups. Particulary, in such a case, the hypothesis of orthogonal orbitals, which is generally admitted and which makes the formalism and the solution of equations far simpler, is not possible in any case. The terms (1s) (ns), n^1S of helium, for n = 2,3 . . . show a simple example where the orbitals can no longer be supposed to be orthogonal. The Hartree-Fock equations were solved for the (1s) (2s), 2^1S state, with the approximation of linear combinations of orbitals of a Slater-type. (auth)

13412 (CLM-R46) ELECTRIC FIELD DISSOCIATION OF H_2^+. Wind, H. (Culham Lab., United Kingdom Atomic Energy Authority, Abingdon (England)). Sept. 1965. 60p. Dep. BIS $1.60. HMSO 8s.

When an electric field of sufficient strength is applied H_2^+ dissociates into $H^0 + H^+$. The probability of this process was computed. For intermediate steps the electronic energy in the field of two coulomb-centers and the energy levels of H_2^+ are also derived. Two methods are described which were used to observe field dissociation. The new data resulting from these are: (1) There is a threshold electric field. This confirms the theory that H_2^+ has a finite number of states. (2) It is possible to detect individual levels. (3) It is possible to estimate the population of these levels. The agreement between theory and experiment is good. (auth)

13413 (CONF-233(Vol.4), pp 538-47) NEW CALCULATIONS OF THE ATOMIC PHOTOEFFECT. Pratt, R. H. (Stanford Univ., Calif. Inst. of Theoretical Physics).

Differential and total cross sections and all polarization correlations between incoming photon and ejected electron were investigated for elements of the range Z = 13 to Z = 92 and of energies from 200 kev to 2 Mev. The numerical methods used are more general than those of previous calculations and will permit inclusion of the screening effects of outer electrons. Calculations are presented for Z = 13, 26, 50, 82, 84, and 92. (M.O.W.)

13414 (JUL-304-RW) ZERSTAEUBUNG VON FESTKOERPERN DURCH IONENBESCHUSS. (Sputtering of Solids by Ion Bombardment). Rie, Kyong-Tschong (Kernforschungsanlage, Juelich (West Germany). Institut fuer Reaktorwerkstoffe). Sept. 1965. 53p. Dep. mn.

The role of the correlative collision in sputtering was investigated by the bombardment of single-crystal Ag and Cd with 1- to 7-kev Ar^+ ions. For the different orientations, the anisotropic emission of the surface atoms and the yield at various ion energies were determined. The structure of the deposition of the emitted atoms was measured for Ag at various temperatures. The experimental results were discussed on the basis of theoretical models. Experimental results of penetration experiments on Ag are included. The results obtained at 2-Mev proton energies were compared with those obtained previously at proton energies of 300 kev. The agreement was good. (tr-auth)

13415 (ORNL-3881) A PROGRAM TO COMPUTE THE CLASSICAL DEFLECTION FUNCTION. Lietzke, M. H.; Menendez, M. G. (Oak Ridge National Lab., Tenn.). Feb. 1966. Contract W-7405-eng-48. 44p. Dep. mn. CFSTI $3.00 cy, $0.50 mn.

A computer program was written which may be useful in the interpretation of (in terms of classical mechanics) angular distributions measured in experiments on molecular beam scattering. The program is written in two parts: the first part is used to adjust the minimum value of the interatomic potential to any desired equilibrium internuclear distance by adjusting the strength of the repulsive portion of the potential, while the second part computes the classical deflection function, the corresponding phase shift, and the angular spacing between the principal rainbow and the second order rainbow. The program is written in both ALGOL and FORTRAN II. (auth)

13416 ON A SIMPLE METHOD OF CALCULATING ATOMIC ONE-ELECTRON EIGENFUNCTIONS. Gombas, P. (Technical Univ., Budapest. Hungarian Academy of Sciences, Budapest). Acta Phys. Acad. Sci. Hung., 19: 295-301(1965).

Starting from a statistical atom model in which electrons are grouped in shells according to the principal quantum number, a method is developed for calculating atomic one-electron eigenfunctions in a simple way. (auth)

13417 ON THE SCATTERING OF SLOW NEUTRONS BY HYDROGEN MOLECULES. Atanasov, A. A.; Ivanov, K. I. (Higher Pedagogical Inst., Plovdiv, Bulgaria). Acta Phys. Pol., 28: 451-7(Oct. 1965).

The scattering of slow neutrons by hydrogen molecules is treated on the basis of Fadeev's equations. In cases when the spin interaction of the neutron and hydrogen molecules is not taken into account and the Fermi potential is used, the problem is reduced to the solution of a system of two integral equations. (auth)

13418 STUDY OF THE ISOTOPIC DISPLACEMENT OF TUNGSTEN, OSMIUM, AND NEODYMIUM. CONTRIBUTION TO THE CLASSIFICATION OF THE ARC SPECTRA OF THESE ELEMENTS. Gluck, Gilbert (Centre National de la Recherche Scientifique, Bellevue, France). Ann. Phys. (Paris) (13), 10: 673-96(Sept.-Oct. 1965). (In French).

The relative isotopic displacements of the 186, 184, 183, 182, and 180 isotopes of W were found to be 1.54 ± 0.02,

2.13 ± 0.02, and 2.92 ± 0.3. An inversion of the odd-even staggering phenomenon, coming from an abnormal position of the 182 isotope, was observed. The arc spectrum of W was studied between 3841 and 6128 Å, and the isotopic displacements of 578 rays were measured. The isotopic displacement of 36 lower even levels (with the configurations $5d^4\ 6s^2$ and $5d^5\ 6s$) and of 12 higher even levels ($5d^4\ 6s\ 7s$) was deduced. The levels 19535 K and 19826 K, classed respectively $5d^5\ 6s\ {}^5G_5$ and $5d^4\ 6s^2\ {}^3G_5$, ought to be exchanged. The isotopic displacement of 152 odd levels ($5d^3\ 6s^2\ 6p$ and $5d^4\ 6s\ 6p$) was deduced. The multiplet $^7P^0$ belongs to the $5d^4\ 6s\ 6p$ and not to $5d^5\ 6p$ configuration. The final rays of the arc spectrum are not $5d^5\ 6s\ {}^7S_3 - 5d^5\ 6p\ {}^7P^0$ transitions but $5d^5\ 6s\ {}^7S_3 - 5d^4\ 6s\ 6p\ {}^7P^0$ transitions. The multiplets $^5F^0$ and $^5D^0$ belong to the $5d^3\ 6s^2\ 6p$ configuration. The systematic investigation of new odd levels was made with an IBM 7094 computer by associating isotopic displacement and differences of the wave numbers of approximately 2000 unclassified or poorly classified rays. 17 new odd levels, $5d^5\ 6p\ {}^7P^0$, were retained. The isotopic displacements of 98 rays of the arc spectrum of Os were measured. The isotopic displacement of 21 lower even levels ($5d^6\ 6s^2\ 6s$ and $5d^7\ 6s$) and 4 higher even levels ($5d^6\ 6s\ 7s$) was deduced, leading to the modification of 4 classifications of lower even levels. The isotopic displacement of 43 odd levels ($5d^6\ 6s\ 6p$, $5d^5\ 6s^2\ 6p$, and $5d^7\ 6p$) was deduced; 8 classifications were modified. For the lower even levels, the comparison of the experimental results with the theoretical results on energies, g values, and preponderant configurations is very satisfactory. The same theoretical study made it possible to discover the first level of the $5d^8$ configuration. The ground configurations of the arc spectra of W and Os were $5d^4\ 6s^2$ and $5d^6\ 6s^2$, showing that the experimental values of the coefficients of isotopic displacement are close. The respective determined values 116 ± 20 mK and 114 ± 14 mK confirm this hypothesis. The isotopic displacements of 56 rays of the arc spectrum of Nd were measured. The incoherence of previous results could not be improved, as only fragmentary results were obtained between 5200 and 6000 Å. (tr-auth)

13419 THE INDUCED INFRARED ABSORPTION SPECTRUM OF SOLID DEUTERIUM AND SOLID HYDROGEN DEUTERIDE. Crane, A.; Gush, H. P. (Univ. of Toronto). Can. J. Phys., 44: 373-98(Feb. 1966).

The fundamental absorption bands of deuterium and hydrogen deuteride were observed in the solid at a temperature of 1.9°K. Features are observed that correspond to rotation-vibration transitions in single molecules, and to molecular transitions accompanied by the creation of phonons. Several features were observed in the HD spectrum that arise from the fact that HD is heteronuclear; one of these was a sharp absorption line due to $\Delta J = 1$ transitions in single molecules. In addition, an unusual split-phonon branch was observed with a minimum of zero absorption a few wave numbers below the frequency of the $\Delta J = 1$ transition. This split-phonon feature is apparently a result of strong interaction between the rotation of the molecule and its translational motion in the lattice. The spectrum of a solid mixture of 10% HD and 90% H_2 was also studied. The phonon branch accompanying the $Q_1(0)$ line of HD and the phonon branch accompanying the $Q_1(0)$ line of H_2 observed in the same crystal have a very different shape, the former exhibiting a distinct minimum as for pure HD. (auth)

13420 SPUTTERING OF GOLD BY LOW-ENERGY INERT GAS IONS. [PART] II. Scott, H. G. (Commonwealth Scientific and Industrial Research Organization, Parkville, Australia). J. Appl. Phys., 37: 287-90(Jan. 1966).

The sputtering of gold by neon and xenon ions with energies from 40 to 100 ev was measured by determining the change in electrical resistance of thin gold films. With xenon ions the yield is proportional to ion energy, and the value at 100 ev (0.14 atoms/ion) is lower than that found previously with argon. It is therefore concluded that factors other than the mass ratio of ion to target atom are important in determining low-energy sputtering yields. The variation of yield with ion current for 40-ev neon ions (cf. Scott, 1962) is confirmed, and pulsed currents were used to investigate the hypothesis that this dependence is due to excitation of an atom followed by ejection: the lifetime of the excited state is estimated to be less than 10^{-6} sec, a value which is inconsistent with the magnitude of the yield. (auth)

13421 IONIZATION OF AN ATOM COLLIDING WITH AN EXCITED ATOM. Smirnov, B. M.; Firsov, O. B. JETP Lett. (USSR) (Engl. Transl.), 2: 297-300(Nov. 15, 1965).

Translated from Zh. Eksp. Teor. Fiz., Pis'ma Redakt., 2: 478-82(Nov. 15, 1965).

The cross section of the reation $A^* + B \rightarrow A + B^+ + e$ with the excitation potential of atom A exceeding the ionization potential of atom B is calculated using the assumption that the cross section of the reaction is determined essentially by collision impact parameters which greatly exceed the dimensions of the colliding atoms. It is shown that if the atom A* is in a resonant excited state from which a transition to the ground state via dipole radiation is possible, then the cross section of the reaction will be larger than in the case of the Penning effect. The results are used to evaluate the cross section of the reaction $Hg(6^1P_1) + Li(Cs) \rightarrow Hg(6^1S_0) + Li^+(Cs^+) + e$. (D.C.W.)

13422 LIFETIME OF THE $4f^6 6s 6p\ z^8P_{5/2}$ STATE OF EUROPIUM. Lange, W.; Luther, J.; Steudel, A.; Walther, H. (Technische Hochschule, Hanover). Phys. Lett., 20: 166-7(Feb. 1, 1966).

The lifetime of the $4f^6 6s 6p\ z^8P_{5/2}$ state of europium was measured by the method of zero field level crossing (Hanle effect). The following preliminary value was derived: $\tau(z^8P_{5/2}) = (0.74 \pm 0.07) \times 10^{-6}$ sec. (auth)

13423 STABILITY AND INSTABILITY OF PLANE-WAVE HARTREE-FOCK SOLUTIONS AND THE HELICAL SPIN ARRANGEMENT. Fukuda, Nobuyuki; Ogawa, Tohru; Soda, Toshio (Tokyo Univ. of Education). [Progr. Theoret. Phys. (Kyoto), 34: Suppl., 492-531(1965)].

The stability condition of the Hartree-Fock states, which are constructed out of the plane waves times spin-up or -down eigenfunctions, i.e., the paramagnetic (P), ferromagnetic (F) and unsaturated ferromagnetic (UF) states, is examined in some detail in the case of repulsive δ-function, Yukawa and Coulomb interactions. The spherical Fermi surface leads of course to the minimum energy in each case; this energy is then minimized as the function of polarization $n = (n^+ - n^-)/(n^+ + n^-)$, $n^\pm$ being the total number of spin-up and -down electrons. The domains of density are determined where each of the three states is most stable. Then the stability of these states against small deformations of one-particle wave functions is examined in their respective domains. In the case of δ-function potential no instability occurs, while for an electron gas the P state ($r_s < 5.45$) is always unstable and the F state ($r_s > 5.45$) is unstable near the critical density. The variational method in the form of canonical transformation is presented to obtain a new Hartree-Fock solution having helical spin structure in case instability occurs. The case of δ-function interaction is worked out for the P state and it is actually shown that such a solution can exist if and only if the P state becomes unstable. This new solution is of nonperturbative nature in the sense that it can never be obtained by perturbation theory starting from the free ground state. (auth)

13424 INVESTIGATION OF SECONDARY ELECTRON EMISSION FROM COPPER-BERYLLIUM BY MEANS OF POSITIVE IONS AT ENERGIES OF 25 kev. Herold, D. (Freie Univ., Berlin). Z. Angew. Phys., 20: 113-18(Dec. 1965). (In German).

After a summary of the few publications dealing with secondary electron emission from metals due to positive ion bombardment measurements with thirty different ions of kev energy are discussed. Those measurements were carried out with an ion converter detector. The mass relation of the secondary emission for single-charged atomic ions shows that within a group of the periodic sys-

tem of elements the secondary emission is critically influenced by the depth of penetration of the ions. There is an additional influence caused by the different electron shells within a period of the system. It is striking, that this latter effect is oriented opposite to the variation of the atomic volume. For multiple-charged atomic ions the secondary emission factor increases linearly with the charge of the ion. A method is indicated to estimate the secondary emission factor for molecular ions from the values for the contained atomic ions and the energy dependence of secondary emission. For diatomic ions this method gives good agreement between measured and estimated values, while aberrations are observed for molecules containing more than two atoms. These aberrations are discussed. (auth)

Cosmic Radiation

See also Elementary Particles and Radiations Nuclear Properties and Reactions

13425 (CEND-3107-249) BURNABLE POISON ADDITION TO UO_2. Progress Report, July 1–September 30, 1965. Brayer, R. C.; Christopher, S. S. (Combustion Engineering, Inc., Windsor, Conn. Nuclear Div.). Nov. 1965. Contract AT(30-1)-3107. 27p. (EURAEC-1539). Dep. mn. CFSTI $2.00 cy, $0.50 mn.

Work Performed under United States–Euratom Joint Research and Development Program.

Two enriched (6%) UO_2 fuel elements containing 500 ppm B_4C were fabricated at Combustion Engineering and were irradiated in the Saxton Reactor to a peak burnup of 1070 MWD/MTU at a peak specific power of 17.2 kw/ft. A post-irradiation evaluation process flow chart and a sampling scheme were finalized in preparation for the hot cell evaluation of the first element. This evaluation is being initiated. The second element will be reinserted into the reactor and will be irradiated to a total peak burnup in excess of 5000 MWD/MTU. Sampling techniques to be used for the evaluation of the irradiated elements were developed and tested inside Westinghouse Waltz Mill hot cells using a full length dummy element identical to the irradiated elements. Analytical techniques for boron are being upgraded. Statistical data indicate that pyrohydrolysis of the fuel mixtures followed by NaOH titration or 1-1′ dianthrimide colorimetric evaluation seems to be superior to the techniques previously used. (auth)

13426 (NASA-TT-F-183) INTENSITY VARIATIONS OF COSMIC RAYS. Kuz'min, A. I. (ed.). Translated from Tr. Yakutskogo Filiala, Akad. Nauk SSSR, Ser. Fiz., No. 4, 4-166(1962). 222p. CFSTI $6.00 cy, $1.25 mn.

Papers (27) dealing with experimental and theoretical observations on intensity variations of cosmic radiation are included. Experimental methods and techniques are covered, together with meteorological effects in the intensity of cosmic rays and the main properties and nature of variations in the intensity of cosmic rays. (D.C.W.)

13427 FLUCTUATIONS OF THE ENERGY FLUXES OF THE NUCLEAR-ACTIVE AND ELECTRON-PHOTON COMPONENTS IN EXTENSIVE AIR SHOWERS. Vernov, S. N.; Belyaeva, I. F.; Vedeneev, O. V.; Dmitriev, V. A.; Nechin, Yu. A.; Khristiansen, G. B. (Moscow State Univ.). Yadern. Fiz., 2: 1075-86(Dec. 1965). (In Russian).

Experimental data are given on the energy flux fluctuations of the nuclear-active and electron-photon components in extensive air showers and on the connection of these fluctuations with each other and with fluctuations of the age parameter s. It is shown that the bulk of these data disagrees with a model previously described. The large role of the experimentally established correlations of the parameter s and other characteristics for the correct setting-up of experiments concerning extensive air-showers is discussed. (auth)

Direct Energy Conversion

Refer also to abstracts 14132 and 14179.

13428 (JAERI–1093) CURRENT DISTRIBUTION IN MHD HALL GENERATORS. Matsunaga, Sakuro (Japan Atomic Energy Research Inst., Tokyo). July 1965. 19p. Dep. mn.

The distributions of the current and field in infinitely long ducts of linear Hall generators were analyzed from the method of conformal mapping under the following assumptions: the magnetic field, conductivity and flow velocity of the gas are independent of the position in the duct. The analysis was made for the case where the electrode length in the gas flow direction is equal to that of the insulator. The results of analysis are as follows. The geometrically opposed electrodes are not in equipotential. In order to make the electrodes in each pair the equipotential, the emitting electrodes must be shifted in the gas flow direction with respect to the anodes. The open circuit voltage of the generator becomes lower than the Hall electromotive force, because of the internal shorting through the boundary layer near the insulators. The shift length, open circuit voltage and internal conductivity of the generator were given as a function of the segment ratio ρ, voltage factor K and Hall parameter $\omega\tau$. Also, the loading characteristic of the generator is discussed with the variation of ρ and $\omega\tau$. The problem of duct end losses was not taken into consideration. (auth)

13429 (N64–32348) DIE SELBSTERREGUNG EINES ELEKTRODENLOSEN MHD-GENERATORS. (Self-Excitation of an Electrodeless MHD-Generator). Peschka, W.; Kelm, S.; Carpetis, C. (Deutsche Versuchsanstalt fuer Luft- und Raumfahrt E. V., Munich (West Germany)). June 1964. 32p. (DVL–319; DLR-FB–64-08). Dep. mn.

For induction generators using iron, a self-excitation is possible. Because of the iron saturation the voltage-current curve is not a straight line. An intersection point between the voltage-current curve of the generator and the voltage-current of the exciting capacitors exists, and therefore a stable self-excitation is possible. If no iron is used in the generator the voltage-current characteristic will also be curved because of the nonlinear behavior of the plasma. Some values for an electrodeless MHD-generator are calculated. Further, the self-excitation of the tranmission-line generator is possible. There is a close formal analogy between the transmission line generator and the high-frequency traveling-wave amplifier. (auth)

13430 (N64–32349) DIE THEORIE DES UNENDLICH LANGEN ELEKTRODENLOSEN MHD-GENERATORS. (Theoretical Studies of an Elektrodeless AC-MHD-Generator of Infinite Length). Peschka, W.; Kelm, S. (Deutsche Versuchsanstalt fuer Luft- und Raumfahrt e. V., Porz (West Germany). Institut fuer Energiewandlung und Elektrische Antriebe). July 1964. 48p. (DVL–316; DLR-FB–64-11). Dep. mn.

The theory of the MHD induction generator of infinite length is outlined. (D.C.W.)

13431 (RT/FI(65)31) LA CONVERSIONE DIRETTA DELL'ENERGIA TERMICA IN ENERGIA ELETTRICA PER VIA MAGNETO-PLASMA-DINAMICA PROGRAMMA DEL C.N.E.N. (The Direct Conversion of Thermal Energy in the Magnetoplasmadynamic Power Generation Program at C.N.E.N.). Bertolini, E.; Boschi, A.; Lo Surdo, C.; Toschi, R. (Comitato Nazionale per l'Energia Nucleare, Rome (Italy)). Sept. 1965. 46p. Dep. mn.

The research program on Magnetoplasmadynamic (MPD) Power Generation to be carried out under the auspices of C.N.E.N. during the period 1965–1969 is outlined. The general features and the state of art of MPD systems in closed cycle are reported. The main object of the theoretical and experimental work to be done during the first two and half years, is the study of the ionization processes in a MPD generator using an alkali seeded noble gas. The two main

experiments, a high speed moving plasma and a steady plasma in a generator duct, are described together with the diagnostic techniques. (auth)

13432 (TID–22419, pp 149-76) PLASMA MAGNETOHYDRODYNAMICS AND ENERGY CONVERSION. Brown, G. A.; Cooper, R. S.; Heiser, W. H.; (and others) (Massachusetts Inst. of Tech., Cambridge. Research Lab. of Electronics).

Results of tests of a steam-water condensing ejector test facility are presented along with results of preliminary experiments with magnetohydrodynamic (MHD) channel flows to determine MHD entry lengths from pilot tube measurements of velocity profiles. Data and discussion are also presented concerning thermionic emission from W monocrystals as function of O_2 pressure. The characteristics of pure alkali-metal vapor plasma are discussed. A summary of work on Brayton cycle MHD power generation is included. (J.R.D.)

13433 RESEARCHES OF THE CEA IN THE FIELD OF MAGNETOHYDRODYNAMICAL CONVERSION. Ricateau, P. (CEN, Saclay, France). Atompraxis, 11: 627-30(Nov.-Dec. 1965). (In German).

During the preliminary period from 1962 up to the end of 1963 the CEA presented the extension of the general plasma studies with regard to feeble ionized gas and characterized the conditions dominating in a MHD-converter by high pressure in the field of magnetohydrodynamical conversion. It is obvious that the weak conductance of feeble ionized gas influences the stated limits of the conversion and that the researches have to be concentrated on an increased ionization, either by displacing the balance between ionization and recombination or by the gas temperature. The displacing of balance is only possible by gases used in a MHD-converter in a closed cycle. The principle of periodical temperature alternation of the beam, frequently signified as conversion in an inhomogenous system, is qualified for a MHD-conversion on combustible gas. In 1963 tests about the characteristic peculiarities on the fuel element gas system were decided. For this reason the CEA joined the association of the French Institute de Pétrole, which disposes of a combustion chamber in its laboratories in Rueil. A program lasting for many years was created and the actual researches are concentrated on the conversion in inhomogeneous system. One part of this research program is the test of ceramic materials and other convenient structures for the conversion on combustible gases. In the domain of a conversion in a closed cycle and its nuclear application, the ionized effects can eliminate the balance, fixed by the electric field and produced in the interior of the converter. The result is a severe drop in temperature, possibly for the heat-source down to a lower limit of 1800°K which is defined by thermodynamic considerations. The tests in the laboratories of the CEA with regard to the physical character of this phenomenon caused the construction of a helium test bend, called TYPHEE. (auth)

13434 STUDIES AND REALIZATIONS OF THE DIRECT ENERGY CONVERSION. Labeyrie, M. (CEN, Saclay, France). Atompraxis, 11: 630-5(Nov.-Dec. 1965). (In German).

The possibilities that can be realized in the field of direct energy conversion in electricity by thermionic or thermoelectric methods are discussed, and a review is given of all results gained during the last years. The various studies of the CEA and the French Industry are presented, and the realized projects, the new research studies, and the recent experiences are mentioned. Finally the principle research programs are indicated in which the CEA is associated with the French Industry. (auth)

13435 SOME EXPERIMENTS ON AN MHD GENERATOR DRIVEN BY A PLASMA JET. Ito, Toshiro; Morikawa, Tetsuya; Murai, Hiroshi (Mitsubishi Electric Corp., Japan). Denki Gakkai Zasshi, 85: 656-64(Apr. 1965). (In Japanese).

Experiments with an MHD generator driven by a plasma jet, the basic components of which were a plasma jet torch, mixing chamber, seeding device, generator duct, diffuser, and magnet, are described. The working fluid (air) was heated in the plasma jet torch. In the mixing chamber, the plasma jet ejected through the main-nozzle was mixed with seeding substances and the cold flow ejected through the sub-nozzle. Thus, the fluid with suitable mass flow, temperature, and conductivity was obtained at the exit port of the chamber. The seeding substance was a potassium acetate-alcohol solution. The generator duct was of constant-area type with an effective length of 90 cm and cross-section of 3.6×10 cm. The electrodes were divided into 20 segments to prevent shortening of the Hall field and allow measurement of the electrical characteristics as they varied along the axis of the duct. Electrical output as high as 15 kw was obtained with the generator and the basic properties of the working fluid were measured both electrically and optically. Among the electrical measurements, open circuit voltage, short circuit current, and power output were estimated on each electrode segment which was connected to a separate set of loads. Among optical measurements, temperature was measured spectroscopically at both ends of the duct. Also, the flow velocity was measured directly by means of the streak photography. It was shown that the experimental results obtained through the measurements on the flow properties at both ends of the duct agreed well with theoretical values indirectly predicted from energy equilibrium and the conservation of mass. However, the electrical characteristics measured in these experiments differed from those predicted from the one-dimensional theory. The discrepancy between them was successfully explained by taking account of the temperature boundary layers developed on the low temperature electrodes. (BBB)

13436 THE PROBLEM OF OPTIMIZATION OF THE FLOW OF A NONEQUILIBRIUM PLASMA IN AN MHD GENERATOR CHANNEL. Ivanov, P. P.; Kovbasyuk, V. I. (High Temperature Research Inst., USSR). Teplofiz. Vysok. Temp., 3: 562-8(July-Aug. 1965). (In Russian).

A theoretical consideration is presented of the dependence of electric power of a Faraday type ideal sectioned generator on the Mach number, at given drag and internal efficiency factors. An example is given of a magnetohydrodynamic generator with a nonequilibrium argon-potassium oxide plasma in the channel. The electron collision section for argon and potassium are taken as 2×10^{-16} and 3×10^{-14} cm^2, respectively. The relative concentrations of the additives are taken as 0.1 and 0.05 mole%, respectively. The inductive magnetic field is 2 webers/m^2. Values of the specific power are calculated as a function of the Mach number. The special characteristics of the operation of a Hall generator are considered from this point of view. The effect of friction is taken into account in the calculations. It is calculated that operating conditions for a magnetohydrodynamic generator with a nonequilibrium plasma in the channel lie in the Mach number range from two up to probably four. Under optimum conditions, the degree of ionization of the additives is almost complete. As a result of the strong dependence of internal efficiency on the Mach number, a magnetohydrodynamic generator is extremely sensitive to dissipation losses in the channel at large Mach numbers. The internal efficiency of such a generator is always less than unity and decreases with a rise in the Mach number. (ATD)

13437 VARIATIONAL PROBLEM OF FLOW IN AN MHD GENERATOR CHANNEL. Medin, S. A. (High Temperature Research Inst., USSR). Teplofiz. Vysok. Temp., 3: 641-4(July-Aug. 1965). (In Russian).

Solutions are presented to two variational problems of flow in a magnetohydrodynamic generator having a minimum length at given values of heat transfer and internal efficiency, with constant velocity or constant Mach number for the flow. A comparison is given between these solutions and the solutions of corresponding nonvariational problems, including the additional condition of the constant value of the efficiency along the length of the channel. It is demonstrated that, under certain limiting conditions, the solution

for a generator with constant Mach number reduces to the solution for a generator with a constant velocity. (ATD)

13438 THERMODYNAMICS OF AN MHD POWER GENERATOR WITH A VAPOR-FILLED INJECTOR. Shpil'rayn, E. E.; Yakimovich, K. A. (Scientific Research Inst. of High Temperatures, USSR). Teplofiz. Vysok. Temp., 3: 757-64(Sept.-Oct. 1965). (In Russian).

The thermodynamics of a vapor-fluid injector are analytically investigated under the assumptions that (1) the whole injector as well as its separate parts are adiabatic; (2) the processes in the nozzle and in the exit cone are not isentropic; and (3) the nonisentropy of the processes in the mixing chamber is determined only by losses due to mixing. The formulas obtained show that the efficiency of the injector and also of the whole device depends on the ratio of the available enthalpy of the flowing fluid to the value of the latent heat of vaporization of the working material. Since calculations show that this ratio is not favorable for otherwise suitable materials, it is suggested that the efficiency of the device could be substantially increased by the use of two-component injectors. (ATD)

13439 A METHOD FOR PRODUCING ALTERNATING ELECTRIC POWER IN A MAGNETO-HYDRODYNAMIC GENERATOR. Brocher, Eric. British Patent 1,013,028. Dec. 15, 1965. Priority date Apr. 16, 1963, Switzerland.

A method of producing alternating electric power in a MHD generator consists of introducing, successively and cyclic, into at least one pair of shock tubes, a first fluid preheated to a temperature of between 1000 and 2000°K and a second fluid preheated to substantially the same temperature but at a static pressure in the order of 2 to 50 times greater than that of the first fluid. The method further consists in that the ionized gas impulse trains that are produced in the form of shock waves in each tube of the pair of tubes is passed through a magnetic field arranged transversely in the tube between at least two electrodes, which are parallel to the field, so as to produce a voltage pulse train between the electrodes of each tube. The electrodes of each pair of tubes are connected to output terminals so as to generate an alternating voltage output whose cycle, i.e., wave form, is formed by two half-waves, each produced by a respective tube of each pair of tubes. The generator is described in detail. (B.L.M.)

13440 MAGNETOHYDRODYNAMIC GENERATORS. (to Siemens-Schuckertwerke AG). British Patent 1,016,117. Jan. 5, 1966. Priority date Sept. 21, 1963, Germany.

A MHD generator includes a first electrode assembly that is hollow and has a substantially cylindrical inner surface. A second electrode assembly having a substantially cylindrical outer surface is coaxial with the first and extends into the first assembly. The outer surface of the second and the inner surface of the first bound a plasma flow-space in which the plasma can be made to flow along helical path. A magnetic field is produced within the flow-space in such a manner that some of the magnetic field lines will pass in one direction, parallel to the axis of the electrode assemblies, through one region of the flow-space and some of the field lines will pass in the opposite direction through a second region of the flow-space. One of the electrode assemblies is made up of a number of separate electrodes spaced angularly from one another about the axis so that in operation relative rotation about the axis can be effected between this electrode assembly and the magnetic field to produce an alternating current output. (B.L.M.)

13441 THERMIONIC CONVERTER. Lawrence, Jackson; Wilson, Volney C. (to General Electric Co.). U. S. Patent 3,223,857. Dec. 14, 1965. Filed Sept. 21, 1961.

A cesium vapor type thermionic converter is described in which both cathode and collector electrode are planar metal surfaces. The electrodes are supported in closely spaced opposed relation and are exposed to the interior of a vacuum tight envelope. The envelope includes a thin metal diaphragm extending from the periphery of the cathode and a peripheral extension of the collector electrode, and the diaphragm and the extension are hermetically bonded together in insulated relation. A tubulation thermally connected with the collector electrode depends on the vacuum tight envelope and communicates with the space between the electrodes. This tubulation includes a section of reduced wall thickness for limiting the transfer of heat from the collector electrode to the remote portion of the tubulation. A quantity of liquid cesium is contained in the tubulation; and the diaphragm and section of reduced thickness operate to maintain the desired temperature differential between the cathode and the collector and between the collector and liquid cesium, respectively, when the cathode is heated to operating temperatures. (B.L.M.)

13442 REGENERATIVE THERMIONIC CONVERTER. Martini, William R. (to North American Aviation, Inc.). U. S. Patent 3,223,858. Dec. 14, 1965. Filed Nov. 30, 1962.

An internally heated fuel-fired thermionic converter includes a cylindrical cathode, an anode circumferentially spaced from the anode, and plasma confined in the space between the electrodes. The cathode defines the sides of an internal combustion chamber, and regenerative heat exchangers define the ends of the chamber. Fuel injecting and air injecting means are provided for separately injecting the fuel and air into the chamber so that mixing of the two occurs only in the chamber to form a combustible mixture that is ignited to generate heat to heat the cathode to electron-emitting temperature. The flow of air into the chamber is controlled in a preselected reversible direction so that each of the regenerative heat exchangers serves alternately to heat the air entering the chamber and to cool the exhaust gases ejected from the chamber to minimize heat losses from the chamber. (B.L.M.)

13443 A.C. MAGNETOHYDRODYNAMIC GENERATOR. Corbitt, Howard E. (to Aerojet-General Corp.). U. S. Patent 3,223,859. Dec. 14, 1965. Filed June 25, 1962.

A MHD generator for the production of a-c current includes a gas flow chamber in which the opposite sides are covered with pieces of a magnetic material. These pieces of magnetic material extend beyond the sides of the gas flow chamber until the adjacent surfaces of the pieces of material face each other defining a sort of chamber. A magnet is mounted rotatably in this chamber, and the rotation of this magnet alternates the flux direction in the magnetic material so that the magnetic field in the gas flow chamber alternates in accordance with the rotation of the magnet. The reluctance between the pieces of magnetic material adjacent to the magnet is high in comparison to the reluctance between the pieces of material covering the sides of the flow chamber. Therefore, the magnetic field induced in the magnetic material is concentrated in the gas flow chamber. Electrodes are positioned in the gas flow chamber, and the alternation of the magnetic field in the chamber causes an alternating potential to be developed on these electrodes. The rotating magnet comprises an armature wrapped with an electric coil, which is connected to a source of direct current to magnetize the armature; and the magnitude of the direct current is selected so that the strength of the alternating magnetic field induced by the rotating magnet is optimized for the most efficient power generation. (B.L.M.)

13444 THERMIONIC CONVERTER. Sidoti, Joseph E. (to Bendix Corp). U. S. Patent 3,227,900. Jan 4, 1966. Filed Jan. 8, 1960.

A thermionic converter consists of an anode and a cathode having an emissive coating of a mixture of UC and ZrC and a filling of Cs vapor between the anode and cathode. A fin-like member is included on the cathode for forming a vacuum type seal between the two electrodes. Cooling means are provided for the anode so that a temperature differential is maintained between the anode and cathode. (B.L.M.)

Elementary Particles and Radiations

See also Field Theory, Scattering Theory, and Symmetries

Refer also to abstracts 13071 and 13835.

13445 (CONF-758-14) THE BRANCHING RATIO OF THE Y_1^*. Kayser, Boris (California Univ., Berkeley. Dept. of Physics); Bloom, Elliott (California Inst. of Tech., Pasadena. Dept. of Physics). [1965]. Contract AT(11-1)-34. 29p. Dep. mn. CFSTI $2.00 cy, $0.50 mn.
From American Physical Society Meeting, New York, Jan. 1965.

The $\pi\Sigma/\pi\Lambda$ branching ratio of the Y_1^* (1385) is smaller than the value predicted on the basis of phase space by a factor of approximately 0.4. It is shown that the difference in the nature (attractive and repulsive) of the forces in the $I = 1$, $J^P = 3/2^+$ $\pi\Lambda$ and $\pi\Sigma$ channels, respectively, contributes strongly to this situation. (D.C.W.)

13446 (DESY-65/9) SEARCH FOR A HEAVY ELECTRON BY ELECTRON-PROTON COINCIDENCE MEASUREMENTS. Behrend, H. J.; Brasse, F. W.; Engler, J.; Ganssauge, E.; Hultschig, H. (Deutsches Elektronen-Synchrotron, Hamburg (West Germany); Galster, S.; Hartwig, G.; Schopper, H. (Techniche Hochschule, Karlsruhe (West Germany). Institut fuer Experimentelle Kernphysik). Aug. 1965. 24p. (KFK-362). Dep. mn.

An attempt was made to observe the production of heavy electrons in the mass region of 500 to 1000 Mev in electron-proton interactions by measuring electron-proton coincidences from the interaction $e + p \rightarrow e^* + p \rightarrow e + \gamma + p$. It was found that no heavy electron exists in this mass region. A rise in the cross section was observed and was identified as the electroproduction of pions around the 2.19-Bev mass of the π-N system. (D.C.W.)

13447 (IC/65/95) ON THE ELECTROMAGNETIC AND WEAK FORM FACTORS OF THE NUCLEON. Cocho, G. (International Centre for Theoretical Physics, Trieste (Italy)). Dec. 31, 1965. 12p. Dep. mn.

The electromagnetic and weak form factors of the nucleon are fitted with a pole model which includes a phenomenological cutoff. The physical masses of the ρ, ω, and ϕ resonances and the coefficient given by $U(6) \otimes U(6)$ are used. (auth)

13448 (JINR-E-2521) ON A RECONSTRUCTION OF THE MESON-NUCLEON SCATTERING MATRIX FROM EXPERIMENTS WITH POLARIZED TARGET. Bilenkii, S. M.; Ryndin, R. M. (Joint Inst. for Nuclear Research, Dubna (USSR). Lab. of Theoretical Physics). 1965. 11p. Dep. mn.

Relativistic formulas were obtained for reconstruction of the meson-nucleon scattering matrix from the experimental data when the angle and energy are fixed (including experiments with a polarized proton target). Pion-nucleon scattering is considered. Relativistic formulas were obtained for reconstruction of amplitudes with total isotopic spin $3/2$ and $1/2$. (auth)

13449 (JINR-P-2433) OTSENKA SECHENIYA VZAIMODEISTVII NESTABIL'NYKH CHASTITS. (Estimation of Interaction Cross Section for Unstable Nuclei). Barashenkov, V. S.; Gudima, K. K.; Truskova, N. F. (Joint Inst. for Nuclear Research, Dubna (USSR). Lab. of Theoretical Physics). 1965. 13p. Dep. mn.

Use is made of the one-meson theory to determine the cross sections of unstable particles π-π and π-K by the experimental data concerning total inelastic three-particle π-N and K-N cross sections. The accuracy of the method is estimated. (auth)

13450 (JINR-P-2488) POISKI NOVYKH SKHEM RASPADA K_2^0-MEZONA. (Search for New Decay Modes of the K_2^0-Mesons). Anikina, M.; Vardenga, G.; Zhuravleva, M.; Kotlyarevskii, D.; Novikov, V.; Okonov, E.; Takhtamyshev, G.; Wu, Tsun-fan; Chkhaidze, L. (Joint Inst. for Nuclear Research, Dubna (USSR). Lab. of High Energy). 1965. 11p. Dep. mn.

The kinematical analysis of the 1116 well measurable K_2^0 decays recorded in a cloud chamber yield no decay of the types $K_2^0 \rightarrow e^+e^-$, $K_2^0 \rightarrow \mu e \nu$ and $K_2^0 \rightarrow \mu^+\mu^-$. This gives $W \lesssim 1.2 \times 10^4\ s^{-1}$ for the upper limit of the probability of these processes. Events of the type $K_2^0 \rightarrow \pi^+\pi^-\gamma$ were not found in which the γ-quantum would have given an electron-positron pair in a lead plate where $W(K_2^0 \rightarrow \pi^+\pi^-\gamma) \lesssim 2 \cdot 10^5\ s^{-1}$. Among the decays analyzed no events with anomalously large decay energy were observed. (auth)

13451 (JINR-P-2505) FORMFAKTORY I MUL'TIPOLI V ELEKTROMAGNITNYKH VZAIMODEISTVIYAKH. (Form-Factors and Multipoles in Electromagnetic Interactions). Dubovik, V. M.; Cheshkov, A. A. (Joint Inst. for Nuclear Research, Dubna (USSR). Lab. of Theoretical Physics). 1965. 9p. Dep. mn.

A definition is given of electric and magnetic multipoles of the first and second kind for particles with arbitrary spins. The parametrization of the electromagnetic current operator is obtained in terms of multipoles and the mean values of their 2n-power distribution radii. The consequences of the conditions which are imposed on the current operator by hermiticity, gauge, and T-invariance are considered in detail. (auth)

13452 (JINR-P-2510) ZARYADOVYE RASPREDELENIYA CHASTITS V ODNOMEZONNOI TEORII NEUPRUGIKH VZAIMODEISTVII PRI VYSOKIKH ENERGIYAKH. (Charge Distributions of Particles in One-Meson Theory of Inelastic Interactions at High Energies). Barashenkov, V. S.; Truskova, H. F. (Joint Inst. for Nuclear Research, Dubna (USSR). Lab. of Theoretical Physics). 1965. 7p. Dep. mn.

A method of calculating the charge distribution of particles produced in inelastic interactions at high energies is outlined. Interactions at 7 Bev are treated as an example to show that the results of the one-meson pole calculations are in good agreement with experimental data and are only slightly sensitive to assumptions concerning the magnitude of the cross sections for unstable particles. (D.C.W.)

13453 (JINR-P-2511) OBRAZOVANIE ZARYAZHENNYKH π-MEZONOV V SOUDARENIYAKH NEITRONOV S PROTONAMI PRI ENERGII NEITRONOV 600 Mev. (Charged Meson Production in Neutron-Proton Collisions at 600 Mev Neutron Energy). Dzhelepov, V. P.; Kiselev, V. S.; Oganesyan, K. O.; Flyagin, V. B. (Joint Inst. for Nuclear Research, Dubna (USSR). Lab. of Nuclear Problems). 1965. 24p. Dep. mn.

The production of mesons ($\pi^\pm$) in n-p interactions at about 600 Mev was investigated using a multichannel magnetic spectrometer. An analysis of the results shows that in spite of the dominating role of resonance pion production, it is necessary to take into account the non-resonance transfer contributions in phenomenological considerations. (D.C.W.)

13454 (UCRL-14100-T(Rev.1)) FINAL STATE ENHANCEMENT AT 1920 Mev in π^-p INELASTIC SCATTERING. Gutay, L. J.; Lannutti, J. E.; Csonka, Paul L.; Moravcsik, Michael J.; Scadron, Michael D. (Lawrence Radiation Lab., Univ. of California, Livermore). [1964]. Contract W-7405-eng-48. 9p. Dep. mn. CFSTI $1.00 cy, $0.50 mn.

It is shown that the 1920-Mev final-state enhancement in the interaction $\pi^- + p \rightarrow \pi^- + \pi^+ + n$ can not be entirely due to a nucleon-exchange process and is possibly the result of interference between meson (ρ) and N^* (1238) production. (D.C.W.)

13455 (UCRL-14240-T) THE SPIN STRUCTURE OF NUCLEON-NUCLEON SCATTERING. Moravcsik, Michael J. (Lawrence Radiation Lab., Univ. of California, Livermore). [nd]. Contract W-7405-eng-48. 26p. (CONF-650928-14). Dep. mn. CFSTI $2.00 cy, $0.50 mn.

From International Conference on Polarization Phenomena of Nucleons, Karlsruhe, Ger.

Nucleon-nucleon scattering is discussed in terms of form factors. The information that can be obtained on the dynamics of the two-nucleon interaction by an experimental determination of the form factors is stressed. (D.C.W.)

13456 (UCRL-16170) RESONANCE PRODUCTION IN PION-PROTON INTERACTIONS AT 3.65 AND 3.7 Bev/c [Thesis]. Shen, Benjamin Ching-chun (Lawrence Radiation Lab., Univ. of California, Berkeley). Sept. 28, 1965. Contract W-7405-eng-48. 154p. Dep. mn. CFSTI $5.00 cy, $1.00 mn.

The interactions of meson (π^+) and meson (π^-) with protons at 3.65 and 3.70 Bev/c, respectively, were investigated using hydrogen bubble chambers. It was found that the double resonance channels in the meson (π^+)-proton experiment involving the simultaneous production of ρ^0N^{*++} and ω^0N^{*++} proceed predominantly via peripheral interactions. The decay distributions of these resonances were investigated in a study of the nature of the exchange mechanism. Evidence that absorption must be included in the one-particle exchange model at this energy was obtained, together with evidence for the observation of multipion states. In particular, the A_1 and A_2 enhancements in the πp system and the B enhancement in the $\pi\omega$ system were studied. (D.C.W.)

13457 (UCRL-16195) TOTAL AND DIFFERENTIAL CROSS SECTIONS FOR $\pi^-p \rightarrow \eta n$ FROM THRESHOLD TO 1300 Mev [Thesis]. Richards, Walter Bruce (Lawrence Radiation Lab., Univ. of California, Berkeley). Nov. 17, 1965. Contract W-7405-eng-48. 165p. Dep. mn. CFSTI $5.00 cy, $1.00 mn.

The reaction $\pi^-p \rightarrow \eta n$ was observed through the decay mode $\eta \rightarrow 2\gamma$ at T_{π^-} = 592, 655, 704, 875, 975, 1117, and 1300 Mev. Details are given of the detection apparatus, a cubic array of six steel-plate spark chambers, completely surrounding a liquid-hydrogen target. Showers produced in the spark chambers by decay photons were recorded photographically for analysis. Events attributed to the decay of an η were identified by the large c.m. opening angle between the two photons. The total cross section for η production was calculated. The differential cross section was obtained by taking the coefficients of a Legendre polynomial fit to the angular distribution of bisectors of selected two shower events, and converting them to the coefficients of the the η c.m. angular distribution. It is suggested that production at threshold is predominantly through an S state, with some P_1 and D_3 waves entering by 655 Mev. Speculation about a possible enhancement in the P_3 wave at 1100 Mev is given. It is suggested that all of the absorption in the S_{11} π-N state can be explained by the η production, and the nature of the η-N S-wave interaction at the η threshold is briefly discussed. (M.O.W.)

13458 (UCRL-16209) PION-PROTON CHARGE-EXCHANGE SCATTERING, 500 TO 1300 Mev [Thesis]. Chiu, Charles Bin (Lawrence Radiation Lab., Univ. of California, Berkeley). Nov. 2, 1965. Contract W-7405-eng-48. 162p. Dep. mn. CFSTI $5.00 cy, $1.00 mn.

Differential cross sections for the reaction $\pi^-p \rightarrow \pi^0n$ were measured at nine incident-pion kinetic energies in the interval from 500 to 1300 Mev. The negative pion beam, obtained from the bevatron, was focused on a liquid hydrogen target surrounded by a cubic array of six steel-plate spark chambers. The spark chambers were triggered on events with neutral final states. Charge-exchange events were identified from the one-shower and two-shower events in the spark chamber pictures. By the Monte Carlo technique, the π^0 distributions were calculated from the bisector distributions of the two-shower π^0 events together with the observed gamma-ray distributions of the one-shower π^0 events. These π^0 distributions were fitted with both Legendre polynomial expansions and power-series expansions by the method of least squares. The extrapolated forward differential cross sections are in good agreement with the dispersion calculations. The Legendre coefficients for the differential cross sections in a pure $I = \frac{1}{2}$ isospin state, and for the differential cross sections due to the interference of $I = \frac{3}{2}$ and $I = \frac{1}{2}$ amplitudes, were obtained by combining our results with the available data on π^+p elastic scattering, in the light of the existing phase-shift solutions, the behavior of these coefficients is discussed. The well-known D_3F_5 interference term that peaks near 900 Mev is verified to be predominantly in a pure $I = \frac{1}{2}$ state. (auth)

13459 (UCRL-16253) TIME REVERSAL, THE FORM FACTOR RATIO, AND THE BRANCHING RATIO IN $K^+_{\mu 3}$ DECAY [Thesis]. Sandler, Carl L. (Lawrence Radiation Lab., Univ. of California, Berkeley). June 1965. Contract W-7405-eng-48. 94p. Dep. mn. CFSTI $3.00 cy, $0.75 mn.

The mesons(μ) kinetic energy spectrum and the branching ratio were measured in the $K^+_{\mu 3}$ decay, $K^+ \rightarrow \pi^0 + \mu^+ + \nu$. Pictures of mesons ($K^+$) stopping in a 30-inch heavy-liquid bubble chamber filled with C_3F_8 yielded 914 observed events with meson(μ) kinetic energy $41 \leq T_\mu \leq 94$ Mev. Assuming time reversal invariance, the data were fitted with a one parameter (V−A) theory to determine from the spectral shape the parameter ξ, the ratio of the form factors, and to determine from the area under the normalized, best-fitting spectral curve, the $K^+_{\mu 3}$ branching ratio, $BR_{K_{\mu 3}}$. In the analysis the χ^2 test of hypothesis was used to determine that the best solution for the purely real or purely imaginary parameter ξ occurred when $\xi = 0^{+2.0}_{-1.0}$, at the point where χ^2 was a minimum. The $K^+_{\mu 3}$ branching ratio, $BR_{K_{\mu 3}} = (2.93 \pm 0.23)\%$, was obtained from the ratio of the total number of $K^+_{\mu 3}$ events to the total number of K^+ mesons, determined from counting K^+_τ decays. A determination of the values of ξ compatible with the data showed that at the 95% confidence level, all values of ξ from −4.0 to +10.0 (the highest value tested) were possible. Restricted values for ξ and the $K^+_{\mu 3}$ branching ratio were found to be $\xi = -0.4 \pm 0.9$ and $BR_{K_{\mu 3}} = (2.9 \pm 0.3)\%$. On the basis of this solution, theories of the $K^+_{\mu 3}$ decay mechanism which predict that the absolute value of ξ is large can be rejected, but no discrimination can be made among those theories that predict ξ near zero. With ξ assumed complex, the same data were analyzed with a two parameter maximum likelihood function to determine ξ_{RE} and ξ_{IM}. The likelihood function is non-Gaussian, but its sensitivity can be indicated by quoting the customary $e^{-0.5}$ and $e^{-2.0}$ of the maximum value: For $L(\xi_{RE}, \xi_{IM}) = e^{-0.5} L_{MAX}$, $\xi_{RE} = 0^{+1.6}_{-1.2}$, and $\xi_{IM} = 0 \pm 1.4$; $L(\xi_{RE}, \xi_{IM}) = e^{-2.0} L_{MAX}$, $\xi_{RE} = 0^{+3.6}_{-2.6}$, and $\xi_{IM} = 0 \pm 2.9$. The likelihood solutions are consistent with the time reversal invariance requirement that $\xi_{IM} = 0$. (auth)

13460 (UCRL-16274) K^--PROTON ELASTIC SCATTERING IN THE MOMENTUM RANGE 700 TO 1400 Mev/c [Thesis]. Holley, William R. (Lawrence Radiation Lab., Univ. of California, Berkeley). Oct. 22, 1965. Contract W-7405-eng-48. 97p. Dep. mn. CFSTI $3.00 cy, $0.75 mn.

Differential cross sections for elastic K^--p scattering were measured at incident-kaon momenta from 700 to 1400 Mev/c. A total of 17,000 elastic events were observed with narrow-gap cylindrical and parallel-plate spark chambers. Least-squares fits of Legendre-polynomial power series to the differential cross sections require fifth-order terms in the region of the suggested 1765- and 1815-Mev resonances. Sixth-order coefficients are not required. The behavior of the coefficients requires a highly elastic resonance near 1815 Mev and is consistent with the existence of an additional enhancement near 1765 Mev. The latter resonance, if it exists, is rather inelastic. Least-squares fits of one or more Breit-Wigner resonance terms with constant backgrounds to the total elastic and total cross sections and a qualitative analysis of the Legendre-polynomial coefficients favor a $J = \frac{5}{2}$ assignment for the 1815-Mev resonance, although $J = \frac{3}{2}$ cannot be completely excluded. (auth)

13461 (UCRL-16365) PION-MASS MEASUREMENT BY CRYSTAL DIFFRACTION OF MESONIC X RAYS

[Thesis]. Shafer, Robert Eugene (Lawrence Radiation Lab., Univ. of California, Berkeley). Dec. 22, 1965. Contract W-7405-eng-48. 88p. Dep. mn. CFSTI $3.00 cy, $0.75 mn.

A value of the mass of the meson (π^-) was obtained from a measurement of the energies of the 4F-3D transitions in pionic Ca and Ti. The conservation of energy in the decay $\pi \rightarrow \mu + \nu$ was studied, and an upper limit of 2.1 Mev (at the 68% confidence level) was assigned to the mass of the muon neutrino. (D.C.W.)

13462 (UCRL-16370) STUDY OF THE REACTION $K^+ + p \rightarrow K + N + \pi$ BETWEEN 0.86 AND 1.58 Bev/c. Bowler, M. G.; Bland, R. W.; Brown, J. L.; Goldhaber, G.; Kadyk, J. A.; Seeger, V.; Trilling, G. H. (Lawrence Radiation Lab., Univ. of California, Berkeley). Dec. 16, 1965. Contract W-7405-eng-48. 20p. (CONF-650945-4). Dep. mn. CFSTI $1.00 cy, $0.50 mn.

From International Conference on Elementary Particles, Oxford.

The interaction $K^+ + p \rightarrow K + N + \pi$ was studied at 0.86, 0.96, 1.20, and 1.58 Bev/c. At all these momenta, the interaction is dominated by resonance formation –N*(1236) at the lower two momenta and both N*(1236) and K*(891) at the higher momenta. The N* production is reasonably well described by the Stodolsky-Sakurai rho-exchange model. The K* production does not fit any simple one-particle exchange model. (auth)

13463 (UCRL–16511, pp 1-53) GENERAL PHYSICS RESEARCH. (Lawrence Radiation Lab., Univ. of California, Berkeley).

Brief summaries of experimental elementary particle research carried out at LRL during this period are presented. The experiments include cross sections and decay mode determinations from various particle interactions. Brief summaries of theoretical research dealing with computer programs, plasma physics, and scattering are presented. (M.O.W.)

13464 NONPERTURBATIVE FIELD-THEORETICAL MODEL OF LEPTONIC WEAK INTERACTIONS. Stern, J. (Technical Univ., Prague). Acta Phys. Acad. Sci. Hung., 19: 223-42(1965).

The problem of the four-leptonic weak processes is studied in the theory with an intermediate vector W-meson. Neglecting $m_{lept.}$ and the part of amplitude containing induced neutral currents, an integral relation between the four-leptonic amplitude and the weak W-meson form factor is found. On the basis of this relation and the unitarity condition the four-leptonic amplitude is evaluated. The solution obtained contains a resonance in the energy channel with the total width about 1 Mev, and decreases as $(1/s^2)$ for $s \rightarrow \infty$. Some consequences of the model are discussed, first of all with regard to the production of an intermediate boson by neutrinos. (auth)

13465 A MULTI-CHANNEL MODEL OF WEAK SCATTERING OF LEPTONS. Vancura, A. (Faculty of Technical and Nuclear Physics, Prague). Acta Phys. Acad. Sci. Hung., 19: 243-51(1965).

A multichannel model of weak scattering is developed, based on the four-fermion theory of weak interactions using Bethe-Salpeter equation. It leads to several relations among the cross sections of different weak scattering processes. In low energy limit the cross sections of all included reactions are expressed with the help of a single constant. (auth)

13466 LEPTONIC DECAYS WITH $\Delta I = 3/2$ AND $\Delta S = 2$ IN THE UNITARY SYMMETRY SCHEME. Nagy, T. (Roland Eoetvoes Univ., Budapest). Acta Phys. Acad. Sci. Hung., 19: 253-6(1965).

A possible generalization of Cabibbo's formalism is investigated in the leptonic decays of the strange particles. (auth)

13467 AN APPLICATION OF THE QUASIPOTENTIAL METHOD TO PION NUCLEON SCATTERING. Isaev, P. S.; Smith, J. (Joint Inst. for Nuclear Research, Dubna USSR). Acta Phys. Acad. Sci. Hung., 19: 259-62(1965).

The quasipotential method developed in Dubna Laboratory was applied to pion-nucleon scattering processes up to the energies 500 Mev, for obtaining the resonance behavior of the P_{33}-phase shift. Although numerical calculations are not completed, the existence of a resonance seems very probable. (auth)

13468 INFLUENCE OF CRYSTALLINITY ON POSITRON-ANNIHILATION ANGULAR CORRELATION IN TEFLON. MacKenzie, I. K.; McKee, B. T. A. (Dalhousie Univ., Halifax, Nova Scotia). Can. J. Phys., 44: 435-41 (Feb. 1966).

Measurements were made to compare the angular correlation of gamma rays produced by positron annihilation in two different Teflon polymers. The changes in the shape of the angular distribution curves can be related to changes in the fraction of positrons that form positronium. Further lifetime measurements to eliminate a possible discrepancy because of different degrees of crystallinity will be carried out. (F.S.A.)

13469 INVESTIGATION OF THE DEPENDENCE OF THE BACKSCATTERING COEFFICIENT OF β RADIATION ON THE ATOMIC NUMBER OF THE SCATTERING MATERIAL. Krivan, V. (Slovak Polytechnic Inst., Bratislava). Chem. Zvesti, 19: 737-54(1965). (In Czech).

A spectrometric scintillation method in an isotropic geometry was used to examine the correlation between the β backscattering coefficient, R, and the order number, Z, of the target. The discrimination curves of ^{32}P, ^{185}W, and ^{32}S allowed the total backscattering coefficients to be derived. In order to eliminate the absorption of radiation in air, the measurements were carried out in an evacuated chamber. The necessary corrections for absorption within the supporting foil and the preparation were made. Much higher values were found for the backscattering coefficients than those reported in the literature. The correlation between the β backscattering coefficient and the atomic number of the target was found to be affected by the energy of the incident radiation: an increase of the energy of the primary radiation resulted in a decrease of the coefficient. The previously reported low values and the nonrecognition of the energy effect is probably attributable to the geometry of the earlier measurements, use of G-M counters, and neglect of the absorption in air. The function $R = f(Z)$ may be expressed as a continuous exponential regression function or, within limits, as a linear function; the two possibilities yield statistically identical values. (TTT)

13470 THE DETERMINATION OF THE IMAGINARY PART OF PHASE SHIFTS IN ELASTIC pp-SCATTERING AT 655 Mev. Vovchenko, V. G. (Ioffe Inst. of Physics and Tech., Leningrad). Dokl. Akad. Nauk SSSR, 163: 1348-51(Aug. 21, 1965). (In Russian).

Phase analysis of the elastic pp scattering under consideration of the meson formation data allowed the determination of only those pp systems in which the meson formation and absorption coefficients were also taken into account. Making use of S. Mandelstam's resonance model, the production cross section of π mesons may be calculated from the original state of the pp system. Examination of the angular distribution of π mesons from the $p + p \rightarrow \pi^+ + d$ reaction at the production threshold and at $E_p = 660$ Mev indicated that the reaction goes from the $^1D_2$ state with an S divergence. In order to determine the parameters at an emitted proton energy of 655 Mev, the meson spectra changes at an angle of 30° in the laboratory system were used. The admixture of μ mesons and electrons in the system was small. The differential cross section of the $p + p \rightarrow \pi^+ + p + n$ reaction was calculated to be $(11.1 \pm 1.1) \times 10^{-27}$ cm^2. The total cross section was found to be $(3.0 \pm 0.23) \times 10^{-27}$ cm^2 for $\sigma(\pi^+pn)/4\pi$ and $\sigma(\pi^+d)$. Values were also obtained for the meson production cross section from other reactions. (TTT)

13471 ELASTIC 180° SCATTERING OF π^+ MESONS BY PROTONS AT HIGH ENERGIES. Vovenko, A. S.; Gus'kov, B. N.; Likhachev, M. F.; Lyubimov, A. L.; Matulenko, Yu. A.; Savin, I. A.; Stavinskii, V. S. (Joint

Inst. of Nuclear Research, Dubna, USSR). JETP Lett. (USSR)(Engl. Transl.), 2: 255-7(Nov. 1, 1965).

Translated from Zh. Eksp. Teor. Fiz., Pis'ma Redakt., 2: 409-13(Nov. 1, 1965).

The differential cross sections for elastic π^+-p scattering in a small solid angle about 180° were measured at meson (π^+) momenta of 3.15, 4.10, and 4.85 Bev/c in the laboratory system. The results for 4.10 and 4.85 Bev/c are presented. (D.C.W.)

13472 INDUCED SYNCHROTRON RADIATION OF ELECTRONS IN CAVITY RESONATORS. Gaponov, A. V.; Gol'denberg, A. L.; Grigor'ev, D. P.; Orlova, I. M.; Pankratova, T. B.; Petelin, M. I. (Gor'kii Radiophysics Research Inst., USSR). JETP Lett. (USSR)(Engl. Transl.), 2: 267-9(Nov. 1, 1965).

Translated from Zh. Eksp. Teor. Fiz., Pis'ma Redakt., 2: 430-5(Nov. 1, 1965).

The self-excitation of electromagnetic oscillations at the electron gyrofrequency was observed in a resonator constituting a 20-cm section of rectangular wave-guide. The induced synchrotron radiation of the electrons at the second harmonic of the gyrofrequency was observed in a barrel-like open resonator. The conditions for self-excitation of electromagnetic oscillations at small longitudinal electron velocities are in satisfactory agreement with theoretical predictions. (D.C.W.)

13473 CP-ODD WEAK INTERACTION. Shabalin, E. P. JETP Lett. (USSR)(Engl. Transl.), 2: 276-8(Nov. 1, 1965).

Translated from Zh. Eksp. Teor. Fiz., Pis'ma Redakt., 2: 446-9(Nov. 1, 1965).

Two radically different consequences of negative CP-parity of weak interactions are outlined. (G.O.Y.)

13474 CONCERNING ONE POSSIBLE METHOD OF DETERMINING ISOBAR PARITY. Dubovikov, M. S. (Moscow Physico-Technical Inst.). JETP Lett. (USSR) (Engl. Transl.), 2: 282-3(Nov. 1, 1965).

Translated from Zh. Eksp. Teor. Fiz., Pis'ma Redakt., 2: 454-6(Nov. 1, 1965).

A method is proposed for determining the parity of isobars produced in interactions of baryons with pseudoscalar mesons. (D.C.W.)

13475 A NOTE ON C-ODD MULTIPOLES. Kobzarev, I. Yu; Okun', L. B.; Terent'ev, M. V. (Inst. of Theoretical and Experimental Physics, Moscow). JETP Lett. (USSR) (Engl. Transl), 2: 289-91(Nov. 15, 1965).

Translated from Zh. Eksp. Teor. Fiz., Pis'ma Redakt., 2: 466-9(Nov. 15, 1965).

The possible existence of C-odd terms in the vertex part of photon emission is discussed for the case of particles with spin $I \geq 1$. (D.C.W.)

13476 LEPTON DECAY OF VECTOR MESONS. Shekhter, V. M. (Ioffe Physico-technical Inst., Leningrad). JETP Lett. (USSR) (Engl. Transl.), 2: 302-4(Nov. 15, 1965).

Translated from Zh. Eksp. Teor. Fiz., Pis'ma Redakt., 2: 486-9(Nov. 15, 1965).

The probabilities of the decay of mesons (ω), (φ), and (ρ^0) into lepton pairs were calculated assuming that strong interactions have unitary symmetry and that the vector mesons interact with conserving currents. (D.C.W.)

13477 DETERMINATION OF THE $\gamma\pi\rho$ INTERACTION CONSTANT. Adamovich, M. I.; Larionova, V. G.; Lebedev, A. I.; Kharlamov, S. P.; Yagudina, F. R. (Lebedev Physics Inst., Moscow). JETP Lett. (USSR) (Engl. Transl.), 2: 305-7(Nov. 15, 1965).

Translated from Zh. Eksp. Teor. Fiz., Pis'ma Redakt., 2: 490-3(Nov. 15, 1965).

The $\gamma\pi\rho$ interaction constant was determined from data on the photoproduction of charged pions on nucleons. The result was used to calculate the width for the radiative decay of the meson (ρ); the value obtained does not contradict the value predicted by the unitary-symmetry hypothesis. (D.C.W.)

13478 CHARGE-PARITY VIOLATING ELECTROMAGNETIC INTERACTION. Dolgov, A. D. (Physico-technical Inst., Academy of Sciences, Ukrainian SSR). JETP Lett. (USSR) (Engl. Transl.), 2: 308-9(Nov. 15, 1965).

Translated from Zh. Eksp. Teor. Fiz., Pis'ma Redakt., 2: 494-6(Nov. 15, 1965).

It was previously shown that the electromagnetic current of particles with spin $J > \frac{1}{2}$ can, in principle, contain both C-odd and C-even terms. The explicit form of the current for particles with $J = 1$ and $\frac{3}{2}$ shows that the contribution of C-even terms to the elastic scattering of electrons by these particles is proportional to the square of the momentum transfer, indicating that the forces which do not conserve C parity are short-range. It is shown that a similar phenomenon occurs for particles with arbitrary spin $J > \frac{1}{2}$. (D.C.W.)

13479 CONSTANTS OF INTERACTION OF VECTOR MESONS WITH NUCLEONS. PHOTOPRODUCTION OF π^0 AND η MESONS ON NUCLEONS AND ELECTROMAGNETIC FORM FACTORS OF NUCLEONS. Rekalo, M. P. (Physico-technical Inst., Academy of Sciences, Ukrainian SSR). JETP Lett. (USSR) (Engl. Transl.), 2: 309-11(Nov. 15, 1965).

Translated from Zh. Eksp. Teor. Fiz., Pis'ma Redakt., 2: 497-9(Nov. 15, 1965).

The ratio of the contributions of various vector mesons to the amplitudes of the interactions $\gamma + P \rightarrow P + \pi^0$ and $\gamma + P \rightarrow P + \eta$ was calculated in the framework of SU(6) symmetry. The predictions of SU(6) symmetry for the constants of interaction between vector mesons and nucleons were tested using experimental data on the electromagnetic form factors of nucleons. (D.C.W.)

13480 THE MUON AND PION SCATTERING IN FREON. Paty, M.; Yoshiki, H. (CERN, Geneva). Nucl. Instrum. Methods, 39: 133-40(Jan. 1966).

The muon scattering cross section in liquid freon and propane is calculated. For the nuclear effects the shell model calculation is done for carbon and fluorine, whereas for bromine the results of the diffused source calculation are used. The results are compared with the pion cross section in these liquids. (auth)

13481 USE OF THE FIALHO METHOD FOR CALCULATING PHASE-SPACE VOLUMES. Childers, R. L.; Galloway, K. F. (Univ. of South Carolina, Columbia). Nucl. Instrum. Methods, 39: 353-4(Jan. 11, 1966).

A technique is given using Failho's results (Phys. Rev. 105, 328 (1957)) which leads quickly to the desired phase-space factors. The calculation can be done using a desk calculator and log tables. The results compare favorably with numerical integrations and are generally better than the results obtained using some simplifying assumptions. (J.F.P.)

13482 PHASE EQUIVALENT POTENTIALS FOR NEUTRON-ALPHA ELASTIC SCATTERING. Pearce, W. A.; Swan, P. (Rice Univ., Houston, Tex.). Nucl. Phys., 78: 433-47(1966). (TID-22105).

A new distorted wave approximation for the deduction of two-body elastic scattering potentials from the phase shifts is applied to the low energy neutron-alpha data. The procedure for smoothing relatively scattered data is discussed and potentials for the interaction are deduced. The potentials found illustrate the strong spin-orbit effects initially evident in the splitting of the P wave phases and do not lead to a bound state for ^{5}He. (auth)

13483 TWO-CHANNEL GENERATION OF THE ρ BY ONE- AND TWO-PARTICLE EXCHANGE FORCES. Gervais, J.-L. (Faculte des Sciences, Orsay, France). Nuovo Cimento, (10), 41A: 329-48(Feb. 1, 1966).

Previous attempts to generate the ρ in the $\pi\pi$ scattering amplitude with elastic unitarity taking into account the exchange of two nonresonating pions, did not lead to any self-consistent solutions. A new calculation is presented based on the same method where the unitarity approximation is improved by adding the $K\bar{K}$ channel to the $\pi\pi$ one. Solutions are found, which appear to be more satisfactory than the results of the model based on one-particle exchange forces. Some general features of the approximate method proposed in order to include two-particle exchange forces into the N/D equations, are also discussed. (auth)

13484 ON THE SCATTERING OF A HEAVY CHARGED PARTICLE AGAINST AN ELECTRON. Edin, K. A.; Eriksson, K. E. (Inst. of Theoretical Physics, Gothenburg). Nuovo Cimento, (10), 41A: 349-59(Feb. 1, 1966).

The cross section for π (μ)-e scattering is calculated to order α^3 for an experimental arrangement in which only the final electron is detected. It is assumed that π (μ) is extremely relativistic but that the momentum transfer to the heavy particle is small enough to allow a static approximation in the calculation of the radiative corrections. The outgoing electron is assumed to be extremely relativistic. (auth)

13485 CHARGE-ASYMMETRY EFFECTS IN Λ-$\mathcal{N}$ SCATTERING. Downs, B. W.; Phillips, R. J. N. (Univ. of Colorado, Boulder). Nuovo Cimento, (10), 41A: 374-9 (Feb. 1, 1966).

A phenomenological, charge-symmetry-breaking (CSB) Λ-$\mathcal{N}$ potential is deduced from the $^4He_\Lambda$–$^4H_\Lambda$ binding-energy difference. This is added to charge-symmetric (CS) potentials deduced from $^3H_\Lambda$ and $^5He_\Lambda$, and applied to Λ-$\mathcal{N}$ scattering for two possible choices of CSB potential parameters. In one case, a CS singlet scattering length –3.5 fermi is changed to –5.4 fermi for Λ-p and to –2.5 fermi for Λ-n. Different combinations of CSB parameters affect the J = 0 ground states and J = 1 excited states of the four-body hypernuclei; observation of the latter could fix the CSB spin-dependence. CSB effects in final-state interactions are also discussed. (auth)

13486 COUPLING-CONSTANT RELATIONS FOR $1^\pm$ AND INDUCED $0^\pm$ MESONS. Cronin, J.; Nambu, Y. (Univ. of Chicago). Nuovo Cimento, (10), 41A: 380-85 (Feb. 1, 1966). (COO-264-275; EFINS-65-72).

A simple model of interactions between vector (pseudovector) and scalar (pseudoscalar) mesons is solved exactly. This allows one to derive the relation $|f|^2 = |G|^2/m_V^2(Z_1 - 1)$, where G and f are the coupling constant of the vector and scalar mesons to an external nucleon current, and Z_1 is the nucleon current renormalization constant. Z_1 (π) is determined using the SU_3 prediction, $-G_A/G_V = 5/3$, and the experimental value, $-G_A/G_V = 1.18$. The coupling constant of a T = 1, Y = 0 axial vector to the nucleon axial vector current is found to be given by $G_{\pi NN}^2/4\pi = 0.03\ (m_\rho^2/m_\pi^2)$. In addition, the model is discussed in the framework of broken SU_3 and used to derive relations between the renormalized coupling constants, masses, and currents of different strangeness. (auth)

13487 APPARENT CORRELATIONS BETWEEN PRODUCTION PROCESSES AND DECAY CHAINS WHICH INCLUDE PIONS. Osborne, W. Z. (Univ. of California, Berkeley). Nuovo Cimento, (10), 41A: 389-94(Feb. 1, 1966).

Four classes of K^- and $K^+_{\pi 2}$ events detected in nuclear emulsions were analyzed in search for correlations between the π-μ-e decay chain and observables of processes that included and preceded creation of a pion. The results of directional measurements are discussed. (L.B.S.)

13488 Y_1^{*+}—Y_1^{*-} MASS DIFFERENCE. Jacob, H.; Bondyopadhyay, D. (Univ. of Delhi). Nuovo Cimento, (10), 41A: 395-8(Feb. 1, 1966).

A one-channel calculation is made of the Y_1^{*+}–Y_1^{*-} mass difference in SU_2-symmetric dynamics, on the assumption of Y_1^* coming in the $^3/_2^+$ state in the π-Λ channel. Several perturbative corrections to the amplitude to which the mass difference is due are taken into account-kinematic corrections, corrections due to photon exchange, corrections due to cross-channel mass splitting, and radiative corrections. A result of –2.99 Mev was obtained. (L.B.S.)

13489 NUCLEON-NUCLEON POTENTIAL WITH A SOFT CORE FOR THE $^1S_0$ STATE IN THE ENERGY REGION 0.17 – 310 Mev. Bystritskii, I.; Legar, F.; Ulegla, I. (Joint Inst. of Nuclear Research, Dubna, USSR). Phys. Lett., 20: 186-7(Feb. 1, 1966).

A nucleon-nucleon potential with a soft core is found which describes well the energy dependence of the $^1S_0$ phase shift in elastic p-p and n-p scattering. However, a simultaneous description of p-p and n-p scattering consistent with the experimental data could not be made with the same potential. (auth)

13490 ELECTRODISINTEGRATION OF THE DEUTERON AT LOW MOMENTUM TRANSFER: MAGNETIC TRANSITIONS. Goldemberg, J.; Schaerf, C. (Stanford Univ., Calif.). Phys. Lett., 20: 193-4(Feb. 1, 1966).

The spectrum of electrons inelastically scattered from a deuterium target at 180° was measured. At this angle the transition is mainly magnetic (spin-flip) and therefore the dominant state of the two nucleons after the transition should be a singlet with zero orbital angular momentum. A liquid deuterium target was used, and measurements were performed at incident electron energies of 54 and 70 Mev. The resulting energy spectrum of the inelastically scattered electrons is shown and compared with theoretical results. The results are very dependent on the folding of experimental resolution. The discrepancy at higher excitation energies can possibly be attributed to inadequate treatment of the final state interaction of the two nucleons or to contributions from meson exchange currents. (J.F.P.)

13491 MODELS OF ELEMENTARY PARTICLES AND ALGEBRA OF CURRENTS. Okubo, S. (Univ. of Rochester, N. Y.). Phys. Lett., 20: 195-8(Feb. 1, 1966).

It is shown that a similar method to that for deriving the exact sum rule using the algebra of currents is applicable for the decay mode $\omega \to \pi_0 + \gamma$ which permits discrimination among various models of elementary particles. It is also shown that a rough estimate seems to favor the Maki Hara model over that of Gell-Mann-Zweig, although the conclusion is not definite due to the many approximations involved. (J.F.P.)

13492 RECENT SINGLE-ENERGY PION-NUCLEON PHASE-SHIFT ANALYSES AND SPIN-FLIP DISPERSION RELATIONS. Draxler, K. D.; Hueper, R. (Technische Hochschule, Karlsruhe, Ger.). Phys. Lett., 20: 199-202 (Feb. 1, 1966).

The consistency of recent phase-shift analyses with dispersion relations for the πN scattering amplitude B_+ in forward direction was checked. The set of Cence does not fulfil these relations. A set of the Saclay group shows fair agreement for $T_\pi < 500$ Mev and systematic deviations for $T_\pi > 500$ Mev. The solution of Donnachie et. al. seems to be in very good agreement. (auth)

13493 THE REAL PART OF THE PROTON-NEUTRON FORWARD SCATTERING AMPLITUDE. Carter, A. A. (Cavendish Lab., Cambridge, Eng.); Bugg, D. V. Phys. Lett., 20: 203-5(Feb. 1, 1966).

The real part of the proton-neutron forward scattering amplitude was evaluated from a dispersion relation. The low energy contribution from the unphysical region may be fitted with a ρ pole alone. (auth)

13494 NUCLEON-ANTINUCLEON CHARGE EXCHANGE IN THE ABSORPTION MODEL. Phillips, R. J. N. (Atomic Energy Research Establishment, Harwell, Eng.); Ringland, G. A. Phys. Lett., 20: 205-6(Feb. 1, 1966).

The results of an absorptive model calculation of the reaction $p + \bar{p} \to n + \bar{n}$ at 3.0 and 3.6 Bev/c are presented. Good agreement with experiment is obtained for $-t \geq 0.1$ (Bev)^2; at smaller angles there is a possible discrepancy. (auth)

13495 K_S AND K_L INTERFERENCE IN THE $\pi^+\pi^-$ DECAY MODE, CP INVARIANCE AND THE K_S–K_L MASS DIFFERENCE. Alff-Steinberger, C.; Heuer, W.; Kleinknecht, K.; Rubbia, C.; Scribano, A.; Steinberger, J.; Tannenbaum, M. J.; Tittel, K. (CERN, Geneva). Phys. Lett., 20: 207-11(Feb. 1, 1966).

The initial results of experiments are reported in which the interference of the mesons (K_S^0) and (K_L^0) in the time dependence of the intensity of the $\pi^+\pi^-$ decay mode is studied. This decay mode is studied as a function of distance from a copper plate placed in a neutral beam at a distance such that the short-lived component has decayed to a negligible level. In the copper a short-lived component of the K^0 beam is regenerated. The experiment consists

of three parts which differ in the type of regenerator: no regenerator, a regenerator of 12 cm of copper of density 8.9 g/cm, and a regenerator of the same dimensions as the second, but consisting of 0.5-mm copper sheets spaced 0.8 cm apart, so that the average density is 0.55 g/c. The mass and angular distributions for the three converter conditions are shown. Also the data are shown treated in such a way that the interference term is isolated. (J.F.P.)

13496 TIME-DEPENDENT INTERFERENCE EFFECTS IN TWO-PION DECAYS OF NEUTRAL KAONS. Bott-Bodenhausen, M.; De Bouard, X.; Cassel, D. G.; (and others) (CERN, Geneva). Phys. Lett., 20: 212-15(Feb. 1, 1966).

Preliminary results from an experiment designed to search for time-dependent interference between short-lived and long-lived neutral mesons (K) are reported. A regenerator was placed in a beam of long-lived neutral mesons (K), and the rate of the $\pi^+\pi^-$ decay mode was observed as a function of distance from the end of the regenerator. The aim of the experiment was the measurement of the beat frequency between the decay amplitudes for this decay mode of the mesons (K_L^0) and the regenerated mesons (K_S^0) and their phase relation. The preliminary results establish the existence of a time-dependent interference pattern. These results demonstrate directly the existence of a CP violation amplitude in the $K_S^0 - K_L^0$ system. (J.F.P.)

13497 ON THE EXISTENCE OF SPIONS FROM K^+ DECAY. Fung, S-Y.; Goldberg, R.; Meyer, S. L.; Plano, R. J. (Rutgers-The State Univ., New Brunswick, N. J.). Phys. Lett., 20: 215-16(Feb. 1, 1966).

A search was made for spin 1 particles arising from the decay of mesons(K). No evidence was seen for either positive or neutral particles of this sort in the τ and τ' decays of K^+. New upper limits for the possible occurrence of these particles are presented. (auth)

13498 DEPOLARIZATION OF POSITIVE MUONS IN SOLIDS. Eisenstein, B.; Prepost, R.; Sachs, A. M. (Columbia Univ., New York). Phys. Rev., 142: 217-27 (Feb. 1966).

When polarized positive mesons(μ) stop in a solid, they may be depolarized prior to their decay. The presence of a magnetic field along the direction of initial polarization will inhibit, or quench, some of this depolarization. Depolarization and quenching was studied in a variety of solids, including semiconductors, at temperatures as low as 4.2°K. No evidence was found that any meson(μ) depolarization is associated with the formation of a muonium atom which is bound for $>10^{-10}$ sec, even in samples at 4.2°K. For many samples and temperatures, the quenching of the observed depolarization is consistent with a model in which the meson(μ) captures and loses electrons repeatedly, forming a succession of briefly bound muonium atoms. In some of the semiconductors at low temperatures, as well as in other samples, a large fraction of the depolarization is quenched by a field of 100 G. This is seen as evidence for another depolarization mechanism. It is also found that the time during which depolarization occurs in boron carbide decreases with decreasing temperature. (auth)

13499 POSITRON LIFETIME SPECTRA IN MOLECULAR SUBSTANCES. Brandt, Werner; Spirn, Irwin (New York Univ., N. Y.). Phys. Rev., 142: 231-7(Feb. 1966).

Earlier quantum-mechanical model calculations show, and experiments have confirmed, that at low and intermediate temperatures the long lifetime of orthopositronium atoms (o-Ps) against electron pickoff in a molecular lattice rises with the free volume, because the overlap between the positron component of the o-Ps wave function and the wave function of the lattice electrons responsible for pickoff decreases with increasing lattice spacing. An extension of this model to higher temperatures, where the influence of lattice vibrations becomes important, predicts a shortening of the pickoff lifetime relative to its value in a cold lattice of the same free volume. In fact, under favorable conditions, on heating, the rise with free volume can be overshadowed by the decline due to thermal density fluctuations such that a maximum in the pickoff life-time develops at a characteristic inversion temperature. In search for such maxima, lifetime spectra of positrons annihilating in three organic insulators (polyethylene, polytetrafluoroethylene, glycerol) were measured with high resolution over wide temperature ranges, and decomposed into three components. On analysis, the data reveal that the relative intensities of the components with the longest and shortest lifetimes, in their dependence on temperature and pressure, vary as the free volume. At elevated temperatures the longest lifetime in polytetrafluoroethylene exhibits a maximum which is interpreted to be a manifestation of the thermal motion of the lattice molecules. (auth)

13500 NEUTRON-PROTON DIFFERENTIAL CROSS SECTION AT 129 AND 150 Mev. Measday, David F. (Harvard Univ., Cambridge, Mass.). Phys. Rev., 142: 584-90 (Feb. 18, 1966).

The differential cross section for neutron-proton scattering was measured from 70 to 180° (center-of-mass system) at energies of 129 ± 1 and 150 ± 1 Mev. A neutron beam was used with an energy width of 6 Mev. The data have relative errors of from 3 to 4%. They were normalized to total-cross-section data with the aid of phase-shift analysis; differences between various solutions imply an uncertainty in the absolute value of these cross-section data of as much as 6.5%. The data at 150 Mev are shown to be more reasonable than previous data in this energy region. The data at 129 Mev agree well with earlier work. (auth)

13501 NONMESIC DECAY OF LIGHT HYPERNUCLEI. STRUCTURE OF THE WEAK INTERACTION $\Lambda + N \rightarrow N + N$. Tamiya, Takanori; Kawaguchi, Masaaki; Sumi, Yoshio (Osaka Univ.). Progr. Theoret. Phys. (Kyoto), 34: 833-42 (Nov. 1965).

Nonmesic decay of light hypernuclei is discussed in order to get maximum direct information on the weak interaction $\Lambda + N \rightarrow N + N$. An octet hamiltonian of the current-current type based on the SU(3) symmetry is discussed in detail. (auth)

13502 WEAK GAMMA DECAYS OF HYPERONS. Itoh, Chiaki (Tokyo Univ. of Education). Progr. Theoret. Phys. (Kyoto), 34: 843-50(Nov. 1965).

Weak gamma decays of hyperons are studied. The gamma rays can have directional asymmetry and polarization, depending on the asymmetry parameter α. Under the assumptions of RP invariance, SU(3), and the pole approximation, two models are discussed: (i) the process hyperon → baryon + ρ^0 (or ω^0), followed by $\rho^0 \rightarrow \gamma$ (or $\omega^0 \rightarrow \gamma$); (ii) the decay amplitude transforming like $A_{\frac{1}{2}} - \frac{1}{2} A_{\frac{3}{2}} - \frac{1}{2} A_{\frac{3}{2}}$. Under one additional condition, the model (i) is reduced to the model (ii). In the model (ii), the decay rate ω ($\Sigma^+ \rightarrow p + \gamma$) has the largest value among many possible weak gamma decays of hyperons. (auth)

13503 SOME CONSIDERATION CONCERNING ENERGY DEPENDENCE OF THE REAL PART OF π-p SCATTERING AMPLITUDE. Minami, Shigeo (Osaka City Univ.). Progr. Theoret. Phys. (Kyoto), 34: 865-6(Nov. 1965).

The experimentally observed decrease of the ratio of the real to the imaginary part of the π-p scattering amplitude with increasing energy is considered. It is found that the real part of the amplitude probably has no effect on the nonshrinkage properties of the elastic diffraction peak. Also, a method for treating the divergence difficulty inherent in field theory is suggested; the matrix element, M(p), for elastic π-p scattering is expressed by the sum of the matrix element, M″(p), due to the damping effect and a matrix element, M′(p), containing the divergence terms, as functions of the cms pion momentum. (M.J.T.)

13504 ON THE MASS OF THE PARTICLES PROPOSED BY TANIKAWA AND WATANABE. Ozaki, Seinosuke (Osaka City Univ.). Progr. Theoret. Phys. (Kyoto), 34: 868-70(Nov. 1965).

The lower limit on the mass of the intermediate boson is discussed, using expressions for the effective cross section and resonance width in the interaction $\nu + n \rightarrow \mu^- + p$ to calculate the muon intensity below ground in terms of

the intermediate boson mass. This equation is compared with the observed upper limit on the muon intensity to obtain a lower limit on the boson mass of $80m_n$. (M.J.T.)

13505 POSSIBLE EXISTENCE OF WRONG G-PARITY INTERACTION IN MUON CAPTURE REACTION. Fujii, Akihiko; Ohtsubo, Hisao (Sophia Univ., Tokyo. Tokyo Inst. of Tech.). Progr. Theoret. Phys. (Kyoto), 34: 873-4(Nov. 1965).

The molecular capture rate of muons in liquid H is evaluated for various choices of the ratio of the axial-vector and vector coupling constants in beta decay, $g_1(0)$, and of the A-radius, ρ_A, by calculating the atomic capture rate and using molecular parameters connecting the molecular and atomic rates. The possible existence of the wrong G-parity interaction is shown. (M.J.T.)

13506 PROBLEMS ON FUNDAMENTAL PHYSICS. Commemoration Issue for the Thirtieth Anniversary of the Meson Theory by Dr. H. Yukawa. [Progr. Theoret. Phys. (Kyoto), 34: Suppl., 1-688 (1965)]. (CONF-650947).

Forty-seven papers are included; separate abstracts were prepared for forty-five. One paper previously appeared in NSA as 3: 1777. The other paper is a reminiscence on the impact of Yukawa's meson theory on workers in Europe. (L.B.S.)

For abstracts of individual papers see: 13353, 13354, 13423, 13507–13514, 13598–13621, 13662–13665, 13876–13880, and 14001.

13507 ON MESONS AND COSMOLOGY. Ivanenko, D. (Moscow State Univ.). [Progr. Theoret. Phys. (Kyoto), 34: Suppl., 161-7(1965)].

The hypothesis of two intermediate bosons is applied for explaining K_2^0 anomalous decay. Some attempts of explaining this anomaly by means of gravitational and cosmological influences are considered, which may contribute to elaboration of unified picture of the universe. (auth)

13508 ROLE OF PARTIALLY CONSERVED AXIAL-VECTOR CURRENT IN THE $\pi_{\mu 2}$ AND $K_{\mu 2}$ DECAYS. Kim, Young Suh; Oneda, Sadao (Univ. of Maryland, College Park). [Progr. Theoret. Phys. (Kyoto), 34: Suppl., 238-49(1965)].

The decay amplitudes for $\pi^+ \rightarrow \mu^+ + \nu$ and $K^+ \rightarrow \mu^+ + \nu$ are evaluated when both the pion and kaon masses are reduced to SU(3) degenerate values, using once-subtracted dispersion relations. An attempt is made to see whether the origin of the axial-vector Cabibbo angle in the symmetry-breaking interaction by constructing a dynamical model in which the symmetry-breaking interaction directly affects the mass spectra whereas all other quantities receive the effect only through mass spectra. It is shown that the Cabibbo angle can be stable even if the generalized Goldberger-Treiman relations are violated to a certain extent. (L.B.S.)

13509 BARYON STRUCTURE AND ELECTROMAGNETIC PROPERTIES. Fenster, Stanley; Nambu, Yoichiro (Univ. of Chicago). [Progr. Theoret. Phys. (Kyoto), 34: Suppl., 250-60(1965)].

A search is made for dynamical consequences of the assumption that the baryon is composed of slowly moving heavy objects (quarks). It is found that the hyperfine structure of hydrogen is relatively sensitive to structure, and the effect tends to reduce the present discrepancy between theory and experiment. It is also pointed out that all neutral baryons will have vanishing charge form factors according to the present model. (auth)

13510 ELEMENTARY PARTICLE STRUCTURES AND MESON-NUCLEON BACKWARD SCATTERINGS. Fujimoto, Yoichi (Waseda Univ., Tokyo); Machida, Shigeru; Namiki, Mikio. [Progr. Theoret. Phys. (Kyoto), 34: Suppl., 304-15(1965)].

Within the framework of the composite particle model, some meson-nucleon large angle scatterings at high energies are qualitatively discussed as the rearrangement collision among constituent particles of meson and nucleon. The purpose is to see the dynamical structure of elementary particles whose characters are never clarified only by the fashionable symmetry argument. The two types of models with the same symmetry are investigated: (i) the "atom-type" of models in which all mesons and baryons are, in the same level, composed of a small number of urbaryons, and (ii) the "molecule-type" of models in which only (all or some) baryons are composed of urbaryons but the other particles (mainly mesons) are composed of the baryons. The backward peaks in the angular distribution of meson-nucleon scattering may be understood as the exchange effect, since the scatterings are analogous to the deuteron-proton scattering in the "molecule-type" of models and to the deuteron-triton scattering in the "atom-type" of model. From this point of view, the two sets of predictions are, correspondingly to the above two types of model, obtained about appearance of the exchange backward peak in various meson-nucleon scatterings at high energies. The existing experiments on $\pi^+ p \rightarrow \pi^+ p$ at 4 Bev and 8 Bev seem to prefer the "molecule-type" of models. Finally discussions are given on the energy dependence of the exchange backward peak and on the related hard core problems. (auth)

13511 PROTON-NEUTRON MASS DIFFERENCE. Miyazawa, Hironari; Oi, Yoshiko; Suzuki, Mahiko (Tokyo Univ.). [Progr. Theoret. Phys. (Kyoto), 34: Suppl., 436-48(1965)].

A method of calculating mass splitting is formulated within the framework of the S-matrix theory. It is applied to calculation of the proton-neutron mass difference. In the approximation of taking the nucleon-antinucleon intermediate states, the result is much the same as that of Feynmann-Speisman picture. In the approximation of taking account of mesonic resonant intermediate states, the predicted value is qualitatively in a good agreement with experiment. The same formulation is also applied to mass splitting of the baryon supermultiplets. (auth)

13512 COMPARISON OF EFFECTIVE RANGES OF n-p AND p-p INTERACTIONS. Breit, G.; Friedman, K. A.; Seamon, R. E. (Yale Univ., New Haven). [Progr. Theoret. Phys. (Kyoto), 34: Suppl., 449-91(1965)]. (YALE-1807-28).

The effective ranges $^1r_0$ in $^1S_0$ states of n-p and p-p interactions are compared on the basis of available data. The results of H. Pierre Noyes regarding the $(^1r_0)_{n-p}$ being about 10% or more smaller than $(^1r_0)_{p-p}$ are confirmed provided the comparison is made for the most probable values of these quantities in the sense of a statistical analysis employing the current values of measured quantities with their small statistical uncertainties such as used by Noyes. Sources of systematic errors in the interpretation of experiments from which the experimental values have been derived are discussed. Among them are dynamic effects of molecular electrons for experiments above the epithermal energy region, effects of molecular binding and intermolecular interactions in experiments on the coherent n-p scattering cross section and possible deviations from the effective range approximation, the meaning of which for the $^3S_1 + {}^3D_1$ state is discussed. A numerical analysis shows that combinations of systematic errors of a reasonable magnitude can result in reducing the difference $(^1r_0)_{p-p} - (^1r_0)_{n-p}$ to a much smaller value than 10%. An alternative less elaborate analysis employing a potential for all but the $^1S_0$ states also admits the possibility of the smaller $(^1r_0)_{p-p} - (^1r_0)_{n-p}$ difference. (auth)

13513 PHENOMENOLOGICAL ANALYSIS OF HIGH ENERGY SCATTERING. Ito, D.; Armoudian, G. A.; Mori, K. (Louisiana State Univ., Baton Rouge). [Progr. Theoret. Phys. (Kyoto), 34: Suppl., 626-36(1965)].

Recent results of the partial wave analysis of π-N and N-N scattering in Bev energy ranges are reviewed, and it is pointed out that these results suggest a saturated Gaussian distribution of inelastic collision matrix elements squared $|M_{jl}|^2$. The gross features of the high-energy scattering are characterized by Gaussian distribution. The large-angle scattering is analyzed in terms of a

relativistic optical potential. A possible form of the potential is suggested from analysis of Orear's formula. The simplest assumption on the interaction via the potential reproduces the experimental results fairly well. Conjecture is made on the origin of the potential. (auth)

13514 HIGH ENERGY NUCLEAR INTERACTIONS AND STRUCTURE OF ELEMENTARY PARTICLES. Taketani, Mituo; Fujimoto, Yoichi (Rikkyo Univ., Tokyo). [Progr. Theoret. Phys. (Kyoto), 34: Suppl., 651-60(1965)].

The dimensional argument by Taketani, Nakamura, and Sasaki on the elementarity and the compositeness of particles is extended and applied to the strongly interacting particles. The internal structure of a meson, being composed of a baryon and an antibaryon, is found to play an essential role in extremely high energy interactions in cosmic ray energy region. A possible effect is looked for in accelerator energy region. It is suggested that the internal structure of a meson becomes effective as soon as the Lorentz factor of incoming particle is larger than λ_π/λ_B, λ_π and λ_B being the Compton wave length of a pion and a baryon. Considerations are extended on the structure of a baryon and its effect on the particle interactions. (auth)

13515 LEPTONIC DECAYS OF K^0 MESONS AND THE POSSIBLE CP VIOLATION. Okonov, E.; Wu, Tsung-fan; Chuvilo, I. (Joint Inst. for Nuclear Research, Dubna, USSR). Yadern. Fiz., 2: 1060-4(Dec. 1965). (In Russian).

The absolute probabilities and the time dependence of the leptonic decays of the K^0-meson are studied in general form. Possible experimental examination of the CP-invariance and the $\Delta Q = \Delta S$ rule is discussed. It is shown that the oscillations in the time dependence of the total number of the K^0_{l3}-decays should mean a large CP-violation in this process. (auth)

13516 PHASE-SHIFT ANALYSIS OF NUCLEON-NUCLEON SCATTERING AT 400 Mev. Kazarinov, Yu. M.; Kiselev, V. S.; Simonov, Yu. N. (Joint Inst. for Nuclear Research, Dubna, USSR). Yadern. Fiz., 2: 1095-1102 (Dec. 1965). (In Russian).

The phase-shift analysis of the nucleon-nucleon scattering at the energy close to 400 Mev was made. Five solutions satisfactorily describing the experimental data are found. Only one of these solutions seems to agree with the set of phase shifts obtained by the interpolation of the solutions for 300 and 600 Mev. (auth)

13517 COVARIANT DESCRIPTION OF POLARIZED PHOTONS. Dubovikov, M. S. (Moscow Inst. of Physics and Tech.). Yadern. Fiz., 2: 1115-21(Dec. 1965). (In Russian).

A covariant density matrix for one and two photons is obtained. The physical meaning of the covariant polarization parameters is established. The photon polarization in electron-positron annihilation is calculated in covariant terms. The results are generalized to bosons with arbitrary spin and zero mass. (auth)

13518 AN ANALYSIS OF Y_1^* PRODUCTION BY 1.15 Bev/C K^- BEAM [Thesis]. Fung, Sun-yiu Samuel. Berkeley, Calif., Univ. of California, 1964. 65p.

The 30-inch propane bubble chamber was used at the Bevatron to investigate Y_1^* production by 1.15-Bev/c K^--meson interaction, $K^- + P \rightarrow Y_1^{*\pm} + \pi^\mp$, $Y_1^{*\pm} \rightarrow \Lambda + \pi^\pm$. The analysis was limited mainly to 548 events where the final state consists of a lambda hyperon and two pions of opposite charge, and which satisfy the hypothesis that the interaction took place in hydrogen. Both the negative and the positive Y_1^* resonance states were observed. These decay strongly into a lambda hyperon and a pion. This Y_1^* state has a mass of 1378 ± 3 Mev and a full width at half maximum of 58 ± 6 Mev for the positively charged state Y_1^{*+}, and 70 ± 8 Mev for the negative one Y_1^{*-}. The ratio of production cross sections, $\sigma(K^- + p \rightarrow Y_1^{*-} + \pi^+)$ to $\sigma(K^- + p \rightarrow Y_1^{*+} + \pi^-)$, is 1.53 ± 0.16. The cross section for production of $\Lambda\pi^-\pi^+$ via Y_1^* is 2.33 ± 0.36 mb. The production angular distributions were fitted to a power series in cos θ_{prod}, where θ_{prod} is the angle between the Y_1^* direction and that of the incoming K^- meson in the center of mass of the K^--p system. This distribution for the Y_1^{*+} system required a fourth order polynomial, while that for the Y_1^{*-} required a third order polynomial. Both imply that at least up to d-wave orbital angular momentum states were present. The spin state of the Y_1^* was studied via its various decay angular distributions. The Y_1^* decay angular distribution relative to the production normal, for Y_1^* production angles near 90° ($|\cos\theta_{prod}| < 0.5$), is not isotropic. This implies that the angular momentum of the Y_1^* state must be equal to or greater than $3/2$. The forward-backward asymmetry of the proton in the lambda decay with respect to the production normal was studied in an attempt to establish whether the Y_1^* state is a p-state resonance or a d-state resonance. The results are not conclusive. (Dissertation Abstr.)

13519 TWO PROBLEMS IN NEUTRINO PHYSICS: MU CAPTURE WITH SIX NUCLEON FORM FACTORS AND NEUTRINO PAIR EMISSION FROM STELLAR PLASMA [Thesis]. Adams, John Barclay. Berkeley, Calif., Univ. of California, 1962. 60p.

The matrix element for μ capture ($\mu^- + p \rightarrow n + \nu$) including not only the effects of vector, axial vector, weak magnetism, and induced pseudoscalar but also two "second-class" couplings has a small dependency on these hitherto undetected couplings. Capture in μ-mesic hydrogen from the S states with both F = 1 and F = 0 is computed, and angular distributions of recoil neutrons and capture rates are given as functions of the six coupling constants. It is found that the second-class terms may contribute as much as weak magnetism and induced pseudoscalar terms. Various current models and generalizations on a universal weak Fermi interaction predict a first order weak coupling between electrons and neutrino-antineutrino pairs. The radiation of such pairs by a hot, partially degenerate star is calculated for temperatures and densities that appear to be relevant for stellar evolution. Neutrino pair emission by collective electron modes, especially transverse plasma oscillations is found to be the main mechanism for neutrino radiation by a dense stellar plasma when electron-positron emission is small either because the temperature is too low ($T \lesssim 10^{9}$°K) or degeneracy suppresses it. The neutrino luminosity of a star can greatly exceed its photon luminosity for a central core temperature greater than 10^{8}°K. (Dissertation Abstr.)

13520 THE ELASTIC SCATTERING OF FAST NEUTRONS BY DEUTERONS [Thesis]. Bonner, Billy Edward. Houston, Tex., Rice Univ., 1965. 104p.

The differential cross section for the elastic scattering of neutrons by deuterons was measured at neutron energies of 5.635 and 9.035 Mev. The D(d,n)^{3}He reaction was used as the source of neutrons, and the scattering sample was a deuterated benzene scintillator coupled to a photomultiplier tube. Both the time-of-flight of the scattered neutron and the recoil energy deposited in the scintillator were measured by using fast coincidence techniques and a two-parameter analyzer. The data were normalized to the n-p scattering cross section. The relative efficiency of the detector was determined by detecting the neutrons scattered from a hydrogenated scintillator. (Dissertation Abstr.)

13521 THE MUON ENERGY SPECTRUM FROM THE $K_{\mu 3}$ DECAY MODE OF THE K MESON [Thesis]. Vanderburg, Vance Dilks. Lafayette, Ind., Purdue Univ., 1965. 71p.

An investigation of the $K_{\mu 3}$ muon energy spectrum was made. The study was carried out in the Powell heavy liquid bubble chamber filled with 45% freon and 55% propane by volume. K^- mesons decaying in flight in the momentum range between 430 and 300 Mev/c were studied. 191 events of the $K_{\mu 3}$ decay mode were observed. A clear understanding of the low-energy behavior of the energy spectrum was obtained. The results indicated that the spectrum rises rapidly at low energy and is consistent with an energy dependence of $T^{1/2}$, where T is the muon kinetic energy. The theoretical description of this decay based on vector coupling involves two nearly constant form factors whose ratio must be: $g_v/f_v = -0.6$ or -3.7. These data dramatically favor the solution of -0.6 with a likelihood ratio of 10^8. The

data were found to be consistent with no tensor admixture to the coupling. (Dissertation Abstr.)

13522 PRODUCTION AND DECAY OF THE $\Lambda\pi$ RESONANCES IN THE K^-n COLLISIONS [Thesis]. Taherzadeh, Moj-taba. Los Angeles, Calif., Univ. of California, 1964. 184p.

The 15-inch deuterium bubble chamber of the Lawrence Radiation Laboratory was exposed to three separated K^--meson beams of momenta of 600, 765, and 850 Mev/c. The effects of the final state pion-hyperon interactions in the collisions of the K^- mesons with neutrons were investigated. The ratio of the cross section of the $K^- + n \rightarrow Y_1^{*0} + \pi^0$ reaction to the cross section of the $K^- + p \rightarrow Y_1^{*\pm} + \pi^{\mp}$ reaction was obtained as a function of the center-of-mass energy. It was found at 850-Mev/c K^- meson momentum that the $K^- + p \rightarrow \Lambda^0 + \pi^+ + \pi^-$ reaction proceeds predominantly through the I = 1 isotopic spin state. It was also found that this ratio was approximately equal to 2 at the center-of-mass energy of 1660 Mev. From the analysis of the production angular distribution of the hyperons of the $K^- + n \rightarrow \Lambda^0 + \pi^-$ reactions, some convincing evidence for the existence of the Y_1^* (1660) resonance was obtained. An attempt to obtain the spin and the parity of the resonance suggests that, if partial waves with $J \geq 5/2$ can be neglected, the data are more consistent with a resonant $P_{3/2}$ amplitude than a resonant $d_{3/2}$ amplitude. The direct and indirect production of the Λ^0 hyperon was investigated. As a result of the analysis of the $K^- + n$ reactions was concluded that the I-spin of the η^0 meson is zero. (Dissertation Abstr.)

13523 HIGH ENERGY $\pi^- + p$ ELASTIC SCATTERING FOR SMALL MOMENTUM TRANSFERS AND FORWARD DISPERSION CALCULATION [Thesis]. Saxer, Howard Irving. Ann Arbor, Mich., Univ. of Michigan, 1965. 89p.

The negative pion-proton elastic differential cross section was measured at incident pion momenta of 2.01, 3.15, 4.13, and 4.95 Bev/c for the range of the square of the four momentum transfer of $0.0008 \leq |t| \leq 0.154$ (Bev/c)^2. The data extended into the region where Coulomb scattering contributions were significant. Experimental values for the real part of the forward nuclear scattering amplitude were calculated using a simple interference model for Coulomb nuclear interaction. The best values found are consistent with dispersion theory predictions in that the sign is negative, indicating destructive interference. Forward dispersion relation calculations were carried out for pion kinetic energies of 1 to 29 Bev using recent $\pi^{\pm} + p$ total cross section results. (Dissertation Abstr.)

13524 PION-PROTON INTERACTIONS AT 450 Mev [Thesis]. Poirier, Charles Philip. Bloomington, Ind., Indiana Univ., 1965. 102p.

A study of $\pi^{\pm}$-p interactions at 450 Mev using the 14 inch Brookhaven National Laboratory liquid hydrogen bubble chamber is reported. The reactions studied are $\pi^{\pm} + p \rightarrow \pi^{\pm} + p$, $\pi^{\pm} + p \rightarrow \pi^{\pm} + \pi^0 + p$, and $\pi^{\pm} + p \rightarrow \pi^{\pm} + \pi^+ + n$. The angular distribution of the elastically scattered positive pions was fit with a fourth order polynomial in $\cos\theta_\pi$. Normalizing the data to a total cross section of 29.44 ± 1.63 mb gives an elastic cross section of 28.11 ± 2.88 mb. A phase shift analysis of the angular distribution with all inelastic parameters set equal to 1 yielded a set of T = 3/2 phase shifts. Introduction of inelastic parameters different from 1 did not produce any substantial changes in the original solutions. The (p + 0)/(+ + n) ratio was found to be 3.57 ± 1.54, which agrees with the ratio 4.9 predicted by the (3,3) pion-nucleon isobar model of Olsson and Yodh. The pion kinetic energy spectra from (p + 0) also supports the isobar model. The angular distribution of the elastically scattered negative pions was fit to a fourth order polynomial in $\cos\theta_\pi$. Normalizing the data to a total cross section of 33.03 ± 0.69 mb gives an elastic cross section of 16.74 ± 1.73 mb. The distribution of events on the Dalitz plot for the (p – 0) production reaction is reasonably well accounted for by the Olsson and Yodh isobar model. However, for the (– + n) production reactions, the model does not describe adequately the distribution of events on the Dalitz plot. Analysis of the (– + n) data in terms of π-n pairings shows that the π^+ production process is dominated by the $(N_{3/2}^*)^-$, and in fact the data are consistent with no $(N_{3/2}^*)^+$ production. Thus, while the (3,3) pion-nucleon isobar is apparently the principal mechanism for single pion production at 450 Mev, the data indicate the existence of some T = 0 two-pion interaction that modifies the simple isobar model. (Dissertation Abstr.)

13525 A MEASUREMENT OF THE FORWARD DIFFERENTIAL CROSS SECTION FOR π^--p ELASTIC CHARGE-EXCHANGE SCATTERING AT 1.03 Bev/C USING THE 72" H_2 BUBBLE CHAMBER AS A NEUTRON DETECTOR [Thesis]. Natapoff, Alan. Berkeley, Calif., Univ. of California, 1964. 163p.

A low statistics measurement of $d\sigma^{ce}(0)/d\Omega$ at 1.03 Bev/c in the 72 in. H_2 bubble chamber is described. The π^- beam comes from the Bevatron and the secondary neutrons are detected when subsequent elastic scatters (n + p → n + p) yield visible stopping protons. The real events were separated from the spurious by a Boolean Algebraic method that reduced the set of all events to a sum of a small number of physically significant sets. The residual background fraction was estimated at 10% by a computer simulation technique using the known beam distribution and a pure sample of background events. The bubble chamber, so used, detects about 5% of the secondary neutrons emitted in the charge-exchange reaction. There were 12 experimental events in three intervals lying in the range $0.84 \leq \cos\theta_{\pi^0}^{cm} \leq 0.96$. A zero constraint, least squares fit of the distribution yielded the estimate $d\sigma^{ce}(0)/d\Omega = (3.65 + 1.93)$ mb/ster. This result is consistent with the predictions based on the dispersion relations. (Dissertation Abstr.)

13526 INELASTIC SCATTERING OF 5 Bev/C MUONS IN NUCLEAR EMULSIONS [Thesis]. Kirk, James Alvah. Seattle, Wash., Univ. of Washington, 1965. 92p.

The inelastic scattering of high-energy muons from emulsion nuclei was measured using a monoenergetic beam of muons produced at the Brookhaven Alternating Gradient Synchrotron. Ilford G-5 stacks were exposed perpendicular to the beam and Ilford K-5 stacks were exposed parallel to the beam. Area scanning resulted in a total of 113 events with four momentum transfers greater than 26 Mev/c. The observed scattering distribution, which extends up to 10 degrees or a momentum transfer of about 900 Mev/c, is in good agreement with the predictions of the electromagnetic theory assuming single photon exchange. There were also observed four events with scattering angles greater than 10 degrees, which is not inconsistent with the theory. Pion production was observed with the major contribution coming from the 3/2, 3/2 resonance. Single "Giant Resonance" protons were observed with a cross section agreement with theory. (Dissertation Abstr.)

13527 THE REACTION $\pi^- + p \rightarrow \pi^- + \pi^+ + n$ FROM 350 TO 800 Mev [Thesis]. Kirz, Janos. Berkeley, Calif., Univ. of California, 1963. 81p.

The reaction $\pi^- + p \rightarrow \pi^- + \pi^+ + n$ is studied in the Lawrence Radiation Laboratory 72-inch hydrogen bubble chamber. Events are located by scanning the pictures for π^+ tracks. Cross sections, Dalitz plots, angular distributions, and $\pi^+\pi^-$ and $\pi^{\pm}n$ mass spectra are given at beam energies of 360, 430, 460, 480, 555, 605, 673, and 780 Mev. No clear evidence is found for $\pi^+\pi^-$ resonances between threshold and $M_{\pi\pi} = 680$ Mev. However, there is a strong preference for high $\pi^+\pi^-$ effective masses, especially at the lowest beam energies. Arguments are given to ascribe this anomaly to the I = 0 state of the π-π system. Production of the $N_{1/2}^*$ (1238) isobar is observed in its negative charge state. (Dissertation Abstr.)

13528 MESON PRODUCTION IN PROTON–DEUTERON COLLISIONS: THE ABC ANOMALY [Thesis]. Klein, Mark Phillip. Bloomington, Ind., Indiana Univ., 1965. 60p.

An attempt was made to calculate the differential cross section for the reaction $p + d \rightarrow {}^3He + 2\pi$ at energies and angles corresponding to those used in an experiment by Abashian, Booth, and Crowe that revealed an anomalous peak that could be interpreted as a strong I = 0, J = 0 final state interaction between the two pions. The recent experimental evidence (which does not support this inter-

pretation) and previous theoretical approaches are reviewed. It is suggested that the large relative p-d angular momentum goes into orbital angular momentum between the final nucleus and the dipion system, and that the resulting momentum-dependent matrix element for the process leads to deviations from pure phase in the forward direction near threshold. An expression for the differential cross section in momentum space is presented using an impulse approximation for the scattering amplitude. The incident proton and final state dipion system are described by plane waves, the deuteron by the Hulthén wave function, and ^{3}He by the Irving and Irving-Gunn wave functions. For the nucleon-nucleon interaction, $2N \rightarrow 2N + 2\pi$, a form characteristic of threshold behavior is written as a sum of partial wave amplitudes and evaluated on the mass shell. Lorentz invariant phase space is used. The matrix elements for the first four partial waves are integrated numerically on an IBM 709 by Monte Carlo techniques, and then combined, taking the partial wave coefficients as parameters, to yield a theoretical cross section that fits the experimental data at a laboratory scattering angle of 11.8°. The same coefficients give a fairly good fit to the 15.7° data near the dipion product-ion threshold. Thus no resonance or attractive dipion scattering length is needed to explain the deviation from phase space — the present theory can reproduce (but does not predict) the anomaly. The peaking of the cross section near threshold can be considered as a manifestation of the angular momentum generated in the production process. (Dissertation Abstr.)

Field Theory, Scattering Theory, and Symmetries

See also Elementary Particles and Radiations

Refer also to abstracts 13163, 13169, 13221, and 13648.

13529 (BNL–8767) LORENTZ COVARIANT DEFINITION OF THE U_6 GROUP FOR FREE PARTICLE STATES. Guersey, F. (Middle East Technical Univ., Ankara (Turkey); Radicati, L. A. (Brookhaven National Lab., Upton, N. Y.). Jan. 1965. Contract AT-30-GEN-16. 10p. Dep. mn. CFSTI $1,00 cy, $0,50 mn.

Two sets of covariantly defined operators X_i^R, X_i^L obeying the covariant commutation laws for the angular momentum are derived. It is shown that X_i^L and X_i^R are the generators of little group transformations for the vectors of the representations $[m,0] \otimes D(s,0)$ and $[m,0] \otimes D(0,s)$ discussed by Shaw. The generators of SU(6) are then constructed as non-hermitian operators in the Shaw representation and hermitian operators in the Wigner representation. Because the little group operators are constants of the motion, they can be represented a three dimensional surface integrals of tensor densities with vanishing divergence. These integrals are given explicitly for a Dirac field. (M.O.W.)

13530 (CERN–65-41) GROUP THEORY AND THE CLASSIFICATION OF THE ELEMENTARY PARTICLES. Lectures Given in the Academic Training Programme of CERN in February 1965. Biedenharn, L. C. (European Organization for Nuclear Research, Geneva (Switzerland)). Dec. 15, 1965. 96p. Dep. mn.

The isospin model is outlined and is generalized to the SU(3) symmetry. The application of SU(3) symmetry and SU(6) symmetry to elementary particles is then demonstrated. (D.C.W.)

13531 (IC/65/17) LECTURES ON THE ANALYTIC STRUCTURE OF MANY-PARTICLE SCATTERING AMPLITUDES. PART I. DISCONTINUITY EQUATIONS. Stapp, Henry P. (International Centre for Theoretical Physics, Trieste (Italy)). Feb. 1965. 44p. Dep. mn.

A dispersion formula is discussed for a function regular in a product of cut planes. A conjecture for the general form of the analytic structure of multiparticle scattering amplitudes is discussed. The elementary discontinuity equation is discussed in some detail. An analytic basis of the back-up rule is presented. Also, maximum analyticity and the generalized Mandelstam representation are discussed. (M.O.W.)

13532 (IC/66/2) DISCRETE DEGENERATE REPRESENTATIONS OF NON-COMPACT ROTATION GROUPS. Raczka, R.; Limic, N.; Niederle, J. (International Centre for Theoretical Physics, Trieste (Italy)). Jan. 24, 1966. 38p. Dep. mn.

The discrete most degenerate principal series of irreducible unitary one-valued representations of an arbitrary non-compact rotation group SO(p,q) are derived. The properties of these representations are discussed and the explicit form of the corresponding harmonic functions is given. (auth)

13533 (IC/66/3) A NEW APPROACH TO ALGEBRA OF CURRENT OPERATORS. Narayanaswamy, P.; Pradhan, T.; Santhanam, T. S. (International Centre for Theoretical Physics, Trieste (Italy)). Jan. 25, 1966. 12p. Dep. mn.

The charge independent interaction between the eight known baryons and mesons is expressed in terms of the eight baryon current densities. The non-relativistic limits of the vector, pseudoscalar, and pseudovector currents were discussed. It is found that with eight baryons one can construct 8 currents which form the SU(3) algebra and also 64 currents which form the U(8) algebra. (M.O.W.)

13534 (IC/66/5) A RELATIVISTIC U(6,6) THEORY. Salam, Abdus; Strathdee, J. (International Centre for Theoretical Physics, Trieste (Italy)). Jan. 31, 1966. 23p. Dep. mn.

Infinite-dimensional unitary representations of the non-compact group U(6,6) are employed to classify elementary particles and, following ideas related to those of Fronsdal, are used to construct relativistic S-matrix elements. Like the previously treated relativistic theories where finite-dimensional representations of U(6,6) were used, a particular S-matrix element shows no symmetry higher than that of the appropriate hybrid subgroup. The overall U(6,6) symmetry may give new relations between form factors for different processes but will not, in general, give anything beyond the results of the previous formulations for the scattering processes. The unitarity of the S-matrix is compatible with the subgroup hierarchy, provided that an infinity of multiplets for elementary particles exists and provided that all such multiplets possess the same mass. The crucial point of the formulation is that if mass differences are introduced, these affect not the relativistic invariance but the unitarity of the S-matrix. (auth)

13535 (IC/66/6) MAXIMAL DEGENERATE SYSTEMS DYNAMICS. Bisiacchi, G.; Budini, P. (International Centre for Theoretical Physics, Trieste (Italy)). Feb. 1966. 11p. Dep. mn.

It is shown that for a "maximal degenerate" system for which the energy multiplet built up a most degenerate representation of the symmetry group, the dynamical problem can be solved with purely group theoretic methods once the spectrum-generating algebra is known. The Casimir operator of this algebra can be reduced in terms of a Cartan operator of the symmetry algebra and of its Casimir operator; this fixes the energy spectrum, the dynamical equations, and Green functions for the system. The method is applied to the N-dimensional harmonic oscillator for which Sp(N,R) is the spectrum-generating algebra. (auth)

13536 (IC/66/7) DIFFERENCE BETWEEN SOURCES AND CHARGES. Krolikowski, W. (International Centre for Theoretical Physics, Trieste (Italy)). Feb. 4, 1966. 9p. Dep. mn.

It is argued that in the case of broken symmetries the concepts of sources and charges are entirely different and cannot refer to the same physical objects, in contradistinction to the familiar case of electrodynamics. The argument contradicts the conjecture of "spontaneous breakdown" of SU(3). A hypothesis of a "partial conservation of tensor current" is suggested. (auth)

13537 (IC/66/8) REMARKS ABOUT THE FUBINI-FURLAN METHOD. Krolikowski, W. (International Centre for Theoretical Physics, Trieste (Italy)). Feb. 4, 1966. 9p. Dep. mn.

Some observations on the Fubini-Furlan approach to the algebra of currents and symmetry breaking are presented. Basic formulas of the Fubini-Furlan method are derived once more without meeting discomfort caused by group generators in remote past and future. A generalization of the condition for "partial conservation of axial vector currents" is gained, which still gives a link between group commutators and transition matrix elements and enables one to derive relations of the Adler-Weisberger type from the algebra of currents. (auth)

13538 (IDO–17142) A NOTE ON INVERTING THE R-MATRIX. Watanabe, T. (Phillips Petroleum Co., Idaho Falls, Idaho. Atomic Energy Div.). Jan. 1966. Contract AT(10-1)-205. 24p. Dep. mn. CFSTI $2.00 cy, $0.50 mn.

The procedure of rank annihilation is applied to the inversion of the R-matrix. It is shown that the method inverts the R-matrix in a way similar to the method of Thomas but that it leads to a different form. The advantage of this particular method and some approximations are discussed. (auth)

13539 (JINR-E–2500) CONDITIONS OF MACROSCOPIC CAUSALITY FOR THE SCATTERING MATRIX. Blokhintsev, D. I.; Kolerov, G. I. (Joint Inst. for Nuclear Research, Dubna (USSR). Lab. of Theoretical Physics). 1965. 14p. Dep. mn.

The macroscopic causality condition is formulated for the scattering matrix. An example of unitary but nonlocal scattering matrix which satisfies macroscopic causality requirements is given. (auth)

13540 (JINR-E–2545) SU(6) AND THE OPERATORS CPT AND C. Ul'mann, A. (Joint Inst. for Nuclear Research, Dubna (USSR). Lab. of Theoretical Physics). 1966. 10p. Dep. mn.

The operators CPT and C are constructed in the SU(6) scheme, supposing that their general structure is already fixed within the domain of validity of SU(6). There is no ambiguity for the electromagnetic charge conjugation. The strong charge conjugation involves, however, a real parameter, that affects states with $B - Y \neq 0$. (auth)

13541 (JINR-P–2419) RADIATSIONNYI RASPAD 1^+-MEZONOV I UNITARNAYA SIMMETRIYA. (Radiative Decay of 1^+ Mesons and Unitary Symmetry). Dao Wong Duc (Joint Inst. for Nuclear Research, Dubna (USSR). Lab. of Theoretical Physics). 1965. 6p. Dep. mn.

A general expression is given for the radiative decay of 1^+ mesons. Relations between widths in the unitary symmetry scheme are presented. (auth)

13542 (JINR-P–2443) OB OB'EDINENII PROSTRANSTVENNOI I VNUTRENNEI SIMMETRII ELEMENTARNYKH CHASTITS. (Problem of Combination of the Space and Internal Symmetries of Elementary Particles). Stoyanov, D. (Joint Inst. for Nuclear Research, Dubna (USSR). Lab. of Theoretical Physics). 1965. 12p. Dep. mn.

The construction of the G group suggested by Michel is considered. This group combines space P and internal S symmetries, S being a normal denominator of G and P = G/S. It is shown that such a construction is obtained in the investigation of the automorphisms of the S group which results in an additional possibility for its equivalent representations (conventionally determined) to be classified according to the factor-group G/S. A general consideration of this problem leads to the fact that any combination S (if it is simple and compact) with the Poincaré group is isomorphic to the direct product of these groups. Finally, the structure of the G group irreducible representation is considered. (auth)

13543 (JINR-P-2474) "OBSHCHII PROPAGATOR" DLYA MEZONOV SO SPINAMI 2,1,0 V TEORII SIMMETRII. ("A General Propagator" for the Mesons With Spin 2,1,0 in Symmetry Theory). Chi, Cao (Joint Inst. for Nuclear Research, Dubna (USSR). Lab. of Theoretical Physics). 1965. 6p. Dep. mn.

The propagators for particles with spins 2,1,0 are obtained with the help of symmetry theory. It is shown that these propagators can be united in a "general propagator" in the case when the considered particles belong to the same representation. It is a new situation that occurs only in symmetry theory. In order to obtain a true propagator for the particle with a definite spin from the "general propagator" the projection operators are introduced. (auth)

13544 (JINR-P–2509) ELEKTROMAGNITNYE SVOISTVA BARIONOV I MEZONOV V NERELYATIVISTSKOI MODELI KVARKOV. (Electromagnetic Properties of Baryons and Mesons in Nonrelativistic Quark Model). Gerasimov, S. B. (Joint Inst. for Nuclear Research, Dubna (USSR). Lab. of Theoretical Physics). 1965. 10p. Dep. mn.

Assuming that the medium-strong interaction-breaking SU(3) symmetry leads to a change in mass and magnetic moment of the "strange" quark, the electromagnetic properties (magnetic moments, electromagnetic mass splitting, radiative decays, electromagnetic radii) of mesons and baryons are treated within the framework of nonrelativistic quark model. (auth)

13545 (JINR-P-2513) ZAMECHANIE O SIMMETRII $SU(6)_w$. (A Remark on $SU(6)_w$ Symmetry). Bokov, O. G. (Joint Inst. for Nuclear Research, Dubna (USSR). Lab. of Theoretical Physics). 1965. 8p. Dep.mn.

$SU(6)_w$ symmetry scheme is discussed. It is shown that the method suggested in Lipkin's and Meshkov's paper (Phys. Rev. Lett., 14: 670(1965)) is non-covariant. The meson-baryon vertex is considered. (auth)

13546 (JINR-P–2519) ASIMPTOTICHESKOE POVEDENIE AMPLITUDY RASSEYANIYA PRI BOL'SHIKH PEREDAVAEMYKH IMPUL'SAKH. (Asymptotic Behaviour of Scattering Amplitude at Large Momentum Transfers). Logunov, A. A.; Mestvirishvili, M. A.; Silin, I. N. (Joint Inst. for Nuclear Research, Dubna (USSR). Lab. of Theoretical Physics). 1965. 29p. Dep. mn.

A phase representation is proposed for form factors and scattering amplitudes in momentum transfer. The representation obtained is applied to approximate the experimental data on electric and magnetic form factors and p-p scattering at high energies. (auth)

13547 (JINR-P–2523) O SIMMETRIYAKH LEPTON-LEPTONNYKH VZAIMODEISTVII. (On Symmetries of Lepton-Lepton Interactions). Achasov, N. N.; Muradyan, R. M. (Joint Inst. for Nuclear Research, Dubna (USSR). Lab. of Theoretical Physics). 1965. 6p. Dep. mn.

Possible symmetries in a system of leptons were studied. The requirement that the lepton-lepton interaction lagrangian is independent of the electric charge is shown to be equivalent to the requirement of muon charge independence only for V–A theory. (auth)

13548 (SLAC–58) INFINITE LADDERS AND THE ALGEBRA OF INTEGRATED CURRENT COMPONENTS. Harari, H. (Stanford Linear Accelerator Center, Stanford Univ., Calif.). Jan. 1966. Contract AT(04-3)-515. 14p. Dep. mn. CFSTI $1.00 cy, $0.50 mn.

Possible relations between various proposed current algebras and some non-compact groups which may generate infinite ladders of particle states are discussed. In particular, the possibility of identifying the compact algebra of currents with the compact version of the non-compact spectrum-generating algebra is studied. Some examples based on the SU(3), SU(4), and SU(6) current algebras are considered, and it is shown that the particles within the first few "levels" of the obtained infinite ladders approximately fall into finite representations of the relevant current algebras. (M.O.W.)

13549 (UCRL–16530) NEW OUTLOOKS IN STRONG INTERACTION PHYSICS. Slansky, Richard C. (Lawrence Radiation Lab., Univ. of California, Berkeley). Oct. 18,

1965. Contract W-7405-eng-48. 48p. Dep. mn. CFSTI $2.00 cy, $0.50 mn.

A typical experiment is described with quantities such as cross sections and branching ratios. The S-matrix is then defined according to quantum mechanics. Relativistic kinematics is also given. From the kinematics and the description of the scattering processes, it is shown how short-lived particles (10^{-24} sec) can be detected. The dynamics of strongly interaction particle processes is treated, and results of quantum mechanics and field theory are used to motivate S-matrix theory. The principle of maximal analyticity is explained. This together with the concept of crossing makes the basis of the bootstrap theory plausible. Equations for the amplitude are derived using analyticity and unitarity. (J.F.P.)

13550 (LA-tr-66-7) ON THE THEORY OF NONLOCALIZED PARTICLES. Vlasov, A. A. Translated by Helen J. Dahlby and John Warren (Los Alamos Scientific Lab., N. Mex.), from Zh. Eksp. Teor. Fiz., 20: 23-6(1950). 9p. Dep. mn. CFSTI $1.00 cy, $0.50 mn. JCL $1.10 fs, $0.80 mf.

A discussion of Vlasov's theory of nonlocalized particles is presented in which objections (particularly those of Tiablikov) to the theory are considered. (D.C.W.)

13551 (LA-tr-66-8) SOME OBSERVATIONS ON THE MANY-BODY PROBLEM IN THE A. A. VLASOV ARRANGEMENT. Tiablikov, S. V. Translated by Helen J. Dahlby and John Warren (Los Alamos Scientific Lab., N. Mex.), from Zh. Eksp. Teor. Fiz., 20: 16-22 (1950). 12p. Dep. mn. CFSTI $1.00 cy, $0.50 mn. JCL $1.60 fs, $0.80 mf.

The applicability of Vlasov's self-consistent field method to systems of interacting particles other than plasma is discussed. (D.C.W.)

13552 ON THE SELF-CONSISTENT METHOD. Umezawa, H. (Istituto di Fisica Teorica, Naples). Acta Phys. Acad. Sci. Hung., 19: 9-28(1965).

A brief account is given of a formulation of the self-consistent method, which was previously proposed by Dell-Antonio and Umezawa. The following subjects are covered: a formulation of the self-consistent method, the V-limit, the asymptotic condition in field theory, broken symmetry and local conservation laws and the Goldstone theorem. (auth)

13553 ON THE UNITARILY INEQUIVALENT REPRESENTATIONS IN THE QUANTUM FIELD THEORY AND THE MANY BODY PROBLEM. Lopuszanski, J. T. (Univ., Wroclaw, Poland). Acta Phys. Acad. Sci. Hung., 19: 29-44 (1965).

The quantum systems of infinitely many degrees of freedom are treated, with special attention given to the unitarily inequivalent representations of the commutation relations that appear only for systems of infinitely many degrees of freedom. The main idea of the theory of inequivalent representations is explained by a simple example of a scalar real field discussed by Haag. Irreducible and reducible representations in the Bogoliubov-BCS model are treated. (L.B.S.)

13554 STRANGE PARTICLES AND THE UNSYMMETRICAL VACUUM. Duerr, H. P. (Max Planck Institut fuer Physik und Astrophysik, Munich). Acta Phys. Acad. Sci. Hung., 19: 47-55(1965).

In Heisenberg's nonlinear theory some new results are presented concerning mainly the properties of strange elementary particles. (auth)

13555 VACUUM DEGENERACY AND BROKEN SYMMETRIES IN NONLINEAR SPINOR THEORIES. Ladanyi, K. (Hungarian Academy of Sciences, Budapest). Acta Phys. Acad. Sci. Hung., 19: 57-65(1965).

The possibility of a spontaneous breakdown of some invariances is discussed by considering three different nonlinear spinor equations. The breakdown of the γ^5-symmetry is considered by using the parity-symmetrized Heisenberg equation. A possible mechanism is suggested for the spontaneous electromagnetic type breakdown of the G-invariance by introducing a simple G-invariant (but not isoinvariant) nonlinear field equation. The third field equation is invariant under the group Sp_6 of unitary symplectic transformations in six dimensions. It is assumed that the medium strong mass splitting operator is due to a spontaneous mixing of the SU_3 singlet (representation 21), the isosinglet member of the SU_3 octet (representation 21), and the Sp_6 singlet (representation 1). (auth)

13556 BROKEN SYMMETRIES IN THE TWO GOLDSTONE MODELS. Kuti, G.; Marx, G. (Roland Eoetvoes Univ., Budapest). Acta Phys. Acad. Sci. Hung., 19: 67-83(1965).

The energy spectra of the two Goldstone models are investigated using the Ritz variational method. More quantum mechanical ground states are obtained, but they do not belong to the same Hilbert space. The eigenvalue problem can be solved using only one Hilbert space, but in this case the ground state does not show all the symmetries possessed by the hamiltonian. (auth)

13557 RELATIVISTIC CALCULATIONS OF THE GREEN'S FUNCTIONS BY MEANS OF THE CONTINUOUS INTEGRATION IN THE CASE OF STRONG COUPLING (APPLICATION TO THE GOLDSTONE-MODEL). Heber, G. (Karl-Marx Univ., Leipzig). Acta Phys. Acad. Sci. Hung., 19: 85-90(1965).

A strong coupling theory is studied for self-coupled meson field with vanishing bare mass by making use of continuous integration. Particularly, the one-particle propagator is discussed. Some remarks are made on the Goldstone model. (auth)

13558 APPROXIMATE SYMMETRIES IN FIELD THEORY. Nagy, K. L.; Nagy, T.; Pocsik, G. (Roland Eoetvoes Univ., Budapest). Acta Phys. Acad. Sci. Hung., 19: 92-7(1965).

Some ideas concerning the broken and approximate symmetries are discussed based on the simplest relativistic field theories satisfying the asymptotic condition. (auth)

13559 ON THE PERTURBATION-THEORETIC CALCULATION OF THE ONE-PARTICLE EXCITATION SPECTRUM IN A LARGE BOSE SYSTEM. Szepfalusy, P. (Roland Eoetvoes Univ., Budapest). Acta Phys. Acad. Sci. Hung., 19: 109-120(1965).

Perturbation theoretic calculation of the one-particle Green's functions is studied for a large system of bosons at zero temperature. First a splitting of the hamiltonian is considered in which the unperturbed part is chosen to be diagonal in the Bogoliubov quasi particle operators. The self-consistent form of the perturbation expansion required by the appearance of inequivalent representations of canonical commutation relations is formulated and discussed. (auth)

13560 RELATIVISTIC FIELD THEORIES WITH SYMMETRY BREAKING SOLUTIONS. Jona-Lasinio, G. (CERN, Geneva). Acta Phys. Acad. Sci. Hung., 19: 139-46(1965).

Following some recent developments in many-body theory, a functional approach to relativistic field theories is suggested particularly suitable to treat the case of symmetry breaking solutions. The method is characterized by the introduction fo a functional of the vacuum expectation value of the field variables which has the property of being stationary around the values produced by the solutions of the theory. To illustrate the formalism the Goldstone theorem is discussed, whose formal derivation becomes very simple in this language. Finally, a stability or degeneracy property of the solutions of a field theory is discussed, which is expressed by the persistence of the stationary conditions if certain infinitesimal variations of the vacuum expectation values of the field are performed. For symmetry breaking solutions, the admissible variations correspond to the superposition of zero mass classical waves of infinitesimal amplitude. (auth)

13561 SUM RULES IN THE QUANTUM FIELD THEORY AND IN THE MANY-BODY PROBLEM. Zawadowski, A. (Central Research Inst. for Physics, Budapest); Pocsik, G. Acta Phys. Acad. Sci. Hung., 19: 148-52(1965).

In case of interacting fermion systems integral restrictions are derived for the spectral functions of the simplest Green's functions. Some applications are shown. (auth)

13562 A GAUGE-INVARIANT METHOD IN THE THEORY OF INTERACTING BOSE SYSTEMS. Hargitai, Cs. (Central Research Inst. for Physics, Budapest). Acta Phys. Acad. Sci. Hung., 19: 153-8(1965).

The pole-approximation method based on the exact sum rules is given for interacting Bose systems. The relations derived here are the same as the ones known from the Valatin–Butler treatment. (auth)

13563 FUNCTIONAL METHODS AND EXACT SOLUTIONS IN FIELD THEORY. Thirring, W. E. (Univ., Vienna). Acta Phys. Acad. Sci. Hung., 19: 171-3(1965).

A theory of charged scalar field with fixed source in a nonperturbative functional approach is studied. In this model for the generator of the boson Green's function a closed expression exists. (auth)

13564 ON ELECTRODYNAMICS OF PARTICLES WITH ZERO SPIN. Fradkin, E. S. (Lebedev Inst. of Physics, Moscow). Acta Phys. Acad. Sci. Hung., 19: 175-98(1965). (In Russian).

The interaction of a vector neutral field with and without mass with a Bose field of zero spin is studied by a functional method. A closed expression for the S-matrix is found, using the operator solution for the producing functional and the operator solution for the Green function in an arbitrary external vector field. A highly detailed modified perturbation theory is developed for finding the asymptotic behavior of the Green function and the cross sections. The asymptotic forms for single-particle, two-particle, and vertex Green functions are investigated. (M.J.T.)

13565 ON SOME RECENT ACHIEVEMENTS IN THE AXIOMATIC APPROACH TO QUANTUM FIELD THEORY. Todorov, I. T. (Joint Inst. for Nuclear Research, Dubna, USSR. Inst. of Physics, Sofia). Acta Phys. Acad. Sci. Hung., 19: 199-211(1965).

Some recent achievements in the general trend of axiomatics are treated. Emphasis is given to asymptotic relations for scattering amplitudes. (auth)

13566 THEORY OF FERMI INTERACTIONS. Domokos, G. (Joint Inst. for Nuclear Research, Dubna, USSR), Suranyi, P.; Vancura, A. Acta Phys. Acad. Sci. Hung., 19: 213-18(1965).

A field theoretical model of Fermi interactions is developed. Explicit expressions are given for lepton scattering amplitudes at high energies. The problem of locality and consistency of a non-renormalizable interaction is discussed. (auth)

13567 REMARKS ON THE CONVERGENCE OF THE PERATIZATION. Montvay, I. (Roland Eoetvoes Univ., Budapest). Acta Phys. Acad. Sci. Hung., 19: 219-21 (1965).

The Feinberg–Pais equation for zero incoming momenta is investigated. In this case it is possible to show the mathematical accuracy and convergence of the peratization method. (auth)

13568 THE RENORMALIZABLE VECTOR BOSON THEORY OF WEAK INTERACTION. Frenkel, A.; Hrasko, P. (Central Research Inst. of Physics, Budapest). Acta Phys. Acad. Sci. Hung., 19: 257-8(1965).

Experimental consequences and some theoretical aspects of the use of the vector boson propagator $[-i/(2\pi)^4]|g_{\mu\nu} - (k_\mu k_\nu/k^2)|(1/k^2 - M_p^2)$ are investigated. (auth)

13569 ON THE CONNECTION BETWEEN VACUUM-LIKE AND LIGHT-LIKE SOLUTIONS OF THE BETHE-SALPETER EQUATION. Bassetto, A.; Ciccariello, S.; Tonin, M. (Univ., Padua). Acta Phys. Acad. Sci. Hung., 19: 269-72(1965).

It is investigated, whether vacuum-like solution of the Bethe–Salpeter equation does imply also light-like solutions. The result is affirmative if there is no degeneracy, in case of degeneracy such conclusion cannot be drawn from the calculations. (auth)

13570 FINITE AND DISCONNECTED SUBGROUPS AND ELEMENTARY PARTICLE SYMMETRIES. Fulton, T. (Johns Hopkins Univ., Baltimore). Acta Phys. Acad. Sci. Hung., 19: 273-80(1965).

The subgroups of the SU_3 group are investigated in connection with elementary particle physics. It is found that the finite and disconnected subgroups of SU_3 cannot account for the elementary particle spectrum. (auth)

13571 A MODIFICATION OF THE NEW SUM RULE. Wit, Romuald (Jagellonian Univ., Krakow). Acta Phys. Pol., 28: 551-3(Oct. 1965).

A convenient form of the sum rule proposed by Khuri and Kinoshita is derived. The symmetrized forward pion-nucleon scattering amplitude $T(E^2)$ is assumed to be bounded for $E \to \infty$, where E is the total energy of the incident pion in the lab system. The function $g(E^2) = \int_1^{E^2} [T(x) - T(o)]\, dx/x\sqrt{x-1}$ is studied in order to derive the relation $\int_0^E dE' \, [\mathrm{Re}T(E') - T(O)]/E^2 > O$. (M.J.T.)

13572 A CONJECTURE OF THE HIGH ENERGY BEHAVIOR OF TWO-PARTICLE SCATTERING AMPLITUDES. Zalewski, Kacper (Inst. of Physical Chemistry, Krakow). Acta Phys. Pol., 28: 563-5(Oct. 1965).

The reaction $A + B \to C + D$ in the s channel and its crossed reactions $A + \overline{D} \to C + \overline{B}$ and $A + \overline{C} \to \overline{B} + D$ in the u and t channels are considered. The three reactions can be described by one amplitude T(s, t, u). Two amplitudes with positive and negative signature are defined. By assuming that in the high energy region the amplitude with either positive or negative signature dominates, it is shown that, for fixed t, $\lim_{s\to\infty} [\,|T(s, t, A-t-s)|/|T(A-t-s, t, s)|] = 1$, and that, for fixed u, $\lim_{s\to\infty} [|T(s, A-s-u, u)|/|T(A-u-s, s, u)|] = 1$, where $A = s + t + u$ is the sum of the squares of the masses of A, B, C, D. (M.J.T.)

13573 QUANTUM STATISTICS IN THE STATISTICAL MODEL OF MULTIPLE PRODUCTION OF PARTICLES. Zalewski, Kacper (Inst. of Physical Chemistry, Krakow). Acta Phys. Pol., 28: 575-84(Nov. 1965).

It is shown that the normalization volume (V_2) which is arbitrary when using the standard versions of the statistical model can be determined from experiment, when quantum statistics are applied to the particles. $V_2 \to \infty$ corresponds to the classical slimit of quantum statistics. Then in the thermodynamic limit Boltzmann's formula should be used. The use of Planck's formula is unjustified. If V_2 is finite and such that Planck's formula applies for average multiplicities, Einstein's condensation should be observed for high multiplicities. The absence of a significant surplus of very low energy pions in high multiplicity events yield a lower bound for V_2. The isospin factor can be separated from the phase space factor only in the classical limit. (auth)

13574 HIGH ENERGY ASYMPTOTIC EXPANSION FOR A SUM OF PHASE SPACE INTEGRALS. Zalewski, Kacper (Inst. of Physical Chemistry, Krakow). Acta Phys. Pol., 28: 639-45(Nov. 1965).

A rigorous, asymptotic, high energy expansion is found for $\Sigma = \sum_{n=2}^{\infty} P(n,E)$, where P(n,E) is the phase space integral for n indistinguishable pions at a center-of-mass energy E. There are two expansion parameters: $x = (24\pi\Omega E^3)^{-1/4}$ and $y = (24\pi\Omega m^4/E)^{1/4}$, where Ω is the interaction volume divided by $(2\pi)^3$ and m is the pion rest mass. The zero order term of the expansion yields the thermodynamic approximation: a Boltzmann formula. The first order approximation reproduces for $y = 0$ the result of Auberson and Escoubès (1965). Three higher order terms are evaluated and, for $\Omega = 4/3\,\pi\,(2\pi m)^{-3}$ and E = 5 Bev, it is found that they reduce the sum by about 20 per cent. Effects of isospin are also discussed. (auth)

13575 THE RAINICH GEOMETRIZATION OF FERMION FIELDS. Kuchar, Karel (Charles Univ., Prague). Acta Phys. Pol., 28: 695-715(Nov. 1965).

The Rainich problem is formulated within Sciama's and Kibble's version of the generally relativistic theory of gravitation and solved for the Dirac bispinor and the Weyl spinor fields. The Rainich equations are given a form of algebraic and differential equations for the canonical energy-momentum tensor and the spin density tensor, which are already geometrized by Kibble's gravitational laws. It is the direct geometrical interpretation of the spin density tensor in terms of torsion, which enables the complete Rainich geometrization of fundamental fermion fields. (auth)

13576 THE COMPLEMENTARY MOMENT OF THE ELECTROMAGNETIC MOMENTUM RADIATED FROM A POINT SOURCE. Zin, Giovanni. Atti Acad. Sci. Torino: I, Cl. Sci. Fis., Mat. Natur., 99: 1149-55(1964-65). (In Italian).

The concept of the complementary moment of the electromagnetic momentum is introduced on the basis of a theorem for vector potential. The complementary moment of the electromagnetic momentum radiated from a point source is then evaluated. (tr-auth)

13577 ON THE CLASSIFICATION OF HIGHER SYMMETRY GROUPS. Mozrzymas, J. (Univ., Wroclaw, Poland). Bull. Acad. Pol. Sci., Ser. Sci. Math. Astron. Phys., 13: 481-5(1965).

The classification is derived for all groups G for which (1) the groups P and S are subgroups of G, (2) the group G is a transitive and primitive group in an (n + 1)-dimensional real Klein space, denoted by T_{n+1} with coordinates x_0, $x_1, \ldots, x_n$, and (3) Minkowski space R_4^1 is a subspace of T_{n+1} and the coordinates x_0, x_1, x_2, x_3 of R_4^1 are the space-time coordinates. Three classes of groups are listed—that consisting of groups with a solvable invariant subgroup, that containing semisimple groups which are a direct product of two locally isomorphic simple groups, and that consisting of the simple groups. The latter is characterized by two theorems on primitive groups in the space T_n. Conclusions related to determining the group G which combines the groups P and S are stated. (M.J.T.)

13578 THE STRUCTURE OF THE DENSITY MATRIX FOR PARTICLES OF HIGHER SPIN VALUES. Konar, W. (Univ., Warsaw). Bull. Acad. Pol. Sci., Ser. Sci. Math. Astron. Phys., 13: 495-8(1965).

The density matrix, ρ, for a beam of particles of spin S is written in terms of (2S + 1)-dimensional matrices Q_N^J: $\rho = [1/(2S+1)] \sum_{J=0}^{2S} \sum_{N=-J}^{J} q_N^J Q_N^J$. The physical meaning of the Q_N^J operators for $J > 1$ is considered. An expression for the Q_N^J by combinations of products of spin operators is derived. (M.J.T.)

13579 ORBITAL-LIKE REPRESENTATION OF SU(6). Krolikowski, W. (Inst. of Nuclear Research, Warsaw. Univ., Warsaw). Bull. Acad. Pol. Sci., Ser. Sci. Math. Astron. Phys., 13: 505-8(1965).

The problem of extending the $SU(6)_S$ group in such a way as to include the orbital angular momentum is discussed. An infinite-dimensional reducible representation of SU(6) is investigated and used to define 35 orbital-like generators of SU(6). These operators are added to 35 spin-like generators of SU(6) to obtain some total angular momentum-like generators. Thus $SU(6)_S$ is extended to a group called $SU(6)_J$, which includes the total angular momentum among its 35 generators. (M.J.T.)

13580 THE $SU_2 \otimes SU_3$ CONTENT OF THE SU_6 REPRESENTATIONS. Grynberg, M.; Pindor, M. (Inst. of Nuclear Research, Warsaw. Univ., Warsaw). Bull. Acad. Pol. Sci., Ser. Sci. Math. Astron. Phys., 13: 509-13 (1965).

A problem arising in the application of the SU(6) group to elementary-particle physics, viz., the reduction of an irreducible representation (IR) of SU(6) regarded as a representation of the group $SU(2) \otimes SU(3)$, is elaborated, using a method based on the link between the linear and the permutation groups. It is found that the IR $\{\lambda', \lambda''\}$ of $SU(2) \otimes SU(3)$ is contained in the IR $\{\lambda\}$ of the SU(6) group as many times as the representation $[\lambda]$ of the group S_k is contained in the product of the $[\lambda']$ and $[\lambda'']$ representations of the S_k group, where k is a number of tensor indices. The graphical method of Hamermesh was used to evaluate the reduction of SU(6) IR's corresponding to tensors of rank 3, 6, and 9, assuming that only tensors of 3m (m integral) have physical meaning. These results are presented, along with three physically interesting representations corresponding to tensors of rank 12. (M.J.T.)

13581 INCONSISTENCY OF THE LOCAL FIELD THEORY OF MASSIVE SPIN-TWO PARTICLES. Adler, David (Atomic Energy Research Establishment, Harwell, Eng.). Can. J. Phys., 44: 289-92(Feb. 1966).

It is shown that the field theory of spin-2 particles, generated by the Lagrange function which reduces to that of linearized gravitational field theory in the limit of zero mass, is inconsistent. (auth)

13582 DISPERSION FOR RELATIVISTIC NONLINEAR EQUATIONS WITH PARTIAL DERIVATIVES. Segal, Irving (Massachusetts Inst. of Tech., Cambridge). Compt. Rend., 261: 5323-6(Dec. 20, 1965). (In French).

A method to establish the existence of the wave operator and the dispersion operator is indicated. As an application it is shown that under certain conditions there exists a unique solution of the nonlinear equation $\Box\varphi = m^2\varphi + F(\varphi)$ which is (a) strongly asymptotic for time $T \to -\infty$ at a given arbitrary solution of the equation $\Box\Psi = m^2\Psi$ whose Fourier transform has compact support and (b) weakly asymptotic for $t \to +\infty$ at another solution of the same equation with finite energy. (tr-auth)

13583 MASS FORMULAS IN THE SUPERMULTIPLET MODEL. Malyuta, Yu. M. (Inst. of Physics, Academy of Sciences, Ukrainian SSR). Dokl. Akad. Nauk SSSR, 163: 335-7(July 11, 1965). (In Russian).

The recently proposed model of strongly interacting particles based on the SU(6) group (F. Gürsey and L. Radicati, Phys. Rev. Lett., 13: 173(1964), A. Pais, ibid. 175) systematizes hadrons according to the F-spin-spin supermultiplets. This model was formulated in the quark language which presents the advantage that diagrams may be used for obtaining the mass formulas. From the quarks, the largest supermultiplets were derived and the energy eigendiagrams were drawn for mesons, baryons, and isobars, taking the perturbation of the SU(6) symmetry into account. The formulas obtained differ from previously reported data. (TTT)

13584 SIMPLE HIGH-ENERGY SCATTERING MODEL. Anisovich, V. V. JETP Lett. (USSR)(Engl. Transl.), 2: 272-4(Nov. 1, 1965).

Translated from Zh. Eksp. Teor. Fiz., Pis'ma Redakt., 2: 439-42(Nov. 1, 1965).

A model is proposed in which elastic forward scattering takes place only by single quark-antiquark or three-quark scattering and for which the only essential quark interactions are those leading to bound states (mesons and baryons). It is assumed that SU(6) symmetry holds. (G.O.Y.)

13585 DISPERSION RELATIONS AND RESONANCE REACTIONS IN MULTI-CHANNEL SCATTERING. Van Winter, Clasine (Univ., Groningen, Netherlands). Nucl. Phys., 77: 99-128(1966).

A parameter expansion is presented for a multi-channel scattering matrix S(z) the elements of which are analytic functions of the energy z. Under the assumption that each matrix element satisfies a dispersion relation, it is shown that S(z) can be written as a Blaschke product times a matrix V(z) the determinant of which does not vanish. The Blaschke product contains the zeros of det S(z), a typical factor being characterized by a zero $E_n + \frac{1}{2}i\Gamma_n$ and a constant unitary matrix u_n. An isolated zero closes to the real axis and gives rise to a resonance with energy E_n and width Γ_n. Given Γ_n, the partial widths are determined by u_n. The analytic properties of a matrix with non-vanishing determinant are discussed in some detail. In particular, it is pointed out that V(z) can be represented by a multiplicative integral. With the help of this representation it is

shown that, in the interval in which S(z) is unitary, V(z) is a slowly varying function of z. From this it follows that V(z) refers to a background scattering. (auth)

13586 SCATTERING BY NON-LOCAL POTENTIALS. Razavy, M. (Univ. of Alberta, Edmonton, Can.). Nucl. Phys., 78: 256-64(1966).

The kernels of a class of non-local potentials are related to the Green functions of the second order differential equations. For these potentials, the integro-differential wave equation may be transformed into a set of coupled ordinary differential equations, which can be solved by a factorization method. A solvable example of the non-separable kernel is given and the variation of the exact wave function with the non-locality of the interaction is studied. The effective mass approximation of Frahn and Lemmer for the optical potential is derived and the connection between the wave function in this approximation and the wave function for the equivalent local potential is discussed. (auth)

13587 STATISTICAL THERMODYNAMICS OF STRONG INTERACTIONS AT HIGH ENERGIES. Hagedorn, R. (CERN, Geneva). Nuovo Cimento, (1), 3: Suppl., 147-86 (1965).

A thermodynamic theory of strong interactions is developed. A high-energy collision is considered as follows: in the first instant a certain volume of thermodynamic equilibrium is established that can be described by statistical thermodynamics of an unlimited and undetermined number of more or less excited hadrons, which then leave the region of interaction and decay strongly through a number of steps in stable form K, π, N, Y, etc. The basic statistical formula is derived, and the self-consistency condition imposed on the system is discussed. The physical interpretation is given, and results are summarized, including some speculations and open problems. (L.B.S.)

13588 THRESHOLD POLES AND LOW-ENERGY SCATTERING. Abbe, W. J.; Kaus, P.; Nath, P.; Srivastava, Y. N. (Univ. of California, Riverside). Nuovo Cimento, (10), 41A: 305-12(Feb. 1, 1966).

The infinitely many threshold poles that approach $\lambda = 0$ as $\nu \to 0$ are shown to produce, using a product representation of the S-matrix obtained recently by Cheng, the correct threshold behavior of the S-matrix; 1 for Re $\lambda > 0$ and $\exp[2\pi i\lambda]$ for Re $\lambda < 0$. Even though the contribution of a single threshold pole to the zero-energy scattering amplitude is vanishingly small, their total contribution is found to be, in general, quite significant. The contribution of these poles to the scattering length is calculated for some soluble cases. For parametrization of low-energy scattering, according to this analysis, a formalism which automatically includes the threshold poles is more reliable than one based on a few Regge poles alone. (auth)

13589 A DYNAMICAL INTERPRETATION OF SPURIONS IN $\tilde{U}_{12}$. Rivers, R. J. (Imperial Coll. of Science and Tech., London). Nuovo Cimento, (10), 41A: 314-28 (Feb. 1, 1966).

The theory of $\tilde{U}_{12}$ is considered from a field-theoretic viewpoint in a four-dimensional space, using noninvariant propagators as a means of providing additional symmetry breaking. The three- and four-point functions are discussed with the aim of giving an interpretation to both the homogeneous and the inhomogeneous $\tilde{U}_{12}$ theory. This gives an alternative way of interpreting the difficulties with unitarity. The way in which spurions arise is discussed, and compared with their phenomenological use in the case of mass splitting. A discussion of the unitarity equations for quark-quark scattering with momentum spurions shows some of the dangers inherent in considering scattering amplitudes as independent of one another, and shows that violation of unitarity is more than infinitesimal. (auth)

13590 REMARKS ON THE BOOTSTRAP CONDITIONS IN A SOLUBLE MODEL. Aramaki, S. (Univ. of Illinois, Urbana). Nuovo Cimento, (10), 41A: 386-8(Feb. 1, 1966).

It is pointed out that the bootstrap conditions in the Lee model with crossing symmetry, which are expressed in different ways in the literature, are nothing but the conditions imposed on the scattering amplitude in the high-energy limit. (L.B.S.)

13591 SIMPLE DERIVATION OF CLUSTER EXPANSIONS FOR MANY-FERMION SYSTEMS. Clark, J. W.; Chakkalakal, D.; Westhaus, P. (Washington Univ., St. Louis). Progr. Theoret. Phys. (Kyoto), 34: 726-33(Nov. 1965).

A simple alternative derivation of conventional cluster expansion formulas of Iwamoto and Yamada and others for the expectation value $\langle H \rangle$ of the energy of a many-fermion system is offered. The assumed trial function is of the general form $F\Phi_p/(F\Phi_p, F\Phi_p)^{1/2}$, where Φ_p is a Slater determinant of appropriate single-particle functions and the factor F is attached to account for the possibility of strong interparticle correlations. The proposed scheme is applicable to finite as well as infinite systems and is easily generalized to the calculation of nondiagonal as well as diagonal matrix elements with respect to the members of the set $[F\Phi_p/(F\Phi_p, F\Phi_p)^{1/2}]$. Explicit results for $\langle H \rangle$ are displayed to second cluster order, contributions being classified according to their assigned order of magnitude in a correlation parameter $\xi = |N\omega|\Omega|$ of the sort introduced by Iwamoto and Yamada and Clark and Westhaus. (auth)

13592 MANY-POLE AMPLITUDES AND ELEMENTARITY. I. ONE ELEMENTARY AND SOME COMPOSITE PARTICLES CASE. Kinoshita, Kisei; Yabuki, Haruichi (Tokyo Univ.). Progr. Theoret. Phys. (Kyoto), 34: 825-32(Nov. 1965).

The relation between the full amplitude and the one-particle irreducible amplitude is investigated when there are an elementary particle and some composite particles in the same channel. While the zeros of the propagator are independent of the coupling constant of the elementary particle, the composite poles depend on it and coincide with the propagator zeros in the limit of the vanishing of the coupling constant. Critical values of the coupling constant, corresponding to the appearances of a ghost pole or a bound-state pole, are obtained. It is impossible to distinguish an elementary particle from composite particles when they co-exist in the same channel. (auth)

13593 A NOTE ON THE ANALYTIC PROPERTY OF A FIFTH ORDER FEYNMAN GRAPH. Nakamura, Morio (Tokyo Univ.). Progr. Theoret. Phys. (Kyoto), 34: 851-5 (Nov. 1965).

The condition for the existence of the fifth order singularity (C^4) by Tarski's notation of a loop diagram is investigated. The condition is explicitly obtained for the simple scattering process of equal particles with equal internal masses. (auth)

13594 RADIATIONLESS CONDITION AND MASS FORMULA. Hokkyo, Noboru (Hitachi Central Research Lab., Ozenji, Japan). Progr. Theoret. Phys. (Kyoto), 34: 856-60(Nov. 1965).

It is pointed out that Nambu's mass formula is obtainable from the radiationless condition for orbiting rigid extended charge distributions. In view of the fact that not all particles obeying Nambu's formula are realized in nature, a model of elementary particles is suggested in which existing long-lived particles are volume or surface distributions of electric and generalized (hyper, baryonic, etc) charge-currents which do not radiate associated field quanta while undergoing small oscillatory motions under the action of no external forces. The additional requirement for the vanishing of the radiation of field quanta from oscillating generalized charge distributions is postulated in a form which relates mass spacings of baryons to strong interaction coupling constants. The problem of the constancy of the mass spectrum of elementary particles is discussed from cosmological viewpoints. It seems that the constancy of the mass spectrum is guaranteed by the laws of conservation of energy and of total charge in the universe. (auth)

13595 THE FORWARD DIFFRACTION PEAK AND THE HIGH-ENERGY BEHAVIOR OF SCATTERING AMPLITUDES. Yamamoto, Yoshitaka (Tokyo Univ.). Progr. Theoret. Phys. (Kyoto), 34: 863-5(Nov. 1965).

The scattering of two equal-mass scalar particles is treated. An expression for the upper bound of the forward scattering amplitude is obtained by connecting the forward diffraction peak of the experimental differential cross section with the high-energy behavior of the scattering amplitude. If shrinkage occurs as predicted by the Regge theory, the upper bound becomes that of Froissart. If there is no shrinkage, the s dependence of the forward amplitude is restricted even more severely. (M.J.T.)

13596 WEAK INTERACTIONS AS DETERMINED BY PERMUTATION SYMMETRY IN ISO-SPACE. Ahrens, Tino (Georgia Inst. of Tech., Atlanta). Progr. Theoret. Phys. (Kyoto), 34: 867-8(Nov. 1965).

The notion of permutation symmetry in three-dimensional isospace is used to predict the occurrence and relative coupling strengths of weak interactions among nucleons and leptons. (M.J.T.)

13597 A MODIFICATION OF THE CURRENT-CURRENT INTERACTION. Kunimasa, Tosaku (Osaka Univ.). Progr. Theoret. Phys. (Kyoto), 34: 870-1(Nov. 1965).

An octet current $J\mu$ is defined by $J\mu = \alpha V\mu + \beta A\mu$, where α and β are arbitrary complex numbers and $V\mu$ and $A\mu$ are the octet vector and axial-vector current matrices, respectively. It is assumed that the nonleptonic weak interaction hamiltonian H_ω is composed of the product of $J\mu$ and its hermitian conjugate and is the sum of the octet components and that CP invariance holds. It is found that $\alpha^*\beta$ is not restricted, permitting $\mathrm{Im}(\alpha^*\beta) \neq 0$ and thus allowing $K_1^0 \to 2\pi$ decay. The restriction $\mathrm{Re}(\alpha^*\beta) = 0$ is investigated, and it is found that (1) the parity-conserving and -violating amplitudes for $|\Delta S| = 1$ processes are correlated, allowing a sum rule for s-wave nonleptonic hyperon decay to be obtained; (2) the parity-violating amplitude for the nonleptonic $\Delta S = 0$ process vanishes; (3) parity conservation is guaranteed when the coupling of $J\mu$ with its hermitian conjugate is extended to the strong interaction hamiltonian. (M.J.T.)

13598 SU_3 TRIPLETS WITH INTEGRAL ELECTRIC CHARGE AND THE BARYON STRUCTURE. Van Hove, L. (CERN, Geneva). [Progr. Theoret. Phys. (Kyoto), 34: Suppl., 14-30(1965)].

In the light of the important results recently obtained in the SU_6 combination of nonrelativistic spin and SU_3 symmetry, the problem of SU_3 triplets, that would be the basic building blocks of mesons and baryons is discussed, concentrating on the case where the basic particles would have integral electric charge. In this case, whereas the SU_3 structure of mesons and baryons is known to be compatible with many different basic triplet models, SU_6 properties reduce the ambiguity to a large degree. If the number of basic triplets is kept to the minimum, which is two in the case of integral charges, one model appears to be strongly preferred on grounds of simplicity. It contains six basic particles of baryon number 1 and spin $\frac{1}{2}$, forming an SU_3 triplet 3 (with charges 1, 0, 0) and an SU_3 triplet 3 (with charges 0, 1, 1). The SU_6 structure of baryons and mesons is studied in the framework of this model. The effect of the supercharge (i.e., of the additional quantum number occurring in the Gell-Mann-Nishijima formula when integrally charged triplets exist) on the baryon magnetic moments is estimated. It is expected to be less than 35% on the proton to neutron moment ratio and less than 20% on the lambda to neutron moment ratio. The rank three Lie groups, which most naturally describe possible higher internal symmetries for the six basic particles (SO_6 and Sp_6), are combined with spin, and the resulting nonrelativistic coupling of all mesons to the baryons is found to belong to one single representation instead of two in the case of SU_6. (auth)

13599 HIGHER SYMMETRY GROUPS WITH PARITY MIXING. Marshak, R. E.; Okubo, S.; Schechter, J.; Wojtaszek, J. (Univ. of Rochester, New York). [Progr. Theoret. Phys. (Kyoto), 34: Suppl., 56-75(1965)]. (UR-875-83).

The properties and some of the consequences of the three groups are examined: USp(6), R(6), and U(6), which follow from a chiral decomposition of a triplet of Dirac fields interacting via the tensor, scalar (or pseudoscalar) and axial vector four-fermion interactions respectively. It is found that USp(6) commutes with the parity operation whereas R(6) and U(6) do not. This has the consequence that SU(3) multiplets of opposite parity appear in the same irreducible representation of the R(6) or the U(6) group but not of the USp(6) group. Furthermore, in the two cases of parity mixing within the same irreducible representation, SU(3) multiplets of zero triality (singlets, octets, etc.) are always accompanied by SU(3) multiplets of opposite parity and non-zero triality (triplets, sextets, etc.). Some sort of triality selection rule could therefore explain the apparent scarcity of particles of the wrong parity (e.g., scalar or axial vector). It is emphasized that all three groups: USp(6), R(6), and U(6) (as well as $\overline{W}(3)$) are consistent with the requirements of Lorentz invariance, unitarity and crossing—in contrast to the $\tilde{U}(12)$ group which mixes spin and unitary spin. It is also found that invariance under R conjugation must hold for the USp(6) and U(6) groups but not for the R(6) group. Since R invariance seems to be badly violated (at least for the baryons), this would tend to favor R(6) as the most promising of the three groups. In comparing the merits of R(6) to the $\overline{W}(3)$ group it is pointed that no triality selection rule is needed for $\overline{W}(3)$ and indeed SU(3) multiplets of zero and non-zero triality are not mixed in the same irreducible representation of $\overline{W}(3)$. On the other hand, the $\overline{W}(3)$ theory definitely predicts the existence of scalar (axial vector) mesons with masses not very different from those of the pseudoscalar (vector) mesons. (L.B.S.)

13600 CAN THE GRAVITATIONAL FIELD PROVE ESSENTIAL FOR THE THEORY OF ELEMENTARY PARTICLES? Markov, M A. (Lebedev Physical Inst., Moscow). [Progr. Theoret. Phys. (Kyoto), 34: Suppl., 85-95(1965)].

The general theory of relativity offers better possibilities than the special theory of relativity for considering the problem of extended particles. Interpretation of the small length ($l_0 = \sqrt{\hbar\kappa/c^3}$) as the fundamental length of the future theory corresponds to the trends of modern systematics to base it on particles of very large masses ("quarks"?). (auth)

13601 A CLASS OF OPTICAL MODELS. Serber, Robert (Columbia Univ., New York). [Progr. Theoret. Phys. (Kyoto), 34: Suppl., 104-7(1965)]. (TID-21883).

A power-law dependent asymptotic form of the amplitude of the scattering wave in shadow scattering at large momentum transfer is obtained, which may be useful for describing the scattering cross sections in the optical model for p-p and π-p scattering. (L.B.S.)

13602 ON BARYON GROUNDSTATES IN YUKAWA THEORIES. Wentzel, Gregor (Univ. of Chicago). [Progr. Theoret. Phys. (Kyoto), 34: Suppl., 108-17(1965)]. (COO-264-261).

Various models of baryons interacting with bosons are reviewed in the static strong-coupling approximation. The nature of the compound single-baryon groundstate may be critically dependent on parameters like the mixture ratio of different types of Yukawa interactions (e.g., F/D). All kinds of special situations are encountered in different models. The major part of this study is devoted to the SU(3)-symmetric scalar theory. (auth)

13603 APPROXIMATION OF REGGE POTENTIALS THROUGH FORM FACTORS. Chew, Geoffrey F. (Univ. of California, Berkeley). [Progr. Theoret. Phys. (Kyoto), 34: Suppl., 118-26(1965)]. (UCRL-16101).

A discussion is given of certain consequences of employing Regge poles rather than fixed-J poles as the source of two-particle generalized potentials. Three qualitative aspects are emphasized. For the purposes of strip approximation dynamics, contrary to common belief, the Regge potential has roughly the same energy dependence as that due to exchange of a fixed-spin particle. The Regge potential, relative to that produced by a corresponding fixed-spin

particle, is damped by an exponential form factor, roughly estimated as $\approx\exp[2\alpha'(t-m^2)]$, where α' is the trajectory slope, t the negative square of momentum transfer, and m the particle mass. Ambiguous zero-range components in the fixed-J potential become replaced by unambiguous short-range components in the Regge potential. (auth)

13604 COMPOSITE MODEL AND PARTICLE PRODUCTION AT SUPERHIGH ENERGIES. Koba, Ziro (Univ. of Copenhagen). [Progr. Theoret. Phys. (Kyoto), 34: Suppl., 168-86(1965)].

The statistical theory of particle production at superhigh energies is reconsidered on the basis of the composite model of particles and resonances. The main difficulties of the statistical approach, namely those concerning the composition and the angular distribution of the produced particles, may be removed by assuming that a statistical equilibrium is reached, within a Lorentz-contracted tiny hot region, between virtual quarks and antiquarks, and not between baryons, antibaryons, and mesons. (auth)

13605 THREE KINDS OF TRIPLET MODEL. Miyamoto, Yoneji (Tokyo Univ. of Education). [Progr. Theoret. Phys. (Kyoto), 34: Suppl., 187-92(1965)].

The spin-statistics problem for fundamental particles is investigated. The sub-baryonic fundamental particles are discussed under the assumptions of the axioms of the conventional field theory: relativity invariance and spin-statistics theorem. (i) Baryons should be antisymmetric with respect to new unitary spin X(3), unitary spin U(3), and angular spin, if fundamental particles are in S states. Three kinds of unitary triplets are introduced to restore the validity of the spin-statistics theorem. (ii) The charge, hypercharge, and baryon number of fundamental particles should be integers. SU(9) is generalized into SU(18), and the subgroups of the 816 irreducible representations of baryons in SU(18) are presented. Finally, the possibility of SU(18) × SU(18) and SU(18) × SU(18) × SU(18) is suggested. (L.B.S.)

13606 DEFORMABLE SPHERE MODEL OF ELEMENTARY PARTICLES AND THE ORIGIN OF INTERNAL SYMMETRIES. Hara, Osamu; Goto, Tetsuo (Nihon Univ., Tokyo). [Progr. Theoret. Phys. (Kyoto), 34: Suppl., 193-206(1965)].

Deformable sphere model of elementary particles is discussed as a generalization of the rigid body model. It is shown that in this model the approximate SU(3) symmetry follows very naturally. (auth)

13607 DYNAMICAL INTERPRETATION OF SPURIONS. Nishijima, K.; Saffouri, M. H. (International Center for Theoretical Physics, Trieste, Italy). [Progr. Theoret. Phys. (Kyoto), 34: Suppl., 207-21(1965)].

The concept of spurions was introduced originally as a formal mathematical tool to express the selection rule $|\Delta I| = \frac{1}{2}$ in the nonleptonic decay of strange particles. It is shown that spurions are of a deeper physical significance in that they can be used not only to express but also to derive selection rules in weak interactions. (auth)

13608 ON THE WEAK INTERMEDIATE BOSON. Ogawa, Shuzo (Hiroshima Univ.). [Progr. Theoret. Phys. (Kyoto), 34: Suppl., 232-7(1965)].

Various aspects of the development of particle physics are reviewed, with emphasis given to the problem of weak interactions. (L.B.S.)

13609 PARTICLES AS COLLECTIVE STATIONARY STATES. Heisenberg, W. (Max-Planck Inst. for Physics and Astrophysics, Munich). [Progr. Theoret. Phys. (Kyoto), 34: Suppl., 298-303(1965)].

The method of Green functions is briefly discussed and is applied to the nonlinear spinor theory of elementary particles. The term Green function is used in the generalized sense as vacuum expectation value of products of some fundamental field operators describing the system. Expressions are derived for calculating coupling constants in scattering processes within this framework. (L.B.S.)

13610 AN IMPACT PARAMETER FORMALISM. Adachi, Toshimi (Tokyo Metropolitan Technical Coll.). Kotani, Tsuneyuki. [Progr. Theoret. Phys. (Kyoto), 34: Suppl., 316-31(1965)].

A relativistic impact-parameter formalism is introduced without any approximation. It is applicable for all physical values of energy and scattering angle. An impact parameter amplitude is defined from an invariant scattering amplitude by the integral with the Bessel function, in place of the Legendre function in the definition of a partial-wave amplitude. It is found that this impact amplitude is an example of a new integral expansion. It is proved that one of the necessary and sufficient conditions that this new expansion is permissible, is that the amplitude should satisfy the Kapteyn equation, which is required in the Webb-Kapteyn theory of the Neumann series expansion of an odd function. The physical interpretation of the amplitude is discussed and cross sections are expressed by simple integrals over the impact parameter without any approximation. The unitarity relation for the amplitude is expressed in the simpler form. Comparison is made with three other relativistic formalisms proposed by Blankenbecler and Goldberger, Ida, and Cottingham and Peierls. In contrast with our formalism, the applications of these three formalisms are limited either to the extremely high energy region or to only the forward angle scattering. (auth)

13611 GENERALIZED ISO-SPIN-SPACE, GENERALIZED GAUGE TRANSFORMATION AND DERIVATION OF MESON. Utiyama, Ryoyu (Osaka Univ.). [Progr. Theoret. Phys. (Kyoto), 34: Suppl., 332-8(1965)].

A four-dimensional fictitious space of Minkowskian type called a ξ-space is introduced in order to describe the isospins of elementary particles in a unified manner. The nucleon field is represented by a set of functions of the ordinary space-time coordinates x and the extra coordinates ξ in the above mentioned ξ-space. The postulate that there are analogies between both x and ξ spaces gives a generalization of the familiar equation of a free nucleon. The replacement of an arbitrary phase of the nucleon field with an arbitrary function of x and ξ leads to the introduction of the triplet scalar meson together with a neutral vector boson. Some further refinements of the theory derive the pseudoscalar triplet meson with the familiar style in its coupling with nucleons. (auth)

13612 SPINOR MODEL OF BARYONS AND MESONS. Takabayasi, Takehiko (Nagoya Univ., Japan). [Progr. Theoret. Phys. (Kyoto), 34: Suppl., 339-82(1965)].

A unified model of baryons and mesons is presented based on the hypothesis that a strongly interacting particle originally has the internal configuration represented by three "triads," where a triad is by definition a light-like vector together with a rotational orientation around it, and the existence of three triads is related to the fact that our Minkowski space allows three independent light-like vectors. The assumed configuration implies twelve (real) independent internal coordinates. The SU(6) symmetry is contained there in conformity with relativity, which requires kinematical couplings to exist between internal and external motions. Characteristic to the model is, beside the SU(6), the existence of generators of a three-dimensional Lorentz group, which represents the extension, dilatation and vibration of the structure. These quantities play particularly important roles of controlling the IR (irreducible representation) of SU(6) and determining the mass operator. Eigenstates of the internal motion are first classified into "shells" by a pair of oscillator quantum numbers, and then each shell is subgrouped into supermultiplets corresponding to IR's of SU(6). The first mesonic shell has odd parity and contains 36 states which are divided into an SU(6) singlet (identified as $X^0(958)$ meson) and an SU(6) 35-plet. The predictions about spin, parity and charge-conjugation parity just agree with observations. In the model the IR's 15 and 20 of SU(6) do not occur in the shells of lower excitation. (auth)

13613 REMARKS ON A NEW CONCEPT OF ELEMENTARY PARTICLES AND THE METHOD OF THE COMPOSITE MODEL. Maki, Ziro; Ohnuki, Yoshio; Sakata, Shoichi (Nagoya Univ., Japan). [Progr. Theoret. Phys. (Kyoto), 34: Suppl., 406-15(1965)].

Remarks are presented concerning the fundamental units of matter previously discussed within the framework of the composite model, the Nagoya model, and the neutrino unified model. Some problems are pointed out on the relation between mesons and baryons, the nature of urbaryons, comparison of various models, and weak interactions. (L.B.S.)

13614 ON THE ABNORMAL SOLUTION OF BETHE-SALPETER EQUATION. A RELATION BETWEEN STATIC AND NON-STATIC SOLUTIONS. Ohnuki, Yoshio; Watanabe, Keiji (Nagoya Univ., Japan). [Progr. Theoret. Phys. (Kyoto), 34: Suppl., 416-35(1965)].

It is shown that the Wick-Cutkosky solution of the covariant Bethe-Salpeter equation has a close connection with that of the static model, that is, the former is a bound state within a potential obtained from the Bethe-Salpeter equation in the static model. Hence the abnormal solution can be understood as a bound state in the physically meaningless potential. Further it is proved that in the case of nonvanishing intermediate boson mass, the covariant equation has no abnormal solution if $\lambda \leqq 1/4$. This corresponds to the fact that the redundant potential, the abnormal energy eigenvalue of the fixed source Bethe-Salpeter equation, does not appear when $\lambda \leqq 1/4$. The correspondence between the static and the non-static models exists also in the norm of the state vector, which is found to be $(-1)^K$ for both cases. (auth)

13615 A RELATION BETWEEN THE MINKOWSKI AND ISOBARIC SPACES. Toyoda, Toshiyuki (Rikkyo Univ., Tokyo). [Progr. Theoret. Phys. (Kyoto), 34: Suppl., 542-7(1965)].

For the purpose of getting an idea of the relation between the Minkowski and isobaric spaces an extension of the conventional Lorentz group is investigated. Particular attention is paid to the structure of the complex Lorentz group proposed by Barut. It is shown explicitly that the maximum compact group contained in the non-compact group is the unitary group U(3). Keeping the same invariant, the complex Lorentz group is widened so as to obtain the generalized Dirac equation, where the Clifford algebra C_8 is utilized. By making use of an adequate representation of the C_8 the compatibility of the conventional space-time transformation and the isobaric one is discussed. (auth)

13616 INELASTIC PROCESS AND THE ONE-BOSON-EXCHANGE MODEL. Kikugawa, Masayoshi (Hiroshima Univ.); Sawada, Shoji; Ueda, Tamotsu; Watari, Wataro; Yonezawa, Minoru. [Progr. Theoret. Phys. (Kyoto), 34: Suppl., 548-56(1965)].

Inelastic process is discussed from the viewpoint of the one-boson-exchange model. A method of unitarizing the amplitudes for multi-channel reaction is given and its effects are investigated in the two channel case. It is pointed out that polarization measurement of the recoil nucleon from $p + p \rightarrow N^* + N$ serves as a test of the ununitarized one-pion-exchange models. (auth)

13617 INTERNAL COORDINATES, SU_3 SYMMETRY AND CHARGE OF ELEMENTARY PARTICLES. Takeda, Gyo (Tohoku Univ., Sendai). [Progr. Theoret. Phys. (Kyoto), 34: Suppl., 557-63(1965)].

A study is made of the necessary variables of the wave function in order to obtain the spin multiplicity and the SU_3 multiplicity of the elementary particles. The transformations of the wave function according to irreducible representations of the SU_3 group are examined for particles of finite rest mass. The internal coordinates of massless particles and elementary particle charge are then considered. (L.B.S.)

13618 A VARIANT TRIPLET MODEL AND INTEGRAL CHARGE. Katayama, Yasuhisa; Umemura, Isao; Yamada, Eiji (Kyoto Univ.). [Progr. Theoret. Phys. (Kyoto), 34: Suppl., 564-77(1965)].

A variant form of Sakata model for elementary particles is proposed. The fundamental triplet is assumed to obey para-Fermi statistics with capacity 3, and to be characterized by the three quantum numbers, the third component of isospin, the strangeness and the triplet number. It is not an eigenstate of electric and hypercharges, while it has definite expectation values for both charges, ($^2/_3$, $-^1/_3$, $-^1/_3$) and ($^1/_3$, $^1/_3$, $-^2/_3$) respectively. The triplet state can be treated as mixture of three sets of sub-triplets which are ordinary fermions with an appropriate description. It is possible to assign them integral eigenvalues for electric and hypercharges. Under the restriction that the physically realizable states should be eigenstates of both charges, it is shown that most of low-lying states are the ones which are actually observed. Although the isolated existence of the triplet state is ruled out, the group theoretical arguments for the realizable states, such as the ratio of magnetic moments of baryons in U(6) symmetry, are not affected. (auth)

13619 PARTICLE DYNAMICS AND SYMMETRIES IN de SITTER SPACE. Tanikawa, Yasutaka (Kobe Univ., Japan). [Progr. Theoret. Phys. (Kyoto), 34: Suppl., 609-20(1965)].

It is attempted to formulate the classical and quantum dynamics of a particle in the de Sitter space on the basis of natural invariance requirement. It is found that a particle motion in the de Sitter space has a remarkable symmetry of the phase space which is a generalization of reciprocal symmetry of particle coordinates and energy-momenta proposed by Born and emphasized by Yukawa. The formal and physical aspects of generalized symmetries in the theory are studied. (auth)

13620 THE REARRANGEMENT OF SYMMETRIES IN DYNAMICAL MAPS. Leplae, L.; Sen, R. N.; Umezawa, H. (Ist. di Fisica Teorica, Naples). [Progr. Theoret. Phys. (Kyoto), 34: Suppl., 637-50(1965)].

An attempt to describe symmetries and broken symmetries simultaneously in field theory leads to a formulation in which the Heisenberg, Schrödinger and interaction representations, as well as the hamiltonian and unphysical particles, are not called upon. The key idea is to start from the formal structure of interacting field equations for basic fields, which define the symmetries and specify the dynamics, and to obtain the possible consistent expressions, called dynamical maps, of the basic fields in terms of incoming fields of observable particles. General principles for the construction of dynamical maps are indicated. The dynamical map determines the commutation properties of the basic fields. The Goldstone theorem is examined for various cases of canonical dynamical maps, and in these cases symmetries of the basic fields appear to be rearranged to the gauge invariance of Goldstone fields. Three examples corroborating the general conclusions are cited of the construction of dynamical maps in the pair approximation. (auth)

13621 QUANTUM NUMBERS OF PARTICLES. Nakamura, Seitaro (Tokyo Univ.). [Progr. Theoret. Phys. (Kyoto), 34: Suppl., 661-84(1965)].

A number of quantum numbers are introduced on the basis of higher symmetry consideration in the two independent charge spaces, one being the extended isotopic spin space ($SU_2 \times SU_2$), the other the hyperspin space ($SU_2 \times SU_2$). A number of new selection rules are derived. In order to accommodate the observed nature of the mass spectrum and selection rules of particles, symmetry breaking interactions are speculated. (auth)

13622 LIMIT OF APPLICABILITY OF THE PERTURBATION THEORY IN WEAK INTERACTIONS. Tu, Pham Quy (Joint Inst. for Nuclear Research, Dubna, USSR). Yadern. Fiz., 2: 1054-9(Dec. 1965). (In Russian).

The unitarity condition is used to estimate the upper limit of the energies, for which the perturbation theory can be applied to weak interactions. (auth)

13623 SOME ELECTROMAGNETIC PROPERTIES OF ELEMENTARY PARTICLES IN THE SU(6) GROUP. Asherova, R. M.; Smirnov, Yu. F.; Yudin, N. P. (Moscow State Univ.). Yadern. Fiz., 2: 1065-8(Dec. 1965). (In Russian).

Relations between magnetic moments and between the nondiagonal elements of the M1 operator are obtained for the meson multiplet in the SU(6) symmetry. The reduction $SU(6) \rightarrow SU(4)_U \otimes SU(2)$, analogous to the use of the U-spin formalism in SU(3), is briefly discussed. (auth)

13624 ELECTROMAGNETIC PROPERTIES OF THE 70-DIMENSIONAL REPRESENTATION IN THE SU(6) SCHEME. Ti, Kao; Tkachev, L. G. (Joint Inst. for Nuclear Research, Dubna, USSR. Saratov State Univ., USSR). Yadern. Fiz., 2: 1069-74(Dec. 1965). (In Russian).

Relations are obtained for the magnetic moments and transition probabilities for resonances in the 70-plet. (auth)

13625 DEGENERATE SU(4) SYMMETRY OF STRONG INTERACTIONS. Vladimirskii, V. V. (Inst. of Theoretical and Experimental Physics, Moscow). Yadern. Fiz., 2: 1087-94(Dec. 1965). (In Russian).

The assumption that the strong interactions are degenerate with respect to one of the quantum numbers of the SU(4) group leads to a significant reduction of the number of states with different masses. The degenerate SU(4) supermultiplets are similar to the SU(3)-supermultiplets. There is only one superfluous mass in the regular 15-dimensional representation in comparison with the octet, two in the 20-dimensional representation, analogous to the baryon octet (Ξ_{1395}, Ω_{1680}), and no superfluous masses in the 20-dimensional representation corresponding to the decuplet. The doubling of the number of K-meson states makes it possible to obtain a phenomenological description of the CP-violation in $K_2^0 \rightarrow 2\pi$ decays. (auth)

13626 RELATIVISTIC OSCILLATOR MODELS OF ELEMENTARY PARTICLES. Ginzburg, V. L.; Manko, V. I. (Lebedev Inst. of Physics, Moscow). Yadern. Fiz., 2: 1103-14(Dec. 1965). (In Russian).

The relativistic invariant equations are considered for the particles described by the center of mass coordinates x^i and three 4-vectors u_i^α ($i = 1,2,3,4$; $\alpha = 1,2,3$) u_i^α are the intrinsic variables which obey the oscillator equations. The solutions of these equations form in the rest system the representations of the group SU(3). It is possible to write the equations which give the solution corresponding to the octet and decuplet for the case of half-integer spin and to the octet and singlet for the case of the integer spin. (auth)

13627 PREDICTIONS FOR THE ELECTROMAGNETIC FORMFACTORS OF BARYONS FROM HYBRID GROUPS. Dosch, H. Guenter; Stech, Berthold (Univ., Heidelberg). Z. Phys., 189: 455-64(1966).

The predictions of the hybrid group $SU_3 \otimes SU_3 \otimes U_1$ for the electromagnetic formfactors of baryons are studied in detail. Surprisingly, this small group leads already to strong restrictions. For example, it gives for the ratio of the magnetic formfactors of neutron and proton $-2/3$ for all values of the momentum transfer variable. The results of the powerful $(SU_6)_W$ hybrid group which involves more speculative assumptions are also quoted. In addition, the theoretical foundation of the hybrid groups is discussed. (auth)

13628 PERTURBATIONAL CALCULATIONS IN THE GAUGE THEORY OF ELEMENTARY PARTICLES [Thesis]. Chand, Prakash. Boston, Mass., Boston Univ. Graduate School, 1965. 103p.

Certain mass differences of elementary particles in second order perturbation theory were calculated within the framework of a gauge invariant theory of interactions. First the mass difference of the electron and the muon was calculated on the assumption that they have some bare mass and have different physical masses as a result of their interaction with a neutral vector meson field whose quantum is the ϕ meson. The calculation gives the mass difference of the muon and the electron in agreement with their experimental value and does not run into any difficulty faced by previous calculations. Secondly, generalizing the meaning of the electromagnetic interaction, the mass differences of the different members of every charge multiplet of the strongly interacting particles were calculated. Only with two adjustable parameters could the mass differences of the seven pairs of particles be predicted. Finally, the origin of the masses of the ϕ and ρ mesons was considered. Using the coupling constants previously introduced, their masses were calculated in agreement with the experimental masses. The same cut-off parameter assumed for the electromagnetic mass splitting was used. (Dissertation Abstr.)

13629 ON THE REPRESENTATIONS ON THE GROUP SU_3 [Thesis]. Resnikoff, Marvin. Ann Arbor, Mich., Univ. of Michigan, 1965. 147p.

The representations $\mathcal{D}^{(\lambda\mu)}(u)$ and the reduction of the direct product representation $\mathcal{D}^{(\lambda_1\mu_1)}(u) \otimes \mathcal{D}^{(\lambda_2\mu_2)}(u)$ for the group SU_3 are examined. The general method of approach is similar to one originated by V. Bargmann for the group SU_2 employing a Hilbert space of base vectors composed of several complex variables. Base vectors $|\lambda\mu;\alpha\rangle$ associated with the representation $\mathcal{D}^{(\lambda\mu)}(u)$ are constructed by means of operators on the Hilbert space and related to the base vectors $|\lambda\mu;\alpha\rangle_c$ associated with the conjugate representation $\overline{\mathcal{D}^{(\lambda\mu)}(u)}$ by an explicit R-conjugation operation on the variables of the base vectors. The general expression for the vector coupling or $3(\lambda\mu)$ coefficient that reduces the product representation, $\mathcal{D}^{(\lambda_1\mu_1)}(\mu) \otimes \mathcal{D}^{(\lambda_2\mu_2)}(u)$, is derived by constructing a function $h_k(k_i)$ in the triple product space of base vectors, which is invariant under a unitary transformation. The explicit $3(\lambda\mu)$ coefficient is then given by taking the inner product of $h_k(k_i)$ with $|\lambda_1\mu_1;\alpha_1\rangle|\lambda_2\mu_2;\alpha_2\rangle|\lambda_3\mu_3;\alpha_3\rangle_c$. The symmetries of the vector coupling coefficients are analyzed. The recoupling or $6(\lambda\mu)$ coefficients are formulated in terms of a generating function, an explicit expression is integrated out for the general non-degenerate case, and a method is prescribed for determining the recoupling coefficients for the degenerate case. The symmetries of the $6(\lambda\mu)$ coefficients are discussed. In addition, the group is parameterized in terms of eight "Euler-like" angles, the group volume element is calculated, and the representations are shown to be irreducible and complete. The primitive characters are constructed, demonstrated to be orthogonal, and several other properties of the characters are noted. (Dissertation Abstr.)

13630 THE THREE-BODY PROBLEM IN QUANTUM MECHANICS [Thesis]. Wessel, William LeRoy. Ann Arbor, Mich., Univ. of Michigan, 1965. 93p.

A non-relativistic, spinless hamiltonian for three charged particles is investigated and it is shown that the neglect of relativistic effects and spin introduces negligible error in the calculation of the three-body interaction energy. Center-of-mass coordinates are eliminated from the hamiltonian and the remaining operator is expressed in terms of the three Euler angles and suitable confocal elliptic coordinates. The wave function is expanded in a finite sum of symmetric top eigenfunctions and the Euler angles are eliminated from the problem, leaving two independent sets of simultaneous, partial differential equations in the confocal elliptic coordinates alone. The solutions to these equations in the case of muonic molecular ions are interpreted physically and those corresponding to bound states identified. Two basis sets are defined, and for each a matrix equation for the expansion coefficients of the wave function is obtained. The elements of these matrices are calculated by taking linear combinations of certain fundamental integrals, which are themselves calculated by recurrence relations. It is only necessary to perform one numerical integration to obtain each matrix. All the bound state energies for the muonic molecular ions, $(p\text{-}\mu\text{-}p)^+$ and $(d\text{-}\mu\text{-}d)^+$, are found, as are expectation values for the internuclear separation, $\langle\rho\rangle$, and muon-nucleon overlap. A theoretical value for the weak interaction capture rate of the muon by one of the protons from the first rotationally excited state of $(p\text{-}\mu\text{-}p)^+$ is calculated to be 484 sec^{-1} as compared to the experimental value of 463 ± 40 sec^{-1}. The energies for the ground state, $1s^2$, and second doubly ex-

cited state, $2p^2$, of the helium atom are calculated as a check of the whole procedure. The total ground state energy of the helium atom was found to be $-637183\ cm^{-1}$ as compared to the experimental value of $-637206.5\ cm^{-1}$. The best bound state energies and expectation values computed for the two muonic molecular ions for each value of the total angular momentum quantum number, K, are given in a table. The probable error in these calculated quantities is on the order of one per cent. (Dissertation Abstr.)

13631 SOME CONSEQUENCES OF THE UNITARITY CONDITION FOR THE ANALYTIC PROPERTIES OF SCATTERING AMPLITUDES [Thesis]. **Dragt, Alexander James. Berkeley, Calif., Univ. of California, 1964. 47p.**

A scattering amplitude may be viewed as an analytic function of several complex variables by extending its energy and angular dependencies to unphysical real and complex values. When such an extension is made, it is found that the analytic structure of a scattering amplitude, i.e., the nature and location of singularities in the several complex variables, is intimately related to the requirement that the scattering amplitude satisfy the unitarity condition. Two particular consequences of the unitarity condition for the analytic properties of scattering amplitudes are discussed. It is first shown that, because of the unitarity condition, the locations and residues of poles appearing in unitarily coupled two-particle scattering amplitudes are not independent and must satisfy the same relations as do poles in perturbation theory. The unitarity condition thus appears as a relation between various singularities of coupled scattering amplitudes. In a second paper, the discussion is extended to general scattering amplitudes involving more than two particles. In this context it is shown that the unitarity condition restricts the locations and types of singularities that can occur. It is found that the general scattering amplitude is free from singularities on the positive real energy axis except for isolated singularities at physical thresholds. The analytic behavior near each such singularity is exhibited. At thresholds for processes involving an even number of particles, this behavior is like a half-integral power; at thresholds involving an odd number of particles, the behavior is logarithmic. (Dissertation Abstr.)

13632 TEORIYA KONECHNYKH FERMI-SISTEM I SVOISTVA ATOMNYKH YADER. (The Theory of Finite Fermi Systems and Properties of Atomic Nuclei). **Migdal, A. B. Moscow, Izdatel'stvo Nauka, 1965. 572p.**

A method is developed for the examination of systems of strongly interacting Fermi particles, which is applied to nuclear theory and could be used for calculating electronic processes in atoms and complex molecules. The Green function method is used to show that, even for strong interactions between the particles, a system can in many cases be considered as a gas of quasiparticles, the interaction between which is determined by several constants. The theory permits the exact relation between the various observed processes to be determined by means of introducing these constants. The general theory of isolated Fermi systems and of Fermi systems in an external field is presented. The results obtained are applied to the theory of the nucleus. Ten articles on nuclear theory are also included. (tr-auth)

13633 THE ANALYTIC PROPERTIES OF THE SCATTERING MATRIX FOR NON-RELATIVISTIC SPIN-DEPENDENT INTERACTIONS [Thesis]. **Rubin, Morton Harold. Princeton, N. J., Princeton Univ., 1964. 68p.**

The Lippmann-Schwinger equation is used to study the scattering matrix for a particle interacting with a static potential through spin-dependent Yukawa forces. It is shown that the on energy-shell scattering matrix is meromorphic in j, the total angular momentum, to the right of the line $\mathrm{Re}\ j = s_{max} - \frac{1}{2}$, where s_{max} is the maximum value of the the spin of the system, and is meromorphic in the energy plane cut from 0 to ∞ and $-\infty$ to $-\mu^2/4$, where μ^{-1} is the range of the longest range force present. The leading Regge pole is shown to approach $s_{max} - 1$ in the small coupling constant or high-energy limit. It is also shown that the "sense" and "nonsense" channels decouple in the limit $j - s_{max} - 1$. To show that the physical scattering matrix is given by the Born-Neumann series at high physical energies, the Fredholm theory of integral equations is extended to Hilbert spaces of functions that are square integrable on a contour. By exploiting the analyticity of the potential matrix in the momentum indices a simple proof of the existence of the physical scattering matrix and the unitarity condition are given. (Dissertation Abstr.)

Fluid Physics and Thermodynamics

See *also* Plasma Physics and Thermonuclear Processes

13634 (AE-210) METHODS FOR THE DETERMINATION OF CURRENTS AND FIELDS IN STEADY TWO-DIMENSIONAL MHD FLOW WITH TENSOR CONDUCTIVITY. **Witalis, E. A. (Aktiebolaget Atomenergi, Stockholm (Sweden)). Dec. 1965. 14p. Dep. mn.**

Rigorous derivations are given of the basic equations and methods available for the analysis of transverse MHD flow when Hall currents are not suppressed. The gas flow is taken to be incompressible and viscous with uniform tensor conductivity and arbitrary magnetic Reynold's number. The magnetic field is perpendicular to the flow and has variable strength. Analytical solutions can be obtained either in terms of the induced magnetic field or from two types of electric potential. The relevant set of suitable simplifications, restrictive conditions, and boundary-value considerations for each method is given. (auth)

13635 (ARL-63-175(Pt.3)) A CRITICAL SURVEY OF MAGNETOFLUID DYNAMICS. PART III. QUASI-ONE-DIMENSIONAL ANALYSIS OF MAGNETOGAS DYNAMICS. **Pai, Shih-I (Maryland Univ., College Park). Mar. 1965. Contract AF33(657)-7805. 62p. CFSTI $3.00 cy, $0.50 mn.**

A critical survey of the flow of an ionized gas in a channel under the influence of transverse electromagnetic fields is presented. First, the exact quasi-one-dimensional equations of magnetogasdynamics are derived. The importance of the various covariance coefficients is pointed out. In the literature, only the cases with covariance coefficients of unity have been reported. A survey of these cases was made which includes inviscid steady flow, steady flow of viscous and heat-conducting fluid, and unsteady flow. Finally, the present understanding of quasi-one-dimensional flow of magnetogasdynamics is summarized and some recommendations are made for future research. (auth)

13636 (IPP-3/24) INTERFEROMETRISCHE UNTERSUCHUNGEN AN ELEKTROMAGNETISCH BESCHLEUNIGTEN STOSSWELLEN. (Interferometric Measurements on Electromagnetically Generated Shock Waves). **Brinkschulte, H. (Institut fuer Plasmaphysik, G.m.b.H. Garching (West Germany)). Dec. 1964. 55p. Dep. mn.**

The phenomena occurring in an electromagnetic shock tube (T-tube) were investigated with the aid of a rotating mirror camera and a Mach-Zehnder interferometer. The test gas used was hydrogen in the pressure range $2.5 < p_0 < 10$ mmHg. The investigations were conducted in the velocity range corresponding to Mach 6 to 20. The luminous phenomena detected with the rotating mirror camera are identical with the plasma already formed between the electrodes during the discharge. This so-called discharge plasma is extremely inhomogeneous and irreproducible. With the interferometer it was possible to show that a non-luminous shock wave is also formed. Unlike the discharge plasma, however, this shock wave is reproducible. The shock front is plane and always precedes the luminous front. As the velocity increases the distance between the two fronts decreases. At velocities exceeding 2.5 cm/μsec the discharge plasma advances right into the shock front. The discontinuity in the density across the front was also measured. This agrees with the value calculated from the Rankine-Hugoniot equations, if thermal equilibrium is assumed.

Since the gas was partially dissociated in the velocity range investigated, it was possible to determine experimentally the refractive index for atomic hydrogen. The shock wave itself runs free and is in an unsteady state (blast wave type). The total time history of the shock wave thus cannot be described with the Rankine-Hugoniot equations, it conforms rather to the homology theory according to von Weizsäcker. Interferometric measurements of both the density drop behind the front and the decrease of the shock front velocity along the tube support this theory. (auth)

13637 (IPP-3/28) ELEKTROMAGNETISCHE ERZEUGUNG VON STOSSWELLEN UND WECHSELWIRKUNG VON STOSSWELLEN MIT ELEKTROMAGNETISCHEN FELDERN. (Electromagnetic Production of Shock Waves and Interaction of Shock Waves With Electromagnetic Fields). Rebhan, Eckhard (Institut fuer Plasmaphysik, G.m.b.H., Garching (West Germany)). Aug. 1965. 68p. Dep. mn.

When a force is suddenly exerted within a confined region of a flow channel on a resting or flowing gas, a shock wave and a rarefaction wave are set up in opposite directions. This situation arises, with heat being generated in addition, when crossed electric and magnetic fields are suddenly applied to an electrically conductive gas at rest, or when a shock wave the region behind which is ionized passes through such a field configuration. This affords the possibility of producing shock waves or influencing a given shock wave electromagnetically. In dependence on the total force P and the total energy input W per second, the asymptotic solutions are investigated toward which the state of flow converges as interaction assumes a steady state. The Mach numbers M obtained when shock waves are produced electromagnetically are proportional to $P^{\frac{1}{3}}$ and $W^{\frac{1}{3}}$ for strong shocks. If the power is supplied by a battery with fixed data, M as a function of the applied magnetic field $\vec{B}$ has a maximum. Influencing a given shock wave electromagnetically causes reflection of shock or rarefaction waves and changes the intensity of the primary shock wave. With heat input only ($P = 0$, $W \geq 0$), the latter is accelerated; with momentum input only ($P \leq 0$, $W = 0$), it is slowed down. If its Mach number is sufficiently great before and after interaction, similar solutions are obtained for $P \sim W^{\frac{1}{3}}$. (auth)

13638 (IPP-6/39) GENERAL INTERCHANGE INSTABILITY. Schlueter, A. (Institut fuer Plasmaphysik, G.m.b.H, Garching (West Germany)). July 1965. 10p. Dep. mn.

Magnetohydrostatic equilibria are considered whose lines of force are interchangeable. The energy change is computed which follows from the interchange of a pair of flux tubes. The separation between the members of the pair and the flux of either tube are kept unspecified. Necessary conditions for stability against interchanges over finite distances are derived and expressed by $p,q = \int dl/B$, and $I = (1/\mu) \int B\, dl$. In the case of infinitesimal interchanges, a necessary and sufficient condition can be derived and considerably simplified by using the equilibrium condition $dI = -q\, dp$. This stability condition is shown to be equivalent to the simultaneous stability against interchange at constant volume and at constant flux. (auth)

13639 (JUL-281-PP) MAGNETISCHE SONDENMESSUNGEN WAEHREND DER VORHEIZPHASE EINES SPINDLE-CUSP-EXPERIMENTES. (Magnetic Probe Measurements During the Preheating Phase of a Spindle-Cusp Experiment). Belitz, H.-J.; Kugler, E. (Kernforschungsanlage, Juelich (West Germany). Institut fuer Plasmaphysik). Aug. 1965. 15p. Dep. mn.

The preheating of the plasma is produced by a fast condenser discharge (0.5 kJ and 800 khz) over the compression coil at the Jülich spindle-cusp experiment. By the use of coil probes, the radial and axial components and the contribution of the magnetic field were measured at various positions of the discharge apparatus. The measurements show the time point of the ignition and the capture of magnetic fields by the plasma. Several layers with opposed field direction are formed and these are only slowly resolved. (tr-auth)

13640 STATISTICAL THERMODYNAMICS WITH HIGHER ORDER TEMPERATURES FOR IDEAL GASES OF BOSONS AND FERMIONS. Ingarden, R. S. (Univ. of Wroclaw, Poland. Inst. of Physics, Polish Academy of Sciences, Wroclaw, Poland); Kossakowski, A. Acta Phys. Pol., 28: 495-511(Oct. 1965).

Ensembles of identical noninteracting bosons and fermions are discussed from the point of view of generalized thermodynamics with higher order temperatures. The generalized Bose, Fermi, and Boltzmann distributions are obtained and applied to the calculation of thermodynamical properties of these gases, whereby the framework of thermodynamical concepts is correspondingly extended. (auth)

13641 PLANE STATIONARY AND IRROTATIONAL HYDRODYNAMIC MOTION OF A FLUID FLOW IN A RIGID CIRCULAR PROFILE. Vacca, Jacopa. Atti Accad. Sci. Torino: I. Cl. Sci. Fis., Mat. Natur., 99: 959-76(1964-65). (In Italian).

The plane and stationary movement of an incompressible electrically conducting fluid, which in the absence of vortices and in presence of uniform magnetic field has a circular rigid profile of radius R, was studied. The velocity, which it is assumed will allow values up to infinity, was determined by the complex potentials. The particular case in which two components of the magnetic field are 0 was examined, and the third component was determined, from which were assigned the values of the circular profile using the method of successive approximations and the hypothesis of small electrical conductivity. (tr-auth)

13642 THE SLOW STATIONARY MOTION OF A VISCOUS ELECTRICALLY CONDUCTING LIQUID CONTAINED IN A SPHERICAL CHANNEL. Vacca, Maria Teresa. Atti Accad. Sci. Torino: I. Cl. Sci. Fis., Mat. Natur., 99: 993-1015(1964-65). (In Italian).

In a viscous electrically conducting liquid contained in a spherical channel and immersed in a uniform magnetic field, the vortex, the conduction current, the induced magnetic field, the velocity, and the pressure were determined with the method of successive approximations, in the case of axial symmetry and under the hypothesis that the viscosity coefficient and the magnetic diffusivity coefficient would be sufficiently small. (tr-auth)

13643 MAGNETOHYDRODYNAMIC FLOWS IN CLOSED REGIONS WITH COMPLETE SYMMETRY ABOUT AN AXIS. Eraslan, Arsev H. (Univ. of Tennessee, Tullahoma). J. Appl. Phys., 37: 98-109(Jan. 1966).

A formal perturbational technique was developed to obtain solutions for magnetohydrodynamic flow problems in closed regions with symmetric properties of flow and boundary conditions about an axis. The system of highly nonlinear partial differential equations, governing the problems of this class, was found to reduce to systems of simultaneous linear partial differential equations, thus creating a possibility of obtaining solutions by classical mathematical methods. The technique used was based on a well-known power series type of perturbational expansion in terms of a small parameter, which in the limit was assumed to become the solution of the original system. The general technique was applied to the magnetohydrodynamic flow in a toroid under the influence of a uniform applied magnetic field along the direction of the main axis of the toroid. It was found that the secondary flow caused by the centrifugal body force on the fluid element due to the curvature created induced electromagnetic components and a pressure variation along the radial direction. The solutions were carried out to include completely the second perturbational equations and the electromagnetic and flow fields were discussed for different values of characteristic parameters appearing in the solutions. (auth)

13644 CALCULATION OF THE HEAT CONDUCTIVITY OF CERTAIN GASES AT TEMPERATURES OF 1000 TO 20,000 K AND ATMOSPHERIC PRESSURES. Krinberg, I. A. (Geochemical Inst., Academy of Sciences, Siberian SSR). Teplofiz. Vysok. Temp., 3: 654-7(July-Aug. 1965). (In Russian).

The thermal conductivities λ of Ar, N, O, and H are calculated, taking into account the heat transfer effects of dissociation λ_D and ionization λ_I reactions: $\lambda = \lambda_0 + \lambda_D + \lambda_T$ (λ_0 = heat transfer by contact and diffusion). The formulas $\lambda_D = (pD_{am}/RT)(\Delta H_D^2/RT^2)[x_a x_m/(1 + x_m)^2]$ and $\lambda_I = (pD_{ia}/RT)(\Delta H_I^2/RT^2)[x_a x_i/(x_a + x_i)^2]$ are used where ΔH_D and ΔH_I are the heat effects of dissociation and ionization reactions; x_m, x_a and x_i are molar portions of molecules, atoms and ions; D_{am} and D_{ia} are coefficients of binary diffusion for atoms and molecules and for ions and atoms. Values for λ_0 for the 1000–8000°K range (<0.1% ionization) were taken from literature. For the 15,000–20,000°K range (>50% ionization), the Spittser formula was used, and values for λ_0 were extrapolated for the intermediate 8000–15,000°K range. Results are compared with previous data, and the reasons for differences are discussed. (ATD)

Geophysics

13645 (AWRE-O-9/66) GEOMAGNETIC MICROPULSATIONS. Orr, D. (Atomic Weapons Research Establishment, Aldermaston (England)). Feb. 1966. 21p. Dep. mn. BIS $0.65. HMSO 3s. 3d.

A survey is presented of various proposed models of the magnetosphere and experimental observations which a successful model must be able to explain. Observations of electromagnetic and hydromagnetic waves which occur within the magnetosphere in the period range for $\frac{1}{5}$ s to 10 min are discussed. Finally proposals are made for experiments which can be performed using data from UKAEA field stations. (auth)

13646 (NASA-SP-3024) MODELS OF THE TRAPPED RADIATION ENVIRONMENT. VOLUME I. INNER ZONE PROTONS AND ELECTRONS. Vette, James I. (Aerospace Corp., El Segundo, Calif.). 1966. Contract AF04 (695)-469. 58p. CFSTI $1.00 cy, $0.75 mn.

A model of the inner radiation belt is described. Electron and proton data obtained with this model are compared in detail with that obtained by various experimenters. (M.O.W.)

13647 TRAPPED PROTONS OF THE INNER RADIATION BELT [Thesis]. Fillius, R. Walker. Iowa City, Iowa, State Univ. of Iowa, 1965. 106p.

Satellite Relay I performed a thorough mapping of the energy spectrum and spatial distribution of protons in the inner zone. New intensity maps are presented for six energy ranges between 1.1 and 63 Mev as of January 1, 1963. With these six distributions and previously published intensities in two more ranges accurate energy spectra at arbitrarily selected locations throughout most of the inner zone can be constructed. In any energy range, the maximum intensity is found at the equator and varies along a line of force near the equator as the third or fourth power of 1/B. There are fewer high-energy than low-energy protons, and they are found closer to the earth. Sample intensities are $j_I = 3.7 \times 10^6$ cm^{-2} sec^{-1} ster^{-1} from 1.1 to 14 Mev at L = 2.2 on the equator and $j_I = 1.6 \times 10^4$ cm^{-2} sec^{-1} ster^{-1} from 18.2 to 25 Mev at L = 1.6 on the equator. Comparison of Relay I data with other experiments demonstrates the value of a comprehensive treatment. Neutron albedo sources, both cosmic-ray and solar proton sources, are weaker than required by as much as three orders of magnitude at 1 Mev. Adiabatic breakdown theories are in disagreement with the spatial dependence of the energy spectrum and cannot be controlling factors. Injection and diffusion of solar wind particles is a possible source, but more theoretical work is needed to clarify the expected results. (Dissertation Abstr.)

Gravitation, Quantum Mechanics, and Relativity Theory

Refer also to abstract 13600.

13648 (ORNL-3877(Rev.)) FORTRAN PROGRAMS FOR THE CLEBSCH-GORDAN AND RACAH COEFFICIENTS AND THE NINE-j SYMBOL. Tamura, Taro (Oak Ridge National Lab., Tenn.). [nd]. Contract W-7405-eng-26. 10p. Dep. mn. CFSTI $1.00 cy, $0.50 mn.

FORTRAN programs for the Clebsch-Gordan and Racah coefficients and 9-j symbol are presented. They are written in a way rather compact and easy to understand. Optimization of the speed of computation was made in these routines. These routines allow for treating the case in which the arguments of these coefficients are very large, and thus can be used, for example, in the analysis of the nuclear reactions of heavy and high energy projectiles. (auth)

13649 QUANTUM THEORY OF SYSTEMS WITH MANY DEGREES OF FREEDOM, SYMPOSIUM AT KESZTHELY [HUNGARY], SEPTEMBER 1964. Acta Phys. Acad. Sci. Hung., 19: 1-363(1965). (CONF-640924).

Thirty-nine papers are presented; separate abstracts were prepared for each. (L.B.S.)

For abstracts of individual papers see: 13348, 13416, 13464–13467, 13552–13570, 13650–13655, 13669–13671, 13789–13792, and 13976.

13650 ON THE ABSTRACT APPROACH TO THE MANY-BODY PROBLEM WITH INFINITE VOLUME. Fano, G. (Univ., Bologna). Acta Phys. Acad. Sci. Hung., 19: 99-108(1965).

After discussing the classification of the possible representations of the canonical commutation and anticommutation relations, the problem of finding the suitable representation for a given hamiltonian is investigated. The consequences of the Galilean invariance of the theory are considered. (auth)

13651 ON SYMPLECTIC-INVARIANT MANY-FERMION PROBLEMS. Gyoergyi, G.; Revai, J. (Central Research Inst. for Physics, Budapest). Acta Phys. Acad. Sci. Hung., 19: 123-7(1965).

A class of symplectic-invariant many-fermion hamiltonians is investigated. A special model hamiltonian is found for which a complete set of "generalized BCS eigenstates" (i.e., eigenstates with definite values of the quasiparticle number) can be constructed. (auth)

13652 GAUGE TRANSFORMATIONS AND INEQUIVALENT REPRESENTATIONS. Leplae, L. (Univ., Naples). Acta Phys. Acad. Sci. Hung., 19: 133-7(1965).

The connection between gauge transformation and inequivalent representations is investigated in a self-consistent way. (auth)

13653 A PROOF OF THE COMPLETENESS OF THE SOLUTIONS OF THE SCHROEDINGER EQUATION IN THE λ-PLANE. Burdet, G.; Giffon, M. (Institut de Physique Nucleaire, Lyon). Acta Phys. Acad. Sci. Hung., 19: 263-7 (1965).

It is proved that the system of solutions of the Schrödinger equation in the complex λ-plane is complete. (auth)

13654 THE PROBABILITY OPERATOR ρ IN MANY BODY PROBLEM. Macke, W. (Technische Univ., Dresden). Acta Phys. Acad. Sci. Hung., 19: 321-37(1965). (In German).

An investigation is made of the totality of all physical problems concerning systems of the type $H = \Sigma_i t_i + \Sigma_{i<j} U_{ij}$. The treatment of nonrelativistic quantum-mechanical many-body problems is characterized by the form of the hamiltonian operator. After formulation of the general problem, equations are derived for the expectation value and the probability operator as functions of time. The reduced probability operator is defined. The use of perturbation-theoretical calculations and approximation methods are discussed. Matrix representations are treated, and, as a special case, the field representation of the many-body problem is considered. (L.B.S.)

13655 ON THE "BEST" APPROXIMATION IN QUANTUM MECHANICS. Hoffmann, T. A. (Central Research Inst. for Physics, Budapest). Acta Phys. Acad. Sci. Hung., 19: 339-48(1965).

In quantum mechanical approximations the difficulty generally arises that the error of calculation cannot be estimated uniquely. By using matrix calculus and the rules of trace calculus the error of approximation is defined

uniquely for any quantum mechanical calculation (in the framework of matrix formalism). This also makes it possible to find a more rapidly convergent method to carry out the calculations. The method is very suitable for use with computers as it contains direct operations only. (auth)

13656 EQUATIONS OF MOTION OF A RELATIVISTIC BI-POINT MODEL OF FREE ELEMENTARY PARTICLE IN AN EXTERNAL GRAVITATIONAL FIELD. Borelowski, Z. (Jagellonian Univ., Krakow). Acta Phys. Pol., 28: 585-97(Nov. 1965).

A particle characterized by its rest mass m_0, coordinates x^α and a vector r^α related to the coordinates is considered, assuming it to be space-like of constant spatial length l in the own reference system of the particle. Motion in Minkowski space is assumed to be determined by the variational principle $\delta\int_{\tau_1}^{\tau_2} L d\tau = 0$, where τ is the proper time of the particle and the Lagrangian L is given by $L = -m_0 c(\sqrt{u_\lambda u^\lambda} + \sqrt{-\dot{r}_\lambda \dot{r}^\lambda}) + \Lambda r_\lambda r^\lambda$. Moreover, c is the velocity of light, u^λ – the four-velocity, $\dot{r}_\lambda \overset{df}{=} dr_\lambda/d\tau$, and Λ – Lagrange's factor to be determined from the equations of motion. The particle is found to be a spin particle. The spin bi-vector is denoted by $s^{\alpha\beta}$ ($s^{\alpha\beta} \sim r^\alpha \dot{r}^\beta - r^\beta \dot{r}^\alpha$). The constant $l(r_\lambda r^\lambda = -l^2)$ is a measure of the particle's diffluence in its own reference system. Considering it as a test particle, a search is made for its equations of motion in an external gravitational field with potentials $g_{\mu\nu}$. In a first approach, the same principle as in Minkowski space is used. In a second approach ideal liquid representation is used, starting from the well-known principle of least action, assuming traditionally action of the field. The equations of motion obtained by the two methods are identical. It results that L is a first integral of the equations of motion, the module of spin ($S^{\lambda\nu}S_{\lambda\nu}$) is constant in the time, and the gravitational field only modifies the shape of the equations to functions $u^\alpha = u^\alpha(\tau)$ (thus modifying motion of the particle as a whole) but does not modify the shape of the equations of motion from which we obtain the dependence $r^\alpha = r^\alpha(\tau)$; this vector and its derivative with respect to the own time generate the bi-vector of spin of our particle. (auth)

13657 UNCERTAINTY RELATION BETWEEN TIME AND ENERGY. Chylinski, Zygmunt (Inst. of Nuclear Research, Krakow). Acta Phys. Pol., 28: 631-8(Nov. 1965).

On the example of a "thought-experiment" proposed by Einstein and analyzed by Bohr, the uncertainty relation between time and energy is considered and another point of view with regard to that experiment is proposed. The main idea consists here in the recognition of the uncertainty relations as an intrinsic property of physical geometry. Thus the uncertainty relations should appear as representing the general nature of the metrical relations of all physical objects rather than a complementary characteristic of our cognition, as Bohr regards them. (auth)

13658 SIMPLIFIED RENORMALIZATION THEORY IN QUANTUM ELECTRODYNAMICS. Bialynicki-Birula, I. (Univ., Warsaw). Bull. Acad. Pol. Sci., Ser. Sci. Math. Astron. Phys., 13: 499-503(1965).

A general theory of renormalization is developed in which the problem of overlapping divergences is solved by a new method. The method is applied to quantum electrodynamics, where the renormalization is simplified by the Ward identity and the absence of the divergent four-photon interaction. The set of Schwinger equations for the time-ordered Green's functions (the electron propagator, the photon propagator, and the vertex function) is rearranged so as to yield renormalized solutions when treated by the perturbation method. (M.J.T.)

13659 THE NUMBER OF QUANTA AS AN INVARIANT OF CLASSICAL ELECTROMAGNETIC FIELD. Zel'dovich, Ya. B. Dokl. Akad. Nauk SSSR, 163: 1359-60(Aug. 21, 1965). (In Russian).

An electromagnetic field E(x), H(x) at t = constant is considered in the absence of charges and fluxes. Such a field may be regarded as a set of electromagnetic waves; by means of its Fourier derivation, the number of quanta of each frequency and the number of quanta of a given field N may be obtained. The expression for N was derived through a coordinate representation of E and H in the Gaussian system of units. The first portion of the expression developed for a classical field, did not contain Planck's constant. The classical value is the integral of the motion of the free field and is a relativistic invariant. Proof of the formula obtained is given by decomposing E and H into transversal waves. A similar expression was obtained by J. A. Wheeler in connection with the probability of a given distribution of H(x) in the fundamental state of the vacuum. (TTT)

13660 TWO-COMPONENT SPINORS IN THE HAMILTONIAN FORMULATION OF GENERAL RELATIVITY. Oliveira, C. G. (Centro Brasileiro de Pesquisas Fisicas, Rio de Janeiro). Nuovo Cimento, (1), 3: Suppl., 192-244 (1965).

The Dirac-Hamiltonian formulation of general relativity is developed in terms of two-component spinors and spin matrices. The basic properties of the standard spinor theory of van der Waerden are briefly reviewed, followed by a brief account of Dirac's Hamiltonian formulation of general relativity in the standard tensor form. The problem of the determination of the dynamical variables is then treated in the framework of the spinor theory of general relativity. The emergence of the new six spin constraints, the meaning of these constraints in terms of infinitesimal canonical transformations, and the associated generators are discussed. Application of the formalism is made to the determination of the classical commutator for infinitesimal separated times, up to the first order. (L.B.S.)

13661 GREEN FUNCTIONS FROM LIE ALGEBRAS. Budini, P. (Univ. Trieste, Italy. International Center for Theoretical Physics, Trieste, Italy). Nuovo Cimento, (10), 41A: 399-401(Feb. 1, 1966).

A method is outlined for solving the dynamic problems of quantum systems in which the Casimir operators of the noncompact algebra can be expressed in well-defined Riemannian spaces as linear differential equations. The dynamic equations thus obtained give both the eigenfunctions and eigenvalues of the mass and Green functions. (L.B.S.)

13662 GEOMETRICAL INTERPRETATION OF ELECTRODYNAMICS. AN ANALYSIS. Froehlich, H. (Univ. of Liverpool). [Progr. Theoret. Phys. (Kyoto), 34: Suppl., 1-13(1965)].

The requirement that generators of local Lorentz transformations of vector fields should exist demands introduction of operators that do not commute with these fields. An analysis shows that electrodynamics in its quantized form contains these generators. They are principally based on the vector potentials. Thus field quantization can be understood as following from geometrical considerations, and the potentials are shifted from an auxiliary to a leading role. (auth)

13663 THE NON-LOCALITY OF FORCE. Wheeler, John Archibald (Princeton Univ., N. J.). [Progr. Theoret. Phys. (Kyoto), 34: Suppl., 127-34(1965)].

According to Einstein's principle of equivalence, the proper measure of the gravitational field is provided, not by the acceleration of one neutral test particle, but by the relative acceleration of two nearby test particles. This relative acceleration is described by the equation of geodesic deviation. In this equation the Riemann curvature tensor provides the mathematical measure for the physically relevant feature of the gravitational field, the "tide-producing force." It is shown that the electromagnetic field can be described by way of a higher-order equation of geodesic deviation based on higher differences between the positions of a whole group of nearby neutral test particles. In this sense the gravitational and electromagnetic field can be regarded as describing nonlocal features of space. Space locally always has Lorentz geometry, no matter how strong the fields may be. (auth)

13664 THE MEASURING PROCESS IN QUANTUM MECHANICS. Rosenfeld, Leon (NORDITA, Copenhagen). [Progr. Theoret. Phys. (Kyoto), 34: Suppl., 222-31(1965)].

It is pointed out that the deficiencies in von Neumann's axiomatic treatment of the measurement problem led to misinterpretations in the translation of Bohr's argument into formal language in an attempt to develop a consistent theory of atomic processes, and that these deficiencies have been completely removed by the discussion of the measuring process in quantum mechanics carried out by Daneri, Loinger and Prosperi. A summary and comment on these works are presented in order to show how the fundamental statistical predictions of the theory closely correspond to the possibilities of determining the physical quantities compatible with the existence of the quantum of action. (L.B.S.)

13665 GRAVITATION PHYSICS. Hiida, Kichiro; Yamaguchi, Yoshio (Tokyo Univ.). [Progr. Theoret. Phys. (Kyoto), 34: Suppl., 261-97(1965)].

Gravitational interactions are generally investigated under the assumptions: the Lorentz invariance (special relativity), (CPT) invariance, gauge invariance, and the weak (gravitation) field approximation. Discussions are given for possible effects of P and T violating gravitational interactions as well as empirical upper limits on the degrees of such violations. (auth)

Low Temperature Physics

Refer also to abstract 13048.

13666 (IPP-4/22) UNTERSUCHUNGEN AN MATERIALIEN FUER SUPRALEITENDE SPULEN. (Tests on Materials for Superconducting Coils). Amenda, W.; Berkl, E. (Institut fuer Plasmaphysik, G.m.b.H., Garching (West Germany)). Apr. 1965. 25p. Dep. mn.

The essential problem involved in the planning of superconducting magnetic coils for high fields is that of the electrical behavior of the conducting material, i.e., the maximum magnetic field strength obtainable with the available conducting material for a given coil geometry without quenching the coil. The I_c–H curves of short samples in an external magnetic field that are usually provided by suppliers allow only very indefinite conclusions regarding the coil behavior, the coil values being lower than the values of the short samples by a factor of 2 and more. This behavior is generally referred to as degradation effect. Measurements of I_c–H curves were made for short samples of commercially available material. All depending on the previous magnetic history, two completely different I_c–H curves were obtained which possibly represent the maximum and minimum of the coil values obtainable. (auth)

13667 (JINR-P-2533) SVERKHPROVODYASHCHII MAGNIT IZ Nb-75 PERCENT Zr NA 85 KGS. (An 85 kG Superconducting Magnet Made of Nb-75 Percent Zr). Goncharov, I. N. (Joint Inst. for Nuclear Research, Dubna (USSR). Lab. of High Energy). 1965. 13p. Dep. mn.

A solenoid made of Nb–Zr wire is described. At about 4.2 and 4.05°K, the maximum magnetic fields in the solenoid are 53.0 and 57.5 kgauss, respectively, with critical currents of 42.5 and 46.0 amp, respectively. The solenoid is very stable; there are no critical current degradation effects. Ferromagnetic poles in the solenoid permit an increase in the field strength up to 85 kgauss in the 1.1-mm gap. (D.C.W.)

13668 (LA-3426) COOLDOWN OF CRYOGENIC TRANSFER LINES. Liebenberg, D. H. (Los Alamos Scientific Lab., Univ. of California, N. Mex.). Nov. 22, 1965. Contract W-7405-eng-36. 22p. Dep. mn. CFSTI $1.00 cy, $0.50 mn.

During the design and planning of the liquid hydrogen transfer lines at Test Cells "A" and "C" at the Nuclear Rocket Development Station in Nevada, LASL instituted a program to study the cooldown of these lines. Included are the several computational techniques developed to predict the cooldown process and the comparison of the computations with measurements made using the completed Test Cell "C" facility. (auth)

13669 A SUPERCONDUCTIVE MODEL WITH TWO KINETIC ENERGIES FOR EVEN AND ODD SYSTEMS. Nemeth, J. (Roland Eoetvoes Univ., Budapest). Acta Phys. Acad. Sci. Hung., 19: 129-31(1965).

A previous discussion (Acta Phys. Hung., 18: 221(1965)) on the superconductive model is continued. The energy of an odd system is determined in the quasispin formalism and is compared with the corrected energy in the BCS approximation. (L.B.S.)

13670 QUASI-PARTICLE OPERATORS FOR THE CONDENSED BOSE SYSTEM. Weller, W. (Karl-Marx-Univ., Leipzig). Acta Phys. Acad. Sci. Hung., 19: 159-62 (1965).

The concept of quasi-particle operators is used for the condensed Bose system. The operators depend on the relative motion of the superfluid and the normal component. (auth)

13671 ON THE RELAXATION TIME FOR NONEQUILIBRIUM STATE OF SUPERFLUID. Iordansky, S. V. (Steklov Mathematical Inst., Moscow). Acta Phys. Acad. Sci. Hung., 19: 163-70(1965).

The idealized problem of spatially homogeneous flow with different velocity of the normal and superfluid components is treated. The aim of the investigation is the development of the expression for the number of vortex rings which reach the critical size in the unit of time. (auth)

13672 MAGNETIC FIELD DISTRIBUTION IN A TYPE II SUPERCONDUCTOR. Cline, H. E.; Rose, R. M.; Wulff, J. (Massachusetts Inst. of Tech., Cambridge). J. Appl. Phys., 37: 1-5(Jan. 1966).

Direct measurements of the magnetic field distribution in the gap between half-ellipsoids of niobium in plastically deformed and annealed states were made using a bismuth thin-film magnetoresistance probe. An empirical equation of the form $r - r_0 = C_0B + C_1(e^{C_2B} - 1)$ for the field distribution in the deformed sample was found. For the annealed sample, a surface discontinuity of the field was observed, which is a boundary condition for the equilibrium magnetization. Flux jumping was observed when the field was not increased slowly. The distribution in the annealed specimen had reproducible irregularities. (auth)

13673 SUPERCONDUCTIVITY OF A COMPOSITE OF FINE NIOBIUM WIRES IN COPPER. Cline, H. E.; Strauss, B. P.; Rose, R. M.; Wulff, J. (Massachusetts Inst. of Tech., Cambridge). J. Appl. Phys., 37: 5-8(Jan. 1966).

Composites consisting of fine Nb filaments in a copper matrix were fabricated, and the following superconducting properties measured: the critical temperature, critical transverse magnetic field as a function of temperature, critical current density at 4.2°K as a function of transverse magnetic field, and magnetization at 4.2°K. The reduction in Nb filament size was checked by optical and electron micrography. Filament diameters ranged down to 100 Å. As the diameter decreased, T_c, $H_c(T)$, and J_c all decreased. This behavior was attributed to the proximity effects of the copper matrix on the Nb. The results are closely comparable to those of investigations of superimposed thin films. It is therefore not expected that high critical fields can be attained by composites involving a type II superconductor in a matrix of a nonsuperconductor. (auth)

13674 ANOMALOUS CRITICAL CURRENTS IN SUPERCONDUCTING NONINDUCTIVE COILS OF Nb-25 percent Zr WIRE. Lubell, M. S. (Westinghouse Electric Corp., Pittsburgh). J. Appl. Phys., 37: 258-62(Jan. 1966).

The critical current vs preset magnetic field was measured for a number of multilayer bifilar noninductive coils wound with cold-worked 0.025-cm-diam Nb–25% Zr wire. In an applied field greater than 8 kG and less than 24 kG the superconducting to normal transitions are not single-valued and show an effect analogous to antitraining. It is

shown that the anomalous critical currents are due to cooling in a constant applied field. The conditions for obtaining, avoiding, and eliminating the different values of critical current were investigated, and the results are compared with short-sample and magnet data. The experimental results suggest the unorthodox view that high transport currents are obtained when induced magnetization currents are initially present and low transport currents are measured when only the reversible magnetization is present in part of the noninductive coil. (auth)

13675 BEHAVIOR OF SUPERCONDUCTING COIL SUBJECTED TO STEADY LOCAL HEATING WITHIN THE WINDINGS. Stekly, Z. J. J. (Avco-Everett Research Lab., Everett, Mass.). J. Appl. Phys., 37: 324-33(Jan. 1966).

The steady-state heat conduction equation in a nonisotropic solid is solved for the relation between local heat imput, the size of the heated region, and the Joule heating in the resultant normal region. The results are used to derive the steady terminal voltage–current characteristics of a superconducting coil with heat generation within the windings. These terminal characteristics exhibit both a positive as well as a negative slope of the voltage versus current curve. A map of the expected behavior of a current carrying superconducting coil with heat generation in the windings shows that the coil can do one of three things: (1) remain fully superconducting; (2) operate in a stable manner with a nonpropagating normal region; (3) go fully normal (quench). The analytical results are compared with measurements taken with a noninductive and an inductive coil. The measured terminal characteristics as well as over-all coil behavior agree well with the result derived analytically. (auth)

13676 CRITICAL TEMPERATURE OF THIN SUPERCONDUCTING FILMS. Kirzhnits, D. A.; Maksimov, E. G. (Lebedev Physics Inst., Moscow). JETP Lett. (USSR)(Engl. Transl.), 2: 274-6(Nov. 1, 1965).

Translated from Zh. Eksp. Teor. Fiz., Pis'ma Redakt., 2: 442-5(Nov. 1, 1965).

The critical temperature of a film with an interaction parameter which is variable over the thickness is studied. (D.C.W.)

13677 A MODEL EXHIBITING TYPE II SUPERCONDUCTIVITY. Griffiths, D. J. (Univ. of Exeter, Eng.). Phys. Lett., 20: 99-100(Feb. 1, 1966).

A charged ideal Bose gas is found to be a type II superconductor. In its "mixed" state an external magnetic field penetrates uniformly. The range of order is reduced to a finite, large value, but the superfluid properties are not entirely destroyed. (auth)

13678 FIELD ENHANCEMENT IN SUPERCONDUCTING TUBES. Gayley, R. I.; Young, E. F. (State Univ. of New York, Buffalo). Phys. Lett., 20: 104-5(Feb. 1, 1966).

An empirical formula, $f_{av} = (o.d./i.d.)^{0.58}$, describing the behavior of a large class of specimens, is presented as evidence of an unexpected regularity in the field enhancement effect. Some clues as to the nature of its explanation are given. (auth)

13679 MAGNETIC HYSTERESIS AND SURFACE SUPERCONDUCTIVITY. Jones, D. P.; Park, J. G. (Imperial Coll. of Science and Tech., London). Phys. Lett., 20: 111-12(Feb. 1, 1966).

Evidence is found which shows that the hysteretic tail in the magnetization curves of four alloys at 3.3°K, which develops with increasing concentration, is due to a persistent surface current flowing in the superconducting region. If the specimen is a cylindrical rod parallel to the field the surface currents will flow around the specimen in closed loops in planes normal to the axis, flowing in one direction or the other depending on whether the field is increasing or decreasing. The hysteresis is also characterized by a splitting of the magnetization curve in the intermediate state close to the critical field; that is, the curves taken in increasing and decreasing field become separated. The suggestion that both the splitting and the tail are due to surface currents is supported by an experiment which is described. (J.F.P.)

13680 CYLINDRICAL JOSEPHSON JUNCTIONS. Tilley, D. R. (Mullard Research Labs., Redhill, Eng.). Phys. Lett., 20: 117-18(Feb. 1, 1966).

In a cylindrical junction, the quantization of flux through the junction area means that the d-c Josephson current must be either its zero field value or else exactly zero. Microwave resonances are possible, but do not appear to be useful. (auth)

13681 ON THE ANGULAR DEPENDENCE OF THE UPPER CRITICAL FIELD IN THIN FILMS. Yamafuji, K.; Kawashima, T.; Irie, F. (Kyushu Univ., Fukuoka, Japan). Phys. Lett., 20: 122-3(Feb. 1, 1966).

The upper critical field in thin films is calculated by applying a perturbation method to the Ginzburg-Landau equation. Tinkham's expression is modified by the present calculation which explains its deviation from the observed data. (auth)

13682 PREFERRED RATES IN HELIUM FILM TRANSFER. Harris-Lowe, R. F. (Ohio State Univ., Columbus); Mate, C. F.; McCloud, K. L.; Daunt, J. C. Phys. Lett., 20: 126-8(Feb. 1, 1966).

Observations of discontinuities in the transfer rate for He II film flow over glass, from 0.4 to 1.5°K, are summarized and their interpretation is discussed. (auth)

13683 SUPERCONDUCTIVITY IN GROUP V^a DICHALCOGENIDES. Van Maaren, M. H.; Schaeffer, G. M. (Philips' Gloeilampenfabrieken, Eindhoven, Netherlands). Phys. Lett., 20: 131(Feb. 1, 1966).

Group V^a dichalcogenides were investigated for superconductivity down to 1.0°K. Besides $NbSe_2$, NbS_2 was found to become superconducting at 6.2°K. Measurements were made on single-crystal specimens. (auth)

13684 ULTRASONIC INVESTIGATION OF FLUX PENETRATION INTO SUPERCONDUCTING NIOBIUM. Gottlieb, M.; Jones, C. K. (Westinghouse Research Labs., Pittsburgh). Phys. Lett., 20: 150-1(Feb. 1, 1966).

The influence of the geometrical parameters, sample shape and magnetic field direction of the field at which initial flux penetration occurs into superconducting niobium was investigated ultrasonically. (auth)

13685 FLUXOID QUANTIZATION AND CRITICAL FIELDS IN SMALL SUPERCONDUCTING SAMPLES. White, R. H. (Univ. of Singapore). Phys. Rev., 142: 241-7(Feb. 1966).

A theoretical treatment of the critical fields of thin superconducting films and related microgeometries is presented. This treatment is based on the Ginzburg-Landau theory and the quantization of the fluxoid. A symmetric superconducting surface state is found which contains fluxoid vortices. This surface state may exist in type-II films in parallel fields or in small samples of thin films in normal fields. For a sample which is infinite in one transverse dimension a critical-field dependence is found which is similar to that previously found theoretically by Saint-James and de Gennes. The model is extended to treat samples which are limited in both transverse dimensions. Excellent qualitative and semiquantitative agreement is found with the experiments of Parks, Mochel, and Surgent which determine the critical field in a microscopic superconducting bridge. (auth)

13686 THERMAL AND ELECTRICAL CONDUCTIVITIES OF Mo–Re ALLOYS IN THE SUPERCONDUCTING AND NORMAL STATES. Lerner, E.; Daunt, J. G. (Ohio State Univ., Columbus). Phys. Rev., 142: 251-8(Feb. 1966).

Details of research carried out on the low-temperature properties of Mo–Re alloys in the superconducting and normal states are given. Measurements were made on a variety of Mo–Re alloys in various states of anneal, the alloys being in the form of fine wires, as suitable for the winding of high-field superconducting solenoids. Micrograph studies were made to determine the percentage of

the various phases present in each specimen. The low-temperature measurements covered observations on the various specimens of the electrical resistivity and the thermal conductivity as functions of temperature and magnetic field. The measurements yielded evaluations of two of the three critical magnetic fields, H_{c2} and H_{c3}, as functions of temperature and alloy constitution, the transition temperatures T_c, and the Landau-Ginzburg parameter κ. Detailed comparisons of the results are made with theoretical predictions and with previous results on similar high-field superconducting alloys. (auth)

13687 TUNNEL-EFFECT MEASUREMENTS ON SUPERIMPOSED LAYERS OF LEAD AND ALUMINUM. Frerichs, R.; Wilson, J. P. (Northwestern Univ., Evanston, Ill.). Phys. Rev., 142: 264-6(Feb. 1966).

Superimposed Al and Pb films are studied using the tunnel effect as an indication of the influence of a normal metal (Al) on a superconductor (Pb). The structures are composed of four layers, $Al/Al_2O_3/Pb/Al$. The Pb and top Al layers were vacuum-evaporated onto 77°K substrates to eliminate diffusion problems. Curves are presented which show the effect of an overlayer on the tunnel-junction I-V characteristic and density-of-states function. The film thicknesses are varied over a wide range. The variation in energy gap with Pb thickness is plotted for a constant Al overlayer of 3100 Å. In addition there are three samples made to determine the critical temperature by resistive measurements with the same structure as a check on the reliability of the tunnel-function results. The energy-gap transition occurs between 300 and 4500 Å of Pb. Comparison with Hauser and Theuerer's results on superimposed Al and Pb films is included in the discussion. (auth)

13688 SPECTRUM OF THE BCS REDUCED HAMILTONIAN IN THE THEORY OF SUPERCONDUCTIVITY. Kato, Yusuke (Kobe Univ., Japan). Progr. Theoret. Phys. (Kyoto), 34: 734-53(Nov. 1965).

The spectrum and eigenstates of Bardeen-Cooper-Schrieffer's reduced hamiltonian in the theory of superconductivity are investigated in a mathematically rigorous manner. The hamiltonian is defined first for a finite number of electrons contained in a finite volume. The interaction hamiltonian is assumed to take a simple form. The hamiltonian after the Bogolyubov transformation (transformed hamiltonian) has a limit in the weak topology of Hilbert space when the volume tends to infinity with the number density of electrons kept constant. In the limit the interaction part vanishes and the free part gives a continuous excitation spectrum of Bogolons (transformed electrons). It should be noticed that the operator norm of the former does not tend to zero and, like the total hamiltonian, has no strong limit. An equivalent boson which consists of two Bogolons with opposite momenta and spins is introduced. In the Fock space for the bosons the hamiltonian has a strong limit for infinite volume. The limit operator has the same excitation spectrum of Bogolons as the free hamiltonian, and the existence of the lower limit of the spectrum is shown for some special class of the interactions. For large volume the limit operator is a good approximation to the transformed hamiltonian. The ground state of the free part of the transformed hamiltonian (i.e., the ground state of Bardeen-Cooper-Schrieffer's calculation) is not the exact eigenstate of the transformed total hamiltonian, and the difference does not vanish when the volume tends to infinity. (auth)

13689 VORTEX THEORY OF SUPERCONDUCTIVE MEMORIES [Thesis]. Pearl, Judea. Brooklyn, N. Y., Polytechnic Inst. of Brooklyn, 1965. 203p.

A physical model that describes storage phenomena in continuous superconducting films is established. The model is based on the Ginsburg-Landau theory and emphasizes the concepts of flux quantization and vortex excitation. With the concepts developed, the operation of superconductive memories employing such films can be formulated in terms of simple rules governed by the principles of vortex mechanics. A special Green's function is developed to handle electromagnetic problems involving thin films. With its aid, the magnetic properties of thin superconductive films versus those of bulk superconductors are discussed and an effective penetration depth for thin films is derived. The function is applied to the solution of a practical problem, namely, the current distribution in a superconducting film under a strip line, which carries a uniform current. Abrikosov's flux tubes model and the stability of vortex structures in thin films made of type I superconductors are discussed. The mechanics of quantized vortices in superconducting films is developed on the basis of the narrow core approximation. The interaction of a superconducting vortex with external magnetic fields and with neighboring vortices is derived. The basic properties of vortices in thin films are derived and compared to those of vortices in bulk superconductors. Vortex pinning, which is responsible for stable storage, is discussed. Expressions are derived for the interactions of a vortex with material defects and with diamagnetic bodies close to the storage film. The transition processes, between states of different vortex configurations, are studied. The applicability of Ginsburg-Douglass formula for the critical field of superconductive films is examined under the geometrical conditions of the memory cell. The role of film defects in triggering instabilities is studied by linearizing the Ginsburg-Landau equations. (Dissertation Abstr.)

13690 AN INVESTIGATION OF THE MAGNETIC EFFECTS OF ROTATING SUPERCONDUCTORS [Thesis]. King, Creston Alexander Jr. Houston, Tex., Rice Univ., 1965. 76p.

The magnetic field inside a superconductor rotating with an angular frequency ω is given by $\underline{B}/\omega = -(2mc/e) = 1.137 \times 10^{-7}$ gauss-sec. Measurements were made on a hollow tin cylinder (length = 22.0 mm, inner diameter = 13.0 mm, outer diameter = 14.3 mm) and a solid tin cylinder (length = 50 mm, diameter = 10 mm) immersed directly in liquid helium and rotating at speeds below 12,000 rpm. The magnetic fields were measured with a modified Hewlett-Packard flux gate magnetometer positioned in the center of the hollow cylinder or within a re-entrant cylindrical cavity in the bottom of the solid cylinder. The magnetometer was calibrated at helium temperature with a possible error of 5%. The rotational frequency was known to 3%, giving an estimated error limit of 8%. A high permeability cylindrical shield constructed from three sheets of 0.014" Conetic-AA was used to reduce the stray field to about 5×10^{-3} gauss. Further reduction of the d-c fields to about 2×10^{-4} gauss was obtained with Helmholtz coils. Plots of the angular speed versus field were made with an x-y recorder and the data were analyzed by the method of least squares. The average of 14 runs gave a slope of $1.08 \pm 0.08 \times 10^{-7}$ gauss-sec. The field trapped in the hollow cylinder was found to depend on the conditions during the normal to superconducting transition. For the solid cylinder preliminary results indicate that the effect is independent of the initial conditions as predicted by London. It is shown that the current distribution produced by uniform rotation of a multiply or singly connected superconductor is the same as that which would be produced by application of an external field $\underline{H} = (2mc/e)\,\omega$, where ω is the angular frequency of rotation. The experimental results are in agreement with this principle, and with the flux conservation law modified to account for the rotation. (Dissertation Abstr.)

13691 AN INVESTIGATION OF THE CHARGED BOSE GAS MODEL OF SUPERCONDUCTIVITY AS APPLIED TO PERSISTENT CURRENTS AND JOSEPHSON TUNNELING [Thesis]. Smith, Todd Iversen. Houston, Tex., Rice Univ., 1965. 89p.

Measurements were made on the stability of persistent currents in long hollow cylinders of tin and mercury. The results indicate that end effects are very important, but the observed stability limits exceed the limits calculated by Bloch and Rorschach, as well as those suggested by Wentzel and by Parikh. Several interesting time effects were observed. These results suggest that lifetime effects may be important and necessary for a complete understanding of persistent currents. The charged Bose gas model was also

used to study Josephson tunneling between superconductors. The usual features of Josephson tunneling are reproduced in the model. In the case of a thin-walled ring with n identical junctions (persistent current loop), the model predicts flux quantization in units of $hc/2e^*$ if n is odd, and in units of hc/e^*, the usual flux quantum, if n is even ($e^* = 2e$ is the charge of a boson). The present experimentally determined upper bound on the voltage across a Josephson junction is of the order of 10^{-5} volts. Using a persistent current loop it should be possible to set an upper limit smaller by several orders of magnitude. The design of apparatus to extend this limit to 10^{-17} volts is discussed. (Dissertation Abstr.)

13692 THE LOW TEMPERATURE SPECIFIC HEAT OF GRAPHITE AND SEVERAL PURE SUPERCONDUCTORS [Thesis]. van der Hoeven, Bernard Jacob Cornelis Jr. Lafayette, Ind., Purdue Univ., 1964. 59p.

Below 1.2°K, the specific heat of natural Madagascar graphite is $C = 13.8\ T + 27.7\ T^3\ \mu$ J/mole deg. The coefficient of the linear term agrees well with theoretical calculations of the electronic specific heat of a pure single crystal of graphite. The T^3 term yields a Debye parameter, Θ_0, of 413°K. For pile graphite, lampblack, and pyrographite it is found that the specific heat is directly dependent on the degree of stacking faults. This is in agreement with the theory that stacking faults will decrease the value of the elastic constant of shear between neighboring layers, which leads to additional modes at low temperatures and thus adds to the specific heat. The specific heats of mercury and thallium were measured between 0.35 and 4.2°K. In the normal state below 0.7°K the mercury results are given by $C_n = 1.79\ T + 5.23\ T^3$ mJ/mole deg. The coefficient, α, of the T^3 term corresponds to a value of the Debye parameter, Θ_0, of 71.9°K. For temperatures higher than 0.7°K, the lattice specific heat deviates above the T^3 law. A plot of $\Theta(T)$ is given. Below 0.6°K, the specific heat of thallium in the normal state is given by $C_n = 1.47\ T + 4.03\ T^3$ mJ/mole deg. The corresponding value of Θ_0 is 78.5°K. Above 0.6°K, the lattice specific heat of thallium shows a deviation below the pure T^3 law. This would imply a deviation in the dispersion curve above the linear portion. A similar effect observed in the specific heat of graphite was explained on the basis of bond bending modes of vibration. Similar modes may explain this behavior for thallium. In the superconducting state the specific heat of both materials can be represented by a sum of the normal lattice term and a superconducting electronic term, C_{es}, of the form $a\gamma T_c \exp(-bT_c/T)$. For mercury, values are a = 15 and b = 1.64 with $T_c = 4.16$°K; for thallium a = 9 and b = 1.52 with $T_c = 2.38$°K. In the case of thallium the critical field as a function of temperature, $H_c(T)$, is determined, with $H_c(0) = 176.5$ gauss. Below 3.3°K the normal state specific heat of niobium, measured in a magnetic field of 17 kG, can be represented by $C_n = 7.79 + 0.094\ T^3$ mJ/mole deg. This corresponds to a value of the Debye parameter at 0°K, Θ_0, of 275°K. The specific heat in the superconducting state does not appear to be anomalous. (Dissertation Abstr.)

13693 CRITICAL CURRENTS IN THIN SUPERCONDUCTING TIN FILMS [Thesis]. Coffey, Howard Thomas. Chapel Hill, N. C., Univ. of North Carolina, 1964. 98p.

The current necessary to restore resistance to plane rectangular films of superconducting tin was measured as a function of temperature. Emphasis was placed on the elimination of heat generated by the measuring current. Superconducting leads and pulsed currents were used to reduce the total heat energy injected into the sample during the measurements. It was shown that there is no advantage to this commonly used type of pulse measurement. A steady current approach was subsequently adopted. The films were thin compared to the 0°K penetration depth. Values of the maximum current density present in the films were calculated assuming the current distribution proposed for this case by Bowers. The temperature dependences of these critical current densities were found to be $(1 - t^2)^{\frac{1}{2}}$ in agreement with the theoretical calculation of Bardeen. The 0°K critical current densities of the films were on the order of 2×10^7 amperes per cm^2. This value agrees in order of magnitude with theoretically predicted values. The thermal conductivity across the interface between a quartz plate and a copper plate was investigated in the temperature range from 1.5 to about 4°K. The rate at which heat energy was transferred across the interface was found to be proportional to the differences in the temperatures of the two surfaces, each temperature being raised to the nth power. The exponent n varied from 2.5 to 3.0. This functional form remained the same although the thermal conductivity was increased by coating the interface with grease and by changing the pressure on the interface. These measurements agree with the conductivity calculated by Little if the parameter m of his calculation is considered to be adjustable. A method of determining the enthalpy and specific heats of materials at low temperatures was proposed and was used to measure the specific heat of crystalline quartz between 2.15 and 3.8°K for the first time. (Dissertation Abstr.)

13694 APPARATUS FOR HEAT CAPACITY MEASUREMENTS IN THE RANGE 0.24 TO 20 deg K AND APPLICATIONS TO SOME TRANSITION METAL SUPERCONDUCTORS AND FERROMAGNETIC-SUPERCONDUCTORS [Thesis]. Batt, Russell Howard. Berkeley, Calif., Univ. of California, 1964. 68p.

An apparatus for heat capacity measurements in the temperature range 0.24 to 20°K, using liquid ^3He, ^4He, or H_2 as cooling agents, is described. The main components of the low-temperature part of the apparatus are a copper block that contains a vapor-pressure bulb and a chamber into which ^3He is condensed, a magnetic thermometer for measuring temperatures below 1°K, and two mechanical heat switches to provide thermal contact between the sample and the copper block and between the block and the liquid ^4He or H_2 bath. The temperature of the copper block can be maintained constant to 0.01% at most temperatures within the range 0.24 to 20°K. The heat capacity of ruthenium was measured from 0.27 to 1.2°K. Several parameters characteristic of the superconducting state are derived from the heat capacity measurements and are compared with those of several other superconductors. This comparison shows no obvious difference between ruthenium and those superconductors that exhibit the isotope effect. A correlation is found to exist between the deviations of these parameters from the BCS values and T_c/θ_0. The heat capacities of Ti, and of Ti containing 0.05%, 0.25%, and 1.0% Fe were measured from 0.24 to 4.2°K. The results show the absence of an ordinary bulk superconducting transition in all of the samples. A reduced superconducting transition is observed in the 1% Fe–Ti alloy at ≈3°K, in agreement with magnetic measurements, but a large linear term in the heat capacity at temperatures below this transition suggests either that the superconductivity is not of the usual kind or that only 15% of the sample participates in the superconducting transition. The present results are compared with related work on Mn–Ti alloys. Heat capacity measurements were made from 0.25 to 20°K on two solid solutions ($Y_{1-x}Gd_xOs_2$) in which superconductivity and ferromagnetic ordering were found by magnetic measurements to coexist. The results indicate that the magnetic and superconducting ordering occur together in the same volume elements of the sample. (Dissertation Abstr.)

13695 THE EFFECT OF STRUCTURE ON THE SUPERCONDUCTING PROPERTIES OF EUTECTIC ALLOYS [Thesis]. Levy, Sander Alvin. Bethlehem, Pa., Lehigh Univ., 1965. 73p.

The superconducting properties of twelve eutectic alloys were studied. The seven alloys that were eutectics between terminal solid solutions were found to behave as Type I superconductors irrespective of the solidification rate. Five other eutectic systems, all of which contained at least one intermetallic compound, were found to behave as Type II superconductors. Measurement of the normal resistivity from room temperature to 1.5°K indicated that the former alloys exhibited low resistivity, and that the resistivity decreased rapidly with decreasing temperature. The latter alloys exhibited high resistivity, which did not decrease

rapidly with temperature. For the Type II alloys a linear variation between the current carrying capacity and the interphase boundary area per unit volume was observed. Of the Type II alloys the two eutectics (Sb–Tl and Pb–Bi) containing one superconducting and one nonsuperconducting phase were found to be the more structure sensitive. Good qualitative agreement with the Anderson-Kim theory of the thermally activated motion of flux lines was obtained. (Dissertation Abstr.)

13696 FILM FREE CONVECTION IN HELIUM II. Rivers, W. J. (San Fernando Valley State Coll., Northridge, Calif.); McFadden, P. W. New York, American Society of Mechanical Engineers, 1965, Preprint No. 65-WA/HT-10, 7p. (CONF-651110-9). ORINS.

From American Society of Mechanical Engineers, Annual Winter Meeting, Chicago.

Free-convection heat transfer from a solid surface to liquid helium(II) in the presence of a film of either liquid helium(I) or helium gas is analyzed mathematically. The analysis includes two heater shapes, a vertical flat plate and a horizontal circular cylinder, each with an isothermal surface. The integral forms of the boundary-layer equations are used to describe the heat transfer and fluid flow processes that occur within the film. The velocity and temperature profiles within the film are approximated by fourth degree polynomials whose coefficients were evaluated by applying a system of boundary conditions which were derived in the usual fashion but are based on assumed discontinuities in both the velocity and temperature profiles at the film-helium(II) interface. Calculated results, which include the film thickness, the heat transfer coefficient, and the mass flow in the film, are presented and discussed. (auth)

Neutron Physics

See also REACTOR TECHNOLOGY — Criticality Studies

Refer also to abstracts 13061, 13088, 13417, 14008, and 14096.

13697 (AEEW-M-605) SCATTER. Broome, J. (Atomic Energy Establishment, Winfrith (England)). Nov. 1965. 8p. Dep. BIS $0.30. HMSO 1s. 9d.

The program SCATTER is a KDF9 program in the EGTRAN dialect of FORTRAN to generate normalized angular distributions for elastically scattered neutrons from data input as the coefficients of a Legendre polynomial series, or from differential cross section data. Also, differential cross section data may be analyzed to produce Legendre polynomial coefficients. (auth)

13698 (DTMB-1820) TET 2—A THERMAL ENERGY TRANSPORT CODE. Dawson, Charles; Battey, Philip E. (David Taylor Model Basin, Carderock, Md.). July 1965. 61p.

TET 2 is a FORTRAN language digital computer program designed to produce numerical solutions to the Boltzmann neutron transport equation. TET 2 was designed primarily for thermal neutron problems but it can also do slowing down problems. The derivation of the equations indicates a way in which equations with higher order spatial terms may be derived. (auth)

13699 (GA-6690) LEGCOEF-3—A PROGRAM TO CALCULATE LEGENDRE EXPANSION COEFFICIENTS FOR THE ANGULAR DISTRIBUTION OF ELASTICALLY SCATTERED NEUTRONS. Smith, C. V.; Drake, M. K. (General Atomic, San Diego, Calif. John Jay Hopkins Lab. for Pure and Applied Science). Sept. 1, 1965. Contract AT(04-3)-167. 38p. Dep. mn. CFSTI $2.00 cy, $0.50 mn.

LEGCOEF-3, a program for the IBM 7044 computer, was written to calculate Legendre expansion coefficients for the angular distribution of elastically scattered neutrons. A supplementary program, GEORGE, was written to calculate the angular distribution of elastically scattered neutrons from the total elastic scattering cross section and a set of Legendre coefficients. Both programs are included. (M.O.W.)

13700 (JAERI-1086) SURVEY AND PROBLEMS IN THE STUDY OF THERMAL NEUTRON SCATTERING. (Japan Atomic Energy Research Inst., Tokyo). Dec. 1964. 115p. (In Japanese). Dep. mn.

The thermal neutron spectrum has become increasingly important in the analysis of thermal reactors, and accurate experiments were extensively carried out on thermal neutron inelastic scatterings, which requires the refined theory of the scattering kernel. Theories and experimental results are described for neutron inelastic scatterings from the solid and liquid materials, organic compounds and hydrogeneous compounds, which are used in reactors as moderators and reflectors. (auth)

13701 (JUL-294-NP) NEUTRONENLEITER: EIN BERICHT UEBER DEN DERZEITIGEN STAND DER ENTWICKLUNG. (Neutron Guides: A Report on the Present State of Development). Alefeld, B.; Christ, J.; Kukla, D.; Scherm, R.; Schmatz, W. (Kernforschungsanlage, Juelich (West Germany). Institut fuer Neutronenphysik). Aug. 1965. 52p. Dep. mn.

For neutrons with the wave length $\lambda = 4$ Å and larger, neutron guides are without doubt the most suitable beam tube. This is true because of the favorable angle of aperture. It is shown that for experiments with good angular resolution neutron guides are also suitable for the range from 0.5 to 2 Å since the loss can be maintained in the range of 30%. For neutron diffraction experiments with 2 and 4 Å neutrons, a construction element with double circular neutron guides is available that suppresses the higher order at low losses. New transmission time methods are available through guide lengths of approximately 100 m. It is shown that the technical difficulties are not as large as was assumed in the first consideration. (tr-auth)

13702 (LA-DC-7594) AN INVESTIGATION OF NEUTRON COLLIMATORS AND THEIR APPLICATION IN NEUTRON RADIOGRAPHY [Thesis]. Morris, Roger A. (Los Alamos Scientific Lab., Univ. of California, N. Mex.). 1965. Contract W-7405-eng-36. 81p. Dep. mn. CFSTI $3.00 cy, $0.75 mn.

Submitted to Univ. of New Mexico, Albuquerque.

A preliminary experimental and theoretical description of a Soller-type collimator for use in neutron radiography is presented. A review of the more important procedures and types of equipment used in neutron radiography is given, followed by a theoretical description of a Soller collimator. A series of experiments that were performed to verify the theoretical predictions is summarized. (D.C.W.)

13703 (MIT-2344-4, pp 17-47) FAST NEUTRON DISTRIBUTIONS. Woodruff, G. L. (Massachusetts Inst. of Tech., Cambridge. Dept. of Nuclear Engineering).

Fast neutron distributions are studied in seven different lattices. These lattices include 1.25-inch, 1.75-inch, and 2.50-inch triangular spacings of 1.027% ^{235}U, 0.25-inch-diameter fuel rods; 1.25-inch and 2.50-inch spacings of 1.143% ^{235}U, 0.25-inch-diameter fuel rods; 1.75-inch spacing, 1.154% ^{235}U, 0.25-inch-diameter fuel rods; and 2.50-inch spacing, 0.947% ^{235}U, 0.75-inch-diameter fuel rods. All the lattices are studied theoretically with two computer codes. The first code, UNCOL, is an uncollided flux approximation. The second code is denoted HEETR (High Energy Events in Thermal Reactors). (auth)

13704 (MIT-2344-4, pp 101-5) OSCILLATING NEUTRON SOURCE EXPERIMENT. Sefchovich, E. (Massachusetts Inst. of Tech., Cambridge. Dept. of Nuclear Engineering).

Problems associated with the production and monitoring of a neutron beam having sinusoidally modulated intensity are discussed. The modulation is produced by sinusoidally varying the area through which a constant-intensity neutron beam is transmitted. (T.F.H.)

13705 (MIT-2344-4, pp 135-44) MEASUREMENT OF THE DIFFUSION COEFFICIENT IN AN ANISOTROPIC MEDIUM. Pilat, E. E.; Gueron, H.; Lanning, D. D. (Massachusetts Inst. of Tech., Cambridge. Dept. of Nuclear Engineering).

An experiment is conducted to provide a test of Benoist's theory of diffusion in an anisotropic medium, unencumbered by the presence of either strong distributed absorption or fission sources and under conditions of anisotropy considerably more extreme than those encountered in most practical reactors. Measurements of the effective thermal neutron diffusion coefficient are made in heavy water containing a regular vertical array of air-filled, Type 1100 aluminum tubes representing a voided volume fraction of 16%. The experiment yields a ratio of radial diffusion coefficient to moderator diffusion coefficient of 1.29 ± 0.02 compared to the theoretical ratio of 1.28. (auth)

13706 (NAA-SR-Memo-10884 and Add.) NAA PROGRAM DESCRIPTION—A PROGRAM TO REFORMAT GRAVE/PRISM PUNCHED OUTPUT. Blaine, R. A. (Atomics International, Canoga Park, Calif.). Jan. 15, 1965. Contract AT-11-1-GEN-8. 43p. Dep. mn. CFSTI $2.00 cy, $0.50 mn.

A computer program that was developed to combine the punched output from the GRAVE and PRISM programs for input to several multigroup library preparation codes is described. (D.C.W.)

13707 (ORNL-TM-1415) CERTAIN DEFINITE INTEGRALS OF BICKLEY AND BESSEL FUNCTIONS. Tobias, Melvin (Oak Ridge National Lab., Tenn.). Nov. 30, 1965. Contract W-7405-eng-26. 5p. Dep. mn. CFSTI $1.00 cy, $0.50 mn.

While investigating the numerical integration of the Boltzmann equation, certain definite integrals of Bickley and Bessel functions, such as $\int_0^{\pi/2} Ki_2(2a \cos \phi)\, d\phi$, $\int_0^{\pi/2} \cos 2\phi\ K_0(2a \cos \phi)\, d\phi$, and $\int_0^{\pi/2} K_1(2a \cos \phi) \cos \phi\, d\phi$, were evaluated analytically. As the results may be useful for other purposes, they are reported together with the derivations. (auth)

13708 (ORNL-TM-1417) A GAUSSIAN QUADRATURE PROCEDURE USEFUL FOR THE NUMERICAL COMPUTATION OF BICKLEY FUNCTIONS AND SIMILAR INTEGRALS; REMARKS ON EXTRAPOLATION IN ITERATIVE PROCEDURES; AN APPROXIMATION TO e^x FOR SMALL x. Tobias, Melvin (Oak Ridge National Lab., Tenn.). Nov. 5, 1965. Contract W-7405-eng-26. 14p. Dep. mn. CFSTI $1.00 cy, $0.50 mn.

Three topics in numerical analysis which arose in the course of investigations into neutron transport theory are discussed. The first is a description of a Gaussian quadrature scheme useful in evaluating Bickley functions and similar integrals of functions of sin θ and cos θ over the range $0 \leq 0 \leq \pi/2$. The methods used in devising this procedure suggested an application to the second topic, extrapolation in iterative procedures. The third subject concerns approximation to e^x for small x; a formula is given which is helpful in evaluating certain expressions which are indeterminate at x = 0. (auth)

13709 (PAEC-IPA(D)PH-652) REMOVAL OF SECOND-ORDER NEUTRONS BY ORIENTED SINGLE CRYSTALS. Iyengar, P. K.; Soni, J. N.; Navarro, Q. O.; Pineda, V. M.; Natera, M. G.; Lee, T. C.; Marsongkohadi; Song, J.; Nimwanadon, T. (Philippine Atomic Research Center, Diliman, Quezon City). May 1965. 27p. Dep. mn.

A method based on Bragg reflection by a single crystal is proposed by which second-order neutrons (1-2Å) can be reflected away from a crystal monochromator without affecting the first-order neutrons (2-4Å). A series of experiments by which the method was verified is summarized. (D.C.W.)

13710 (STI/PUB/104(Vol. 1)) PULSED NEUTRON RESEARCH. VOL. I. Proceedings Series. Proceedings of the Symposium held at Karlsruhe, 10-14 May 1965. (International Atomic Energy Agency, Vienna (Austria)). Aug. 1965. 705 p. (CONF-650504(Vol. 1)). IAEA: $14.00; S 294,-; £4.4.0; F Fr 56,-; DM 49,-.

Separate abstracts are prepared for 16 of the 40 papers presented. The remaining 24 papers were previously abstracted in NSA (19: 19355, 25457, 25458, 27387-27389, 29169, 29177, 31195, 31196, 33216-33218, 33223-33229, 33231, 33672, 37762, and 45222). (C.E.S.)

For abstracts of individual papers see: 13726-13741.

13711 (STI/PUB/104(Vol. 2)) PULSED NEUTRON RESEARCH. VOL. II. Proceedings Series. Proceedings of the Symposium held at Karlsruhe, 10-14 May 1965. (International Atomic Energy Agency, Vienna (Austria)). Oct. 1965. 925p. (CONF-650504(Vol. 2)). IAEA: $18.00; S 378,-; £5.8.0; F Fr 72,-; DM 63,-.

Separate abstracts are prepared for 30 of the 47 papers presented. The remaining 17 papers were previously abstracted in NSA (19: 19360, 27390, 27752, 31607, 33219-33222, 33230, 33232, 33574, 33645, 33671, 38128, 38273, and 43251 and 20: 10425). (C.E.S.)

For abstracts of individual papers see: 13719-13725, 14075-14089, 14096, 14162, 14163, and 14199-14203.

13712 A PHYSICAL REMARK ON THE GREY ROD EXTRAPOLATION DISTANCE. Bonalumi, R. (CISE, Segrate, Italy). Energia Nucl. (Milan), 13: 39-40(1966).

An attempt is made to justify Kushneriuk-McKay's approximation on physical grounds for the extrapolation distance of an infinitely long cylindrical rod of radius a imbedded in an infinite moderator. It is shown that for a rod blackness $\beta = 1$, the extrapolation distance is a function of a Σ_m only, where Σ_m is the moderator transport cross section. (L.B.S.)

13713 DIGITAL SPEED AND PHASE CONTROL SYSTEM FOR THREE-ROTOR TYPE NEUTRON CHOPPERS. Ohno, E.; Kawabata, T. (Mitsubishi Electric Corp., Amagasaki, Japan). Nucl. Instrum. Methods, 39: 109-18 (Jan. 1966).

Three-rotor type neutron beam choppers have been successfully phase-controlled when driven by 400 w d-c motors. A novel, simple, and accurate method for the control of the speed and the phase difference of three motors is described. The first motor is accurately speed controlled by a digital speed controller, while the second and third motor are phase controlled by digital phase controllers so as to follow the first motor, keeping arbitrary phase differences among them. This new chopper drive system is simpler to operate, less expensive and more accurate than the ordinary system, using synchronous motors. In this system digital techniques are adapted to the essential parts of the control system and the monitor system, so this system is suitable for program control and data processing by a central digital computer. High absolute accuracy and stability are guaranteed by the digital system. All components used in this chopper controller are solid state devices, and high reliability can be expected. (auth)

13714 THE ROOM SCATTERED BACKGROUND PRODUCED BY A NEUTRON SOURCE IN A LABORATORY WITH CONCRETE WALLS. White, P. H. (Atomic Weapons Research Establishment, Aldermaston, Eng.). Nucl. Instrum. Methods, 39: 256-60(Jan. 11, 1966).

The neutron backgrounds present in a laboratory containing a neutron source, due to the scattering in the walls, were measured for fission detectors and for a BF_3 neutron detector and agree to within a factor 2 with the backgrounds calculated on the continuous slowing down model. For a fission detector containing thermally fissile material the relative background at a distance of 20 cm from a neutron source in a cubical laboratory of 10 m side is typically 20%. (auth)

13715 AN INDIRECT METHOD FOR MONITORING 2.5 Mev NEUTRONS, PRODUCED BY A 150 kv ACCELERATOR. Mangialajo, M. (CISE, Milan). Nucl. Instrum. Methods, 39: 345-6(Jan. 11, 1966).

A method was developed for monitoring 2.5-Mev neutrons from a 150-kev accelerator. It consists in counting the protons produced on the deuterium target by the reaction D(d,p)T. Total and differential cross sections of

D(d,n)^{3}He and D(d,p)T reactions are compared. A semiconductor detector is mounted on the target assembly and detects protons produced on a deuterium target in a backward direction. Comparison between energies of incoming deuterons and outcoming protons ensures that no protons are lost by target absorption. The apparatus allows the direct counting of protons. A typical spectrum is shown. (J.F.P.)

13716 MEASUREMENTS OF NEUTRON CROSS SECTIONS OF Fe, Al, AND CF_2 BY A RATIO METHOD. Langsdorf, A. Jr.; Monahan, J. E.; Lane, R. O.; Elwyn, A. J. (Argonne National Lab., Ill.). Phys. Rev., 142: 643-56(Feb. 18, 1966).

When the number of neutrons scattered by a sample and the number transmitted through it are measured simultaneously, the ratio of scattering to transmission can be used to determine the neutron total cross section. This ratio method is free from some of the time-dependent and other systematic errors characteristic of customary transmission measurements. The method may also reduce statistical errors. It is used to reduce spurious fluctuations in measured cross sections and thereby to aid in interpreting cross-section measurements upon Fe, Al, and CF_2 (Teflon) in the neutron-energy interval from about 130 to 160 kev. The results are compared with a more conventional analysis of part of the same data. (auth)

13717 SCATTERING OF 262-kev POLARIZED NEUTRONS BY ^{4}He. Jewell, R. W.; John, W.; Sherwood, J. E.; White, D. H. (Univ. of California, Livermore). Phys. Rev., 142: 687-9(Feb. 18, 1966). (UCRL-14257).

The analyzing power of ^{4}He for 262-kev polarized neutrons was measured at a scattering angle of 89° cm. Neutrons of known polarization were obtained from a radioactive ^{24}Na-D photoneutron source. The left-right asymmetry in the scattering from a liquid helium target was observed. Neutron spins were inverted by precession in a solenoid. The result, $P = +0.21 \pm 0.06$, is slightly higher than, but consistent with, new phase shifts calculated by Roper from available n-^{4}He data. (auth)

13718 THERMAL NEUTRON DIFFUSION LENGTH MEASUREMENTS IN POISONED ORGANIC MATERIAL. Matsubara, T.; Tada, H.; Mukoyama, T.; Hatanaka, T. Sumitomo Elec. Rev., No. 84, 93-8(Mar. 1964). (In Japanese).

When poisoning of moderator materials is used for reactor control, the nuclear data of the poisoned moderator are fundamentally important. The diffusion length of thermal neutrons was measured in organic material (Santowax-R) poisoned with boron, and its temperature dependence was studied. The values of the diffusion lengths are 6.3, 7.4, and 8.9 cm at 200, 300, and 360°C, respectively, for $\Sigma_\alpha = 0.0265$ cm^{-1} and 7.3 cm at 200°C for $\Sigma_\alpha = 0.0212$ cm^{-1}. (auth)

13719 CONTRIBUTION TO THE STUDY OF FAST NEUTRON NON-MULTIPLYING ASSEMBLIES BY THE PULSED NEUTRON TECHNIQUE. Deconninck, G. (Centre de Physique Nucleaire Louvain); d'Oultremont, P.; Stievenart, M. pp 493-510 of STI/PUB/104(Vol. 2).

Pulsed neutrons experiments were performed on non-multiplying and poorly moderating materials (Fe, Cu, C). The energy of the source neutrons was chosen to be 1400, 1100, 890, and 670 kev. The time variations of the leakage flux were measured for different locations of the detector. The former was shown to be strongly dependent on the latter. A systematic study of these experiments was done by the Monte Carlo method using a semi-continuous energy model. The results given by this method are in good agreement with the experimental results and, moreover, the Monte Carlo method is a very useful tool to study the energetic degradation of the primary neutrons. The propagation of the incident neutrons in such assemblies was also studied by the time-dependent P_1 approximation. This method gives analytical results which are also in good agreement with the experimental results. (auth)

13720 THE GENERATION OF NEUTRON PULSES AND MODULATED NEUTRON FLUXES WITH SEALED OFF NEUTRON TUBES. Elenga, C. W.; Reifenschweiler, O. (Philips Research Labs., Eindhoven, Netherlands). pp 609-22 of STI/PUB/104(Vol. 2).

Results of experiments with sealed-off neutron tubes are reported with particular reference to the generation of neutron pulses and modulated neutron fluxes. The mean neutron output of the normal (Philips) tube during continuous and pulsed operation was from 1 to 5×10^8 n/s. The output during pulses was 10^9 n/s, the pulse duration within the range from 5 μs to 10 s. The life of the tested tubes was several 1000 h. Experiments were carried out on the modulation of the neutron output in accordance with an arbitrary time function. It was found possible to generate, for example, sinusoidal modulated fluxes in the frequency range between 1 and 1000 c/s. A special tube for pulsed operation, based on the normal tube, has been developed. With a mean output of 1 to 2.5×10^8 n/s this tube yields about 5×10^{10} n/s during pulses in the range from 3 to 500 μs. These neutron tubes have a wide range of application by reason of their reliability, their long life, their simplicity, ruggedness and small size (diameter 7 cm, length about 50 cm). (auth)

13721 CONTROLLABLE PULSE FREQUENCY AND WIDTH SYSTEM FOR PULSING AND MODULATING FAST-NEUTRON CORE ASSEMBLIES. Duquesne, M.; Gerbier, R.; Lyon, F.; Schmitt, A. (Centre d'Etudes Nucleaires, Cadarache, France). pp 635-52 of STI/PUB/104(Vol. 2). (In French).

A system for producing neutron bursts of independently controllable width and frequency is described. The rise and quenching times of these bursts are of the order of a few nanoseconds. The system is applied to high-frequency pulsed and modulated experiments. Rapidly quenched neutron bursts are produced by deflection of a pure deuteron beam which has previously been accelerated and sorted. Ions other than atomic deuterons are removed after acceleration in a 10° magnetic sorting field. Consideration is also being given to a pre-acceleration sorting system offering the advantage of reduced bulk. The deuteron beam passes through the space between two plates where there is normally an electrostatic field which deflects the beam onto the surfaces of a diaphragm. Application of a very high potential pulse to the first plate cancels the field and thus brings the beam rapidly onto the neutron-producing target (beginning of the burst). The second plate then receives a pulse of the same type which restores the field and removes the beam from the target (end of the burst). The pulse rise time is of the order of 10 ns; disappearance from the target is faster. The duration of the burst can be controlled as required within reasonable limits by suitably increasing the interval between the two pulses. In some cases ion transit time in the plates is not negligible in relation to the duration of the step applied to them. In such cases, one of the plates is replaced by a travelling wave line to which the two pulses are applied successively. The potential pulse thus accompanies the deuteron cluster producing the burst. The burst times can thus be reduced below 4 ns. The first stages of the voltage step generators are transistorized. The output tubes are sealed-disc valves providing a 1500-v step in a few nanoseconds. A 50-MHz double tetrode is employed for pulses for the delay line. A detection system comprises a scintillator-photomultiplier device incorporating a coincidence-anticoincidence unit, a time analyzer and a digital data recorder. (auth)

13722 EXCITATION OF NEUTRON WAVES BY MODULATED AND PULSED SOURCES. Perez, R. B.; Booth, R. S. (Univ. of Florida, Gainesville). pp 701-28 of STI/PUB/104(Vol. 2).

Placement of either a sinusoidally modulated or pulsed source of thermal neutrons at one of the boundaries of a nuclear assembly creates a disturbance which can be analyzed in terms of wave components, propagating away from the localized source with frequency-dependent attenuation factors and wave velocities. The dispersive properties of the assembly are expressed through the dispersion relation, connecting the inverse complex relaxation length (or complex wave number), $\rho(\omega)$, to the frequency of the excitation and the nuclear parameters of the system. Experiments

were performed using graphite as the moderating material. Two different sources of thermal neutrons were used. In one case 14-Mev neutrons generated by a Cockcroft-Walton machine were thermalized in a tank containing several layers of iron, lead, and graphite immersed in water. The University of Florida 4-Mev Van de Graaff accelerator produced 29-kev neutrons from the (Li-p) reaction which were thermalized in a few inches of paraffin. In both instances the ion beams could be modulated sinusoidally or pulsed. Fourier analysis of the slow pulses showed very good agreement with the results obtained from the sinusoidal excitation of the waves. (auth)

13723 COMPARATIVE STUDY OF SEVERAL TYPES OF PULSED AND MODULATED EXPERIMENTS ON FAST MULTIPLYING MEDIA. Cadilhac, M.; Govaerts, P.; Hammer, P.; Moore, M.; Nicolaenko, B.; Storrer, F. (EURATOM-CEA, Cadarache, France). pp 729-57 of STI/PUB/104(Vol. 2).

A distinction is made between two types of kinetic experiment (pulsed or modulated) according to the configuration of the assembly and the source position: (1) critical or slightly subcritical assembly with the source in or near the core; (2) greatly subcritical mass fed by a source on one face, exactly as in an exponential experiment. In both cases, the law governing the variation of the source as a function of time can be: a Dirac function or one closely similar. In this case, it is a pulsed experiment; a sinusoidal wave or at least a periodical function in which the fundamental component is dominant. It is then a modulated experiment; or an aleatory or pseudo-aleatory function. A comparative study of the two aspects of these various types of experiment is presented: fundamental integral experiments to check the basic data or methods of calculation by comparing the theoretical and experimental results; and experiments designed to determine important parameters of projected or existing reactors (e.g., determination of α-β/l and reactivity by the classical pulsed method, or material buckling by an exponential experiment). As the phenomenon is perfectly linear, it is obvious that the same information can be obtained, in principle, by the method based on modulation over the entire frequency range and the pulsed method, whose spectral analysis contains all the frequencies. In practice, one or the other of these methods may be preferable, according to the purpose of the experiment. Both theoretical and experimental factors enter into the choice (e.g., accuracy of measurement and time necessary). Only some of the outstanding points are covered, e.g., for type (1) experiments, the pulsed method is generally used. It takes advantage of the fact that often only the basic decay mode is measured. In this case, the neutron burst need not be an exact Dirac function. Even for a core assembly, the existence of a discrete fundamental mode is exceptional. Generally, there is a continuous spectrum of decay constants which, in certain cases, may present a very marked peak, so that a "pseudo-fundamental" mode can be defined. Even for type (1) experiments, modulation may be preferable to pulsation. This is true, for example, for the area method. Whereas this method is very difficult to apply by means of a pulsed technique, it should be possible to obtain the same result much more easily by single frequency modulation (some tens of cycles per second). For type (2) experiments, modulation appears preferable because it is the natural extension of the classic exponential experiment, which is merely a zero frequency modulation, and because, like it, it produces an asymptotic mode, characteristic of the assembly, remote from the boundaries and sources. In this case also, a discrete asymptotic mode is not the most general one. In some cases, pulsation may be preferable for this type of experiment, if only because it gives the response to all frequencies in one operation. (auth)

13724 A SIMPLE CROSS-CORRELATION METHOD FOR THE STUDY OF THE NEUTRON PULSE TRANSFER FUNCTION IN MEDIA USING A STATISTICALLY PULSED NEUTRON SOURCE. Haas, R.; Matthes, W.; Weckermann, B. (EURATOM, C.C.R., Ispra, Italy). pp 849-59 of STI/PUB/104(Vol. 2).

The cross-correlation between the fission process in a fission neutron source and a neutron detector yields the pulse transfer function of the medium between source and detector position. Because of the low background obtainable, the asymptotic behavior and the short time behavior of the decay curve, which results from space and energy transients, can be measured even with rather weak sources. The reported measurements are considered as a survey to determine the experimental possibilities of this method. The time constant for thermalization (the neutron energy decay) in paraffin is measured as (5 ± 1) μs. Some fundamental aspects of the application of this correlation method to multiplying media are discussed. (auth)

13725 SUMMARY OF THE SYMPOSIUM ON PULSED NEUTRON RESEARCH. Nelkin, M. (Cornell Univ., Ithaca, N. Y.). pp 885-98 of STI/PUB/104(Vol. 2).

The main aspects of the symposium are outlined under the topics: experiments in nonmultiplying systems, theory for nonmultiplying systems, neutron thermalization and spectra, thermal multiplying systems, fast neutron systems, and pulsed reactors and neutron sources. (C.E.S.)

13726 EXTRAPOLATION DISTANCES FOR PULSED NEUTRON EXPERIMENTS. Walker, J.; Brown, J. B. C.; Wood, J. (Univ. of Birmingham, Eng.). pp 49-63 of STI/PUB/104(Vol. 1).

Attention has been drawn in earlier work to the effect of uncertainty in extrapolation distance on the results of pulsed neutron experiments and hence to the need for more accurate knowledge of this parameter. The extrapolated endpoints can be obtained from flux plots and the value for large systems can be deduced from diffusion coefficients. Information from both approaches is given and the dependence of extrapolated endpoint on temperature and on buckling is discussed. Decay times and time-dependent flux plots were measured in pulsed source experiments on small, accurately-known, volumes of water and Dowtherm A (thermex) by the use of a small scintillation detector and a time analyzer; a separate scintillation detector or a BF_3 counter was used as a monitor. Spatial harmonic analysis of the flux plots was performed by the method of least squares to obtain the extrapolated endpoints once appropriate corrections have been made to the recorded counts. Some consideration was given to the possibility of testing for the effect of flux distortion near the boundary by successive removal of the outer points and to the effects on extrapolated endpoint of the flux perturbation produced by the detector. The results presented are mainly for measurements at 20°C in 4-in. and 7-in. cubic containers lined with cadmium, but very preliminary information was obtained for water at temperatures up to 80°C and equipment is being designed to extend the range of temperatures still further. (auth)

13727 STUDY OF GRAPHITE AND BERYLLIUM OXIDE USING THE PULSED NEUTRON SOURCE METHOD. Cuny, G.; Deniz, V.; Lalande, J.; Le Ho, J. G.; Sagot, M. (Centre d'Etudes Nucleaires, Cadarache, France). pp 89-104 of STI/PUB/104(Vol. 1). (In French).

Diffusion parameter values (λ_t, C, F) for graphite, obtained from measurements made in the buckling range of 5.6 to 190 m^{-2} and supplemented by determination of anisotropy, are presented. The results of a systematic study (based on output current measurements) of the spectral stabilization of a neutron burst in relation to the stack dimensions and, for large stacks, in relation to the position of the point of measurement are taken into account. The value of the transport mean free path for beryllium oxide is also given. (auth)

13728 NEUTRON SLOWING-DOWN TIME AND THERMALIZATION TIME CONSTANT IN GRAPHITE. Kaneko, Y.; Sumita, K. (Japan Atomic Energy Research Inst., Tokyo). pp 139-53 of STI/PUB/104(Vol. 1).

Extended models including phonon exchange between the neutron and moderator lattice are discussed. In order to prove their validity, a series of pulsed neutron experiments was performed to investigate neutron moderation and thermalization in a graphite pile. The graphite pile is of nuclear reactor grade with density 1.54 and is 240 cm in height and 120 cm in a side of its hexagonal cross section. Bursts of neutrons of width 1 microsecond were generated at the cen-

ter of the pile. The slowing-down and diffusing neutrons were detected by bare and energy-selective, filter-covered BF_3 counters and analyzed with a 256-channel time analyzer. By interpreting that the increment of the difference of the events between the bare and the filter-covered counter is due to the contribution made by that fraction of the neutrons slowing down at the time of measurement below the cut-off energy of the filter, slowing-down times in graphite were determined. As the results of the experiment, slowing-down times below 1.46, 0.61, 0.50, 0.41, and 0.21 ev were determined as 23, 36.9, 41.6, 45.8, and 87.5 μs respectively. The thermalization time constant in graphite was also determined as (296 ± 50) μs by using the silver filter transmission method. It is concluded that the crystal model is capable of describing most satisfactorily the slowing-down and thermalization phenomena in graphite. (auth)

13729 DATA EVALUATION PROBLEMS IN THE PULSED NEUTRON SOURCE METHOD. Pal, L.; Bod, L.; Szatmary, Z. (Central Research Inst. of Physics, Budapest). pp 165-84 of STI/PUB/104(Vol. 1).

Results of measurements in water, benzene, toluene, xylene, cyclohexane, n-hexane, and diphenyl are reported and the methods by which the diffusion parameters of interest can be evaluated from the measured data with the least error are discussed. The time-of-flight effect, manifesting itself, for technical reasons, in the investigation of moderators at elevated temperatures and influencing the value of the decay constant, is investigated in detail both theoretically and experimentally, and the geometrical conditions under which proper accuracy can be achieved are given. The effect of the dead-time of the neutron detector and amplifier system on the value of the decay constant is also determined and it is shown that the effect of dead-time can be neglected when $[i(t)\ \tau]^2 \ll 1$, where i (t) dt is the number of neutrons detected in the time interval (t, t + dt) and τ is the dead-time. For the evaluation of the decay constant the maximum likelihood method is used. For unambiguous determination of the likelihood function, the multi-channel analyzer was operated in such a way as to store a maximum of one pulse per analyzing cycle and per channel. It is of primordial importance to incorporate the parameter characterizing the background into the likelihood function. The parameters of the maximum likelihood function were evaluated by Newton iteration on a computer. If the background is not properly taken into account, this may cause apparent higher harmonic contamination, while higher harmonic contamination, in turn, may be taken for an apparent background. Therefore, it is particularly important to determine the parameter characterizing the background directly from the decay data obtained at several delay times. The diffusion parameters were computed by the weighted least-squares method using the decay constants of minimum standard deviation evaluated from the maximum liklihood function. Since, for the materials investigated, the values of the transport mean free path were not known, a fast converging iteration procedure was elaborated for the determination of the transport mean free path. The computer evaluation made it possible to determine the coefficients of the B^6 and higher order terms of the decay constant. The diffusion parameters of the hydrogenous materials investigated were calculated by the Radkowsky prescription from the energy dependence of the integral scattering cross sections. The calculations have shown that the Radkowsky prescription is a useful empirical method for the evaluation of the transport mean free path of numerous hydrogenous materials. (auth)

13730 MEASUREMENT OF M_2 IN ORGANIC LIQUIDS. Sancho, L.; Garcia-Castaner, B.; Verdaguer, F. (Junta de Energia Nuclear, Madrid). pp 185-90 of STI/PUB/104 (Vol. 1). (In Spanish).

The experimental study, using the pulsed neutron source method, of the effect of non-1/v capture on the diffusion parameters of organic liquids is discussed. Cadmium is used to introduce the non-1/v capture, cadmium iodide being dissolved in tributyl phosphate and then dissolved in the liquid. The study is made with six different concentrations of cadmium, in addition to measuring the pure liquid. Benzene, a non-polar liquid, was used for the first measurement, and chlorobenzene, a polar liquid, for the following one. Measurements are carried out with internal counters situated at zero of the first harmonic; successive measurements are made with four, three, two and one counters, thus making it possible to determine the interference caused by the counters. The results of the measurements enable the value of M_2, the mean-square energy transfer, to be calculated for the liquid used. (auth)

13731 THEORETICAL INTERPRETATION OF PULSED NEUTRON PHENOMENA. Corngold, N. (Brookhaven National Lab., Upton, N. Y.). pp 199-217 of STI/PUB/104 (Vol. 1).

Transient effects in the variation of neutron distributions in space, time, and energy are discussed. In the analysis, particular attention is given to the pulsed neutron experiment in non-multiplying media, and to its interpretation in terms of space-energy modes and (time) decay constants. Theoretical research in this field has been built upon the exact solution of several special problems, and approximate, numerical solutions in more realistic situations. Recently, a unified point of view, based on the Van Hove-Glauber theory of the scattering of slow neutrons, has been proposed. It has been found that the long-time behavior of the pair-correlation function, which enables one to distinguish between different types of moderating materials, also controls the type of decay-constant spectrum that one finds. The case of infinite medium solutions that are proportional to $\exp(i\vec{B} \cdot \vec{r})$, in media having 1/v absorption is emphasized. The analytical work is concerned with modal solutions, proportional to $\exp(\lambda t)$ as well, while the numerical work is directed at the full, "life-history" solution, as well as the modal solutions. Phenomena encountered when the absorption is not 1/v and when the moderator sample is so small that the long-time solutions are no longer separable in space and energy are also considered. The bearing of these recent developments upon the interpretation of pulsed experiments is discussed. Particular reference is made to the measurement of diffusion and diffusion cooling coefficients, and to the nature of the approach to the asymptotic distribution. (auth)

13732 GRAPHIC METHOD OF SOLVING A CERTAIN CLASS OF NEUTRON PHYSICS PROBLEM. Stepanov, A. V. (Lebedev Inst. of Physics, Moscow). pp 339-54 of STI/PUB/104(Vol. 1). (In Russian).

The passage of neutrons through an inhomogeneous moderator with scattering properties which undergo space-time fluctuations is considered. A graphic method is devised for solving a Boltzmann equation possessing parameters which vary in an irregular manner, i.e., are random functions. An equation is derived for averaged neutron density and the problem is formulated in terms of the characteristic values for a heterogeneous moderator system. It is shown in particular that the relaxation length of neutron density in an inhomogeneous moderator differs from the relaxation length calculated for systems with averaged, "leveled" properties. (auth)

13733 INVESTIGATIONS RELATED TO THE THEORY OF THE PASSAGE OF COLD NEUTRONS THROUGH MATTER. Stepanov, A. V. (Lebedev Inst. of Physics, Moscow). pp 355-69 of STI/PUB/104(Vol. 1). (In Russian).

A study was made of the passage of cold neutrons through matter, account being taken of quantum effects. A solution was obtained for the wave equation of Schrödinger which describes the development of a pulse of neutrons of low energy in time. It is shown that correlation of the fluctuations in the scattering properties of the medium leads to a change in the law of dispersion and to additional attenuation of the neutron wave. (auth)

13734 POSSIBLE METHOD FOR STUDYING THE ANALYTICAL DEPENDENCE OF NEUTRON DISTRIBUTION ON PARAMETERS OF THE SCATTERING NUCLEUS. Kazarnovskii, M. V.; Kenzhebaev, Sh. (Lebedev Inst. of

Physics, Moscow). pp 371-80 of STI/PUB/104(Vol. 1). (In Russian).

One of the possible models for the scattering nucleus—$W_s(v,v')$—convenient for studying the analytical properties of the functions of neutron distributions—is the expression $W_s(v,v')$ in the form of a superposition of the scattering nuclei represented by a gaseous model corresponding to different masses. Even in the simplest case involving the sum of two terms this superposition satisfies the general requirements (asymptotic character at high energies and the condition of detailed balance) and contains two arbitrary parameters. Within the framework of the multi-velocity theory the total information on the law of scattering which is necessary to calculate the neutron distributions is contained in the set of parameters γ_{ik} ($\gamma_{ik} + \gamma_{ki}$, $\gamma_{io} = \gamma_{oi} = \gamma_{oo} = 0$). If these are known it is relatively easy to consider the behavior of the neutron distributions in the thermal range. Within the framework of the gaseous (and consequently also the superposition) model the parameters γ_{ik} can be calculated in an analytical form (in the paper expressions are quoted for γ_{11}, γ_{12} and γ_{22}). The advantages, the drawbacks, and the physical justification for the superposition model are discussed. (auth)

13735 REVIEW OF THE APPLICATION OF PULSED SOURCES TO THE MEASUREMENT OF NEUTRON SPECTRA IN MODERATORS AND REACTOR LATTICES. Poole, M. J. (Atomic Energy Research Establishment, Harwell, Eng.). pp 425-63 of STI/PUB/104(Vol. 1).

The employment of pulsed sources for neutron spectrum measurements is described with reference to applications for which the method is suitable. Emphasis is placed on the use of pulsed sources for basic studies of the process of neutron moderation. Various scattering laws which have been proposed for common moderators are mentioned and the corresponding predicted energy spectra are compared with experimental measurements. (auth)

13736 MEASUREMENT OF THE TIME-DEPENDENT SPECTRUM IN HEAVY WATER. Poole, M. J. (Atomic Energy Research Establishment, Harwell, Eng.); Wydler, P. pp 535-44 of STI/PUB/104(Vol. 1).

The spectrum of neutrons emerging from the center of a cylindrical tank containing 280 l of pure heavy water was measured between 40 μs and 1.2 ms after the injection of a fast neutron pulse. A chopper time-of-flight spectrometer and magnetic tape recording and analyzing facilities were used. Theoretical spectra calculated in the diffusion approximation using a scattering kernel for heavy water suggested by Honeck agree well with the experimental results. (auth)

13737 MEASUREMENTS OF NEUTRON SPECTRA IN HYDROGENOUS MODERATORS. Kallfelz, J.; Reichardt, W. (Kernforschungszentrum, Karlsruhe, Ger.). pp 545-66 of STI/PUB/104(Vol. 1).

Measurements of neutron spectra were made in various hydrogenous moderators, using a 400-kev Cockcroft-Walton pulsed neutron source, a slow chopper, and a 3-m flight path. The spectra measured include the following types: Asymptotic leakage spectra normal to the surface for water, benzene and Dowtherm A, for slab geometries with thickness varying from 2 to 15 cm. Asymptotic leakage spectra in water at various angles from the normal of the surface, for an effectively infinite geometry. Time-dependent spectra from the middle of an ice moderator at liquid nitrogen and liquid hydrogen temperatures, and from the middle and surface of a block of zirconium hydride ($ZrH_{1.65}$) at room temperature. Spectra calculations were made using theoretical and experimental scattering kernels. Among the programs used is a FORTRAN II code, ADALS, for the calculation of angular-dependent asymptotic leakage spectra. The scattering kernels used include the Nelkin and Haywood kernels for water, and kernels for benzene and Dowtherm A derived from scattering-law measurements made at Karlsruhe. The calculated spectra are compared with the experimental results. (auth)

13738 EXPERIMENTAL STUDY OF THE NEUTRON-THERMALIZATION PROCESS IN TIME IN GRAPHITE AND BERYLLIUM. Mostovoi, V. I.; Sadikov, I. P.; Chernyshov, A. A.; Ishmaev, S. N.; Yudkevich, M. S.; Nozik, V. A. (Lebedev Inst. of Physics, Moscow). pp 623-41 of STI/PUB/104(Vol. 1). (In Russian).

A description is given of an experimental facility for studying the establishment of an equilibrium neutron energy spectrum in various media. Short pulses of fast neutrons were produced in the moderators under study by means of a high-current electron linear accelerator. At various intervals following the production of the fast-neutron pulse, the neutron spectra were measured in a beam extracted from the moderator by means of a mechanical chopper phased to the operation of the accelerator. The optimum resolution in spectrum measurement was 2.5 μs/m and the minimum uncertainty in the measurement of slowing-down time was 3.5 μs. Results are given for the measurement of non-stationary spectra in graphite ($B^2 = 8.9 \times 10^{-3}$ cm^{-2}) and in beryllium ($B^2 = 9.7 \times 10^{-3}$, 24×10^{-3}, 43×10^{-3} cm^{-2}) for slowing-down times of between 30 and about 2500 μs. The results measured in beryllium were compared with calculations of non-stationary spectra performed with double-differential cross sections computed on the basis of experimental data on the energy spectrum of Be lattice vibrations. The chemical binding and the thermal agitation of the atoms of the moderator were found to have a marked effect on the speed at which the neutron spectrum approaches the equilibrium spectrum even at times of about 30 μs, which corresponds to an average spectrum energy of about 1 ev for graphite and about 0.2 ev for beryllium. The total time needed to establish an equilibrium neutron spectrum was about 2000 μs in graphite and about 1000 μs in beryllium. The shape assumed by the neutron spectrum in small beryllium blocks is determined to a considerable extent by the effects of coherent scattering, the latter leading to the formation of so-called neutron traps which slow up the establishment of an equilibrium energy spectrum. (auth)

13739 EXPERIMENTAL STUDY OF THE PROCESS OF NEUTRON THERMALIZATION IN TIME IN AQUEOUS MODERATORS. Ishmaev, S. N.; Mostovoi, V. I.; Sadikov, I. P.; Chernyshov, A. A. (Lebedev Inst. of Physics, Moscow). pp 643-56 of STI/PUB/104(Vol. 1). (In Russian).

Non-stationary neutron spectra were measured in zirconium hydride and in water at room temperature as a function of slowing-down time, with a resolution of 3.5 μs. The spectra measured in a large ZrH prism ($B^2 = 3.8 \times 10^{-2}$ cm^2) belong to a slowing-down time range ($t > 30$ μs) in which the mean neutron energy is less than 0.13 ev and the energy exchange between neutron gas and the medium is caused mainly by the excitation of acoustic lattice vibrations. In this range thermalization proceeds at a comparatively slow rate and the time required to establish an equilibrium neutron spectrum is of the order of 400 μs. In a small ZrH assembly ($B^2 \simeq 20 \times 10^{-2}$ cm^{-2}) a strong diffusion-cooling effect is observed. The spectra measured at long slowing-down times are found to differ considerably from the Maxwellian distribution with the temperature of the medium. The time required to establish an equilibrium energy distribution increases with decreasing system size. The neutron energy spectra in water ($B^2 = 2.56 \times 10^{-2}$ cm^{-2}) are presented for slowing-down times of over 13 μs, where distortions from resolutions are insignificant. The shape of the spectrum is only fully consistent with the Maxwellian distribution at room temperature after about 100 μs following a fast neutron burst. The time required to establish an equilibrium neutron spectrum in this experiment is three to four times longer than the values calculated by others. The possible reasons for this discrepancy are discussed. (auth)

13740 NEUTRON THERMALIZATION IN A GRAPHITE-WATER SYSTEM AT LARGE TEMPERATURE GRADIENTS. Maiorov, L. B.; Mostovoi, V. I.; Safin, Yu. A.; Trukhanov, G. Ya. (Lebedev Inst. of Physics, Moscow). pp 657-68 of STI/PUB/104(Vol. 1). (In Russian).

Measurements were made of the space-energy distribution of thermal neutrons in a graphite-water system at graphite temperatures of 443–823°K and a water temperature of 303°K. The system investigated consisted of a graphite prism measuring 100 cm × 100 cm × 59.5 cm and an aluminum tank of water measuring 175 cm × 175 cm ×

50 cm, separated by a thermal screen. The WWR-2 reactor was used as the external neutron source. Neutron beams were extracted from different points in the graphite and the water in the direction of the neutron flux from the reactor incident on the graphite prism. The neutron spectra in the extracted beams were measured by the time-of-flight method by means of a mechanical chopper with a resolution of 20 μs/m. The measured spectra were compared with the spectra calculated in accordance with a T-2 program (P-1 approximation, 40 energy groups), use being made of the differential cross sections for an ideal gas and the differential cross sections obtained taking into account the chemical binding. On the basis of the measured spectra, the neutron rethermalization cross section in the graphite and the water was calculated as a function of graphite temperature. The experimental results were compared with the data obtained by others. (auth)

13741 MODERATION OF NEUTRONS EMITTED BY A PULSED SOURCE AND NEUTRON SPECTROMETRY BASED ON SLOWING-DOWN TIME. Bergman, A. A.; Isakov, A. I.; Kazarnovskii, M. V.; Popov, Yu. P.; Shapiro, F. L. (Lebedev Inst. of Physics, Moscow). pp 671-93 of STI/PUB/104(Vol. 1). (In Russian).

Over the past ten years research has been going on at the P. N. Lebedev Physics Institute on the non-stationary moderation of neutrons in heavy media, the development of a method of neutron spectrometry based on the slowing-down time and the use of this method in studying the energy dependence of the cross sections of nuclear reactions produced by neutrons with energy up to 30 kev. This work is reviewed, and the results achieved are discussed. The theory of the non-stationary moderation and thermalization of neutrons and the results of experimental studies of neutron moderation in graphite, iron and lead, and of neutron thermalization in lead are discussed. Using a pulsed neutron source and resonance detectors the distribution of slowing-down times was measured up to a series of fixed values for final neutron energy. The results are compared with theory, which takes into account the thermal motion of the moderator atoms; in the case of lead this thermal motion leads to a measurable spread in the slowing-down times at energies below 10 ev. The relation between the mean velocity of neutrons in lead and the slowing-down time is measured in the sub-cadmium energy range and a comparison made with multigroup theory. The procedure for determining the energy dependence of neutron reaction cross sections by slowing-down time is described and the potentialities of this method of spectrometry discussed. There follows a brief discussion of the results obtained in two fields of spectrometric measurement. Firstly, precise measurement of the relative excitation functions of the following reactions: $^{3}He(n,p)$, $^{6}Li(n,\alpha)$, $^{10}B(n,\alpha)$, and $^{14}N(n,p)$—the most interesting results being the discovery of a constant negative component of the reaction cross section and indications of the existence of an excited ^{4}He level. Secondly, measurement of the energy dependence of averaged radiative capture cross sections. Measurements carried out on a large number of substances, including separated isotopes, have led to the discovery of hitherto unknown resonance levels with small neutron widths and have made it possible to determine for many nuclei the magnitude of the force function for the capture of neutrons with orbital angular momentum $l = 1$. (auth)

13742 THE CONTRIBUTION OF FLOOR RETURNS TO NEUTRON INTERACTION. Brydon, D.; Parker, J. B.; Pendlebury, E. D. (Atomic Weapons Research Establishment, Aldermaston, Eng.). Vienna, International Atomic Energy Agency, 1965, Preprint No. SM-70/3, 22p. (CONF-651103-14). ORINS.

From IAEA Symposium on Criticality Control of Fissile Materials, Stockholm.

A Monte Carlo method was used to estimate the proportion of neutrons reflected from a floor, simulated by a concrete slab, as a function of position and angle of emergence, from an isotropic source of fission neutrons situated 2 feet 6 inches above the surface of the concrete. A selection of the results from the Monte Carlo calculation are given. Using a secondary program the proportion of neutrons reaching a spherical target situated anywhere above the concrete can be calculated from the results of the Monte Carlo calculation. Results for the case of a unit target sphere situated at the same height as the source are given for different distances of separation between the source and the target and compared with contribution from the neutrons which reach the target direct from the source. The results are discussed in relation to simplified models in which the neutrons are assumed to leave the concrete isotropically. (auth)

13743 NEUTRON GENERATOR. Tawara, Hiroyuki (to Hitachi, Ltd.). Japanese Patent 1964-18487. Aug. 31, 1964. Filed Feb. 25, 1963.

A portable neutron generator includes a hot cathode discharge tube connected to the primary winding of the pulse transformer through a condenser, and the secondary output is fed to the neutron generating tube. Both ends of the primary winding and the middle part of the secondary winding are grounded. The plate and cathode are arranged opposedly in the neutron generating tube, and the discharge between them produces tritium ions from the tritium adsorbed in the tube. (TCO)

13744 NEUTRON GENERATOR. Suematsu, Sigeru (to Hitachi, Ltd.). Japanese Patent 1964-27174. Nov. 27, 1964. Filed Jan. 18, 1964.

A neutron generator is proposed in which the temperature of a target material can be kept automatically below a predetermined value. The neutrons are produced by bombarding the target material with the ions accelerated by several hundred kv—several Mv potential. A temperature indicator is installed at the target, and the accelerated ion beam is controlled by the output of this indicator. (NSA of Japan)

13745 PULSED NEUTRON GENERATOR. Iwashita, Fumio (to Tokyo Shibaura Electric Co., Ltd.). Japanese Patent 1964-30364. Dec. 26, 1964. Filed Oct. 15, 1963.

A pulsed neutron generator is proposed, which can easily and rapidly select a pulsed neutron beam in the pulse width range from microsecond to millimicrosecond orders. The generator consists of an ion source, a target, a deflector placed between the ion source and the target, and a first and a second slit, movable perpendicular to the path of the ions. (NSA of Japan)

Nuclear Properties and Reactions

Refer also to abstracts 12920, 13062, 13070, 13076, 13099, 13101, 13632, 13741, and 14059.

13746 (AD-626681) ELECTRIC MONOPOLE TRANSITIONS AND BETA BANDS IN EVEN NUCLEI. Davidson, J. P. (Naval Radiological Defense Lab., San Francisco, Calif.). Nov. 5, 1965. 31p. (USNRDL-TR-926).

Reduced transition probabilities for electric monopole transitions ρ^2 were calculated using a collective model with deformation vibrations but no asymmetry vibrations. Both ρ^2 and $X = \rho^2 R_0^4/B(E2)$ were evaluated within the context of the model by exact numerical methods for transitions within positive as well as negative parity rotational bands of even nuclei. Comparison of experiment with theory shows quite good agreement in the actinide deformed region; however, for the rare earths theoretical predictions are generally an order of magnitude greater than the measured values. (auth)

13747 (AECD/EP/7) TABLES FOR NEUTRON ENERGY AS A FUNCTION OF BOMBARDING ENERGY AND EMISSION ANGLE FOR THE REACTIONS $^{7}Li(p,n)^{7}Be$, $T(p,n)^{3}He$, $D(d,n)^{3}He$ AND $T(d,n)^{4}He$. Ahmed, Motaheruddin (Atomic Energy Centre, Dacca (Pakistan). Experimental Physics Div.). Oct. 1, 1965. 31p. Dep. mn.

Tabulations are presented for incident beam energies of 0.05 to 3.00 Mev and for emission angles of 0 to 90°. (M.O.W.)

13748 (AECL–2510) NEUTRON ABSORPTION CROSS SECTION OF GROSS FISSION PRODUCTS OF ^{233}U, ^{235}U, AND ^{239}Pu. Okazaki, A.; Durham, R. W.; Lounsbury, M. (Atomic Energy of Canada Ltd., Chalk River (Ontario)). Nov. 1965. 16p. Dep. AECL $0.50.

The thermal and resonance neutron absorption cross sections of the gross fission products of ^{233}U, ^{235}U, and ^{239}Pu were measured. Aluminum alloy samples, irradiated to about 2.5×10^{21} n/cm^2, were measured by the pile oscillator method in the PTR reactor. After the pile oscillator measurements the samples were analyzed for U and Pu content by isotope dilution, electrochemical and alpha counting methods. Pile oscillator measurements were also made on calibration samples containing fissile material and boron. The measured cross sections are lower than the calculated cross sections based on the cross section and fission yield of most of the individual fission products. (auth)

13749 (AEEW-M–502) THE REACTIONS OF NEUTRONS WITH ^{235}U: AN INTERIM REVISION OF THE FILE IN THE U. K. NUCLEAR DATA LIBRARY. Freemantle, R. G. (Atomic Energy Establishment, Winfrith (England)). May 1965. 44p. Dep. BIS $1.20. HMSO 6s.

An interim revision (dated June 1964) of the neutron cross sections of ^{235}U was carried out for inclusion in the U.K. Nuclear Data Library; the new Data File Number is 48. The preliminary experimental data employed in this evaluation were subsequently amended and the effect on this evaluation is discussed. (auth)

13750 (AEEW-M–553) EDITOR: A PROGRAMME FOR EDITING BCD DATA ON MAGNETIC TAPE IN THE FORMAT OF THE U.K.A.E.A. NUCLEAR DATA LIBRARY. Pope, A. L. (Atomic Energy Establishment, Winfrith (England)). May 1965. 14p. Dep. BIS $0.50. HMSO 2s. 6d.

The description and operating instructions of EDITOR are presented. EDITOR is written in the S2 FORTRAN dialect for the IBM 7030 computer. Its purpose is to prepare data library tapes for the U.K.A.E.A. nuclear data library by copying prescribed data files in BCD from one or more input data tapes, or from card decks, onto a single output tape. (auth)

13751 (AEEW-M–606) SLP—A SINGLE LEVEL BREIT-WIGNER CROSS-SECTION GENERATING PROGRAMME. Doherty, G. (Atomic Energy Establishment, Winfrith (England)). June 1965. 10p. Dep. BIS $0.50. HMSO 2s. 6d.

Unbroadened cross-sections are calculated from a single level Breit-Wigner approximation which allows for resonance-potential interference but not resonance-resonance interference. Doppler broadening and instrumental resolution broadening for thin samples are optionally performed by successive numerical convolutions. An energy point selection and discard system enables the cross section over a specified energy range to be represented to a required degree of accuracy using the minimum number of energy points. An energy grid prepared by the user can be incorporated in the calculation but the program will usually be more efficient if only the end points of the energy range of interest are specified by the user and the intermediate energy points left to the program to organize. The capacity of the program varies with the energy range and type of resonance (narrow or broad). About fifty resonances may be sufficient to generate an energy grid of 4000 energy points, which is the maximum allowable energy vector. The program is written in KDF9 EGTRAN (a FORTRAN dialect); output is printed and may be copied on cards, and intermediate results are stored on magnetic disc. (auth)

13752 (ANL–7096) ADDITIONAL YIELD DATA FOR TRANSPLUTONIUM ELEMENT PRODUCTION IN THERMAL REACTORS. Milsted, J.; Macias, E. S.; Basile, L. J.; Anderson, R. W.; Stewart, D. C. (Argonne National Lab., Ill.). Oct. 1965. Contract W-31-109-eng-38. 13p. Dep. mn. CFSTI $1.00 cy, $0.50 mn.

Calculated yields of the heaviest nuclides as formed in various plutonium targets by multiple neutron capture in thermal reactors are presented. Yields of ^{242}Pu, ^{243}Am, ^{244}Cm, ^{246}Cm, ^{252}Cm are given for neutron fluxes of 7×10^{13}, 3×10^{14}, 7×10^{14}, 2×10^{15}, and 1×10^{16} neutrons/cm^2/sec. (M.O.W.)

13753 (BNL–961) THE NEUTRON CROSS SECTION OF SODIUM BELOW 40 Kev. Stephenson, Thomas E. (Brookhaven National Lab., Upton, N. Y.). Dec. 1965. Contract AT-30-2-GEN-16. 23p. (EANDC(US)–82(U)). Dep. mn. CFSTI $2.00 cy, $0.50 mn.

The neutron cross section of sodium from 1 to 40 kev is calculated using the single level formula and BNL-325 resonance parameters for the 2.85-kev level. A good fit to the data is obtained with the spin-dependent scattering radii $R'_+ = 5.85$ f and $R'_- = 5.18$ f. A good fit to the experimental data throughout the region was not found using a spin-independent scattering radius. The excess absorption resonance integral is calculated to be 0.072 barns and is in good agreement with experimental values. The scattering resonance integral is calculated to be 72 barns which compares favorably with an evaluated experimental result. The low energy potential scattering is described by spin-dependent square potential wells. (auth)

13754 (CONF-233(Vol.4)) ROLE OF ATOMIC ELECTRONS IN NUCLEAR TRANSFORMATIONS. Proceedings of International Conference. (International Union of Pure and Applied Physics. International Atomic Energy Agency, Vienna (Austria). Nuclear Energy Information Center, Warsaw (Poland). Polish Academy of Sciences, Warsaw). Sept. 28, 1963. 204p. Dep. ORAU.

Separate abstracts were prepared for 14 of the 16 included papers. The remaining two papers appeared previously in NSA as 18: 34837 and 19: 27438. (M.O.W.)

For abstracts of individual papers see: 13413 and 13755–13767.

13755 (CONF-233(Vol.4), pp 548-60) L, M, and N PHOTO-ELECTRIC CROSS SECTION MEASUREMENTS IN URANIUM FOR $h\nu = 122$ kev. Boyd, H. W.; Brantley, W. H.; Hamilton, J. H. (Vanderbilt Univ., Nashville, Tenn.).

The internal-external conversion method was used to find the L, M, and N photoelectric cross sections for $h\nu = 122$ kev. The conversion coefficient of this transition in ^{152}Sm is well known so that the photoelectric cross section for the L shell may be obtained. Results obtained are: $\tau_L = 360 \pm 40$ b/atom, $\tau_{L_I+L_{II}}/\tau_{L_{III}} = 3.1 \pm 0.35$, $\tau_L/\tau_M = 4.55 \pm 0.55$, and $\tau_M/\tau_{N+} = 2.5 \pm 0.3$. The τ_L value is higher than that predicted from τ_K when the τ_K/τ_L ratio is assumed to be energy independent. The $\tau_{L_I+L_{II}}/\tau_{L_{III}}$ and τ_M/τ_{N+} ratios are in agreement with other results. (auth)

13756 (CONF-233(Vol.4), pp 562-94) SCATTERING OF 662-kev γ-RAYS ON BOUND ELECTRONS. Di Lazzaro, M. A.; Missoni, G. (Istituto Superiore di Sanitá, Rome (Italy). Laboratori di Fisica).

Measurements were made of the incoherent scattering cross section for 662-kev photons, by K and L electrons of gold and uranium. Measurements were also made of coherent scattering cross section by atoms of gold for scattering angles ranging from 4 to 90°. Finally energy distribution of the photons incoherently scattered by the K and L shell electrons of gold and K shell electrons of uranium were determined. (M.O.W.)

13757 (CONF-233(Vol.4), pp 595-608) SCATTERING CROSS SECTIONS WITH AND WITHOUT ATOMIC EXCITATION FOR 50-500 Kev ELECTRONS. Motz, J. W.; Placious, R. C.; Dick, C. E. (National Bureau of Standards, Washington, D. C.).

Experimental results are given for some of the important processes responsible for electron scattering in the energy region from 50 to 500 kev. For scattering without atomic excitation ("elastic") of 50, 100, 200, and 400 kev electrons at 20 to 110 degrees from thin gold targets, the experimental cross sections show good agreement with the Lin, Sherman, and Percus phase shift calculations including Hartree screening for the exact Mott cross section. For scattering with atomic excitation ("inelastic")

of 500 kev electrons at 100 degrees from thin gold and aluminum targets, the experimental cross sections in the 300 kev energy region for the scattered electron are approximately an order of magnitude larger than the sum of the theoretical cross sections evaluated with the Born calculations of Racah and of Weber, Deck, and Mullin for the respective processes of bremsstrahlung and of atomic K-shell ionization. This disagreement can be attributed to the breakdown in this energy region of both the high energy approximation in the latter calculation and the Born approximation in both calculations. (auth)

13758 (CONF-233(Vol.4), pp 609-13) INVESTIGATIONS ON THE INTERNAL BREMSSTRAHLUNG ACCOMPANYING THE NON-UNIQUE SECOND-FORBIDDEN ELECTRON CAPTURE DECAY OF ^{36}Cl. Berenyi, D. (Magyar Tudomanyos Akademia Atommag Kutato Intezet, Debrecen).

The internal bremsstrahlung accompanying the non-unique second forbidden electron capture decay of ^{36}Cl to ^{36}S ($2^+ \rightarrow 0^+$ transition) is discussed. Brief results from a study of this spectra are discussed. (M.O.W.)

13759 (CONF-233(Vol.4), pp 614-24) INTERNAL BREMSSTRAHLUNG ACCOMPANYING THE ELECTRON CAPTURE DECAY OF MEDIUM HEAVY NUCLEI. Sujkowski, Z.; Jastrzebski, J.; Zglinski, A.; Zylicz, J. (Institute of Nuclear Research, Swierk (Poland)).

The radiative electron capture decay of ^{165}Er and ^{159}Dy is studied. The singles and the K x-ray coincidence spectra are obtained and compared with the theory of Glauber and Martin. Good agreement with the theory is obtained for the shapes as well as for the intensities of the IS spectra (the radiative K capture). The intensities of the P spectra, however, seem to be appreciably lower than the predicted ones. (auth)

13760 (CONF-233(Vol.4), pp 637-55) CUSP OF THE INTERNAL BREMSSTRAHLUNG SPECTRA NEAR $2M_e$ DUE TO THE SURFACE OF THE COULOMB-DISTORTED NEGATIVE ENERGY SEA. Koh, Yujiro (Osaka City Univ. (Japan)).

With the intention to clarify differences and relations between the spectra of the internal bremsstrahlung due to the orbital electron capture and the ordinary beta spectra, two topics are discussed; an anomaly of the internal bremsstrahlung at an energy slightly less than $2M_e$, i.e., a cusp of the spectrum attributed to the existence of the surface of intermediate negative energy sea of electrons in the Coulomb field; and the correspondence of the multipole expansions. A method of the numerical calculation for the precise shape of the cusp is presented which is at least necessary as a new correction for the precise determination of the disintegration energy of the proton excess nuclei near $2M_e$. Promising test nuclei suitable for observing such anomaly are discussed. (auth)

13761 (CONF-233(Vol.4), pp 656-68) THE INTERNAL BREMSSTRAHLUNG IN β-DECAY. Bienlein, J. K. (Erlangen Univ. (West Germany). Physikalisches Institut); Felsner, G. (Erlangen Univ. (West Germany). Institut fuer Theoretische Physik).

The theory of internal bremsstrahlung in β-decay is briefly discussed. Some measurements of the internal bremsstrahlung spectra in the decay of ^{6}He, ^{90}Sr, and ^{90}Y were made. The results are discussed. (M.O.W.)

13762 (CONF-233(Vol.4), pp 700-9) THE INVESTIGATION OF INTERNAL PAIR FORMATION FOLLOWING NEUTRON CAPTURE. Meyer, L. (Zentralinstitut fuer Kernphysik, Rossendorf bei Dresden (East Germany)).

Techniques for studying internal pair production by neutron capture reactions are discussed. The energy spectrum of the pairs from the ^{35}Cl(n,λ)^{36}Cl reaction was obtained using a cloud chamber. (M.O.W.)

13763 (CONF-233(Vol.4), pp 710-19) MAGNETIC INTERACTION OF THE ^{155}Gd NUCLEUS IN THE 87-Kev EXCITED STATE. Bozek, E.; Hrynkiewicz, A. Z.; Ogaza, S.; Styczen, J. (Institute of Nuclear Physics, Krakow (Poland)).

The experimental technique for investigating the magnetic interaction of the ^{155}Gd nucleus in the 87-kev state is discussed. In particular, the half life of the 87-kev state, the time dependence of the attenuation coefficients, decoupling by the longitudinal magnetic field, and decoupling of the hfs-interaction by the transverse magnetic field are discussed. (M.O.W.)

13764 (CONF-233(Vol.4), pp 720-2) A METHOD TO DERIVE ELECTRIC QUADRUPOLE MOMENTS OF 2^+ ROTATIONAL STATUS OF RARE EARTH NUCLEI FROM THE ATTENUATION PARAMETERS λ_2 AND λ_4 OF $\gamma\gamma$-ANGULAR CORRELATIONS. Bodenstedt, E.; Guenther, Ch. (Bonn Univ. (West Germany). Institut fuer Strahlen und Kernphysik).

The theory of A. Abragam and R. V. Pound (Phys. Rev. 92: 943(1953)) is discussed and its weaknesses are pointed out. A brief discussion of the considerations which must be taken into account is presented. (M.O.W.)

13765 (CONF-233(Vol.4), pp 723-5) g FACTORS OF THE ROTATIONAL BANDS IN ^{177}Lu AND ^{177}Hf. Boehm, F.; Alexander, P.; Kankeleit, E. (California Inst. of Tech., Pasadena).

A study of the branching ratios of the crossover-to-cascade transitions $\lambda = T_\gamma(E2)/[T_\gamma(E2) + T_\gamma(M1)]$ was made. The branching ratio λ and the quantity $[(g_K - g_R)/Q_0]^2$ as derived from the branching ratio are given for the transitions in the $K = 7/2$ band of ^{177}Lu and in the $K = 7/2^-$ and $K = 9/2^+$ bands of ^{177}Hf. The symbols g_K and g_R are the g factors for the intrinsic and rotational nuclear motion respectively. (M.O.W.)

13766 (CONF-233(Vol.4), pp 726-9) THE M4 ISOMERISM IN ^{205}Pb. Bergkvist, K. E.; Stockendal, R. (Nobel Inst. of Physics, Stockholm (Sweden)).

Previous experiments do not agree on the γ transition probability in the decay of ^{205}Bi. Internal conversion measurements were carried out on ^{205}Bi in order to measure the M4 transition probability. It was shown that there exists two transitions in ^{205}Pb with an energy near 1014 kev. (M.O.W.)

13767 (CONF-233(Vol.4), pp 730-42) THE DECAY OF ^{184}Ta. Verheul, H.; Blok, J.; Boddendijk, H. G.; Dulfer, G. H. (Vrije Universiteit, Amsterdam (Netherlands). Natuurkundig Laboratorium).

The beta decay of ^{184}Ta to the excited states of ^{184}W was investigated by $\beta - \gamma$ coincidence experiments. Data are compared with previous experimental data. (M.O.W.)

13768 (CONF-650410-40) ANGULAR-CORRELATION MEASUREMENTS FOR THE ^{26}Mg(d,pγ)^{27}Mg REACTION. Tilley, D. R. (Mullard Research Labs., Reigate (England)). [nd]. 9p. ORAU.

From American Physical Society, Washington, D. C.

The energy levels of ^{27}Mg were studied by measuring p-γ angular correlations in the reaction ^{26}Mg(d,pγ)^{27}Mg. The data were analyzed using plane-wave stripping theory. Spin assignments were made for low-lying levels of ^{27}Mg. (D.C.W.)

13769 (DP-949) ENERGY SPECTRA OF NEUTRONS AND GAMMA RAYS FROM SPONTANEOUS FISSION OF ^{244}Cm. Herold, T. Richard (Du Pont de Nemours (E. I.) and Co., Aiken, S. C. Savannah River Lab.). July 1965. Contract AT(07-2)-1. 23p. Dep. mn. CFSTI $2.00 cy, $0.50 mn.

The energy spectrum of the neutrons from the spontaneous fission of ^{244}Cm was measured from 0.5 to 6 Mev with a solid state ^{3}He spectrometer. The spectrum shows a maximum at about 0.75 Mev and decreases exponentially above 2 Mev. The energy spectrum of the gamma rays that were emitted within 180 nanoseconds of the spontaneous fission neutrons was measured from 0.1 to 2.5 Mev with a gamma ray spectrometer that included the ^{3}He spectrometer in a coincidence circuit. The gamma ray spectrum shows a dual-peak maximum at about 200 kev and decreases exponentially above 800 kev. Both measured spectra are similar to the corresponding spectra from the spontaneous fission of ^{252}Cf. The measurements were made with a purified sample of 95.5 wt % ^{244}Cm that was produced in a Savannah River reactor. (auth)

13770 (GA-6576) A COMPILATION AND EVALUATION OF THE NUCLEAR DATA AVAILABLE FOR THE MAJOR PLUTONIUM ISOTOPES. Drake, M. K.; Dyos, M. W. (General Atomic, San Diego, Calif. John Jay Hopkins Lab. for Pure and Applied Science). July 30, 1965. Contracts AT(04-3)-167; AT(04-3)-187. 173p. Dep. mn. CFSTI $5.00 cy, $1.00 mn.

The available data for ^{239}Pu, ^{240}Pu, ^{241}Pu, and ^{242}Pu were compiled and evaluated for neutron energies between thermal and 15 Mev. The data obtained from this evaluation are presented in the form used in the General Atomic data library. A best set of single level resonance parameters was obtained, over the resolved resonance region for each of the above nuclides, in order that some estimate of the Doppler coefficient of reactivity can be made. (auth)

13771 (IA-1050) FURTHER STUDY OF NUCLEAR RESONANT SCATTERING USING NEUTRON-CAPTURE GAMMA RAYS. Ben-David, G.; Arad, B.; Balderman, J.; Schlesinger, Y. (Israel Atomic Energy Commission, Yavne. Soreq Nuclear Research Center). Aug. 1965. 35p. Dep. mn.

The study of resonance scattering of neutron capture gamma rays was extended using 22 capture gamma sources and 57 scattering targets. About fifty resonance scattering events were observed in 23 elements and the effective cross sections evaluated. Some cases of complex spectra are described. The association of the scattering with nuclei in the region of closed shells is clearly shown. Problems of minimum observable cross sections are discussed and some further applications of the technique are suggested. (auth)

13772 (IEA-99) PARAMAGNETIC STUDIES OF HOLMIUM BY NEUTRON TOTAL CROSS SECTION MEASUREMENTS. Mattos, Marieta C. (Instituto de Energia Atomica, Sao Paulo (Brazil)). Aug. 1965. 12p. (CONF-650804-31). Dep. mn.

From 5th Rare Earth Research Conference, Ames, Iowa.

The total neutron cross section for holmium was measured for neutron wavelengths between 0.20 and 9.00 Å. The IEA crystal spectrometer was used together with a mechanical velocity selector to eliminate higher order reflections from the crystal. Powder samples of Ho_2O_3 were prepared in high purity, taking particular care to eliminate contamination by the rare earths of high neutron cross section. Although paramagnetic form factors are usually determined by differential cross section measurements with one neutron wavelength, accurate total cross section measurements for a wide range of known wavelengths give definite information on the radius of the 4f electron orbits. Measurements indicate a radius different from the one used by Blume, Freeman and Watson, who calculated the form factor assuming hydrogenic wave functions. The possible choice of different screening constant is discussed. (auth)

13773 (IKF-13) KERNSPEKTROSKOPISCHE UNTERSUCHUNGEN MIT HILFE VON (n,pγ)- UND (n,αγ)-REAKTIONEN. (Nuclear-Spectroscopic Investigations Using (n,pγ)- and (n,αγ)-Reactions). Bass, R. (Institut fuer Kernphysik, Universitaet Frankfurt (West Germany)). 1965. 84p. Dep. mn.

A method of using a scintillation crystal both as target and detector for neutron-induced reactions was extended by the observation and analysis of coincident γ-radiation. Thereby improved separation and identification of individual final states as well as information on their modes of γ-deexcitation could be obtained. K(Tl) and Na(Tl) crystals were employed at various neutron bombarding energies between 4 and 14 Mev. Low-lying states of the final nuclei ^{39}Ar, ^{36}Cl, ^{23}Ne and ^{20}F, produced in (n,p) or (n,α) reactions of the target nuclei ^{39}K and ^{23}Na, were studied. Pulse-shape-discrimination was used where necessary to identify the reaction products and to eliminate background. In addition to normal p-γ or α-γ coincidence measurements, triple coincidence measurements were performed with the sumcoincidence technique. For selected final states absolute production cross sections and γ-ray angular distributions were measured, and analyzed by appropriate theories assuming a compound nucleus reaction mechanism. (M.O.W.)

13774 (JAERI-1096) PROGRAM ELIESE-1: FORTRAN-II PROGRAM FOR ANALYSES OF ELASTIC AND INELASTIC SCATTERING CROSS SECTIONS. (Japan Atomic Energy Research Inst., Tokyo). Nov. 1965. 87p. Dep. mn.

The program ELIESE-1 can be used for calculating any kinds of cross sections for elastic and inelastic scatterings of neutrons, protons and alpha particles by means of the optical model and of the Hauser-Feshbach's method in the compound nuclear process. (auth)

13775 (JINR-P-2490) NEUPRUGOE RASSEYANIE ELEKTRONOV NA YADRAKH S VOZBUZHDENIEM KOLLEKTIVNYKH UROVNEI. (Inelastic Scattering of Electrons on Nuclei With Collective Level Excitation). Petkov, I. Zh., Luk'yanov, V. K.; Pol, Yu. S. (Joint Inst. for Nuclear Research, Dubna (USSR). Lab. of Theoretical Physics). 1965. 18p. Dep. mn.

Inelastic scattering of electrons on medium-weight and heavy nuclei was treated in the adiabatic approximation. A distortion of the electron wave in the field of the nucleus is taken into account in the high energy approximation. An analytical expression was obtained for the scattering amplitude in terms of the sum of residues in the poles of the Fermi distribution of the charge density in the nucleus. The effect of "multiple" transitions on the elastic scattering cross section is estimated. It turns out that they may not be taken into account. The calculations made by the obtained analytical formulas are compared with experiment. (auth)

13776 (JINR-P-2499) OBNARUZHENIE SPONTANNO DELYASHCHEGOSYA IZOMERA S $T_{½}$ = 2.6 MIN V YADERNYKH REAKTSIYAKH $^{233}U + ^{11}B$ I $^{233}U + ^{10}B$. (An Observation of Spontaneously Fissionable Isomer with $T_{½}$ = 2.6 min in the Nuclear Reaction $^{233}U + ^{11}B$ and $^{233}U + ^{10}B$). Kuznetsov, V. I.; Skobelev, N. K.; Flerov, G. N. (Joint Inst. for Nuclear Research, Dubna (USSR). Lab. of Nuclear Reactions). 1965. 6p. Dep. mn.

In the nuclear reactions $^{233}U + ^{10}B$ and $^{233}U + ^{11}B$ a spontaneously fissionable product with $T_{½}$ = (2.6 ± 0.2) min was observed. The excitation function of this product in the reaction $^{233}U + ^{11}B$ was investigated. The magnitude of the maximum production cross section was found to be 2.10^{-33} cm^2. A conclusion was drawn that the nucleus of Am or of another lighter element with mass number A ≤ 236 undergoes a spontaneous fission with $T_{½}$ = 2.6 min. (auth)

13777 (JINR-E-2515) ON THE STRUCTURE OF SPONTANEOUSLY FISSIONING ISOMERS. Malov, L. A.; Polikanov, S. M.; Soloviev, V. G. (Joint Inst. for Nuclear Research, Dubna (USSR)). 1965. 15p. Dep. mn.

The possibility of the existence of isomeric states with deformations larger than those of nuclei in the ground state was studied. Under the assumption that spontaneously fissioning isomers are two-quasi-particle states of odd-odd nuclei with the equilibrium deformation δ_i= 0.31 to 0.33 and an excitation energy with respect to the ground state of the nucleus at δ_0 of the order of 1.0 to 1.5 Mev, the probabilities of the spontaneous fission of such isomers in odd-odd nuclei were estimated. The possibility of the existence of spontaneously fissioning isomers in odd-A and even-even nuclei was also considered. (D.C.W.)

13778 (JINR-P-2525) PERIOD POLURASPADA IZOTOPA 102 ELEMENTA S MASSOVYM CHISLOM 256. (Half-Life of an Isotope of Element 102 With Mass Number 256). Kuznetsov, V. I.; Lobanov, Yu. V.; Perelygin, V. P. (Joint Inst. for Nuclear Research, Dubna (USSR). Lab. of Nuclear Reactions). 1965. 7p. Dep. mn.

By bombarding a ^{242}Pu target with accelerated ^{18}O ions the half-life of the isotope of element 102 with mass number 256 was measured to be (8.2 ± 1.0) s. The measurement of the half-life was made by spontaneous fission. Charged particle detectors were used. (auth)

13779 (JINR-P-2465) NOVYI IZOTOP ^{216}Ac. (A New Isotope ^{216}Ac). Rotter, Kh.; Demin, A. G.; Pashchenko, L. P.; Brinkmann, Kh. F. (Joint Inst. for Nuclear Research, Dubna (USSR). Lab. of Nuclear Reactions). 1965. 12p. Dep. mn.

A new short-lived isotope ^{216}Ac created via the reaction

$^{209}Bi(C^{-12}, 5n)^{216}Ac$ was observed. The measured values of half-life and energy of α particles $T_{½} = (0.39 \pm 0.03)$ ms and $E_\alpha = (9.14 \pm 0.03)$ Mev, agree with the α-decay systematics of nuclei with N = 127. The α-particle energies of ^{213}Rn, ^{214}Fr and ^{215}Ra were also measured. Under some assumptions concerning the decay scheme of these nuclei reduced widths of α decay of nuclei with N = 127 were calculated and their relative behavior is discussed. (auth)

13780 (KFK–358) ZWEI NEUE ISOTOPE DES TECHNETIUMS, ^{106}Tc UND ^{107}Tc. (Two New Isotopes of Technetium, ^{106}Tc and ^{107}Tc). Feuerstein, Horst (Kernforschungszentrum, Karlsruhe (West Germany). Institut fuer Radiochemie). Aug. 1965. 68p. Dep. mn.

A method for the fast and quantitative separation of Tc from Mo, Ru, Rh, and Pd by extraction was developed. By means of this separation method it is possible to separate within 60 sec radiochemically pure technetium from the fission product mixture. In addition to the γ lines given earlier of the isotopes ^{103}Tc, ^{104}Tc, and ^{105}Tc, in the γ spectrum of ^{105}Tc two additional γ lines were found so that now 3 lines, at 80, 108 and 144 kev, are known. The half lives given by Kienle of the 3 isotopes ^{103}Tc, ^{104}Tc, and ^{105}Tc were confirmed. The values found were for ^{103}Tc, $t_{½} = 50 \pm 4$ sec, for ^{104}Tc $t_{½} = 18.0 \pm 0.1$ min, and for ^{105}Tc $t_{½} = 8.0 \pm 0.02$ min. The half lives of the two previously unknown Tc isotopes were for ^{106}Tc $t_{½} = 38 \pm 3$ sec and for ^{107}Tc $t_{½} = 29 \pm 3$ sec. The γ spectrum of Tc preparations taken 80 sec after the end of the irradiation shows a marked γ line at 0.28 Mev which decays with a half life of 38 sec and is assigned with high probability to ^{106}Tc. The cumulative yields of ^{105}Tc, ^{106}Tc, and ^{107}Tc were determined and the Z_p values for these mass numbers for the fission of ^{235}U and ^{239}Pu with thermal neutrons were determined. The Z_p values found lie only slightly above the values calculated using the Talot-Erben function. Investigations on ^{108}Tc, ^{109}Tc, ^{106}Mo, and ^{107}Mo showed that these isotopes must have half lives of less than 10 sec. (tr-auth)

13781 (NASA-CR-354) INVESTIGATIONS OF ELECTRON INTERACTIONS WITH MATTER. PART 1. BREMSSTRAHLUNG PRODUCTION IN ALUMINUM AND IRON. PART 2. ELECTRON SCATTERING IN ALUMINUM. Dance, William E.; Baggerly, Leo L.; Rester, David H.; Rainwater, Walter J. Jr. (LTV Research Center, Dallas, Tex.). Dec. 1965. Contract NASw-948. 92p. CFSTI $3.00 cy, $0.75 mn.

Part 1 by Dance and Baggerly. Part 2 by Rester and Rainwater.

The experimental intensity spectra, differential in photon energy and angle, for thick targets of aluminum and iron in the energy range 0.5 to 3.0 Mev are presented. The spectra integrated over photon angle are given for Al and Fe as a function of incident electron energy. The cross section for Coulomb scattering of electrons by Al without atomic excitation are given for incident electron energies of 0.1 to 3.0 Mev at scattering angles from 30 to 150°. (M.O.W.)

13782 (ORNL-P-1927) EXCITATION AND DISINTEGRATION OF NUCLEI BY LOW-ENERGY ELECTRONS AND X-RAYS. Guth, E. (Oak Ridge National Lab., Tenn.); Edge, R. D. (South Carolina Univ., Columbia). [1965]. Contract W-7405-eng-26. 8p. (CONF-651118-5). Dep. mn. CFSTI $1.00 cy, $0.50 mn.

From American Physical Society, Gatlinburg, Tenn.

The purposes and uses of low energy (E < 30 Mev) electron studies are briefly discussed. Examples are given of ^{7}Li and ^{115}In excitation by low energy electrons and x rays for energy level determinations. (M.O.W.)

13783 (ORNL-TM-1333) INDEPENDENT YIELDS OF ^{95}Zr FROM THERMAL NEUTRON FISSION OF ^{235}U AND ^{233}U [Thesis]. Niece, Lawrence H. (Oak Ridge National Lab., Tenn.). Dec. 1965. Contract W-7405-eng-26. 118p. Dep. mn. CFSTI $4.00 cy, $0.75 mn.

Submitted to Missouri Univ., Columbia.

Independent fission yields of ^{95}Zr from thermal neutron fission of ^{235}U and ^{233}U are determined to be 0.0040 ± 0.006 and 0.034 ± 0.009 respectively. From the values obtained, together with previously measured yields, the width of the charge dispersion for mass-95 fission products in ^{235}U fission is found to be 0.53 ± 0.03 in terms of the width parameter σ of the normal Gaussian curve. This small value suggests that the forty-proton subshell does not enhance the independent yield of ^{95}Zr. The small σ value, when compared to other known σ values, suggests a small decrease in σ with fission product mass. An empirical σ function is formulated to describe the variation of σ with fission product mass. An upper limit of 0.56 for σ in the case of mass-95 products from ^{233}U fission indicates that charge dispersion in this system is similar to that for ^{235}U. Incidental to this research, half lives of 6 ± 2 sec and 16.82 ± 0.5 hr are determined for ^{97}Y and ^{97}Zr, respectively. (auth)

13784 (ORNL-TM-1336) NUCLEAR STRUCTURE STUDIES IN ZIRCONIUM WITH 65-Mev ALPHA PARTICLES [Thesis]. Bingham, Carrol R. (Oak Ridge National Lab., Tenn.). Jan. 1966. Contract W-7405-eng-26. 132p. Dep. mn; CFSTI $4.00 cy, $1.00 mn.

Submitted to Univ. of Tennessee, Knoxville.

Optical-model analysis of elastic scattering from ^{92}Zr yielded a distinct minimum in χ^2 at a real well depth of 34.6 Mev. A continuous ambiguity was found indicating the importance of the surface region of the potential. Collective-model calculations for the inelastic scattering showed no preference among the ambiguous potentials, and predictions were generally in good agreement with the data. Shell model and distorted wave calculations were also made. The ^{90}Zr (α,He-3) angular distribution showed sensitivity to the choice of optical-model parameters. (J.F.P.)

13785 (ORNL-TM-1374) NUCLEAR GROUND STATE PROPERTIES OF ^{16}O BY AN EXTENSION OF THE EDEN-EMERY METHOD [Thesis]. MacKellar, Alan Douglas (Oak Ridge National Lab., Tenn.). Feb. 1966. Contract W-7405-eng-26. 149p. Dep. mn. CFSTI $4.00 cy, $1.00 mn.

A Brueckner theory calculation of the nuclear ground state properties of ^{16}O is performed. The method employed is an extension of the calculations of Eden and Emery, and Eden, Emery, and Sampanthar. The Bethe-Goldstone equation is solved using harmonic oscillator unperturbed single particle wave functions and the Eden-Emery approximation of the effect of the Exclusion Principle. Explicit equations are derived for the Brueckner-Hartree-Fock single particle potential and ground state binding energy for doubly closed-shell nuclei using the transformation properties of harmonic oscillator functions from single particle to relative and center-of-mass coordinates. However, in the numerical calculation for ^{16}O, the Eden-Emery-Sampanthar approximation to self consistency is kept, which adds an adjustable state-dependent constant to the harmonic oscillator potential and employs an approximate variational calculation to determine the harmonic oscillator range parameter. The two-nucleon interactions studied are the standard hard core potential of Moszkowski and Scott (SHC), the Brueckner-Gammel-Thaler potential (BGT), the Hamada-Johnston potential (HJ), and the Yale potential. The resulting calculated binding energy per nucleon for ^{16}O is −5.1 Mev for SHC, −9.2 Mev for BGT, −8.0 Mev for HJ, and −5.1 Mev for Yale. Single particle levels are calculated and in general are more tightly bound than the levels calculated by Brueckner, Lockett, and Rotenberg applying the "local density" approximation to nuclear matter t-matrix elements. The calculated $p_{½} - p_{⅜}$ splitting is found to be larger and the model rms radius smaller than the experimental values for all cases. (M.O.W.)

13786 (ORNL-TM-1396) RCS-2—A FORTRAN PROGRAM FOR THE CALCULATION OF CROSS SECTIONS FROM RESONANCE PARAMETERS. Thomas, W. E.; Tsagaris, M. E. (Oak Ridge National Lab., Tenn.). July 7, 1965. Contract W-7405-eng-26. 23p. Dep. mn. CFSTI $1.00 cy, $0.50 mn.

The program evaluates point microscopic absorption, fission, scattering, and total cross sections from resonance parameters by the Breit-Wigner single level formula. All cross sections are computed in the laboratory

system of coordinates. Options are available for normalizing absorption cross sections to an input 2200 m/s value, computing 1/E flux weighted average group cross sections for any desired group structure, and evaluating the parameters E_0 and Γ_n for a possible "negative energy resonance." RCS-2 is written in FORTRAN for the IBM 7090. (auth)

13787 (TID–22637) [REACTION CROSS SECTIONS]. Final Report. Pilger, Richard C. (Notre Dame Univ., Ind.). Jan. 1966. Contract AT(11-1)-834. 58p. Dep. mn. CFSTI $3.00 cy, $0.75 mn.

The excitation functions and cross sections were calculated for the following reactions; $^{165}Ho(\alpha,3n)^{166}Tm$, $^{165}Ho(\alpha,4n)^{165}Tm$, $^{165}Ho(\alpha,2n)^{167}Tm$, $^{165}Ho(\alpha,n)^{168}Tm$, $^{164}Er(\alpha,2n)^{166}Yb$, $^{166}Er(\alpha,4n)^{166}Yb$, $^{164}Er(\alpha,3n)^{165}Yb$, $^{164}Er(\alpha,n)^{167}Yb$, $^{166}Er(\alpha,3n)^{167}Yb$, $^{167}Er(\alpha,4n)^{167}Yb$, $^{166}Er(\alpha,pn)^{168}Tm$, and $^{167}Er(\alpha,p2n)^{168}Tm$. The results are presented. (M.O.W.)

13788 (ORNL-tr-1062) TRANSITION RADIATION OF A CHARGED RELATIVISTIC PARTICLE IN THE OPTICAL FREQUENCY RANGE. Pafomov, V. E.; Frank, I. M. (Akademiya Nauk SSSR, Moscow. Institut Fiziki). Translated for Oak Ridge National Lab., Tenn., from report A-76. 1965. 19p. Dep. mn. CFSTI $1.00 cy, $0.50 mn. JCL $1.60 fs, $0.80 mf.

The transition radiation is examined for a charged relativistic particle in the optical frequency range. The results of calculations of radiation intensity are reported, as a function of the magnitude of the real and imaginary parts of the refractive index. The problem of the possibility of using transition radiation for measuring the optical properties of metals is discussed. (M.O.W.)

13789 BETHE-SALPETER EQUATION AND CONSERVATION LAWS IN NUCLEAR PHYSICS. Brenig, W. (Max Planck Institut fuer Physik, Munich. Technische Hochschule, Munich). Acta Phys. Acad. Sci. Hung., 19: 281-7(1965).

Finite nuclei are considered with the method of interacting quasiparticles. The justification of this description is based on the application of the Bethe-Salpeter technique. The number of free parameters are reduced with the help of invariance properties. (auth)

13790 MANY-BODY FOUNDATIONS OF THE NUCLEAR SHELL MODEL. Brandow, B. H. (Inst. for Theoretical Physics, Copenhagen). Acta Phys. Acad. Sci. Hung., 19: 289-94(1965).

It is shown how the general features of the shell model emerge when the Brueckner-Bethe-Goldstone theory of nuclear matter is extended to the case of finite nuclei. The basic idea is to use perturbation theory, together with suitable partial summations. The starting point is $H_0 = T + V_{SM}$, where V_{SM} is a one-body operator chosen to optimize convergence of the expansion. After some comments on perturbation theory, it is indicated how the Brueckner reaction matrix can be calculated within the finite geometry defined by the above H_0. Finally, the form of V_{SM} that leads to a rapid convergence of the linked-cluster expansion is discussed. (auth)

13791 THE METHOD OF EFFECTIVE INTERACTION IN NUCLEAR PHYSICS. Mittelstaedt, P. (Max-Planck-Institut fuer Physik und Astrophysik, Munich). Acta Phys. Acad. Sci. Hung., 19: 303-14(1965).

In the nuclear two-body problem the Gammel-Thaler hard core potential can be replaced by any one of an infinite number of equivalent non local potentials, which are regular everywhere. Such potentials can easily be constructed. It is investigated, to what degree equivalent two-body potentials are also equivalent for the nuclear many body problem, and can therefore be used as effective interaction in the many-body hamiltonian. (auth)

13792 NUCLEAR MATTER WITH MOMENTUM-DEPENDENT NUCLEAR FORCES. Rennert, P. (Technical Univ., Dresden). Acta Phys. Acad. Sci. Hung., 19: 357-9 (1965).

Nuclear matter with momentum-dependent nuclear forces are investigated with the result that those forces are suitable to explain certain properties of atomic nuclei and nuclear scattering experiments. (auth)

13793 THE SECOND VIBRATIONAL STATE OF EVEN-EVEN SPHERICAL NUCLEI. Chlebowska, Daniela; Zielinska, Malgorzata (Inst. for Nuclear Research, Warsaw). Acta Phys. Pol., 28: 523-32(Oct. 1965).

The energy of the second vibrational state (the triplet 0^+, 2^+, 4^+) in spherical even-even nuclei is estimated from the poles of the four-particle Green function. The two-phonon approximation is used, taking into account the correction arising from the particle-hole interaction. The one-phonon functions are calculated by solving the equations given by Belyaev. The energy of the levels of the triplet is calculated numerically for several nuclei with double magic core. (auth)

13794 ON INELASTIC SCATTERING OF COMPLEX NUCLEI WITH LARGE CHARGES. Grabovskii, Ya.; Ivanova, S. P.; Kalinkhin, B. N. (Joint Inst. for Nuclear Research, Dubna, USSR). Acta Phys. Pol., 28: 783-8 (Dec. 1965). (In Russian).

The effect of dynamic deformation on the process of inelastic scattering of heavy ions by complex nuclei is studied for the range of energies under the Coulomb barrier. Results of calculations are presented for $^{69}Ga + {}^{132}Xe \rightarrow {}^{69*}Ga + {}^{132}Xe$, giving the ^{69}Ga quadrupole deformation as a function of the internuclear distance and the total collision cross section of the ^{69}Ga single-particle level 1 $f_{\frac{5}{2}}$ as a function of the collision energy and of a parameter representing the terms not included in the Nilsson hamiltonian. (M.J.T.)

13795 THE PHOTOEMISSION OF NEUTRONS AT 6 TO 80 Mev FROM ^9Be. Costa, S.; Minetti, B. Molino, C.; Pasqualini, L.; Piragino, G. Atti Accad. Sci. Torino: I. Cl. Sci. Fis., Mat. Natur., 99: 1157-64(1964-65). (In Italian).

The cross section for the photoproduction of neutrons at 6 to 80 Mev by ^9Be was measured using the 31-Mev betatron and the 100-Mev synchrotron at Turin. The results obtained indicate the presence of a region between 25 and 40 Mev in which the photon absorption is considerable. The levels of ^9Be in this energy region, recently predicted, were partially confirmed. (tr-auth)

13796 SPIN ASSIGNMENTS FOR THREE RESONANCES IN ^{191}Ir. Bhat, M. R. (Atomic Energy of Canada Ltd., Chalk River, Ont.). Can. J. Phys., 44: 399-408(Feb. 1966). (AECL-2381).

Resonant scattering of neutrons by iridium was studied with samples of three different thicknesses. The scattering cross section for the 5.36-, 30-, and 51.3-ev resonances of ^{191}Ir was measured. These measurements combined with the published transmission data and the fact that the target nucleus has a spin of $\frac{3}{2}$ give the spins of these resonances. The 5.36-ev resonance is found to have a spin of 2, while each of the other two resonances has a spin of 1. (auth)

13797 THE ELECTRON CAPTURE TO NEGATIVE ELECTRON EMISSION BRANCHING RATIO FOR ^{142}Pr DECAY. Crocker, I. H.; Werner, R. D.; Cherrin, W. (Atomic Energy of Canada Ltd., Chalk River, Ont.). Can. J. Phys., 44: 409-14(Feb. 1966). (AECL-2379).

The ratio of electron capture to negative electron emission for the decay of ^{142}Pr was found to be $(1.64 \pm 0.08) \times 10^{-4}$. The half life for electron capture, relative to the accepted beta emission half life of 19.2 hours, is 13.3 ± 0.6 years. The ratio was found by mass-spectrometric stable isotope dilution determinations of the quantities of ^{142}Ce and ^{142}Nd produced by the decay. (auth)

13798 A FORMALISM BASED ON A SYMMETRIC INTERACTION IN THE INPUT AND OUTPUT METHODS FOR REARRANGEMENT COLLISIONS. Lafoucriere, Joseph; Pigeon, Jacques; El-Baz, Edgard (Institut de Physique Nucleaire, Lyon). Compt. Rend., 261: 5327-9 (Dec. 20, 1965). (In French).

The study of the first "post" and "prior" terms of the Born series makes it possible to propose a formalism based on a symmetric interaction in the input and output

paths for a rearrangement collision. This formalism makes it possible to resolve, in particular, the problem of orthogonality of the initial and final states. (tr-auth)

13799 CONTRIBUTION TO THE STUDY OF ^{57}Co. Moreau, Gerard; Ambrosino, Georges (C.E.N., Gif-sur-Yvette, France). Compt. Rend., 261: 5438-41(Dec. 20, 1965). (In French).

The internal conversion lines of the two γ rays at 122 and 136 Kev which follow the electron-capture decay of ^{57}Co were studied. The internal conversion coefficients α_K and α of the γ radiation at 14 kev were determined. (tr-auth)

13800 APPLICATION OF THE OVERHAUSER EFFECT AND OF SPIN DECOUPLING TO STUDIES ON ^{13}C. Imbaud, Jean-Pierre (Faculte des Sciences, Clermont-Ferrand, France). Compt. Rend., 261: 5442-5(Dec. 20, 1965). (In French).

An apparatus with Overhauser effect for the study of ^{13}C was developed. Some results relative to different organic liquids with spin decoupling by radiofrequency are reported and analyzed. (tr-auth)

13801 ELECTRIC QUADRUPOLE TRANSITIONS BETWEEN ROTARY STATES WITH LARGE SPINS IN EVEN NUCLEI. Davydov, A. S.; Ovcharenko, V. I. (Inst. of Physics, Academy of Sciences, Ukrainian SSR). Dokl. Akad. Nauk SSSR, 163: 329-31(July 11, 1965). (In Russian).

Study of the energy spectra of the high-spin rotational states of nine nonspheroidal even nuclei indicated that the rotational state energy agrees with theoretical predictions; the deformability of the nucleus during rotation was derived from the nonadiabaticity parameter μ. The law that governs the energy relations of the subsequent rotational levels in the absolutely rigid ($\mu = 0$) axially symmetrical, even nuclei is changed in the case of "soft" ($\mu = 1$) nuclei; at the same time the probability of the E2 cascade transitions from the excited to the ground state is also changed. Calculations were carried out to determine the probability of the E2 transitions between neighboring states of even, axial nuclei without using the adiabatic approximation. The calculations indicated that in deformable nuclei, where $\mu \neq 0$, a special factor becomes larger than 1, increasing with the spin of the rotational state. On the basis of μ values of 0.24, 0.27, 0.28, 0.29, 0.30, 0.31, 0.35, 0.33, and 0.38, corresponding to ^{172}Hf, ^{168}Yb, ^{176}W, ^{170}Hf, ^{174}W, ^{164}Yb, ^{168}Hf, ^{172}W, and ^{166}Hf, it was shown that the change in the relative probability of the E2 cascade transitions due to the rotation-induced deformation of the nucleus is quite marked. It is recommended to prove this conclusion experimentally. (TTT)

13802 CORRELATION OF INTERNAL-CONVERSION ELECTRON POLARIZATION. Boldyshev, V. F. JETP Lett. (USSR)(Engl. Transl.), 2: 280-1(Nov. 1, 1965).

Translated from Zh. Eksp. Teor. Fiz., Pis'ma Redakt., 2: 451-4(Nov. 1, 1965).

The polarization dependence of the correlation function for the directions of emission of the conversion electrons and photons was studied using the Furry-Maue-Sommerfeld approximation. (D.C.W.)

13803 DETERMINATION OF THE MIXING PARAMETER OF M1 AND E2 RADIATION FOR THE 0.341-Mev TRANSITION IN ^{49}Ti. Bogdanov, A. P.; Tadeush, V. N.; Firsov, E. I. (Physics Inst., Academy of Sciences Belorussian SSR). JETP Lett. (USSR) (Engl. Transl.), 2: 326-8(Dec. 1, 1965).

Translated from Zh. Eksp. Teor. Fiz., Pis'ma Redakt., 2: 522-6(Dec. 1, 1965).

The mixing parameter of M1 and E2 radiation for the 0.341-Mev transition in ^{49}Ti was measured using a fast-slow coincidence technique. (G.O.Y.)

13804 THE ACCELERATION OF HEAVY IONS AND THE PRODUCTION OF THE HEAVIEST CHEMICAL ELEMENTS. Smend, F. (Univ., Goettingen, Ger.). Naturwissenschaften, 52: 632-5(1965). (In German).

The methods used for the production of beams of heavy ions (hydrogen, helium, nitrogen, carbon, and neon) are indicated. The nuclear reactions used to produce the transuranic elements are briefly discussed. (J.S.R.)

13805 ABSOLUTE MEASUREMENT OF RADIOACTIVE SOURCE STRENGTH BY MEANS OF A GENERAL COINCIDENCE METHOD: COINCIDENCE BETWEEN TWO RADIATION GROUPS, DISCUSSION OF DEAD TIME EFFECTS. Kowalski, E. (Univ., Bern). Nucl. Instrum. Methods, 39: 93-103(Jan. 1966). (In German).

In the absolute measurement of source strength by means of a general form of the coincidence method, the influence of angular correlation, coincidences by scattering, and sum-event pulses are evaluated. The results are extended to the case of an isotope with a complicated decay scheme. On certain conditions it is possible to divide the radiations emitted into two groups and to measure the source-strength using the coincidences between these groups instead of coincidences between single radiations. These conditions are specified and the interference of the so called self-coincidences will be discussed. Self-coincidences are coincident events whose both partners belong to the same radiation group. A treatment of dead time effects is given. (auth)

13806 A DIGITAL COMPUTER SYSTEM FOR THE EXECUTIVE CONTROL OF A FAST NEUTRON LABORATORY. Whalen, J. F.; Roge, R.; Smith, A. B. (Argonne National Lab., Ill.). Nucl. Instrum. Methods, 39: 185-93 (Jan. 11, 1966).

The rationale governing the on-line application of a small digital computer to executive control of a fast neutron laboratory inclusive of a Van de Graaff accelerator is discussed. Domains and methods of productive application are defined. The logical concept of the system, the system components and operation are detailed in the context of present and future requirements. As an illustrative example, the application of the system to the automated determination of fast neutron total cross sections is described. Benefits and drawbacks of the system are discussed in the light of extensive laboratory experience. (auth)

13807 THE THERMAL NEUTRON ABSORPTION CROSS SECTION OF THE AERE BORON STANDARD. Wynchank, S. A. R.; Cox, A. E.; Collie, C. H. (Oxford Univ.). Nucl. Instrum. Methods, 39: 350(Jan. 11, 1966).

Information is given pertinent to the results of the measurement of thermal neutron absorption cross section of the new AERE boron standard (σ_B AERE). For the isotopic composition, the results of a mass spectrometric measurement on this and other boron standard indicates that the ^{10}B content of the AERE boron standard is 19.744 ± 0.093%. Also σ_B AERE is predicted as being 756. ± 4.1 barn. Further details are given of the chemical analysis of the solutions in which measurements were made of thermal neutron lifetime. (J.F.P.)

13808 THE ^{10}B(^{3}He,n)^{12}N REACTION. Zafiratos, C. D. (Los Alamos Scientific Lab., N. Mex.); Ajzenberg-Selove, F.; Dietrich, F. S. Nucl. Phys., 77: 81-91(1966).

Time-of-flight neutron spectra from the bombardment of ^{10}B targets by 2.6, 3.0, 4.0, and 5.8 Mev ^{3}He particles show neutron groups corresponding to the ground state of ^{12}N and to excited states at $E_x = 0.959 \pm 0.020$ ($\Gamma < 50$ kev), 1.24 ± 0.03 ($\Gamma = 140 \pm 40$ kev), 2.4 ± 0.1, 3.14 ± 0.08 ($\Gamma = 280 \pm 80$ kev), and 3.57 ± 0.08 Mev ($\Gamma = 270 \pm 80$ kev). There is also some indication of additional low intensity neutron groups. The ground state Q-value is measured to be 1.568 ± 0.020 Mev, corresponding to a ^{12}N atomic mass excess of 17.358 ± 0.020 Mev. The angular distributions at $E(^3He) = 4$ and 5.8 Mev show the influence of direct interaction. The results are discussed in terms of the known information on the T = 1 states in the A = 12 isobaric triad. (auth)

13809 PHOTOFISSION ANGULAR ANISOTROPY AND THE PARITY OF THE GROUND STATE OF ^{239}Pu. Rabotnov, N. S.; Smirenkin, G. N.; Soldatov, A. S.; Usachov, L. N.; Kapitza, S. P.; Tsipenyuk, Yu. M. (Inst. of Physics and Power Engineering, Obninsk, USSR. Inst. for Physical Problems, Moscow). Nucl. Phys., 77: 92-8(1966).

The angular distributions of ^{239}Pu photofission fragments

produced by 5.4-7.9 Mev endpoint energy bremsstrahlung γ quanta from a microtron are measured. Anisotropic angular distributions of the form $W(\vartheta) = a + b \sin^2 \vartheta$ were observed for E_{max} = 5.4, 5.65 and 5.9 Mev. The greatest anisotropy which corresponded to b/a = −0.192 was recorded for E_{max} = 5.65 Mev. Comparison of the results with those on neutron-induced fission of ^{238}Pu yields the parity of the ground state of ^{239}Pu with respect to that of the ground state of the even nucleus. The fission data are in agreement with the positive parity of ^{239}Pu derived from spectroscopic data. (auth)

13810 THE ^{7}Li(p,γ)^{8}Be* REACTION AND SINGLE-PARTICLE LEVELS IN ^{8}Be. Marion, Jerry B.; Wilson, Mark (Univ. of Maryland, College Park). Nucl. Phys., 77: 129-48(1966).

The ^{7}Li(p,γ)^{8}Be* reaction was studied by observing the α particles from the decay of the ^{8}Be levels at 16.62 and 16.92 Mev by means of a magnetic spectrometer. The yields to both levels are resonant at E_p = 0.44 Mev, the well-known (p,γ) resonance. In addition, the 16.62 Mev level is populated by a direct capture process, confirming the expectation based on ^{7}Li(d,n)^{8}Be threshold and stripping measurements that this level is a single-proton state. The present results, when combined with information from previous experiments, strongly suggest that the 16.62 and 16.92 Mev levels are both single-particle states of different character and that an isobaric spin description of these levels is inappropriate. (auth)

13811 THE EQUIVALENT LOCAL POTENTIAL AND THE PEREY EFFECT. Fiedeldey, H. (South African Atomic Energy Board, Pelindaba). Nucl. Phys., 77: 149-56(1966).

The equivalent local potential and the reduction factor for the non-local wave function compared to the equivalent local wave function inside the nucleus are calculated in the Perey-Saxon approximation in such a way that the wave function does not appear explicitly in the formulas obtained. The equivalent local potential and the reduction factor only depend on the equivalent local potential of Perey and Buck. The result is in good agreement with Perey's numerical comparisons. (auth)

13812 ANGULAR DISTRIBUTION OF THE PHOTOPROTONS FROM CARBON. Parikh, Vastupal (Laboratoire de l'Accelerateur Lineaire, Orsay, France. Physical Research Lab., Ahmedabad, India). Nucl. Phys., 77: 157-60(1966).

The 34.2-Mev proton angular distribution resulting from the photodisintegration of carbon is measured employing the 55-Mev electron beam of the linear accelerator. The results are compared with the theoretical values based on the quasi-deuteron, the quasi-alpha particle and the independent particle models. (auth)

13813 ABSOLUTE POLARIZATION MEASUREMENTS IN PROTON SCATTERING IN THE 140 Mev ENERGY RANGE. Jarvis, O. N.; Rose, B.; Scanlon, J. P. (Atomic Energy Research Establishment, Harwell, Eng.). Nucl. Phys., 77: 161-81(1966).

The polarization of the proton beam extracted from the 279 cm synchrocyclotron was determined to an accuracy of ±1% using two independent techniques. Measurements with this beam have shown that the absolute calibrations of all the published proton-nucleus polarization data in the energy range between 50 and 150 Mev are considerably in error. This fact means that the published proton-proton polarization data are also in error. The appropriate correction factors to be applied to the published experimental results are given. (auth)

13814 TWO-NUCLEON STRIPPING PROCESSES. Abul-Magd, A. Y.; El-Nadi, M. (Atomic Energy Establishment, Cairo). Nucl. Phys., 77: 182-92(1966).

The theory of two-nucleon stripping reactions is developed in the distorted wave Born approximation. The two-nucleon forces responsible for the reaction are taken to be spin and isospin dependent and of finite range. Expressions for the angular distribution and polarization of the emitted particles are given. The angular correlation and circular polarization of γ-rays following the reaction are considered. (auth)

13815 THE DECAY OF ^{56}Ni AND ^{57}Ni. Piluso, C. J.; Wells, D. O.; McDaniels, D. K. (Univ. of Oregon, Eugene). Nucl. Phys., 77: 193-201(1966).

The energies and relative intensities of the gamma radiations following the decays of ^{56}Ni to ^{56}Co and ^{57}Ni to ^{57}Co were measured using a 3 mm depletion-depth lithium-drifted germanium detector. Gamma rays of the following energies were observed in ^{56}Co (relative intensities in parentheses): 0.1583 (96.1), 0.2696 (38.4), 0.4807 (39.8), 0.7506 (52.2), and 1.5625 (12.3) Mev. Gamma rays populating the levels at 1.008 and 1.105 Mev were not observed. For ^{57}Co the following gamma rays were observed: 0.1272 (12.3), 1.3781 (82.2), 1.7577 (5.7), and 1.9202 (12.1) Mev. No evidence was found for a level at 1.59 Mev. The level schemes are compared with simple shell-model calculations. (auth)

13816 STRIPPING VIA CORE EXCITATION. Kozlowsky, B.; De-Shalit, A. (Weizmann Inst. of Science, Rehovoth, Israel). Nucl. Phys., 77: 215-24(1966).

Stripping processes in which the target nucleus is excited through its interaction with the outgoing particle in the exit channel are considered. It is shown that the angular distribution is very similar to that obtained from a usual stripping process, but the magnitude of the cross-section is very sensitive to small variations in the optical potential parameters. The case of ^{62}Ni(^{3}He,d)^{63}Cu is discussed in some detail. (auth)

13817 OPTICAL MODEL WAVE FUNCTIONS FOR NUCLEONS. Amos, K. A. (Univ. of California, Davis). Nucl. Phys., 77: 225-38(1966).

The optical model wave functions for nucleons on ^{13}C, ^{19}F, and ^{118}Sn are shown in magnitude and phase diagrams. From these, necessary features of approximate calculations are defined. It is shown that the focus remains an important feature even at higher incident energies of nucleons and that phase variation should be included in these approximate calculations. (auth)

13818 A NOTE ON THE MEASUREMENT OF THE ENERGIES OF GAMMA RAYS FROM THE DECAY OF ^{66}Ga. Cote, R. E. (Argonne National Lab., Ill.); Guso, R.; Raboy, S.; Carrigan, R. A. Jr.; Gaigalas, A.; Sutton, R. B.; Trail, C. C. Nucl. Phys., 77: 239-40(1966).

The energies of the most energetic gamma rays from the decay of ^{66}Ga were measured to be 4832 ± 7, 4485 ± 10, 4313 ± 10, and 4132 ± 11 kev. (auth)

13819 ANGULAR CORRELATION STUDIES USING THE ^{13}C(^{3}He,pγ)^{15}N REACTION. Pelte, D.; Povh, B.; Scholz, W. (Univ., Frieburg i.B.). Nucl. Phys., 78: 241-55(1966).

Levels in ^{15}N up to 8.57 Mev excitation energy were studied using the ^{13}C(^{3}He,pγ)^{15}N reaction at ^{3}He energies of 4.95 and 5.25 Mev. Angular correlations between protons and gamma rays were measured with the proton counter either at 0 or 180°. The spin assignments for the 7.16, 7.57 and 8.57 Mev states were found to be J = 5/2, J = 1/2 and J = 3/2, respectively. The possible spin assignments for the 8.31 Mev state are J = 1/2 or J = 3/2. Branching ratios were measured for all states. The 6.33 Mev $J^{\pi} = 3/2^{-}$ and the 7.31 Mev $J^{\pi} = 3/2^{+}$ states decay to the ground state only. The 7.16 and the 7.57 Mev state decay to the 5.28 Mev state only with quadrupole to dipole amplitude ratios $\delta = -0.04 \pm 0.05$ and $\delta = -0.04 \pm 0.01$, respectively. The octupole to quadrupole amplitude ratio for the transition from the 5.28 Mev $J^{\pi} = 5/2^{+}$ state to the ground state is $\rho = -0.09 \pm 0.02$ or 4.5 ± 0.3. The 8.31 Mev state decays to the ground state, the 5.3 Mev doublet, the 6.33 Mev state and the 7.31 Mev state with branching ratios of 70:12:12:≦6. The 8.57 Mev state decays to the ground state, the 5.28 Mev state and the 6.33 Mev state with branching ratios of 27:66:≦7. For the quadrupole to dipole amplitude ratio of the transition from the 8.57 Mev state to the 5.28 Mev state $\delta = 0.03 \pm 0.05$ was obtained. The results are discussed in the framework of Lane's weak-coupling model and compared with shell model predictions. (auth)

13820 OCTUPOLE VIBRATION AND E1 ($\Delta K = 0$) TRANSITION PROBABILITIES IN ODD-MASS NUCLEI IN THE RARE EARTH REGION. Monsonego, G.; Piepenbring, R. (Center de Recherches Nucleaires, Strasborg). Nucl. Phys., 78: 265-72(1966). (In French).

The E1 transitions in the odd-mass, deformed rare-earth nuclei with $\Delta K = 0$ are in general in reasonable agreement with the Nilsson estimate. Reduction factors introduced by pairing correlations deteriorate markedly this agreement. A simple model is constructed taking into account octupole vibrations and octupole quasi-particle interaction. In the framework of this model $\Delta K = 0$ transitions are computed and good agreement is obtained. (auth)

13821 AN INVESTIGATION OF SOME OF THE LOW-LYING STATES OF ^{40}Ca. Grace, M. A.; Poletti, A. R. (Dept. of Nuclear Physics, Oxford). Nucl. Phys., 78: 273-97(1966).

Inelastic proton scattering were used to excite states in the nucleus ^{40}Ca and magnetic spectrometer measurements have established the positions of all those below 9.3 Mev which are strongly excited. The decay modes of the majority of the states below 7 Mev were studied and a proton-gamma angular correlation method involving the detection of the protons inelastically scattered through (nearly) 180° was used to determine the spins of the states and the mixing ratios in the gamma ray transitions. The spins of the second, third and fourth excited states at 3.73, 3.90 and 4.48 Mev were verified as being 3,2 and 5, respectively. Unique spin assignments were made to the states at 5.24(2), 5.27(4), 5.62(2), 5.90(1) and 6.03 Mev (3). The spin of the state at 5.20 Mev is most probably J = 0 but J = 1 cannot be entirely excluded. Both J = 2 and 3 were found to be compatible with the experimental angular distributions observed for the decay of the 6.28 Mev level. This result together with the possible assignments of J = 3 or 4 by Leenhouts and Endt determines the spin of the 6.28 Mev level to be J = 3. (auth)

13822 A STUDY OF SOME EXCITED STATES OF ^{19}F BY AN ANGULAR CORRELATION TECHNIQUE. Thomas, M. F.; Lopes, J. S.; Ollerhead, R. W.; Poletti, A. R.; Warburton, E. K. (Nuclear Physics Lab., Oxford). Nucl. Phys., 78: 298-318(1966).

Decay schemes for the states in ^{19}F between 2 Mev and 5 Mev above the ground state were determined by particle γ-ray coincidence studies. The particle γ-ray angular correlation method of Litherland and Ferguson was used to gain information upon the spin values and the γ-ray mixing ratios of these states which were excited by the reaction ^{19}F(p,p')^{19}F* using incident bombarding energies in the range 7.5–8.5 Mev. The spin of the 2.79 Mev level was rigorously limited to the values $\frac{9}{2}$, $\frac{5}{2}$. States at 3.91 and 4.57 Mev were established as $\frac{3}{2}$, a model dependent argument being presented to assign negative and positive parities, respectively. Limitations were imposed upon the spins of the states at 4.00, 4.04, 4.39, and 4.70 Mev and upon the value of the mixing ratio in the transitions 2.70 Mev → 0.198 Mev, 4.39 Mev → 0.198 Mev. The results are compared to the predictions of the shell model and a unified model. (auth)

13823 A STUDY OF SOME LOW-LYING EXCITED STATES IN ^{32}S. Poletti, A. R.; Grace, M. A. (Nuclear Physics Lab., Oxford). Nucl. Phys., 78: 319-36(1966).

The spins and decay modes of eight of the first 11 excited states of ^{32}S were investigated by the use of the particle-gamma angular correlation method of Litherland and Ferguson. The ^{32}S(p,p')^{32}S reaction was used at bombarding energies between 7.5 and 10.7 Mev. Protons were detected in an annular counter at 180° to the beam and gamma rays at angles between 20 and 90° to the beam. Decay modes are given for all states studied. Spin assignments were made to the levels at 4.29(2), 4.70(1), 5.41(3), 5.55(2), 5.80(1), and 6.23 Mev (2), and that of the 4.46-Mev level was limited to 2,3 or 4. (auth)

13824 CORRELATED WIDTH FLUCTUATION FACTOR. Ullah, Nazakat (Tata Inst. of Fundamental Research, Bombay). Nucl. Phys., 78: 337-40(1966).

The width fluctuation factor is calculated using the correlated multichannel distribution. A closed form expression is obtained for the two-channel case, which shows that the width fluctuation factor approaches unity as the correlation between the two channels increases. An approximate result is derived for the case of a large number of channels. (auth)

13825 A NOTE ON COUPLING SCHEMES IN ODD-MASS NUCLEI. Kisslinger, L. S. (Univ. of California, Berkeley. Western Reserve Univ., Cleveland). Nucl. Phys., 78: 341-52(1966). (UCRL-16341).

A representation which utilizes second-quantized operators for the three quasi-particle states is introduced. In this representation the pairing plus quadrupole interaction is approximately diagonalized in a j-shell. The main prediction is that associated with the opposite parity state of large spin in the major shells of medium and heavy nuclei there will appear extra low-lying states which do not arise from particle-phonon coupling. The states are characterized by forbidden M1 transition rates. (auth)

13826 SELF-CONSISTENT FIELD AND METHOD OF PROJECTION. Rouhaninejad, H.; Yoccoz, J. (Centre de Recherches Nucleaires, Strasbourg). Nucl. Phys., 78: 353-68(1966). (In French).

The projection method is investigated in relation to the definition of the Hartree-Fock field. It is shown that, when the variational principle is applied correctly, the mass in the center-of-mass motion comes out correctly, and the corrections to the self-consistent field due to this motion are calculated. In the rotation case, it is shown that, as long as we keep the condition of a unique generating function with K = 0, the Peierls–Yoccoz formula for the moment of inertia is valid, but may be modified if we take into account band mixing with K = 1. (auth)

13827 ENERGY DEPENDENCE OF THE NUCLEAR LEVEL DENSITY BELOW THE NEUTRON BINDING ENERGY. Tsukada, K.; Tanaka, S.; Maruyama, M.; Tomita, Y. (Japan Atomic Energy Research Inst., Tokyo). Nucl. Phys., 78: 369-84(1966).

The energy spectra of neutrons inelastically scattered from Co, Ag, In, Ta and Au were measured in the energy range 3.5–8.5 Mev (every 0.5 Mev step) of incident neutrons by means of the time-of-flight technique with pulsed-beam Van de Graaff accelerators and an ion buncher of the Mobley type. The relations between the level density and the excitation energy are obtained in the 2–8 Mev range. The inverse compound nucleus formation cross sections for several forms of the optical model potential are used in the derivation. For Co and Ag, the relations agree with the prediction of the Fermi gas model. For In, Ta and Au, there are obvious breaks in the observed relations at 4–5 Mev excitation. Below the breaks the observed points fit to the curves calculated by the constant temperature model. Above the breaks they fit those based on the Fermi gas or constant temperature model. (auth)

13828 THE PARITY OF THE 6.89 Mev LEVEL IN ^{14}C. Riess, F.; Trost, W. (Univ., Freiburg i. B.). Nucl. Phys., 78: 385-8(1966).

The plane polarization of the 6.89–6.09 Mev gamma transition in ^{14}C was measured in coincidence with the 6.09 Mev ground state transition using a Compton polarimeter. The 6.89 Mev level was fed by the reaction ^{13}C(d,p)^{14}C. The parity of the 6.89 Mev level was determined to be negative. (auth)

13829 ELASTIC AND INELASTIC SCATTERING OF FAST NEUTRONS FROM Ag, In AND Cd. Vonach, W. G.; Smith, A. B. (Argonne National Lab., Ill.). Nucl. Phys., 78: 389-408(1966).

The differential elastic and inelastic neutron scattering cross sections of Ag, In and Cd were measured at ten scattering angles for incident neutron energies between 0.3 and 1.5 Mev. The incident neutron energy spread was ≈20 kev and pulsed beam time-of-flight techniques were utilized to resolve the elastically and the inelastically scattered neutron groups. The inelastic excitation of states in Ag at 0.09, 0.33, 0.42, 0.71, 0.78, 0.95 and 1.15 Mev; in In

at 0.33, 0.58, 0.83, 0.96 and 1.10 Mev; and in Cd at 0.31 and 0.62 Mev was observed. The measured differential elastic scattering cross sections were compared with the results of optical model calculations employing the surface absorption potential of Moldauer. Hauser-Feshbach calculations, including corrections for width fluctuations, were carried out and the results are discussed in the context of the experimental measurements. (auth)

13830 NEUTRON TRANSFER IN HEAVY ION REACTIONS. Buttle, P. J. A.; Goldfarb, L. J. B. (Univ. of Manchester, Eng.). Nucl. Phys., 78: 409-32(1966).

A DWBA treatment of the heavy-ion neutron transfer reaction is given which is suitable for energies below the Coulomb barrier where the transition amplitude may be evaluated with reasonable accuracy. Consideration is given of the post-prior paradox, virtual Coulomb excitation and of effects associated with antisymmetrization. The $^{14}N(^{14}N, ^{13}N)^{15}N$ reaction is taken as an example and calculations are made of angular distributions and total cross section for several energies. The results are very similar to those obtained using the tunnelling theory of Breit et al. Good agreement is also obtained with the experimental data of Hiebert, Couch and McIntyre, which thus points further to the feasibility of estimations of single-particle neutron reduced widths, based on the study of heavy-ion reactions. (auth)

13831 MATRIX ELEMENTS OF BETA TRANSITIONS IN THE NILSSON MODEL. Berthier, J. (Faculte des Sciences, Grenoble, France); Lipnik, P. Nucl. Phys., 78: 448-64(1966). (In French).

Using Nilsson model wave functions, expressions for the non-relativistic nuclear matrix elements of beta transitions are obtained. As an illustration, these formulas are applied to some selected cases, for which the model predictions are compared with the experimental data. It is suggested to analyze the beta decay results in terms of the model parameters. (auth)

13832 THE EXCITATION OF GIANT MULTIPOLE RESONANCES IN HEAVY NUCLEI BY INELASTIC ELECTRON SCATTERING. Drechsel, Dieter (Univ., Frankfurt am Main). Nucl. Phys., 78: 465-75(1966).

The electroexcitation of various giant multipole resonances (E1, E2, E0) is discussed. The relative strength of the cross sections was derived in Born approximation. It is shown that the E2 giant resonance should be observed experimentally very clearly at scattering angles of the electron of about 40–50°, if the primary energy of the electrons is about 200 Mev. At these angles the tail of the strong E1 giant resonance can be depressed nearly completely. Since the cross sections for the excitation of E2 and E0 giant multipoles behave quite similarly as functions of the scattering angles, it seems impossible to distinguish between them. The monopole excitation cross section was also calculated exactly by a phase shift analysis and compared with the results of the Born approximation. (auth)

13833 THE $^{12}C(p,pn)^{11}C$ REACTION FROM 50 TO 160 Mev. Measday, David F. (Harvard Univ., Cambridge, Mass.). Nucl. Phys., 78: 476-80(1966).

The production of ^{11}C activity by the reaction $^{12}C(p,pn)^{11}C$ was studied in the region of 50 to 160 Mev. The measurements are relative but have been normalized to an absolute determination at 98.1 Mev. The results have a relative error of 2.5% with a normalizing error of 0.5%. These data are more accurate than previously published work in this region and they span a larger energy range as well. In addition, studies were made of the loss of radioactive gas from Pilot B plastic scintillator. The thinnest samples were 27 mg/cm^2; the effect was largest for these but the activity lost was only 1.5 ± 1.0%. (auth)

13834 ON THE EXISTENCE OF THE ^{4}He EXCITED LEVELS AND OF OTHER LIGHT NUCLIDES. Argan, P. E. (Univ. Naples. Istituto Nazionale di Fisica Nucleare, Naples); Mantovani, G. C.; Marazzini, P.; Piazzoli, A.; Scannicchio, D. Nuovo Cimento, (1), 3: Suppl., 245-80(1965).

Some general considerations are given to methods used for revealing the existence of excited states of ^{4}He. Summaries are presented of experimental research for various ranges of excitation energy. Experiments on ^{4}H and ^{5}H stability against dissociation, ^{4}H instability against dissociation, ^{3}n and ^{4}n and ^{4}Li are also briefly reviewed. Two theoretical problems are discussed: the application of the pairing-energy argument in order to obtain previsions on the existence of some light nuclear systems, and the assignment of the isotopic spin to the ^{4}He excited levels with its possible consequences. (L.B.S.)

13835 COULOMB CORRECTIONS CONCERNING A TEST FOR TIME REVERSAL VIOLATION IN NEUTRINO-INDUCED REACTIONS. Kokkedee, J. J. J. (CERN, Geneva). Nuovo Cimento, (10), 41A: 293-304(Feb. 1, 1966).

Recently it was proposed to test time reversal invariance in weak interactions through the measurement of the transversal polarization of the muon in the reaction $\nu(\bar{\nu})$ + nucleus → $\mu^-(\mu^+)$ + all final states. Neglecting Coulomb corrections this transversal polarization must be zero if time reversal invariance holds, but for heavy nuclei it is not clear whether or not, in this connection, the effect of Coulomb final-state interactions of the muon is negligible. An upper limit for the amount of transverse polarization due to Coulomb interactions is derived under some rather general assumptions. It is found that for muon energies of 500 Mev or higher this amount of polarization will be below 1%, the effects being smaller the higher the energy of the muon. (auth)

13836 THE EIGENVALUES OF THE LIPPMANN-SCHWINGER KERNEL FOR YUKAWA AND NUCLEON-NUCLEON POTENTIALS. Warburton, A. E. A. (Atomic Energy Research Establishment, Harwell, Eng.). Nuovo Cimento, (10), 41A: 360-73(Feb. 1, 1966).

Numerical results are obtained for the eigenvalues of the Lippmann-Schwinger kernel for a single Yukawa potential, and for a nucleon-nucleon triplet s-state potential. An asymptotic series for the eigenvalues is developed for potentials of a class including sums of Yukawas, and useful approximations derived from these series by Padé approximants. The phase shifts for any single Yukawa potential may be readily deduced. (auth)

13837 ALLOWED, BUT INHIBITED BETA DECAYS OF ^{43}K AND ^{45}K. Zamick, L. (Princeton Univ., N. J.). Phys. Lett., 20: 168-70(Feb. 1, 1966). (PUC-937-184).

Various reasons are considered for the long lifetime of the transitions in potassium-43 and -45 beta decays. Emphasis is placed on the degree of mixing of different basic states in calcium-43 which is required to obtain the correct lifetime. The isotopic spin decompositions of the wave functions of potassium-43 and calcium-43 are considered. (J.F.P.)

13838 MAGNETIC MOMENT CORRECTIONS TO SECOND ORDER IN PERTURBATION THEORY. Mavromatis, H. A.; Zamick, L. (Princeton Univ., N. J.). Phys. Lett., 20: 171-3(Feb. 1, 1966).

It is proved that, with a central residual interaction, the correction to the magnetic moment of ^{17}O due to configuration mixing is equal in magnitute and opposite in sign to the correction for its mirror ^{17}F; likewise for all mirror pairs consisting of one particle or one hole beyond a closed major shell. This is tested with the mirror pairs ^{15}O and ^{15}N, ^{17}O and ^{17}F, and it is found indeed that the corrections from the Schmidt moments are almost equal and opposite. The small discrepancy can be explained by using an interaction with a tensor part (Hamada-Johnson interaction). It is found that configuration mixing quenches the magnetic moment of a nucleus with one particle beyond a closed major shell, i.e., ^{17}O, ^{41}Ca, but anti-quenches the magnetic moment of a nucleus with one hole beyond a closed shell, i.e., ^{15}O, ^{39}Ca. (auth)

13839 THE ROLE OF DEFORMED STATES IN THE ^{42}Ca SPECTRUM. Federman, P. (Weizmann Inst. of Science, Rehovoth, Israel). Phys. Lett., 20: 174-5(Feb. 1, 1966).

Starting from a shell-model description of ^{50}Ti and including the interplay with deformed states in ^{42}Ca, it is shown that a consistent picture of these two nuclei can be made. (auth)

13840 NUCLEAR BINDING ENERGY PARAMETERS IN TERMS OF REALISTIC TWO-NUCLEON-POTENTIALS. Zamick, L. (Princeton Univ., N. J.). Phys. Lett., 20: 176-9(Feb. 1, 1966).

Effective forces are derived from realistic two-body forces, and renormalizations coming from excitation of closed shells are shown to be important in achieving agreement with empirical binding energies. (auth)

13841 CONCERNING THE POSSIBILITY OF A PARITY ADMIXTURE IN THE 57.6 kev TRANSITION IN ^{180m}Hf. Hager, R.; Seltzer, E. (California Inst. of Tech., Pasadena). Phys. Lett., 20: 180-1(Feb. 1, 1966).

The anomalies in the L-subshell internal conversion intensities in the 57.6 kev transition in ^{180m}Hf, which were recently interpreted as evidence for parity impurities in the nulcear levels, are shown to be entirely understood with the inclusion of nuclear structure dependent terms in the internal conversion process. (auth)

13842 MAGNETIC MOMENT OF NUCLEI FOR A MOMENTUM-DEPENDENT INTERNUCLEON FORCE. Bhaduri, R. K. (Theoretical Physics Dept. Oxford. McMaster Univ., Hamilton, Ont.); Van Leuven, P. Phys. Lett., 20: 182-4(Feb. 1, 1966).

There is a correction to the magnetic-moment operator of nuclei if explicit momentum-dependence is contained in the two-nucleon potential. A simple calculation for this correction in ^{209}Bi shows that it is of the order of +0.55 n.m. This is enough to remove most of the discrepancy from the experimental value that remains after making the corrections for the polarization of the core and the spin-orbit force. (auth)

13843 INTERNAL PAIR FORMATION OF THE 12.33 Mev TRANSITION IN ^{28}Si. Spring, E. (Univ. of Helsinki). Phys. Lett., 20: 184-6(Feb. 1, 1966).

The internal pair formation coefficient Γ of the 12.33-Mev transition in ^{28}Si was measured. The transition originates from the ^{27}Al(p, γ)^{28}Si reaction at a proton energy of 773 kev. The result was $\Gamma = (2.7 \pm 0.6) \times 10^{-3}$. (auth)

13844 POSITIVE PARITY STATES IN ^{16}O. Wong, S. S. M. (Univ. of Rochester, N. Y. Oak Ridge National Lab., Tenn.). Phys. Lett., 20: 188-90(Feb. 1, 1966).

The ^{16}O (0 + 2) $\hbar\omega$ configurations were investigated using the shell model. Large particle-hole components are found in the ground state. The level spectrum up to 20 Mev is fairly well given but not the strongly-enhanced E2 rates. Extended calculations are in progress. (auth)

13845 EXCITED STATES IN ^{6}Be. Eccles, S. F.; Wong, C.; Anderson, J. D. (Univ. of California, Livermore). Phys. Lett., 20: 190-3(Feb. 1, 1966). (UCRL-14623).

In order to clarify the low-lying states in ^{6}Be, the results of two experiments are reported. In the first experiment ^{3}He particles of 26-Mev incident energy were used to bombard a target of ^{4}He, and the resulting neutron spectrum was analyzed by time-of-flight techniques. In addition, a ^{4}He beam at 28 Mev was used to bombard a target of ^{3}He. The combination of these two bombardments gave reaction neutrons throughout the complete angular range. A second experiment involved the ^{6}Li(p,n) reaction and used incident protons of 11.6 and 12.6 Mev. The angular distribution of neutrons leading to the ground state of ^{6}Be appears to be more or less isotropic from the ^{4}He(He-3,n) reaction within the rather large errors in the determination of the cross sections. A typical value for the cross section is 0.3 mb/sr. The intensity of the excited state in ^{6}Be is much larger, in both reactions, than the ground state. (J.F.P.)

13846 ANGULAR DISTRIBUTIONS FOR THE REACTION ^{12}C(^{6}Li,α)^{14}N BETWEEN 2 AND 3 Mev. Bergman, Clark; Hobbie, Russell K. (Univ. of Minnesota, Minneapolis). Phys. Rev., 142: 575-8(Feb. 18, 1966).

Angular distributions were measured for ^{12}O(^{6}Li,α)^{14}N when the ^{14}N is left in its ground state and 3.9-Mev second excited state. These extended our previous measurements from 3 Mev down to 2 Mev. The discrepancy between these results and some measurements at 1.7 Mev is discussed. (auth)

13847 GAMMA-RAY CASCADES FROM NUCLEI WITH HIGH SPIN. Sperber, Daniel (Illinois Inst. of Tech., Chicago). Phys. Rev., 142: 578-83(Feb. 18, 1966).

The spectra and angular distribution for a cascade of gamma rays from nuclear states with high spin were calculated. Calculations based on the single-particle and liquid-drop model are presented. It is shown how the angular distribution can be used to determine the appropriate model for the states under consideration. (auth)

13848 INELASTIC ALPHA SCATTERING AND ASSOCIATED GAMMA RADIATION. II. Inglis, David R. (Argonne National Lab., Ill.). Phys. Rev., 142: 591-8 (Feb. 18, 1966).

The rotational excitation of a deformed nucleus by inelastic alpha scattering gives rise to a gamma radiation pattern whose orientation, as the alpha angle is varied, sometimes displays a remarkable reverse rotation determined by the relative phase of the excited rotational states. This arises from the motion of beats occurring where the incoming and outgoing waves overlap at the surface of the nucleus, as has been qualitatively explained in previous communications. The nuclear excitation and subsequent radiation are discussed somewhat more thoroughly, again in the two-dimensional model with the aim of exploring the essentials of the mechanism and not hiding them in computation. (auth)

13849 ASYMMETRIC-ROTATOR MODEL IN THE s-d SHELL. Bar-Touv, J. (Weizmann Inst. of Science, Rehovoth, Israel); Kelson, I. Phys. Rev., 142: 599-602 (Feb. 18, 1966).

The asymmetric-rotator model based on the non-axially-symmetric Hartree-Fock field is applied to ^{24}Mg, to ^{32}S, and to their odd-even neighbors. Relations between the earlier particle-hole treatment and the asymmetric-rotator model for the K = 2 band of ^{24}Mg are investigated. (auth)

13850 PROJECTION OPERATORS IN THE UNIFIED REACTION THEORY. Hahn, Yukap (New York Univ., N. Y. Yale Univ., New Haven). Phys. Rev., 142: 603-7 (Feb. 18, 1966).

A simple form of the projection operators applicable for general rearrangement and exchange processes with full recoil effect is constructed for the unified reaction theory of Feshbach. Channels of different cluster configurations are not orthogonal and the overlap of their wave functions is important. Multidimensional generalization of the wave functions and corresponding wave equations takes this effect into account in a simple way without the complication of solving the integral equations with overlap kernels. Introduction of the projection operators makes it possible to reduce the multiparticle scattering problem in a natural way to that of multiclusters and the dispersive part which involves intermediate states of the compound system. The formalism is compared with the Faddeev equations for the case of three-particle two-cluster reactions, and also with other theories. (auth)

13851 CALCULATIONS OF DEUTERON STRIPPING IN A SOLUBLE MODEL. Aaron, R.; Shanley, P. E. (Northeastern Univ., Boston). Phys. Rev., 142: 608-11 (Feb. 18, 1966).

Preliminary results are presented of calculations based on a soluble three-body model recently proposed by Amado. Angular distributions for the deuteron stripping process are presented for several energies and the results are compared with the general behavior of experimental stripping patterns although no attempt is made to describe the particular nucleus. Various approximation schemes such as the Butler theory and the distorted-wave Born approximation are applied to our model amplitudes. The possibility of describing real nuclei with this model is also discussed. (auth)

13852 ^{7}Li AND ALPHA PARTICLES FROM THE ^{6}Li + ^{9}Be REACTION. Sahai, Baldev (Univ. of Chicago). Phys. Rev., 142: 612-24(Feb. 18, 1966).

The kinetic-energy spectra of ^{7}Li nuclei and alpha particles formed as a result of the nuclear reaction between ^{6}Li projectiles of energies 3.0–3.75 Mev and ^{9}Be targets were studied by a particle-selection system using a gas proportional counter (ΔE) with a very thin window (~35 $\mu g/cm^2$) and solid-state detectors to measure the energy. No evidence could be found for discrete ^{7}Li energy groups such as would result from a two-product reaction producing ^{8}Be in its ground state or first excited state. The ^{7}Li spectrum is an energy continuum, whereas the alpha-particle spectrum has discrete energies as well as an energy continuum. Absolute values of $d^2\sigma/dE\,d\Omega$ were obtained for these continua in the barycentric system. By extrapolation of the observed results, the total cross section σ_t for the ^{7}Li continuum is estimated to be 24 ± 8 mb, whereas σ_t for the alpha continuum, which has contributions from some other reactions also, is estimated to be 103 ± 30 mb. The reaction is interpreted as predominantly a direct three-body breakup $^{9}Be + {}^{6}Li \rightarrow {}^{7}Li + 2\alpha$ and sequential decay through highly excited states in ^{11}B. Absolute differential cross sections for the four highest alpha groups from the concomitant reaction $^{9}Be(^{6}Li,\alpha)^{11}B$ are also given. (auth)

13853 ^{46}Ca(d,p)^{47}Ca REACTION AT 7-Mev BOMBARDING ENERGY. Belote, T. A. (Massachusetts Inst. of Tech., Cambridge.); Chen, H. Y.; Hansen, Ole; Rapaport, J. Phys. Rev., 142: 624-32(Feb. 18, 1966). (MIT–2098-173).

The ^{46}Ca(d,p)^{47}Ca reaction was investigated using the MIT-ONR electrostatic generator. The broad-range, multiple-gap spectrograph was used in the detection of the reaction protons. Twenty-seven excited levels were identified in ^{47}Ca below an excitation energy of 6.1 Mev, and a Q value of 5.047 ± 0.010 Mev was measured for the ground-state transition. The angular distributions to the corresponding levels were measured and analyzed by means of the distorted-wave Born approximation. Unperturbed single-particle energies were extracted from the strengths and energies of the levels using the shell-model sum rules. An $I_n = 2$ and an $I_n = 0$ transition were observed to the 2.580- and 2.600-Mev levels, respectively. The ^{46}Ca ground-state configuration is discussed in terms of these results. (auth)

13854 ENERGY LEVELS IN ^{49}Sc FROM ^{48}Ca (^{3}He,d) ^{49}Sc AND OTHER REACTIONS PROCEEDING FROM ^{48}Ca. Erskine, J. R.; Marinov, A.; Schiffer, J. P. (Argonne National Lab., Ill.). Phys. Rev., 142: 633-7(Feb. 18, 1966).

The ^{48}Ca(^{3}He,d)^{49}Sc reaction at $E_{^3He}$ = 12.00 Mev was studied with a broad-range magnetic spectrograph. Twenty-four energy levels were identified up to an excitation energy of 7 Mev. Distorted-wave Born-approximation calculations were used to assign l values and extract spectroscopic factors for most of the transitions. Some information obtained with the $^{48}Ca(^{3}He,\alpha)^{47}Ca$, ^{48}Ca(d,t)^{47}Ca, ^{48}Ca(d,p)^{49}Ca, and $^{48}Ca(\alpha,p)^{51}Sc$ reactions is also given. (auth)

13855 NUCLEAR-SPIN, HYPERFINE-STRUCTURE, AND MAGNETIC-MOMENT INVESTIGATIONS ON ^{61}Cu, ^{62}Cu, AND ^{64}Cu. Dodsworth, Barbara M.; Shugart, Howard A. (Univ. of California, Berkeley). Phys. Rev., 142: 638-42(Feb. 18, 1966). (UCRL–16327).

Atomic-beam magnetic-resonance experiments on the $^{2}S_{½}$ ground state of three radioactive copper isotopes, ^{61}Cu, ^{62}Cu, and ^{64}Cu, are described. The results are summarized. The nuclear magnetic moments are calculated from the Fermi-Segrè formula by using known constants of ^{63}Cu and ^{65}Cu. A 1% error is quoted on the ^{64}Cu moment to bracket a possible hyperfine-structure anomaly. (auth)

13856 DECAY PROPERTIES OF ^{86}Zr. Hyde, E. K.; Treytl, W. J.; Siivola, A.; Sisson, D. H.; Horen, D. K. (Univ. of California, Berkeley). Phys. Rev., 142: 657-63 (Feb. 18, 1966). (UCRL–16337).

The radiations of 16.5-h ^{86}Zr were reinvestigated within lithium-drifted germanium and silicon detectors and with a NaI crystal spectrometer. Besides x rays, there are gamma rays of 28, 243, and 612 kev in relative intensity 21, 100, and 5.4. No other gamma rays were detected. No annihilation radiation was present. There is no evidence for formation of 48-min ^{86m}Y in the decay of ^{86}Zr. The K-conversion coefficient of the 243-kev transition was found to be 0.035 ± 0.003. The lifetime was measured as 29 ± 3 nsec. These properties agree well with an E2 multipolarity. The lifetime and conversion coefficient of the 28-kev transition are <10 nsec and 3.8 ± 0.5, respectively, which corresponds to an E1 multipolarity. A decay scheme is constructed and reasonable shell-model assignments are made to all levels except the 2– level of ^{86}Y, whose character is uncertain. (auth)

13857 TRIPLE CORRELATIONS IN THE $^{56}Fe(p,\gamma\gamma)^{57}Co$ REACTION. August, L. S.; Gosset, C. R.; Treado, P. A. (Naval Research Lab., Washington, D. C.). Phys. Rev., 142: 664-72(Feb. 18, 1966).

Approximately seventy resonances were observed for the $^{56}Fe(p,\gamma)^{57}Co$ reaction in the range of proton energy from 1300 to 1800 kev. Gamma-ray energy measurements performed with scintillation and lithium-drift silicon spectrometers yield 6.040 ± 0.030 Mev for the Q value of the $^{56}Fe(p,\gamma)^{57}Co$ reaction and show the existence of intermediate states in ^{57}Co at 1.381 ± 0.010, 1.506 ± 0.020, 1.760 ± 0.020, 1.921 ± 0.020, 2.136 ± 0.020, 2.60 ± 0.03, 2.74 ± 0.03, 2.80 ± 0.03, 2.88 ± 0.03, 3.11 ± 0.03, 3.18 ± 0.03, 3.27 ± 0.03, and 3.52 ± 0.03 Mev. Triple-correlation measurements performed with a double sum-coincidence spectrometer permit J^π assignments of $^{3}/_{2}^{-}$, $^{5}/_{2}^{-}$, $^{5}/_{2}^{-}$, and $^{5}/_{2}^{+}$ to the intermediate states in ^{57}Co at 1.38, 1.76, 1.92, and 2.14 Mev, respectively. These measurements were performed at resonance energies of 1525, 1598, 1622, 1637, 1645, and 1800 kev, where the capturing states at the 1637- and 1800-kev resonances are assigned a J^π value of $^{5}/_{2}^{+}$, and for the others J^π is $^{3}/_{2}^{-}$. Ambiguities exist for the E2/M1 amplitude ratios for all of the mixed secondary gamma-ray transitions observed in these studies. All measurements were in agreement with the established value of $^{7}/_{2}^{-}$ for the ground state of ^{57}Co. (auth)

13858 NUCLEAR-REACTION STUDIES IN THE NICKEL ISOTOPES: THE $^{58}Ni(p,p')^{58}Ni$ AND $^{58}Ni(d,p)^{59}Ni$ REACTIONS. Cosman, E. R.; Paris, C. H.; Sperduto, A; Enge, H. A. (Massachusetts Inst. of Tech., Cambridge). Phys. Rev., 142: 673-86(Feb. 18, 1966). (MIT–2098-171).

The reactions $^{58}Ni(p,p')^{58}Ni$ and $^{58}Ni(d,p)^{59}Ni$ were studied at a bombarding energy of 7.0 Mev using the MIT–ONR Van de Graaff generator and both the single-gap and multi-gap broad-range spectrographs. With an energy resolution of better than 10 kev, fourteen levels in ^{58}Ni were observed up to 4.2-Mev excitation; and in ^{59}Ni, 173 levels were observed up to an excitation energy of 7.5 Mev. Q values and positions of energy levels for both reactions were measured with accuracies between 5 and 10 kev using a single-gap spectrograph. In the $^{58}Ni(d,p)^{59}Ni$ investigation, simultaneous proton spectra were obtained at 24 reaction angles with the multiple-gap spectrograph. The angular distribution of the proton groups showing stripping characteristics were analyzed by use of the distorted-wave Born approximation. Absolute differential cross sections for all levels have been measured, and the values of l_n, the orbital angular momentum of the transferred neutron, and the strength functions $(2J + 1)S_{l_n,j}$ for the stripping levels were obtained. A sum-rule analysis is made, and the results are compared with shell-model predictions. (auth)

13859 GAMMA RAYS FROM THE DECAY OF 35-DAY ^{95}Nb. Church, L. B. (Carnegie Inst. of Tech., Pittsburgh); Gaigalas, A.; Sutton, R. B.; Cote, R. E.; Raboy, S.; Trail, C. C. Phys. Rev., 142: 690-1(Feb. 18, 1966).

The gamma spectrum from the decay of ^{95}Nb was obtained. No evidence was found for a gamma ray reported at 753 kev; if it is present at all, its intensity cannot be as great as ½% of that of the gamma ray at 765 kev. The en-

ergy of the latter was measured to be 765.8 ± 0.4 kev. (auth)

13860 PHOTOFISSION OF ^{238}U INDUCED BY 17.5-Mev MONOENERGETIC GAMMA RAYS. Meason, J. L.; Kuroda, P. K. (Univ. of Arkansas, Fayetteville). Phys. Rev., 142: 691-5(Feb. 18, 1966).

Fission yields were determined radiochemically using low-level counting techniques for fourteen mass chains from photofission of ^{238}U induced by 17.5-Mev monoenergetic gamma rays from the $^{7}Li(p,\gamma)^{2}4He$ reaction. Fine structure in the mass-yield curve in the region A = 131-135 was observed, with the peak occurring at A = 132. A striking similarity was noted between the photofission mass-yield curve in the mass-130-136 region and the relative abundance pattern of the excess fission xenon recently observed in certain meteorites. (auth)

13861 KINETIC ENERGY-MASS DISTRIBUTIONS FROM THE FISSION OF NUCLEI LIGHTER THAN RADIUM. Plasil, F.; Burnett, D. S.; Britt, H. C.; Thompson, S. G. (Univ. of California, Berkeley). Phys. Rev., 142: 696-715(Feb. 18, 1966). (UCRL-11954).

The distributions in masses and total kinetic energies of fission fragments from a number of elements ranging from erbium to bismuth were measured. The nuclei undergoing fission were produced by bombarding a variety of targets with projectiles ranging from ^{4}He to ^{16}O. The energies of coincident fission fragments were measured using solid-state counters. The energy data were transformed to give mass-total kinetic energy density-of-events distributions. These distributions were compared with those calculated from an approximate version of the liquid-drop model which applies to this region of elements. General agreement in the shapes and widths of the distributions was found, particularly in the cases which involved small angular momenta and small nuclear temperatures. The dependence of the widths of the experimental distributions on the nuclear temperature was found to differ from that predicted by the theory, but uncertainties in the evaluation of nuclear temperatures for the reactions investigated may be large. Analysis of these uncertainties indicated that they were not large enough to alone account for the discrepancy, although this analysis was subjected to some error. Angular momentum effects were studied by using certain combinations of targets and projectiles to give the compound nucleus ^{186}Os at the same excitation energy but with different angular momenta. The effect of increasing angular momentum was to broaden and change the shape of the experimental distributions. (auth)

13862 SEARCH FOR RADIOCHEMICAL EVIDENCE FOR TERNARY FISSION OF ^{235}U BY THERMAL NEUTRONS. Stoenner, R. W.; Hillman, Manny (Brookhaven National Lab., Upton, N. Y.). Phys. Rev., 142: 716-19 (Feb. 18, 1966). (BNL-9625).

Upper limits for yields of certain isotopes of argon from fission of ^{235}U by thermal neutrons were determined radiochemically as follows: ^{37}Ar, $\leq 1 \times 10^{-7}\%$; ^{39}Ar, $\leq 4 \times 10^{-7}\%$; ^{41}Ar, $\leq 3 \times 10^{-9}\%$; ^{42}Ar, $\leq 3 \times 10^{-11}\%$ The upper limit for the fission yield of ^{56}Co (daughter of ^{56}Ni) was determined as $\leq 8 \times 10^{-8}\%$. The yields of these isotopes are three to seven orders of magnitude lower than those expected from thermal-neutron-induced ternary fission of ^{235}U as described by Muga. (auth)

13863 DECAY OF ^{183}Hf AND THE NUCLEAR SPECTROSCOPY OF ^{183}Ta. Bakhru, H.; Mukherjee, S. K. (Saha Inst. of Nuclear Physics, Calcutta, India). Phys. Rev., 142: 719-24(Feb. 18, 1966).

The decay of ^{183}Hf is studied after bombarding tungsten with 14-Mev neutrons, separating the Hf fraction by radiochemistry and using standard scintillation-counter techniques. The beta measurements show three beta groups of energies 2.21, 1.87, and 1.35 Mev. The first two groups decay with a half-life of 91 days and the last one decays with a half-life of 64 min. The gamma measurements show eight gamma rays of energies 95, 250, 345, 405, 500, 590, 750, and 930 kev. The 95-, 250-, and 340-kev gamma-rays are found to decay with half-lives of 64 min and 91 days; and the 345-, 405-, and 750-kev gamma rays decay with a half-life of 64 min only. A metastable state of ^{183}Hf decays with a half-life of about 91 days; the ground state of ^{183}Hf is found to decay with a half-life of 64 min. An electron conversion line of energy 640 kev is observed to decay with a half-life of 91 days only. The γ-γ and β-γ coincidences and the sum-coincidence studies were performed, and based on these results a decay scheme of ^{183}Hf and ^{183m}Hf is proposed and results discussed. (auth)

13864 ^{141}Nd AND ITS PRODUCTION IN THE (n,2n) REACTION. Grissom, J. T. (Army Missile Command, Redstone Arsenal, Ala.); Koehler, D. R.; Alford, W. L. Phys. Rev., 142: 725-8(Feb. 18, 1966).

Several properties of the production and decay of ^{141}Nd from the nuclear reactions $^{142}Nd(n,2n)^{141g}Nd$, ^{141m}Nd were studied. The parameters measured were the isomeric yield ratio, the half-lives of the isomeric state and the ground state, the positron branching ratio of the ground state decay, and the $^{142}Nd(n,2n)^{141}Nd$ cross section. The values obtained for these quantities are 0.689 ± 0.069, 64.7 ± 1.3 sec, 2.42 ± 0.09 h, 2.73% ± 0.27%, and 1650 ± 165 mb, respectively. In addition, an upper limit on the ratio of the $^{142}Nd(n,\alpha)^{139}Ce$ cross section to the $^{142}Nd(n,2n)^{141}Nd$ cross section was determined to be 1.5×10^{-3}. This leads to an upper limit on the $^{142}Nd(n,\alpha)$ cross section of approximately 2.5 mb. This work was performed using 14.7-Mev neutrons from the $T(d,n)^{4}He$ reaction. (auth)

13865 SPECTROSCOPIC FACTORS FROM DEUTERON STRIPPING REACTIONS LEADING TO GROUND AND FIRST EXCITED STATES OF EVEN SPHERICAL NUCLEI. Sorensen, Raymond A. (Carnegie Inst. of Tech., Pittsburgh); Lin, E. K.; Cohen, B. L. Phys. Rev., 142: 729-34 (Feb. 18, 1966).

Deuteron stripping reactions on odd-neutron targets from Cr to Sm leading to the ground and first excited states of the even system are analyzed with distorted-wave Born approximation calculations. Theoretical spectroscopic factors are computed for these reactions using wave functions derived from the pairing-plus-$P^{(2)}$ model. One such factor is calculated and measured for the ground-state transition, while for the first excited state the analysis is in terms of several spectroscopic factors corresponding to several l values for the transferred neutron. For the ground state, the agreement between experiment and theory is excellent. For the excited state the agreement is not so good, but most of the spectroscopic factors are in agreement to about a factor of 2. (auth)

13866 $^{90}Zr(p,p')$ REACTION AT 18.8 Mev AND THE NUCLEAR-SHELL MODEL. Gray, W. S. (Univ. of Colorado, Boulder); Kenefick, R. A.; Kraushaar, J. J.; Satchler, G. R. Phys. Rev., 142: 735-48(Feb. 18, 1966). (UCOL-535-550).

The elastic and inelastic scattering of 18.8-Mev protons from ^{90}Zr was studied. Angular distributions for the elastic and 17 inelastic groups were measured. An optical-model analysis of the elastic scattering was performed. The inelastic scattering was compared with the predictions of the shell model using a simple two-body interaction between the incident and target nucleons. A Yukawa potential with a range of about 1 F and a strength of about 200 Mev gives a good fit to the excitation of the states of the $g_{9/2}^{2}$ configuration. Excitation of the other states is discussed in terms of the shell-model configurations expected to contribute. Arguments are given for the spin-flip strength being small. (auth)

13867 SHELL-MODEL FORM FACTORS FOR THE $^{90}Zr(p,p')$ REACTION. Johnson, M. B.; Owen, L. W.; Satchler, G. R. (Oak Ridge National Lab., Tenn.). Phys. Rev., 142: 748-57(Feb. 18, 1966). (ORNL-P-1641).

The application of the shell model to the $^{90}Zr(p,p')$ reaction is described. The nuclear matrix elements, and particularly the radial form factors, are discussed. Interactions of Gaussian and Yukawa form between projectile and target nucleons are used. They are assumed to be central, but spin and isospin dependence is included. The shell-model orbitals are calculated for a potential of the Woods-

Saxon shape. The effects of parameter variations and of corrections such as may be due to nonlocality of the potentials are studied in some detail. It is shown how the data for the $^{90}Zr(p,p')$ reaction favor a Yukawa interaction with a range of about 1 F. (auth)

13868 POLARIZATION AND DIFFERENTIAL CROSS SECTIONS IN THE SMALL-ANGLE SCATTERING OF NEUTRONS BY URANIUM. Elwyn, A. J.; Monahan, J. E.; Lane, R. O.; Langsdorf, A. Jr.; Mooring, F. P. (Argonne National Lab., Ill.). Phys. Rev., 142: 758-67(Feb. 18, 1966).

A measurement of the polarization as well as the differential cross section of 0.83-Mev neutrons scattered from uranium through angles of 1.65, 2.35, 4.6, and 10° is described. The observed increase in the differential cross section with decreasing angle is greater (by more than a standard deviation for the three smallest angles) than that expected from nuclear plus Schwinger scattering alone. No corresponding anomalous polarization effects are seen, however. The results of these and previous measurements suggest that this anomalous scattering may be coupled to the fission process. The importance of correcting the measured differential cross sections for finite-solid-angle effects is discussed. (auth)

13869 ELECTRON-CAPTURE RATIO AND INTERNAL BREMSSTRAHLUNG IN ^{181}W DECAY. Rao, P. Venugopala; Crasemann, Bernd (Univ. of Oregon, Eugene). Phys. Rev., 142: 768-74(Feb. 18, 1966). (RLO-1921-3).

A capture ratio $P_L/P_K = 0.27 \pm 0.05$ was determined for the decay of ^{181}W to the ground state and 6-kev level of ^{181}Ta, on the basis of an x-ray intensity ratio $I_L/I_K = 0.311 \pm 0.006$ and a measured partial L-shell fluorescence yield $\omega_{LL} = 0.225 \pm 0.010$. This value of ω_{LL}, determined from coincidences between L x rays and γ rays, is shown to apply for L capture to the 0- and 6-kev levels as well as to the 136- and 159-kev levels. The decay energy of ^{181}W is found to be 187 ± 10 kev from an analysis of the internal bremsstrahlung associated with 1s-electron capture, observed in coincidence with K x rays, and the internal bremsstrahlung spectrum produced in 2s-electron capture, measured with a Ge(Li) spectrometer. For this transition energy, the theoretical capture ratio is somewhat higher than the measured value, but lies within the error limits of the measurement. (auth)

13870 EXCITATION OF A 3- COLLECTIVE STATE BY LOW-ENERGY NEUTRON SCATTERING. Cranberg, L. (Los Alamos Scientific Lab., N. Mex. Univ. of Virginia, Charlottesville); Zafiratos, C. D. Phys. Rev., 142: 775-8(Feb. 18, 1966).

The well-known octupole state at 2.6-Mev excitation in the region of A = 208 was excited by inelastic neutron scattering. At 8-Mev incident-neutron energy a distorted-wave Born-approximation analysis of the data yields a value of the deformation β_3 in agreement with the results of other measurements. The reaction mechanism changes rapidly between 6- and 4-Mev incident-neutron energy from dominance of direct interaction to dominance of a compound-nucleus mechanism. (auth)

13871 ^{233}U FISSION CROSS SECTION MEASURED USING A NUCLEAR EXPLOSION IN SPACE. Albert, Richard D. (Univ. of California, Livermore). Phys. Rev., 142: 778-87(Feb. 18, 1966). (UCRL-14176-T).

A high-altitude nuclear explosion in 1962 was used as a neutron source in an experiment to measure the fission cross section of ^{233}U relative to ^{235}U in the 30-ev to 5-Mev energy region. Fission data were telemetered to the ground station at Kauai, Hawaii from sounding rockets carrying the fission counters which were near their apogee at the time the nuclear explosion occurred over Johnston Island. The flight path for the neutron time-of-flight experiment was 1280 km. The ^{233}U fission-cross-section results indicated average values about 20% lower in the 2-Mev energy region and about 30-40% higher in the 30-500-ev energy region than the average of previously obtained values. The results also fill the gap in ^{233}U fission-cross-section data which existed between previous high-energy Van de Graaff and low-energy time-of-flight measurements in the 1-20-kev region. (auth)

13872 STUDIES OF (d,d') REACTIONS ON Sn, Cd, Te, AND Mo ISOTOPES. Kim, Y. S.; Cohen, B. L. (Univ. of Pittsburgh). Phys. Rev., 142: 788-?(Feb. 18, 1966).

Energy spectra were obtained from inelastic scattering of 15-Mev deuterons by various isotopes of Sn, Cd, Te, and Mo. The 2^+ and 3^- collective states are located, and the systematics of their excitation energies and cross sections are studied. Crude estimates are obtained for the octupole vibrational deformation parameter β_3 for these isotopes and for isotopes of Zn, Se, Zr, and Pd studied previously. Many other (noncollective) levels are catalogued, and some information is obtained on their parities. (auth)

13873 DYNAMICAL CORRELATIONS AND THE NUCLEAR PHOTOEFFECT. Wang, Tso-Pin; Clark, John W. (Washington Univ., St. Louis). Progr. Theoret. Phys. (Kyoto), 34: 776-813(Nov. 1965).

The dipole sum rules of Levinger and Bethe are used to estimate the influence of strong dynamical correlations, generated by realistic 2-nucleon potentials, on the photoeffect in heavy nuclei. The description of the nuclear ground state is an asymptotic one, based on a complete set of correlated functions $\{F\Phi_m\}$, where F is a product of 2-body correlation factors f appropriate to a system with strong short-range repulsions and $\{\Phi_m\}$ a complete set of Fermi-gas model functions satisfying periodic boundary conditions over a fundamental volume Ω identified with the (assumed large) nuclear volume. The integral of the photonuclear cross section over all photon energies, $\sigma_{int} = \int\sigma(W)dW$, is estimated in zeroth cluster order for Hamada-Johnston, Brueckner-Gammel-Thaler, Gammel-Christian-Thaler, and Ohmura-Morita-Yamada potentials with a ground-state wave function constructed from the $F\Phi_m$ via a first-order perturbation theory. The bremsstrahlung-weighted cross section, $\sigma_b = \int\sigma(W)W^{-1}dW$, is calculated with the unperturbed wave function $F\Phi_0$, where Φ_0 is the wave function of the degenerate Fermi gas; here first-order cluster corrections are included. The first energy moment of the cross section, $\sigma_1 = \int\sigma(W)WdW$, is also evaluated using $F\Phi_0$, but keeping only lowest cluster contributions. Variation of these three energy moments of $\sigma(W)$ with an inverse range parameter γ in f and with the nuclear radius parameter r_0 is studied. It is found that σ_{int} and σ_1, which depend explicitly on the 2-nucleon potential and are sensitive to the short-range behavior of f, are substantially increased, and σ_b, which is sensitive to the long-range behavior of f, may be appreciably diminished, compared to their respective values for a Fermi-gas model and well-behaved central potentials fitting the low energy scattering data. In particular, for all potentials tested and for reasonable parameter choices, σ_{int} is enhanced by roughly a factor 2 over the TRK value. It is anticipated that, in the future, the Levinger-Bethe sum rules may emerge as important tools for probing the validity of favored models of the nuclear ground state and of the 2-nucleon potential. (auth)

13874 THE ABSORPTION OF π MESONS AND THE (p,pd) REACTION. Sakamoto, Yoshiyuki; Cheon, Il-Tong (Kyoto Univ.). Progr. Theoret. Phys. (Kyoto), 34: 814-24(Nov. 1965).

The absorption of π mesons is considered to occur on a correlated nucleon pair in the nucleus (N). The proton-neutron pair absorbs a π meson leaving the residual nucleus (N-2) behind. This process gives information about the momentum distribution of the center of mass of the proton-neutron pair with respect to that of other nucleons of the nucleus. The information about the momentum distribution is also studied by the (p,pd) reaction. The similarity of the expression for the absorption of the stopped π^- meson by ^{12}C to that for the $^{12}C(p,pd)$ reaction is shown when the residual nucleus ^{10}B is left in low-lying states. It is also shown that a knocked-out deuteron at the zero momentum transfer in the $^{12}C(p,pd)$ reaction and two neutrons emitted at the angle of 180° to each other in the $^{12}C(\pi^-,2n)$ reaction are hardly observed when the

residual nucleus ^{10}B is left in the ground and first excited states. (auth)

13875 $^{9}Be(\alpha,2\alpha)^{5}He$ REACTION AND ALPHA-PARTICLE MODEL. Hiura, Jun; Shimodaya, Ichiro (Hokkaido Univ., Sapporo). Progr. Theoret. Phys. (Kyoto), 34: 861-3(Nov. 1965).

The $^{9}Be(\alpha,2\alpha)^{5}He$ reaction is investigated in the framework of the modified alpha-particle model, which takes into account the effects of the Pauli principle and introduces α-α and n-α potentials as the basic interactions. A two-step process—the emission of two α particles by the α-^{9}Be collision and the subsequent breakup of the residual ^{5}He nucleus into a neutron and an α particle—is assumed. Expressions are obtained for the differential cross section and the momentum distribution function, and results of numerical calculations are given for the coplaner and symmetric scattering cases for initial energy of 28 Mev. (M.J.T.)

13876 NUCLEAR FORCE AND THE BETHE-SALPETER EQUATION. Kawaguchi, Masaaki (Osaka Univ.). [Progr. Theoret. Phys. (Kyoto), 34: Suppl., 76-84(1965)].

Bound states of two nucleons are discussed based on the Bethe-Salpeter equation. A general method is developed to obtain the eigenvalue of the coupling constant and the four-dimensional wave function for a given binding energy. (auth)

13877 POSSIBLE G-PARITY NONCONSERVATION IN MUON CAPTURE REACTIONS. ANGULAR DISTRIBUTION OF RECOILS. Morita, Masato (Kyoto Univ.); Morita, Reiko; Shirafuji, Takeshi. [Progr. Theoret. Phys. (Kyoto), 34: Suppl., 96-103(1965)].

Induced effects in muon capture reactions are investigated under the assumption of possible G-parity nonconservation. An explicit formula of the angular distribution of the recoils in muon capture is given for unique n-th forbidden transitions [spin change $0 \rightarrow J$, $J = n + 1$; parity change $(-)^{J+1}$]. (auth)

13878 ON THE ELECTROMAGNETIC STRUCTURE OF THE YUKAWA MESON. Schiff, L. I. (Univ. of Stanford, Calif.). [Progr. Theoret. Phys. (Kyoto), 34: Suppl., 400-5(1965)].

A discussion is presented of a recent proposal of Hofstadter for the measurement of the electromagnetic form factor of the Yukawa meson, by comparing the elastic scattering of positive and negative pions on an isoscalar nucleus. A formalism is developed which permits Coulomb effects to be calculated to first order without the use of Coulomb wave functions. In particular, it is shown that the Coulomb–Born amplitude is not enough in itself, but that there are additional first order Coulomb effects that arise from distortion of the pion wave function by the nuclear interaction. (auth)

13879 A POSSIBLE ORIGIN OF REPULSIVE CORE IN NUCLEAR FORCES. Otsuki, Shoichiro; Tamagaki, Ryozo; Yasuno, Masaru (Nagoya Univ., Japan). [Progr. Theoret. Phys. (Kyoto), 34: Suppl., 578-601(1965)].

A dynamical treatment is made of an originating mechanism of repulsive core provided that the nucleon is a few urfermion system with hard internal structure, by investigating N-N interaction in parallel with α-α one. It is clarified that the originating mechanism of such a structural core is closely related, above all, with the internal structure of the composed state of two nucleons (corresponding to ^{8}Be in the α-α case). A typical exchange kernel expected by the few urfermion structure is proposed, whose effect is almost equivalent to the observed hard core. Some phenomenological aspects of such structural core are discussed. (auth)

13880 EMISSION OF LIGHT FRAGMENTS FROM HEAVY NUCLEI IN HIGH ENERGY NUCLEAR REACTIONS. Miyazima, Tatsuoki; Nakamura, Kosuke; Futami, Yasuhiko (Tokyo Univ. of Education). [Progr. Theoret. Phys. (Kyoto), 34: Suppl., 621-5(1965)].

The importance of the apparent reduction of the Coulomb barrier for light fragments emitted from heavy nuclei bombarded by high-energy projectiles is pointed out and a new model is presented. Some discussions are also given on the relation between emitted high-energy particles and nucleonic clusters. (auth)

13881 INTERNAL CONVERSION ELECTRON SPECTRA IN (α,n) AND $(\alpha,2n)$ NUCLEAR REACTIONS ON THE ISOTOPES ^{92}Mo AND ^{98}Mo. Chikhladze, V. L. Yadern. Fiz., 2: 961-5(Dec. 1965). (In Russian).

A method is described for measuring conversion spectra by means of a β spectrometer. The targets are continuously bombarded by α particles and serve as sources of internal conversion electrons in the spectrometer. The K- and L-conversion lines of the $E_\gamma = 256 \pm 4$ kev γ transition were observed when a ^{92}Mo target was irradiated. The measured value of the internal conversion coefficient shows that this is an isomer transition in ^{95}Ru. When a ^{98}Mo target was irradiated the K- and L-conversion lines of the $E_\gamma = 224 \pm 4$ kev γ transition were observed. The measured value of the internal conversion coefficient shows that this is an M2 type transition. The transition was identified as an isomer transition in ^{101}Ru. Possible decay schemes of the isomer states ^{95}Ru, ^{97}Ru and ^{101}Ru are suggested. (auth)

13882 DECAY OF ^{138}Pr. Basina, A. S.; Badica, T.; Gromov, K. Ya.; Dzhelepov, B. S.; Lebedev, N. A.; Morozov, V. A.; Novgorodov, A. F. (Joint Inst. for Nuclear Research, Dubna, USSR. Leningrad State Univ.). Yadern. Fiz., 2: 966-73(Dec. 1965). (In Russian).

The γ-spectrum, $\gamma\gamma$- and $\beta^+\gamma$-coincidence spectra and the conversion electron spectra of praseodymium samples obtained from the products created by irradiating Ta, Tb and Er by 660 Mev protons, were measured. Intensive γ-trasitions with the energies 303, 789 and 1047 kev were observed in the ^{138}Pr γ-ray spectrum and their relative intensities were determined. The $\gamma\gamma$-coincidence experiments give evidence for a cascade of transitions 303–1047–789 kev. Measured $\beta^+\gamma$-coincidences did not confirm the existence of the β^+ -decay in ^{138}Pr to the level 1840 kev. The conversion electrons of the transitions 303 ± 1 and 789 ± 3 kev were investigated on a lens β-spectrometer. The internal conversion coefficients $\alpha_{K303} = 0.14 \pm 0.02$ and $\alpha_{K789} = 3.42 \times 10^{-3}$ were determined. The first coefficient makes it possible to conclude, that the 303 kev transition is of the type E3, the second does not contradict the assumption, that the 789 kev transition is pure E2. The quantum characteristics of the excited states of ^{138}Ce are discussed. (auth)

13883 INTERNAL CONVERSION COEFFICIENTS FOR NUCLEAR TRANSITIONS IN ^{132}Xe. Ivanov, Yu. F.; Rumer, I. A. (Inst. of Biophysics, Ministry of Public Health, USSR). Yadern. Fiz., 2: 974-7(Dec. 1965). (In Russian).

Photoconversion methods are used to determine the internal conversion coefficients for the nuclear transitions in ^{132}Xe with the energies 523; 630; 667.8; 772.9 and 954.5 kev. The conversion electron and photoelectron spectra were investigated with the help of a magnetic $\pi\sqrt{2}$-focusing β spectrometer. Platinum targets 6 and 11 mg · cm^{-2} thick, calibrated according to γ-rays from ^{198}Au and ^{137}Cs were used in the photoelectron spectrum investigations. The relative intensities of these γ transitions in ^{132}Xe were determined. The multipolarities of the 523; 630; 667.8 and 772.9 kev transitions were determined to be E2, that of the 954.5 kev transition–E1. This is in agreement with the level scheme suggested by Hamilton and Boyd. The parity of the levels 1963.7 and 2070.9 is positive, of 2395.2–negative. (auth)

13884 ABSORPTION OF π^- MESONS AND γ QUANTA AND NUCLEON CORRELATIONS IN ^{4}He. Kopaleyshvili, T. I.; Machabeli, I. Z. (Tbilissi State Univ., USSR). Yadern. Fiz., 2: 978-85(Dec. 1965). (In Russian).

The reactions (π^-,nn), (π^-,n), (γ,np), and (γ,N) on the ^{4}He nucleus are investigated theoretically, assuming a direct interaction mechanism between the π^- mesons and γ quanta and individual nucleons or nucleon pairs in the nucleus. Use is made of wave functions taking pairing correlations into account, determined with the help of a variational prob-

lem for the ^{4}He nucleus. One of them corresponds to a nucleon–nucleon potential with a repulsive core, the second to a velocity-dependent potential. The obtained results are: a) the energy dependence of the (γ,np) and (γ,N) cross sections; b) the distribution with respect to the relative energies of the emitted nucleons and to the recoil deuteron energies in the (π^-,nn) process; c) the probability of π^- meson absorption with the emission of one or two neutrons. A comparison with experimental data shows that the wave function corresponding to a velocity dependent potential gives a better fit to the whole complex of experimental data on all the considered processes. (auth)

13885 EVAPORATION OF NEUTRONS FROM COMPOUND NUCLEI WITH LARGE ANGULAR MOMENTA. Yungclaussen, G. (Joint Inst. for Nuclear Research, Dubna, USSR). Yadern. Fiz., 2: 986-91(Dec. 1965). (In Russian).

A simple method of measuring nuclear temperatures with the help of threshold indicators is described. The method is applicable to reactions with heavy ions for large values of the momentum transfered to the target nucleus. Results of the measurements, obtained when Ti, Cu, and Mo were bombarded by Ar and Ne ions are given. The level density parameter and moment of inertia of compound nuclei are determined. (auth)

13886 INFLUENCE OF STRONG INTERACTIONS BETWEEN NUCLEONS IN NUCLEI ON ALLOWED β DECAY. Rapoport, L. P.; Kopytin, I. V. (Voronezh State Univ., USSR). Yadern. Fiz., 2: 992-1001(Dec. 1965). (In Russian).

Strong interactions between nucleons, taken into account according to the Fermi-liquid theory, induce a β-decay form factor, strongly dependent on the nuclear structure. Formulas are obtained for the total probability and various correlation effects in β decay. The results are compared with experiments. (auth)

13887 ALLOWED NUCLEAR β TRANSITIONS IN THE THEORY OF FINITE FERMI SYSTEMS. Gaponov, Yu. V. Yadern. Fiz., 2: 1002-8(Dec. 1965). (In Russian).

Allowed β transitions in odd nuclei between A = 11 and A = 63 are studied on the basis of the theory of finite fermi-systems. It is shown that the theory explains the absolute decrease of the matrix elements for A > 40 and gives a good description of their behavior in mirror transitions and in the 2p-subshell. In the region where states strongly degenerate with respect to ($1f_{\frac{7}{2}}$, $1g_{\frac{9}{2}}$) are being filled, it is necessary to take the configurations into account more exactly. (auth)

13888 ON THE COHERENT EXCITATION OF NUCLEI MOVING THROUGH CRYSTALS. Okorokov, V. V. (Inst. of Theoretical and Experimental Physics, Moscow). Yadern. Fiz., 2: 1009-14(Dec. 1965). (In Russian).

Some arguments for the existence of the coherent Coulomb excitation of nuclei moving through crystals are given. (auth)

13889 EVAPORATION REACTIONS OF SEVERAL NEUTRONS PRODUCED BY IRRADIATION OF ^{238}U BY THE ACCELERATED IONS ^{18}O, ^{19}F, AND ^{22}Ne. Donets, E. D.; Shchegolev, V. A.; Ermakov, V. A. (Joint Inst. for Nuclear Research, Dubna, USSR). Yadern. Fiz., 2: 1015-23(Dec. 1965). (In Russian).

The energy dependence of the production cross section of the isotopes of the 100, 101 and the 102 elements for the following reactions is studied: ^{238}U(^{18}O,xn)($4 \leq x \leq 8$), ^{238}U(^{19}F,xn)($5 \leq x \leq 7$), ^{238}U(^{22}Ne,xn)($4 \leq x \leq 6$). The obtained results demonstrate a strong dependence of the quantity $(\overline{\Gamma_n}/\overline{\Gamma_f})$ for the given compound nucleus upon the incident ion energy and show a decrease of the average quantity $(\overline{\Gamma_n}/\overline{\Gamma_f})$ when increasing Z of the compound nucleus. (auth)

13890 INELASTIC SCATTERING OF COMPLEX NUCLEI ACCOMPANIED BY THE EXCITATION OF COLLECTIVE LEVELS. Kalinkin, B. N.; Grabovski, Ya. (Joint Inst. for Nuclear Research, Dubna, USSR). Yadern. Fiz., 2: 1024-9(Dec. 1965). (In Russian).

The relative role of the Coulomb and nuclear mechanisms in the excitation of collective levels in the inelastic scattering of complex nuclei is established for energies above the barrier. (auth)

13891 MECHANISMS OF THE REACTIONS $^{12}C + {}^{10}B \rightarrow {}^{10}B + 3\alpha$ AND $^{14}N + {}^{10}B \rightarrow {}^{12}C + 3\alpha$. Shumilov, S. N.; Klyucharev, A. P.; Rutkevich, N. Ya. Yadern. Fiz., 2: 1030-41(Dec. 1965). (In Russian).

The interactions of 100 Mev ^{10}B ions with carbon and nitrogen nuclei in photoemulsion were investigated. The use of discriminating photoemulsions, a complete measurement of the parameters and a detailed analysis of the star kinematics made it possible to identify the reactions $^{12}C + {}^{10}B \rightarrow {}^{10}B + 3\alpha + 7.3$ Mev, $^{14}N + {}^{10}B \rightarrow {}^{12}C + 3\alpha + 7.6$ Mev. The excitation functions, angular and energy distributions of ^{10}B, ^{12}C and α-particles were measured for these reactions. The angular distributions of ^{10}B nuclei created in the first reaction and ^{12}C in the second have a maximum at large angles. The dominating mechanism of the reactions is the transfer of a deuteron. (auth)

13892 DISTRIBUTION OF KNOCK-OUT NUCLEONS AS A FUNCTION OF NUCLEAR VOLUME, EXCITATION ENERGY, AND NUCLEAR RECCIL MOMENTUM DISTRIBUTIONS IN CASCADE PROCESSES. Denisov, F. P.; Milovanov, V. P.; Latypova, R. A.; Cherenkov, P. A. (Lebedev Inst. of Physics, Moscow). Yadern. Fiz., 2: 1042-8(Dec. 1965). (In Russian).

The discussion of the results of previous calculations is continued. The distributions of the knocked-out nucleons in the volume of the nucleus, the excitation energies of the residual nuclei and the momentum distribution of the recoil nuclei. (auth)

13893 COHERENT INELASTIC INTERACTIONS BETWEEN HIGH-ENERGY π^- MESONS AND HEAVY NUCLEI IN PHOTOEMULSION. Azimov, S. A.; Beter, E. V.; Gulyamov, U. G.; Eroshkina, N. B.; Levin, A. Ya. (Inst. of Nuclear Physics, Academy of Sciences, Uzbek SSR). Yadern. Fiz., 2: 1049-53(Dec. 1965). (In Russian).

The characteristics of interactions assumed to be the coherent inelastic reactions $\pi^- + A \rightarrow \pi^+ + \pi^- + \pi^- + A'$ on heavy nuclei in photoemulsion are investigated for 17.2 Bev/C pion momenta. The cross section of this process is estimated to be 5.4 ± 1.4 mb. Compared with the corresponding value for carbon, this indicates a dependence of the cross-section on the atomic number of the type $A^{1/3}$ or $A^{2/3}$. (auth)

13894 THE THREE-NUCLEON SYSTEM [Thesis]. Simpson, Wilburn Dwain. Houston, Tex., Rice Univ., 1965. 160p.

The three-nucleon system was studied experimentally by the ^{2}H(p,2p)n reaction at E_p = 9.0 and 10.5 Mev, and by the ^{1}H(d,2p)n reaction at E_d = 10.5 Mev. The two protons in the final state were detected in coincidence and energy-analyzed by use of a two-parameter pulse-height analyzer, thus completely specifying the kinematics of the reaction. The distinction between sequential and simultaneous decay for the three-nucleon system was investigated. The sequential decay of this system via the virtual deuteron was observed, and decay via the singlet di-proton seems likely. A preliminary theoretical analysis of the data using the generalized density-of-states describes the observed decay via the virtual deuteron, but the same analysis does not predict the observed yield due to decay via a di-proton system. (Dissertation Abstr.)

13895 ENERGY LEVELS OF ^{211}Bi [Thesis]. Mead, Richard Oliver. Davis, Calif., Univ. of California, 1965. 54p.

The gamma spectrum from the decay of ^{211}Pb was studied with NaI crystals (using singles, gamma-gamma coincidence and sum-coincidence techniques) and with a germanium semiconductor detector. The energies and relative gamma-ray intensities are reported for 16 transitions in ^{211}Bi. Using a precision magnetic beta-ray spectrometer, the energy

and relative intensity of the most intense conversion electron lines were measured. From the gamma-ray and electron-conversion transition energies as well as gamma-gamma coincidence measurements a consistent level diagram for ^{211}Bi is proposed, which has levels at 404.84 ± .04, 766.34 ± .07, 831.83 ± .04, 1020 ± 3, 1076 ± 3, 1104 ± 2, 1188 ± 2 and 1265 ± 2 kev. (Dissertation Abstr.)

13896 EXPERIMENTAL STUDY OF THE REACTION ^{3}He(γ,π^+)^{3}H UP TO 260 Mev [Thesis]. O'Fallon, John Robert. Urbana, Ill., Univ. of Illinois, 1965. 97p.

The differential cross section for the reaction ^{3}He(γ,π^+)^{3}H was measured for photon energies of 180 to 260 Mev (momentum transfer 1.2 F^{-1} to 1.9 F^{-1}). A target of gaseous ^{3}He at 20.4°K and approximately one atmosphere pressure was irradiated by a 270-Mev bremsstrahlung x-ray beam. The reaction was observed by detecting π^+–^{3}H coincidences. The counter telescopes consisted of seven plastic scintillators for the pions and four transmission type semiconductor detectors for the tritons. Pulses from the semiconductor detectors and the scintillators were displayed on a dual beam oscilloscope and photographed. E and dE/dx relations were used for particle identification. Tritons with energies between 9.7 and 24.5 Mev were observed at laboratory angles of 26, 30, 35, and 40°. At 26° the cross sections in the center of mass system ranged from 2.55 ± 0.34 μb/ster to 0.78 ± 0.16 μb/ster, decreasing with increasing photon energy. An impulse approximation calculation was performed to relate the cross section to the matter form factor of the 3-nucleon system under the assumption of identical wave functions for ^{3}He and ^{3}H. Values for the matter form factor obtained using this relation and the cross sections of this experiment were found to lie below the values obtained from the results of electron scattering experiments. Several plausible arguments may be presented to explain this discrepancy. Under the condition of proximity of two nucleons which depends on the internal momentum distribution, phase space considerations (Wilson model) favor two-nucleon ejection over free pion production. Pions may be scattered or absorbed before they escape the nucleus. Alternatively, the pion production amplitude may have a many-body aspect; that is, it may depend on the coordinates of more than one nucleon. (Dissertation Abstr.)

13897 AN EXPERIMENTAL STUDY OF SUB-BARRIER PROTON EMISSION IN COMPOUND NUCLEAR REACTIONS [Thesis]. Parkinson, Ernest Roland. Seattle, Wash., Univ. of Washington, 1965. 318p.

Measurements of low-energy (sub-Coulomb-barrier) proton emission probabilities were carried out under experimental conditions dominated by contributions from a compound nuclear reaction mechanism. Differential cross sections for (p,p′) reactions at 10.5-Mev incident energy were measured for ^{27}Al, Ti, ^{59}Co, Ni, and ^{63}Cu targets. Using a particle identification method that combined the advantages of dE/dx–E and time-of-flight methods, proton emission spectra were measured down to an energy threshold of about 2 Mev. Comparisons of the angular distributions, spectrum shapes, and absolute magnitudes of the observed spectra with statistical theory predictions confirmed that a majority of the observed events, especially at low emission energy, were due to a statistical reaction mechanism. Calculations of the spectrum shape were based on both optical model and continuum theory values of the inverse reaction cross section, and showed good agreement with observed low-energy proton spectra from all targets except Al. The relative probability of low-energy proton emission and gamma-ray emission from states near 8-Mev excitation energy in ^{63}Cu was examined separately. The differential cross section for the ^{63}Cu (p,2p)^{62}Ni reaction was measured in an experiment in which the coincident proton energies were observed. Assuming the reaction took place via the sequential decay of a ^{64}Zn compound nucleus, the ratio of the ^{63}Cu(p,2p) and ^{63}Cu(p,p′) cross sections provided an experimental measure of proton-gamma ray competition. The probability for second proton emission was found to be 0.12 ± 0.05, when the available second-proton kinetic energy was 2.08 Mev. This value was compared with the statistical theory to obtain the relative proton and gamma emission widths as a function of the spin and excitation of the emitting level, and such values were found to be consistent with absolute values of proton and gamma ray emission widths predicted by the statistical theory. (Dissertation Abstr.)

13898 STATES IN ^{17}O FROM ^{13}C + α [Thesis]. Barnes, Barry Keith. Houston, Tex., Rice Univ., 1965. 113p.

The ^{13}C(α,α)^{13}C cross sections were measured at 54.7°, 107.9°, 142.6°, and 169.6° (cms) from 2 to 3.5 Mev. The ^{13}C(α,n)^{16}O cross sections at 0° were measured for the same energy range. A dispersion theory analysis was carried out to assign parities, obtain consistent partial widths, and resolve ambiguities in spin assignments to states of the compound nucleus ^{17}O. The spin and parity assignments determined or confirmed were $\frac{1}{2}^-$, $\frac{3}{2}^+$, $\frac{3}{2}^-$, $\frac{1}{2}^+$, $\frac{5}{2}^+$, $\frac{1}{2}^+$, $\frac{5}{2}^-$, $\frac{3}{2}^-$, $\frac{3}{2}^+$, $(\frac{7}{2}, \frac{9}{2})^-$, and $\frac{7}{2}^-$ to levels at 7.97, 8.06, 8.20, 8.33, 8.39, 8.46, 8.50, 8.68, 8.87, 8.88, and 8.94 Mev respectively. The level at 8.88 has not been previously seen, since it is observed only in the elastic scattering. The 8.46-Mev level exhibited a quite strong elastic scattering resonance. States in ^{14}N in the region of excitation energy between 12.2 and 15.0 Mev were investigated by bombarding ^{13}C with protons. The elastic scattering cross sections were measured at θ_{cms} 170.8° and 150.8° from E_p 5.0 to 8.1 Mev. The reaction cross sections for d, p_1, p_2, and p_3 reaction groups were measured at θ_{lab} 170.0°, 148.5°, 80.0°, and 58.5° for the same energy range. Angular distributions were measured for the reaction groups at 15 energies in the same energy range. The coefficients for the expansion of the angular distributions in a series of Legendre polynomials were determined by a least squares fitting method. From these coefficients maximum spin values were determined for 8 levels of ^{14}N in this energy region. (Dissertation Abstr.)

13899 THE POLARIZATION OF PROTONS ELASTICALLY SCATTERED FROM ^{12}C [Thesis]. Clegg, Thomas Boykin. Houston, Tex., Rice Univ., 1965. 114p.

Position-sensitive solid state detectors were incorporated into a polarimeter to use in double scattering experiments with solid targets. Two of these detectors count simultaneously particles scattered through second scattering angles from 36° to 144°. Left-right asymmetries are measured by rotating the polarimeter to opposite sides of the incident beam. A digital computer is used to accumulate data as two-parameter spectra, the two parameters being the positions and energies of the detected particles. Events are labeled to indicate in which detector they occurred. The polarimeter was used initially to double scatter protons from ^{12}C in the energy range 5.76–6.67 Mev. Angular distributions of asymmetry were measured near 6.22 Mev and 5.76 Mev. Curves of relative polarization were obtained by normalizing the asymmetry to Wisconsin values for the polarization of the protons first scattered at 50°. Absolute cross section measurements for p + ^{12}C elastic scattering were measured near the same energies by scattering protons from a methane gas target in a differentially pumped, gas scattering chamber. A phase shift analysis of the cross section data and some of the polarization data was performed. (Dissertation Abstr.)

13900 FINAL STATE INTERACTIONS IN THE ^{3}He(^{3}He,2p)^{4}He REACTION [Thesis]. Aldridge III, Jack Paxton. Houston, Tex., Rice Univ., 1965. 118p.

The ^{3}He(^{3}He,2p)^{4}He reaction was studied at a bombarding energy near 4.9 Mev by observation of both proton–proton coincidences and proton–alpha particle coincidences. The ^{3}He gas target was contained in a cell filled to 20 cm Hg pressure, provided with a 1.9 mg/cm^2 thick molybdenum foil entrance window. The particles emerged from the cell through a Mylar exit window and were detected with lithium-drifted silicon detectors. The pulse height spectra were recorded by an on-line, two-dimensional computer analyzer system. Measurements of the spectra of (p,p) and (p,α) coincidences were made at eight different angle settings for the detectors in order to study the angular variation of the reaction cross sections. The angle settings used were

(60°, 40°), (60°, 60°), (60°, 75.1°), (60°, 80°), (60°, 100°), (60°, 70°), (119.8°, 30°), and (103.2°, 40°). The detectors were located on opposite sides of the beam. The spectra indicate that the reaction proceeds predominantly via sequential two-body decay through the broad $P_{\frac{3}{2}}$ and $P_{\frac{1}{2}}$ levels in ^{5}Li and through the $^1S_0$ state of ^{2}He. Preliminary comparisons of the spectra to predictions of the generalized density of states function formulation of sequential decay processes are presented. (Dissertation Abstr.)

Plasma Physics and Thermonuclear Processes

See also Fluid Physics and Thermodynamics

Refer also to abstracts 13428 and 13432.

13901 (CEA-R-2822) CONTRIBUTION A L'ETUDE DES INSTABILITES A HAUTE FREQUENCE DANS LA DECHARGE REFLEX A CATHODES FROIDES [Theses]. (Study of High-Frequency Instabilities on a Cold Cathode Reflex Discharge [Thesis]). Gregoire, Michel (Commissariat a l'Energie Atomique, Saclay (France). Centre d'Etudes Nucleaires). 1965. 76p. Dep. mn.

Submitted to Paris Univ. (France). Faculte des Sciences.

The cold cathode reflex discharge develops a cathode sheath of several hundreds of volts, which accelerates electrons released from the cathode to high velocities along the lines of the axial magnetic field. On the studied pressure range (4×10^{-4} torr $< p < 2 \times 10^{-2}$ torr) the plasma density is about 10^{11} cm^{-3}. Under certain conditions high frequency (1–5000 MHz) instabilities appear. These instabilities are found to profoundly modify the mean characteristics of the discharge. In particular, particle flow across the lines of magnetic field is found to be considerably greater than that predicted by classical diffusion theory. Theoretical considerations are presented with complementary experimental results. They show that the high frequency instabilities are a result of the fast electronic assembly accelerated through the cathode sheath. (auth)

13902 (CEA-R-2898) EXTENSION DE LA LOI DE CHILD LANGMUIR A UN FAISCEAU DE PARTICULES ANIME D'UNE VITESSE DIRIGEE. (Extension of the Child-Langmuir Law to a Beam of Particles Having an Initial Velocity). Geller, Richard (Commissariat a l'Energie Atomique, Saclay (France). Centre d'Etudes Nucleaires). Nov. 1965. 24p. Dep. mn.

A d-c ion current of 50 mamp/cm^2 was obtained with approximately 100 volts extraction from the plasma created by the CIRCE device, and a still stronger electron current was obtained with a still lower extraction. These results are an order of magnitude higher than the ordinary characteristics. In the neutral plasma beam produced in the CIRCE device, the ions have mainly longitudinal energy whereas the electron energy is transverse. This situation makes the charge separation easier. This result is explained on a basis of current increase due to the initial velocity of the particles. (auth)

13903 (CLM-R51) MICROWAVE EMISSION FROM PLASMAS AT HARMONICS OF THE ELECTRON CYCLOTRON FREQUENCY. Boyd, T. J. M. (Culham Lab., United Kingdom Atomic Energy Authority, Abingdon (England)). Aug. 1965. 24p. Dep. BIS $0.80. HMSO 4s.

A mechanism is proposed to account for the anomalously large microwave emission from certain plasmas in the region of harmonics of the electron cyclotron frequency. This mechanism involves the scattering of electron plasma waves propagating almost orthogonally to the magnetic field by fluctuations in the ion plasma density; a wave-wave interaction leads to the conversion from one wave type (primarily longitudinal) to another (transverse). A kinetic theory calculation based on this model gives an emission spectrum which may be compared with the observations. (auth)

13904 (CLM-R52) THE EFFECT OF COULOMB COLLISIONS ON THE SCATTERING OF LIGHT BY PLASMAS. Boyd, T. J. M. (Culham Lab., United Kingdom Atomic Energy Authority, Abingdon (England)). Oct. 1965. 14p. Dep. BIS $0.60. HMSO 3s.

The effect of Coulomb collisions on the low-frequency ion acoustic resonance is calculated using a simple hydrodynamic approach, and the line profile obtained is compared with that found by DuBois and Gilinsky in the limit of collision-dominated plasmas. In the region of the ion acoustic resonance, the results from the two approaches are identical, but the line shape in the region of zero frequency predicted by the DuBois-Gilinsky calculation is distinct from that obtained by the hydrodynamic approach. The main result is that the low-frequency ion feature narrows significantly in collision-dominated plasmas. The contribution of Coulomb collisions to the broadening of the feature at the electron plasma frequency (sometimes called the "plasma line" or "satellite feature") is also calculated and is compared, over a range of parameters, with the contribution due to the Landau damping in a collisionless plasma. It is shown that over the range of parameters covered by the Culham experiments, collision effects are not important. (auth)

13905 (CONF-651056-1) NONLINEAR MECHANICS OF PLASMA-LIKE DISTRIBUTED MEDIA. Lashinsky, Herbert (Maryland Univ., College Park). Jan. 1966. Contract AT(40-1)-2405. 25p. (BN-432). Dep. mn. CFSTI $1.00 cy, $0.50 mn.

From Symposium on the Dynamics of Plasmas and Fluids, College Park, Md.

The finite-amplitude controlled oscillations produced in a thermal-plasma device (Q-machine) as a result of the universal instability provide a useful tool for experimental research in the nonlinear mechanics of plasma-like distributed systems i.e., systems in which the pertinent physical parameters are distributed in one or more of the coordinate variables (position and velocity) used to describe the system, rather than lumped, as in more familiar vacuum-tube or mechanical configurations. Results obtained in such experiments were analyzed by extending techniques of nonlinear mechanics to distributed systems. In particular, nonlinear phenomena such as mode competition and mode locking were examined and the relation between these phenomena in plasmas and in related systems such as the gaseous optical maser was delineated. The current status of this work is reviewed with particular emphasis being given to the analysis of mode locking and the implications of this effect for turbulence in plasmas. (auth)

13906 (IPP-1/40) ANWENDBARKEIT ELEKTRISCHER SONDEN IN HEISSEN PLASMEN. (Electrostatic Double Probes and Their Applicability in Hot Plasmas). Combecher, D. (Institut fuer Plasmaphysik, G.m.b.H. Garching (West Germany)). July 1965. 22p. Dep. mn.

Density measurements were made in a 7.5-kJ theta pinch using double electric probes. Measurements were also made using a Mach-Zehnder interferometer. The line density obtained from the probe measurements along the axis of the discharge tube was much lower than the result obtained interferometrically. The discrepancy was attributed to the fact that the magnetic field of the discharge does not penetrate the probe material deeply because of its high frequency. The vaporization of the probe material was studied spectroscopically. (D.C.W.)

13907 (IPP-2/42) MEASUREMENT OF THE ANISOTROPY IN THE RADIAL NEUTRAL GAS PRESSURE. Cattanei, G. (Institut fuer Plasmaphysik, G.m.b.H. Garching (West Germany)). June 1965. 14p. Dep. mn.

The rate of the transport of radial momentum by the neutral gas from a plasma beam to the walls of the container (i.e., the anisotropy in the radial pressure of the neutral gas) was measured by observing the force exerted on the plate of a torsion balance. The force was plotted as a function of the gas pressure and of the magnetic field strength. (D.C.W.)

13908 (IPP-2/44) HELIOS-CONSIDERATIONS FOR THE PRODUCTION AND CONTAINMENT OF A HIGH-TEMPERATURE PLASMA. Boeschoten, F. (Institut fuer Plasmaphysik, G.m.b.H. Garching (West Germany)). Aug. 1965. 27p. Dep. mn.

The HELIOS project is discussed in detail. Electrons are to be heated by electron cyclotron resonance in a magnetic mirror field, after which the ions will be heated by ion cyclotron resonance. The hot plasma is to be stabilized with minimum-B fields and is to be subjected to adiabatic compression. The plasma properties and instabilities are considered in detail. (D.C.W.)

13909 (IPP-6/40) ERHALTUNGSGROESSEN UND MIKROSKOPISCHE STABILITAET DES PLASMAS. (Conservation Laws and Microscopic Stability of the Plasma). Voelk, H. (Institut fuer Plasmaphysik, G.m.b.H. Garching (West Germany)). Aug. 1965. 55p. Dep. mn.

The problem is discussed to sidestep the direct solution of the linearized Vlasov-equation and to treat the microscopic stability problem in employing constants of the motion. In the case of plane equilibria a number of conservation laws is derived in the electrostatic approximation. All these conserved quantities are quadratic expressions in the perturbations. They embrace especially the energy and momentum to second order. For some special equilibria the the positive-definiteness of the total energy yields a sufficient stability criterion, analogous to the situation in the hydromagnetic theory of static equilibria. A variational principle due to Dawson and Oberman is discussed, which attempts to give a sufficient criterion also in more general cases. It is demonstrated that this extremum principle, at least in the homogeneous case without magnetic field, is equivalent to the evaluation of marginal solutions of the Vlasov-equations, but does not lead to a minimum of the functional varied. Its numerical treatment leads back to the explicit solution of the dynamical equations. In this variational principle use is made of conservation of energy and momentum only. If one takes into account the entirety of the conservation laws derived, one can get a necessary and sufficient stability criterion in the sense of an energy principle. But it turns out, that one in general needs the continuum of conservation laws, except the fore mentioned special cases. So the practical usefulness of this constant of motion method seems doubtful. (auth)

13910 (JUL-297-MA) UEBER EIN ANFANGSWERT-PROBLEM FUER DIE STATIONAERE BOLTZMANN-VLASOV-GLEICHUNG. (An Initial Value Problem for the Stationary Boltzmann-Vlasov Equation). Neunzert, H. (Kernforschungsanlage, Juelich (West Germany). Zentral-institut fuer Angewandte Mathematik). Nov. 1965. 53p. Dep. mn.

The physical origin of the problem is given, and the requirements placed on functions of the equation are discussed. The principles used in the formal construction of the solution are given and are proved. The formal construction is demonstrated on the basis of an example. (J.S.R.)

13911 (JUL-336-PP) BESCHLEUNIGUNG EINES PLASMAS DURCH EINEN MAGNETISCHEN KOLBEN NACH DEM "FREE PARTICLE" MODELL. (Acceleration of a Plasma Through a Magnetic Bottle According to the Free-Particle Model). Bieger, W.; Graeff, P.; Tuczek, H. (Kernforschungsanlage, Juelich (West Germany)). Institut fuer Plasmaphysik). Nov. 1965. 15p. Dep. mn.

The acceleration of a plasma by means of a magnetic bottle was described by a one-dimensional free-particle model. The thermal energy of the plasma was assumed to be small with respect to the translation energy in the direction of motion, so that the initial state is given sufficiently by the statement of the line density and the translation energy at each position of the acceleration gap. (J.S.R.)

13912 (LGI-65/21 and App.) ON THE THEORY OF QUASISTATIONARY PLASMAS IN CONTACT WITH A WALL. Cavaliere, A.; Engelmann, F.; Onori, G. (Laboratorio Gas Ionizzati, Comitato Nazionale per l'Energia Nucleare, Frascati (Italy)). Aug. 1965. 135p. Dep. mn.

The problem of a quasistationary plasma in contact with a wall is treated by the boundary layer technique using a kinetic description for the motion of the ions. As typical examples, a low pressure discharge and a spherical electrostatic plasma probe are considered. The logical structure of the method is displayed, and a set of conditions is derived which insures a consistent matching between the plasma and sheath regions and generalizes the classical Bohm criterion. The universal character of the properties of the space charge dominated boundary layer is demonstrated, and it is shown that if a sheath is present, under very general conditions the electric field at the plasma edge as given by the boundary layer technique is formally infinite. Furthermore, it is discussed when a boundary layer has to appear. The general theory is applied to some simple models. (auth)

13913 (MATT-317) SCATTERING OF ELECTROMAGNETIC WAVES FROM "MARGINALLY STABLE" PLASMA WAVES. Arunasalam, V. (Princeton Univ., N. J. Plasma Physics Lab.). Dec. 1964. Contract AT(30-1)-1238. 9p. Dep. mn; CFSTI $1.00 cy, $0.50 mn.

From the energy density associated with any longitudinal plasma wave and the energy density of any longitudinal electrostatic density wave from classical electromagnetic theory, the structure factor appropriate to the boundary waves is found. A modification gives the expression for marginal stability. These results are compared with the corresponding results for acoustic ion plasma wave instability. Since, the plasma waves under study have an acoustic type dispersion relation, the cross section for the transfer of energy from the incident electromagnetic wave to the marginally stable plasma wave is found. It is seen that the cross sections for the scattering of electromagnetic waves from the density fluctuations associated with the marginally stable plasma waves are very much larger than the Thomson cross section. (J.F.P.)

13914 (MATT-318) SCATTERING ELECTROMAGNETIC WAVES FROM "MARGINALLY STABLE" ACOUSTIC ION PLASMA WAVES OF A BEAM-PLASMA SYSTEM. Arunasalam, V. (Princeton Univ., N. J. Plasma Physics Lab.). Dec. 1964. Contract AT(30-1)-1238. 20p. Dep. mn; CFSTI $1.00 cy, $0.50 mn.

The conditions for the existence of the low-frequency acoustic ion plasma wave instability in beam-plasma systems are discussed. It is shown that when the drift velocity of the "beam-electrons" is in the neighborhood of the phase velocity of the acoustic ion plasma mode, the beam-plasma system exhibits a behavior analogous to that found in phase-transitions. The cross-sections for the scattering of electromagnetic waves from "marginally-stable" acoustic ion plasma waves are shown to exhibit a very large increase in a form somewhat analogous to the critical opalescence for a liquid-gas phase transition. The earlier results for a current-carrying plasma are recovered by setting the "plasma-electron" density equal to zero. (auth)

13915 (MATT-402) MULTI-PROBE MEASUREMENTS OF FLUCTUATING AZIMUTHAL DENSITY VARIATIONS. Bol, K.; Prelec, K. (Princeton Univ., N. J. Plasma Physics Lab.). Dec. 1965. Contract AT(30-1)-1238. 22p. Dep. mn. CFSTI $1.00 cy, $0.50 mn.

The evolution of azimuthal density fluctuations in the Etude Stellarator was studied by surrounding the plasma column with a ring of probes. Very rapid changes in the amplitudes of large-scale perturbations were observed, indicating kink instabilities. (D.C.W.)

13916 (MATT-412) ROADBLOCKS IN THE PATH OF CONTROLLED FUSION. Bishop, A. S. (Princeton Univ., N. J. Plasma Physics Lab.). Jan. 1966. Contract AT(30-1)-1238. 30p. (CONF-650827-3). Dep. mn. CFSTI $2.00 cy, $0.50 mn.

From Western Electronics Show and Conference, San Francisco.

A survey of the various approaches to controlled fusion is presented. Some of the more important recent developments in the US program are outlined, together with the difficulties encountered in each approach. (D.C.W.)

13917 (NASA-TN-3250) BASIC STUDIES OF A LOW-DENSITY HALL CURRENT ION ACCELERATOR. Chubb, Donald L.; Seikel, George R. (National Aeronautics and Space Administration, Cleveland, Ohio. Lewis Research Center). Feb. 1966. 56p. CFSTI $3.00 cy, $0.50 mn.

An experimental and theoretical investigation of a low density annular Hall current ion accelerator operating with argon gas was carried out. The variation of electron temperature and number density, ion current density, and plasma potential through the accelerator was experimentally determined as a function of the magnetic field strength. Azimuthal electron Hall current was also measured. Experimentally determined values of the axial electron current density parallel to the applied electric field were much larger than those predicted by classical electron diffusion, and the ratio of the azimuthal Hall current to the axial current was much smaller than expected. As a result, it was concluded that an anomalous electron diffusion mechanism exists. The variation of the electric field could be reasonably predicted by an anomalous electron diffusion analysis that made use of the experimentally determined value of the Hall parameter (electron cyclotron frequency/electron collision frequency). The experimental results indicate that energy and momentum transfer to the accelerator walls are the primary loss mechanisms for the accelerator. (auth)

13918 (NASA-TN-D-3255) ERROR IN INDUCED ELECTRIC FIELD MODES UNDER STIX COIL RESULTING FROM ASSUMPTION OF ORTHOGONALITY OF NATURAL PLASMA MODES. Woollett, Richard R. (National Aeronautics and Space Administration, Cleveland, Ohio. Lewis Research Center). Feb. 1966. 30p. CFSTI $2.00 cy, $0.50 mn.

When the Bessel function representing the induced electric field in a plasma under a Stix coil is expanded in terms of the natural plasma modes, the coefficients of the expansion may be approximated by assuming that the eigenfunctions are orthogonal. However, the eigenfunctions are not orthogonal. When the orthogonality assumption is not used, there results an infinite system of equations involving an infinite set of unknowns. Kantorovich developed a technique that can be adapted to this problem. The technique produces both a deficient and an excessive value of the coefficient. Because the correct value lies between these two limits, the greatest error resulting from the orthogonality assumption can be obtained. In the cases tested it was found that the errors involved in determining the coefficients using the orthogonality assumption were less than 0.1 percent for the fundamental mode. (auth)

13919 (NP–15703) PROPAGATION AND DISPERSION OF HYDROMAGNETIC AND ION CYCLOTRON WAVES IN PLASMAS IMMERSED IN MAGNETIC FIELDS. Semi-annual Status Report No. 5, January 15, 1965–July 14, 1965. Dougal, Arwin A. (Texas Univ., Austin. Plasma Dynamics Research Lab.). July 15, 1965. 94p.

Separate abstracts were prepared for the three included papers. (M.O.W.)

For abstracts of individual papers see: 13920–13922.

13920 (NP–15703, pp 1-51) RESONANCES AND WAVES IN ONE-AND TWO-ION SPECIES PLASMAS SUBJECTED TO INTENSE MAGNETIC FIELDS. Kristiansen, Magne; Harris, Franklin C.; Dodge, Nathan B.; Melton, Jimmy G. (Texas Univ., Austin. Plasma Dynamics Research Lab.).

Plasma heating by excitation and absorption of ion cyclotron waves was successfully investigated experimentally. The effect of thermalizing the wave energy in a slowly decreasing magnetic field region was investigated from diamagnetic and r-f magnetic probe measurements, and r-f power absorption measurements. Emphasis was on diamagnetic probe measurements of the transverse plasma temperature along the plasma column for various experimental conditions. The experimental arrangement and instrumentation were further improved. Both the magnetic field capability and the vacuum system were expanded. The shock preheater was modified. Additional equipment for spectroscopic studies of plasma temperature and possible plasma impurities was added. A Faraday shield was placed under the r-f excitation coil. Theoretical considerations and design of laser diagnostic equipment for plasma density measurements are outlined. Interpretations of diamagnetic probe signals and techniques of magnetic field shaping are discussed. Transverse temperature measurements are reported for various B-fields, neutral gas pressures, and axial probe positions. Grounding the ends of the discharge tube in some cases led to plasma fluctuations. Transverse temperature measurements with r-f preionization demonstrate the generation, propagation and thermalization of ion cyclotron waves. The existence of an optimum density for coupling r-f power into ion cyclotron waves is indicated, in agreement with theoretical calculations. Collisional broadening of the resonance curve is observed as the neutral gas pressure is increased. Calculations indicate plasma densities as high as 5.7×10^{13} cm^{-3} and ion temperatures in the range of 2–20 ev. Spatial measurements of wave magnetic fields also verify the generation, propagation, and damping of the ion cyclotron waves in this experimental arrangement. (auth)

13921 (NP–15703, pp 52-63) SHOCK IONIZATION FOR ION-CYCLOTRON WAVE EXPERIMENT. Melton, Jimmy G.; Kristiansen, Magne; Harris, Franklin C. (Texas Univ., Austin. Plasma Dynamics Research Lab.).

Experimental data are presented for arc-driven ionizing shock waves. Shock velocities from 0.6 cm/μs to 2.5 cm/μs are produced by a conical shock tube operating in the 1 to 70 micron Hg pressure range with external magnetic fields from 0 to 9000 gauss. The effects of driving a shock through through a magnetic mirror are considered. Theoeretical estimates of temperature and ion density vs. shock velocity indicate that the minimum shock velocity for full ionization in the low pressure range is 6.0 cm/μs. A possible means of generating faster shock waves at low pressures using a coaxial electrode arrangement is discussed. An inexpensive high voltage vacuum feedthrough is described. (auth)

13922 (NP–15703, pp 64-81) PLASMA SHEATH DYNAMICS. Friedrich, Otto M. Jr.; Weigl, Frederic (Texas Univ., Austin. Plasma Dynamics Research Lab.).

Dynamic plasma sheaths in magnetoplasmas are investigated experimentally and analytically. A parallel plate accelerator with 6 cm wide × 8 cm long stainless steel electrodes spaced 3.4 cm apart, immersed in a several kilogauss multipole magnetic field is used to produce relatively flat 3 × 4 cm plasma sheaths in hydrogen, deuterium, and argon. In a second experimental geometry, cylindrical plasma sheaths with radial velocities of several times 10^4 m/sec are produced in an extremely high temperature, 5 cm ID, 20 cm long, theta pinch. Infrared maser and optical interferometry (Mach-Zehnder Interferometer) techniques employed to obtain quantitative space and time resolved electron densities are described. Based on a two-fluid model, the plasma variables and the electromagnetic field variables for the theta pinch are calculated on a high speed digital computer. A set of five partial differential equations for the electron energy, ion energy, momentum, mass conservation, and the electromagnetic fields is solved numerically. Lagrangian coordinates and an implicit integration method are employed. The calculated position of peak density vs. time is in agreement with measured values obtained from Kerr cell photographs. The calculated ion temperatures are higher than the calculated electron temperatures. Computer calculations show that the sign, as well as the magnitude, of the bias, magnetic field is very important during the initial pinch and subsequent radial oscillations of the plasma column. (auth)

13923 (TID–22419, pp 77-84) PLASMA PHYSICS. Brown, S. C.; Allis, W. P.; Bekefi, G.; (and others) (Massachusetts Inst. of Tech., Cambridge. Research Lab. of Electronics).

The time and spatial decay of pulsed P.I.G. discharges were studied. Results indicate that the electron density and temperature both decay initially by radial diffusion. After 100 to 200 μsec, electron-ion collisions become an

important cooling mechanism. The ion cyclotron experiment was modified so that it operates in high Q modes. A model which accounts for the majority of effects in these modes was developed. (J.R.D.)

13924 (TID–22419, pp 85-98) GASEOUS ELECTRONICS. Brown, S. C.; Allis, W. P.; Bekefi, G.; (and others) (Massachusetts Inst. of Tech., Cambridge. Research Lab. of Electronics).

The usefulness of operator methods for dealing with problems involving Vlasov's equation in its more general linearized form is examined. Emphasis is placed on applications of these methods to inhomogeneous bounded anisotropic plasmas. An evaluation is presented for the complex susceptance of resonance-probe-plasma systems in which sheath regions around conducting dipole spheres were regarded as vacuums and the surrounding plasmas extended to infinity. By using a computer, the solution for the susceptance was evaluated for several values of the parameters f and νc, where f is the ratio of the sheath cavity radius to the probe radius, and νc is the collision frequency normalized to plasma frequency. (J.R.D.)

13925 (TID–22419, pp 99-147) PLASMA ELECTRONICS. Haus, H. A.; Bers, A.; Getty, W. D.; (and others) (Massachusetts Inst. of Tech., Cambridge. Research Lab. of Electronics).

Results of a quantum-mechanical analysis of the interactions between acoustic phonons and electrons drifting along external magnetic fields are presented. The coupling between electrons and phonons is taken through the deformation potential. It is found that stimulated emission of phonons, with electrons making transitions between Landau levels, has a threshold magnetic field. An analysis of longitudinal interactions of electrons with phonons in magnetic fields is included. An analysis is also included concerning damping of instabilities arising in transelectromagnetic waves propagating along applied magnetic fields in plasmas with anisotropic electron velocity distributions. These instabilities are considered to arise from finite electron temperature along the magnetic field. Results of studies concerning instabilities of quasi-static waves propagating perpendicular to static uniform magnetic fields in infinite plasmas composed of stationary ions and electrons are presented. Research and development summaries are included concerning quasi-linear interactions of filamentary electron beams with plasma-filled waveguides, dispersion of hot-electron plasmas, nonadiabatic diffusion of electrons in toroidal geometries, interactions of particles with circularly polarized waves in plasmas, nonadiabatic magnetic traps, laser radiation Thompson-scattered by electron beams, and incoherent scattering of light from plasmas. (J.R.D.)

13926 (UCRL-16517) ON FINITE GYRO-RADIUS CORRECTIONS TO THE HYDROMAGNETIC EQUATIONS FOR A VLASOV PLASMA [Thesis]. Macmahon, Alan (Lawrence Radiation Lab., Univ. of California, Berkeley). Oct. 15, 1965. Contract W-7405-eng-48. 178p. Dep. mn. CFSTI $5.00 cy, $1.00 mn.

A systematic procedure for expanding velocity moments of the Vlasov equation in the mass-to-charge ratio is presented and its relation to the strong magnetic field expansion of the Vlasov equation and to the guiding center description of the particle motion is discussed. It is shown that the expansion of the Vlasov equation implies a condition on the form of the distribution function at the initial time. Scaling of these and Maxwell's equations is studied, and both the ordering scheme leading to ordinary hydromagnetics and the so-called "finite gyro-radius" (FGR) ordering are considered. A hydromagnetic description of a two-component plasma is easily found from the moment equations for the separate components. For the first of the above orderings FGR effects produce small corrections to ordinary hydromagnetics which are found through first order for an arbitrary plasma configuration. For FGR ordering, "finite gyro-radius" terms, which include second-order corrections to the pressure tensor, appear in even the lowest-order approximation to the moment equations. The corresponding modified hydromagnetic equations are derived and, for the special case of low plasma pressure and uniform magnetic field, previous results are recovered. Because of transport along the field lines, closed moment equations are not obtained in general for either ordering. In addition, for FGR ordering and non-uniform magnetic field, an analogous but independent closure problem arises because of transport across the field lines. For this reason applicability of the hydromagnetic equations for FGR ordering to finite-pressure systems is limited. Closed hydromagnetic equations are obtained, however, for low-frequency, finite-pressure interchange modes, and these equations are used to find finite-pressure modifications of the well known FGR stabilization of these modes. Closed equations are also obtained for the (finite-pressure) "firehose" instability and FGR corrections to the condition of marginal stability are found. A hydromagnetic description of finite-pressure "long-term" equilibria, and "minimum-B" configurations in particular, is also obtained. (auth)

13927 (UCRL–16557) USE OF THE BETHE-SALPETER EQUATION IN TRANSPORT THEORY AND THE DERIVATION OF A CONVERGENT KINETIC EQUATION FOR A CLASSICAL PLASMA [Thesis]. Gould, Harvey Allen (Lawrence Radiation Lab., Univ. of California, Berkeley). Nov. 23, 1965. Contract W-7405-eng-48. 161p. Dep. mn. CFSTI $5.00 cy, $1.00 mn.

The response of a normal many-body system to a weak external electric field is expressed in terms of the change in the one-particle distribution function. The basis of the treatment is the relation between the response and an appropriately defined two-particle Green's function. Making extensive use of the temperature-dependent diagram technique and the method of analytic continuation, a general transport equation valid for low frequencies and long wavelengths is derived. The derivation is based on a reordering of the perturbation expansion of the two-particle Green's function leading to the formulation of the temperature-dependent Bethe-Salpeter equation. Full advantage is taken of the analytic properties of G_2. The collision integral involves the imaginary part of the self-energy and various discontinuities of the kernel of the Bethe-Salpeter equation. The general transport equation is used to derive a kinetic equation for the electron gas not subject to the usual short-range divergence and is exact to first-order in the plasma parameter. The method is based on the direct analogy with the well known equilibrium theory of the electron gas and does not lead to a divergent equation of state. No arbitrary separations or cutoffs are necessary. The collision integral is a sum of three terms: a Lenard-Balescu integral involving the dynamically screened Coulomb potential, a Boltzmann term and a Fokker-Planck term both with the Debye shielded potential. (auth)

13928 (AD–625070) METHOD OF RETAINING AND ACCUMULATING HIGH TEMPERATURE PLASMA IN A TRAP. Lomnev, S. P.; Pereslavtsev, E. B.; Shatunov, V. M. Translation of Russian Patent 167260. Apr. 25, 1963. 4p. (FTD-TT–65-1168). CFSTI.

A method of retaining and accumulating hot plasma is proposed in which a dipole magnetic field that increases in time is used. The rate and magnitude of the increase of the field are determined by the parameters of the specific arrangement. (D.C.W.)

13929 (NP-tr–1340) INSTABILITY AND RELATED MACROSCOPIC EFFECTS IN TOROIDAL DISCHARGES. Kadomtsev, B. B.; Pogutse, O. P. (Institut Atomnoi Energii, Gosudarstvennyi Komitet po Ispol'zovaniyu Atomnoi Energii SSSR, Moscow). Translation of paper No. CN–21/127 presented at the Conference on Plasma Physics and Controlled Nuclear Fusion Research, Culham, England, September 6–10, 1965. 18p. (CTO/230). Dep. mn. CFSTI $1.00 cy, $0.50 mn. JCL $1.60 fs, $0.80 mf.

The various plasma instabilities in toroidal systems are analyzed on the basis of their macroscopic effects. The nonlinear convection of a plasma due to the instabilities is considered briefly, and the coefficients of diffusion and thermal conductivity are evaluated. (D.C.W.)

13930 (NP-tr-1343) CLOSED MINIMUM-B CONFIGURATIONS. Solovev, L. S.; Shafranov, V. D. (Institut Atomnoi Energii, Gosudarstvennyi Komitet po Ispol'zovaniyu Atomnoi Energii SSSR, Moscow). Translation of paper No. CN-21/133 presented at the Conference on Plasma Physics and Controlled Nuclear Fusion Research, Culham, England, September 6–10, 1965. 27p. (CTO/229). Dep. mn. CFSTI $2.00 cy, $0.80 mn. JCL $2.60 fs, $1.01 mf.

The possibility of producing closed minimum-B configurations by relatively simple means is studied. Homogeneous configurations with circular magnetic axes and with spatial magnetic axes are considered. (D.C.W.)

13931 (NP-tr-1348) OSCILLATIONS AND INSTABILITY OF A WEAKLY TURBULENT PLASMA. Vedenov, A. A.; Gordeev, A. V.; Rudakov, L. I. Translation of paper No. CN-21/155, presented to the Conference on Plasma Physics and Controlled Nuclear Fusion Research, Culham, England, September 6–10, 1965. 23p. (CTO/237). Dep. mn. CFSTI $1.00 cy, $0.50 mn. JCL $2.60 fs, $0.89 mf.

The possibility is discussed of describing effects associated with the interaction of collective oscillations of a plasma by means of a self-consistent system of equations: a kinetic equation for the distribution function of high-frequency waves (in six-dimensional coordinate- and wave-vector space) and equations describing the slow motion of a plasma under the action of high-frequency pressure. (M.O.W.)

13932 ON THE THEORY OF WAVE PROPAGATION IN A BOUNDED COMPRESSIBLE PLASMA. Wait, James R. (Inst. for Telecommunication Sciences and Aeronomy, Boulder). Can. J. Phys., 44: 293-302(Feb. 1966).

The influence of boundaries on wave propagation in a compressible plasma is considered. Although the models chosen are highly idealized, a number of interesting complexities arise that may be significant in actual bounded plasma configurations. For example, it is demonstrated that a perfectly conducting metallic boundary will support a surface wave in the plasma. However, if the boundary is not perfectly rigid, the surface wave will be attenuated even when the plasma is collisionless. Certain aspects of multiple reflections between two parallel boundaries are also treated. (auth)

13933 RADIAL HYDROMAGNETIC OSCILLATIONS OF A ROTATING PLASMA CYLINDER. Curzon, F. L. (Univ. of British Columbia, Vancouver). Can. J. Phys., 44: 433-5(Feb. 1966).

Rotation in the early stages can be resolved by observing the effect of the angular velocity on radial oscillation of the plasma cylinder. It should be possible to study angular rotation by observing radial hydromagnetic oscillations. By studying the damping of these oscillations, the viscosity of the plasma might be evaluated. (F.S.A.)

13934 STUDY OF A SYNTHESIS PLASMA BY AN EMISSIVE PROBE. Spiess, Gerard (Centre d'Etudes Nucleaires de Saclay, Gif-sur-Yvette, France). Compt. Rend., 261: 5362-5(Dec. 20, 1965). (In French).

A summary theory of a plane emissive probe, assumed infinite, is presented. The experimental characteristics obtained confirm this theory and permit the measurement of the plasma potential at ±0.1 v in cases where the interpretation of the characteristics of the Langmuir probe would be delicate. The perturbations caused to the plasma are shown to be negligible. (tr-auth)

13935 NON-COLLISIONAL DAMPINGS IN THE RESONANCE OF A HIGH-FREQUENCY PROBE. Rolland, Paul (Centre d'Etudes Nucleaires de Saclay, Gif-sur-Yvette, France). Compt. Rend., 261: 5366-9(Dec. 20, 1965). (In French).

The resonances of h-f and d-c currents are modified by two types of noncollisional damping due to the reflection of electrons in the sheath and to the time of transit of the electrons across the sheath. The model of Messiaen is corrected to take these phenomena into consideration. (tr-auth)

13936 STUDY OF SHOCK WAVES BY THE MICROWAVE TECHNIQUES. Nakai, Sadao; Yamanaka, Chiyoe (Osaka Univ.). Denki Gakkai Zasshi, 85: 289-98(Feb. 1965). (In Japanese).

A new method of the microwave measurement for plasma studies was developed, which is based on measurement of reflection, and it was applied to the study of electromagnetically driven shock waves. The microwave reflection coefficient was calculated from the sharply bounded plasma as a function of the electron density, collision frequency, and cyclotron frequency with an electrical digital computer (MADIC II-A) and vector charts were developed from the microwave reflection coefficient. From this calculation, it was shown that the reflection method is suitable and fairly accurate in the range of $100 > \eta > 1$, where $\eta = (\omega_p/\omega)^2$ and in the range of $\eta > 100$; the penetration depth is so small that the reflected microwave is not sensitive to the collision frequency of electrons in plasma. An automatic measuring apparatus was constructed for measuring the reflection coefficient. By applying the experimental vector patterns to the calculated chart, it is possible to read out the electron density and collision frequency of plasma under various conditions of magnetic fields. Results of preliminary measurements on shock waves generated in air and argon with a T-shaped shock tube are discussed. (TCO)

13937 HYSTERESIS PHENOMENON NEAR B_c IN THE POSITIVE COLUMN IN A MAGNETIC FIELD. Imazu, Shingo; Yano, Masaaki; Nakano, Yoshiei (Tokyo Inst. of Tech.). Denki Gakkai Zasshi, 85: 1439-43(Aug. 1965). (In Japanese).

Experiments are described in which measurements of E_z, the electric field, were made in the axial direction of a hot cathode helium-filled tube. Under some discharge conditions (radius x pressure < 1 cm mm Hg), hysteresis effects of the critical field B_c exist, above which the positive column is unstable. That is, there are two critical magnetic fields, B_{c1} and B_{c2}, which correspond to the critical points with increasing and decreasing B, respectively. This phenomenon was investigated. The results showed that, above B_c, the instability results in oscillations which lead to an increase in flux of charged particles striking the walls. Temperature of charged particles increases with increasing particle and energy losses. Since the boundary between plasma and wall sheath varies with the temperatures of charged particles, the plasma region in the tube decreases with increasing temperature. Then, E_z increases with decreasing plasma. According to the explanation of F. C. Hoh, the displacement ΔE, the electric field that increases taking account of sheath, makes "helical instability" develop easily. Therefore, with decreasing B, these instabilities are readily maintained by ΔE. Thus, a hysteresis effect in the curve represented by $B\text{-}E_z$ exists. Conditions for helical oscillations were determined taking into account the wall sheath, and these theoretical values were compared with experimental results. It is shown that this hysteresis effect can be explained by the effect on the development of helical oscillations. (BBB)

13938 DIFFUSION AND CONDUCTIVITY OF PLASMAS IN STRONG EXTERNAL FIELDS. Green, H. S.; Leipnik, R. B. (Univ. of Florida, Gainesville). Int. J. Eng. Sci., 3: 491-514(Oct. 1965).

Methods of studying the coefficients of diffusion and the electrical conductivity of a plasma based on Boltzmann's equation are discussed. The diffusion tensors of a plasma in strong external fields are derived from first principles. A pair of integro-differential equations, which are the first members of a chain analogous to Yvon's hierarchy, is obtained, together with the required boundary conditions and an approximation, called the disjunctive approximation, which makes the solution determinate. It is shown how the diffusion tensors can be calculated from the solution of these equations. A study is made of the influence of the external fields on the encounters between charged particles in a plasma. A generalization of Boltzmann's equation is

obtained, which takes into account many-body interactions in the plasma and the effect of the external field on the collision integral. Explicit expressions are obtained for the friction tensors, the diffusion tensors, and the electrical conductivity tensor, for a plasma subject to a strong external magnetic field. (BBB)

13939 NOBLE GAS PLASMA PRODUCED BY FISSION FRAGMENTS. Leffert, Charles B.; Rees, David B.; Jamerson, Frank E. (General Motors Corp., Warren, Mich.). J. Appl. Phys., 37: 133-42(Jan. 1966).

The generation of a plasma by fission-fragment ionization of noble gases is reported. The experimental data consist of steady-state current–voltage (I-V) characteristics obtained with ceramic–metal ionization tubes which were operated in the high neutron flux region of a nuclear reactor. The observed dependence of I on $V^{1/2}$ for applied potentials <100 v is shown to be consistent with the theory that the predominant charge loss in the plasma is volume recombination of diatomic ions and electrons. The ion generation rate is calculated from the energy loss rate of the fission fragments in the gas and I-V characteristics for the noble gases are computed. These characteristics, which do not contain any adjustable parameters, are in agreement with the experimental data within ±10%. Data are presented for neon, argon, xenon, and neon–argon ($Ar/Ne = 10^{-3}$) for gas pressures in the range 30 to 400 torr. Typically, for a gas pressure of 240 torr and a neutron flux of 10^{13} $cm^{-2} \cdot sec^{-1}$, the computed values for ion generation rate and electron density in the pure gases were $\approx 5 \times 10^{16}$ $cm^{-3} \cdot sec^{-1}$ and $\approx 3 \times 10^{11}$ cm^{-3}, respectively. For the neon–argon mixture, the electron density was estimated to be $\approx 7 \times 10^{11}$ cm^{-3}. This higher density arises not only because of additional production of Ar^+ ions via neon metastables encountering argon neutrals, but also because of a reduction in the formation rate of Ar_2^+ ions (followed promptly by dissociative recombination). The point is that $Ar^+ + Ar + Ne \rightarrow Ar_2^+$ is unlikely compared with $Ne^+ + 2Ne \rightarrow Ne_2^+$, for a small argon admixture. (auth)

13940 LOW-FREQUENCY IMPEDANCE CHARACTERISTICS OF A LANGMUIR PROBE IN A PLASMA. Crawford, F. W.; Grard, R. (Stanford Univ., Calif.). J. Appl. Phys., 37: 180-3(Jan. 1966).

Measurement of the low-frequency impedance of a Langmuir probe in a plasma can give the local electron density and temperature. Such diagnostic methods have been employed in ionospheric probing, but the interpretation of the results based on simplified theory has not been entirely satisfactory. Laboratory plasma studies designed to investigate the validity of the simplified theory are described. Good agreement is obtained between results obtained by two different impedance techniques and conventional Langmuir probe data reduction. It is concluded that the methods could provide additional methods of measurement in laboratory plasmas, with some inherent advantages, but that a more detailed theory and extensive experimental verification are required before they can be applied with confidence to more complicated conditions in the ionosphere. (auth)

13941 EFFECT OF MAGNETIC FIELD ON RESONANCES OF SURFACE WAVES PROPAGATING ALONG A CYLINDRICAL PLASMA COLUMN. Akao, Yasuo; Ida, Yoshio (Nagoya Univ., Japan). J. Appl. Phys., 37: 290-4(Jan. 1966).

The effect of axial magnetic field on the resonances of surface waves propagating along a cylindrical plasma is examined. When the magnetic field is increased and the exciting frequency maintained constant, the resonance peaks in the symmetric mode are shifted towards the lower discharge current side whereas the peaks in the dipolar mode split into two peaks with increasing separations. A method for determining plasma density by use of surface wave resonances is thus extended to the case of magnetoplasma columns. (auth)

13942 OPTICAL FREQUENCY PLASMA RESONANCE IN GASES. Minck, R. W.; Rado, W. G. (Ford Motor Co., Dearborn, Mich.). J. Appl. Phys., 37: 355-8(Jan. 1966).

An intense optical beam was reflected backwards from a laser-induced spark in argon and nitrogen gas at high pressures. The reflected beam was about 10% as intense, diverged with a comparable angle, and had the same frequency (to within about 0.01 cm^{-1}) as the incident beam. By simultaneously focusing a weak second harmonic beam onto the discharge, the reflectivity at the higher frequency was measured. One percent of the incident harmonic beam was reflected in a nearly collimated beam, and with no apparent frequency shift (less than 0.05 cm^{-1}). The proposed model is that a stationary region having very high electron density ($n_e \approx 2 \times 10^{21}$ electrons/cm^3) is created in the focal volume and exhibits plasma resonance at the laser frequency. The resonance would appear quite damped due to the high collision rate. Experiments were performed which support the hypothesis and discriminate against several other possible explanations such as reflection from the mismatch of index of refraction at the shock front, stimulated Brillouin scattering, and stimulated plasma-wave scattering. (auth)

13943 ANOMALOUS DIFFUSION AND INSTABILITIES OF AN ARGON PLASMA IN A STRONG MAGNETIC FIELD. Chen, Che Jen (California Inst. of Tech., Pasadena). J. Appl. Phys., 37: 419-25(Jan. 1966).

The electron density decay with time in an argon discharge tube energized with a capacitor bank of energy up to 3000 J in a magnetic field up to 30 kG parallel to the axis of the tube is measured by using electron continuum intensity, ion current probe, and microwave techniques. The electron temperature decay is obtained by the spectral line intensity ratio method. The oscillation or instability in the plasma is monitored with electrostatic and magnetic probes. The coefficient of ambipolar diffusion is evaluated from the decay data obtained in the diffusion dominated region. The data thus obtained indicate that the coefficient of ambipolar diffusion agrees with the prediction of the collision theory up to a critical magnetic field of about 1000 G. Beyond 1000 G, the onset of oscillations is detected, and the coefficient of diffusion is much higher than the collision theory prediction. For B > 1000 G, the coefficient of diffusion varies as B^{-1}, and the absolute values are quite close to Bohm's. It is thought that the mechanism responsible for the anomalous diffusion is the onset of instabilities in the plasma, ion oscillations dominating at low magnetic fields, and the universal drift instability at high magnetic fields. (auth)

13944 POSITIVE COLUMN STRIATIONS IN A MAGNETIC FIELD. McNichols, J. L.; Cory, J. S. (Douglas Aircraft Co., Inc., Santa Monica, Calif.). J. Appl. Phys., 37: 433-4(Jan. 1966).

Narrow, stable, two-dimensional striations were observed in the positive column of a diffuse-mode discharge in a 95% He–5% H_2 mixture in a uniform magnetic field; pressures ranged from 5 to 20 torr, total discharge current from 50 to 200 mamp, and magnetic field strength from 300 to 1100 G. A model for interpreting the striation curvature is proposed, in which the thin striation curve is bounded by curves of constant electrostatic potential. The agreement between observed striation curvature and results of computer calculations of the potential curvature and the reasonable electron collision times predicted tend to confirm the model. (M.J.T.)

13945 SURFACE AND INTERFACE WAVES IN PLASMA GAPS. Davis, C. (RCA Labs., Princeton, N. J.); Tamir, T. J. Appl. Phys., 37: 461-2(Jan. 1966).

The waveguiding properties of the boundary interface produced by a gap in a plasma medium are examined. It is found that interface waves tightly bound to the boundary may occur; some of these waves show backward-wave characteristics which may be responsible for plasma instabilities. These backward waves occur when a small gap is associated with a thick plasma. (M.J.T.)

13946 RESONANT HEATING OF A PLASMA BY A HIGH-FREQUENCY FIELD. Chechkin, V. V.; Vasil'ev, M. P.; Grigor'eva, L. I.; Longinov, A. V.; Smerdov, B. I. JETP Lett. (USSR)(Engl. Transl.), 2: 260-2(Nov. 1, 1965).

Translated from Zh. Eksp. Teor. Fiz., Pis'ma Redakt., 2: 418-22(Nov. 1, 1965).

The preliminary results of experiments on heating of a dense hydrogen (or helium) plasma with powerful h-f pulses under conditions in which a fast magnetic-sound wave is resonantly excited in the plasma are presented. The temperature calculated from the energy balance under the assumption that the entire energy absorbed by the plasma goes into its heating is in good agreement with the experimental data. (G.O.Y.)

13947 INFLUENCE OF THE MIRROR RATIO ON PLASMA HEATING BY AN ELECTRON BEAM IN A PROBKOTRON. Blinov, P. I.; Zakatov, L. P.; Plakhov, A. G.; Chikin, R. V.; Shapkin, V. V. JETP Lett. (USSR) (Engl. Transl.), 2: 264-6(Nov. 1, 1965).

Translated from Zh. Eksp. Teor. Fiz., Pis'ma Redatk., 2: 426-30(Nov. 1, 1965).

The interaction between an electron beam and a highly ionized plasma was investigated by simultaneously injecting the plasma and the electron beam into a trap with magnetic mirrors. It was found that the efficiency with which the plasma electrons are heated by the beam depends substantially on the mirror ratio. (D.C.W.)

13948 PLASMA HEATING BY A STOCHASTIC FIELD. Shapiro, V. D. (Physico-technical Inst., Academy of Sciences, Ukrainian SSR). JETP Lett. (USSR) (Engl. Transl.), 2: 291-4(Nov. 15, 1965).

Translated from Zh. Eksp. Teor. Fiz., Pis'ma Redakt., 2: 469-73(Nov. 15, 1965).

The acceleration of plasma particles to high energies is treated as a particular case of interaction between a plasma and a stochastic field, the harmonic of which have a finite correlation time. The case of a circularly polarized electromagnetic wave propagating along an external magnetic field is considered. (D.C.W.)

13949 INVESTIGATIONS ON THE OCCURRENCE OF SELF-LUMINESENCE COLLISION FRONTS IN ELECTROMAGNETICALLY OPERATING SHOCK TUBES. Hermel, A.; Seliger, K. Monatsber. Deut. Akad. Wiss. Berlin, 7: 287-96(1965). (In German).

At Mach numbers of approximately 16 in Ar and between 13 and 16 in He a self-luminating collision front from the discharge plasma front is released in the electromagnetically operating T tube or in a shock tube that operates with an electrodeless ring discharge. Whereas the self-luminating collision front is flat, the following discharge plasma front shows sharp irregularities. Time spectroscopic pictures show that the radiation behind the collision front arises from impurities from the walls. The Mach number at which the resolution of the collision front occurs is independent of the type of generation of the discharge plasma (T tube or electrodless discharge) and of the special electrical parameters and the tube diameter. (tr-auth)

13950 LONGITUDINAL PLASMA WAVES AND LANDAU DAMPING. Hopman, H. J. (F.O.M.-Laboratorium voor Massascheiding, Amsterdam). Ned. Tijdschr. Natuur., 31: 266-85(Aug. 1965). (In Dutch).

A representation is given of plasma oscillations in a plasma without thermal motion, and then the alterations occurring at a definite temperature are shown. A derivation of the Landau damping is given. The investigation performed by Wong and Motley to test the theory is described. (J.S.R.)

13951 A SPECTROSCOPIC INVESTIGATION OF TWO BEAM INSTABILITY. Kennedy, W. T.; Emeleus, K. G. (Queen's Univ., Belfast). Phys. Lett., 20: 165-6(Feb. 1, 1966).

Probe and phenomenological studies of turbulent instability of counter-streaming electron beams in a low pressure plasma were extended by study of the optical spectra, using lines with high excitation potentials to show the location of fast electrons. (auth)

13952 DISAPPEARANCE OF THE CHARGE CARRIERS IN A PLASMA MOVING IN AN ELECTRIC FIELD. Musin, A. K.; Tyulina, M. A. (All-Union Electrotechnical Inst., USSR). Teplofiz. Vysok. Temp., 3: 501-9(July-Aug. 1965). (In Russian).

The formation and the disintegration of space charges during the passage of an electric current through a stream of ionized gas moving in a transverse electric field are studied. In a quasineutral plasma in an electric field, the charge carriers can disappear by recombination within the volume and on the walls, and also during the passage of an electric current through the plasma. If the electrodes are sufficiently long, the charged component of the plasma finally disappears, since the electrons in the plasma move to the anode, and the positive ions to the cathode. Experimental determinations were made of the volt-ampere characteristics of a nonselfsustaining current in a disintegrating plasma, and a formula is derived for the rate of disappearance of the charge carriers. This formula is valid only under conditions of mobility and in the absence or disappearance of the charged particles due to ambipolar diffusion and of recombination within the volume. These conditions are met only in a sufficiently weakly ionized plasma. (ATD)

13953 USE OF EMISSION SPECTRA OF THE COPPER ATOM FOR DIAGNOSTICS OF A PLASMA. Bakanovich, G. I.; Grechikhin, L. I. (Inst. of Physics, Academy of Sciences, USSR). Teplofiz. Vysok. Temp., 3: 520-3(July-Aug. 1965). (In Russian).

Since copper pairs formed by erosion of electrodes are present in all types of plasma apparatus, work was carried out on selection of the corresponding spectral lines, fixing their basic constants (transition probability and Stark and van der Waals constants), evaluating the effect of various factors on the width of the selected lines, and explaining errors in the measurement of temperature and concentration of the charged particles. The experiments were carried out with a direct current arc (8 amp) between copper or brass electrodes under water. The temperature of the arc was determined from two pairs of copper lines: 5105.5 : 5153.2 Å and 5105.5 : 4530.8 Å. A value of $(1.3 \pm 0.3)\ 10^{16}\ cm^{-3}$ was found for the concentration of charged particles in a plasma in a direct current arc between copper electrodes under water. The concentration of charged particles increased compared to the same arc in the atmosphere, for which a value of $10^{15}\ cm^{-3}$ is given. The temperature rises to approximately 1500°K. (ATD)

13954 EXPERIMENTAL INVESTIGATION OF ELECTRIC CONDUCTIVITY IN A STREAM OF ARGON CONTAINING POTASSIUM OXIDE. Maslennikov, N. M.; Germanyuk, V. N. (All-Union Electrotechnical Inst., USSR). Teplofiz. Vysok. Temp., 3: 524-9(July-Aug. 1965). (In Russian).

The effect of discharge conditions, temperature, cathode, material, and parameters of gas flow on the electric conductivity of the plasma space as a whole was studied. Argon was heated to the required temperature and fed into the mixing chamber, and a mixture of argon and potassium oxide was fed into the same chamber. The walls of the mixing chamber were cooled with water, and a metallic screen prevented condensation of the potassium oxide. The gas then entered the measuring section through rectangular openings. The material of the heated electrodes was molybdenum, tantalum, and tungsten, with a thickness of 0.1 to 0.2 mm. Gas feed was 2 grams/sec, and the flow rate between electrodes varied from 20 to 40 m/sec, depending on gas temperature. Experimental results showed that, with a nonselfsustaining discharge at a gas temperature of 2500 to 3000°K, the measured electric conductivity of the space was less than the electric conductivity of the space calculated with respect to the equilibrium conductivity of the plasma and was limited by emissions from the cathode. Under conditions of a nonselfsustaining discharge, at a gas temperature of 1800°K and a potassium oxide temperature greater than 2570°K, measurements of electric conductivity were hundreds of times greater than the electric conductivity of the space calculated with respect to the equilibrium electric conductivity of the plasma. (ATD)

13955 EXPERIMENTAL INVESTIGATION OF THE CONTINUOUS SPECTRUM OF AN ARGON PLASMA. Asinovskii, E. I.; Batenin, V. M. (Research Inst. for High Temperatures, USSR). Teplofiz. Vysok. Temp., 3: 530-5(July-Aug. 1965). (In Russian).

An experimental investigation was performed of the continuous spectrum of an argon plasma at atmospheric pressure, temperatures of 10,000 to 15,000°K, and wavelengths of 2500 to 7500 Å. The experimental unit used an electric arc operating at atmospheric pressure and stabilized by cooled copper walls. The coefficient of continous irradiation was measured by comparing the spectral brightness of the plasma source with a standard. The experimental data were compared with the Biberman-Norman theory of the continous spectrum of low-temperature plasma. A relation was established between the displacement of the threshold of photoionization in the plasma and the brightness of the continuum, and the photoionization cross section from the 4s level was evaluated. (ATD)

13956 DERIVATION OF A BALANCE EQUATION FOR A NONEQUILIBRIUM PLASMA. Ul'yanov, K. N. (All-Union Electrotechnical Inst., USSR). Teplofiz. Vysok. Temp., 3: 536-46(July-Aug. 1965). (In Russian).

An attempt is made to derive a mathematical formulation of the state of a plasma when thermodynamic equilibrium is not present. The required balance equations are obtained directly from the kinetic equations, taking into account deviation from thermodynamic equilibrium due to nonequilibrium conditions in the radiation field. The following equations are successively derived: a kinetic equation for electrons, a balance equation for free electrons, a balance equation for the energy of the electrons, and a kinetic equation for heavy particles. The balance equations for the particles and the energies obtained from the kinetic equations make it possible to calculate the changes with time of the parameters of the plasma, if the function of the electron velocity distribution is known. Thus, the problem reduces to the simultaneous solution of the balance equations and the kinetic equation for the electrons, into which the concentrations of the atoms and the electrons enter as parameters. However, for solution of the balance equations, just as for solution of the kinetic equation, the dependence of the section on the energies of the initial and final states must be known. (ATD)

13957 COLLISION INTEGRALS FOR THE LITHIUM–HYDROGEN SYSTEM. VISCOSITY OF MIXTURES OF LITHIUM–HYDROGEN. Belov, V. A.; Klyuchnikov, N. I. (High Temperature Research Inst., USSR). Teplofiz. Vysok. Temp., 3: 645-8(July-Aug. 1965). (In Russian).

In the calculation of the kinetic coefficients of rarefied gases, use is made of collision integrals $\Omega_{ji}^{(l,s)}$. Calculations are given of the integrals $\Omega(2,2)_{Li-H}$, $\Omega(2,2)_{Li-Li}$, $\Omega(2,2)_{H-H}$, $\Omega(1,1)_{H-H^+}$, $\Omega(2,2)_{H-H^+}$, and the viscosity of a weakly ionized plasma in the temperature interval 1000 to 10,000°K, and at pressures of 1, 10, 10^2, 10^5 newtons/m^2. Calculations were also made for mixtures of lithium and hydrogen based on the obtained experimental data. In the high temperature regions from 3000 to 8000 and 9000 to 10,000°K, where the mixture is almost binary, the error is estimated at 50%. These results are completely suitable for use. In the temperature intervals 1000 to 3000 and 8000 to 9000°K, the composition changes very sharply, and it is very difficult to calculate the viscosity accurately, even if accurately calculated collision integrals are available. These results illustrate the general course of the viscosity curve in these temperature intervals, and the errors here can be very substantial. (ATD)

13958 RADIATION BY A UNIFORMLY ROTATING LINE CHARGE IN A PLASMA [Thesis]. Gianzero, Stanley C. Jr. Brooklyn, N. Y., Polytechnic Inst. of Brooklyn, 1965. 78p.

A theoretical investigation is conducted for the radiation produced by a linear distribution of electric charge executing circular motion both inside and outside a cylindrical plasma column. The analysis includes the effects of compressibility and anisotropy of the plasma upon the radiation characteristics of the charge distribution. In the incompressible isotropic case, a dipole resonance phenomenon is exhibited for the first harmonic of the angular frequency of rotation of the charge when the charge moves at nonrelativistic velocities. If the charge moves at extremely small velocities, the resonance becomes a singularity. The influence of compressibility upon these radiation characteristics is discussed and is shown to be negligible. In the case of the presence of a magnetic field, i.e., for an anisotropic plasma, the dipole resonance is shifted. Moreover, a multipole resonance is possible for a sufficiently higher order harmonic. Furthermore, in a frequency range just above this multipole resonance, Čerenkov radiation contributes to the existent bremsstrahlung radiation for a single harmonic in the neighborhood of the singularity of the index of refraction. Thereafter, the radiation contribution of the remaining harmonics is negligible. (Dissertation Abstr.)

13959 THE HELICAL INSTABILITY PRODUCED IN GASEOUS MAGNETOPLASMAS BY THE GYRO-INTERACTION OF MICROWAVES [Thesis]. Cherrington, Blake Edward. Urbana, Ill., Univ. of Illinois. 181p.

The non-uniform absorption of gyro-resonant microwave energy by an electron gas is used to produce the helical instability in gaseous magnetoplasmas. This helical instability is examined both theoretically and experimentally. Stability criteria for the existence of the helix and the dependence of the properties of the helix on the plasma parameters are derived from the two-fluid magnetohydrodynamic equations for electrons and ions. The experimental examination of the instability is accomplished by the development of a suitable diagnostic procedure using low power (~50 microwatt), nonresonant microwave sensing signals. The detailed examination of the properties of the helical instability verifies the theoretical predictions. Where it has been possible to measure the properties of the plasma discharge exactly, such as helix rotational frequency and discharge tube radius, excellent quantitative agreement between theory and experiment is found. Where it has only been possible to estimate the plasma parameters, such as electron temperature and longitudinal gradients, good qualitative agreement between theory and experiment is found. (Dissertation Abstr.)

13960 NONLINEAR MAGNETOPLASMADYNAMICS [Thesis]. Sandler, Melvin. Brooklyn, N. Y., Polytechnic Inst. of Brooklyn, 1965. 98p.

A number of devices involving magnetoplasma interactions are studied with the aid of a one-dimensional model. Analytic solutions to limiting cases provide insight and aid in the formulation of a general numerical technique. A study is made of the stability of the resulting finite difference scheme and a viewpoint is presented for choosing computation schemes in complex problems. The one-dimensional model consists of a plasma of finite extent with crossed electric and magnetic fields perpendicular to the direction of flow. Stress is placed on the study of the generation of electric pulses, plasma acceleration, and plasma compression. The limiting cases considered include the incompressible fluid, steady flow and large disturbance to steady flow, and infinite electrical conductivity. A detailed study of an electromechanical pulse generator, which illustrates the effects of load and plasma on the pulse shape, is included. The steady flow solutions exhibit motoring, generating, and braking phenomena. In one case a closed form solution to this nonlinear problem is obtained. In addition an approximate solution of closed form clearly depicts the development of a shock wave from a large disturbance to the steady flow. The numerical technique consists of breaking the plasma into a set of slabs of constant mass. This simplifies the application of boundary conditions to the moving boundaries. The stability problem in the resulting finite difference

scheme is reduced to the solution for the roots of a complex polynomial. An approximate solution for the roots and subsequent higher order corrections enable one to choose a scheme such that the roots fall within a circle of convergence. Once the proper finite difference scheme has been established, the resulting numerical solutions are compared with the analytic solutions to the limiting cases. Effects such as compressibility and conductivity are made evident. (Dissertation Abstr.)

13961 VZAIMODEISTVIE PUCHKOV ZARYAZHENNYKH CHASTITS S PLAZMOI. (Charged Particle Beam Interactions with Plasma). Sinel'nikov, K. D. (ed.). Kiev, Naukova Dumka, 1965. 275p.

Twenty-eight articles are included on the results of experimental and theoretical studies of the interactions of charged-particle beams with plasma, excitation of plasma oscillations by electron and ion beams, instabilities arising from plasma-beam interactions, excitation and propagation of electromagnetic and acoustic waves, plasma waveguides, plasma in magnetic fields, acceleration in plasma, and gas discharges. (M.J.T.)

13962 IMPROVEMENTS IN OR RELATING TO METHODS OF HEATING IONS IN A PLASMA. Hamberger, Sydney Maxwell (to United Kingdom Atomic Energy Authority). British Patent 1,014,382. Dec. 22, 1965. Filed Aug. 24, 1962.

A method for heating ions in a plasma contained by a magnetic field and having an ion cyclotron frequency consists of subjecting the plasma to two radio frequency electromagnetic waves each of a frequency high enough to penetrate the plasma effectively and differing by a frequency that resonates with the ion cyclotron frequency. The apparatus for carrying out the method is described in detail. (B.L.M.)

13963 PLASMA ACCELERATOR. Gorowitz, Bernard; Park, Elkins; Gloersen, Per (to General Electric Co.). U. S. Patent 3,221,212. Nov. 30, 1965. Filed Oct. 27, 1961.

A device is described for controlling the time of occurrence and the duration of a plasma discharge without the necessity of controlling the gas flow correspondingly and without the necessity of switching the high-power source required to produce a high energy electric discharge through the plasma. Preliminary ionizing control means are provided in the vicinity of the gas stream before its entrance into the region of the main electric field, which is made insufficient in magnitude to initiate ionization. (B.L.M.)

Shielding

Refer also to abstract 14180.

13964 (ORNL-3746) A GENERAL CATEGORY OF SOLUBLE NUCLEON-MESON CASCADE EQUATIONS. Alsmiller, F. S. (Oak Ridge National Lab., Tenn.). Dec. 1965. Contract W-7405-eng-26. 36p. Dep. mn; CFSTI $2.00 cy, $0.50 mn.

The set of coupled equations describing a one-dimensional nucleon-meson cascade fed by arbitrary space and energy-dependent sources is reduced to quadrature under the following assumptions: charged-particle stopping, meson decay, and deviation of the nonelastic collision cross sections from a single constant value are neglected for the secondary particles produced in the cascade; the secondary particle differential production spectra, $F_{jk}(E,E')$, which give the number per unit energy, E, of j-type particles produced in a nonelastic collision of a k-type particle of energy E' with a target nucleus are taken to be of the general form: $F_{jk}(E,E') = [g_k(E')/g_j(E)]\{K_j(E,E') + h(E)k(E')\delta_{jk}\}$ with the restriction, $\Sigma_j K_j(E,E') + h(E)k(E') = H(E) + L(E')$. The functions $g_j(E)$, $H(E)$, and $L(E')$ are arbitrary. Examples are given. Solutions are given for a variety of assumptions concerning the form of the primary particle spectra. (auth)

13965 (ORNL-RSIC-11) SPACE AND ACCELERATOR SHIELDING. BIBLIOGRAPHY, SUBJECT INDEX, AND AUTHOR INDEX OF THE LITERATURE EXAMINED BY THE RADIATION SHIELDING INFORMATION CENTER. Gurney, J. (ed.) (Oak Ridge National Lab., Tenn.). Nov. 1965. Contract W-7405-eng-26. 69p. Dep. ORNL Free.

The bibliography contains only articles of the review or summary type and deals with the primary areas of space radiation sources, cross section data, particle transport, and shielding. (M.O.W.)

13966 (UNC-5140) GAMMA SPECTRAL DATA FOR SHIELDING AND HEATING CALCULATIONS. Summary Report. Celnik, J.; Spielberg, D. (United Nuclear Corp., Elmsford, N. Y.). Nov. 30, 1965. Contract NAS3-2600. 65p. (NASA-CR-54794).

Spectra of gamma rays following neutron absorption and inelastic-scattering events in H, Be, C, O, Al, Cr, Fe, Ni, Zr, natural W and the W isotopes, ^{235}U, and ^{238}U are tabulated. The gamma thermal capture spectra for Cd and Sm are presented. A detailed study of the prompt and delayed fission gammas (both intensities and time variations) is also given. Descriptions are given of the sources of information and the calculations performed. In addition, an evaluation of reliability of the data is made. (auth)

13967 MEASURE OF THE COEFFICIENT OF ABSORPTION OF ELECTRONS ACCELERATED BY VOLTAGES BETWEEN 100 AND 1200 KILOVOLTS. Dupouy, Gaston; Perrier, Frantz; Uyede, Ryozi; Ayroles, Rene; Mazel, Annie (C.N.R.S., Toulouse). J. Microscop., 4: 429-50 (Aug. 1965). (In French).

The curve giving the intensity of the transmitted beam, I, against the thickness, t, of an MgO crystal varies periodically. This curve is tangent to two others, the difference of which, I_t, is given by $I_t = I_0 \exp(-\mu_0 t)$, in which I_0 is the incident beam intensity and μ_0 is the mean absorption coefficient. The values for μ_0 at various voltages are: 100 kv, 993 $Å^{-1}$; 300 kv, 1509 $Å^{-1}$; 500 kv, 2076 $Å^{-1}$; 750 kv, 2526 $Å^{-1}$; 1000 kv, 2663 $Å^{-1}$; 1200 kv, 2741 $Å^{-1}$. These figures are mean values for dark and light fields and have standard deviations of 5–10%. They were determined by determining I_t/I_0 from darkening of photographic plates on electron impact for a crystal thickness t, while a constant effective aperture was maintained. Results are in slight disagreement with theory. (BBB)

13968 THEORY OF MULTIPLE SCATTERING. [PART] II. Dolginov, A. Z.; Gnedin, Yu. N. (Ioffe Inst. of Physics and Tech., Leningrad). Nucl. Phys., 77: 202-14(1966).

The problem of multiple scattering of particles or quanta on a plane slab of matter is considered in the case of anisotropic scattering at a single center of force. The solution of the transport equation in explicit analytical form is obtained for the cases when the expansion of the cross section in Legendre polynomials has a finite number of terms and when the cross section has a sharp maximum at small angles (Coulomb scattering). (auth)

13969 THE CHANGE OF RELATIVE LINEAR ENERGY TRANSFER WITH THE PENETRATION DEPTH OF 14-Mev ELECTRONS IN PLEXIGLASS. Hagemann, G. (Univ., Marburg, Ger.). Z. Angew. Phys., 20: 83-5 (Nov. 1965). (In German).

Utilizing the Cherenkov effect the electron density distribution in the beam axis of an electron beam in lucite for electrons with energies between 631 kev and 13.8 Mev was measured. By means of some calculated corrections the energy range in the lower boundary was extended to 10 kev. The energy dose distribution was then divided by the corrected electron density distribution yielding the distribution of the relative linear energy transfer. The maximum value of 4.2 ± 0.3 was in fairly good agreement with the theoretical value of 4.6. (auth)

Solid State Physics

See also CHEMISTRY — Inorganic and Physical Chemistry
METALS, CERAMICS, AND OTHER MATERIALS — Properties and Structure

Refer also to abstracts 13025, 13130, 13423, and 13788.

13970 (AD-611432, pp 135-47) A PARAMAGNETIC RESONANCE STUDY OF NITROGEN ATOMS TRAPPED IN X-IRRADIATED ALKALI AZIDES. Carlson, Frederick F. (Army Engineer Research and Development Labs., Fort Belvoir, Va.).

The nitrogen atoms in NaN_3, KN_3, RbN_3, and CsN_3 were studied by EPR spectroscopy. The experimental methods and results are discussed. A brief review of the current theory is presented. It is noted that nitrogen atoms in the alkali azides provide an excellent system in which to study the spectroscopy of S state atoms. (M.O.W.)

13971 (AD-625834) STACKING FAULTS. Final Report. Adler, R. P. I. (Martin Co., Orlando, Fla.). Dec. 1965. Contract Nonr-3706(00). 14p. (OR-6891). CFSTI $1.00 cy, $0.50 mn.

All original experimental, analytical, and theoretical work performed on stacking faults in crystalline materials are summarized. Highlights of the project are listed and references are made to publications in the open literature, abstracts, dicussions, and invited presentation where details are elaborated. Experimental work was primarily performed using x-ray diffraction and electron microscopy techniques. Materials investigated included 70:30 brass, Cu-6.6 atomic percent Si, niobium, tantalum, cerium, α-uranium, carbon, and boron. Theoretical and analytical studies were also performed to identify the contribution of faults, twins, and thin platelets to diffraction phenomena and to standarize the terminology in indexing the hexagonal system. (auth)

13972 (IA-1056) PARAMAGNETIC RESONANCE SPECTRUM OF Co^{1+} IN SINGLE CRYSTALS OF CALCIUM OXIDE. Low, W.; Suss, J. T. (Israel Atomic Energy Commission, Yavne. Soreq Nuclear Research Center). Oct. 1965. 7p. Dep. mn.

The paramagnetic resonance spectrum of Co^+ in CaO was investigated. Co^+ was obtained by γ irradiation of crystals containing Co^{2+}. The resonance results are: $A = (31.6 \pm 0.3) \times 10^{-4} cm^{-1}$; $g = 2.2743 \pm 0.0008$ at 20°K and $g = 2.2756 \pm 0.0008$ at 12°K. A comparison of effective core polarization between Co^+ in MgO, Co^+ in CaO and Ni^{2+} in MgO is given. (auth)

13973 (NYO-3033-1) RADIATION EFFECTS IN SOLIDS. Report for the Period, April 1, 1965–March 31, 1966. (Carnegie Inst. of Tech., Pittsburgh., Pa. Dept. of Physics). Jan. 28, 1966. Contract AT(30-1)-3033. 20p. Dep. mn. CFSTI $1.00 cy, $0.50 mn.

The types and properties of defects produced in alkali halide crystals by x radiation were investigated. The thermal stability of defects was studied, and an attempt was made to observe optical transitions associated with interstitials. The electronic properties of defects were investigated by observing absorption, emission, and excitation spectra. The change in the creep rate of LiF during exposure to x radiation at room temperature under a constant load was also measured. (D.C.W.)

13974 (STI/PUB/21/16) THE MOESSBAUER EFFECT. Bibliographical Series No. 16. (International Atomic Energy Agency, Vienna (Austria)). 1965. 140p. IAEA: $3.00; S63,-; 18/-stg; F Fr 12,-; DM 10.50.

Abstracts of papers on various aspects of the Mössbauer effect are included. Theoretical and experimental papers are listed. Applications of the Mössbauer effect in nuclear physics, solid-state physics, and general physics are included. (M.O.W.)

13975 (TID-21571) THE POWER DEPENDENCE OF THE SATURATION OF THE EPR SPECTRUM OF THE F-CENTER AT 4 deg K. Noble, Gordon A.; Stungis, G. E. (IIT Research Inst., Chicago, Ill. Physics Div.). [1962]. Contract AT(11-1)-578. 36p. Dep. mn. CFSTI $2.00 cy, $0.50 mn.

A new method of observing an inhomogeneously broadened line is described. The saturation of the electron paramagnetic resonance of F-centers in KCl at 4°K is measured as a function of the saturating power and the separation between the field during saturation and the instantaneous magnetic field during observation. A saturation factor can be defined for these experiments and it has a fundamental non-symmetry. The growth of the saturated portion of the spectrum occurs only during the application of microwave power and is independent of the concentration of the F-centers. Some structure is observed in the saturation. The experimental results are compared with the predictions of a simple theory based on the spin packet model. There is no agreement with this theory because each upper level cannot be paired with a single lower level. The introduction of only discrete types of transition cannot explain the results. A continuous distribution for the transition probabilities does explain the results. (auth)

13976 THE EFFECT OF EXCHANGE INTERACTION ON PARAMAGNETIC RESONANCE. Potapkov, N. A. (Steklova Mathematical Inst., Moscow). Acta Phys. Acad. Sci. Hung., 19: 349-55(1965). (In Russian).

The widening of the resonance line due to the change of the exchange interaction caused by the thermal oscillations of the crystal lattice is investigated. (auth)

13977 MODIFICATIONS OF THE DENSITY AND MOBILITY OF MAJORITY CARRIERS IN N-TYPE GERMANIUM BOMBARDED BY PROTONS AT 600 Mev. Daspet, Danielle; Cambou, Francis; de Lafond, Yann Gervais (Faculte des Sciences, Toulouse). Compt. Rend., 261: 5416-19(Dec. 20, 1965). (In French).

Samples of N-type germanium of resistivity 1.1 Ω cm were irradiated at room temperature with an integral flux of 3×10^{14} protons/cm^2 at 600 Mev. The variations of the resistivity, the Hall coefficient, and the mobility during the irradiation were determined. The resistivity and Hall coefficient curves show conversion of the n-type semiconductor into p-type. The agreement between the calculated and theoretical mean effective radius is good. (J.S.R.)

13978 ELECTRON MICROSCOPIC OBSERVATION OF STACKING FAULTS IN TWIN CRYSTALS OF BERYLLIUM. Antolin, Jacqueline; Poirier, Jean-Paul; Dupouy, Jean-Michel (Centre d'Etudes Nucleaires, Saclay, France). Compt. Rend., 261: 5477-8(Dec. 20, 1965). (In French).

Stacking faults and dislocations of the Burgers vectors outside of the base plane in mechanical twin crystals of beryllium were observed by electron microscope. The faults are situated on the base plane of the twin crystal and the Burgers vector of the associated imperfect dislocations is of the type $1/6\ \langle 20\bar{2}3 \rangle$. (tr-auth)

13979 HIGH-TEMPERATURE STUDY OF CHANGES OF THE CRYSTALLINE FORM OF NEODYMIUM SESQUIOXIDE. Foeex, Marc; Traverse, Jean-Pierre; Coutures, Juliette (Centre National de la Recherche Scientifique, Montlouis, France). Compt. Rend., 261: 5497-5500 (Dec. 20, 1965). (In French).

The study of neodymium sesquioxide by thermal analysis and x-ray diffraction at high temperatures shows two transformations of this oxide near 2100 and 2200°C respectively. The first of these transformations seems to correspond to a sharp change of the crystalline parameters of the hexagonal form. (tr-auth)

13980 ANISOTROPY OF THE SNOEK PHENOMENON IN NIOBIUM. Hoffman, R. A.; Wert, C. A. (Univ. of Illinois, Urbana). J. Appl. Phys., 37: 237-40(Jan. 1966).

The anisotropy of the strength of the Snoek relaxation was measured for both oxygen and nitrogen in niobium. Single crystals of niobium of extreme orientations, [100], and [111], as well as several intermediate orientations

were grown in an electron beam melter. The height of the Snoek peaks of the residual oxygen and nitrogen was measured at 80 kcps using a quartz transducer. The orientation for which the peak height is maximum is [100]; the orientation for which it is minimum is [111]—it is actually zero for this orientation. This result shows that the interstitial site is symmetrical about [111], but it alone does not differentiate between occupancy by the interstitial of the octahedral and tetrahedral sites. (auth)

13981 LEED BEAM BROADENING AS A RESULT OF SPUTTERING DAMAGE. Park, Robert L. (Brown Univ., Providence). J. Appl. Phys., 37: 295-8(Jan. 1966).

Investigations of sputtering damage based only on changes in LEED (low energy electron diffraction) intensities are unable to distinguish between lattice distortions resulting from bombardment atoms imbedded in the lattice and localized structural defects such as vacancies. Such a distinction can be made on the basis of beam broadening. The observed beam broadening due to bombardment of a clean annealed (100) nickel surface with 500-ev argon ions can be accounted for by assuming that a strain of 0.05 is introduced by occluded argon atoms. As a result of the finite beam width, plots of the intensity of the beam as a function of electron energy are affected by the mechanics of recording and reducing the data. It is shown that the correct intensity can be obtained regardless of beam width by superimposing plots of collector current versus electron energy for all values of the collector angle. (auth)

13982 EFFECT OF CARRIER TRAPS IN POLYETHYLENE UNDER GAMMA-RAY IRRADIATION. Yahagi, Kichinosuke (Waseda Univ., Tokyo); Shinohara, Kenichi. J. Appl. Phys., 37: 310-15(Jan. 1966).

Stimulated currents are detected with increasing temperature in polyethylene films following irradiation with high-energy electron beams at 77°K. A peak current occurs at about 200°K in low-density specimens and 250°K in high-density ones. Induced currents I under gamma irradiation of polyethylene at room temperature depend on dose rate R via $I \propto R^{\Delta}$. In high-density polyethylene preirradiation by electron beams of about 5×10^7 rads at room temperature Δ increases from 0.5 to 0.84 and is accompanied by a decrease of induced current. In the low-density specimens Δ decreases from 0.8 to 0.6 and the induced current increases with the same preirradiation. After boiling the preirradiated specimen for 5 min, Δ becomes 0.5 in both cases, and in the high-density specimens the induced current I returns to that of the nonirradiated sample. This behavior suggests that the increase and decrease of carrier traps by these treatments influence the induced current characteristics. Another factor influencing the induced conductivity is the crystallinity; with decreasing crystallinity the induced conductivity of all specimens decreases, while in most cases Δ values increase. This behavior suggests the domination of electrons as charge carriers and the hypothesis is that they are able to flow more easily in the crystalline parts than in the amorphous parts. (auth)

13983 INVERSION OF POLE FIGURES FOR MATERIALS HAVING ORTHORHOMBIC SYMMETRY. Morris, Peter R. (National Lead Co. of Ohio, Cincinnati). J. Appl. Phys., 37: 359-64(Jan. 1966).

A method for obtaining inverse pole figures from pole figures for materials having orthorhombic symmetry is presented. The method entails expansion of the axis distribution function in a series of spherical surface harmonics of appropriate symmetry, even in x_1, x_2, x_3. Truncation of the series at order n = 2, 4, 6, . . ., 2m, where m is a nonnegative integer, gives rise to $\frac{1}{2}n$ systems of 2,3, $(\frac{1}{2}n) + 1$ simultaneous linear equations in a like number of variables, requiring a minimum of $(\frac{1}{2}n) + 1$ pole figures for solution. A method for evaluating the goodness of fit is suggested. Data obtained by Mueller and Knott for alpha uranium are used to illustrate the method. (auth)

13984 PRODUCTION BY FISSION FRAGMENTS OF LARGE TRACKS IN CRYSTALS. Caspar, P. E. (Cambridge Univ., Eng.). J. Appl. Phys., 37: 427-30(Jan. 1966).

Thin crystals of two nonmetallic compounds were irradiated with uranium fission fragments and the resulting damage investigated using the electron microscope. The light-contrast tracks observed were wider by a factor of over two than any previously reported and appeared to be directly produced by the passage of the fission fragments. Considerations of the rate of energy loss strongly suggest that the damage was produced by an ionization mechanism and that even these track widths are not the maximum which may be observed. (auth)

13985 ULTRA-THIN SECTIONS OF CsI SINGLE CRYSTALS. Granzer, F.; Haase, G.; Zoergiebel, F. (Univ., Frankfurt am Main). J. Appl. Phys., 37: 457-8 (Jan. 1966).

Tl-activated CsI thin slices, prepared by a Leitz ultramicrotome with a diamond knife, were examined in the electron microscope. The slices were found free from large lattice distortions and possessed the same dislocation density as in the bulk crystals, showing that microtoming is a suitable technique for the preparation of slices for studies of the effect of dislocations on the scintillation efficiency. (M.J.T.)

13986 EFFECT OF HARD RADIATION ON THE OPTICAL CENTERS OF TR^{3+} IONS IN CRYSTALS. Voron'ko, Yu. K.; Kaminskii, A. A.; Osiko, V. V. (Lebedev Physics Inst., Moscow). JETP Lett. (USSR) (Engl. Transl.), 2: 294-7(Nov. 15, 1965).

Translated from Zh. Eksp. Teor. Fiz., Pis'ma Redakt., 2: 473-8(Nov. 15, 1965).

The effects of ^{60}Co gamma rays on the absorption spectra of the crystals $CaF_2:Er^{3+}$, $CaF_2:Eu^{3+}$, and $CaF_2:Nd^{3+}$ were investigated. It is concluded that gamma irradiation changes the structure of the optical TR^{3+} centers; some centers (M and N) disintegrate and are replaced by other centers. Two possible mechanisms for the transformation of the TR^{3+} centers are outlined. (D.C.W.)

13987 RADIATION DAMAGE IN GERMANIUM. Ishino, Shiori (Tokyo Univ.). Kinzoku Butsuri, 9: 102-14(1963). (In Japanese).

Heavy particle bombardment of n-type Ge results in decrease of conductive electrons and change to p-type. An effect of bombardment is the formation of vacant states which introduce a new state in the forbidden energy band. Earlier ideas concerning energy levels associated with lattice defects were based on single ionization of lattice vacancies and interstitial atoms. The vacancy behaves as an acceptor whereas the interstitial atom behaves as a donor. Later, the damage in bombardment of Ge was known to be much more complicated. A study of the electron spin resonance of silicon showed that the radiation-induced defect could be produced by irradiation at room temperature and the lattice vacancy was affected by the nature of the impurity. Different spectra were observed depending on the Fermi level in the irradiated sample. The energy levels found in Ge irradiated by different heavy particles seemed at first to be mutually inconsistent; however, it was possible tentatively to reconcile the differences by consideration of clustering and association of defects. Four levels are ascribed to single vacancies and interstitials. A crude theory is constructed to explain these levels, particularly their asymmetrical distribution in the energy gap, and to assign each to a definite defect. It differs somewhat from Lark-Horovitz's theory. Some problems relating to damage and subthreshold energy, introduction rate and temperature, and annealing of radiation damage in Ge are also discussed. (BBB)

13988 THE FERMI SURFACE. Tan, D. S. (Univ., Amsterdam). Ned. Tijdschr. Natuur., 31: 257-65(Aug. 1965). (In Dutch).

A brief description is given of the behavior of electrons on the Fermi surface. A review is presented of the existing techniques for the determination of its topology. (J.S.R.)

13989 IONIZATION DEFECTS OF ENERGETIC ^{28}Al ATOMS IN SILICON. Morgenstern, H.; Hilscher, D.; Scheer, J. (Hahn-Meitner-Institut fuer Kernforschung, Berlin). Nucl. Instrum. Methods, 39: 347-9(Jan. 11, 1966).

The ionization defect for nuclei passing through matter was observed as a by-product of measurements of the angular distribution of protons and alpha particles from neutron-induced reactions in silicon. Neutrons at 13.95 Mev impinged on two solid-state detectors facing each other, the common center line forming angles with the incoming neutron direction. Only coincident pulses were registered from charged particles from the reaction $^{28}Si(n,p)^{28}Al$ and $^{28}Si(n,\alpha)^{25}Mg$ leaving one detector and hitting the other. By varying the angle the angular distribution could be obtained. The pulse-height spectra of protons from the first reactions and the ionization defects as a function of the recoil energy are given. (J.F.P.)

13990 THE EFFECT OF RADIATION DAMAGE AT ROOM TEMPERATURE ON THE THERMOLUMINESCENCE CHARACTERISTIC OF SINGLE CRYSTALS OF ZINC SULPHIDE. Bryant, F. J.; Cox, A. F. J. (Univ. of Hull, Eng.). Phys. Lett., 20: 108-9(Feb. 1, 1966).

A study of the thermoluminescence curves of single crystals of zinc sulphide before and after bombardment with monoenergetic electrons in the range 100-400 kev reveals a threshold energy at 240-250 kev above which a new trapping state is formed. (auth)

13991 VALENCY CHANGES IN CERIUM COMPOUNDS. Busch, G.; Vogt, O. (Laboratorium fuer Festkorperphysik, Zurich). Phys. Lett., 20: 152-4(Feb. 1, 1966).

The magnetic susceptibilities versus temperature and magnetic moments versus applied fields of CeP, CeAs and CeSb were measured. At low enough temperatures magnetic order is observed. The valency state of the Ce ion depends on temperature. (auth)

13992 MOESSBAUER EFFECT IN ^{161}Dy IN $DyCo_2$ AND $DyNi_2$. Ofer, S.; Segal, E. (Hebrew Univ., Jerusalem). Phys. Rev., 141: 448-51(Jan. 1966).

The recoilless absorption spectra of the 26-kev γ rays from ^{161m}Dy situated in $DyNi_2$ and in $DyCo_2$ were measured at various temperatures. A value of (-866 ± 30) Mc/sec was found for the magnetic hyperfine constant ($g_0\mu_n H_{eff}$) of the ground state of ^{161}Dy in $DyCo_2$ at 4°K. This value is about 4% higher than the free-ion value calculated for the Dy^{3+} ions in the fully magnetized state ($J_z = J$) from data on electron spin resonance in dilute salts. For ^{161}Dy in $DyNi_2$, a value of (-818 ± 30) Mc/sec was found for $g_0\mu_n H_{eff}$ at 4°K. This value corresponds to an ionic magnetic moment of $(9.8 \pm 0.3)\ \mu_B$, which is higher than that obtained by magnetic measurements ($7.1\ \mu_B$) and indicates probably that the Ni sublattice contributes to the total magnetization by an antiferromagnetic coupling. The isomeric shifts of Dy metal, $DyFe_2$, $DyNi_2$, and $DyCo_2$ absorbers were found to be the same within the experimental errors (1.9 ± 0.2 mm/sec relative to Dy_2O_3). (auth)

13993 LONG-RANGE MAGNETIC ORDER IN MnO. Blech, I. A.; Averbach, B. L. (Massachusetts Inst. of Tech., Cambridge). Phys. Rev., 142: 287-90(Feb. 1966).

Neutron diffraction measurements on powder samples confirm that the magnetic moments in MnO are arrayed in ferromagnetic sheets parallel to {111} planes, with neighboring planes coupled in an antiferromagnetic fashion. The long-range order parameter S increases progressively with decreasing temperature below the Néel temperature, but complete order is apparently not reached even at very low temperatures. The magnetic unit cell is rhombohedral, and the rhombohedral angle changes progressively as the temperature is lowered. The change in rhombohedral angle is shown to be related to the long-range order parameter, and it is deduced from this that the distance between antiparallel spins is less than the distance between parallel spins by 0.8%. (auth)

13994 SPIN CORRELATIONS IN IRON. Spooner, Stephen; Averbach, B. L. (Massachusetts Inst. of Tech., Cambridge). Phys. Rev., 142: 291-9(Feb. 1966).

Measurements of diffuse magnetic neutron scattering from an iron single crystal show that there is strong ferromagnetic short-range order above the Curie temperature. The associated small-angle scattering is spherically symmetric and decreases smoothly in reciprocal space, indicating that there is no systematic orientation relationship between spin clusters. Correlation coefficients, defined as $\gamma_r = (S \cdot S')_r/S(S+1)$ where S and S′ are spin vectors with spin quantum number S separated by the vector r, were obtained from a quasielastic analysis of the data. The correlation coefficients follow the relationship $\gamma_r = A \exp.(-r/\delta)$ at short correlation distances. Beyond 15 Å the Van Hove relationship, $\gamma_r = (B/r) \exp(-\kappa r)$, is followed. The quantities δ and $1/\kappa$ are correlation ranges, and the factors A and B are related to the strength of the correlation. The first-neighbor spin coupling energy was calculated from nearest-neighbor correlation coefficients and magnetic specific-heat data. The resultant exchange energy, $J_1 = 0.012$ ev, and this is in good agreement with recent calculations for a Heisenberg ferromagnet above the Curie temperature. Observations of small-angle scattering show that the spin disorder persists well below the Curie temperature. Measurements were made of the total diffuse magnetic scattering in the vicinity of the Curie temperature, and these data also demonstrate the gradual and continuous onset of spin disorder as the temperature is raised toward the critical point. (auth)

13995 NUCLEAR SPIN-LATTICE RELAXATION IN FERROMAGNETIC INSULATORS AT LOW TEMPERATURES. Honma, Akio (Brookhaven National Lab., Upton, N. Y.). Phys. Rev., 142: 306-17(Feb. 1966). (BNL-9403).

A theoretical study of the nuclear spin-lattice relaxation in cubic ferromagnetic insulators at ultralow temperatures is presented. Calculations are performed for nuclei which belong to the magnetic atoms, considering only the direct processes. Three mechanisms are considered: the relaxation to mixed magnon-phonon modes, indirect nuclear-spin interaction modulated by lattice vibrations, and nuclear quadrupole energy modulated by lattice vibrations. The first two mechanisms lead to a relaxation time T_1 which depends on both the temperature T and the external field H_0 with $T_1 \sim H_0^2/T$ for $H_0 \gg$ magnetization and the anisotropy field. For a field comparable to the magnetization or the anisotropy field, the relaxation time is proportional to H_0^n, n being larger or smaller than 2 depending on the shape of the single-crystal sample. The last mechanism does not lead to a field-dependent T_1. Comparison with experiments performed on powdered EuS is also presented. (auth)

13996 SPACE-TIME SYMMETRY OF TRANSPORT COEFFICIENTS. Kleiner, W. H. (Massachusetts Inst. of Tech., Lexington). Phys. Rev., 142: 318-26(Feb. 1966).

The symmetry properties of linear transport coefficients are derived treating time inversion and spatial transformations on the same footing. The possible presence of a uniform external magnetic field is taken into account. The method used can be applied more generally—to nonlinear transport coefficients, for example. It is shown that the usual Onsager reciprocity relations do not in general apply in practice to magnetic crystals; appropriate generalized Onsager relations are given. The 1651 3-dimensional space groups which exist when time inversion is taken into account fall into three categories: (a) 230 which contain time inversion as an element, (b) 230 which do not involve time inversion, and (c) 1191 which contain time inversion only in combination with spatial transformations; (a) refers to nonmagnetic crystals and (b) and (c) refer to magnetic crystals. Onsager's relations are shown to apply in their usual form to crystals in category (a), not at all to crystals in category (b), and in general only in a modified form to crystals in category (c). As an application, the equations derived which determine the symmetry restrictions are used to obtain symmetry-restricted matrices for the thermogalvanomagnetic coefficients for each of the 1651 space-group symmetries, and the results are tabulated. (auth)

13997 SOME PROPERTIES OF SUPPORTED SMALL α-Fe_2O_3 PARTICLES DETERMINED WITH THE MOESS-

BAUER EFFECT. Kuendig, Walter (Univ. of California, Los Angeles); Boemmel, Hans; Constabaris, G.; Lindquist, R. H. Phys. Rev., 142: 327-33(Feb. 1966).

Mössbauer spectra of ^{57}Fe in α-Fe_2O_3 were measured as a function of particle size and temperature. Bulk α-Fe_2O_3 shows a change in the sign of the quadrupole interaction in going through the Morin transition temperature, 263°K. Analyses of the spectra show that the magnetization vector is in the c plane above the transition temperature and parallel to the c axis below it. In contrast, finely divided α-Fe_2O_3 particles, supported on a high-area silica, do not undergo a Morin transition. The spectra show that the magnetization vector remains perpendicular to the c axis at least down to 10°K. It is evident that the spins are pinned by the surface in small particles. When the particle size is less than 135 Å, the room-temperature spectrum consists only of a quadrupole-split center line corresponding to superparamagnetic α-Fe_2O_3. As the particle size is gradually increased, a 6-line hyperfine spectrum of increasing intensity appears. This transition from superparamagnetic to ferromagnetic behavior, coupled with a measurement of the average particle size by x-ray line broadening, leads to a calculated value of the crystalline anisotropy constant in the c plane of $(4.7 \pm 1.1) \times 10^4$ erg per cm^3. A sample with an average particle size just below that required for ferromagnetic behavior at room temperature, when cooled, displays an increasing fraction of ferromagnetic material as the temperature is decreased. From these data the particle size distribution of the α-Fe_2O_3 is determined. In addition, these data are used to calculate an independent value of the anisotropy constant of $(4.1 \pm 1.1) \times 10^4$ erg per cm^3. Careful measurements on the series of samples with varying particle sizes show that the quadrupole splitting increases from the bulk value of 0.42 mm sec^{-1} to a value of 0.98 mm sec^{-1} for particles with an undetermined average size of less than 100 Å. (auth)

13998 INFRARED ABSORPTION SPECTRA OF OXYGEN-DEFECT COMPLEXES IN IRRADIATED SILICON. Ramdas, A. K.; Rao, M. G. (Purdue Univ., Lafayette, Ind.). Phys. Rev., 142: 451-6(Feb. 1966).

The infrared-active localized modes of oscillation of defect-oxygen complexes in electron-irradiated and neutron-irradiated silicon containing oxygen are reported. Behavior with heat treatment and relative intensities show the existence of a large number of complexes besides the Si-B1 center responsible for the line at 835 cm^{-1}. Neutron-irradiated silicon exhibits satellite lines close to the 835 cm^{-1} line when such specimens are annealed above 473°K. Isochronal-annealing studies indicate that the satellite centers are not associated with the Si-B1 center. Multiple-vacancy centers in association with dispersed oxygen may account for the satellites. (auth)

13999 VACANCY-PRODUCTION EFFICIENCIES IN KBr AT LOW TEMPERATURES. Ritz, Victor H. (Naval Research Lab., Washington, D. C.). Phys. Rev., 142: 505-13(Feb. 1966).

The growth of the prominent absorption bands (alpha, F, H, 2300 Å) produced by low-energy x ray and 2.0-Mev electron irradiation was studied in KBr at temperatures between 5 and 9°K. The growth curves are not, in general, linear when plotted as a function of absorbed dose. The total vacancy production (F plus alpha centers) is a smooth but nonlinear function of absorbed dose. The α/F ratio is not constant as the irradiation progresses. The ratio is initially 4:1 and reaches a maximum 9:1 at an F-center concentration of 5×10^{16} (F centers)/cm^3. Continued irradiation causes the α/F ratio to drop to about 4:1 at 3×10^{17} (F centers)/cm^3. This variation in the α/F ratio is the same for all types or "qualities" of radiation when plotted as a function of the F-center concentration. The intensity dependence of vacancy production was investigated by varying the beam current by a factor of 120 for the 2.0-Mev electron irradiations. More energy is required to produce a vacancy at higher intensities, but the α/F ratio is unaffected. The variation of total vacancy production efficiency in KBr with radiation "quality" parallels the F-center efficiencies reported earlier. One is led to the same conclusion reached previously, i.e., the low-temperature coloration process is dominated by mechanisms of the sort proposed by Klick and by Williams which involve the single ionization of two adjacent halide ions. (auth)

14000 ON THE INFLUENCE OF IRRADIATION WITH SMALL X-RAY DOSES ON THE BLEACHING OF KCl CRYSTALS WITH F CENTERS. Froehlich, F.; Grau, P. (Univ., Halle, Ger.). Phys. Status Solidi, 12: 421-8(1965).

It is shown that the rate of F-center production at the beginning of the growth curve is greatly enhanced by repeated low intensity x irradiation for short periods followed by bleaching with white light. The defects responsible for this behavior are found to anneal in two distinct stages with activation energies of 0.68 ev and 0.9 to 1.0 ev. The relation between the two stages depends on the prior treatment of the specimen. The effective defects are connected with OH-impurities, which probably enhance the growth rate of F-centers by a U-center mechanism and increase the real concentration of anion vacancies by an enhanced production of colloids. (auth)

14001 THE THEORY OF CORRELATED CRYSTALS. Brueckner, Keith A.; Frohberg, Jobst (Univ. of California, San Diego, La Jolla). [Progr. Theoret. Phys. (Kyoto), 34: Suppl., 383-99(1965)].

The theory of the correlated crystal is developed using two alternative methods. The first is based on a variational wave function and requires the development of a cluster expansion that has a number of features peculiar to the crystal. The second approximation method starts from the Raleigh-Schrödinger perturbation theory in the Hartree basis representation and by selective summation in the perturbation series, develops results similar to the cluster expansion. Previous results and the degree of their validity are discussed. The solution to the generalized equation is considered, and various approximations suitable for explicit evaluation are presented. (L.B.S.)

14002 THE TRANSPORT OF HOT ELECTRONS IN THIN ALUMINUM FILMS. Thompson, Ch. Z. Angew. Phys., 20: 1-10(Nov. 1965).

The complete range-energy relation and the mean free paths of hot electrons in evaporated thin aluminum films were measured. Correlation of electron-electron and electron-phonon interactions with the experimentally determined range of analytic expressions were obtained. The photoheating vacuum-collection experiments were made to enable the determination of the range for electrons with excitation energy above the work function, while the photoheating internal-collection measurements across the Schottky barriers of Al–GaP contacts gave the ranges for electrons with an energy 1 to 2 ev above the Fermi level. The thickness of Al films varied from 50 to 10,000 Å. The range was determined from a plot of response per absorbed photon vs thickness. The electron-electron mean free path l_e decreased in the same energy region. This extremely strong dependence of l_e on initial energy agreed qualitatively with the theoretical calculations based on self-consistent, dielectric, constant approach, and screened potential formulation. (auth)

14003 GENERATION OF ACOUSTIC WAVES AT MICROWAVE FREQUENCIES IN THIN FILMS OF DYSPROSIUM METAL [Thesis]. Maley, Martin Paul. Houston, Tex., Rice Univ., 1965. 85p.

Microwave phonons at 1 Gc/sec were generated in thin films of dysprosium metal vacuum-deposited onto the ends of polished quartz rods. The effect is observed by the pulse-echo technique previously employed in studies on thin films of nickel, cobalt, and their various alloys. It involves converting magnetic energy in the form of excited magnons into acoustic energy through the magnetostrictive coupling. Acoustic generation was observed between the temperatures of 4.2 and 130°K at values of the applied magnetic field that require that the dysprosium be in its ferromagnetic phase. The effect does not begin to saturate at the highest fields attainable (20 kOe), and is present at fields much lower than those theoretically predicted for

FMR in single crystals. Various possible mechanisms are discussed. (Dissertation Abstr.)

14004 CHARACTERISTIC ENERGY LOSS STUDIES OF ELECTRON-BOMBARDED Al, Cd, In, Mg, AND Zn FOILS WITH VACUUM ULTRAVIOLET SPECTROSCOPY [Thesis]. **Herickhoff, Robert John. Nashville, Tenn., Vanderbilt Univ., 1965. 79p.**

The possibility that some characteristic energy losses originate in plasma oscillations of the conduction electrons and the subsequent prediction that the radiation is emitted from the decay of these oscillations prompted the present investigation of ultraviolet light emitted by electron-bombarded metal foils. Optical emission studies were carried out by bombarding Al, Mg, Cd, In, and Zn foils 500 to 1000 Å in thickness with 60- to 100-kev electrons, and analyzing the light emitted at 30° from the foil normal with a Seya-Namioka vacuum ultraviolet spectrometer and a sodium salicylate-coated EMI 6256B photomultiplier as a detector. A sharp peak at 15.2 ev and a broad peak at 8.85 ev were found in the spectra of Al and Mg, respectively. A sharp, intense peak with a half width of 0.9 ev was observed in Cd at 9.1 ev, and a less intense peak was observed in In at 11.8 ev. In Zn only an edge at 8.6 ev was observed with the intensity dropping sharply at higher energies. These results agree reasonably well with characteristic energy-loss experiments. Al, Mg, and In show good agreement between the optical emission peaks and the theoretical plasma energies, whereas for Cd and Zn there is considerable discrepancy between these values. Theoretical x-ray energies of Cd and Zn were comparable to the energy of peak emission, with the conclusion that either the emissions may be due to interband transitions or interband transitions are seriously affecting the plasma interaction in these metals. Since the optical constants were known for Al and In, the theoretical transition radiation spectra were calculated for these elements and showed good agreement with the experimental spectra. (Dissertation Abstr.)

14005 CONFIGURATION INTERACTION IN THE RARE EARTHS AND ITS EFFECT ON THE STARK LEVELS OF $PrCl_3$ AND $GdCl_3 \cdot 6H_2O$ [Thesis]. **Rajnak, Katheryn Edmonds. Berkeley, Calif., Univ. of California, 1963. 122p.**

The techniques of Racah were used to obtain expressions for the matrix elements of the Coulomb interaction between the configuration $4f^2$ and the excited configurations 4f6p and 4f5f, and between $4f^7$ and $4f^6$6p. Approximate SCF radial wave functions were computed for Pr^{+3} and Tm^{+3} and used to calculate the necessary radial integrals. A second-order crystal field interaction between the configurations $4f^2$ and 4f5d was also considered. While these mechanisms lead to rather large shifts in some of the Stark levels of Pr^{+3} in $PrCl_3$, no one mechanism gives shifts large enough to explain the observed discrepancy between the experimental levels of the $^1D_2$ and those calculated by Margolis. The interaction of $4f^7$ with $4f^6$6p is not large enough to explain the splitting of the $^6P_{\frac{7}{2}}$ and $^6P_{\frac{5}{2}}$ levels of $GdCl_3 \cdot 6H_2O$ observed by Dieke and Leopold. (Dissertation Abstr.)

REACTOR TECHNOLOGY

General

Refer also to abstract 13752.

14006 (ANL–7122) REACTOR DEVELOPMENT PROGRAM PROGRESS REPORT, NOVEMBER 1965. (Argonne National Lab., Ill.). Dec. 27, 1965. Contract W-31-109-eng-38. 102p. Dep. mn; CFSTI $4.00 cy, $0.75 mn.

Four sections are included; separate abstracts have been prepared for each. (T.F.H.)

For abstracts of individual sections see: 14007–14009 and 14179.

14007 (ANL–7122, pp 1-41) LIQUID-METAL-COOLED REACTORS. (Argonne National Lab., Ill.).

A review is presented of the operations and analyses of several liquid-metal-cooled reactors, including EBR-2, FARET, SEFOR, and ZPR-3 and -9. Phase studies and irradiation testing of U–Pu–Zr, U–Pu–Ti, U–Pu Fissium, and UC–PuC systems are reported. The distribution coefficient of U between $MgCl_2$ and Cu–Mg alloy is measured. The performance of V–Ti, SS 304, SS 316, Hastelloy X, Hastelloy X280, Nb–Zr, Nb–V, V, W, carbon steel 1020, chromium steel 4130, SS 405, Ta, V–Ti–Mo, and V–Cr–Al in liquid–Na and fused-chloride–liquid-metal environments (the latter consisting in Al–Mg–$MgCl_2$–KCl–NaCl) is evaluated. The wetting of the surfaces of a vitreous C crucible by a fused-chloride–liquid-metal system consisting of Cu–Mg–$MgCl_2$–KCl–NaCl–U is determined. (T.F.H.)

14008 (ANL–7122, pp 42-69) GENERAL REACTOR TECHNOLOGY. (Argonne National Lab., Ill.).

Measurements of the neutron resonance absorption integrals of C, Al, Fe, Co, Cu, Zn, Se, Cd, Sn, Pb, Lucite, LiF, B_4C, and the oxides of Mg, Al, Ca, Ti, V, Mn, Cu, Zn, Zr, Ba, and Ta are tabulated. Experimental and theoretical studies are reported on: the criticality parameters for the Hi–C Critical Experiment; infinite-slab calculations of interactions of coupled reactors; the ARC computation system for reactor kinetics; the thermal expansion of UC; phase studies on U–UP; reactions of UP with phosphoric acid; phase studies on U–UO_2; vapor pressure of U–UO_2 systems at 1580 to 2400°K; Ta corrosion by flowing liquid Sn at 800 to 1100°C; reactivity of EBWR with Pu fuel loading; Na_2O concentration measurements in coolant loops of Na-cooled reactors; fluorination of UO_2–PuO_2–fission product mixtures on alumina fluidized beds; BrF_5 reactions with U_3O_8 at 250 to 400°C; corrosion of Ni and Ni alloys by TeF_6 and MoF_6–F_2 mixtures at 500°C; fluorination of PuO_2–UO_2 mixtures to PuF_6–UF_6, and subsequent separation of the components by decomposition of PuF_6 to solid PuF_4; and preparation of UC and UC–PuC mixtures from hydrides. (T.F.H.)

14009 (ANL–7122, pp 82-90) NUCLEAR SAFETY. (Argonne National Lab., Ill.).

Reports are given on: TREAT operations; corrosion of EBR-II Mark I prototype fuel pins (stainless-steel clad) by liquid sodium in TREAT loops; kinetics studies in fast reactors; ionization effects in the equations of state of Pu and UO_2 around 2000 atm and at 5000 to 10,000°K; and the reactions of type 304 stainless steel with steam at 1400°C and 1 to 12 atm. (T.F.H.)

14010 (BNWL–183) SOME NOVEL PLUTONIUM FUELING METHODS FOR THERMAL REACTORS. (Battelle-Northwest, Richland, Wash. Pacific Northwest Lab.). Nov. 1965. Contract AT(45-1)-1830. 105p. Dep. mn. CFSTI $4.00 cy, $1.00 mn.

Separate abstracts were prepared for the five included sections. (M.O.W.)

For abstracts of individual sections see: 14011, 14057, 14102, 14117, and 14118.

14011 (BNWL–183, Sect.V) CONSERVATION ECONOMICS AND REACTOR TECHNOLOGY. Neef, W. I.; Jones, E. D. (Battelle-Northwest, Richland, Wash. Pacific Northwest Lab.). 18p. (CONF-651101–60).

The conservation of natural uranium resources is discussed with respect to future development of breeder and converter reactors. (M.O.W.)

14012 (IA-1048) DETERMINATION OF THE GAMMA FLUX IN A NUCLEAR REACTOR BY THE $^{1414}N_2$–$^{1515}N_2$ ISOTOPIC EXCHANGE REACTION. Anbar, M.; Perlstein, P. (Israel Atomic Energy Commission, Yavne. Soreq Nuclear Research Center). Sept. 1965. 10p. Dep. mn.

The γ flux of the IRR-1 research reactor was determined using the $^{14}N_2$ – $^{15}N_2$ isotopic exchange reaction as a dosimeter. The application of this exchange reaction as a dosimeter for high γ fluxes, including nuclear reactors, is discussed. (auth)

14013 (IDO–17123) SPERT PROJECT. Quarterly Technical Report, April–June 1965. Crocker, J. G. (ed.) (Phillips Petroleum Co., Idaho Falls, Idaho. Atomic Energy Div.). Jan. 1966. Contract AT(10-1)-205. 66p. Dep. mn. CFSTI $3.00 cy, $0.75 mn.

The design and fabrication of a capsule for use in in-pile tests of Capsule Driver Core (CDC) fuel were completed; and a series of out-of-pile tests was performed using chemical explosives to investigate the effect of explosive energy releases on the CDC fuel rods, the CDC support structure, power chambers, and the Spert IV reactor vessel. An analysis of fuel failure mechanisms in UO_2 fuel rods was also made. In addition, several prototype PBF fuel samples were encapsulated and irradiated during the 0.6-msec-period KIWI destructive test. The validity of the point kinetic equations was also studied; the results obtained using the point kinetic equations were compared with the results obtained by solution of the space-time diffusion equations. (D.C.W.)

14014 (MIT–2344-4) HEAVY WATER LATTICE PROJECT ANNUAL REPORT. Thompson, T. J.; Kaplan, I.; Clikeman, F. M.; Driscoll, M. J. (eds.) (Massachusetts Inst. of Tech., Cambridge. Dept. of Nuclear Engineering). Sept. 30, 1965. Contract AT(30-1)-2344. 165p. (MITNE-65). Dep. mn; CFSTI $5.00 cy, $1.00 mn.

Twelve sections are included; separate abstracts have been prepared for all. A bibliography consisting of 49 references to material on heavy water lattices is appended. (T.F.H.)

For abstracts of individual sections see: 13703–13705, 14065–14070, 14103, 14185, and 14186.

14015 (ORNL-TM-1075) VELOCITY AND MASS-DIFFUSION MEASUREMENTS FOR BEDS OF LARGE, UNIFORM-DIAMETER SPHERES RANDOMLY PACKED IN A FULL-SCALE MODEL OF A PEBBLE-BED NUCLEAR REACTOR CORE [Thesis]. Bundy, Roy Dale (Oak Ridge National Lab., Tenn.). Feb. 1966. Contract W-7405-eng-26. 323p. Dep. mn. CFSTI $7.00 cy, $1.50 mn.

Submitted to Univ. of Tennessee, Knoxville.

Velocity profiles and total radial mass diffusivities were determined for shallow beds of randomly packed spheres to provide information needed for the hot-spot analysis of pebble-bed nuclear reactors. The void fractions of the beds and the angles of repose of the spheres along the sides of the fill cones were also obtained to provide auxiliary information of use in interpreting the velocity and diffusion data. (auth)

14016 (STI/PUB/21/17) ORGANIC COOLANTS AND MODERATORS. Bibliographical Series No. 17. (International Atomic Energy Agency, Vienna (Austria)). 1965. 176p. IAEA: $4.00; S84,-; £1.4.0; F Fr 16,-; DM 14,-.

References (540) with abstracts are presented for literature on organic coolants and moderators. Author and subject indexes are included. (D.C.W.)

14017 (STI/PUB/105(Vol.2)) NON-DESTRUCTIVE TESTING IN NUCLEAR TECHNOLOGY. Vol. II. Proceedings Series. Proceedings of a Symposium held in Bucharest, 17-21 May 1965. (International Atomic Energy Agency, Vienna (Austria)). 1965. 448p. (CONF-650509(Vol.2)) IAEA: $9.00; S 189,-; £2.14.0; F Fr 36,-; DM 31,50.

Separate abstracts were prepared for 20 of the 25 included papers. The remaining 5 papers appeared previously in NSA as: 19: 20126, 22508, 22510, 29643, and 38823. (M.O.W.)

For abstracts of individual papers see: 12811, 12812, 13318–13321, 13343, 14032–14034, 14158–14161, 14168, and 14194–14198.

14018 THE SECURITY OF REACTORS. Bourgeois, J. (CEN, Saclay, France). Atompraxis, 11: 639-45(Nov.-Dec. 1965). (In German).

In France the safety of reactors presents great problems to constructors and researchers. Safety will be affected according to the stated regulations, without influence on the development of the program. The chief stress lies in technical tests, in which safety is proved by normal functionalism and possible accidents. (auth)

14019 A TRIAL OF A REACTOR POWER METER BY MEASURING ^{16}N ACTIVITY IN COOLANT. Lin, Chia-Shi; Sun, Jin-Bor; Yuan, Liq-Ji (National Tsing Hua Univ., Hsinchu, Taiwan). Ho Tsu K'o Hsueh, 4: No. 3-4, 55-64 (Aug. 1965).

A precise indication of the reactor power level is essential for the safety operation of the reactor. A conventional compensated ionization chamber which is usually installed in the neighborhood of the reactor core responds to the local flux which depends strongly on the core geometry as well as control blade configuration thereby giving rise only to the relative indication leaving the actual power level uncertain. For an aqueous reactor, the radioactive nuclides of ^{16}N are produced as a result of (n,p) reaction of ^{16}O and by monitoring the dose rate of decay gamma of ^{16}N, a precise indication of the power level independent of the core geometry can be obtained. A Victoreen ionization chamber of Model 716A which is originally supplied as an area monitor was modified and mounted at a certain location in the primary coolant circulation loop. The output current of the ionization chamber was then calibrated against the temperature differential measurement across the core. The result of the measurements shows an excellent linearity in the interval between 200 to 1,000 kw and the reading of the ionization chamber is indeed independent of the control blade configuration. (auth)

14020 OPTIMAL CONTROL OF NUCLEAR-REACTOR PROCESSES [Thesis]. Mohler, Ronald Rutt. Ann Arbor, Mich., Univ. of Michigan, 1965. 151p.

The two problem areas analyzed in this study are (1) the minimum-time control of a nuclear reactor fission process and (2) the optimal control of a direct-cycle heat-exchange process to minimize the consumption of coolant. The minimum-time optimal control problems are analyzed using the maximum principle of Pontryagin. Considered first is a reactor with no precursor groups and with amplitude and velocity-limited reactivity control; the time optimal control in going from one neutron level to another consists of continuous application of maximum-effort control. Next a single precursor model is considered with symmetrical positive and negative limits on reactivity; the time-optimal control to go from one equilibrium state to another is shown to be a bang-bang process with one switching. Finally, the time-optimal control to go from a given equilibrium state to a higher neutron level with amplitude-constrained reactivity is shown to be a maximum effort control with no switching. For both the single and six-precursor models this maximum-effort control is followed by a continuous reactivity control that maintains the neutron level at the desired terminal value. It is shown that this terminal control is in the allowable control set. To avoid instability it must be implemented by means of a closed-loop system. Both continuous and dither-type closed-loop terminal controls are analyzed using Nyquist and describing-function techniques. The problem of optimal control of a direct-cycle heat-exchange process to minimize the coolant consumption is analyzed using a one-stage model for the heat exchanger (no axial or radial subdivisions). In this case there are two control components, an amplitude-constrained reactivity and coolant flow rate with upper and lower bounds. The optimal control is shown to consist of both the time-optimal neutronic control process derived previously and a bang-bang control in coolant flow rate. Additional constraints due to the propellant pumping system are also considered. (Dissertation Abstr.)

14021 IMPROVEMENTS IN OR RELATING TO HIGH TEMPERATURE GAS COOLED REACTORS. Lothe, Johan (to United Kingdom Atomic Energy Authority). British Patent 1,013,102. Dec. 15, 1965. Filed Mar. 28, 1962.

In a high-temperature gas-cooled reactor, means are provided for limiting the catalytic activity of certain fission products in promoting corrosion reactions between graphite or carbides of elements and impurities in the coolant. Small quantities of a corrosion inhibitor, such as oxides of Si, Zr, or Al are incorporated into those graphitic components that are located in the core near the point of entry of the coolant into the core. (B.L.M.)

14022 REACTOR SIMULATOR. Arai, Osamu (to Hitachi, Ltd.). Japanese Patent 1964-18483. Aug. 31, 1964. Filed Dec. 19, 1961.

A reactor simulator consists of a potentiometer for simulating the reactivity of a reactor; a second potentiometer, linked to the first, for indicating the position of a control rod; a device to give a negative reactivity proportional to the deflection of the first potentiometer when the control rod is completely inserted; and a switch for opening the circuit of the second potentiometer. The control rod is in the state of complete insertion when the negative reactivity has been given. (NSA of Japan)

Auxiliaries and Components

Refer also to abstract 13231.

14023 (AD-611432, pp 221-35) CLOSED CYCLE GAS TURBINE. Crim, W. M. Jr. (Nuclear Power Field Office, Fort Belvoir, Va.).

A summary of the concept, theories explored, design, fabrication, construction, and initial testing of the first experimental compact closed cycle thermodynamic system is presented. (M.O.W.)

14024 (APDA-182) QUARTERLY TECHNICAL PROGRESS REPORT ON AEC-SPONSORED ACTIVITIES, OCTOBER-DECEMBER 1965. (Atomic Power Development Associates, Inc., Detroit, Mich.). Contract AT(11-1)-865. 62p. Dep. mn. CFSTI $3.00 cy, $0.75 mn.

Particulars of the following projects are reported; (1) paste concept for fast reactor blanket application, (2) small leak sodium-water reaction, (3) sodium technology loop, (4) fuel element flow stability studies, (5) under sodium scanner, (6) compilation of Fermi experience, (7) Fast Flux Test Facility, and (8) the structural materials irradiation subassembly. Under (1), the loop operation with uranium carbide particles was investigated. Various measurements are presented. In (2), the stability and response of the oxygen and rhometers to sodium monoxide injections in the sodium loop were reported. In (5), further transducer studies for sonic inspection of sodium were made. Only brief discussions of the other projects are presented. (M.O.W.)

14025 (DP-944) DESCRIPTION OF A TEMPERATURE MONITOR FOR LARGE REACTORS. PART III. PERFORMANCE. Byrd, Joseph S.; Dexter, Arthur H.; Goosey, Malcolm H.; Hutter, Carl R.; Leep, Richard W.; Wilson, John N. (Du Pont de Nemours (E. I.) and Co.,

Aiken, S. C. Savannah River Lab.). Jan. 1965. Contract AT(07-2)-1. 32p. Dep. mn. CFSTI $2.00 cy, $0.50 mn.

The results of accuracy and reliability tests on a monitor that was developed to scan large numbers of thermocouples are presented. (D.C.W.)

14026 (EUR–2299.e) RESEARCH ON THE INFLUENCE ON THE CONDITIONS OF FLOW, SUBCOOLING AND COMPOSITION, ON THE BURN-OUT HEAT FLUX OF POLYPHENYL REACTOR COOLING AGENTS. Van Gasselt, M. L. G.; Van Meel, D. A. (Nederlandse Organisatie voor Toegepast Natuurwetenschappelijk Onderzoek, The Hague. Centraal Technisch Instituut). 1965. 23p. Dep. mn.

A description is given of the experimental investigations carried out since 1961 on the burn-out heat flux of organic coolants mainly composed of terphenyl isomers. The burnout was studied for upward forced flow through a vertical round stainless steel tube heated by the Joule effect using direct current. The dimensions of the tube were: internal diameter 5 mm, wall thickness 0.25 mm, length 500 mm. The experiments were limited to the condition of subcooled boiling at the heating surface. To be able to establish the degree of subcooling of complex mixtures a vapor pressure apparatus was developed. Vapor pressures are reported of mixtures of terphenyls and benzene or diphenyl. Burnout heat sources as a function of mass velocity and degree of subcooling are presented for the Progil terphenyl mixtures OM2 and OM1 which were directly pressurized with nitrogen, for degassed OM2, and for the systems OM2-benzene and OM2-biphenyl. (auth)

14027 (EURAEC–909) HYDRODYNAMIC INSTABILITIES LIMITING THE POWER OF BOILING WATER REACTORS. Fabrega, S. (Commissariat a l'Energie Atomique, Grenoble (France). Centre d'Etudes Nucleaires). 1965. Contract 076-61-12 RDF. 105p. Dep. mn. CFSTI $6.00 cy, $0.75 mn.

Work Performed Under United States–Euratom Joint Research and Development Program.

The investigation was carried out at atmospheric pressure and at a pressure of about 8 atmospheres, in channels heated electrically by a constant and uniform specified current. In the tests at 8 atmospheres the channel was a round tube of approximately 6 mm interior diameter. At 1 atmosphere a ring-section channel was used, 10 × 20 mm in diameter, with an inner heating tube and an outer tube of pyrex. It was possible to operate with natural convection and also with forced convection with test-channel by-pass. The study consists of 3 parts: preliminary determination of the laws governing pressure-drop during boiling; determination of the fronts at which oscillation appears, within a wide range of the parameters involved; and a descriptive study of the oscillations and measurement of the periods. The oscillation fronts are given with natural and forced convection for various values of the singular pressure drop at the channel inlet and for various riser lengths. (M.O.W.)

14028 (IITRI–578P22-14) STUDIES OF REACTOR CONTAINMENT STRUCTURES. Summary Report. Salmon, M. A.; Chiapetta, R. L.; Schuyler, F. L. (IIT Research Inst., Chicago, Ill.). [1964]. Contract AT(11-1)-578. 334p. Dep. mn. CFSTI $7.00 cy, $1.50 mn.

The following areas of reactor containment structures were investigated: analysis of the response of containment vessels, the effect of openings on the strength of containment vessels, and the behavior of cylinders of finite length under internal pressure. Data on the mechanical properties of materials, plastic strength of thin cylindrical shells with various end closures under internal pressure, and the transmission and attenuation of disturbances in generalized media are discussed. (M.O.W.)

14029 (NASA-CR-54788) PNEUMATIC NUTATOR ACTUATOR MOTOR. Final Report. Howland, G. R. (Bendix Products Aerospace Div., Bendix Corp., South Bend, Ind.). Oct. 17, 1965. Contract NAS3-5214. 138p. (BPAD–863-16719R).

The design, development, and test of a new type of low-speed, high-torque motor designed for manipulating the control drums of nuclear rocket engines similar to NERVA are described. The motor consists of a pair of bevel gears with an unequal number of teeth. Rotational output is obtained from nutational motion of the input gear driven by pressurized bellows located around its periphery. Flow to the bellows is commutated by vortex amplifiers operating in a closed loop logic sequence. The pneumatic logic circuit operates without moving mechanical parts. (auth)

14030 PRESTRESSED CONCRETE PRESSURE VESSELS OF NUCLEAR REACTORS. David, Milan. Jad. Energ., 11: 402-10(Nov. 1965). (In Czech).

The engineering problems of prestressed concrete reactor pressure vessels are considered. Technical and economic comparisons with steel vessels are presented. Experience with concrete vessels is reported. The evaluation indicated the need of solving problems in connection with the realization of the Czechoslovakian program of nuclear power development. (auth)

14031 CONTAINMENT FOR NUCLEAR REACTORS. Malay, F. L. (Westinghouse Electric Corp., Pittsburgh); Chave, C. T. Mech. Eng., 87: 30-5(Aug. 1965).

Features of the design of nuclear power reactor plants are discussed in regard to public safety under certain postulated accidents. The two hazards associated with core meltdown and attendant fission-product release (direct radiation, and ingestion and inhalation of radioactive material) are examined and adequate protection means are discussed. Structural design of a double containment system is illustrated and described in detail. The containment vessel is a vertical, cylindrical, reinforced-concrete structure with a concrete bottom and hemispherical concrete dome. The bottom is a soil-bearing flat-mat foundation that provides support for the containment vessel. The reinforced-concrete vessel has certain inherent safety features that are not found in steel-plate vessels. The result of the test indicates that the properties of popcorn concrete are satisfactory. Membranes, penetrations through the containment vessel, and subsystems are also considered. It is concluded that the double containment adequately ensures there would be essentially no leakage of radioactive gases from the containment under postulated accident conditions as long as the evacuating compressors were operated and even for at least one hour after they had ceased to function. Even assuming the vacuum in the popcorn-concrete envelope were lost, this honeycombed structure provides a large surface for the plating out of radioiodine. It is considered to be as fully effective as underground containment in regard to absorbing fission products. (TCO)

14032 THE ECONOMICAL APPLICATION OF NONDESTRUCTIVE TESTING TO REACTOR COMPONENTS, ESPECIALLY JACKET TUBING. Renken, C. J. (Argonne National Lab., Ill.). pp 125-37 of STI/PUB/105(Vol. II).

The economical testing of plates and tubes, especially the latter, is discussed in detail. The discussion is centered around components of stainless steel, Zircaloy, and certain refractory metal alloys. It is shown through various examples that although the use of radiography and penetrants may be useful or even essential steps in the testing, critical inspection of thin-wall tubing must usually be made by either an ultrasonic or an electromagnetic method for technical as well as economic reasons. The optimum area of application of these two methods is explained as well as the large area of overlap where results produced by well-designed and properly operated equipment of both types are essentially equivalent. Spurious defect indications contribute directly to increased component costs, so an evaluation of these effects for both the ultrasonic and the electromagnetic test methods is included for several commonly encountered sources of spurious defect signals. The experience in the application of these methods at Argonne National Laboratory on relatively large quantities of tubing from various sources are recounted from the standpoint of the lowest possible inspection cost

per unit-length of tubing. This section also summarizes experience gained at Argonne with the newer pulsed electromagnetic test methods. The critical but generally unappreciated role of tube diameter and wall thickness on tube inspection cost is discussed. Since the question of economical inspection is closely related to allowable defect levels, defect levels and standards in use at Argonne are covered. Finally, the practical and theoretical barriers to reduced component inspection costs are enumerated and a projection of what possible reductions in cost might be attainable in the future with the ultrasonic and electromagnetic test methods is attempted. (auth)

14033 EDDY-CURRENT TESTING OF THIN-WALLED CLADDING TUBES. Verstappen, C.; Deknock, R.; Neider, R.; Brabers, M.; de Meester, P. (Studiecentrum voor Kernenergie, Mol, Belg.). pp 195-209 of STI/PUB/105 (Vol. II).

In view of an extended program on the evaluation of properties and defects of stainless steel and Zircaloy thin-walled tubes, a basic study was made of the optimum test conditions for applying eddy current test methods. An electronic apparatus was built to define these conditions for a great variety of test problems. Therefore, it was necessary to have the possibility of changing the frequency over a wide range and to measure the two components of the complex impedance of the test coil separately. This has the advantage over a measurement of the absolute value of the impedance change since this value has little meaning in view of the change of the properties of the test object. The actual apparatus allows the precise and sensitive measurement of the real and imaginary components of any test coil in a frequency range from 0.1 to 500 kHz. A special type of modulation device was developed. The apparatus is not considered as an actual testing apparatus; by determining optimum conditions for each case, it enables a relatively simple and specific apparatus to be built. Up to now, a detailed study of relationships between physical and electrical properties of a specimen and the test coil impedance was performed for tubular fuel cladding materials. Frequency and coil configurations are established for wall thickness measurements and a particular apparatus was constructed; the accuracy is better than 1% and changes between inner and outer diameter variations can be discriminated. Other specific apparatus are studied and proposed. (auth)

14034 THE DEVELOPMENT OF FLAW-DETECTION TECHNIQUES AT HARWELL. Sharpe, R. S. (Atomic Energy Research Establishment, Harwell, Eng.). pp 351-64 of STI/PUB/105(Vol. II).

In the field of radiography, attention at Harwell recently has been directed towards high-speed techniques, methods of dealing with highly active components and x-ray microscopy. Panoramic radiography, projection fluoroscopy, and a radiopaque penetrant technique were developed to meet the particular needs of reactor components. The characteristics of an image converter system for radiography are described and the results of applying a novel design of ultrasonic converter tube to fuel plate bond evaluation are illustrated. Other ultrasonic techniques described were developed for detecting structural and dimensional flaws in thin-walled fuel sheathing. It is shown how emphasis was placed on improving inspection techniques by concentrating attention on data presentation. Facsimile recording of test signals has been widely applied to ultrasonic and eddy current methods of inspection. By a novel form of signal processing (quantizing) it is shown how these recordings were made considerably more informative. (M.O.W.)

14035 HEAT EXCHANGE UNIT. Rodwell, William (to United Kingdom Atomic Energy Authority). British Patent 1,013,084. Dec. 15, 1965. Filed Dec. 6, 1963.

A heat exchange unit comprises two parallel headers and tubular elements that form a parallel flow array and interconnect the headers. Each tubular element is arranged as a pair of coils in series, one encircling each header, of opposite rotation and lying in a single plane perpendicular to the headers. The turns of one element are arranged between the turns of the other so that each element is of the same length. These heat exchange units may be incorporated into a heat exchanger that is housed with the reactor within a single reactor housing in an arrangement in which the headers of the various units are spaced circumferentially around an annular plenum co-axial with the core and the vessel and aligned axially of the plenum. (B.L.M.)

14036 IMPROVEMENTS IN AND RELATING TO FUELLING ARRANGEMENTS FOR NUCLEAR REACTORS. Tattersall, John Owen; Jones, Geoffrey; Davies, Peter John (to Nuclear Power Plant Co. Ltd. A.E.I.-John Thompson Nuclear Energy Co. Ltd.). British Patent 1,013,255. Dec. 15, 1965. Filed Apr. 8, 1963.

A core access system that does not require a moveable charging chute is described for reactors of the type in which nuclear fuel is located in channels or bores in a neutron-moderating core. The core of the reactor is enclosed in a vessel through which standpipes pass to permit access to the inside of the vessel. Tubular members extend from the standpipes, and at least some of the tubular members each has a number of extensions branching off from it. Each extension extends into or abuts a fuel channel in the core, and a plug is inserted in each of the extensions where they branch off from the tubular member. The plugs are so shaped that any one can be removed to permit fuel to pass from the standpipe into the tubular extension and thence into the channel while the remainder of the plugs remain in place. (B.L.M.)

14037 IMPROVEMENTS IN AND RELATING TO NUCLEAR REACTORS. Beck, Ainslie Rogers; Yovell, Frederick Peter; Taylor, Roderick (to Nuclear Power Plant Co. Ltd. A.E.I.-John Thompson Nuclear Energy Co. Ltd.). British Patent 1,013,926. Dec. 22, 1965. Filed Mar. 29, 1962.

A gas-cooled, graphite-moderated reactor comprises a pressure vessel containing the core and heat exchangers for working fluid for a power plant outside the pressure vessel. A radiation shield wall formed of layers of neutron-moderating material and thermal neutron and gamma ray absorbing material separate the core from the heat exchangers. The shield has one or more passages subdivided by ribs of radiation shielding material extending along the passage, and each passage includes an inlet and an outlet part substantially parallel to one another. Guide vanes extending between the ribs in the passage to reduce the pressure loss are placed in the bends of the passages. (B.L.M.)

14038 IMPROVEMENTS IN OR RELATING TO NUCLEAR REACTORS. Oliver, John; Blair, John Austin Incledon (to Nuclear Power Plant Co. Ltd. A.E.I.-John Thompson Nuclear Energy Co. Ltd.). British Patent 1,014,784. Dec. 31, 1965. Filed May 15, 1963.

A core restraint system is provided for a reactor having a core comprising an assembly of blocks of interlocking neutron-moderating material located within a vessel. The system includes two sets of restraint members disposed at intervals around the sides of the core. One set of members is attached at the coolant inlet face and extends around the sides to a free end adjacent to the outlet face of the core while the second set is fixed at the outlet face and extends around the core to a free end at the inlet face. One set of members supports the sides of the core while the other set supports circumferential restraining rings surrounding the core and spaced from one another at intervals. Temperature compensating means in the form of wedges or links transmit the forces between the set of members supporting the sides of the core and the circumferential rings while permitting relative movement in the longitudinal and radial directions of the structural members of both sets of support members and relative movement in a radial direction of the restraining rings and the structural members supporting the sides of the core. (B.L.M.)

14039 CONCRETE PRESSURE VESSEL. Spruce, Thomas William (to Nuclear Power Plant Co., Ltd. A.E.I.-John Thompson Nuclear Energy Co., Ltd.). British Patent 1,014,872. Dec. 31, 1965. Filed June 8, 1962.

A concrete pressure vessel for a reactor includes a liner on its inner surface that is keyed to the concrete by keys in

the form of ribs projecting from and extending over the outer surface of the liner so that the liner and concrete are rigidly secured together, at least over certain regions of the vessel. Various arrangements for the keys are described in detail. Cooling pipes for cooling the liner are secured to the keys. The pressure vessel is particularly suitable for use with a gas cooled, graphite-moderated reactor. (B.L.M.)

14040 NUCLEAR REACTOR. Jervis, Max William (to Nuclear Power Plant Co. Ltd. A.E.I.-John Thompson Nuclear Energy Co. Ltd.). British Patent 1,014,790. Dec. 31, 1965. Filed Jan. 23, 1964.

In a nuclear reactor having a concrete pressure vessel enclosing a reactive core and having heat exchangers disposed around the core and within the vessel, instruments for measurement of neutron flux are located in the bottom wall of the vessel. The bottom wall has a passage in it extending from the side of the reactor to permit access to the instruments, and a secondary radiation shield is incorporated in the passage. (B.L.M.)

14041 IMPROVEMENTS IN AND RELATING TO VAPOUR GENERATORS. Heathcote, John (to Foster Wheeler Ltd.). British Patent 1,015,912. Jan. 5, 1966. Filed May 28, 1962.

A vapor generator in which the input energy is derived from a liquid coolant of a nuclear reactor comprises a vertical casing having a removable closure at the upper end and having within it a number of clusters of U-tubes to provide the heating surface. The two sets of legs of the U-tubes are connected to the inlet and outlet manifolds disposed at the upper end of the casing. The inlet and outlet pass through the closure so that the tube assembly can be removed with the closure as one unit. Each manifold serves only one tube cluster and is connected as appropriate to an inlet to or an outlet from the casing at the upper end for the fluid to be heated and the heating fluid, respectively. This generator is adapted for operation with a liquid heating fluid in which the tubes extend downward into an open-topped shell arranged within the casing where the liquid level is maintained below the open end of the inner shell. The space within the casing can be divided into compartments that are interconnected in series by tubes to provided economizer, steam heating, steam generating, and superheating sections. (B.L.M.)

14042 IMPROVEMENTS IN OR RELATING TO NUCLEAR REACTORS. Foure, Claude Desire; Moussez, Claude Henri Charles (to Societe Nationale d'Etude et de Construction de Moteurs d'Aviation). British Patent 1,016,113. Jan. 5, 1966. Priority date May 31, 1963, France.

A core sub-assembly for a heterogeneous reactor comprises a group or cluster of parallel fuel elements located at the apices of a regular polygon lattice and immersed in the cooling fluid. A control unit consisting of a series of control elements that have a cross section substantially identical to that of the fuel elements are spaced apart at a distance equal to the spacing of the fuel elements in the lattice. The control elements are disposed along lines that are parallel to those on which the fuel elements are located and are provided with an actuating mechanism for simultaneous actuation of all the control elements in the unit. The control elements maintain a constant cross sectional area of passage for the coolant irrespective of their condition. Coolant deflector members are located in the channels for dividing the coolant flow in a series of helical streams, and each deflector member has its axis parallel to the fuel elements and occupies one channel limited either by fuel elements alone or by fuel elements and control elements. A number of these assemblies arranged in parallel order constitute a reactor core. (B.L.M.)

14043 IMPROVEMENTS IN OR RELATING TO RETARDING DEVICES. Dean, John Robert (to United Kingdom Atomic Energy Authority). British Patent 1,016,261. Jan. 5, 1966. Filed Nov. 10, 1961.

A retarding device is described chiefly for application to nucleonic control rods of the type that are arranged for insertion into the reactor from above and depending from a cable attached to a winding gear mounted above the reactor. The device includes an energy absorbing rotary member that is driven by the weight and means operative in response to the degree of rotation of the member for varying its moment of inertia. The moment of inertia is varied by effecting a change in the radius of gyration of the member. (B.L.M.)

14044 SUPPORT STRUCTURE FOR VERTICAL STACK OF SOLID MODERATOR. Dupuy, Gerard (to Commissariat a l'Energie Atomique). Canadian Patent 725,279. Jan. 4, 1966.

In a heterogeneous gas-cooled reactor, it is desirable to maintain a constant lattice pitch between the fuel rods. Seven columns of graphite blocks with holes in the center of each are arranged in a hexagon with the central column containing a structural support rod. The six peripheral columns are joined to each other and to the central column by interlocking keys. Fuel rods penetrate the six peripheral columns. A seven column unit is supported on a base or "tile." This tile is in turn supported by pillars underneath thermally insulated from the tile. Hexagonal support plates or tiles are spaced so that each seven column unit may expand independently. Thus, swelling from radiation or expansion because of temperature variations with height, does not disturb the lattice pitch at any elevation. (F.S.A.)

14045 EMERGENCY SHUTDOWN DEVICES FOR NUCLEAR REACTORS. Kumpf, Hermann (to Siemens-Schuckertwerke AG). German Patent 1,204,346. Nov. 4, 1965. Filed July 18, 1961.

The safety device is described, which consists of a thimble mounted on a flange of the reactor vessel, a closed storage vessel containing a neutron absorbing gas which is slidably arranged within the thimble, a fixed pierce at the open end of the thimble and opposite a weakened zone of the storage vessel, and a compressed air tank connected to the closed end of the thimble via a valve. (Gmelin Inst.)

14046 SHUTDOWN APPARATUS FOR GAS COOLED NUCLEAR REACTORS. Nye, Anthony Edward Thomas (to Associated Electrical Industries Ltd.). German Patent 1,204,756. Nov. 11, 1965. Priority date Oct. 26, 1956, Great Britain.

The shutdown apparatus for gas-cooled nuclear reactors comprises means for obtaining a first signal voltage representative of the nuclear power output of the reactor, means for obtaining a second signal voltage representative of the total gas flow in the reactor, means for comparing said signals and means for actuating shutdown devices for the reactor when the ratio of the first signal voltage to the second signal voltage exceeds a predetermined value. (Gmelin Inst.)

14047 PNEUMATIC DRIVE FOR NUCLEAR REACTOR CONTROL RODS. Gerard, Victor Jean; Martin, Jean Antoine (to Groupement Atomique Alsacienne Atlantique). German Patent 1,205,205. Nov. 18, 1965. Priority date June 15, 1961, France.

A pneumatic drive is designed, which comprises a pressure cylinder and a piston slidably disposed within the cylinder and engaged to a hollow rod that connects the piston with the control rod. The lower end of the hollow rod extends downward from the piston and through an opening in the bottom of the cylinder having a suitable pressure seal. The hollow rod is provided with radially directed and axially spaced openings. An exit opening at the lower end of the cylinder equipped with a return valve is connected to a container which communicates with the atmosphere via a calibrated opening. (Gmelin Inst.)

14048 COOLING SYSTEM FOR THE SHIELD OF A REACTOR. Kurata, Chikara (to Hitachi, Ltd.). Japanese Patent 1964-30380. Dec. 26, 1964. Filed Nov. 27, 1961.

An emergency cooling system for a reactor shield is provided to take care of abrupt temperature rises in the shield due to an unusual rise of the reactor output. The usual cooling circuit with piping running through the shield

is provided, and a head tank in which a given water level and stationary head are maintained is connected to the circuit near the entrance of cooling water into the shield. Near the exit from the shield, a discharge pipe for the water from the head tank is connected to the closed circuit. When the temperature of the shield exceeds the predetermined value, the circulation of cooling water through the closed circuit is stopped, and a new cooling circuit is established from the head tank, through the regular piping in the shield and to the discharge pipe, which is opened. Thus, the desired adequate cooling of the shield of higher temperature is achieved. (TCO)

14049 FLANGED JOINT. Moberg, Carl Ake (to Aktiebolaget Atomenergi). U. S. Patent 3,219,370. Nov. 23, 1965. Priority date Feb. 1, 1962, Sweden.

A flanged joint is described for connecting different parts of containers, receivers, pipes, or particularly different parts of a reactor pressure vessel. The joint is substantially free from stressing caused by either the forces keeping the parts together or by the large internal pressure or temperature differences that may occur between the different parts of the joint. The two flanges are fixed by welding to the parts to be joined and several tension members (e.g., bolts) extend obliquely from each flange and outside the adjacent one. Each tension member is connected with a thrust member resting against the adjacent flange and also connected with two adjacent identical thrust elements associated with two adjacent tension members from the other flange, preferably through special spacing members. A part of the common face between the flanges is designed to act as a packing area and is taken up by a seal. (B.L.M.)

14050 NUCLEAR REACTOR CORE UNIT CELL. Stoker, Donald J. (to North American Aviation, Inc.). U. S. Patent 3,220,926. Nov. 30, 1965. Filed June 16, 1960.

A reactor core unit cell consists of a solid moderator block having a number of sides. A peripheral, longitudinal recess in each of the sides defines a fuel element channel segment, which forms a fuel channel when the moderator blocks are stacked together; and an unclad fuel element(s) is disposed in the fuel channel. At least one coolant tube is provided for each of the segments with the tube being disposed in a bore extending longitudinally through the block substantially parallel and immediately adjacent to the fuel channel. The coolant tube for each fuel channel segment communicates with a common coolant inlet tube at one end of the moderator block and with a common coolant outlet tube at the other end of the block. (B.L.M.)

14051 METHOD OF PURIFYING PRIMARY FLUID OF NUCLEAR REACTOR CIRCUIT. Maldague, Pierre Edmund Jules Marie (to Societe Anglo-Belge Vulcain, Societe Anonyme). U. S. Patent 3,222,255. Dec. 7, 1965. Priority date Aug. 11, 1962, Belgium.

A method is proposed for the purification of a fluid used in a reactor as a coolant and/or a moderator, and/or a reflector, and/or a regulating fluid, and/or an intermediary fluid while the reactor is operating and at power during which time the fluid circulates and accumulates either dissolved or suspended impurities. A portion of the fluid is separated and then distilled at a total pressure substantially equal to the pressure prevailing in the fluid circuit when the reactor is at power. After the distillation forms vapor of the fluid and a residual concentrate containing the impurities, the vapor is returned to the primary fluid circuit and the residue is discarded. (B.L.M)

14052 REGULATING METHOD AND APPARATUS FOR NUCLEAR REACTORS. Ziegler, Albert (to Siemens-Schuckertwerke Aktiengesellschaft). U. S. Patent 3,223,589. Dec. 14, 1965. Priority date Jan. 30, 1960, Germany.

A method and apparatus are described for regulating a reactor having a core with fuel channels cooled separately from the rest of the core and a movable neutron-absorptive floatable control means. Coolant liquid is caused to boil to vapor in a selected fuel channel at a given operating condition below full power. The vapor is condensed in a chamber separate from the fuel channel, and the control means is variably displaced into various degrees of immersed condition within the condensation chamber relative to the core depending upon the boiling in the channel. (B.L.M.)

14053 ELECTRIC PROTECTION SYSTEM FOR NUCLEAR REACTORS. Troeger, Herbert (to Siemens-Schuckertwerke Aktiengesellschaft). U. S. Patent 3,223,590. Dec. 14, 1965. Priority date June 1, 1962, Germany.

A reactor safety circuit comprises three probes for separately responding to the same reactor condition to be sensed. Each probe has three contacts; and three lines are provided in mutually parallel relation, each including one contact from each trio of probe means. Each line means forms two parallel branches having a relay coil in series with the branches. The three contacts in each line means is distributed among the branches in a manner differing from the distribution in the branches of the other line means. Relay switches respond to the relay coils and are adapted to be series connected between a reactor control and a source so as to cut off the reactor if two out of three of the relay coils are unenergized. Each branch includes a low inductance check relay means. (B.L.M.)

14054 GASEOUS REACTOR CONTAINER. McLafferty, George H. (to United Aircraft Corp.). U. S. Patent 3,223,591. Dec. 14, 1965. Filed Aug. 27, 1962.

A nuclear energy conversion system is described in which thermal radiation rather than convection is used as the primary means of heat transfer. The device includes a container having walls of a material of the group consisting of quartz, fused silica, sapphire, CaF_2, and LiF, which are transparent to thermal radiation. The container is provided with an inlet and means for conducting a fluid nuclear fuel into the container through the inlet. Moderator-reflector means adjacent to the container induce a nuclear reaction in the fuel to produce high temperatures and thermal radiation. A focusing reflector outside the container and spaced from it receives the thermal radiation and reflects the energy created to a point remote from the container. Cooling means are provided for the container and reflecting means. (B.L.M.)

Criticality Studies

Refer also to abstracts 13005, 13019, 13020, 13069, 13700, 13703, 13723, 13735, 14127, and 14163.

14055 (AEEW-R-445) ARGOSY 4: A PROGRAMME FOR LATTICE CALCULATIONS. Macdougall, J. D. (Atomic Energy Establishment, Winfrith (England)). July 1965. 75p. Dep. BIS $2.20. HMSO 11s.

The methods of calculation that are used in the Argosy 4 program are described, together with the input requirements and output of the program. The equations that are solved by the program are included. (D.C.W.)

14056 (AWRE-O-99/65) SWAN—A MULTI-GROUP ONE-DIMENSIONAL DIFFUSION CODE FOR THE IBM-7030. Brickstock, A.; Davies, A. R. (Atomic Weapons Research Establishment, Aldermaston (England)). Jan. 1966. 46p. Dep. mn. BIS $1.40. HMSO 7s.

SWAN is a code for solving the multi-group diffusion equations in one-dimension. Spherical, cylindrical, or slab geometry is allowed, the last two requiring values of buckling to take account of leakage in directions transverse to the one being considered. Variable dimension arrays are used throughout so that the only restriction is on total problem size. The code is designed to take resonance self-shielding into account automatically and also to make approximate corrections for heterogeneity. (M.O.W.)

14057 (BNWL-183, Sect.I) MONTE CARLO CALCULATIONS OF OPTIMUM LOADING OF PLUTONIUM IN THERMAL REACTOR FUELS. Merrill, E. T. (Battelle-Northwest, Richland, Wash. Pacific Northwest Lab.). 17p. (CONF-651101-56).

The theoretical benefits of placing plutonium in the center of natural uranium fuel rods of thermal reactors are discussed. The RBU Monte Carlo code was used to estimate the interrelation of fissile content, fissile placement, and the ratio of water-to-fuel volume to the α of fissile isotopes. The discussion is based upon 80 calculations representing four enrichments of plutonia in natural urania (0.5, 1, 2, and 4%), four configurations of these enrichments, and five water volume to fuel volume ratios (0.625, 0.94, 1.18, 1.44, and 1.72) of these enrichments and configurations. (M.O.W.)

14058 (GEAP–4690) EXPERIMENTAL PLAN FOR THE PLUTONIUM SUBCRITICAL PROGRAM. Carver, J. G. (General Electric Co., San Jose, Calif. Atomic Power Equipment Dept.). Aug. 2, 1965. Contract AT (04-3)-189. 22p. (EURAEC–1559). Dep. mn. CFSTI $1.00 cy, $0.50 mn.

Work Performed under United States–Euratom Joint Research and Development Program.

The experimental studies to be performed during this program are outlined. Included are descriptions of subcritical lattice and the pressurized system. (M.O.W.)

14059 (IDO–17104) NUCLEAR TECHNOLOGY BRANCHES QUARTERLY REPORT, JANUARY 1–MARCH 31, 1965. (Phillips Petroleum Co., Idaho Falls, Idaho. Atomic Energy Div.). Dec. 1965. Contract AT (10-1)-205. 80p. Dep. mn. CFSTI $3.00 cy, $0.75 mn.

ATRC measurements in the A and B holes using zinc as a detector showed that the maximum fast flux in the ATR operating with a 40–50–60 MW power split will be 4.1×10^{14} n/cm^2-sec. Other ATRC measurements showed that the accidental voiding of a flux trap will produce a reactivity effect less than one dollar. Irradiation of aluminum cermet fuels of interest to high performance test reactors continued in the PAED-G-12 ETR water loop. Temperature measurements obtained during ETR Cycle 69 showed an alumina formation rate corresponding to that measured in ex-reactor experiments. Post-irradiation annealing tests on aluminum-clad sample fuel plates indicate that blistering occurs at considerably lower temperatures for oxide fuels than those containing the uranium-aluminide intermetallic compound. Prototype MTR and ETR fuel elements using powdered UAl_3 as a fuel material have performed satisfactorily in the reactor. Beryllium irradiated at 750°C to an integrated flux of 7.5×10^{20} n/cm^2 > 1 Mev shows little increase in compression yield strength and a decrease in ultimate compression strength and ductility. There is a release of gas from the beryllium of 0.223 cc He (STP) per cc beryllium. The application of the microprobe to the examination of irradiated fuel materials to determine the presence and distribution of fission products and plutonium was continued and extended. An unirradiated PuO_2-nichrome cermet fuel material was also examined. The study of the decay of Nd-149 was essentially completed. Energies of intensities are reported for conversion electrons and gamma-ray transition. Experimental and theoretical conversion coefficients are compared. A decay scheme is proposed. Two problems were studied on the analog computer. The first was concerned with the primary coolant system of the proposed Experimental Organic Cooled Reactor, and the second was a study of the design parameters of air pulsers used with extraction pulse columns at the Idaho Chemical Processing Plant (ICPP). In addition to these studies, a tape programmer for the In-Pile Fatigue Tester; a high-speed, ultra-reliable, pulse-counting system for use in the critical facilities; and instrumentation required for the detection, amplification, and counting of fringes produced by a gas-phase laser mirror combination were developed. (D.C.W.)

14060 (IDO–17114) IREKIN—PROGRAM FOR THE NUMERICAL SOLUTION OF THE REACTOR KINETICS EQUATIONS. Wagner, R. J. (Phillips Petroleum Co., Idaho Falls, Idaho. Atomic Energy Div.). Jan. 1966. Contract AT(10-1)-205. 84p. Dep. mn. CFSTI $3.00 cy, $0.75 mn.

The IREKIN program solves the one-group, space-independent, differential equations that describe the power behavior of a nuclear reactor in response to an arbitrary function of reactivity. In addition, the code yields numerical solutions to other ordinary differential equations which might be used to describe a particular model of reactor behavior. These additional differential equations may describe feedback mechanisms representing the dependence of the reactivity of the system upon time, reactor power, and energy release. The reactivity can be represented as an arbitrary function of time, power, energy, and the other variables which may have been specified in the differential equations. Operation and use of the code on the IBM 7040 are described. (M.O.W.)

14061 (IDO–17127) XKINEQ—A TWO-GROUP, TWO-DIMENSIONAL, MULTIREGION COMPUTER CODE FOR EXAMINING FLUX STABILITY IN NUCLEAR REACTORS IN THE PRESENCE OF ^{135}Xe. Sandquist, Gary M. (Phillips Petroleum Co., Idaho Falls, Idaho. Atomic Energy Div.). Jan. 1966. Contract AT(10-1)-205. 98p. Dep. mn. CFSTI $3.00 cy, $0.75 mn.

XKINEQ is a FORTRAN coded digital computer program for examining the stability of the neutron flux distribution in time in a reactor core under the influence of xenon-135. The program simulates kinetic equations which employ two-energy-group diffusion theory to describe the neutron flux and describes the two-dimensional radial-axial time behavior in multiregion reactor cores with cylindrical geometry and any two-dimensional time behavior in multiregion cores with rectangular geometry. (auth)

14062 (JUL–214-RG) MULTIGRUPPEN-WIRKUNGSQUERSCHNITTE FUER DIE STRUKTUR-, LOESUNGS- UND BRUTMATERIALIEN DES MOSEL-REAKTORS. (Multigroup Effective Cross Sections for the Structural, Solution, and Breeding Materials of the Mosel Reactor). Jung, Hans H. (Kernforschungsanlage, Juelich (West Germany). Institut fuer Reaktorentwicklung). Dec. 1964. 40p. Dep. mn.

Group cross sections for 68-group structure of the GAM-1 code for absorption, fission, and (n,2n) processes for the structural solution, and breeding materials of the Mosel Reactor concept (Ni, Mo, Cr, Fe, Na, Be, F, and Th) are given. The sources of the basic data are compiled. (tr-auth)

14063 (KAPL-M–6528) MEASUREMENT AND CALCULATION OF RELATIVE POISON-TO-FUEL CAPTURE RATIOS IN SLAB CORES. Heffley, R. A.; Watson, R. A.; Skolnik, Willard (Knolls Atomic Power Lab., Schenectady, N. Y.). Nov. 1965. Contract W-31-109-eng-52. 56p. Dep. mn. CFSTI $3.00 cy, $0.50 mn.

A method is described for measuring relative neutron capture rates between lumped burnable ^{10}B poison and fuel, using the gamma activity of ^{64}Ni as an indicator of the ^{10}B captures. The application of the method to a series of water-moderated critical assembly experiments with a metal-water ratio of 1.5, $\beta\gamma = 1.0$, a poison optical thickness of 1.4 (at 0.025 ev.), and various poison-plate and water-gap configurations is described. The experimental capture ratios are compared with both DRAM Monte Carlo and KARE diffusion theory calculations. The DRAM calculations agree with the measured values, within the experimental error, for most of the cases examined, but are about 10-12% lower than experiment when a large discrete water region is located near the poison. (auth)

14064 (LA–3427) DPC: A TWO-DIMENSIONAL DATA PREPARATION CODE. Hannum, W. H.; Carmichael, B. M. (Los Alamos Scientific Lab., Univ. of California, N. Mex.). June 28, 1965. Contract W-7405-eng-36. 64p. Dep. mn. CFSTI $3.00 cy, $0.75 mn.

The DPC code prepares input in R-Z geometry for two-dimensional neutronic codes. The input to the code is a free-format reactor description, based on data in a form available from engineering drawings. A general description of regions, in terms of multiple subregions, allows for explicit consideration of detailed structural forms. During the transformation of data, general thermal expansions are included. Also, considerable data checking and

evaluation are performed. Combined with the flexible narrative input, these features make the code useful in the preparation of error-free input for complex problems. (auth)

14065 (MIT–2344-4, pp 4-16) MATERIAL BUCKLING AND INTRACELLULAR THERMAL NEUTRON DISTRIBUTIONS. Barch, J.; Berube, N.; Kelley, B.; Supple, A.; Clikeman, F. M. (Massachusetts Inst. of Tech., Cambridge. Dept. of Nuclear Engineering).

Standard methods are developed to measure the material buckling and the intracellular thermal neutron distributions for lattices studied in the M. I. T. Lattice Facility. Results are obtained by these techniques on three lattices of uranium rods in D_2O. Results are given for 1.143% ^{235}U-enriched, 0.25-inch-diameter rods in triangular lattice spacings of 1.75 and 2.50 inches, and 0.947% ^{235}U-enriched, 0.75-inch-diameter uranium rods in a 2.50-inch triangular spacing. (auth)

14066 (MIT–2344-4, pp 63-9) PULSED NEUTRON STUDIES. Bliss, H. E. (Massachusetts Inst. of Tech., Cambridge. Dept. of Nuclear Engineering).

Work is described in three areas: pulsed neutron source die-away measurements to determine lattice parameters in clean, poisoned and substituted lattices; data analyses to obtain an accurate value of the fundamental mode die-away constant and, possibly, estimates for one or more higher harmonics; and measurements with and without a cadmium plate in the bottom of the lattice tank in an attempt to determine an effective return coefficient (albedo) for the lattice cavity. (auth)

14067 (MIT–2344-4, pp 80-8) SINGLE ROD EXPERIMENTS IN THE THERMAL ENERGY REGION. Pilat, E. E. (Massachusetts Inst. of Tech., Cambridge. Dept. of Nuclear Engineering).

Relative thermal fluxes are measured as function of horizontal distance from a single fuel rod immersed in heavy water in the MITR exponential facility. The fuel rod studied has a diameter of 1.010 in., and is made of natural uranium metal. The analysis of these data to obtain lattice and fuel parameters is carried out using a computer program (ONE-ROD) and an age-theory line source kernel. (T.F.H.)

14068 (MIT–2344-4, pp 89-100) TWO-REGION LATTICES. Gosnell, J. (Massachusetts Inst. of Tech., Cambridge. Dept. of Nuclear Engineering).

A study is carried out to determine the validity of physics measurements made in small central test regions of two-region, heavy-water lattices. Several lattices are studied experimentally. Each comprises a central test region surrounded axisymmetrically by an outer region. The test region has a central rod, surrounded by 2, 3, 4, or 5 rings of identical rods, of diameter 0.25 or 0.75 in. The outer region is comprised of 0.25-in.-diameter rods. Either region may have a lattice pitch of 1.25, 1.75, or 2.50 in. The 0.75-in.-diameter rods are 0.947%-^{235}U enriched U, and the 0.25-in.-diameter rods are either 1.027 or 1.143%-^{235}U enriched U. The parameters specifically studied include spatial variations of the Au–Cd ratios, and the radial variations of the axial relaxation lengths. (T.F.H.)

14069 (MIT–2344-4, pp 106-14) MINIATURE LATTICE STUDIES. Sefchovich, E. (Massachusetts Inst. of Tech., Cambridge. Dept. of Nuclear Engineering).

The applicability of miniature-lattice analyses of heavy-water reactors is investigated, with the goal of refining and extending this applicability. Both experimental and theoretical studies are carried out on heavy-water-moderated lattices of 0.25-in.-diameter U rods, at lattice pitches of 1.25, 1.75, and 2.50 in. and ^{235}U enrichments of 1.143 and 1.027%. The experimental and theoretical results are compared where possible. (T.F.H.)

14070 (MIT–2344-4, pp 115-34) RETURN COEFFICIENT MEASUREMENTS. Goebel, D. M. (Massachusetts Inst. of Tech., Cambridge. Dept. of Nuclear Engineering).

To facilitate the interpretation of lattice experiments, it is desirable to have well-defined boundary conditions. In the M. I. T. lattice, this is effected for thermal neutrons by wrapping the sides of the core tank with 0.020-inch-thick cadmium. However, epicadmium neutrons can still leak into and out of the core. In order to determine the extent and consequences of this "room return" effect, a series of experiments is made. The experiments yield the return coefficient for the M. I. T. lattice as a function of vertical distance along the core tank. (auth)

14071 (RL-SA–45A and Suppl.) SPATIAL KINETICS IN LARGE REACTORS. Hamric, J. P. (General Electric Co., Richland, Wash. Hanford Atomic Products Operation). 1965. Contract AT(45-1)-1350. 26p. (CONF-651101–62). Dep. mn. CFSTI $2.00 cy, $0.50 mn.

From 13th Conference on Remote Systems Technology, Washington, D. C.

The importance of spatial dependence in kinetics calculations was studied for reactivity changes $\ll B/2$ per second. The results show that the point kinetics model can lead to significant errors in evaluating even very small reactivity changes. (D.C.W.)

14072 MEASUREMENT OF THE NEUTRON FLUX DISTRIBUTION IN A HOMOGENEOUS SUSPENSION REACTOR. Bruynesteyn, W. Atoomenergie Haar Toepass., 7: 182-90(Sept. 1965). (In Dutch).

The problems in the measurement of the neutron flux distribution in a homogeneous liquid reactor were considered. A flow diagram is given of the method developed for the measurement of the neutron flux distribution. Some of the results obtained are reported. (tr-auth)

14073 ONE-GROUP PARAMETERS BY NEUTRON WAVE MEASUREMENTS. Mueller, K.-H. (CCR, EURATOM, Ispra, Italy). Nucl. Instrum. Methods, 39: 355 (Jan. 11, 1966).

It is shown that the neutron wave technique makes it possible to determine the parameters for a one-group representation of the neutron flux by means of the measurement of the relaxation length and the corresponding propagation time. (J.F.P.)

14074 APPLICATION OF ADIABATIC APPROXIMATION TO THE SPACE-DEPENDENT KINETICS OF BOILING WATER REACTORS [Thesis]. Nishihara, Hideaki. Ann Arbor, Mich., Univ. of Michigan, 1965. 171p.

The adiabatic approximation implies that the flux distribution at an instant of time can be replaced by the steady state flux distribution if the reactor is made critical with the reactor constants at that time by changing the mean number of neutrons born per fission. Instead of solving the diffusion equation at each time interval, the flux distribution and the reactivity are obtained by the following steps: (1) determine the steady state flux distributions and the reactivity for various conditions the reactor may assume during the transient, (2) express these quantities as functions of the reactor conditions, and (3) solve the reactor kinetic equations that describe the neutron flux level, the correlations obtained in step (2), and the feedback equations appropriate to the reactor system. An analytical model was formulated following these three steps. The numerical calculations were performed on the IBM-7090 computer for the sample boiling reactor whose core height is 200 cm and whose rated power is 200 Mw (th). In step (1) over one hundred void distribution patterns were assumed and steady-state diffusion calculations were performed for these distributions. In step (2) the correlations of the flux and reactivity to the void distribution were obtained by the stepwise regression code. In step (3) a computer program that carries out the numerical solution was written. The space-time behavior of the sample boiling reactor was studied for three kinds of external perturbations: (1) a step increase in reactivity of 90 cents, (2) sinusoidal variations in reactivity with amplitude of ten cents and (3) sinusoidal variations in vertical acceleration with amplitude of 0.5 g. For the step increase in reactivity a large distortion in the neutron flux distribution was observed; in the latter two cases, however, the space-dependent effect was of little importance. It agrees with experi-

mental observations of the Dresden boiling water reactor. (Dissertation Abstr.)

14075 SURVEY OF PULSED NEUTRON SOURCE METHODS FOR MULTIPLYING MEDIA. Garelis, E. (General Electric Co., Pleasanton, Calif.). pp 3-23 of STI/PUB/104(Vol. 2).

The methods by which the reactivity is derived from the α-measurement, e.g., the α-delayed critical measurement and the recent ($k\beta/l$) method, are discussed. The fundamental modal treatments are examined in the light of the theory of the pulsed neutron source techniques as developed for the ($k\beta/l$) model. The implications of the pulsed neutron source theory to obtain precise decay constants and suitable data for the analysis of pulsed systems are considered. Experimental work is reviewed that shows the advantages as well as the limitations of the ($k\beta/l$) technique. The use of pseudo-random impulse response methods with cross correlation between the input and output for the determination of the Green's function of a multiplying assembly is also discussed. It is shown that the information obtained by the pseudo-random method is identical to that obtained from the repetitively pulsed method. Thus, this makes it possible to apply the methods developed for the repetitive to that of the pseudo-random technique. (auth)

14076 PULSED-SOURCE EXPERIMENTS WITH MULTIPLYING AND NON-MULTIPLYING HEAVY WATER SYSTEMS. Utzinger, E.; Heer, W.; Lutz, H. R. (Swiss Federal Inst. for Reactor Research, Wuerenlingen). pp 119-36 of STI/PUB/104(Vol. 2).

An extensive series of measurements with a pulsed source of the $^3T(d,n)^4He$ type was performed at the subcritical facility MINOR. Three types of experiments were carried out to measure: decay constants of prompt neutron modes in natural and slightly enriched lattices; subcritical reactivity by means of the prompt decay and delayed neutron tails in natural and slightly enriched lattices; and anisotropy of the thermal diffusion constant in D_2O containing different numbers of parallel empty tubes of various size. The time-dependent thermal neutron flux was measured in each system at different axial positions to obtain decay constants of the prompt modes for different axial bucklings (Fourier analysis) without changing the actual height of the D_2O level. The experimental values were compared with theoretical two-group parameters. Limitations of the technique are discussed. In addition, reactivity in highly subcritical systems with $\rho \geq -40$ \$ was measured directly by utilizing the delayed neutron tail of the pulses. Results are compared with static measurements and show rather good agreement. (auth)

14077 STUDY OF HOMOGENEOUS CORE ASSEMBLIES USING PULSED NEUTRON SOURCES. Bruna, J. G.; Brunet, J. P.; Buchet, J.; Houelle, M.; Tellier, H. (Centre d'Etudes Nucleaires, Saclay, France). pp 157-78 of STI/PUB/104(Vol. 2). (In French).

The pulsed neutron technique was applied to the study of light-water-moderated homogeneous core assemblies. Using fissile materials in solution form it is easy to achieve large variations in geometrical buckling and moderation ratio. In the initial series of experiments, the fuel consisted of ^{235}U or ^{233}U in the form of uranyl nitrate. The solution concentrations used varied from 44 to 326 g of uranium per liter. Adoption of a coherent series of cross sections made it possible to deduce, from the variations in the prompt neutron decay constant as a function of geometrical buckling, data on the non-leakage probability and the slowing-down area. Effective cross sections calculated on the basis of assimilating light water to a secondary differential thermalizer were adopted. Interesting comparisons are made possible by the use of two fissile materials with markedly different η and resonance capture values. In a second series of experiments, devoted mainly to safety measures, the maximum permissible concentrations in various containers at processing plants were deduced by measuring the prompt neutron decay constants in weak plutonium nitrate solutions. (auth)

14078 THE COMMON BELGONUCLEAIRE-CEN PROGRAMME FOR THE SURVEY STUDY OF UO_2–PUO_2–H_2O LATTICES BY THE PULSED NEUTRON TECHNIQUE. Debrue, J. (Centre d'Etude de l'Energie Nucleaire, Mol, Belg.); Motte, F.; Delrue, R.; Fossoul, E.; Stievenart, M.; Tavernier, G. pp 181-91 of STI/PUB/104(Vol. 2).

In the frame of the work performed on plutonium recycling in light water reactors, a good deal of effort is devoted to the determination of the $PuO_2-UO_2-H_2O$ lattice nuclear parameters. The scarcity and the cost of plutonium at high 240 content is such that one must rely on experimental methods involving small quantities of fuel, in other words, subcritical assemblies. The pulsed neutrons technique was chosen as a valuable, handy and fast tool for survey studies of plutonium-fueled lattices. Such a survey aims at the measurement of several integral parameters such as infinite multiplication factor, material bucklings, temperature coefficients, etc., for different kinds of fuel (U-enrichment, Pu content, ^{240}Pu isotopic content, etc.), lattices (rod diameter, water-to-fuel ratio poisoning, etc.), and temperatures. As a first step in the program, a 5% enriched UO_2 lattice was studied by the proposed technique, and preliminary results pertaining to that particular experiment are given. (auth)

14079 KINETIC AND STEADY-STATE MEASUREMENTS OF VARIABLE-PITCH ENRICHED URANIUM, LIGHT WATER LATTICES. Gavin, P. H. (Univ., Lausanne, Switzerland). pp 219-30 of STI/PUB/104(Vol. 2). (In French).

The decay of the neutron flux in a subcritical reactor after a sudden shutdown (following steady-state operation) can be analyzed into a series of spatial and time harmonics. Spatial harmonics can be deduced from steady-state operation. The time constants of exponentials are characteristic of the core assembly and in a two-group theory the lattice and reactivity parameters can be deduced from measurements of flux in relation to time. These parameters are determined experimentally for various bare cores composed of enriched UO_2 rods in light water and are used to study a variable-pitch lattice and predict its kinetic and steady-state behavior. (auth)

14080 PULSED NEUTRON STUDIES OF BeO-NATURAL URANIUM LATTICES. Joshi, B. V.; Nargundkar, V. R.; Subbarao, K. (Atomic Energy Establishment Trombay, Bombay). pp 231-37 of STI/PUB/104(Vol. 2).

The use of the pulsed neutron method for determination of the diffusion parameters and multiplication constants of lattices is described. The diffusion parameters and multiplication constants of BeO-natural uranium lattices are obtained by this method. The uranium rods used were 2.92 cm diameter clad in aluminum 0.072 cm thick and were arranged vertically in channels of square cross section 5 × 5 cm, in a square lattice of pitch 15 cm. The neutron bursts were produced from a cascade accelerator by pulsing the ion source and using the Be(d,n) reaction. The detectors were enriched boron trifluoride proportional counters. The space and time harmonics were eliminated. The decay constant of the fundamental mode was determined for several bucklings, far from criticality. In these calculations the effect of diffusion cooling and anisotropy was taken into account. All the diffusion and multiplication constants were determined by the method of least squares fit by three different approaches. The prompt critical buckling was determined by solving the decay constant equation for $\lambda = 0$. (auth)

14081 SUBCRITICALITY DETERMINATION ON A REFLECTED GRAPHITE SYSTEM BY THE PULSED NEUTRON METHOD. Sumita, K.; Kaneko, Y. (Japan Atomic Energy Research Inst., Osaka). pp 241-59 of STI/PUB/104(Vol. 2).

The usual concept of reactivity is based on the treatment of a persisting mode of neutron multiplication. The experimental methods for reactivity measurement in a highly subcritical system which are based on the measurement of the persisting mode have theoretical and experimental difficulties. The other reactivity measurement methods, which are based on that of the prompt mode (pulsed neutron experiment, Rossi-α method, etc.), have other difficulties, because the prompt neutron lifetime changes depending on subcriti-

cality, and the relation with the method based on persisting mode is very complicated in a reflected system. An attempt is made to establish another concept to avoid this problem, and to describe exactly the situation of neutron multiplication in a reflected subcritical system. The concept is that the prompt neutron decay constant of fundamental mode α should be used directly as a measure of neutron multiplication, because this quantity satisfies the following two sufficient, fundamental requirements: to be uniquely free from space dependence and detector specification, and to be calculable from the fundamental Boltzmann equations. To prove that α does satisfy these requirements, a series of pulsed experiments was made at various subcritical states in a reflected graphite-moderated enriched fuel system (SHE). The experimental results confirmed that α_{00} has the same value at any point of core and reflector, by means of the separation of spatial harmonics, using bare and cadmium-covered BF_3 counters. The state of SHE is changed by diminishing the core with or without a center control rod and by adding distributed poison to the core or to the reflector. The multigroup subcritical kinetics of the reflected reactor were extended, and a direct comparison between the experimental results from pulsed neutron experiments and the calculated values from multigroup treatment using P_1 and S_4 approximation with regard to the systems was made to investigate this concept. Calculated values of α_{00} for the core-diminished subcritical status with and without a control rod showed fairly good agreement with the measured values. In addition the time-dependent spectra changes of the subcritical systems were also investigated in the experiments. (auth)

14082 PULSED NEUTRON REACTIVITY MEASUREMENTS IN THE NEAR-CRITICAL STATE. Einfeld, K.; Hennies, H.; Memmert, G.; Ullrich, W. (Interatom, Bensberg, Ger.). pp 299-312 of STI/PUB/104(Vol. 2).

Measured and calculated thermal neutron decay constants λ are reported for various 5% enriched zirconium hydride moderated lattices, using UO_2 and $ZrH_{1.7}$ rods in an aluminum matrix. By performing measurements in the critical and in near-critical states values of β/l could be determined. The resulting β/l values were used to calculate reactivity worths of different absorber rods and absorber arrangements from the measured decay constants. Several measurements were evaluated applying the modified pulsed source technique of Garelis and Russell. (auth)

14083 PULSED NEUTRON EXPERIMENTS ON FAST AND INTERMEDIATE SYSTEMS. Storrer, F. (Centre d'Etudes Nucleaires, Cadarache, France). pp 317-36 of STI/PUB/104(Vol. 2).

Experimental and theoretical aspects of the work which has been done on the pulsing of fast and intermediate assemblies are critically reviewed. It is indicated that much less work has been done on the theoretical analysis of such experiments than has been the case for thermal neutron systems. The essential differences between the experimental and theoretical aspects of pulsed experiments on fast and thermal systems are indicated; the areas where research is in progress and where more research is called for are outlined. Special emphasis is placed on the comparison between different types of kinetic experiments. It is shown that all these experiments, including the modulated experiments, the noise experiments and also static source amplification experiments, can be considered as special cases of a more general class of experiments in which the neutron density is a function of time, space, and energy. The different objectives of such experiments are discussed as well as the choice of the experiment which will best meet any particular objective. (auth)

14084 PULSED NEUTRON MEASUREMENTS IN FAST ASSEMBLIES. Comte, R.; Massieux, J.; Roche, M. (Centre d'Etudes Nucleaires, Saclay, France). pp 337-56 of STI/PUB/104(Vol. 2). (In French).

Kinetic measurements with pulsed neutrons were performed in fast subcritical assemblies with a plutonium core and a uranium or copper reflector. The apparatus is described, and the data are presented and discussed. The results obtained by the pulsed neutron and by conventional methods are compared. A discussion of some aspects of the signal-to-noise ratio and the performance of the accelerator and electronics system, with a view to improving accuracy of the method, is included. (auth)

14085 DETERMINATION OF NEUTRON LIFETIMES AND REACTIVITIES IN THE FAST CRITICAL FR-0 ASSEMBLY. Bergstroem, A.; Brunfelter, B.; Kockum, J. (Research Inst. of National Defence, Stockholm). pp 357-71 of STI/PUB/104(Vol. 2).

The pulsed source technique was used to measure negative reactivities ranging from 0.05 to 10% in the first core of the fast critical assembly FR-0. The loading contains a 20% enriched uranium metal core with a thick copper reflector. The decay constant of the main mode was deduced by a least squares fitting to the measured data, approximating the higher modes with one second exponential decay. The reactivities were calculated. The decay constant is determined with a relative statistical uncertainty of about ±3%, the reactivity with an uncertainty of ±4%. Comparisons were made with Rossi-α measurements. When trying to evaluate the lifetime with the aid of one-region kinetic equations, it is found that the lifetime increases 40% between criticality and 1% subcriticality. The value of the lifetime obtained is about 60% too high compared to 14-group calculations. Two-region kinetic equations using separate lifetimes in core and reflector give closer agreement between theory and experiment. (auth)

14086 SOME MEASUREMENTS OF FAST REACTOR SPECTRA BY THE TIME-OF-FLIGHT TECHNIQUE USING A PULSED NEUTRON SOURCE. Paterson, W. J.; McCormick, W. B.; Weale, J. W. (Atomic Weapons Research Establishment, Aldermaston, Eng.). pp 417-33 of STI/PUB/104(Vol. 2).

The zero-energy fast reactor VERA is equipped with a pulsed neutron source and a 50-m neutron flight path and these facilities were used for time-of-flight neutron spectrometry in the energy range 100 ev to 50 kev. The results are discussed and are compared with calculated values. (auth)

14087 THEORETICAL CONSIDERATIONS CONCERNING THE PULSATION OF FAST SUBCRITICAL ASSEMBLIES. Stievenart, M. (Societe Belge pour l'Industrie Nucleaire, Brussels). pp 461-77 of STI/PUB/104(Vol. 2).

The use of a punctual multigroup energy model for interpreting time eigenvalues measured on fast neutrons subcritical bare assemblies is discussed. The inadequacies of this model are pointed out. The definition of a punctual continuous energy model is given, and the possibility of treating adequately inelastic and elastic scattering is discussed. It is also shown that the continuous energy model presented can be reduced, in some particular cases, to simpler and more classical models used in reactor physics. The energy-space-time problem is also emphasized. The possibility of using a multigroup multinodal model is discussed for interpreting the time eigenvalue measured in pulsed neutron experiments. (auth)

14088 CONTRIBUTION TO THE THEORY OF PULSED AND MODULATED EXPERIMENTS ON FAST NEUTRON MULTIPLYING MEDIA. Cadilhac, M.; Govaerts, P.; Hammer, P.; Moore, M.; Nicolaenko, B.; Storrer, F. (Centre d'Etudes Nucleaires, Cadarache, France). pp 479-91 of STI/PUB/104(Vol. 2).

The structure of the analytical function $k(p)$ is studied to disclose the core conditions which it may be possible to obtain in the course of pulsed and modulated experiments. In the case of pulsed experiments, the existence of a well-defined persistent exponential mode cannot necessarily be assumed at the outset. The initial formula used is one in which energy is viewed continuously, so as to obviate the artificial features introduced by the usual multigroup method. Using quite general hypotheses, it can be shown that $k(p)$ takes the form: $k(p) = \int_{\lambda_0}^{\lambda_1} [\kappa(\lambda)d\lambda]/(\lambda + p)$. From this, it can be deduced that the time distribution of pulse-triggered fissions is only dominated asymptotically by a pure exponential mode for core assemblies. The multigroup method provides a stepped approximation of the cu-

mulant of $\kappa(\lambda)$. It is useful to consider the synthetic forms of $\kappa(\lambda)$, involving a few parameters whose values have to be adjusted. For example, $\kappa(\lambda)$ can be considered proportional to $(\lambda - \lambda_0)^r(\lambda_1 - \lambda)^s$, especially as this expression is suggested by rigorous calculation of $\kappa(\lambda)$ in a model in which the slowing-down is expressed by a nucleus of the Wigner or Greuling-Goertzel type and the cross sections obey certain simple analytical laws. Various illustrations and applications of the methods described are given. (auth)

14089 MEASUREMENTS OF THE PROMPT NEUTRON DECAY CONSTANT OF THE VERA REACTOR USING THE PULSED SOURCE METHOD. Weale, J. W.; Paterson, W. J.; Goodfellow, H.; McTaggart, M. H. (Atomic Weapons Research Establishment, Aldermaston, Eng.). pp 759-74 of STI/PUB/104(Vol. 2).

The prompt neutron decay constant was measured by the pulsed source method for a number of uranium- and plutonium-fueled fast reactor assemblies. The results are discussed and are compared with values obtained on the same systems using the Rossi-α method. (auth)

14090 A STUDY ON INTERACTION OF SUBCRITICAL ASSEMBLIES. Kiyose, R.; Shimazaki, Y.; Enomoto, S. (Tokyo Univ.). Vienna, International Atomic Energy Agency, 1965, Preprint No. SM-70/24, 12p. (CONF-651103-23). ORINS.

From IAEA Symposium on Criticality Control of Fissile Materials, Stockholm.

Simplified expressions for critical conditions of interacting sub-critical assemblies are derived for several cases of pairs of identical slabs and cylinders. The applied theory is a one-group diffusion theory coupled with a simplified boundary condition, which uses a fraction ρ of neutrons emitted through the interacting surface entering the other surface as a key parameter. As an example, the criticality condition for pairs of identical slabs is treated. For the purpose of estimating the fraction ρ experimentally without the use of critical experiment, a pulsed neutron technique is applied to a pair of coaxial, identical cylinders. Taking a system of known neutronic parameters, i.e., a pair of graphite cylinders in this case, the effective geometrical buckling B^2g and then the fraction ρ are estimated from the measured values of the decay constant corresponding to the fundamental mode. The pulsed neutron is generated by D-T reaction, using a 150 kv Cockcroft-Walton accelerator. Decay constants are measured by a BF_3 counter and a 32-channel time analyzer. The measured values of B^2g and ρ are compared with the values calculated by the method mentioned in the previous paragraphs. The pulsed neutron measurement gives somewhat lower values for B^2g and higher values for ρ. (auth)

14091 SOME QUESTIONS OF NUCLEAR SAFETY. Dubovskii, B. G.; Kamaev, A. V.; Vladykov, G. M.; Bogatyrev, V. K.; Gurin, V. N.; Diev, L. V.; Kuznetsov, F. M.; Sviridenko, V. Ya. (Physico-Energetics Inst., Obninsk, USSR). Vienna, International Atomic Energy Agency, 1965, Preprint No. SM-70/46, 17p. (In Russian). (CONF-651103-25). ORINS.

From IAEA Symposium on Criticality Control of Fissile Materials, Stockholm.

Results of experiments and calculations to determine the effectiveness of annular absorbing inserts and absorber rod grids in homogeneous, water-uranium critical assemblies are given. The effectiveness was estimated from the change in critical volume (critical height or critical mass) of a solution of uranium when an absorber is introduced into the core and also in reactivity units. The experiments to determine the effectiveness of absorbing inserts were performed with aqueous solutions of the salt $UO_2(NO_3)_2$ (90% enriched uranium) in the concentration range 34-500 g/l. The effectiveness was studied for thin absorbing inserts with cadmium and boroncarbide and of cadmium-water and steel inserts in cylindrical vessels, with water reflectors and without reflectors. The diameters of the cores are 400, 500, 650, and 700 mm. The dependence of effectiveness on the geometrical dimensions of the inserts, the diameter of the core and the uranium concentration in the solution was studied. The maxium effectiveness was found to be possessed by annular inserts with a mean radius $r = (0.4 - 0.5)R_e$, where R_e, is the equivalent radius of the assembly. Experiments to determine the effectiveness of absorber rod grids were carried out with aqueous solutions of $UO_2(NO_3)_2$ (uranium enriched to 90, 10, and 5%) in a cylindrical tank of diameter 1100 mm. Grids of boron carbide rods occupied 10 to 40% of the core volume. The critical mass in this reactor amounted to 100 kg of U^{235}. Multigroup calculations of the effectiveness of inserts and rod grids were made in a P_1 approximation; there was satisfactory agreement with the experiment. It is shown that the use of absorbing inserts and grids of rods constitutes an efficient method of ensuring nuclear safety in the processing and storing of large volumes of solutions of fissile materials. An account is also given of methods of calculating the critical parameters of bodies of irregular shape. A general method is proposed for calculating the geometrical parameter of a body of arbitrary shape. Calculations of the critical size of bodies in the form of cones, hemispheres and intersecting cylinders are compared with experimental values. A table of integrals is given for calculating geometrical parameters. (auth)

14092 ADMINISTRATIVE ASPECTS OF THE CRITICALITY CONTROLS USED IN PROGRAMS FOR BASIC CRITICALITY RESEARCH, REACTOR DEVELOPMENT, AND MATERIALS PROCESSING. Wood, D. P.; Giessing, D. F. (Atomic Energy Commission, Albuquerque, N. Mex.). Vienna, International Atomic Energy Agency, 1965, Preprint No. SM-70/48, 13p. (CONF-651103-26). ORINS.

From IAEA Symposium on Criticality Control of Fissile Materials, Stockholm.

The administrative and procedural aspects of criticality controls used by a field office of the United States Atomic Energy Commission (USAEC) in programs that include reactor criticals, research and materials testing reactors, and power reactor development are described. Situations encountered include handling, storing, and processing large quantities of uranium-235 and plutonium-239 of various configurations and compositions in laboratories and operations which gather basic criticality data, processing of fissile material, and varied reactor research and development programs including fuel materials. Similar situations exist for uranium-233 and plutonium-238 on a smaller laboratory scale. The administrative controls and interactions of the USAEC field office and the operating contractors, who operate these installations for the USAEC, are outlined. (auth)

14093 THE GEM MONTE CARLO CODE AND ITS USE IN SOLVING CRITICALITY PROBLEMS. Longworth, T. C. (United Kingdom Atomic Energy Authority, Risley, Eng.). Vienna, International Atomic Energy Agency, 1965, Preprint No. SM-70/7, 23p. (CONF-651103-17). ORINS.

From IAEA Symposium on Criticality Control of Fissile Materials, Stockholm.

The criticality assessment of chemical and metallurgical plants processing fissile materials, and of the storage and transport of these materials, requires a program capable of handling very complicated geometrical arrangements. The only method which readily lends itself to such complexity is the Monte Carlo method of calculation. The latest version of the GEM code, written for the IBM 7090, is designed to facilitate neutron tracking through systems of any specified geometry. The tracking cycle is defined by dividing the system into a "Core" and a "Reflector" by selecting a boundary across which the distribution of neutrons settles quickly. The method of tracking is then designed so as to yield directly the surface multiplication, M, of the core, and the reflection, R, of the reflector. Thus the parameter MR, an immediate measure of criticality, is readily determined. Many other counts are taken during the tracking, and if desired an estimate of K-effective may be obtained by the program from a simple formula. A general description of the methods used in the GEM program is given, including some of the more recent developments, showing examples of the sort of systems which may be handled by GEM. Examples are given of several problems

of varying geometrical complexity which have been solved using the GEM code, such as storage arrays, transport containers, etc. (auth)

14094 THE USE OF THE ADJOINT TRANSPORT EQUATION IN SOLVING CRITICALITY PROBLEMS. Pendlebury, E. D. (Atomic Weapons Research Establishment, Aldermaston, Eng.). Vienna, International Atomic Energy Agency, 1965, Preprint No. SM-70/4, 14p. (CONF-651103-15). ORINS.

From IAEA Symposium on Criticality Control of Fissile Materials, Stockholm.

Some criticality problems can most conveniently be solved by calculating a suitable adjoint problem, leading to a considerable saving in computer time. Such is the case, for example, if one wishes to know the surface multiplication of a proposed transport container, containing fissile material, for a specified incident angular distribution as a function of incident neutron energy. In problems of this kind the computer time required may be reduced by a factor of order 10 by solving the appropriate adjoint problem. The kinds of criticality problem which can be solved by solving a suitable adjoint problem are discussed together with the method of choosing the appropriate adjoint problem. Some numerical examples, computed with the S_n program STRAINT, are given to demonstrate how the method works in practice. (auth)

14095 CIRCUIT ARRANGEMENT FOR THE MEASUREMENT OF THE RECIPROCAL OF THE PERIOD OF A NUCLEAR REACTOR. Amano, Noboru (to Nihon Genshiryoku Kenkyu Sho). German Patent 1,205,206. Nov. 18, 1965. Priority date Nov. 7, 1961, Japan.

A neutron detector is directly connected to one or two oscillator circuits (multivibrators) the frequency of which is proportional to the signal of the detector. Means are provided for differentiating the oscillator frequency. (Gmelin Inst.)

Design and Feasibility

14096 THE PULSED FAST REACTOR AS A SOURCE FOR PULSED NEUTRON EXPERIMENTS. Raievski, V. (EURATOM, Ispra, Italy); Kley, W.; Haas, R.; (and others). pp 553-73 of STI/PUB/104(Vol. 2).

The physics layout of a pulsed fast reactor is discussed in detail and the choices of the free reactor parameters in relation to reactor physics, the experimental needs and metallurgical limitations are explained. It is shown that even with the very conservative values of fuel burnup chosen, mean specific power production and pulsation device safety, the performance figures for pulsed neutron experiments in the thermal and sub-thermal energy region compare favorably with those obtained at high flux reactors, which are close to the upper limits of possible development. The optimization of the moderators, which serve as sources for thermal and cold neutrons, and the interaction of the moderators on the reactor performance characteristics are discussed. The epithermal neutron source is also described. Finally, some safety considerations, which are specific for the pulsed nature of the reactor, are presented. (auth)

14097 IMPROVEMENTS IN OR RELATING TO APPARATUS AND METHOD FOR PRODUCING CONTROLLABLE SLOW NEUTRON CHAIN REACTION. Martin, Arthur Francis (to Hercules Powder Co.). British Patent 1,016,048. Jan. 5, 1966. Filed July 22, 1964.

A reaction system for producing a controllable slow neutron chain reaction comprises a reactor core containing a critical mass of fissionable material suspended as a powder in the coolant gas, a moderator substantially surrounding the reactor core, and a number of heat exchangers located outside of the reactor core and moderators. Conduit means connect the core with each heat exchanger for the passage of the suspension of fissionable material from the core to the heat exchangers, while return conduit means carry the suspension from the heat exchanger to the core. In each reactor core-heat exchanger circuit in which the suspension of fissionable material is circulated, means are provided for continuously cycling the suspension therein and throughout the system. Provision is made for the addition of both fissionable material and coolant gas to the system and for the removal of fissionable material and fission products from the system for processing. (B.L.M.)

14098 BOILING WATER REACTORS, NUCLEAR REACTORS, ESPECIALLY WITH EXCHANGEABLE FUEL ELEMENTS. Zapff, Joachim (to VEB Atomkraftwerk Rheinsberg mit Betriebsteil, Berlin). German Patent 1,205,204. Nov. 18, 1965. Filed Apr. 13, 1960.

A boiling water reactor is described, which comprises a hexagonally shaped core which is rotable about a horizontal axis and is composed of six equal triangular pyramids. Control of the nuclear reactor is achieved by neutron absorbing plates located at the periphery of the core. (Gmelin Inst.)

14099 METHOD OF CONTROLLING THE REACTIVITY OF A NUCLEAR REACTOR. Maldague, Pierre Edmond Jules Marie; de Waegh, Francois Albert (to Societe Anglo-Belge Vulcain, Societe Anonyme). U. S. Patent 3,222,254. Dec. 7, 1965. Filed Feb. 5, 1963.

A method of controlling the reactivity of a nuclear reactor having a core through which a water coolant-moderator flows consists of varying the light to heavy water ratio to control reactivity variations and modifying during normal power operation the concentration of a poison in response to the water temperature to maintain a combined effect upon reactivity of ^{135}Xe and poison substantially equal to that of ^{135}Xe equilibrium poisoning at reactor full power. A portion of the primary fluid is deviated through a separate circuit in which the poison is removed by distillation. Boron in the form of boric acid is a suitable poison. (B.L.M.)

14100 HETEROGENEOUS NUCLEAR REACTOR LIQUID MODERATED AND COOLED. Bernard, Jean A.; Bunge, Joachim; Dufresne, Jacques; Volta, Giuseppe (to European Atomic Energy Community-Euratom). U. S. Patent 3,226,301. Dec. 28, 1965. Filed Oct. 2, 1963.

A liquid moderated (heavy water) and liquid cooled (organic liquid) heterogeneous reactor comprises a tank with a heat insulating shield dividing the tank into an upper compartment for the heavy water and a lower collector compartment for the heat carrying organic liquid. A hollow completely closed heat insulated collector mounted in the collection compartment is partially filled with the heat carrying fluid. A number of reactor channels are vertically mounted in the tank. Each channel has an inner power tube of sintered Al and an outer calender tube of Al or zircaloy coaxial with and spaced from the power tube. Both the tubes extend through the heat insulating shield and the wall of the collector and have their ends immersed in the organic liquid. Gas is delivered under pressure into the space between the tank and the collector, and the pressure in the space is maintained at a valve between that of the heat-carrying fluid at the outlet for the tubes and that of the fluid in the collector. Inlet and outlet means for the gas are provided on the tubes interconnecting the space between the tank and the collector and the space above the liquid in the collector. An expansion joint is provided below the inlet means to permit the power tube to expand axially without stress. (B.L.M.)

14101 HETEROGENEOUS ATOMIC REACTOR. Hargoe, Bernt Torsten Allan; Dahlgren, Dick Gilbert (to Aktiebolaget Atomenergi). U. S. Patent 3,227,621. Jan. 4, 1966. Priority date May 11, 1960, Sweden.

A self-regulating heterogeneous nuclear reactor of the pressurized water type designed to operate at temperatures in excess of 100°C comprises a pressure vessel, means for introducing heavy water into the bottom of the vessel, and an outlet for the heated heavy water adjacent to the upper end of the vessel. The fuel is in the form of spaced, parallel, cylindrical rods of fissionable material distributed over the entire cross section of the vessel and extend in the direction of flow of the heavy water. The rods each have a diameter of less than 20mm and are so spaced that the ratio of the volume of heavy water to volume of fuel is more than

5 to 1. The spaces between the columns of fuel elements are substantially free of partitions so that the heavy water filling the spaces serves both as coolant and moderator and is free to move in all directions. (B.L.M.)

Fuels

14102 (BNWL–183, Sect.II) A NEW FUEL CONFIGURATION TO INCREASE PLUTONIUM VALUE. Deonigi, D. E.; Nail, J. H. (Battelle-Northwest, Richland, Wash. Pacific Northwest Lab.). 19p. (CONF-651101–57).

The burnup characteristics and the value effects of concentrating plutonium in the core of fuel rods of water moderated reactors were investigated. A zero-dimensional version of the ALTHAEA burnup code was used to assess the effect that reduced cross sections and alphas would have both on the value of plutonium in thermal reactors and on the burnup characteristics of tight pencil fuel. The reactivity and the power distribution of tight pencil fuel are compared with normal uniformly mixed, or homogeneous, fuel. (M.O.W.)

14103 (MIT–2344-4, pp 48-62) MEASUREMENT OF INTEGRAL PARAMETERS IN FUEL RODS. Papay, L. T.; Robertson, C. G.; Hellman, S. P.; Driscoll, M. J. (Massachusetts Inst. of Tech., Cambridge. Dept. of Nuclear Engineering).

Bare and Cd-covered foil irradiations in heavy-water lattices are used to measure the $^{238}U/^{235}U$ fission-rate ratios, the ^{238}U total-capture/epicadmium-capture ratios, the ^{235}U epicadmium/subcadmium fission-rate ratios, and the ^{238}U-capture/^{238}U-capture/^{235}U-fission rate ratios in these lattices. Details of the measurements and their uses in determination of the desired ratios are given for two cases: 0.25-in.-diam, 1.143%-enriched-U rod lattices; and 0.75-in.-diam, 0.947%-enriched-U rod lattices. (T.F.H.)

14104 (ORNL–3885, pp 244-50) FAST REACTOR DEVELOPMENT. (Oak Ridge National Lab., Tenn.).

Two types of fuel elements were investigated for fast gas-cooled reactors. The design and planned operating conditions for both elements are summarized. (M.O.W.)

14105 FUEL ELEMENTS AND PRIMARY MATERIALS. REPORT PRESENTED TO THE FORATOM CONGRESS. Leger, Jean-Etienne. Bull. Inform. A.T.E.N. (Ass. Tech. Energ. Nucl.), No. 56, 20-30(Nov.-Dec. 1965). (In French).

The production capacities now in existence or under construction for the preparation of fuel elements are summarized. The existing and projected capacities for the reprocessing of fuel elements are indicated, and data are given on the estimation of reprocessing costs. The fuel cycles are then considered from an economic viewpoint. The long-term French needs in primary nuclear materials are outlined, and the position of France with respect to the long-term supply of natural uranium is discussed. The price of natural U, Pu, and enriched U is considered. Uranium reserves, both known and prospective, are considered. (J.S.R.)

14106 A STUDY OF THE THERMAL STRESSES IN FUEL ELEMENT. Wang, Pin-Fu (National Tsing Hua Univ., Hsinchu, Taiwan). Ho Tsu K'o Hsueh, 4: No. 3-4, 65-80(Aug. 1965).

The concept of the effect of temperature increment in developing thermal stresses and strains in the fuel element of a nuclear reactor is presented and discussed. Equations of temperature distribution and thermal stress are developed for the three different types of fuel elements. Temperature and thermal stress distributions are pictured and compared. Some conclusions of practical significance are drawn from this comparison. (auth)

14107 IMPROVEMENTS IN FUEL ELEMENT CANS FOR NUCLEAR REACTORS. Wallis, John Dawtrey; Dixon, Laurence Charles Ward; Tindale, John Valentine; Arms, Henry Shull (to English Electric Co. Ltd.). British Patent 1,013,541. Dec. 15, 1965. Filed Apr. 6, 1961.

A reactor fuel assembly for insertion into a fuel channel includes a hollow fuel can having a heat transfer surface consisting of helical cooling fins. The surface of the fins is divided into substantially separate zones by radial splitters of greater radial depth than the fins and extending generally lengthwise with respect to the can. The assembly is provided with at least one pair of deflector vane arranged diametrically opposite. Portions of the vanes are inclined parallel with each other and obliquely to a plane containing the axis of the assembly so as to deflect flow of coolant and create an asymmetrical pressure distribution around the assembly to create a lateral stabilizing force on the assembly when the assembly is in position in the channel of the reactor. (B.L.M.)

14108 IMPROVEMENTS IN OR RELATING TO NUCLEAR REACTORS. Worley, Norman George (to Babcock and Wilcox Ltd.). British Patent 1,013,922. Dec. 22, 1965. Filed Mar. 21, 1961.

In a nuclear fuel pin cluster for a liquid-cooled reactor, the pins are provided with helical fins and are arranged in a matrix with a series of flow spaces between the fuel pins. Four fuel pins are associated with each flow space, and the fins of adjacent fuel pins at the sides of the flow space are of opposite hands and touch at their edges. (B.L.M.)

14109 IMPROVEMENTS IN OR RELATING TO NUCLEAR REACTORS. Carlson, Walter Berndt; Worley, Norman George (to Babcock and Wilcox Ltd.). British Patent 1,014,822. Dec. 31, 1965. Filed Mar. 21, 1961.

A fuel pin cluster for a liquid-cooled reactor has the fuel pins arranged in a matrix defining a number of regular polygons. The pins associated with any polygon are disposed about a flow space located within the polygon, and the fuel pins are united in the groups by ferrules disposed in the flow spaces. The pins are fitted with pins, and the ferrules are provided internally with fins; and all the fins are adapted to produce whirling of coolant flow longitudinally through the flow space. The direction of whirl in any cluster is the same as that produced by fins of other such finning means in each of the other flow spaces in the cluster. (B.L.M.)

14110 METHOD FOR THE COMPENSATION OF BURNUP IN A NUCLEAR REACTOR WITH A SOLID MODERATOR. Bagge, Erich (to Rolf Schlottau). German Patent 1,204,347. Nov. 2, 1965. Filed Sept. 17, 1964.

Fuel burnup is compensated for by exchanging zirconium hydride and/or zirconium deuteride rods with different moderating qualities. (Gmelin Inst.)

14111 METHOD FOR MOUNTING ARMOURING ON THE ENDS OF A NUCLEAR REACTOR FUEL ELEMENT CAN. Gauthorn, Maurice; Ringot, Claude (to Commissariat a l'Energie Atomique). German Patent 1,205,203. Nov. 18, 1965. Priority date July 7, 1959, France.

The ends of a fuel can are armored by covering the outside of the welded end caps, the weld, and at least part of the can with a metallic mass (stainless steel, beryllium, sintered aluminum, magnesium–thorium alloy) according to the method of Shoop and of shaping the mass into a cylindrical body with a plane face. (Gmelin Inst.)

14112 FUEL ELEMENTS FOR NUCLEAR REACTORS. Bauer, Stefan George (to Rolls-Royce Ltd.). U. S. Patent 3,220,927. Nov. 30, 1965. Priority date Oct. 13, 1961, Great Britain.

A fuel element assembly comprises inner and outer hollow, concentric sheathing members defining an elongated annulus between them. A number of wedge-shaped fuel elements composed of UC, UN, or UO_2 are disposed within the annulus in spaced relation from one another and from the sheath. The elements taper toward the inner sheathing member and are metallic bonded to the internal wall of the sheath. The metallic bond comprises a layer of material having a low neutron absorption and a melting point above the temperature of reactor operation. The sheath that is substantially free from chemical attack by the metallic bond has a number of parts welded together and has projections extending from it into engagement with the inner and outer members to maintain the spaced relationship. (B.L.M.)

14113 NUCLEAR FUEL ELEMENT WITH IMPROVED END CAP ASSEMBLY. Fletcher, Frederick Owen; Taylor, Alan Frederick (to United Kingdom Atomic Energy Authority). U. S. Patent 3,222,256. Dec. 7, 1965. Priority date Mar. 24, 1961, Great Britain.

An end cap assembly is described for a reactor fuel element in which the fissile material is enclosed in a sheath closed by end caps. Each end cap is joined to the sheath by a first circumferential edge weld, while screw threads mechanically join each of the end caps to the sheath. A shroud member is provided at each end of the element enclosing the first edge welds and joined to the sheath by a second circumferential edge weld and to the end caps by screw threads. A circumferential ridge provided adjacent to the second circumferential edge member projects radially by at least the amount of the projection of the edge weld to prevent damage of the fuel elements during loading into the reactor. (B.L.M.)

Power and Power-Breeder Reactors

14114 (BAW-393-2) THORIUM FUEL CYCLE FOR HEAVY WATER MODERATED ORGANIC COOLED REACTORS. Quarterly Technical Report No. 2, April–June 1965. (Babcock and Wilcox Co., Lynchburg, Va. Atomic Energy Div.). Contract AT(38-1)-393. 325p. Dep. mn. CFSTI $7.00 cy, $1.75 mn.

Fuel element design and fuel cycle analysis were emphasized, and some effort was directed toward reactor and steam plant designs that are compatible with the chosen reference core design. Three fuel element designs were developed and evaluated. One design uses thorium oxide in a fuel pin; the other two designs use thorium metal in nested-cylinder arrangements of four and six cylinders. Study of many factors resulted in selection of the six-ring nested-cylinder design for the reference core. This design has several important advantages over the others that were studied: low fuel costs, reduced capital costs, high conversion ratio, and good potential for enlargement and economic improvement in the future. The studies and experiments which led to the selection of this design are described. (auth)

14115 (BAW-3576-1) ZERO POWER TESTS—PM-3A CORE III. Batch, M. L. (Babcock and Wilcox Co., Lynchburg, Va. Critical Experiment Lab.). Jan. 1966. Contract AT(30-1)-3576. 32p. Dep. mn. CFSTI $3.00 cy, $0.50 mn.

Detector response was measured at specific locations during core submersion and approach to criticality. The temperature coefficient was measured up to 170 F. The results fit the linear function; $d\rho/dT = -0.087\ T - 0.37$ (in units of cents/F). Stuck-rod criteria and core uniformity were confirmed. Total excess reactivity was measured using boric acid techniques; the result is 9.92% $\Delta k/k$. All tests except core submersion detector response were performed with stainless steel mockups of thermal shields and the pressure vessel. (M.O.W.)

14116 (BNWL-177) PROPOSED TUBE POWER LIMITS FOR THE PRTR 58-INCH MK I FUEL ELEMENT. Hesson, G. M. (Battelle-Northwest, Richland, Wash. Pacific Northwest Lab.). Dec. 1965. Contract AT(45-1)-1830. 19p. Dep. mn. CFSTI $1.00 cy, $0.50 mn.

The factors that affect the possibility of the occurrence of boiling burnout were evaluated. The numerical values assigned to the factors were used to calculate the boiling burnout tube power limit for several flow rates and inlet coolant temperatures. (D.C.W.)

14117 (BNWL-183, Sect.III) A COMPARISON OF FUEL CYCLES FOR CROSSED-PROGENY FUELS IN CONVENTIONAL AND NOVEL CONFIGURATIONS. Deonigi, D. E. (Battelle-Northwest, Richland, Wash. Pacific Northwest Lab.). 18p. (CONF-651101-58).

Fuel cycle costs for plutonium-thorium and ^{233}U-natural uranium systems were investigated. The studies indicate that plutonium-thorium may be attractive for a D_2O moderated reactor and that ^{233}U-natural uranium may be attractive for pressurized water reactors. (M.O.W.)

14118 (BNWL-183, Sect.IV) THE CALIBRATION OF A HIGH SPEED BURNUP CODE FOR NUCLEAR FUEL SURVEYS. Porath, W. W.; Deonigi, D. E.; Merrill, E. T. (Battelle-Northwest, Richland, Wash. Pacific Northwest Lab.). 23p. (CONF-651101-59).

Calibration of the ALTHAEA computer program is discussed. ALTHAEA is a four group, one-dimensional code with a zero-dimensional option, and uses the Westcott formalism for cross section representation. This code was altered to allow better fitting of burnup data, with the strong restraint that computation time should be less than 20 seconds of 7090 time for a 20,000 Mwd/T burnup. (M.O.W.)

14119 (CEND/PRWRA-257) BOILING NUCLEAR SUPERHEATER (BONUS) POWER STATION: STARTUP SUMMARY REPORT, FEBRUARY 1966. (Combustion Engineering, Inc., Windsor, Conn. Puerto Rico Water Resources Authority, San Juan). Contracts AT(40-1)-2674; AT(40-1)-2672. 600p. Dep. mn. CFSTI $9.00 cy, $2.50 mn.

The startup and initial operation of the BONUS power plant are summarized. The nuclear and thermal characteristics of the integral boiling superheater core, the performance of the auxiliary and emergency systems of the reactor, the performance of the generating part of the plant, and the problems that had to be resolved for the various systems and controls during the startup period are discussed. (D.C.W.)

14120 (COO-1454-1) PRIMARY PIPING FLEXIBILITY ANALYSIS FOR LIQUID-METAL-COOLED FAST BREEDER REACTORS. McKeon, J. T. (Kellogg (M. W.) Co., Jersey City, N. J.). Aug. 20, 1965. Contract AT(11-1)-1454. 54p. (RD-65-1084). Dep. mn. CFSTI $3.00 cy, $0.50 mn.

Design standards and technological problems involved in the flexibility analysis of primary coolant piping systems for a 1000-Mwe liquid-metal-cooled fast breeder reactor are detailed. The effects of the nuclear environment on the design requirements are studied. Theoretical and phenomenological analyses of the stresses in this type of piping are carried out. (T.F.H.)

14121 (EUR-2453.f) ETUDE ECONOMIQUE DE L'INTEGRATION DE CENTRALES NUCLEAIRES DANS LES RESEAUX DE PRODUCTION ET DE DISTRIBUTION D'ELECTRICITE. (Economic Study of the Integration of Nuclear Power Plants in Electricity Generation and Distribution Networks). (Bureau d'Etudes Nucleaires, S. A., Brussels (Belgium). Societe Belge d'Economie et de Mathematique Appliquees, S. A., Brussels). Aug. 1965. Contract 018-63-9 ECIB. 176p. Dep. mn.

Despite the inaccuracy of the economic data on the cost of installing and operating nuclear plants, it would seem that nuclear power stations, even when financed on an industrial basis, are in numerous cases more economical than conventional units. It also appears that the availability of these plants is very satisfactory and close to that of conventional units. In view of these costs, an ideal complex of power generating installations should include a large proportion of nuclear plants—of the order of 50 ± 20%, depending on the network under consideration and the financing conditions. However, two conditions have to be fulfilled in view of the considerable proportions of nuclear power plants. On the one hand, in order to ensure that a large number of these units are satisfactorily operated throughout their lifetime, special turbines must be used and nuclear groups and units installed which can economically cope with the peak load. Pumping stations and installations using aircraft turbo-jets seem to be best suited to this role at present. On the other hand, it was shown that, as the installed capacity of nuclear power plants increases, an ever larger number of them can be used first for weekend and then for night-time modulation, when those units do not always lend themselves to this

method of exploitation. The economic appeal of nuclear power plants is also dampened by another factor when they become too numerous. Nuclear installations are more sensitive than conventional groups to the effect which their dimensions have at high power levels. Economic nuclear plants will therefore necessarily be of large size (500 Mw and over) and accordingly what is required is not that supply-line construction programs be stepped up but that their schedule be put forward. This additional cost should be taken into consideration in any comparison of the profitability of nuclear and conventional installations. (auth)

14122 (GA-4451) ADVANCED BERYLLIUM OXIDE CONCEPTS. Progress Report, April 1–June 30, 1963. (General Atomic, San Diego, Calif. John Jay Hopkins Lab. for Pure and Applied Science). Sept. 17, 1963. Contract AT(04-3)-187. 68p. Dep. mn. CFSTI $3.00 cy, $0.75 mn.

Research during this period was concentrated on a 200-Mw(e) reactor using a BeO spine, $BeO-UO_2-ThO_2$ fuel compact, and a graphite sleeve. The preliminary engineering-design work is presented together with an estimated capital cost for the plant. The physics work was concentrated on the determination of the fuel-cycle costs, and the materials effort centered on the determination of the fuel-fabrication costs for the plant. The second area of interest centered on the Pu-fueled system. A homogeneous concept was developed which appeared to yield excellent burnup-lifetime characteristics and a large prompt negative temperature coefficient, and in addition, used fuel which had isotopic concentrations typical of singly cycled fuel in low-enrichment uranium reactors. The feasibility of adding small volume fractions of ZrH_n to the core in order to achieve similarly good lifetime and temperature coefficient characteristics from a smaller core was investigated. (M.O.W.)

14123 (GAMD-1561(Rev.)) CORE PERFORMANCE CODE (COPE CODE). Katz, R. (General Atomic, San Diego, Calif. John Jay Hopkins Lab. for Pure and Applied Science). Mar. 21, 1963. Contract AT(04-3)-187. 47p. Dep. mn. CFSTI $2.00 cy, $0.50 mn.

The computer program, COPE, which calculates the steady-state temperature and pressure distribution in the fuel elements of a multichannel, gas-cooled, reactor core, is described. The temperature calculations include the coolant, the fuel-cladding surface, and an internal fuel temperature. The axial distributions of heat flux, dynamic pressure, Reynolds number, heat transfer coefficient, and friction coefficient are also printed in the output. Options are available for determining orificing schedules for the fuel elements to obtain either equal coolant outlet temperatures from each element or a constant fuel-cladding surface temperature in each element. The geometry of the fuel element is arbitrary and may be different for each fuel element comprising the core. (auth)

14124 (GAMD-6859) NEUTRON PRODUCTION IN UNIRRADIATED EBOR FUEL ELEMENTS DUE TO THE (α,n) REACTION. McWhirter, A. D. (General Atomic, San Diego, Calif. John Jay Hopkins Lab. for Pure and Applied Science). Dec. 13, 1965. Contract AT(04-3)-187. 17p. Dep.mn. CFSTI $1.00 cy, $0.50 mn.

The neutron activities due to the (α,n) reaction of two sample fuel pellets of EBOR fuel having different grain sizes are measured. The total neutron source in the fully loaded EBOR core is calculated from these measurements to be 5.48×10^5 neuts/sec maximum and 1.92×10^5 neuts/sec minimum. It is concluded that this source is not strong enough to interfere significantly with the initial loading and zero power testing of EBOR, but may be sufficient as a source for normal startup. (auth)

14125 (GEAP-4898) BLOWOUT, HEAT TRANSFER, PRESSURE DROP, AND MAXIMUM FLOW TESTS CONDUCTED ON A PROTOTYPE MARK III FUEL BUNDLE. Jones, L. T.; Rebman, H. P. (General Electric Co., San Jose, Calif. Atomic Power Equipment Dept.). June 25, 1965. Contract AT(04-3)-189. 90p. Dep. mn. CFSTI $3.00 cy, $0.75 mn.

An EVESR MK III modified fuel bundle was fully instrumented and was operated intermittently for a 3-month period at the Moss Landing Power Plant. The test bundle was operated at 1000 psi with steam flows from 660 to over 18,100 lb/h and steam inlet temperatures up to 760°F. Data were recorded for blowout, flow distribution, heat transfer, pressure drop, and maximum flow. (auth)

14126 (JUL-276-RG) EINE BEWERTUNG VON THORIUM-BRENNSTOFFKREISLAEUFEN. (An Evaluation of Thorium Fuel Cycles). Kasten, Paul R. (Kernforschungsanlage, Juelich (West Germany). Institut fuer Reaktorentwicklung). June 1965. 163p. Dep. mn.

The reasons for development of reactor systems with a high fuel utilization are discussed. Fuel cycles are evaluated with respect to fuel recharging in present reactor types: gas-cooled graphite-moderated reactors, gas-cooled BeO-moderated reactors, heavy-water-moderated reactors, molten-salt reactors, fast reactors with solid fuel, and thermal breeders. The technological problems in the development of reactor systems with high fuel utilization are considered. The molten salt reactor concept, the pebble-bed reactor concept, and the heavy water reactors are compared. (J.S.R.)

14127 (JUL-291-RG) MOSEL: VERGLEICH VON SPEKTREN UND SPEKTRAL GEMITTELTEN GROESSEN EINER ZWEIKOMPONENTEN-SALZSCHMELZE. (MOSEL: Comparison of Spectra and Spectrally Determined Parameters of a Two-Component Salt Melt). Barthold, W.; Wolf, L.; Graf, I. (Kernforschungsanlage, Juelich (West Germany). Institut fuer Reaktorentwicklung). July 1965. 59p. Dep. mn.

Within the framework of a study on the nuclear properties of an epithermal or fast fused-salt reactor with internal cooling through the blanket melt, the effect of core size, melt composition, and uranium enrichment on the spectrum of the reactor was investigated. The effects of the use of the same carrier salt for fuel material and breeding material was considered. (tr-auth)

14128 (JUL-296-RG) MOSEL: ALLGEMEINE STUDIE UEBER TEMPERATUREN, LEISTUNGSDICHTE UND WAERMEUEBERGANG. (MOSEL: General Study on Temperatures, Power Density, and Heat Transfer). Gat, Uri (Kernforschungsanlage, Juelich (West Germany). Institut fuer Reaktorentwicklung). Aug. 1965. 71p. Dep. mn.

A review of the construction possibilities of a fused salt reactor is given with respect to power density and temperatures. On the basis of economic grounds as high a power density as possible was desired. There are construction limitations with respect to building dimensions and heat flux. Both plates and tubes were considered as fuel elements. The power density limitations were indicated. It is shown that for laminar flowing fuel materials the limitation is dependent on the maximum possible temperature difference between fuel element center and wall and the heat conductivity. In turbulent flow, the limitation of the power density is dependent only on the structural material properties. The structural materials were considered with respect to their influence on the temperature pattern. Volume ratios of fuel material to structural material and coolant were shown as a function of the building materials. Heat flux limitation and wall densities were determined from other works. Both fused salts and sodium were considered as coolant. A formula was developed that shows the relation between core dimensions, heat flux, and heating-up time. The mutual effects of the three zones (fuel, structural material, and coolant) were determined principally by the heat flux. The corresponding proposal for the calculation of a core is given. Sodium and fused salt coolants were compared. An evaluation of the decisive factors for a selection between the two coolants was discussed. (tr-auth)

14129 (JUL-315-RG) MOSEL: VERGLEICH VON SPEKTREN UND SPEKTRAL GEMITTELTEN GROESSEN EINER DREIKOMPONENTEN ($NaF-BeF_2$)-SALZSCHMELZE. (MOSEL: Comparison of Spectra and Spectrally Determined Magnitudes of a Two-Component Salt

Melt ($NaF–BeF_2$)). Barthold, W. P.; Wolf, L. A.; Graf, I. (Kernforschungsanlage, Juelich (West Germany). Institut fuer Reaktorentwicklung). Oct. 1965. 87p. Dep. mn.

Within the framework of studies on the nuclear properties of an epithermal or fast molten-salt reactor with internal cooling by blanket melts, the effects of core size, fluoride concentrations, and uranium enrichment on the spectrum of the reactor system were investigated. Mixtures of equal parts of NaF and BeF_2 were considered as the carrier salts for the fuel material and the breeding material. (tr-auth)

14130 (KFK–366) KERNBRENNSTOFFBEDARF UND KOSTEN VERSCHIEDENER REAKTORTYPEN IN DEUTSCHLAND. (Demand for Nuclear Fuels and Costs of Different Reactor Types in Germany). Gruemm, H.; Gupta, D.; Haefele, W.; Jansen, P.; Schmidt, E.; Seetzen, J. (Kernforschungszentrum, Karlsruhe (West Germany). Institut fuer Angewandte Reaktorphysik). Sept. 1965. 70p. Dep. mn.

An estimation of the need of installed nuclear power indicated that in the year 2000 about 130 Mw(e) would be expected. In 1975 about 1 billion DM per year would accrue to the total annual nuclear energy costs. In 1970 about 500 kg of Pu would be produced in Germany; in 1980 this value would be between 10 and 20 tons. If in the Republic not more than a total of 200 up to 300×10^3 tons of natural U were used, the introduction of breeders is essential. By the year 2000 the natural uranium needs would be in the millions of tons. Such a quantity can be obtained only from the sea if it is technically and economically possible. The possibility of constructing a generation of fast breeders with initial use of ^{235}U is not considered in this study. If the Pu needs of the fast breeder generation is obtained from converter reactors, the U needs of each conceivable convertor/breeder combination is under 200×10^3 tons if a breeder rate of 1.4 is obtained. Then, no supplementary generation of high converting reactors is necessary. From the viewpoint of conservation of U resources it is better to combine a low converting convertor with a good breeder than the reverse. If the total consumption in each case remains under 200×10^3 tons, then a breeder rate of at least 1.4 in the fast breeder and the construction of a supplementary generation of D_2O reactors is necessary. The fast breeder has the most favorable cost potential in the framework of the data presented. The maximum installation of convertors was expected in the 1990's. If light water reactors are considered, then the capacity would be expected to be 45 Mw(e). The necessary processing capacity in reactors with enriched U in relatively small (about 4500 ton/year in 2000). For natural U convertors a capacity up to 20,000 ton/yr is necessary. In the case of two reactor types (both light and heavy water) this difference is no longer very large (4700 or 7600 ton/yr). (J.S.R.)

14131 (KR–98) PREBOLO: DESCRIPTION OF THE HIGH PRESSURE BOILING LOOP AT KJELLER. Kjelland-Fosterud, E. (Institutt for Atomenergi, Kjeller (Norway)). Aug. 1965. 39p. Dep. mn.

The high pressure boiling loop in the Engineering Laboratory at Kjeller is described. The overall design is given as well as assembly drawings of the major components. The experimental programs are stated in sufficient detail to justify the design. The instrumentation is fully reviewed, especially the temperature measuring equipment. The capacity of the heat exchanger is regulated by the rate of flow of cooling water which is admitted, and this evaporates partially. Due to this design the heat removed in the condenser and subcooler cannot be measured on the secondary side, and a reliable and accurate temperature measurement procedure is therefore essential. The operation and staffing of the loop is briefly described. (auth)

14132 (LA–3368) NUCLEAR REACTOR MAGNETOHYDRODYNAMIC POWER GENERATION. Cooper, Ralph S.; Booth, Lawrence A.; Fries, R. J.; Salgado, P. G.; Kirkbride, L. D.; Rhodes, C. A.; Rosa, R. J.; Crowe, W. E. (Los Alamos Scientific Lab., Univ. of California, N. Mex.). Aug. 1965. Contract W-7405-eng-36. 47p. Dep. mn. CFSTI $3.00 cy, $0.50 mn.

A preliminary survey was conducted to evaluate nuclear magnetohydrodynamics (MHD) as a field for future Los Alamos Scientific Laboratory research. The survey of MHD application to large-scale electrical power generation for central stations is presented. (auth)

14133 (NP–15587) ON PROBLEMS REGARDING THE COMPETITIVENESS OF NUCLEAR POWER REACTORS. Nicholas Ridley (Council of Europe). Oct. 21, 1964. 50p. Dep. mn.

The competitiveness of nuclear power plants with conventional hydro and thermal power plants for producing electric power is discussed from a long time economic point of view. Conclusions are discussed. (M.O.W.)

14134 (NYO–3379-2) OPERATING CHARACTERISTICS OF THE PRESENT PM-TYPE REACTOR INSTRUMENTATION. TASK 2 TOPICAL REPORT. Lenk, Pedro A.; McCreary, Joseph C.; Bazarnic, P. Rockne; Wurster, D. E. (Bailey Meter Co., Wickliffe, Ohio). Jan. 31, 1966. Contract AT(30-1)-3379. 434p. Dep. mn. CFSTI $7.34 cy, $2.00 mn.

An analysis of the equipment presently utilized at the PM installations is presented. Specific areas amenable to improvement in both the design and implementation of the reactor instrumentation system are determined by analyzing the instrumentation on both a modular and system basis. This operational analysis is correlated with an analysis of the effect of failures on the equipment and historical experience with the equipment. (M.O.W.)

14135 (ORNL–3885) GAS-COOLED REACTOR PROGRAM SEMIANNUAL PROGRESS REPORT FOR PERIOD ENDING SEPTEMBER 30, 1965. (Oak Ridge National Lab. Tenn.). Feb. 1966. Contract W-7405-eng-26. 319p. Dep. mn. CFSTI $7.00 cy, $1.50 mn.

Separate abstracts were prepared for the nine included sections. (M.O.W.)

For abstracts of individual sections see: 13215, 13261, 13262, 14104, 14136–14140.

14136 (ORNL–3885, pp 150–94) STUDIES FOR AVR-GERMAN PEBBLE-BED REACTOR. McCurdy, H. C.; Sisman, O.; Coobs, J. H. (Oak Ridge National Lab., Tenn.).

Pyrolytic carbon-coated $ThC_2–UC_2$ fuels were irradiation tested for the AVR reactor. Results from three different tests are presented. In addition, the fission gas release from AVR production particles and the performance of the fueled graphite spheres are discussed. (M.O.W.)

14137 (ORNL–3885, pp 236–43) STUDIES FOR ADVANCED SYSTEMS. Perry, A. M.; Witt, F. J. (Oak Ridge National Lab., Tenn.).

The effect on high temperature gas-cooled reactor conversion ratios and fuel-cycle cost of using a fuel that rapidly releases the fission products instead of retaining them was investigated. Diagrams show the net conversion ratios at a power density of 7 w/cm^3 and doubling times for the total fission inventory. The fuel-cycle costs at a power density of 7 w/cm^3 are given. In addition, a brief summary of results from mechanical experiments on nozzle-to-spherical shell attachments is presented. (M.O.W.)

14138 (ORNL–3885, pp 253–67) PERFORMANCE ANALYSES. Perry, A. M.; Cottrell, W. B. (Oak Ridge National Lab., Tenn.).

Results of graphite-air oxidation studies in the EGCR are presented. Discussions are presented on the core cooling requirements and nitrogen purge effectiveness for extreme coolant piping ruptures and the effect of increased oxidation rate, higher initial temperatures, and increased oxidation depth on required air coolant flow. (M.O.W.)

14139 (ORNL–3885, pp 268–83) COMPONENT DEVELOPMENT AND TESTING. Savage, H. W.; Coobs, J. H. (Oak Ridge National Lab., Tenn.).

The development and testing of the following components for the EGCR are discussed: compressor shaft seals, control rod drive test, charge-machine cylinder-seal develop-

ment, and special fuel assemblies for flux mapping. In addition, brief summaries of experimental studies of steam-graphite reactions and failure of the 42-in. bellows between the EGCR containment shell and the experimenters shell are presented. (M.O.W.)

14140 (ORNL–3885, pp 284–93) IRRADIATION TESTING OF COMPONENTS AND MATERIALS. McCurdy, H. C.; Coobs, J. H.; Sisman, O.; Wechsler, M. S. (Oak Ridge National Lab., Tenn.).

Results of irradiation testing of prototype fuels for the EGCR are presented. In addition, a brief summary of the pressure vessel surveillance program for the EGCR is presented. (M.O.W.)

14141 (ORNL–3910) BONUS REACTOR SUPERHEATER FUEL ASSEMBLIES—AN INVESTIGATION OF FAILURE AND METHOD OF CORRECTION. Cunningham, J. E.; Long, E. L. Jr.; Franco-Ferreira, E. A.; Harman, D. G. (Oak Ridge National Lab., Tenn.). Dec. 1965. Contract W-7405-eng-26. 173p. Dep. mn; CFSTI $5.00 cy, $1.00 mn.

A superheater assembly that incurred a fission break when accidently subjected to a modest temperature transient during full-core testing of the BONUS Reactor at a power level of 5 Mw was examined. The techniques used to locate the source of fission-product leakage and establish the nature and extent of damage to the Inconel-clad UO_2 fuel rods are described. Significant observations made during in-cell inspection, component disassembly, gamma scanning, dimensional measurements, gas sampling and analysis, leak testing, and metallographic examination are recorded and discussed. The supporting laboratory and analytical data obtained to facilitate the identification of cause and mode of failure are presented. Fabrication studies undertaken to delineate corrective measures are described. The failure was caused primarily by leak holes that resulted in welds from a faulty welding practice that left hot cracks. Water or steam leaked into the element, so that overheating suddenly increased the pressure, rupturing the cladding. (auth)

14142 (ORNL-TM–1378) POSTIRRADIATION EXAMINATION OF EGCR PROTOTYPE CAPSULE 03A-6. Morgan, J. G.; Osborne, M. F.; Long, E. L. Jr. (Oak Ridge National Lab., Tenn.). Feb. 1966. Contract W-7405-eng-26. 21p. Dep. mn. CFSTI $1.00 cy, $0.50 mn.

Capsule 03A-6 was irradiated at a design cladding temperature of 1300°F and heat rating of 30,000 Btu/hr · ft. The element contained Westinghouse EGCR production UO_2 pellets and was clad with 304H stainless steel. After a fuel burnup of 10,000 Mwd/mt UO_2, the capsule was examined. The cladding had collapsed around the fuel. Bowing was nominal and a gamma scan showed no shifting of the fuel. Metallographic examination of the fuel and cladding showed no detrimental structural changes. (auth)

14143 (PAPP–6401) PATHFINDER ATOMIC POWER PLANT REACTOR BUILDING INTEGRATED LEAKAGE RATE TEST. Williams, L. P.; Davie, R. L. (Northern States Power Co., Sioux Falls, S. Dak.). Nov. 18, 1963. Revised Aug. 1964. 137p. (ACNP–65522; DOCKET–50-130). Dep. mn. CFSTI $4.00 cy, $1.00 mn.

The Pathfinder reactor building leakage rate test is discussed. The entire testing program including test procedures, measurements, data analysis, discussion of results, and conclusions is discussed. Three separate approaches are taken to verify a building fractional leakage rate, including uncertainty limits. The reference system method was used to determine the primary leakage rate, which will normally be the building fractional leakage rate. Other tests included an individual leakage source survey and a reactor building controlled leakage rate test. All values of leakage rate determined by these separate methods are in close agreement with each other. The total fractional leakage rate under test conditions is concluded to be no more than .083%/24 hours. This value includes leakage through the reactor safety valve discharge line isolation-valve, which was not installed at the time of the test. The multi-tube temperature compensating reference system was proven very effective. All other test apparatus was equally suitable for this type of test but one improvement is recommended. A controlled leakage rate test was performed in addition to the primary leakage rate test to confirm the accuracy of the error analysis calculations. The results of the two tests compared to within 3% of each other, in units of maximum allowable leakage rate. (M.O.W.)

14144 (PEL–77) VERBRANDINGSBEREKENINGE TEN OPSIGTE VAN TERMIESE KRAGREAKTORE MET NATURIUMKOELING. (Burnup Calculations for Thermal Power Reactors With Sodium Cooling). Engelbrecht, C. A.; Fiedeldey, H. (Atomic Energy Board, Pelindaba, Pretoria (South Africa)). June 1965. 21p. Dep. mn.

The methods used and the results obtained in the calculation of the burnup in a thermal power reactor with natural uranium fuel, heavy water reflector, and sodium coolant are reported. (J.S.R.)

14145 (TID–22595) ARMY GAS-COOLED REACTOR SYSTEMS PROGRAM. ML-1-IM DESIGN REPORT. (Aerojet-General Nucleonics, San Ramon, Calif.). Dec. 1965. Contract AT(10-1)-880. 238p. (AN-AGCR–958). Dep. mn. CFSTI $6.00 cy, $1.25 mn.

Design analysis and developmental testing are discussed. Design analysis covers the neutronic, thermal, and mechanical analytical efforts performed for the design of ML-1-IM and concludes with a summary of the basic characteristics of the ML-1-I and ML-1-I/-IM cores. Developmental testing covers the material, mechanical, and in-pile tests performed in the development of the ML-1-I and ML-1-II fuel elements as applied to the ML-1-IM design (no development or tests were performed specifically to support the ML-1-IM design). The appendixes provide supplemental neutronic information, properties of materials, mechanical design and stress calculations, and the ML-1-IM drawing list. (M.O.W.)

14146 (TID–22596) ARMY GAS-COOLED REACTOR SYSTEMS PROGRAM. OFF-NORMAL SCRAM SYSTEM. Final Design Report. Malmstrom, S. A. (Aerojet-General Nucleonics, San Ramon, Calif.). Dec. 1965. Contract AT(10-1)-880. 54p. (AN-AGCR–962). Dep. mn. CFSTI $3.00 cy, $0.50 mn.

The final design of the automatic shutdown system for the ML-1 is presented. The scram system was developed to prevent excessive core temperatures during periods of transient operation. Component specifications are given. Results of functional and environmental testing are presented. (M.O.W.)

14147 (UCRL–16394) EFFECT OF NATURAL CONVECTION UPON THE TEMPERATURE TRANSIENT FOLLOWING A LOSS-OF-COOLANT ACCIDENT IN A NUCLEAR POWER REACTOR [Thesis]. Omberg, Ronald Paul (Lawrence Radiation Lab., Univ. of California, Berkeley). Sept. 1965. Contract W-7405-eng-48. 118p. Dep. mn. CFSTI $4.00 cy, $0.75 mn.

The effect of natural convection upon the temperature transient following a loss-of-coolant accident was analyzed for a typical power reactor configuration. The system of equations developed was then solved using the design parameters of the Loss-of-Fluid Test Reactor (LOFT). It was found that natural convection will prevent melting of either the fuel or cladding at low power levels. At the maximum power density allowable in the LOFT, the time to fuel melting was nearly twice that for an adiabatic transient. The solution was based on the one-dimensional quasi-steady state flow conservation equations coupled to the lumped capacity transient energy equation for small axial sections of fuel. The time dependence of the decay heat source was considered; the frictional losses and heat transfer were assumed to be adequately represented by the relations for turbulent pipe flow. A constant radial power density was assumed. The system of equations was amenable to machine calculation using an iterative scheme. It was found that natural convection has a pronounced effect, as compared to the adiabatic case, upon the temperature transient. With a constant radial power

density, it was found that the cladding will not melt at power levels below 38 Mw and that the fuel will not melt at power levels below 68.5 Mw. (auth)

14148 (WCAP-3385-5) SAXTON PLUTONIUM PROGRAM. Fifth Quarterly Progress Report for the Period Ending September 30, 1965. (Westinghouse Electric Corp., Pittsburgh, Pa. Atomic Power Div.). Oct. 1965. Contract AT(30-1)-3385. 104p. (EURAEC-1465). Dep. mn; CFSTI $4.00 cy, $0.75 mn.

Work Performed under United States-Euratom Joint Research and Development Program.

A summary of the Saxton Pu program is presented. All fuel was fabricated and Core II was shipped to Saxton during the period. Alpha monitoring equipment was installed and calibrated. Fuel design and fabrication were completed. Planning and analysis of critical experiments were completed along with safeguards analyses. Plans for zero power tests and startup tests were completed, and a past irradiation sampling plan was prepared. (J.R.D.)

14149 (ORNL-tr-900) FAST NEUTRONS. Report of Activities of 2nd Quarter 1965. (Commissariat a l'Energie Atomique, Cadarache (France). Centre d'Etudes Nucleaires. Commissariat a l'Energie Atomique, Paris (France). Centre d'Etudes Nucleaires). Translated by G. L. Boisvert (Oak Ridge National Lab., Tenn.). 106p. Dep. mn. JCL $9.10 fs, $3.38 mf.

The status of the Rapsodie reactor, the Harmonie research reactor, and the Masurca critical assembly is summarized, together with fuel studies, studies of neutron physics, safety studies, and other associated studies. (D.C.W.)

14150 THE HEAVY WATER GAS GOOLED REACTOR IN THE FRENCH PROGRAM. Naudet, R. (CEN, Saclay, France). Atompraxis, 11: 612-15(Nov.-Dec. 1965). (In German).

The choice of heavy water as moderator for a second program of thermal reactors has proved better conditions for natural uranium than in a graphite reactor. The choice of a certain type of fuel-element-cycle results not only from commodiousness or independence from provision, but it emerges from the conviction that the economical advantages are of great importance. In the first part various advantages of the principle of the fuel-element-cycle, obtained by a heavy-water-reactor, are mentioned. It is specially pointed out that the sensitivity of an additional gram of uranium-235 is dependent on the neutron balance. The second part shows that the cooling by gas associated with the moderator, shows also interesting characteristics and presents the advantage of industrial success. (auth)

14151 ECONOMIC PROSPECTS OF NUCLEAR ENERGY. Gaussens, J. (CEA, Paris). Atompraxis, 11: 646-53(Nov.-Dec. 1965). (In German).

The utilization of nuclear energy for naval propulsion radioisotopes, production of sweet water, the civil utilization of nuclear explosions is discussed. The economical aspects for the production of electricity is treated. The advantage of the research program on natural-uranium-graphite-gas (production of plutonium, securing of provision, costs) are stressed and a comparative study of an enriched uranium-reactor is suggested. Actual exploitations or constructions would permit the French to bring nuclear industry to international context. (auth)

14152 THE DEVELOPMENT OF GRAPHITE-GAS RESEARCH. Cabanius, J.; Horowitz, J. Atompraxis, 11: 609-12(Nov.-Dec. 1965). (In German).

By the end of 1964 the French Government agreed upon the program: "The production of Electricity of Nuclear Origin" for the period of 1966 up to 1970 (Vème-Plan); a minimal program of 2500 Mwe completed by an additional program of 1500 Mwe. This is provided in natural-uranium-graphite-gas research and will be realized by the majority of nuclear power stations. After having pointed out the experiences gained in France with the reactors of the actual research programs (G2, G3, EDF1, EDF2), the characteristic principles are shown as the economical aspects of these two types which represent the base of this five year plan: EDF4 (St Laurent 1, St Laurent 2) which represents a certain development degree, proved on the technical- and competitive on the economic sector; the annular nuclear fuel reactor (Bugey 1) which stimulates the unit power of the nuclear power stations and moreover exploits all possibilities of this program. (auth)

14153 IMPROVEMENTS MADE TO THE CONTROL DRIVE WINCHES FOR THE EDF-1 CONTROL RODS. Grauvogel, M. A. Bull. Inform. A.T.E.N. (Ass. Tech. Energ. Nucl.), No. 56, 31-7(Nov.-Dec. 1965). (In French).

The principles for the control of the EDF-1 reactor are outlined. The design of the original installations for the winch control and the improvements made in this control are described in some detail. (J.S.R.)

14154 AUTOMATIC CONTROL EQUIPMENT OF THE DRAGON REACTOR. Franchi, M.; Garroni, A.; Sciuto, F. (C.C.R., EURATOM, Ispra, Italy). Energia Nucl. (Milan), 13: 1-11(1966).

The DRAGON reactor automatic control equipment for power and cooling gas outlet temperature is described. The special purpose electronic control system is based entirely on solid state components. (auth)

14155 THE THERMAL NUCLEAR ELECTRICITY CENTERS OF FRANCE. Genie Civil, 142: 291-300 (July 15, 1965). (In French).

The first three centers, EDF 1, EDF 2, and EDF 3 are located at Chinon and produce 70, 200, and 400 Mw respectively. The fourth, EDF 4, produces 480 Mw and is located at St.-Laurent-des-Eaux, near Blois; the fifth, Bugey, on the Rhone, comprises five units of 500 Mw. A joint unit with Belgium at Chooz in the Ardennes produces 266 Mw; a small station at Brennelis, in the Monts d'Arree, operates at reduced level (75 Mw) and uses heavy water instead of graphite as moderator, and is called EL 4. Plans of each of the three centers at Chinon are illustrated, with some detail given of the operation of each unit. Transverse sections of EDF 2 and the reactor of EDF 3 are given. A distinction between EDF 4 and the larger earlier units lies in the placement of the heat exchangers; price per kw from this unit is competitive with classically produced energy. Several sections of units and elements are illustrated. A description of the EL 4 test center is given; the Franco-Belgian unit is of an American design, using enriched U. (BBB)

14156 A CORRELATOR FOR INVESTIGATING RANDOM FLUCTUATIONS IN NUCLEAR POWER REACTORS. Boardman, F. D. (Dounreay Experimental Reactor Establishment, Caithness, Scotland); Harrington, E. L. E.; Carswell, D. J. A. Radio Electron. Eng., 30: 161-74 (Sept. 1965).

As in most physical processes, fluctuations are observed in various parameters (such as power and temperature) of a nuclear power reactor operating at a nominally constant power. The cross-correlation between simultaneous recordings of these fluctuations can give information on the kinetics of the reactor system without disturbing its normal operation. An apparatus was built to explore the practical possibilities of the technique and some of its design principles, practical implementation, and the results of tests are described. Some typical results obtained on the Dounreay Fast Reactor are also given. The equipment records the fluctuations in four channels on magnetic tape, the correlation functions being obtained subsequently by analogue computing techniques in an accelerated time scale. A novel feature is the use of a continuously-rotating magnetic drum with multiple heads to delay one signal relative to another. Delays equivalent to 25 sec in recording time can be obtained, the smallest delay being 0.05 sec. Tests with sinusoidal signals show that frequencies can be measured to better than 2% and the r.m.s. error of all points on the correlation curve is less than 2% of full scale. These errors are shown to be considerably less than the statistical errors due to the finite recording time. The possibility

of detecting and measuring small resonances in the presence of considerably greater noise was proved, which could be useful in detecting an incipient instability in the reactor system. It also appears possible to obtain some information from the cross-correlation function of two parameters in the presence of 20 times as much uncorrelated noise. It is concluded that an on-line monitor of the reactor kinetics using noise analysis techniques is feasible. (BBB)

14157 DESIGN FEATURES OF THE SAN ONOFRE NUCLEAR STATION. von Hollen, H. J.; Currey, C. F. (Westinghouse Electric Corp., Pittsburgh). Westinghouse Eng., 25: 142-7(Sept. 1965).

Some new design concepts that have been incorporated in the Southern California nuclear plant, with significant improvements in simplification and overall performance, are described and illustrated. The pressurized water reactor (PWR) coolant system, turbine generators and cycle efficiency, and advanced control-rod concept are described. Plant output is 450 Mw gross. The core contains about 150,000 lb of sintered uranium-oxide pellets, 0.380 in. in dia, of an average 3.5% initial enrichment. The pellets are sealed into 125-in. long stainless steel fuel tubes. Descriptions and diagrams are also provided of reactor coolant pumps, the safety injection system, and instrumentation and control features. (TCO)

14158 POTENTIALITIES OF GAMMA-SPECTROMETRY IN NON-DESTRUCTIVE MEASUREMENTS ON FUEL ELEMENTS. Engelmann, Ch.; Brebant, C.; Gosset, J.; Monier, J.; Roussel, E. (CEN, Saclay, France). pp 139-49 of STI/PUB/105(Vol. II). (In French).

The application of gamma spectrometry to the problems of nondestructive determination of the burn-up of irradiated fuels was investigated. Research shows: (1) that ^{144}Pr, the daughter element of ^{144}Ce with a half life of 290 d, can be particularly recommended for determining the number of fissions ascribable to ^{235}U. Its gamma radiation, of very high energy, is such that it can easily be detected in the presence of other fission products after a short cooling period. (2) That in the same conditions, taking into account the fission yields, ^{106}Rh, the daughter of ^{106}Ru with half-life 370 d, can be used to measure the fissions characteristic of ^{239}Pu. Thus, simultaneous measurement of the γ-ray intensities of ^{144}Pr and ^{106}Rh would make it possible to determine the burnup of ^{235}U; and the ^{239}Pu content of the fuel. The reasons which led to the choice of the two gamma emitters mentioned are discussed. The equipment which has been installed is described. An account is also given of the results already obtained, and of the practical possibilities and the limitations of the method. (auth)

14159 THE APPLICATION OF NON-DESTRUCTIVE TECHNIQUES IN THE QUALITY CONTROL INSPECTION AND TESTING OF FUEL MATERIALS FOR THE DRAGON REACTOR EXPERIMENT. Conde, J. F. G.; Pointud, R.; Holliday, J.; Good, P. D. (Atomic Energy Establishment, Winfrith, Eng.). pp 167-94 of STI/PUB/105(Vol. II).

The O.E.C.D. high-temperature gas-cooled reactor experiment, Dragon, is graphite-moderated and helium-cooled and employs fission product-retaining fuel of the coated-particle type. The development and use of this new type of fuel have required the application of a variety of nondestructive techniques for quality control, inspection and testing. Methods which are employed in the inspection of fuel materials both in the development phase and subsequently in production are described. Physical methods of analysis are used for control of the chemical analysis of fuel cartridges and assessment of fuel contamination of fuel particle coatings, and particular gamma spectrometric and alpha scintillation counting techniques are described. The general quality of coated particles is assessed and metrology of coatings performed by means of micro-radiography with the x-ray projection microscope; the procedure is outlined and typical results are presented. Fuel cartridges which consist of fuel particles in a graphite matrix are inspected for homogeneity of fuel distribution and freedom from defects by fluoroscopy and panoramic slit-scanning radiography. Color radiography is also employed to a limited extent and the various techniques are presented together with illustrative examples of the results obtained. The fuel elements are fabricated almost entirely from various grades of graphite, and eddy-current nondestructive testing techniques are being developed to permit inspection of raw materials and finished machined components for freedom from significant defects. A brief description of these techniques is given. (auth)

14160 LIMITS TO THE RECOGNIZABILITY OF FLAWS IN NON-DESTRUCTIVE TESTING STEAM-GENERATOR TUBES FOR NUCLEAR-POWER PLANTS. Kuhlmann, A.; Adamsky, F.-J. (Technischer Ueberwachungs-Verein Reinland e.V., Cologne). pp 213-23 of STI/PUB/105 (Vol. II).

In the Federal Republic of Germany there are nuclear reactors under construction with steam generators inside the reactor pressure vessel. As a result design repairs of steam generator tubes are very difficult and cause large shutdown times of the nuclear power plant. It is known that numerous troubles in operating conventional power plants are results of steam generator tube damages. Because of the high total costs of these reactors it is necessary to construct the steam generators especially in such a manner that the load factor of the power plant is as high as possible. The Technischer Überwachungs-Verein Rheinland was charged to supervise and to test fabrication and construction of the steam generators to see that this part of the plant was as free of defects as possible. The experience gained during this work is of interest for manufacture and construction of steam generators for nuclear power plants in general. The efficiency limits of non-destructive testing steam generator tubes were investigated. The following tests performed are discussed in detail; automatic ultrasonic testing of the straight tubes in the production facility, combined ultrasonic and radiographic testing of the bent tubes and tube weldings, and other non-destructive tests. (auth)

14161 THE NON-DESTRUCTIVE TESTING OF FUEL ELEMENTS AND THEIR COMPONENTS FOR THE UNITED KINGDOM POWER-REACTOR DEVELOPMENT PROGRAMME. Mann, C. A.; Campsie, I. C. (United Kingdom Atomic Energy Authority, Preston, Eng.). pp 365-83 of STI/PUB/105(Vol. II). (TRG-Report-1031).

The test procedures are described which were developed in the Reactor Fuel Element Laboratories as part of the Reactor Group's development program on fuel pins for a number of reactor systems. The sheaths of these pins are tubes in the range 5 to 15 mm diam; the materials are stainless steels and zirconium alloys. Flaw detection in tubes is described in terms of ultrasonic and eddy current inspection. Dimensional inspection of tubes and pellets is also discussed. Various mechanical, pneumatic, nuclear and electronic methods of measuring the tube dimensions are compared and the arrangements to prevent the scratching of the tubes are described. Techniques for measuring pellet diameter and circumferences are explained and it is suggested that with thin walled tubes a more realistic approach to the pellet/gap problems can be obtained by comparing circumferences. (M.O.W.)

14162 AN EXPERIMENTAL STUDY OF THE ($k\beta/l$) PULSED NEUTRON SOURCE TECHNIQUE IN LIGHT WATER ASSEMBLIES. Meyer, P. (General Electric Co., Pleasanton, Calif.). pp 25-48 of STI/PUB/104(Vol.2).

A new pulsed neutron model and experimental technique have been investigated in light water reflected cores with special emphasis on application in large central station power reactors. The pulsed neutron source method is based upon a bare, monoenergetic diffusion theory model. It uses the complete neutron density versus time profile of a pulsed assembly to obtain the parameters α and ($k\beta/l$) from a single measurement. The distinguishing feature of this method is that all spatial modes are taken into account, as opposed to the usual fundamental mode treatment. A new pulsing method that simplifies the ex-

periments to obtain reliable data for both the α and $(k\beta/l)$ measurement has also been experimentally verified. The results of a test program performed in the Vallecitos Thermal Critical Assembly to investigate the range of validity of the $(k\beta/l)$ model in various lattices are discussed. The dependence of $(k\beta/l)$ upon the relative source and detector position over a large range of subcriticality is shown. It has been established that the new technique eliminates the need for a separate α-delayed critical, (β/l) determination, a measurement which, particularly in large power reactors, is at best difficult and expensive to perform. The experimental results indicate that the $(k\beta/l)$ theory yields meaningful results for reasonably small reflected cores down to at least 3.5 dollars subcritical. In large cores the reflector problem is minimized since the importance of the reflector is decreased and reasonable results can be expected at even lower subcriticalities. This is confirmed by experiments which were carried out in a 150 Mw(t) boiling water reactor before and after full power operation, and the 12.5 Mw(t) Vallecitos Experimental Superheat Reactor at room and design temperatures and design pressure. Both of these facilities exhibited the multi-core effect that is found in large power reactor cores and an interpretation of these pulsed measurements is made possible by the proper placement of pulsed source and detectors. (auth)

14163 CALIBRATION OF CONTROL RODS IN NATURAL URANIUM–GRAPHITE LATTICES. **Fuster, S.; Sagot, M.; Tarabella, A.; Tellier, H. (Centre d'Etudes Nucleaires, Saclay, France). pp 261-79 of STI/PUB/104(Vol. 2). (In French).**

Application of the pulsed neutron technique to natural uranium, graphite-moderated lattices raises some problems as regards both experimentation and interpretation. The large amount of fuel results in background due to the numerous spontaneous fissions and necessitates the use of sources which are powerful enough but which do not disturb the lattice. As a result of their large size, graphite reactors, when used as pulsed sources, have spatial harmonics which decrease with constants close to that of the fundamental mode, so that the sources and detectors have to be carefully sited. Neutron lifetime is relatively long and the induced flux falls off sufficiently slowly for the decay of the first delayed neutron groups to be detectable during the analysis. All these problems were studied in a series of preliminary measurements carried out on the MARIUS experimental critical stack, during which several prototype control rods were calibrated in various lattices. The experiments were subsequently extended to power reactors by measuring the negative reactivity of a number of rod clusters at the EDF2 nuclear power station. (auth)

14164 DEVELOPMENT OF AN ELEVATED-TEMPERATURE CENTRIFUGAL PUMP FOR A MOLTEN-SALT NUCLEAR REACTOR. **Smith, P. G.; Wilson, L. V. (Oak Ridge National Lab., Tenn.). New York, American Society of Mechanical Engineers, 1965, Preprint No. 65-WA/FE-27, 11p., $1.50. (CONF-651110-6). ORINS.**

From American Society of Mechanical Engineers, Annual Winter Meeting, Chicago.

An elevated-temperature (up to 1400 deg F) centrifugal pump was developed for the Molten Salt Reactor Experiment, a small nuclear power reactor. Hydraulic performance of the pump was predictable from water-test performance. The range of off-design operation of the pump was limited by the running clearances. Back-diffusion tests with Kr-85 indicate that the shaft purge flow is effective in maintaining the Kr concentration in the shaft-seal oil-leakage region below that in the pump tank by a factor of a least 35,000. Pumps of this design are installed in the MSRE, and have circulated 1200 deg F nonfissionable salt and an enriched salt at criticality. (auth)

Process Heat Reactors

Refer also to abstract 12877.

14165 (ANL–7035) A PRELIMINARY EVALUATION OF THE USE OF HIGH-TEMPERATURE PROCESS HEAT AS PART OF A TOTAL NUCLEAR-ENERGY SOURCE. **Gordon, L. J.; Marchaterre, J. F. (Argonne National Lab., Ill.). Sept. 1965. Contract W-31-109-eng-38. 46p. Dep. mn. CFSTI $3.00 cy, $0.50 mn.**

A preliminary study of the use of high-temperature (1500-3000°F) process heat as part of a multipurpose complex was carried out. The conclusions of the study indicate that in addition to conventional electric power generation, nuclear energy might be useful in alumina and aluminum production; in cement production as part of a complex; and in calcining and/or sintering ores such as taconite. The main factor that could make high-temperature, nuclear, process heat attractive is the potential of developing specially designed multipurpose reactors. The multipurpose reactor appears to be a possible way in which high temperature process heat could be economically supplied. Most uses of high-temperature process heat that appear attractive would necessitate the development of heat exchangers to heat air to 2200–2700°F. (auth)

14166 (TID–22330(Vol.3)) ENGINEERING AND ECONOMIC FEASIBILITY STUDY FOR A COMBINATION NUCLEAR POWER AND DESALTING PLANT. SUMMARY. **(Bechtel Corp., San Francisco, Calif.). Dec. 1965. 199p. Dep. mn. CFSTI $1.25 cy, $1.25 mn.**

The economics, plant analysis, siting analysis, and feasibility of a combination nuclear-desalting and power-producing plant on the California coast are reviewed and evaluated. (T.F.H.)

Production Reactors

14167 (HW–70878) N REACTOR ANALOG SIMULATION FEASIBILITY STUDY. **Trumble, R. E.; DeVoss, H. G.; Harvey, R. A. (General Electric Co., Richland, Wash. Hanford Atomic Products Operation). Aug. 25, 1961. Contract AT(45-1)-1350. 37p. Dep. mn. CFSTI $2.00 cy, $0.50 mn.**

A description of the required facility is presented. Various other brief discussions are presented on the use of the facility, economics, procurement schedule, administration, experience with analog simulation, why existing facilities are inadequate, and consequences of not having an NPR simulator. (M.O.W.)

14168 A FAST TEST FOR EXCESSIVE ^{235}U CONCENTRATIONS IN ENRICHED FUEL ELEMENTS. **McEachern, A. D. (Atomic Energy of Canada Ltd., Chalk River, Ont.). pp 387-97 of STI/PUB/105(Vol. II).**

A nondestructive method of detecting areas of enriched fuel elements containing excessive ^{235}U, and an instrument designed to inspect uranium-aluminum alloy fuel for the NRU reactor using the new method are described. The new method is as precise as conventional methods but is much faster. Alternatively, the method may be used to improve the precision of the test without increasing the testing time. The method may be used when the ^{235}U concentration in selected areas of a fuel element is estimated by measuring the intensity of 184-kev γ rays (from the natural decay of ^{235}U) and when an area is considered acceptable if the measured intensity from it is less than a limiting intensity equivalent to the maximum allowable ^{235}U concentration. If the measured intensity is much less or much greater than the limiting intensity, much less time is required to make this decision than when they are nearly the same The new method takes advantage of this. It thus inspects each area only as long as is necessary to make a decision with the required confidence. The average time taken in practical cases is less than that taken by conventional methods which inspect each area for a preselected time ohosen to give the required confidence in the most difficult cases–when the measured and limiting intensities are nearly the same. The new method is based on sequential sampling theory. It may also be used to detect areas with undesirably low ^{235}U concentration. (auth)

Propulsion and Space

See also ENGINEERING — Space Propulsion

Refer also to abstract 14029.

14169 (AFWL-TDR-64-75) PARTICLE DISINTEGRATION STUDY FOR RE-ENTERING NUCLEAR AUXILIARY POWER SYSTEMS. Final Report. Littman, F. E.; Bell, L. E.; Koppang, R. R.; Malinovsky, A. H.; Silvestri, R. (Douglas Aircraft Co., Inc., Newport Beach, Calif. Astropower Lab.). Sept. 1964. Contract AF29 (601)-5004. 93p. (AD-607410). CFSTI $3.00 cy, $0.75 mn.

The oxidation behavior of molten zirconium-10% uranium alloy particles was investigated in the presence of air or its components. A theoretical analysis of the aerodynamic and thermodynamic conditions affecting the droplets was carried out. The reaction of molten droplets of 50 to 8000 micron size with nitrogen, oxygen and air was studied at pressures ranging from 3 to 760 torr. The results indicate that the particles of all sizes react more or less completely with the surrounding atmosphere. The reaction of the larger particles is quiet and smooth. The smaller droplets react with explosive violence, disintegrating into very small particles. Only in the latter case, which appears to be limited to particles initially smaller than 400 microns, does the reaction with air contribute to further decrease in particle size. (auth)

14170 (EGG-1183-2019) TCC CONTROL SYSTEMS: TRANSDUCER EVALUATION, WIRE EVALUATION, AND CALORIMETRIC DETECTOR DEVELOPMENT. Final Report. (Edgerton, Germeshausen and Grier, Inc., Santa Barbara, Calif.). Mar. 3, 1964. Contract AT(29-1)-1183. 93p. Dep. mn. CFSTI $3.00 cy, $0.75 mn.

Strain gage and potentiometer transducers were operated in known radiation environments, simulating typical nuclear rocket environments, and were calibrated for electrical output versus the pressure imposed. The effects of radiation on the operating performance of the transducers were determined. A calorimetric detector was tested under similar conditions and the results of this analysis are also presented. In addition, the performance of various wire insulators under intense radiation was studied. Results are presented. (M.O.W.)

14171 (LA-3388) PIN TECHNIQUE FOR DISPLACEMENT MEASUREMENTS IN KIWI TNT. Washburn, Beverly; Hudson, C. E. (Los Alamos Scientific Lab., Univ. of California, N. Mex.). June 8, 1965. Contract W-7405-eng-36. 19p. Dep. mn. CFSTI $1.00 cy, $0.50 mn.

A pin technique used to measure relatively small, early outward displacements of the TNT reactor core and reflector cylinder components during the Kiwi Transient Nuclear Test is described. Considerations necessary to adapt this method to the environment of the reactor transient and the results are presented. An experiment to determine the times of closing of selected propellant passages using coaxial wires is also outlined. (auth)

14172 (LA-3397) RADIATION MEASUREMENTS OF THE EFFLUENT FROM THE KIWI B4D-202 AND B4E-301 REACTORS. Henderson, R. W.; Fultyn, R. V. (Los Alamos Scientific Lab., Univ. of California, N. Mex.). Aug. 12, 1965. Contract W-7405-eng-36. 88p. Dep. mn. CFSTI $3.00 cy, $0.75 mn.

The results are presented of documentation studies on the effluent from the Kiwi B4D-202 and Kiwi B4E-301 reactors during full power tests. A description of procedures and equipment is also given. An analysis of the environmental effects due to the passage and deposition of released material is given as well as deposition velocities measured at various locations. (auth)

14173 (TID-22416) SNAPSHOT PROGRAM RELIABILITY LIFE TEST. (Lockheed Missiles and Space Co., Sunnyvale, Calif.). Oct. 8, 1965. Contract AF04(695)-136. 115p. (LMSC-A763154; AD-476321). Dep. mn. CFSTI $4.00 cy, $0.75 mn.

The results of a test of SNAPSHOT subsystem equipment are presented. (D.C.W.)

14174 (TID-22417) SNAPSHOT AGENA POSTFLIGHT DESIGN REVIEW. (Lockheed Missiles and Space Co., Sunnyvale, Calif.). Oct. 15, 1965. Contract AF04(695)-136. 61p. (LMSC-A769348; AD-476322). Dep. mn. CFSTI $3.00 cy, $0.75 mn.

Design of the Snapshot Agena as represented by the 7001 flight vehicle was evaluated for the purpose of determining possibilities of improving vehicle performance. Design changes which should be made are discussed for the following components: residual propellant disposal, propellant pressurization, altitude control junction box, surge battery requirements, voltage regulator fuses, voltage regulator redundancy, transmitter and tape recorder redundancy, submultiplexer Type IX, tape recorder Type VIII, multiplexer Type IV, operational controls, power control unit Type XIX, instrumentation, SNAP-10A interface, ion engine interface, and the antenna and altitude monitor systems. (M.O.W.)

14175 (TID-22418) SNAP 10A FLIGHT VEHICLE NUCLEAR ENVIRONMENT AND RADIATION EFFECTS. Bennett, C. M.; Krakar, J. J.; Kruse, W. G. (Lockheed Missiles and Space Co., Sunnyvale, Calif.). Oct. 15, 1965. Contract AF04(695)-136. 188p. (LMSC-A764793; AD-476320). Dep. mn. CFSTI $5.00 cy, $1.00 mn.

The results of measurements of gamma and neutron distributions in the SNAP 10A-Agena space vehicle are presented, and an analysis of radiation effects on SNAPSHOT equipment is made. Recommendations for future SNAP flights are included. (D.C.W.)

14176 THE STUDIES ABOUT NUCLEAR NAVAL PROPULSION IN FRANCE. Chevallier, J. (CEN, Saclay, France). Atompraxis, 11: 635-9(Nov.-Dec. 1965). (In German).

The construction of a reactor prototype for naval propulsion was concluded in 1960. The studies and constructions of this prototype were finished within 4 years. The reactor became critical for the first time on August 14, 1964, and received its nominal power some days later. The tests about stability and actual performances were satisfying and they guarantee to the first naval propulsion reactor the same functionalism like most modern foreign reactors. France has made the first step forward to nuclear naval propulsion. (auth)

14177 SNAP 10A, FIRST REACTOR IN SPACE. Johnson, Richard A.; Morgan, William T.; Rocklin, Sol R. (Atomics International, Canoga Park, Calif.). New York, Society of Automotive Engineers, Inc., 1965, Preprint No. 650793, 12p. (CONF-651034-3). ORINS.

From Society of Automotive Engineers, National Aeronautic and Space Engineering and Mfg. Meeting, Los Angeles.

SNAP 10A was designed to provide 500 electrical watts of power in space. It employs a compact nuclear reactor as the heat source, and converts the heat directly into electricity through thermoelectric conversion. It is the first complete powerplant of this type which has progressed through the design, development, and flight test stage. As part of the development program for SNAP 10A, complete systems were operated in a simulated space environment on the ground. One such system, designated FS-3, was sequentially tested through a complete environmental cycle, including shock and vibration, automatic reactor startup, and long-term endurance in a space chamber. As of Aug. 1, 1965, the unit had accumulated, satisfactorily, 190 continuous days of full power operation. Flight testing of the SNAP 10A unit took place on April 3, 1965, with the unit being brought to power in orbit at 1:45 a.m. Sunday morning, April 4. Startup of SNAP 10A in orbit occurred uneventfully and the unit operated continuously for 43 consecutive days. During this time, the performance of the system met or exceeded the design requirements in all respects and correlated closely with ground test data. On May 16, 1965, 43 days after startup, ground contact with the spacecraft was lost. Subsequent review of the data, while not totally

complete, indicates premature shutdown of the SNAP 10A system as a result of failures in some of the onboard electronic devices. (auth)

Research and Test Reactors

Refer also to abstract 12914.

14178 (AE–207) EXPERIMENTAL STUDIES ON ASSEMBLIES 1 AND 2 OF THE FAST REACTOR FRO. PART 2. Hellstrand, E.; Andersson, T. L.; Brunfelter, B.; Kockum, J.; Londen, S-O.; Tiren, L. I. (Aktiebolaget Atomenergi, Stockholm (Sweden)). Dec. 1965. 56p. Dep. mn.

Control rod calibrations were made using the positive-period, the inverse-multiplication, the rod-drop, and the pulsed-source techniques; the results show satisfactory agreement between the various methods. The reactivity worths of samples of different materials and different sizes were measured at the core center. Comparisons with perturbation calculations show that the regular and adjoint fluxes are well predicted in the central region of the core. The variation in the prompt neutron lifetime with reactivity was studied by means of the pulsed source and the Rossi-α techniques. Comparison with one-region calculations reveals large discrepancies, indicating that this simple model is inadequate. Some investigations of streaming effects in an empty channel in the reactor and of interaction effects between channels were made and were compared with theoretical estimates. Measurements of the reactivity worth of an air gap between the reactor halves and of the temperature coefficient are also described. (auth)

14179 (ANL–7122, pp 70–81) ADVANCED SYSTEMS RESEARCH AND DEVELOPMENT. (Argonne National Lab., Ill.).

Experimental and theoretical reactor physics, fuel and materials development, primary systems and components, control rod drive mechanisms, and general development activities are reported for the Argonne Advanced Research Reactor. The development and testing of Na–Pb bimetallic regenerative electrolytic emf cells is also reported. (T.F.H.)

14180 (COO–1430-1) SHIELDING ANALYSIS FOR THE FAST FLUX TEST FACILITY. DeFelice, Joseph (Nuclear Technology Corp., White Plains, N. Y.). June 30, 1965. Contract AT(11-1)-1430. 49p. (NTC–126). Dep. mn. CFSTI $2.00 cy, $0.50 mn.

For Battelle-Northwest, Richland, Wash.

The shielding requirements for the FFTF were investigated and an initial specification of required types and thicknesses of shield materials was obtained. The radial shield specification was 3.5 ft of iron plus 5 ft of graphite. The axial shield was specified to consist of 3 ft of iron above the 30-ft sodium pool. A number of alternate materials for the shield were also investigated. The best of these alternate materials was found to consist of a 5 ft layer of borated Fe_2O_3 in place of the 5 ft radial graphite shield. The borated Fe_2O_3 produced a secondary sodium activation about a factor of 8 less than the graphite shield. Furthermore, the use of borated Fe_2O_3 could very possibly result in a cost saving of approximately one million dollars by the elimination of the graphite and its associated inert gas systems. Complete neutron flux traverse calculations for the axial shield and the radial shield are presented both for the reference design and for a number of alternate materials. The results of parametric studies on a number of alternate shield materials are also presented. The results of variations in shield thickness for the reference design are also given. (auth)

14181 (COO–1430-2) ANALYSIS OF THE MAXIMUM HYPOTHETICAL ACCIDENT. DeFelice, Joseph (Nuclear Technology Corp., White Plains, N. Y.). June 30, 1965. Contract AT(11-1)-1430. 10p. (NTC–127). Dep. mn. CFSTI $1.00 cy, $0.50 mn.

For Battelle-Northwest, Richland, Wash.

An analysis of the maximum hypothetical accident in the FFTF is presented. The method used for the calculation is discussed. (M.O.W.)

14182 (COO–1430-3) FAST TEST REACTOR HYPOTHETICAL MELTDOWN ACCIDENT. Progress Report, October 1965–December 1965. DeFelice, Joseph; Hyland, Michael (Nuclear Technology Corp., White Plains, N. Y.). Jan. 21, 1966. Contract AT(11-1)-1430. 71p. (NTC–129). Dep. mn. CFSTI $3.00 cy, $0.75 mn.

For Battelle Northwest, Richland, Wash.

A study of the energy yield from a hypothetical meltdown accident for the FTR is in progress. Particular emphasis was placed on the effect of design variables and problem input parameters on this energy yield. One of the important design variables—the use of fuel zoning in the core—was explored in detail. Two available mathematical tools, the AX-1 and Weak Explosion computer codes, were used for this and the rest of the analyses. The AX-1 calculations have indicated a smaller increase in energy release due to fuel zoning than expected. The Weak Explosion code results in a large increase in energy release with fuel zoning. However, its lack of treatment of surface effects undoubtedly overestimates the effect of fuel zoning. Work is continuing to get a definitive result. Efforts on the refinement of core material physical properties and an estimate of the effect of core Doppler coefficient are in progress to firm up the meltdown accident energy release estimate. (auth)

14183 (DP–1037) FINAL SAFETY ANALYSIS OF THE MAXIMUM CREDIBLE ACCIDENT IN THE HEAVY WATER COMPONENTS TEST REACTOR. Arnett, L. M.; Ross, Charles P.; Rusche, Ben C.; Taylor, Charles D. (Du Pont de Nemours (E. I.) and Co., Aiken, S. C. Savannah River Lab.). Dec. 1965. Contract AT(07-2)-1. 30p. Dep. mn. CFSTI $2.00 cy, $0.50 mn.

The maximum credible accident in the HWCTR is analyzed for the conditions that exist since iodine absorbers were installed in the containment building. The absorbers remove radioiodine isotopes to the extent that the thyroid and whole-body doses at the Savannah River Plant boundary would be less by factors of six and twenty-five, respectively, than the allowable limits set forth in the Code of Federal Regulations (10 CFR 100). (auth)

14184 (JUL–236-RE) ERGEBNISSE DER ANFAHR-EXPERIMENTE AM REAKTOR FRJ-2. (Results of Start-up Experiments on the FRJ-2 Reactor). Fassbender, J.; Kraemer, H.; Meister, G. (Kernforschungsanlage, Juelich (West Germany). Zentralabteilung Forschungsreaktoren). July 1965. 213p. Dep. mn.

The physical experiments and measurements which were carried out on the FRJ-2 Reactor during the startup phase from November 13, 1962 to December 12, 1963, are reported in detail. The reactor plant is briefly described, but the individual elements are considered only to the point necessary for understanding of the experiments and the measurement results reported. The experimental part of the report begins with the description of the methods used in the first complete charging of the reactor with unirradiated fuel elements. In the following sections methods are discussed which were used for the measurement of the reactivity values with respect to their limits of error and the optimization of the measurement devices. The pulse source method is treated in some detail as most reactivity values were measured with this method. Measurement results are reported which give indications on the limits of error of this method. In addition to the pulse source measurements, reactivity values were determined from the subcritical neutron multiplication, multiplication time, and rod-drop measurements. The results of the various methods are compared. The reactivity absorption of the shutdown and control absorber, the reactivity of the top reflector, the temperature coefficient of the reactivity, reactivity losses through Xe and Sm poisoning, the reactivity values of individual fuel elements, and the distribution of the statistical weight in the reactor core for a weak neutron absorber were also measured. The in-hour relation of the reactor was experimentally determined by rod-drop measurements. The distribution of the thermal, epithermal, and fast neutron flux in the reactor core and in the experimental devices

were measured by probe activation. The methods used for these measurements and the devices are described and the results discussed. The measured flux distribution curves are compiled. The results of the power calibration from the fission rate determined by probe activation are compared with the results of the thermal power calibration. (tr-auth)

14185 (MIT-2344-4, pp 70-9) USE OF NEUTRON ABSORBERS IN THE DETERMINATION OF LATTICE PARAMETERS. Harrington III, J. (Massachusetts Inst. of Tech., Cambridge. Dept. of Nuclear Engineering).

A series of experiments is carried out on heavy-water-moderated sub-critical lattices to which varying amounts of thermal neutron absorber (Cu rods) are added. The purpose of these experiments is to obtain precise measurements of lattice parameters. Three lattices having widely varying moderator-to-fuel ratios are investigated. (T.F.H.)

14186 (MIT-2344-4, pp 145-8) EPITHERMAL NEUTRON STUDIES. D'Ardenne, W. H. (Massachusetts Inst. of Tech., Cambridge. Dept. of Nuclear Engineering).

The dependence of the effective resonance integral on the fuel-to-moderator ratio in MITR is to be examined. (auth)

14187 (NP-15836) AIR FORCE NUCLEAR ENGINEERING TEST FACILITY. (Air Force Inst. of Tech., Wright-Patterson AFB, Ohio). [1965]. 72p.

A general description of the Air Force Nuclear Engineering Test Facility (AF NETF) is presented. A detailed description of the facilities available at the AF NETF for the conduct of experiments is included. The procedures which an experimenter should use in requesting the use of the AF NETF are outlined. The ways in which a research or test reactor can be used as a tool of inquiry in support of the various scientific and engineering disciplines are discussed. (M.O.W.)

14188 (RT/FI(65)40) SU UNA MISURA DEL COEFFICIENTE DI TEMPERATURA DEL REATTORE RC-1 (TRIGA). (Temperature Coefficient Measurements of the RC-1 Reactor (Triga)). Focaccia, G.; Marseguerra, M. (Comitato Nazionale per l'Energia Nucleare, Rome (Italy)). Oct. 1965. 31p. Dep. mn.

Temperature coefficient measurements of the RC-1 reactor are presented. An experimental method is given permitting the determination of all the total coefficient components. The results of the method are in accordance with the General Atomic experimental measurements. (auth)

14189 (RT/FI(65)43) ESAME DEL METODO SPERIMENTALE DEL PCTR PER RETICOLI A PLUTONIO MODERATI CON ACQUA LEGGERA. (Feasibility Studies of PCTR Measurements With Light Water Moderated Plutonium Fueled Lattices). Cardosi, G.; Santandrea, E. (Comitato Nazionale per l'Energia Nucleare, Rome (Italy)). Nov. 1965. 21p. Dep. mn.

The feasibility of carrying on experiments of PCTR type with plutonium light water moderated lattices is analyzed from the physics point of view. The main difficulties found in the measurements come from the following characteristics: noticeable spectrum differences between the lattices to be tested and the driver, necessity of great quantities of poison with consequent deformation of the thermal spectrum and of the average values of σ and η, and noticeable epithermal contribution to the multiplication factor. The influence of these peculiar characteristics on the accuracy of the measurements is evaluated, and the improvements obtainable by means of some modifications of the traditional measurement system are analyzed. (auth)

14190 (UJV-1446/65) THE RESEARCH WORK ON THE WATER LOOP IN THE WWR-S REACTOR. Zajic, V. (Ustav Jaderneho Vyzkumu, Ceskoslovenska Akademie Ved, Rez). 1965. 34p. (CONF-651123-19). Dep. mn.

From Conference on Reactor Physics and Engineering, Budapest.

The equipment and operation of an experimental water loop inserted into the core of the WWR-S research reactor are described. At present the loop facility is used for the investigation of water corrosion on carbon steels intended for application in construction of the biological shield vessel for the heavy water reactor of the first Czechoslovak nuclear power plant. The influence of the reactor radiation on the process of corrosion and on the stability of water solutions with corrosion inhibitors are investigated in the loop. Some results of research carried out are given and further possibilities of water loop exploitation are outlined. (auth)

14191 (BNL-tr-60) PULSED RESEARCH REACTOR OF THE JOINT INSTITUTE FOR NUCLEAR RESEARCH AND FEASIBILITY OF PULSED REACTOR APPLICATION IN NEUTRON SPECTROSCOPY. Anan'ev, V. D.; Matora, I. M.; Pogodaev, G. N.; Rudenko, V. T.; Shabalin, E. P.; Shapiro, F. L.; Frank, I. M. (Joint Inst. for Nuclear Research, Dubna (USSR). Lab. of Neutron Physics). Translated by Stephen J. Amoretty (Brookhaven National Lab., Upton, N. Y.), from a report, 1965. 35p. Dep. mn. CFSTI $2.00 cy, $0.50 mn. JCL $3.60 fs, $1.45 mf.

The operation of the pulsed reactor at higher power is discussed, and the final design of the SORA high-power reactor is outlined. The experimental capabilities of pulsed reactors are compared with those of other types of pulsed neutron sources. (D.C.W.)

14192 REACTOR TYPES WITH FAST NEUTRONS IN FRANCE. Wustner, R. (CEN, Saclay, France). Atompraxis, 11: 616-20(Nov.-Dec. 1965). (In German).

After recalling the importance of the fast neutron reactor program in the French nuclear equipment schedule and the reasons for the selected trend, the great lines of action and some specific aspects of the studies pursued by the Euratom-CEA Association are discussed. After the completion on test reactor RAPSODIE and the HARMONIE and MASURCA installations, the next target of these studies is the reactor PHENIX which is to establish the possibilities of this new line of concepts. (auth)

14193 BREEDER REACTOR FEATURES SODIUM COOLANT, FUEL REPROCESSING PLANT. Mod. Power Eng., 60: 44-7(Jan. 1966).

The Experimental Breeder Reactor II at Idaho Falls is described with illustrations. In a brief outline, the fuel, unique fuel reprocessing facility, protection against intense radioactivity, and handling of 89,000 gallons of liquid sodium, are covered. Power is 1 Mw per litre of core volume. (F.S.A.)

14194 ULTRASONIC TESTING OF METALLIC URANIUM. Nakamura, Y.; Tateishi, Y. (Atomic Fuel Corp., Tokyo). pp 23-35 of STI/PUB/105(Vol. II).

The development of ultrasonic testing and the results of routine inspection on cast billets and rolled rods for JRR-3 fuel elements are described. The reactor is a domestic made, heavy-water-moderated and cooled, research reactor of 10 MW capacity, with aluminium-clad metallic uranium fuel elements. Cast billets of 3-in diam. were rolled to rods of 1-in diam. Ultrasonic testing was applied for detecting internal voids and cracks and for evaluating random orientation and grain size after heat treatment. The ultrasonic testing of uranium was very difficult because of its high acoustic impedance, and the high sensitivity of the transducers and special beam mask were necessary for the water-immersed transmission method. A set of brass billets with artificial defects was used as the standard. During the development of these standards, several kinds of Cu-Zn alloy were examined for their acoustic properties. Any internal defects greater than 2 mm and 0.5 mm equivalent diameter were rejected in the case of billets and rolled rods respectively. Two billets which included typical voids were rolled to size, and ultrasonic testing and radiography with Betatron were carried out at several stages to find the behavior of the voids during fabrication. The attenuation of ultrasonic waves is affected by the grain size, and is particularly large if the ultrasonic wavelength is comparable to the grain size. This was used for the detection of unsatisfactory heat treatment. The ultrasonic wave speed is different in the parallel and

perpendicular rolling directions in as-rolled state. This difference decreased as the temperature of heat treatment is increased; however, a small difference was observed in a beta-quenched specimen, and real acoustic isotropy was obtained by gamma-quenching. (auth)

14195 ULTRASONIC WATER-GAP MEASUREMENTS IN MTR FUEL ELEMENTS. Deknock, R. (S.C.K./C.E.N., Mol, Belg.). pp 37-46 of STI/PUB/105(Vol. II).

The high thermal fluxes, which are usual in the latest materials testing reactors, impose suitable paths for uniform heat transfer and a reliable heat removal avoiding bulk-vapor formation. Furthermore, to control the overall swelling and reactor fuel behavior, water-gap measurements will also be performed in post-irradiation experiments on spent fuel elements. For that purpose, a probe for measuring the 3-mm water-gap of the BR-2 fuel element over a 1-m length, based on the principle of ultrasonics, was developed. In the case of post-irradiation experiments, the measuring probe should operate in a fuel element by being immersed in a water pool at a depth of at least 6 m. The probe can withstand prolonged immersion in water and is not affected by normal gamma-irradiation doses. Although operating on the usual pulse-reflection method, the system allows emitted and reflected pulses to be separated by a 10-MHz ferro-electric crystal with high inherent energy dissipation. Oscilloscope read-out can be used, whereby the time is displayed on the horizontal axis, the scanning speed being adjusted to bear a direct relation to the velocity of wave propagation, i.e., the gap distance. This type of read-out is satisfactory where the number of measurements is restricted, but chart recorder read-out is obviously desirable. In this case, emitted and reflected pulses are shaped and fed to a time-voltage converter using transistor logic techniques. The instrument allows continuous adjustment of output zero for any arbitrary gap distance between 2 and 4 mm thereby permitting zero-center-recording. Furthermore, any desired 100-μm gap distance variation can give a stable 1-V output voltage to a recorder. An accuracy of 5-μm gap-distance variation is easily obtained. Several fuel elements were measured. The results and reproducibility were very satisfactory. (auth)

14196 ASSESSMENT OF END-PLUG WELDING OF FUEL ELEMENTS. Nakamura, Y.; Aoki, T. (Atomic Fuel Corp., Tokyo). pp 265-76 of STI/PUB/105(Vol. II).

Several kinds of assessments in out-of-pile state were carried out simulating the in-reactor conditions. Some details of these assessments on JRR-3 fuel elements are described. The reactor is a heavy-water-moderated and cooled research reactor of 10-Mw capacity, with aluminum-clad metallic uranium fuel elements. As the elements have only mechanical bonding between cladding and core, there might be a tensile stress at the end plug as a result of irradiation growth of the uranium core. Thermal cycling will cause a similar stress in the welds. Preferential corrosion by hot water might occur in the vicinity of the welds because of the difference of micro structure. It is essential to keep leak tightness during and after the reactor service. Specially designed specimens were used for tensile testing, high-temperature creep testing, thermal cycling, and corrosion testing. Many sorts of weld characters were examined nondestructively before the tests and leak checked at intervals of the tests. Evaluations of these results may be used for the establishment of inspection standards such as x-ray radiography and visual inspection of the end plug welding. Some other results on Magnox-clad and Zircaloy-clad fuel elements are also described. (auth)

14197 THE ROLE OF NON-DESTRUCTIVE TESTING IN TEST-REACTOR OPERATION AT THE NATIONAL REACTOR TESTING STATION. Francis, W. C.; Brown, E. S.; Burdick, E. E.; Gibson, G. W.; Tingey, F. H. (Phillips Petroleum Co., Idaho Falls, Idaho). pp 331-49 of STI/PUB/105(Vol. II).

The various nondestructive testing methods in use at the National Reactor Testing station are discussed. The performance and uses of ultrasonics, gamma scanning, eddy current, and mechanical probing techniques are discussed. (M.O.W.)

14198 FUEL LOCATION, HOMOGENEITY AND AMOUNT IN FLAT AND TUBULAR CONFIGURATIONS. de Meester, P. (Studiecentrum voor Kernenergie, Mol, Belg.). pp 413-36 of STI/PUB/105(Vol. II).

The fuel elements for the materials testing reactor BR-2 can be assembled either with plates obtained by the picture frame process, or with tubes obtained by coextrusion. In the course of the fabrication and before reactor loading the fuel disposition, the homogeneity and the absolute amount have to be checked or measured. Radiography at about 80 to 90 kev, autoradiography and gammagraphy with a thulium-170 source were done. By radiographing the fuel tubes a lead mandrel with the x-ray film fixed to it was placed inside the tube and subsequent x-ray shots at different angles were taken. A radioactive source scanning the fuel tube along its center line in combination with a film around the tube showed records with a high resolution. The fuel homogeneity is to be controlled in view of a safe reaction operation, i.e., on the one hand to avoid exaggerated fuel concentrations that could give rise to vapor formation in the operating PWR, and on the other hand to guarantee a sufficient and evenly spread fuel load. Radiographs can be used for a visual check. However, if a quantitative analysis is needed, a better device is a scintillation gamma spectrometer measuring the proper radiation emitted by the ^{235}U. An analysis of the results on some 400 fuel plates and on a first batch of fuel tubes is given. Forming characteristics and typical end forms can be controlled. Digital results from static measurements and continuous recording are discussed. The fuel amount as an absolute quantity should be known per zone for actual reactor operation calculations and per complete element for reasons of fuel accounting and for comparison with post-irradiation burnup evaluation. The fabrication and the use of the different standards are considered. Accuracy and elimination of errors are discussed. Some possible future improvements in the tests are proposed. (auth)

14199 MODIFIED PULSED SOURCE TECHNIQUES. Gozani, T. (Atomic Energy Commission, Tel Aviv, Israel); Demarmels, P.; Huerlimann, T.; Winkler, H. pp 49-62 of STI/PUB/104(Vol. 2).

The modified pulsed source techniques of Gozani and of Garelis and Russell were checked experimentally at the swimming pool reactor SAPHIR. These methods are characterized by the simultaneous experimental determination of negative reactivity and generation time. Both quantities obtained by these methods are in units of dollar (i.e., β_{eff}) and therefore are independent of arbitrary theoretical definitions. Measurements were carried out for several subcritical states. Various proposed correction terms were scrutinized experimentally. The effects of the finite width of the neutron pulses were investigated. Measurements were carried out for a variety of delayed neutron states at the beginning and end of the experiment. All corrected reactivity values agreed well within their statistical errors. Systematic errors caused by spatial harmonics were studied by varying the position of the detector. It is shown that in the presence of positive harmonics (normally close to the source) the evaluation procedure proposed by Gozani generally gave results slightly below the correct reactivity values, whereas the procedure proposed by Garelis and Russell resulted in slightly larger ones. For negative harmonics the situation is reversed. Thus, the two methods may be used to bracket the correct values of reactivity and generation time. The reactivity of a state near -10 \$ was measured in this manner with a precision of 2%. (auth)

14200 REACTIVITY MEASUREMENT BY THE PULSED NEUTRON METHOD. Scott, S. A. (Israel Inst. of Tech., Haifa). pp 63-76 of STI/PUB/104(Vol. 2).

An extensive series of subcritical reactivity measurements was carried out with the IRR-I swimming pool reactor, to test the applicability of the pulsed neutron method to a fully reflected core heavily contaminated with fission

products. A Kaman pulsed neutron source was located on the grid plate, and up to 11 $ negative reactivity was obtained by completely inserting the control rods, both singly and in groups. Each subcritical reactivity level was determined by the pulsed neutron technique and compared to stable period and rod drop measurements. The pulsed neutron data was analyzed in three ways: (1) The prompt neutron decay period α was determined at each reactivity level, including the value α_0 at delayed critical. The reactivity in $ is then given by $\alpha = \alpha_0 (1 + \$)$ where $\alpha_0 = k/l^*$. A correction is applied to account for the dependence on reactivity of the reduced prompt neutron average lifetime l^*. (2) The method of Garelis and Russell. It is shown that serious errors are introduced by this method of analysis if the prompt neutron density reaches the constant background level before the arrival of the following pulse. The effect is particularly important in situations close to delayed critical. A suitable correction term is developed and applied to the analysis. (3) On the assumption that only the fundamental harmonic term is present, the Garelis and Russell form of analysis is simplified to $\$ = AR/D\alpha$ where A/D is the saturated prompt-to-delayed neutron ratio during the pulse. A detailed evaluation of these forms of analysis is presented, and the experimental results are compared with those obtained by the "conventional" techniques of stable period and rod drop. Finally a composite form of analysis is recommended, in which the improved Garelis and Russell method is used to obtain α_0, which is then used in the decay period method for reactivity measurements. (auth)

14201 FAR SUBCRITICALITY MEASUREMENTS BY THE PULSED NEUTRON TECHNIQUE. Petrovic, M. (Boris Kidric Inst. of Nuclear Science, Belgrade). pp 281-6 of STI/PUB/104(Vol. 2).

Subcriticality measurements of the Argonaut reactor were performed with the reactivity as far as −15 $. Data are obtained by measuring the time and space distribution of the decaying neutron after the injected burst. The reactor was made subcritical with dummy fuel plates inserted into the system instead of fuel plates. Dummy fuel plates were made with the same absorption cross section as the fuel. The Kaman Pulsatron was used as the pulsed neutron source. To minimize generation of the higher modes in the initial flux distribution, attention was paid to the positioning of the neutron source. The BF_3 counters and the TMC multichannel analyzer were used for detection, time analysis and registration. The data were processed using the ZUSE Z-23 digital computer. The results of measurements show the limit of the method. (auth)

14202 FAST-REACTOR PHYSICS PARAMETERS FROM A PULSED SOURCE. Kato, W. Y. (Argonne National Lab., Ill); Meister, H. H.; Main, G. W.; Russell, J. L. Jr.; Crosbie, K. L. pp 373-97 of STI/PUB/104(Vol. 2).

To evaluate the feasibility of measuring fast neutron spectra from a core using time-of-flight techniques, an experiment was performed to measure the equilibrium spectrum in a large block of depleted uranium using the linac facilities. A ten-metric-ton block of depleted uranium was assembled to form a 81-cm cube. This block of uranium was pulsed by electron bombardment of a uranium target imbedded in the block. The spectra from various sections of the block were measured using time-of-flight techniques for a 50-m flight path. Spectral indices, such as the ratio of the fission rates of $^{238}U/^{235}U$, $^{233}U/^{235}U$, $^{234}U/^{235}U$, $^{237}Np/^{235}U$, $^{239}Pu/^{235}U$, were also measured. In addition, measurements of the ^{238}U capture rates were obtained in various parts of the block. The techniques used to obtain these reactor physics parameters are described. The experimental results such as the spectra and spectral indices are also compared with those obtained from theoretical considerations using multigroup transport theory analysis. The pulsed neutron technique is also applicable for the measurement of such parameters as: β/l, where β is the effective delayed neutron fraction and l is the lifetime; neutron importance; and k_{eff}. A discussion on the proposed application of a pulsed neutron source for the measurement of some of these parameters on fast reactor cores constructed on ZPR-VI, the Argonne Fast Critical Facility is included. (auth)

14203 THE TRANSIENT CHARACTERISTICS OF A NEW PULSE RESEARCH REACTOR. MacPhee, J. (American Machine and Foundry Co., York, Pa.); Lumb, R. F. pp 573-88 of STI/PUB/104(Vol. 2).

A new concept in research reactors has recently been proof-tested. The new core was designed by AMF Atomics to be compatible with existing physical facilities and replaces a highly-enriched uranium-aluminum plate-type core. Called PULSTAR for ease of reference, the new core consists of uranium dioxide, enriched 6% in the isotope ^{235}U. Sintered oxide pellets clad with Zircaloy comprise the fuel rods, 25 of which, in a 5 × 5 array, are incorporated in the 3 in. × 3 in. box of the fuel assembly. An eccentric nosepiece on the fuel assembly provides two orientations on the grid plate. Adjacent assemblies rotated 180° generate half-inch water gaps in which the six silver-indium-cadmium control blades operate. The pulsing capability is accomplished by fixing one control blade to the piston of a pneumatic cylinder. Standard AMF cantilever rod drives, as originally installed, are utilized to position all rods. PULSTAR was designed for 5-Mw steady state operation capable of pulsing to 10,000-Mw peak power in a burst with a width, at half height, of less than 10 ms. The Doppler broadening of the ^{238}U resonance absorption peak provides the prompt shutdown. The heavily loaded, undermoderated core which results from these specifications provides some unique operating characteristics. Detailed physics parameters, such as prompt neutron lifetime, void, temperature and power coefficients of reactivity, and the assets accruing from low xenon poisoning are presented. The transient characteristics are described including data on period versus reactivity, power versus period, energy versus period, burst shape parameters, and fuel and clad temperatures. Also included are neutron spectrum data and flux distribution in the experimental facilities. (auth)

14204 SWIMMING POOL TYPE REACTOR. Hasegawa, Toru (to Hiatchi, Ltd.). Japanese Patent 1964-27165. Nov. 27, 1964. Filed Aug. 13, 1962.

In the swimming pool reactor proposed, in order to prevent the diffusion of radioactivity in the "warm water layer," the downward current is produced in the layer. The compartment containing the reactor core at the bottom extends vertically open to the atmosphere and separates the cooling water in the compartment from the rest pool water. The warm water layer is formed in the top of this compartment, and the warm water is supplied from the top. A ring-shaped pipe with many holes is placed in the lower part of the layer and is connected to the external pump. Thus, the slightly radioactive hot-water layer can always be supplied with fresh water, and the downward current can be maintained. (NSA of Japan)

14205 SWIMMING POOL TYPE REACTOR. Yoshiyanagi, Kiyomi (to Hitachi, Ltd.). Japanese Patent 1964-27170. Nov. 27, 1964. Filed Sept. 11, 1962.

In the swimming pool reactor, the forced circulation of cooling water can easily be changed to the natural circulation at the time of an accident. The water tank with the reactor core extending vertically separates the coolant system from the pool water. An entrance and exit for the forced circulation are located at the top and bottom of the reactor core. A warm-water layer is provided in the top of the tank. A natural circulation system is installed through the exit and entrance. In the entrance of circulation water in the natural circulation system, a means is provided for preventing the counter-flow. By the hydraulic pressure of the forced circulation, the natural circulation is interrupted, and the forced circulation system operates. When the pressure of the forced circulation becomes lower than the predetermined value, this circulation is stopped by the pressure of the natural circulation, and the latter system starts to operate. (NSA of Japan)

14206 DEVICE FOR ADJUSTING THE POSITION OF ELEMENTS IN A NUCLEAR REACTOR TANK. Jouin, Jacques (to Commissariat a l'Energie Atomique). U. S. Patent 3,220,573. Nov. 30, 1965. Priority date Apr. 13, 1962, France.

A device is described for adjusting the position of fuel

elements in a nuclear reactor tank and thus for modifying the neutron-flux characteristics of the reactor. The device makes it possible to arrange a number of fuel elements in a uniform lattice having a variable pitch, whether square, rectangular, or triangular, particularly in the tank of a swimming pool reactor. The device is also applicable to the positioning of reflector elements or the like inside a reactor tank. (B.L.M.)

WASTE DISPOSAL AND PROCESSING

See also BIOLOGY AND MEDICINE — Ecology
CHEMISTRY — Radiochemistry
CHEMISTRY — Separation Processes and Procedures
HEALTH AND SAFETY

Refer also to abstract 12928.

14207 (IDO-14670) STABILITY STUDIES OF HIGHLY RADIOACTIVE ALUMINA CALCINE DURING HIGH TEMPERATURE STORAGE. Wilding, M. W.; Rhodes, D. W. (Phillips Petroleum Co., Idaho Falls, Idaho. Atomic Energy Div.). Jan. 1966. Contract AT(10-1)-205. 13p. Dep. mn. CFSTI $1.00 cy, $0.50 mn.

Stability of highly radioactive alumina calcine from the Waste Calcining Facility was studied in a temperature range from 600 to 1200°C. Strontium-90 and cerium-144 were not volatile. Cesium-137, ruthenium-106, boron, mercury, and nitrate were volatile to some degree over this temperature range. The alumina produced in the WCF was amorphous but converted to alpha alumina at 800°C and higher temperatures. (auth)

14208 (ORNL-P-1926) ESTIMATED COSTS OF HIGH-LEVEL WASTE MANAGEMENT. Blomeke, J. O.; Salmon, R.; Roberts, J. T.; Bradshaw, R. L.; Perona, J. J. (Oak Ridge National Lab., Tenn.). [nd]. Contract W-7405-eng-26. 21p. (CONF-660208-1). Dep. mn. CFSTI $1.00 cy, $0.50 mn.

From Symposium on Solidification and Long-Term Storage of Highly Radioactive Wastes, Richland, Wash.

The costs of perpetual tank storage of both acid and alkaline wastes were estimated as a function of tank size, tank life, and fission product concentration in the waste for three representative types of financing. For acid wastes, the optimum tank capacity is about a million gallons, and minimum total costs range from 0.0165 to 0.0272 mill/kwhr. For alkaline wastes, the optimum tank capacity is 2.5 million gallons, and minimum total costs range from 0.0177 to 0.0294 mill/kwhr. Reducing the volume of wastes, as stored, by doubling the concentration of fission products reduces the total costs between 15 and 30%. The minimum total costs for management by the series of operations consisting of interim liquid storage, pot calcination, interim solid storage, shipment, and disposal in salt mines, are estimated to range from 0.017 to 0.020 mill/kwhr when carried out over a 30-year period. (auth)

14209 (RT/PROT(65)29) A STUDY ON THE SORPTION PROPERTIES OF THE NATURAL TUFFS OCCURRING IN THE LAKE BRACCIANO REGION (ROME). Report No. 2. Boenzi, D.; Dlouhy, Z.; Lenzi, G. (Comitato Nazionale per l'Energia Nucleare, Rome (Italy)). Oct. 1965. 16p. Dep. mn.

Samples of 85 different materials were studied with respect to their sorption capacity for microamounts of ^{137}Cs and ^{89}Sr from low-activity waste solutions. The materials studied were classified according to certain criteria, chiefly as regards the influence on sorption of grain size, of pH, of the contact time, and of the concentration of competing Na^+ and Ca^{2+} ions. On a limited number of particularly interesting samples, sorption kinetics were also briefly studied. The classification of a total of 175 samples, tuffs (90 in the first and 85 in this second part of the work), has led to the identification of a number of very promising materials, predominantly volcanic tuffs, which meet the requirements of good natural sorbents and which may be used to advantage in the treatment of contaminated liquids. (tr-auth)

14210 HANDLING AND FILTRATION OF RADIOACTIVE SLUDGES. Pearce, K. W.; Smyth, M. J. (Atomic Energy Research Establishment, Harwell, Eng.). Filtr. Sep., 90-4(Mar.-Apr. 1965).

Two processes for treatment of radioactive sludges were developed: pressure filtration at 30 to 35 psig and freezing-thawing followed by vacuum or centrifugal filtration. (M.C.G.)

14211 TREATMENT OF RADIOACTIVE WASTE. Hwang, Yin-Si; Huang, An-I (National Tsing Hua Univ., Hsinchu, Taiwan). Ho Tsu K'o Hsueh, 4: No. 3-4, 85-90 (Aug. 1965).

Attempts were made to investigate the feasibility of disposing radioactive liquid wastes from ^{131}I and ^{60}Co produced in the radioisotope laboratory of the National Tsing Hua University. In particular much effort was devoted to finding a simple method of disposal of the liquid waste resulting from the production of ^{131}I and the recovery of telluric acid. It was found that the pH adjustment of liquid waste as well as the addition of precipitant (sodium phosphate : calcium hydroxide = 1 : 0.6) is effective to decontaminate the radioactivity of the liquid waste. The nitric acid precipitation method and the alcohol precipitation method were tried for the recovery of telluric acid from the liquid waste. For the ^{60}Co liquid waste mixed reagent, sodium carbonate : calcium hydroxide = 1 : 1 was found to be effective. (auth)

14212 RADIOACTIVE WASTE MATERIAL INCINERATOR. Berghout, Christian F.; Dauer, Maxwell; Lanard, Francis W.; Minx, Ramon P.; Senoski, Walter E.; Ward, Ural T. (to U. S. Army). U. S. Patent 3,218,997. Nov. 30, 1965. Filed Feb. 6, 1963.

In a proposed incinerator for combustible radioactive material, the combustion chamber has charging means for the waste material, fuel injection means, means to support the material, and air supply means. A controlled ash disposal means at the base of and contiguous to the combustion chamber includes an ash chute, a control valve in and for the ash chute, means for liquid spraying the ash in the chute, and dust removal means for disposal of the dust created by the combustion by discharging the contents of the combustion chamber. Dynamic precipitation means purify the waste gases emitted from the combustion chamber, and water cooled exhaust conduit means are provided between the combustion chamber and the dynamic precipitation means. A controlled precipitation disposal means are provided contiguous to the precipitation means and includes a valve controlled hopper and dust removal means. A radiation detector alarm and recording device is mounted in the stack and at the ash disposal means. (B.L.M.)

GENERAL AND MISCELLANEOUS

14213 (ACF–15) FILAMENT WOUND JOINT DESIGN STUDY. Underwood, W. F. (ACF Industries, Inc., Albuquerque, N. Mex.). Oct. 13, 1965. Contract AT(29-1)-1352. 100p. (ACF–412-256). Dep. mn. CFSTI $3.00 cy, $0.75 mn.

Studies were made to establish the type of joints in filament wound structures which made the most effective contribution to joint strength and integrity. The problem of bonding dissimilar materials, such as fiberglass to metal, was investigated. Basic data concerning bond strengths, cleaning procedures for bonding, ultimate laminate shear and bearing stresses, and various joint concepts are presented. (auth)

14214 (BNL–8564) THE HISTOPATHOLOGY OF HEREDITARY CONCENITAL DEAFNESS IN WHITE MINK. Saunders, L. Z. (Brookhaven National Lab., Upton, N. Y.). [nd]. Contract AT(30-2)-Gen-16. 15p. Dep. mn. CFSTI $1.00 cy, $0.50 mn.

The histology of the ear of minks is described. Comparison is made of the histology of the ears of brown mink and that of the congenitally deaf white mink of the Hedlund strain. (C.H.)

14215 (BNL–8643) QUIESCENT CENTER OF THE PRIMARY ROOT OF GLYCINE MAX. Miksche, Jerome P.; Greenwood, Michael (Brookhaven National Lab., Upton, N. Y.). [1964]. Contract AT(30-2)-Gen-16. 12p. Dep. mn. CFSTI $1.00 cy, $0.50 mn.

Seeds of Glycine max were sown in vermiculite under controlled growth room conditions and were treated at various times from 24 to 120 hr after the beginning of germination by soaking for one hr in a solution of 10 μc/ml of tritiated thymidine. The quiescent zone, defined as regions of cells that did not display DNA synthesis 24 hr after planting, was located by autoradiography of sections of germinating seeds and seedlings. The quiescent center was observed to change in size at various times after sowing. It increased in size during early development, then decreased with a corresponding reduction of the cell population of the root. Delimitation of quiescent center boundaries was difficult in view of dramatic changes in size of regions of non-DNA synthesis within the primary root. (C.H.)

14216 (BNL–9859) TIME AND TEMPERATURE TOLERANCES OF MAIZE SEEDS. Briggs, Robert W. (Brookhaven National Lab., Upton, N. Y.). [nd]. Contract AT(30-2)-Gen-16. 9p. (CONF-660101–1). Dep. mn. CFSTI $1.00 cy, $1.00 cy, $0.50 mn.

From 1st International Mutation Group Meeting, Vienna.

The length of time that maize seeds can remain viable when soaked in water at different temperatures with different gas contents and then dried back to a dormant state was studied. Biological effects of gases at 3° and 45°C were found to be related to their solubility in water. At these temperatures carbon dioxide was the most soluble of those tested and gave the greatest effect. These results are compatible with Henry's law. However, at 25°, increased metabolic activity in the presence of oxygen and air apparently gave the greatest biological effect. The oxygen treatment was the least effective at 3 and 45°C. This response follows neither Henry's law nor the data on solubility of gases in water. Since nitrogen is the least soluble gas used and would not be expected to increase metabolic activity, it should give the least damage. Since this was not so it appears that these anaerobic conditions are more detrimental than aerobic conditions at 3 and 45°C. (P.C.H.)

14217 (COO–888-43) ION UPTAKE BY CELLS ENZYMICALLY ISOLATED FROM GREEN TOBACCO LEAVES. Jyung, Woon H.; Wittwer, Sylvan H.; Bukovac, Martin J. (Michigan State Univ., East Lansing. Dept. of Horticulture). Sept. 21, 1964. Contract AT(11-1)-888. 19p. Dep. mn. CFSTI $1.00 cy, $0.50 mn.

An improved method for the enzymic separation of cells from green tobacco leaves is described. The isolated cells appropriately suspended and incubated in aqueous solution were utilized for studies of Rb and phosphate uptake. Cells from leaves, stems, and roots of bean seedlings were also isolated and relative rates of Rb uptake estimated. Absorption of Rb by green tobacco leaf cells was temperature dependent. Energy sources such as light, and succinate and bicarbonate as a source of CO_2 for photosynthesis promoted uptake. Absorption rates in the light for green leaf cells exceeded by almost 100 per cent those isolated from the pith. Rb uptake was sensitive to NaN_3 and DNP, and was essentially non-exchangeable. The inhibitory effect of DNP on Rb uptake was negated by the addition of ATP. Phosphate absorption by isolated leaf cells was also temperature dependent, and suppressed by NaN_3 and DNP. The DNP effect on phosphate uptake, however, was not altered by the exogenous application of ATP. Temperature coefficients (Q_{10}) for Rb and phosphate uptake were significantly reduced by the addition of decenylsuccinic acid, but this was also accompanied by a marked suppression in total phosphate absorbed, with a slight increase in Rb uptake. The results suggest that the coupling between absorption and metabolism occurs at the cellular level during the overall course of foliar absorption of mineral nutrients. (auth)

14218 (COO–888-44) THE EFFECTS OF UREA ON ION PENETRATION THROUGH ISOLATED CUTICULAR MEMBRANES AND ION UPTAKE BY LEAF CELLS. Yamada, Y.; Jyung, W. H.; Wittwer, S. H.; Bukovac, M. J. (Michigan State Univ., East Lansing). [1965]. Contract AT(11-1)-888. 10p. Dep. mn. CFSTI $1.00 cy, $0.50 mn.

Urea at a concentration of 10 millimolar enhanced the permeation of both rubidium and chloride ions through astomatous cuticular membranes enzymically isolated from ripe tomato fruit. Similarly, urea facilitated the absorption of rubidium by cells (palisade, spongy parenchyma) separated from green tobacco leaf laminae, but there was no effect on chloride uptake. The potentiations of cuticular permeability and cellular absorption of mineral nutrients induced by urea may explain reports of the increased effectiveness of nutrient sprays in the presence of urea. (auth)

14219 (COO–888-47) PATHWAYS AND MECHANISMS FOR FOLIAR ABSORPTION OF MINERAL NUTRIENTS—A REVIEW. Jyung, W. H.; Wittwer, S. H.; Yamada, Y.; Bukovac, M. J. (Michigan State Univ., East Lansing. Dept. of Horticulture). [1964]. Contract AT(11-1)-888. 21p. Dep. mn. CFSTI $1.00 cy, $0.50 mn.

Existing data on the mechanisms of nutrient absorption by plant leaves are summarized. Topics discussed include the role of enzyme kinetics in ion uptake by leaves, the relation of nutrient uptake and cellular metabolism, pathways of penetration of nutrients, the function of carriers in nutrient uptake, criteria for active foliar absorption of mineral nutrients, the energetics and kinetics of foliar absorption, and a comparison of mechanisms in foliar and root absorption of nutrients. 38 references. (C.H.)

14220 (COO–888-48) UPTAKE AND TRANSPORT OF ^{59}Fe BY INTACT LEAVES AND ENZYMICALLY ISOLATED LEAF CELLS OF THE BEAN PLANT (PHASEOLUS VULGARIS). De, Rajat; Wittwer, S. H.; Kannan, S. (Michigan State Univ., East Lansing. Dept. of Horticulture). [1965]. Contract AT(11-1)-888. 12p. Dep. mn. CFSTI $1.00 cy, $0.50 mn.

Absorption and mobility of ^{59}Fe applied as $FeSO_4$, FeEDTA, FeEDDHA and $FeSO_4$ in the presence of urea were evaluated utilizing the primary leaves of intact greenhouse-grown bean plants, the leaf immersion and washing technique, and enzymically isolated cells from the lamina of the primary leaves. Urea greatly enhanced

the absorption of ^{59}Fe from $FeSO_4$ and its mobility within the treated leaf. Iron absorption from FeEDDHA was greatly depressed both with intact leaves and isolated leaf cells, but mobility of the absorbed iron in the intact plants was greatly increased. The effects of EDTA both on the absorption of iron by isolated cells and mobility of the foliar absorbed iron within the intact plant were intermediate between $FeSO_4$ and EDDHA. (auth)

14221 (COO–1198-230) PRESSURE AND THE ELECTRONIC STRUCTURE OF SOLIDS. Drickamer, H. G. (Illinois Univ., Urbana). [1964]. Contract AT(11-1)-1198. 21p. Dep. mn; CFSTI $1.00 cy, $0.50 mn.

The use of very high pressure to elucidate the electronic structure of solids is illustrated. Three examples are included. The first topic is the approach to the metallic state in insulators and semiconductors. It is shown that this can be a continuous process as in iodine or it can involve a first order phase transition as it does for silicon, germanium, and a large number of III–V and II–VI compounds with related structure. The second topic is the so called electronic transition wherein the energies of outer electronic states of an element are modified as the interatomic distance decreases. The example presented involves the alkali metals. In cesium, in rubidium, and apparently ultimately in potassium the conduction electron which is normally an s electron is scattered into a d state, entirely changing the outer electronic structure of the atom. The final topic concerns the electronic structure of iron. At 130 kilobars there is a first order phase transition to the hcp structure. Mössbauer measurements show that the hcp is not ferromagnetic. It is also possible to describe the effect of pressure on the internal magnetic field of the bcc phase, as well as the changing character of the valence electrons in the two phases and at the transition. (auth)

14222 (NP–15612) THIRTEENTH ANNUAL REPORT FOR THE YEAR ENDING JUNE 30, 1965. (Australian Atomic Energy Commission). 100p. Dep. mn; Australian AEC Free.

The Commission recommended the continuation of exploration for U in the Northern Territory, and has encouraged private producers in Australia to resume exploration. Uranium concentrate in Australia is produced at the Rum Jungle plant. The main research program continued to be a study of the technical and economic feasibility of a high temperature, gas cooled reactor concept (H.T.G.C.R.) of the pebble-bed type in which the core is composed of ceramic materials—oxides of U, Pu, Th, and Be. During the year, these studies were concerned largely with fundamental research in the fields of materials, nuclear and reactor physics, and nuclear engineering. Efforts directed to the production and application of radioisotopes are summarized. The reactor HIFAR is particularly suitable for the production of isotopes with a high specific activity, such as ^{60}Co. Sources of ^{60}Co with activities up to 250 curies per gram were prepared for hospital use. Other radioisotopes were also produced for use in research, medicine, agriculture, and industry. New laboratories to house irradiation research facilities were completed during the period and work began on the construction of radiochemical laboratories for development and production of processed radioisotopes to meet medical and scientific requirements. Extensive gamma irradiation facilities were set up using ^{60}Co and irradiated fuel elements from HIFAR, and also a 1.3 Mev electron accelerator. During the year under review the Commission continued to receive a satisfactory flow of information from overseas and reports of the work done by the Commission's officers and by university research staff under contract to the Commission have received a wide circulation overseas. Australia participated in developments relating to the international transport of radioactive materials, including a major revision of the International Atomic Energy Agency Regulations for the Safe Transport of Radioactive Materials. The Commission installed an IBM 7040/1401 digital computing system at the Research Establishment at Lucas Heights. The major use of the computer has been the running of large programs to solve complex physics and engineering problems associated with the reactor study. (J.R.D.)

14223 (NP–15723) RAPPORT ANNUEL, 1964. (Annual Report, 1964). (Commissariat a l'Energie Atomique, Paris (France)). 192p. Dep. mn.

The activities of the CEA during 1964 with respect to the production of base materials for the nuclear industry, scientific and technical research, nuclear reactors, artificial radioelements, military applications, relations of CEA with industry, international relations, instruction, and finances are summarized. The general structure of the CEA with respect to the research centers and the production centers is described. In the production of base materials the emphasis is on mining, concentration, and processing of natural uranium and recovery enriched uranium. The technical and scientific research included studies on general physics, reactor physics, reactor chemistry, nuclear fuels, nuclear materials, physical chemistry, chemical and isotopic analysis, radiobiology, and radiological protection. Operations of the research, training, production, and power reactors are outlined. The industrial applications of radioisotopes are discussed. Examples are given of research on possible military applications of nuclear energy. (J.S.R.)

14224 (TID–21562) THE PREMEIOTIC STAGES OF SPERMATOGENESIS. Hannah-Alava, Aloha (Turku Univ. (Finland). Dept. of Genetics). [1964]. Contract AT(30-1)-2690. 91p. Dep. mn. CFSTI $3.00 cy, $0.75 mn.

A review is presented on germ-cell maturation primarily in D. melanogaster. The subjects discussed include: maintenance of the germ-line and spermatogonial multiplication; relating temporal and spatial patterns of spermatogenesis; and radiosensitivity of spermatogonia. 175 references are cited. (P.C.H.)

14225 (TID–21577) PYRIDINE COMPLEXES OF NICKEL(II). Rosenthal, Michael R.; Drago, Russell S. (Noyes Lab. of Chemistry, Univ. of Illinois, Urbana). [1964]. Contract AT(11-1)-758. 19p. Dep. mn. CFSTI $1.00 cy, $0.50 mn.

Evidence for the existence of $Ni(C_5H_5N)_6^{2+}$ is presented for the first time. This permits direct calculation of the spectrochemical parameters for pyridine. The complexes $Ni(C_5H_5N)_4(ClO_4)_2$ and $Ni(C_5H_5N)_4(BF_4)_2$ were prepared and found to be high-spin at room temperature with coordinated perchlorate and tetrafluoroborate. A nitrate complex of formula $Ni(C_5H_5N)_3(NO_3)_2$ was also prepared. The behavior of these complexes in solution and their reactions in solution with excess pyridine are reported. (auth)

14226 (TID–21586) DETERMINATION OF THE DONOR SITES IN LEWIS ACID ADDUCTS OF ANISOLE AND THIOANISOLE. Wayland, Bradford; Drago, Russell S. (Noyes Lab. of Chemistry, Univ. of Illinois, Urbana). [1964]. Contract AT(11-1)-758. 17p. Dep. mn. CFSTI $1.00 cy, $0.50 mn.

In solution the donors anisole and thioanisole each form two distinct 1:1 complexes with the acid phenol. For each donor-phenol system two distinct O-H stretching vibrations assignable to the complex were observed in the infrared spectrum. For one of these bands, the frequency shift of the phenol upon complexation, $\Delta\Lambda_{O\text{-}H}$, was found to lie on a linear plot of $\Delta\Lambda_{OH}$ versus the Hammett substituent constant for a series of donors consisting of substituted phenyl compounds. This result was interpreted to indicate that one of the donor sites in anisole and thioanisole is the phenyl ring. Arguments are presented to substantiate the assignment of the donor site in the second complex to the n-electrons of sulfur or oxygen. Symmetry arguments are presented which indicate that prior conclusions proposing the existence of two complexes because two charge transfer bands were found in some anisole and thioanisole adducts are not valid. An alternate interpretation exists. Conditions which can lead to the simultaneous existence of two distinct complexes are outlined. (auth)

14227 (TID–22419) QUARTERLY PROGRESS REPORT NO. 79 [ON ELECTRONICS]. Zimmermann, H. J.; Harvey, G. G. (Massachusetts Inst. of Tech., Cambridge. Research Lab. of Electronics). Oct. 15, 1965. Contracts AT(30-1)-1842; AT(30-1)-3285. 277p. Dep. mn; CFSTI $6.00 cy, $1.50 mn.

Research and development progress is reported in 17 sections. Separate abstracts were prepared for each of 4 sections. Sections for which no abstracts were prepared are concerned with molecular beams, microwave spectroscopy, radio astronomy, geophysics, noise and electron devices, physical electronics and surface physics, physical acoustics, statistical communication theory, processing and transmission of information, cognitive information processing, communications biophysics, and computation research. (J.R.D.)

For abstracts of individual sections see: 13432 and 13923–13925.

14228 (TID–22527) X-RAY DIFFRACTION STUDIES OF AQUEOUS ALKALI METAL HALIDE SOLUTIONS [Thesis]. Lawrence, Richard Manley (Arkansas Univ., Fayetteville). 1965. Contract AT(40-1)-2096. 136p. Dep. mn. CFSTI $4.00 cy, $1.00 mn.

In order to determine the sizes, hydration, and association of alkali metal and halide ions in concentrated aqueous solutions x-ray-diffraction techniques were utilized. Radial distribution functions (RDF's) were derived and interpreted in terms of the sizes and environments of the ions. From the positions of the ion-water peaks in the RDF's the sizes of the aqueous ions were found to be given by their usual crystal radii. The number of primary waters of hydration was relatively independent of the concentration of the solution and appeared to slightly increase with increasing size of the halide ion. Correlation of ripples in the RDF's with particular ions indicated an ordering of water molecules beyond the first hydration spheres for both the positive and negative ions studied. For the alkali metal ions the volume of the ordered region was found to decrease with increasing concentration of the solution and with increasing size of the ion. From the positions of the ripples in the RDF's the primary waters of hydration were found to be oriented about a positive ion with the ion on their dipolar axes. The negative ions were found to lie on hydrogen–oxygen bond axes of the hydrated water molecules. No evidence for ion association either of the water-bridging or direct-contact type was found for the lithium or sodium halide solutions. However, for 2.50, 5.00, and 10.0 molal cesium chloride, 2.50 and 5.00 molal cesium bromide, and 2.50 molal cesium iodide increasing direct contact among ions occurred with increasing concentration of the solution and with decreasing size of the halide ion. (P.C.H.)

14229 (JPRS–33605) TRANSLATIONS ON COMMUNIST CHINA'S SCIENCE AND TECHNOLOGY NO. 274. Translated from K'o Hsueh Tung Pao, No. 9, 753–9; 775–98; 805–10; 831–2; Kuang-ming Jih-Pao, 1–(Oct. 21, 1965). 70p. (TT–66–30049). CFSTI $3.00 cy, $0.75 mn.

For an abstract of the individual paper see: 13268.

14230 (ORNL-tr–972) THERMONUCLEAR EXPLOSIONS AT GREAT ALTITUDE. Pretre, S. Translated for Oak Ridge National Lab., Tenn., from Preprint Neue Zuercher Zeitung, Nos. 270, 271(Jan. 22, 1964). 21p. Dep. mn. JCL $2.60 fs, $0.83 mf.

The effects of nuclear explosions at altitudes >30 km are outlined. The case of a nuclear attack on Switzerland is treated as an example. Civil-defense measures are briefly considered, as well as counterstrike possibilities and the usefulness of antimissile weapons. (D.C.W.)

CORPORATE AUTHOR INDEX

This index contains entries for this period for all report literature and, in addition, for certain published literature items for which it is felt that a corporate approach is especially desirable, e.g., symposia, conference proceedings, and meetings.

Each entry under a corporate author is a shortened version of the title of the publication, followed by the *NSA* volume and abstract number. Report numbers are given in parentheses.

The phrase "Progress report" is abbreviated as "Prog. rpt.," permitting a more rapid and complete alphabetical arrangement of the titles without changing the location of the progress report titles in relation to the other titles.

A

ACF INDUSTRIES, INC., ALBUQUERQUE, N. MEX.
Filament-wound joint design study, 20: 14213 (ACF-15)

AEROJET-GENERAL CORP., AZUSA, CALIF.
Cryogenic irradiation of resistance temperature transducers for NERVA, 20: 13127 (CONF-651101-61)

AEROJET-GENERAL NUCLEONICS, SAN RAMON, CALIF.
AGCR off normal scram system, 20: 14146 (TID-22596)
Forced convection condensing heat transfer for rubidium and cesium, 20: 13232 (AGN-8162)
ML-1-IM design report, 20: 14145 (TID-22595)

AEROPROJECTS, INC., WEST CHESTER, PA.
Prog. rpt. on ultrasonic instrumentation for nuclear applications, 10/1–11/30/65, 20: 13031 (NYO-2910-13)

AEROSPACE CORP., EL SEGUNDO, CALIF.
Models of trapped radiation environment. I., 20: 13646 (NASA-SP-3024)

AGRICULTURAL AND TECHNICAL COLL. OF NORTH CAROLINA, GREENSBORO.
Prog. rpt. on studies of x-irradiated mice following bone marrow injections, final, 10/65, 20: 12720 (TID-22466)

AIR FORCE INST. OF TECH., WRIGHT-PATTERSON AFB, OHIO.
Air Force Nuclear Engineering Test Facility, 20: 14187 (NP-15836)

AKADEMIYA NAUK SSSR, MOSCOW. INSTITUT FIZIKI.
Transition radiation of charged relativistic particle in optical frequency range, 20: 13788 (ORNL-tr-1062)

AKTIEBOLAGET ATOMENERGI, STOCKHOLM (SWEDEN).
Experimental studies on assemblies 1 and 2 of fast reactor FRO, 20: 14178 (AE-207)
Methods for determination of currents and fields in steady two-dimensional MHD flow, 20: 13634 (AE-210)

ALBERT EINSTEIN COLL. OF MEDICINE, YESHIVA UNIV., BRONX, N. Y.
Prog. rpt. on cytochemical and electron microscopic studies of radiation damage, final, 1965, 20: 12635 (NYO-2786-1)

AMES LAB., IOWA STATE UNIV. OF SCIENCE AND TECH.
Bismuth–zirconium alloy system, 20: 13252 (IS-1269)
Calcium–ytterbium system, 20: 13254 (IS-T-70)
Deformation behaviors of niobium and tantalum at low temperatures, 20: 13253 (IS-T-65)
Isotopic exchange study of tungsten in sodium metatungstate–sodium orthotungstate aqueous system, 20: 12822 (IS-T-68)
Partial molal heat capacities of aqueous rare-earth chloride solutions at 25°C, 20: 12818 (IS-T-52)
Phase study of dysprosium–dysprosium(III) chloride system, 20: 12821 (IS-T-62)
Prog. rpt. on reactor materials development, 10–12/65, 20: 13180 (IS-RD-4)
Stability constants of rare earths with some carboxylic acids, 20: 12817 (IS-1311)
Structures of the ethyl Grignard reagent in diethyl ether and a tropoeoid photo-oxidation product, 20: 12819 (IS-T-53)
Trans-effect in hydrolysis reactions of trichloroammineplatinate(II) ion, 20: 12820 (IS-T-57)

ARGONNE NATIONAL LAB., ILL.
Advanced systems research and development, 20: 14179 (ANL-7122, pp 70-81)
Critical temperatures and densities of alkali metals, 20: 12815 (ANL-7025)
Engineering development of fluid-bed fluoride volatility processes. III., 20: 12923 (ANL-6898)
Environmental radioactivity at Argonne National Lab., 1964, 20: 12998 (ANL-7104)
Fabrication and evaluation of thoria–urania fuel material, 20: 13207 (ANL-6893)
Fabrication and testing of depleted uranium blanket slugs for EBR-II, 20: 13206 (ANL-6417)
General reactor technology, 20: 14008 (ANL-7122, pp 42-69)
Glassy materials for reactor applications, 20: 13209 (ANL-7062)
Liquid-metal-cooled reactors, 20: 14007 (ANL-7122, pp 1-41)
Neutron-diffraction study of $UO_2(NO_3)_2 \cdot 6H_2O$, 20: 13233 (ANL-6943)
Nuclear safety, 20: 14009 (ANL-7122, pp 82-90)
Pilot-plant development of process for U alloy fuels. VIII., 20: 12924 (ANL-6973)
Production of PuC, 20: 13208 (ANL-6969)
Prog. rpt. on applied mathematics, 7/64–6/65, 20: 13163 (ANL-7129)
Prog. rpt. on reactor development, 11/65, 20: 14006 (ANL-7122)
Review of status of self-diffusion in US, UN, UO_2, and UC, 20: 13234 (ANL-7094)
Three-dimensional stress concentration around cylindrical hole in semi-infinite elastic body, 20: 12943 (ANL-7097)
Use of high-temperature process heat as part of total-energy source, 20: 14165 (ANL-7035)
Yield data for transplutonium element production in thermal reactors, 20: 13752 (ANL-7096)

ARKANSAS UNIV., FAYETTEVILLE.
X-ray-diffraction studies of aqueous alkali metal halide solutions, 20: 14228 (TID-22527)

ARMY ENGINEER RESEARCH AND DEVELOPMENT LABS., FORT BELVOIR, VA.
Paramagnetic resonance study of nitrogen atoms trapped in x-irradiated alkali azides, 20: 13970 (AD-611432, pp 135-47)

ATOMIC BOMB CASUALTY COMMISSION, HIROSHIMA (JAPAN).
Active tuberculosis in leukemia, malignant lymphoma, and myelofibrosis, 20: 12639 (TID-21517)

ATOMIC ENERGY BOARD, PELINDABA, PRETORIA (SOUTH AFRICA).
Burnup calculations for thermal power reactors with sodium cooling, 20: 14144 (PEL-77)
Determination of C in UC, 20: 12773 (PEL-80)

ATOMIC ENERGY CENTRE, DACCA (PAKISTAN).
500-Curie irradiation facility, 20: 12911 (AECD/HP/3)

ATOMIC ENERGY CENTRE, DACCA (PAKISTAN). CHEMISTRY DIV.
Calibration of ^{60}Co gamma cell, 20: 12910 (AECD/CH/3)

ATOMIC ENERGY CENTRE, DACCA (PAKISTAN). EXPERIMENTAL PHYSICS DIV.
Installation of a 3 Mev Van de Graaff at Dacca, 20: 13356 (AECD/EP/6)
Tables for neutron energy for reactions $^7Li(p,n)^7Be$, $T(p,n)^3He$, $D(d,n)^3He$, and $T(d,n)^4He$, 20: 13747 (AECD/EP/7)

ATOMIC ENERGY ESTABLISHMENT, WINFRITH (ENGLAND).
ARGOSY 4: program for lattice calculations, 20: 14055 (AEEW-R-445)
EDITOR: program for editing BCD data on magnetic tape, 20: 13750 (AEEW-M-553)

Experimental system for thermoluminescent dosimetry, 20: 13059 (AEEW-R-411)
KDF9 program EDIT 1, 20: 13344 (AEEW-M-604)
Reactions of neutrons with ^{235}U, 20: 13749 (AEEW-M-502)
Scatter, 20: 13697 (AEEW-M-605)
SLP—single level Breit-Wigner cross-section generating program, 20: 13751 (AEEW-M-606)

ATOMIC ENERGY OF CANADA LTD., CHALK RIVER (ONTARIO).
Neutron absorption cross section of gross fission products of ^{233}U, ^{235}U, and ^{239}Pu, 20: 13748 (AECL-2510)

ATOMIC ENERGY OF CANADA LTD., PINAWA (MANITOBA). WHITESHELL NUCLEAR RESEARCH ESTABLISHMENT.
Fate of terphenyl in the rat, 20: 12589 (AECL-2507)

ATOMIC ENERGY RESEARCH ESTABLISHMENT, HARWELL (ENGLAND).
Advanced course in principles of radiation protection. I., 20: 12732 (AERE-R-5084)
Determination of Pa-231 in urine, 20: 12761 (AERE-R-4911)

ATOMIC POWER DEVELOPMENT ASSOCIATES, INC., DETROIT, MICH.
Prog. rpt. on reactor engineering, 10–12/65, 20: 14024 (APDA-182)

ATOMIC WEAPONS RESEARCH ESTABLISHMENT, ALDERMASTON (ENGLAND).
Bibliography on ultrasonic welding, 1960–65, 20: 13210 (AWRE/LIB/BIB/13)
Geomagnetic micropulsations, 20: 13645 (AWRE-O-9/66)
SWAN—multi-group one-dimensional diffusion code for the IBM-7030, 20: 14056 (AWRE-O-99/65)

ATOMICS INTERNATIONAL, CANOGA PARK, CALIF.
NAA program description—a program to reformat grave/prism punched output, 20: 13706 (NAA-SR-Memo-10884 and Add.)

AUSTRALIAN ATOMIC ENERGY COMMISSION.
Prog. rpt., annual, 7/64–6/65, 20: 14222 (NP-15612)

B

BABCOCK AND WILCOX CO., LYNCHBURG, VA. ATOMIC ENERGY DIV.
Prog. rpt. on Th fuel cycle for HWR, 4–6/65, 20: 14114 (BAW-393-2)

BABCOCK AND WILCOX CO., LYNCHBURG, VA. CRITICAL EXPERIMENT LAB.
Zero power tests—PM-3A Core III, 20: 14115 (BAW-3576-1)

BAILEY METER CO., WICKLIFFE, OHIO.
Operating characteristics of the present PM-type reactor instrumentation, 20: 14134 (NYO-3379-2)

BATTELLE MEMORIAL INST., COLUMBUS, OHIO.
Phase equilibria in uranium–tungsten–oxygen system, 20: 13235 (BMI-1755)
Prog. rpt. on civilian applications, 11/65, 20: 13171 (BMI-1751)

BATTELLE-NORTHWEST, RICHLAND, WASH. PACIFIC NORTHWEST LAB.
Analysis of maximum hypothetical accident, 20: 14181 (COO-1430-2)
Calibration of high-speed burnup code for nuclear fuel surveys, 20: 14118 (BNWL-183, Sect.IV)
Comparison of fuel cycles for crossed-progeny fuels in conventional and novel configurations, 20: 14117 (BNWL-183, Sect.III)
Conservation economics and reactor technology, 20: 14011 (BNWL-183, Sect.V)
Continuous separation of Ce from trivalent rare earths, 20: 12762 (BNWL-173)
Double cantilever beam specimen for determining plane strain fracture toughness of metals, 20: 12972 (BNWL-168)
Electrochemistry of Pu(III) in molten alkali chlorides, 20: 12816 (BNWL-158)
Monte Carlo calculations of optimum loading of plutonium in thermal reactor fuels, 20: 14057 (BNWL-183, Sect.I)
New fuel configuration to increase plutonium value, 20: 14102 (BNWL-183, Sect.II)
Nickel electroplating on U, 20: 13211 (BNWL-124)
Plutonium fueling methods for thermal reactors, 20: 14010 (BNWL-183)
Prog. rpt. on fast test reactor hypothetical meltdown accident, 10–12/65, 20: 14182 (COO-1430-3)
Proposed tube power limits for PRTR 58-inch Mk I fuel element, 20: 14116 (BNWL-177)
Radiation-induced dimensional changes of raw-coke graphites, 20: 13322 (BNWL-178)
Shielding analysis for Fast Flux Test Facility, 20: 14180 (COO-1430-1)

BECHTEL CORP., SAN FRANCISCO, CALIF.
Engineering and economic feasibility study for a combination nuclear power and desalting plant, 20: 14166 (TID-22330(Vol.3))

BENDIX CORP., SOUTHFIELD, MICH. RESEARCH LABS. DIV.
Analytical study of feasibility of pneumatic neutron flux detector, 20: 13069 (NASA-CR-54468)

BENDIX PRODUCTS AEROSPACE DIV., BENDIX CORP., SOUTH BEND, IND.
Pneumatic nutator actuator motor, 20: 14029 (NASA-CR-54788)

BONN UNIV. (WEST GERMANY). INSTITUT FUER STRAHLEN UND KERNPHYSIK.
Method to derive electric quadrupole moments of 2+ rotational status of rare earth nuclei, 20: 13764 (CONF-233(Vol.4), pp 720-2)

BROOKHAVEN NATIONAL LAB., UPTON, N. Y.
Aperture and cell-size effects on shunt impedance of alternating periodic structures, 20: 13358 (BNL-9944)
Effect of x irradiation and thermal trauma on intestinal mucosa, 20: 12630 (BNL-8383)
Histopathology of hereditary congenital deafness in white mink, 20: 14214 (BNL-8564)
Liquid fuel synthesis using nuclear power in a mobile energy depot system, 20: 12877 (BNL-955)
Lorentz covariant definition of the U_6 group for free particle states, 20: 13529 (BNL-8767)
Neutron cross section of sodium below 40 kev, 20: 13753 (BNL-961)
Positron scanner for brain tumors, 20: 12734 (BNL-9911)
Quiescent center of primary root of Glycine max, 20: 14215 (BNL-8643)
Time and temperature tolerances of maize seeds, 20: 14216 (BNL-9859)

BRUSSELS UNIV. (BELGIUM). LABORATOIRE DE ZOOLOGIE ET BIOLOGIE.
Prog. rpt. on selective absorption of Sr by Acantharia, annual, 2/62–3/64, 20: 12591 (EUR-2475.f)

BUREAU D'ETUDES NUCLEAIRES, S. A., BRUSSELS (BELGIUM).
Economic study of integration of nuclear power plants in electricity generation and distribution networks, 20: 14121 (EUR-2453.f)

BUREAU OF MINES, RENO, NEV. RENO METALLURGY RESEARCH CENTER.
Reaction rate of U metal with UF_4 in molten fluoride solutions, 20: 13170 (BM-RI-6736)

C

CALIFORNIA INST. OF TECH., PASADENA.
g Factors of the rotational bands in ^{177}Lu and ^{177}Hf, 20: 13765 (CONF-233(Vol.4), pp 723-5)

CALIFORNIA INST. OF TECH., PASADENA. DEPT. OF PHYSICS.
Branching ratio of the Y_1^+, 20: 13445 (CONF-758-14)

CALIFORNIA UNIV., BERKELEY. DEPT. OF PHYSICS.
Branching ratio of the Y_1^+, 20: 13445 (CONF-758-14)

CALIFORNIA UNIV., DAVIS. DEPT. OF POMOLOGY.
Comparative inactivation of conidia, mycellia, and sclerotia of Botrytis cinerea by γ radiation, 20: 13149 (UCD-34P80-3, pp 176-89)
Effect of γ irradiation on fresh prunes, 20: 13144 (UCD-34P80-3, pp 69-74)
Effect of γ irradiation on lemon fruits, 20: 13145 (UCD-34P80-3, pp 75-83)
Effect of γ irradiation on ripening of bananas, 20: 13146 (UCD-34P80-3, pp 84-91)
Effect of γ irradiation on peaches, 20: 13147 (UCD-34P80-3, pp 92-8)
Effect of γ irradiation on post-harvest behavior of tomato fruits, 20: 13148 (UCD-34P80-3, pp 99-175)
Gamma-ray radiosynthesis of ozone from air, 20: 12885 (UCD-34P80-3, pp 59-68)
Gas exchange in Bartlett pears in relation to γ irradiation, 20: 13140 (UCD-34P80-3, pp 27-47)
Interaction of γ irradiation, sealed packages, and controlled atmosphere on incidence of Botrytis rot in strawberries, 20: 13139 (UCD-34P80-3, pp 9-26)
Mn^{2+} in ^{60}Co γ-irradiated strawberries, 20: 13143 (UCD-34P80-3, pp 55-7)
Prog. rpt. on radiation technology in extending shelf life of fruits and vegetables, annual, 2/64–1/65, 20: 13138 (UCD-34P80-3)
Sensory evaluation of irradiated cherries, 20: 13141 (UCID-34P80-3, pp 48-51)
Thiamine and niacin analysis of irradiated strawberries, 20: 13142 (UCD-34P80-3, pp 52-4)

CARNEGIE INST. OF TECH., PITTSBURGH, PA. DEPT. OF PHYSICS.
Prog. rpt. on radiation effects in solids, 4/65–3/66, 20: 13973 (NYO-3033-1)

CATANIA UNIV. (ITALY). ISTITUTO DI GENETICA.
Mutability of polygenes and utilization of induced genetic variability, 20: 12541 (TID-22582)

CENTRE D'ETUDE DE L'ENERGIE NUCLEAIRE, BRUSSELS (BELGIUM).
Prog. rpt. on use of Pu as reactor fuel, 1–6/64, 20: 13176 (EURAEC-1503)
Prog. rpt. on use of Pu as reactor fuel, 7–12/64, 20: 13177 (EURAEC-1504)

CENTRE D'ETUDE DE L'ENERGIE NUCLEAIRE, MOL (BELGIUM).
Prog. rpt. on reprocessing irradiated fuels, 1–3/65, 20: 12925 (EURAEC-

1446)
COMBUSTION ENGINEERING, INC., WINDSOR, CONN.
BONUS power station startup summary report, 2/66, 20: 14119 (CEND/PRWRA-257)
COMBUSTION ENGINEERING, INC., WINDSOR, CONN. NUCLEAR DIV.
Prog. rpt. on burnable poison additions to UO_2, 7–9/65, 20: 13425 (CEND-3107-249)
COMISION NACIONAL DE ENERGIA ATOMICA, BUENOS AIRES (ARGENTINA).
Preparation of ^{131}I-Allyl-Inulin, 20: 12912 (CNEA-161)
Separation of ^{131}I-rose bengal by thin-layer chromatography, 20: 12763 (CNEA-162)
COMITATO NAZIONALE PER L'ENERGIA NUCLEARE, ROME (ITALY).
Behavior of fission gas bubbles, 20: 13329 (RT/FI(65)46)
Direct conversion of thermal energy in MPD power generation program at C.N.E.N., 20: 13431 (RT/FI(65)31)
Feasibility studies of PCTR measurements with light-water-moderated plutonium-fueled lattices, 20: 14189 (RT/FI(65)43)
Reversed-phase partition chromatography and its application, 20: 12776 (RT/PROT(65)33)
Semiconductor detectors of surface-barrier type, 20: 13072 (RT/EL(65)7)
Sorption properties of natural tuffs occurring in Lake Bracciano region (Rome), 20: 14209 (RT/PROT(65)29)
Temperature coefficient measurements of the RC-1 reactor (TRIGA), 20: 14188 (RT/FI(65)40)
COMMISSARIAT A L'ENERGIE ATOMIQUE, CADARACHE (FRANCE). CENTRE D'ETUDES NUCLEAIRES.
Prog. rpt. on fast neutrons, 1965, 20: 14149 (ORNL-tr-900)
COMMISSARIAT A L'ENERGIE ATOMIQUE, FONTENAY-AUX-ROSES (FRANCE). CENTRE D'ETUDES NUCLEAIRES.
Determination of oxygen in sodium by liquid ammonia, 20: 12780 (ORNL-tr-931)
Prog. rpt. on radioactive contamination levels in environment and food chain, annual, 1964, 20: 13000 (EUR-2520.f)
Recovery and radio-resistance in mice after external irradiation, 20: 12631 (CEA-R-2776)
COMMISSARIAT A L'ENERGIE ATOMIQUE, GRENOBLE (FRANCE). CENTRE D'ETUDES NUCLEAIRES.
Hydrodynamic instabilities limiting the power of boiling water reactors, 20: 14027 (EURAEC-909)
Vegetative rhythms of woody species, 20: 12590 (CEA-R-2825)
COMMISSARIAT A L'ENERGIE ATOMIQUE, PARIS (FRANCE).
Fabrication of second set of U–Pu fuel elements for substitution experiments, 20: 13214 (EURAEC-1484)
Investigation on radioactive contamination of foodstuffs stemming from animals, 20: 12979 (EUR-2287.d)
Prog. rpt., annual, 1964, 20: 14223 (NP-15723)
COMMISSARIAT A L'ENERGIE ATOMIQUE, PIERRELATTE (FRANCE).
Inspection of professional personnel exposedto ionizing radiation, 20: 12999 (CEA-R-2746)
COMMISSARIAT A L'ENERGIE ATOMIQUE, SACLAY (FRANCE). CENTRE D'ETUDES NUCLEAIRES.
Extension of Child-Langmuir law to beam of particles having initial velocity, 20: 13902 (CEA-R-2898)
Fuel cycle optimization: marginal values of losses, 20: 13212 (CEA-R-2866)
Method for calorimetric analysis in variable conditions, 20: 13236 (CEA-R-2797)
Neutron dosimetry by means of proportional counters with tissue-equivalent walls, 20: 13060 (CEA-R-2891)
Prog. rpt. on fast neutrons, 1965, 20: 14149 (ORNL-tr-900)
Study of high-frequency instabilities on cold cathode reflex discharge, 20: 13901 (CEA-R-2822)
Study of the 2^1S state of helium using Hartree-Fock method, 20: 13411 (CEA-R-2855)
COMPAGNIE POUR L'ETUDE ET LA REALISATION DE COMBUSTIBLES ATOMIQUES, BONNEUIL-SUR-MARNE (FRANCE).
Fuel cycle optimization: marginal values of losses, 20: 13212 (CEA-R-2866)
COUNCIL OF EUROPE.
Problems regarding the competitiveness of nuclear power reactors, 20: 14133 (NP-15587)
CULHAM LAB., UNITED KINGDOM ATOMIC ENERGY AUTHORITY, ABINGDON (ENGLAND).
Effect of Coulomb collisions on scattering of light by plasmas, 20: 13904 (CLM-R52)
Electric field dissociation of H_2^+, 20: 13412 (CLM-R46)
Microwave emission from plasmas at harmonics of electron cyclotron frequency, 20: 13903 (CLM-R51)
CZECHOSLOVAK ACADEMY OF SCIENCES, BRNO. INST. OF BIOPHYSICS.
Prog. rpt. on protective substances during irradiation and study of damage to bacteriophage, 20: 12617 (NP-15863)

D

DAVID TAYLOR MODEL BASIN, CARDEROCK, MD.
TET-2—thermal energy transport code, 20: 13698 (DTME-1820)
"DEMOCRITUS" NUCLEAR RESEARCH CENTER, ATHENS (GREECE).
Effect of chemical sensitizers on radiation resistance of fruit-spoilage fungi, 20: 13137 (NP-15360)
DEUTSCHE VERSUCHSANSTALT FUER LUFT- UND RAUMFAHRT E. V., MUNICH (WEST GERMANY).
Self-excitation of an electrodeless MHD generator, 20: 13429 (N64-32348)
Theoretical studies of electrodeless MHD generator of infinite length, 20: 13430 (N64-32349)
DEUTSCHES ELEKTRONEN-SYNCHROTRON, HAMBURG (WEST GERMANY).
Search for a heavy electron by electron-proton coincidence measurements, 20: 13446 (DESY-65/9)
DIVISION OF REACTOR DEVELOPMENT AND TECHNOLOGY (AEC), WASHINGTON, D. C.
Fuels and materials development under reactor programs, 20: 13183 (TID-6506(Pt.2, 3rd Ed.))
Nuclear fuels and materials development, 20: 13184 (TID-11295(Pt.1, 4th Ed.))
DIVISION OF RESEARCH (AEC), WASHINGTON, D. C.
Summaries of programs in metallurgy, solid state physics, and ceramics, 1965, 20: 13182 (TID-4005(Pt.1, 9th Ed.))
DIVISION OF TECHNICAL INFORMATION EXTENSION, (AEC), OAK RIDGE, TENN.
Summaries of programs in metallurgy, solid state physics, and ceramics, 1965, 20: 13182 (TID-4005(Pt.1, 9th Ed.))
DOUGLAS AIRCRAFT CO., INC., NEWPORT BEACH, CALIF. ASTROPOWER LAB.
Particle disintegration study for re-entering nuclear auxiliary power systems, 20: 14169 (AFWL-TDR-64-75)
DU PONT DE NEMOURS (E. I.) & CO., AIKEN, S. C. SAVANNAH RIVER LAB.
Chemical separation of reactor-produced ^{171}Tm, 20: 12764 (CONF-660305-8)
Description of temperature monitor for large reactors. III., 20: 14025 (DP-944)
Determination of fluoride by pyrohydrolysis and automated colorimetry, 20: 12765 (DP-1004)
Energy spectra of neutrons and γ rays from spontaneous fission of ^{244}Cm, 20: 13769 (DP-949)
Final safety analysis of maximum credible accident in the HWCTR, 20: 14183 (DP-1037)

E

EDGERTON, GERMESHAUSEN AND GRIER, INC., SANTA BARBARA, CALIF.
DASA fallout and transit dose rate measurement system, 20: 12978 (AD-627077)
Radiation calibration of a 20-Mev linac, 20: 13361 (EGG-1183-2066)
TCC control systems: transducer evaluation, wire evaluation, and calorimetric detector development, 20: 14170 (EGG-1183-2019)
ERLANGEN UNIV. (WEST GERMANY). INSTITUT FUER THEORETISCHE PHYSIK.
Internal bremsstrahlung in β decay, 20: 13761 (CONF-233(Vol.4), pp 656-68)
ERLANGEN UNIV. (WEST GERMANY). PHYSIKALISCHES INSTITUT.
Internal bremsstrahlung in β decay, 20: 13761 (CONF-233(Vol.4), pp 656-68)
EUROPEAN ATOMIC ENERGY COMMUNITY.
Conditions affecting burnout heat flux of polyphenyl cooling agents, 20: 14026 (EUR-2299.e)
Development of a chalk-dust measuring device, 20: 13024 (EUR-2544.d)
Economic study of integration of nuclear power plants in electricity generation and distribution networks, 20: 14121 (EUR-2453.f)
Frittotal (Al–Al_2O_3) and nuclear applications, 20: 13213 (EUR-2447.f)
Investigation on radioactive contamination of foodstuffs stemming from animals, 20: 12979 (EUR-2287.d)
Prog. rpt. effects of mutagenic substances, annual, 1964, 20: 12632 (EUR-2546.f)
Prog. rpt. on radioactive contamination levels in environment and food chain, annual, 1964, 20: 13000 (EUR-2520.f)
Prog. rpt. on selective absorption of Sr by Acantharia, annual, 2/63–3/64, 20: 12591 (EUR-2475.f)
EUROPEAN COMPANY FOR THE CHEMICAL PROCESSING OF IRRADIATED FUELS, MOL (BELGIUM).
Electrodeless conductivity meter for on-stream measurements, 20: 12927

(NP-15756)

EUROPEAN ORGANIZATION FOR NUCLEAR RESEARCH, GENEVA (SWITZERLAND).
Focusing and chromatic aberrations in a periodic AG beam transport system, 20: 13360 (CERN-65-42)
Group theory and classification of elementary particles, 20: 13530 (CERN-65-41)
Septum magnets with 10- and 20-kg fields for slow and fast ejection from the CPS, 20: 13359 (CERN-65-36)

F

FEDERAL COUNCIL FOR SCIENCE AND TECHNOLOGY, WASHINGTON, D. C. COORDINATING COMMITTEE ON MATERIALS RESEARCH AND DEVELOPMENT.
Federal materials research program—opportunities, roadblocks, and problems, 20: 13185 (TID-22424)

FLORIDA UNIV., GAINESVILLE. DEPT. OF METALLURGICAL AND MATERIALS ENGINEERING.
Effects of prestrain on mechanical properties of Zr, 20: 13246 (CONF-651017-13)

FRANKFURT UNIV. (WEST GERMANY).
Bibliography on accelerators, 11/65, 20: 13357 (AED-C-18-06)

G

GENERAL ATOMIC, SAN DIEGO, CALIF. JOHN JAY HOPKINS LAB. FOR PURE AND APPLIED SCIENCE.
Compilation and evaluation of nuclear data available for major plutonium isotopes, 20: 13770 (GA-6576)
Core performance code COPE, 20: 14123 (GAMD-1561(Rev.))
LEGCOEF-3—program to calculate Legendre expansion coefficients, 20: 13699 (GA-6690)
Neutron production in unirradiated EBOR fuel elements due to the (α,n) reaction, 20: 14124 (GAMD-6859)
Prog. rpt. on advanced graphite fuel systems, 8/15–11/14/65, 20: 13247 (GA-6831)
Prog. rpt. on advanced BeO concepts, 4–6/63, 20: 14122 (GA-4451)

GENERAL ELECTRIC CO., CINCINNATI, OHIO. NUCLEAR MATERIALS AND PROPULSION OPERATION.
High-temperature reactor materials research, 20: 13249 (GEMP-55A, pp 29-53)
High-temperature thermocouple and electric materials research, 20: 13250 (GEMP-55A, pp 55-6)
Oxidation-resistant fuel element materials research, 20: 13179 (GEMP-55A, pp 13-28)
Prog. rpt. on high-temperature materials, 10/15–12/15/65, 20: 13178 (GEMP-55A)
Refractory-metal alloy research and development, 20: 13251 (GEMP-55A, pp 57-82)

GENERAL ELECTRIC CO., CINCINNATI, OHIO. SPACE POWER AND PROPULSION SECTION.
Prog. rpt. on K corrosion test loop development, 4/15–7/15/65, 20: 13192 (NASA-CR-54843)
Prog. rpt. on refractory alloy corrosion loop program, 7/15–10/15/65, 20: 13193 (NASA-CR-54845)
Prog. rpt. on studies of alkali metal corrosion on materials for advanced space power systems, 3–6/65, 20: 13191 (NASA-CR-54476)

GENERAL ELECTRIC CO., RICHLAND, WASH. HANFORD ATOMIC PRODUCTS OPERATION.
N reactor analog simulation feasibility study, 20: 14167 (HW-70878)
Programmed tube to tubesheet welding on heat exchangers used in nuclear processing service, 20: 13219 (RL-SEP-710)
Spatial kinetics in large reactors, 20: 14071 (RL-SA-45A and Suppl.)

GENERAL ELECTRIC CO., SAN JOSE, CALIF. ATOMIC POWER EQUIPMENT DEPT.
Blowout, heat transfer, pressure drop, and maximum flow tests conducted on prototype Mark III fuel bundle, 20: 14125 (GEAP-4898)
Experimental plan for the plutonium subcritical program, 20: 14058 (GEAP-4690)
Fracture mechanics and the stability of engineering structures, 20: 13248 (GEAP-4678)
Irradiation of 0.5-inch-diameter, solid-pellet UO_2 fuel rods, 20: 13326 (GEAP-5100C)
Prog. rpt. on stainless steel failure, 7–9/65, 20: 13325 (GEAP-4968)
Prog. rpt. on two-phase flow, 7–9/65, 20: 12962 (GEAP-4959)
Single-rod, forced-flow, transition boiling heat transfer from smooth and finned surfaces, 20: 12961 (GEAP-4786)
Sodium mass transfer. VII., 20: 12766 (GEAP-4178)
Sodium mass transfer. XVII., 20: 12767 (GEAP-4833)

GOODYEAR ATOMIC CORP., PIKETON, OHIO.
Radiation alarm instrument instruction manual, 20: 13001 (GAT-T-1222)

H

HUGHES RESEARCH LABS., MALIBU, CALIF.
Prog. rpt. on research on single-crystal high-resistivity CdTe for use as γ spectrometer, annual, 6/65, 20: 13073 (SAN-549-1)

I

IIT RESEARCH INST., CHICAGO, ILL.
Studies of reactor containment structures, 20: 14028 (IITRI-578P22-14)

IIT RESEARCH INST., CHICAGO, ILL. METALS RESEARCH DIV.
Yield-point occurrence in polycrystalline alpha zirconium, 20: 13245 (CONF-651017-7)

IIT RESEARCH INST., CHICAGO, ILL. PHYSICS DIV.
Power dependence of saturation of EPR spectrum of F center at 4°K, 20: 13975 (TID-21571)

ILLINOIS UNIV., URBANA.
Pressure and the electronic structure of solids, 20: 14221 (COO-1198-230)

ILLINOIS UNIV., URBANA. DIGITAL COMPUTER LAB.
Novel family of digital circuits, 20: 13164 (COO-415-1028)

INSTITUT ATOMNOI ENERGII, GOSUDARSTVENNYI KOMITET PO ISPOL'ZOVANIYU ATOMNOI ENERGII SSSR, MOSCOW.
Closed minimum-B configurations, 20: 13930 (NP-tr-1343)
Instability and related macroscopic effects in toroidal discharges, 20: 13929 (NP-tr-1340)

INSTITUT FUER KERNPHYSIK, UNIVERSITAET FRANKFURT (WEST GERMANY).
Nuclear-spectroscopic investigations using (n,pγ)- and (n,αγ)-reactions, 20: 13773 (IKF-13)

INSTITUT FUER PLASMAPHYSIK, G.M.B.H. GARCHING (WEST GERMANY).
A-c method for measuring the characteristic data of a field emission point, 20: 13025 (IPP-2/37)
Conservation laws and microscopic stability of plasma, 20: 13909 (IPP-6/40)
Electromagnetic production of shock waves and interaction of shock waves with electromagnetic fields, 20: 13637 (IPP–3/28)
Electrostatic double probes and their applicability in hot plasmas, 20: 13906 (IPP-1/40)
General interchange instability, 20: 13638 (IPP-6/39)
Interferometric measurements on electromagnetically generated shock waves, 20: 13636 (IPP-3/24)
Lighting of very high voltage spark gaps by means of light triggering, 20: 13027 (IPP-4/24)
Measurement of anisotropy in radial neutral gas pressure, 20: 13907 (IPP-2/42)
Production and containment of high-temperature plasma, 20: 13908 (IPP-2/44)
Tests on materials for superconducting coils, 20: 13666 (IPP-4/22)
Two-chamber ionization gage, 20: 13026 (IPP-2/39)

INSTITUT NATIONAL DE RECHERCHE AGRONOMIQUE, DIJON (FRANCE). STATION D'AMELIORATION DES PLANTES.
Prog. rpt. effects of mutagenic substances, annual, 1964, 20: 12632 (EUR-2546.f)

INSTITUTE FOR NUCLEAR STUDY, TOKYO UNIV. (JAPAN).
Prog. rpt. on nuclear research, annual, 1964, 20: 13345 (NP-15772)

INSTITUTE OF NUCLEAR PHYSICS, KRAKOW (POLAND).
Magnetic interaction of ^{155}Gd nucleus in 87-kev excited state, 20: 13763 (CONF-233(Vol.4), pp 710-19)

INSTITUTE OF NUCLEAR RESEARCH, SWIERK (POLAND).
Internal bremsstrahlung accompanying electron capture decay of medium heavy nuclei, 20: 13759 (CONF-233(Vol.4), pp 614-24)
New calculations of the atomic photoeffect, 20: 13413 (CONF-233(Vol.4), pp 538-47)

INSTITUTO DE ENERGIA ATOMICA, SAO PAULO (BRAZIL).
Activation analysis of gold in ores samples, 20: 12769 (IEA-98)
Determination of Cl and Cu in high-purity water by radioactivation, 20: 12768 (IEA-97)
Gamma-gamma cascades in disintegration of compound nuclei formed by neutron capture, with aid of Hoogenboom circuit, 20: 13062 (IEA-96)
Paramagnetic studies of holmium by neutron total cross section measurements, 20: 13772 (IEA-99)
Radiochemistry activities in research reactor centers, 20: 12914 (IEA-100)

INSTITUTT FOR ATOMENERGI, KJELLER (NORWAY).
PREBOLO: description of high-pressure boiling loop at Kjeller, 20: 14131 (KR-98)

INSTITUTUL DE FIZICA ATOMICA, ACADEMIA R. P. R., BUCHAREST (ROMANIA).
Bibliography of ^{14}C measurements. II., 20: 12770 (IFA/CO/28)

INTERNATIONAL ATOMIC ENERGY AGENCY, VIENNA (AUSTRIA).
Bibliography on Moessbauer effect, 20: 13974 (STI/PUB/21/16)

Bibliography on organic coolants and moderators, 20: 14016 (STI/PUB/21/17)
Conference on pulsed neutron research, Karlsruhe, 5/65. I., 20: 13710 (STI/PUB/104(Vol. 1))
Conference on pulsed neutron research, Karlsruhe, 5/65. II., 20: 13711 (STI/PUB/104(Vol.2))
Conference on role of atomic electrons in nuclear transformations, Warsaw, 9/63, 20: 13754 (CONF-233(Vol.4))
Decay of ^{184}Ta, 20: 13767 (CONF-233(Vol.4), pp 730-42)
g Factors of the rotational bands in ^{177}Lu and ^{177}Hf, 20: 13765 (CONF-233(Vol.4), pp 723-5)
Internal bremsstrahlung accompanying non-anique second-forbidden electron capture decay of ^{36}Cl, 20: 13758 (CONF-233(Vol.4), pp 609-13)
Internal bremsstrahlung accompanying electron capture decay of medium heavy nuclei, 20: 13759 (CONF-233(Vol.4), pp 614-24)
Internal bremsstrahlung near 2 M_e, 20: 13760 (CONF-233(Vol.4), pp 637-55)
Internal bremsstrahlung in β decay, 20: 13761 (CONF-233(Vol.4), pp 656-68)
Internal pair formation following neutron capture, 20: 13762 (CONF-233(Vol.4), pp 700-9)
L, M, and N photoelectric cross section measurements in uranium for $h\nu = 122$ kev, 20: 13755 (CONF-233(Vol.4), pp 548-60)
Magnetic interaction of ^{155}Gd nucleus in 87-kev excited state, 20: 13763 (CONF-233(Vol.4), pp 710-19)
Method to derive electric quadrupole moments of 2+ rotational status of rare earth nuclei, 20: 13764 (CONF-233(Vol.4), pp 720-2)
M4 isomerism in ^{205}Pb, 20: 13766 (CONF-233(Vol.4), pp 726-9)
New calculations of the atomic photoeffect, 20: 13413 (CONF-233(Vol.4), pp 538-47)
Scattering cross sections for 50- to 500-kev electrons, 20: 13757 (CONF-233(Vol.4), pp 595-608)
Scattering of 662-kev γ rays on bound electrons, 20: 13756 (CONF-233(Vol.4), pp 562-94)
Symposium on nondestructive testing in nuclear technology, Bucharest, 5/65, 20: 14017 (STI/PUB/105(Vol.2))

INTERNATIONAL CENTRE FOR THEORETICAL PHYSICS, TRIESTE (ITALY).
A new approach to algebra of current operators, 20: 13533 (IC/66/3)
Analytic structure of many-particle scattering amplitudes. I., 20: 13531 (IC/65/17)
Difference between sources and charges, 20: 13536 (IC/66/7)
Discrete degenerate representations of non-compact rotation groups, 20: 13532 (IC/66/2)
Electromagnetic and weak form factors of the nucleon, 20: 13447 (IC/65/95)
Maximal degenerate systems dynamics, 20: 13535 (IC/66/6)
Relativistic U(6,6) theory, 20: 13534 (IC/66/5)
Remarks about the Fubini-Furlan method, 20: 13537 (IC/66/8)

INTERNATIONAL UNION OF PURE AND APPLIED PHYSICS.
Conference on role of atomic electrons in nuclear transformations, Warsaw, 9/63, 20: 13754 (CONF-233(Vol.4))
Decay of ^{184}Ta, 20: 13767 (CONF-233(Vol.4), pp 730-42)
g Factors of the rotational bands in ^{177}Lu and ^{177}Hf, 20: 13765 (CONF-233(Vol.4), pp 723-5)
Internal bremsstrahlung accompanying non-unique second-forbidden electron capture decay of ^{36}Cl, 20: 13758 (CONF-233(Vol.4), pp 609-13)
Internal bremsstrahlung accompanying electron capture decay of medium heavy nuclei, 20: 13759 (CONF-233(Vol.4), pp 614-24)
Internal bremsstrahlung near 2 M_e, 20: 13760 (CONF-233(Vol.4), pp 637-55)
Internal bremsstrahlung in β decay, 20: 13761 (CONF-233(Vol.4), pp 656-68)
Internal pair formation following neutron capture, 20: 13762 (CONF-233(Vol.4), pp 700-9)
L, M, and N photoelectric cross section measurements in uranium for $h\nu = 122$ kev, 20: 13755 (CONF-233(Vol.4), pp 548-60)
Magnetic interaction of ^{155}Gd nucleus in 87-kev excited state, 20: 13763 (CONF-233(Vol.4), pp 710-19)
Method to derive electric quadrupole moments of 2+ rotational status of rare earth nuclei, 20: 13764 (CONF-233(Vol.4), pp 720-2)
M4 isomerism in ^{205}Pb, 20: 13766 (CONF-233(Vol.4), pp 726-9)
New calculations of the atomic photoeffect, 20: 13413 (CONF-233(Vol.4), pp 538-47)
Scattering cross sections for 50- to 500-kev electrons, 20: 13757 (CONF-233(Vol.4), pp 595-608)
Scattering of 662-kev γ rays on bound electrons, 20: 13756 (CONF-233(Vol.4), pp 562-94)

INTERNATIONALE ATOMREAKTORBAU G.M.B.H., BENSBERG (WEST GERMANY).
Development of a chalk-dust measuring device, 20: 13024 (EUR-2544.d)

IONICS, INC., WATERTOWN, MASS. RESEARCH DIV.
Advanced study of milk decontamination by electrodialysis, 20: 12997 (AD-626210)

ISRAEL ATOMIC ENERGY COMMISSION, YAVNE. SOREQ RESEARCH ESTABLISHMENT.
Mechanism of radiolysis of CO_2, 20: 12882 (IA-1065)

ISRAEL ATOMIC ENERGY COMMISSION, YAVNE. SOREQ NUCLEAR RESEARCH CENTER.
Determination of γ flux in reactor by ^{14}N–^{15}N isotopic exchange reaction, 20: 14012 (IA-1048)
Nuclear resonant scattering using neutron-capture γ rays, 20: 13771 (IA-1050)
Paramagnetic resonance spectrum of Co^{1+} in single crystals of CaO, 20: 13972 (IA-1056)

ISTITUTO DI RICERCHE FARMACOLOGICHE MARIO NEGRI, MILAN (ITALY).
Prog. rpt. on selective protection of damages induced by x irradiation and radiomimetic drugs, 11/64–1/65, 20: 12717 (NP-15666)
Prog. rpt. on selective protection of damages induced by x irradiation and radiomimetic drugs, annual, 9/15/64, 20: 12718 (NP-15667)
Prog. rpt. on selective protection of damages induced by x irradiation and radiomimetic drugs, final, 9/65, 20: 12719 (NP-15668)

ISTITUTO SUPERIORE DI SANITA', ROME (ITALY). LABORATORI DI FISICA.
Scattering of 662-kev γ rays on bound electrons, 20: 13756 (CONF-233(Vol.4), pp 562-94)

J

JAPAN ATOMIC ENERGY RESEARCH INST., TOKYO.
Bibliography on accidents in nuclear facilities, 20: 13002 (JAERI-4034)
Characteristics of gamma-block stilbene detector, 20: 13063 (JAERI-1092)
Comparison of methods of personnel-monitoring dosimetry practised in nuclear establishments of different countries, 20: 13003 (JAERI-4035)
Current distribution in MHD Hall generators, 20: 13428 (JAERI-1093)
ELIESE-1: FORTRAN-II program for analyses of elastic and inelastic scattering cross sections, 20: 13774 (JAERI-1096)
Survey and problems in study of thermal neutron scattering, 20: 13700 (JAERI-1086)

JOINT INST. FOR NUCLEAR RESEARCH, DUBNA (USSR).
Structure of spontaneously fissioning isomers, 20: 13777 (JINR-E-2515)

JOINT INST. FOR NUCLEAR RESEARCH, DUBNA (USSR). LAB OF HIGH ENERGY.
An 85-kG superconducting magnet made of Nb-75% Zr, 20: 13667 (JINR-P-2533)
Diaphragmed waveguide as a deflection system of high-frequency separator, 20: 13362 (JINR-P-2503)
Search for new decay modes of K^0_2 mesons, 20: 13450 (JINR-P-2488)
Waves with complex propagation constants in diaphragmed waveguide, 20: 13363 (JINR-P-2507)

JOINT INST. FOR NUCLEAR RESEARCH, DUBNA (USSR). LAB. OF NEUTRON PHYSICS.
Pulsed research reactor and feasibility of pulsed reactor application in neutron spectroscopy, 20: 14191 (BNL-tr-60)

JOINT INST. FOR NUCLEAR RESEARCH, DUBNA (USSR). LAB OF NUCLEAR PROBLEMS.
Charged meson production in neutron-proton collisions at 600-Mev neutron energy, 20: 13453 (JINR-P-2511)
Magnetic β spectrometer with two-fold focusing at the angle $\pi\sqrt{2}$, 20: 13064 (JINR-E-2494)

JOINT INST. FOR NUCLEAR RESEARCH, DUBNA (USSR). LAB OF NUCLEAR REACTIONS.
Half life of an isotope of element 102 with mass number 256, 20: 13778 (JINR-P-2525)
New isotope ^{216}Ac, 20: 13779 (JINR-P-2465)
Spontaneously fissionable isomer with $T_{1/2} = 2.6$ min in reactions of ^{233}U with ^{11}B and ^{10}B, 20: 13776 (JINR-P-2499)

JOINT INST. FOR NUCLEAR RESEARCH, DUBNA (USSR). LAB OF THEORETICAL PHYSICS.
Asymptotic behavior of scattering amplitude at large momentum transfers, 20: 13546 (JINR-P-2519)
Charge distributions of particles in one-meson theory of inelastic interactions at high energies, 20: 13452 (JINR-P-2510)
Conditions of macroscopic causality for the scattering matrix, 20: 13539 (JINR-E-2500)
Electromagnetic properties of baryons and mesons in nonrelativistic quark model, 20: 13544 (JINR-P-2509)
Estimation of interaction cross section for unstable nuclei, 20: 13449 (JINR-P-2433)
Form factors and multipoles in electromagnetic interactions, 20: 13451 (JINR-P-2505)
General propagator for mesons with spin 2,1,0 in symmetry theory, 20: 13543 (JINR-P-2474)
General structure of an operator which is multiplicative with respect to a

symmetry group, 20: 13165 (JINR-E-2542)
Inelastic scattering of electrons on nuclei with collective level excitation, 20: 13775 (JINR-P-2490)
Problem of combination of space and internal symmetries of elementary particles, 20: 13542 (JINR-P-2443)
Radiative decay of 1^+ mesons and unitary symmetry, 20: 13541 (JINR-P-2419)
Reconstruction of meson-nucleon scattering matrix from experiments with polarized target, 20: 13448 (JINR-E-2521)
SU(6) and the operators CPT and C, 20: 13540 (JINR-E-2545)
$SU(6)_w$ symmetry, 20: 13545 (JINR-P-2513)
Symmetries of lepton-lepton interactions, 20: 13547 (JINR-P-2523)

JUNTA DE ENERGIA NUCLEAR, MADRID (SPAIN). SECCION DE INVESTIGACION.
Considerations on the genesis of uraniferous deposits. II., 20: 12996 (JEN-155-SIG/I-4)

K

KELLOGG (M. W.) CO., JERSEY CITY, N. J.
Primary piping flexibility analysis for liquid-metal-cooled fast breeder reactors, 20: 14120 (COO-1454-1)

KERNFORSCHUNGSANLAGE, JUELICH (WEST GERMANY). INSTITUT FUER NEUTRONENPHYSIK.
High-resolution spectrometer for slow neutrons for use on sources of very high flux reactor, 20: 13065 (JUL-295-NP)
Neutron guides: report on present state of development, 20: 13701 (JUL-294-NP)

KERNFORSCHUNGSANLAGE, JUELICH (WEST GERMANY). INSTITUT FUER PHYSIKALISCHE CHEMIE.
Comparative investigations on counting methods for the absolute determination of activity of α emitters, 20: 13066 (JUL-298-PC)

KERNFORSCHUNGSANLAGE, JUELICH (WEST GERMANY). INSTITUT FUER PLASMAPHYSIK.
Acceleration of plasma through magnetic bottle according to free-particle model, 20: 13911 (JUL-336-PP)
Magnetic probe measurements during the preheating phase of a spindle-cusp experiment, 20: 13639 (JUL-281-PP)

KERNFORSCHUNGSANLAGE, JUELICH (WEST GERMANY). INSTITUT FUER REAKTORBAUELEMENTE.
Gamma spectrometry with semiconductor detectors, 20: 13067 (JUL-308-RB)

KERNFORSCHUNGSANLAGE, JUELICH (WEST GERMANY). INSTITUT FUER REAKTORENTWICKLUNG.
Evaluation of Thorium Fuel Cycles, 20: 14126 (JUL-276-RG)
MOSEL: comparison of spectra and spectrally determined parameters of a two-component salt melt, 20: 14127 (JUL-291-RG)
MOSEL: comparison of spectra and spectrally determined magnitudes of a two-component salt melt ($NaF-BeF_2$), 20: 14129 (JUL-315-RG)
MOSEL: general study on temperatures, power density, and heat transfer, 20: 14128 (JUL-296-RG)
Multigroup effective cross sections for structural, solution, and breeding materials of Mosel, 20: 14062 (JUL-214-RG)

KERNFORSCHUNGSANLAGE, JUELICH (WEST GERMANY). INSTITUT FUER REAKTORWERKSTOFFE.
Sputtering of solids by ion bombardment, 20: 13414 (JUL-304-RW)

KERNFORSCHUNGSANLAGE, JUELICH (WEST GERMANY). ZENTRALABTEILUNG FORSCHUNGSREAKTOREN.
Startup experiments on FRJ-2 reactor, 20: 14184 (JUL-236-RE)

KERNFORSCHUNGSANLAGE, JUELICH (WEST GERMANY). ZENTRALINSTITUT FUER ANGEWANDTE MATHEMATIK.
Initial value problem for stationary Boltzmann-Vlasov equation, 20: 13910 (JUL-297-MA)

KERNFORSCHUNGSZENTRUM, KARLSRUHE (WEST GERMANY). INSTITUT FUER ANGEWANDTE KERNPHYSIK.
MESPRO 64—a program for on-line computer MIDAS, 20: 13166 (KFK-371)

KERNFORSCHUNGSZENTRUM, KARLSRUHE (WEST GERMANY). INSTITUT FUER ANGEWANDTE REAKTORPHYSIK.
Nuclear fuels and costs of different reactor types in Germany, 20: 14130 (KFK-366)

KERNFORSCHUNGSZENTRUM, KARLSRUHE (WEST GERMANY). INSTITUT FUER RADIOCHEMIE.
Two new isotopes of technetium, ^{106}Tc and ^{107}Tc, 20: 13780 (KFK-358)

KNOLLS ATOMIC POWER LAB., SCHENECTADY, N. Y.
Fatigue characteristics of Ni–Cr–Fe alloys with emphasis on pressure-vessel cladding, 20: 13255 (KAPL-3108)
Measurement and calculation of relative poison-to-fuel capture ratios in slab cores, 20: 14063 (KAPL-M-6528)
Measurement of characteristic kernels of a class of nonlinear systems, 20: 13023 (CONF-660206-1)
Reference table for W–3% Re vs. W–25% Re thermocouples, 20: 13028 (KAPL-M-6498)

L

LABORATOIRE DE L'ACCELERATEUR LINEAIRE, UNIV. DE PARIS, ORSAY (FRANCE).
Prog. rpt., 4/15–10/15/65, 20: 13364 (LAL-1148)

LABORATORIO GAS IONIZZATI, COMITATO NAZIONALE PER L'ENERGIA NUCLEARE, FRASCATI (ITALY).
Theory of quasistationary plasmas in contact with a wall, 20: 13912 (LGI-65/21 and App.)

LAWRENCE RADIATION LAB., UNIV. OF CALIFORNIA, BERKELEY.
Absorption spectrum of Cf^{+3} and crystallography of Cf_2O_3 and $CfCl_3$, 20: 12831 (UCRL-16516)
Accelerator operation and development, 20: 13368 (UCRL-16511, pp 54-8)
Accelerator radiation monitoring and shielding, 20: 13367 (UCRL-16445(Rev.))
Cross sections for $\pi^- p \rightarrow \eta n$ from threshold to 1300 Mev, 20: 13457 (UCRL-16195)
Effect of natural convection upon temperature transient following a loss-of-coolant accident, 20: 14147 (UCRL-16394)
General physics research, 20: 13463 (UCRL-16511, pp 1-53)
K⁻-proton elastic scattering at 700 to 1400 Mev/c, 20: 13460 (UCRL-16274)
Low-background concrete, 20: 12946 (UCRL-11674)
New outlooks in strong interaction physics, 20: 13549 (UCRL-16530)
On finite gyro-radius corrections to hydromagnetic equations for Vlasov plasma, 20: 13926 (UCRL-16517)
Pion-mass measurement by crystal diffraction of mesonic x rays, 20: 13461 (UCRL-16365)
Pion-proton charge-exchange scattering at 500 to 1300 Mev, 20: 13458 (UCRL-16209)
Prog. rpt. on physics, semiannual, 5–10/65, 20: 13347 (UCRL-16511)
Reaction $K^+ + p \rightarrow K + N + \pi$ between 0.86 and 1.58 Bev/c, 20: 13462 (UCRL-16370)
Resonance production in pion-proton interactions at 3.65 and 3.7 Bev/c, 20: 13456 (UCRL-16170)
Time reversal, form factor ratio, and branching ratio in $K_{\mu 3}$ decay, 20: 13459 (UCRL-16253)
Use of Bethe-Salpeter equation in transport theory and derivation of convergent kinetic equation for classical plasma, 20: 13927 (UCRL-16557)

LAWRENCE RADIATION LAB., UNIV. OF CALIFORNIA, LIVERMORE.
Final-state enhancement at 1920 Mev in $\pi^- p$ inelastic scattering, 20: 13454 (UCRL-14100-T(Rev.1))
Purification of Be and its properties, 20: 13175 (CONF-170, pp 214-20)
Spin structure of nucleon-nucleon scattering, 20: 13455 (UCRL-14240-T)
Vapor pressure and evaporation coefficient studies of beryllium nitride decomposition reaction, 20: 12830 (UCRL-7802)

LEDGEMONT LAB., KENNECOTT COPPER CORP., LEXINGTON, MASS.
Air Force-sponsored Be research and development program, 20: 13174 (CONF-170, pp 184-213)

LOCKHEED MISSILES AND SPACE CO., PALO ALTO, CALIF.
Discussion of an account of deformation and fracture in single- and polycrystalline beryllium between 20 and 450°C by A. Moore and G. C. Ellis, 20: 13241 (CONF-179, pp 121-5)

LOCKHEED MISSILES AND SPACE CO., SUNNYVALE, CALIF.
SNAP-10A flight vehicle nuclear environment and radiation effects, 20: 14175 (TID-22418)
SNAPSHOT Agena postflight design review, 20: 14174 (TID-22417)
SNAPSHOT program reliability life test, 20: 14173 (TID-22416)

LOS ALAMOS SCIENTIFIC LAB., UNIV. OF CALIFORNIA, N. MEX.
Cooldown of cryogenic transfer lines, 20: 13668 (LA-3426)
Criticality control in operations with fissile material, 20: 13005 (LA-3366)
DPC: two-dimensional data preparation code, 20: 14064 (LA-3427)
Fabrication of precision lead collimators, 20: 13030 (LA-3443)
Investigation of neutron collimators and their application in neutron radiography, 20: 13702 (LA-DC-7594)
Molecular and principal series absorption in cesium–argon mixtures, 20: 12823 (LA-3391)
Nuclear reactor magnetohydrodynamic power generation, 20: 14132 (LA-3368)
Pin technique for displacement measurements in Kiwi-TNT, 20: 14171 (LA-3388)
Plutonium dispersal by low-order detonation of atomic weapons, 20: 13004 (LA-1981(Rev.))
Radiation measurements of effluent from Kiwi B4D-202 and B4E-301 reactors, 20: 14172 (LA-3397)
Spectra of ion exchangers containing absorbed cobalt(II) chloride, 20: 12824 (LA-DC-6749)
Ultrahigh vacuum thermobalance for Langmuir vaporization studies, 20: 13029 (LA-3423)

LTV RESEARCH CENTER, DALLAS, TEX.

Electron interactions with matter. I., 20: 13781 (NASA-CR-334)

LYON UNIV. (FRANCE).
Inspection of professional personnel exposed to ionizing radiation, 20: 12999 (CEA-R-2746)

M

MAGYAR TUDOMANYOS AKADEMIA ATOMMAG KUTATO INTEZET, DEBRECEN.
Internal bremsstrahlung accompanying non-unique second-forbidden electron capture decay of ^{36}Cl, 20: 13758 (CONF-233(Vol.4), pp 609-13)

MARTIN CO., ORLANDO, FLA.
Stacking faults, 20: 13971 (AD-625834)

MARYLAND UNIV., COLLEGE PARK.
Critical survey of magnetofluid dynamics, 20: 13635 (ARL-63-175(Pt.3))

MARYLAND UNIV., COLLEGE PARK. INST. FOR FLUID DYNAMICS AND APPLIED MATHEMATICS.
Nonlinear mechanics of plasma-like distributed media, 20: 13905 (CONF-651056-1)

MASSACHUSETTS INST. OF TECH., CAMBRIDGE.
Measurement of characteristic kernels of a class of nonlinear systems, 20: 13023 (CONF-660206-1)

MASSACHUSETTS INST. OF TECH., CAMBRIDGE. DEPT. OF NUCLEAR ENGINEERING.
Epithermal neutron studies, 20: 14186 (MIT-2344-4, pp 145-8)
Fast neutron distributions, 20: 13703 (MIT-2344-4, pp 17-47)
Material buckling and intracellular thermal neutron distributions, 20: 14065 (MIT-2344-4, pp 4-16)
Measurement of diffusion coefficient in an anisotropic medium, 20: 13705 (MIT-2344-4, pp 135-44)
Measurement of integral parameters in fuel rods, 20: 14103 (MIT-2344-4, pp 48-62)
Miniature lattice studies, 20: 14069 (MIT-2344-4, pp 106-14)
Oscillating neutron source experiment, 20: 13704 (MIT-2344-4, pp 101-5)
Prog. rpt. on D_2O lattice project, annual, 9/65, 20: 14014 (MIT-2344-4)
Pulsed neutron studies, 20: 14066 (MIT-2344-4, pp 63-9)
Return coefficient measurements, 20: 14070 (MIT-2344-4, pp 115-34)
Single rod experiments in thermal energy region, 20: 14067 (MIT-2344-4, pp 80-8)
Two-region lattices, 20: 14068 (MIT-2344-4, pp 89-100)
Use of neutron absorbers in determination of lattice parameters, 20: 14185 (MIT-2344-4, pp 70-9)

MASSACHUSETTS INST. OF TECH., CAMBRIDGE. RESEARCH LAB. OF ELECTRONICS.
Gaseous electronics, 20: 13924 (TID-22419, pp 85-98)
Plasma electronics, 20: 13925 (TID-22419, pp 99-147)
Plasma magnetohydrodynamics and energy conversion, 20: 13432 (TID-22419, pp 149-76)
Plasma physics, 20: 13923 (TID-22419, pp 77-84)
Prog. rpt. on electronics, 10/15/65, 20: 14227 (TID-22419)

MASSACHUSETTS UNIV., AMHERST. DEPT. OF FOOD SCIENCE AND TECHNOLOGY.
Prog. rpt. on stability of food lipids to ionizing radiation, 2–8/65, 20: 12618 (TID-22399)

MAX-PLANCK-INSTITUT FUER BIOPHYSIK, FRANKFURT AM MAIN (WEST GERMANY).
Bibliography on radiation effects on living tissues and organisms, 7/65, 20: 12629 (AED-C-04-22)

MIAMI UNIV., FLA. DEPT. OF PATHOLOGY.
Factors in uptake, physiology, and retention of ^{65}Zn in male reproductive system of the rat, 20: 12601 (TID-22526)

MICHIGAN STATE UNIV., EAST LANSING.
The effects of urea on ion penetration through isolated cuticular membranes and ion uptake by leaf cells, 20: 14218 (COO-888-44)

MICHIGAN STATE UNIV., EAST LANSING. DEPT. OF HORTICULTURE.
Ion uptake by cells enzymically isolated from green tobacco leaves, 20: 14217 (COO-888-43)
Pathways and mechanisms for foliar absorption of mineral nutrients, 20: 14219 (COO-888-47)
Uptake and transport of ^{59}Fe by intact leaves and enzymically isolated leaf cells of the bean plant, 20: 14220 (COO-888-48)

MIDDLE EAST TECHNICAL UNIV., ANKARA (TURKEY).
Lorentz covariant definition of the U_6 group for free particle states, 20: 13529 (BNL-8767)

MISSOURI UNIV., COLUMBIA.
Independent yields of ^{95}Zr from thermal neutron fission of ^{235}U and ^{233}U, 20: 13783 (ORNL-TM-1333)

MONTPELLIER UNIV. (FRANCE). FACULTE DE MEDECINE.
Synthesis of double-labeled cholesteryl linolenate and arachidonate, 20: 12913 (EUR-2446.f)

MOUND LAB., MIAMISBURG, OHIO.
Coincidence corrections in proportional counter. III., 20: 13068 (MLM-1263)

MULLARD RESEARCH LABS., REIGATE (ENGLAND).
Angular-correlation measurements for the $^{26}Mg(d,p\gamma)^{27}Mg$ reaction, 20: 13768 (CONF-650410-40)

N

NATIONAL AERONAUTICS AND SPACE ADMINISTRATION, CLEVELAND, OHIO. LEWIS RESEARCH CENTER.
Basic studies of a low-density Hall current ion accelerator, 20: 13917 (NASA-TN-3250)
Error in induced electric field modes under Stix coil from assumption of orthogonality of natural plasma modes, 20: 13918 (NASA-TN-D-3255)
Influence of orientation of grains in tungsten on its friction characteristics, 20: 13258 (NASA-TN-D-3238)
Mechanical properties and recrystallization behavior of electron-beam-melted W, 20: 13257 (NASA-TN-D-3232)
Ultrahigh-vacuum creep behavior of Nb and Ta alloys at 2000 and 2200°F, 20: 13256 (NASA-TN-D-3222)

NATIONAL BUREAU OF STANDARDS, WASHINGTON, D. C.
Scattering cross sections for 50- to 500-kev electrons, 20: 13757 (CONF-233(Vol.4), pp 595-608)

NATIONAL INST. FOR RESEARCH IN NUCLEAR SCIENCE, CHILTON (ENGLAND). RUTHERFORD HIGH ENERGY LAB.
Joint kinematical and geometrical analysis of bubble chamber events, 20: 13071 (RHEL/R-111)

NATIONAL LEAD CO. OF OHIO, CINCINNATI.
Effects of various grades of graphite electrodes in carrier distillation of impurities in U_3O_8, 20: 12771 (NLCO-967)
Study of as-cast and heat-treated U–UC alloys, 20: 13259 (NLCO-962)

NAVAL RADIOLOGICAL DEFENSE LAB., SAN FRANCISCO, CALIF.
Bone marrow as source of immunologically competent cells in the mouse, 20: 12716 (AD-626682)
Calculated response of air-wall dosimeters or Geiger-Mueller tubes to monoenergetic photons between 1 and 10 Mev, 20: 13055 (AD-626998)
Characteristics of ^{40}K distributed sources in water, 20: 13056 (AD-627000)
Cobalt-60 γ radiolysis of deuterium–oxygen mixtures, 20: 12881 (AD-626609)
Dose rate and spectral measurements from pulsed x-ray generators, 20: 13057 (AD-627567)
Electric monopole transitions and β bands in even nuclei, 20: 13746 (AD-626681)
General orbit program for sector-focused cyclotrons, 20: 13355 (AD-626999)
Germanium (lithium) detector fabrication, 20: 13058 (AD-627930)
Longevity in neutron-exposed guinea pigs, 20: 12628 (AD-626997)
Quantitative radiochemical determination of ^{63}Ni in seawater, 20: 12779 (USNRDL-TR-924)

NEDERLANDSE ORGANISATIE VOOR TOEGEPAST NATUURWETENS. CHAPPELIJK ONDERZOEK, THE HAGUE. CENTRAAL TECHNISCH INSTITUUT.
Conditions affecting burnout heat flux of polyphenyl cooling agents, 20: 14026 (EUR-2299.e)

NEW MEXICO UNIV., ALBUQUERQUE.
Investigation of neutron collimators and their application in neutron radiography, 20: 13702 (LA-DC-7594)

NEW YORK STATE AGRICULTURAL EXPERIMENT STATION, GENEVA.
Study of radiation-induced softening of plant tissues, 20: 13135 (AD-625482)

NEW YORK STATE VETERINARY COLL., ITHACA, N. Y. DEPT. OF PHYSICAL BIOLOGY.
Prog. rpt. on metabolism of selected radionuclides, final, 6/64–6/65, 20: 12588 (AD-626320)

NOBEL INST. OF PHYSICS, STOCKHOLM (SWEDEN).
M4 isomerism in ^{205}Pb, 20: 13766 (CONF-233(Vol.4), pp 726-9)

NORTH CAROLINA STATE UNIV., RALEIGH. DEPT. OF TEXTILE CHEMISTRY.
Radiation-induced oxidation of hydrocarbons, 20: 12883 (ORO-634)

NORTHERN STATES POWER CO., SIOUX FALLS, S. DAK.
Pathfinder reactor building integrated leakage rate test, 20: 14143 (PAPP-6401)

NOTRE DAME UNIV., IND.
Prog. rpt. on reaction cross sections, final, 10/59–10/64, 20: 13787 (TID-22637)

NOYES LAB. OF CHEMISTRY, UNIV. OF ILLINOIS, URBANA.
Determination of donor sites in Lewis acid adducts of anisole and thioanisole, 20: 14226 (TID-21586)
Pyridine complexes of nickel(II), 20: 14225 (TID-21577)
Transition metal ion-ligand covalency from NME contact shifts, 20: 12828 (TID-21587)

NUCLEAR ENERGY INFORMATION CENTER, WARSAW (POLAND).
Conference on role of atomic electrons in nuclear transformations,

Warsaw, 9/63, 20: 13754 (CONF-233(Vol.4))
Decay of ^{184}Ta, 20: 13767 (CONF-233(Vol.4), pp 730-42)
g Factors of the rotational bands in ^{177}Lu and ^{177}Hf, 20: 13765 (CONF-233(Vol.4), pp 723-5)
Internal bremsstrahlung accompanying non-unique second-forbidden electron capture decay of ^{36}Cl, 20: 13758 (CONF-233(Vol.4), pp 609-13)
Internal bremsstrahlung accompanying electron capture decay of medium heavy nuclei, 20: 13759 (CONF-233(Vol.4), pp 614-24)
Internal bremsstrahlung near 2 M_e, 20: 13760 (CONF-233(Vol.4), pp 637-55)
Internal bremsstrahlung in β decay, 20: 13761 (CONF-233(Vol.4), pp 656-68)
Internal pair formation following neutron capture, 20: 13762 (CONF-233(Vol.4), pp 700-9)
L, M, and N photoelectric cross section measurements in uranium for $h\nu$ = 122 kev, 20: 13755 (CONF-233(Vol.4), pp 548-60)
Magnetic interaction of ^{155}Gd nucleus in 87-kev excited state, 20: 13763 (CONF-233(Vol.4), pp 710-19)
Method to derive electric quadrupole moments of 2+ rotational status of rare earth nuclei, 20: 13764 (CONF-233(Vol.4), pp 720-2)
M4 isomerism in ^{205}Pb, 20: 13766 (CONF-233(Vol.4), pp 726-9)
New calculations of the atomic photoeffect, 20: 13413 (CONF-233(Vol.4), pp 538-47)
Scattering cross sections for 50- to 500-kev electrons, 20: 13757 (CONF-233(Vol.4), pp 595-608)
Scattering of 662-kev γ rays on bound electrons, 20: 13756 (CONF-233(Vol.4), pp 562-94)

NUCLEAR POWER FIELD OFFICE, FORT BELVOIR, VA.
Closed-cycle gas turbine, 20: 14023 (AD-611432, pp 221-35)

NUCLEAR TECHNOLOGY CORP., WHITE PLAINS, N. Y.
Analysis of maximum hypothetical accident, 20: 14181 (COO-1430-2)
Prog. rpt. on fast test reactor hypothetical meltdown accident, 10–12/65, 20: 14182 (COO-1430-3)
Shielding analysis for Fast Flux Test Facility, 20: 14180 (COO-1430-1)

O

OAK RIDGE GASEOUS DIFFUSION PLANT, TENN.
Alloy powder preparation by flame reduction techniques, 20: 13181 (K-L-6076)

OAK RIDGE NATIONAL LAB., TENN.
Ageing effects on beryllium single crystals, 20: 13237 (CONF-170, pp 29-47)
Air Force-sponsored Be research and development program, 20: 13174 (CONF-170, pp 184-213)
AVR-German pebble-bed reactor, 20: 14136 (ORNL-3885, pp 150-94)
Ball-milling of graphite-base reactor fuel, 20: 13218 (ORNL-TM-1412)
Basal plane fracture of beryllium single crystals, 20: 13238 (CONF-170, pp 48-68)
Bibliography on space and accelerator shielding, 20: 13965 (ORNL-RSIC-11)
BONUS superheater fuel assemblies—failure and method of correction, 20: 14141 (ORNL-3910)
Burger's vectors in beryllium and their effect on ductility, 20: 13242 (CONF-170, pp 126-37)
Cell ventilation monitor for fission products development laboratory building, 20: 13006 (ORNL-TM-1384)
Certain definite integrals of Bickley and Bessel functions, 20: 13707 (ORNL-TM-1415)
Component development and testing, EGCR, 20: 14139 (ORNL-3885, pp 268-83)
Conference on physical metallurgy of Be, Gatlinburg, Tenn., 4/30–5/1/63, 20: 13172 (CONF-170)
Deformation and fracture in single- and polycrystalline beryllium between 20 and 450°C, 20: 13240 (CONF-170, pp 102-20)
Discussion of an account of deformation and fracture in single- and polycrystalline beryllium between 20 and 450°C by A. Moore and G. C. Ellis, 20: 13241 (CONF-170, pp 121-5)
Effect of irradiation on stress-rupture characteristics of a Nb-stabilized stainless steel, 20: 13328 (ORNL-TM-1359)
Effects of neutron irradiation on mechanical properties of hot-pressed and extruded Be, 20: 13323 (CONF-170, pp 138-59)
Equilibrium solid solutions of N in Nb–1% Zr between 1200 to 1800°C, 20: 13263 (ORNL-TM-1355)
Estimated costs of high-level waste management, 20: 14208 (ORNL-P-1926)
Excitation and disintegration of nuclei by low-energy electrons and x-rays, 20: 13782 (ORNL-P-1927)
Fabrication of aluminum-base irradiation test plates, 20: 13217 (ORNL-TM-1377)
Fast reactor development, 20: 14104 (ORNL-3885, pp 244-50)
FORTRAN programs for Clebsch-Gordan and Racah coefficients and the NINE-j symbol, 20: 13648 (ORNL-3877(Rev.))
Fueled-graphite development, 20: 13215 (ORNL-3885, pp 3-86)
Fueled-graphite systems, 20: 13261 (ORNL-3885, pp 87-149)
Gaussian quadrature procedure for computation of Bickley functions, 20: 13708 (ORNL-TM-1417)
General category of soluble nucleon-meson cascade equations, 20: 13964 (ORNL-3746)
Heat transfer in the design of large radioisotopic heat sources, 20: 13157 (ORNL-P-1945)
Independent yields of ^{95}Zr from thermal neutron fission of ^{235}U and ^{233}U, 20: 13783 (ORNL-TM-1333)
Interaction of multiple coils on cylindrical induction heating load, 20: 13032 (ORNL-TM-1352)
Irradiation testing of components and materials, EGCR, 20: 14140 (ORNL-3885, pp 284-93)
Large-scale preparation of high purity ^{131}I and ^{133}Xe by sorption techniques, 20: 12772 (ORNL-3840)
Machine to remotely fill and compact nuclear fuel tubes by vibration, 20: 12945 (ORNL-TM-1383)
Minimum bias designs for an exponential response, 20: 13167 (ORNL-3873)
Moderator materials, 20: 13262 (ORNL-3885, pp 195-235)
Nuclear ground state properties of ^{160}, 20: 13785 (ORNL-TM-1374)
Nuclear structure studies in Zr with 65-Mev α particles, 20: 13784 (ORNL-TM-1336)
Oak Ridge, Tennessee, flora: I. Vascular plants, 20: 12567 (ORNL-TM-1232)
Performance analyses, EGCR, 20: 14138 (ORNL-3885, pp 253-67)
Postirradiation examination of EGCR prototype capsule, 20: 14142 (ORNL-TM-1378)
Preparation of isotopic metallic foils and bulk isotopic metals from oxides, 20: 13216 (ORNL-P-1899)
Prog. rpt. on chemical separations processes, 4–6/65, 20: 12928 (ORNL-3868)
Prog. rpt. on GCR program, semiannual, 9/65, 20: 14135 (ORNL-3885)
Program to compute the classical deflection function, 20: 13415 (ORNL-3881)
Purification of Be metal by distillation process, 20: 13173 (CONF-170, pp 1-5)
Purification of Be and its properties, 20: 13175 (CONF-170, pp 214-20)
RCS-2—FORTRAN program for calculation of cross sections from resonance parameters, 20: 13786 (ORNL-TM-1396)
Recent source developments with aerospace utility, 20: 13129 (ORNL-P-1948)
Recombination and trapping in ^{60}Co γ-irradiated n-type Ge, 20: 13327 (ORNL-TM-1354)
Recrystallization characteristics of wrought ingot beryllium sheet, 20: 13243 (CONF-170, pp 160-83)
Structural application of beryllium in the U. K., 20: 13244 (CONF-170, pp 221-44)
Studies for advanced systems, 20: 14137 (ORNL-3885, pp 236-43)
The effect of purification and recontamination on slip in beryllium single crystals, 20: 13239 (CONF-170, pp 90-101)
Velocity and mass-diffusion measurements for full-scale model of pebble-bed reactor core, 20: 14015 (ORNL-TM-1075)

OFFICE, CHIEF OF RESEARCH AND DEVELOPMENT (ARMY), WASHINGTON, D. C.
Army science conference, West Point, N. Y., 6/64. I., 20: 12760 (AD-611432)
Closed-cycle gas turbine, 20: 14023 (AD-611432, pp 221-35)
Paramagnetic resonance study of nitrogen atoms trapped in x-irradiated alkali azides, 20: 13970 (AD-611432, pp 135-47)

ORGANISMO INTERNACIONAL REGIONAL DE SANIDAD AGROPECUARIA, SAN SALVADOR (EL SALVADOR).
Prog. rpt. on insect control by radiation, 7/63–6/64, 20: 12633 (NP-15348)
Prog. rpt. on insect control by radiation, 6/64–3/65, 20: 12634 (NP-15349)

OSAKA CITY UNIV. (JAPAN).
Internal bremsstrahlung near 2 M_e, 20: 13760 (CONF-233(Vol.4), pp 637-55)

P

PARIS UNIV. (FRANCE). FACULTE DES SCIENCES.
Study of high-frequency instabilities on cold cathode reflex discharge, 20: 13901 (CEA-R-2822)

PARIS UNIV., ORSAY (FRANCE). FACULTE DES SCIENCES.
Neutron dosimetry by means of proportional counters with tissue-equivalent walls, 20: 13060 (CEA-R-2891)

PAVIA UNIV. (ITALY). ISTITUTO DI GENETICA.
Mutability of polygenes and utilization of induced genetic variability, 20: 12641 (TID-22582)

PENNSYLVANIA STATE UNIV., UNIVERSITY PARK. MATERIALS

RESEARCH LAB.
Prog. rpt. on crystal chemistry, 5/13–3/13/65, 20: 13260 (NP-15852)
PHILIPPINE ATOMIC RESEARCH CENTER, DILIMAN, QUEZON CITY.
Removal of second-order neutrons by oriented single crystals, 20: 13709 (PAEC-IPA(D)PH-652)
PHILLIPS PETROLEUM CO. IDAHO FALLS, IDAHO., ATOMIC ENERGY DIV.
Compilation of resolutions and intensities of slow neutron, inelastic scattering, time-of-flight instruments, 20: 13061 (IDO-17134)
Inverting the R matrix, 20: 13538 (IDO-17142)
IREKIN—program for numerical solution of reactor kinetics equations, 20: 14060 (IDO-17114)
Prog. rpt. on nuclear technology, 1–3/65, 20: 14059 (IDO-17104)
Prog. rpt. on Spert, 4–6/65, 20: 14013 (IDO-17123)
Stability of highly radioactive alumina calcine, 20: 14207 (IDO-14670)
Uranium recovery from aluminum-alloyed fuel, 20: 12926 (IDO-14669)
XKINEQ—two-group, two-dimensional, multiregion computer code for examining flux stability in reactors, 20: 14061 (IDO-17127)
POLISH ACADEMY OF SCIENCES, WARSAW.
Conference on role of atomic electrons in nuclear transformations, Warsaw, 9/63, 20: 13754 (CONF-233(Vol.4))
Decay of ^{184}Ta, 20: 13767 (CONF-233(Vol.4), pp 730-42)
g Factors of the rotational bands in ^{177}Lu and ^{177}Hf, 20: 13765 (CONF-233(Vol.4), pp 723-5)
Internal bremsstrahlung accompanying non-unique second-forbidden electron capture decay of ^{36}Cl, 20: 13758 (CONF-233(Vol.4), pp 609-13)
Internal bremsstrahlung accompanying electron capture decay of medium heavy nuclei, 20: 13759 (CONF-233(Vol.4), pp 614-24)
Internal bremsstrahlung near 2 M_0, 20: 13760 (CONF-233(Vol.4), pp 637-55)
Internal bremsstrahlung in β decay, 20: 13761 (CONF-233(Vol.4), pp 656-68)
Internal pair formation following neutron capture, 20: 13762 (CONF-233(Vol.4), pp 700-9)
L, M, and N photoelectric cross section measurements in uranium for $h\nu = 122$ kev, 20: 13755 (CONF-233(Vol.4), pp 548-60)
Magnetic interaction of ^{155}Gd nucleus in 87-kev excited state, 20: 13763 (CONF-233(Vol.4), pp 710-19)
Method to derive electric quadrupole moments of 2+ rotational status of rare earth nuclei, 20: 13764 (CONF-233(Vol.4), pp 720-2)
M4 isomerism in ^{205}Pb, 20: 13766 (CONF-233(Vol.4), pp 726-9)
New calculations of the atomic photoeffect, 20: 13413 (CONF-233(Vol.4), pp 538-47)
Scattering cross sections for 50- to 500-kev electrons, 20: 13757 (CONF-233(Vol.4), pp 595-608)
Scattering of 662-kev γ rays on bound electrons, 20: 13756 (CONF-233(Vol.4), pp 562-94)
PRATT AND WHITNEY AIRCRAFT, MIDDLETOWN, CONN. CONNECTICUT ADVANCED NUCLEAR ENGINEERING LAB.
Solubility of helium in liquid lithium and potassium, 20: 12827 (TID-21583)
PRINCETON UNIV., N. J. PLASMA PHYSICS LAB.
Multi-probe measurements of fluctuating azimuthal density variations, 20: 13915 (MATT-402)
Roadblocks in the path of controlled fusion, 20: 13916 (MATT-412)
Scattering EM waves from "marginally stable" acoustic ion plasma waves of a beam-plasma system, 20: 13914 (MATT-318)
Scattering of EM waves from "marginally stable" plasma waves, 20: 13913 (MATT-317)
PRODUCTION GROUP, UNITED KINGDOM ATOMIC ENERGY AUTHORITY, SELLAFIELD (ENGLAND).
Determination of ^{144}Ce in reactor fuel solutions, 20: 12774 (PG-Report-685)
PUERTO RICO WATER RESOURCES AUTHORITY, SAN JUAN.
BONUS power station startup summary report, 2/66, 20: 14119 (CEND/PRWRA-257)

R

RADIATION RESEARCH LABS., MELLON INST., PITTSBURGH, PA.
Prog. rpt., 10–12/65, 20: 12884 (RRL-2310-171)
REACTIVE METALS, INC., ASHTABULA, OHIO.
Prog. rpt. on [extrusion of U], 7–9/64, 20: 13220 (RMI-3)
REACTOR CENTRUM NEDERLAND, PETTEN.
Activation methods for determination of intermediate neutron spectra, 20: 13070 (RCN-40)
REACTOR GROUP, UNITED KINGDOM ATOMIC ENERGY AUTHORITY, RISLEY (ENGLAND).
Steels data manual, 20: 13186 (TRG-Report-840)
RENSSELAER POLYTECHNIC INST., TROY, N. Y.
Prog. rpt. on radiation damage in semiconductor materials, 5–7/65, 20: 13128 (NP-15835(Suppl.))
ROCHESTER UNIV., N. Y. DEPT. OF PHYSICS AND ASTRONOMY.
Charged particle counting system, with particle separation, 20: 13076 (UR-875-117)
ROCKY FLATS DIV., DOW CHEMICAL CO., GOLDEN, COLO.
Pyrohydrolysis of PuF_4, 20: 12775 (RFP-601)
ROENTGEN TECHNISCHE DIENST N. V., ROTTERDAM (NETHERLANDS).
Prog. rpt. on non-destructive weld studies, 7–9/65, 20: 12973 (EURAEC-1519)

S

SANDIA CORP., ALBUQUERQUE, N. MEX.
Combustion and explosion of zirconium droplets ignited by flash heating, 20: 12826 (SC-RR-65-569)
Mie scattering functions computer program description, 20: 13346 (SC-RR-65-396)
Radiation effects in electronics, 20: 13130 (SC-DC-65-1892)
SCOTTISH RESEARCH REACTOR CENTRE, EAST KILBRIDE (SCOTLAND).
Shadow-shielded whole-body counter of high sensitivity, 20: 13074 (SRRC-11/65)
SOCIETA RICERCHE IMPIANTI NUCLEARI, SLUGGIA (ITALY). CENTRO RICERCHE NUCLEARI.
Prog. rpt. on influence of nitrogen in Fe and steel under fast neutron irradiation, 7–9/65, 20: 13324 (EURAEC-1529)
SOCIETE BELGE D'ECONOMIE ET DE MATHEMATIQUE APPLIQUEES, S. A., BRUSSELS.
Economic study of integration of nuclear power plants in electricity generation and distribution networks, 20: 14121 (EUR-2453.f)
SOCIETE BELGE POUR L'INDUSTRIE NUCLEAIRE, BRUSSELS.
Prog. rpt. on use of Pu as reactor fuel, 1–6/64, 20: 13176 (EURAEC-1503)
Prog. rpt. on use of Pu as reactor fuel, 7–12/64, 20: 13177 (EURAEC-1504)
SOCIETE NATIONALE D'ETUDE ET DE CONSTRUCTION DE MOTEURS D'AVIATION, SURESNES (FRANCE). DIVISION ATOMIQUE.
Swirl flows in boiling water, 20: 12960 (EURAEC-1515)
SOCIETE TREFIMETAUX, ARGENTEUIL (FRANCE).
Frittoxal ($Al-Al_2O_3$) and nuclear applications, 20: 13213 (EUR-2447.f)
SOUTH CAROLINA UNIV., COLUMBIA.
Excitation and disintegration of nuclei by low-energy electrons and x-rays, 20: 13782 (ORNL-P-1927)
STANFORD LINEAR ACCELERATOR CENTER, STANFORD UNIV., CALIF.
Infinite ladders and algebra of integrated current components, 20: 13548 (SLAC-58)
Magnetic field measurement and spectroscopy in multipole fields, 20: 13365 (SLAC-39(Rev.))
Prog. rpt. on two-mile accelerator, 7–9/65, 20: 13366 (SLAC-53)
STANFORD UNIV., CALIF. INST. OF THEORETICAL PHYSICS.
New calculations of the atomic photoeffect, 20: 13413 (CONF-233(Vol.4), pp 538-47)
SWIFT AND CO., CHICAGO, ILL.
Determination of equivalence between sterilization process and commercial thermal process for cured meats, 20: 13134 (AD-625252)
SYLVANIA ELECTRONIC SYSTEMS, WALTHAM, MASS. APPLIED RESEARCH LAB.
Prog. rpt. on plasma-covered slot antennas, 11/62–9/65, 20: 13022 (AFCRL-65-859)

T

TAIWAN PROVINCIAL CHUNG-HSING UNIV., TAICHUNG (CHINA). DEPT. OF AGRONOMY.
Prog. rpt. on application of isotopes and radiation in rice cultivation, 2/65, 20: 12592 (NP-15671)
Prog. rpt. on application of isotopes and radiation in rice cultivation, final, 8/65, 20: 12593 (NP-15672)
TECHNICHE HOCHSCHULE, KARLSRUHE (WEST GERMANY). INSTITUT FUER EXPERIMENTELLE KERNPHYSIK.
Search for a heavy electron by electron-proton coincidence measurements, 20: 13446 (DESY-65/9)
TEMPLE UNIV., PHILADELPHIA, PA. RESEARCH INST.
Densities, volume, expansion, compressibility and pressure coefficients and derived functions of metallic Hg for its entire liquid range, 20: 12825 (NYO-2082-1)
TENNESSEE UNIV., KNOXVILLE.
Nuclear structure studies in Zr with 65-Mev α particles, 20: 13784 (ORNL-TM-1336)
Velocity and mass-diffusion measurements for full-scale model of pebble-bed reactor core, 20: 14015 (ORNL-TM-1075)
TEXAS ENGINEERING EXPERIMENT STATION, COLLEGE STATION.
Effects of pre- and postnatal γ irradiation on reproduction in the albino

rat, 20: 12640 (TID-22378)

TEXAS UNIV., AUSTIN. PLASMA DYNAMICS RESEARCH LAB.

Plasma sheath dynamics, 20: 13922 (NP-15703, pp 64-81)

Prog. rpt. on propagation and dispersion of hydromagnetic and ion cyclotron waves in plasmas immersed in magnetic fields, 1/15–7/14/65, 20: 13919 (NP-15703)

Resonances and waves in one- and two-ion species plasmas subjected to intense magnetic fields, 20: 13920 (NP-15703, pp 1-51)

Shock ionization for ion-cyclotron wave experiment, 20: 13921 (NP-15703, pp 52-63)

TORONTO UNIV. (ONTARIO). BANTING AND BEST DEPT. OF MEDICAL RESEARCH.

Effect of x irradiation and thermal trauma on intestinal mucosa, 20: 12630 (BNL-8383)

TRACERLAB/WEST, RICHMOND, CALIF.

Prototype radioisotope inspection system to measure residual flux on automatically processed electronic circuit boards, 20: 13033 (TLW-1110)

TUFTS UNIV., MEDFORD, MASS. DEPT. OF CHEMISTRY.

Dissociation pressure of system Yb–YbH_2, 20: 12829 (TID-22502)

TURKU UNIV. (FINLAND). DEPT. OF GENETICS.

Premeiotic stages of spermatogenesis, 20: 14224 (TID-21562)

Rates of visible mutations as related to maturity of male germ cells of Drosophila, 20: 12636 (TID-21459)

Spermatogenesis of adult Drosophila males after treatment with x rays, 20: 12637 (TID-21466)

U

UNION CARBIDE CORP., OAK RIDGE, TENN. Y-12 PLANT.

Fabrication of miniaturized hardware for space equipment, 20: 12642 (Y-IA-17)

High-volume, air-monitor calibration facility, 20: 13077 (Y-1503)

UNITED ELECTRODYNAMICS, INC., PASADENA, CALIF.

Cavity stability instrumentation and observation, 20: 12989 (NVO-1312-1(Vol.1))

Cavity stability instrumentation and observation, 20: 12990 (NVO-1312-1(Vol.2))

UNITED NUCLEAR CORP., ELMSFORD, N. Y.

Gamma spectral data for shielding and heating calculations, 20: 13966 (UNC-5140)

UNITED STATES–EURATOM JOINT RESEARCH AND DEVELOPMENT PROGRAM.

Experimental plan for the plutonium subcritical program, 20: 14058 (GEAP-4690)

Fabrication of second set of U–Pu fuel elements for substitution experiments, 20: 13214 (EURAEC-1484)

Hydrodynamic instabilities limiting the power of boiling water reactors, 20: 14027 (EURAEC-909)

Irradiation of 0.5-inch-diameter, solid-pellet UO_2 fuel rods, 20: 13326 (GEAP-5100C)

Prog. rpt. on influence of nitrogen in Fe and steel under fast neutron irradiation, 7–9/65, 20: 13324 (EURAEC-1529)

Prog. rpt. on non-destructive weld studies, 7–9/65, 20: 12973 (EURAEC-1519)

Prog. rpt. on reprocessing irradiated fuels, 1–3/65, 20: 12925 (EURAEC-1446)

Prog. rpt. on Saxton Pu program, 7–9/65, 20: 14148 (WCAP-3385-5)

Prog. rpt. on use of Pu as reactor fuel, 1–6/64, 20: 13176 (EURAEC-1503)

Prog. rpt. on use of Pu as reactor fuel, 7–12/64, 20: 13177 (EURAEC-1504)

Single-rod, forced-flow, transition boiling heat transfer from smooth and finned surfaces, 20: 12961 (GEAP-4786)

Swirl flows in boiling water, 20: 12960 (EURAEC-1515)

USTAV JADERNEHO VYZKUMU, CESKOSLOVENSKA AKADEMIE VED, REZ.

Application of highly sensitive integrator in gas chromatography, 20: 12777 (UJV-1431/65)

Concentration-dependent distribution methods for determination of Zr in submicrogram amounts, 20: 12778 (UJV-1434/65)

Research work on the water loop in the WWR-S reactor, 20: 14190 (UJV-1446/65)

Time selector for two-dimensional analysis, 20: 13075 (UJV-1450/65)

V

VANDERBILT UNIV., NASHVILLE, TENN.

L, M, and N photoelectric cross section measurements in uranium for $h\nu = 122$ kev, 20: 13755 (CONF-233(Vol.4), pp 548-60)

VIRGINIA UNIV., CHARLOTTESVILLE. RADIOBIOLOGY AND BIOPHYSICS LAB.

Study of DNA-labeled cells at different times after high doses of radiation, 20: 12638 (TID-21474)

VRIJE UNIVERSITEIT, AMSTERDAM (NETHERLANDS). NATUURKUNDIG LABORATORIUM.

Decay of ^{184}Ta, 20: 13767 (CONF-233(Vol.4), pp 730-42)

W

WABASH COLL., CRAWFORDSVILLE, IND. DEPT. OF BIOLOGY.

Rates and pattern of radioisotope release from fresh tree litter at three levels of mesic forest development, 20: 12566 (COO-1006-4)

WELLESLEY COLL., MASS. DEPT. OF BIOLOGICAL SCIENCES.

Prog. rpt. on effects of radiation on migratory orientation of salamanders, 5/65–2/66, 20: 12568 (TID-22639)

WESTINGHOUSE ELECTRIC CORP., PITTSBURGH, PA. ASTRONUCLEAR LAB.

Modified transient and/or steady-state digital heat transfer code, 20: 12963 (WANL-TME-1108)

Prog. rpt. on pilot production and evaluation of Ta alloy sheet, 4/25/64–10/30/65. III., 20: 13205 (AD-626622)

Prog. rpt. on weldability and stability of refractory alloys, 3/21–6/20/65, 20: 13264 (WANL-PR(P)-008)

WESTINGHOUSE ELECTRIC CORP., PITTSBURGH, PA. ATOMIC POWER DIV.

Prog. rpt. on Saxton Pu program, 7–9/65, 20: 14148 (WCAP-3385-5)

Y

YUGOSLAV ACADEMY OF SCIENCES AND ARTS, ZAGREB. INST. FOR MEDICAL RESEARCH.

Prog. rpt. on mammalian retention of radioactive Sr, 10/61–3/62, 20: 12594 (NP-15679)

Prog. rpt. on mammalian retention of radioactive Sr, 10/62–3/63, 20: 12596 (NP-15681)

Prog. rpt. on mammalian retention of radioactive Sr, 4–6/63, 20: 12597 (NP-15682)

Prog. rpt. on mammalian retention of radioactive Sr, 7/63–3/64, 20: 12598 (NP-15683)

Prog. rpt. on mammalian retention of radioactive Sr, 4–6/64, 20: 12599 (NP-15684)

Prog. rpt. on mammalian retention of radioactive Sr, final, 10/61–9/64, 20: 12600 (NP-15685)

Prog. rpt. on mammalian retention of radioactive Sr, 4–9/62, 20: 12595 (NP-15680)

Z

ZENTRALINSTITUT FUER KERNPHYSIK, ROSSENDORF BEI DRESDEN (EAST GERMANY).

Internal pair formation following neutron capture, 20: 13762 (CONF-233(Vol.4), pp 700-9)

ZENTRALSTELLE FUER ATOMKERNENERGIE-DOKUMENTATION, GMELIN-INSTITUT FUER ANORGANISCHE CHEMIE UND GRENZGEBIETE, FRANKFURT AM MAIN (WEST GERMANY).

Bibliography on nuclear medicine, 9/65, 20: 12733 (AED-C-10-04)

Bibliography on radiation effects on food, 6/65, 20: 13136 (AED-C-02-06)

PERSONAL AUTHOR INDEX

Each entry after an author's name is a shortened version of the title of the report or article, followed by the *NSA* volume and abstract number. Report numbers are given in parentheses.

The phrase "Progress report" is abbreviated as "Prog. rpt.," permitting a more rapid and complete alphabetical arrangement of the titles without changing the location of the progress report titles in relation to the other titles.

Because of problems involving the mechanical preparation of this index, all accent marks are omitted. The following changes in spelling have been introduced to reduce some of the confusion which might result from omitting the accents:

ä	becomes	ae
ö		oe
ø		oe
ü		ue (except in transliterated Chinese names)

A

AARON, R., Calculations of deuteron stripping in soluble model, 20: 13851

ABBE, W. J., Threshold poles and low-energy scattering, 20: 13588

ABDEL-KADER, Adel S., Effect of γ irradiation on post-harvest behavior of tomato fruits, 20: 13148 (UCD-34P80-3, pp 99-175)

ABDULLAH, S. Abu, 500-Curie irradiation facility, 20: 12911 (AECD/HP/3)

ABECASIS, S. M., Separation of Nb and Mo by solvent extraction, 20: 12933

ABRAHAMSON II, E. P., Lattice parameters and solubility limits of alpha Fe as affected by binary transition-element additions, 20: 13317

ABRAO, Alcidio, Activation analysis of gold in ores samples, 20: 12769 (IEA-98)

ABUL-MAGD, A. Y., Two-nucleon stripping processes, 20: 13814

ACHASOV, N. N., Symmetries of lepton-lepton interactions, 20: 13547 (JINR-P-2523)

ACREE, E. H., Large-scale preparation of high purity ^{131}I and ^{133}Xe by sorption techniques, 20: 12772 (ORNL-3840)

ADACHI, Takeshi, Accelerating tube for particle accelerator, 20: 13394

ADACHI, Toshimi, Impact parameter formalism, 20: 13610

ADAM, I., Magnetic β spectrometer with two-fold focusing at the angle $\pi\sqrt{2}$, 20: 13064 (JINR-E-2494)

ADAMOVICH, M. I., Determination of the $\gamma\pi p$ interaction constant, 20: 13477

ADAMS, John Barclay, Two problems in neutrino physics, 20: 13519

ADAMSKY, F.-J., Limits to flaw recognition in nondestructive testing steam-generator tubes for nuclear plants, 20: 14160

ADLER, David, Inconsistency of local field theory of massive spin-two particles, 20: 13581

ADLER, R. P. I., Stacking faults, 20: 13971 (AD-625834)

AGEEV, N. V., Heterogeneous phases of $Nb_3(Al, Ge, and Sn)$, 20: 13275

AGRON, Paul A., Xenon hexafluoride: crystallographic data and phase transitions, 20: 12844

AHMED, Motaheruddin, Tables for neutron energy for reactions $^{7}Li(p,n)^{7}Be$, $T(p,n)^{3}He$, $D(d,n)^{3}He$ and $T(d,n)^{4}He$, 20: 13747 (AECD/EP/7)

AHRENS, Tino, Weak interactions as determined by permutation symmetry in isospace, 20: 13596

AJZENBERG-SELOVE, F., Reaction $^{10}B(^{3}He,n)^{12}N$, 20: 13808

AKAISHI, Jun, Bibliography on accidents in nuclear facilities, 20: 13002 (JAERI-4034)

AKAO, Yasuo, Effect of magnetic field on resonances of surface waves propagating along cylindrical plasma columns, 20: 13941

ALAN, J. J., Bean mutant induced by ionizing radiation. I., 20: 12709

ALAN, J. J., Bean mutant induced by ionizing radiation. II., 20: 12710

ALBERT, Philippe, Determination of sulfur in copper by neutron activation, 20: 12793

ALBERT, Richard D., Uranium-233 fission cross section measured using nuclear explosion in space, 20: 13871

ALBERTI, Giulio, Spectrofluorometric trace determination of Sn, Eu, Tb, and Dy in Na tungstate solutions, 20: 12787

ALBUQUERQUE, H. A., Survey of radioactive content of food grown on Brazilian areas of high natural radioactivity, 20: 12988

ALDRIDGE III, Jack Paxton, Final-state interactions in $^{3}He(^{3}He,2p)^{4}He$ reaction, 20: 13900

ALECU, M., Nondestructive testing methods applicable to sintered materials, 20: 13319

ALEFELD, B., Neutron guides: report on present state of development, 20: 13701 (JUL-294-NP)

ALEKSANDROV, I. A., Diaphragmed waveguide as deflection system of high-frequency separator, 20: 13362 (JINR-P-2503)

ALEKSANDROV, I. A., Waves with complex propagation constants in diaphragmed waveguide, 20: 13363 (JINR-P-2507)

ALEKSANDROV, O. M., Kinetics of $MoSi_2$ oxidation at 1500 to 1800°C, 20: 13195

ALEKSANDROV, O. M., Oxidation of WSi_2 at 1500 to 1800°C, 20: 13196

ALEKSANDROV, O. M., Oxidation of $TaSi_2$ in temperature range from 1400 to 1800°C, 20: 13197

ALEXANDER, P., g Factors of the rotational bands in ^{177}Lu and ^{177}Hf, 20: 13765 (CONF-233(Vol.4), pp 723-5)

ALEXANDER, P., Reaction of radicals induced in E. coli by γ rays with cysteamine and with oxygen, 20: 12622

ALEXANDER, W. D., Clinical significance of complement-fixation test in thyrotoxicosis, 20: 12744

ALFF-STEINBERGER, C., K-meson decay and CP invariance, 20: 13495

ALFORD, W. L., Neodymium-141 and its production in the (n,2n) reaction, 20: 13864

ALLEN, Donald R., Cell for the production of uranium, 20: 12876

ALLEN, R., Programmed spot automatic scanning system for spark chambers, 20: 13106

ALLENDEN, Dennis, Low-count-rate radioactivity alarm systems, 20: 13122

ALLIS, W. P., Gaseous electronics, 20: 13924 (TID-22419, pp 85-98)

ALLIS, W. P., Plasma physics, 20: 13923 (TID-22419, pp 77-84)

ALSMILLER, F. S., General category of soluble nucleon-meson cascade equations, 20: 13964 (ORNL-3746)

ALTER, Henry Ward, Irradiated fuel reprocessing, 20: 12940

ALTHAUS, William A., Study of as-cast and heat-treated U–UC alloys, 20: 13259 (NLCO-968)

ALYAMOVSKAYA, K. V., Reactions of zirconia with rubidium carbonate and silicate, 20: 12851

ALYBAKOV, A. A., Mechanical properties of U-activated NaF single crystals, 20: 13277

AMANO, Noboru, Measurement of the reciprocal of the period of a reactor, 20: 14095

AMATO, I., Grain growth in pure and titania-doped UO_2, 20: 13297

AMBROSINO, Georges, Contribution to study of ^{57}Co, 20: 13799

AMENDA, W., Tests on materials for superconducting coils, 20: 13666 (IPP-4/22)

AMENU-KPODO, Kwasi, Influence of temperature on F-center absorption in NaF, 20: 12892

AMEZQUITA, Refael, Effect of γ irradiation on ripening of bananas, 20: 13146 (UCD-34P80-3, pp 84-91)

AMIEL, Jean-Louis, Induction of tolerance to allogenic grafts, 20: 12656

AMMON, R. L., Prog. rpt. on pilot production and evaluation of Ta alloy sheet, 4/25/64–10/30/65. III., 20: 13205(R) (AD-626622)

AMOS, K. A., Optical model wave functions for nucleons, 20: 13817

ANAN'EV, V. D., Pulsed research reactor and feasibility of pulsed reactor application in neutron spectroscopy, 20: 14191 (BNL-tr-60)
ANASTASIA, L. J., Engineering development of fluid-bed fluoride volatility processes. III., 20: 12923 (ANL-6898)
ANBAR, M., Determination of γ flux in reactor by $^{14}N-^{15}N$ isotopic exchange reaction, 20: 14012 (IA-1048)
ANBAR, M., Mechanism of radiolysis of CO_2, 20: 12882 (IA-1065)
ANDERSON, Cleve R., Irradiated fuel reprocessing, 20: 12940
ANDERSON, J. D., Excited states in ^{6}Be, 20: 13845
ANDERSON, J. R., Clinical significance of complement-fixation test in thyrotoxicosis, 20: 12744
ANDERSON, R. W., Yield data for transplutonium element production in thermal reactors, 20: 13752 (ANL-7096)
ANDERSON, Robert E., Active tuberculosis in leukemia, malignant lymphoma, and myelofibrosis, 20: 12639 (TID-21517)
ANDERSON, Robert E., Hexosamine: collagen ratio as measure of biochemical age in Hiroshima atomic bomb survivors, 20: 12644
ANDERSSON, T. L., Experimental studies on assemblies 1 and 2 of fast FRO. II., 20: 14178 (AE-207)
ANDREESCU, N., Nondestructive testing methods applicable to sintered materials, 20: 13319
ANDRYSEK, O., Macroautoradiography with radiophosphorus in stomach cancer, 20: 12742
ANIKINA, M., Search for new decay modes of $K^{\pm}_{2}$ mesons, 20: 13450 (JINR-P-2488)
ANISOVICH, V. V., Simple high-energy scattering model, 20: 13584
ANNEKE, S., Cell for the production of uranium, 20: 12876
ANSELMO, Vincent C., Complex polyphosphates in irradiated phosphorus oxy-anions, 20: 12902
ANTOLIN, Jacqueline, Electron microscopic observation of stacking faults in twin crystals of Be, 20: 13978
ANTONESCU, E., Spectrometric determination of rare earths, 20: 12806
ANTONOVA, M. M., Chemical bond in transition metal hydrides, 20: 12847
ANTOSZEWSKA, L., Ascorbic acid in crown-gall tumor tissue of Nictoiana tabacum under influence of ^{60}Co γ rays, 20: 12649
AOKI, T., Assessment of end-plug welding of fuel elements, 20: 14196
APERS, D. J., Comparison of ^{51}Cr annealing kinetics in neutron-irradiated and in ^{51}Cr(III)-doped potassium chromate, 20: 12904
ARAD, B., Nuclear resonant scattering using neutron-capture γ rays, 20: 13771 (IA-1050)
ARAI, Osamu, Reactor simulator, 20: 14022
ARAKI, Fumio, Carcinostatic effect of extracts from human gastric cancer, 20: 12625
ARAMAKI, S., Bootstrap conditions in a soluble model, 20: 13590
ARGAN, P. E., Existence of ^{4}He excited levels and of other light nuclides, 20: 13834
ARIEL, Irving M., Intra-arterial administration of Y-90 radiating microspheres for treatment of liver and pancreatic cancers, 20: 12738
ARIMIZU, Nobuo, Gonad dose of patients in x-ray treatment of benign tumors, 20: 13013
ARMOUDIAN, G. A., Phenomenological analysis of high-energy scattering, 20: 13513
ARMS, Henry Shull, Improvements in reactor fuel element cans, 20: 14107
ARMSTRONG, Arthur A. Jr., Radiation-induced oxidation of hydrocarbons, 20: 12883 (ORO-634)
ARNETT, L. M., Final safety analysis of maximum credible accident in the HWCTR, 20: 14183 (DP-1037)
ARUNASALAM, V., Scattering of EM waves from "marginally stable" plasma waves, 20: 13913 (MATT-317)
ARUNASALAM, V., Scattering EM waves from "marginally stable" acoustic ion plasma waves of a beam-plasma system, 20: 13914 (MATT-318)
ASGHAR, M., Neutron resonance scattering measurements with ^{6}Li glass detectors, 20: 13090
ASHEROVA, R. M., Electromagnetic properties of elementary particles in the SU(6) group, 20: 13623
ASHWOOD-SMITH, M. J., Effect of hypothermia on induction of chromosomal mutations by acute x irradiation of mice, 20: 12693
ASINOVSKII, E. I., Continuous spectrum of an argon plasma, 20: 13955
ASPINALL, K., Criticality detection and alarm systems—design principles, 20: 13115
ATANASOV, A. A., Scattering of slow neutrons by hydrogen molecules, 20: 13417
ATTAS, V., Determination of oxygen in sodium by liquid ammonia, 20: 12780 (ORNL-tr-931)
AUERBACH, S. I., Radionuclide cycling: current status and future needs, 20: 12573
AUGUST, L. S., Triple correlations in $^{56}Fe(p,\gamma\gamma)^{57}Co$ reaction, 20: 13857
AULT, John Douglas, Improvements in or relating to luminescent materials, 20: 12921
AUSLOOS, P., Gas-phase radiolysis of cyclobutane, 20: 12894
AVERBACH, B. L., Long-range magnetic order in MnO, 20: 13993
AVERBACH, B. L., Spin correlations in iron, 20: 13994
AYROLES, Rene, Coefficient of absorption of electrons accelerated by voltages between 100 and 1200 kv, 20: 13967
AZIMOV, M. A., Investigation of total absorption lead-glass Cherenkov γ spectrometer in energy range 0.25 to 4.0 Bev, 20: 13105
AZIMOV, S. A., Coherent inelastic interactions between high-energy π-mesons and heavy nuclei in photoemulsion, 20: 13893

B

BADICA, T., Decay of ^{136}Pr, 20: 13882
BADIELLO, R., Gamma irradiation of solid-state N and C terminally protected oligopeptides and amino acids. Carbobenzoxy derivatives and esters of amino acids, 20: 12889
BAEUMLER, J. G., Lighting of very high voltage spark gaps by means of light triggering, 20: 13027 (IPP-4/24)
BAGGE, Erich, Compensation of burnup in a nuclear reactor with a solid moderator, 20: 14110
BAGGERLY, Leo L., Electron interactions with matter. I., 20: 13781 (NASA-CR-334)
BAHNSEN, A., Charged particle counting system, with particle separation, 20: 13076 (UR-875-117)
BAILY, N. A., Prog. rpt. on research on single-crystal high-resistivity CdTe for use as γ spectrometer, annual, 6/65, 20: 13073 (SAN-549-1)
BAKANOVICH, G. I., Use of emission spectra of the copper atom for diagnostics of a plasma, 20: 13953
BAKER, A., Reaction of radicals induced in E. coli by γ rays with cysteamine and with oxygen, 20: 12622
BAKER, D. G., Effect of x irradiation and thermal trauma on intestinal mucosa, 20: 12630 (BNL-8383)
BAKER, D. G., Simulated fallout studies in conifers—preliminary report, 20: 12671
BAKER, N. F., Comparative metabolism of Sr, Ca, and Cs in deer and sheep, 20: 12609
BAKER, T. W., X-ray thermal expansion of near-stoichiometric UO_2, 20: 13300
BAKHRU, H., Decay of ^{183}Hf and the nuclear spectroscopy of ^{183}Ta, 20: 13863
BAKKEN, K., High-temperature low-cycle fatigue of extruded Al–Si–Mg–Ni alloy, 20: 13308
BALAZARI, A. Petruccioli, Grain growth in pure and titania-doped UO_2, 20: 13297
BALDERMAN, J., Nuclear resonant scattering using neutron-capture γ rays, 20: 13771 (IA-1050)
BALDOCK, P. J., X-ray thermal expansion of near-stoichiometric UO_2, 20: 13300
BALDWIN, W. F., Radiosensitivity of female germ cell stages of Dahlbominus, 20: 12691
BAMBYNEK, W., Precision (1%) absolute counting of x rays of low energy, 20: 13092
BANAIGS, J., Particle optics inside an absorber, 20: 13350
BANAS, Julius, Continuous recording of spectra with DRg-140 recording instrument and NZG-319 single-crystal γ scintillation spectrometer, 20: 13086
BANCZYKOWNA, Krystyna, Rapid method of obtaining cerium of very high purity. II., 20: 12935
BAQUE, P., Safety of use of Mg alloy cladding in reactors cooled by CO_2, 20: 13199
BARASHENKOV, V. S., Charge distributions of particles in one-meson theory of interelastic interactions at high energies, 20: 13452 (JINR-P-2510)
BARASHENKOV, V. S., Estimation of interaction cross section for unstable nuclei, 20: 13449 (JINR-P-2433)
BARBANO, P. G., Rapid separation of ^{231}Pa from its daughters, 20: 12937
BARCH, J., Material buckling and intracellular thermal neutron distributions, 20: 14065 (MIT-2344-4, pp 4-16)
BARDOU, L., Synthesis of double-labeled cholesteryl linolenate and arachidonate, 20: 12913 (EUR-2446.f)
BARGHUSEN, John J., Pilot-plant development of process for U alloy fuels. VIII., 20: 12924 (ANL-6973)
BARNES, Barry Keith, States in ^{17}O from $^{13}C + \alpha$, 20: 13898
BARNES, R. D., Comparative metabolism of Sr, Ca, and Cs in deer and sheep, 20: 12609
BARTH, G., Bone-marrow transfusion in the whole-body irradiated, tumor-bearing rat, 20: 12651
BARTHOLD, W., MOSEL: comparison of spectra and spectrally determined parameters of a two-component salt melt, 20: 14127 (JUL-291-RG)
BARTHOLD, W. P., MOSEL: comparison of spectra and spectrally determined magnitudes of a two-component salt melt ($NaF–BeF_2$), 20: 14129 (JUL-315-RG)
BAR-TOUV, J., Asymmetric-rotator model in s-d shell, 20: 13849
BASHIRUZZAMAN, Mohammad, Calibration of ^{60}Co gamma cell, 20: 12910 (AECD/CH/3)
BASILE, L. J., Yield data for transplutonium element production in thermal

reactors, 20: 13752 (ANL-7096)
BASINA, A. S., Decay of ^{139}Pr, 20: 13882
BASKIN, Y., Phase studies in system UP–UO_2, 20: 13285
BASS, R., Nuclear-spectroscopic investigations using (n,pγ)- and (n,αγ)-reactions, 20: 13773 (IKF-13)
BASSETTO, A., Connection between vacuum-like and light-like solutions of the Bethe-Salpeter equation, 20: 13569
BATCH, M. L., Zero power tests—PM-3A Core III, 20: 14115 (BAW-3576-1)
BATEMAN, A. J., Effects of x rays on female germ cells of Drosophila. II., 20: 12689
BATENIN, V. M., Continuous spectrum of an argon plasma, 20: 13955
BATT, Russell Howard, Apparatus for heat capacity measurements in range 0.24 to 20°K, 20: 13694
BATTEY, Philip E., TET2—thermal energy transport code, 20: 13698 (DTMB-1820)
BATTISTONE, G. C., Sample handling conveniences for activation analysis, 20: 12795
BAUER, Stefan George, Fuel elements for nuclear reactors, 20: 14112
BAYER, H., Thyroid scintigraphy with Tc-99m, 20: 12749
BAZARNIC, P. Rockne, Operating characteristics of the present PM-type reactor instrumentation. Task 2 topical report, 20: 14134 (NYO-3379-2)
BEAN, C. H., Fabrication and testing of depleted uranium blanket slugs for EBR-II, 20: 13206 (ANL-6417)
BEASLEY, D., Ageing effects on beryllium single crystals, 20: 13237 (CONF-170, pp 29-47)
BEATLEY, Janice C., Effects of radioactive and nonradioactive dust on Larrea divaricata, 20: 12670
BEATTY, Alvin V., Reduction of radiation damage to Tradescantia chromosomes by adenosine triphosphate, proline, and histidine, 20: 12728
BEATTY, Joanne W., Reduction of radiation damage to Tradescantia chromosomes by adenosine triphosphate, proline, and histidine, 20: 12728
BECK, Ainslie Rogers, Improvements in and relating to nuclear reactors, 20: 14037
BECKER, Christo, Influencing of respiratory center by x radiation, 20: 12702
BECKER, Hans-Wolfgang, Influencing of respiratory center by x radiation, 20: 12702
BEDNAR, B., Macroautoradiography with radiophosphorus in stomach cancer, 20: 12742
BEGHI, G., Thermal transformations of aluminas extracted from Al–Al_2O_3 composites, 20: 13296
BEHREND, H. J., Search for a heavy electron by electron-proton coincidence measurements, 20: 13446 (DESY-65/9)
BEKEFI, G., Gaseous electronics, 20: 13924 (TID-22419, pp 85-98)
BEKEFI, G., Plasma physics, 20: 13923 (TID-22419, pp 77-84)
BELITZ, H.-J., Magnetic probe measurements during the preheating phase of a spindle-cusp experiment, 20: 13639 (JUL-281-PP)
BELL, Alan, Improvements in and relating to shell and tube heat exchangers, 20: 12970
BELL, L. E., Particle disintegration study for re-entering nuclear auxiliary power systems, 20: 14169 (AFWL-TDR-64-75)
BELLER, M., Liquid fuel synthesis using nuclear power in a mobile energy depot system, 20: 12877 (BNL-955)
BELOKONSKI, I., Radiosensitivity of guinea pigs with hypocatalasia, 20: 12643 (ANL-Trans-264)
BELOTE, T. A., Reaction $^{46}Ca(d,p)^{47}Ca$ at 7 Mev, 20: 13853
BELOV, V. A., Collision integrals for the Li–H system. Viscosity of mixtures, 20: 13957
BELYAEVA, I. F., Fluctuations of energy fluxes of nuclear-active and electron-photon components in extensive air showers, 20: 13427
BEN-DAVID, G., Nuclear resonant scattering using neutron-capture γ rays, 20: 13771 (IA-1050)
BENDER, Michael L., Manganese nodules: their evolution, 20: 12976
BENNETT, C. M., SNAP-10A flight vehicle nuclear environment and radiation effects, 20: 14175 (TID-22418)
BENO, M., Effect of carrier on pulmonary retention of radiocerium, 20: 12615
BENZ, R., Phase equilibria in uranium–nitrogen system, 20: 13286
BEN-ZEEV, Nehama, Viability of heterozygotes for induced mutations in Drosophila. II., 20: 12661
BERENYI, D., Internal bremsstrahlung accompanying non-unique second-forbidden electron capture decay of ^{36}Cl, 20: 13758 (CONF-233(Vol.4) pp 609-13)
BERG, R. E., Measurement of high-energy γ rays with Ge(Li) detectors, 20: 13095
BERGHOUT, Christian F., Radioactive waste material incinerator, 20: 14212
BERGKVIST, K. E., M4 isomerism in ^{205}Pb, 20: 13766 (CONF-233(Vol.4), pp 726-9)
BERGMAN, A. A., Moderation of neutrons emitted by pulsed source, 20: 13741
BERGMAN, Clark, Angular distributions for reaction $^{12}C(^6Li,\alpha)^{14}N$ between 2 and 3 Mev, 20: 13846
BERGSTROEM, A., Neutron lifetimes and reactivities in FR-0, 20: 14085
BERKL, E., Tests on materials for superconducting coils, 20: 13666 (IPP-4/22)
BERMAN, R. M., Homogenization of two-phase mixtures of ZrO_2–UO_2 by irradiation, 20: 13330
BERMAN, R. M., Metallographic and x-ray study of limits of oxygen solubility in UO_2–ThO_2 system, 20: 13301
BERNARD, Jean A., Heterogeneous reactor liquid moderated and cooled, 20: 14100
BERRY, P. F., Radioisotope x-ray backscatter gage, 20: 13050
BERS, A., Plasma electronics, 20: 13925 (TID-22419, pp 99-147)
BERTHIER, Guy, Method for calorimetric analysis in variable conditions, 20: 13236 (CEA-R-2797)
BERTHIER, J., Matrix elements of β transitions in the Nilsson model, 20: 13831
BERTOLINI, E., Direct conversion of thermal energy in MPD power generation program at C.N.E.N., 20: 13431 (RT/FI(65)31)
BERUBE, N., Material buckling and intracellular thermal neutron distributions, 20: 14065 (MIT-2344-4, pp 4-16)
BETER, E. V., Coherent inelastic interactions between high-energy π⁻ mesons and heavy nuclei in photoemulsion, 20: 13893
BETHGE, K., Negative H and Li ions in a duoplasmatron, 20: 13376
BHADURI, R. K., Magnetic moment of nuclei for a momentum-dependent internucleon force, 20: 13842
BHARATHAN, K. G., Radioactivity of plants from high radiation areas of Kerala coast and adjoining regions. II., 20: 12987
BHAT, M. R., Spin assignments for three resonances in ^{191}Ir, 20: 13796
BHATTACHARJEE, Jnanendra K., Genetic integrity of upgraded and downgraded alleles in Saccharomyces, 20: 12655
BIAIS, R., Frittoxal (Al–Al_2O_3) and nuclear applications, 20: 13213 (EUR-2447.f)
BIALYNICKI-BIRULA, I., Simplified renormalization theory in quantum electrodynamics, 20: 13658
BIEDENHARN, L. C., Group theory and classification of elementary particles, 20: 13530 (CERN-65-41)
BIEGER, W., Acceleration of plasma through magnetic bottle according to free-particle model, 20: 13911 (JUL-336-PP)
BIEKER, Richard J., Study of as-cast and heat-treated U–UC alloys, 20: 13259 (NLCO-968)
BIENEK, Guenther, Instrument for measurement of dose rate of γ radiation and detection of β radiation, 20: 13120
BIENLEIN, J. K., Internal bremsstrahlung in β decay, 20: 13761 (CONF-233(Vol.4), pp 656-68)
BIJWAARD, G., Prog. rpt. on two-phase flow, 7–9/65, 20: 12962 (GEAP-4959)
BILENKII, S. M., Reconstruction of meson-nucleon scattering matrix from experiments with polarized target, 20: 13448 (JINR-E-2521)
BINGHAM, Carrol R., Nuclear structure studies in Zr with 65-Mev α particles, 20: 13784 (ORNL-TM-1336)
BINGO, Kazuyoshi, Comparison of methods of personnel-monitoring dosimetry practiced in nuclear establishments of different countries, 20: 13003 (JAERI-4035)
BISCOVEANU, I., Nondestructive testing methods applicable to sintered materials, 20: 13319
BISHOP, A. S., Roadblocks in the path of controlled fusion, 20: 13916 (MATT-412)
BISHOP, W. N., Production of Y-87 and a Sr-87m generator, 20: 12917
BISIACCHI, G., Maximal degenerate systems dynamics, 20: 13535 (IC/66/6)
BISWAS, A. B., Thermogravimetric analysis of La, Ce, Pr, and Nd oxalates in air and in CO_2, 20: 12862
BLACKADDER, W. H., Nondestructive determination of burnup by means of ^{144}Pr 2.18-Mev γ-activity, 20: 12812
BLADEL, B. O., Determination of equivalence between sterilization process and commercial thermal process for cured meats, 20: 13134 (AD-625252)
BLAINE, R. A., NAA program description—a program to reformat grave/prism punched output, 20: 13706 (NAA-SR-Memo-10884 and Add.)
BLAIR, John Austin Ischeden, Improvements in or relating to nuclear reactors, 20: 14038
BLANC, D., Cloud chambers filled with dielectric liquid, 20: 13112
BLANCHARD, Richard L., Rapid determination of ^{210}Pb and ^{210}Po in environmental samples by deposition on nickel, 20: 12785
BLAND, R. W., Reaction $K^+ + p \rightarrow K + N + \pi$ between 0.86 and 1.58 Bev/c, 20: 13462 (UCRL-16370)
BLANKENBURG, S. A., Efficiency of secondary electron emission monitors for 70-Mev electrons, 20: 13103
BLASSE, G., New compositions with K_2NiF_4 structure, 20: 12865
BLAUTH, E. W., Two-chamber ionization gage, 20: 13026 (IPP-2/39)
BLAYLOCK, B. Gordon, Chromosomal polymorphism in irradiated natural populations of Chironomus, 20: 12662

BLECH, I. A., Long-range magnetic order in MnO, 20: 13993
BLIGH, A. S., Pituitary implantation for pituitary tumors, 20: 12753
BLINOV, P. I., Influence of mirror ratio on plasma heating by an electron beam in a probkotron, 20: 13947
BLISS, H. E., Pulsed neutron studies, 20: 14066 (MIT-2344-4, pp 63-9)
BLOK, J., Decay of ^{184}Ta, 20: 13767 (CONF-233(Vol.4), pp 730-42)
BLOKHINTSEV, D. I., Conditions of macroscopic causality for the scattering matrix, 20: 13539 (JINR-E-2500)
BLOMEKE, J. O., Estimated costs of high-level waste management, 20: 14208 (ORNL-P-1926)
BLOOM, Elliot, Branching ratio of the Y_1^0, 20: 13445 (CONF-758-14)
BLOOM, Justin L., Thermal neutron flux measuring device using two boron thermistors, 20: 13126
BLUM, Pierre, Process for preparation of UC powder, 20: 13190
BLUMBERG, L. N., Polarized-proton scattering facility at the Oak Ridge Isochronous Cyclotron, 20: 13375
BOARDMAN, F. D., Correlator for investigating random fluctuations in power reactors, 20: 14156
BOD, L., Data evaluation problems in pulsed neutron source method, 20: 13729
BODDENDIJK, H. G., Decay of ^{184}Ta, 20: 13767 (CONF-233(Vol.4), pp 730-42)
BODDY, Keith, Shadow-shielded whole-body counter of high sensitivity, 20: 13074 (SRRC-11/65)
BODENSTEDT, E., Method to derive electric quadrupole moments of 2+ rotational states of rare earth nuclei, 20: 13764 (CONF-233(Vol.4), pp 720-2)
BODERGAT, R., Prog. rpt. on effects of mutagenic substances, annual, 1964, 20: 12632 (EUR-2546.f)
BOEHM, F., g Factors of the rotational bands in ^{177}Lu and ^{177}Hf, 20: 13765 (CONF-233(Vol.4), pp 723-5)
BOEHM, H., Changes of mechanical properties of Cr–Ni steel and Ni alloys after neutron irradiation, 20: 13333
BOEMMEL, Hans, Properties of supported small α-Fe_2O_3 particles determined with Moessbauer effect, 20: 13997
BOENZI, D., Sorption properties of natural tuffs occurring in Lake Bracciano region (Rome), 20: 14209 (RT/PROT(65)29)
BOERNER, W., Thyroid scintigraphy with Tc-99m, 20: 12749
BOERNER, Wilhelm, Radioiodine test for thyroid function with simultaneous estimation of peripheral hormonal iodide supply, 20: 12746
BOESCHOTEN, F., Production and containment of high-temperature plasma, 20: 13908 (IPP-2/44)
BOGATYREV, V. K., Some questions of nuclear safety, 20: 14091
BOGDANOV, A. P., Determination of mixing parameter of M1 and E2 radiation for 0.341-Mev transition in ^{49}Ti, 20: 13803
BOISVERT, Gregory L., Determination of oxygen in sodium by liquid ammonia, 20: 12780 (ORNL-tr-931)
BOIZIAU, C., Radioactive source manometer, 20: 13045
BOKOV, O. G., SU(6)w symmetry, 20: 13545 (JINR-P-2513)
BOKROS, J. C., Prog. rpt. on advanced graphite fuel systems, 8/15–11/14/65, 20: 13247 (GA-6831)
BOL, K., Multi-probe measurements of fluctuating azimuthal density variations, 20: 13915 (MATT-402)
BOLDYSHEV, V. F., Correlation of internal-conversion electron polarization, 20: 13802
BONALUMI, R., Grey rod extrapolation distance, 20: 13712
BONDYOPADHYAY, D., Y_1^{0+} and Y_1^{0-} mass difference, 20: 13488
BONNER, Billy Edward, Elastic scattering of fast neutrons by deuterons, 20: 13520
BOOCOCK, Peter Munro, Improvements in or relating to tube joints, 20: 12951
BOOTH, Lawrence A., Nuclear reactor magnetohydrodynamic power generation, 20: 14132 (LA-3368)
BOOTH, R. S., Excitation of neutron waves by modulated and pulsed sources, 20: 13722
BOQUET, P. L., Origin of urinary excretion of taurine by the rat irradiated with ^{60}Co. I., 20: 12648
BOREK, Ernest, Alterations in transfer ribonucleic acid methylases after bacteriophage infection or induction, 20: 12619
BORELOWSKI, Z., Relativistic bi-point model of free elementary particle in external gravitational field, 20: 13656
BORKOWSKA, Aleksandra, Rapid method of obtaining cerium of very high purity. II., 20: 12935
BORKOWSKI, Bogusław, Rapid method of obtaining cerium of very high purity. II., 20: 12935
BORLERA, Maria Lucco, Systems between niobium oxide and oxides of aluminum and chromium, 20: 12833
BOSCHI, A., Direct conversion of thermal energy in MPD power generation program at C.N.E.N., 20: 13431 (RT/FI(65)31)
BOSIO, F., Delayed effects of ionizing radiation: changes in seminal tissue, 20: 12686
BOTT-BODENHAUSEN, M., Time-dependent interference effects in two-pion decays of neutral kaons, 20: 13496
BOTTER, Fernando, Capillary chromatography in analysis of isomers and isotopes of hydrogen, 20: 12792
BOTTINO, Paul J., Radiosensitivity studies on an interspecific grass hybrid, 20: 12679
BOUDIER, C., Determination of oxygen in sodium by liquid ammonia, 20: 12780 (ORNL-tr-931)
BOURDEAU, Philippe, Movement of fallout in irrigated ecosystems of Po Valley, Italy, 20: 12986
BOURGEOIS, J., Security of reactors, 20: 14018
BOWERS, M. T., Vibration-rotation spectra of monomeric HCl, DCl, HBr, DBr, and HI in rare-gas lattices and N_2-doping experiments in rare-gas lattices, 20: 12857
BOWLER, M. G., Reaction $K^+ + p \rightarrow K + N + \pi$ between 0.86 and 1.58 Bev/c, 20: 13462 (UCRL-16370)
BOWMAN, M. G., Phase equilibria in uranium–nitrogen system, 20: 13286
BOYD, Camille, Effect of γ irradiation on fresh prunes, 20: 13144 (UCD-34P80-3, pp 69-74)
BOYD, Camille, Effect of γ irradiation on lemon fruits, 20: 13145 (UCD-34P80-3, pp 75-83)
BOYD, Camille, Effect of γ irradiation on peaches, 20: 13147 (UCD-34P80-3, pp 92-8)
BOYD, Camille, Sensory evaluation of irradiated cherries, 20: 13141 (UCD-34P80-3, pp 48-51)
BOYD, Camille, Thiamine and niacin analysis of irradiated strawberries, 20: 13142 (UCD-34P80-3, pp 52-4)
BOYD, H. W., L, M, and N photoelectronic cross section measurements in uranium for $h\nu = 122$ kev, 20: 13755 (CONF-233(Vol.4), pp 548-60)
BOYD, T. J. M., Effect of Coulomb collisions on scattering of light by plasmas, 20: 13904 (CLM-R52)
BOYD, T. J. M., Microwave emission from plasmas at harmonics of electron cyclotron frequency, 20: 13903 (CLM-R51)
BOZEK, E., Magnetic interaction of ^{155}Gd nucleus in 87-kev excited state, 20: 13763 (CONF-233(Vol.4), pp 710-19)
BOZZO, S. R., Positron scanner for brain tumors, 20: 12734 (BNL-9911)
BRABERS, M., Eddy-current testing of thin-walled cladding tubes, 20: 14033
BRADLEY, L. B., Programmed tube to tubesheet welding on heat exchangers used in nuclear processing service, 20: 13219 (RL-SEP-710)
BRADLEY, W. F., Vatcrite-type ABO_3 rare-earth borates, 20: 12837
BRADSHAW, R. L., Estimated costs of high-level waste management, 20: 14208 (ORNL-P-1926)
BRANDOW, B. H., Many-body foundations of the nuclear shell model, 20: 13790
BRANDT, R. J., Cavity stability instrumentation and observation, 20: 12989 (NVO-1312-1(Vol.1))
BRANDT, R. J., Cavity stability instrumentation and observation, 20: 12990 (NVO-1312-1(Vol.2))
BRANDT, Werner, Positron lifetime spectra in molecular substances, 20: 13499
BRANTLEY, W. H., L, M, and N photoelectric cross section measurements in uranium for $h\nu = 122$ kev, 20: 13755 (CONF-233(Vol.4), pp 548-60)
BRASS, W., Clinical significance of complement-fixation test in thyrotoxicosis, 20: 12744
BRASSE, F. W., Search for a heavy electron by electron-proton coincidence measurements, 20: 13446 (DESY-65/9)
BRATER, D. C., Alloy powder preparation by flame reduction techniques, 20: 13181 (K-L-6076)
BRAUN, Heribert, Influence of body burden on radiation sensitivity of rats, 20: 12703
BRAUN, J. Z., Coincidence corrections in proportional counter. III., 20: 13068 (MLM-1263)
BRAYER, R. C., Prog. rpt. on burnable poison additions to UO_2, 7–9/65, 20: 13425 (CEND-3107-249)
BREBANT, C., Dimensional measurements and flaw detection, 20: 13343
BREBANT, C., Potentialities of γ spectrometry in nondestructive measurements on fuel elements, 20: 14158
BRECCIA, A., Gamma irradiation of solid-state N and C terminally protected oligopeptides and amino acids. Carbobenzoxy derivatives and esters of amino acids, 20: 12889
BREIT, G., Comparison of effective ranges of n-p and p-p interactions, 20: 13512
BRENIG, W., Bethe-salpeter equation and conservation laws in nuclear physics, 20: 13789
BRESSERS, J., Preparation of uranium sulfide single crystals, 20: 12856
BRICKSTOCK, A., SWAN—multi-group one-dimensional diffusion code for the IBM-7030, 20: 14056 (AWRE-O-99/65)
BRIGGS, Robert W., Effects of x radiation on intracistron recombination at the waxy locus in maize, 20: 12678
BRIGGS, Robert W., Time and temperature tolerances of maize seeds, 20: 14216 (BNL-9859)
BRILL, Edward F., Heat exchange system, 20: 12971
BRINKMANN, Kh. F., New isotope ^{216}Ac, 20: 13779 (JINR-P-2465)
BRINKSCHULTE, H., Interferometric measurements on electromagnetically

generated shock waves, 20: 13636 (IPP-3/24)
BRITT, H. C., Kinetic energy-mass distributions from fission of nuclei lighter than radium, 20: 13861
BRITZ, E. J., Determination of C in UC, 20: 12733 (PEL-80)
BROCHER, Eric, Producing alternating electric power in an MHD generator, 20: 13439
BROECKER, Wallace S., Manganese nodules: their evolution, 20: 12976
BRONISZ, S. E., Electron fractographic study of alpha Pu, 20: 13293
BROOKS, C. R., Specific heat of Zircaloy-2 from 50 to 700°C, 20: 13310
BROOKS, F. D., Neutron resonance scattering measurements with ^{6}Li glass detectors, 20: 13090
BROOME, J., Scatter, 20: 13697 (AEEW-M-605)
BROWN, D. S., Prog. rpt. on radiation technology in extending shelf life of fruits and vegetables, annual, 2/64–1/65, 20: 13138 (UCD-34P80-3)
BROWN, E. S., Nondestructive testing in test-reactor operation at NRTS, 20: 14197
BROWN, G. A., Plasma magnetohydrodynamics and energy conversion, 20: 13432 (TID-22419, pp 149-76)
BROWN, I. G., Kinetics of $\beta \rightarrow \alpha$ phase change in U–1 at.% Pt alloy, 20: 13307
BROWN, J. B. C., Extrapolation distances for pulsed neutron experiments, 20: 13726
BROWN, J. E., DASA fallout and transit dose rate measurement system, 20: 12978 (AD-627077)
BROWN, J. L., Reaction $K^{+} + p \rightarrow K + N + \pi$ between 0.86 and 1.58 Bev/c, 20: 13462 (UCRL-16370)
BROWN, S. C., Gaseous electronics, 20: 13924 (TID-22419, pp 85-98)
BROWN, S. C., Plasma physics, 20: 13923 (TID-22419, pp 77-84)
BRUECKNER, Keith A., Theory of correlated crystals, 20: 14001
BRUGGER, R. M., Compilation of resolutions and intensities of slow neutron, inelastic scattering, time-of-flight instruments, 20: 13061 (IDO-17134)
BRUK, Z. V., Calorimetric detector for measuring energy of an ionized beam, 20: 13114
BRUNA, J. G., Study of homogeneous core assemblies using pulsed neutron sources, 20: 14077
BRUNER, Fabrizio, Gas chromatography of isotopic molecules on open tubular columns, 20: 12930
BRUNET, J. P., Study of homogeneous core assemblies using pulsed neutron sources, 20: 14077
BRUNFELTER, B., Experimental studies on assemblies 1 and 2 of fast reactor FRO. II., 20: 14178 (AE-207)
BRUNFELTER, B., Neutron lifetimes and reactivities in FR-0, 20: 14085
BRUYNESTEYN, W., Measurement of neutron flux distribution in a homogeneous suspension reactor, 20: 14072
BRYANT, F. J., Effect of radiation damage on ZnS single crystals, 20: 13990
BRYANT, T. H. E., Grid field dosimetry for ^{60}Co beams, 20: 13010
BRYDON, D., Contribution of floor returns to neutron interaction, 20: 13742
BRYER, Robert George, Improvements in or relating to radiation-sensitive devices, 20: 13117
BUCHANAN, W. Watson, Clinical significance of complement-fixation test in thyrotoxicosis, 20: 12744
BUCHET, J., Study of homogeneous core assemblies using pulsed neutron sources, 20: 14077
BUCKLEY, Donald H., Influence of orientation of grains in tungsten on its friction characteristics, 20: 13258 (NASA-TN-D-3238)
BUCKLEY, Patricia M., Comparative inactivation of conidia, mycellia, and sclerotia of Botrytis cinerea by γ radiation, 20: 13149 (UCD-34P80-3, pp 176-89)
BUDINI, P., Green functions from Lie algebras, 20: 13661
BUDINI, P., Maximal degenerate systems dynamics, 20: 13535 (IC/66/6)
BUDINI, R., Gamma irradiation of solid-state N and C terminally protected oligopeptides and amino acids. Carbobenzoxy derivatives and esters of amino acids, 20: 12889
BUGG, D. V., Real part of the proton-neutron forward scattering amplitude, 20: 13493
BUIKO, V. M., Mechanical properties of U-activated NaF single crystals, 20: 13277
BUKOVAC, M. J., Pathways and mechanisms for foliar absorption of mineral nutrients, 20: 14219 (COO-888-47)
BUKOVAC, M. J., The effects of urea on ion penetration through isolated cuticular membranes and ion uptake by leaf cells, 20: 14218 (COO-888-44)
BUKOVAC, Martin J., Ion uptake by cells enzymically isolated from green tobacco leaves, 20: 14217 (COO-888-43)
BUNDY, Roy Dale, Velocity and mass-diffusion measurements for full-scale model of pebble-bed reactor core, 20: 14015 (ORNL-TM-1075)
BUNGE, Joachim, Heterogeneous reactor liquid moderated and cooled, 20: 14100
BUNSHAH, R. F., Purification of Be and its properties, 20: 13175 (CONF-170, pp 214-20)
BUNTING, W. R., Simulated fallout studies in conifers—preliminary report, 20: 12671
BURBACH, Werner, Thickness measurement with γ beams, 20: 13151
BURDESE, Aurelio, Systems between niobium oxide and oxides of aluminum and chromium, 20: 12833
BURDET, G., Proof of completeness of solutions of the Schroedinger equation in the λ plane, 20: 13653
BURDICK, E. E., Nondestructive testing in test-reactor operation at NRTS, 20: 14197
BURGER, C., Dose dependence of annealing stage II in neutron-irradiated aluminum, 20: 13340
BURNETT, D. S., Kinetic energy-mass distributions from fission of nuclei lighter than radium, 20: 13861
BURNETT, D. S., Strontium–rubidium age of an iron meteorite, 20: 12992
BURNS, John H., Refinement of crystal structure of Li_2BeF_4, 20: 12834
BUROV, I. V., Rare earth alloys and compounds, 20: 13280
BURT, W. R. Jr., Fabrication and testing of depleted uranium blanket slugs for EBR-II, 20: 13206 (ANL-6417)
BUSCH, G., Valency changes in cerium compounds, 20: 13991
BUSSEL, Joseph, Gas exchange in Bartlett pears in relation to γ irradiation, 20: 13140 (UCD-34P80-3, pp 27-47)
BUTTLE, P. J. A., Neutron transfer in heavy ion reactions, 20: 13830
BYRD, Joseph S., Description of temperature monitor for large reactors. III., 20: 14025 (DP-944)
BYSTRITSKII, I., Nucleon-nucleon potential with a soft core for $^{1}S_0$ state at 0.17 to 310 Mev, 20: 13489

C

CABANIUS, J., The development of graphite–gas research, 20: 14152
CADILHAC, M., Pulsed and modulated experiments on fast multiplying media, 20: 13723
CADILHAC, M., Theory of pulsed and modulated experiments on fast neutron multiplying media, 20: 14088
CAHILL, T. A., Electric dissociation of the H^- ion near 2.4 Mev, 20: 13380
CALAIS, D., Diffusion in the Pu–U system, 20: 13313
CALMON, Calvin, Radioactive fallout treatment kit, 20: 12942
CALUSARU, A., Thermal annealing and role of water of crystallization in potassium trioxalatoferrate irradiated with neutrons, 20: 12903
CAMBOU, Francis, Modifications of density and mobility of majority carriers in n-type Ge bombarded by protons at 600 Mev, 20: 13977
CAMIN, Leopoldo, Separation of ^{131}I-rose bengal by thin-layer chromatography, 20: 12763 (CNEA-162)
CAMIN, Leopoldo L., Preparation of ^{131}I-allyl-inulin, 20: 12912 (CNEA-161)
CAMPBELL, Milton H., Gas-chromatographic analysis of solvent used in fuel reprocessing and fission-product recovery, 20: 12789
CAMPSIE, I. C., Nondestructive testing of fuel elements, 20: 14161
CANNON, D. D., Machine to remotely fill and compact nuclear fuel tubes by vibration, 20: 12945 (ORNL-TM-1383)
CARDOSI, G., Feasibility studies of PCTR measurements with light-water-moderated plutonium-fueled lattices, 20: 14189 (RT/FI(65)43)
CARLSON, Frederick F., Paramagnetic resonance study of nitrogen atoms trapped in x-irradiated alkali azides, 20: 13970 (AD-611432, pp 135-47)
CARLSON, Walter Berndt, Improvements in or relating to nuclear reactors, 20: 14109
CARMICHAEL, B. M., DPC: two-dimensional data preparation code, 20: 14064 (LA-3427)
CARNAHAN, Brice, Radiation-induced cracking of pentanes and dimethyl-butanes, 20: 12908
CARPETIS, C., Self-excitation of an electrodeless MHD generator, 20: 13429 (N64-32348)
CARRIGAN, R. A. Jr., Measurement of energies of γ rays from decay of ^{66}Ga, 20: 13818
CARROLL, R. M., In-pile fission-gas release from fine-grain UO_2, 20: 13290
CARSWELL, D. J. A., Correlator for investigating random fluctuations in power reactors, 20: 14156
CARTER, A. A., Real part of the proton-neutron forward scattering amplitude, 20: 13493
CARTER, D., Aperture and cell-size effects on shunt impedance of alternating periodic structures, 20: 13358 (BNL-9944)
CARTONI, Gian Paolo, Gas chromatography of isotopic molecules on open tubular columns, 20: 12930
CARVER, J. G., Experimental plan for the plutonium subcritical program, 20: 14058 (GEAP-4690)
CASE, F. N., Large-scale preparation of high purity ^{131}I and ^{133}Xe by sorption techniques, 20: 12772 (ORNL-3840)
CASE, F. N., Recent source developments with aerospace utility, 20: 13129 (ORNL-P-1943)
CASPAR, P. E., Production by fission fragments of large tracks in crystals, 20: 13984
CASSEL, D. G., Time-dependent interference effects in two-pion decays of neutral kaons, 20: 13496

CATTANEI, G., Measurement of anisotropy in radial neutral gas pressure, 20: 13907 (IPP-2/42)
CAVALIERE, A., Theory of quasistationary plasmas in contact with a wall, 20: 13912 (LGI-65/21 and App.)
CAVALLORO, Raffaele, Movement of fallout in irrigated ecosystems of Po Valley, Italy, 20: 12986
CAZALIS, Jean Pierre, Improvements in hot cells, 20: 12953
CAZZANIGA, E., Thermal transformations of aluminas extracted from Al–Al_2O_3 composites, 20: 13296
CELEDA, J., Kinetics and mechanism of dissolution of uranous-uranic oxide in sulfuric acid in presence of ferric ion, 20: 12863
CELNIK, J., Gamma spectral data for shielding and heating calculations, 20: 13966 (UNC-5140)
CERCY, Colette, Capillary chromatography in analysis of isomers and isotopes of hydrogen, 20: 12792
CHAKKALAKAL, D., Simple derivation of cluster expansions for many-fermion systems, 20: 13591
CHALABREYSSE, Jacques, Inspection of professional personnel exposed to ionizing radiation, 20: 12999 (CEA-R-2746)
CHALMERS, J. H., Boron poisoning of plutonium solutions, 20: 13019
CHALUTZ, Edo, Interaction of γ irradiation, sealed packages, and controlled atmosphere on incidence of Botrytis rot in strawberries, 20: 13139 (UCD-34P80-3, pp 9-26)
CHAMBERLAIN, Richard H., Radiation hazards: an exercise in value judgment, 20: 12752
CHAMBRE, P. L., Release of fission gas from an evaporating fuel body, 20: 13336
CHAN, Yau W., Series expansion of a determinant and solution of secular equation, 20: 13168
CHAND, Prakash, Perturbational calculations in gauge theory of elementary particles, 20: 13628
CHANDLEY, A. C., Effects of x rays on female germ cells of Drosophila. II., 20: 12689
CHANDRA, Hombe Gowda Sharat, Cytogenetic studies following high-dosage irradiation in the mealy bug, 20: 12715
CHASE, L. H., Cell ventilation monitor for fission products development lab. building, 20: 13006 (ORNL-TM-1384)
CHAVE, C. T., Containment for nuclear reactors, 20: 14031
CHAZOT, Henri, Improvements in installations for spectrophotometric analysis of radioactive solutions, 20: 12813
CHECHKIN, V. V., Resonant heating of plasma by high-frequency field, 20: 13946
CHEER, D. A., Recrystallization characteristics of wrought ingot beryllium sheet, 20: 13243 (CONF-170, pp 160-83)
CHEN, Che Jen, Anomalous diffusion and instabilities of argon plasma in strong magnetic field, 20: 13943
CHEN, H. Y., Reaction $^{46}Ca(d,p)^{47}Ca$ at 7 Mev, 20: 13853
CHENOUARD, J., Determination of Pu by double-tracer isotopic dilution, 20: 12811
CHEON, Il-Tong, Absorption of π mesons and (p,pd) reaction, 20: 13874
CHERENKOV, P. A., Distribution of knock-out nucleons as a function of nuclear volume, excitation energy, and nuclear recoil momentum distributions in cascade processes, 20: 13892
CHERNYSHOV, A. A., Neutron-thermalization process in time in graphite and beryllium, 20: 13738
CHERNYSHOV, A. A., Neutron thermalization in time in aqueous moderators, 20: 13739
CHERPENTIER, C., Ultrasonic inspection following heat treatment of uranium alloys, 20: 13318
CHERRIN, W., Electron capture to negative electron emission branching ratio for ^{142}Pr decay, 20: 13797
CHERRINGTON, Blake Edward, Helical instability produced in gaseous magnetoplasmas by gyro-interaction of microwaves, 20: 13959
CHESHKOV, A. A., Form factors and multipoles in electromagnetic interactions, 20: 13451 (JINR-P-2505)
CHEVALLIER, J., Studies about nuclear naval propulsion in France, 20: 14176
CHEW, Geoffrey F., Approximation of Regge potentials through form factors, 20: 13603
CHI, Cao, General propagator for mesons with spin 2,1,0 in symmetry theory, 20: 13543 (JINR-P-2474)
CHIAPETTA, R. L., Studies of reactor containment structures, 20: 14028 (IITRI-578P22-14)
CHIKHLADZE, V. L., Internal conversion electron spectra in (α,n) and (α,2n) nuclear reactions on Mo-92 and Mo-98, 20: 13881
CHIKIN, R. V., Influence of mirror ratio on plasma heating by an electron beam in a probkotron, 20: 13947
CHILDERS, R. L., Use of Fialho method for calculating phase-space volumes, 20: 13481
CHIU, Charles Bin, Pion-proton charge exchange scattering at 500 to 1300 Mev, 20: 13458 (UCRL-16209)
CHKHAIDZE, L., Search for new decay modes of K_2^0 mesons, 20: 13450 (JINR-P-2488)
CHLEBOWSKA, Daniela, Second vibrational state of even-even spherical nuclei, 20: 13793
CHO, Tong Y., Dissociation pressure of system Yb–YbH_2, 20: 12829 (TID-22502)
CHRIST, J., Neutron guides: report on present state of development, 20: 13701 (JUL-294-NP)
CHRISTIAN, John E., Properties of a diuretic agent in swine by in vivo whole-body counting, 20: 12613
CHRISTOPHER, S. S., Prog. rpt. on burnable poison additions to UO_2, 7–9/65, 20: 13425 (CEND-3107-249)
CHUBB, Donald L., Basic studies of a low-density Hall current ion accelerator, 20: 13917 (NASA-TN-3250)
CHUKHLANTSEV, V. G., Reactions of zirconia with rubidium carbonate and silicate, 20: 12851
CHUKHLANTSEV, V. G., Triangulation of the Na_2O–ZrO_2–SiO_2 system, 20: 13284
CHUKHLINTSEV, V. G., Systems BaO–ZrO_2 rich in BaO, 20: 13282
CHUMIN, V. G., Magnetic β spectrometer with two-fold focusing at the angle $\pi\sqrt{2}$, 20: 13064 (JINR-E-2494)
CHURCH, Bruce W., Trophic level effect on ^{137}Cs concentration, 20: 12611
CHURCH, L. B., Gamma rays from decay of 35-day ^{95}Nb, 20: 13859
CHUVILO, I., Leptonic decays of K^0 mesons and possible CP violation, 20: 13515
CHYLINSKI, Zygmunt, Uncertainty relation between time and energy, 20: 13657
CICCARIELLO, S., Connection between vacuum-like and light-like solutions of the Bethe-Salpeter equation, 20: 13569
CIESLAK, E., Observation of fission events in mica sandwiches, 20: 13099
CIMORELLI, L., Measurement of void fraction with impedance gauge technique, 20: 12964
CITRON, A., Particle optics inside an absorber, 20: 13350
CITTADINI, E., Intra-operative detection of pelvic lymph nodes by radioactive isotopes, 20: 12751
CITTADINI, G., Response to whole-body irradiation of mice pretreated with stimulating drugs, 20: 12685
CLARK, G. M., Simulated fallout studies in conifers—preliminary report, 20: 12671
CLARK, J. W., Simple derivation of cluster expansions for many-fermion systems, 20: 13591
CLARK, John W., Dynamical correlations and the nuclear photoeffect, 20: 13873
CLEARY, R. E., Solubility of helium in liquid lithium and potassium, 20: 12827 (TID-21583)
CLEGG, Thomas Boykin, Polarization of protons elastically scattered from ^{12}C, 20: 13899
CLENDENEN, R. L., Effect of very high pressure on structure of some hcp 20: 13316
CLIKEMAN, F. M., Material buckling and intracellular thermal neutron distributions, 20: 14065 (MIT-2344-4, pp 4-16)
CLIKEMAN, F. M., Prog. rpt. on D_2O lattice project, annual, 9/65, 20: 14014 (MIT-2344-4)
CLINE, H. E., Magnetic field distribution in type II superconductor, 20: 13672
CLINE, H. E., Superconductivity of composite of fine niobium wires in copper, 20: 13673
CLINE, J. F., Mineral transfer in a greasewood community and ion uptake by grasses, 20: 12575
COBAS, Amador, Detection of radiation damage in anthracene crystals by space-charge-limited current measurements, 20: 12893
COBB, J. K., Efficiency of secondary electron emission monitors for 70-Mev electrons, 20: 13103
COBB, J. K., Magnetic field measurement and spectroscopy in multipole fields, 20: 13365 (SLAC-39(Rev.))
COCHO, G., Electromagnetic and weak form factors of the nucleon, 20: 13447 (IC/65/95)
COFFEY, Howard Thomas, Critical currents in thin superconducting tin films, 20: 13693
COHEN, B. L., Reactions (d,d') on Sn, Cd, Te, and Mo isotopes, 20: 13872
COHEN, B. L., Spectroscopic factors from deuteron stripping reactions, 20: 13865
COHEN, I., Metallographic and x-ray study of limits of oxygen solubility in UO_2–ThO_2 system, 20: 13301
COIANTE, D., Semiconductor detectors of surface-barrier type, 20: 13072 (RT/EL(65)7)
COLE, L. J., Bone marrow as source of immunologically competent cells, 20: 12716 (AD-626682)
COLEMAN, James S., Spectra of ion exchangers containing absorbed cobalt(II) chloride, 20: 12824 (LA-DC-6749)
COLI, M., Sensitive, 100-MHz pulse discriminator and shaping circuit, 20: 13043

COLLIE, C. H., Thermal neutron absorption cross section of the AERE boron standard, 20: 13807
COLLINS, C. H., Comparison of ^{51}Cr annealing kinetics in neutron-irradiated and in ^{51}Cr(III)-doped potassium chromate, 20: 12904
COLLINS, Donnell Michael Jr., Novel family of digital circuits, 20: 13164 (COO-415-1028)
COLLINS, K. E., Comparison of ^{51}Cr annealing kinetics in neutron-irradiated and in ^{51}Cr(III)-doped potassium chromate, 20: 12904
COLOMBO, R. L., Grain growth in pure and titania-doped UO_2, 20: 13297
COMAR, C. L., Prog. rpt. on metabolism of selected radionuclides, final, 6/64–6/65, 20: 12588 (AD-626320)
COMBECHER, D., Electrostatic double probes and their applicability in hot plasmas, 20: 13906 (IPP-1/40)
COMER, R. H., Pulsed electron beam system, 20: 13034
COMMANDER, R. E., Uranium recovery from aluminum-alloyed fuel, 20: 12926 (IDO-14669)
COMTE, R., Pulsed neutron measurements in fast assemblies, 20: 14084
CONARD, R. A., Growth status of children exposed to fallout radiation on Marshall Islands, 20: 13011
CONDE, J. F. G., Quality control inspection and testing of fuel materials for Dragon, 20: 14159
CONSOLI, Terenzio, Method and apparatus for accelerating ionized gas, 20: 12952
CONSTABARIS, G., Properties of supported small α-Fe_2O_3 particles determined with Moessbauer effect, 20: 13997
COOBS, J. H., AVR-German pebble-bed reactor, 20: 14136 (ORNL-3885, pp 150-94)
COOBS, J. H., Component development and testing, EGCR, 20: 14139 (ORNL-3885, pp 268-83)
COOBS, J. H., Fueled-graphite development, 20: 13215 (ORNL-3885, pp 3-86)
COOBS, J. H., Irradiation testing of components and materials, 20: 14140 (ORNL-3885, pp 284-93)
COOBS, J. H., Moderator materials, 20: 13262 (ORNL-3885, pp 195-235)
COOK, Marlin M., Study of as-cast and heat-treated U–UC alloys, 20: 13259 (NLCO-968)
COOPER, R. S., Plasma magnetohydrodynamics and energy conversion, 20: 13432 (TID-22419, pp 149-76)
COOPER, Ralph S., Nuclear reactor magnetohydrodynamic power generation, 20: 14132 (LA-3368)
CORBETT, L., Bibliography on ultrasonic welding, 1960–65, 20: 13210 (AWRE/LIB/BIB/13)
CORBITT, Howard E., A-c magnetohydrodynamic generator, 20: 13443
CORELLI, John C., Prog. rpt. on radiation damage in semiconductor materials, 5–7/65, 20: 13128 (NP-15835(Suppl.))
CORNGOLD, N., Theoretical interpretation of pulsed neutron phenomena, 20: 13731
CORY, J. S., Positive column striations in magnetic field, 20: 13944
COSMAN, E. R., Nuclear-reaction studies in Ni isotopes, 20: 13858
COSTA, S., Device for detection of neutrons at energies up to 50 Mev, 20: 13081
COSTA, S., Photoemission of neutrons at 6 to 80 Mev from ^{9}Be, 20: 13795
COTE, R. E., Gamma rays from decay of 35-day ^{95}Nb, 20: 13859
COTE, R. E., Measurement of energies of γ rays from decay of ^{66}Ga, 20: 13818
COTTER, David J., Recovery of hardwood stands 3 to 5 years following acute irradiation, 20: 12675
COTTRELL, W. B., Performance analyses, EGCR, 20: 14138 (ORNL-3885, pp 253-67)
COUTURES, Juliette, High-temperature study of changes of the crystalline form of Nd_2O_3, 20: 13979
COWGILL, Dale Stephen, Deformation behaviors of niobium and tantalum at low temperatures, 20: 13253 (IS-T-65)
COX, A. E., Thermal neutron absorption cross section of the AERE boron standard, 20: 13807
COX, A. F. J., Effect of radiation damage on ZnS single crystals, 20: 13990
CRANBERG, L., Excitation of a 3-collective state by low-energy neutron scattering, 20: 13870
CRANE, A., Induced infrared absorption spectrum of solid deuterium and solid hydrogen deuteride, 20: 13419
CRASEMANN, Bernd, Electron-capture ratio and internal bremsstrahlung in ^{181}W decay, 20: 13869
CRASTES DE PAULET, A., Synthesis of double-labeled cholesteryl linolenate and arachidonate, 20: 12913 (EUR-2446.f)
CRAVEN, B. M., Neutron diffraction study of orthoboric acid $D_3{}^{11}BO_3$, 20: 12836
CRAWFORD, B. R., Wilzbach tritiation studies. II., 20: 12878
CRAWFORD, F. W., Low-frequency impedance characteristics of Langmuir probe in a plasma, 20: 13940
CRILE, George Jr., Radioactive iodine treatment of Graves' disease, 20: 12736
CRIM, W. M. Jr., Closed-cycle gas turbine, 20: 14023 (AD-611432, pp 221-35)
CRISTOFOLINI, G., Oak Ridge, Tennessee, flora: I. vascular plants, 20: 12567 (ORNL-TM-1232)
CRISTOFOLINI, S., Oak Ridge, Tennessee, flora: I. vascular plants, 20: 12567 (ORNL-TM-1232)
CROCKER, I. H., Electron capture to negative electron emission branching ratio for ^{142}Pr decay, 20: 13797
CROCKER, J. G., Prog. rpt. on Spert, 4–6/65, 20: 14013 (IDO-17123)
CRONIN, J., Coupling-constant relations for vector and scalar mesons, 20: 13486
CROOKS, J., Clinical significance of complement-fixation test in thyrotoxicosis, 20: 12744
CROSBIE, K. L., Fast-reactor physics parameters from pulsed source, 20: 14202
CROSSLEY, D. A. Jr., Radiocesium dispersion in a cryptozoan food web, 20: 12576
CROWE, W. E., Nuclear reactor magnetohydrodynamic power generation, 20: 14132 (LA-3368)
CSANYI, Piroska, Measurement of isotopes emitting soft β radiation with aid of liquid scintillator in single-channel measuring instrument. III., 20: 12801
CSONKA, Paul L., Final-state enhancement at 1920 Mev in π^-p inelastic scattering, 20: 13454 (UCRL-14100-T(Rev.1))
CUNNINGHAM, J. E., BONUS superheater fuel assemblies—failure and method of correction, 20: 14141 (ORNL-3910)
CUNNINGHAM, J. R., Tissue-air ratios and scatter functions for large field sizes for ^{60}Co γ radiation, 20: 13009
CUNY, G., Study of graphite and beryllium oxide using pulsed neutron source method, 20: 13727
CURREY, C. F., Design features of the San Onofre nuclear station, 20: 14157
CURZON, F. L., Radial hydromagnetic oscillations of rotating plasma cylinder, 20: 13933
CUYPERS, Jacqueline, Determination of sulfur in copper by neutron activation, 20: 12793
CUYPERS, Marc, Determination of sulfur in copper by neutron activation, 20: 12793
CZERWONKO, Anna, Formation and thermal bleaching of color centers in sodium chlorate crystals irradiated by γ rays, 20: 12900
CZUBEK, J. A., Physical possibilities of γ-γ logging, 20: 12993

D

DAHL, A. H., Factors influencing accumulation of fallout ^{137}Cs in Colorado mule deer, 20: 12984
DAHLBERG, E. P., Effects of prestrain on mechanical properties of Zr, 20: 13246 (CONF-651017-13)
DAHLBY, Helen J., Observations on the many-body problem in the A. A. VLASOV arrangement, 20: 13551 (LA-tr-66-8)
DAHLBY, Helen J., Theory of nonlocalized particles, 20: 13550 (LA-tr-66-7)
DAHLGREN, Dick Gilbert, Heterogeneous atomic reactor, 20: 14101
DAKOWSKI, M., Observation of fission events in mica sandwiches, 20: 13099
DAMM, Jozef Zbigniew, Formation and thermal bleaching of color centers in sodium chlorate crystals irradiated by γ rays, 20: 12900
DANCE, William E., Electron interactions with matter. I., 20: 13781 (NASA-CR-334)
DANFORTH, H. P., Cell ventilation monitor for fission products development lab. building, 20: 13006 (ORNL-TM-1384)
DANIEL, H., First-order theory of high-dispersion spectrometer with winding magnetic field, 20: 13087
DANIELS, J., Criticality detection and alarm systems—design principles, 20: 13115
DANIELS, J. T., Management and operational control of criticality, 20: 13020
DAO WONG DUC, Radiative decay of 1^+ mesons and unitary symmetry, 20: 13541 (JINR-P-2419)
D'ARDENNE, W. H., Epithermal neutron studies, 20: 14186 (MIT-2344-4, pp 145-8)
DARRAS, R., Safety of use of Mg alloy cladding in reactors cooled by CO_2, 20: 13199
DA SILVA FILHO, Joaquim G., Activation analysis of gold in ores samples, 20: 12769 (IEA-98)
DA SILVA FILHO, Joaquim G., Determination of Cl and Cu in high-purity water by radioactivation, 20: 12768 (IEA-97)
DASPET, Danielle, Modifications of density and mobility of majority carriers in n-type Ge bombarded by protons at 600 Mev, 20: 13977
DATTA, Bidyut Kumar, Universe admitting a four-parameter group of motions, 20: 13406
DAUER, Maxwell, Radioactive waste material incinerator, 20: 14212
DAUNT, J. C., Preferred rates in helium film transfer, 20: 13682
DAUNT, J. G., Thermal and electrical conductivities of Mo–Re alloys in

superconducting and normal states, 20: 13686
DAVID, Milan, Prestressed concrete pressure vessels of nuclear reactors, 20: 14030
DAVIDSON, J. P., Electric monopole transitions and β bands in even nuclei, 20: 13746 (AD-626681)
DAVIE, R. L., Pathfinder reactor building integrated leakage rate test, 20: 14143 (PAPP-6401)
DAVIES, A. R., SWAN—multi-group one-dimensional diffusion code for the IBM-7030, 20: 14056 (AWRE-O-99/65)
DAVIES, D. Roy, Repair mechanisms and variations in uv sensitivity within the cell cycle, 20: 12687
DAVIES, Peter John, Improvements in and relating to fueling arrangements for nuclear reactors, 20: 14036
DAVIES, V. De L., High-temperature low-cycle fatigue of extruded Al–Si–Mg–Ni alloy, 20: 13308
DAVIS, C., Surface and interface waves in plasma gaps, 20: 13945
DAVIS, F. C., Machine to remotely fill and compact nuclear fuel tubes by vibration, 20: 12945 (ORNL-TM-1383)
DAVTYAN, I. A., Systems Nd_2O_3–ZrO_2 rich in neodymium oxides, 20: 13283
DAVYDOV, A. S., Electric quadrupole transitions between rotary states with large spins in even nuclei, 20: 13801
DAWSON, Charles, TET2—thermal energy transport code, 20: 13698 (DTMB-1820)
DAYTON, Russell W., Prog. rpt. on civilian applications, 11/65, 20: 13171 (BMI-1751)
DE, Rajat, Uptake and transport of ^{59}Fe by intact leaves and enzymically isolated leaf cells of the bean plant, 20: 14220 (COO-888-48)
DE ABREU, Manoel Americo Nogueira, Gamma-gamma cascades in disintegration of compound nuclei formed by neutron capture, with aid of Hoogenboom circuit, 20: 13622 (IAE-96)
DE AGAZIO, E., Low-background β detector for solid sample assay, 20: 13102
DEAN, C., Reaction of radicals induced in E. coli by γ rays with cysteamine and with oxygen, 20: 12622
DEAN, John Robert, Improvements in or relating to retarding devices, 20: 14043
DE BACCI, M. A., Thermal and electrical conductivity of SAP, 20: 13306
DE BOUARD, X., Time-dependent interference effects in two-pion decays of neutral kaons, 20: 13496
DEBRUE, H., Study of UO_2–PuO_2–H_2O lattices by pulsed neutron techniques, 20: 14078
DE CAROLIS, M., Electrodeless conductivity meter for on-stream measurements, 20: 12927 (NP-15756)
DECONNINCK, G., Fast neutron non-multiplying assemblies, 20: 13719
DE DOMINICIS, Raffaella, Changes of small bowel mucosa in patients irradiated over the abdomen, 20: 12700
DE FELICE, Joseph, Analysis of maximum hypothetical accident, 20: 14181 (COO-1430-2)
DE FELICE, Joseph, Prog. rpt. on fast test reactor hypothetical meltdown accident, 10–12/65, 20: 14182 (COO-1430-3)
DE FELICE, Joseph, Shielding analysis for Fast Flux Test Facility, 20: 14180 (COO-1430-1)
DEIKE, S., Impulse generator for adjustment and testing of coincidence systems with crossover circuits, 20: 13044
DE KERVILER, Herve, Neutron dosimetry by means of proportional counters with tissue-equivalent walls, 20: 13060 (CEA-R-2891)
DEKNOCK, R., Eddy-current testing of thin-walled cladding tubes, 20: 14033
DEKNOCK, R., Ultrasonic water-gap measurements in MTR fuel elements, 20: 14195
DE LAFOND, Yann Gervais, Modifications of density and mobility of majority carriers in n-type Ge bombarded by protons at 600 Mev, 20: 13977
DE LASTEYRIE, Bernard, Fuel cycle optimization: marginal values of losses, 20: 13212 (CEA-R-2866)
DELLA ROSA, R. J., Comparative metabolism of Sr, Ca, and Cs in deer and sheep, 20: 12609
DE LOTTO, J., Pile-up effects in time measurements, 20: 13041
DELRIO, G., Prog. rpt. on selective absorption of Sr by Acantharia, annual, 2/63–3/64, 20: 12591 (EUR-2475.f)
DELRUE, R., Study of UO_2–PuO_2–H_2O lattices by pulsed neutron techniques, 20: 14078
DEMARMELS, P., Modified pulsed source techniques, 20: 14199
DE MEESTER, P., Eddy-current testing of thin-walled cladding tubes, 20: 14033
DE MEESTER, P., Fuel location, homogeneity, and amount in flat and tubular configurations, 20: 14198
DEMIN, A. G., New isotope ^{216}Ac, 20: 13779 (JINR-P-2465)
DENISIK, S. A., Solving nuclear geophysics problems by Monte Carlo method, 20: 12994
DENISOV, F. P., Distribution of knock-out nucleons as a function of nuclear volume, excitation energy, and nuclear recoil momentum distributions in cascade processes, 20: 13892
DENISOV, Yu. N., Magnetic β spectrometer with two-fold focusing at the angle $\pi\sqrt{2}$, 20: 13064 (JINR-E-2494)
DENIZ, V., Study of graphite and beryllium oxide using pulsed neutron source method, 20: 13727
DEONIGI, D. E., Calibration of high speed burnup code for nuclear fuel surveys, 20: 14118 (BNWL-183, Sect.IV)
DEONIGI, D. E., Comparison of fuel cycles for crossed-progeny fuels in conventional and novel configurations, 20: 14117 (BNWL-183, Sect.III)
DEONIGI, D. E., New fuel configuration to increase plutonium value, 20: 14102 (BNWL-183, Sect.II)
DE-SHALIT, A., Stripping via core excitation, 20: 13816
DESTRIBATS, Marie-Therese, Ultrasonic inspection following heat treatment of uranium alloys, 20: 13318
DE VOSS, H. G., N reactor analog simulation feasibility study, 20: 14167 (HW-70878)
DE WAEGH, Francois Albert, Controlling reactivity of a reactor, 20: 14099
DEXTER, Arthur H., Description of temperature monitor for large reactors. III., 20: 14025 (DP-944)
DICK, C. E., Scattering cross sections for 50- to 500-kev electrons, 20: 13757 (CONF-233(Vol.4), pp 595-608)
DIENST, W., Changes of mechanical properties of Cr–Ni steel and Ni alloys after neutron irradiation, 20: 13333
DIETRICH, F. S., Reaction $^{10}B(^3He,n)^{12}N$, 20: 13808
DIEV, L. V., Some questions of nuclear safety, 20: 14091
DI GIUGNO, G., Synchrotron radiation and observation of bunches in storage rings, 20: 13378
DI LAZZARO, M. A., Scattering of 662-Kev γ rays on bound electrons, 20: 13756 (CONF-233(Vol.4), pp 562-94)
DILLON, Ira G., Critical temperatures and densities of alkali metals, 20: 12815 (ANL-7025)
DIMITROV, O., Elimination of defects in Al irradiated by fast neutrons in liquid nitrogen, 20: 13338
DINGELDEIN, W. H., Effects of various grades of graphite electrodes in carrier distillation of impurities in U_3O_8, 20: 12771 (NLCO-967)
DINKLOH, H., Problem of combined radiologic and surgical injuries, 20: 12684
DIVON, B., Random pulse generator, 20: 13037
DIXON, Laurence Charles Ward, Improvements in reactor element cans, 20: 14107
DLOUHY, Z., Sorption properties of natural tuffs occurring in Lake Bracciano region (Rome), 20: 14209 (RT/PROT(65)29)
DMITRIEV, V. A., Fluctuations of energy fluxes of nuclear-active and electron-photon components in extensive air showers, 20: 13427
DODGE, Nathan B., Resonances and waves in one- and two-ion species plasmas subjected to intense magnetic fields, 20: 13920 (NP-15703, pp 1-51)
DODSWORTH, Barbara M., Nuclear-spin, hyperfine-structure, and magnetic-moment investigations on ^{61}Cu, ^{62}Cu, and ^{64}Cu, 20: 13855
DOEPKER, R. D., Gas-phase radiolysis of cyclobutane, 20: 12894
DOHERTY, G., KDF9 program EDIT 1, 20: 13344 (AEEW-M-604)
DOHERTY, G., SLP—single level Breit-Wigner cross-section generating program, 20: 13751 (AEEW-M-606)
DOI, Yoshihiko, Particle size of submicron W and WC powders for WC–Co alloy, 20: 13226
DOLAN, K. W., Performance studies of Phillips 56 AVP and XP 1020 photomultiplier tubes, 20: 13100
DOLAND, Michael F., Protection of lethally irradiated guinea pigs with leukocytes, 20: 12727
DOLGINOV, A. Z., Theory of multiple scattering. II., 20: 13968
DOLGOV, A. D., Charge-parity violating electromagnetic interaction, 20: 13478
DOLL, R., High-sensitivity helium magnetometer for use at low temperatures, 20: 13046
DOMMERGUES, P., Prog. rpt. on effects of mutagenic substances, annual, 1964, 20: 12632 (EUR-2546.f)
DOMOKOS, G., Theory of Fermi interactions, 20: 13566
DOMOTO, K., Measurement of internal friction of nuclear materials, 20: 13321
DONETS, E. D., Evaporation reactions of neutrons produced by irradiation of ^{238}U by accelerated ions ^{16}O, ^{19}F, and ^{22}Ne, 20: 13889
DONSKOI, A. V., Special characteristics of processes for growing high-melting crystals in high-frequency plasma burners, 20: 13189
DORSETT, Robert S., Determination of fluoride by pyrohydrolysis and automated colorimetry, 20: 12765 (DP-1004)
DOSCH, H. Guenter, Predictions for the electromagnetic formfactors of baryons from hybrid groups, 20: 13627
DOTTI, D., Pile-up effects in time measurements, 20: 13041
DOUGAL, Arwin A., Prog. rpt. on propagation and dispersion of hydromagnetic and ion cyclotron waves in plasmas immersed in magnetic fields, 1/15–7/14/65, 20: 13919 (NP-15703)
DOUGLASS, D. L., Electron fractographic study of alpha Pu, 20: 13293
D'OULTREMONT, P., Fast neutron non-multiplying assemblies, 20: 13719

DOUMERC, Jean, Fuel cycle optimization: marginal values of losses, 20: 13212 (CEA-R-2866)
DOWNS, B. W., Charge-asymmetry effects in Λ-N, 20: 13485
DRAGO, Russell S., Determination of donor sites in Lewis acid adducts of anisole and thioanisole, 20: 14226 (TID-21586)
DRAGO, Russell S., Pyridine complexes of nickel(II), 20: 14225 (TID-21577)
DRAGO, Russell S., Transition metal ion-ligand covalency from NMR contact shifts, 20: 12828 (TID-21587)
DRAGT, Alexander James, Some consequences of the unitarity condition for the analytic properties of scattering amplitudes, 20: 13631
DRAGULESCU, C., Complexes of carminic acid with ter- and tetravalent metals. I., 20: 12870
DRAKE, M. K., Compilation and evaluation of nuclear data available for major plutonium isotopes, 20: 13770 (GA-6576)
DRAKE, M. K., LEGCOEF-3—program to calculate Legendre expansion coefficients, 20: 13699 (GA-6690)
DRAXLER, K. D., Recent single-energy π-N phase-shift analyses and spin-flip dispersion relations, 20: 13492
DRECHSEL, Dieter, Excitation of giant multipole resonances in heavy nuclei by inelastic electron scattering, 20: 13832
DRESVIN, S. V., Special characteristics of processes for growing high-melting crystals in high-frequency plasma burners, 20: 13189
DRICKAMER, H. G., Effect of very high pressure on structure of some hcp metals and alloys, 20: 13316
DRICKAMER, H. G., Pressure and the electronic structure of solids, 20: 14221 (COO-1198-230)
DRISCOLL, M. J., Measurement of integral parameters in fuel rods, 20: 14103 (MIT-2344-4, pp 48-62)
DRISCOLL, M. J., Prog. rpt. on D_2O lattice project, annual, 9/65, 20: 14014 (MIT-2344-4)
DUBOVIK, V. M., Form factors and multipoles in electromagnetic interactions, 20: 13451 (JINR-P-2505)
DUBOVIKOV, M. S., Covariant description of polarized photons, 20: 13517
DUBOVIKOV, M. S., Determining isobar parity, 20: 13474
DUBOVSKII, B. G., Some questions of nuclear safety, 20: 14091
DUERR, H. P., Strange particles and the unsymmetrical vacuum, 20: 13554
DUERRSCHNABEL, W., System Nb–N. III. Outgassing in high vacuum, 20: 13202
DUERRSCHNABEL, W., System Nb–N. I., 20: 13302
DUERRSCHNABEL, W., System Nb–N. II., 20: 13303
DUFRESNE, Jacques, Heterogeneous reactor liquid moderated and cooled, 20: 14100
DULFER, G. H., Decay of ^{184}Ta, 20: 13767 (CONF-233(Vol.4), pp 730-42)
DUPOUY, Gaston, Coefficient of absorption of electrons accelerated by voltages between 100 and 1200 kv, 20: 13967
DUPOUY, Jean-Michel, Electron microscopic observation of stacking faults in twin crystals of Be, 20: 13978
DUPUY, Gerard, Support structure for vertical stack of solid moderator, 20: 14044
DUPUY, M., Diffusion in the Pu–U system, 20: 13313
DUQUESNE, M., Controllable pulse frequency and width system for pulsing and modulating fast-neutron core assemblies, 20: 13721
DURHAM, R. W., Neutron absorption cross section of gross fission products of ^{233}U, ^{235}U, and ^{239}Pu, 20: 13748 (AECL-2510)
DURST, R. A., Photopolarographic behavior of inorganic depolarizers, 20: 12798
DUTINA, D., Sodium mass transfer. XVII., 20: 12767 (GEAP-4833)
DYMLING, John-Fredrik, External counting of ^{85}Sr and ^{47}Ca in localized bone infections, 20: 12735
DYOS, M. W., Compilation and evaluation of nuclear data available for major plutonium isotopes, 20: 13770 (GA-6576)
DYSON, E. D., Advanced course in principles of radiation protection. I., 20: 12732 (AERE-R-5084)
DZHELEPOV, B. S., Decay of ^{138}Pr, 20: 13882
DZHELEPOV, V. P., Charged meson production in neutron-proton collisions at 600-Mev neutron energy, 20: 13453 (JINR-P-2511)

E

EAGER, R. L., Mean lifetime of free radical chains in ^{60}Co γ-irradiated chloral hydrate and bromal hydrate solutions, 20: 12887
ECCLES, S. F., Excited states in ^{6}Be, 20: 13845
EDGE, R. D., Excitation and disintegration of nuclei by low-energy electrons and x-rays, 20: 13782 (ORNL-P-1927)
EDIN, K. A., Scattering of a heavy charged particle against an electron, 20: 13484
EDWARDS, D. K., Simultaneous radiation, conduction, and convection in spectrally selective, emitting, and scattering porous bed, 20: 12969
EDWARDS, George C., Computers and simulators of atomic radiation, 20: 13021
EDWARDS, R. J., Kinetics of $\beta \rightarrow \alpha$ phase change in U–1 at.% Pt alloy, 20: 13307
EFIMENKO, L. N., Oxidation of lower W and Mo silicides, 20: 13198
EINFELD, K., Pulsed neutron reactivity measurements in the near-critical state, 20: 14082
EINFELD, Klaus, Method and apparatus for measuring fissionable isotope concentration, 20: 12814
EISENSTEIN, B., Depolarization of positive muons in solids, 20: 13498
EL-BAZ, Edgard, Formalism based on symmetric interaction in input and output methods for rearrangement collisions, 20: 13798
ELENGA, C. W., Generation of neutron pulses and modulated neutron fluxes with sealed-off neutron tubes, 20: 13720
ELIAS, D., Advanced radioisotope thermoelectric space power system, 20: 13158
ELLINGER, F. H., System plutonium–carbon–oxygen, 20: 13291
ELLIS, G. C., Deformation and fracture in single- and polycrystalline beryllium between 20 and 450°C, 20: 13240 (CONF-170, pp 102-20)
ELLIS, G. C., Structural application of beryllium in the U.K., 20: 13244 (CONF-170, pp 221-44)
EL-NADI, M., Two-nucleon stripping processes, 20: 13814
ELWYN, A. J., Measurements of neutron cross sections of Fe, Al, and CF_2 by a ratio method, 20: 13716
ELWYN, A. J., Polarization and differential cross sections in small-angle scattering of neutrons by uranium, 20: 13868
ELYUTIN, O. P., Physical and mechanical properties of Ti–Nb–Al alloys, 20: 13271
EMELEUS, K. G., Spectroscopic investigation of two-beam instability, 20: 13951
EMMERSON, J. McL., Unfolding apparatus function from data of low statistical accuracy, 20: 13038
ENGE, H. A., Nuclear-reaction studies in Ni isotopes, 20: 13858
ENGELBRECHT, C. A., Burnup calculations for thermal power reactors with sodium cooling, 20: 14144 (PEL-77)
ENGELMANN, Ch., Potentialities of γ spectrometry in nondestructive measurements on fuel elements, 20: 14158
ENGELMANN, F., Theory of quasistationary plasmas in contact with a wall, 20: 13912 (LGI-65/21 and App.)
ENGLE, G. B., Prog. rpt. on advanced graphite fuel systems, 8/15–11/14/65, 20: 13247 (GA-6831)
ENGLER, J., Search for a heavy electron by electron-proton coincidence measurements, 20: 13446 (DESY-65/9)
ENOMOTO, S., Interaction of subcritical assemblies, 20: 14090
EPSTEIN, I. S., Treatment of polycythemia vera and thrombocythemia with Myleran, 20: 12743
ERASLAN, Arsev H., MHD flows in closed regions with complete symmetry about an axis, 20: 13643
ERIKSSON, K. E., Scattering of a heavy charged particle against an electron, 20: 13484
ERMAKOV, V. A., Evaporation reactions of neutrons produced by irradiation of ^{238}U by accelerated ions ^{18}O, ^{19}F, and ^{22}Ne, 20: 13889
EROSHKINA, N. B., Coherent inelastic interactions between high-energy π⁻ mesons and heavy nuclei in photoemulsion, 20: 13893
ERSKINE, J. R., Energy levels in ^{49}Sc from ^{48}Ca(^{3}He,d) and other reactions, 20: 13854
EVANS, E. P., Effect of hypothermia on induction of chromosomal mutations by acute x irradiation of mice, 20: 12693
EYRE, B. L., Formation and behavior of point defect clusters in neutron-irradiated uranium carbide, 20: 13332
EYRING, Henry, Significant-structure theory applied to water and heavy water, 20: 12858
EZAKI, Haruo, Carcinostatic effect of extracts from human gastric cancer, 20: 12625

F

FABIANI, F., Technique of n-γ discrimination, 20: 13111
FABREGA, S., Hydrodynamic instabilities limiting the power of boiling water reactors, 20: 14027 (EURAEC-909)
FAHN, Abraham, Radiological method for determination of cambial activity, 20: 12614
FALK, Fred W., Computers and simulators of atomic radiation, 20: 13021
FALK, Raphael, Viability of heterozygotes for induced mutations in Drosophila. II., 20: 12661
FANO, G., Abstract approach to the many-body problem with infinite volume, 20: 13650
FARMELO, Donald R., Compact 1900°F resistance-wound combustion furnace for remote operation, 20: 12790
FARRIS, G. C., Factors influencing accumulation of fallout ^{137}Cs in Colorado mule deer, 20: 12984
FASSBENDER, J., Startup experiments on FRJ-2 reactor, 20: 14184 (JUL-236-RE)
FAYET, Jean-Claude, EPR study of x-irradiated $KClO_3$, 20: 12888
FEDERER, J. I., Diffusion studies of ^{95}Nb in polycrystalline UO_2 between 1100 and 2100°C, 20: 13289
FEDERMAN, P., Role of deformed states in ^{42}Ca spectrum, 20: 13839

FEDOROV, T. F., Ternary systems Hf–Nb–C, Zr–Nb–C, and Ti–Nb–C, 20: 13272
FEIST, I., Application of highly sensitive integrator in gas chromatography, 20: 12777 (UJV-1431/65)
FELBER, J.-P., Radioimmunologic method of determination of insulin, 20: 12754
FELBER, J.-P., Radioimmunologic method for determination of thyroid-stimulating hormone, 20: 12755
FELDMAN, M. H., Sample handling conveniences for activation analysis, 20: 12795
FELDMANN, Hans-Helmut, Measurement of phasing of an ion bunch in orbital path in isochronous cyclotron, 20: 13387
FENSTER, Stanley, Baryon structure and electromagnetic properties, 20: 13509
FERGUSON, C., Development of high-temperature molten lithium pump, 20: 12948
FERRERO, F., Device for detection of neutrons at energies up to 50 Mev, 20: 13081
FERRIS, L. M., Ball-milling of graphite-base reactor fuel, 20: 13218 (ORNL-TM-1412)
FEUERSTEIN, Horst, Two new isotopes of technetium, ^{106}Tc and ^{107}Tc, 20: 13780 (KFK-358)
FIALA, J., Effect of radiation on phagocytic activity of leukocytes in preserved blood, 20: 12698
FIEDELDEY, H., Burnup calculations for thermal power reactors with sodium cooling, 20: 14144 (PEL-77)
FIEDELDEY, H., Equivalent local potential and the Perey effect, 20: 13811
FILIPPI, A. M., Prog. rpt. on pilot production and evaluation of Ta alloy sheet, 4/25/64–10/30/65. III., 20: 13205 (AD-626622)
FILLIUS, R. Walker, Trapped protons of the inner radiation belt, 20: 13647
FINGER, M., Magnetic β spectrometer with two-fold focusing at the angle $\pi\sqrt{2}$, 20: 13064 (JINR-E-2494)
FIOCCHI, R., Effect of surface diffusion on separation efficiency in Breton-Massignon's theory, 20: 13160
FIRSOV, E. I., Determination of mixing parameter of M1 and E2 radiation for 0.341-Mev transition in ^{49}Ti, 20: 13803
FIRSOV, O. B., Ionization of atom colliding with an excited atom, 20: 13421
FISCHELL, R. E., Effect of artificial radiation belt on solar power systems, 20: 13131
FISHER, C. R., Forced convection condensing heat transfer for rubidium and cesium, 20: 13232 (AGN-8162)
FLEROV, G. N., Spontaneously fissionable isomer with T = 2.6 min in reactions of ^{233}U with ^{11}B and ^{10}B, 20: 13776 (JINR-P-2499)
FLETCHER, Frederick Owen, Nuclear fuel element with improved end cap assembly, 20: 14113
FLORMANN, Paul, Thickness measurement with γ beams, 20: 13151
FLYAGIN, V. B., Charged-meson production in neutron-proton collisions at 600-Mev neutron energy, 20: 13453 (JINR-P-2511)
FLYGARE, W. H., Vibration-rotation spectra of monomeric HCl, DCl, HBr, DBr, and HI in rare-gas lattices and N_2-doping experiments in rare-gas lattices, 20: 12857
FOCACCIA, G., Temperature coefficient measurements of the RC-1 Reactor (TRIGA), 20: 14188 (RT/FI(65)40)
FOEEX, Marc, High-temperature study of changes of the crystalline form of Nd_2O_3, 20: 13979
FORREST, A. P. M., Pituitary implantation for pituitary tumors, 20: 12753
FORREST, A. P. M., Plasma-growth-hormone levels in untreated acromegaly and after radioactive implants into pituitary, 20: 12748
FORST, H. C., Pulsed electron beam system, 20: 13034
FORSYTH, R. S., Nondestructive determination of burnup by means of ^{144}Pr 2.18-Mev γ activity, 20: 12812
FORTLAGE, R. J., Comparative inactivation of conidia, mycellia, and sclerotia of Botrytis cinerea by γ radiation, 20: 13149 (UCD-34P80-3, pp 176-89)
FOSSOUL, E., Study of UO_2–PuO_2–H_2O lattices by pulsed neutron techniques, 20: 14078
FOURE, Claude Desire, Improvements in or relating to nuclear reactors, 20: 14042
FRADKIN, E. S., Electrodynamics of particles with zero spin, 20: 13564
FRANCA, E. Penna, Survey of radioactive content of food grown on Brazilian areas of high natural radioactivity, 20: 12988
FRANCHI, M., Automatic control equipment of Dragon, 20: 14154
FRANCIS, W. C., Nondestructive testing in test-reactor operation at NRTS, 20: 14197
FRANCO-FERREIRA, E. A., BONUS superheater fuel assemblies—failure and method of correction, 20: 14141 (ORNL-3910)
FRANK, I. M., Pulsed research reactor and feasibility of pulsed reactor application in neutron spectroscopy, 20: 14191 (BNL-tr-60)
FRANK, I. M., Transition radiation of charged relativistic particle in optical frequency range, 20: 13788 (ORNL-tr-1062)
FREDERICKSON, A. Robb, Prog. rpt. on radiation damage in semiconductor materials, 5–7/65, 20: 13128 (NP-15835(Suppl.))
FREEDMAN, A. H., High-remelt-temperature brazing of Ta using diffusion sink concept, 20: 13224
FREEDMAN, M. S., Response of NaI, anthracene, and plastic scintillators to electrons, 20: 12899
FREEMANTLE, R. G., Reactions of neutrons with ^{235}U: 20: 13749 (AEEW-M-502)
FRENCH, Norman R., Radiation and animal populations: problems, progress, and projections, 20: 12584
FRENKEL, A., Renormalizable vector boson theory of weak interactions, 20: 13568
FRERICHS, R., Tunnel-effect measurements on superimposed layers of lead and aluminum, 20: 13687
FRIDDLE, R. J., Effects of high pressure and temperature on microstructure of Pu, 20: 13292
FRIEDMAN, K. A., Comparison of effective ranges of n-p and p-p interactions, 20: 13512
FRIEDRICH, Otto M. Jr., Plasma sheath dynamics, 20: 13922 (NP-15703, pp 64-81)
FRIES, R. J., Nuclear reactor magnetohydrodynamic power generation, 20: 14132 (LA-3368)
FRIES, R. Jay, Ultrahigh vacuum thermobalance for Langmuir vaporization studies, 20: 13029 (LA-3423)
FRITSCH, C. A., Radiative heat-transfer through an absorbing boundary layer, 20: 12966
FROEHLICH, F., Influence of irradiation with small x-ray doses on bleaching of KCl crystals with F centers, 20: 14000
FROEHLICH, H., Geometrical interpretation of electrodynamics, 20: 13662
FROHBERG, Jobst, Theory of correlated crystals, 20: 14001
FROIS, C., Elimination of defects in Al irradiated by fast neutrons in liquid nitrogen, 20: 13338
FROMAGEOT, P., Origin of urinary excretion of taurine by the rat irradiated with ^{60}Co. I., 20: 12648
FRONDEL, C., Strontium–rubidium age of an iron meteorite, 20: 12992
FRONIA, J., Pulse generator (μsec) with 10-Mw pulse power at 200-kv pulse voltage, 20: 13035
FRONTEAU, J., Particle optics inside an absorber, 20: 13350
FUJII, Akihiko, Possible existence of wrong G-parity interaction in muon capture, 20: 13505
FUJIMOTO, Yoichi, Elementary particle structures and meson-nucleon backward scatterings, 20: 13510
FUJIMOTO, Yoichi, High-energy nuclear interactions and structure of elementary particles, 20: 13514
FUJIZAKI, Tetsuo, Device for irradiating vertically, 20: 12957
FUKUDA, Nobuyuki, Stability and instability of planewave Hartree-Fock solutions and the helical spin arrangement, 20: 13423
FULTON, T., Finite and disconnected subgroups and elementary particle symmetries, 20: 13570
FULTYN, R. V., Radiation measurements of effluent from Kiwi B4D-202 and B4E-301 reactors, 20: 14172 (LA-3397)
FUNAOKA, Hiroaki, Carcinostatic effect of extracts from human gastric cancer, 20: 12625
FUNG, S-Y., Existence of spions from K^+ decay, 20: 13497
FUNG, Sun-yiu Samuel, Analysis of Y_1^* production by 1.15-Bev/c K^- beam, 20: 13518
FURMAN, Daniel W., Nuclear blast and overpressure detection and recording system, 20: 12995
FUSS, Fred N., Preanodization of tantalum electrodes, 20: 13204
FUSTER, S., Calibration of control rods in natural uranium–graphite lattices, 20: 14163
FUTAMI, Yasuhiko, Emission of light fragments from heavy nuclei in high-energy nuclear reactions, 20: 13880

G

GABBE, E. E., Hamburg 4π large-volume radioactivity detector with liquid organic scintillator. II., 20: 13079
GABOR, J. D., Engineering development of fluid-bed fluoride volatility processes. III., 20: 12923 (ANL-6898)
GAGNAIRE, Janine, Vegetative rhythms of woody species, 20: 12590 (CEA-R-2825)
GAIGALAS, A., Gamma rays from decay of 35-day ^{95}Nb, 20: 13859
GAIGALAS, A., Measurement of energies of γ rays from decay of ^{66}Ga, 20: 13818
GAINOTTI, A., Methods of measurement of low intermetallic diffusion coefficients, 20: 13270
GAITANIS, N., Modification of RCL 512-channel analyzer for time-of-flight analysis, 20: 13097
GALAKTIONOV, Yu. V., Investigation of Bev-neutron registration efficiency by scintillation counters, 20: 13109
GALEJS, J., Prog. rpt. on plasma-covered slot antennas, 11/62–9/65, 20: 13022 (AFCRL-65-859)

GALKIN, Yu. M., Systems BaO–ZrO_2 rich in BaO, 20: 13282
GALLOWAY, K. F., Use of Fialho method for calculating phase-space volumes, 20: 13481
GALSTER, S., Search for a heavy electron by electron-proton coincidence measurements, 20: 13446 (DESY-65/9)
GANSSAUGE, E., Search for a heavy electron by electron-proton coincidence measurements, 20: 13446 (DESY-65/9)
GAPONOV, A. V., Induced synchrotron radiation of electrons in cavity resonators, 20: 13472
GAPONOV, Yu. V., Allowed nuclear β transitions in theory of finite Fermi systems, 20: 13887
GARATTINI, S., Prog. rpt. on selective protection of damages induced by x irradiation and radiomimetic drugs, 11/64–1/65, 20: 12717 (NP-15666)
GARATTINI, S., Prog. rpt. on selective protection of damages induced by x irradiation and radiomimetic drugs, annual, 9/15/64, 20: 12718 (NP-15667)
GARATTINI, S., Prog. rpt. on selective protection of damages induced by x irradiation and radiomimetic drugs, final, 9/65, 20: 12719 (NP-15668)
GARAULT, Yves, Study of class of guided electromagnetic waves: the EH waves, 20: 13370
GARCIA, Gilbert, Improvements in installations for spectrophotometric analysis of radioactive solutions, 20: 12813
GARCIA-CASTANER, B., Measurement of M_2 in organic liquids, 20: 13730
GARELIS, E., Survey of pulsed neutron source methods for multiplying media, 20: 14075
GARNETT, J. L., Wilzbach tritiation studies. II., 20: 12878
GARRONI, A., Automatic control equipment of Dragon, 20: 14154
GAT, Uri, MOSEL: General study on temperatures, power density, and heat transfer, 20: 14128 (JUL-296-RG)
GATTI, E., Synthesis of an optimum filter for timing scintillation pulses, 20: 13104
GAUSSENS, J., Economic prospects of nuclear energy, 20: 14151
GAUSSENS, Jacques, Fuel cycle optimization: marginal values of losses, 20: 13212 (CEA-R-2866)
GAUTHORN, Maurice, Mounting armoring on ends of a reactor fuel element can, 20: 14111
GAUTSCH, O., Controlled expansion of UC pellets by surface oxidation in cladding, 20: 13188
GAVIN, P. H., Kinetic and steady-state measurements of variable-pitch enriched uranium, light water lattices, 20: 14079
GAYLEY, R. I., Field enhancement in superconducting tubes, 20: 13678
GEBAUHR, W., Separation process for use in activation analysis. I., 20: 12803
GEBHARDT, E., System Nb–N. III. Outgassing in high vacuum, 20: 13202
GEBHARDT, E., System Nb–N. I., 20: 13302
GEBHARDT, E., System Nb–N. II., 20: 13303
GEERTS, S. J., Conference on genetics, The Hague, 9/63. II., 20: 12564
GEERTS, S. J., Conference on genetics, The Hague, 9/63. III., 20: 12565
GELLER, Richard, Extension of Child-Langmuir law to beam of particles having initial velocity, 20: 13902 (CEA-R-2898)
GELLES, S. H., Air Force-sponsored Be research and development program, 20: 13174 (CONF-170, pp 184-213)
GEMMILL, Wayne J., Process for making high-purity radioactive ^{131}I, 20: 12922
GENKIN, Ye. E., X-ray emission spectra of Nb and Zr and character of their interatomic bond, 20: 12846
GENUNCHE, Ana, Bibliography of ^{14}C measurements. II., 20: 12770 (IFA/CO/28)
GEORGE, E., Experimental system for thermoluminescent dosimetry, 20: 13059 (AEEW-R-411)
GEORGE, W. D., Radiation calibration of a 20-Mev linac, 20: 13361 (EGG-1183-2066)
GEORGIADOU, E., Effect of chemical sensitizers on radiation resistance of fruit-spoilage fungi, 20: 13137 (NP-15360)
GEORGII, Axel, General pathogenesis of leukemia, 20: 12707
GEORGOPOULOS, S. G., Effect of chemical sensitizers on radiation resistance of fruit-spoilage fungi, 20: 13137 (NP-15360)
GERARD, Victor Jean, Pneumatic drive for reactor control rods, 20: 14047
GERASIMOV, S. B., Electromagnetic properties of baryons and mesons in nonrelativistic quark model, 20: 13544 (JINR-P-2509)
GERBIER, R., Controllable pulse frequency and width system for pulsing and modulating fast-neutron core assemblies, 20: 13721
GERMANYUK, V. N., Electric conductivity in stream of argon containing potassium oxide, 20: 13954
GERONTOPULOS, P. Th., Rapid separation of ^{231}Pa from its daughters, 20: 12937
GERVAIS, J.-L., Two-channel generation of the ρ meson by one- and two-particle exchange forces, 20: 13483
GESSEL, Stanley P., Mineral cycling in a Douglas fir forest stand, 20: 12574
GETTY, W. D., Plasma electronics, 20: 13925 (TID-22419, pp 99-147)
GHOOS, Y. F., Comparison of ^{51}Cr annealing kinetics in neutron-irradiated and in ^{51}Cr(III)-doped potassium chromate, 20: 12904
GIAMBASTIANI, Romolo, Determination of Cl and Cu in high-purity water by radioactivation, 20: 12768 (IEA-97)
GIANZERO, Stanley C. Jr., Radiation by uniformly rotating line charge in a plasma, 20: 13958
GIBB, T. R. P. Jr., Dissociation pressure of system Yb–YbH_2, 20: 12829 (TID-22502)
GIBSON, G. W., Nondestructive testing in test-reactor operation at NRTS, 20: 14197
GIESSING, D. F., Administrative aspects of criticality controls, 20: 14092
GIFFON, M., Proof of completeness of solutions of the Schroedinger equation in the λ plane, 20: 13653
GILBERT, R. W., Tempered structures of Zr–2.5 wt.% Nb alloy, 20: 13304
GILCHRIST, E. J., Cryogenic irradiation of resistance temperature transducers for NERVA, 20: 13127 (CONF-651101-61)
GILLESPIE, D. E., Laser-stimulated nucleation in a bubble chamber, 20: 13084
GILLOT, J., Prog. rpt. on effects of mutagenic substances, annual, 1964, 20: 12632 (EUR-2546.f)
GILWOOD, Martin E., Radioactive fallout treatment kit, 20: 12942
GINZBURG, V. L., Relativistic oscillator models of elementary particles, 20: 13626
GLADYSHEVSKII, E. I., Ternary systems Hf–Nb–C, Zr–Nb–C, and Ti–Nb–C, 20: 13272
GLASS, Werner, Advanced study of milk decontamination by electrodialysis, 20: 12997 (AD-626210)
GLAZOV, V. V., Temperature dependence of electroconductivity of titanium and zirconium suboxides, 20: 12850
GLAZOVA, V. V., Nature of chemical bond in titanium and zirconium suboxides, 20: 12848
GLOERSEN, Per, Plasma accelerator, 20: 13963
GLUCK, Gilbert, Isotopic displacement of tungsten, osmium, and neodymium, 20: 13418
GLUSHKOVA, V. B., Systems Nd_2O_3–ZrO_2 rich in neodymium oxides, 20: 13283
GNEDIN, Yu. N., Theory of multiple scattering. II., 20: 13968
GODBEE, Herschel W., Thermal conductivities of MgO, Al_2O_3, and ZrO_2 powders to 850°C. I., 20: 12854
GODBEE, Herschel W., Thermal conductivities of MgO, Al_2O_3, and ZrO_2 powders to 850°C. II., 20: 12855
GODER, G., Histological changes in irradiated malignant intraocular tumors, 20: 12740
GOEBEL, D. M., Return coefficient measurements, 20: 14070 (MIT-2344-4, pp 115-34)
GOEDDEL, W. V., Prog. rpt. on advanced graphite fuel systems, 8/15–11/14/65, 20: 13247 (GA-6831)
GOLDBERG, R., Existence of spions from K^+ decay, 20: 13497
GOLDBLITH, Samuel A., Effect of ionizing radiation on flavor of whole-egg magma, 20: 12660
GOLDEMBERG, J., Electrodisintegration of the deuteron at low momentum transfer: magnetic transitions, 20: 13490
GOL'DENBERG, A. L., Induced synchrotron radiation of electrons in cavity resonators, 20: 13472
GOLDFARB, L. J. B., Neutron transfer in heavy ion reactions, 20: 13830
GOLDHABER, G., Reaction $K^+ + p \rightarrow K + N + \pi$ between 0.86 and 1.58 Bev/c, 20: 13462 (UCRL-16370)
GOLDMAN, Marvin, Comparative metabolism of Sr, Ca, and Cs in deer and sheep, 20: 12609
GOLDONI, Gino, Thermal conductivity in rotating cylinder exposed to radiation, 20: 13349
GOLDSTEIN, N., Dose rate and spectral measurements from pulsed x-ray generators, 20: 13057 (AD-627567)
GOLDZAHL, L., Particle optics inside an absorber, 20: 13350
GOLLEY, Frank B., Effect of acute γ radiation on opossium, gray fox, raccoon, and bobcat, 20: 12667
GOMBAS, P., Method of calculating atomic one-electron eigenfunctions, 20: 13416
GONCHAROV, I. N., An85-kG superconducting magnet made of Nb-75% Zr, 20: 13667 (JINR-P-2533)
GOOD, P. D., Quality control inspection and testing of fuel materials for Dragon, 20: 14159
GOODALE, Edmund E., Device for measuring biological effect of radiation, 20: 13121
GOODFELLOW, H., Prompt neutron decay constant of VERA reactor, 20: 14089
GOOSEY, Malcolm H., Description of temperature monitor for large reactors. III., 20: 14025 (DP-944)
GOPAL, N. G. S., Control of radiochemical purity of organic radiopharmaceuticals labeled with ^{131}I, 20: 12918
GOPAL-AYENGAR, A. R., Radioactivity of plants from high radiation areas of Kerala coast and adjoining regions. II., 20: 12987
GORDEEV, A. V., Oscillations and instability of a weakly turbulent

plasma, 20: 13931 (NP-tr-1348)
GORDON, E. Kent, Refinement of crystal structure of Li_2BeF_4, 20: 12834
GORDON, L. J., Use of high-temperature process heat as part of total-energy source, 20: 14165 (ANL-7035)
GOROWITZ, Bernard, Plasma accelerator, 20: 13963
GOSNELL, J., Two-region lattices, 20: 14068 (MIT-2344-4, pp 89-100)
GOSSET, J., Potentialities of γ spectrometry in nondestructive measurements on fuel elements, 20: 14158
GOSSETT, C. R., Triple correlations in $^{56}Fe(p,\gamma\gamma)^{57}Co$ reaction, 20: 13857
GOTO, Tetsuo, Deformable sphere model of elementary particles and origin of internal symmetries, 20: 13606
GOTTLIEB, M., Ultrasonic investigation of flux penetration into superconducting niobium, 20: 13684
GOUDIE, R. B., Clinical significance of complement-fixation test in thyrotoxicosis, 20: 12744
GOULD, Harvey Allen, Use of Bethe-Salpeter equation in transport theory and derivation of convergent kinetic equation for classical plasma, 20: 13927 (UCRL-16557)
GOVAERTS, P., Pulsed and modulated experiments on fast multiplying media, 20: 13723
GOVAERTS, P., Theory of pulsed and modulated experiments on fast neutron multiplying media, 20: 14088
GOYA, H. A., Quantitative radiochemical determination of ^{63}Ni in seawater, 20: 12779 (USNRDL-TR-924)
GOZANI, T., Modified pulsed source techniques, 20: 14199
GRABOVSKI, Ya., Inelastic scattering of complex nuclei accompanied by excitation of collective levels, 20: 13890
GRABOVSKII, Ya., Inelastic scattering of complex nuclei with large charges, 20: 13794
GRACE, M. A., Low-lying states of ^{40}Ca, 20: 13821
GRACE, M. A., Low-lying excited states in ^{32}S, 20: 13823
GRAEBNER, H., Bone-marrow transfusion in the whole-body irradiated, tumor-bearing rat, 20: 12651
GRAEFF, P., Acceleration of plasma through magnetic bottle according to free-particle model, 20: 13911 (JUL-336-PP)
GRAF, D. L., Vaterite-type ABO_3 rare-earth borates, 20: 12837
GRAF, I., MOSEL: comparison of spectra and spectrally determined parameters of a two-component salt melt, 20: 14127 (JUL-291-RG)
GRAF, I., MOSEL: comparison of spectra and spectrally determined magnitudes of a two-component salt melt ($NaF-BeF_2$), 20: 14129 (JUL-315-RG)
GRAF, P., High-sensitivity helium magnetometer for use at low temperatures, 20: 13046
GRANZER, F., Ultra-thin sections of CsI single crystals, 20: 13985
GRARD, R., Low-frequency impedance characteristics of Langmuir probe in a plasma, 20: 13940
GRAU, P., Influence of irradiation with small x-ray doses on bleaching of KCl crystals with F centers, 20: 14000
GRAUVOGEL, M. A., Improvements made to control drive winches for EDF-1 control rods, 20: 14153
GRAY, I. L., Advanced radioisotope thermoelectric space power system, 20: 13158
GRAY, K. G., Clinical significance of complement-fixation test in thyrotoxicosis, 20: 12744
GRAY, W. S., Reaction $^{90}Zr(p,p')$ at 18.8 Mev and the shell model, 20: 13866
GREATOREX, John L., Advanced study of milk decontamination by electrodialysis, 20: 12997 (AD-626210)
GREBTSEV, N. V., Recrystallization of high-melting metals in welding and soldering, 20: 13267 (AD-624909)
GRECHI, G., Changes of small bowel mucosa in patients irradiated over the abdomen, 20: 12700
GRECHIKHIN, L. I., Use of emission spectra of the copper atom for diagnostics of a plasma, 20: 13953
GREEN, H. S., Diffusion and conductivity of plasmas in strong external fields, 20: 13938
GREEN, J. L., Absorption spectrum of Cf^{+3} and crystallography of CF_2O_3 and $CfCl_3$, 20: 12831 (UCRL-16516)
GREENBERG, R. A., Determination of equivalence between sterilization process and commercial thermal process for cured meats, 20: 13134 (AD-625252)
GREENE, M. W., Production of Y-87 and a Sr-87m generator, 20: 12917
GREENHOW, W. A., Cryogenic irradiation of resistance temperature transducers for NERVA, 20: 13127 (CONF-651101-61)
GREENWOOD, F. C., Pituitary implantation for pituitary tumors, 20: 12753
GREENWOOD, F. C., Plasma-growth-hormone levels in untreated acromegaly and after radioactive implants into pituitary, 20: 12748
GREENWOOD, Michael, Quiescent center of primary root of Glycine max, 20: 14215 (BNL-8643)
GREESON, R. L., Electrolytic swab etching for metallography of Pu, 20: 13187
GREGOIRE, Michel, Study of high-frequency instabilities on cold cathode reflex discharge, 20: 13901 (CEA-R-2822)
GREGOIRE, Pierre, Reaction U + C → UC. II., 20: 13223
GREGOR, O., Macroautoradiography with radiophosphorus in stomach cancer, 20: 12742
GRIFFITH, K. M., Growth status of children exposed to fallout radiation on Marshall Islands, 20: 13011
GRIFFITHS, D. J., A model exhibiting type II superconductivity, 20: 13677
GRIGOR'EV, D. P., Induced synchrotron radiation of electrons in cavity resonators, 20: 13472
GRIGOR'EVA, L. I., Resonant heating of plasma by high-frequency field, 20: 13946
GRIM, Alfred C., Effect of ionizing radiation on flavor of whole-egg magma, 20: 12660
GRISSOM, J. T., Neodymium-141 and its production in the (n,2n) reaction, 20: 13864
GROMOV, K. Ya., Decay of ^{138}Pr, 20: 13882
GROMOV, K. Ya., Magnetic β spectrometer with two-fold focusing at the angle $\pi\sqrt{2}$, 20: 13064 (JINR-E-2494)
GROSH, Joe, Significant-structure theory applied to water and heavy water, 20: 12858
GROSH, R. J., Radiative heat-transfer through an absorbing boundary layer, 20: 12966
GROSS, E. E., Polarized-proton scattering facility at the Oak Ridge Isochronous Cyclotron, 20: 13375
GROSSE, Aristid V., Densities, volume, expansion, compressibility and pressure coefficients and derived functions of metallic Hg for its entire liquid range, 20: 12825 (NYO-2082-1)
GRUEMM, H., Demand for nuclear fuels and costs of different reactor types in Germany, 20: 14130 (KFK-366)
GRYNBERG, M., $SU_2 \otimes SU_3$ content of the SU_6 representations, 20: 13580
GSCHAIDER, Siegfried, Modification of electron structure of gold by α irradiation and subsequent recovery, 20: 13339
GUAITANI, A., Prog. rpt. on selective protection of damages induced by x irradiation and radiomimetic drugs, 11/64–1/65, 20: 12717 (NP-15666)
GUAITANI, A., Prog. rpt. on selective protection of damages induced by x irradiation and radiomimetic drugs, annual, 9/15/64, 20: 12718 (NP-15667)
GUAITANI, A., Prog. rpt. on selective protection of damages induced by x irradiation and radiomimetic drugs, final, 9/65, 20: 12719 (NP-15668)
GUDIMA, K. K., Estimation of interaction cross section for unstable nuclei, 20: 13449 (JINR-P-2433)
GUENTHER, Ch., Method to derive electric quadrupole moments of 2+ rotational states of rare earth nuclei, 20: 13764 (CONF-233(Vol.4), pp 720-2)
GUENTHER, Karl-Georg, Mass spectrometer with particular ion source for analysis of solid bodies, 20: 13053
GUERON, H., Measurement of diffusion coefficient in an anisotropic medium, 20: 13705 (MIT-2344-4, pp 135-44)
GUERSEY, F., Lorentz covariant definition of the U_6 group for free particle states, 20: 13529 (BNL-8767)
GUETLICH, Ph., Rate of heterogeneous isotopic exchange on surfaces of ionic crystals, 20: 12869
GUGGENBERGER, Lloyd Joseph, Structures of the ethyl Grignard reagent in diethyl ether and a troponoid photo-oxidation product, 20: 12819
GUILLAUMONT, Robert, Physical chemistry of protactinium, 20: 12832 (UCRL-Trans-1244(L))
GULYAMOV, U. G., Coherent inelastic interactions between high-energy π^- mesons and heavy nuclei in photoemulsion, 20: 13893
GUNN, Samuel A., Factors in uptake, physiology, and retention of ^{65}Zn in male reproductive system of the rat, 20: 12601 (TID-22526)
GUPTA, D., Demand for nuclear fuels and costs of different reactor types in Germany, 20: 14130 (KFK-366)
GUPTA, S. K., Tissue-air ratios and scatter functions for large field sizes for ^{60}Co γ radiation, 20: 13009
GURIN, V. N., Some questions of nuclear safety, 20: 14091
GURNEY, J., Bibliography on space and accelerator shielding, 20: 13965 (ORNL-RSIC-11)
GUSH, H. P., Induced infrared absorption spectrum of solid deuterium and solid hydrogen deuteride, 20: 13419
GUS'KOV, B. N., Elastic 180° scattering of π^+ mesons by protons at high energies, 20: 13471
GUSO, R., Measurement of energies of γ rays from decay of ^{66}Ga, 20: 13818
GUTAY, L. J., Final-state enhancement at 1920 Mev in π^-p inelastic scattering, 20: 13454 (UCRL-14100-T(Rev.1))
GUTH, E., Excitation and disintegration of nuclei by low-energy electrons and x-rays, 20: 13782 (ORNL-P-1927)
GYFTOPOULOS, Elias P., Measurement of characteristic kernels of a class of nonlinear systems, 20: 13023 (CONF-660206-1)
GYORGYI, G., Symplectic-invariant many-fermion problems, 20: 13651

H

HAAS, P. A., Prog. rpt. on chemical separations processes, 4–6/65,

20: 12928 (ORNL-3868)
HAAS, R., Cross-correlation method for study of neutron pulse transfer function, 20: 13724
HAAS, R., Pulsed fast reactor as source for pulsed neutron experiments, 20: 14096
HAASE, G., Ultra-thin sections of CsI single crystals, 20: 13985
HABEL, Dan William, Surgical complications in irradiated patients, 20: 12646
HABERER, K., Improvement in direct measurement of β activity in liquid scintillation counters, 20: 13080
HABIBULLAH, A. K. M., 500-Curie irradiation facility, 20: 12911 (AECD/HP/3)
HADDRELL, V. J., Diffusion creep deformation in magnesium reactor component, 20: 13309
HADLEY, Wayne B., Luminescence processes generated by ionizing radiation in KI and KI:Tl, 20: 12891
HAEFELE, W., Demand for nuclear fuels and costs of different reactor types in Germany, 20: 14130 (KFK-366)
HAENLEIN, Walter, Mass spectrometer with particular ion source for analysis of solid bodies, 20: 13053
HAGEDORN, R., Statistical thermodynamics of strong interactions at high energies, 20: 13587
HAGEMANN, G., Change of relative linear energy transfer with the penetration depth of 14-Mev electrons in Plexiglass, 20: 13969
HAGER, R., Possibility of parity admixture in the 57.6-kev transition in Hf-180m, 20: 13841
HAHN, Yukap, Projection operators in the unified reaction theory, 20: 13850
HAIMSON, J., Electron bunching in traveling-wave linear accelerators, 20: 13374
HAISSINSKI, J., Synchrotron radiation and observation of bunches in storage rings, 20: 13378
HAKAMADA, Koichi, New products of irradiated polyethylene, 20: 12905
HALIK, J., Toxicity of modern radioactive luminous compounds, 20: 12603 (JPRS-33958, pp 1-7)
HALL, D., Crystal structure of dicesium tetrachlorodioxouranium (VI), 20: 12835
HALL, Richard B., Method and apparatus for accelerating ionized gas, 20: 12952
HALL, Robert W., Ultrahigh-vacuum creep behavior of Nb and Ta alloys at 2000 and 2200°F, 20: 13256 (NASA-TN-D-3222)
HALPERN, Bernard, Preservation by phytohemagglutinin of medullo-restoring and hematopoietic properties of medullary cells, 20: 12726
HAMAL, Karel, Characteristics of a high-frequency electron linear accelerator, 20: 13373
HAMBERGER, Sydney Maxwell, Improvements in or relating to methods of heating ions in a plasma, 20: 13962
HAMILTON, C. B., Bismuth–zirconium alloy system, 20: 13252 (IS-1269)
HAMILTON, J. H., L, M, and N photoelectric cross section measurements in uranium for $h\nu = 122$ kev, 20: 13755 (CONF-233(Vol.4), pp 548-60)
HAMMER, P., Pulsed and modulated experiments on fast multiplying media, 20: 13723
HAMMER, P., Theory of pulsed and modulated experiments on fast neutron multiplying media, 20: 14088
HAMRIC, J. P., Spatial kinetics in large reactors, 20: 14071 (RL-SA-45A and Suppl.)
HAN, Won-lung, Rare earth oxides–BeO system, 20: 13268 (JPRS-33605, pp 64-7)
HANDWERK, J. H., Fabrication and evaluation of thoria–urania fuel material, 20: 13207 (ANL-6893)
HANIK, L., Macroautoradiography with radiophosphorus in stomach cancer, 20: 12742
HANNAH-ALAVA, Aloha, Premeiotic stages of spermatogenesis, 20: 14224 (TID-21562)
HANNAH-ALAVA, Aloha, Rates of visible mutations as related to maturity of male germ cells of Drosophila, 20: 12636 (TID-21459)
HANNUM, W. H., DPC: two-dimensional data preparation code, 20: 14064 (LA-3427)
HANSEN, Ole, Reaction $^{46}Ca(d,p)^{47}Ca$ at 7 Mev, 20: 13853
HANSON, W. C., Seasonal cycle of ^{137}Cs in some Alaskan natives and animals, 20: 12983
HANSTOCK, R. F., Nondestructive examination of heat-affected zone of welded Zr–Nb alloy, 20: 13320
HAQ, A. M. Sirajul, 500-Curie irradiation facility, 20: 12911 (AECD/HP/3)
HARA, Osamu, Deformable sphere model of elementary particles and origin of internal symmetries, 20: 13606
HARAM, Sevrin Andrew, Neutron irradiation apparatus, 20: 12954
HARARI, H., Infinite ladders and algebra of integrated current components, 20: 13548 (SLAC-58)
HARDY, Harriet L., Beryllium poisoning—lessons in control of man-made disease, 20: 13016
HARGITAI, Cs., Gauge-invariant method in theory of interacting Bose systems, 20: 13562
HARGOE, Bernt Torsten Allen, Heterogeneous atomic reactor, 20: 14101
HARGREAVES, F., Long-term compatibility of thermionic converter materials with cesium, 20: 13203
HARKER, Y. D., Compilation of resolutions and intensities of slow neutron, inelastic scattering, time-of-flight instruments, 20: 13061 (IDO-17134)
HARMAN, D. G., BONUS superheater fuel assemblies—failure and method of correction, 20: 14141 (ORNL-3910)
HARRINGTON, David E., Determination of fluoride by pyrohydrolysis and automated colorimetry, 20: 12765 (DP-1004)
HARRINGTON, E. L. E., Correlator for investigating random fluctuations in power reactors, 20: 14156
HARRINGTON III, J., Use of neutron absorbers in determination of lattice parameters, 20: 14185 (MIT-2344-4, pp 70-9)
HARRIS, Franklin C., Resonances and waves in one- and two-ion species plasmas subjected to intense magnetic fields, 20: 13920 (NP-15703, pp 1-51)
HARRIS, Franklin C., Shock ionization for ion-cyclotron wave experiment, 20: 13921 (NP-15703, pp 52-63)
HARRIS, P. S., Plutonium dispersal by low-order detonation of atomic weapons, 20: 13004 (LA-1981(Rev.))
HARRIS-LOWE, R. F., Preferred rates in helium film transfer, 20: 13682
HARRISON, R. G., Enzymic processes and vascular changes in skin radiation reaction, 20: 12623
HARRISON, R. W., Prog. rpt. on studies of alkali metal corrosion on materials for advanced space power systems, 3–6/65, 20: 13191 (NASA-CR-54476)
HARRISON, R. W., Prog. rpt. on refractory alloy corrosion loop program, 7/15–10/15/65, 20: 13193 (NASA-CR-54845)
HARROD, D. L., Prog. rpt. on pilot production and evaluation of Ta alloy sheet, 4/25/64–10/30/65. III., 20: 13205 (AD-626622)
HART, James L., Extraction of metal values from acid solutions, 20: 12941
HARTWIG, G., Search for a heavy electron by electron-proton coincidence measurements, 20: 13446 (DESY-65/9)
HARVEY, G. G., Prog. rpt. on electronics, 10/15/65, 20: 14227 (TID-22419)
HARVEY, R. A., N reactor analog simulation feasibility study, 20: 14167 (HW-70878)
HASEGAWA, Isao, Fabrication of UO_2 fuel element by vibratory compaction, 20: 13225
HASEGAWA, Toru, Swimming-pool-type reactor, 20: 14204
HASHIMOTO, Kenjiro, Apparatus for moving radiation source, 20: 12956
HASIGUTI, R. R., Measurement of internal friction of nuclear materials, 20: 13321
HATANAKA, T., Thermal neutron diffusion length measurements in poisoned organic material, 20: 13718
HATTULA, J., Gamma-spectrometer systems employing anti-Compton annulus, 20: 13098
HAUCK, H., Changes of mechanical properties of Cr–Ni steel and Ni alloys after neutron irradiation, 20: 13333
HAUS, H. A., Plasma electronics, 20: 13925 (TID-22419, pp 99-147)
HAYAKAWA, Satio, Atomism and cosmology, 20: 13354
HAYASHI, Chushiro, Thermal and dynamical properties of a protostar and its contraction to stage of quasi-static equilibrium, 20: 13408
HAYASHI, Miyoko, Absolute dose-rate measurements of very soft and weak x rays by means of a G-M counter, 20: 13085
HAYASHI, Miyoko, X rays from color television receivers, 20: 13014
HAYASHI, Satori, Absolute dose-rate measurements of very soft and weak x rays by means of a G-M counter, 20: 13085
HAYASHI, Satori, X rays from color television receivers, 20: 13014
HEATHCOTE, John, Improvements in and relating to vapour generators, 20: 14041
HEBER, G., Relativistic calculations of Green's functions, 20: 13557
HEDBERG, Kenneth, Structure of gaseous XeF_6, 20: 12860
HEER, W., Pulsed-source experiments with multiplying and non-multiplying D_2O systems, 20: 14076
HEFFLEY, R. A., Measurement and calculation of relative poison-to-fuel capture ratios in slab cores, 20: 14063 (KAPL-M-6528)
HEINRICH, H. C., Hamburg 4π large-volume radioactivity detector with liquid organic scintillator. II., 20: 13079
HEINZ, W., Pulse generator (μsec) with 10-Mw pulse power at 200-kv pulse voltage, 20: 13035
HEINZ, W., Pulsed injector for large current and voltage, 20: 13036
HEISENBERG, W., Particles as collective stationary states, 20: 13609
HEISER, W. H., Plasma magnetohydrodynamics and energy conversion, 20: 13432 (TID-22419, pp 149-76)
HELLMAN, S. P., Measurement of integral parameters in fuel rods, 20: 14103 (MIT-2344-4, pp 48-62)
HELLSTRAND, E., Experimental studies on assemblies 1 and 2 of fast reactor FRO. II., 20: 14178 (AE-207)
HELM, J. W., Radiation-induced dimensional changes of raw-coke graphites, 20: 13322 (BNWL-178)
HELSETH, Frank, Movement and distribution of radionuclides on granitic

outcrops within Georgia piedmont, 20: 12985
HENDERSON, J. Frank, Selective elution of scintillation phosphors from chromatography paper, 20: 12929
HENDERSON, R. W., Radiation measurements of effluent from Kiwi B4D-202 and B4E-301 reactors, 20: 14172 (LA-3397)
HENNIES, H., Pulsed neutron reactivity measurements in the near-critical state, 20: 14082
HENRIE, T. A., Reaction rate of U metal with UF_4 in molten fluoride solutions, 20: 13170 (BM-RI-6736)
HERDLY, J., Cicatrization after telecobalt therapy in surgery of neck and buccal cavity, 20: 12653
HERENGUEL, J., Frittoxal ($Al-Al_2O_3$) and nuclear applications, 20: 13213 (EUR-2447.f)
HERICKHOFF, Robert John, Characteristic energy loss studies of electron-bombarded Al, Cd, In, Mg, and Zn foils, 20: 14004
HERMAN, M., Basal plane fracture of beryllium single crystals, 20: 13238 (CONF-170, pp 48-68)
HERMANN, Guenter, 25 years of nuclear fission. II., 20: 12920
HERMANN, Horst, Manipulator arm, 20: 12958
HERMEL, A., Occurrence of self-luminescence collision fronts in electromagnetically operating shock tubes, 20: 13949
HEROLD, D., An ion converter detector with gate connections for mass spectrometric investigations, 20: 13047
HEROLD, D., Secondary electron emission from Cu–Be by positive ions at energies of 25 kev, 20: 13424
HEROLD, T. Richard, Energy spectra of neutrons and γ rays from spontaneous fission of ^{244}Cm, 20: 13769 (DP-949)
HESSON, G. M., Proposed tube power limits for PRTR 58-inch MK I fuel element, 20: 14116 (BNWL-177)
HEUER, W., K-meson decay and CP invariance, 20: 13495
HEWITT, Harold B., Effect of cell survival of inhalation of oxygen during irradiation of solid mouse sarcoma, 20: 12725
HICKMAN, B. S., Effect of neutron irradiation on Al_2O_3, 20: 13337
HIIDA, Kichiro, Gravitation physics, 20: 13665
HILLIGES, Dieter, Material requirements for reinforced Maxwell bodies with small reinforcing members. II., 20: 12944
HILLMAN, M., Production of Y-87 and a Sr-87m generator, 20: 12917
HILLMAN, Manny, Search for radiochemical evidence for ternary fission of ^{235}U by thermal neutrons, 20: 13862
HILSCHER, D., Ionization defects of energetic ^{28}Al atoms in silicon, 20: 13989
HIRATA, Masashi, Effects due to low-dose irradiation in utero, 20: 12683
HIREL, Renee, Electron grouping system at input of linear accelerator and coefficients of space harmonics of accelerating structure, 20: 13369
HIRSCH, Roland Felix, Analytical aspects of chemistry of technetium, 20: 12808
HIURA, Jun, Reaction $^9Be(\alpha,2\alpha)^5He$ and α-particle model, 20: 13875
HLINIAKOWA, I., Rectal complications following radium treatment of uterine carcinoma, 20: 12696
HOAGLAND, R. G., Double cantilever beam specimen for determining plane strain fracture toughness of metals, 20: 12972 (BNWL-168)
HOBBIE, Russell K., Angular distributions for reaction $^{12}C(^6Li,\alpha)^{14}N$ between 2 and 3 Mev, 20: 13846
HODDENBACH, G. A., Growth of lizards in natural populations exposed to γ irradiation, 20: 12669
HODGKINS, B., Biological importance of uv-induced DNA-protein cross-links in E. coli, 20: 12621
HOEKSTRA, H., Crystal structure of high-pressure UO_3, 20: 13269
HOENIG, Clarence L., Vapor pressure and evaporation coefficient studies of beryllium nitride decomposition reaction, 20: 12830 (UCRL-7802)
HOEPFNER, A., Hydrogen bonding and vapor pressure isotope effects in n-deuterated methyl and ethyl amines, 20: 12879
HOERZ, G., System Nb–N. III. Outgassing in high vacuum, 20: 13202
HOERZ, G., System Nb–N. I., 20: 13302
HOERZ, G., System Nb–N. II., 20: 13303
HOFFMAN, E. E., Prog. rpt. on K corrosion test loop development, 4/15–7/15/65, 20: 13192 (NASA-CR-54843)
HOFFMAN, R. A., Anisotropy of Snoek phenomenon in niobium, 20: 13980
HOFFMANN, T. A., Approximation in quantum mechanics, 20: 13655
HOFFMANN, W., Measurement of low-energy β emitters in heterogeneous phases with liquid scintillators, 20: 12804
HOKKYO, Nobuo, Radiationless condition and mass formula, 20: 13594
HOLLEY, William R., K^--proton elastic scattering at 700 to 1400 Mev/c, 20: 13460 (UCRL-16274)
HOLLIDAY, J., Quality control inspection and testing of fuel materials for Dragon, 20: 14159
HOLLIDAY, Robin, Radiation-sensitive mutants of Ustilago maydis, 20: 12694
HOLMES, John T., Pilot-plant development of process for U alloy fuels. VIII., 20: 12924 (ANL-6973)
HONMA, Akio, Nuclear spin-lattice relaxation in ferromagnetic insulators at low temperatures, 20: 13995
HOOPER, E. W., Purification of Be metal by distillation process, 20: 13173 (CONF-170, pp 1-5)
HOOPER, Richard J., Measurement of characteristic kernels of a class of nonlinear systems, 20: 13023 (CONF-660206-1)
HOPMAN, H. J., Longitudinal plasma waves and Landau damping, 20: 13950
HOREN, D. K., Decay properties of ^{86}Zr, 20: 13856
HORI, Ippei, Effects due to low-dose irradiation in utero, 20: 12683
HORNSBY, J., Particle optics inside an absorber, 20: 13350
HORNUNG, Guenter, Influence of body burden on radiation sensitivity of rats, 20: 12703
HOROWITZ, J., The development of graphite–gas research, 20: 14152
HORTON, J. C., Mass spectrometric analysis of BF_3, 20: 12786
HORTON, R. W., Prog. rpt. on chemical separations processes, 4–6/65, 20: 12928 (ORNL-3868)
HOUELLE, M., Study of homogeneous core assemblies using pulsed neutron sources, 20: 14077
HOWART, Sheila, Resistance to bactericidal effect of uv radiation conferred on enterobacteria by the colicine factor Col. I, 20: 12677
HOWELL, Carol-Joyce, Radiosensitivity of guinea pigs with hypocatalasia, 20: 12643 (ANL-Trans-264)
HOWLAND, G. R., Pneumatic nutator actuator motor, 20: 14029 (NASA-CR-54788)
HRASKO, P., Renormalizable vector boson theory of weak interactions, 20: 13568
HRYNKIEWICZ, A. Z., Magnetic interaction of ^{155}Gd nucleus in 87-kev excited state, 20: 13763 (CONF-233(Vol.4), pp 710-19)
HSIEH, Jack J. C., Autoradiography: Technique for drastic reduction of exposure time to α particles, 20: 12563
HSU, T. H., Associated particle time-of-flight system for use with D-D neutrons, 20: 13088
HUANG, An-I, Treatment of radioactive waste, 20: 14211
HUBBELL, Stephen P., Radiotracer, gravimetric, and calorimetric studies of ingestion and assimilation rates of an isopod, 20: 12610
HUDSON, C. E., Pin technique for displacement measurements in Kiwi-TNT, 20: 14171 (LA-3388)
HUEPER, R., Recent single-energy π-N phase-shift analyses and spin-flip dispersion relations, 20: 13492
HUERLIMANN, T., Modified pulsed source techniques, 20: 14199
HUESCHEN, Robert E., Vanadium window for an atomic particle and radiation-emitting device, 20: 13052
HUGHES, Kenneth John, Study of PrO_2 prepared by acetic acid leaching, 20: 12874
HUILLERY, R., Dimensional measurements and flaw detection, 20: 13343
HULTSCHIG, H., Search for a heavy electron by electron-proton coincidence measurements, 20: 13446 (DESY-65/9)
HUNGATE, F. P., Autoradiography: Technique for drastic reduction of exposure time to α particles, 20: 12563
HUNT, Stanley Ernest, Improvements relating to radiation detectors, 20: 13116
HURLEY, J. P., Germanium (lithium) detector fabrication, 20: 13058 (AD-627930)
HURLEY, J. P., Performance studies of Phillips 56 AVP and XP 1020 photomultiplier tubes, 20: 13100
HUSSAIN, Md. Emdad, Installation of a 3-Mev Van de Graaff at Dacca, 20: 13356 (AECD/EP/6)
HUTTER, Carl R., Description of temperature monitor for large reactors. III., 20: 14025 (DP-944)
HWANG, Donna S., Genetic integrity of upgraded and downgraded alleles in Saccharomyces, 20: 12655
HWANG, Yin-Si, Treatment of radioactive waste, 20: 14211
HYDE, E. K., Decay properties of ^{86}Zr, 20: 13856
HYLAND, Michael, Fast test reactor hypothetical meltdown accident, 10–12/65, 20: 14182 (COO-1430-3)

I

IBA, Shozo, Gonad dose of patients in x-ray treatment of benign tumors, 20: 13013
IDA, Yoshio, Effect of magnetic field on resonances of surface waves propagating along cylindrical plasma columns, 20: 13941
IGATA, N., Measurement of internal friction of nuclear materials, 20: 13321
IHLE, H., Comparative investigations on counting methods for absolute determination of activity of α emitters, 20: 13066 (JUL-298-PC)
IIJIMA, Toshitetsu, Bibliography on accidents in nuclear facilities, 20: 13002 (JAERI-4034)
IKEDA, Mariko, Behavior of sulfhydryl groups of sea urchin eggs, 20: 12624
IKEDA, Masamichi, Measurement of leakage tritium from tritium self-luminous paints, 20: 13153
IKENAGA, Mitsuo, Comparative studies of mutation frequencies induced by ^{32}P treatment and γ irradiation in male silkworm, 20: 12692
IKEYA, Motoji, Neutron activation analysis of divalent ions in alkali halide crystals, 20: 12805

ILBERY, P. L. T., Thymic, lymphoid, and marrow inocula in cytogenetic repopulation studies of irradiated mice, 20: 12647
IMAMURA, Yoshinori, Studies on lymph node and thymus tissue culture. I., 20: 12682
IMAZU, Shingo, Hysteresis phenomenon near B_c in positive column in a magnetic field, 20: 13937
IMBAUD, Jean-Pierre, Application of Overhauser effect and of spin decoupling to studies on ^{13}C, 20: 13800
INGARDEN, R. S., Statistical thermodynamics with higher order temperatures for ideal gases of bosons and fermions, 20: 13640
INGLIS, David R., Inelastic alpha scattering and associated gamma radiation. II., 20: 13848
INMAN, Fred W., Transition radiation from relativistic electrons crossing dielectric boundaries, 20: 13352
INOUYE, H., Equilibrium solid solutions of N in Nb–1% Zr between 1200 to 1800°C, 20: 13263 (ORNL-TM-1355)
IORDANSKY, S. V., Relaxation time for nonequilibrium state of superfluids, 20: 13671
IRIE, F., Angular dependence of upper critical field in thin films, 20: 13681
IRIE, Hideo, Influence of radioprotective substances on damages to bone growth in rats, 20: 12729
IRVINE, W. J., Prognostic significance of thyroid antibodies in management of thyrotoxicosis, 20: 12626
ISAEV, P. S., Application of quasipotential method to pion-nucleon scattering, 20: 13467
ISAKOV, A. I., Moderation of neutrons emitted by pulsed source, 20: 13741
ISEBECK, K., Dose dependence of annealing stage II in neutron-irradiated aluminum, 20: 13340
ISENHOUR, T. L., Determination of boron by thermal neutron activation analysis using a modulation technique, 20: 12784
ISENHOUR, T. L., Modulation technique for neutron-capture γ measurements in activation analysis, 20: 12783
ISHIDA, Ryuichi, Fabrication of UO_2 fuel element by vibratory compaction, 20: 13225
ISHIHARA, Takehiko, Chemical degradation of kerosene diluent with nitric acid, 20: 12934
ISHINO, Shiori, Radiation damage in germanium, 20: 13987
ISHMAEV, S. N., Neutron thermalization in time in aqueous moderators, 20: 13739
ISHMAEV, S. N., Neutron-thermalization process in time in graphite and beryllium, 20: 13738
ISRAEL, J., Thermoelectric properties of Pt–Ru alloys, 20: 13299
ITAKURA, Tadashi, Removal of fission products with diatomaceous earth of Ishikawa prefecture, 20: 12938
ITANI, Koichi, Fabrication study of uranium nitride fuel, 20: 13227
ITO, D., Phenomenological analysis of high-energy scattering, 20: 13513
ITO, Toshiro, Experiments on MHD generator driven by plasma jet, 20: 13435
ITOH, Chiaki, Weak γ decays of hyperons, 20: 13502
IVAN, Eugenia, Formation of complex erbium halides by refractometry in aqueous solutions, 20: 12871
IVANENKO, D., Mesons and cosmology, 20: 13507
IVANOV, K. I., Scattering of slow neutrons by hydrogen molecules, 20: 13417
IVANOV, P. P., Optimization of flow of nonequilibrium plasma in MHD generator channel, 20: 13436
IVANOV, V. E., Kinetics of $MoSi_2$ oxidation at 1500 to 1800°C, 20: 13195
IVANOV, V. E., Oxidation of WSi_2 at 1500 to 1800°C, 20: 13196
IVANOV, V. E., Oxidation of $TaSi_2$ in temperature range from 1400 to 1600°C, 20: 13197
IVANOV, Yu. F., Internal conversion coefficients for nuclear transitions in ^{132}Xe, 20: 13883
IVANOVA, S. P., Inelastic scattering of complex nuclei with large charges, 20: 13794
IWAMI, F. S., Environmental radioactivity at Argonne National Lab., 1964, 20: 12998 (ANL-7104)
IWASAKI, Motoo, Chemical analysis of BrF_3, 20: 12797
IWASHITA, Fumio, Betatron, 20: 13404
IWASHITA, Fumio, Deflector for pulsed charged particles, 20: 13405
IWASHITA, Fumio, Particle accelerator with electric-shock preventing device, 20: 13399
IWASHITA, Fumio, Particle accelerator, 20: 13401
IWASHITA, Fumio, Particle accelerator, 20: 13396
IWASHITA, Fumio, Particle accelerator, 20: 13398
IWASHITA, Fumio, Pulsed neutron generator, 20: 13745
IYENGAR, P. K., Removal of second-order neutrons by oriented single crystals, 20: 13709 (PAEC-IPA(D)PH-652)
IZUMI, M., Irradiation effects on polyvinyl chloride and applications for wire insulation, 20: 12907

J

JACKSON, R. J., Electrolytic swab etching for metallography of Pu, 20: 13187
JACOB, H., Y_1^{+} and Y_1^{-} mass difference, 20: 13488
JACOBSON, Martin I., Discussion of "an account of deformation and fracture in single- and polycrystalline beryllium between 20 and 450°C" by A. Moore and G. C. Ellis, 20: 13241 (CONF-170, pp 121-5)
JAEGER, Robert G., Measuring techniques serving radiation protection, 20: 12730
JAGIELAK, J., Investigations on self-diffusion of In by absorption method, 20: 13315
JAMERSON, Frank E., Noble gas plasma produced by fission fragments, 20: 13939
JANSEN, P., Demand for nuclear fuels and costs of different reactor types in Germany, 20: 14130 (KFK-366)
JARVIS, O. N., Absolute polarization measurements in proton scattering at 140-Mev, 20: 13813
JASTRZEBSKI, J., Internal bremsstrahlung accompanying electron capture decay of medium heavy nuclei, 20: 13759 (CONF-233(Vol.4), pp 614-24)
JEFFERSON, Sidney, Improvements in or relating to interlocks, 20: 12955
JEHENSON, P., Frittoxal ($Al-Al_2O_3$) and nuclear applications, 20: 13213 (EUR-2447.f)
JENKINS, James H., Effect of acute γ radiation on opossum, gray fox, raccoon, and bobcat, 20: 12667
JERVIS, Max William, Nuclear reactor, 20: 14040
JEWELL, R. W., Scattering of 262-kev polarized neutrons by ^4He, 20: 13717
JHON, Mu Shik, Significant-structure theory applied to water and heavy water, 20: 12858
JOHN, W., Scattering of 262-kev polarized neutrons by ^4He, 20: 13717
JOHNS, W. L., Electrolytic swab etching for metallography of Pu, 20: 13187
JOHNSON, Carol F., Effect of γ irradiation on fresh prunes, 20: 13144 (UCD-34P80-3, pp 69-74)
JOHNSON, Carol F., Effect of γ irradiation on ripening of bananas, 20: 13146 (UCD-34P80-3, pp 84-91)
JOHNSON, Carol F., Effect of γ irradiation on peaches, 20: 13147 (UCD-34P80-3, pp 92-8)
JOHNSON, Carol F., Sensory evaluation of irradiated cherries, 20: 13141 (UCD-34P80-3, pp 48-51)
JOHNSON, Carroll K., Xenon hexafluoride: crystallographic data and phase transitions, 20: 12844
JOHNSON, K. A., System plutonium–carbon–oxygen, 20: 13291
JOHNSON, M. B., Shell-model form factors for $^{90}Zr(p,p')$ reaction, 20: 13867
JOHNSON, Richard A., SNAP-10A, first reactor in space, 20: 14177
JOLLES, B., Enzymic processes and vascular changes in skin radiation reaction, 20: 12623
JONA-LASINIO, G., Relativistic field theories with symmetry-breaking solutions, 20: 13560
JONES, C. K., Ultrasonic investigation of flux penetration into superconducting niobium, 20: 13684
JONES, D. C., Longevity in neutron-exposed guinea pigs, 20: 12628 (AD-626997)
JONES, D. P., Magnetic hysteresis and surface superconductivity, 20: 13679
JONES, E. D., Conservation economics and reactor technology, 20: 14011 (BNWL-183, Sect. V)
JONES, Geoffrey, Improvements in and relating to fueling arrangements for nuclear reactors, 20: 14036
JONES, Kenneth Cecil, Partial molal heat capacities of aqueous rare-earth chloride solutions at 25°C, 20: 12818 (IS-T-52)
JONES, L. T., Blowout, heat transfer, pressure drop, and maximum flow tests conducted on prototype Mark III fuel bundle, 20: 14125 (GEAP-4898)
JONES, Yvonne Marie, Isotopic exchange study of tungsten in sodium metatungstate–sodium or thotungstate aqueous system, 20: 12822 (IS-T-68)
JOSHI, B. V., Pulsed neutron studies of BeO–natural uranium lattices, 20: 14080
JOUIN, Jacques, Device for adjusting position of elements in reactor tank, 20: 14206
JUNG, Hans H., Multigroup effective cross sections for structural, solution, and breeding materials of Mosel, 20: 14062 (JUL-214-RG)
JURCSIK, Istvan, Problems in determination of uranium with Arsenazo III, 20: 12799
JURKIEWICZ, L., Radiometric determination of spatial concentration of inhomogeneous fluid in pipe lines, 20: 13049
JURY, S. H., Interaction of multiple coils on cylindrical induction heating load, 20: 13032 (ORNL-TM-1352)
JYUNG, W. H., Pathways and mechanisms for foliar absorption of mineral nutrients, 20: 14219 (COO-888-47)
JYUNG, W. H., The effects of urea on ion penetration through isolated cuticular membranes and ion uptake by leaf cells, 20: 14218 (COO-888-44)
JYUNG, Woon H., Ion uptake by cells enzymically isolated from green tobacco leaves, 20: 14217 (COO-888-43)

K

KACHI, S., Prog. rpt. on crystal chemistry, 5/13–8/13/65, 20: 13260 (NP-15852)

KADLECEK, J. A., Reference table for W–3% Re vs. W–25% Re thermocouples, 20: 13028 (KAPL-M-6498)

KADOMTSEV, B. B., Instability and related macroscopic effects in toroidal discharges, 20: 13929 (NP-tr-1340)

KADYK, J. A., Reaction $K^+ + p \rightarrow K + N + \pi$ between 0.86 and 1.58 Bev/c, 20: 13462 (UCRL-16370)

KAERCHER, Karl Heinz, Importance of biochemical investigations of connective tissue components during radiotherapy. I., 20: 12756

KAKEHI, Hirotake, Gonad dose of patients in x-ray treatment of benign tumors, 20: 13013

KALININ, G. P., Physical and mechanical properties of Ti–Nb–Al alloys, 20: 13271

KALINKHIN, B. N., Inelastic scattering of complex nuclei with large charges, 20: 13794

KALINKIN, B. N., Inelastic scattering of complex nuclei accompanied by excitation of collective levels, 20: 13890

KALLFELZ, J., Measurements of neutron spectra in hydrogenous moderators, 20: 13737

KAMAEV, A. V., Some questions of nuclear safety, 20: 14091

KAMEMOTO, Y., Preparation of xenon compound by activation processes for fluoride system, 20: 12898

KAMINSKI, A., Isotopic exchange of iodine in aluminum iodide–ethyl iodide liquid system, 20: 12864

KAMINSKII, A. A., Effect of hard radiation on optical centers of TR^{3+} ions in crystals, 20: 13986

KANEKO, Y., Neutron slowing-down time and thermalization time constant in graphite, 20: 13728

KANEKO, Y., Subcriticality determination of reflected graphite system, 20: 14081

KANKELEIT, E., g Factors of the rotational bands in ^{177}Lu and ^{177}Hf, 20: 13765 (CONF-233(Vol.4), pp 723-5)

KANNAN, S., Uptake and transport of ^{59}Fe by intact leaves and enzymically isolated leaf cells of the bean plant, 20: 14220 (COO-888-48)

KANTELE, J., Gamma-spectrometer systems employing anti-Compton annulus, 20: 13098

KAPELNER, S. M., Solubility of helium in liquid lithium and potassium, 20: 12827 (TID-21583)

KAPITZA, S. P., Photofission angular anisotropy and parity of ^{239}Pu ground state, 20: 13809

KAPLAN, I., Prog. rpt. on D_2O lattice project, annual, 9/65, 20: 14014 (MIT-2344-4)

KARAYANNIS, M., Comparative investigations on counting methods for absolute determination of activity of α emitters, 20: 13066 (JUL-298-PC)

KASAMATSU, Toshio, Fabrication of UO_2 fuel element by vibratory compaction, 20: 13225

KASAMATSU, Toshio, Fabrication study of uranium nitride fuel, 20: 13227

KASHY, E., Measurement of high-energy γ rays with Ge(Li) detectors, 20: 13095

KASTEN, Paul R., Evaluation of thorium fuel cycles, 20: 14126 (JUL-276-RG)

KATAYAMA, Yasuhisa, Variant triplet model and integral charge, 20: 13618

KATO, W. Y., Fast-reactor physics parameters from pulsed source, 20: 14202

KATO, Yusuke, Spectrum of the BCS-reduced Hamiltonian in theory of superconductivity, 20: 13688

KATSUYA, Hiroo, Fabrication study of uranium nitride fuel, 20: 13227

KATZ, R., Core performance code COPE, 20: 14123 (GAMD-1561(Rev.))

KAUFMAN, H. L., Alloy powder preparation by flame reduction techniques, 20: 13181 (K-L-6076)

KAUFMAN, R. Gilbert, Luminescence processes generated by ionizing radiation in KI and KI:Tl, 20: 12891

KAUS, P., Threshold poles and low-energy scattering, 20: 13588

KAWABATA, T., Digital speed and phase control system for three-rotor type neutron choppers, 20: 13713

KAWAGUCHI, Masaaki, Nonmesic decay of light hypernuclei, 20: 13501

KAWAGUCHI, Masaaki, Nuclear force and Bethe-Salpeter equation, 20: 13876

KAWAI, Keiji, Neutron activation analysis of divalent ions in alkali halide crystals, 20: 12805

KAWAMURA, Fumio, Protection mechanisms of non-malignant and malignant cells against ionizing radiation. I., 20: 12680

KAWASHIMA, M., Measurement of electron beam current, 20: 13383

KAWASHIMA, Mazumi, Application of large accelerator to produce irradiated polyethylene products, 20: 12906

KAWASHIMA, T., Angular dependence of upper critical field in thin films, 20: 13681

KAYS, W. M., Heat transfer in parallel rod arrays, 20: 12967

KAYSER, Boris, Branching ratio of the Y_1^+, 20: 13445 (CONF-758-14)

KAZARINOV, Yu. M., Phase-shift analysis of nucleon-nucleon scattering at 400 Mev, 20: 13516

KAZARNOVSKII, M. V., Method for studying analytical dependence of neutron distribution on parameters of scattering nucleus, 20: 13734

KAZARNOVSKII, M. V., Moderation of neutrons emitted by pulsed source, 20: 13741

KAZATO, Kenji, Ion source for use in a mass spectrometer, 20: 13051

KECKI, Zbigniew, Primary processes in radiation chemistry as studied by mass spectrometry. IV, 20: 12901

KEEN, N. J., Purification of Be metal by distillation process, 20: 13173 (CONF-170, pp 1-5)

KELER, E. K., Systems Nd_2O_3–ZrO_2 rich in neodymium oxides, 20: 13283

KELLER, Donald E., Phase equilibria in uranium–tungsten–oxygen system, 20: 13235 (BMI-1755)

KELLEY, B., Material buckling and intracellular thermal neutron distributions, 20: 14065 (MIT-2344-4, pp 4-16)

KELLY, R. W., Development of high-temperature molten lithium pump, 20: 12948

KELM, S., Self-excitation of an electrodeless MHD generator, 20: 13429 (N64-32348)

KELM, S., Theoretical studies of electrodeless MHD generator of infinite length, 20: 13430 (N64-32349)

KELSON, I., Asymmetric-rotator model in s-d shell, 20: 13849

KENEFICK, R. A., Reaction $^{90}Zr(p,p')$ at 18.8 Mev and the shell model, 20: 13866

KENNA, B. T., Neutron activation: relationship of sample mass to self-shielding factor, 20: 12794

KENNEDY, W. T., Spectroscopic investigation of two-beam instability, 20: 13951

KENZHEBAEV, Sh, Method for studying analytical dependence of neutron distribution on parameters of scattering nucleus, 20: 13734

KEPPLER, E., Effect of x irradiation on crossing populations of barley in M1 and M2 generations, 20: 12714

KERBY, Carey C., Protection of lethally irradiated guinea pigs with leukocytes, 20: 12727

KERTESZ, Z. I., Study of radiation-induced softening of plant tissues, 20: 13135 (AD-625483)

KESSER, Gwendolyn, Spectrophotometric determination of Ru with 1-nitroso-2-naphthol, 20: 12788

KESSLER, Wayne V., Properties of a diuretic agent in swine by in vivo whole-body counting, 20: 12613

KHACHATURYAN, M. N., Investigation of total absorption lead-glass Cherenkov γ spectrometer in energy range 0.25 to 4.0 Bev, 20: 13105

KHAPAEV, M. M., Nonlinear theory of motion of fast charged particles in helical toroidal magnetic fields, 20: 13371

KHARLAMOV, S. P., Determination of the *ymp* interaction constant, 20: 13477

KHRISTIANSEN, G. B., Fluctuations of energy fluxes of nuclear-active and electron-photon components in extensive air showers, 20: 13427

KICK, H., Spectroscopic ^{15}N determination with use of step filter for Q24 Zeiss spectrograph, 20: 12807

KIEL, K., Biometeorology—medical meteorology—anthropometeorology, 20: 13015

KIKUGAWA, Masayoshi, Inelastic process and one-boson-exchange model, 20: 13616

KIM, Y. S., Reactions (d,d') on Sn, Cd, Te, and Mo isotopes, 20: 13872

KIM, Young Suh, Role of partially conserved axial-vector current in $\pi_{\mu 2}$ and $K_{\mu 2}$ decays, 20: 13508

KIMELDORF, D. J., Longevity in neutron-exposed guinea pigs, 20: 12628 (AD-626997)

KING, Creston Alexander Jr., Investigation of magnetic effects of rotating superconductors, 20: 13690

KING, H. J., A status report on an ion engine development program, 20: 12975

KINOSHITA, Kisei, Many-pole amplitudes and elementarity. I., 20: 13592

KIRBY, G. W., Deuterium and tritium exchange reactions of phenols, 20: 12880

KIRBY, H. W., Coincidence corrections in proportional counter. III., 20: 13068 (MLM-1263)

KIRILYOK, Yu. I., Radioactivity of waters of the Pacific Ocean, 20: 13007 (NP-tr-1336)

KIRK, James Alvah, Inelastic scattering of 5-Bev/c muons in nuclear emulsions, 20: 13526

KIRKBRIDE, L. D., Nuclear reactor magnetohydrodynamic power generation, 20: 14132 (LA-3368)

KIRZ, Janos, Reaction $\pi^- + p \rightarrow \pi^- + \pi^+ + n$ from 350 to 800 Mev, 20: 13527

KIRZHNITS, D. A., Critical temperature of thin superconducting films, 20: 13676

KISELEV, V. S., Charged meson production in neutron-proton collisions at 600-Mev neutron energy, 20: 13453 (JINR-P-2511)

KISELEV, V. S., Phase-shift analysis of nucleon-nucleon scattering at 400 Mev, 20: 13516

KISSLINGER, L. S., Coupling schemes in odd-mass nuclei, 20: 13825
KITAO, Takaya, X rays from color television receivers, 20: 13014
KITCHINGMAN, W. J., Kinetics of $\beta \rightarrow \alpha$ phase change in U–1 at.% Pt alloy, 20: 13307
KIYOSE, R., Interaction of subcritical assemblies, 20: 14090
KIZER, Donald E., Phase equilibria in uranium–tungsten–oxygen system, 20: 13235 (BMI-1755)
KJELLAND-FOSTERUD, E., PREBOLO: description of high-pressure boiling loop at Kjeller, 20: 14131 (KR-98)
KLEBANOV, G. N., Recrystallization of high-melting metals in welding and soldering, 20: 13267 (AD-624909)
KLEIN, Mark Phillip, Meson production in proton-deuteron collisions: the ABC anomaly, 20: 13528
KLEINER, W. H., Space-time symmetry of transport coefficients, 20: 13996
KLEINKNECHT, K., K-meson decay and CP invariance, 20: 13495
KLEITMAN, David, Properties of Ge under 9.6-Mev deuteron irradiation, 20: 13342
KLEMENT, Alfred W. Jr., Radioactive fallout phenomena and mechanisms, 20: 12981
KLEY, W., Pulsed fast reactor as source for pulsed neutron experiments, 20: 14096
KLOPP, William D., Mechanical properties and recrystallization behavior of electron-beam-melted W, 20: 13257 (NASA-TN-D-3232)
KLYUCHAREV, A. P., Mechanisms of reactions $^{12}C + {}^{10}B \rightarrow {}^{10}B + 3\alpha$ and $^{14}N + {}^{10}B \rightarrow {}^{12}C + 3\alpha$, 20: 13891
KLYUCHNIKOV, N. I., Collision integrals for the Li–H system. Viscosity of mixtures, 20: 13957
KNAPTON, J. D., Pulsed electron beam system, 20: 13034
KNECHTEL, G., Influence of network defects on optical characteristics of glasses, 20: 13341
KNOWLES, D. J., Cell ventilation monitor for fission products development lab. building, 20: 13006 (ORNL-TM-1384)
KOBA, Ziro, Composite model and particle production at superhigh energies, 20: 13604
KOBAYASHI, Hiroo, Bibliography on accidents in nuclear facilities, 20: 13002 (JAERI-4034)
KOBAYASHI, Jindo, Protection mechanisms of non-malignant and malignant cells against ionizing radiation. I., 20: 12680
KOBAYASHI, Yasuko, Chemical analysis of BrF_3, 20: 12797
KOBAYASHI, Yukichi, Bibliography on accidents in nuclear facilities, 20: 13002 (JAERI-4034)
KOBISK, E. H., Preparation of isotopic metallic foils and bulk isotopic metals from oxides, 20: 13216 (ORNL-P-1899)
KOBZAREV, I. Yu., C-odd multipoles, 20: 13475
KOCH, L., Separation of Cd and In from fission product mixtures, 20: 12936
KOCKUM, J., Experimental studies on assemblies 1 and 2 of fast reactor FRO. II., 20: 14178 (AE-207)
KOCKUM, J., Neutron lifetimes and reactivities in FR-0, 20: 14085
KOEHLER, D. R., Neodymium-141 and its production in the (n,2n) reaction, 20: 13864
KOELLE, W., Improvement in direct measurement of β activity in liquid scintillation counters, 20: 13080
KOELSCH, Eckehart, Difference in photoreactivation of uv damage between genes in repressed and derepressed states, 20: 12713
KOELSCH, Eckehart, Difference in uv sensitivity between genes in repressed and derepressed states, 20: 12712
KOH, Yujiro, Internal bremsstrahlung near $2m_e$, 20: 13760 (CONF-233(Vol.4, pp 637-55))
KOHN, A. Moisture control in mixture for agglomeration using neutron probe, 20: 13156
KOKKEDEE, J. J. J., Coulomb corrections concerning test for time reversal violation in neutrino-induced reactions, 20: 13835
KOLEROV, G. I., Conditions of macroscopic causality for the scattering matrix, 20: 13539 (JINR-E-2500)
KOMAI, Kenichiro, Accelerating tube for linear accelerator, 20: 13403
KOMAI, Kenichiro, Charged-particle source, 20: 13400
KOMAI, Kenichiro, Device for controlling particle accelerator, 20: 13395
KOMAI, Kenichiro, Linear accelerator, 20: 13402
KONAR, W., Structure of density matrix for particles of higher spin values, 20: 13578
KONDO, Sohei, Comparative studies of mutation frequencies induced by ^{32}P treatment and γ irradiation in male silkworm, 20: 12692
KONISHI, Chugo, Fabrication of UO_2 fuel element by vibratory compaction, 20: 13225
KOPALEYSHVILI, T. I., Absorption of π^- mesons and γ quanta and nucleon correlations in ^4He, 20: 13884
KOPPANG, R. R., Particle disintegration study for re-entering nuclear auxiliary power systems, 20: 14169 (AFWL-TDR-64-75)
KOPYTIN, I. V., Influence of strong interactions between nucleons in nuclei on allowed β decay, 20: 13886
KORANDA, John J., Persistence of tritium and ^{14}C in Pacific Proving Ground, 20: 12579
KORBEL, K., Radiometric determination of spatial concentration of inhomogeneous fluid in pipe lines, 20: 13049
KORNILOV, I. I., Equilibrium diagram of quasi-ternary system Ti_3Al–Ti_3Sn–Zr, 20: 13273
KORNILOV, I. I., Nature of chemical bond in titanium and zirconium suboxides, 20: 12848
KORNILOV, I. I., Temperature dependence of electroconductivity of titanium and zirconium suboxides, 20: 12850
KOROLEV, G. K., Distribution of certain radioactive substances upon their inhalation, 20: 12604 (JPRS-33958, pp 8-19)
KORSUNSKII, M. I., X-ray emission spectra of Nb and Zr and character of their interatomic bond, 20: 12846
KOSINA, Zdenek, Time selector for two-dimensional analysis, 20: 13075 (UJV-1450/65)
KOSKI, W. S., ESR study of x-irradiated binary mixtures of benzene and alcohols, 20: 12890
KOSSAKOWSKI, A., Statistical thermodynamics with higher order temperatures for ideal gases of bosons and fermions, 20: 13640
KOSTIKAS, A., Modification of RCL 512-channel analyzer for time-of-flight analysis, 20: 13097
KOSTIKOV, V. I., Constitution diagram of ZrB_2–Cr, 20: 13276
KOTANI, Tsuneyuki, Impact parameter formalism, 20: 13610
KOTLYAREVSKII, D., Search for new decay modes of K_2^0 mesons, 20: 13450 (JINR-P-2488)
KOTOV, V. I., Diaphragmed waveguide as deflection system of high-frequency separator, 20: 13362 (JINR-P-2503)
KOTOV, V. I., Waves with complex propagation constants in diaphragmed waveguide, 20: 13363 (JINR-P-2507)
KOUTRAS, D. A., Clinical significance of complement-fixation test in thyrotoxicosis, 20: 12744
KOVBASYUK, V. I., Optimization of flow of nonequilibrium plasma in MHD generator channel, 20: 13436
KOWALSKI, E., Absolute measurement of radioactive source strength, 20: 13805
KOWALSKI, Emil, Ionization-chamber-type radiation dosimeter, 20: 13123
KOZLOWSKY, B., Stripping via core excitation, 20: 13816
KRAEMER, H., Startup experiments on FRJ-2 reactor, 20: 14184 (JUL-236-RE)
KRAKAR, J. J., SNAP-10A flight vehicle nuclear environment and radiation effects, 20: 14175 (TID-22418)
KRASZNAI, Istvan, Effects of whole-body irradiation and bone marrow irradiation on osmotic resistance of reserve leukocytes, 20: 12705
KRAUSHAAR, J. J., Reaction $^{90}Zr(p,p')$ at 18.8 Mev and the shell model, 20: 13866
KRINBERG, I. A., Calculation of thermal conductivity of certain gases at temperatures of 1000 to 20,000°K and atmospheric pressures, 20: 13644
KRISE, George M., Effects of pre- and postnatal γ irradiation on reproduction in the albino rat, 20: 12640 (TID-22378)
KRISTIANSEN, Magne, Resonances and waves in one- and two-ion species plasmas subjected to intense magnetic fields, 20: 13920 (NP-15703, pp 1-51)
KRISTIANSEN, Magne, Shock ionization for ion-cyclotron wave experiment, 20: 13921 (NP-15703, pp 52-63)
KRIVAN, V., Dependence of backscattering coefficient of β radiation on atomic number of scattering material, 20: 13469
KRIVAN, V., Influence of preparation pressure factors for powders on β backscattering results, 20: 13221
KRIVORUCHKO, V. M., Kinetics of $MoSi_2$ oxidation at 1500 to 1800°C, 20: 13195
KRIVORUCHKO, V. M., Oxidation of WSi_2 at 1500 to 1800°C, 20: 13196
KRIVORUCHKO, V. M., Oxidation of $TaSi_2$ in temperature range from 1400 to 1800°C, 20: 13197
KROH, J., Ascorbic acid in crown-gall tumor tissue of Nictoiana tabacum under influence of ^{60}Co γ rays, 20: 12649
KROKOWSKI, Ernst, Changes in radiosensitivity by preirradiation, 20: 12701
KROLIKOWSKI, W., Difference between sources and charges, 20: 13536 (IC/66/7)
KROLIKOWSKI, W., Orbital-like representation of SU(6), 20: 13579
KROLIKOWSKI, W., Remarks about the Fubini-Furlan method, 20: 13537 (IC/66/8)
KRTIL, J., Ion exchange properties of vanadium ferrocyanide. II., 20: 12932
KRUEGER, G., MESPRO 64—program for on-line computer MIDAS, 20: 13166 (KFK-371)
KRUG, M. P., Composition and crystallographic data for the highest boride of tungsten, 20: 12838
KRUSE, W. G., SNAP-10A flight vehicle nuclear environment and radiation effects, 20: 14175 (TID-22418)
KU, Teh-Lung, Manganese nodules: their evolution, 20: 12976
KUBOSE, D. A., Cobalt-60 γ radiolysis of deuterium–oxygen mixtures, 20: 12881 (AD-626609)
KUCHAR, Karel, Rainich geometrization of fermion fields, 20: 13575
KUENDIG, Walter, Properties of supported small α-Fe_2O_3 particles

determined with Moessbauer effect, 20: 13997
KUGLER, E., Magnetic probe measurements during the preheating phase of a spindle-cusp experiment, 20: 13639 (JUL-281-PP)
KUHLMANN, A., Limits to flaw recognition in nondestructive testing steam-generator tubes for nuclear plants, 20: 14160
KUKLA, D., Neutron guides: report on present state of development, 20: 13701 (JUL-294-NP)
KUMPF, Hermann, Emergency shutdown devices for nuclear reactors, 20: 14045
KUNIMASA, Tosaku, Modification of the current-current interaction, 20: 13597
KUPELWIESER, Elisabeth B., Effects of x-irradiated feeder layers on mitotic activity and development of aneuploidy in mouse-embryo cells, 20: 12654
KUPRIANOV, S. E., Mass-spectrometric detection of reactions between highly excited hydrogen atoms and ethylene molecules, 20: 12886 (SC-T-66-0706)
KURATA, Chikara, Cooling system for shield of reactor, 20: 14048
KURODA, P. K., Photofission of ^{238}U induced by 17.5-Mev monoenergetic γ rays, 20: 13860
KUTI, G., Broken symmetries in two Goldstone models, 20: 13556
KUZDOWICZ, A., Disturbances in microsporogenesis caused by x rays in sugar beet di- and tetraploids, 20: 12676
KUZ'MIN, A. I., Intensity variations of cosmic rays, 20: 13426 (NASA-TT-F-183)
KUZNETSOV, F. M., Some questions of nuclear safety, 20: 14091
KUZNETSOV, V. I., Half life of an isotope of element 102 with mass number 256, 20: 13778 (JINR-P-2525)
KUZNETSOV, V. I., Spontaneously fissionable isomer with $T_{1/2}$= 2.6 min in reactions of ^{233}U with ^{11}B and ^{10}B, 20: 13776 (JINR-P-2499)
KUZNETSOVA, M. Ya., Magnetic β spectrometer with two-fold focusing at the angle $\pi\sqrt{2}$, 20: 13064 (JINR-E-2494)
KYRS, M., Concentration-dependent distribution methods for determination of Zr in submicrogram amounts, 20: 12778 (UJV-1434/65)

L

LABBE, J., Civil engineering problems raised by building the Cadarache Nuclear Studies Center, 20: 12947
LABEYRIE, M., Studies and realizations of direct energy conversion, 20: 13434
LABUSCA, Elena, Nondestructive testing methods applicable to sintered materials, 20: 13319
LACKS, Sanford, Integration efficiency and genetic recombination in pneumococcal transformation, 20: 12665
LACONI, A., Intra-operative detection of pelvic lymph nodes by radio-active isotopes, 20: 12751
LADANYI, K., Vacuum degeneracy and broken symmetries in nonlinear spinor theories, 20: 13555
LADNER, H. A., Feasibility of surgery after whole-body x irradiation and administration of radioprotective agent, 20: 12645
LADU, M., Liquid dielectric ionization chamber as means to study mixed radiation fields, 20: 13107
LAFOUCRIERE, Joseph, Formalism based on symmetric interaction in input and output methods for rearrangement collisions, 20: 13798
LAI, M. G., Quantitative radiochemical determination of ^{63}Ni in seawater, 20: 12779 (USNRDL-TR-924)
LAL, M., Annealing processes after nuclear recoil in metal complexes, 20: 12896
LALANDE, J., Study of graphite and beryllium oxide using pulsed neutron source method, 20: 13727
LALEGERIE, Pierre, Superstructure of adenohypophysial tumors from combined effects of I-131 and chlorpromazine, 20: 12657
LANARD, Francis W., Radioactive waste material incinerator, 20: 14212
LANDGRAF, W. C., Mn^{2+} in ^{60}Co γ-irradiated strawberries, 20: 13143 (UCD-34P80-3, pp 55-7)
LANDSBERG, L. G., Investigation of Bev-neutron registration efficiency by scintillation counters, 20: 13109
LANE, R. O., Measurements of neutron cross sections of Fe, Al, and CF_2 by a ratio method, 20: 13716
LANE, R. O., Polarization and differential cross sections in small-angle scattering of neutrons by uranium, 20: 13868
LANGE, W., Lifetime of excited state of europium, 20: 13422
LANGHAM, W. H., Plutonium dispersal by low-order detonation of atomic weapons, 20: 13004 (LA-1981(Rev.))
LANGMANN, H. J., Fabrication and study of thick-base surface-barrier detectors, 20: 13093
LANGSDORF, A. Jr., Measurements of neutron cross sections of Fe, Al, and CF_2 by a ratio method, 20: 13716
LANGSDORF, A. Jr., Polarization and differential cross sections in small-angle scattering of neutrons by uranium, 20: 13868
LANKARD, Judy M., Defense mechanisms of cysteamine and AET for intestinal radiation death, 20: 12721 (BNWL-tr-11)
LANNING, D. D., Measurement of diffusion coefficient in an anisotropic medium, 20: 13705 (MIT-2344-4, pp 135-44)
LANNOM, J. R. Jr., Growth of lizards in natural populations exposed to γ irradiation, 20: 12669
LANNUTTI, J. E., Final-state enhancement at 1920 Mev in π^-p inelastic scattering, 20: 13454 (UCRL-14100-T(Rev.1))
LARA, J. Gomez, Kinetics and mechanism of dissolution of uranous-uranic oxide in sulfuric acid in presence of ferric ion, 20: 12863
LARIONOVA, V. G., Determination of the $\gamma n p$ interaction constant, 20: 13477
LARSEN, R. P., Spectrophotometric determination of Ru with 1-nitroso-2-naphthol, 20: 12788
LASHINSKY, Herbert, Nonlinear mechanics of plasma-like distributed media, 20: 13905 (CONF-651056-1)
LASHKAREV, G. V., Physical properties and chemical bond in rare earth chalcogenides, 20: 12849
LATYPOVA, R. A., Distribution of knock-out nucleons as a function of nuclear volume, excitation energy, and nuclear recoil momentum distributions in cascade processes, 20: 13892
LAUE, H. J., Changes of mechanical properties of Cr–Ni steel and Ni alloys after neutron irradiation, 20: 13333
LAWRENCE, C. W., Effect of dose duration in influence of irradiation on recombination in Chlamydomonas, 20: 12688
LAWRENCE, Jackson, Thermionic converter, 20: 13441
LAWRENCE, Richard Manley, X-ray-diffraction studies of aqueous alkali metal halide solutions, 20: 14228 (TID-22527)
LEACH, Charles M., Detection of ultraviolet-absorbing substances in living mycelium of fungi, 20: 12695
LEBEAUPIN, Denis, Improvements in hot cells, 20: 12953
LEBEDEV, A. I., Determination of the $\gamma n p$ interaction constant, 20: 13477
LEBEDEV, N. A., Decay of ^{138}Pr, 20: 13882
LEBEDEV, V. E., Solving nuclear geophysics problems by Monte Carlo method, 20: 12994
LE COUVIOUR, M., Prog. rpt. on effects of mutagenic substances, annual, 1964, 20: 12632 (EUR-2546.f)
LEE, T. C., Removal of second-order neutrons by oriented single crystals, 20: 13709 (PAEC-IPA(D)PH-652)
LEEP, Richard W., Description of temperature monitor for large reactors. III., 20: 14025 (DP-944)
LEFEVRE, G. Jr., Cytogenetic studies of the white locus in Drosophila, 20: 12664
LEFEVRE, G. Jr., Mutation frequencies detected following irradiation of Drosophila females, 20: 12663
LEFFERT, Charles B., Noble gas plasma produced by fission fragments, 20: 13939
LEFORT, Guy, Improvements in hot cells, 20: 12953
LEGAR, F., Nucleon-nucleon potential with a soft core for $^1S_0$ state at 0.17 to 310 Mev, 20: 13489
LEGER, Jean-Etienne, Fuel elements and primary materials. Report to FORATOM congress, 20: 14105
LE GUILLOU, Sylvain, Recovery and radio-resistance in mice after external irradiation, 20: 12631 (CEA-R-2776)
LE HERICY, Jacques, Determination of sulfur in copper by neutron activation, 20: 12793
LE HO, J. G., Study of graphite and beryllium oxide using pulsed neutron source method, 20: 13727
LEIPNIK, R. B., Diffusion and conductivity of plasmas in strong external fields, 20: 13938
LEISTNER, L., Radioactive contamination of foodstuffs stemming from animals, 20: 12979 (EUR-2287.d)
LEITTEN, C. F. Jr., Fabrication of aluminum-base irradiation test plates, 20: 13217 (ORNL-TM-1377)
LEMARCHANG-BERAUD, Th., Radioimmunologic method for determination of thyroid-stimulating hormone, 20: 12755
LENGEMANN, F. W., Prog. rpt. on metabolism of selected radionuclides, final, 6/64–6/65, 20: 12588 (AD-626320)
LENK, Pedro A., Operating characteristics of the present PM-type reactor instrumentation. Task 2 topical report, 20: 14134 (NYO-3379-2)
LENZI, G., Sorption properties of natural tuffs occurring in Lake Bracciano region (Rome), 20: 14209 (RT/PROT(65)29)
LEONE, J. A., ESR study of x-irradiated binary mixtures of benzene and alcohols, 20: 12890
LEPLAE, L., Gauge transformations and inequivalent representations, 20: 13652
LEPLAE, L., Rearrangement of symmetries in dynamical maps, 20: 13620
LERCH, O., Precision (1%) absolute counting of x rays of low energy, 20: 13092
LERNER, E., Thermal and electrical conductivities of Mo–Re alloys in superconducting and normal states, 20: 13686
LEROY, Jean-Marie, Hydrates and thermal decomposition of uranium sulfate, 20: 12843
LESSMANN, G. G., Prog. rpt. on weldability and stability of refractory alloys, 3/21–6/20/65, 20: 13264 (WANL-PR(P)-008)

LEUNG, A. T., Simultaneous radiation, conduction, and convection in spectrally selective, emitting, and scattering porous bed, 20: 12969
LEVAY, Bela, Measurement of isotopes emitting soft β radiation with aid of liquid scintillator in single-channel measuring instrument. III., 20: 12801
LEVIN, A. Ya., Coherent inelastic interactions between high-energy π^- mesons and heavy nuclei in photoemulsion, 20: 13893
LEVINSKII, Yu. V., Investigations of interactions in Nb–N–C and Ta–N–C systems, 20: 12845
LEVY, Henri A., Xenon hexafluoride: crystallographic data and phase transitions, 20: 12844
LEVY, Sander Alvin, Effect of structure on superconducting properties of eutectic alloys, 20: 13695
LEWIS, D., Strain-induced activity in thoria and its relief with temperature, 20: 13295
LIACOPOULOS-BRIOT, Monique, Preservation by phytohemagglutinin of medullo-restoring and hematopoietic properties of medullary cells, 20: 12726
LIBERTI, Arnaldo, Gas chromatography of isotopic molecules on open tubular columns, 20: 12930
LICCIARDELLO, J. J., Storage of eviscerated haddock in refrigerated sea water treated with γ radiation, 20: 13152
LICHTENSTEIN, Roland M., Prog. rpt. on radiation damage in semiconductor materials, 5–7/65, 20: 13128 (NP-15835(Suppl.))
LIDEN, Kurt, Transport of ^{137}Cs from lichen to animal and man, 20: 12578
LIEBENBERG, D. H., Cooldown of cryogenic transfer lines, 20: 13668 (LA-3426)
LIESER, K. H., Rate of heterogeneous isotopic exchange on surfaces of ionic crystals, 20: 12869
LIETZKE, M. H., Program to compute the classical deflection function, 20: 13415 (ORNL-3881)
LIKHACHEV, M. F., Elastic 180° scattering of π^+ mesons by protons at high energies, 20: 13471
LIMA, Fausto W., Activation analysis of gold in ores samples, 20: 12769 (IEA-98)
LIMA, Fausto W., Determination of Cl and Cu in high-purity water by radioactivation, 20: 12768 (IEA-97)
LIMA, Fausto W., Radiochemistry activities in research reactor centers, 20: 12914 (IEA-100)
LIMIC, N., Discrete degenerate representations of non-compact rotation groups, 20: 13532 (IC/66/2)
LIN, Chie-Shi, Test of reactor power meter by measuring ^{16}N activity in coolant, 20: 14019
LIN, Chien-Cheng, Recovery of telluric acid from ^{131}I production waste, 20: 12916
LIN, E. K., Spectroscopic factors from deuteron stripping reactions, 20: 13865
LINDEGREN, Carl C., Genetic integrity of upgraded and downgraded alleles in Saccharomyces, 20: 12655
LINDER, A., Generalized variational principles in classical mechanics, 20: 13351
LINDLEY, M. W., Strain-induced activity in thoria and its relief with temperature, 20: 13295
LINDQUIST, R. H., Properties of supported small α-Fe_2O_3 particles determined with Moessbauer effect, 20: 13997
LINDSAY, H. M., Dislocation vectors related to the ductility of Be, 20: 13305
LIPNIK, P., Matrix elements of β transitions in the Nilsson model, 20: 13831
LIPTAI, R. G., Effects of high pressure and temperature on microstructure of Pu, 20: 13292
LITT, Benjamin, Process for assembling concentrically spaced nuclear fuel elements, 20: 13231
LITTMAN, F. E., Particle disintegration study for re-entering nuclear auxiliary power systems, 20: 14169 (AFWL-TDR-64-75)
LLOYD, L. T., Effects of high pressure and temperature on microstructure of Pu, 20: 13292
LLOYD, Ray D., Trophic level effect on ^{137}Cs concentration, 20: 12611
LOBANOV, Yu. V., Half life of an isotope of element 102 with mass number 256, 20: 13778 (JINR-P-2525)
LOCKHART, R. W., Sodium mass transfer. VII., 20: 12766 (GEAP-4178)
LOGUNOV, A. A., Asymptotic behavior of scattering amplitude at large momentum transfers, 20: 13546 (JINR-P-2519)
LOMMATZSCH, P., Histological changes in irradiated malignant intraocular tumors, 20: 12740
LOMNEV, S. P., Method of retaining and accumulating high-temperature plasma in a trap, 20: 13928 (AD-625070)
LONDEN, S.-O., Experimental studies on assemblies 1 and 2 of fast reactor FRO. II., 20: 14178 (AE-207)
LONDRES, H., Survey of radioactive content of food grown on Brazilian areas of high natural radioactivity, 20: 12988
LONG, E. L. Jr., BONUS superheater fuel assemblies—failure and method of correction, 20: 14141 (ORNL-3910)
LONG, E. L. Jr., Postirradiation examination of EGCR prototype capsule, 20: 14142 (ORNL-TM-1378)
LONGHURST, W. M., Comparative metabolism of Sr, Ca, and Cs in deer and sheep, 20: 12609
LONGINOV, A. V., Resonant heating of plasma by high-frequency field, 20: 13946
LONGO, G., Technique of n-γ discrimination, 20: 13111
LONGWORTH, T. C., GEM Monte Carlo code and its use in solving criticality problems, 20: 14093
LOONEY, W. B., Study of DNA-labeled cells at different times after high doses of radiation, 20: 12638 (TID-21474)
LOPATA, S. L., Lattice parameters and solubility limits of alpha Fe as affected by binary transition-element additions, 20: 13317
LOPATO, L. M., Investigation of the optical properties of compounds formed in La_2O_3–SrO and La_2O_3–BaO systems, 20: 13278
LOPES, J. S., Excited states of ^{19}F by angular correlation technique, 20: 13822
LOPUSZANSKI, J. T., Unitarily inequivalent representations in quantum field theory and the many-body problem, 20: 13553
LORY, JACQUELINE, Participation of an excitonic mechanism in formation of latent image in an ionographic emulsion, 20: 13082
LOSERIES, Hans-Georg, Instrument for measurement of dose rate of γ radiation and detection of β radiation, 20: 13120
LO SURDO, C., Direct conversion of thermal energy in MPD power generation program at C.N.E.N., 20: 13431 (RT/FI(65)31)
LOTHE, Johan, Improvements in or relating to high-temperature gas-cooled reactors, 20: 14021
LOUNSBURY, M., Neutron absorption cross section of gross fission products of ^{233}U, ^{235}U, and ^{239}Pu, 20: 13748 (AECL-2510)
LOVELL, G. H. B., Determination of C in UC, 20: 12773 (PEL-80)
LOW, W., Paramagnetic resonance spectrum of Co^{1+} in single crystals of CaO, 20: 13972 (IA-1056)
LOWE, J. N., Recrystallization characteristics of wrought ingot beryllium sheet, 20: 13243 (CONF-170, pp 160-83)
LU, Si-ting, Magnetic β spectrometer with two-fold focusing at the angle $\pi\sqrt{2}$, 20: 13064 (JINR-E-2494)
LUBELL, M. S., Anomalous critical currents in superconducting noninductive coils of Nb-25% Zr wire, 20: 13674
LUCAS, Monique, Determination of Pu by double-tracer isotopic dilution, 20: 12811
LUECK, Hosse, Bibliography on radiation effects on food, 6/65, 20: 13136 (AED-C-02-06)
LUKHININSKII, B. E., Solving nuclear geophysics problems by Monte Carlo 20: 12994
LUKIN, E. S., Vaporization of pure-oxide ceramics at high temperatures, 20: 13265 (AD-623208)
LUK'YANOV, V. K., Inelastic scattering of electrons on nuclei with collective level excitation, 20: 13775 (JINR-P-2490)
LUMB, R. F., Transient characteristics of a new pulse research reactor, 20: 14203
LUNDQUIST, J. R., Nickel electroplating on U, 20: 13211 (BNWL-124)
LUSTINEC, Jiri, 500-Curie irradiation facility, 20: 12911 (AECD/HP/3)
LUTHER, J., Lifetime of excited state of europium, 20: 13422
LUTZ, H. R., Pulsed-source experiments with multiplying and nonmultiplying D_2O systems, 20: 14076
LYNCH, Charles T., Hot pressing zirconia, 20: 13230
LYNCH, E. D., Fabrication and evaluation of thoria–urania fuel material, 20: 13207 (ANL-6893)
LYNCH, E. D., Glassy materials for reactor applications, 20: 13209 (ANL-7062)
LYNCH, R. W., Effect of very high pressure on structure of some hcp metals and alloys, 20: 13316
LYON, F., Controllable pulse frequency and width system for pulsing and modulating fast-neutron core assemblies, 20: 13721
LYONS, M. F., Irradiation of 0.5-inch-diameter, solid-pellet UO_2 fuel rods, 20: 13326 (GEAP-5100C)
LYUBIMOV, A. L., Elastic 180° scattering of π^+ mesons by protons at high energies, 20: 13471
LYUBIMOV, V. A., Investigation of Bev-neutron registration efficiency by scintillation counters, 20: 13109

M

MAC DOUGALL, J. D., ARGOSY 4: program for lattice calculations, 20: 14055 (AEEW-R-445)
MACGREGOR, A. G., Prognostic significance of thyroid antibodies in management of thyrotoxicosis, 20: 12626
MACHABELI, I. Z., Absorption of π^- mesons and γ quanta and nucleon correlations in ^{4}He, 20: 13884
MACHIDA, Shigeru, Elementary particle structures and meson-nucleon backward scatterings, 20: 13510
MACIAS, E. S., Yield data for transplutonium element production in thermal reactors, 20: 13752 (ANL-7096)
MACKE, W., Probability operator ρ in many-body problems, 20: 13654

MACKELLAR, Alan Douglas, Nuclear ground state properties of ^{16}O, 20: 13785 (ORNL-TM-1374)
MAC KENZIE, I. K., Influence of crystallinity on positron-annihilation angular correlation in teflon, 20: 13468
MACMAHON, Alan, On finite gyro-radius corrections to hydromagnetic equations for Vlasov plasma, 20: 13926 (UCRL-16517)
MAC PHEE, J., Transient characteristics of a new pulse research reactor, 20: 14203
MACRIS, B., Effect of chemical sensitizers on radiation resistance of fruit-spoilage fungi, 20: 13137 (NP-15360)
MAEKAWA, Akitsugu, Charged particle accelerator, 20: 13390
MAIN, G. W., Fast-reactor physics parameters from pulsed source, 20: 14202
MAIOROV, L. B., Neutron thermalization in graphite-water system at large temperature gradients, 20: 13740
MAJLE, Tadeusz, Recent opinions on effects of ionizing radiation on human population, 20: 12699
MAKI, Ziro, New concept of elementary particles and method of the composite model, 20: 13613
MAKIN, M. J., Burger's vectors in beryllium and their effect on ductility, 20: 13242 (CONF-170, pp 126-37)
MAKSIMOV, E. G., Critical temperature of thin superconducting films, 20: 13676
MALAY, F. L., Containment for nuclear reactors, 20: 14031
MALDAGUE, Pierre Edmond Jules Marie, Controlling reactivity of a reactor, 20: 14099
MALDAGUE, Pierre Edmund Jules Marie, Method of purifying primary fluid of nuclear reactor circuit, 20: 14051
MALEY, Martin Paul, Generation of acoustic waves at microwave frequencies in thin films of dysprosium metal, 20: 14003
MALININ, Theodore I., Protection of lethally irradiated guinea pigs with leukocytes, 20: 12727
MALINOVSKY, A. H., Particle disintegration study for re-entering nuclear auxiliary power systems, 20: 14169 (AFWL-TDR-64-75)
MALMSTROM, S. A., AGCR off-normal scram system, 20: 14146 (TID-22596)
MALOV, L. A., Structure of spontaneously fissioning isomers, 20: 13777 (JINR-E-2515)
MALYUTA, Yu. M., Mass formulas in the supermultiplet model, 20: 13583
MAMONTOVSKAYA, L. V., Physical and mechanical properties of Ti–Nb–Al alloys, 20: 13271
MANESCHI, M., Intra-operative detection of pelvic lymph nodes by radioactive isotopes, 20: 12751
MANFREDI, D. V., Development of high-temperature molten lithium pump, 20: 12948
MANGIALAJO, M., Monitoring 2.5-Mev neutrons produced by a 150-kv accelerator, 20: 13715
MANKO, V. I., Relativistic oscillator models of elementary particles, 20: 13626
MANN, C. A., Nondestructive testing of fuel elements, 20: 14161
MANSON, A. R., Minimum bias designs for an exponential response, 20: 13167 (ORNL-3873)
MANTOVANI, G. C., Existence of ^{4}He excited levels and of other light nuclides, 20: 13834
MARAZZINI, P., Existence of ^{4}He excited levels and of other light nuclides, 20: 13834
MARCHATERRE, J. F., Use of high-temperature process heat as part of total-energy source, 20: 14165 (ANL-7035)
MARCHESI, F., Intra-operative detection of pelvic lymph nodes by radioactive isotopes, 20: 12751
MARIA, Alain, Improvements in installations for spectrophotometric analysis of radioactive solutions, 20: 12813
MARIN, P., Synchrotron radiation and observation of bunches in storage rings, 20: 13378
MARINOV, A., Energy levels in ^{49}Sc from $^{48}Ca(^{3}He,d)$ and other reactions, 20: 13854
MARION, Jerry B., Reaction $^{7}Li(p,\gamma)^{8}Be^{*}$ and single-particle levels in ^{8}Be, 20: 13810
MARKOV, M. A., Can the gravitational field prove essential for the theory of elementary particles?, 20: 13600
MARKOVA, I. A., Rare earth alloys and compounds, 20: 13280
MARSEGUERRA, M., Temperature coefficient measurements of the RC-1 Reactor (TRIGA), 20: 14188 (RT/FI(65)40)
MARSHAK, R. E., Higher symmetry groups with parity mixing, 20: 13599
MARSONGKOHADI, Removal of second-order neutrons by oriented single crystals, 20: 13709 (PAEC-IPA(D)PH-652)
MARTIN, Arthur Francis, Apparatus and method for producing controllable slow neutron chain reaction, 20: 14097
MARTIN, D. H., Ion beam analysis by an electrostatic technique, 20: 13372
MARTIN, Jean Antoine, Pneumatic drive for reactor control rods, 20: 14047
MARTIN, M. M., Fabrication of aluminum-base irradiation test plates, 20: 13217 (ORNL-TM-1377)
MARTIN, W. R., Irradiation embrittlement of stainless steel, 20: 13335
MARTIN, William E., Interception and retention of fallout by desert shrubs, 20: 12572
MARTINI, William R., Regenerative thermionic converter, 20: 13442
MARTTILA, O. J., Gamma-spectrometer systems employing anti-Compton annulus, 20: 13098
MARUYAMA, M., Energy dependence of nuclear level density below the neutron binding energy, 20: 13827
MARUYAMA, M., 5.5-Mev ion buncher of Mobley type, 20: 13379
MARUYAMA, Masuo, Particle accelerator, 20: 13393
MARX, G., Broken symmetries in two Goldstone models, 20: 13556
MASLENNIKOV, N. M., Electric conductivity in stream of argon containing potassium oxide, 20: 13954
MASSE, Jean-Leon, Study of $2^{1}S$ state of helium using Hartree-Fock method, 20: 13411 (CEA-R-2855)
MASSET, M., Distribution of Sr and Ca in Pisum sativum, 20: 12605
MASSEY, L. M. Jr., Study of radiation-induced softening of plant tissues, 20: 13135 (AD-625483)
MASSIEUX, J., Pulsed neutron measurements in fast assemblies, 20: 14084
MASSUCCI, Maria A., Spectrofluorometric trace determination of Sm, Eu, Tb, and Dy in Na tungstate solutions, 20: 12787
MATE, C. F., Preferred rates in helium film transfer, 20: 13682
MATHE, Georges, Induction of tolerance to allogenic grafts, 20: 12656
MATHE, Gy., Improved particle separation with pulse-shape discrimination in case of CsI(Tl) scintillator, 20: 13110
MATHIESEN, J. M., Germanium (lithium) detector fabrication, 20: 13058 (AD-627930)
MATHIESEN, J. M., Performance studies of Phillips 56 AVP and XP 1020 photomultiplier tubes, 20: 13100
MATHIEU, J., Cloud chambers filled with dielectric liquid, 20: 13112
MATORA, I. M., Pulsed research reactor and feasibility of pulsed reactor application in neutron spectroscopy, 20: 14191 (BNL-tr-60)
MATSUBARA, T., Thermal neutron diffusion length measurements in poisoned organic material, 20: 13718
MATSUDA, Michinori, Effects due to low-dose irradiation in utero, 20: 12683
MATSUNAGA, Sakuro, Current distribution in MHD Hall generators, 20: 13428 (JAERI-1093)
MATSUURA, T., Dynamic extraction of recoil products from complex ions adsorbed on an ion exchanger, 20: 12897
MATTHES, W., Cross-correlation method for study of neutron pulse transfer function, 20: 13724
MATTOS, Marieta C., Paramagnetic studies of holmium by neutron total cross section measurements, 20: 13772 (IEA-99)
MATULENKO, Yu. A., Elastic 180° scattering of π^{+} mesons by protons at high energies, 20: 13471
MATVEEVA, I. I., Calorimetric detector for measuring energy of an ionized beam, 20: 13114
MAUSBERG, W., Bibliography on accelerators, 11/65, 20: 13357 (AED-C-18-06)
MAVROMATIS, H. A., Magnetic moment corrections to second order in perturbation theory, 20: 13838
MAXIE, E. C., Comparative inactivation of conidia, mycellia, and sclerotia of Botrytis cinerea by γ radiation, 20: 13149 (UCD-34P80-3, pp 176-89)
MAXIE, E. C., Effect of γ irradiation on fresh prunes, 20: 13144 (UCD-34P80-3, pp 69-74)
MAXIE, E. C., Effect of γ irradiation on lemon fruits, 20: 13145 (UCD-34P80-3, pp 75-83)
MAXIE, E. C., Effect of γ irradiation on ripening of bananas, 20: 13146 (UCD-34P80-3, pp 84-91)
MAXIE, E. C., Effect of γ irradiation on peaches, 20: 13147 (UCD-34P80-3, pp 92-8)
MAXIE, E. C., Effect of γ irradiation on post-harvest behavior of tomato fruits, 20: 13148 (UCD-34P80-3, pp 99-175)
MAXIE, E. C., Gamma-ray radiosynthesis of ozone from air, 20: 12885 (UCD-34P80-3 pp 59-68)
MAXIE, E. C., Gas exchange in Bartlett pears in relation to γ irradiation, 20: 13140 (UCD-34P80-3, pp 27-47)
MAXIE, E. C., Interaction of γ irradiation, sealed packages, and controlled atmosphere on incidence of Botrytis rot in strawberries, 20: 13139 (UCD-34P80-3, pp 9-26)
MAXIE, E. C., Mn^{2+} in ^{60}Co γ-irradiated strawberries, 20: 13143 (UCD-34P80-3, pp 55-7)
MAXIE, E. C., Prog. rpt. on radiation technology in extending shelf life of fruits and vegetables, annual, 2/64–1/65, 20: 13138 (UCD-34P80-3)
MAXIE, E. C., Sensory evaluation of irradiated cherries, 20: 13141 (UCD-34P80-3, pp 48-51)
MAXIE, E. C., Thiamine and niacin analysis of irradiated strawberries, 20: 13142 (UCD-34P80-3, pp 52-4)
MAYO, G. T. J., Long-term compatibility of thermionic converter materials with cesium, 20: 13203
MAYS, Charles W., Trophic level effect on ^{137}Cs concentration, 20: 12611
MAZEL, Annie, Coefficient of absorption of electrons accelerated by voltages between 100 and 1200 kv, 20: 13967
MC CARTHY, G. J., Prog. rpt. on crystal chemistry, 5/13–8/13/65,

20: 13260 (NP-15852)
MC CLOUD, K. L., Preferred rates in helium film transfer, 20: 13682
MC COLLUM, Bill Crews, Phase study of dysprosium–dysprosium(III) chloride system, 20: 12821 (IS-T-62)
MC CORMICK, J. Frank, Interactions of γ radiation and other environmental stresses on pine seeds and seedlings, 20: 12673
MC CORMICK, W. B., Measurements of fast reactor spectra, 20: 14086
MC CREARY, Joseph C., Operating characteristics of the present PM-type reactor instrumentation. Task 2 topical report, 20: 14134 (NYO-3379-2)
MC CURDY, H. C., AVR-German pebble-bed reactor, 20: 14136 (ORNL-3885, pp 150-94)
MC CURDY, H. C., Fueled-graphite development, 20: 13215 (ORNL-3885, pp 3-86)
MC CURDY, H. C., Irradiation testing of components and materials, EGCR, 20: 14140 (ORNL-3885, pp 284-93)
MC CURDY, H. C., Moderator materials, 20: 13262 (ORNL-3885, pp 195-235)
MC DANIELS, D. K., Decay of ^{56}Ni and ^{57}Ni, 20: 13815
MC EACHERN, A. D., Fast test for excessive ^{235}U concentrations in enriched fuel elements, 20: 14168
MC FADDEN, P. W., Film free convection in helium II, 20: 13696
MC GINNIS, John T., Recovery of hardwood stands 3 to 5 years following acute irradiation, 20: 12675
MC GOWAN, R. D., Fabrication and testing of depleted uranium blanket slugs for EBR-II, 20: 13206 (ANL-6417)
MC HENRY, R. E., Heat transfer in the design of large radioisotopic heat sources, 20: 13157 (ORNL-P-1945)
MC INTOSH, H. W., Hyperpigmentation and pituitary tumor as sequelae of surgical treatment of Cushing's syndrome, 20: 12737
MC INTOSH, R. G., Mean lifetime of free radical chains in ^{60}Co γ-irradiated chloral hydrate and bromal hydrate solutions, 20: 12887
MC JUNKIN, Robert E., Interactions of γ radiation and other environmental stresses on pine seeds and seedlings, 20: 12673
MC KEE, B. T. A., Influence of crystallinity on positron-annihilation angular correlation in teflon, 20: 13468
MC KENZIE, A. D., Hyperpigmentation and pituitary tumor as sequelae of surgical treatment of Cushing's syndrome, 20: 12737
MC KEON, J. T., Primary piping flexibility analysis for liquid-metal-cooled fast breeder reactors, 20: 14120 (COO-1454-1)
MC LAFFERTY, George H., Gaseous reactor container, 20: 14054
MC NICHOLS, J. L., Positive column striations in magnetic field, 20: 13944
MC REE, P. C., High-volume, air-monitor calibration facility, 20: 13077 (Y-1503)
MC TAGGART, M. H., Prompt neutron decay constant of VERA reactor, 20: 14089
MC WHIRTER, A. D., Neutron production in unirradiated EBOR fuel elements due to the (α,n) reaction, 20: 14124 (GAMD-6859)
MEAD, Richard Oliver, Energy levels of ^{211}Bi, 20: 13895
MEAKER, R. E., Reaction rate of U metal with UF_4 in molten fluoride solutions, 20: 13170 (BM-RI-6736)
MEASDAY, David F., Neutron-proton differential cross section at 129 and 150 Mev, 20: 13500
MEASDAY, David F., Reaction $^{12}C(p,pn)^{11}C$ from 50 to 160 Mev, 20: 13833
MEASON, J. L., Photofission of ^{238}U induced by 17.5-Mev monoenergetic γ rays, 20: 13860
MECHAM, W. J., Engineering development of fluid-bed fluoride volatility processes. III., 20: 12923 (ANL-6898)
MEDIN, S. A., Variational problem of flow in an MHD generator channel, 20: 13437
MEERSON, G. A., Structure and physical and mechanical properties of WC–NbC–Co systems, 20: 13274
MEISSNER, H., Dose dependence of annealing stage II in neutron-irradiated aluminum, 20: 13340
MEISTER, G., Startup experiments on FRJ-2 reactor, 20: 14184 (JUL-236-RE)
MEISTER, H. H., Fast-reactor physics parameters from pulsed source, 20: 14202
MELCHING, H. J., Problem of combined radiologic and surgical injuries, 20: 12684
MELCHING, Hans-Joachim, Investigations on combination injuries. IV., 20: 12704
MELTON, Jimmy G., Resonances and waves in one- and two-ion species plasmas subjected to intense magnetic fields, 20: 13920 (NP-15703, pp 1-51)
MELTON, Jimmy G., Shock ionization for ion-cyclotron wave experiment, 20: 13921 (NP-15703, pp 52-63)
MEMMERT, G., Pulsed neutron reactivity measurements in the near-critical state, 20: 14082
MENENDEZ, M. G., Program to compute the classical deflection function, 20: 13415 (ORNL-3881)
MENGELKAMP, Bernhard, Density measurement with radioactive beams in explosion-possible atmospheres, 20: 13150
MENTZONI, M., Prog. rpt. on plasma-covered slot antennas, 11/62–9/65, 20: 13022 (AFCRL-65-859)
MENZEL, R. G., Soil-plant relationships of radioactive elements, 20: 12608
MERCER, Nina J. H., Selective elution of scintillation phosphors from chromatography paper, 20: 12929
MERCIER, C., Fabrication of second set of U–Pu fuel elements for substitution experiments, 20: 13214 (EURAEC-1484)
MERICLE, L. W., Reassessing biological role of background terrestrial radiation as a constituent of the natural environment, 20: 12587
MERICLE, R. P., Reassessing biological role of background terrestrial radiation as a constituent of the natural environment, 20: 12587
MERINFELD, G., Prog. rpt. on selective absorption of Sr by Acantharia, annual, 2/63–3/64, 20: 12591 (EUR-2475.f)
MERRILL, E. T., Calibration of high speed burnup code for nuclear fuel surveys, 20: 14118 (BNWL-183, Sect.IV)
MERRILL, E. T., Monte Carlo calculations of optimum loading of plutonium in thermal reactor fuels, 20: 14057 (BNWL-183, Sect.I)
MESSENGER, G. C., Displacement damage in MOS transistors, 20: 13133
MESSER, C. E., Dissociation pressure of system Yb–YbH_2, 20: 12829 (TID-22502)
MESSERSCHMIDT, O., Problem of combined radiologic and surgical injuries, 20: 12684
MESSERSCHMIDT, Otfried, Investigations on combination injuries. IV., 20: 12704
MESTVIRISHVILI, M. A., Asymptotic behavior of scattering amplitude at large momentum transfers, 20: 13546 (JINR-P-2519)
METZGER, Charles Frederick, Sorption of Cs by montmorillonite, 20: 12873
MEYER, D. I., Programmed spot automatic scanning system for spark chambers, 20: 13106
MEYER, L., Internal pair formation following neutron capture, 20: 13762 (CONF-233(Vol.4), pp 700-9)
MEYER, O., Fabrication and study of thick-base surface-barrier detectors, 20: 13093
MEYER, P., Experimental study of the $k\beta/l$ pulsed neutron source technique in light water assemblies, 20: 14162
MEYER, R. J., Spectrophotometric determination of Ru with 1-nitroso-2-naphthol, 20: 12788
MEYER, S. L., Existence of spions from K^+ decay, 20: 13497
MIA, M. Mohtazuddin, 500-Curie irradiation facility, 20: 12911 (AECD/HP/3)
MICHALOWICZ, J., Semiconductor detectors of surface-barrier type, 20: 13072 (RT/EL(65)7)
MIGDAL, A. B., Theory of finite fermi systems and properties of atomic nuclei, 20: 13632
MIKSCHE, Jerome P., Quiescent center of primary root of Glycine max, 20: 14215 (BNL-8643)
MIKULSKI, Jan, Electrolytic preparation of lead targets from stable isotopes ^{206}Pb and ^{207}Pb in sulfates form, 20: 12867
MIKUS, E. B., High-remelt-temperature brazing of Ta using diffusion sink concept, 20: 13224
MILICH, J. J., Development of high-temperature molten lithium pump, 20: 12948
MILLARD, Rosemary E., Abnormalities of human chromosomes following therapeutic irradiation, 20: 12658
MILLER, Lee N., Changes in radiosensitivity of pine seedlings subjected to water stress during chronic γ irradiation, 20: 12674
MILNE, George Angus, Improvements in or relating to tube joints, 20: 12951
MILOVANOV, V. P., Distribution of knock-out nucleons as a function of nuclear volume, excitation energy, and nuclear recoil momentum distributions in cascade processes, 20: 13892
MILSTED, J., Yield data for transplutonium element production in thermal reactors, 20: 13752 (ANL-7096)
MINAMI, Shigeo, Energy dependence of the real part of π-p scattering amplitude, 20: 13503
MINCK, R. W., Optical frequency plasma resonance in gases, 20: 13942
MINETTI, B., Photoemission of neutrons at 6 to 80 Mev from ^{9}Be, 20: 13795
MINGARRO, E., Considerations on the genesis of uraniferous deposits. II., 20: 12996 (JEN-155-SIG/I-4)
MINNIGERODE, B., Unilateral insertion of ^{60}Co implants in thyroid cartilage for laryngeal carcinoma, 20: 12758
MINX, Ramon P., Radioactive waste material incinerator, 20: 14212
MIRION, L., Nondestructive testing methods applicable to sintered materials, 20: 13319
MISSONI, G., Scattering of 662-Kev γ rays on bound electrons, 20: 13756 (CONF-233(Vol.4), pp 562-94)
MISTRY, K. B., Radioactivity of plants from high radiation areas of Kerala coast and adjoining regions. II., 20: 12987
MITCHELL, G. M., Pituitary implantation for pituitary tumors, 20: 12753
MITROFANOV, A. S., Kinetics of $MoSi_2$ oxidation at 1500 to 1800°C, 20: 13195

MITROFANOV, A. S., Oxidation of WSi_2 at 1500 to 1800°C, 20: 13196
MITROFANOV, A. S., Oxidation of $TaSi_2$ in temperature range from 1400 to 1800°C, 20: 13197
MITSUHASHI, Tadashi, Iron core, having many legs, for a betatron, 20: 13392
MITTA, Aldo E. A., Preparation of ^{131}I-allyl-inulin, 20: 12912 (CNEA-161)
MITTA, Aldo E. A., Separation of ^{131}I-rose bengal by thin-layer chromatography, 20: 12763 (CNEA-162)
MITTAL, M. L., Electrometric studies on compositions of uranyl vanadates, 20: 12796
MITTELSTAEDT, P., Method of effective interaction in nuclear physics, 20: 13791
MIYAMOTO, Yoneji, Three kinds of triplet model, 20: 13605
MIYANAGA, Ichiro, Comparison of methods of personnel-monitoring dosimetry practiced in nuclear establishments of different countries, 20: 13003 (JAERI-4035)
MIYAZAWA, Hironari, Proton-neutron mass difference, 20: 13511
MIYAZIMA, Tetsuoki, Emission of light fragments from heavy nuclei in high-energy nuclear reactions, 20: 13880
MIYOSHI, Akiyoshi, Particle size of submicron W and WC powders for WC–Co alloy, 20: 13226
MOBERG, Carl Ake, Flanged joint, 20: 14049
MOH, C. C., Bean mutant induced by ionizing radiation. I., 20: 12709
MOH, C. C., Bean mutant induced by ionizing radiation. II., 20: 12710
MOHAI, Miklos, Problems in determination of uranium with Arsenazo III, 20: 12799
MOHLER, Ronald Rott, Optimal control of nuclear reactor processes, 20: 14020
MOISAN, J., Frittoxal ($Al–Al_2O_3$) and nuclear applications, 20: 13213 (EUR-2447.f)
MOLINO, C., Photoemission of neutrons at 6 to 80 Mev from ^{9}Be, 20: 13795
MOLL, E., Thyroid scintigraphy with Tc-99m, 20: 12749
MONAHAN, J. E., Measurements of neutron cross sections of Fe, Al, and CF_2 by a ratio method, 20: 13716
MONAHAN, J. E., Polarization and differential cross sections in small-angle scattering of neutrons by uranium, 20: 13868
MONATERI, P. C., Delayed effects of ionizing radiation: changes in seminal tissue, 20: 12686
MONGON, A., Electrodeless conductivity meter for on-stream measurements, 20: 12927 (NP-15756)
MONIER, J., Potentialitites of γ spectrometry in nondestructive measurements on fuel elements, 20: 14158
MONREAU, Claude, Process for preparation of UC powder, 20: 13190
MONSONEGO, G., Octupole vibration and E1 transition probabilities in odd-mass nuclei in the rare earth region, 20: 13820
MONTVAY, I., Convergence of peratization, 20: 13567
MOODY, A. J., Radioimmunologic method of determination of insulin, 20: 12754
MOORE, A., Ageing effects on beryllium single crystals, 20: 13237 (CONF-170, pp 29-47)
MOORE, A., Deformation and fracture in single- and polycrystalline beryllium between 20 and 450°C, 20: 13240 (CONF-170, pp 102-20)
MOORE, A., Structural application of beryllium in the U.K., 20: 13244 (CONF-170, pp 221-44)
MOORE, A., The effect of purification and recontamination on slip in beryllium single crystals, 20: 13239 (CONF-170, pp 90-101)
MOORE, M., Pulsed and modulated experiments on fast multiplying media, 20: 13723
MOORE, M., Theory of pulsed and modulated experiments on fast neutron multiplying media, 20: 14088
MOORING, F. P., Polarization and differential cross sections in small-angle scattering of neutrons by uranium, 20: 13868
MORALES, E., Prog. rpt. on insect control by radiation, 7/63–6/64, 20: 12633 (NP-15348)
MORALES, E., Prog. rpt. on insect control by radiation, 6/64–3/65, 20: 12634 (NP-15349)
MORAN, W. H., Uranium–molybdenum alloy for use in prompt-burst reactor, 20: 13287
MORAVCSIK, Michael J., Final-state enhancement at 1920 Mev in π^-p inelastic scattering, 20: 13454 (UCRL-14100-T(Rev.1))
MORAVCSIK, Michael J., Spin structure of nucleon-nucleon scattering, 20: 13455 (UCRL-14240-T)
MOREAU, Gerard, Contribution to study of ^{57}Co, 20: 13799
MORGAN, Eric L., Effect of acute γ radiation on opossum, gray fox, raccoon, and bobcat, 20: 12667
MORGAN, J. G., Postirradiation examination of EGCR prototype capsule, 20: 14142 (ORNL-TM-1378)
MORGAN, William T., SNAP-10A, first reactor in space, 20: 14177
MORGENSTERN, H., Ionization defects of energetic ^{28}Al atoms in silicon, 20: 13989
MORI, K., Phenomenological analysis of high-energy scattering, 20: 13513
MORIGUCHI, E., Transforming activity and integrity of DNA as revealed by ultraviolet flow dichroism, 20: 12620
MORIKAWA, Tetsuya, Experiments on MHD generator driven by plasma jet, 20: 13435
MORITA, Masato, Possible G-parity nonconservation in muon capture reactions, 20: 13877
MORITA, Reiko, Possible G-parity nonconservation in muon capture reactions, 20: 13877
MOROZOV, V. A., Decay of ^{138}Pr, 20: 13882
MORRIS, L. L., Effect of γ irradiation on post-harvest behavior of tomato fruits, 20: 13148 (UCD-34P80-3, pp 99-175)
MORRIS, Peter R., Inversion of pole figures for materials having orthorhombic symmetry, 20: 13983
MORRIS, Roger A., Investigation of neutron collimators and their application in neutron radiography, 20: 13702 (LA-DC-7594)
MORRISON, G. H., Determination of boron by thermal neutron activation analysis using a modulation technique, 20: 12784
MORRISON, G. H., Modulation technique for neutron-capture γ measurements in activation analysis, 20: 12783
MORROW, Lewis B., Active tuberculosis in leukemia, malignant lymphoma, and myelofibrosis, 20: 12639 (TID-21517)
MOSTOVOI, V. I., Neutron-thermalization process in time in graphite and beryllium, 20: 13738
MOSTOVOI, V. I., Neutron thermalization in time in aqueous moderators, 20: 13739
MOSTOVOI, V. I., Neutron thermalization in graphite-water system at large temperature gradients, 20: 13740
MOTTE, F., Study of $UO_2–PuO_2–H_2O$ lattices by pulsed neutron techniques, 20: 14078
MOTZ, J. W., Scattering cross sections for 50- to 500-kev electrons, 20: 13757 (CONF-233(Vol.4), pp 595-608)
MOUSSEZ, Claude Henri Charles, Improvements in or relating to nuclear reactors, 20: 14042
MOWBRAY, D. F., Fatigue characteristics of Ni–Cr–Fe alloys with emphasis on pressure-vessel cladding, 20: 13255 (KAPL-3108)
MOZRZYMAS, J., Classification of higher symmetry groups, 20: 13577
MUELLER, K.-H., One-group parameters by neutron wave measurements, 20: 14073
MUELLER, M. H., Neutron-diffraction study of $UO_2(NO_3)_2 \cdot 6H_2O$, 20: 13233 (ANL-6943)
MUELLER-BUSCHBAUM, Hk., Structure investigations on La_2O_3, 20: 12872
MUENZEL, H., Separation of Cd and In from fission product mixtures, 20: 12936
MUETTERTIES, E. L., Chelate chemistry. IV., 20: 12853
MUKHERJEE, S. K., Decay of ^{183}Hf and the nuclear spectroscopy of ^{183}Ta, 20: 13863
MUKOYAMA, T., Thermal neutron diffusion length measurements in poisoned organic material, 20: 13718
MULFORD, R. N. R., System plutonium–carbon–oxygen, 20: 13291
MULLER, O., Prog. rpt. on crystal chemistry, 5/13–8/13/65, 20: 13260 (NP-15852)
MURADYAN, R. M., Symmetries of lepton-lepton interactions, 20: 13547 (JINR-P-2523)
MURAI, Hiroshi, Experiments on MHD generator driven by plasma jet, 20: 13425
MURAY, J. J., Efficiency of secondary electron emission monitors for 70-Mev electrons, 20: 13103
MURAY, J. J., Magnetic field measurement and spectroscopy in multipole fields, 20: 13365 (SLAC-39(Rev.))
MURRENHOFF, A., Comparative investigations on counting methods for absolute determination of activity of α emitters, 20: 13066 (JUL-298-PC)
MURTHY, Gopala K., Comparison of ^{90}Sr component of human and cows' milk, 20: 13012
MUSIN, A. K., Disappearance of charge carriers in plasma moving in an electric field, 20: 13952
MUSTACCHI, C., Controlled expansion of UC pellets by surface oxidation in cladding, 20: 13188
MUSTARD, G. L., Radiation alarm instrument instruction manual, 20: 13001 (GAT-T-1222)
MYTTENAERE, C., Distribution of Sr and Ca in Pisum sativum, 20: 12605
MYTTENAERE, Constant, Movement of fallout in irrigated ecosystems of Po Valley, Italy, 20: 12986

N

NAGASAKI, Ryukichi, Metallographic observations of creep deformation of Magnox AL 80, 20: 13311
NAGY, K. L., Approximate symmetries in field theory, 20: 13558
NAGY, T., Approximate symmetries in field theory, 20: 13558
NAGY, T., Leptonic decays in the unitary symmetry scheme, 20: 13466
NAIL, J. H., New fuel configuration to increase plutonium value, 20: 14102 (BNWL-183, Sect.II)
NAKAGAWA, Shigeru, Effects due to low-dose irradiation in utero,

20: 12683
NAKAI, Sadao, Study of shock waves by microwave techniques, 20: 13936
NAKAMURA, Kosuke, Emission of light fragments from heavy nuclei in high-energy nuclear reactions, 20: 13880
NAKAMURA, Morio, Analytic property of fifth-order Feynman graph, 20: 13593
NAKAMURA, Seitaro, Quantum numbers of particles, 20: 13621
NAKAMURA, Y., Assessment of end-plug welding of fuel elements, 20: 14196
NAKAMURA, Y., Measurement of internal friction of nuclear materials, 20: 13321
NAKAMURA, Y., Ultrasonic testing of metallic uranium, 20: 14194
NAKANO, Takenori, Thermal and dynamical properties of a protostar and its contraction to stage of quasi-static equilibrium, 20: 13408
NAKANO, Yoshiei, Hysteresis phenomenon near B_C in positive column in a magnetic field, 20: 13937
NAMBU, Y., Coupling-constant relations for vector and scalar mesons, 20: 13486
NAMBU, Yoichiro, Baryon structure and electromagnetic properties, 20: 13509
NAMIKI, Mikio, Elementary particle structures and meson-nucleon backward scatterings, 20: 13510
NARAYANASWAMY, P., A new approach to algebra of current operators, 20: 13533 (IC/66/3)
NARGUNDKAR, V. R., Pulsed neutron studies of BeO–natural uranium lattices, 20: 14080
NARITA, Masakuni, After-pulses of the G-M counter dependent upon intensity of nuclear radiation, 20: 13083
NARITA, Yuichi, After-pulses of the G-M counter dependent upon intensity of nuclear radiation, 20: 13083
NARITOMI, Tatsuo, Fabrication of UO_2 fuel element by vibratory compaction, 20: 13225
NARTOVA, T. T., Equilibrium diagram of quasi-ternary system Ti_3Al–Ti_3Sn–Zr, 20: 13273
NASCUTIU, T., Paper chromatography of inorganic substances. III., 20: 12939
NASEBAND, A., Development of a chalk-dust measuring device, 20: 13024 (EUR-2544.d)
NATAPOFF, Alan, Differential cross section for π^--p elastic charge-exchange scattering, 20: 13525
NATERA, M. G., Removal of second-order neutrons by oriented single crystals, 20: 13709 (PAEC-IPA(D)PH-652)
NATH, P., Threshold poles and low-energy scattering, 20: 13588
NAUDET, R., Heavy water gas-cooled reactor in the French program, 20: 14150
NAUMKIN, O. P., Rare earth alloys and compounds, 20: 13280
NAVARRO, Q. O., Removal of second-order neutrons by oriented single crystals, 20: 13709 (PAEC-IPA(D)PH-652)
NAWAR, Wassef W., Prog. rpt. on stability of food lipids to ionizing radiation, 2–8/65, 20: 12618 (TID-22399)
NECHIN, Yu. A., Fluctuations of energy fluxes of nuclear-active and electron-photon components in extensive air showers, 20: 13427
NECHIPORENKO, E. P., Kinetics of $MoSi_2$ oxidation at 1500 to 1800°C, 20: 13195
NECHIPORENKO, E. P., Oxidation of WSi_2 at 1500 to 1800°C, 20: 13196
NECHIPORENKO, E. P., Oxidation of $TaSi_2$ in temperature range from 1400 to 1800°C, 20: 13197
NEEF, W. I., Conservation economics and reactor technology, 20: 14011 (BNWL-183, Sect. V)
NEIDER, R., Eddy-current testing of thin-walled cladding tubes, 20: 14033
NELKIN, M., Summary of symposium on pulsed neutron research, 20: 13725
NELSON, L. S., Combustion and explosion of zirconium droplets ignited by flash heating, 20: 12826 (SC-RR-65-569)
NELSON, P. A., Critical temperatures and densities of alkali metals, 20: 12815 (ANL-7025)
NELSON, R. C., Irradiation of 0.5-inch-diameter, solid-pellet UO_2 fuel rods, 20: 13326
NELSON, R. S., Atomic collision sequences and thermal spikes in α uranium, 20: 13334
NEMETH, J., Superconductive model with two kinetic energies for even and odd systems, 20: 13669
NETZ, V., Determining optimal layer thickness for C/H analysis by means of neutrons, 20: 12791
NEUBERT, Theodore J., Influence of temperature on F-center absorption in NaF, 20: 12892
NEUNZERT, H., Initial value problem for stationary Boltzmann-Vlasov equation, 20: 13910 (JUL-297-MA)
NEUSTADT, M., Displacement damage in MOS transistors, 20: 13133
NGUYEN-LONG-DEN, Separation of radiocesium by effect of thermoionization, 20: 13159
NICHOLAS, Ridley, Problems regarding the competitiveness of nuclear power reactors, 20: 14133 (NP-15587)
NICKERSON, J. T. R., Storage of eviscerated haddock in refrigerated sea water treated with γ radiation, 20: 13152
NICODEMI, W., Zircaloy-2–stainless steel diffusion bonds, 20: 13222
NICOLAENKO, B., Pulsed and modulated experiments on fast multiplying media, 20: 13723
NICOLAENKO, B., Theory of pulsed and modulated experiments on fast neutron multiplying media, 20: 14088
NIECE, Lawrence H., Independent yields of ^{95}Zr from thermal neutron fission of ^{235}U and ^{233}U, 20: 13783 (ORNL-TM-1333)
NIEDERLE, J., Discrete degenerate representations of non-compact rotation groups, 20: 13532 (IC/66/2)
NIELSEN, J. M., Cosmic-ray produced radionuclides in the environment, 20: 12571
NIMWANADON, T., Removal of second-order neutrons by oriented single crystals, 20: 13709 (PAEC-IPA(D)PH-652)
NISHI, Tatsuo, Comparison of methods of personnel-monitoring dosimetry practiced in nuclear establishments of different countries, 20: 13003 (JAERI-4035)
NISHIHARA, Hideaki, Application of adiabatic approximation to space-dependent kinetics of boiling water reactors, 20: 14074
NISHIJIMA, K., Dynamical interpretation of spurions, 20: 13607
NISHIKAWA, T., Aperture and cell-size effects on shunt impedance of alternating periodic structures, 20: 13358 (BNL-9944)
NISHITA, H., Decay characteristics of neutron-induced radioactivity in soils, 20: 12582
NISHIYAMA, Atsushi, Fabrication of UO_2 fuel element by vibratory compaction, 20: 13225
NISHIYAMA, Atsushi, Fabrication study of uranium nitride fuel, 20: 13227
NISSEN, D. A., Electrochemistry of Pu(III) in molten alkali chlorides, 20: 12816 (BNWL-158)
NOBILI, D., Thermal and electrical conductivity of SAP, 20: 13306
NOBLE, Gordon A., Power dependence of saturation of EPR spectrum of F center at 4°K, 20: 13975 (TID-21571)
NOJIRI, Toshiaki, Study of intensification of front lead screen for γ radiography, 20: 12974
NOSHKIN, V. E., Low-background β detector for solid sample assay, 20: 13102
NOVGORODOV, A. F., Decay of ^{138}Pr, 20: 13882
NOVIKOFF, Alex B., Prog. rpt. on cytochemical and electron microscopic studies of radiation damage, final, 1965, 20: 12635 (NYO-2786-1)
NOVIKOV, V., Search for new decay modes of K^0_2 mesons, 20: 13450 (JINR-P-2488)
NOZIK, V. A., Neutron-thermalization process in time in graphite and beryllium, 20: 13738
NYBERG, R. A., Characteristics of ^{40}K distributed sources in water, 20: 13056 (AD-627000)
NYE, Anthony Edward Thomas, Shutdown apparatus for gas-cooled reactors, 20: 14046

O

ODUM, Eugene P., Feedback between radiation ecology and general ecology, 20: 12570
OEFF, K., Bibliography on nuclear medicine, 9/65, 20: 12733 (AED-C-10-04)
O'FALLON, John Robert, Reaction $^3He(\gamma,\pi^+)^3H$ up to 260 Mev, 20: 13896
OFER, S., Moessbauer effect in ^{161}Dy in $DyCo_2$ and $DyNi_2$, 20: 13992
OFFUTT, G. F., Uranium recovery from aluminum-alloyed fuel, 20: 12926 (IDO-14669)
OGANESYAN, K. O., Charged meson production in neutron-proton collisions at 600-Mev neutron energy, 20: 13453 (JINR-P-2511)
OGAWA, Shuzo, Weak intermediate boson, 20: 13608
OGAWA, Tohru, Stability and instability of planewave Hartree-Fock solutions and the helical spin arrangement, 20: 13423
OGAZA, S., Magnetic interaction of ^{155}Gd nucleus in 87-kev excited state, 20: 13763 (CONF-233(Vol.4), pp 710-19)
OGUNKOYA, L., Deuterium and tritium exchange reactions of phenols, 20: 12880
OHNO, Akira, Study of intensification of front lead screen for γ radiography, 20: 12974
OHNO, E., Digital speed and phase control system for three-rotor type neutron choppers, 20: 13713
OHNUKI, Yoshio, Abnormal solution of Bethe-Salpeter equation, 20: 13614
OHNUKI, Yoshio, New concept of elementary particles and method of the composite model, 20: 13613
OHSE, Roland W., High-temperature vapor-pressure studies of UO_2 by the effusion method and its thermodynamic interpretation, 20: 13288
OHTSUBO, Hisao, Possible existence of wrong G-parity interaction in muon capture, 20: 13505
OHWADA, Ken, Chemical degradation of kerosene diluent with nitric acid, 20: 12934
Oi, Yoshiko, Proton-neutron mass difference, 20: 13511
OKADA, Tsuichi, Neutron activation analysis of divalent ions in alkali halide crystals, 20: 12805

OKANO, Kotoyuki, Characteristics of gamma-block stilbene detector, 20: 13063 (JAERI-1092)
OKAZAKI, A., Neutron absorption cross section of gross fission products of ^{233}U, ^{235}U, and ^{239}Pu, 20: 13748 (AECL-2510)
OKI, Iwashiro, X rays from color television receivers, 20: 13014
OKONOV, E., Leptonic decays of K^0 mesons and possible CP violation, 20: 13515
OKONOV, E., Search for new decay modes of K_2^0 mesons, 20: 13450 (JINR-P-2488)
OKOROKOV, V. V., Coherent excitation of nuclei moving through crystals, 20: 13888
OKUBO, S., Higher symmetry groups with parity mixing, 20: 13599
OKUBO, S., Models of elementary particles and algebra of currents, 20: 13491
OKUN', L. B., C-odd multipoles, 20: 13475
O'LEARY, M. E., Biological importance of uv-induced DNA-protein cross-links in E. coli, 20: 12621
OLIPHANT, G. W., Fabrication of miniaturized hardware for space equipment, 20: 12642 (Y-IA-17)
OLIVEIRA, C. G., Two-component spinors in Hamiltonian formulation of general relativity, 20: 13660
OLIVER, John, Improvements in or relating to nuclear reactors, 20: 14038
OLLERHEAD, R. W., Excited states of ^{19}F by angular correlation technique, 20: 13822
OLSON, J. S., Oak Ridge, Tennessee, flora, I. vascular plants, 20: 12567 (ORNL-TM-1232)
OLSON, Jerry S., Equations for cesium transfer in a Liriodendron forest, 20: 12577
OMBERG, Ronald Paul, Effect of natural convection upon temperature transient following a loss-of-coolant accident, 20: 14147 (UCRL-16394)
ONEDA, Sadao, Role of partially conserved axial-vector current in $\pi_{\mu 2}$ and $K_{\mu 2}$ decays, 20: 13508
ONORI, G., Theory of quasistationary plasmas in contact with a wall, 20: 13912 (LGI-65/21 and App.)
OPAUSZKY, Istvan, Determination of ^{18}O content in small samples of water by mass spectrometry, 20: 12800
ORLOVA, I. M., Induced synchrotron radiation of electrons in cavity resonators, 20: 13472
ORMAI, Sandor, Effects of whole-body irradiation and bone marrow irradiation on osmotic resistance of reserve leukocytes, 20: 12705
ORMEROD, M. G., Reaction of radicals induced in E. coli by γ rays with cysteamine and with oxygen, 20: 12622
ORR, D., Geomagnetic micropulsations, 20: 13645 (AWRE-O-9/66)
OSBORNE, M. F., Postirradiation examination of EGCR prototype capsule, 20: 14142 (ORNL-TM-1378)
OSBORNE, W. Z., Apparent correlations between production processes and decay chains which include pions, 20: 13487
OSBURN, W. S., Primordial radionuclide distribution, movement, and ecosystem effects, 20: 12982
OSHINO, Akira, X rays from color television receivers, 20: 13014
OSIKO, V. V., Effect of hard radiation on optical centers of TR^{3+} ions in crystals, 20: 13986
OSIUMI, Yosihiko, Influence of radioprotective substances on damages to bone growth in rats, 20: 12729
OTSUKI, Shoichiro, Possible origin of repulsive core in nuclear forces, 20: 13879
OUANG, T. Y., Prog. rpt. on application of isotopes and radiation in rice cultivation, final, 8/65, 20: 12593 (NP-15672)
OVCHARENKO, V. I., Electric quadrupole transitions between rotary states with large spins in even nuclei, 20: 13801
OWEN, L. W., Shell-model form factors for $^{90}Zr(p,p')$ reaction, 20: 13867
OZAKI, Seinosuke, Masses of particles proposed by Tanikawa and Watanabe, 20: 13504
OZAWA, Yasutomo, After-pulses of the G-M counter dependent upon intensity of nuclear radiation, 20: 13083
OZERNOI, L. M., Magnetic bremsstrahlung in variable field as mechanism behind the changing radiance of quasistellar radio sources, 20: 13407

P

PACER, Richard Arnold, Analytical chemistry of technetium, 20: 12809
PADERNO, Yu. B., Physical properties and chemical bond in rare earth chalcogenides, 20: 12849
PADGETT, R. A. Jr., Diffusion studies of ^{95}Nb polycrystalline UO_2 between 1100 and 2100°C, 20: 13289
PAFOMOV, V. E., Transition radiation of charged relativistic particle in optical frequency range, 20: 13788 (ORNL-tr-1062)
PAI, R. H., Departure from nucleate boiling in steam–water mixtures flowing in vertical round tubes, 20: 12968
PAI, Shih-I, Critical survey of magnetofluid dynamics, 20: 13635 (ARL-63-175(Pt.3))
PAL, Imre, Effects of whole-body irradiation and bone marrow irradiation on osmotic resistance of reserve leukocytes, 20: 12705
PAL, L., Data evaluation problems in pulsed neutron source method, 20: 13729
PALMA, V., Prog. rpt. on selective protection of damages induced by x irradiation and radiomimetic drugs, 11/64–1/65, 20: 12717 (NP-15666)
PALMA, V., Prog. rpt. on selective protection of damages induced by x irradiation and radiomimetic drugs, annual, 9/15/64, 20: 12718 (NP-15667)
PALMA, V., Prog. rpt. on selective protection of damages induced by x irradiation and radiomimetic drugs, final, 9/65, 20: 12719 (NP-15668)
PALMER, H. E., Seasonal cycle of ^{137}Cs in some Alaskan natives and animals, 20: 12983
PANFILOV, A. S., Effect of pressure on magnetic susceptibility of Mn and Sc, 20: 13312
PANKRATOVA, T. B., Induced synchrotron radiation of electrons in cavity resonators, 20: 13472
PANOV, V. S., Structure and physical and mechanical properties of WC–NbC–Co systems, 20: 13274
PANTUJEV, V. S., Investigation of total absorption lead-glass Cherenkov γ spectrometer in energy range 0.25 to 4.0 Bev, 20: 13105
PAPAY, L. T., Measurement of integral parameters in fuel rods, 20: 14103 (MIT-2344-4, pp 48-62)
PAPEZIK, F., Ultrasonic inspection following heat treatment of uranium alloys, 20: 13318
PAPKOW, A., Penning ion source for increased ion currents, 20: 13384
PAPROCKI, Stan J., Prog. rpt. on civilian applications, 11/65, 20: 13171 (BMI-1751)
PARDI, A. J., Effects of various grades of graphite electrodes in carrier distillation of impurities in U_3O_8, 20: 12771 (NLCO-967)
PARIKH, Vastupal, Angular distribution of photoprotons from carbon, 20: 13812
PARIS, C. H., Nuclear-reaction studies in Ni isotopes, 20: 13858
PARIS, Oscar H., Radiotracer, gravimetric, and calorimetric studies of ingestion and assimilation rates of an isopod, 20: 12610
PARISI PRESICCE, L., Semiconductor detectors of surface-barrier type, 20: 13072 (RT/EL(65)7)
PARK, Elkins, Plasma accelerator, 20: 13963
PARK, J. G., Magnetic hysteresis and surface superconductivity, 20: 13679
PARK, Robert L., Leed beam broadening as a result of sputtering damage, 20: 13981
PARKER, D. R., Chromosome pairing and induced exchange in Drosophila, 20: 12690
PARKER, J. B., Contribution of floor returns to neutron interaction, 20: 13742
PARKER, Raymond C., Effects of x-irradiated feeder layers on mitotic activity and development of aneuploidy in mouse-embryo cells, 20: 12654
PARKINSON, Ernest Roland, Sub-barrier proton emission in compound nuclear reactions, 20: 13897
PASCARD, Roger, Fabrication of sintered compounds based on uranium and plutonium, 20: 13229
PASHCHENKO, L. P., New isotope ^{216}Ac, 20: 13779 (JINR-P-2465)
PASHOS, T. J., Irradiation of 0.5-inch-diameter, solid-pellet UO_2 fuel rods, 20: 13326 (GEAP-5100C)
PASHOS, T. J., Prog. rpt. on stainless steel failure, 7–9/65, 20: 13325 (GEAP-4968)
PASINT, D., Departure from nucleate boiling in steam–water mixtures flowing in vertical round tubes, 20: 12968
PASQUALINI, L., Photoemission of neutrons at 6 to 80 Mev from ^{9}Be, 20: 13795
PATERSON, W. J., Measurements of fast reactor spectra, 20: 14086
PATERSON, W. J., Prompt neutron decay constant of VERA reactor, 20: 14089
PATTERSON, H. Wade, Accelerator radiation monitoring and shielding, 20: 13367 (UCRL-16445(Rev.))
PATY, M., Muon and pion scattering in freon, 20: 13480
PAWLICKI, G., Investigations on self-diffusion of In by absorption method, 20: 13315
PAXTON, H. C., Criticality control in operations with fissile material, 20: 13005 (LA-3366)
PEARCE, K. W., Handling and filtration of radioactive sludges, 20: 14210
PEARCE, W. A., Phase-equivalent potentials for neutron-α elastic scattering, 20: 13482
PEARL, Judea, Vortex theory of superconductive memories, 20: 13689
PEARSON, J. D., Use of ^{51}Cr-labeled hemoglobin and ^{47}Sc as inert fecal markers, 20: 12612
PELLICCIONI, M., Liquid dielectric ionization chamber as means to study mixed radiation fields, 20: 13107
PELTE, D., Angular correlation studies using the $^{13}C(^{3}He,p\gamma)^{15}N$ reaction, 20: 13819
PENDLEBURY, E. D., Contribution of floor returns to neutron interaction, 20: 13742
PENDLEBURY, E. D., Use of the adjoint transport equation in solving

criticality problems, 20: 14094
PENDLETON, Robert C., Trophic level effect on ^{137}Cs concentration, 20: 12611
PEPPER, C. E., Effects of various grades of graphite electrodes in carrier distillation of impurities in U_3O_8, 20: 12771 (NLCO-967)
PEREC, Miecyslaw, Production of UO_2 by reduction of U(VI) in sodium carbonate solutions. I., 20: 12868
PERELYGIN, V. P., Half life of an isotope of element 102 with mass number 256, 20: 13778 (JINR-P-2525)
PERESLAVTSEV, E. B., Method of retaining and accumulating high-temperature plasma in a trap, 20: 13928 (AD-625070)
PEREZ, R. B., Excitation of neutron waves by modulated and pulsed sources, 20: 13722
PEREZ-ALBUERNE, E. A., Effect of very high pressure on structure of hcp metals and alloys, 20: 13316
PERKINS, R. W., Cosmic-ray produced radionuclides in the environment, 20: 12571
PERKINS, W. C., Chemical separation of reactor-produced ^{171}Tm, 20: 12764 (CONF-660305-8)
PERLSTEIN, P., Determination of γ flux in reactor by $^{14}N-^{15}N$ isotopic exchange reaction, 20: 14012 (IA-1048)
PERLSTEIN, P., Mechanism of radiolysis of CO_2, 20: 12882 (IA-1065)
PERONA, G., Zircaloy-2–stainless steel diffusion bonds, 20: 13222
PERONA, J. J., Estimated costs of high-level waste management, 20: 14208 (ORNL-P-1926)
PERRIER, Frantz, Coefficient of absorption of electrons accelerated by voltages between 100 and 1200 kv, 20: 13967
PERRY, A. M., Performance analyses, EGCR, 20: 14138 (ORNL-3885, pp 253-67)
PERRY, A. M., Studies for advanced systems, 20: 14137 (ORNL-3885, pp 236-43)
PERRY, K. E. G., Experimental system for thermoluminescent dosimetry, 20: 13059 (AEEW-R-411)
PERRY, Robert P., Quantitative autoradiography, 20: 12616
PERRY, Vernon P., Protection of lethally irradiated guinea pigs with leukocytes, 20: 12727
PESCHKA, W., Self-excitation of an electrodeless MHD generator, 20: 13429 (N64-32348)
PESCHKA, W., Theoretical studies of electrodeless MHD generator of infinite length, 20: 13430 (N64-32349)
PETELIN, M. I., Induced synchrotron radiation of electrons in cavity resonators, 20: 13472
PETERSEN, Kurt-Friedrich, Investigations on combination injuries. IV., 20: 12704
PETERSON, Steven H., Structure of gaseous XeF_6, 20: 12860
PETERSON, Vern LeRoy, Beta-decay inhibition and stellar abundance ratios in nucleosynthesis, 20: 13410
PETKAU, A., Fate of terphenyl in the rat, 20: 12589 (AECL-2507)
PETKOV, B., Radiosensitivity of guinea pigs with hypocatalasia, 20: 12643 (ANL-Trans-264)
PETKOV, I. Zh., Inelastic scattering of electrons on nuclei with collective level excitation, 20: 13775 (JINR-P-2490)
PETRANYI, Gyorgy Jr., Defense mechanisms of cysteamine and AET for intestinal radiation death, 20: 12721 (BNWL-tr-11)
PETREANU, E., Infrared absorption of 75% ^{18}O-barium phosphate, 20: 12861
PETRI, H., Gamma spectrometry with semiconductor detectors, 20: 13067 (JUL-308-RB)
PETROV, R., Transplantation immunity and radiative chimeras, 20: 12731
PETROVIC, M., Far subcriticality measurements by pulsed neutron technique, 20: 14201
PETTY, R. O., Rates and pattern of radioisotope release from fresh tree litter at three levels of mesic forest development, 20: 12566 (COO-1006-4)
PFLEGERS, L., Therapy of angiomas, 20: 12745
PHILLIPS, R. D., Longevity in neutron-exposed guinea pigs, 20: 12628 (AD-626997)
PHILLIPS, R. J. N., Charge-asymmetry effects in Λ-N, 20: 13485
PHILLIPS, R. J. N., Nucleon-antinucleon charge exchange in the absorption model, 20: 13494
PIATTI, G., Thermal transformations of aluminas extracted from $Al-Al_2O_3$ composites, 20: 13296
PIAZZOLI, A., Existence of ^4He excited levels and of other light nuclides, 20: 13834
PICKUP, J., Gamma-spectrum stabilizer with compensation for effects of detector temperature variation, 20: 13094
PICKWICK, K. M., Kinetics of $\beta \rightarrow \alpha$ phase change in U–1 at.% Pt alloy, 20: 13307
PICTON, G., Corrosion and ignition behavior of some U–Pu–Fe alloys, 20: 13200
PIEKARZ, H., Observation of fission events in mica sandwiches, 20: 13099
PIEKARZ, J., Observation of fission events in mica sandwiches, 20: 13099
PIEPENBRING, R., Octupole vibration and E1 transition probabilities in odd-mass nuclei in the rare earth region, 20: 13820
PIERCE, B. L., Modified transient and/or steady-state digital heat transfer code, 20: 12963 (WANL-TME-1108)
PIERCE, J. T., Switching characteristics of small geometry thin film superconductors, 20: 13048
PIGEON, Jacques, Formalism based on symmetric interaction in input and output methods for rearrangement collisions, 20: 13798
PIGEON, M., Ultrasonic inspection following heat treatment of uranium alloys, 20: 13318
PILAT, E. E., Measurement of diffusion coefficient in an anisotropic medium, 20: 13705 (MIT-2344-4, pp 135-44)
PILAT, E. E., Single rod experiments in thermal energy region, 20: 14067 (MIT-2344-4, pp 80-8)
PILGER, Richard C., Prog. rpt. on reaction cross sections, final, 10/59–10/64, 20: 13787 (TID-22637)
PILUSO, C. J., Decay of ^{56}Ni and ^{57}Ni, 20: 13815
PINCHAS, S., Infrared absorption of 75% ^{18}O-barium phosphate, 20: 12861
PINDOR, M., $SU_2 \otimes SU_3$ content of the SU_6 representations, 20: 13580
PINEDA, V. M., Removal of second-order neutrons by oriented single crystals, 20: 13709 (PAEC-IPA(D)PH-652)
PIRAGINO, G., Photoemission of neutrons at 6 to 80 Mev from ^9Be, 20: 13795
PLACIOUS, R. C., Scattering cross sections for 50- to 500-kev electrons, 20: 13757 (CONF-233(Vol.4), pp 595-608)
PLAKHOV, A. G., Influence of mirror ratio on plasma heating by an electron beam in a probkotron, 20: 13947
PLANIOL, Therese, Radioisotopes and afflictions of central nervous system, 20: 12759
PLANO, R. J., Existence of spions from K^+ decay, 20: 13497
PLASIL, F., Kinetic energy-mass distributions from fission of nuclei lighter than radium, 20: 13861
PLATT, Robert B., Radiation effects on plant populations and communities: research status and potential, 20: 12586
PLESKOVA, A., Effect of carrier on pulmonary retention of radiocerium, 20: 12615
PLOSTINARU, S., Spectrometric determination of rare earths, 20: 12806
PLUMMER, Gaylord L., Movement and distribution of radionuclides on granitic outcrops within Georgia piedmont, 20: 12985
POCSIK, G., Approximate symmetries in field theory, 20: 13558
POCSIK, G., Sum rules in quantum field theory and in the many-body problem, 20: 13561
POGODAEV, G. N., Pulsed research reactor and feasibility of pulsed reactor application in neutron spectroscopy, 20: 14191 (BNL-tr-60)
POGUTSE, O. P., Instability and related macroscopic effects in toroidal discharges, 20: 13929 (NP-tr-1340)
POINTUD, R., Quality control inspection and testing of fuel materials for Dragon, 20: 14159
POIRIER, Charles Philip, Pion-proton interactions at 450 Mev, 20: 13524
POIRIER, Jean-Paul, Electron microscopic observation of stacking faults in twin crystals of Be, 20: 13978
POL, Yu. S., Inelastic scattering of electrons on nuclei with collective level excitation, 20: 13775 (JINR-P-2490)
POLACZEK, A., Isotopic exchange of iodine in aluminum iodide–ethyl iodide liquid system, 20: 12864
POLETTI, A. R., Excited states of ^{19}F by angular correlation technique, 20: 13822
POLETTI, A. R., Low-lying states of ^{40}Ca, 20: 13821
POLETTI, A. R., Low-lying excited states in ^{32}S, 20: 13823
POLEZHAEV, Yu. M., Triangulation of the $Na_2O-ZrO_2-SiO_2$ system, 20: 13284
POLICEC, Septimia, Complexes of carminic acid with ter- and tetravalent metals. I., 20: 12870
POLIKANOV, S. M., Structure of spontaneously fissioning isomers, 20: 13777 (JINR-E-2515)
POLTAVTSEV, N. S., Kinetics of $MoSi_2$ oxidation at 1500 to 1800°C, 20: 13195
POLUBOYARINOV, D. N., Vaporization of pure-oxide ceramics at high temperatures, 20: 13265 (AD-623208)
POOLE, M. J., Measurement of time-dependent spectrum in D_2O, 20: 13736
POOLE, M. J., Pulsed sources for neutron spectra measurement, 20: 13735
POPE, A. L., EDITOR: program for editing BCD data on magnetic tape, 20: 13750 (AEEW-M-553)
POPOV, Yu. P., Moderation of neutrons emitted by pulsed source, 20: 13741
POPOVA, N. M., Ternary systems Hf–Nb–C, Zr–Nb–C, and Ti–Nb–C, 20: 13272
PORATH, W. W., Calibration of high speed burnup code for nuclear fuel surveys, 20: 14118 (BNWL-183, Sect.IV)
PORTER, Bernard, Reaction rate of U metal with UF_4 in molten fluoride solutions, 20: 13170 (BM-RI-6736)
PORTER, F. T., Response of NaI, anthracene, and plastic scintillators to electrons, 20: 12899

POSEY, J. C., Heat transfer in the design of large radioisotopic heat sources, 20: 13157 (ORNL-P-1945)
POTAPKOV, N. A., Effect of exchange interaction on paramagnetic resonance, 20: 13976
POTSAID, Majic S., Radiation dosimeter with radiochromic couple suspended in an essentially anhydrous solid translucent matrix, 20: 13125
POVAROVA, K. B., Properties and uses of rhenium, 20: 13266 (AD-624905)
POVH, B., Angular correlation studies using the $^{13}C(^3He,py)^{15}N$ reaction, 20: 13819
POWELL, J. L., Isotopic composition of Sr in four carbonate vein-dikes, 20: 12980
POWELL, Jack E., Stability constants of rare earths with some carboxylic acids, 20: 12817 (IS-1311)
PRADHAN, T., A new approach to algebra of current operators, 20: 13533 (IC/66/3)
PRATT, R. H., New calculations of the atomic photoeffect, 20: 13413 (CONF-233(Vol.4), pp 538-47)
PRAVECZKI, E., New method for calculation of temperature averages, 20: 13348
PRELEC, K., Multi-probe measurements of fluctuating azimuthal density variations, 20: 13915 (MATT-402)
PREMOLI, A., Measurement of void fraction with impedance gauge technique, 20: 12964
PREOPOST, R., Depolarization of positive muons in solids, 20: 13498
PRESCOTT, D., Quantitative autoradiography, 20: 12616
PRESCOTT, J. R., Statistical model for photomultiplier single-electron statistics, 20: 13096
PRETRE, S., Thermonuclear explosions at great altitude, 20: 14230 (ORNL-tr-972)
PRICE, Keith R., Field method for studying root systems, 20: 12581
PRICE, R. J., Prog. rpt. on advanced graphite fuel systems, 8/15–11/14/65, 20: 13247 (GA-6831)
PRITCHARD, J. P. Jr., Switching characteristics of small geometry thin film superconductors, 20: 13048
PRUITT, J. S., Secondary electron trajectories in Faraday-cup magnetic field, 20: 13382
PRZEWLOCKI, K., Radiometric determination of spatial concentration of inhomogeneous fluid in pipe lines, 20: 13049
PUECHL, K. H., Criticality control program in Pu processing and fabrication plant, 20: 13018
PURO, Jaakko A., Spermatogenesis of adult Drosophila males after treatment with x rays, 20: 12637 (TID-21466)

Q

QUARTARARO, P., Intra-operative detection of pelvic lymph nodes by radioactive isotopes, 20: 12751
QUINN, E. P., Single-rod, forced-flow, transition boiling heat transfer from smooth and finned surfaces, 20: 12961 (GEAP-4786)
QUITTNER, G., Error propagation in resolution correction, 20: 13040

R

RABOTNOV, N. S., Photofission angular anisotropy and parity of ^{239}Pu ground state, 20: 13809
RABOY, S., Gamma rays from decay of 35-day ^{95}Nb, 20: 13859
RABOY, S., Measurement of energies of γ rays from decay of ^{66}Ga, 20: 13818
RACZKA, R., Discrete degenerate representations of non-compact rotation groups, 20: 13532 (IC/66/2)
RADEV, T., Radiosensitivity of guinea pigs with hypocatalasia, 20: 12643 (ANL-Trans-264)
RADICATI, L. A., Lorentz covariant definition of the U_6 group for free particle states, 20: 13629 (BNL-8767)
RADO, W. G., Optical frequency plasma resonance in gases, 20: 13942
RAE, A. D., Crystal structure of dicesium tetrachlorodioxouranium (VI), 20: 12835
RAE, Henry, Thiamine and niacin analysis of irradiated strawberries, 20: 13142 (UCD-34P80-3, pp 52-4)
RAE, Henry L., Effect of γ irradiation on lemon fruits, 20: 13145 (UCD-34P80-3, pp 75-83)
RAE, Henry L., Effect of γ irradiation on peaches, 20: 13147 (UCD-34P80-3, pp 92-8)
RAGONESE, P., Intra-operative detection of pelvic lymph nodes by radioactive isotopes, 20: 12751
RAHMAN, Abdur, Calibration of ^{60}Co gamma cell, 20: 12910 (AECD/CH/3)
RAIEVSKI, V., Pulsed fast reactor as source for pulsed neutron experiments, 20: 14096
RAINWATER, Walter J. Jr., Electron interactions with matter. I., 20: 13781 (NASA-CR-334)
RAIS, Pistek, Concentration-dependent distribution methods for determination of Zr in submicrogram amounts, 20: 12778 (UJV-1434/65)
RAJNAK, Katheryn Edmonds, Configuration interaction in the rare earths, 20: 14005
RAKOW, Adelbert, Measurement of standard ion doses for x and γ radiation between 50 kev and 3 Mev. II., 20: 13113
RAMDAS, A. K., Infrared absorption spectra of oxygen-defect complexes in irradiated silicon, 20: 13998
RAMEY, James T., Progress and problems in radiation standards and radioactive waste disposal, 20: 13017
RAND, R. E., Design of 180° electron scattering facility, 20: 13089
RAO, M. G., Infrared absorption spectra of oxygen-defect complexes in irradiated silicon, 20: 13998
RAO, P. Venugopala, Electron-capture ratio and internal bremsstrahlung in ^{181}W decay, 20: 13869
RAO, R. V. G., Thermogravimetric analysis of La, Ce, Pr, and Nd oxalates in air and in CO_2, 20: 12862
RAPAPORT, J., Reaction $^{46}Ca(d,p)^{47}Ca$ at 7 Mev, 20: 13853
RAPOPORT, L. P., Influence of strong interactions between nucleons in nuclei on allowed β decay, 20: 13886
RAU, G., Negative H and Li ions in a duoplasmatron, 20: 13376
RAU, R. C., Further replica electron microscopy studies of irradiated BeO, 20: 13331
RAUBER, Ernest L., Effect of acute γ radiation on opossum, gray fox, raccoon, and bobcat, 20: 12667
RAYNER, H. L., Fate of terphenyl in the rat, 20: 12589 (AECL-2507)
RAZAVY, M., Scattering by nonlocal potentials, 20: 13586
REBHAN, Eckhard, Electromagnetic production of shock waves and interaction of shock waves with electromagnetic fields, 20: 13637 (IPP-3/28)
REBMAN, H. P., Blowout, heat transfer, pressure drop, and maximum flow tests conducted on prototype Mark III fuel bundle, 20: 14125 (GEAP-4898)
REDMOND, A., Calculated response of air-wall dosimeters or Geiger-Mueller tubes to monoenergetic photons between 1 and 10 Mev, 20: 13055 (AD-626998)
REE, Taikyue, Significant-structure theory applied to water and heavy water, 20: 12858
REED-HILL, R. E., Effect of prestrain on mechanical properties of Zr, 20: 13246 (CONF-651017-13)
REES, David B., Noble gas plasma produced by fission fragments, 20: 13939
REGENSTREIF, E., Focusing and chromatic aberrations in a periodic AG beam transport system, 20: 13360 (CERN-65-42)
REICHARDT, W., Measurements of neutron spectra in hydrogenous moderators, 20: 13737
REICHLE, David E., Radiocesium dispersion in a cryptozoan food web, 20: 12576
REIFENSCHWEILER, O., Generation of neutron pulses and modulated neutron fluxes with sealed-off neutron tubes, 20: 13720
REKALO, M. P., Constants of interaction of vector mesons with nucleons, 20: 13479
REME, H., Effects of radiation injury on intestine and ureter, 20: 12739
REMMENGA, E. E., Factors influencing accumulation of fallout ^{137}Cs in Colorado mule deer, 20: 12984
RENAULT, Henri, Ultrastructure of experimental adenohypophysial thyrotropic tumors after radiothyroidectomy, 20: 12652
RENKEN, C. J., Economical application of nondestructive testing to reactor components, especially jacket tubing, 20: 14032
RENNERT, A., Ascorbic acid in crown-gall tumor tissue of Nictoiana tabacum under influence of ^{60}Co γ rays, 20: 12649
RENNERT, P., Nuclear matter with momentum-dependent nuclear forces, 20: 13792
RESNIKOFF, Marvin, Representations on the group SU_3, 20: 13629
RESTER, David H., Electron interactions with matter. I., 20: 13781 (NASA-CR-334)
REVAI, J., Symplectic-invariant many-fermion problems, 20: 13651
REYERS-DEGLI INNOCENTI, I., Prog. rpt. on selective protection of damages induced by x irradiation and radiomimetic drugs, final, 9/65, 20: 12719 (NP-15668)
REYERS-DEGLI INNOCENTI, I., Prog. rpt. on selective protection of damages induced by x irradiation and radiomimetic drugs, annual, 9/15/64, 20: 12718 (NP-15667)
REYERS-DEGLI INNOCENTI, I., Prog. rpt. on selective protection of damages induced by x irradiation and radiomimetic drugs, 11/64–1/65, 20: 12717 (NP-15666)
REYNOLDS, M. B., Fracture mechanics and the stability of engineering structures, 20: 13248 (GEAP-4678)
REZVANOV, R. A., Solving nuclear geophysics problems by Monte Carlo method, 20: 12994
RHODES, C. A., Nuclear reactor magnetohydrodynamic power generation, 20: 14132 (LA-3368)
RHODES, D. W., Stability of highly radioactive alumina calcine, 20: 14207 (IDO-14670)
RIBEIRO, C. Costa, Survey of radioactive content of food grown on Brazilian areas of high natural radioactivity, 20: 12988

RICATEAU, P., CEA research in magnetohydrodynamic conversion, 20: 13433
RICE, William L. R., Fuels and materials development under reactor programs, 20: 13183 (TID-6506(Pt.2, 3rd Ed.))
RICE, William L. R., Nuclear fuels and materials development, 20: 13184 (TID-11295(Pt.1, 4th Ed.))
RICHARDS, Keith C., Control of plasma, 20: 12959
RICHARDS, P., Production of Y-87 and a Sr-87m generator, 20: 12917
RICHARDS, Walter Bruce, Cross sections for $\pi^- p \to \eta n$ from threshold to 1300 Mev, 20: 13457 (UCRL-16195)
RICHARDSON, G. L., Continuous separation of Ce from trivalent rare earths, 20: 12762 (BNWL-173)
RICHARDSON, J. Reginald, Electric dissociation of the H^- ion near 2.4 Mev, 20: 13380
RICHARDSON, Paul E., Detection of radiation damage in anthracene crystals by space-charge-limited current measurements, 20: 12893
RICKARD, W. H., Mineral transfer in a greasewood community and ion uptake by grasses, 20: 12575
RIE, Kyong-Tschong, Sputtering of solids by ion bombardment, 20: 13414 (JUL-304-RW)
RIEKERK, Hans, Mineral cycling in a Douglas fir forest stand, 20: 12574
RIENECKER, F., Uranium–molybdenum alloy for use in prompt-burst reactor, 20: 13287
RIEPE, G., Gamma spectrometry with semiconductor detectors, 20: 13067 (JUL-308-RB)
RIESS, F., Parity of the 6.89-Mev level in ^{14}C, 20: 13828
RIGALI, L., Rapid separation of ^{231}Pa from its daughters, 20: 12937
RINGLAND, G. A., Nucleon-antinucleon charge exchange in the absorption model, 20: 13494
RINGOT, Claude, Mounting armoring on ends of a reactor fuel element can, 20: 14111
RITZ, Victor H., Vacancy-production efficiencies in KBr at low temperatures, 20: 13999
RIVERS, R. J., Dynamical interpretation of spurions in $\bar{U}_{12}$, 20: 13589
RIVERS, W. J., Film free convection in helium II, 20: 13696
ROBBINS, Robert, Photographic representation of isodose patterns by application of Sabattier effect, 20: 13008
ROBERTS, J. T., Estimated costs of high-level waste management, 20: 14208 (ORNL-P-1926)
ROBERTSON, C. G., Measurement of integral parameters in fuel rods, 20: 14103 (MIT-2344-4, pp 48-62)
ROBERTSON, J. S., Positron scanner for brain tumors, 20: 12734 (BNL-9911)
ROBINSON, Lawrence B., Hot pressing zirconia, 20: 13230
ROBSON, J. M., Associated particle time-of-flight system for use with D-D neutrons, 20: 13088
ROCHE, M., Pulsed neutron measurements in fast assemblies, 20: 14084
ROCHLIN, Robert S., Device for measuring biological effect of radiation, 20: 13121
ROCKLIN, Sol R., SNAP-10A, first reactor in space, 20: 14177
RODIER, D., Cicatrization after telecobalt therapy in surgery of neck and buccal cavity, 20: 12653
RODWELL, William, Heat exchange unit, 20: 14035
ROESSLE, E., Method for measurements of total neutron cross sections, 20: 13101
ROGE, R., Digital computer system for executive control of fast neutron laboratory, 20: 13806
ROGERS, Frank, Improvements in or relating to irradiation plant, 20: 12950
ROLANDO, Piero, Systems between niobium oxide and oxides of aluminum and chromium, 20: 12833
ROLLAND, Paul, Non-collisional dampings in resonance of high-frequency probe, 20: 13935
ROMANS, P. A., Composition and crystallographic data for the highest boride of tungsten, 20: 12838
RONGSTAD, Orrin J., Calcium-45 labeling of mammals for use in population studies, 20: 12583
ROSA, R. J., Nuclear reactor magnetohydrodynamic power generation, 20: 14132 (LA-3368)
ROSE, B., Absolute polarization measurements in proton scattering at 140-Mev, 20: 13813
ROSE, R. M., Magnetic field distribution in type II superconductor, 20: 13672
ROSE, R. M., Superconductivity of composite of fine niobium wires in copper, 20: 13673
ROSENBAUM, I., Rate of heterogeneous isotopic exchange on surfaces of ionic crystals, 20: 12869
ROSENFELD, Leon, The measuring process in quantum mechanics, 20: 13664
ROSENTHAL, Michael R., Pyridine complexes of nickel(II), 20: 14225 (TID-21577)
ROSHANMANESH, Ali, Genetic integrity of upgraded and downgraded alleles in Saccharomyces, 20: 12655
ROSS, Charles P., Final safety analysis of maximum credible accident in the HWCTR, 20: 14183 (DP-1037)
ROSS, Joseph F., Gordon Wilson lecture: ionizing radiation and development and survival of life, 20: 12708
ROSSIN, F., Prog. rpt. on influence of nitrogen in Fe and steel under fast neutron irradiation, 7–9/65, 20: 13324 (EURAEC-1529)
ROSUE, A., Swirl flows in boiling water, 20: 12960 (EURAEC-1515)
ROTH, R. S., Vaterite-type ABO_3 rare-earth borates, 20: 12837
ROTHFELS, Klaus H., Effects of x-irradiated feeder layers on mitotic activity and development of aneuploidy in mouse-embryo cells, 20: 12654
ROTHWELL, E., Causes of high-temperature substoichiometry in sintered UO_2, 20: 13294
ROTTER, Kh., New isotope ^{210}Ac, 20: 13779 (JINR-P-2465)
ROUHANINEJAD, H., Self-consistent field and method of projection, 20: 13826
ROUSSEL, E., Dimensional measurements and flaw detection, 20: 13343
ROUSSEL, E., Potentialities of γ spectrometry in nondestructive measurements on fuel elements, 20: 14158
ROY, R. M., Simulated fallout studies in conifers—preliminary report, 20: 12671
ROY, Rustum, Prog. rpt. on crystal chemistry, 5/13–8/13/65, 20: 13260 (NP-15852)
ROYAL, George C. Jr., Prog. rpt. on studies of x-irradiated mice following bone marrow injections, final, 10/65, 20: 12720 (TID-22466)
ROYAL, Gladys W., Prog. rpt. on studies of x-irradiated mice following bone marrow injections, final, 10/65, 20: 12720 (TID-22466)
ROZEN, S., Random pulse generator, 20: 13037
RUBBIA, C., K-meson decay and CP invariance, 20: 13495
RUBENSTEIN, Daniel, Gamma-ray degradation of chloroplast structure and photoreduction, 20: 12627
RUBIN, Morton Harold, Analytic properties of the scattering matrix for nonrelativistic spin-dependent interactions, 20: 13633
RUDAKOV, L. I., Oscillations and instability of a weakly turbulent plasma, 20: 13931 (NP-tr-1348)
RUDENKO, V. T., Pulsed research reactor and feasibility of pulsed reactor application in neutron spectroscopy, 20: 14191 (BNL-tr-60)
RUESS, Hermann M., Fabrication of precision lead collimators, 20: 13030 (LA-3443)
RUGH, Roberts, Effect of ionizing radiations, including radioisotopes, on the placenta and embryo, 20: 12650
RUMER, I. A., Internal conversion coefficients for nuclear transitions in ^{132}Xe, 20: 13883
RUSCHE, Ben C., Final safety analysis of maximum credible accident in the HWCTR, 20: 14183 (DP-1037)
RUSEV, G., Radiosensitivity of guinea pigs with hypocatalasia, 20: 12643 (ANL-Trans-264)
RUSH, J. J., Low-frequency motions and barrier to rotation in phosphonium iodide, 20: 12859
RUSI, A., Thermal annealing and role of water of crystallization in potassium trioxalatoferrate irradiated with neutrons, 20: 12903
RUSSELL, J. L. Jr., Fast-reactor physics parameters from pulsed source, 20: 14202
RUSSELL, R. Scott, Interception and retention of airborne material on plants, 20: 12607
RUTHERFORD, William M., Preparation of elemental ^{13}C in high yield from $^{13}CO_2$, 20: 12852
RUTKEVICH, N. Yu., Mechanisms of reactions $^{12}C + {}^{10}B \to {}^{10}B + 3\alpha$ and $^{14}N + {}^{10}B \to {}^{12}C + 3\alpha$, 20: 13891
RUTKOWSKI, W., Properties of boron carbide sintered under pressure, 20: 13314
RYAN, Robert R., Structure of gaseous XeF_6, 20: 12860
RYNDIN, R. M., Reconstruction of meson-nucleon scattering matrix from experiments with polarized target, 20: 13448 (JINR-E-2521)
RYON, A. D., Prog. rpt. on chemical separations processes, 4–6/65, 20: 12928 (ORNL-3868)

S

SABINE, T. M., Neutron diffraction study of orthoboric acid $D_3{}^{11}BO_3$, 20: 12836
SABOL, W. W., Sodium mass transfer. VII., 20: 12766 (GEAP-4178)
SACHS, A. M., Depolarization of positive muons in solids, 20: 13498
SACKMAN, J. F., Corrosion and ignition behavior of some U–Pu–Fe alloys, 20: 13200
SADIKOV, I. P., Neutron-thermalization process in time in graphite and beryllium, 20: 13738
SADIKOV, I. P., Neutron thermalization in time in aqueous moderators, 20: 13739
SAFFOURI, M. H., Dynamical interpretation of spurions, 20: 13607
SAFIN, Yu. A., Neutron thermalization in graphite-water system at large temperature gradients, 20: 13740
SAGOT, M., Calibration of control rods in natural uranium–graphite lattices, 20: 14163
SAGOT, M., Study of graphite and beryllium oxide using pulsed neutron

source method, 20: 13727
SAHAI, Baldev, Lithium-7 and α particles from $^{6}Li + {}^{9}Be$ reaction, 20: 13852
SAKAMOTO, Yoshiyuki, Absorption of π mesons and (p,pd) reaction, 20: 13874
SAKATA, Shoichi, New concept of elementary particles and method of the composite model, 20: 13613
SAKURAI, Tsutomu, Chemical analysis of BrF_3, 20: 12797
SALAM, Abdus, Relativistic U(6,6) theory, 20: 13534 (IC/66/5)
SALGADO, P. G., Nuclear reactor magnetohydrodynamic power generation, 20: 14132 (LA-3368)
SALMON, M. A., Studies of reactor containment structures, 20: 14028 (IITRI-578P22-14)
SALMON, R., Estimated costs of high-level waste management, 20: 14208 (ORNL-P-1926)
SALOMON, M., Reaction rate and separation factor isotope effects in hydrogen evolution reaction, 20: 12840
SAMARINA, V. A., Phase components in ZrO_2–$PrO_{1.83}$ system, 20: 13279
SANCHO, L., Measurement of M_2 in organic liquids, 20: 13730
SANDALLS, F. J., Determination of Pa-231 in urine, 20: 12761 (AERE-R-4911)
SANDERS, Merwyn, High-volume, air-monitor calibration facility, 20: 13077 (Y-1503)
SANDIFER, C. W., Radiation calibration of a 20-Mev linac, 20: 13361 (EGG-1183-2066)
SANDLER, Carl L., Time reversal, form factor ratio, and branching ratio in K_{l3} decay, 20: 13459 (UCRL-16253)
SANDLER, Melvin, Nonlinear magnetoplasmadynamics, 20: 13960
SANDQUIST, Gary M., XKINEQ—two-group, two-dimensional, multiregion computer code for examining flux stability in reactors, 20: 14061 (IDO-17127)
SANO, Kikuro, Electron-bombardment ion source, 20: 13386
SANTANDREA, E., Feasibility studies of PCTR measurements with light-water-moderated plutonium-fueled lattices, 20: 14189 (RT/FI(65)43)
SANTHANAM, T. S., A new approach to algebra of current operators, 20: 13533 (IC/66/3)
SANTOS, P. L., Survey of radioactive content of food grown on Brazilian areas of high natural radioactivity, 20: 12988
SAPORETTI, F., Technique of n-γ discrimination, 20: 13111
SASAO, N., Measurement of internal friction of nuclear materials, 20: 13321
SATCHLER, G. R., Reaction $^{90}Zr(p,p')$ at 18.8 Mev and the shell model, 20: 13866
SATCHLER, G. R., Shell-model form factors for $^{90}Zr(p,p')$ reaction, 20: 13867
SATO, Taichi, Extraction of U(VI) and Th from HNO_3 solutions by tri-n-butyl phosphate, 20: 12931
SATOMI, Yoshiyasu, Density operational amplifier and application to γ density gage for inspection of fuel rod, 20: 13154
SAULYS, A., Programmed spot automatic scanning system for spark chambers, 20: 13106
SAUNDERS, L. Z., Histopathology of hereditary congenital deafness in white mink, 20: 14214 (BNL-8564)
SAUTER, Eugen, Solid probe capable of being activated for nuclear reactors, 20: 13119
SAVAGE, H. W., Component development and testing, EGCR, 20: 14139 (ORNL-3885, pp 268-83)
SAVAGE, H. W., Fueled-graphite systems, 20: 13261 (ORNL-3885, pp 87-149)
SAVIDGE, R. E., Fatigue characteristics on Ni–Cr–Fe alloys with emphasis on pressure-vessel cladding, 20: 13255 (KAPL-3108)
SAVIN, I. A., Elastic 180° scattering of π^+ mesons by protons at high energies, 20: 13471
SAVITSKII, E. M., Rare earth alloys and compounds, 20: 13280
SAWADA, Shoji, Inelastic process and one-boson-exchange model, 20: 13616
SAXENA, R. S., Electrometric studies on compositions of uranyl vanadates, 20: 12796
SAXER, Howard Irving, High-energy $\pi^- + p$ elastic scattering for small momentum transfers and forward dispersion calculation, 20: 13523
SCADRON, Michael D., Final-state enhancement at 1920 Mev in $\pi^- p$ inelastic scattering, 20: 13454 (UCRL-14100-T(Rev.1))
SCANLON, J. P., Absolute polarization measurements in proton scattering at 140-Mev, 20: 13813
SCANNICCHIO, D., Existence of ^{4}He excited levels and of other light nuclides, 20: 13834
SCHAEFFER, G. M., Superconductivity in group V^{a} dichalcogenides, 20: 13683
SCHAERF, C., Electrodisintegration of the deuteron at low momentum transfer: magnetic transitions, 20: 13490
SCHARMANN, A., Influence of network defects on optical characteristics of glasses, 20: 13341
SCHECHTER, J., Higher symmetry groups with parity mixing, 20: 13599
SCHEER, J., Ionization defects of energetic ^{28}Al atoms in silicon, 20: 13989
SCHENZ, R. F., Cryogenic irradiation of resistance temperature transducers for NERVA, 20: 13127 (CONF-651101-61)
SCHERM, R., High-resolution spectrometer for very slow neutrons for use on cold sources of very high flux reactor, 20: 13065 (JUL-295-NP)
SCHERM, R., Neutron guides: report on present state of development, 20: 13701 (JUL-294-NP)
SCHEUERBRANDT, Goenter, Automatic determination of decarboxylase for aromatic amino acids in mouse liver, 20: 12782
SCHIFF, L. I., Electromagnetic structure of the Yukawa meson, 20: 13878
SCHIFFER, J. P., Energy levels in ^{49}Sc from $^{48}Ca(^{3}He,d)$ and other reactions, 20: 13854
SCHILLING, W., Dose dependence of annealing stage II in neutron-irradiated aluminum, 20: 13340
SCHLESINGER, Y., Nuclear resonant scattering using neutron-capture γ rays, 20: 13771 (IA-1050)
SCHLUETER, A., General interchange instability, 20: 13638 (IPP-6/39)
SCHMATZ, W., Neutron guides: report on present state of development, 20: 13701 (JUL-294-NP)
SCHMIDT, E., Demand for nuclear fuels and costs of different reactor types in Germany, 20: 14130 (KFK-366)
SCHMIDT, K., Development of a chalk-dust measuring device, 20: 13024 (EUR-2544.d)
SCHMIDTKE, H.-H., Nephelauxetic effect in rare earth complexes illustrated for Pr(III), 20: 12866
SCHMITT, A., Controllable pulse frequency and width system for pulsing and modulating fast-neutron core assemblies, 20: 13721
SCHMUTZLER, F., First-order theory of high-dispersion spectrometer with winding magnetic field, 20: 13087
SCHNUERER, E., Crystal counter investigations of CdS cleavage cells by γ excitation, 20: 13132
SCHOEB, Virginia R., Stability constants of rare earths with some carboxylic 20: 12817 (IS-1311)
SCHOENHEIT, E., An ion converter detector with gate connections for mass spectrometric investigations, 20: 13047
SCHOENIG, F. C., Reference table for W–3% Re vs. W–25% Re thermocouples, 20: 13028 (KAPL-M-6498)
SCHOLZ, W., Angular correlation studies using the $^{13}C(^{3}He,p\gamma)^{15}N$ reaction, 20: 13819
SCHOPPER, H., Search for a heavy electron by electron-proton coincidence measurements, 20: 13446 (DESY-65/9)
SCHRICKER, K. Th., Bone-marrow transfusion in the whole-body irradiated, tumor-bearing rat, 20: 12651
SCHULTE-BRINKMANN, Wolfgang, Radiation exposure of patients and radiological employees in heart probes. I., 20: 12757
SCHULZ, R. K., Soil chemistry of radionuclides, 20: 12915
SCHUMACHER, O. Peter, Radioactive iodine treatment of Graves' disease, 20: 12736
SCHUYLER, F. L., Studies of reactor containment structures, 20: 14028 (IITRI-578P22-14)
SCHWEIKERT, C. H., Feasibility of surgery after whole-body x irradiation and administration of radioprotective agent, 20: 12645
SCHWEIMER, W., Circuit for pulse-shape discrimination, 20: 13108
SCIUTO, F., Automatic control equipment of Dragon, 20: 14154
SCOSSIROLI, R. E., Mutability of polygenes and utilization of induced genetic variability, 20: 12641 (TID-22582)
SCOTT, B. B., Separation of Nb and Mo by solvent extraction, 20: 12933
SCOTT, H. G., Sputtering of gold by low-energy inert gas ions. II., 20: 13420
SCOTT, S. A., Reactivity measurement by pulsed neutron method, 20: 14200
SCOTT, V. D., Dislocation vectors related to the ductility of Be, 20: 13305
SCRIBANO, A., K-meson decay and CP invariance, 20: 13495
SEAMON, R. E., Comparison of effective ranges of n-p and p-p interactions, 20: 13512
SEARCY, Alan W., Vapor pressure and evaporation coefficient studies of beryllium nitride decomposition reaction, 20: 12830 (UCRL-7802)
SEARLE, A. G., Effect of hypothermia on induction of chromosomal mutations by acute x irradiation of mice, 20: 12693
SEBESTIK, V., Effect of radiation on phagocytic activity of leukocytes in preserved blood, 20: 12698
SEBESTIK, V., Thermostability of rat erythrocytes irradiated in vitro, 20: 12697
SEDDON, B. J., Steels data manual, 20: 13186 (TRG-Report-840)
SEDLET, J., Environmental radioactivity at Argonne National Lab., 1964, 20: 12998 (ANL-7104)
SEDMAN, E. C., Joint kinematical and geometrical analysis of bubble chamber events, 20: 13071 (RHEL/R-111)
SEEGER, V., Reaction $K^+ + p \rightarrow K + N + \pi$ between 0.86 and 1.58 Bev/c, 20: 13462 (UCRL-16370)
SEETZEN, J., Demand for nuclear fuels and costs of different reactor types in Germany, 20: 14130 (KFK-366)
SEFCHOVICH, E., Miniature lattice studies, 20: 14069 (MIT-2344-4, pp 106-14)

SEFCHOVICH, E., Oscillating neutron source experiment, 20: 13704 (MIT-2344-4, pp 101-5)
SEGAL, E., Moessbauer effect in ^{161}Dy in $DyCo_2$ and $DyNi_2$, 20: 13992
SEGAL, Irving, Dispersion for relativistic nonlinear equations with partial derivatives, 20: 13582
SEGRE, G. J., Behavior of fission gas bubbles, 20: 13329 (RT/FI(65)46)
SEIKEL, George R., Basic studies of a low-density Hall current ion accelerator, 20: 13917 (NASA-TN-3250)
SEKI, Masatoshi, Electron microscopic studies on normal mouse spleen and its morphological changes after total-body irradiation, 20: 12681
SEKI, Yoshinaga, Deflector for charged particles, 20: 13397
SEKIGUCHI, Morimasa, Induction of tolerance to allogenic grafts, 20: 12656
SEKIYAMA, Shigeteke, Electron microscopic studies on normal mouse spleen and its morphological changes after total-body irradiation, 20: 12681
SELIGER, K., Occurrence of self-luminescence collision fronts in electromagnetically operating shock tubes, 20: 13949
SELTZER, E., Possibility of parity admixture in the 57.6-kev transition in Hf-180m, 20: 13841
SELUCKY, P., Concentration-dependent distribution methods for determination of Zr in submicrogram amounts, 20: 12778 (UJV-1434/65)
SEN, R. N., Rearrangement of symmetries in dynamical maps, 20: 13620
SENOSKI, Walter E., Radioactive waste material incinerator, 20: 14212
SERBER, Robert, Class of optical models, 20: 13601
SESHADRI, S., Prog. rpt. on plasma-covered slot antennas, 11/62–9/65, 20: 13022 (AFCRL-65-859)
SESINI, R., Zircaloy-2–stainless steel diffusion bonds, 20: 13222
SEYFRIED, P., Impulse generator for adjustment and testing of coincidence systems with crossover circuits, 20: 13044
SHABALIN, E. P., CP-odd weak interaction, 20: 13473
SHABALIN, E. P., Pulsed research reactor and feasibility of pulsed reactor application in neutron spectroscopy, 20: 15191 (BNL-tr-60)
SHAFER, Robert Eugene, Pion-mass measurement by crystal diffraction of mesonic x rays, 20: 13461 (UCRL-16365)
SHAFRANOV, V. D., Closed minimum-B configurations, 20: 13930 (NP-tr-1343)
SHAH, J., Gamma-ray radiosynthesis of ozone from air, 20: 12885 (UCD-34P80-3 pp 59-68)
SHAH, J., Mn^{2+} in ^{60}Co γ-irradiated strawberries, 20: 13143 (UCD-34P80-3, pp 55-7)
SHAMRAI, V. F., Heterogeneous phases of Nb_3(Al, Ge, and Sn), 20: 13275
SHAMSUDDIN, A. K., Calibration of ^{60}Co gamma cell, 20: 12910 (AECD/CH/3)
SHAMYRKANOV, Y., Mechanical properties of U-activated NaF single crystals, 20: 13277
SHANKAR, J., Annealing processes after nuclear recoil in metal complexes, 20: 12896
SHANLEY, P. E., Calculations of deuteron stripping in soluble model, 20: 13851
SHAPIRO, F. L., Moderation of neutrons emitted by pulsed sources, 20: 13741
SHAPIRO, F. L., Pulsed research reactor and feasibility of pulsed reactor application in neutron spectroscopy, 20: 14191 (BNL-tr-60)
SHAPIRO, V. D., Plasma heating by a stochastic field, 20: 13948
SHAPKIN, V. V., Influence of mirror ratio on plasma heating by an electron beam in a probkotron, 20: 13947
SHARPE, R. S., Development of flaw-detection techniques at Harwell, 20: 14034
SHATUNOV, V. M., Method of retaining and accumulating high-temperature plasma in a trap, 20: 13928 (AD-625070)
SHAW, L., General orbit program for sector-focused cyclotrons, 20: 13355 (AD-626999)
SHAW, Stanley M., Properties of a diuretic agent in swine by in vivo whole-body counting, 20: 12613
SHBYDCHENKO, A. G., Oxidation of lower W and Mo silicides, 20: 13198
SHCHEGOLEV, V. A., Evaporation reactions of neutrons produced by irradiation of ^{238}U by accelerated ions ^{18}O, ^{19}F, and ^{22}Ne, 20: 13889
SHEKHTER, V. M., Lepton decay of vector mesons, 20: 13476
SHEN, Benjamin Ching-chun, Resonance production in pion-proton interactions at 3.65 and 3.7 Bev/c, 20: 13456 (UCRL-16170)
SHERMAN, I. S., Response of NaI, anthracene, and plastic scintillators to electrons, 20: 12899
SHERRY, E., Crystal structure of high-pressure UO_3, 20: 13269
SHERWOOD, J. E., Scattering of 262-kev polarized neutrons by ^{4}He, 20: 13717
SHIELDS, L., Ag I and Ag III from solvated Ag II by radiation-chemical conversion, 20: 12895
SHIMAZAKI, Y., Interaction of subcritical assemblies, 20: 14090
SHIMODAYA, Ichiro, Reaction ^{9}Be(α,2α)^{5}He and α-particle model, 20: 13875
SHINOHARA, Koichi, Effect of carrier traps in polyethylene under γ irradiation, 20: 13982
SHINOZAKI, Yoshiharu, Measurement of leakage tritium from tritium self-luminous paints, 20: 13153
SHIPMAN, T. L., Plutonium dispersal by low-order detonation of atomic weapons, 20: 13004 (LA-1981(Rev.))
SHIRAFUJI, Takeshi, Possible G-parity nonconservation in muon capture reactions, 20: 13877
SHIRAISHI, Kensuke, Metallographic observations on creep deformation of Magnox AL 80, 20: 13311
SHITIKOVA, M. G., Comparative study of action of polyglucine by various molecular weights on acute radiation sickness, 20: 12723 (JPRS-33766, pp 3-7)
SHOOP, C. Robert, Prog. rpt. on effects of radiation on migratory orientation of salamanders, 5/65–2/66, 20: 12568 (TID-22639)
SHOPAUSKAS, K. K., Determination of parameters of natural radioactive aerosol removal from air, 20: 12977
SHPIL'RAYN, E. E., Thermodynamics of MHD power generator with vapor-filled injector, 20: 13438
SHUGART, Howard A., Nuclear-spin, hyperfine-structure, and magnetic-moment investigations on ^{61}Cu, ^{62}Cu, and ^{64}Cu, 20: 13855
SHUMILOV, S. N., Mechanisms of reactions $^{12}C + {}^{10}B \rightarrow {}^{10}B + 3\alpha$ and $^{14}N + {}^{10}B \rightarrow {}^{12}C + 3\alpha$, 20: 13891
SIDDIQI, Axix Ahmed, 500-Curie irradiation facility, 20: 12911 (AECD/HP/3)
SIDOTI, Joseph E., Thermionic converter, 20: 13444
SIEGEL, S., Crystal structure of high-pressure UO_3, 20: 13269
SIEGERT, W., Effect of x irradiation on crossing populations of barley in M1 and M2 generations, 20: 12714
SIGALOVICH, V. V., Contract reaction of titanium with niobium carbide on graphite, 20: 13194
SIIVOLA, A., Decay properties of ^{88}Zr, 20: 13856
SIKORA, Anne, Radiotracer, gravimetric, and calorimetric studies of ingestion and assimilation rates of an isopod, 20: 12610
SILIN, I. N., Asymptotic behavior of scattering amplitude at large momentum transfers, 20: 13546 (JINR-P-2519)
SILVESTRI, R., Particle disintegration study for re-entering nuclear auxiliary power systems, 20: 14169 (AFWL-TDR-64-75)
SIMONESCU, T., Complexes of carminic acid with ter- and tetravalent metals. I., 20: 12870
SIMONOV, Yu. N., Phase-shift analysis of nucleon-nucleon scattering at 400 Mev, 20: 13516
SIMPSON, J. L., Sodium mass transfer. XVII., 20: 12767 (GEAP-4833)
SIMPSON, Wilbur Dwain, Three-nucleon system, 20: 13894
SINEL'NIKOV, K. D., Charged particle beam interactions with plasma, 20: 13961
SINHA, S. P., Nephelauxetic effect in rare earth complexes illustrated for Pr(III), 20: 12866
SISMAN, O., AVR-German pebble-bed reactor, 20: 14136 (ORNL-3885, pp 150-94)
SISMAN, O., Fueled-graphite development, 20: 13215 (ORNL-3885, pp 3-86)
SISMAN, O., Fueled-graphite systems, 20: 13261 (ORNL-3885, pp 87-149)
SISMAN, O., In-pile fission-gas release from fine-grain UO_2, 20: 13290
SISMAN, O., Irradiation testing of components and materials, EGCR, 20: 14140 (ORNL-3885, pp 284-93)
SISSON, D. H., Decay properties of ^{88}Zr, 20: 13856
SISTEK, L., Macroautoradiography with radiophosphorus in stomach cancer, 20: 12742
SKOBELEV, N. K., Spontaneously fissionable isomer with T = 2.6 min in reactions of ^{233}U with ^{11}B and ^{10}B, 20: 13776 (JINR-P-2499)
SKOLNIK, Willard, Measurement and calculation of relative poison-to-fuel capture ratios in slab cores, 20: 14063 (KAPL-M-6528)
SKORKO-TRYBULA, Zofia, Colorimetric determination of vanadium in uranium compounds using p-methoxybenzothiohydroxamic acid, 20: 12802
SLANSKY, Richard C., New outlooks in strong interaction physics, 20: 13549 (UCRL-16530)
SLAWOV, L., Cytological test for diagnosis of radioresistant carcinoma of cervix uteri, 20: 12659
SLAY, B. G., Switching characteristics of small geometry thin film superconductors, 20: 13048
SLOTNICK, H., Solubility of helium in liquid lithium and potassium, 20: 12827 (TID-21583)
SMEND, F., Acceleration of heavy ions and production of heaviest chemical elements, 20: 13804
SMERDOV, B. I., Resonant heating of plasma by high-frequency field, 20: 13946
SMETANINA, L. I., Calorimetric detector for measuring energy of an ionized beam, 20: 13114
SMILEY, S. H., Alloy powder preparation by flame reduction techniques, 20: 13181 (K-L-6076)
SMIRENKIN, G. N., Photofission angular anisotropy and parity of ^{239}Pu ground state, 20: 13809
SMIRNOV, B. M., Ionization of atom colliding with an excited atom, 20: 13421

SMIRNOV, Yu. F., Electromagnetic properties of elementary particles in the SU(6) group, 20: 13623
SMITH, A. B., Digital computer system for executive control of fast neutron laboratory, 20: 13806
SMITH, A. B., Elastic and inelastic scattering of fast neutrons from Ag, In and Cd, 20: 13829
SMITH, C. V., LEGCOEF-3—program to calculate Legendre expansion coefficients, 20: 13699 (GA-6690)
SMITH, Harold H., Effects of x radiation on intracistron recombination at the waxy locus in maize, 20: 12678
SMITH, J., Application of quasipotential method to pion-nucleon scattering, 20: 13467
SMITH, K. C., Biological importance of uv-induced DNA-protein crosslinks in E. coli, 20: 12621
SMITH, P. G., Centrifugal pump for a molten-salt nuclear reactor, 20: 14164
SMITH, Roy A., Phase equilibria in uranium–tungsten–oxygen system, 20: 13235 (BMI-1755)
SMITH, Tennyson, Kinetics and mechanism of H permeation of oxide films on Zr, 20: 13201
SMITH, Todd Iverson, Investigation of the charged Bose gas model of superconductivity, 20: 13691
SMYTH, M. J., Handling and filtration of radioactive sludges, 20: 14210
SNELLING, G. F., Gamma-spectrum stabilizer with compensation for effects of detector temperature variation, 20: 13094
SNYDER, A. William, Radiation effects in electronics, 20: 13130 (SC-DC-65-1892)
SOBASZEK, A., Investigations on self-diffusion of In by absorption method, 20: 13315
SOCHOR, Vaclav, Characteristics of a high-frequency electron linear accelerator, 20: 13373
SODA, Toshio, Stability and instability of planewave Hartree-Fock solutions and the helical spin arrangement, 20: 13423
SODERQUIST, Sven Dale, Calcium–ytterbium system, 20: 13254 (IS-T-70)
SOJKA, B., Application of highly sensitive integrator in gas chromatography, 20: 12777 (UJV-1431/65)
SOKOL, G. J., Fatigue characteristics of Ni–Cr–Fe alloys with emphasis on pressure-vessel cladding, 20: 13255 (KAPL-3108)
SOLDATOV, A. S., Photofission angular anisotropy and parity of ^{239}Pu ground state, 20: 13809
SOLE, M. J., Formation and behavior of point defect clusters in neutron-irradiated uranium carbide, 20: 13332
SOLLID, J. E., Molecular and principal series absorption in cesium-argon mixtures, 20: 12823 (LA-3391)
SOLOVEV, L. S., Closed minimum-B configurations, 20: 13930 (NP-tr-1343)
SOLOVIEV, V. G., Structure of spontaneously fissioning isomers, 20: 13777 (JINR-E-2515)
SOMMER, K., Spectroscopic ^{15}N determination with use of step filter for Q24 Zeiss spectrograph, 20: 12807
SOMMER, N. F., Comparative inactivation of conidia, mycellia, and sclerotia of Botrytis cinerea by γ radiation, 20: 13149 (UCD-34P80-3, pp 176-89)
SOMMER, N. F., Interaction of γ irradiation, sealed packages, and controlled atmosphere on incidence of Botrytis rot in strawberries, 20: 13139 (UCD-34P80-3, pp 9-26)
SOMMER, N. F., Prog. rpt. on radiation technology in extending shelf life of fruits and vegetables, annual, 2/64–1/65, 20: 13138 (UCD-34P80-3)
SONG, J., Removal of second-order neutrons by oriented single crystals, 20: 13709 (PAEC-IPA(D)PH-652)
SONI, J. N., Removal of second-order neutrons by oriented single crystals, 20: 13709 (PAEC-IPA(D)PH-652)
SORENSEN, Raymond A., Spectroscopic factors from deuteron stripping reactions, 20: 13865
SOWINSKI, M., Observation of fission events in mica sandwiches, 20: 13099
SPACU, P., Formation of complex erbium halides by refractometry in aqueous solutions, 20: 12871
SPACU, P., Spectrometric determination of rare earths, 20: 12806
SPANGLER, G. E., Basal plane fracture of beryllium single crystals, 20: 13238 (CONF-170, pp 48-68)
SPEIDEL, Edward O., Phase equilibria in uranium–tungsten–oxygen system, 20: 13235 (BMI-1755)
SPERBER, Daniel, Gamma cascades from nuclei with high spin, 20: 13847
SPERDUTO, A., Nuclear-reaction studies in Ni isotopes, 20: 13858
SPERNOL, A., Precision (1%) absolute counting of x rays of low energy, 20: 13092
SPIELBERG, D., Gamma spectral data for shielding and heating calculations, 20: 13966 (UNC-5140)
SPIESS, Gerard, Study of synthesis plasma by an emissive probe, 20: 13934
SPINDLER, W. E., X-ray thermal expansion of near-stoichiometric UO_2, 20: 13300
SPINKS, J. W. T., Mean lifetime of free radical chains in ^{60}Co γ-irradiated chloral hydrate and bromal hydrate solutions, 20: 12887
SPIRN, Irwin, Positron lifetime spectra in molecular substances, 20: 13499
SPOGLIA, U., Semiconductor detectors of surface-barrier type, 20: 13072 (RT/EL(65)7)
SPOONER, Stephen, Spin correlations in iron, 20: 13994
SPRING, E., Internal pair formation of 12.33-Mev transition in ^{28}Si, 20: 13843
SPRUCE, Thomas William, Concrete pressure vessel, 20: 14039
SRINIVASAN, P. R., Alterations in transfer ribonucleic acid methylases after bacteriophage infection or induction, 20: 12619
SRIVASTAVA, Y. N., Threshold poles and low-energy scattering, 20: 13588
STAHLHOFEN, W., Bibliography on radiation effects on living tissues and organisms, 7/65, 20: 12629 (AED-C-04-22)
STALLMAN, R. F., Effect of γ irradiation on peaches, 20: 13147 (UCD-34P80-3, pp 92-8)
STAMBERG, R. C., Laser-stimulated nucleation in a bubble chamber, 20: 13084
STANGLER, Ferdinand, Modification of electron structure of gold by α irradiation and subsequent recovery, 20: 13339
STANSBURY, E. E., Specific heat of Zircaloy-2 from 50 to 700°C, 20: 13310
STAPP, Henry P., Analytic structure of many-particle scattering amplitudes. I., 20: 13531 (IC/65/17)
STARLINGER, Peter, Difference in uv sensitivity between genes in repressed and derepressed states, 20: 12712
STARLINGER, Peter, Difference in photoreactivation of uv damage between genes in repressed and derepressed states, 20: 12713
STAUB, F. W., Prog. rpt. on two-phase flow, 7–9/65, 20: 12962 (GEAP-4959)
STAVINSKII, V. S., Elastic 180° scattering of π^+ mesons by protons at high energies, 20: 13471
STECH, Berthold, Predictions for the electromagnetic formfactors of baryons from hybrid groups, 20: 13627
STEELE, Bernard Robert, Improvements in or relating to fuel for reactors, 20: 13228
STEELE, E. J., Displacement damage in MOS transistors, 20: 13133
STEIGER, R. H., Lead isotopes and age of the earth, 20: 12991
STEIN, Wayne Alfred, Continuum electromagnetic radiation from solar flares, 20: 13409
STEINBERG, M., Liquid fuel synthesis using nuclear power in a mobile energy depot system, 20: 12877 (BNL-955)
STEINBERGER, J., K-meson decay and CP invariance, 20: 13495
STEKLY, Z. J. J., Behavior of superconducting coil subjected to steady local heating within windings, 20: 13675
STEPANOV, A. V., Graphic method of solving neutron physics problem, 20: 13732
STEPANOV, A. V., Theory of passage of cold neutrons through matter, 20: 13733
STEPHENSON, Thomas E., Neutron cross section of sodium below 40 kev, 20: 13753 (BNL-961)
STERLINSKI, Slawomir, Regression and correlation in scintillation γ spectrometry of short-lived radioisotopes, 20: 12781
STERLINSKI, Slawomir, Relation between lower limit of detection of radioactivity counter and time of measurement, 20: 13078
STERMAN, L. S., Critical heat flux on submerged surfaces during boiling of organic coolants, 20: 12965
STERN, J., Nonperturbative field-theoretical model of leptonic weak interactions, 20: 13464
STERNBERG, Eli, Three-dimensional stress concentration around cylindrical hole in semi-infinite elastic body, 20: 12943 (ANL-7097)
STETHERS, Howard, Pilot-plant development of process for U alloy fuels. VIII., 20: 12924 (ANL-6973)
STEUDEL, A., Lifetime of excited state of europium, 20: 13422
STEVENS, Walton E., Radiation therapy in lung cancer, 20: 12741
STEWART, D. C., Yield data for transplutonium element production in thermal reactors, 20: 13752 (ANL-7096)
STEWART, H. J., Pituitary implantation for pituitary tumors, 20: 12753
STEWART, Helen J., Plasma-growth-hormone levels in untreated acromegaly and after radioactive implants into pituitary, 20: 12748
STIEVENART, M., Fast neutron non-multiplying assemblies, 20: 13719
STIEVENART, M., Pulsation of fast subcritical assemblies, 20: 14087
STIEVENART, M., Study of UO_2–PuO_2–H_2O lattices by pulsed neutron techniques, 20: 14078
STOCKENDAL, R., M4 isomerism in ^{205}Pb, 20: 13766 (CONF-233(Vol.4), pp 726-9)
STOENNER, R. W., Search for radiochemical evidence for ternary fission of ^{235}U by thermal neutrons, 20: 13862
STOKER, Donald Jr., Nuclear reactor core unit cell, 20: 14050
STONE, L. H., High-remelt-temperature brazing of Ta using diffusion sink concept, 20: 13224
STONER, D. R., Prog. rpt. on weldability and stability of refractory alloys, 3/21–6/20/65, 20: 13264 (WANL-PR(P)-008)
STORRER, F., Pulsed and modulated experiments on fast multiplying

media, 20: 13723
STORRER, F., Pulsed neutron experiments on fast and intermediate systems, 20: 14083
STORRER, F., Theory of pulsed and modulated experiments on fast neutron multiplying media, 20: 14088
STOYANOV, D., Problem of combination of space and internal symmetries of elementary particles, 20: 13542 (JINR-P-2443)
STRATHDEE, J., Relativistic U(6,6) theory, 20: 13534 (IC/66/5)
STRAUB, Conrad P., Comparison of ^{90}Sr component of human and cows' milk, 20: 13012
STRAUSS, B. P., Superconductivity of composite of fine niobium wires in copper, 20: 13673
STREKALOVSKII, V. N., Phase components in ZrO_2–$PrO_{1.83}$ system, 20: 13279
STROMATT, R. W., Nickel electroplating on U, 20: 13211 (BNWL-124)
STRUTHERS, D. R., Automatic-control-system design for Berkeley 88-inch cyclotron, 20: 13381
STUART, A. E., Prognostic significance of thyroid antibodies in management of thyrotoxicosis, 20: 12626
STUART, C., Response to whole-body irradiation of mice pretreated with stimulating drugs, 20: 12685
STUNGIS, G. E., Power dependence of saturation of EPR spectrum of F center at 4°K, 20: 13975
STURMAN, I., Prototype radioisotope inspection system to measure residual flux on automatically processed electronic circuit boards, 20: 13033 (TLW-1110)
STYCZEN, J., Magnetic interaction of ^{155}Gd nucleus in 87-kev excited state, 20: 13763 (CONF-233(Vol.4), pp 710-19)
STYRA, B. J., Determination of parameters of natural radioactive aerosol removal from air, 20: 12977
SUAREZ, C., Preparation of sulfides and elemental sulfur labeled with ^{35}S from neutron-irradiated KCl, 20: 12919
SUBBARAO, K., Pulsed neutron studies of BeO–natural uranium lattices, 20: 14080
SUBBA RAO, V. V., Thermogravimetric analysis of La, Ce, Pr, and Nd oxalates in air and in CO_2, 20: 12862
SUDDATH, J. C., Prog. rpt. on chemical separations processes, 4–6/65, 20: 12928 (ORNL-3868)
SUEMATSU, Sigeru, Neutron generator, 20: 13744
SUGIHARA, Yoshio, Carcinostatic effect of extracts from human gastric cancer, 20: 12625
SUGIMOTO, Shun, Protective device for accelerating tube, 20: 13388
SUITA, Tokuo, Neutron activation analysis of divalent ions in alkali halide crystals, 20: 12805
SUJKOWSKI, Z., Internal bremsstrahlung accompanying electron capture decay of medium heavy nuclei, 20: 13759 (CONF-233(Vol.4), pp 614-24)
SUMI, Yoshio, Nonmesic decay of light hypernuclei, 20: 13501
SUMITA, K., Neutron slowing-down time and thermalization time constant in graphite, 20: 13728
SUMITA, K., Subcriticality determination of reflected graphite system, 20: 14081
SUN, Jia-Bor, Test of reactor power meter by measuring ^{16}N activity in coolant, 20: 14019
SUPPLE, A., Material buckling and intracellular thermal neutron distributions, 20: 14065 (MIT-2344-4, pp 4-16)
SURANYI, P., Theory of Fermi interactions, 20: 13566
SUSS, J. T., Paramagnetic resonance spectrum of Co^{1+} in single crystals of CaO, 20: 13972 (IA-1056)
SUTHERLAND, W. A., Heat transfer in parallel rod arrays, 20: 12967
SUTOW, W. W., Growth status of children exposed to fallout radiation on Marshall Islands, 20: 13011
SUTTON, R. B., Gamma rays from decay of 35-day ^{95}Nb, 20: 13859
SUTTON, R. B., Measurement of energies of γ rays from decay of ^{66}Ga, 20: 13818
SUZUKI, F., Irradiation effects on polyvinyl chloride and applications for wire insulation, 20: 12907
SUZUKI, K., Transforming activity and integrity of DNA as revealed by ultraviolet flow dichroism, 20: 12620
SUZUKI, Mahiko, Proton-neutron mass difference, 20: 13511
SVECHKAREV, I. V., Effect of pressure on magnetic susceptibility of Mn and Sc, 20: 13312
SVELTO, V., Synthesis of an optimum filter for timing scintillation pulses, 20: 13104
SVENSSON, Goeran K., Transport of ^{137}Cs from lichen to animal and man, 20: 12578
SVIRIDENKO, V. Ya., Some questions of nuclear safety, 20: 14091
SWAN, P., Phase-equivalent potentials for neutron-α elastic scattering, 20: 13482
SWANSON, B. S., Critical temperatures and densities of alkali metals, 20: 12815 (ANL-7025)
SWINDELLS, N., Solubility of Fe in solid U between 0.003 and 0.3 wt.% Fe, 20: 13298
SYSOYEV, N. N., Radioactivity of waters of the Pacific Ocean, 20: 13007 (NP-tr-1336)
SZATMARY, Z., Data evaluation problems in pulsed neutron source method, 20: 13729
SZAVITS, O., Analog-to-digital converter nonlinearity due to the loss current, 20: 13042
SZEGLOWSKI, Zdzislaw, Electrolytic preparation of lead targets from stable isotopes ^{206}Pb and ^{207}Pb in sulfates form, 20: 12867
SZEPFALUSY, P., Perturbation-theoretic calculation of one-particle excitation spectrum in a large Bose system, 20: 13559
SZMANT, H. Harry, Detection of radiation damage in anthracene crystals by space-charge-limited current measurements, 20: 12893
SZTEKE, W., Properties of boron carbide sintered under pressure, 20: 13314

T

TADA, H., Thermal neutron diffusion length measurements in poisoned organic material, 20: 13718
TADEUSH, V. N., Determination of mixing parameter of M1 and E2 radiation for 0.341-Mev transition in ^{49}Ti, 20: 13803
TAENZER, Volker, Changes in radiosensitivity by preirradiation, 20: 12701
TAHERZADEH, Moj-taba, Production and decay of the Λ-π resonances in the K^-n collisions, 20: 13522
TAKABAYASI, Takehiko, Spinor model of baryons and mesons, 20: 13612
TAKAYAMA, Kazuo, Dose distribution of rotation therapy of cervical cancer with 15-Mev betatron, 20: 12747
TAKEDA, Gyo, Internal coordinates, SU_3 symmetry, and charge of elementary particles, 20: 13617
TAKETANI, Mituo, High-energy nuclear interactions and structure of elementary particles, 20: 13514
TAKHTAMYSHEV, G., Search for new decay modes of K^0_2 mesons, 20: 13450 (JINR-P-2488)
TAMAGAKI, Ryozo, Possible origin of repulsive core in nuclear forces, 20: 13879
TAMAS, Jozsef, Determination of ^{18}O content in small samples of water by mass spectrometry, 20: 12800
TAMBOISE, Edmond, Superstructure of adenohypophysial tumors from combined effects of I-131 and chlorpromazine, 20: 12657
TAMIR, T., Surface and interface waves in plasma gaps, 20: 13945
TAMIYA, Takenori, Nonmesic decay of light hypernuclei, 20: 13501
TAMURA, Taro, FORTRAN programs for Clebsch-Gordan and Racah coefficients and the NINE-j symbol, 20: 13648 (ORNL-3877(Rev.))
TAN, D. S., Fermi surface, 20: 13988
TANAKA, Osamu, Betatron, 20: 13391
TANAKA, S., Energy dependence of nuclear level density below the neutron binding energy, 20: 13827
TANAKA, S., 5.5-Mev ion buncher of Mobley type, 20: 13379
TANG, M. D., Quick method for calibrating the electron of an electron accelerator, 20: 13377
TANIKAWA, Yasutaka, Particle dynamics and symmetries in de Sitter space, 20: 13619
TANNENBAUM, M. J., K-meson decay and CP invariance, 20: 13495
TANOOKA, Hiroshi, Comparison of methods of personnel-monitoring dosimetry practiced in nuclear establishments of different countries, 20: 13003 (JAERI-4035)
TARABELLA, A., Calibration of control rods in natural uranium–graphite lattices, 20: 14163
TATEISHI, Y., Ultrasonic testing of metallic uranium, 20: 14194
TATTERSALL, John Owen, Improvements in and relating to fueling arrangements for nuclear reactors, 20: 14036
TAUBER, M., Method for measurements of total neutron cross sections, 20: 13101
TAUSCHER, L., First-order theory of high-dispersion spectrometer with winding magnetic field, 20: 13087
TAVERNIER, G., Study of UO_2–PuO_2–H_2O lattices by pulsed neutron techniques, 20: 14078
TAWARA, Hiroyuki, Neutron generator, 20: 13743
TAYLOR, Alan Frederick, Nuclear fuel element with improved end cap assembly, 20: 14113
TAYLOR, Charles D., Final safety analysis of maximum credible accident in the HWCTR, 20: 14183 (DP-1037)
TAYLOR, J. C., Neutron-diffraction study of $UO_2(NO_3)_2 \cdot 6H_2O$, 20: 13233 (ANL-6943)
TAYLOR, J. K., Photopolarographic behavior of inorganic depolarizers, 20: 12798
TAYLOR, Roderick, Improvements in and relating to nuclear reactors, 20: 14037
TEITAKOWSKI, M., Survey of radioactive content of food grown on Brazilian areas of high natural radioactivity, 20: 12988
TELLIER, H., Calibration of control rods in natural uranium–graphite lattices, 20: 14163
TELLIER, H., Study of homogeneous core assemblies using pulsed neutron sources, 20: 14077

TEREKHOVA, V. F., Rare earth alloys and compounds, 20: 13280
TERENT'EV, M. V., C-odd multipoles, 20: 13475
TERNINI, John P., Radioactive fallout treatment kit, 20: 12942
TESTA, C., Reversed-phase partition chromatography and its application, 20: 12776 (RT/PROT(65)33)
THERET, Claude, Superstructure of adenohypophysial tumors from combined effects of I-131 and chlorpromazine, 20: 12657
THERET, Claude, Ultrastructure of experimental adenohypophysial thyrotropic tumors after radiothyroidectomy, 20: 12652
THIEBLEMONT, Bernard, EPR study of x-irradiated $KClO_3$, 20: 12888
THIRRING, W. E., Functional methods and exact solutions in field theory, 20: 13563
THOMAS, A. C., Long-term compatibility of thermionic converter materials with cesium, 20: 13203
THOMAS, J. P., Pituitary implantation for pituitary tumors, 20: 12753
THOMAS, M. F., Excited states of ^{19}F by angular correlation technique, 20: 13822
THOMAS, W. E., RCS-2—FORTRAN program for calculation of cross sections from resonance parameters, 20: 13786 (ORNL-TM-1396)
THOMAS, W. R. G., Pituitary implantation for pituitary tumors, 20: 12753
THOMPSON, Ch., Transport of hot electrons in thin aluminum films, 20: 14002
THOMPSON, Leonard R., Hemangioma associated with thrombocytopenia, 20: 12750
THOMPSON, S. G., Kinetic energy-mass distributions from fission of nuclei lighter than radium, 20: 13861
THOMPSON, T. J., Prog. rpt. on D_2O lattice project, annual, 9/65, 20: 14014 (MIT-2344-4)
TI, Kao, Electromagnetic properties of the 70-dimensional representation in the SU(6) scheme, 20: 13624
TIABLIKOV, S. V., Observations on the many-body problem in the A. A. VLASOV arrangement, 20: 13551 (LA-tr-66-8)
TILLEY, D. R., Angular-correlation measurements for the $^{26}Mg(d,p\gamma)^{27}Mg$ reaction, 20: 13768 (CONF-650410-40)
TILLEY, D. R., Cylindrical Josephson junctions, 20: 13680
TILTON, G. R., Lead isotopes and age of the earth, 20: 12991
TIMMERMAN, Robert, Cross-linking of polyvinylidene fluoride, 20: 12909
TINDALE, John Valentine, Improvements in reactor fuel element cans, 20: 14107
TINGEY, F. H., Nondestructive testing in test-reactor operation at NRTS, 20: 14197
TINKLE, Donald W., Effects of radiation on population of lizards, 20: 12585
TIREN, L. I., Experimental studies on assemblies 1 and 2 of fast reactor FRO. II., 20: 14178 (AE-207)
TITRAN, Robert H., Ultrahigh-vacuum creep behavior of Nb and Ta alloys at 2000 and 2200°F, 20: 13256 (NASA-TN-D-3222)
TITTEL, K., K-meson decay and CP invariance, 20: 13495
TKACHEV, L. G., Electromagnetic properties of the 70-dimeasional representation in the SU(6) scheme, 20: 13624
TOBIAS, Melvin, Certain definite integrals of Bickley and Bessel functions, 20: 13707 (ORNL-TM-1415)
TOBIAS, Melvin, Gaussian quadrature procedure for computation of Bickley functions, 20: 13708 (ORNL-TM-1417)
TOCHILIN, E., Dose rate and spectral measurements from pulsed x-ray generators, 20: 13057 (AD-627567)
TODOROV, I. T., Recent achievements in axiomatic approach to quantum field theory, 20: 13565
TOLMIE, R. W., Radioisotope x-ray backscatter gage, 20: 13050
TOMISELLI, G., Response to whole-body irradiation of mice pretreated with stimulating drugs, 20: 12685
TOMITA, Y., Energy dependence of nuclear level density below the neutron binding energy, 20: 13827
TOMITA, Y., 5.5-Mev ion buncher of Mobley type, 20: 13379
TOMIN, M., Connection between vacuum-like and light-like solutions of the Bethe-Salpeter equation, 20: 13569
TONOMAE, R., Measurement of internal friction of nuclear materials, 20: 13321
TOPE, William G., Production of PuC, 20: 13208 (ANL-6969)
TORRES, L., Cloud chambers filled with dielectric liquid, 20: 13112
TOSCHI, R., Direct conversion of thermal energy in MPD power generation program at C.N.E.N., 20: 13431 (RT/FI(65)31)
TOURNIER, G., Swirl flows in boiling water, 20: 12960 (EURAEC-1515)
TOUVIN, H., Prog. rpt. on effects of mutagenic substances, annual, 1964, 20: 12632 (EUR-2546.f)
TOWNER, Joseph W., Effect of radioactive fallout at the Nevada Test Site on chromosomes of the pocket mouse, 20: 12666
TOYODA, Toshiyuki, Relation between the Minkowski and isobaric spaces, 20: 13615
TRAIL, C. C., Gamma rays from decay of 35-day ^{95}Nb, 20: 13859
TRAIL, C. C., Measurement of energies of γ rays from decay of ^{66}Ga, 20: 13818
TRAVERSE, Jean-Pierre, High-temperature study of changes of the crystalline form of Nd_2O_3, 20: 13979
TREADO, P. A., Triple correlations in $^{56}Fe(p,\gamma\gamma)^{57}Co$ reaction, 20: 13857
TRESTER, Seymour, Detection of radiation damage in anthracene crystals by space-charge-limited current measurements, 20: 12893
TRESVYATSKII, S. G., Investigation of the optical properties of compounds formed in La_2O_3–SrO and La_2O_3–BaO systems, 20: 13278
TREYTL, W. J., Decay properties of ^{86}Zr, 20: 13856
TRIDOT, Gabriel, Hydrates and thermal decomposition of uranium sulfate, 20: 12843
TRILLING, G. H., Reaction $K^+ + p \rightarrow K + N + \pi$ between 0.86 and 1.58 Bev/c, 20: 13462 (UCRL-16370)
TRISTEM, C. E. R., The effect of purification and recontamination on slip in beryllium single crystals, 20: 13239
TRNOVEC, T., Effect of carrier on pulmonary retention of radiocerium, 20: 12615
TROEGER, Herbert, Electric protection system for nuclear reactors, 20: 14053
TROST, W., Parity of the 6.89-Mev level in ^{14}C, 20: 13828
TRUKHANOV, G. Ya., Neutron thermalization in graphite-water system at large temperature gradients, 20: 13740
TRUMBLE, R. E., N reactor analog simulation feasibility study, 20: 14167 (HW-70878)
TRUNOV, V. K., X-ray investigations of binary oxides of zirconium and niobium, 20: 13281
TRUSKOVA, N. F., Charge distributions of particles in one-meson theory of interelastic interactions at high energies, 20: 13452 (JINR-P-2510)
TRUSKOVA, N. F., Estimation of interaction cross section for unstable nuclei, 20: 13449 (JINR-P-2433)
TSAGARIS, M. E., RCS-2—FORTRAN program for calculation of cross sections from resonance parameters, 20: 13786 (ORNL-TM-1396)
TSIEN, K. C., Photographic representation of isodose patterns by application of Sabattier effect, 20: 13008
TSIPENYUK, Yu. M., Photofission angular anisotropy and parity of ^{239}Pu ground state, 20: 13809
TSUJI, Yoshio, Application of large accelerator to produce irradiated polyethylene products, 20: 12906
TSUKADA, K., Energy dependence of nuclear level density below the neutron binding energy, 20: 13827
TSUKADA, K., 5.5-Mev ion buncher of Mobley type, 20: 13379
TU, Pham Quy, Limit of applicability of the perturbation theory in weak interactions, 20: 13622
TUCKER, Mary Ann, Trans-effect in hydrolysis reactions of trichloro-ammineplatinate(II) ion, 20: 12820 (IS-T-57)
TUCZEK, H., Acceleration of plasma through magnetic bottle according to free-particle model, 20: 13911 (JUL-336-PP)
TURNER, F. B., Growth of lizards in natural populations exposed to γ irradiation, 20: 12669
TYAN, M. L., Bone marrow as source of immunologically competent cells, 20: 12716 (AD-626682)
TYLKINA, M. A., Properties and uses of rhenium, 20: 13266 (AD-624905)
TYULINA, M. A., Disappearance of charge carriers in plasma moving in an electric field, 20: 13952

U

UEDA, Tamotsu, Inelastic process and one-boson-exchange model, 20: 13616
ULEGLA, I., Nucleon-nucleon potential with a soft core for $^1S_0$ state at 0.17 to 310 Mev, 20: 13489
ULLAH, Nazakat, Correlated width fluctuation factor, 20: 13824
ULLRICH, W., Pulsed neutron reactivity measurements in the near-critical state, 20: 14082
UL'MANN, A., General structure of an operator which is multiplicative with respect to a symmetry group, 20: 13165 (JINR-E-2542)
UL'MANN, A., SU(6) and the operators CPT and C., 20: 13540 (JINR-E-2545)
UL'YANOV, K. N., Balance equation for nonequilibrium plasma, 20: 13956
UMEMURA, Isao, Variant triplet model and integral charge, 20: 13618
UMEZAWA, H., Rearrangement of symmetries in dynamical maps, 20: 13620
UMEZAWA, H., Self-consistent method, 20: 13552
UMIASTOWSKI, K., Radiometric determination of spatial concentration of inhomogeneous fluid in pipe lines, 20: 13049
UMLAUF, Harry J. Jr., Hemangioma associated with thrombocytopenia, 20: 12750
UMSTAETTER, H. H., Septum magnets with 10- and 20-kg fields for slow and fast ejection from the CPS, 20: 13359 (CERN-65-36)
UNDERWOOD, W. O., Filament-wound joint design study, 20: 14213 (ACF-15)
UPOR, Endre, Problems in determination of uranium with Arsenazo III, 20: 12799
USACHOV, L. N., Photofission angular anisotropy and parity of ^{239}Pu ground state, 20: 13809

UTIYAMA, Ryoyu, Generalized isospin-space, generalized gauge transformation and derivation of the meson, 20: 13611
UTZINGER, E., Pulsed-source experiments with multiplying and non-multiplying D_2O systems, 20: 14076
UYEDE, Ryozi, Coefficient of absorption of electrons accelerated by voltages between 100 and 1200 kv, 20: 13967

V

VACCA, Jacopo, Plane stationary and irrotational hydrodynamic motion of a fluid flow in a rigid circular profile, 20: 13641
VACCA, Maria Teresa, Slow stationary motion of a viscous electrically conducting liquid contained in a spherical channel, 20: 13642
VACHER, Robert, Improvements in installations for spectrophotometric analysis of radioactive solutions, 20: 12813
VAGIN, V. A., Diaphragmed waveguide as deflection system of high-frequency separator, 20: 13362 (JINR-P-2503)
VAGIN, V. A., Waves with complex propagation constants in diaphragmed waveguide, 20: 13363 (JINR-P-2507)
VAHLDIEK, Fred W., Hot pressing zirconia, 20: 13230
VALERIOTE, F. A., Effect of x irradiation and thermal trauma on intestinal mucosa, 20: 12630 (BNL-8383)
VANCURA, A., Multi-channel model of weak scattering of leptons, 20: 13465
VANCURA, A., Theory of Fermi interactions, 20: 13566
VANDERBURG, Vance Dilks, Muon energy spectrum from $K_{\mu 3}$ decay mode, 20: 13521
VAN DER HOEVEN, Bernard Jacob Cornelis Jr., Low-temperature specific heat of graphite and several pure superconductors, 20: 13692
VAN DER WALT, C. M., Burger's vectors in beryllium and their effect on ductility, 20: 13242 (CONF-170, pp 126-37)
VAN DER WOUDE, A., Polarized-proton scattering facility at the Oak Ridge Isochronous Cyclotron, 20: 13375
VAN DOMELEN, B. H., Neutron activation: relationship of sample mass to self-shielding factor, 20: 12794
VAN DYNE, George M., Application of operations research techniques to food chain analysis problems, 20: 12580
VANECKOVA, O., Macroautoradiography with radiophosphorus in stomach cancer, 20: 12742
VAN GASSELT, M. L. G., Conditions affecting burnout heat flux of polyphenyl cooling agents, 20: 14026 (EUR-2299.e)
VAN HOVE, L., SU_3 triplets with integral electric charge and the baryon structure, 20: 13598
VAN LEUVEN, P., Magnetic moment of nuclei for a momentum-dependent internucleon force, 20: 13842
VAN LIERDE, W., Preparation of uranium sulfide single crystals, 20: 12856
VAN MAAREN, M. H., Superconductivity in group V^a dichalcogenides, 20: 13683
VAN MEEL, D. A., Conditions affecting burnout heat flux of polyphenyl cooling agents, 20: 14026 (EUR-2299.e)
VANNOTTI, A., Radioimmunologic method for determination of thyroid-stimulating hormone, 20: 12755
VAN WINTER, Cleoine, Dispersion relations and resonance reactions in multi-channel scattering, 20: 13585
VARDENGA, G., Search for new decay modes of K_2^0 mesons, 20: 13450 (JINR-P-2488)
VARNER, Donald E., Measuring property of magnetizable workpiece using nuclear radiation, 20: 13054
VASIL'EV, M. P., Resonant heating of plasma by high-frequency field, 20: 13946
VAUBEL, Ekkehard, Induction of tolerance to allogenic grafts, 20: 12656
VEBRA, E. Yu., Determination of parameters of natural radioactive aerosol removal from air, 20: 12977
VEDENEEV, O. V., Fluctuations of energy fluxes of nuclear-active and electron-photon components in extensive air showers, 20: 13427
VEDENOV, A. A., Oscillations and instability of a weakly turbulent plasma, 20: 13931 (NP-tr-1348)
VEJVODA, E., Pyrohydrolysis of PuF_4, 20: 12775 (RFP-601)
VENARD, J. T., Effect of irradiation on stress-rupture characteristics of a Nb-stabilized stainless steel, 20: 13328 (ORNL-TM-1359)
VENTURINI, G., Technique of n-γ discrimination, 20: 13111
VENUS, G., Two-chamber ionization gage, 20: 13026 (IPP-2/39)
VERBA, J. W., Electric dissociation of the H⁻ ion near 2.4 Mev, 20: 13380
VERBINSKI, Victor V., Device for measuring biological effect of radiation, 20: 13121
VERDAGUER, F., Measurement of N_2 in organic liquids, 20: 13730
VERFAILLIE, Georges, Movement of fallout in irrigated ecosystems of Po Valley, Italy, 20: 12986
VERHEUL, H., Decay of ^{184}Ta, 20: 13767 (CONF-233(Vol.4), pp 730-42)
VERKHOROBIN, L. F., Kinetics of $MoSi_2$ oxidation at 1500 to 1800°C, 20: 13195
VERKHOROBIN, L. F., Oxidation of lower W and Mo silicides, 20: 13198
VERMANDE, P., Cloud chambers filled with dielectric liquid, 20: 13112
VERNICKEL, H., A-c method for measuring the characteristic data of a field emission point, 20: 13025 (IPP-2/37)
VERNOV, S. N., Fluctuations of energy fluxes of nuclear-active and electron-photon components in extensive air showers, 20: 13427
VERSTAPPEN, C., Eddy-current testing of thin-walled cladding tubes, 20: 14033
VERTUT, Jean, Improvements in hot cells, 20: 12953
VETTE, James I., Models of trapped radiation environment. I., 20: 13646 (NASA-SP-3024)
VILEMAS, Yu. V., Critical heat flux on submerged surfaces during boiling of organic coolants, 20: 12965
VILNAT, Jacqueline, Effects of gaseous atmospheres on emission spectrographic analysis of rare earths, 20: 12810
VLADAR, M., Effect of carrier on pulmonary retention of radiocerium, 20: 12615
VLADIMIRSKII, V. V., Degenerate SU(4) symmetry of strong interactions, 20: 13625
VLADYKOV, G. M., Some questions of nuclear safety, 20: 14091
VLASOV, A. A., Theory of nonlocalized particles, 20: 13550 (LA-tr-66-7)
VOELK, H., Conservation laws and microscopic stability of plasma, 20: 13909 (IPP-6/40)
VOGT, O., Valency changes in cerium compounds, 20: 13991
VOIGT, A. F., Prog. rpt. on reactor materials development, 10–12/65, 20: 13180 (IS-RD-4)
VOLCHENKOVA, Z. S., Phase components in ZrO_2–$PrO_{1.83}$ system, 20: 13279
VOLF, V., Effect of phosphates, carbonates, and MgO on intestinal absorption of ^{85}Sr in rats, 20: 12606
VOLKOVA, G. A., Contact reaction of titanium with niobium carbide on graphite, 20: 13194
VOLTA, Giuseppe, Heterogeneous reactor liquid moderated and cooled, 20: 14100
VOLYNETS, F. K., Special characteristics of processes for growing high-melting crystals in high-frequency plasma burners, 20: 13189
VONACH, W. G., Elastic and inelastic scattering of fast neutrons from Ag, In and Cd, 20: 13829
VON HOLLEN, H. J., Design features of the San Onofre nuclear station, 20: 14157
V[ON] SCHNERING, H. G., Structure investigations on La_2O_3, 20: 12872
VORONIN, K. K., Special characteristics of processes for growing high-melting crystals in high-frequency plasma burners, 20: 13189
VORON'KO, Yu. K., Effect of hard radiation on optical centers of TR^{3+} ions in crystals, 20: 13986
VOUK, V. B., Prog. rpt. on mammalian retention of radioactive Sr, 10/61–3/62, 20: 12594 (NP-15679)
VOUK, V. B., Prog. rpt. on mammalian retention of radioactive Sr, 4–9/62, 20: 12595 (NP-15680)
VOUK, V. B., Prog. rpt. on mammalian retention of radioactive Sr, 10/62–3/63, 20: 12596 (NP-15681)
VOUK, V. B., Prog. rpt. on mammalian retention of radioactive Sr, 4–6/63, 20: 12597 (NP-15682)
VOUK, V. B., Prog. rpt. on mammalian retention of radioactive Sr, 7/63–3/64, 20: 12598 (NP-15683)
VOUK, V. B., Prog. rpt. on mammalian retention of radioactive Sr, 4–6/64, 20: 12599 (NP-15684)
VOVCHENKO, V. G., Determination of imaginary part of phase shifts in elastic p-p scattering at 655 Mev, 20: 13470
VOVENKO, A. S., Elastic 180° scattering of π^+ mesons by protons at high energies, 20: 13471

W

WADA, A., Transforming activity and integrity of DNA as revealed by ultraviolet flow dichroism, 20: 12620
WAGNER, F. Jr., Response of NaI, anthracene, and plastic scintillators to electrons, 20: 12899
WAGNER, R. J., IREKIN—program for numerical solution of reactor kinetics equations, 20: 14060 (IDO-17114)
WAHL, H., Controlled expansion of UC pellets by surface oxidation in cladding, 20: 13188
WAINFAN, Elsie, Alterations in transfer ribonucleic acid methylases after bacteriophage infection or induction, 20: 12619
WAISEL, Yoav, Radiological method for determination of cambial activity, 20: 12614
WAIT, James R., Theory of wave propagation in bounded compressible plasma, 20: 13932
WAKEFIELD, R. H., Ion beam analysis by an electrostatic technique, 20: 13372
WALKER, D. C. B., Nondestructive examination of heat-affected zone of welded Zr–Nb alloy, 20: 13320
WALKER, D. G., Effect of neutron irradiation on Al_2O_3, 20: 13337
WALKER, J., Extrapolation distances for pulsed neutron experiments,

20: 13726
WALLIS, John Dewitney, Improvements in reactor fuel element cans, 20: 14107
WALSH, William K., Radiation-induced oxidation of hydrocarbons, 20: 12883 (ORO-634)
WALTER, C. M., Review of status of self-diffusion in US, UN, UO_2, and UC, 20: 13234 (ANL-7094)
WALTERS, G. P., Burger's vectors in beryllium and their effect on ductility, 20: 13242 (CONF-170, pp 126-37)
WALTERS, G. P., Effects of neutron irradiation on mechanical properties of hot-pressed and extruded, 20: 13323 (CONF-170, pp 138-59)
WALTHER, H., Lifetime of excited state of europium, 20: 13422
WANG, Pin-Fu, Thermal stresses in fuel elements, 20: 14106
WANG, Tso-Pin, Dynamical correlations and the nuclear photoeffect, 20: 13873
WARBURTON, A. E. A., Eigenvalues of Lippmann-Schwinger kernel for Yukawa and nucleon-nucleon potentials, 20: 13836
WARBURTON, E. K., Excited states of ^{19}F by angular correlation technique, 20: 13822
WARD, Ural T., Radioactive waste material incinerator, 20: 14212
WARNKE, D. F., Mie scattering functions computer program description, 20: 13346 (SC-RR-65-396)
WARREN, John, Observations on the many-body problem in the A. A. VLASOV arrangement, 20: 13551 (LA-tr-66-8)
WARREN, John, Theory of nonlocalized particles, 20: 13550 (LA-tr-66-7)
WASHBURN, Beverly, Pin technique for displacement measurements in Kiwi-TNT, 20: 14171 (LA-3388)
WASSERBURG, G. J., Strontium–rubidium age of an iron meteorite, 20: 12992
WASSERMANN, Felix E., Effect of uv radiation on HeLa cells infected with adenovirus, 20: 12711
WASSERMANN, Marien, Ion source for generation of a concave ion beam, 20: 13385
WATANABE, Keiji, Abnormal solution of Bethe-Salpeter equation, 20: 13614
WATANABE, Satosi, Conditional probability in physics, 20: 13353
WATANABE, T., Inverting the R matrix, 20: 13538 (IDO-17142)
WATARI, Wataro, Inelastic process and one-boson-exchange model, 20: 13616
WATERS, T. N., Crystal structure of dicesium tetrachlorodioxouranium (VI), 20: 12835
WATSON, C. D., Prog. rpt. on chemical separations processes, 4–6/65, 20: 12928 (ORNL-3868)
WATSON, G. M., Fueled-graphite systems, 20: 13261 (ORNL-3885, pp 87-149)
WATSON, G. M., Moderator materials, 20: 13262 (ORNL-3885, pp 195-235)
WATSON, R. A., Measurement and calculation of relative poison-to-fuel capture ratios in slab cores, 20: 14063 (KAPL-M-6528)
WAYLAND, Bradford, Determination of donor sites in Lewis acid adducts of anisole and thioanisole, 20: 14226 (TID-21586)
WAYLAND, Bradford B., Transition metal ion-ligand covalency from NMR contact shifts, 20: 12828 (TID-21587)
WEALE, J. W., Measurements of fast reactor spectra, 20: 14086
WEALE, J. W., Prompt neutron decay constant of VERA reactor, 20: 14089
WEBB, R. I. A., DASA fallout and transit dose rate measurement system, 20: 12978 (AD-627077)
WECHSLER, M. S., Irradiation testing of components and materials, EGCR, 20: 14140 (ORNL-3885, pp 284-93)
WECKERMANN, B., Cross-correlation method for study of neutron pulse transfer function, 20: 13724
WEIDENBAUM, B., Irradiation of 0.5-inch-diameter, solid-pellet UO_2 fuel rods, 20: 13326 (GEAP-5100C)
WEIGL, Frederic, Plasma sheath dynamics, 20: 13922 (NP-15703, pp 64-81)
WEINSTEIN, D., Yield-point occurrence in polycrystalline alpha zirconium, 20: 13245 (CONF-651017-7)
WEINSTOCK, Bernard, Structure of gaseous XeF_6, 20: 12860
WEIR, J. R., Effect of irradiation on stress-rupture characteristics of a Nb-stabilized stainless steel, 20: 13328 (ORNL-TM-1359)
WEIR, J. R., Irradiation embrittlement of stainless steel, 20: 13335
WEISZ, S. Z., Detection of radiation damage in anthracene crystals by space-charge-limited current measurements, 20: 12893
WELLER, W., Quasi-particle operators for the condensed Bose system, 20: 13670
WELLS, D. O., Decay of ^{56}Ni and ^{57}Ni, 20: 13815
WENDEBERG, Bo, External counting of ^{85}Sr and ^{47}Ca in localized bone infections, 20: 12735
WENTWORTH, R. A., Prog. rpt. on metabolism of selected radionuclides, final, 6/64–6/65, 20: 12588 (AD-626320)
WENTZEL, Gregor, Baryon ground states in Yukawa theories, 20: 13602
WENZL, H., Dose dependence of annealing stage II in neutron-irradiated aluminum, 20: 13340
WERNER, R. D., Electron capture to negative electron emission branching ratio for ^{142}Pr decay, 20: 13797
WERNER, W. J., Fabrication of aluminum-base irradiation test plates, 20: 13217 (ORNL-TM-1377)
WERT, C. A., Anisotropy of Snoek phenomenon in niobium, 20: 13980
WESLEY, E. J., Characteristics of ^{40}K distributed sources in water, 20: 13056 (AD-627000)
WESSEL, William LeRoy, Three-body problem in quantum mechanics, 20: 13630
WEST, R. W., Charged particle counting system, with particle separation, 20: 13076 (UR-875-117)
WESTERKOWSKY, Kurt, Circuit arrangement for radiation dose measurement, 20: 13124
WESTHAUS, P., Simple derivation of cluster expansions for many-fermion systems, 20: 13591
WESTHEAD, James W., Prog. rpt. on radiation damage in semiconductor materials, 5–7/65, 20: 13128 (NP-15835(Suppl.))
WHALEN, J. F., Digital computer system for executive control of fast neutron laboratory, 20: 13806
WHANG, D. H., Hamburg 4π large-volume radioactivity detector with liquid organic scintillator. II., 20: 13079
WHATLEY, M. E., Prog. rpt. on chemical separations processes, 4–6/65, 20: 12928 (ORNL-3868)
WHEELER, B. R., Uranium recovery from aluminum-alloyed fuel, 20: 12926 (IDO-14669)
WHEELER, John Archibald, Nonlocality of force, 20: 13663
WHICKER, F. H., Factors influencing accumulation of fallout ^{137}Cs in Colorado mule deer, 20: 12984
WHITE, D. H., Scattering of 262-kev polarized neutrons by ^4He, 20: 13717
WHITE, J. L., Prog. rpt. on advanced graphite fuel systems, 8/15–11/14/65, 20: 13247 (GA-6831)
WHITE, P. H., Room scattered background produced by a neutron source, 20: 13714
WHITE, R. H., Fluxoid quantization and critical fields in small superconducting samples, 20: 13685
WHITE, W. B., Prog. rpt. on crystal chemistry, 5/13–8/13/65, 20: 13260 (NP-15852)
WHITEHOUSE, W. J., Advanced course in principles of radiation protection. I., 20: 12732 (AERE-R-5084)
WHITTAKER, J. K., Simple current generator, 20: 13039
WILDIN, M. W., Radiative heat-transfer through an absorbing boundary layer, 20: 12966
WILDING, M. W., Stability of highly radioactive alumina calcine, 20: 14207 (IDO-14670)
WILHELM, H. A., Bismuth–zirconium alloy system, 20: 13252 (IS-1269)
WILKINS, M. D., Cytogenetic studies on the white locus in Drosophila, 20: 12664
WILL, Wolfram, Measurement of standard ion doses for x and γ radiation between 50 kev and 3 Mev. II., 20: 13113
WILLARD, H. James Jr., Prog. rpt. on radiation damage in semiconductor materials, 5–7/65, 20: 13128 (NP-15835(Suppl.))
WILLARD, William K., Long-term effects of acute low-level x rays on population dynamics of yellow fever mosquito, 20: 12668
WILLIAMS, C. D., Tempered structures of Zr–2.5 wt.% Nb alloy, 20: 13304
WILLIAMS, D., Gamma-spectrum stabilizer with compensation for effects of detector temperature variation, 20: 13094
WILLIAMS, E. C. Jr., Rates and pattern of radioisotope release from fresh tree litter at three levels of mesic forest development, 20: 12566 (COO-1006-4)
WILLIAMS, L. P., Pathfinder reactor building integrated leakage rate test, 20: 14143 (PAPP-6401)
WILLS, Stanley Charles Frederick, Sealing means for providing seal between two relatively movable parts, 20: 12949
WILSON, C. R., Irradiation of 0.5-inch-diameter, solid-pellet UO_2 fuel rods, 20: 13326 (GEAP-5100C)
WILSON, J. P., Tunnel-effect measurements on superimposed layers of lead and aluminum, 20: 13687
WILSON, John N., Description of temperature monitor for large reactors. III., 20: 14025 (DP-944)
WILSON, L. V., Centrifugal pump for a molten-salt nuclear reactor, 20: 14164
WILSON, Mark, Reaction $^7Li(p,\gamma)^8Be^*$ and single-particle levels in ^8Be, 20: 13810
WILSON, S. A., Autoradiography: Technique for drastic reduction of exposure time to α particles, 20: 12563
WILSON, Volney C., Thermionic converter, 20: 13441
WINCEL, Henryk, Primary processes in radiation chemistry as studied by mass spectrometry. IV., 20: 12901
WIND, H., Electric field dissociation of H_2^+, 20: 13412 (CLM-R46)
WINKLER, H., Modified pulsed source techniques, 20: 14199
WIT, Romuald, Modification of the new sum rule, 20: 13571
WITALIS, E. A., Methods for determination of currents and fields in steady two-dimensional MHD flow, 20: 13634 (AE-210)
WITHERSPOON, John P., Radiation damage to forest surrounding an

unshielded fast reactor, 20: 12672
WITT, F. J., Moderator materials, 20: 13262 (ORNL-3885, pp 195-235)
WITT, F. J., Studies for advanced systems, 20: 14137 (ORNL-3885, pp 236-43)
WITTE, H. O., Ball-milling of graphite-base reactor fuel, 20: 13218 (ORNL-TM-1412)
WITTE, S., Bone-marrow transfusion in the whole-body irradiated, tumor-bearing rat, 20: 12651
WITTWER, S. H., Pathways and mechanisms for foliar absorption of mineral nutrients, 20: 14219 (COO-888-47)
WITTWER, S. H., The effects of urea on ion penetration through isolated cuticular membranes and ion uptake by leaf cells, 20: 14218 (COO-888-44)
WITTWER, S. H., Uptake and transport of ^{59}Fe by intact leaves and enzymically isolated leaf cells of the bean plant, 20: 14220 (COO-888-48)
WITTWER, Sylvan H., Ion uptake by cells enzymically isolated from green tobacco leaves, 20: 14217 (COO-888-43)
WITZKE, Walter R., Mechanical properties and recrystallization behavior of electron-beam-melted W, 20: 13257 (NASA-TN-D-3232)
WOJTASZEK, J., Higher symmetry groups with parity mixing, 20: 13599
WOLF, L., MOSEL: comparison of spectra and spectrally determined parameters of a two-component salt melt, 20: 14127 (JUL-291-RG)
WOLF, L. A., MOSEL: comparison of spectra and spectrally determined magnitudes of a two-component salt melt ($NaF-BeF_2$), 20: 14129 (JUL-315-RG)
WOLFF, H., Hydrogen bonding and vapor pressure isotope effects in a-deuterated methyl and ethyl amines, 20; 12879
WOLLENBERG, Harold A., Low-background concrete, 20: 12946 (UCRL-11674)
WONG, C., Excited states in ^{6}Be, 20: 13845
WONG, S. S. M., Positive parity states in ^{16}O, 20: 13844
WOOD, D. P., Administrative aspects of criticality controls, 20: 14092
WOOD, G. M., Development of high-temperature molten lithium pump, 20: 12948
WOOD, J., Extrapolation distances for pulsed neutron experiments, 20: 13726
WOOD, R. G., Pituitary implantation for pituitary tumors, 20: 12753
WOOD, R. G., Plasma-growth-hormone levels in untreated acromegaly and after radioactive implants into pituitary, 20: 12748
WOODRUFF, G. L., Fast neutron distributions, 20: 13703 (MIT-2344-4, pp 17-47)
WOOLLETT, Richard R., Error in induced electric field modes under Stix coil from assumption of orthogonality of natural plasma modes, 20: 13918 (NASA-TN-D-3255)
WOOLLEY, F. M., Bibliography on ultrasonic welding, 1960--65, 20: 13210 (AWRE/LIB/BIB/13)
WORKER, J. M., Structural application of beryllium in the U.K., 20: 13244 (CONF-170, pp 221-44)
WORLEY, Norman George, Improvements in or relating to nuclear reactors, 20: 14108
WORLEY, Norman George, Improvements in or relating to nuclear reactors, 20: 14109
WOZNIAKOWSKA, Z., Rectal complications following radium treatment of uterine carcinoma, 20: 12696
WRIGHT, I. J., Prototype radioisotope inspection system to measure residual flux on automatically processed electronic circuit boards, 20: 13033 (TLW-1110)
WU, Tsun-fan, Search for new decay modes of K_2^0 mesons, 20: 13450 (JINR-P-2488)
WU, Tsung-fan, Leptonic decays of K^0 mesons and possible CP violation, 20: 13515
WULFF, J., Magnetic field distribution in type II superconductor, 20: 13672
WULFF, J., Superconductivity of composite of fine niobium wires in copper, 20: 13673
WURSTER, D. E., Operating characteristics of the present PM-type reactor instrumentation. Task 2 topical report, 20: 14134 (NYO-3379-2)
WUSTNER, R., Reactor types with fast neutrons in France, 20: 14192
WYDLER, P., Measurement of time-dependent spectrum in D_2O, 20: 13736
WYNCHANK, S. A. R., Thermal neutron absorption cross section of the AERE boron standard, 20: 13807

Y

YABUKI, Hanichi, Many-pole amplitudes and elementarity. I., 20: 13592
YAGI, K., Reduction of resolution in uniform-field magnetic analyzer system, 20: 13091
YAGUDINA, F. R., Determination of the *ynp* interaction constant, 20: 13477
YAHAGI, Kichinosuke, Effect of carrier traps in polyethylene under γ irradiation, 20: 13982
YAKIMOVICH, K. A., Thermodynamics of MHD power generator with vapor-filled injector, 20: 13438
YAMADA, Eiji, Variant triplet model and integral charge, 20: 13618
YAMADA, Y., Pathways and mechanisms for foliar absorption of mineral nutrients, 20: 14219 (COO-888-47)
YAMADA, Y., The effects of urea on ion penetration through isolated cuticular membranes and ion uptake by leaf cells, 20: 14218 (COO-888-44)
YAMAFUJI, K., Angular dependence of upper critical field in thin films, 20: 13681
YAMAGUCHI, Yoshio, Gravitation physics, 20: 13665
YAMAMOTO, Hozumu, Comparison of methods of personnel-monitoring dosimetry practiced in nuclear establishments of different countries, 20: 13003 (JAERI-4035)
YAMAMOTO, Yoshitake, Forward diffraction peak and high-energy behavior of scattering amplitudes, 20: 13595
YAMANAKA, Chiyoe, Study of shock waves by microwave techniques, 20: 13936
YANAGI, Takako, Measurement of leakage tritium from tritium self-luminous paints, 20: 13153
YANO, Masaaki, Hysteresis phenomenon near B_C in positive column in a magnetic field, 20: 13937
YAREMENKO, Z. A., Investigation of the optical properties of compounds formed in La_2O_3–SrO and La_2O_3–BaO systems, 20: 13278
YASUNO, Masaru, Possible origin of repulsive core in nuclear forces, 20: 13879
YATA, Minoru, Fabrication of UO_2 fuel element by vibratory compaction, 20: 13225
YERANOS, W. A., Normal coordinate analysis of $XeOF_4$ in the Urey-Bradley field, 20: 12841
YERANOS, W. A., Vibrational analysis of IO_4^- and XeO_4, 20: 12842
YOCCOZ, J., Self-consistent field and method of projection, 20: 13826
YONEYAMA, Tatsuo, Electron microscopic studies on normal mouse spleen and its morphological changes after total-body irradiation, 20: 12681
YONEZAWA, Minoru, Inelastic process and one-boson-exchange model, 20: 13616
YOSHIDA, Yoshinori, Linear accelerator using multi-cavity type speed-modulation tube oscillator, 20: 13389
YOSHIHARA, Hidetosi, Influence of radioprotective substances on damages to bone growth in rats, 20: 12729
YOSHIKI, H., Muon and pion scattering in freon, 20: 13480
YOSHIYANAGI, Kiyomi, Swimming-pool-type reactor, 20: 14205
YOUNG, E. F., Field enhancement in superconducting tubes, 20: 13678
YOUNGBLADE, Walter, Influence of temperature on F-center absorption in NaF, 20: 12892
YOUNGDAHL, Carl K., Three-dimensional stress concentration around cylindrical hole in semi-infinite elastic body, 20: 12943 (ANL-7097)
YOVELL, Frederick Peter, Improvements in and relating to nuclear reactors, 20: 14037
YUAN, Liq-Ji, Test of reactor power meter by measuring ^{16}N activity in coolant, 20: 14019
YUDIN, N. P., Electromagnetic properties of elementary particles in the SU(6) group, 20: 13623
YUDKEVICH, M. S., Neutron-thermalization process in time in graphite and beryllium, 20: 13738
YUNGCLAUSSEN, G., Evaporation of neutrons from compound nuclei with large angular momenta, 20: 13885
YURI, T., Irradiation effects on polyvinyl chloride and applications for wire insulation, 20: 12907

Z

ZADORI, Ernoe, Effects of whole-body irradiation and bone marrow irradiation on osmotic resistance of reserve leukocytes, 20: 12705
ZADUBAN, Milan, Continuous recording of spectra with DRg-140 recording instrument and NZG-319 single-crystal γ scintillation spectrometer, 20: 13086
ZAFIRATOS, C. D., Excitation of a 3-collective state by low-energy neutron scattering, 20: 13870
ZAFIRATOS, C. D., Reaction $^{10}B(^{3}He,n)^{12}N$, 20; 13808
ZAJIC, V., Research work on the water loop in the WWR-S Reactor, 20: 14190 (UJV-1446/65)
ZAKATOV, L. P., Influence of mirror ratio on plasma heating by an electron beam in a probkotron, 20: 13947
ZAKRZEWSKI, J., Observation of fission events in mica sandwiches, 20: 13099
ZALEWSKI, Kacper, Conjecture of the high-energy behavior of two-particle scattering amplitudes, 20: 13572
ZALEWSKI, Kacper, High-energy asymptotic expansion for sum of phase space integrals, 20: 13574
ZALEWSKI, Kacper, Quantum statistics in statistical model of multiple production of particles, 20: 13573
ZAMBROW, John L., Process for assembling concentrically spaced nuclear fuel elements, 20: 13231
ZAMICK, L., Allowed, but inhibited β decays of ^{43}K and ^{45}K, 20: 13837
ZAMICK, L., Magnetic moment corrections to second order in perturbation theory, 20: 13838

ZAMICK, L., Nuclear binding energy parameters in terms of realistic two-nucleon potentials, 20: 13840
ZAPFF, Joachim, Boiling water reactors with exchangeable fuel elements, 20: 14098
ZARETSKAYA, Yu., Transplantation immunity and radiative chimeras, 20: 12731
ZAWADOWSKI, A., Sum rules in quantum field theory and in the many-body problem, 20: 13561
ZECCHINA, L., Methods of measurement of low intermetallic diffusion coefficients, 20: 13270
ZEIDLER, M. D., Reorientation times, transition times, and quadrupole coupling in organic fluids, 20: 12839
ZEL'DOVICH, Ya. B., Number of quanta as an invariant of classical electromagnetic fields, 20: 13659
ZGLINSKI, A., Internal bremsstrahlung accompanying electron capture decay of medium heavy nuclei, 20: 13759 (CONF-233(Vol.4), pp 614-24)
ZHELOBENKO, D. P., Lectures on Lie group theory, 20: 13169
ZHURAVLEVA, M., Search for new decay modes of K^0_1 mesons, 20: 13450 (JINR-P-2488)
ZIEGLER, Albert, Regulating method and apparatus for reactors, 20: 14052
ZIEGLER, Waldemar T., Thermal conductivities of MgO, Al_2O_3, and ZrO_2 powders to 850°C. I., 20: 12854
ZIEGLER, Waldemar T., Thermal conductivities of MgO, Al_2O_3, and ZrO_2 powders to 850°C. II., 20: 12855
ZIELINSKA, Malgorzata, Second vibrational state of even-even spherical nuclei, 20: 13793
ZIJP, W. L., Activation methods for determination of intermediate neutron spectra, 20: 13070 (RCN-40)
ZIMMERMAN, R. L., A status report on an ion engine development program, 20: 12975
ZIMMERMANN, H. J., Prog. rpt. on electronics, 10/15/65, 20: 14227 (TID-22419)
ZIMMERMANN, W. E., Newer therapeutic possibilities for thermonuclear injuries, 20: 12724
ZIN, Giovanni, Complementary moment of electromagnetic momentum radiated from a point source, 20: 13576
ZINGELMANN, W. J., Determination of equivalence between sterilization process and commercial thermal process for cured meats, 20: 13134 (AD-625252)
ZIPF, G., MESPRO 64—program for on-line computer MIDAS, 20: 13166 (KFK-371)
ZMII, V. I., Kinetics of $MoSi_2$ oxidation at 1500 to 1800°C, 20: 13195
ZMII, V. I., Oxidation of WSi_2 at 1500 to 1800°C, 20: 13196
ZMII, V. I., Oxidation of $TaSi_2$ in temperature range from 1400 to 1600°C, 20: 13197
ZOELLER, Wolfgang W., Reactions of embryos to irradiation of extraembryonal region of hens, 20: 12706
ZOERGIEBEL, F., Ultra-thin sections of CsI single crystals, 20: 13985
ZOJA, R., Zircaloy-2–stainless steel diffusion bonds, 20: 13222
ZSEBOEK, Zoltan B., Defense mechanisms of cysteamine and AET for intestinal radiation death, 20: 12721 (BNWL-tr-11)
ZUBER, N., Prog. rpt. on two-phase flow, 7–9/65, 20: 12962 (GEAP-4959)
ZUCKER, A., Polarized-proton scattering facility at the Oak Ridge Isochronous Cyclotron, 20: 13375
ZYLICZ, J., Internal bremsstrahlung accompanying electron capture decay of medium heavy nuclei, 20: 13759 (CONF-233(Vol.4), pp 614-24)

SUBJECT INDEX

Main entries in this index are generally specific materials, things, and processes. These are followed by modifiers that describe the properties of, and processes applied to, the main entries.

The number preceding the colon is the *NSA* volume number, and the number following is the abstract number. The designation (R) following the abstract number indicates that the abstract is of a progress report; (P) indicates a patent; and (T) indicates a translation. Abstracts for reports other than progress reports carry no letter designation. References to report numbers, where appropriate, are included after the abstract number of the citation. Published literature (journal article or book) is identifiable by the absence of a report number.

The user should bear in mind that the ideas presented in the original literature, rather than key words, have been indexed. The indexers have tried to select what seemed the most probable and logical place to look for typical information. Since it is not possible to anticipate where a user would look for information, numerous cross references are included in cumulative indexes to assist him in his search.

Experience in using an index of this type will be the best guide in obtaining the desired information, and a consideration of synonymous or closely related terms will prove valuable.

Information must be so indexed as to be of the greatest use to the greatest number of users. This requires that a topic be indexed to headings that most specifically describe it and not ordinarily to the headings that describe its ultimate use, nor to the general class headings that include the specific headings. For example, information on the treatment of thyroid disease with I-131 would be indexed under Thyroid Gland and under Iodine Isotopes I-131, but not necessarily under Radiotherapy. A study of the effects of x radiation on hair would be indexed under both X Radiation and Hair. However, the information would not be indexed under the experimental animal, e.g., Rats, unless the report discusses the effects on rat hair as compared with the effect on the hair of other animals.

The broad, general class headings are used only for general information or for comprehensive reports or articles.

Subject Heading Styles

Generally, the direct form of subject entry is used rather than inverted headings, e.g., Amino Acids rather than Acids, Amino; Helium Isotopes He-4 rather than Helium—isotopes He-4 or Helium—He-4 isotopes. Note, however, that in some cases parenthetic modifying terms or inverted headings of the form Neutrons, Fast are used in preference to a direct entry that would result in the scattering of information. Organic compounds are usually entered in the index in the inverted form so that substituted compounds can be listed near the parent compound; e.g., Benzene, Bromo- rather than Bromobenzene. In general, the style of nomenclature used is that of Chemical Abstracts, except that some items listed in that publication as subheadings are elevated to form part of the main heading; e.g., Butyric Acid, Methyl Ester rather than Butyric Acid—methyl ester.

Alphabetization

Main headings are alphabetized word-by-word. A parenthetic qualifier following a main heading is disregarded in alphabetizing unless there are two or more headings identical except for the parenthetic qualifier, in which case the qualifier determines the order. Headings involving Greek letters are arranged as if the names of the letters were spelled out.

Examples:

M-Capture
  see Electron Capture
Magnesium
Magnesium Alloys
Manganese Fluorides
Manganese(II) Fluorides
Mesons
Mesons (π)
Mesons (ρ)
3-Pentanol, 2,4-Dimethyl-
2-Pentanol, 2-Methyl-
2-Pentanol, 4-Methyl-

Nomenclature of Inorganic Compounds

Inorganic compounds are indexed in the direct form, listing cations in the order of increasing valence in the case of polycationic salts of varying valence and in alphabetic order for polycationic salts in which all cations have the same valence; e.g., Sodium Aluminum Silicates and Potassium Sodium Sulfates.

Multicomponent Alloys and Other Systems

Multicomponent alloys, except well-known trade names, are indexed under a main heading in the form "element alloy" for each element in the alloy. The modifier begins with element symbols for each component arranged alphabetically as if the English name for the element were spelled out.

Example: Copper-Gold Alloy is indexed
  Copper Alloys
    Cu-Au...
  Gold Alloys
    Cu-Au...

Well-known alloys such as Zircaloy-2 are indexed directly to the trade name; cross references referring from each component of the alloy to the entry for the trade name appear in cumulative indexes.

Multicomponent systems of non-metallic elements are indexed in a manner similar to alloys except the main heading used contains the word "Systems" in place of "Alloys."

Example: Silicon–Tungsten Systems are indexed
  Silicon Systems
    Si-W...
  Tungsten Systems
    Si-W...

Multicompound systems and mixtures of compounds are indexed under the main heading for each component com-

pound; the modifiers begin with an alphabetical listing of compound formulas.

Example: Lead Titanate–Lead Zirconate is indexed
Lead Titanates
$PbTiO_3$-$PbZrO_3$...
Lead Zirconates
$PbTiO_3$-$PbZrO_3$...

A mixed system of compounds and elements is indexed using a combined form of the above conventions, e.g., a dispersion of copper and alumina would be indexed

Aluminum Oxides
Al_2O_3-Cu...
Copper Systems
Al_2O_3-Cu..

Physical States and Configurations of Materials

Specification of the physical state, if other than normal, or geometric configuration of the material is included in the modifying phrase, i.e., liquid metals would be indexed to the metal with "liquid" in the modifier, and carbon crucibles would be indexed to Carbon with "crucibles" appropriately placed in the modifier and also to Crucibles if appropriate.

Modifying Phrases

The modifiers appearing under a main heading are written specifically to describe the relation of the item being indexed to that main heading. The modifier, therefore, will generally contain more useful information about that relation than will a title or a phrase written to be used under every main heading assigned to the item. Effort is exerted to begin the modifier with the word judged to be of greatest use to the greatest number of users; this, however, does not obviate the need to consider all modifiers under the main heading(s) of interest.

Modifiers are usually intended to form a meaningful phrase when combined with the main heading. Some are intended to be read following the main heading, e.g., the entry Hydrogen—sorption by charcoal is read "hydrogen sorption by charcoal"; however, as a result of placing the important word first, many modifiers must be arranged for smooth reading, e.g., Formaldehyde—yields in radiolysis of ethyl ether, effects of deuterium on is read "effects of deuterium on formaldehyde yields in radiolysis of ethyl ether" and Uranium—crystal structure of, effect of cooling rate on allotropic transformations in is read "effect of cooling rate on allotropic transformations in crystal structure of uranium." Prepositions are sometimes omitted if no ambiguity results.

Special characters are added to modifiers in the field of physics; if the modifier does not establish the experimental or theoretical character of a reference, a symbol (E), (T), or (E/T) is placed immediately after the modifying phrase and before the journal reference number. The value of this identification has been established by the American Institute of Physics.

A

ABSTRACTS
on Mössbauer effect, 20: 13974 (STI/PUB/21/16)
ACCELERATOR TUBES
design, 20: 13394(P)
design for linear accelerators, 20: 13403(P)
protective device for, 20: 13388(P)
ACCELERATORS
beam current measurement methods for electron, 20: 13383
beam deflection system for, 20: 13405(P)
beam separators for, properties of diaphragmed waveguide, 20: 13362 (JINR-P-2503)
beam transport system for, focusing and chromatic aberrations in alternating-gradient, (T), 20: 13360 (CERN-65-42)
beams from, energy calibration of electron, (E), 20: 13377
bibliography, 20: 13357 (AED-C-18-06)
control system for, 20: 13395(P)
design, 20: 13390(P)
design, 20: 13393(P)
design, 20: 13398(P)
design for ionized gas, 20: 12952(P)
design of charged particle, with improved vacuum system, 20: 13396(P)
design of plasma, 20: 13963(P)
design with electric shock preventing device, 20: 13399(P)
irradiation facility design for, vertical low-temperature, 20: 12957(P)
operation and development, 20: 13347(R) (UCRL-16511)
radiation monitoring and shielding studies, (E), 20: 13367 (UCRL-16445(Rev.))
shielding of, bibliography on, 20: 13965 (ORNL-RSIC-11)
use for production of irradiated polyethylene products, 20: 12906
ACCIDENTS
radiation hazards to personnel from, bibliography on, 20: 13002 (JAERI-4034)
ACETAMIDE, IODO-
effects on radiosensitivity of fruit-spoilage fungi, 20: 13137 (NP-15360)
ACETATES
properties of, chemisorbed on praseodymium, 20: 12874
ACETIC ACID
nuclear magnetic resonance spin-lattice relaxation times in, deuteron and proton, 20: 12839
use in praseodymium oxide preparation, 20: 12874
yields in radioinduced oxidation of ethane using hydrobromic acid catalyst, 20: 12883 (ORO-634)
ACETIC ACID, [(CARBOXYMETHYLIMINO) BIS(ETHYLENENITRILO)] TETRA-
effects on toxicity in rats, 20: 12594(R) (NP-15679)
ACETIC ACID, (1,2-CYCLOPENTYLENEDINITRILO) TETRA-
complexes with calcium and strontium, stability of, 20: 12595(R) (NP-15680)
effects on strontium-85 retention by female rat skeleton, 20: 12596(R) (NP-15681)
preparation, 20: 12595(R) (NP-15680)
stability constant for, 20: 12596(R) (NP-15681)
ACETIC ACID, (1,3-CYCLOPENTYLENEDINITRILO)TETRA-
effects on strontium-85 removal from rats, 20: 12598(R) (NP-15683)
effects on strontium-85 removal from rats, 20: 12600(R) (NP-15685)
preparation, 20: 12595(R) (NP-15680)
ACETIC ACID, [1,2-DIMETHYLETHYLENE)DINITRILO]TETRA-
complexes with barium, calcium, magnesium, and strontium, stability of, 20: 12594(R) (NP-15679)
effects on strontium-85 retention by female rat skeleton, 20: 12596(R) (NP-15681)
effects on strontium-85 removal from rats, 20: 12598(R) (NP-15683)
effects on strontium-85 removal from rats, 20: 12600(R) (NP-15685)
effects on toxicity in rats, 20: 12594(R) (NP-15679)
preparation and properties of, 20: 12594(R) (NP-15679)
ACETIC ACID, (ETHYLENEDIAMINE) TETRA-
effects on iron-59 uptake and transport by bean leaf cells and leaves, 20: 14220 (COO-888-48)
effects on strontium-85 removal from rats, 20: 12598(R) (NP-15683)
effects on strontium-85 removal from rats, 20: 12600(R) (NP-15685)
effects on toxicity in rats, 20: 12594(R) (NP-15679)
ACETIC ACID, (ETHYLENEDIIMINO)BIS($_o$-HYDROXYPHENYL)-
effects on iron-59 uptake and transport by bean leaf cells and leaves, 20: 14220 (COO-888-48)
ACETIC ACID, (*N*-HYDROXYETHYLETHYLENEDIAMINE) TRI-
effects on toxicity in rats, 20: 12594(R) (NP-15679)
solvent properties for thulium-171, 20: 12764 (CONF-660305-8)
ACETIC ACID, (PHENYLETHYLENEDINITRILO)TETRA-
preparation of, method for, 20: 12596(R) (NP-15681)
ACETIC ACID, (PROPYLENEDINITRILO)TETRA-
effects on strontium-85 retention by female rat skeleton, 20: 12596(R) (NP-15681)
effects on strontium-85 removal from rats, 20: 12598(R) (NP-15683)
effects on strontium-85 removal from rats, 20: 12600(R) (NP-15685)
effects on toxicity in rats, 20: 12594(R) (NP-15679)
preparation and properties of, 20: 12594(R) (NP-15679)
ACETONE
nuclear magnetic resonance spin-lattice relaxation times in, deuteron and proton, 20: 12839
solvent properties for POPOP and PPO phosphors, 20: 12929
yields in radioinduced oxidation of propane using hydrobromic acid catalyst, 20: 12883 (ORO-634)
ACETONITRILE
nuclear magnetic resonance spin-lattice relaxation times in, deuteron and proton, 20: 12839
ACETYLENE
pyrolysis for carbon deposition on uranium carbide particles, 20: 13215(R) (ORNL-3885, pp 3-86)
yields from gas-phase radiolysis of cyclobutane, 20: 12894
yields in radiolysis of liquid argon–ethylene, 20: 12884(R) (RRL-2310-171)
ACID PHOSPHATES
uptake of phosphorus-32-labeled super-, by rice, 20: 12592(R), (NP-15671)
ACOUSTIC WAVES
generation at microwave frequencies in dysprosium films, 20: 14003
propagation in plasma, 20: 13961
ACTINIDES
energy level transitions in even, E0, (T), 20: 13746 (AD-626681)
ACTINIUM ISOTOPES Ac-216
half life, (E), 20: 13779 (JINR-P-2465)
production in carbon-12 reactions with bismuth-209, (E), 20: 13779 (JINR-P-2465)
ACTIVATION ANALYSIS
development, 20: 14222(R) (NP-15612)
methods for, by neutron capture gamma measurements, 20: 12783
sample-handling equipment for, 20: 12795
self-shielding effects in neutron, 20: 12794
separation process for use in, 20: 12803
use of modulation technique in thermal-neutron, 20: 12784
ACTIVATION DETECTORS
design for neutron leakage and return counting in heavy-water reactors, 20: 14070(R) (MIT-2344-4, pp 115-34)
design of boron-trifluoride, for neutron-beam monitoring, 20: 13704(R) (MIT-2344-4, pp 101-5)
performance of lithium-6-glass, for neutron counting, (E), 20: 13090
use for intermediate neutron spectra determination, review of, 20: 13070 (RCN-40)
ADENOSINEPHOSPHORIC ACIDS
effects on phosphate and rubidium uptake by isolated cells of bean seedlings and tobacco leaves, 20: 14217 (COO-888-43)
effects on recovery in x-irradiated Tradescantia, 20: 12728
ADVANCED REACTIVITY MEASUREMENT FACILITY
reactivity measurement errors in, power dependence of, 20: 14059(R) (IDO-17104)
reactivity of, neutron scattering effects on, 20: 14059(R) (IDO-17104)
ADVANCED TEST REACTOR
fuel elements for, fabrication of aluminum–uranía dispersion, 20: 13217 (ORNL-TM-1377)
neutron flux in, fast, 20: 14059(R) (IDO-17104)
reactivity effects of voids in ATRC, 20: 14059(R) (IDO-17104)
AEROSOL GENERATORS
development for controlled-size particles, 20: 12928(R) (ORNL-3868)
AEROSOLS
inhalation of radioactive, distribution after, 20: 12604(T) (JPRS-33958, pp 8-19)
light scattering by spherical, computer program for, 20: 13346 (SC-RR-65-396)
metabolism by plants, effects on radiation dose to ecosystems, 20: 12607
particle sizes in, measurement of, by light scattering, 20: 12928(R) (ORNL-3868)
separation of radioactive, from air by accumulation on cloud droplets, 20: 12977
AGE
effects on cesium–potassium ratios in animals, 20: 12611
radiosensitivity effects on eye color mutations in Dahlbominus, γ, 20: 12691
AGE ESTIMATION
lead isotope ratios for, of Earth, 20: 12991
strontium–rubidium method for, in iron meteorite, 20: 12992
thorium-230 method for, of manganese nodules and adjacent deep-sea sediments, 20: 12976

AGING
radiation effects on, in Hiroshima and Nagasaki, 20: 12644
AIR
air–Al–D_2O, neutron diffusion in air-filled aluminum-tube lattices in heavy water, (E/T), 20: 13705(R) (MIT-2344-4, pp 135-44)
corrosive effects on iron–platonium–uranium alloy, effects of casting conditions and iron content on, 20: 13200
effects on thermal decomposition of cerium, lanthanum, neodymium, and praseodymium oxalates at 30 to 1100°C, 20: 12862
monitoring equipment for, facility for calibrating, 20: 13077 (Y-1503)
radiation effects on ozone formation in flowing and static, gamma, 20: 12885(R) (UCD-34P80-3, pp 59-68)
reactions with molten uranium–zirconium particles, disintegration properties of, 20: 14169 (AFWL-TDR-64-75)
reactions with uranium carbide, factors affecting, 20: 12925(R) (EURAEC-1446)
air–H_2O, swirl flows in tubes, (E/T), 20: 12960 (EURAEC-1515)
AIR FORCE NUCLEAR ENGINEERING TEST FACILITY
design and uses, 20: 14187 (NP-15836)
ALANINE
N,N-bis(2-chloroethyl)-, effects on tumor-bearing mice receiving radioprotective drugs, 20: 12719(R) (NP-15668)
ALANINE, 3-(3,4-DIHYDROXYPHENYL)-
labeling with deuterium and tritium, 20: 12880
ALARM SYSTEMS
design for continuous radioactivity monitor, 20: 13122(P)
design of criticality, for gaseous diffusion, 20: 13001 (GAT-T-1222)
design principles for criticality detection, 20: 13115
ALASKA
cesium-137 content in animals and natives of, 20: 12983
ALGAE
radiation effects on genetic recombination in Chlamydomonas, effects of dose duration on γ, 20: 12688
radiosensitivity of cell stages in Chlamydomonas, effects of repair mechanisms on uv, 20: 12687
ALKALI METAL HALIDES
analysis of single crystals of, activation, 20: 12805
radioinduced defects in crystals of, x, (E), 20: 13973(R) (NYO-3033-1)
ALKALI METALS
properties of plasma of, (E), 20: 13432(R) (TID-22419, pp 149-76)
separation by ion exchange using vanadium ferrocyanide, 20: 12932
ALKANES
radiolysis of, scavenging effects of hydriodic acid on, 20: 12884(R) (RRL-2310-171)
ALKENES
effects on exchange of iodine-131 in aluminum iodide–iodoethane system, 20: 12864
ALLENES
yields from gas-phase radiolysis of cyclobutane, 20: 12894
ALLOYS
fracture toughness of, double cantilever beam testing method for, 20: 12972 (BNWL-168)
research and development programs on, opportunities, roadblocks, and problems in, 20: 13185 (TID-22424)
superconductivity of eutectic, effects of structure on, 20: 13695
ALPHA PARTICLES
detection and measurement at Saxton plutonium project, 20: 14148(R) (WCAP-3385-5)
detection and measurement using proportional counters and liquid scintillators, 20: 13066 (JUL-298-PC)
detection of, performance of dielectric liquid-filled cloud chamber for, 20: 13112
detection using scintillation detectors with pulse-shape discriminators, 20: 13110
effects on electron structure of gold foil at 78°K, 20: 13339
emission by plants growing in areas of high natural radioactivity, 20: 12987
emission from lithium-6 reactions (Li-6,Li-7) reactions with beryllium-9 at 3 to 3.75 Mev, spectra of, (E), 20: 13852
interactions with neutrons, phase equivalent potentials for elastic, (T), 20: 13482
interactions with protons in final state of helium-3 (He-3,2p) reaction, (E), 20: 13900
interactions with alpha particles in beryllium-8, repulsive forces in, (T), 20: 13879
reactions (α,He-3) with zirconium isotopes at 65 Mev, nuclear structure analysis from, (E/T), 20: 13784 (ORNL-TM-1336)
reactions (α,n) and (α,2n) with molybdenum-92, conversion electron spectra from, (E), 20: 13881
reactions (α,n) with molybdenum-98, conversion electron spectra from, (E), 20: 13881
reactions (α,n) with beryllium-9, neutron spectra from, (E), 20: 13063 (JAERI-1092)
reactions (α,p) with calcium-48, (E), 20: 13854
reactions (α,xn) with rare earth nuclei, cross sections and excitation functions for, (T), 20: 13787(R) (TID-22637)
reactions (α,xn) with rubidium at 35 Mev, yttrium-87 production in, 20: 12917
reactions (α,2α) with beryllium-9, angular and momentum distributions from, (T), 20: 13875
reactions with carbon-13 at 2 to 3.5 Mev, oxygen-17 levels from, (E), 20: 13898
scattering by deformed nuclei, rotational excitation and gamma angular pattern from inelastic, (T), 20: 13848
scattering by zirconium-90, -91, and -92 at 65 Mev, nuclear structure from, (E/T), 20: 13784 (ORNL-TM-1336)
scattering cross sections for, computer program for calculating, 20: 13774 (JAERI-1096)
ALTERNATING-GRADIENT FOCUSING
beam chromatic aberration in, 20: 13360 (CERN-65-42)
ALUMINUM
analysis for rare earths, emission spectrographic, 20: 12810
electron absorption by, use for Mev-range energy calibrations, (E), 20: 13377
electron and gamma energy losses in cascade showers from, (E), 20: 13345(R) (NP-15772)
electron inelastic scattering at 500 kev, cross sections for, (E/T), 20: 13757 (CONF-233(Vol.4), pp 595-608)
electron propagation through vacuum boundary with, relative transition radiation yields from, (E), 20: 13352
electron ranges in, effects of energy on, 20: 14002
electron scattering at 0.5 to 3.0 Mev, bremsstrahlung production in, (E), 20: 13781 (NASA-CR-334)
electron scattering at 0.5 to 3.0 Mev, cross sections for, (E), 20: 13781 (NASA-CR-334)
electron secondary emission from thin foils of, (E), 20: 13103
electron tunneling in superconducting lead film laminates with normal, (E), 20: 13687
neutron absorption and inelastic scattering by, gamma spectra from, 20: 13966 (UNC-5140)
neutron diffraction at high pressures, 20: 14059(R) (IDO-17104)
neutron reflection by oriented single crystals of, (E/T), 20: 13709 (PAEC-IPA(D)PH-652)
neutron resonance absorption integral of, (E), 20: 14008(R) (ANL-7122, pp 42-69)
neutron scattering at 130 to 160 kev, ratio method for cross sections for, (E), 20: 13716
photoelectron production cross sections from 0.2 to 2 Mev, (T), 20: 13413 (CONF-233(Vol.4), pp 538-47)
properties of bonded joints of, with aluminum and fiberglass, 20: 14213 (ACF-15)
proton scattering at 140 Mev, absolute polarization from, (E), 20: 13813
radiation effects on electric conductivity of, dose dependence of stage II annealing of neutron, 20: 13340
radioinduced defects in, annealing of, 20: 13338
reactions with uranium dioxide, 20: 14059(R) (IDO-17104)
separation from other inorganic ions by paper chromatography, 20: 12939
ultraviolet emission from electron-bombarded foils of, 20: 14004
ALUMINUM ALLOYS
Al–Cr–Fe–Y, diffusion of uranium through cladding of, 20: 13179(R) (GEMP-55A, pp 13-28)
Al–Cr–Fe–Y, impact properties of powder-metallurgy, effects of atomized powders on, 20: 13179(R) (GEMP-55A, pp 13-28)
Al–Cr–Fe–Y, radiation effects on tensile properties of, fast-neutron, 20: 13179(R) (GEMP-55A, pp 13-28)
Al–Cr–V, development of refractory, for use in oxygen-contaminated sodium systems, (E), 20: 14007(R) (ANL-7122, pp 1-41)
Al–Ge–Nb–Sn, phase studies, 20: 13275
Al–Nb, phase studies, 20: 13275
Al–Nb–Ti, properties of, mechanical and physical, 20: 13271
Al–Pu, analysis for cerium-144 by bis(2-ethylhexyl) phosphate extraction and beta counting, 20: 12774 (PG-Report-685)
Al–Sn–Ti–Zr, phase studies, 20: 13273
Al–U, analysis for cerium-144 by bis(2-ethylhexyl) phosphate extraction and beta counting, 20: 12774 (PG-Report-685)
Al–U, flowsheet for uranium separation from, 20: 12926 (IDO-14669)
Al–U, fluid-bed fluoride volatility process for uranium separation from, 20: 12924 (ANL-6973)
Al–U, testing of reactor fuel elements of UAl_3, 20: 14059(R) (IDO-17104)
Al–U, uranium-235 concentration in, nondestructive method for determining excess, 20: 14168
ALUMINUM IODIDES
iodine-131 exchange with iodoethane, 20: 12864
ALUMINUM ISOTOPES Al-27
deuteron reactions (d,n) with, neutron spectra from, (E), 20: 13063

(JAERI-1092)
proton reactions (p,γ) at 773 kev, silicon-28 internal-pair formation coefficient from, (E), 20: 13843
proton reactions (p,p') at 10.5 Mev, cross sections for, (E), 20: 13897
ALUMINUM ISOTOPES Al-28
recoil from silicon-28 (n,p) reactions in silicon, ionization defects from, (E), 20: 13989
ALUMINUM OXIDES
compatibility with cesium at 550°C, 20: 13203
moisture control in agglomeration mixtures of, using neutron probe, 20: 13156
neutron resonance absorption integral of, (E), 20: 14008(R) (ANL-7122, pp 42-69)
properties of sintered, methods for determining, 20: 13319
radioinduced swelling in, fast-neutron, 20: 13337
stability of highly radioactive calcine of, during high-temperature storage, 20: 14207 (IDO-14670)
thermal conductivity of powders of, at 100 to 850°C, 20: 12854
thermal conductivity of powders of, at 100 to 850°C, (T), 20: 12855
use as corrosion inhibitor in high-temperature gas-cooled reactors, 20: 14021(P)
vaporization of, to 2300°C, 20: 13265(T) (AD-623208)
Al–Al_2O_3, phase transformations in composites of, effects of liquid aluminum on, 20: 13296
Al–Al_2O_3, properties and technology of sintered, 20: 13213 (EUR-2447.f)
Al_2O_3–Nb_2O_5, phase studies, 20: 12833
ALUMINUM SYSTEMS
air–Al–D_2O, neutron diffusion in air-filled aluminum-tube lattices in heavy water, (E/T), 20: 13705(R) (MIT-2344-4, pp 135-44)
Al–Al_2O_3, phase transformations in composites of, effects of liquid aluminum on, 20: 13296
Al–Al_2O_3, properties and technology of sintered, 20: 13213 (EUR-2447.f)
Al–Mg–$MgCl_2$–KCl–NaCl, corrosive effects on steels and tantalum at 500 to 800°C, (E), 20: 14007(R) (ANL-7122, pp 1-41)
Al–Mg–Ni–Si, fatigue properties at 250 to 350°C, low-cycle, 20: 13308
Al–UO_2–ZrH, reactivity measurements in lattices of, near-critical, (E), 20: 14082
AMERICIUM ISOTOPES Am-243
neutron fission of, yields from, 20: 13752 (ANL-7096)
production in thermal reactors, yield data for, 20: 13752 (ANL-7096)
AMINES
analysis and calibration as solvent of, by gas chromatography, 20: 12789
amine–ether, solvent properties for metals in acid solutions, 20: 12941(P)
AMINO ACIDS
radiolysis of derivatives and esters of, gamma, 20: 12889
AMMINES
complexes with cobalt, radiolysis of, extraction of recoil products from, 20: 12897
AMMONIA
effects on gas-phase radiolysis of cyclobutane and deuterated cyclobutane, 20: 12894
separation from mass transfer samples, methods for, 20: 12766 (GEAP-4178)
AMMONIUM CHLORIDES
methyltrioctyl-, use of, in separation of protactinium from bismuth, polonium, radium, radon, and thorium, 20: 12937
AMMONIUM CITRATES
solvent properties for cobalt-60 recoil products from irradiated cobalt complexes, 20: 12897
AMMONIUM COMPOUNDS, QUATERNARY
analytical use of aliquot-336 in reversed-phase chromatography, 20: 12776 (RT/PROT(65)33)
solvent properties for molybdenum and niobium, 20: 12933
use of, in separation of protactinium from bismuth, polonium, radium, radon, and thorium, 20: 12937
AMMONIUM SULFATES
uptake of nitrogen-15-labeled, by rice, 20: 12592(R) (NP-15671)
uptake of nitrogen-15-labeled, by rice, 20: 12593(R) (NP-15672)
AMPLIFIERS
design for use with gamma density gages, 20: 13154
development of low-noise fast, 20: 13345(R) (NP-15772)
ANIMAL CELLS
neoplastic transformation in mouse, effects of x-irradiated feeder layers on, 20: 12654
radiation effects on cytoplasm of, uv and x, 20: 12635(R) (NYO-2786-1)
radiation effects on osmotic resistance of rat bone marrow, β, 20: 12705
radiation effects on survival of mouse sarcoma, effects of oxygen inhalation on x, 20: 12725
radiation effects on tumorous, protective effects of MEA against, 20: 12680
role of splenic reticular, in erythropoiesis and lymphocytopoiesis, 20: 12681
ANIMAL REPRODUCTION
radiation effects on, in rats following pre- and post-natal exposure, 20: 12640 (TID-22378)
radiation effects on lizard, after gonadal exposure, 20: 12585
ANIMAL RESPIRATION
radiation effects on, in man, x, 20: 12702
ANIMALS
carbon-14 contamination of Pacific Proving Ground, 12 years after weapons tests, 20: 12579
cesium–potassium ratios in, effects of age and diet on, 20: 12611
cesium-137 content in food of cryptozoan, in Liriodendron forests, 20: 12576
genetic studies on, applications in breeding programs, 20: 12565
radioactive contamination of, role in human food contamination, 20: 12979 (EUR-2287.d)
tritium contamination of Pacific Proving Ground, 12 years after weapons tests, 20: 12579
ANISOLE
spectra of donor sites in Lewis acid adducts of, infrared, 20: 14226 (TID-21586)
ANODES
effects of graphite, on carrier distillation of impurities in uranium(IV-VI) oxides, 20: 12771 (NLCO-967)
ANTENNAS
properties of plasma-covered, (E/T), 20: 13022(R) (AFCRL-65-859)
ANTHRACENE
radiation effects on crystals of, space-charge-limited current measurements of, 20: 12893
scintillation response to 5- to 1000-kev electrons, (E), 20: 12899
ANTIBODIES
radiation effects on titers of, in hyperthyroid patients, beta, 20: 12626
radiation effects on, in mice, 20: 12631 (CEA-R-2776)
titers in hyperthyroid patients, prognostic value for iodine-131 therapy, 20: 12626
ANTIMONY
separation from other inorganic ions by paper chromatography, 20: 12939
ANTIMONY ALLOYS
Sb–Ag, crystal structure of, effect of high pressure on, (E), 20: 13316
Sb–Ce, cerium ion valency changes in intermetallic compounds of, (E), 20: 13991
Sb–Ga, radiation effects on, deuteron, 20: 13342
Sb–In, radiation effects on, deuteron, 20: 13342
ANTINEUTRINOS
reactions ($\bar{\nu},\mu^+$) with nuclei, test for time reversal violation in, (T), 20: 13835
ANTIPROTONS
interactions with protons at 3.0 and 3.6 Bev/c, absorptive model for charge exchange in, (T), 20: 13494
ARACHIDONIC ACID
preparation of double-labeled cholesteryl esters of, method for, 20: 12913 (EUR-2446.f)
ARGON
analysis for carbon, hydrogen, and nitrogen in loop-cover, by diffusion gasometry, 20: 12767 (GEAP-4833)
diffusion and instability of plasma of, in strong magnetic field, (E), 20: 13943
effects on emission spectrographic determination of rare earths, 20: 12810
electric conductivity of plasma of, seeded with potassium oxide, (E), 20: 13954
flow velocity optimization in MHD generator channel, (T), 20: 13436
ionization by fission fragments, plasma production in, (E/T), 20: 13939
neutron inelastic scattering by liquid and solid, thermal, 20: 14059(R) (IDO-17104)
properties of plasma sheath of, (E/T), 20: 13922(R) (NP-15703, pp 64-81)
resonance in laser-induced plasma of, optical frequency, (E/T), 20: 13942
shock fronts in electromagnetic tubes, self-luminescence, (E), 20: 13949
shock propagation in plasma of, microwave reflection technique for, 20: 13936
spectra of hydrobromic, hydrochloric, and hydriodic acids in, deuterium effects on, 20: 12857
spectra of plasma of, at 2500 to 7500 Å, (E), 20: 13955
thermal conductivity at 1000 to 20,000°K, (T), 20: 13644
ARGON IONS
analysis of components of beam of, electrostatic technique for spatial, 20: 13372
reactions with copper, molybdenum, and titanium, nuclear temperatures from, (E), 20: 13885
sputtering on cadmium and silver at 1 to 7 kev, (E/T), 20: 13414

(JUL-304-RW)
sputtering on nickel, electron diffraction analysis of damage from, (E/T), 20: 13981
ARGON ISOTOPES Ar-37
yield in thermal neutron ternary fission of uranium-235, (E), 20: 13862
ARGON ISOTOPES Ar-39
energy levels of, parity and spin of, (E/T), 20: 13773 (IKF-13)
yield in thermal neutron ternary fission of uranium-235, 20: 13862
ARGON ISOTOPES Ar-41
yield in thermal neutron ternary fission of uranium-235, 20: 13862
ARGON ISOTOPES Ar-42
yield in thermal neutron ternary fission of uranium-235, 20: 13862
ARGON SYSTEMS
Ar–Cs, absorption spectra of gaseous, 20: 12823 (LA-3391)
Ar–ethylene, radiolysis yields in liquid, 20: 12884(R) (RRL-2310-171)
Ar–Ne, plasma production by fission-fragment ionization of, (E/T), 20: 13939
ARGONAUT REACTOR
reactivity of, pulsed-source measurements of far subcritical, (E), 20: 14201
ARGONNE ADVANCED RESEARCH REACTOR
design and development, 20: 14179(R) (ANL-7122, pp 70-81)
ARGONNE FAST REACTOR EXPERIMENT TEST
development and safety analysis, (E), 20: 14007(R) (ANL-7122, pp 1-41)
ARGONNE NATIONAL LAB., LEMONT, ILL.
environs monitoring, 1964, 20: 12998 (ANL-7104)
ARMY REACTORS (ML-1)
design analysis and developmental testing of ML-1-IM, (E/T), 20: 14145 (TID-22595)
fuel element design for ML-1-IM, 20: 14145 (TID-22595)
neutron flux in ML-1-IM, 20: 14145 (TID-22595)
shutdown system for, design of off-normal, 20: 14146 (TID-22596)
ARMY REACTORS (PM-1)
instrumentation performance analysis for, 20: 14134 (NYO-3379-2)
ARMY REACTORS (PM-2)
instrumentation performance analysis for, 20: 14134 (NYO-3379-2)
ARMY REACTORS (PM-3)
criticality testing of PM-3A, zero-power, 20: 14115 (BAW-3576-1)
instrumentation performance analysis for, 20: 14134 (NYO-3379-2)
ARSENAZO III
analytical use for photometric determination of uranium in ores, 20: 12799
ARSENIC
separation from other inorganic ions by paper chromatography, 20: 12939
ASCORBIC ACID
radiation effects on content in tobacco crown-gall tumors, γ, 20: 12649
radiosterilization effects on content of, in lemons in nonrefrigerated storage, 20: 13145(R) (UCD-34P80-3, pp 75-83)
ATMOSPHERE
cesium-137 content in Colorado, 20: 12984
effects on incidence of Botrytis rot in radiosterilized strawberries, 20: 13139(R) (UCD-34P80-3, pp 9-26)
fallout behavior in, 20: 12981
radioactive aerosol separation from, by accumulation on cloud droplets, 20: 12977
radioactivity in, alarm system for use in monitoring, 20: 13122(P)
radioactivity in, of EURATOM countries, 1964, 20: 13000(R) (EUR-2520.i)
radioactivity of, effects on health, 20: 13015
ATMOSPHERES
effects on maize seeds in water at 3 to 45°C, biological, 20: 14216 (BNL-9859)
ATOMIC BEAMS
developments in, annual report of CEA, 20: 14223(R) (NP-15723)
ATOMIC ENERGY
uses of, annual report of CEA on military, 20: 14223(R) (NP-15723)
ATOMIC ENERGY COMMISSION
criticality research programs of, controls for, 20: 14092
ATOMIC EXPLOSIONS
detection of, device for, 20: 12995(P)
effects on aging in persons exposed to, 20: 12644
fallout from, in Pacific Proving Grounds 12 yrs after detonation, 20: 12579
plutonium dispersal in, health hazards from, 20: 13004 (LA-1981(Rev.))
review of, 20: 12981
yields of, device for determining, 20: 12995(P)
ATOMIC PHYSICS
cosmological foundations of, 20: 13354
developments in, annual report of CEA, 20: 14223(R) (NP-15723)
ATOMS
energy levels of, method of calculating one-electron eigenfunctions for, 20: 13416
ionization in collisions with excited atoms, (T), 20: 13421(T)
scattering from solids, model of, 20: 14227(R) (TID-22419)
transmission through crystals, coherent nuclear Coulomb excitation in, (T), 20: 13888
AUDITORY ORGANS
histology of mink, 20: 14214 (BNL-8564)
AUSTRALIA
Atomic Energy Commission annual report 1964–1965, 20: 14222(R) (NP-15612)
AUTORADIOGRAPHY
development of high-speed, gross, alpha, 20: 12563
review on quantitative, 20: 12616
use of macro-, in diagnosis of tumors and ulcers of stomach, 20: 12742
AVR REACTOR
fuel irradiation testing for, 20: 14136(R) (ORNL-3885, pp 150-94)

B

BACTEREMIA
etiology of, in irradiated mice, 20: 12704
BACTERIOPHAGES
effects of hydroxylamine on function of, 20: 12617(R) (NP-15863)
radiation effects on, recovery from x, 20: 12617(R) (NP-15863)
radiation effects on function, uv and x, 20: 12617(R) (NP-15863)
radioinduced T1 and T2, effects on *E. coli* levels of base-specific t-RNA methylases, uv, 20: 12619
radiosensitivity of, effects of radioprotective compounds on, x, 20: 12617(R) (NP-15863)
BALANCES
design of ultrahigh vacuum thermo-, for vapor pressure measurements, 20: 13029 (LA-3423)
BALLOONS
operation of remote-control, (E), 20: 13345(R) (NP-15772)
BARITE CONCRETES
radioactivity determination for low-background counting facilities, 20: 12946 (UCRL-11674)
BARIUM
determination in potassium chloride and sodium chloride single crystals, activation, 20: 12805
separation from other inorganic ions by paper chromatography, 20: 12939
BARIUM CARBONATES
reactions with zirconium oxide, 20: 13282
BARIUM COMPLEXES
with [(1,2-dimethylethylene)dinitrilo]- and (propylenedinitrilo)-tetraacetic acids, stability of, 20: 12594(R) (NP-15679)
BARIUM ISOTOPES Ba-138
energy levels of, second-vibrational, (T), 20: 13793
BARIUM ISOTOPES Ba-140
exchange between barium sulfate crystals, rate of, 20: 12869
BARIUM OXIDES
neutron resonance absorption integral of, (E), 20: 14008(R) (ANL-7122, pp 42-69)
reactions with zirconium oxide, 20: 13282
$BaO–Dy_2O_3$, optical properties of compounds formed in, 20: 13278
$BaO–Er_2O_3$, optical properties of compounds formed in, 20: 13278
$BaO–Eu_2O_3$, optical properties of compounds formed in, 20: 13278
$BaO–Gd_2O_3$, optical properties of compounds formed in, 20: 13278
$BaO–Ho_2O_3$, optical properties of compounds formed in, 20: 13278
$BaO–Lu_2O_3$, optical properties of compounds formed in, 20: 13278
$BaO–Sc_2O_3$, optical properties of compounds formed in, 20: 13278
$BaO–Sm_2O_3$, optical properties of compounds formed in, 20: 13278
$BaO–Tb_2O_3$, optical properties of compounds formed in, 20: 13278
$BaO–Tm_2O_3$, optical properties of compounds formed in, 20: 13278
$BaO–Yb_2O_3$, optical properties of compounds formed in, 20: 13278
$BaO–Y_2O_3$, optical properties of compounds formed in, 20: 13278
BARIUM PHOSPHATES
spectra of, effects of oxygen-18 on infrared, 20: 12861
BARIUM SULFATES
barium-140 and sulfur-35 exchange between crystals of, rate of, 20: 12869
BARIUM ZIRCONATES
production in reactions of barium carbonate or barium oxide with zirconium oxide at 1150 to 1350°C, 20: 13282
BARLEY
radioinduced mutations in, x, 20: 12714
sodium uptake by, growing in soils from greasewood forests, 20: 12575
BARRIERS
diffusion through porous, Breton-Massignon's theory for gaseous, 20: 13160
BARYONS
electromagnetic properties and structure of, (T), 20: 13509
electromagnetic properties of, nonrelativistic quark model for, (T), 20: 13544 (JINR-P-2509)
form factors for, hybrid group predictions of electromagnetic, 20: 13627

interactions with pseudoscalar mesons, isobar parity in, (T), 20: 13474(T)
interactions with mesons, models for, 20: 13602
mass formulas in supermultiplet model for, 20: 13583
model of, spinor, 20: 13612
structure of, effects in high-energy interactions, 20: 13514
structure of, SU(3) triplet model for SU(6), 20: 13598
BARYONS, RESONANCE
decay of Y_1^*(1385), branching ratio in, (T), 20: 13445 (CONF-758-14)
mass of Y_1^{*+} and Y_1^{*-}, difference in, (T), 20: 13488
production and properties of Y_1^*, in meson (K^-)-proton interactions at 1.15 Bev/c, (E), 20: 13518
production in meson (π^+)-proton interactions at 3.65, 20: 13456 (UCRL-16170)
production of N*(1920), (T), 20: 13454 (UCRL-14100-T(Rev.1))
production of $N_{3/2}^*$ (1238) in meson (π^-)-proton interactions, (E), 20: 13527
production of N*, in meson (K^+)-proton interactions at 0.86 to 1.58 Bev/c, (E), 20: 13462 (UCRL-16370)
production of N_{33}^*, in meson (π)-proton interactions at 450 Mev, (E), 20: 13524
production of Y_1^* (1660), in meson (K^-)-neutron interactions at 600 to 850 Mev/c, (E), 20: 13522
BAUXITE
moisture control in agglomeration mixtures of, using neutron probe, 20: 13156
BEANS
iron-59 uptake and transport by leaf cells and leaves of, effects of chelating agents and urea on, 20: 14220 (COO-888-48)
radioinduced mutation in *Phaseolus vulgaris*, γ, 20: 12709
radioinduced mutations in *Phaseolus vulgaris*, γ, 20: 12710
rubidium uptake by cells of, effects of chemicals, light, and temperature on, 20: 14217 (COO-888-43)
BEHAVIOR
genetic factors affecting, 20: 12565
BELGIAN REACTOR-2
fuel element testing of, nondestructive methods for, 20: 14198
fuel elements of, ultrasonic water-gap measurements in, 20: 14195
BENZENE
boiling of, critical heat flux on submerged surfaces during, 20: 12965
neutron diffusion parameters for, pulsed, (E), 20: 13729
neutron spectra in, pulsed-source measurements of, (E/T), 20: 13737
nuclear magnetic resonance spin-lattice relaxation times in, deuteron and proton, 20: 12839
benzene–Cd, pulsed neutron diffusion in, effects of non–1/v capture on, (E), 20: 13730
benzene–ethanol, radiation effects on, at 77°K, ESR and tracer studies of x, 20: 12890
benzene–methanol, radiation effects on, at 77°K, ESR and tracer studies of x, 20: 12890
benzene–terphenyl, boiling burnout properties of, 20: 14026 (EUR-2299.e)
BENZENE, CHLORO-
Cd–chlorobeazene, pulsed neutron diffusion in, effects of non–1/v capture on, (E), 20: 13730
BENZOIC ACID, 3,5-DIACTAMIDO-2,4,6-TRIIODO-
purification of iodine-131-labeled, by electrophoresis and chromatography, 20: 12918
BERKELIUM ISOTOPES Bk-249
production in thermal reactors, yield data for, 20: 13752 (ANL-7096)
BERYLLIUM
deformation and fracture in mono- and polycrystalline, at 20 to 450°C, 20: 13240 (CONF-170, pp 102-20)
deformation properties at –200 to 100°C, 20: 13241 (CONF-170, pp 121-5)
ductility of single-crystal, effects of purification and recontamination on, 20: 13239 (CONF-170, pp 90-101)
ductility of, effects of aging treatments on, 20: 13237 (CONF-170, pp 29-47)
ductility of, relation of Burger's vectors to, 20: 13242 (CONF-170, pp 126-37)
ductility of, relation of dislocation structures to, 20: 13305
electron secondary emission from thin foils of, (E), 20: 13103
fracture of single-crystal, basal plane, 20: 13238 (CONF-170, pp 48-68)
lattices in twin crystals of, stacking faults in, (E), 20: 13978
neutron absorption by, gamma spectra from, 20: 13966 (UNC-5140)
neutron cross sections for, 20: 14062 (JUL-214-RG)
neutron thermalization processes in, pulsed-source investigations of, (E), 20: 13738
physical metallurgy of, conference on, Gatlinburg, Tenn., Apr. 30 to May 1, 1963, 20: 13172 (CONF-170)
properties and structural uses of, 20: 13244 (CONF-170, pp 221-44)
purification by crucible-free vacuum melting and distillation, 20: 13175 (CONF-170, pp 214-20)
purification by distillation, 20: 13173 (CONF-170, pp 1-5)
radiation effects at 750°C, 20: 14059(R) (IDO-17104)
radiation effects on mechanical properties of, neutron, 20: 13323 (CONF-170, pp 138-59)
radioinduced expansion, 20: 14059(R) (IDO-17104)
recrystallization properties of wrought, 20: 13243 (CONF-170, pp 160-83)
research and development programs on, summary of Air Force sponsored, 20: 13174 (CONF-170, pp 184-213)
separation from other inorganic ions by paper chromatography, 20: 12939
BERYLLIUM ALLOYS
Be–Cu, ion reactions at 25 kev with, secondary electron emission in positive, (E), 20: 13424
BERYLLIUM FLUORIDES
BeF_2–NaF, use in molten-salt reactors, 20: 14129 (JUL-315-RG)
BERYLLIUM ISOTOPES Be-6
energy levels of, structure of low-lying, (E), 20: 13845
BERYLLIUM ISOTOPES Be-8
alpha decay of excited, from proton reactions (p,γ) with lithium-7, (E), 20: 13810
energy levels of, single-particle, (E), 20: 13810
BERYLLIUM ISOTOPES Be-9
alpha reactions (α,2α) with, angular and momentum distributions from, (T), 20: 13875
alpha reactions (α,n) with neutron spectra from, (E), 20: 13063 (JAERI-1092)
bremsstrahlung reactions (γ,n) at 6 to 80 Mev, cross sections for, (E), 20: 13795
energy levels, (E), 20: 13795
helium-3 reactions (He-3,n) with, neutron spectra from, (E), 20: 13063 (JAERI-1092)
lithium-6 reactions (Li-6,Li-7) at 3 to 3.75 Mev, lithium-7 and alpha spectra from, (E), 20: 13852
BERYLLIUM NITRIDES
thermodynamic properties and vaporization of, 20: 12830 (UCRL-7802)
BERYLLIUM OXIDE REACTOR EXPERIMENT
design of, using plutonium and thorium–uranium fuel cycles, 20: 14122(R) (GA-4451)
neutron production in fuel elements of, from (α,n) reactions, (E), 20: 14124 (GAMD-6859)
BERYLLIUM OXIDES
energy storage in neutron-irradiated, calorimetric measurement of, 20: 13236 (CEA-R-2797)
neutron diffusion in, pulsed, 20: 13727
radiation effects on microstructure, 20: 13331
vaporization of, to 2300°C, 20: 13265(T) (AD-623208)
BeO–Gd_2O_3, phase studies, 20: 13268(T) (JPRS-33605, pp 64-7)
BeO–graphite, compatibility, 20: 13262(R) (ORNL-3885, pp 195-235)
BeO–U, neutron diffusion parameters and multiplication constants of lattices of, pulsed, (E/T), 20: 14080
BeO–ZrH, reactivity effects on plutonium-fueled reactors, 20: 14122(R) (GA-4451)
BERYLLIUM POISONING
control of, 20: 13016
BETA DECAY
bremsstrahlung emission in, (T), 20: 13761 (CONF-233(Vol.4), pp 656-68)
form factors for, nuclear-structure-dependent, (T), 20: 13886
matrix element for, Nilsson model, 20: 13831
rates in stars, effects on stellar element abundances, 20: 13410
transitions in odd nuclei ($11 \leq A \leq 63$), theory of finite Fermi systems for, 20: 13887
BETA PARTICLES
design analysis for high-dispersion, with winding magnetic field, (T), 20: 13087
detection and measurement using liquid-organic scintillation counter with added sodium naphthylamine sulfonate, 20: 13080
detection of low-background, for solid sample assay, 20: 13102
dosimetry of, instrument design for, 20: 13120(P)
effects on antibody titers and thyroglobulin after hyperthyroid therapy, 20: 12626
effects on electrophoretic pattern of acid mucopolysaccharides, 20: 12756
effects on growth of lymph node and thymus cells in culture, 20: 12682
effects on lung tumors, therapeutic, 20: 12741
effects on osmotic resistance of rat bone marrow cells, 20: 12705
effects on pancreatic and liver cancer, 20: 12738
effects on pituitary of mice, effects of chlorpromazine on carcinogenic, 20: 12657
effects on production of pituitary hormones, 20: 12748
effects on rat pituitaries, development histologically of, 20: 12652
effects on silkworm, frequency of mutagenic, 20: 12692
scattering by pressed powders, effects of compaction pressure on back-, 20: 13221
scattering of, effects of energy and atomic number of scattering material

on back-, 20: 13469
BETA SOURCES
implantation for pituitary ablation, 20: 12753
use in radiometric devices for measuring chalk dust density, 20: 13024 (EUR-2544.d)
use of gold-198, for brachytherapy of lung tumors, 20: 12741
use of isotope, in simulation of electron energy distribution and flux in space, 20: 13129 (ORNL-P-1943)
BETA SPECTROMETERS
design for studies of electrons scattered through 180°, (E), 20: 13089
design of double-focusing $\pi\sqrt{2}$, 20: 13064 (JINR-E-2494)
design of magnetic multichannel, 20: 13118(P)
BETA SPECTROSCOPY
equipment development for, 20: 13345(R) (NP-15772)
BETATRONS
beam injector for, 20: 13391(P)
design of, with improved iron core, 20: 13392(P)
design of, with self-contained core handling equipment, 20: 13404(P)
BEVATRON
radiation monitoring and shielding studies, (E), 20: 13367 (UCRL-16445(Rev.))
BIBLIOGRAPHIES
on accelerator and space shielding, 20: 13965 (ORNL-RSIC-11)
on accelerators, 20: 13357 (AED-C-18-06)
on accidents in nuclear facilities, 20: 13002 (JAERI-4034)
on carbon-14 measurements, 20: 12770 (IFA/CO/28)
on combustion and explosion of zirconium droplets ignited by flash heating, 20: 12826 (SC-RR-65-569)
on critical temperatures and densities of alkali metals, 20: 12815 (ANL-7025)
on deformation behavior of niobium and tantalum at low temperatures, 20: 13253 (IS-T-65)
on dysprosium–dysprosium trichloride system, 20: 12821 (IS-T-62)
on fallout data, 20: 12981
on fracture mechanics and stability of engineering structures, 20: 13248 (GEAP-4678)
on heavy water lattices, 20: 14014(R) (MIT-2344-4)
on Mössbauer effect, 20: 13974 (STI/PUB/21/16)
on nuclear medicine, 20: 12733 (AED-C-10-04)
on organic coolants and moderators, 20: 14016 (STI/PUB/21/17)
on radiation effects on fish lipids, 20: 12618(R) (TID-22399)
on radiation effects on living organisms and tissues, 20: 12629 (AEC-C-04-22)
on radiation resistance and recovery in mice, 20: 12631 (CEA-R-2776)
on radioactive contamination of food, 20: 13136 (AED-C-02-06)
on radiopreservation of food, 20: 13136 (AED-C-02-06)
on self-diffusion in uranium carbide, dioxide, nitride, and sulfide, 20: 13234 (ANL-7094)
on spermatogenesis in insects, 20: 14224 (TID-21562)
on stability constants of rare earths with carboxylic acids, 20: 12817 (IS-1311)
on structure of ethyl Grignard reagent and a troponoid photooxidation product, 20: 12819 (IS-T-53)
on Tokyo university publications, 20: 13345(R) (NP-15772)
on ultrasonic welding, 20: 13210 (AWRE/LIB/BIB/13)
BINDERS
effects on pitch-, on physical properties and radiation damage in molded graphite, 20: 13247(R) (GA-6831)
BINDING ENERGY
calculation of nuclear, using two-nucleon potentials, 20: 13840
BIOLOGICAL STRESS
effects on recovery from radiation injuries, 20: 12684
radiation effects on environmental, 20: 12982
radiosensitivity effects in rats, 20: 12703
radiosensitivity effects of water, on pine seedlings, 20: 12674
BIOMETRY
computerization in ecological studies, 20: 12580
BIPHENYL
boiling of, critical heat flux on submerged surfaces during, 20: 12965
neutron diffusion parameters for, pulsed, (E), 20: 13729
neutron flux distributions in Dowtherm A, extrapolation distances from pulsed, (E), 20: 13726
neutron spectra in Dowtherm A, pulsed-source measurements of, (E/T), 20: 13737
biphenyl–phenyl ether, critical heat flux on submerged surfaces during boiling of, 20: 12965
BIPHENYL, ISOPROPYL-
boiling of, critical heat flux on submerged surfaces during, 20: 12965
BISMUTH
separation from other inorganic ions by paper chromatography, 20: 12939
separation from protactinium by solvent extraction using methyltrioctylammonium chloride, 20: 12937
BISMUTH ALLOYS
Bi–Zr, preparation and phase studies on, 20: 13252 (IS-1269)
BISMUTH ISOTOPES Bi-205
beta decay of, gamma transitions in, (E), 20: 13766 (CONF-233(Vol.4), pp 726-9)
BISMUTH ISOTOPES Bi-209
carbon-12 reactions (C-12,5n) with, actinium-216 production in, (E), 20: 13779 (JINR-P-2465)
ion fission of, fragment energy and mass distributions from, (E), 20: 13861
nuclear magnetic moment correction for, for momentum dependent internucleon force, (T), 20: 13842
BISMUTH ISOTOPES Bi-211
energy levels from lead-211 decay, (E), 20: 13895
BLOOD FORMATION
role of reticular cells in lymphocytic, 20: 12681
BLOOD PICTURE
radiation effects on dog, effects of polyglucin on x, 20: 12723(T) (JPRS-33766, pp 3-7)
radiation effects on, low-dose x, 20: 12999 (CEA-R-2746)
BLOOD PLASMA SUBSTITUTES
effects of polyglucin, in x-irradiated dogs, 20: 12723(T) (JPRS-33766, pp 3-7)
molecular weight of polyglucin, selection of optimal, 20: 12722(T) (JPRS-33766)
use of polyglucin, for treating traumatic shock, 20: 12722(T) (JPRS-33766)
BLOOD PLATELETS
radiation effects on thrombocytopenia of, after hemangioma therapy in children, 20: 12750
BLOOD VESSELS
radiotherapy of tumors in children's, x, 20: 12750
BODY WATER
radiation and/or thermal trauma effects on content of, in rat intestinal mucosa, 20: 12630 (BNL-8383)
BOILERS
design of once-through, 20: 14041(P)
sodium–water reactions in sodium-heated, 20: 14149(T,R) (ORNL-tr-900)
tubes for, nondestructive testing of, 20: 14160
BOILING
burnout in steam-water mixtures in vertical tubes, empirical correlation for, 20: 12968
burnout of polyphenyl reactor coolants, properties of, 20: 14026 (EUR-2299.e)
heat transfer from finned and smooth fuel rods in forced flow, 20: 12961 (GEAP-4786)
void fraction in subcooled, impedance gage for measuring, 20: 12964
BOILING REACTORS
control element design for, floating, 20: 14052(P)
coolant flow in, hydrodynamic instabilities of, (E/T), 20: 14027 (EURAEC-909)
design with rotatable hexagonal core, 20: 14098(P)
fuel element testing of, loop design for, 20: 14131 (KR-98)
kinetics of, adiabatic approximation to space-dependent, 20: 14074
BONE MARROW
diseases of, effects on tuberculosis incidence in Hiroshima, 20: 12639 (TID-21517)
effects on immune reactions in irradiated mice, 20: 12716 (AD-626682)
effects on radiation injuries in mice, 20: 12720(R) (TID-22466)
protective effects of grafts of, against radiation injuries in rats, 20: 12651
protective effects of injected, against radiation injuries, effects of hemagglutinins on, 20: 12726
radiation effects on osmotic resistance of cells of rat, β, 20: 12705
transplantation after radiation injury, 20: 12731
viability of, maintained in tissue culture, effects of hemagglutinins on, 20: 12726
BONES
radiation effects on growth of rat, protective effects of MEG against, 20: 12729
radiodiagnosis of infections of, using calcium-47 and strontium-85, 20: 12735
BORIC ACID
crystal structure of boron-11- and deuterium-labeled ortho-, 20: 12836
use as soluble poison for reactor control, 20: 14099(P)
BORON
defects in crystals of, stacking-fault, (E/T), 20: 13971 (AD-625834)
determination by thermal-neutron activation methods, 20: 12784
effects on plutonium nitrate and plutonium-239 solutions, criticality-concentration limit relaxation for poisoning, (T), 20: 13019
neutron absorption cross section of standard natural, thermal, (E), 20: 13807
volatility of, in radioactive alumina calcine during high-temperature

storage, 20: 14207 (IDO-14670)
BORON CARBIDES
meson (μ^+) stopping in, depolarization and quenching in, (E), 20: 13498
neutron absorption by inserts of, in uranyl nitrate critical assembly, (E), 20: 14091
neutron resonance absorption integral of, (E), 20: 14008(R) (ANL-7122, pp 42-69)
properties of pressure-sintered, 20: 13314
B_4C–UO_2, radiation effects on fuel elements of, 20: 13425(R) (CEND-3107-249)
BORON FLUORIDES
analysis for boron isotopes, mass spectrometric, 20: 12786
BORON ISOTOPES
abundance ratios in boron trifluoride, mass spectrometric determination of, 20: 12786
BORON ISOTOPES B-10
determination in boron trifluoride, mass spectrometric, 20: 12786
helium-3 reactions (He-3,n) at 2.6 to 5.8 Mev, nitrogen-12 energy levels from, (E), 20: 13808
neutron capture by, in slab cores, (E/T), 20: 14063 (KAPL-M-6528)
neutron reactions (n,α) with, excitation functions for, (E), 20: 13741
reactions (B-10,3α) with carbon-12 and nitrogen-14 in photoemulsions at 100 Mev, mechanisms of, (E), 20: 13891
reactions with uranium-233, spontaneously fissionable isomer production in, 20: 13776 (JINR-P-2499)
use in thermistors for thermal neutron flux measurements, 20: 13126(P)
BORON ISOTOPES B-11
effects on crystal structure of orthoboric acid, 20: 12836
neutron scattering length for, in orthoboric acid, 20: 12836
reactions with uranium-233, spontaneously fissionable isomer production in, 20: 13776 (JINR-P-2499)
BORON SYSTEMS
B–Fe, performance for neutron shielding, 20: 14180 (COO-1430-1)
B–Fe_2O_3, performance for neutron shielding, 20: 14180 (COO-1430-1)
B–graphite, performance for neutron shielding, 20: 14180 (COO-1430-1)
BOSONS
electrodynamics of zero-spin, functional method for, 20: 13564
form factor of intermediate W, in model of leptonic weak interactions, 20: 13464
Green function generator in theory of charged scalar field for, 20: 13563
interaction coupling constants and mass for, method of calculating, 20: 13554
interactions at zero temperature, perturbation theory for one-particle Green's functions for, 20: 13559
interactions in many-body systems of, gauge-invariant method in, (T), 20: 13562
interactions of weak intermediate, review on, 20: 13608
mass of intermediate vector, from neutrino-neutron interactions, (T), 20: 13504
polarization of zero mass, covariant formalism for, (T), 20: 13517
production of intermediate W, in neutrino interactions, 20: 13464
production of spin-1, in meson (K^+) decay, (E), 20: 13497
superconductivity of gases, model for type-II, (T), 20: 13677
theory of vector, for weak interactions, renormalizable, 20: 13568
thermodynamics for ideal gases of, statistical, 20: 13640
BRAIN
research programs on dynamics of, 20: 14227(R) (TID-22419)
BRAIN TUMORS
localization of, using positron-emitting isotopes and multi-detector scanner, 20: 12734 (BNL-9911)
radiodiagnosis of, techniques for, 20: 12759
BRAKES
design for reactor control rods, 20: 14043(P)
BRASS
defects in crystals of, stacking-fault, (E/T), 20: 13971 (AD-625834)
BRAZIL
radioactivity of foods grown on monazite sands and volcanic intrusions in, 20: 12988
BREEDER REACTORS
economics for uranium conservation, 20: 14011 (BNWL-189, Sect.V)
fuel cycle for, evaluation of thorium, 20: 14126 (JUL-276-RG)
fuel development for fast, uranium carbide paste, 20: 14024(R) (APDA-182)
fuel processing for molten-salt, flowsheet for, 20: 12928(R) (ORNL-3868)
kinetics and operations of ZPR-9, (E), 20: 14007(R) (ANL-7122, pp 1-41)
BREMSSTRAHLUNG
polarization of coherent, from electron-silicon reactions, (E), 20: 13345(R) (NP-15772)
production by electron reactions with silicon, spectra of, (E), 20: 13345(R) (NP-15772)
production in electron reactions with aluminum and iron at 0.5 to 3.0 Mev, (E), 20: 13781 (NASA-CR-334)
production in 20-Mev electron linac, spectral distribution of, (E), 20: 13361 (EGG-1183-2066)
reactions (γ,n) with beryllium-9 at 6 to 80 Mev, energy levels and cross sections for, 20: 13795
reactions (γ,p) with carbon-12 below 55 Mev, angular distributions from, (E), 20: 13812
spectra from electron-capture decay, determination of, (T), 20: 13760 (CONF-233(Vol.4), pp 637-55)
spectra of internal, in beta decay, (T), 20: 13761 (CONF-233(Vol.4), pp 656-68)
use of off-axis, in production of polarized gamma radiation, (E), 20: 13345(R) (NP-15772)
BREMSSTRAHLUNG SOURCES
use in radiometric devices for measuring chalk dust density, 20: 13024 (EUR-2544.d)
BRITISH REACTORS
fuel elements for, nondestructive testing of, 20: 14161
BROMAL
radiolysis of, mean lifetime of free radical chains from gamma, 20: 12887
BROMINE
determination in bromine fluorides, 20: 12797
meson (μ) and (π) scattering cross sections of, (T), 20: 13480
BROMINE FLUORIDES
analysis for bromine, fluorine, and impurities, 20: 12797
reactions with uranium(IV-VI) oxide at 250 to 400°C, (E), 20: 14008(R) (ANL-7122, pp 42-69)
BUBBLE CHAMBERS
film scanning systems for, development of, 20: 13163(R) (ANL-7129)
nucleation in freon, laser-stimulated, 20: 13084
particle tracks in, computer program for analysis of, 20: 13071 (REEL/R-111)
BUILDING MATERIALS
fracture mechanics and stability of engineering structures, review on, 20: 13248 (GEAP-4678)
BUTADIENE
yields from gas-phase radiolysis of cyclobutane, 20: 12894
BUTANE
n-butane–ethylamine, vapor pressure of, deuterium isotope effects on, 20: 12879
BUTANE, 2,2-DIMETHYL-
radioinduced cracking of, 20: 12908
BUTANE, 2,3-DIMETHYL-
radioinduced cracking of, 20: 12908
1-BUTENE
yields from gas-phase radiolysis of cyclobutane, 20: 12894
BUTYL PHOSPHATES
analysis and calibration as solvent of, by gas chromatography, 20: 12789
analytical use in reversed-phase chromatographic separations, 20: 12776 (RT/PROT(65)33)
kerosene–TBP, solvent properties for thorium and uranium, 20: 12931
kerosene–TBP, solvent properties for fission products and uranium, effects of chemical degradation of kerosene on, 20: 12934

C

CADARACHE REACTORS
facilities for, civil engineering problems in construction of, 20: 12947
CADARACHE REACTORS (RAPSODIE)
development status of, 20: 14192
status, 20: 14149(T,R) (ORNL-tr-900)
CADMIUM
deuteron inelastic scattering at 15 Mev, energy spectra from, (E), 20: 13872
neutron absorption by inserts of, in uranyl nitrate critical assembly, (E), 20: 14091
neutron absorption by, gamma spectra from, 20: 13966 (UNC-5140)
neutron resonance absorption integral of, (E), 20: 14008(R) (ANL-7122, pp 42-69)
neutron scattering at 0.3 to 1.5 Mev, differential cross sections for, (E), 20: 13829
separation from other fission products by solvent extraction using dithizone, 20: 12936
separation from other inorganic ions by paper chromatography, 20: 12939
sputtering by argon ions at 1 to 7 kev, (E/T), 20: 13414 (JUL-304-RW)
sputtering by protons at 2 and 300 Mev, (E), 20: 13414 (JUL-304-RW)
ultraviolet emission from electron-bombarded foils of, 20: 14004
CADMIUM ALLOYS
Cd–Ag, crystal structure of, effect of high pressure on, (E), 20: 13316
Cd–Mg, crystal structure of, effect of high pressure on, (E), 20: 13316
CADMIUM ISOTOPES
separation from isotopes of other elements, summary of, 20: 13345(R)

(NP-15772)
CADMIUM OXIDES
CdO–Cr_2O_3–O, phase studies on, 20: 13260(R) (NP-15852)
CADMIUM SULFIDES
radiation effects on current pulse height in crystal counters of, gamma, 20: 13132
CADMIUM SYSTEMS
benzene–Cd, pulsed neutron diffusion in, effects of non–1/v capture on, (E), 20: 13730
Cd–chlorobenzene, pulsed neutron diffusion in, effects of non–1/v capture on, (E), 20: 13730
CADMIUM TELLURIDES
use of single crystals of, in gamma spectrometers, 20: 13073(R) (SAN-549-1)
CALCIUM
effects of dietary, on calcium-45 and strontium-85 retention by rats, 20: 12598(R) (NP-15683)
effects of dietary, on strontium-85 retention by rat skeleton labeled *in utero*, 20: 12599(R) (NP-15684)
metabolism in deer and sheep, tracer study of, 20: 12609
metabolism in *Pisum sativum*, tracer study, 20: 12605
preparation of isotopic bulk materials and foils of, from oxide, 20: 13216 (ORNL-P-1899)
separation from other inorganic ions by paper chromatography, 20: 12939
uptake and transport by spruce trees during yearly vegetative cycle, tracer study, 20: 12590 (CEA-R-2825)
x-ray transition energies in pi mesic atoms of, (E), 20: 13461 (UCRL-16365)
CALCIUM ALLOYS
Ca–Yb, phase studies on, by differential thermal analysis, 20: 13254 (IS-T-70)
Ca–Zn, thermodynamic properties, 20: 13180(R) (IS-RD-4)
CALCIUM COMPLEXES
with [(1,2-dimethylethylene)dinitrilo]- and (propylenedinitrilo)-tetraacetic acids, stability of, 20: 12594(R) (NP-15679)
with (1,2-cyclopentylenedinitrilo)tetraacetic acid, stability of, 20: 12595(R) (NP-15680)
CALCIUM FLUORIDES
radiation effects on optical centers of trivalent rare-earth ions in crystals of, 20: 13986(T)
CALCIUM IONS
effects of interlayer of, on cesium sorption by montmorillonite, 20: 12873
CALCIUM ISOTOPES Ca-39
nuclear magnetic moment corrections for, perturbation theory for, 20: 13838
CALCIUM ISOTOPES Ca-40
helium-3 reactions (He-3,α) at 24.4 Mev, momentum spectra from, (E), 20: 13345(R) (NP-15772)
proton inelastic scattering at 13.065 Mev, energy levels from, (E), 20: 13821
proton reactions (p,p'γ) at 7.5 to 9.6 Mev, energy levels from, (E), 20: 13821
CALCIUM ISOTOPES Ca-41
nuclear magnetic moment corrections for, perturbation theory for, 20: 13838
CALCIUM ISOTOPES Ca-42
energy levels of, deformed, (T), 20: 13839
preparation of bulk materials and foils of, from oxide, 20: 13216 (ORNL-P-1899)
CALCIUM ISOTOPES Ca-43
energy level transitions in, mixing of, (T), 20: 13837
CALCIUM ISOTOPES Ca-45
energy level transitions in, mixing of, (T), 20: 13837
excretion in rat feces and urine, effects of dietary phosphorus on, 20: 12594(R) (NP-15679)
excretion in rat feces and urine, effects of dietary phosphorus on, 20: 12596(R) (NP-15681)
incorporation in mammals for population studies, 20: 12583
retention by rat skeleton, effects of phosphorus and strontium in diet on, 20: 12595(R) (NP-15680)
retention by rat skeleton, effects of dietary phosphorus and strontium on, 20: 12594(R) (NP-15679)
retention by rats, effects of calcium and phosphate in diet on, 20: 12598(R) (NP-15683)
transport in Douglas-fir forests, 20: 12574
uptake by barley seedlings, effects of greasewood forest soil on, 20: 12575
CALCIUM ISOTOPES Ca-46
deuteron reactions (d,p) at 7 Mev, calcium-47 levels from, (E), 20: 13853
CALCIUM ISOTOPES Ca-47
energy levels from deuteron reactions (d,p) with calcium-46 at 7 Mev, (E), 20: 13853
metabolism and retention by rats, effects of dietary phosphorus on, 20: 12600(R) (NP-15685)
metabolism in rats, effects of dietary phosphorus on, 20: 12596(R) (NP-15681)
retention by rat, effects of dietary phosphorus on, 20: 12597(R) (NP-15682)
use as tracer in metabolism studies in deer and sheep, techniques for, 20: 12609
use in diagnosing bone infections, 20: 12735
CALCIUM ISOTOPES Ca-48
alpha reactions (α,p) with, (E), 20: 13854
deuteron reactions (d,t) with, (E), 20: 13854
deuteron reactions (d,p) with, (E), 20: 13854
helium-3 reactions (He-3,d) at 12 Mev, scandium-49 levels from, (E), 20: 13854
helium-3 reactions (He-3,α) with, (E), 20: 13854
CALCIUM OXIDES
cobalt ion EPR spectra in, univalent, (E), 20: 13972 (IA-1056)
moisture control in agglomeration mixtures of, using neutron probe, 20: 13156
neutron resonance absorption integral of, (E), 20: 14008(R) (ANL-7122, pp 42-69)
properties as insulators for tungsten–5 rhenium thermocouples at 2450°C, 20: 13250(R) (GEMP-55A, pp 56-6)
vaporization of, to 2300°C, 20: 13265(T) (AD-623208)
CALIBRATION
facility for air monitors, high-volume, 20: 13077 (Y-1503)
CALIFORNIUM CHLORIDES
preparation, spectra, and structure of, 20: 12831 (UCRL-16516)
CALIFORNIUM IONS
spectra of, absorption, 20: 12831 (UCRL-16516)
CALIFORNIUM ISOTOPES Cf-249
preparation and purification of, method for, 20: 12831 (UCRL-16516)
CALIFORNIUM ISOTOPES Cf-252
neutron fission of, yields from, 20: 13752 (ANL-7096)
production in thermal reactors, yield data for, 20: 13752 (ANL-7096)
CALIFORNIUM OXIDES
preparation, spectra, and structure of, 20: 12831 (UCRL-16516)
CALORIMETERS
construction and operation of, for measuring ion-beam energy, 20: 13114
design and performance for gamma and neutron detection, 20: 14170 (EGG-1183-2019)
design and performance of adiabatic, for measuring specific heats of aqueous solutions at 25°C, 20: 12818 (IS-T-52)
CALORIMETRY
method for radiation dose-rate measurements, 20: 12908
use for solid state structure transformations and thermal diffusivity studies, method for, 20: 13236 (CEA-R-2797)
CARBOHYDRATES
analysis for carbon and hydrogen, optimal layer thickness for neutron-scattering, 20: 12791
CARBON
defects in crystals of, stacking-fault, (E/T), 20: 13971 (AD-625834)
deposition of pyrolytic, on uranium carbide particles, 20: 13215(R) (ORNL-3885, pp 3-86)
deposition on graphite, from helium–methane–water vapor mixtures, 20: 13262(R) (ORNL-3885, pp 195-235)
deposition on nuclear fuel particles, fluidized-bed process for, 20: 12875(P)
deposition on plutonia spheres, parameters for pyrolytic, 20: 13171(R) (BMI-1751)
determination in carbohydrates, optimal layer thickness for neutron-scattering, 20: 12791
determination in loop-cover argon by diffusion gasometry, 20: 12767 (GEAP-4833)
determination in sodium loop transfer samples, methods for, 20: 12766 (GEAP-4178)
determination in uranium monocarbide, combustion method for, 20: 12773 (PEL-80)
effects on ductility and porosity of welds in tungsten–rhenium–molybdenum alloys, 20: 13251(R) (GEMP-55A, pp 57-82)
fission product recoil in pyrolytic, 20: 13261(R) (ORNL-3885, pp 87-149)
meson (μ) and (π) scattering cross sections of, (T), 20: 13480
neutron absorption and inelastic scattering by, gamma spectra from, 20: 13966 (UNC-5140)
neutron resonance absorption integral of, (E), 20: 14008(R) (ANL-7122, pp 42-69)
neutron transport in, pulsed fast, (E/T), 20: 13719
performance of vitreous, as containers for copper–magnesium–magnesium-chloride–potassium-chloride–sodium-chloride–uranium systems at 800°C, (E), 20: 14007(R) (ANL-7122, pp 1-41)
photon reactions with, deuteron production in, (E), 20: 13345(R) (NP-15772)

production in reactions between ethylene and excited hydrogen atoms, 20: 12886(T) (SC-T-66-0706)
proton scattering at 140 Mev, absolute polarization from, (E), 20: 13813
radiation effects on coatings of pyrolytic, 20: 13215(R) (ORNL-3885, pp 3-86)
radiation effects on properties and structure of pyrolytic, 20: 13247(R) (GA-6831)
reactions with nitrogen and niobium or tantalum at 1150 to 2370°C, 20: 12845
reactions with plutonium at 1610 to 1650°C, preparation of plutonium monocarbide by, 20: 13208 (ANL-6969)
reactions with uranium nitride at 1900°C, 20: 13171(R) (BMI-1751)
reactions with uranium, mechanisms of, 20: 13223
temperature effects on coating of pyrolytic, 20: 13215(R) (ORNL-3885, pp 3-86)
thermal expansion and preferred orientation of non-graphitic, 20: 13247(R) (GA-6831)

CARBON DIOXIDES
compatibility with magnesium alloys in gas-cooled reactors, 20: 13199
effects on maize seeds in water at 3 to 45°C, biological, 20: 14216 (BNL-9859)
effects on thermal decomposition of cerium, lanthanum, neodymium, and praseodymium oxalates at 30 to 1100°C, 20: 12862
radiolysis of, in exchange reactions between labeled carbon dioxide and oxygen, 20: 12882 (IA-1065)
reduction of carbon-13-labeled, to elemental carbon-13, 20: 12852

CARBON IONS
production and acceleration of beams of, 20: 13804

CARBON ISOTOPES C-11
production in proton reactions (p,pn) with carbon-12 at 50 to 160 Mev, cross sections for, (E), 20: 13833

CARBON ISOTOPES C-12
boron-10 reactions (B-10,3α) at 100 Mev in photoemulsions, mechanism of, (E), 20: 13891
bremsstrahlung reactions (γ,p) below 55 Mev, angular distributions from, (E), 20: 13812
deuteron reactions (d,p) at 4 Mev, emission spectra from, (E), 20: 13076 20: 13076 (UR-875-117)
lithium-6 reactions (Li-6,α) at 2 to 3 Mev, angular distributions from, (E), 20: 13846
meson (π^-) reactions (π^-,2N) with, momentum distribution from, (T), 20: 13874
proton elastic scattering at 5.76 to 6.67 Mev, polarization in, (E), 20: 13899
proton reactions (p,pn) at 50 to 160 Mev, cross sections for, (E), 20: 13833
proton reactions (p,pd) with, momentum distribution from, (T), 20: 13874
reactions (C-12, 5n) with bismuth-209, actinium-216 production in, (E), 20: 13779 (JINR-P-2465)
reactions with nuclei ($176 \leq A \leq 209$), fission fragment energy and mass distributions from, (E), 20: 13861

CARBON ISOTOPES C-13
alpha reactions (α,α) and (α,n) at 2 to 3.5 Mev, cross sections for, (E), 20: 13898
alpha reactions at 2 to 3.5 Mev, oxygen-17 levels from, (E), 20: 13898
deuteron reactions (d,p) at 3 Mev, parity of 6.89-Mev level in carbon-14 from, (E), 20: 13828
helium-3 reactions (He-3,pγ) at 4.95 and 5.25 Mev, nitrogen-15 level from, (E), 20: 13819
nuclear magnetic resonance of, Overhauser effect and spin decoupling for, (E), 20: 13800
nucleon reactions with, optical-model wave functions for, (T), 20: 13817
preparation from labeled carbon dioxide, efficiency of, 20: 12852
proton reactions at 5.0 to 8.1 Mev, nitrogen-14 levels from, (E), 20: 13898

CARBON ISOTOPES C-14
content in Pacific Proving Ground 12 yrs after weapons tests, 20: 12579
determination by mass spectroscopy and liquid scintillation counting, 20: 12801
determination in heterogeneous phases by liquid scintillators, 20: 12804
energy levels from deuteron reactions (d,p) with carbon-13 at 3 Mev, parity of 6.89 Mev, (E), 20: 13828
incorporation in cholesteryl arachidonate and linolenate with tritium, 20: 12913 (EUR-2446.f)
measurements, bibliography on, 20: 12770 (IFA/CO/28)
use in plant physiology studies, 20: 12614

CARBON MONOXIDES
reactions with zirconium droplets, flash heating effects on combustion and explosive, 20: 12826 (SC-RR-65-569)
yields in radiolysis of carbon dioxide in exchange reactions with oxygen, 20: 12882 (IA-1065)

CARBON STEEL
corrosion of type 1020, by aluminum–magnesium–magnesium-chloride–potassium-chloride–sodium-chloride systems at 500 to 800°C, 20: 14007(R) (ANL-7122, pp 1-41)
heat flux on submerged, during boiling of organic coolants, 20: 12965
iodine deposition on wires of, properties of, 20: 13261(R) (ORNL-3885, pp 87-149)

CARBON SYSTEMS
C–Hf–Nb, phase diagrams, 20: 13272
C–Hf–Ta, Fabrication and properties of sheets of, 20: 13205(R) (AD-626622)
C–Hf–Ta–W, creep behavior in ultrahigh vacuum at 2000 and 2200°F, 20: 13256 (NASA-TN-D-3222)
C–Hf–Ta–W, fabrication and properties of sheets of T-222, 20: 13205(R) (AD-626622)
C–Hf–Ta–W, weldability of T-222, effects of oxygen contamination on, 20: 13264(R) (WANL-PR(P)-008)
C–Nb–Ti, phase diagrams, 20: 13272
C–Nb–W–Y–Zr, weldability of D-43Y, 20: 13264(R) (WANL-PR(P)-008)
C–Nb–W–Zr, corrosion of D-43, by potassium at 2450°F, stress-, 20: 13191(R) (NASA-CR-54476)
C–Nb–W–Zr, creep behavior in ultrahigh vacuum at 2000 and 2200°F, 20: 13256 (NASA-TN-D-3222)
C–Nb–Zr, phase diagrams, 20: 13272
C–O–Pu, phase studies, 20: 13291
C–Y, phase studies, 20: 13180(R) (IS-RD-4)

CARBONATES
effects on phosphate and rubidium uptake by isolated cells of bean seedlings and tobacco leaves, 20: 14217 (COO-888-43)
effects on strontium-85 metabolism by rats, 20: 12606
strontium-86 to strontium-87 ratios in veins and vein-dikes of, Idaho, Montana, and Ontario, 20: 12980

CARCINOGENESIS
radiation effects on, by gastric tumor extracts, x, 20: 12625

CARCINOMAS
effects of radiomimetic agents on mouse, effects of drugs on, 20: 12719(R) (NP-15668)
radioinduced morphological changes in cervical, γ and x, 20: 12659
radiotherapy of cervical, rectal complications from γ, 20: 12696
radiotherapy of laryngeal, γ, 20: 12758

CARMINIC ACID
complexes with thorium, preparation and composition of, 20: 12870

CASCADE SHOWERS
properties of meson-nucleon one-dimensional, equations for, (T), 20: 13964 (ORNL-3746)

CASTLE OPERATION
fallout from, effects on growth of Marshall Island children, 20: 13011

CATHODE-RAY TUBES
x-ray emission by Japanese, 20: 13014

CATION EXCHANGE MATERIALS
use for separation of cesium-137 and strontium-90 from milk, 20: 12997 (AD-626210)

CATS
radiation injuries of, protective effects of tris(hydroxymethyl) aminomethane against, 20: 12724

CATTLE
metabolism by, cesium-134 and strontium-85, 20: 12588(R) (AD-626320)

CAVES
materials evaluation for low-background, 20: 12946 (UCRL-11674)
penetration sealing device for, 20: 12953(P)

CAVITY RESONATORS
electron synchrotron radiation in, (E), 20: 13472(T)
impedance of, aperture and cell size effects on shunt, (T), 20: 13358 (BNL-9944)

CELLULOSE
analytical use in reversed-phase chromatographic separations, 20: 12776 (RT/PROT(65)33)

CEMENTS
radioactivity determination for low-background counting facilities, 20: 12946 (UCRL-11674)

CENTRIFUGAL PUMPS
design and performance of high-temperature, for MSRE, 20: 14164

CERAMIC MATERIALS
research and development programs on, opportunities, roadblocks, and problems in, 20: 13185 (TID-22424)
research programs on, summaries of USAEC, 20: 13182 (TID-4005(Pt.1, 9th Ed.))

CERIUM
defects in crystals of, stacking-fault, (E/T), 20: 13971 (AD-625834)
determination by spectrometry using 4,5-dihydroxy-3-[(p-sulfophenyl)azo]-2,7-naphthalenedisulfonic acid, 20: 12806
determination in glass, emission spectrographic, 20: 12810
preparation of high-purity, 20: 12935
separation from alkali metals by ion exchange using vanadium ferrocyanide, 20: 12932

separation from other inorganic ions by paper chromatography, 20: 12939
separation from rare earths by persulfate oxidation and bis(2-ethylhexyl) phosphate extraction, 20: 12762 (BNWL-173)
solvent properties for tantalum, 20: 13180(R) (IS-RD-4)

CERIUM ALLOYS
Sb–Ce, cerium ion valency changes in intermetallic compounds of, (E), 20: 13991

CERIUM COMPLEXES
with dilactic, mandelic, and quinic acids, formation and stability constants of, 20: 12817 (IS-1311)

CERIUM ISOTOPES Ce-138
energy levels from praseodymium-138 decay spectra, (E), 20: 13882

CERIUM ISOTOPES Ce-144
deposition in lungs of rats, effects of carrier on, 20: 12615
determination in fission products by bis(2-ethylhexyl) phosphate extraction and beta counting, 20: 12774 (PG-Report-685)
separation from aqueous solutions by sorption on diatomaceous earth, 20: 12938
uptake by plants in Georgia piedmont, 20: 12985
volatility of, in radioactive alumina calcine during high-temperature storage, 20: 14207 (IDO-14670)

CERIUM OXALATES
thermal decomposition in air and carbon dioxide at 30 to 1100°C, 20: 12862

CERIUM PHOSPHIDES
cerium ion valency changes in, (E), 20: 13991

CERIUM SELENIDES
cerium ion valency changes in, (E), 20: 13991

CERMETS
heat treatment of nichrome–plutonium dioxide, 20: 14059(R) (IDO-17104)
radiation effects on aluminum–uranium, 20: 14059(R) (IDO-17104)

CESIUM
compatibility with metals and ceramics at 550°C, 20: 13203
critical temperature and densities of liquid and vaporous, 20: 12815 (ANL-7025)
electron band structure of, high-pressure determination of, 20: 14221 (COO-1198-230)
heat transfer properties, 20: 13232 (AGN-8162)
ionization in collisions with excited atoms, (T), 20: 13421(T)
metabolism in deer and sheep, tracer study of, 20: 12609
performance in multistrip contact ion engines, 20: 12975
ratio to potassium in animals, effects of age and diet on, 20: 12611
separation from other alkali metals by ion exchange using vanadium ferrocyanide, 20: 12932
separation from other inorganic ions by paper chromatography, 20: 12939
sorption by montmorillonites, mechanism of, 20: 12873
thermophysical properties, 20: 13232 (AGN-8162)
transport in Liriodendron forests, model for, 20: 12577
use in thermionic cells, 20: 13444(P)

CESIUM AZIDES
radioinduced nitrogen free radicals in, EPR spectra of x, 20: 13970 (AD-611432, pp 135-47)

CESIUM BROMIDES
ion association and hydration in aqueous solutions of, x-ray diffraction studies on, 20: 14228 (TID-22527)

CESIUM CHLORIDES
ion association and hydration in aqueous solutions of, x-ray diffraction studies on, 20: 14228 (TID-22527)

CESIUM IODIDES
ion association and hydration in aqueous solutions of, x-ray diffraction studies on, 20: 14228 (TID-22527)
performance of thallium-activated, with pulse-shape discriminator, 20: 13110
preparation of thin slices for electron microscopic study, microtoming for, 20: 13985

CESIUM ISOTOPES
separation by thermoionization effect, 20: 13159

CESIUM ISOTOPES Cs-134
metabolism by cows, goats, and hogs, 20: 12588(R) (AD-626320)

CESIUM ISOTOPES Cs-137
content in Alaskan animals and natives, 20: 12983
content in Colorado mule deer, factors affecting, 20: 12984
content in cows' and human milk, 1959 to 1961, 20: 13012
content in Pacific Ocean off coasts of California and Japan, 20: 13007(T) (NP-tr-1336)
content in Po Valley rice, effects of crop irrigation on, 20: 12986
distribution in cryptozoan food chain, 20: 12576
distribution in forest ecosystems after tree inoculation, 20: 12566 (COO-1006-4)
effects on mammals, 20: 12667
separation from aqueous solution by sorption on diatomaceous earth, 20: 12938
separation from fission products by ion exchange using vanadium ferrocyanide, 20: 12932
separation from milk by electrodialysis, pilot plant study of, 20: 12997 (AD-626210)
sorption by clays and sands, 20: 14209 (RT/PHOT(65)29)
uptake by lichens in Sweden, 20: 12578
uptake by plants in Georgia piedmont, 20: 12985
use as gamma source in radiography, 20: 12974
use as tracer in metabolism studies in deer and sheep, techniques for, 20: 12609
volatility of, in radioactive alumina calcine during high-temperature storage, 20: 14207 (IDO-14670)

CESIUM ISOTOPES Cs-144
content in Po Valley rice, effects of crop irrigation on, 20: 12986

CESIUM SYSTEMS
Ar–Cs, absorption spectra of gaseous, 20: 12823 (LA-3391)

CESIUM URANYL CHLORIDES
crystal structure, 20: 12835

CHALKS
density of dusts of, radiometric devices for measuring, 20: 13024 (EUR-2544.d)

CHARCOAL
sorptive properties for xenon-133 in fission product mixtures, 20: 12772 (ORNL-3840)

CHARGED PARTICLE BEAMS
book: *Charged Particle Beam Interactions with Plasma*, 20: 13961
current calculation by Child-Langmuir law, effect of initial velocity on, (T), 20: 13902 (CEA-R-2898)
deflection of, electric and magnetic device for, 20: 13405(P)
energy of, calorimeter detector for measuring, 20: 13114
focusing in alternating-gradient magnetic fields, chromatic aberration in, (T), 20: 13360 (CERN-65-42)
interactions with plasma, dispersion diagrams for, (E/T), 20: 13925(R) (TID-22419, pp 99-147)

CHARGED PARTICLES
absorption and interactions in matter, (T), 20: 13350
deflector design for, 20: 13397(P)
detection of magnetically analyzed, equipment for, 20: 13345(R) (NP-15772)
detection using emulsions, exciton mechanism for image formation in, (T), 20: 13082
effects of heavy, on germanium crystals, 20: 13987
electromagnetic-wave emission by ultrarelativistic, in deflectors, (E/T), 20: 13370
interactions of, quantum mechanics of three-body, 20: 13630
interactions with circularly polarized waves in plasma, (E/T), 20: 13925(R) (TID-22419, pp 99-147)
motion in electromagnetic fields, generalized variational principles for, 20: 13351
motion in helical toroidal magnetic field, nonlinear theory of, 20: 13371
motion in sector-focused cyclotrons, computer program for orbit, 20: 13355
reactions with heavy-nuclei at high-energy, light fragment emission in, (T), 20: 13880
reactions with metals, transition radiation from relativistic, (E/T), 20: 13788(T) (ORNL-tr-1062)
spectroscopy of, resolution of magnetic uniform-field analyzers for, (T), 20: 13091

CHELATES
effects of acetic acid, on strontium-85 removal from rats, 20: 12600(R) (NP-15685)

CHEMICAL ANALYSIS
furnace design for remote operations in, 20: 12790

CHEMICAL ENGINEERING
radioisotope uses in, 20: 13155

CHEMICAL RADIATION DETECTORS
design using chromic couple suspended in anhydrous translucent matrix, 20: 13125(P)
performance of gaseous ethylene and nitrous oxide, 20: 12884(R) (RRL-2310-171)

CHEMISTRY
developments in, annual report of CEA, 20: 14223(R) (NP-15723)
research, 20: 12760 (AD-611432)
research in, using swimming pool reactors, 20: 12914 (IEA-100)

CHICKENS
radiation effects on embryos of, pathological x, 20: 12706

CHIMERAS
radiation effects on genetic homogeneity of fruit-tree, 20: 12632(R) (EUR-2546.f)
stability in fruit-tree, 20: 12632(R) (EUR-2546.f)

CHINON REACTORS (EDF-1)
control rods for, drive winches for, 20: 14153

CHINON REACTORS (EDF-2)
control rod calibration in, using pulsed sources, (E/T), 20: 14163

CHLORAL
radiolysis of, mean lifetime of free radical chains from gamma, 20: 12887
CHLORIDES
permeation through cuticular membranes of fruits and leaves, effects of urea on, 20: 14218 (COO-888-44)
CHLORINE
determination in water, activation, 20: 12768 (IEA-97)
CHLORINE FLUORIDES
reactions with sintered plutonia and uranía, factors affecting, 20: 12925(R) (EURAEC-1446)
reactions with uranía, corrosive effects on container materials for, 20: 12925(R) (EURAEC-1446)
CHLORINE ISOTOPES Cl-35
neutron capture by, internal electron pair production in, (E), 20: 13762 (CONF-233(Vol.4), pp 700-9)
CHLORINE ISOTOPES Cl-36
decay of, internal bremsstrahlung spectra from electron-capture, (E), 20: 13758 (CONF-233(Vol.4), pp 609-13)
electron pair emission from, spectra of, (E), 20: 13762 (CONF-233(Vol.4), pp 700-9)
energy levels of, parity and spin of, (E/T), 20: 13773 (IKF-13)
exchange between silver chloride crystals, rate of, 20: 12869
CHLOROPHYLLS
radioinduced mutations for wheat, classification of, 20: 12632(R) (EUR-2546.f)
CHLOROPLASTS
isolation and treatment of, techniques for, 20: 12627
radiation effects on photoreduction and structure of, gamma, 20: 12627
CHROMATOGRAPHY
isotope seperation by gas, 20: 12930
reversed-phase, use of, for rare earth separations, 20: 12776 (RT/PROT(65)33)
use of sensitive integrator in gas, 20: 12777 (UJV-1431/65)
CHROMIUM
determination in sodium loop transfer samples, methods for, 20: 12766 (GEAP-4178)
neutron absorption and inelastic scattering by, gamma spectra from, 20: 13966 (UNC-5140)
neutron cross sections for, 20: 14062 (JUL-214-RG)
separation from other inorganic ions by paper chromatography, 20: 12939
CHROMIUM ALLOYS
Al–Cr–Fe–Y, diffusion of uranium through cladding of, 20: 13179(R) (GEMP-55A, pp 13-28)
Al–Cr–Fe–Y, impact properties of powder-metallurgy, effects of atomized powders on, 20: 13179(R) (GEMP-55A, pp 13-28)
Al–Cr–Fe–Y, radiation effects on tensile properties of, fast-neutron, 20: 13179(R) (GEMP-55A, pp 13-28)
Al–Cr–V, development of refractory, for use in oxygen-contaminated sodium systems, (E), 20: 14007(R) (ANL-7122, pp 1-41)
Cr–Fe–Ni, fatigue tests on pressure vessel cladding of, 20: 13255 (KAPL-3108)
CHROMIUM ISOTOPES Cr-51
decay in potassium chromate, annealing of radiation effects from, 20: 12904
determination in mass transfer samples, methods for, 20: 12766 (GEAP-4178)
metabolism and fecal excretion by man, after oral administration, 20: 12612
reactions of recoil, in potassium chromate, annealing of, 20: 12904
CHROMIUM ISOTOPES Cr-52
energy levels of, second-vibrational, (T), 20: 13793
proton reactions (p,n) at 14.2 Mev, angular distributions, Q values, and spectra from, (E), 20: 13345(R) (NP-15772)
CHROMIUM OXIDES
CdO–Cr_2O_3–O, phase studies on, 20: 13260(R) (NP-15852)
Cr_2O_3–MgO–O, phase studies on, 20: 13260(R) (NP-15852)
Cr_2O_3–Nb_2O_5, phase studies, 20: 12833
Cr_2O_3–NiO–O, phase studies on, 20: 13260(R) (NP-15852)
CHROMIUM STEEL
corrosion of type 4130, by aluminum–magnesium–magnesium-chloride–potassium-chloride–sodium-chloride systems at 500 to 800°C, 20: 14007(R) (ANL-7122, pp 1-41)
properties of 12%, 20: 13186 (TRG-Report-840)
Cr–Mo, properties, 20: 13186 (TRG-Report-840)
Cr–Ni–Nb, radiation effects on stress-rupture of, 20: 13328 (ORNL-TM-1359)
CHROMIUM SYSTEMS
Cr–UO_2, diffusion of uranium through iron-base alloy cladding from fuel of, 20: 13179(R) (GEMP-55A, pp 13-28)
Cr–ZrB_2, phase studies, evidence for existence of $CrZrB_2$ in, 20: 13276
CHROMOSOMES
function and structure, 20: 12564
ploidy in mouse tissue cultures of, effects of x-irradiated feeder layers on, 20: 12654
radiation effects on X, in female Drosophila, x, 20: 12690
radiation effects on, in mealy bugs, 20: 12715
radiation effects on ploidy and structure of leukocytic, after abdominal or pelvic therapy, x, 20: 12658
radiation effects on mean viability of Drosophila autosomal, x, 20: 12661
radioinduced aberrations in Perognathus, chronic-exposure, 20: 12666
radioinduced aberrations in maize, x, 20: 12678
radioinduced aberrations in forage grass, γ, 20: 12679
radioinduced crossing-over in Drosophila X, x, 20: 12689
radioinduced mutations in mouse, effects of hypothermia on x, 20: 12693
CIRCUITS
design and performance of pulse-shape discriminator, 20: 13108
design for x-ray dosimetry, 20: 13124(P)
soldering flux on circuit boards, system for measuring, 20: 13033 (TLW-1110)
CIVIL ENGINEERING
problems in, for Cadarache Nuclear Centre, 20: 12947
CIVILIAN DEFENSE
against high-altitude thermonuclear explosions, 20: 14230(T) (ORNL-tr-972)
CLAYS
sorptive properties of Italian, for cesium-137 and strontium-89, 20: 14209 (RT/PHOT(65)29)
CLOSTRIDIUM
radiosensitivity of spores of *Cl. botulinum*, in canned chopped ham, γ, 20: 13134 (AD-625252)
CLOUD CHAMBERS
properties of dielectric liquid-filled, for alpha, gamma, and neutron radiation, 20: 13112
CLOUD-ION CHAMBERS
performance for accelerator monitoring, 20: 13367 (UCRL-16445(Rev.))
CLOUDS
radioactive aerosol accumulation on droplets in, in atmosphere, 20: 12977
COATINGS
deposition on nuclear fuel particles, fluidized-bed process for, 20: 12875(P)
COBALT
neutron inelastic scattering at 3.5 to 8.5 Mev, energy dependence of level density parameters from, (E), 20: 13827
neutron resonance absorption integral of, (E), 20: 14008(R) (ANL-7122, pp 42-69)
separation from other inorganic ions by paper chromatography, 20: 12939
COBALT ALLOYS
properties of die inserts of Stellite, for extrusion of uranium, 20: 13220(R) (BMI-3)
Co–Dy, dysprosium-161 Mössbauer effect in, (E), 20: 13992
Co–Dy, dysprosium-161 isomer shift in, 20: 13992
Co–Hf, phase studies, 20: 13180(R) (IS-RD-4)
COBALT(II) CHLORIDES
spectra of complexes of, in ion exchangers, 20: 12824 (LA-DC-6749)
COBALT COMPLEXES
radiation effects on, absorbed on ion exchanger, extraction of recoils formed in, 20: 12897
with hexamethylphosphoramide, NMR contact shifts in, 20: 12828 (TID-21587)
with 3,3-diacetyl-2,4-pentanedione, radiation effects on, annealing of chemical recoil damage in, 20: 12896
COBALT GLASS
reduction of, site population of cobalt ions in, 20: 13260(R) (NP-15852)
COBALT IONS
electron paramagnetic resonance spectra of univalent, in monocrystalline calcium oxide, (E), 20: 13972 (IA-1056)
photopolarographic reduction, uv, 20: 12798
spectra of, in cobalt glass during reduction, 20: 13260(R) (NP-15852)
COBALT ISOTOPES Co-56
energy levels of, parity and spin of, (E), 20: 13815
yield in thermal neutron ternary fission of uranium-235, 20: 13862
COBALT ISOTOPES Co-57
beta decay scheme, (T), 20: 13805
decay of, gamma spectra from electron-capture, (E), 20: 13799
energy levels from proton reactions (p,γγ) with iron-56 at 1.3 to 1.8 Mev, parity and spin of, 20: 13857
energy levels of, parity and spin of, (E), 20: 13815
COBALT ISOTOPES Co-59
proton reactions (p,p′) at 10.5 Mev, cross sections for, (E), 20: 13897
COBALT ISOTOPES Co-60
calibration of gamma sources of, 20: 13107
determination in mass transfer samples, methods for, 20: 12766 (GEAP-4178)
gamma emission from, measurement of air to tissue ratios and scatter

functions for, 20: 13009
gamma emissions from, dosimetry of, 20: 13008
production of, disposal of waste from, 20: 14211
separation of recoil, from irradiated cobalt complexes adsorbed on ion exchangers, 20: 12897
use as gamma source in radiography, 20: 12974
use in contact therapy of laryngeal carcinomas, 20: 12758
use in therapy, grid design for, 20: 13010
COBALT SYSTEMS
Co–NbC–WC, mechanical properties of, effects of composition on, 20: 13274
WC–Co, tungsten carbide grain size in, methods of controlling, 20: 13226
COILS
interactions of multiple induction heating, in waste calciners, (T), 20: 13032 (ORNL-TM-1352)
COINCIDENCE CIRCUITS
testing of, pulse generator for, 20: 13044
COINCIDENCE COUNTERS
design for positron scanning of brain tumors, 20: 12734 (BNL-9911)
performance of proportional, corrections for, (T), 20: 13068 (MLM-1263)
COINCIDENCE MEASUREMENTS
performance for absolute determination of radiation source strengths, (T), 20: 13805
COKE
moisture control in agglomeration mixtures of, using neutron probe, 20: 13156
COLICINS
radiosensitivity effects of factor Col I, on bacteria, 20: 12677
COLLAGEN
radiation effects on ratio of, to hexosamine in man, 20: 12644
COLLIMATORS
fabrication of precision lead, technique for, 20: 13030 (LA-3443)
neutron intensity distribution from Soller-type, (E/T), 20: 13702 (LA-DC-7594)
properties of neutron, review of, 20: 13701 (JUL-294-NP)
COLORADO
cesium-137 content in deer of, factors affecting, 20: 12984
COMBUSTION
effects of flash heating on, of zirconium droplets, 20: 12826 (SC-RR-65-569)
COMMUNICATION SYSTEMS
research programs on, 20: 14227(R) (TID-22419)
COMMUNICATION THEORY
research programs on, 20: 14227(R) (TID-22419)
COMPACTS
beta scattering by, effects of pressure in sample preparation on, 20: 13221
fabrication of hard dense, hot-pressing method and apparatus for, 20: 13230(P)
COMPUTER PROGRAMS
ALTHAEA, for reactor fuel burnup, 20: 14118 (BNWL-183, Sect.IV)
ARGOSY 4, for analysis of reactor kinetics, 20: 14055 (AEEW-R-445)
CAMOUT, for reflected neutron bombardment of unit spherical target, 20: 13742
CLEB, for Clebsch-Gordan coefficients, FORTRAN for CDC 1604, 20: 13648 (ORNL-3877(Rev.))
COPE, for calculation of core performance in gas-cooled reactors, FORTRAN for IBM 7090, 20: 14123 (GAMD-1561(Rev.))
development at ANL, 20: 13163(R) (ANL-7129)
DPC, for reactor neutronic data preparation, FORTRAN, 20: 14064 (LA-3427)
DWBA2, for nucleon transfer and scattering cross sections, 20: 13345(R) (NP-15772)
DWBA3, for knock-on, pickup, and stripping reactions, 20: 13345(R) (NP-15772)
EDITOR, for editing nuclear data on magnetic tape, S2-FORTRAN for IBM 7030, 20: 13750 (AEEW-M-553)
EDIT1, for nuclear data editing, KDF9-FORTRAN, 20: 13344 (AEEW-M-604)
ELIESE-1, for scattering cross sections, FORTRAN II for IBM-7090, 20: 13774 (JAERI-1096)
for analysis of bubble chamber events, FORTRAN II for IBM-7090, 20: 13071 (REEL/R-111)
for automatic spot scanning for spark chambers, 20: 13106
for charged particle orbits in sector-focused cyclotrons, SAP for IBM 704, 20: 13355
for classical deflection function calculations for molecular beam scattering, ALGOL and FORTRAN II, 20: 13415 (ORNL-3881)
for coincidence counter correction determinations, in FORTRAN, 20: 13068 (MLM-1263)
for preparation of neutron cross section libraries, FORTRAN IV for IBM 7094, 20: 13705 (NAA-SR-Memo-10884 and Add.)
GEM, for criticality problems, 20: 14093
GEORGE, for Legendre expansion coefficients, FORTRAN for IBM 7044, 20: 13699 (GA-6690)
HEETR, for fast-neutron distributions in enriched-uranium heavy-water lattices, 20: 13703(R) (MIT-2344-4, pp 17-47)
IREKIN, for reactor kinetics, MAP for IBM 7040, 20: 14060 (IDO-17114)
LASER, for plutonia–urania critical experiment analyses, 20: 14148(R) (WCAP-3385-5)
LEGCOEF-3, for Legendre expansion coefficients, FORTRAN for IBM 7044, 20: 13699 (GA-6690)
LEOPARD, for plutonia–urania critical experiment analyses, 20: 14148(R) (WCAP-3385-5)
MSF, for Mie scattering functions, FORTRAN for CDC 3600, 20: 13346 (SC-RR-65-396)
NINEJ, for 9-J coefficients, FORTRAN for CDC 1604, 20: 13648 (ORNL-3877(Rev.))
ONE-ROD, for neutronic properties of single fuel rods in heavy water, for IBM 7094, (T), 20: 14067(R) (MIT-2344-4, pp 80-8)
QUIXOT DULCIN, for polynomial root-finding, 20: 14227(R) (TID-22419)
RAC 7, for Racah coefficients, FORTRAN for CDC 1604, 20: 13648 (ORNL-3877(Rev.))
RATIO, for analysis of neutron spectra calculated by HEETR program, 20: 13703(R) (MIT-2344-4, pp 17-47)
RCS-2, for neutron cross sections from resonance parameters, FORTRAN for IBM 7090, 20: 13786 (ORNL-TM-1396)
SCATTER, for neutron elastic scattering angular distributions, EGTRAN-FORTRAN, 20: 13697 (AEEW-M-605)
SLP, for neutron cross sections, KDF9 EGTRAN-FORTRAN, 20: 13751 (AEEW-M-606)
SWAN, for neutron diffusion, IBM 7030, 20: 14056 (AWRE-O-99/65)
TET 2, for Boltzman neutron transport equation, FORTRAN, 20: 13698 (DTMB-1820)
TOSS, for analysis of steady-state and transient heat transfer, 20: 12963 (WANL-TME-1108)
UNCOL, for fast-neutron distributions in enriched-uranium heavy water lattices, 20: 13703(R) (MIT-2344-4, pp 17-47)
XKINEQ, for neutron flux stability in reactors containing xenon-135, FORTRAN IV, 20: 14061 (IDO-17127)
COMPUTERS
description of MIDAS installation, 20: 13166 (KFK-371)
design for cyclotron control, 20: 13381
design of ARC system for reactor kinetics calculations, (E), 20: 14008(R) (ANL-7122, pp 42-69)
feasibility of analog, for N reactor simulation, 20: 14167 (HW-70878)
logic circuits for, family of, 20: 13164 (COO-416-1028)
performance for fast neutron laboratory executive control, 20: 13806
performance of digital, for fast neutron data analysis, 20: 13806
systems development at ANL, 20: 13163(R) (ANL-7129)
use for fallout radiation field simulation, 20: 13021(P)
CONCRETE AGGREGATES
radioactivity determination for low-background counting facilities, 20: 12946 (UCRL-11674)
CONCRETES
neutron reflection from slab of, Monte Carlo Method for determining, 20: 13742
radioactivity determination for low-background counting facilities, 20: 12946 (UCRL-11674)
stresses in hollow spheres of steel-reinforced, (T), 20: 12944
testing prestressed, for reactor pressure vessels, 20: 14030
CONDENSERS
testing steam–water ejector, facility for, 20: 13432(R) (TID-22419, pp 149-76)
CONFERENCES
see also introduction to Report Number Index
Genetics Today, Vol. 2, The Netherlands, 1963, 20: 12564
Physical Metallurgy of Beryllium, Conference on, Gatlinburg, Tenn., Apr. 30 to May 1, 1963, 20: 13172 (CONF-170)
CONNECTIVE TISSUE
radiation effects on, biochemical, 20: 12756
CONTACTORS
design and performance of stacked-clone, for solvent extraction, 20: 12928(R) (ORNL-3868)
CONTAMINATION
bibliography on food, 20: 13136 (AED-C-02-06)
CONVERSION ELECTRONS
polarization of, correlation of, (T), 20: 13802(T)
spectra of, from (p,2n) reactions on odd-Z nuclei, (E/T), 20: 13345(R) (NP-15772)
COPPER
analysis for sulfur, activation, 20: 12793
argon-ion reactions with, nuclear temperature from, (E), 20: 13885
compatibility with cesium at 550°C, 20: 13203
corrosion by chlorine trifluoride–urania reaction-gas mixtures,

20: 12925(R) (EURAEC-1446)
determination in sodium loop transfer samples, methods for, 20: 12766 (GEAP-4178)
determination in water, activation, 20: 12768 (IEA-97)
effects on crystal structure of alpha-iron, 20: 13317
electron and gamma energy losses in cascade showers from, (E), 20: 13345(R) (NP-15772)
electron secondary emission from thin foils of, (E), 20: 13103
neutron resonance absorption integral of, (E), 20: 14008(R) (ANL-7122, pp 42-69)
neutron transport in, pulsed fast, (E/T), 20: 13719
niobium wire superconducting properties in matrix of, 20: 13673
performance as neutron absorber rods for subcritical-lattice analyses, (E), 20: 14185(R) (MIT-2344-4, pp 70-9)
separation from other inorganic ions by paper chromatography, 20: 12939
solubility in alpha-iron at 600 to 900°C, 20: 13317
spectra in arc discharges, plasma diagnostics using emission, (E), 20: 13953
thermal conductivity across interface between quartz and, at 1.5 to 4°K, 20: 13693

COPPER ALLOYS
Be–Cu, ion reactions at 25 kev with, secondary electron emission in positive, (E), 20: 13424
Cu–Mg, uranium distribution between liquid, and fused magnesium chloride, (E), 20: 14007(R) (ANL-7122, pp 1-41)

COPPER COMPLEXES
with hexamethylphosphoramide, NMR contact shifts in, 20: 12828 (TID-21587)

COPPER ISOTOPES Cu-61
hyperfine structure, magnetic moment, and nuclear spin of, (E), 20: 13855

COPPER ISOTOPES Cu-62
hyperfine structure, magnetic moment, and nuclear spin of, (E), 20: 13855

COPPER ISOTOPES Cu-63
proton reactions (p,p') and (p,2p), cross sections for, (E), 20: 13897

COPPER ISOTOPES Cu-64
hyperfine structure, magnetic moment, and nuclear spin of, (E), 20: 13855
use for localization of brain tumors, 20: 12734 (BNL-9911)

COPPER OXIDES
neutron resonance absorption integral of, (E), 20: 14008(R) (ANL-7122, pp 42-69)

COPPER SYSTEMS
Cu–Mg–$MgCl_2$–KCl–NaCl–U, chemical compatibility with vitreous carbon containers at 800°C, (E), 20: 14007(R) (ANL-7122, pp 1-41)
Cu–Si, stacking faults in crystals of, (E/T), 20: 13971 (AD-625834)

CORROSION INHIBITORS
use of oxide, in gas-cooled reactors, 20: 14021(P)

CORROSION LOOPS
design for WWR-S, 20: 14190 (UJV-1446/65)
development of potassium, 20: 13192(R) (NASA-CR-54843)
development of potassium, constructed of T-111 tantalum alloy, 20: 13193(R) (NASA-CR-54845)

CORROSION-RESISTANT ALLOYS
fracture toughness of, double cantilever beam testing method for, 20: 12972 (BNWL-168)
research and development programs on, opportunities, roadblocks, and problems in, 20: 13185 (TID-22424)

COSMIC ELECTRONS
energy flux in extensive air showers, (E), 20: 13427

COSMIC NUCLEONS
interactions of high-energy, with nuclear emulsions, (E), 20: 13345(R) (NP-15772)

COSMIC PARTICLES
environmental contamination by, 20: 12571
interactions of, effect of elementary-particle structure in, 20: 13514

COSMIC PHOTONS
energy flux in extensive air showers, (E), 20: 13427

COSMIC RADIATION
intensity variations, (E/T), 20: 13426(T)
intensity variations of, methods for long-term measurement, (E), 20: 13345(R) (NP-15772)

COSMIC SHOWERS
analysis of high-energy jet, methods for, (E), 20: 13345(R) (NP-15772)
composition and properties of air, (E/T), 20: 13345(R) (NP-15772)
energy flux of electron-photon and nuclear-active components in extensive, (E), 20: 13427
measurement of air, electronic equipment for, (E), 20: 13345(R) (NP-15772)
measurements of air, in Bolivian joint experiment, (E), 20: 13345(R) (NP-15772)
occurrence frequency of extensive, (E), 20: 13426(T)

COSMOLOGY
model of universe admitting four-parameter group of motions, 20: 13406
structure of universe, physical laws from, 20: 13354

COUNTING DEVICES
design of fast, 20: 14059(R) (IDO-17104)

CREEP
deformation in magnesium alloy, example of diffusion, 20: 13309
equations, evaluation of transient, 20: 13249(R) (GEMP-55A, pp 29-53)

CRITICAL ASSEMBLIES
control element effectiveness in homogeneous uranium–water, annular and rod-grid, (E), 20: 14091
criticality parameters of Hi–C, (E/T), 20: 14008(R) (ANL-7122, pp 42-69)
fast neutron distributions in enriched-uranium heavy-water lattices, 20: 13703(R) (MIT-2344-4, pp 17-47)
fuel elements for Super Kukla, testing of, 20: 13287
kinetics and operations of ZPR-9, (E), 20: 14007(R) (ANL-7122, pp 1-41)
kinetics of heavy-water-moderated, miniature-lattice analysis of, (E/T), 20: 14069(R) (MIT-2344-4, pp 106-14)
kinetics of heavy-water-moderated, pulsed-neutron analyses of, (E), 20: 14066(R) (MIT-2344-4, pp 63-9)
kinetics of two-region heavy-water-moderated, (E), 20: 14068(R) (MIT-2344-4, pp 89-100)
neutron decay constant of VERA, pulsed-source measurements of prompt, (E), 20: 14089
neutron flux in ATRC, fast, 20: 14059(R) (IDO-17104)
neutron flux in, one-group parameters for thermal, (T), 20: 14073
neutron kinetics in intermediate and fast, pulsed, 20: 14083
neutron kinetics in copper or uranium reflected plutonium, fast pulsed, (E/T), 20: 14084
neutron lifetimes in FR-0, pulsed-source measurements of, (E/T), 20: 14085
neutron parameters of enriched-uranium heavy-water lattices, 20: 14065(R) (MIT-2344-4, pp 4-16)
neutron parameters of single heavy-water-moderated uranium rods in, (T), 20: 14067(R) (MIT-2344-4, pp 80-8)
neutron spectra in VERA, pulsed-source measurements of fast, (E/T), 20: 14086
parameters of heavy-water sub-, analysis using absorber rods, (E), 20: 14185(R) (MIT-2344-4, pp 70-9)
reactivity measurements in KNK, in near-critical state, (E), 20: 14082
reactivity measurements in Swedish FRO, 20: 14178 (AE-207)
reactivity of FR-0, pulsed-source measurements of negative, (E/T), 20: 14085
reactivity of Saxton, 20: 14148(R) (WCAP-3385-5)
reactivity of SHE, pulsed-source measurements of, (E/T), 20: 14081
status of Masurca, 20: 14149(T,R) (ORNL-tr-900)
uses of ZPR-3 for SEFOR analyses, (E), 20: 14007(R) (ANL-7122, pp 1-41)

CRITICALITY STUDIES
control analysis for operations with fissile material, 20: 13005 (LA-3366)
controls for, administrative and procedural, 20: 14092
problems in, adjoint transport equation for solution of, (T), 20: 14094
problems in, Monte Carlo program for solving, 20: 14093

CRUCIBLES
performance of vitreous-carbon, for copper–magnesium–magnesium-chloride–potassium-chloride–sodium-chloride–uranium systems at 800°C, (E), 20: 14007(R) (ANL-7122, pp 1-41)

CRUSTACEA
metabolism in isopod, comparison of methods for measuring, 20: 12610
strontium-85 excretion by isopod, under field and laboratory conditions, 20: 12610

CRYOGENICS
transport lines for liquid hydrogen, cooldown from, (E/T), 20: 13668 (LA-3426)

CRYSTALS
atom transmission through, coherent nuclear Coulomb excitation in, 20: 13888
defects in, stacking-fault, (E/T), 20: 13971 (AD-625834)
Fermi surface of, (T), 20: 13988
fission fragment tracks in, (E/T), 20: 13984
growth of high-melting, using h-f plasma burners, 20: 13189
lattice orientation of orthorhombic, inversion of pole figures for preferred, (T), 20: 13983
lattice oscillations in, effect of exchange interactions on paramagnetic resonance from, (T), 20: 13976
sputtering by ions, electron diffraction analysis of damage from, (E/T), 20: 13981
theory of correlated, 20: 14001
transport coefficients for magnetic, space-time symmetry of, 20: 13996

CURIUM ISOTOPES Cm-244
fission of, gamma and neutron spectra from spontaneous, (E), 20: 13769 (DP-949)
neutron fission of, yields from, 20: 13752 (ANL-7096)
production in thermal reactors, yield data for, 20: 13752 (ANL-7096)

CURIUM ISOTOPES Cm-246
neutron fission of, yields from, 20: 13752 (ANL-7096)
production in thermal reactors, yield data for, 20: 13752 (ANL-7096)
CURIUM ISOTOPES Cm-248
production in thermal reactors, yield data for, 20: 13752 (ANL-7096)
CURRENT INTEGRATORS
use with ionization chamber in gas chromatography, 20: 12777 (UJV-1431/65)
CYCLOBUTANE
decomposition of, mercury-photosensitized, 20: 12884(R) (RRL-2310-171)
radiolysis of deuterated, effects of ammonia, hydrogen sulfide, nitrogen oxide, oxygen, and organic compounds on gas-phase, 20: 12894
radiolysis of, effects of ammonia, hydrogen sulfide, nitrogen oxide, oxygen, and organic compounds on gas-phase, 20: 12894
CYCLOHEXANE
neutron diffusion parameters for, pulsed, (E), 20: 13729
nuclear magnetic resonance spin-lattice relaxation times in, deuteron and proton, 20: 12839
CYCLOTRON RADIATION
emission by electrons in cavity resonators, (E), 20: 13472(T)
properties of, from electron beam storage rings, 20: 13378
CYCLOTRONS
beam orbit in sector-focused, computer program for calculating, 20: 13355
beam-bunch phasing in isochronous, induction probes for measurement of, 20: 13387(P)
control of 88-inch, system design for automatic, 20: 13381
design and operation of fixed-frequency, 20: 13345(R) (NP-15772)
development and operation, 20: 13368(R) (UCRL-16511, pp 54-8)
radiation monitoring and shielding studies, (E), 20: 13367 (UCRL-16445(Rev.))
CYLINDERS
fracture mechanics and stability of, review on, 20: 13248 (GEAP-4678)
radiation effects on temperature distribution in rotating, 20: 13349
CYSTEINE
effects on damages induced in mouse tumors by radiomimetic agents 20: 12719(R) (NP-15668)
effects on effects of radiomimetic agents in tumor-bearing mice, 20: 12717(R) (NP-15666)
effects on effects of radiomimetic agents in tumor-bearing mice, 20: 12718(R) (NP-15667)
CYTOLOGY
methods for, combined enzyme chemistry and electron microscopic, 20: 12635(R) (NYO-2786-1)
of genetics, 20: 12564
CYTOPLASM
radiation effects on, in animal cells, 20: 12635(R) (NYO-2786-1)
radiation effects on mouse spleen, x, 20: 12681

D

DATA RECORDING SYSTEMS
description of digital computer, for fast neutron laboratory, 20: 13806
design for in-pile fatigue testing, 20: 14059(R) (IDO-17104)
stabilization of gamma-spectrum measurements, 20: 13094
testing for SNAPSHOT vehicle, 20: 14173 (TID-22416)
DATA TABULATIONS
electromotive force-temperature tables for tungsten-3% rhenium/tungsten-25% rhenium thermocouples, 20: 13028 (KAPL-M-6498)
gamma spectral data for heating and shielding calculations, 20: 13966 (UNC-5140)
neutron energies from (d,n) and (p,n) reactions with deuterium, lithium-7, and tritium, 20: 13747 (AECD/EP/7)
properties of steels used in reactors, 20: 13186 (TRG-Report-840)
thermodynamic functions for uranium carbides, 20: 13215(R) (ORNL-3885, pp 3-86)
DEER
cesium-137 contamination in, transfer to man of, 20: 12578
cesium-137 content in Colorado, factors affecting, 20: 12984
cesium-137 uptake by, from lichens, 20: 12578
metabolism in, tracer studies of, 20: 12609
DENSITOMETERS
design for chalk dust, 20: 13024 (EUR-2544.d)
development of radiometric, for explosive atmospheres, 20: 13150
development of radiometric, for spatial concentration of inhomogeneous fluid in pipe lines, 20: 13049
use for fuel rod inspection, amplifier for, 20: 13154
DEUTERIUM
deuteron reactions (d,n) at 0.05 to 3.00 Mev, neutron energies from, 20: 13747 (AECD/EP/7)
effects on crystal structure of orthoboric acid, 20: 12836
effects on hydrogen evolution at platinum and palladium cathodes, 20: 12840
effects on rotation-vibration spectra of, hydrobromic, hydrochloric, and hydriodic acids in rare gas lattices, 20: 12857
effects on vapor pressure of *n*-butane–ethylamine, ethylamine–*n*-hexane, and methylamine–*n*-hexane systems, 20: 12879
incorporation in phenols by isotopic exchange in alkaline solutions, 20: 12880
photon reactions at 500 to 700 Mev, meson(π^0) production in, (E), 20: 13345(R) (NP-15772)
properties of plasma sheath of, (E/T), 20: 13922(R) (NP-15703, pp 64-81)
proton reactions (p,2p) at 9.0 and 10.5 Mev, three-nucleon systems in, (E/T), 20: 13894
separation from hydrogen, design of exchange column for, 20: 13161(P)
separation from hydrogen, design of exchange column for, 20: 13162(P)
spectra of solid, induced infrared absorption, (E), 20: 13419
use in reactor flux probes, 20: 13119(P)
DEUTERIUM HYDRIDES
spectra of solid, induced infrared absorption, (E), 20: 13419
DEUTERIUM SYSTEMS
D–O, radiolysis yields in gaseous, 20: 12881 (AD-626609)
DEUTERON BEAMS
production of pulsed, ion buncher for, 20: 13379
DEUTERONS
binding energy and coupling constant for, Bethe-Salpeter equation for, 20: 13876
effects on properties of n- and p-type germanium, 20: 13342
interactions with electrons at 54 and 70 Mev, energy spectrum from inelastic, (E), 20: 13490
interactions with protons, meson (π) production in, (T), 20: 13528
interactions with neutrons at 5.635 and 9.035 Mev, cross sections for elastic, (E), 20: 13520
interactions with mesons (μ^-), quantum mechanics of, 20: 13630
momentum distribution from (p,pd) reactions, (T), 20: 13874
nuclear magnetic resonance spin-lattice relaxation times of, in organic liquids, 20: 12839
photoproduction on carbon, (E), 20: 13345(R) (NP-15772)
quadrupole coupling constants of, in organic liquids, 20: 12839
reactions (d,n) with deuterium and tritium at 0.05 to 3.00 Mev, neutron energies from, 20: 13747 (AECD/EP/7)
reactions (d,n) with aluminum-27, neutron spectra from, (E), 20: 13063 (JAERI-1092)
reactions (d,pγ) with magnesium-26 at 4.28 Mev, angular correlations in, (E), 20: 13768 (CONF-650410-40)
reactions (d,p) with carbon-12 at 4 Mev, emission spectra from, (E), 20: 13076 (UR-875-117)
reactions (d,p) with carbon-13 at 3 Mev, parity of 6.89-Mev level in carbon-14 from, (E), 20: 13828
reactions (d,p) with calcium-46 at 7 Mev, calcium-47 levels from, (E), 20: 13853
reactions (d,p) with calcium-48, (E), 20: 13854
reactions (d,p) with nickel-58 at 7 Mev, cross sections and nickel-59 levels from, (E), 20: 13858
reactions (d,t) with calcium-48, (E), 20: 13854
reactions (d,2p) with hydrogen at 10.5 Mev, three-nucleon system in, (E/T), 20: 13894
reactions with nuclei, angular distribution calculations in model for stripping, (T), 20: 13851
reactions with odd-n nuclei, spectroscopic factors from stripping, (T), 20: 13865
scattering by cadmium, molybdenum, tellurium, and tin at 15 Mev, energy spectra from inelastic, (E), 20: 13872
DIABETES
diagnosis, 20: 12754
DIATOMACEOUS EARTH
sorptive properties for fission products, 20: 12938
DIDO REACTORS
operation of Australian, 20: 14222(R) (NP-15612)
reactivity of FRJ-2, 20: 14184 (JUL-236-RE)
startup of FRJ-2, 20: 14184 (JUL-236-RE)
DIET
effects of calcium and phosphorus in, on strontium-85 retention by rat skeleton labeled *in utero*, 20: 12599(R) (NP-15684)
effects of phosphorus in, on calcium-47 and strontium-85 retention by rats, 20: 12597(R) (NP-15682)
effects of phosphorus and strontium, on calcium-45 and strontium-85 retention by rat skeleton, 20: 12594(R) (NP-15679)
effects of phosphorus and strontium in, on calcium-45 and strontium-85 retention by rat skeleton, 20: 12595(R) (NP-15680)
effects of phosphorus in, on calcium-47 and strontium-85 metabolism in rats, 20: 12596(R) (NP-15681)
effects of phosphorus in, on calcium-47 and strontium-85 metabolism and retention by rats, 20: 12600(R) (NP-15685)
effects on cesium–potassium ratios in animals, 20: 12611
DIETHYLAMINE, 2,2'-DICHLORO-N-METHYL-

effects on tumor-bearing mice, effects of radioprotective drugs on, 20: 12719(R) (NP-15668)
DIFFERENTIAL EQUATIONS
solution of initial-value problem for Boltzmann-Vlasov equation, 20: 13910 (JUL-297-MA)
solution of, error control in, 20: 13163(R) (ANL-7129)
DIFFUSION
coefficients of, methods of measuring very low, 20: 13270
DIODRAST
purification of iodine-131-labeled, by electrophoresis and chromatography, 20: 12918
DIPHENYLAMINE, 2,2',4,4',6,6'-HEXANITRO-
analytical use in reversed-phase chromatographic separations, 20: 12776 (RT/PROT(65)33)
DISEASES
radiotherapy of Cushing's, x, 20: 12737
radiotherapy of thyrotoxicosis, using iodine-131, 20: 12744
DISPLACEMENT GAGES
design and performance for Project Dribble, 20: 12990 (NVO-1312-1 (Vol.2))
DITHIZONE
solvent properties for cadmium and indium, 20: 12936
DIURETICS
properties in swine, tracer study, 20: 12613
DOGS
radiation effects on, effects of polyglucin on x, 20: 12723(R) (JPRS-33766, pp 3-7)
radiation effects on, pathological x, 20: 12645
DOORS
design for irradiation facilities, 20: 12950(P)
lock system for, to radioactive areas, 20: 12955(P)
DOSIMETERS
calibration of fast neutron, 20: 14222(R) (NP-15612)
circuits for x-ray, 20: 13124(P)
data read-out system for lithium fluoride finger-tip, design of, 20: 13059 (AEEW-R-411)
design and performance for fallout monitoring, 20: 12978 (AD-627077)
design for beta and gamma radiation, 20: 13120(P)
design using radiochromatic couple suspended in anhydrous translucent matrix, 20: 13125(P)
feasibility of pneumatic, for neutron flux in reactors, 20: 13069 (NASA-CR-54468)
performance of nitrogen isotopic exchange, for reactor gamma flux, 20: 14012 (IA-1048)
reader design for glass, 20: 13117(P)
sensitivity for x radiation, 20: 13057 (AD-627567)
DOUNREAY FAST REACTOR
kinetics of, correlator for random fluctuations for analysis of, 20: 14156
DROSOPHILA
radiation effects on early stages of spermatogenesis of adult male, 20: 12637 (TID-21466)
radiation effects on X chromosomes in, x, 20: 12690
radiation effects on mean viability of autosomes in, x, 20: 12661
radiation effects on mutation frequency in inseminated and virgin female, x, 20: 12663
radioinduced crossing-over in X chromosome of, x, 20: 12689
radioinduced mutation in germ cells of male, effects of age on, 20: 12636 (TID-21459)
radioinduced mutations for white locus in, cytogenetic use of, 20: 12664
spermatogenesis in, maintenance, patterns, and radiosensitivity of, 20: 14224 (TID-21562)
DRUGS
radiosensitivity effects of central-nervous-system-stimulating, in mice, 20: 12685
DUSTS
density measurements on chalk, radiometric devices for, 20: 13024 (EUR-2544.d)
effects of radioactive, on *Larrea divaricata* leaves, 20: 12670
DYSPROSIUM
acoustic wave generation at microwave frequencies in films of, 20: 14003
determination in aqueous solutions, effects of sodium tungstate on spectrofluorometric, 20: 12787
dysprosium-161 isomeric shift in metallic, 20: 13992
DYSPROSIUM ALLOYS
Co–Dy, dysprosium-161 Mössbauer effect in, (E), 20: 13992
Co–Dy, dysprosium-161 isomer shift in, 20: 13992
Dy–Fe, dysprosium-161 isomeric shift in, 20: 13992
Dy–Ni, dysprosium-161 Mössbauer effect in, (E), 20: 13992
Dy–Ni, dysprosium-161 isomer shift in, 20: 13992
DYSPROSIUM CHLORIDES
thermal capacity of aqueous solutions of, at 25°C, 20: 12818 (IS-T-52)
Dy–$DyCl_3$, phase studies on, 20: 12821 (IS-T-62)
DYSPROSIUM COMPLEXES
with dilactic, mandelic, and quinic acids, formation and stability constants of, 20: 12817 (IS-1311)
DYSPROSIUM ISOTOPES Dy-159
decay of, internal bremsstrahlung spectra from electron-capture, (E/T), 20: 13759 (CONF-233(Vol.4), pp 614-24)
DYSPROSIUM ISOTOPES Dy-161
Mössbauer effect in cobalt–dysprosium and dysprosium–nickel alloys, (E), 20: 13992
DYSPROSIUM OXIDES
BaO–Dy_2O_3, optical properties of compounds formed in, 20: 13278
Dy_2O_3–ReO_2, preparation and ferromagnetic properties of phases in, 20: 13260(R) (NP-15852)
Dy_2O_3–SrO, optical properties of compounds formed in, 20: 13278
DYSPROSIUM SYSTEMS
Dy–$DyCl_3$, phase studies on, 20: 12821 (IS-T-62)

E

ECOLOGY
conference on radiation and terrestrial, 20: 12569
genetic studies on animal and plant, 20: 12564
inventory of vascular plants in East Tennessee, alphabetic, 20: 12567 (ORNL-TM-1232)
mathematical methods in food chain analysis, 20: 12580
radiation effects on animal population, 20: 12584
radiation effects on plant, review of research on ionizing, 20: 12586
radiation effects on plant, background, 20: 12587
radiation effects on, background, 20: 12982
radiobiological research in, 20: 12570
radioisotope contamination in, effects of cosmic spallation on, 20: 12571
radioisotope distribution in forest ecosystems, 20: 12566 (COO-1006-4)
radioisotope transport mechanisms for, 20: 12573
EGGS
radiation effects on flavor of, effects of dose and irradiation temperature on γ, 20: 12660
radiation effects on sulfhydryl groups in sea urchin, thermal and uv, 20: 12624
EINSTEINIUM ISOTOPES E_{S}-254
production in thermal reactors, yield data for, 20: 13752 (ANL-7096)
ELECTRIC ARCS
switches for high-voltage, design of, 20: 13027 (IPP-4/24)
ELECTRIC CHARGES
decay and production in plasma moving in electric field, (E/T), 20: 13952
radiation from rotating linear, in plasma, (T), 20: 13958
ELECTRIC CONDUCTIVITY
measurement of solutions in radiochemical processing plants, instrument for, 20: 12927 (NP-15756)
ELECTRIC CURRENTS
generation of pulsed, in magnetoplasma, 20: 13960
production of 40- and 400-mamp, generators for, 20: 13039
stability of persistent, in mercury and tin cylinders, 20: 13691
ELECTRIC DISCHARGE
chamber design for, with vanadium foil window, 20: 13052(P)
plasma heating by, magnetic probe measurements in, (E), 20: 13639 (JUL-281-PP)
plasma instabilities in cold cathode, high frequency, (E/T), 20: 13901 (CEA-R-2822)
striations in positive column of diffuse-mode, in magnetic field, (E/T), 20: 13944
ELECTRIC FIELDS
effects on radiolysis of cyclobutane, 20: 12894
ELECTRIC GENERATORS
design of 40- and 400-mamp current generators, 20: 13039
ELECTRIC INSULATORS
electron work function for, a-c method for measuring, 20: 13025 (IPP-2/37)
radiation effects on polyvinyl chloride, 20: 12907
radiation testing of inorganic and organic, 20: 14170 (EGG-1183-2019)
ELECTRIC METERS
performance for sodium purity monitoring, 20: 14024(R) (APDA-182)
ELECTRIC PROBES
electric impedance characteristics of Langmuir, for plasma diagnostics, (T), 20: 13940
performance of plane emissive, for study of synthesis plasma, (E/T), 20: 13934
resonance damping of h-f and d-c, noncollisional, (T), 20: 13935
susceptance of plasma, evaluation of, (E/T), 20: 13924(R) (TID-22419, pp 85-98)
use of double, for plasma diagnostics, (E), 20: 13906 (IPP-1/40)
ELECTRICITY
production by nuclear plants, economics for, 20: 14133 (NP-15587)
ELECTRODES

anodizing tantalum, pre-, 20: 13204(P)
ELECTRODYNAMICS
field quantization for geometrical interpretation of, 20: 13662
ELECTROLYTIC CELLS
development and testing of regenerative lead–sodium bimetallic emf, 20: 14179(R) (ANL-7122, pp 70-81)
ELECTROMAGNETIC FIELDS
interactions with shock waves, properties of, (T), 20: 13637 (IPP-3/28)
particle motion in, generalized variational principles for, 20: 13351
plasma acceleration by, (T), 20: 13911 (JUL-336-PP)
plasma heating by stochastic, (T), 20: 13948(T)
quantization of classical, (T), 20: 13659
theory of nonlocality of, equation of geodesic deviation in, 20: 13663
ELECTROMAGNETIC LENSES
magnetic field measurements in strong-focusing, of Stanford Linear Accelerator, (E/T), 20: 13365 (SLAC-39(Rev.))
ELECTROMAGNETIC WAVES
propagation across magnetic fields, instabilities in, (E/T), 20: 13925(R) (TID-22419, pp 99-147)
propagation along magnetic fields in plasmas, mechanisms of instability damping in, (E/T), 20: 13925(R) (TID-22419, pp 99-147)
propagation in magnetosphere, properties of, 20: 13645 (AWRE-O-9/66)
propagation in plasma, 20: 13961
propagation of EH, in waveguides, (E/T), 20: 13370
scattering by ion acoustic waves in plasma, (T), 20: 13914 (MATT-318)
scattering by marginally stable plasma waves, energy transfer in, (T), 20: 13913 (MATT-317)
scattering by spherical bodies, computer program for, 20: 13346 (SC-RR-65-396)
ELECTROMAGNETISM
cosmological foundations of, 20: 13354
theory of complementary moment of electromagnetic momentum from point source, 20: 13576
ELECTRON BEAMS
bunching and deflection in linear accelerators, (T), 20: 13369
current calculation by Child-Langmuir law, effect of initial velocity on, (T), 20: 13902 (CEA-R-2898)
current measurement using Hall-element and ionization-chamber methods, 20: 13383
current monitors for 70-Mev, secondary emission foils for, 20: 13103
diagnostics in storage rings using synchrotron radiation, 20: 13378
diffraction by crystals damaged by sputtering, beam broadening in, (E/T), 20: 13981
diffusion in toroidal fields, nonadiabatic, (E/T), 20: 13925(R) (TID-22419, pp 99-147)
dosimetry of, method for, 20: 13008
effects on carrier trapping centers in polyethylene, (E), 20: 13982
effects on oxygen-defect complex formation in silicon, infrared absorption spectra of, (E), 20: 13998
effects on solar-cell power systems, 20: 13131
effects on vacancy center formation in potassium bromides at low temperature, (E), 20: 13999
energy calibration method for Mev-range, (E), 20: 13377
interactions with plasma in waveguides, (E), 20: 13925(R) (TID-22419, pp 99-147)
interactions with maser radiation, (E/T), 20: 13925(R) (TID-22419, pp 99-147)
interactions with plasma, 20: 13961
phase analysis of, in traveling-wave linacs, (T), 20: 13374
production of high-current pulsed, (E), 20: 13036
production of pulsed, system design for, 20: 13034
stability of counter-streaming, in low-pressure plasma, (E), 20: 13951
ELECTRON PAIRS
annihilation of, covariant formalism for photon polarization in, (T), 20: 13517
spectra of, methods for determining, (E), 20: 13762 (CONF-233(Vol.4), pp 700-9)
ELECTRON SOURCES
design of high-current pulsed, (E), 20: 13036
ELECTRON TUBES
development of klystrons for Stanford Linear Accelerator, 20: 13366(R) (SLAC-53)
ELECTRONIC EQUIPMENT
radiation effects on, transient, 20: 13130 (SC-DC-65-1892)
radiation effects on SNAPSHOT, 20: 14175 (TID-22418)
soldering flux on circuit boards, system for measuring, 20: 13033 (TLW-1110)
testing for SNAPSHOT vehicle, 20: 14173 (TID-22416)
ELECTRONIC FILTERS
development of optimum, for timing scintillation pulses, 20: 13104
ELECTRONS
absorption by magnesium oxide crystals at 100 to 1200 kv, coefficients for, (E), 20: 13967
acceleration of pulsed, device for, 20: 13402(P)
attenuation by plexiglass at 631 kev to 13.8 Mev, LET variations with, 20: 13969
density in plasma, laser interferometric measurement of, (E), 20: 13923(R) (TID-22419, pp 77-84)
detection and measurement at 5 to 1000 kev, performance of phosphors for, (E), 20: 12899
detection of 70-Mev, using secondary emission foils, 20: 13103
distributions in inner Van Allen belts, model for, 20: 13646 (NASA-SP-3024)
effects on p-type silicon, transient, (E), 20: 13128(R) (NP-15835 (Suppl.))
effects on zinc sulfide single-crystal thermoluminescent properties, (E), 20: 13990
emission from beryllium–copper alloys in positive ion reactions at 25 kev, secondary, (E), 20: 13424
emission of secondary, from thin metallic foils, (E), 20: 13103
energy distribution and flux in space, simulation using radioisotope sources, 20: 13129 (ORNL-P-1943)
energy levels in gases of, Hartree-Fock solutions and helical spin arrangement for, 20: 13423
energy losses in cascade showers from aluminum, copper and lead, (E), 20: 13345(R) (NP-15772)
energy states in atoms, Hartree eigenvalues for, 20: 13416
heating by electron beams in magnetic mirror machines, mirror ratio effect on, (E), 20: 13947(T)
injection into betatron, device for, 20: 13391(P)
interactions with magnetic fields, phonon emission from, (E/T), 20: 13925(R) (TID-22419, pp 99-147)
interactions with phonons in magnetic fields, (E/T), 20: 13925(R) (TID-22419, pp 99-147)
interactions with mesons (μ) and (π), cross section for, (T), 20: 13484
interactions with deuterons at 54 and 70 Mev, energy spectrum from inelastic, (E), 20: 13490
interactions with protons, meson(π^0) production in, (E), 20: 13345(R) (NP-15772)
mass relative to mesons (μ), calculation using perturbation theory, 20: 13628
motion of secondary, in Faraday-cup magnetic field, (E), 20: 13382
photoproduction on uranium, cross sections for, (E), 20: 13755 (CONF-233(Vol.4), pp 548-60)
production of heavy, in electron-proton interactions at high energies, (E), 20: 13446 (DESY-65/9)
propagation through dielectric-vacuum boundaries, transition radiation yields from, (E), 20: 13352
ranges in aluminum, effects of energy on, 20: 14002
reactions with metal foils, uv emission in, 20: 14004
reactions with nuclei at low energies, excitation in, 20: 13782 (ORNL-P-1927)
reactions with silicon, bremsstrahlung spectra from, (E), 20: 13345(R) (NP-15772)
scattering by aluminum and gold at 50 to 500 kev, cross sections for, (E/T), 20: 13757 (CONF-233(Vol.4), pp 595-608)
scattering by aluminum and iron at 0.5 to 3.0 Mev, bremsstrahlung production in, (E), 20: 13781 (NASA-CR-334)
scattering by aluminum at 0.5 to 3.0 Mev, cross sections for, (E), 20: 13781 (NASA-CR-334)
scattering by heavy nuclei, excitation of giant multipole resonances in inelastic, (T), 20: 13832
scattering by nuclei, amplitudes for inelastic, (T), 20: 13775 (JINR-P-2490)
scattering by nuclei, analysis near 180°, (E), 20: 13089
spectra in photomultiplier tubes, models for, 20: 13096
tunneling in normal-superconducting film laminates, (E), 20: 13687
work functions for, a-c method for measuring, 20: 13025 (IPP-2/37)
ELECTROPHORESIS
method of, for irradiated acid mucopolysaccharides, 20: 12756
ELECTROSTATIC ANALYZERS
development of ion beam components, 20: 13372
ELEMENTARY PARTICLES
binding energy of interacting, static Bethe-Salpeter equation for, 20: 13614
charge, internal coordinates and SU(3) symmetry of, 20: 13617
conference on problems in fundamental physics, 20: 13506
density matrix for $J > 1$, (T), 20: 13578
electromagnetic properties in SU(6) group, 20: 13623
electromagnetic properties of 70-plet representation in SU(6) scheme for, 20: 13624
field theory for, symmetry breakdown and vacuum degeneracy in nonlinear, 20: 13555
field theory of massive spin-2, inconsistency of local, 20: 13581
form factors of, phase representation for, (T), 20: 13546 (JINR-P-2519)
interactions at high energies, statistical thermodynamics of strong, (T),

20: 13587
interactions at high energies, charge distribution in inelastic, (T), 20: 13452 (JINR-P-2510)
interactions at high energy, effect of meson and baryon structure in, 20: 13514
interactions at high energies, model for, (T), 20: 13584(T)
interactions of quarks, high-energy, (T), 20: 13584(T)
interactions of quarks with momentum spurions, unitary equations for, (T), 20: 13589
interactions of scalar, high-energy behavior of forward amplitude for, (T), 20: 13595
interactions of, analytic property of fifth-order Feynman diagram for, 20: 13593
interactions of, bootstrap theory for strong, (T), 20: 13549 (UCRL-16530)
interactions of, CP invariance in electromagnetic, (T), 20: 13475(T)
interactions of, CP invariance violation in electromagnetic, (T), 20: 13478(T)
interactions of, CP invariance in modified V-A, 20: 13597
interactions of, dispersion relations and resonance reactions in multichannel, (T), 20: 13585
interactions of, degenerate SU(4) symmetry of strong, 20: 13625
interactions of, elementarity and many-pole amplitudes for, (T), 20: 13592
interactions of, form factors and multipoles in electromagnetic, (T), 20: 13451 (JINR-P-2505)
interactions of, Fubini-Furlan theory for, 20: 13537 (IC/66/8)
interactions of, form-factor approximation of Regge potentials for, 20: 13603
interactions of, high-energy behavior of amplitudes for two-body, (T), 20: 13572
interactions of, limits on use of perturbation theory for weak, (T), 20: 13622
interactions of, matrix for nonrelativistic spin-dependent, 20: 13633
interactions of, negative CP-parity in weak, (T), 20: 13473(T)
interactions of, one-boson-exchange model for inelastic, 20: 13616
interactions of, phase-space volumes for, (T), 20: 13481
interactions of, research on, (E/T), 20: 13463(R) (UCRL-16511, pp 1-53)
interactions of, renormalizable vector boson theory for weak, 20: 13568
interactions of, representation of SU(3) group in, 20: 13629
interactions of, sum rule for amplitudes of, (T), 20: 13571
isospin space for, generalized gauge transformation in, 20: 13611
kinetics and symmetries in de Sitter space, 20: 13619
mass differences of, calculation using perturbation theory, 20: 13628
mass formulas in supermultiplet model for, 20: 13583
model for long-lived, Nambu mass formula for radiationless, 20: 13594
model for, bootstrap conditions in Lee, 20: 13590
model of, spinor, 20: 13612
models for, current algebras for comparing, (T), 20: 13491
models for, triplet, 20: 13605
models of, relativistic oscillator, 20: 13626
motion in external gravitational field, relativistic bi-point model of free, 20: 13656
production at superhigh energies, composite model for, 20: 13604
production of, quantum statistics in model of multiple, 20: 13573
properties of fundamental units of matter in composite model for, 20: 13613
properties of strange, Heisenberg's nonlinear theory for, 20: 13554
properties of, charge mixture in variant triplet model for, 20: 13618
properties of, Minkowski and isobaric spaces for, 20: 13615
quantum numbers and selection rules for, higher-symmetry, 20: 13621
scattering by plane slab of matter, transport equation solution for anisotropic multiple, (T), 20: 13968
structure from meson-nucleon backward scattering, 20: 13510
symmetries for, combination of internal and space, (T), 20: 13542 (JINR-P-2443)
symmetries for, infinite ladders and current components of, 20: 13548 (SLAC-58)
symmetries of, current operators for, 20: 13533 (IC/66/3)
symmetries of, deformable sphere model for internal, 20: 13606
symmetries of, lectures on, (T), 20: 13530 (CERN-65-41)
symmetry for, dynamic interpretation of spurions in $\bar{U}_{12}$, 20: 13589
symmetry for, electric charges and sources in broken, 20: 13536 (IC/66/7)
symmetry for, Lie group theory in, 20: 13169
symmetry for, SU(2) ⊗ SU(3) reduction of irreducible representation of SU(6), 20: 13580
symmetry for, total angular momentum-like representation of SU(6), 20: 13579
symmetry group for, Lorentz covariant definition of U(6), 20: 13529 (BNL-8767)
symmetry group for, relativistic U(6,6), 20: 13534 (IC/66/5)
symmetry group for, operators CPT and C for SU(6), (T), 20: 13540 (JINR-E-2545)
symmetry group for, $SU(6)_w$, 20: 13545 (JINR-P-2513)
symmetry groups for, discrete degenerate representations of noncompact rotation, (T), 20: 13532 (IC/66/2)
symmetry groups for, dynamics of maximal degenerate, 20: 13535 (IC/66/6)
symmetry groups for, finite and disconnected subgroups of SU(3), 20: 13570
symmetry groups for, classification of higher, 20: 13577
symmetry groups with parity mixing for, higher, 20: 13599
symmetry of, dynamic mapping in field theory for, 20: 13620
theory for, general relativity, 20: 13600
theory of collective stationary states for, Green function method in, 20: 13609
theory of nonlocalized, 20: 13550(T) (LA-tr-66-7)
theory of systems of interacting, Vlasov method in, 20: 13551(T) (LA-tr-66-8)
wave equations for, dispersion for relativistic partial-differential, 20: 13582

ELEMENTS
abundance in stars, effects of beta-decay and neutron capture rates on, 20: 13410

EMBRYOS
radiation effects on chick, pathological x, 20: 12706
radiation effects on mealy bug, 20: 12715
radiation effects on developing mouse, pathological x, 20: 12650

ENDOXAN
effects on tumor-bearing mice, effects of radioprotective drugs on, 20: 12717(R) (NP-15666)
effects on tumor-bearing mice, effects of radioprotective drugs on, 20: 12718(R) (NP-15667)
effects on tumor-bearing mice, effects of radioprotective drugs on, 20: 12719(R) (NP-15668)

ENGINEERING TEST REACTOR
fuel element testing for, 20: 14059(R) (IDO-17104)

ENTHALPY
measurement at low temperatures, method for, 20: 13693

ENZYMES
content in *E. coli* of base-specific t-RNA methylase, effects of uv-induced phage induction on, 20: 12619
radiation effects on activity of decarboxylase, in mouse livers, automatic determination of, 20: 12782
role of protease, in radioinduced inflammations, 20: 12623

EQUIPMENT AND PROCEDURES
design and testing of, for studying radiation effects on weightless leukocytes, 20: 12642 (Y-1A-17)

ERBIUM
crystal structure of, effect of high pressure on, (E), 20: 13316
determination by spectrometry using 4,5-dihydroxy-3-[(p-sulfophenyl)azo]-2,7-naphthalenedisulfonic acid, 20: 12806
neutron absorption resonance integrals, 20: 14059(R) (IDO-17104)
preparation and purification of, process development for, 20: 13180(R) (IS-RD-4)
preparation of isotopic bulk materials and foils of, from oxide, 20: 13216 (ORNL-P-1899)
separation from other inorganic ions by paper chromatography, 20: 12939

ERBIUM BROMIDES
$ErBr_3$–KBr, complex formation in, 20: 12871
$ErBr_3$–NaBr, complex formation in, 20: 12871

ERBIUM CHLORIDES
thermal capacity of aqueous solutions of, at 25°C, 20: 12818 (IS-T-52)
$ErCl_3$–KCl, complex formation in, 20: 12871
$ErCl_3$–NaCl, complex formation in, 20: 12871
$ErCl_3$–RbCl, complex formation in, 20: 12871

ERBIUM COMPLEXES
with dilactic, mandelic, and quinic acids, formation and stability constants of, 20: 12817 (IS-1311)

ERBIUM ISOTOPES
preparation of bulk materials and foils of, from oxide, 20: 13216 (ORNL-P-1899)

ERBIUM ISOTOPES Er-164
alpha reactions (α,xn) with, cross sections and excitation functions for, (T), 20: 13787(R) (TID-22637)

ERBIUM ISOTOPES Er-165
decay of, internal bremsstrahlung spectra from electron-capture, (E/T), 20: 13759 (CONF-233(Vol.4), pp 614-24))

ERBIUM ISOTOPES Er-166
alpha reactions (α,xn) with, cross sections and excitation functions for, (T), 20: 13787(R) (TID-22637)

ERBIUM ISOTOPES Er-167
alpha reactions (α,xn) with, cross sections and excitation functions for, (T), 20: 13787(R) (TID-22637)

ERBIUM ISOTOPES Er-170
ion fission of, fragment energy and mass distributions from, (E),

20: 13861
ERBIUM OXIDES
thulium-171 separation from, by complexing with HEDTA, 20: 12764 (CONF-660305-8)
BaO–Er_2O_3, optical properties of compounds formed in, 20: 13278
Er_2O_3–ReO_2, preparation and ferromagnetic properties of phases in, 20: 13260(R) (NP-15852)
Er_2O_3–SrO, optical properties of compounds formed in, 20: 13278
ERYTHROCYTES
radiation effects on thermal hemolysis in rat, x, 20: 12697
ERYTHROPOIESIS
role of reticular cells in, 20: 12681
ERYTHROSIN
purification of iodine-131-labeled, by electrophoresis and chromatography, 20: 12918
ESCHERICHIA COLI
radiation damage in, effects of genes on photoreactivation of uv, 20: 12713
radiation effects on, effects of colicine factor on uv, 20: 12677
radiation effects on ESR in, effects of temperature on γ, 20: 12622
radioinduced free radicals in, effects of MEA and oxygen on γ, 20: 12622
radioinduced phage induction in, effects on base-specific t-RNA methylase levels, uv, 20: 12619
radiosensitivity of, uv, 20: 12712
radiosensitivity of, effects of nutritional restriction on uv, 20: 12621
ETHANE
neutron inelastic scattering at small angles, 20: 14059(R) (IDO-17104)
radioinduced oxidation of, using hydrogen bromide catalyst, yields in gamma, 20: 12883 (ORO-634)
separation of normal and deuterated, by gas chromatography, 20: 12930
yields from gas-phase radiolysis of cyclobutane, 20: 12894
ETHANE, HEXAFLUORO-
radiolysis of solid, ESR spectra of fluorinated ethyl radicals during, 20: 12884(R) (RRL-2310-171)
ETHANE, IODO-
iodine-131 exchange with aluminum iodide, 20: 12864
ETHANETHIOL, 2-AMINO-
effects on damages induced in mouse tumors by radiomimetic agents, 20: 12719(R) (NP-15668)
effects on effects of radiomimetic agents in tumor-bearing mice, 20: 12717(R) (NP-15666)
effects on effects of radiomimetic agents in tumor-bearing mice, 20: 12718(R) (NP-15667)
effects on radiation effects on intestinal death in rats, 20: 12721(T) (BNWL-tr-11)
radiosensitivity effects on tumor cells, mechanism for, 20: 12680
radiosensitivity effects on free radical formation in *E. coli*, γ, 20: 12622
ETHANOL
nuclear magnetic resonance spin-lattice relaxation times in, deuteron and proton, 20: 12839
benzene–ethanol, radiation effects on, at 77°K, ESR and tracer studies of x, 20: 12890
ETHERS
amine–ether, solvent properties for metals in acid solutions, 20: 12941(P)
ETHYL ACETATE
solvent properties for molybdenum and niobium, 20: 12933
ETHYL RADICALS
radioinduced in hexafluoroethane, ESR spectra of fluorinated, 20: 12884(R) (RRL-2310-171)
ETHYLAMINE
ethylamine–*n*-hexane, vapor pressure of, deuterium isotope effects on, 20: 12879
n-butane–ethylamine, vapor pressure of, deuterium isotope effects on, 20: 12879
ETHYLENE
radiation effects on production of, in pears, effects of nitrogen atmosphere on, 20: 13140(R) (UCD-34P80-3, pp 27-47)
radiation effects on gaseous, yields in, 20: 12884(R) (RRL-2310-171)
radiopreservation effects on production of, in tomatoes, 20: 13148(R) (UCD-34P80-3, pp 99-175)
reactions with excited hydrogen atoms, mass spectrometric detection of, 20: 12886(T) (SC-T-66-0706)
separation of normal and deuterated, by gas chromatography, 20: 12930
yields from gas-phase radiolysis of cyclobutane, 20: 12894
Ar–ethylene, radiolysis yields in liquid, 20: 12884(R) (RRL-2310-171)
ETHYLENE, CHLORO- POLYMERS
radiation effects on properties of, 20: 12907
ETHYLENE, CHLOROTRIFLUORO- POLYMERS
analytical use in reversed-phase chromatographic separations, 20: 12776 (RT/PROT(65)33)
ETHYLENE, DIFLUORO- POLYMERS
radioinduced cross-linking of, 20: 12909(P)
ETHYLENE POLYMERS
positron lifetime in, (E), 20: 13499
production of irradiated, use of large accelerator for, 20: 12906
radiation effects on chemical and physical properties of, 20: 12905
radiation effects on carrier trapping centers in, electron and gamma, (E), 20: 13982
uses of irradiated, 20: 12905
ETHYLENE, TETRAFLUORO- POLYMERS
neutron scattering at 130 to 160 kev, ratio method for cross sections for, (E), 20: 13716
positron annihilation in, effect of crystallinity on angular distributions from, 20: 13468
positron lifetime in, (E), 20: 13499
ETHYLENEDIAMINE COMPLEXES
with cobalt, radiolysis of, extraction of recoil products from, 20: 12897
EUROPIUM
determination by spectrometry using 4,5-dihydroxy-3-[(*p*-sulfophenyl)azo]-2,7-naphthalenedisulfonic acid, 20: 12806
determination in aqueous solutions, effects of sodium tungstate on spectrofluorometric, 20: 12787
energy levels of, lifetime of excited, (E), 20: 13422
preparation of isotopic bulk materials and foils of, from oxide, 20: 13216 (ORNL-P-1899)
separation from cerium by persulfate oxidation and bis(2-ethylhexyl) phosphate extraction, 20: 12762 (BNWL-173)
separation from other inorganic ions by paper chromatography, 20: 12939
solvent properties for tantalum, 20: 13180(R) (IS-RD-4)
EUROPIUM ALLOYS
Eu–Pb, phase studies, 20: 13180(R) (IS-RD-4)
EUROPIUM COMPLEXES
with dilactic, mandelic, and quinic acids, formation and stability constants of, 20: 12817 (IS-1311)
EUROPIUM ISOTOPES
preparation of bulk materials and foils of, from oxide, 20: 13216 (ORNL-P-1899)
EUROPIUM OXIDES
BaO–Eu_2O_3, optical properties of compounds formed in, 20: 13278
Eu_2O_3–SrO, optical properties of compounds formed in, 20: 13278
EUROPIUM SULFIDES
nuclear spin-lattice relaxation in insulators of, at low temperature, (T), 20: 13995
EUTECTICS
superconductivity of, effects of structure on, 20: 13695
EXPERIMENTAL BOILING WATER REACTOR
reactivity of plutonium-loaded, (E), 20: 14008(R) (ANL-7122, pp 42-69)
EXPERIMENTAL BREEDER REACTOR-II
breeding elements for, fabrication and testing of depleted uranium slugs for use in, 20: 13206 (ANL-6417)
description of, 20: 14193
development and operations of, (E), 20: 14007(R) (ANL-7122, pp 1-41)
fuel pins for, corrosion testing of Mark I, (E), 20: 14009(R) (ANL-7122, pp 82-90)
EXPERIMENTAL GAS COOLED REACTOR
component development for, 20: 14139(R) (ORNL-3885, pp 268-83)
coolant system ruptures in, nitrogen purge effectiveness for, 20: 14138(R) (ORNL-3885, pp 253-67)
fuel element irradiation testing for, 20: 14142 (ORNL-TM-1378)
fuel irradiation testing for, 20: 14140(R) (ORNL-3885, pp 284-93)
moderator oxidation studies, 20: 14138(R) (ORNL-3885, pp 253-67)
moderator structural testing for, graphite, 20: 13262(R) (ORNL-3885, pp 195-235)
EXPERIMENTAL ORGANIC COOLED REACTOR
coolant flow transients in, simulation using analog computer, 20: 14059(R) (IDO-17104)
EXPLOSIONS
effects of flash heating on, of zirconium droplets, 20: 12826 (SC-RR-65-569)
EXPONENTIAL PILES
criticality conditions for interacting cylinder and slab, one-group diffusion theory for, 20: 14090
criticality studies on plutonium dioxide–uranium dioxide–water, using pulsed sources, (E), 20: 14078
neutron kinetics in fast, pulsed, (T), 20: 14087
neutron kinetics in, modulated and pulsed experiments for prompt, (T), 20: 14088
reactivity measurements in MINOR, using pulsed sources, (E), 20: 14076
reactivity of variable-pitch enriched uranium-water, kinetic and steady-state measurements of, (E/T), 20: 14079
EYES
radioinduced mutations for color in male Dahlbominus, effects of maternal age at irradiation on γ, 20: 12691
radiotherapy of intraocular tumors in, γ and x, 20: 12740

F

FALLOUT
characteristics of, 20: 12981
content in Colorado mule deer, factors affecting, 20: 12984
content in human food, factors affecting, 20: 12979 (EUR-2287.d)
content in Pacific Proving Ground 12 yrs after weapons tests, 20: 12579
content in Po Valley rice, effects of crop irrigation on, 20: 12986
effects on chromosomes in Perognathus, aberrant, 20: 12666
effects on growth of Marshall Island children exposed in 1954, 20: 13011
effects on *Larrea divaricata* populations, 20: 12670
effects on man, review on, 20: 12708
monitoring of, dose rate system for, 20: 12978 (AD-627077)
radiation field from, computer simulation of, 20: 13021(P)
separation from water, treatment kit for ion exchange, 20: 12942(P)
uptake by desert shrubs, 20: 12572
uptake by lichens in Sweden, 20: 12578
uptake by plants in Georgia piedmont, 20: 12985
FAST FLUX TEST FACILITY
accident analysis of, maximum hypothetical, 20: 14181 (COO-1430-2)
shield design and analysis for, (E/T), 20: 14180 (COO-1430-1)
FAST REACTORS
breeding blanket development for, uranium carbide paste, 20: 14024(R) (APDA-182)
cooling systems for 1000-Mw(e) liquid-metal-cooled power breeders, stress analysis of piping in, 20: 14120 (COO-1454-1)
design of pulsed, 20: 14096
development in France, 20: 14192
development of liquid-metal-cooled power-breeder, 20: 14149(T,R) (ORNL-tr-900)
fuel cycle for, evaluation of thorium, 20: 14126 (JUL-276-RG)
fuel element design and testing for gas-cooled, 20: 14104(R) (ORNL-3885, pp 244-50)
kinetics and operations of ZPR-9, (E), 20: 14007(R) (ANL-7122, pp 1-41)
reactivity effects in Swedish FRO, 20: 14178 (AE-207)
FAST TEST REACTOR
core meltdown accident, hypothetical, 20: 14182(R) (COO-1430-3)
FECES
chromium-51 content in, after oral administration, 20: 12612
excretion of calcium-45 and strontium-85 in rat, effects of dietary phosphorus on, 20: 12594(R) (NP-15679)
excretion of calcium-45 and strontium-85 in rat, effects of dietary phosphorus on, 20: 12596(R) (NP-15681)
radium content in rat, after radium chloride implantation, 20: 12603(T) (JPRS-33958, pp 1-7)
radium content in rat, after ingesting radium dyes, 20: 12603(T) (JPRS-33958, pp 1-7)
scandium-47 content in, after oral administration, 20: 12612
FERMIONS
book: *The Theory of Finite Fermi Systems and Properties of Atomic Nuclei*, 20: 13632
field theory for, Rainich geometrization in, 20: 13575
Hartree-Fock field and method of projection for system of, 20: 13826
interaction coupling constants and mass for, method of calculating, 20: 13554
interaction hamiltonian for many-body systems of, sympletic-invariant, 20: 13651
interactions in many-body systems of, sum rules for, (T), 20: 13561
interactions in many-body systems of, cluster expansions for, (T), 20: 13591
interactions of, field-theoretical model for, 20: 13566
theory of many-body systems of, Hartree-Fock solutions and helical spin arrangement in, 20: 13423
thermodynamics for ideal gases of, statistical, 20: 13640
FERMIUM ISOTOPES
production in oxygen-18 reactions (0-18,xn) with uranium-238, cross sections for, (E), 20: 13889
FERMIUM ISOTOPES Fm-255
production in thermal reactors, yield data for, 20: 13752 (ANL-7096)
FERRICYANIDES
radiation effects on photoreduction by chloroplasts, gamma, 20: 12627
FERROMAGNETIC MATERIALS
nuclear spin-lattice relaxation in insulators of, at low temperature, (T), 20: 13995
FERTILIZERS
foliar spray application of, effects of urea on permeation in, 20: 14218 (COO-888-44)
uptake of nitrogen-15-labeled ammonium sulfate, by rice, 20: 12592(R) (NP-15671)
uptake of nitrogen, effects of amount and time of application on rice, 20: 12593(R) (NP-15672)
uptake of phosphorus-32-labeled superphosphate, by rice, 20: 12592(R) (NP-15671)
FETUSES
radiation effects on developing mouse, neutron and x, 20: 12683
radiation effects on developing mouse, pathological x, 20: 12650
FIELD THEORY
Bethe-Salpeter equation in quantum, vacuum- and light-like solutions of, 20: 13569
Bethe-Salpeter equation in quantum, static and nonstatic solutions of, 20: 13614
dispersion for relativistic nonlinear equations with partial derivatives, 20: 13582
fermions in, Rainich geometrization of, 20: 13575
Feynman diagrams in, analytic property of fifth-order, 20: 13593
formalism for many-body quantum systems, inequivalent representations in, 20: 13553
formalism of charged scalar, functional methods and exact solutions in, 20: 13563
interactions of Bose and vector neutral fields, functional method for, 20: 13564
meson coupling in, relativistic Green's functions from streng, 20: 13557
peratization method in, convergence in, 20: 13567
quantum, self-consistent method in, 20: 13552
sum rules for many-fermion systems in quantum, 20: 13561
symmetries in relativistic, broken and approximate, 20: 13558
symmetry breakdown and vacuum degeneracy from nonlinear spinor equations in, 20: 13555
symmetry breakdown in Goldstone models in, 20: 13556
symmetry breaking solutions in relativistic, 20: 13560
symmetry rearrangement in dynamical maps in, 20: 13620
FILMS
critical fields in thin superconducting, fluxoid quantization and Ginsburg-Landau theory for, 20: 13685
flow transfer rates for liquid helium II, preferred, (E), 20: 13682
superconducting transition temperature of thin, (T), 20: 13676(T)
FILTERS
sorptive properties of molecular sieves for xenon-133 in fission product mixtures, 20: 12772 (ORNL-3840)
testing ventilation, for radiochemical laboratories, 20: 12925(R) (EURAEC-1446)
FILTRATION
methods development for radioactive sludges, 20: 14210
FINNED TUBES
design for reactor fuel canning, 20: 14107(P)
FISH
radiation effects on lipids in, gamma, 20: 12618(R) (TID-22399)
storage life of storage in γ-irradiated sea water, 20: 13152
FISSION CHAMBERS
use for neutron detection in concrete-walled laboratory, background determination for, 20: 13714
FISSION FRAGMENTS
angular distributions from plutonium-239 photofission, (E), 20: 13809
effects on ionization of rare gases for plasma production, (E/T), 20: 13939
energy and mass distributions from ion fission of nuclei ($176 \leq A \leq 209$), (E), 20: 13861
mass yields in uranium-238 photofission at 17.5 Mev, (E), 20: 13860
reactions in crystals, track production in, (E/T), 20: 13984
yield in thermal neutron ternary fission of uranium-235, 20: 13862
yields from heavy nuclei, analysis using mica sandwiches, 20: 13099
yields in neutron fission of plutonium-239, uranium-233, and uranium-235, 20: 14059(R) (IDO-17104)
FISSION PRODUCTS
analysis for cerium-144 by bis(2-ethylhexyl) phosphate extraction and beta counting, 20: 12774 (PG-Report-685)
containment by sodium coolant in meltdown accidents, 20: 14149(T,R) (ORNL-tr-900)
diffusion from evaporating fuel bodies, gaseous, 20: 13336
diffusion from iron–uranía cermet fuels, 20: 13179(R) (GEMP-55A, pp 13-28)
diffusion of gaseous, from uranium dioxide, effects of lattice defects on, 20: 13290
diffusion of gaseous, in irradiated uranium dioxide fuel elements, 20: 13329 (RT/FI(65)46)
distribution in irradiated reactor fuels, 20: 14059(R) (IDO-17104)
effects on hardwood-pine forests, effects of age and dose on recovery from, 20: 12675
neutron absorption cross sections for plutonium-239 and uranium-233 and -235, (E/T), 20: 13748 (AECL-2510)
release from ceramic coated fuels during postirradiation annealing, 20: 13261(R) (ORNL-3885, pp 87-149)
release from irradiated carbon-coated uranium dioxide particles, 20: 13261(R) (ORNL-3885, pp 87-149)
separation from aqueous solution by sorption on diatomaceous earth,

20: 12938
separation from irradiated fuels, analysis of organic solvents used in, 20: 12789
separation from plutonium–uranium halide process gases by trapping, 20: 12925(R) (EURAEC-1446)
separation from plutonium and uranium in aqueous solutions, process for, 20: 12940(P)
separation from uranium by solvent extraction using TBP–kerosene, effects of chemical degradation of kerosene on, 20: 12934
separation of cadmium and indium from, by solvent extraction using dithizone, 20: 12936
separation of cesium-137 from, by ion exchange using vanadium ferrocyanide, 20: 12932
separation of iodine-131 and xenon-133 from uranium-235, by sorption, 20: 12772 (ORNL-3840)
separation of technetium from, 20: 12808
yields from low-energy fission of heavy nuclei, methods of determining, 20: 12920
yields of transplutonium, in thermal reactors, 20: 13752 (ANL-7096)

FISSIONABLE MATERIAL
analysis of mixed, radiometric, 20: 12814(P)
criticality of, computer program for, 20: 14093
criticality of, detection systems for, 20: 13115
criticality of, management and operational control of, 20: 13020
handling and processing of, criticality control for, 20: 13005 (LA-3366)

FISSIUM
fissium–Pu–U, radiation effects on, in-pile testing of, (E), 20: 14007(R) (ANL-7122, pp 1-41)
fissium–UO_2, reactions with chlorine trifluoride, 20: 12925(R) (EURAEC-1446)

FLANGES
design for reactor pressure vessels, 20: 14049(P)
design for tubes of different diameters and thermal expansion coefficients, 20: 12951(P)

FLUID FLOW
analysis of MHD generator, variational, 20: 13437
hydrodynamic and magnetohydrodynamic, research on, 20: 14227(R) (TID-22419)
hydrodynamics of two-phase swirling, (E/T), 20: 12960 (EURAEC-1515)
in randomly packed beds of large spheres, mass transfer and velocity profiles in, 20: 14015 (ORNL-TM-1075)
magnetohydrodynamic, in channel in transverse electromagnetic fields, (T), 20: 13635 (ARL-63-175(Pt.3))
magnetohydrodynamic, in rigid circular profile, (T), 20: 13641
magnetohydrodynamic, in closed regions with axial symmetry, (T), 20: 13643
oscillation mechanisms in two-phase boiling, 20: 12962(R) (GEAP-4959)
relaxation times and vortex rings for nonequilibrium state of superfluid, (T), 20: 13671
stability in BWR coolant channels, 20: 14027 (EURAEC-909)
void fraction in two-phase, impedance gage for measuring, 20: 12964

FLUID FLOW (TURBULENT)
heat transfer in parallel rod arrays, solutions for, (T), 20: 12967

FLUID FUEL REACTORS
design using powdered fuel-coolant gas suspension, 20: 14097(P)

FLUIDIZATION
fluid flow in randomly packed beds of large spheres, mass transfer and velocity profiles in, 20: 14015 (ORNL-TM-1075)

FLUIDS
void fraction of two-phase, impedance gage technique for measuring, 20: 12964

FLUORIDE VOLATILITY PROCESSES
design for reactor fuel processing, 20: 12940(P)
development of fluid-bed, for uranium hexafluoride production from uranium dioxide pellets, 20: 12923 (ANL-6898)
development of fluid-bed, for fuel element decladding and uranium dioxide fluorination, 20: 12923 (ANL-6898)
development of fluid-bed, for uranium separation from fuel elements, 20: 12924 (ANL-6973)
uses for recovery of tungsten–rhenium alloy scrap, economics and technology of, 20: 13181 (K-L-6076)

FLUORIDES
determination in liquids and solids by automated colorimetry and pyrohydrolysis, 20: 12765 (DP-1004)

FLUORINATION
process development for plutonia–urania–fission product mixtures, on alumina fluidized beds, (E), 20: 14008(R) (ANL-7122, pp 42-69)
process for plutonia–urania mixtures, to hexafluorides, (E), 20: 14008(R) (ANL-7122, pp 42-69)

FLUORINE
corrosive effects on nickel and nickel alloys at 500°C, (E), 20: 14008(R) (ANL-7122, pp 42-69)
determination in bromine fluorides by titration with thorium nitrate, 20: 12797
determination in plutonium tetrafluoride using pyrohydrolysis, 20: 12775 (RFP-601)
meson (μ) and (π) scattering cross sections of, (T), 20: 13480
neutron cross sections for, 20: 14062 (JUL-214-RG)
neutron scattering at 130 to 160 kev, ratio method for cross sections for, (E), 20: 13716

FLUORINE ISOTOPES F-17
nuclear magnetic moment corrections for, perturbation theory for, 20: 13838

FLUORINE ISOTOPES F-19
nucleon reactions with, optical-model wave functions for, (T), 20: 13817
proton reactions ($p,p'\gamma$) at 7.5 to 8.5 Mev, spin and M3/E2 mixing ratios for excited levels in, (E), 20: 13822
reactions (F-19,xn) with uranium-238, cross sections for, (E), 20: 13889

FLUORINE ISOTOPES F-20
energy levels of, parity and spin of, (E/T), 20: 13773 (IKF-13)

FOILS
electric conductivity of thin, nondestructive testing of, 20: 13066 (JUL-298-PC)
electron secondary emission from thin metallic, (E), 20: 13103

FONTENAY-AUX-ROSES REACTORS
control rod calibration in MARIUS, using pulsed sources, (E/T), 20: 14163

FOOD
cesium-137 content in cryptozoan, in tagged Liriodendron forest, 20: 12576
radiation processing of canned chopped ham, effects on viability of spores of *Cl. botulinum*, 20: 13134 (AD-625252)
radioactive contamination of, bibliography on, 20: 13136 (AED-C-02-06)
radioactivity in human, role of environmental and animal activity in, 20: 12979 (EUR-2287.d)
radioactivity of, grown on monazite sands and volcanic intrusions, 20: 12988
radiopreservation of fruits and vegetables, 20: 13138(R) (UCD-34P80-3)
radiopreservation of, bibliography on, 20: 13136 (AED-C-02-06)
radiosterilization effects on appearance, flavor, and texture of cherries, 20: 13141(R) (UCD-34P80-3, pp 48-51)
radiosterilization effects on incidence of Botrytis rot in strawberries, effects of atmosphere and temperature on, 20: 13139(R) (UCD-34P80-3, pp 9-26)
transit time in gastrointestinal tract, 20: 13000(R) (EUR-2520.1)
use of, equations for problems in, 20: 12580

FORESTS
cesium transport in Liriodendron, model for, 20: 12577
cesium-137 in tagged Liriodendron, uptake by cryptozoan food chain of, 20: 12576
mineral transport in Douglas-fir, tracer study, 20: 12574
radiation effects on hardwood-pine, recovery from fission-product, 20: 12675
radiation effects on conifer-hardwood, effects of environmental factors on fast-neutron, 20: 12672
radioisotope release from fresh tree litter of, 20: 12566 (COO-1006-4)

FORMIC ACID
morpholinodithio-, effects on effects of radiomimetic agents in tumor-bearing mice, 20: 12717(R) (NP-15666)
morpholinodithio-, effects on effects of radiomimetic agents in tumor-bearing mice, 20: 12718(R) (NP-15667)
morpholinodithio-, effects on damages induced in tumor-bearing mice by radiomimetic agents, 20: 12719(R) (NP-15668)
2-methylpiperazinedithio-, effects on effects of radiomimetic agents in tumor-bearing mice, 20: 12718(R) (NP-15667)
2-methylpiperazinedithio-, effects on damages induced in tumor-bearing mice by radiomimetic agents, 20: 12719(R) (NP-15668)
2-methylpiperazinedithio-, effects on effects of radiomimetic agents in tumor-bearing mice, 20: 12717(R) (NP-15666)

FRANCE
Cadarache Nuclear Centre in, civil engineering problems in construction of, 20: 12947
nuclear power economics in, 20: 14151

FRANCIUM ISOTOPES Fr-214
alpha decay, (E), 20: 13779 (JINR-P-2465)

FREE RADICALS
formation of stable, in radiolysis of solid-state N-carbobenzoxy derivatives and esters of amino acids, 20: 12889
radioinduced in *E. coli*, effects of MEA and oxygen on, 20: 12622
yields and lifetime in gamma radiolysis of bromal and chloral hydrates, 20: 12887

FRENCH REACTORS
description and operation of, for power, 20: 14155
development for propulsion, 20: 14176

development of graphite-gas power, 20: 14152
development status of fast, 20: 14192
economics of heavy-water gas-cooled, 20: 14150
safety program for, 20: 14018
FRUITS
radiation effects on gas exchange in pears, effects of nitrogen atmosphere on, 20: 13140(R) (UCD-34P80-3, pp 27-47)
radiation processing of, biochemistry and physiology of tissue softening in, 20: 13135 (AD-625483)
radiopreservation, 20: 13138(R) (UCD-34P80-3)
radiopreservation effects on prunes, gamma, 20: 13144(R) (UCD-34P80-3, pp 69-74)
radiopreservation effects on ripening of bananas, gamma, 20: 13146(R) (UCD-34P80-3, pp 84-91)
radiopreservation effects on flavor of peaches exposed when green and ripe, 20: 13147(R) (UCD-34P80-3, pp 92-8)
radiosensitivity of conidia, mycellia, and sclerotia of Botrytis rot on, 20: 13149(R) (UCD-34P80-3, pp 176-89)
radiosensitivity of fungi on, effects of chemical sensitizers on, 20: 13137 (NP-15360)
radiosterilization effects on incidence of Botrytis rot in strawberries, effects of atmosphere and temperature on, 20: 13139 (UCD-34P80-3, pp 9-26)
radiosterilization effects on appearance, flavor, and texture of cherries, 20: 13141(R) (UCD-34P80-3, pp 48-51)
radiosterilization effects on niacin and thiamine content in strawberries, 20: 13142(R) (UCD-34P80-3, pp 52-4)
radiosterilization effects on manganese content in, gamma, 20: 13143(R) (UCD-34P80-3, pp 55-7)
radiosterilization effects on lemons in nonrefrigerated storage, 20: 13145(R) (UCD-34P80-3, pp 75-83)
FUEL CELLS
development and testing of regenerative lead–sodium bimetallic emf, 20: 14179(R) (ANL-7122, pp 70-81)
FUNGI
radiation effects on sporogenesis of, uv, 20: 12695
radioinduced mutations in, uv, 20: 12694
radiosensitivity of conidia, mycellia, and sclerotia of, in fruits, 20: 13149(R) (UCD-34P80-3, pp 176-89)
radiosensitivity of fruit-spoilage, effects of chemical sensitizers on, 20: 13137 (NP-15360)
sporogenesis in, photochemical mechanisms of, 20: 12695
FURNACES
design of resistance-wound combustion, for remote operation, 20: 12790

G

GADOLINIUM
determination by spectrometry using 4,5-dihydroxy-3-[(*p*-sulfophenyl)azo]-2,7-naphthalenedisulfonic acid, 20: 12806
preparation of isotopic bulk materials and foils of, from oxide, 20: 13216 (ORNL-P-1899)
GADOLINIUM ALLOYS
Gd–Os–Y, magnetic and superconducting ordering in, 20: 13694
Gd–Os–Y, thermal capacity at 0.25 to 20°K, 20: 13694
GADOLINIUM CHLORIDES
Stark levels of, effects of configuration interaction on, 20: 14005
GADOLINIUM COMPLEXES
with dilactic, mandelic, and quinic acids, formation and stability constants of, 20: 12817 (IS-1311)
GADOLINIUM ISOTOPES
preparation of bulk materials and foils of, from oxide, 20: 13216 (ORNL-P-1899)
GADOLINIUM ISOTOPES Gd-155
energy levels of, magnetic interaction of 87-kev, (E), 20: 13763 (CONF-233(Vol.4), pp 710-19)
GADOLINIUM OXIDES
$BaO–Gd_2O_3$, optical properties of compounds formed in, 20: 13278
$BeO–Gd_2O_3$, phase studies, 20: 13268(T) (JPRS-33605, pp 64-7)
$Gd_2O_3–SrO$, optical properties of compounds formed in, 20: 13278
GALLIUM
separation from other inorganic ions by paper chromatography, 20: 12939
GALLIUM ALLOYS
Sb–Ga, radiation effects on, deuteron, 20: 13342
GALLIUM ISOTOPES Ga-66
gamma spectra, (E), 20: 13818
GALLIUM ISOTOPES Ga-69
reactions with xenon-132, dynamic deformation in, (T), 20: 13794
GAMMA RADIATION
angular distribution from positron annihilation in teflon, effect of crystallinity on, 20: 13468
detection and measurement using single crystals of cadmium telluride, 20: 13073 (SAN-549-1)
detection and measurement of low-level, performance of 4π liquid-organic scintillation detector for, 20: 13079
detection and measurement using lithium-drift germanium detectors, 20: 13095
detection by dielectric liquid ionization chambers, 20: 13107
detection of, calorimeter performance for, 20: 14170 (EGG-1183-2019)
detection of, performance of dielectric liquid-filled cloud chamber for, 20: 13112
discrimination of, in neutron detectors, 20: 13111
dosimetry in cobalt-60 grid therapy, 20: 13010
dosimetry of cobalt-60, measurement of air to tissue ratios and scatter functions for, 20: 13009
dosimetry of wedge-filtered, method for, 20: 13008
dosimetry of, instrument design for, 20: 13120(P)
dosimetry of, performance of ionization chambers for, 20: 13113
effects on angiomas, effects of age on, 20: 12745
effects on anthracene crystals, 20: 12893
effects on antibodies in mice, 20: 12631 (CEA-R-2776)
effects on ascorbic acid content of tobacco crown-gall tumors, 20: 12649
effects on bromal and chloral hydrates, 20: 12887
effects on carrier trapping centers in polyethylene, (E), 20: 13982
effects on cervical carcinomas, cytological, 20: 12659
effects on chloroplast photoreduction and structure, 20: 12627
effects on current pulse height in cadmium sulfide crystal counters, 20: 13132
effects on electronic equipment, transient, 20: 13130 (SC-DC-65-1892)
effects on electrophoretic pattern of acid mucopolysaccharides, 20: 12756
effects on ESR in *E. coli*, effects of temperature on, 20: 12622
effects on eye color in male progeny of irradiated Dahlbominus females, mutagenic, 20: 12691
effects on fish lipids, 20: 12618(R) (TID-22399)
effects on flavor of whole-egg magma, effects of dose and irradiation temperature on, 20: 12660
effects on forage grass, lethal, 20: 12679
effects on gas exchange in pears, effects of nitrogen atmosphere on, 20: 13140(R) (UCD-34P80-3, pp 27-47)
effects on gaseous deuterium–oxygen mixtures, yields in, 20: 12881 (AD-626609)
effects on genetic recombination in Chlamydomonas, effects of dose duration on, 20: 12688
effects on growth of transplanted tumors in rats, 20: 12651
effects on growth in lizards, chronic-exposure, 20: 12669
effects on guinea pigs, effects of leukocytes on, 20: 12727
effects on hardwood-pine forests, effects of age and dose on recovery from, 20: 12675
effects on intestinal mucosa after uterine cancer therapy, 20: 12700
effects on intraocular tumors, therapeutic, 20: 12740
effects on mammals, 20: 12667
effects on manganese content in strawberries, 20: 13143(R) (UCD-34P80-3, pp 55-7)
effects on mice, leukemogenic, 20: 12647
effects on n-type germanium, annealing of, 20: 13327 (ORNL-TM-1354)
effects on optical centers of trivalent rare-earth ions in crystals of calcium fluorides, 20: 13986(T)
effects on oxidation of butane, isobutane, and propane, yields from, 20: 12883 (ORO-634)
effects on ozone formation in flowing and static air, 20: 12885(R) (UCD-34P80-3, pp 59-68)
effects on *Phaseolus vulgaris*, genetic, 20: 12709
effects on *Phaseolus vulgaris*, genetic, 20: 12710
effects on pine seedlings subjected to water stress, 20: 12674
effects on pines after seed or seedling exposure, effects of post-irradiation environment on, 20: 12673
effects on pituitary tumors, 20: 12737
effects on pressure transducers, 20: 14170 (EGG-1183-2019)
effects on recovery following mouth and neck cancer surgery, 20: 12653
effects on rectum after cervical carcinoma therapy, 20: 12696
effects on reproduction in rats, following pre- and post-natal exposure, 20: 12640 (TID-22378)
effects on reproductive capacity of Mediterranean fruit flies, 20: 12633(R) (NP-15348)
effects on reproductive capacity of Mediterranean fruit flies, 20: 12634(R) (NP-15349)
effects on ripening of bananas, 20: 13146(R) (UCD-34P80-3, pp 84-91)
effects on sea water used to store fish, 20: 13152
effects on seed germination and seedling survival in conifers, 20: 12671
effects on silkworms, frequency of mutagenic, 20: 12692
effects on silver(II) salt solutions at 77°K, 20: 12895
effects on sodium chlorate crystals, 20: 12900
effects on solid-state N-carbobenzoxy derivatives and esters of amino acids, 20: 12889
effects on taurine excretion, 20: 12648

effects on ternary plutonium–uranium alloys and plutonium-carbide–uranium-carbide fuels, in-pile, (E), 20: 14007(R) (ANL-7122, pp 1-41)
effects on viability of *Cl. botulinum* spores in canned chopped ham, 20: 13134 (AD-625252)
effects on vitamin B and nicotinic acid in strawberries, 20: 13142(R) (UCD-34P80-3, pp 52-4)
effects on wholesomeness of prunes, 20: 13144(R) (UCD-34P80-3, pp 69-74)
effects on wholesomeness of tomatoes, 20: 13148(R) (UCD-34P80-3, pp 99-175)
effects on wound healing after surgical resection for tumors, 20: 12646
emission by plants growing in areas of high natural radioactivity, 20: 12987
emission from high-spin levels in nuclei, angular distribution and spectra of, (T), 20: 13847
emission in alpha inelastic scattering by deformed nuclei, rotational excitation and angular pattern of, 20: 13848
emission in compound nuclear reactions, (E), 20: 13897
emission in neutron capture reactions, method for analysis of, (E), 20: 13062 (IEA-96)
energy determination using photomultiplier tubes, 20: 13100
energy losses in cascade showers from aluminum, copper and lead, (E), 20: 13345(R) (NP-15772)
flux in reactors, isotopic exchange method for determining, 20: 14012 (IA-1048)
interactions with protons at 200 to 800 Mev, Compton cross sections for, (E), 20: 13345(R) (NP-15772)
production by high-energy cosmic nucleons in nuclear emulsions, spectra of, (E), 20: 13345(R) (NP-15772)
production of polarized, using off-axis bremsstrahlung, (E/T), 20: 13345(R) (NP-15772)
reactions (γ,e) with uranium at 133 kev, cross sections for, (E), 20: 13755 (CONF-233(Vol.4), pp 548-60)
reactions (γ,N) and (γ,np) with helium-4, cross sections for, (T), 20: 13884
reactions (γ,π+) with helium-3 at 180 to 260 Mev, cross sections for, (E), 20: 13896
reactions with plutonium-239 at 5.4 to 7.9 Mev, fission fragment angular distribution anisotropy from, (E), 20: 13809
reactions with uranium-238 at 17.5 Mev, fission-mass yields in, (E), 20: 13860
scattering by gold and uranium at 662 kev, cross sections for, (E), 20: 13756 (CONF-233(Vol.4), pp 562-94)
scattering by nuclei, resonance, (E), 20: 13771 (IA-1050)
use in density measurements, 20: 13154
use in thickness measurements, 20: 13151
use in well logging, for determination of heavy element concentration in rocks, 20: 12993

GAMMA SOURCES
calibration of cobalt-60, using Fricke dosimetry, 20: 12910 (AECD/CH/3)
calibration of cobalt-60, 20: 13107
design and construction of 500-Curie, 20: 12911 (AECD/HP/3)
use in contact therapy of laryngeal carcinomas, 20: 12758
use in radiography, lead screen intensification factors for, 20: 12974
use in radiometric devices for measuring chalk dust density, 20: 13024 (EUR-2544.d)

GAMMA SPECTRA
measurement and recording of, electronic stabilizer for, 20: 13094

GAMMA SPECTROMETERS
data recording system for single-crystal, 20: 13086
design for two-dimensional neutron capture studies, 20: 13075 (UJV-1450/65)
development using single crystals of cadmium telluride, 20: 13073(R) (SAN-549-1)
performance of germanium, silicon, and sodium iodide crystals, 20: 13067 (JUL-308-RB)
performance of total-absorption lead-glass Cherenkov, 20: 13105
performance using anti-Compton annulus, 20: 13098
stabilization of recording electronic systems for, 20: 13094
uses for determination of homogeneity of plutonia–urania fuel rods, 20: 13176(R) (EURAEC-1502)

GAMMA SPECTROSCOPY
correlation coefficient and regression line in scintillation, of short-lived radioisotopes, (T), 20: 12781
equipment development for, 20: 13345(R) (NP-15772)
use for reactor fuel element burnup determination, 20: 12812
use for reactor fuel burnup analysis, 20: 14158

GAS COOLED REACTORS
control apparatus for, design of shutdown, 20: 14046(P)
core performance in, computer program for calculating, 20: 14123 (GAMD-1561(Rev.))
corrosion inhibitors for, 20: 14021(P)
design of Australian HTGCR, 20: 14222(R) (NP-15612)
design of beryllium oxide moderated thorium–uranium fueled helium, 20: 14122(R) (GA-4451)
development, 20: 14135(R) (ORNL-3885)
development of graphite moderated power, in France, 20: 14152
economics of heavy-water, in France, 20: 14150
fuel conversion ratios and economics for, fission product releasing, 20: 14137(R) (ORNL-3885, pp 236-43)
fuel cycle for, evaluation of thorium, 20: 14126 (JUL-276-RG)
fuel element design and testing for fast, 20: 14104(R) (ORNL-3885, pp 244-50)
magnesium alloy fuel cladding compatibility with carbon dioxide in, 20: 13199
pressure vessels design with liner for, 20: 14039(P)
shielding design for graphite-moderated, 20: 14037(P)

GAS FLOW
heat transfer in, simultaneous conductive, convective, and radiative, (T), 20: 12969
magnetohydrodynamic, with tensor conductivity, (T), 20: 13634 (AE-210)

GASEOUS DIFFUSION PLANTS
criticality alarm system for, design of, 20: 13001 (GAT-T-1222)

GASEOUS DIFFUSION PROCESS
separation efficiency in, Breton-Massignon's theory for surface diffusion effect on, 20: 13160

GASEOUS FUEL REACTORS
containment vessel for, 20: 14054(P)

GASES
acceleration of ionized, equipment and method for, 20: 12952(P)
analysis for nitrogen-15 by spectrography, step-filters for, 20: 12807
diffusion through porous barriers, Breton-Massignon's theory for, 20: 13160
electric discharges in, instabilities from cold cathode, (E/T), 20: 13901 (CEA-R-2822)
separation of mixed, design of column for, 20: 13161(P)
separation of mixed, design of column for, 20: 13162(P)

GASTROINTESTINAL TRACT
food transit time in, 20: 13000(R) (EUR-2520.i)
radiation dose to, from contaminated foods, 20: 13000(R) (EUR-2520.i)
radiation effects on rectal, after cervical carcinoma therapy, γ, 20: 12696
radioactive particle sorption by, review, 20: 12604(T) (JPRS-33958, pp 8-19)
retention of calcium-47 and strontium-85 by rat, effects of dietary phosphorus on, 20: 12597(R) (NP-15682)
retention of calcium-47 and strontium-85 in rat, effects of dietary phosphorus on, 20: 12600(R) (NP-15685)

GEIGER-MUELLER TUBES
design and performance of low-background beta, for solid sample assay, 20: 13102
performance for 1- to 15-Mev photons, 20: 13055 (AD-626998)
properties in soft x-ray dosimetry, 20: 13085
response to high-intensity radiation, occurrence of after-pulses in, 20: 13083

GENES
cytogenetics of Drosophila white locus, 20: 12664
effects on photoactivation of uv-damage in *E. coli*, 20: 12713
function and structure, 20: 12564
radioinduced mutations in Saccharomyces, at meleritose locus, 20: 12655
radioinduced mutations for Drosophila white locus, 20: 12664
radiosensitivity effects in *Escherichia coli*, uv, 20: 12712

GENETICS
conference on, 20: 12564
Genetics Today, Vol. 3, The Netherlands, 1963, 20: 12565
radiation effects on variability of, in maize and wheat, 20: 12641 (TID-22582)
radiation effects on Chlamydomonas, effects of dose duration on γ, 20: 12688
radiation effects on human, 20: 12699
radiation effects on human, review on, 20: 12708
radiation effects on Pneumococci, uv, 20: 12665
radiation effects on plant, background, 20: 12587

GEOMAGNETIC FIELDS
pulsations in, micro-, 20: 13645 (AWRE-O-9/66)

GEOPHYSICS
research programs on, 20: 14227(R) (TID-22419)

GEORGIA
fallout uptake by plants in piedmont area of, 20: 12985

GERMAN REACTORS
economics, 20: 14130 (KFK-366)

GERMANIUM
fabrication of semiconductor detectors using lithium-drifted, 20: 13058 (AD-627930)
performance of lithium-drifted semiconductors of, for gamma spectroscopy, 20: 13067 (JUL-308-RB)

performance of lithium-drifted, for gamma counting, 20: 13095
radiation effects on n-type, annealing of, 20: 13327 (ORNL-TM-1354)
radiation effects on density and mobility of majority carriers in n-type, proton, (E), 20: 13977
radiation effects on n- and p-type, deuteron, 20: 13342
radioinduced defects in mechanism of heavy-particle, 20: 13987
GERMANIUM ALLOYS
Al–Ge–Nb–Sn, phase studies, 20: 13275
Ge–Nb, phase studies, 20: 13275
GERMANY
reactor fuel economics in, 20: 14130 (KFK-366)
GERMINATION
radiation effects on conifer seed, gamma, 20: 12671
GLASS
analysis for rare earths, emission spectrographic, 20: 12810
radiation effects on optical properties of silicate, 20: 13341
spectra of nickel ions in nickel, after reduction, 20: 13260(R) (NP-15852)
GLASS TEXTILES
properties of bonded joints of, with aluminum and fiberglass, 20: 14213 (ACF-15)
GLOBULIN
radiation effects on thyro-, in hyperthyroid patients, beta, 20: 12626
GLOVE BOXES
design for fabrication of alpha-and beta-emitting materials, 20: 14059(R) (IDO-17104)
GLYCEROL
positron lifetime in, (E), 20: 13499
GOATS
metabolism by, cesium-134 and strontium-85, 20: 12588(R) (AD-626320)
GOLD
determination in ores, activation, 20: 12769 (IEA-98)
electron propagation through vacuum boundary with absolute transition radiation yield from, (E), 20: 13352
electron scattering at 50 to 400 kev, cross sections for, (E/T), 20: 13757 (CONF-233(Vol.4), pp 595-608)
electron secondary emission from thin foils of, (E), 20: 13103
gamma scattering at 662 kev, cross sections for, (E), 20: 13756 (CONF-233(Vol.4), pp 562-94)
neutron inelastic scattering at 3.5 to 8.5 Mev, energy dependence of level density parameters from, (E), 20: 13827
radiation effects on electron structure of foils of, at 78°K, alpha, 20: 13339
separation from other inorganic ions by paper chromatography, 20: 12939
sputtering by neon and xenon at 40 to 100 ev, yields from, (E/T), 20: 13420
GOLD ISOTOPES Au-198
implantation for pituitary ablation, 20: 12753
use as beta source for brachytherapy of lung tumors, 20: 12741
use in pituitary gland ablation, 20: 12748
GONADS
radiation dose to medical personnel and patient, from benign tumor therapy, x, 20: 13013
radiation effects on histology of rat, following pre- and post-natal exposure, 20: 12640 (TID-22378)
radiation effects on testis, pathological, 20: 12686
zinc uptake by rat, 20: 12601 (TID-22526)
GRAPHITE
carbon deposition on, from helium–methane–water vapor mixtures, 20: 13262(R) (ORNL-3885, pp 195-235)
dimensional stability of, temperature effects on, 20: 13262(R) (ORNL-3885, pp 195-235)
effects of electrodes of, on carrier distillation of impurities in uranium(IV-VI) oxides, 20: 12771 (NLCO-967)
grinding reactor fuels of, evaluation of ball-milling for, 20: 13218 (ORNL-TM-1412)
mechanical properties of, 20: 13262(R) (ORNL-3885, pp 195-235)
neutron diffusion in, pulsed, 20: 13727
neutron moderation in, pulsed-source measurements of, (E), 20: 13741
neutron slowing-down and thermalization time constants for, pulsed, (E), 20: 13728
neutron thermalization in, wave excitation in, (E/T), 20: 13722
neutron thermalization processes in, pulsed-source investigations of, (E), 20: 13738
oxidation in EGCR, 20: 14138(R) (ORNL-3885, pp 253-67)
physical properties of molded bodies of, effects of pitch-binder content on, 20: 13247(R) (GA-6831)
pressing of, evaluation of binders for cold-, 20: 13171(R) (BMI-1751)
properties of sintered, methods for determining, 20: 13319
radiation effects on molded bodies of, effects of pitch-binder content on, 20: 13247(R) (GA-6831)
radiation effects on length and preferred orientation in polycrystalline, 20: 13247(R) (GA-6831)
radiation effects on creep of, 20: 13262(R) (ORNL-3885, pp 195-235)
radioinduced dimensional changes in raw-coke, neutron, 20: 13322 (BNWL-178)
thermal capacity below 1.2°K, 20: 13692
thermal conductivity, 20: 13262(R) (ORNL-3885, pp 195-235)
graphite–H_2O, neutron thermalization in, at large temperature gradients, (E), 20: 13740
graphite–UO_2, reactivity of semi-homogeneous systems of, pulsed source measurements of, (E/T), 20: 14081
GRAPHITE (IMPREGNATED)
processing coated particulate, grind-leach method for, 20: 12928(R) (ORNL-3868)
GRAPHITE MODERATED REACTORS
development of gas-cooled power, in France, 20: 14152
shield design for gas-cooled, 20: 14037(P)
GRAPHITE SYSTEMS
BeO–graphite, compatibility, 20: 13262(R) (ORNL-3885, pp 195-235)
B–graphite, performance for neutron shielding, 20: 14180 (COO-1430-1)
GRASS
radiosensitivity of forage, γ, 20: 12679
sodium uptake by cheat-, growing in greasewood forests, 20: 12575
GRAVIMETRIC ANALYSIS
use for biosynthetic measurement, comparison with tracer techniques, 20: 12610
GRAVITATION
constant of, determination from structure of universe, 20: 13354
elementary particle motion in external field of, relativistic bi-point model of free, 20: 13656
interactions of fields of, effects of P and T violation in, (T), 20: 13665
theory of nonlocality of, equation of geodesic deviation in, 20: 13663
GRIGNARD REAGENTS
structure of ethylmagnesium bromide in ethyl ether, 20: 12819 (IS-T-53)
GRINDING
use of ball-milling for, of graphite reactor fuels, 20: 13218 (ORNL-TM-1412)
GUINEA PIGS
radiation effects on life span of, neutron, 20: 12628 (AD-626997)
radiation effects on, effects of leukocyte transplants on γ, 20: 12727
radioinduced inflammations in, mechanism for x, 20: 12623
radiosensitivity of hypocatalasic, role of hydrogen peroxide in, 20: 12643(T) (ANL-Trans-264)

H

HAFNIUM
effects on crystal structure of alpha-iron, 20: 13317
separation from other inorganic ions by paper chromatography, 20: 12939
solubility in alpha-iron at 600 to 900°C, 20: 13317
HAFNIUM ALLOYS
Co–Hf, phase studies, 20: 13180(R) (IS-RD-4)
Hf–Ta–W, creep behavior in ultrahigh vacuum at 2000 and 2200°F, 20: 13256 (NASA-TN-D-3222)
Hf–Ta–W, development of potassium corrosion test loop constructed of T-111, 20: 13193(R) (NASA-CR-54845)
Hf–Ta–W, weldability of T-111, effects of oxygen contamination on, 20: 13264(R) (WANL-PR(P)-008)
HAFNIUM HYDRIDES
chemical bonds in, properties of, 20: 12847
HAFNIUM ISOTOPES Hf-177
energy levels of, g factors for rotational, (T), 20: 13765 (CONF-233 (Vol.4), pp 723-5)
HAFNIUM ISOTOPES Hf-180
isomeric transition in, parity admixture in 57.6-kev, (E), 20: 13841
HAFNIUM ISOTOPES Hf-183
beta decay of, coincidence and spectral measurements of, (E), 20: 13863
HAFNIUM SYSTEMS
C–Hf–Nb, phase diagrams, 20: 13272
C–Hf–Ta, fabrication and properties of sheets of, 20: 13205(R) (AD-626622)
C–Hf–Ta–W, creep behavior in ultrahigh vacuum at 2000 and 2200°F, 20: 13256 (NASA-TN-D-3222)
C–Hf–Ta–W, fabrication and properties of sheets of T-222, 20: 13205(R) (AD-626622)
C–Hf–Ta–W, weldability of T-222, effects of oxygen contamination on, 20: 13264(R) (WANL-PR(P)-008)
HALDEN BOILING REACTOR
fuel element testing of, loop design for, 20: 14131 (KR-98)
HALL EFFECT
properties in crossed-field plasma jets, (E/T), 20: 13917 (NASA-TN-3250)
HANFORD PRODUCTION REACTORS (N)
fuel element for, nondestructive testing of, 20: 14168
simulation of, feasibility of analog, 20: 14167 (HW-70878)

HARDNESS
measurement of, radiation-reflection method for, 20: 13054(P)
HASTELLOY X
performance as cladding for alloy and carbide fuels, (E), 20: 14007(R) (ANL-7122, pp 1-41)
performance of X208, as cladding for plutonium–uranium fuel alloys, (E), 20: 14007(R) (ANL-7122, pp 1-41)
HEALTH PHYSICS
hazards from plutonium release in nuclear explosions, 20: 13004 (LA-1981(Rev.))
HEAT
effects of thermal trauma with and without x irradiation on intestinal mucosa in rats, 20: 12630 (BNL-8383)
HEAT EXCHANGERS
design for inclusion within reactor pressure vessels, 20: 14035(P)
design of molten slag-air, for use in MHD electric power plant, 20: 12971(P)
design of shell-and-tube, 20: 12970(P)
welding tube to tubesheet for, automated process for, 20: 13219 (EL-SEP-710)
HEAT-RESISTING ALLOYS
fracture toughness of, double cantilever beam testing method for, 20: 12972 (BNWL-168)
phase diagrams, electron-concentration, 20: 13251(R) (GEMP-55A, pp 57-82)
research and development programs on, opportunities, roadblocks, and problems in, 20: 13185 (TID-22424)
weld ductility of niobium-base and tantalum-base, comparison of, 20: 13264(R) (WANL-PR(P)-008)
weld porosity in, causes and effects of, 20: 13264(R) (WANL-PR(P)-008)
HEAT TRANSFER
analysis of steady-state and transient, computer program for, 20: 12963 (WANL-TME-1108)
by freon-22 in two-phase flow, 20: 12962(R) (GEAP-4959)
control of reactor, optimal, 20: 14020
from finned and smooth fuel rods, boiling, 20: 12961 (GEAP-4786)
in large radioisotope thermal radiation sources, 20: 13157 (ORNL-P-1945)
in loss-of-coolant accidents in power reactors, by natural convection, 20: 14147 (UCRL-16394)
in parallel rod arrays, solutions for turbulent-flow, (T), 20: 12967
in porous bed, simultaneous conductive, convective, and radiative, (T), 20: 12969
radiative, through absorbing boundary layer, (T), 20: 12966
HEAT TRANSFER SYSTEMS
design for BWR studies, 20: 14131 (KR-98)
HEAVY WATER REACTORS
bibliography, 20: 14014(R) (MIT-2344-4)
control of, use of moderator mixing, soluble poison, and xenon for, 20: 14099(P)
criticality studies on enriched-uranium lattices, 20: 14065(R) (MIT-2344-4, pp 4-16)
design of organic-cooled, 20: 14100(P)
design of self-regulating pressurized, 20: 14101(P)
development, 20: 14014(R) (MIT-2344-4)
economics of gas-cooled, in France, 20: 14150
fast neutron distributions in enriched-uranium lattices in, 20: 13703(R) (MIT-2344-4, pp 17-47)
fuel cycle cost for, plutonium–thorium, 20: 14117 (BNWL-183, Sect.III)
fuel cycle for, evaluation of thorium, 20: 14126 (JUL-276-RG)
fuel rod criticality parameters in subcritical, (T), 20: 14067(R) (MIT-2344-4, pp 80-8)
kinetics of subcritical, analysis using absorber rods, (E), 20: 14185(R) (MIT-2344-4, pp 70-9)
kinetics of two-region subcritical, (E), 20: 14068(R) (MIT-2344-4, pp 89-100)
kinetics of, miniature-lattice analysis of, (E/T), 20: 14069(R) (MIT-2344-4, pp 106-14)
kinetics of, pulsed-neutron analyses of, (E), 20: 14066(R) (MIT-2344-4, pp 63-9)
neutron effective resonance integrals in MITR, effects of fuel/moderator ratio on, (E), 20: 14186(R) (MIT-2344-4, pp 145-8)
neutron leakage and return fluxes in, (E), 20: 14070(R) (MIT-2344-4, pp 115-34)
neutron reactions with uranium isotopes in, (E), 20: 14103(R) (MIT-2344-4, pp 48-62)
HELIUM
effects on emission spectrographic determination of rare earths, 20: 12810
energy levels of, Hartree-Fock formalism for, (T), 20: 13411 (CEA-R-2855)
energy levels of, quantum mechanical calculation of ground-state, 20: 13630
flow transfer rates for films of liquid II, preferred, (E), 20: 13682
heat transfer to liquid II, film-free convective, (T), 20: 13696
operators for liquid II, quasi-particle, (T), 20: 13670
reactions with uranium-238, fission mass-yield curves from, (E), 20: 13345(R) (NP-15772)
shock fronts in electromagnetic tubes, self-luminescence, (E), 20: 13949
solubility in liquid lithium at 871°C, 20: 12827 (TID-21583)
solubility in liquid potassium at 704°C, 20: 12827 (TID-21583)
stability of discharge plasma of, hysteresis effects in helical, (E), 20: 13937
use in high-sensitivity magnetometer for low temperatures, 20: 13046
HELIUM IONS
production and acceleration of beams of, 20: 13804
HELIUM ISOTOPES He-2
production as intermediate in helium-3 (He-3,2p) reaction, (E), 20: 13900
HELIUM ISOTOPES He-3
gamma reactions (γ,π^+) at 180 to 260 Mev, sections for cross sections for, (E), 20: 13896
helium-3 reactions (He-3,2p) at 4.9 Mev, mechanism of, (E), 20: 13900
helium-4 reactions (He-4,n) at 28 Mev, beryllium-6 excited states from, (E), 20: 13845
neutron reactions (n,p) with, excitation functions for, (E), 20: 13741
reactions (He-3,α) with calcium-48, (E), 20: 13854
reactions (He-3,α) with calcium-40 at 24.4 Mev, momentum spectra from, (E), 20: 13345(R) (NP-15772)
reactions (He-3,d) with nickel-62, core excitation in, (T), 20: 13816
reactions (He-3,d) with magnesium-24, scandium-45, and silicon-28 at 24.4 Mev, momentum spectra from, (E), 20: 13345(R) (NP-15772)
reactions (He-3,d) with calcium-48 at 12 Mev, scandium-49 levels from, (E), 20: 13854
reactions (He-3,n) with boron-10 at 2.6 to 5.8 Mev, nitrogen-12 energy levels from, (E), 20: 13808
reactions (He-3,n) with helium-4 at 26 Mev, beryllium-6 excited states from, (E), 20: 13845
reactions (He-3,n) with beryllium-9, neutron spectra from, (E), 20: 13063 (JAERI-1092)
reactions (He-3, pγ) with carbon-13 at 4.95 and 5.25 Mev, nitrogen-15 levels from, (E), 20: 13819
HELIUM ISOTOPES He-4
energy levels in, isotopic spin of excited, (T), 20: 13834
gamma reactions (γ,N) and (γ,np) with, cross sections for, (T), 20: 13884
helium-3 reactions (He-3,n) at 26 Mev, beryllium-6 excited states from, (E), 20: 13845
mesons (π^-) reactions (π^-,nn) and (π^-,n) with, nucleon correlations in, (T), 20: 13884
neutron scattering at 262 kev, polarization in, (E), 20: 13717
reactions (He-4,n) with helium-3 at 28 Mev, beryllium-6 excited states from, (E), 20: 13845
reactions with nuclei ($176 \leq A \leq 209$), fission fragment energy and mass distributions from, (E), 20: 13861
HELIUM ISOTOPES He-6
beta decay of, bremsstrahlung spectra in, (E), 20: 13761 (CONF-233 (Vol.4), pp 656-68)
HELIUM SYSTEMS
He–H, striations in positive column of diffuse-mode discharge in, (E/T), 20: 13944
HEMAGGLUTININS
effects on viability of bone marrow cells maintained in culture, 20: 12726
HEMATOPOIETIC SYSTEM
effects of tissue transplants of, on incidence of radioinduced leukemia in mice, 20: 12647
transplantation of tissues of, after radiation injury, 20: 12731
HEMOGLOBIN
sorption of chromium-51-labeled, after oral administration to man, tracer studies of, 20: 12612
HEMOLYSIS
radiation effects on thermally-induced erythrocyte, x, 20: 12697
HEPTANE
performance in liquid dielectric ionization chambers for mixed radiation fields, 20: 13107
HETEROGENEOUS REACTORS
design of liquid-moderated and -cooled, 20: 14100(P)
design of self-regulating, pressurized heavy water, 20: 14101(P)
HEXANE
neutron diffusion parameters for, pulsed, (E), 20: 13729
performance in liquid dielectric ionization chambers for mixed radiation fields, 20: 13107
ethylamine–n-hexane, vapor pressure of, deuterium isotope effects on, 20: 12879
n-hexane–methylamine, vapor pressure of, deuterium isotope effects on, 20: 12879

HEXOSAMINES
radiation effects on ratio of, to collagen in man, 20: 12644
HIGH-ALTITUDE EXPLOSIONS
effects of July 1962, on satellite solar-cell power systems, 20: 13131
effects of thermonuclear, 20: 14230(T) (ORNL-tr-972)
use for determining uranium-233 fission cross section at 30 ev to 5 Mev, (E), 20: 13871
HIGH TEMPERATURE GAS COOLED REACTOR EXPERIMENT
control of, equipment for automatic, 20: 14154
fuels for Dragon, nondestructive methods for testing, 20: 14159
HIROSHIMA
incidence of tuberculosis in cases of leukemia, malignant lymphoma, and myelofibrosis in, 20: 12639 (TID-21517)
radioinduced aging in, hexosamine-collgen ratio for detecting, 20: 12644
HISTIDINE
effects on recovery in x-irradiated Tradescantia, 20: 12728
HOLMIUM
crystal structure of, effect of high pressure on, (E), 20: 13316
neutron cross section for, (E), 20: 13772 (ISA-99)
preparation of isotopic bulk materials and foils of, from oxide, 20: 13216 (ORNL-P-1899)
HOLMIUM COMPLEXES
with dilactic, mandelic, and quinic acids, formation and stability constants of, 20: 12817 (IS-1311)
HOLMIUM ISOTOPES
preparation of bulk materials and foils of, from oxide, 20: 13216 (ORNL-P-1899)
HOLMIUM ISOTOPES Ho-165
alpha reactions (α,xn) with, cross sections and excitation functions for, (T), 20: 13787(R) (TID-22637)
conversion bremsstrahlung spectra from erbium-165 decay, (E/T), 20: 13759 (CONF-233(Vol.4), pp 614-24)
HOLMIUM OXIDES
$BaO–Ho_2O_3$, optical properties of compounds formed in, 20: 13278
$Ho_2O_3–ReO_2$, preparation and ferromagnetic properties of phases in, 20: 13260(R) (NP-15852)
$Ho_2O_3–SrO$, optical properties of compounds formed in, 20: 13278
HOMOGENEOUS REACTORS
neutron flux distribution in, (E), 20: 14072
HUMIDITY
radiosensitivity effects on conifer-hardwood forests, fast-neutron, 20: 12672
radiosensitivity effects on pines, after seed or seedling exposure, gamma, 20: 12673
HYDRIODIC ACID
effects on radiolysis of saturated alkanes, 20: 12884(R) (RRL-2310-171)
spectra in rare gas lattices, rotation-vibration, 20: 12857
HYDROAROMATIC COMPOUNDS
effects on exchange of iodine-131 in aluminum iodide–iodoethane system, 20: 12864
HYDROBROMIC ACID
effects as catalyst on radioinduced oxidation of ethane, isobutane, and propane, 20: 12883 (ORO-634)
spectra in rare gas lattices, deuterium effects on rotation-vibration, 20: 12857
HYDROCARBONS
analysis and calibration as solvent of, by gas chromatography, 20: 12789
thermal decomposition in fluidized-bed process for coating reactor fuel particles, 20: 12875(P)
HYDROCHLORIC ACID
spectra in argon lattice, effects of nitrogen on, 20: 12857
spectra in rare gas lattices, deuterium effects on rotation-vibration, 20: 12857
HYDROFLUORIC ACID
reactions with uranium carbide, factors affecting, 20: 12925(R) (EURAEC-1446)
HYDROGEN
determination in carbohydrates, optimal layer thickness for neutron-scattering, 20: 12791
determination in loop-cover argon by diffusion gasometry, 20: 12767 (GEAP-4833)
determination in sodium from mass transfer loops by diffusion gasometry, 20: 12767 (GEAP-4833)
determination of isomers of, by capillary chromatography, 20: 12792
deuteron reactions (d,2p) at 10.5 Mev, three-nucleon system in, (E/T), 20: 13894
diffusion in zirconium oxide films, kinetics of, 20: 13201
dissociation pressure in ytterbium–ytterbium hydride system, 20: 12829 (TID-22502)
effects on phase transformations in vanadium, 20: 13180(R) (IS-RD-4)
effects on tritium iodide photolysis in hexane solutions, 20: 12884(R) (RRL-2310-171)
evolution at platinum and palladium cathodes, deuterium effects on, 20: 12840
hyperfine structure of, effect of baryon structure on, (T), 20: 13509
meson (μ^-) capture in liquid, G-parity in rates of, (T), 20: 13505
neutron absorption by, gamma spectra from, 20: 13966 (UNC-5140)
neutron scattering by molecular, Fadeev equations for slow, (T), 20: 13417
photon reactions in phase II, meson (π^+) and (π^-) spectra from, (E), 20: 13345(R) (NP-15772)
properties of plasma sheath of, (E/T), 20: 13922(R) (NP-15703, pp 64-81)
reactions of excited, with ethylene molecules, 20: 12886(T) (SC-T-66-0706)
reactions with uranium, 20: 13227
reactions with zirconium droplets, flash heating effects on combustion and explosive, 20: 12826 (SC-RR-65-569)
separation from deuterium, design of exchange column for, 20: 13161(P)
separation from deuterium, design of column for, 20: 13162(P)
thermal conductivity at 1000 to 20,000°K, (T), 20: 13644
transport lines for liquid, cooldown from, (E/T), 20: 13668 (LA-3426)
yields in radiolysis of gaseous ethylene, 20: 12884(R) (RRL-2310-171)
HYDROGEN IONS H^+
dissociation of molecular, electric field, (T), 20: 13412 (CLM-R46)
dissociation of negative, electric, (E), 20: 13380
energy levels of molecular, (T), 20: 13412 (CLM-R46)
production and acceleration of beams of, 20: 13804
production of negative, in duoplasmatron ion source, 20: 13376
HYDROGEN ISOTOPES
determination and separation by capillary chromatography, 20: 12792
HYDROGEN ISOTOPES H-4
production of stable, (T), 20: 13834
HYDROGEN ISOTOPES H-5
production of stable, (T), 20: 13834
HYDROGEN PEROXIDES
effects on radiation sickness in hypocatalasic guinea pigs, 20: 12643(T) (ANL-Trans-264)
HYDROGEN SULFIDES
effects on gas-phase radiolysis of cyclobutane and deuterated cyclobutane, 20: 12894
labeling with sulfur-35, 20: 12919
HYDROGEN SYSTEMS
He–H, striations in positive column of diffuse-mode discharge in, (E/T), 20: 13944
H–Li, collision integrals and viscosity of weakly ionized plasma of, (E/T), 20: 13957
HYDROMAGNETIC WAVES
propagation in magnetosphere, properties of, 20: 13645 (AWRE-0-9/66)
propagation in plasma, properties of, (E/T), 20: 13919(R) (NP-15703)
HYDROQUINONE
tetrachloro-, analytical use in reversed-phase chromatography, 20: 12776 (RT/PROT(65)33)
HYDROXYLAMINE
effects on bacteriophages, 20: 12617(R) (NP-15863)
HYPERFRAGMENTS
decay of light, SU(3) symmetry for nonmesic, (T), 20: 13501
HYPERONS
decay of, models for weak gamma, (T), 20: 13502
HYPERONS (Λ)
interactions with nucleons, charge-asymmetry effects in, (T), 20: 13485
production in Y_1^* decay, (E), 20: 13518
HYPERONS (Λ^0)
decay of, models for weak gamma, (T), 20: 13502
interactions with nucleons, hypernucleus nonmesic decay for, (T), 20: 13501
HYPERONS (Σ^+)
decay of, models for weak gamma, (T), 20: 13502
HYPERONS (Ξ^-)
decay of, models for weak gamma, (T), 20: 13502
HYPERONS (Ω^-)
decay of, models for weak gamma, (T), 20: 13502
HYPERTHYROIDISM
radiodiagnosis of, using iodine-132, 20: 12746
radiotherapy using iodine-131 in children, 20: 12736
HYPOTHYROIDISM
radiotherapy of, effects on antibody titers and thyroglobulin of beta, 20: 12626

I

ICE
neutron spectra in, pulsed-source measurements of, (E/T), 20: 13737
IDAHO (LEMHI CO.)
strontium-86 to strontium-87 ratios in carbonate veins and vein-dikes in,

20: 12980
ILMENITE CONCRETES
radioactivity determination for low-background counting facilities, 20: 12946 (UCRL-11674)
IMMUNE REACTIONS
effects of bone marrow cells on, in irradiated mice, 20: 12716 (AD-626682)
radiation effects on, to tissue transplants, 20: 12645
radiation effects on, to allogenic skin grafts in mice, effects of isogenic grafts on, 20: 12656
radiation effects on, in rats, x, 20: 12701
to insulin, 20: 12754
IMMUNITY
genetic factors affecting, 20: 12565
IMPEDANCE BRIDGES
use in void fraction determinations in two-phase flow, 20: 12964
IN-PILE LOOPS
design of corrosion, for WWR-S, 20: 14190 (UJV-1446/65)
INCINERATORS
design for radioactive wastes processing, 20: 14212(P)
INCONEL
corrosion by chlorine trifluoride–uranium reaction-gas mixtures, 20: 12925(R) (EURAEC-1446)
radiation effects on mechanical properties of types 600 and X-750, neutron, 20: 13333
INDIA
radioactivity of plants growing in areas of high background in, 20: 12987
INDIUM
diffusion of, tracer studies of self-, 20: 13315
neutron inelastic scattering at 3.5 to 8.5 Mev, energy dependence of level density parameters from, (E), 20: 13827
neutron scattering at 0.3 to 1.5 Mev, differential cross sections for, (E), 20: 13829
separation from other fission products by solvent extraction using dithizone, 20: 12936
separation from other inorganic ions by paper chromatography, 20: 12939
ultraviolet emission from electron-bombarded foils of, 20: 14004
INDIUM ALLOYS
In–Ag, crystal structure of, effect of high pressure on, (E), 20: 13316
In–Sn, magnetic field enhancement in superconducting tubes of, empirical formula for, (E/T), 20: 13678
In–Sn, superconducting surface current effects on magnetic hysteresis of, (E), 20: 13679
Mg–In, crystal structure of, effect of high pressure on, (E), 20: 13316
Sb–In, radiation effects on, deuteron, 20: 13342
INDIUM ISOTOPES In-115
electron scattering at low energies, excitation in, (E/T), 20: 13782 (ORNL-P-1927)
INDOLE,3-(2-AMINOETHYL)-
effects on damages induced in tumor-bearing mice by radiomimetic agents, 20: 12719(R) (NP-15668)
effects on effects of radiomimetic agents in tumor-bearing mice, 20: 12717(R) (NP-15666)
effects on effects of radiomimetic agents in tumor-bearing mice, 20: 12718(R) (NP-15667)
INDOPHENOLS
dichloro-, radiation effects on photoreduction by chloroplasts, gamma, 20: 12627
INFECTIONS
etiology of, in x irradiated mice with skin wounds, 20: 12704
incidence of Botrytis rot in strawberries, effects of atmosphere and temperature on, radiosterilization effects on, 20: 13139(R) (UCD-34P80-3)
radiodiagnosis of bone, using calcium-47 and strontium-85, 20: 12735
INFLAMMATION
radioinduced guinea pig and rabbit, mechanism for x, 20: 12623
INSECTS
behavior of Mediterranean fruit fly, tracer study, 20: 12633(R) (NP-15348)
effects of paternal irradiation on female mealy bug progeny, cytogenetic, 20: 12715
phosphorus-32 uptake by forest, after tree inoculation, 20: 12566 (COO-1006-4)
population control of Mediterranean fruit fly by release of radiosterilized adults, 20: 12633(R) (NP-15348)
population control of Mediterranean fruit fly by release of radiosterilized adults, 20: 12634(R) (NP-15349)
radioinduced chromosomal polymorphism in populations of chironomus, background, 20: 12662
radioinduced mutations for eye color in male Dahlbominus, effects of maternal age at irradiation on γ, 20: 12691
spermatogenesis in, maintenance, patterns, and radiosensitivity of, 20: 14224 (TID-21562)
INSTRUMENTATION
design and performance for Project Dribble, 20: 12990 (NVO-1312-1 (Vol.2))
design for laser experiments, 20: 14059(R) (IDO-17104)
design for low-noise radiation damage tests, 20: 13128(R) (NP-15835 (Suppl.))
development for Stanford Linear Accelerator, 20: 13366(R) (SLAC-53)
properties of nonlinear, cross correlation determination of, 20: 13023 (CONF-660206-1)
INSTRUMENTS
apparatus functions for low-accuracy measurements, unfolding of, (T), 20: 13038
design for measurement of electric conductivity of solutions in radiochemical processing plants, 20: 12927 (NP-15756)
INSULIN
content in blood, tracer method for measurement, 20: 12754
immune reactions to, comparison of labeled and unlabeled, 20: 12754
labeling with iodine-131, 20: 12754
INTERFEROMETERS
use for shock wave measurements, (E), 20: 13636 (IPP-3/24)
use of laser, for plasma electron density measurements, (E), 20: 13923(R) (TID-22419, pp 77-84)
INTERMETALLIC COMPOUNDS
diffusion in, methods for measuring coefficients of, 20: 13270
INTERNAL COMBUSTION ENGINES
fuel for, methanol synthesis using nuclear power in mobile energy depot system, 20: 12877 (BNL-955)
INTERNAL CONVERSION
electron polarization in, correlation of, (T), 20: 13802(T)
INTESTINE
radiation and/or thermal trauma effects on mucosa in rat, 20: 12630 (BNL-8383)
radiation effects on rat, protective effects of AET and cysteamine against, 20: 12721(T) (BNWL-tr-11)
radiation effects on mucosa of, after uterine cancer therapy of, gamma, 20: 12700
radiation effects on permeability of walls of, to bacteria, 20: 12704
radiation injuries of, induced by radiotherapy, 20: 12739
INULIN
allyl-, preparation of iodine-131-labeled, 20: 12912 (CNEA-161)
IODATES
spectra and potential of, analysis of vibrational, 20: 12842
IODINE
deposition on carbon steel, stainless steel, and silver surfaces, properties of, 20: 13261(R) (ORNL-3885, pp 87-149)
metabolism in children, 20: 13000(R) (EUR-2520.i)
IODINE ISOTOPES I-125
use in backscatter gage for fiber thickness measurements, 20: 13050
IODINE ISOTOPES I-127
proton reactions (p,2n) at 8.7 Mev, conversion electrons from, 20: 13345(R) (NP-15772)
IODINE ISOTOPES I-131
effects on antibody titers and thyroglobulin after hyperthyroid therapy, 20: 12626
effects on rat pituitaries, development histologically of, 20: 12652
exchange between aluminum iodide and iodoethane, effects of aromatics and alkenes on, 20: 12864
incorporation in allylinulin, 20: 12912 (CNEA-161)
incorporation in insulin, 20: 12754
incorporation into thyrotropin, 20: 12755
production by thermal-neutron irradiation of heated tellurium dioxide, 20: 12922(P)
production of, disposal of waste from, 20: 14211
production of, telluric acid recovery from waste from, 20: 12916
separation from uranium-235 fission products by sorption on platinum, 20: 12772 (ORNL-3840)
tracer use for root systems, 20: 12581
uptake by desert shrubs, 20: 12572
use for therapy of hyperthyroidism in children, 20: 12736
use in thyrotoxicosis therapy, 20: 12744
IODINE ISOTOPES I-132
use in thyroid function tests, 20: 12746
ION BEAMS
analysis of components of positive, electrostatic technique for spatial, 20: 13372
current calculation by Child-Langmuir law, effect of initial velocity on, (T), 20: 13902 (CEA-R-2898)
effects on atom ejection from alpha-uranium, krypton, 20: 13334
interactions with plasma, 20: 13961
measurement of, ion converter for, 20: 13047
production and acceleration of heavy, 20: 13804
production in mercury electron-bombardment and multistrip cesium contact engines, 20: 12975

production of concave, source for, 20: 13385(P)
production of negative hydrogen and lithium, in duoplasmatron sources, 20: 13376

ION EXCHANGE MATERIALS
performance of Permutit SK resin, for processing plutonia wastes, 20: 13176(R) (EURAEC-1503)
spectra of, containing cobalt(II) chloride, 20: 12824 (LA-DC-6749)

ION EXCHANGE PROCESSES
design for reactor fuel processing, 20: 12940(P)

ION SOURCES
design for mass spectrometers, 20: 13051(P)
design for production of concave ion beams, 20: 13385(P)
design of cold-cathode electron-collision, for mass spectrometers, 20: 13053(P)
design of electron-bombardment, 20: 13386(P)
design of PIG, for beams to 10 mamp, 20: 13384
design of, with plural of sub-sources, 20: 13400(P)
ion extraction from duoplasmatron, negative hydrogen and lithium, 20: 13376
properties of low-density Hall current, (E/T), 20: 13917 (NASA-TN-3250)

IONIZATION CHAMBERS
calibration for measurements in liquid and solid media, 20: 13113
design of boron-trifluoride, for neutron-beam monitoring, 20: 13704(R) (MIT-2344-4, pp 101-5)
efficiency for x-ray counting, (E), 20: 13092
performance for γ and x dosimetry, 20: 13113
response of dielectric liquid, to gamma and neutron mixed fields, 20: 13107

IONS
cyclotron resonance effects on plasma heating, (E), 20: 13920(R) (NP-15703, pp 1-51)
emission from tungsten monocrystals, effects of oxygen pressure on, (E), 20: 13432(R) (TID-22419, pp 149-76)
reactions with beryllium–copper alloys at 25 kev, secondary electron emission in positive, (E), 20: 13424
reactions with nuclei ($176 \leq A \leq 209$), fission fragment energy and mass distributions from, (E), 20: 13861
scattering by complex nuclei, dynamic deformation in inelastic, (T), 20: 13794
scattering by lead-208, nickel-58, and tin-118, collective level excitation in inelastic, (T), 20: 13890

IRIDIUM ISOTOPES Ir-191
neutron resonant scattering by, cross sections and spin assignments for, (E), 20: 13796

IRIDIUM ISOTOPES Ir-192
use as gamma source in radiography, 20: 12974

IRON
crystal structure of alpha-, effects of transition metals on, 20: 13317
determination in sodium loop transfer samples, methods for, 20: 12766 (GEAP-4178)
effects on colorimetric determination of vanadium in uranium compounds, 20: 12802
effects on photometric determination of uranium in ores using Arsenazo III, 20: 12799
electron band structure of, high-pressure determination of, 20: 14221 (COO-1198-230)
electron scattering at 0.5 to 3.0 Mev, bremsstrahlung production in, (E), 20: 13781 (NASA-CR-334)
moisture control in agglomeration mixtures of, using neutron probe, 20: 13156
neutron absorption and inelastic scattering by, gamma spectra from, 20: 13966 (UNC-5140)
neutron cross sections for, 20: 14062 (JUL-214-RG)
neutron magnetic scattering on, spin correlations from diffuse, (E), 20: 13994
neutron moderation in, pulsed-source measurements of, (E), 20: 13741
neutron resonance absorption integral of, (E), 20: 14008(R) (ANL-7122, pp 42-69)
neutron scattering at 130 to 160 kev, ratio method for cross sections for, (E), 20: 13716
neutron transport in, pulsed fast, (E/T), 20: 13719
photoelectron production cross sections from 0.2 to 2 Mev, (T), 20: 13413 (CONF-233(Vol.4), pp 538-47)
radiation effects on tensile properties of, effects of nitrogen content on fast-neutron, 20: 13324(R) (EURAEC-1529)
separation from other inorganic ions by paper chromatography, 20: 12939
solubility in uranium in solid state, 20: 13298
solvent properties of alpha-, for transition metals at 600 to 900°C, 20: 13317

IRON ALLOYS
fracture mechanics and stability of, review on, 20: 13248 (GEAP-4678)
Al–Cr–Fe–Y, diffusion of uranium through cladding of, 20: 13179(R) (GEMP-55A, pp 13-28)
Al–Cr–Fe–Y, impact properties of powder-metallurgy, effects of atomized powders on, 20: 13179(R) (GEMP-55A, pp 13-28)
Al–Cr–Fe–Y, radiation effects on tensile properties of, fast-neutron, 20: 13179(R) (GEMP-55A, pp 13-28)
Cr–Fe–Ni, fatigue tests on pressure vessel cladding of, 20: 13255 (KAPL-3108)
Dy–Fe, dysprosium-161 isomeric shifts in, 20: 13992
Fe–Pu–U, corrosion by air, effects of casting conditions and iron content on, 20: 13200
Fe–Ti, radiation effects on tensile properties of, effects of nitrogen content on fast-neutron, 20: 13324(R) (EURAEC-1529)
Fe–Ti, superconductivity in, 20: 13694
Fe–Ti, thermal capacity at 0.24 to 4.2°K, 20: 13694
Fe–U, phase studies at 660 to 800°C, 20: 13298

IRON CHLORIDES
corrosive effects on type 304 stainless steel, effects of reactor irradiation on, 20: 13325(R) (GEAP-4968)

IRON COMPLEXES
with nitrogen oxide, kinetics of formation of, 20: 12884(R) (RRL-2310-171)

IRON(II) COMPLEXES
with hexamethylphosphoramide, NMR contact shifts in, 20: 12828 (TID-21587)

IRON IONS
effects of trivalent, on dissolution of uranium(IV-VI) oxide in sulfuric acid, 20: 12863

IRON ISOTOPES Fe-54
energy levels of, second-vibrational, (T), 20: 13793

IRON ISOTOPES Fe-56
proton reactions (p,n) at 14.2 Mev, angular distributions, Q values, and spectra from, 20: 13345(R) (NP-15772)
proton reactions (p,$\gamma\gamma$) at 1.3 to 1.8 Mev, cobalt-57 levels from, (E), 20: 13857

IRON ISOTOPES Fe-57
energy level transitions, (T), 20: 13805
gamma spectra of, from cobalt-57 electron-capture decay, (E), 20: 13799
Mössbauer effect in alpha-iron oxides, effect of particle size and temperature on, 20: 13997

IRON ISOTOPES Fe-59
determination in mass transfer samples, methods for, 20: 12766 (GEAP-4178)
uptake and transport by bean leaf cells and leaves, effects of chelating agents and urea on, 20: 14220 (COO-888-48)

IRON(III) OXIDES
iron-57 Mössbauer effect in alpha-phase, effect of particle size and temperature on, (E), 20: 13997
B–Fe_2O_3, performance for neutron shielding, 20: 14180 (COO-1430-1)

IRON PERCHLORATES
radiolysis of, transient absorption in pulse, 20: 12884(R) (RRL-2310-171)

IRON(II) SULFATES
sensitivity of, for calibration of 500-Curie gamma source, 20: 12911 (AECD/HP/3)

IRON SYSTEMS
B–Fe, performance for neutron shielding, 20: 14180 (COO-1430-1)
Fe–UO_2, diffusion of uranium through iron-base alloy cladding from fuel of, 20: 13179(R) (GEMP-55A, pp 13-28)
Fe–UO_2, fission product diffusion from cermet fuels of, 20: 13179(R) (GEMP-55A, pp 13-28)

IRRADIATION FACILITIES
design and construction of 500-Curie gamma, 20: 12911 (AECD/HP/3)
design for paraffin cracking, 20: 12908
design of neutron, 20: 12954(P)
design of vertical low-temperature, for accelerated charged particles, 20: 12957(P)
door design for, 20: 12950(P)
lock system for, 20: 12955(P)
source moving apparatus for, 20: 12956(P)

ISOTOPE EFFECTS
of deuterium on rotation-vibration spectra of hydrobromic, hydrochloric, and hydriodic acids in rare gas lattices, 20: 12857
of deuterium on vapor pressure of n-butane–ethylamine, ethylamine–n-hexane, and n-hexane–methylamine systems, 20: 12879
of oxygen-18 on infrared spectra of barium phosphate, 20: 12861
on hydrogen evolution at platinum and palladium cathodes, 20: 12840

ISOTOPE SEPARATION METHODS
exchange, column design for, 20: 13161(P)
exchange, column design for, 20: 13162(P)

ISOTOPES
separation at 77°K by gas chromatography, 20: 12930

ISOTOPIC EXCHANGE
kinetics of heterogeneous, on surfaces of ionic crystals, 20: 12869

of iodine-131 in aluminum iodide–iodoethane system, effects of aromatics and alkenes on, 20: 12864
use of nitrogen-14 and -15, for gamma flux determination in reactors, 20: 14012 (IA-1048)
ITALY
geology of Lake Bracciano region of, 20: 14209 (RT/PHOT(65)29)
radionuclide contamination of rice in Po Valley, effects of irrigation on, 20: 12986

J

JAPAN
radiation monitoring of personnel in, equipment and procedures for, 20: 13003 (JAERI-4035)
television equipment manufactured in, x-ray emission by, 20: 13014
JOINTS
design and properties of filament-wound, 20: 14213 (ACF-15)
design for tubes of different diameters and thermal expansion coefficients, 20: 12951(P)
properties of bonded fiberglass/fiberglass, fiberglass/metal, and metal/metal, 20: 14213 (ACF-15)
seals for movable, 20: 12949(P)

K

KEROSENE
decomposition in Purex Process, effects of nitric acid on, 20: 12934
kerosene–TBP, solvent properties for thorium and uranium, 20: 12931
kerosene–TBP, solvent properties for fission products and uranium, effects of chemical degradation of kerosene on, 20: 12934
KIDNEYS
retention of calcium-47 and strontium-85 by rat, effects of dietary phosphorus on, 20: 12597(R) (NP-15682)
retention of calcium-47 and strontium-85 by rat, effects of dietary phosphorus on, 20: 12600(R) (NP-15685)
KILNS
heating coils for, interactions of, (T), 20: 13032 (ORNL-TM-1352)
KRYPTON
spectra of hydrobromic, hydrochloric, and hydriodic acids in, deuterium effects on, 20: 12857
KRYPTON IONS
effects on atom ejection from alpha-uranium, 20: 13334

L

LABORATORIES
design of mobile-van, for testing radiation effects on weightless leukocytes, 20: 12642 (Y-IA-17)
development and operation of pilot plant for radiochemical, 20: 12925(R) (EURAEC-1446)
neutron background in concrete-walled, room-scattered, (E/T), 20: 13714
ventilation system exhaust monitoring equipment for, 20: 13006 (ORNL-TM-1384)
LABORATORY EQUIPMENT
design of, for rapid sample handling in activation analysis, 20: 12795
LACTIC ACID COMPLEXES
with lanthanum, rare earths, and yttrium, formation and stability constants of, 20: 12817 (IS-1311)
LANTHANUM
determination in glass, emission spectrographic, 20: 12810
separation from other inorganic ions by paper chromatography, 20: 12939
solvent properties for tantalum, 20: 13180(R) (IS-RD-4)
LANTHANUM CHLORIDES
thermal capacity of aqueous solutions of, at 25°C, 20: 12818 (IS-T-52)
LANTHANUM COMPLEXES
with dilactic, mandelic, and quinic acids, formation and stability constants of, 20: 12817 (IS-1311)
LANTHANUM OXALATES
thermal decomposition in air and carbon dioxide at 30 to 1100°C, 20: 12862
LANTHANUM OXIDES
crystal structure of A-type, 20: 12872
LARVAE
radiation effects on *Aedes aegypti*, x, 20: 12668
LARYNX
radiotherapy of cancer of, effects on recovery from subsequent surgery of, 20: 12653
radiotherapy of carcinomas of, γ, 20: 12758
LEAD
critical current density in superconducting switch of, 20: 13048
determination by deposition on nickel and beta counting of bismuth-210 daughter, 20: 12785
determination in rocks, gamma-gamma logging method for, 20: 12993
development and testing of regenerative lead–sodium bimetallic emf cells, (E), 20: 14179(R) (ANL-7122, pp 70-81)
electron and gamma energy losses in cascade showers from, (E), 20: 13345(R) (NP-15772)
electron tunneling in aluminum film laminates with superconducting, (E), 20: 13687
neutron moderation in, pulsed-source measurements of, (E), 20: 13741
neutron resonance absorption integral of, (E), 20: 14008(R) (ANL-7122, pp 42-69)
photoelectron production cross sections from 0.2 to 2 Mev, (T), 20: 13413 (CONF-233(Vol.4), pp 538-47)
preparation of high-purity, by double electrolysis, 20: 12867
LEAD ALLOYS
Eu–Pb, phase studies, 20: 13180(R) (IS-RD-4)
Pb–Y, phase studies, 20: 13180(R) (IS-RD-4)
Pb–Yb, phase studies, 20: 13180(R) (IS-RD-4)
LEAD GLASS
preparation and devitrification properties of fuel- and neutron absorbent-bearing, 20: 13209 (ANL-7062)
LEAD ISOTOPES Pb-202
energy levels of, second-vibrational, (T), 20: 13793
LEAD ISOTOPES Pb-204
energy levels of, second-vibrational, (T), 20: 13793
LEAD ISOTOPES Pb-205
energy level transitions in, M4, (E), 20: 13766 (CONF-233(Vol.4), pp 726-9)
LEAD ISOTOPES Pb-206
energy levels of, second-vibrational, (T), 20: 13793
preparation of high-purity irradiation targets of, by double electrolysis, 20: 12867
LEAD ISOTOPES Pb-207
nuclear magnetic moment correction for, for momentum dependent internucleon force, (T), 20: 13842
preparation of high-purity irradiation targets of, by double electrolysis, 20: 12867
LEAD ISOTOPES Pb-208
ion inelastic scattering by, collective level excitation in complex, (T), 20: 13890
LEAD ISOTOPES Pb-211
decay of, gamma spectra from, (E), 20: 13895
LEAVES
iron-59 uptake and transport by bean, effects of chelating agents and urea on, 20: 14220 (COO-888-48)
nutrient absorption by, mechanisms for, 20: 14219 (COO-888-47)
nutrient permeation through cuticular membranes of, effects of urea on, 20: 14218 (COO-888-44)
radiation effects on *Larrea divaricata*, fallout, 20: 12670
radioisotope release from, 20: 12566 (COO-1006-4)
uptake of phosphate and rubidium by isolated cells in bean and tobacco, factors affecting, 20: 14217 (COO-888-43)
LECTURES
on symmetries of elementary particles, (T), 20: 13530 (CERN-65-41)
LEPTONS
interaction amplitudes for, field-theoretical model for, 20: 13566
interactions of, convergence of perstization method for, (T), 20: 13567
interactions of, multichannel model of weak, 20: 13465
interactions of, nonperturbative field-theoretical model of weak, 20: 13464
interactions of, symmetries for, (T), 20: 13547 (JINR-P-2523)
interactions with leptons and nucleons, permutation symmetry in isospace for weak, 20: 13596
LEUKEMIA
effects on tuberculosis incidence in Hiroshima, 20: 12639 (TID-21517)
pathogenesis of, 20: 12707
radioinduced human, review on, 20: 12708
radioinduced in mice, effects of hematopoietic tissue transplants on incidence of, 20: 12647
radioinduced, etiology of, 20: 12707
LEUKOCYTES
effects of transplants of, on survival in γ-irradiated guinea pigs, 20: 12727
radiation effects on weightless, equipment for testing, 20: 12642 (Y-IA-17)
radiation effects on phagocytic activity of, x, 20: 12698
radiation effects on osmotic resistance of rat, x, 20: 12705
radiation effects on chromosomal ploidy and structure in, after abdominal or pelvic therapy, x, 20: 12658
LEVEL INDICATORS
testing ultrasonic, for molten metals, 20: 13031(R) (NYO-2910-13)
LICHENS
cesium-137 content in Alaskan, 20: 12983
cesium-137 uptake by, transfer to reindeer following, 20: 12578
fallout uptake by, in Georgia piedmont, 20: 12985

LIFE SPANS
radiation effects on guinea pig, neutron, 20: 12628 (AD-626997)
LIGHT
effects on rubidium uptake by isolated cells of bean seedlings and tobacco leaves, 20: 14217 (COO-888-43)
effects on sporogenesis of fungi, 20: 12695
intensity and polarization of, from solar corona, 20: 13409
radiosensitivity effects on pines, after seed or seedling exposure, gamma, 20: 12673
scattering by aerosols, particle size determination from, 20: 12928(R) (ORNL-3868)
scattering by plasma, incoherent, (E/T), 20: 13925(R) (TID-22419, pp 99-147)
scattering by plasma, effect of Coulomb collisions on, (T), 20: 13904 (CLM-R52)
LINEAR ACCELERATORS
beam bunching and deflection in electron, (T), 20: 13369
beam bunching in traveling-wave electron, (T), 20: 13374
beam handling system calibration of 20-Mev electron, (E), 20: 13361 (EGG-1183-2066)
cavity resonators for, aperture and cell size effects on shunt impedance of, (T), 20: 13358 (BNL-9944)
design for variable electron current with constant energy, 20: 13402(P)
design using multi-cavity speed-modulation oscillator, 20: 13389(P)
development and operation, 20: 13368(R) (UCRL-16511, pp 54-8)
development and research at Orsay, 20: 13364(R) (LAL-1148)
performance of high-frequency electron, evaluation of, 20: 13373
radiation monitoring and shielding studies, (E), 20: 13367 (UCRL-16445(Rev.))
tube design for, 20: 13403(P)
waveguides for, spatial harmonic coefficients of, (E), 20: 13369
LINOLEIC ACID
preparation of double-labeled cholesteryl esters of, method for, 20: 12913 (EUR-2446.f)
LIPIDS
radiation effects on fish, gamma, 20: 12618(R) (TID-22399)
LIQUID FLOW
magnetohydrodynamic, in spherical channels, (T), 20: 13642
LIQUID METAL COOLED REACTORS
boiler design for, 20: 14041(P)
cooling systems for 1000-Mw(e) fast power breeders, stress analysis of piping in, 20: 14120 (COO-1454-1)
cooling systems for, sodium oxide determination in, (E), 20: 14008(R) (ANL-7122, pp 42-69)
fuel burnup calculations for thermal sodium, 20: 14144 (PEL-77)
LITHIUM
circulation of molten, pump for, 20: 12948
determination in sodium loop transfer samples, methods for, 20: 12766 (GEAP-4178)
ionization in collisions with excited atoms, (T), 20: 13421(T)
separation from other inorganic ions by paper chromatography, 20: 12939
solvent properties for helium at 871°C, 20: 12827 (TID-21583)
LITHIUM BERYLLIUM FLUORIDES
crystal structure, 20: 12834
LITHIUM BROMIDES
ion association and hydration in aqueous solutions of, x-ray diffraction studies on, 20: 14228 (TID-22527)
LITHIUM CHLORIDES
ion association and hydration in aqueous solutions of, x-ray diffraction studies on, 20: 14228 (TID-22527)
LITHIUM COBALT LANTHANUM OXIDES
crystal structure, 20: 12865
LITHIUM FLUORIDES
neutron resonance absorption integral of, (E), 20: 14008(R) (ANL-7122, pp 42-69)
performance for x dosimetry, 20: 13057 (AD-627567)
radioinduced defects in crystals of, x, (E), 20: 13973(R) (NYO-3033-1)
reactions between uranium and uranium tetrafluoride in, mechanism and rate of, 20: 13170 (BM-RI-6736)
LiF–UO_2, radiation effects on, xenon fluoride production by neutron, 20: 12898
LITHIUM IODIDES
ion association and hydration in aqueous solutions of, x-ray diffraction studies on, 20: 14228 (TID-22527)
LITHIUM IONS
production of negative, in duoplasmatron ion source, 20: 13376
LITHIUM ISOTOPES Li-4
production of, (T), 20: 13834
LITHIUM ISOTOPES Li-5
production as intermediate in helium-3 (He-3,2p) reaction, (E), 20: 13900
LITHIUM ISOTOPES Li-6
neutron reactions (n,α) with, excitation functions for, (E), 20: 13741
photoneutron emission from, performance of detector for, 20: 13081
proton reactions (p,n) at 11.6 and 12.6 Mev, beryllium-6 excited states from, (E), 20: 13845
reactions (Li-6,α) with carbon-12 at 2 to 3 Mev, angular distributions from, (E), 20: 13846
reactions (Li-6,Li-7) with beryllium-9 at 3 to 3.75 Mev, lithium-7 and alpha spectra from, (E), 20: 13852
LITHIUM ISOTOPES Li-7
electron scattering at low energies, excitation in, (E/T), 20: 13782 (ORNL-P-1927)
emission from lithium-6 reactions (Li-6,Li-7) with beryllium-9 at 3 to 3.75 Mev, spectra of, (E), 20: 13852
proton reactions (p,n) at 1.90 to 3.00 Mev, neutron energies from, 20: 13747 (AECD/EP/7)
proton reactions (p,γ) at 0.4 to 2.4 Mev, beryllium-8 single-particle levels from, (E), 20: 13810
LITHIUM LANTHANUM NICKEL OXIDES
crystal structure, 20: 12865
LITHIUM SYSTEMS
H–Li, collision integrals and viscosity of weakly ionized plasma of, (E/T), 20: 13957
LIVER
radiation effects on DNA synthesis in rat, as function of time, 20: 12638 (TID-21474)
radiation effects on decarboxylase activity for aromatic amino acids and protein content in mouse, 20: 12782
radiotherapy of cancer of, using yttrium-90 microspheres, 20: 12738
LOOPS
design and operation of two-phase-flow, 20: 12962(R) (GEAP-4959)
design of high pressure boiling, for fuel element testing, 20: 14131 (KR-98)
development for sodium-water reaction tests, 20: 14024(R) (APDA-182)
LUMINESCENT MATERIALS
preparation of granular, 20: 12921(P)
LUNGS
cerium-144 deposition in rat, effects of carrier on, 20: 12615
radiotherapy of tumors of, 20: 12741
LUTETIUM
preparation of isotopic bulk materials and foils of, from oxide, 20: 13216 (ORNL-P-1899)
separation from other inorganic ions by paper chromatography, 20: 12939
LUTETIUM BORATES
crystal structure of vaterite-type, polymorphism in, 20: 12837
LUTETIUM COMPLEXES
with dilactic, mandelic, and quinic acids, formation and stability constants of, 20: 12817 (IS-1311)
LUTETIUM ISOTOPES
preparation of bulk materials and foils of, from oxide, 20: 13216 (ORNL-P-1899)
LUTETIUM ISOTOPES Lu-177
energy levels of, g factors for rotational, (T), 20: 13765 (CONF-233 (Vol.4), pp 723-5)
LUTETIUM OXIDES
BaO–Lu_2O_3, optical properties of compounds formed in, 20: 13278
Lu_2O_3–SrO, optical properties of compounds formed in, 20: 13278
LYMPH SYSTEM
node localization in, tracer method for, 20: 12751
radiation effects on growth of node cells of, in tissue culture, β, 20: 12682

M

MAGNESIUM
corrosion by chlorine trifluoride–urania reaction-gas mixtures, 20: 12925(R) (EURAEC-1446)
crystal structure of, effect of high pressure on, (E), 20: 13316
neutron diffraction at high pressures, 20: 14059(R) (IDO-17104)
preparation of isotopic bulk materials and foils of, from oxide, 20: 13216 (ORNL-P-1899)
separation from other inorganic ions by paper chromatography, 20: 12939
ultraviolet emission from electron-bombarded foils of, 20: 14004
MAGNESIUM ALLOYS
compatibility with carbon dioxide in gas-cooled reactors, 20: 13199
Cd–Mg, crystal structure of, effect of high pressure on, (E), 20: 13316
Cu–Mg, uranium distribution between liquid, and fused magnesium chloride, (E), 20: 14007(R) (ANL-7122, pp 1-41)
Mg–Ag, crystal structure of, effect of high pressure on, (E), 20: 13316
Mg–In, crystal structure of, effect of high pressure on, (E), 20: 13316
Mg–Mn, creep in, diffusion, 20: 13309
Mg–Sn, crystal structure of, effect of high pressure on, (E), 20: 13316
Mg–Sn, infrared reflectivity of, effects of temperature on, 20: 14227(R) (TID-22419)
Mg–Zn, analysis for ruthenium using 1-nitroso-2-naphthol, spectrophotometric, 20: 12788

MAGNESIUM CHLORIDES
uranium distribution between fused, and liquid copper–magnesium alloy, (E), 20: 14007(R) (ANL-7122, pp 1-41)
Al–Mg–$MgCl_2$–KCl–NaCl, corrosive effects on steels and tantalum at 500 to 800°C, (E), 20: 14007(R) (ANL-7122, pp 1-41)
Cu–Mg–$MgCl_2$–KCl–NaCl–U, chemical compatibility with vitreous carbon containers at 800°C, (E), 20: 14007(R) (ANL-7122, pp 1-41)
MAGNESIUM COMPLEXES
with [(1,2-dimethylethylene)dinitrilo]- and (propylenedinitrilo)-tetraacetic acids, stability of, 20: 12594(R) (NP-15679)
MAGNESIUM ISOTOPES
separation from isotopes of other elements, summary of, 20: 13345(R) (NP-15772)
MAGNESIUM ISOTOPES Mg-24
energy levels of, asymmetric-rotator model for rotational, (T), 20: 13849
helium-3 reactions (He-3,d) at 24.4 Mev, momentum spectra from, (E), 20: 13345(R) (NP-15772)
preparation of bulk materials and foils of, from oxide, 20: 13216 (ORNL-P-189)
MAGNESIUM ISOTOPES Mg-25
recoil from silicon-28 (n,α) reactions in silicon, ionization defects from, (E), 20: 13989
MAGNESIUM ISOTOPES Mg-26
deuteron reactions (d,pγ) at 4.28 Mev, angular correlations in, (E), 20: 13768 (CONF-650410-40)
MAGNESIUM ISOTOPES Mg-27
energy levels, 20: 13768 (CONF-650410-40)
MAGNESIUM OXIDES
effects on strontium-85 metabolism by rats, 20: 12606
electron absorption coefficients at 100 to 1200 kv, (E), 20: 13967
moisture control in agglomeration mixtures of, using neutron probe, 20: 13156
neutron resonance absorption integral of, (E), 20: 14008(R) (ANL-7122, pp 42-69)
thermal conductivity of powders of, at 100 to 850°C, 20: 12854
thermal conductivity of powders of, at 100 to 850°C, (T), 20: 12855
vaporization of, to 2300°C, 20: 13265(T) (AD-623208)
Cr_2O_3–MgO–O, phase studies on, 20: 13260(R) (NP-15852)
MAGNESIUM STRONTIUM COBALT LANTHANUM OXIDES
crystal structure, 20: 12865
MAGNESIUM SYSTEMS
Al–Mg–$MgCl_2$–KCl–NaCl, corrosive effects on steels and tantalum at 500 to 800°C, (E), 20: 14007(R) (ANL-7122, pp 1-41)
Al–Mg–Ni–Si, fatigue properties at 250 to 350°C, low-cycle, 20: 13308
Cu–Mg–$MgCl_2$–KCl–NaCl–U, chemical compatibility with vitreous carbon containers at 800°C, (E), 20: 14007(R) (ANL-7122, pp 1-41)
MAGNET COILS
heating effects on properties of superconducting, (E/T), 20: 13675
materials for superconducting, testing of, 20: 13666 (IPP-4/22)
MAGNETIC FIELDS
charged particle beam focusing in alternating-gradient, chromatic aberrations in, (T), 20: 13360 (CERN-65-42)
charged particle motion in, in magnetic analyzers, (T), 20: 13091
charged-particle motion in helical toroidal, nonlinear theory of fast, 20: 13371
development of nonadiabatic, for trapping thermonuclear plasma, (E/T), 20: 13925(R) (TID-22419, pp 99-147)
effects on excited gadolinium-155 γ–γ angular correlations, (E), 20: 13763 (CONF-233(Vol.4), pp 710-19)
effects on resonances of surface waves propagating along cylindrical plasma column, (T), 20: 13941
electron motion in Faraday-cup, secondary, (E), 20: 13382
induction in superconducting cylinders by rotation, 20: 13690
interactions with electrons, phonon production in, (E/T), 20: 13925(R) (TID-22419, pp 99-147)
measurement of multipole, (E/T), 20: 13365 (SLAC-39(Rev.))
plasma containment by dipole, (T), 20: 13928(T) (AD-625070)
plasma heating by h-f, resonant, (E), 20: 13946(T)
plasma stability in toroidal discharges, (T), 20: 13929(T) (NP-tr-1340)
production of closed minimum-B, (T), 20: 13930(T) (NP-tr-1343)
use in acoustic wave generation at microwave frequencies in dysprosium films, 20: 14003
MAGNETIC MIRROR MACHINES
gas pressure in, anisotropy of radial, (E), 20: 13907 (IPP-2/42)
plasma heating by electron beams, mirror ratio effect on, (E), 20: 13947(T)
plasma heating in, (E/T), 20: 13908 (IPP-2/44)
plasma instability in, nonlinear mechanics of, (T), 20: 13905 (CONF-651056-1)
MAGNETIC MIRRORS
shock wave propagation in, effects of, (E), 20: 13921(R) (NP-15703, pp 52-63)
MAGNETIC PROBES
use for plasma measurements in electric discharges, (E), 20: 13639 (JUL-281-PP)
MAGNETIC RESONANCE
spectral line broadening in EPR, effect of crystal lattice thermal oscillations on, (T), 20: 13976
MAGNETOHYDRODYNAMIC CELLS
design of a-c, 20: 13439(P)
design of a-c, 20: 13440(P)
design of a-c, 20: 13443(P)
development of Brayton cycle, (E), 20: 13432(R) (TID-22419, pp 149-76)
development of, C.N.E.N. program for, 20: 13431 (RT/FI(65)31)
feasibility for use in nuclear power plants, 20: 14132 (LA-3368)
flow velocity optimization in channel with argon–potassium oxide plasma, (T), 20: 13436
fluid flow in, variational analysis of, 20: 13437
performance of plasma-jet driven, (E), 20: 13435
plasma current distribution in linear Hall, (T), 20: 13428 (JAERI-1093)
properties of electrodeless, self-excitation, (T), 20: 13429 (N64-32348)
research on, CEA, 20: 13433
theory of electrodeless a-c, 20: 13430 (N64-32349)
MAGNETOHYDRODYNAMICS
channel flow velocity profiles and entry lengths, (T), 20: 13432(R) (TID-22419, pp 149-76)
fluid flow in channel in transverse electromagnetic fields, (T), 20: 13635 (ARL-63-175(Pt.3))
fluid flow in closed regions with axial symmetry, perturbational technique for, (T), 20: 13643
gas flow with tensor conductivity, two-dimensional, (T), 20: 13634 (AE-210)
magnetic flux interchange instabilities in, (T), 20: 13638 (IPP-6/39)
plasma dynamics in, model and numerical technique for, 20: 13960
thermodynamics of, with vapor-fluid injector, (T), 20: 13438
MAGNETOMETERS
design and performance of helium, for low temperatures, 20: 13046
MAGNETOSPHERE
electromagnetic and hydromagnetic waves in, properties of, 20: 13645 (AWRE-O-9/66)
MAGNETS
design and performance of septum, for fast and slow particle ejection from CERN proton synchrotron, 20: 13359 (CERN-65-36)
design of betatron, 20: 13392(P)
design of superconducting, 20: 13667 (JINR-P-2533)
development for Stanford Linear Accelerator, 20: 13366(R) (SLAC-53)
field measurements in multipole, (E/T), 20: 13365 (SLAC-39(Rev.))
MAGNOX ALLOYS
creep deformation of AL 80, grain boundary migration in, 20: 13311
MAIZE
effects of gases at 3 to 45°C on seed of, biological, 20: 14216 (BNL-9859)
radiation effects on genetic variability in, 20: 12641 (TID-22582)
MALEIC ACID
effects on radiosensitivity of fruit-spoilage fungi, 20: 13137 (NP-15360)
MALEIMIDE, *N*-ETHYL-
effects on radiosensitivity of fruit-spoilage fungi, 20: 13137 (NP-15360)
MAMMALS
cesium-137 content in Alaskan caribou, 20: 12983
radiation effects on, gamma, 20: 12667
radiation injuries of testis of, delayed, 20: 12686
MAN
cesium-137 content in Alaskan, 20: 12983
cesium-137 uptake by, from reindeer, 20: 12578
chromium-51 metabolism and fecal excretion by, after oral administration, 20: 12612
genetic factors in, identification of, 20: 12565
radiation dose to gonads in, from benign tumor therapy during childhood, 20: 13013
radiation dose to, from contaminated foods, 20: 13000(R) (EUR-2520.i)
radiation effects on, 20: 12699
radiation effects on respiratory center of, x, 20: 12702
radiation effects on, leukemogenic, 20: 12707
radiation effects on, review, 20: 12708
radiation effects on growth of children of Marshall Islands exposed to fallout in 1954, 20: 13011
radiation exposure of, living in areas of high natural radioactivity, 20: 12988
radioactivity in foods of, factors affecting, 20: 12979 (EUR-2287.d)
radioinduced aging in, 20: 12644
scandium-47 metabolism and fecal administration by, after oral administration, 20: 12612
MANDELIC ACID
complexes with lanthanum, rare earths, and yttrium, formation and

stability constants of, 20: 12817 (IS-1311)

MANGANESE
determination in deep-sea nodules and sediments, activation, 20: 12976
determination in potassium chloride and sodium chloride single crystals, activation, 20: 12805
determination in sodium loop transfer samples, methods for, 20: 12766 (GEAP-4178)
magnetic susceptibility of, pressure effects on, (E), 20: 13312(T)
radiosterilization effects on content of, in strawberries, gamma, 20: 13143(R) (UCD-34P80-3, pp 55-7)
separation from other inorganic ions by paper chromatography, 20: 12939

MANGANESE ALLOYS
Mg–Mn, creep in, diffusion, 20: 13309

MANGANESE COMPLEXES
with hexamethylphosphoramide, NMR contact shifts in, 20: 12828 (TID-21587)

MANGANESE ISOTOPES Mn-54
content in Po Valley rice, effects of crop irrigation on, 20: 12986
determination in mass transfer samples, methods for, 20: 12766 (GEAP-4178)
uptake by plants in Georgia piedmont, 20: 12985

MANGANESE ISOTOPES Mn-55
proton reactions (p,n) at 14.2 Mev, angular distributions, Q values, and spectra from, 20: 13345(R) (NP-15772)

MANGANESE OXIDES
magnetic structure of, long-range, (E), 20: 13993
neutron resonance absorption integral of, (E), 20: 14008(R) (ANL-7122, pp 42-69)

MANGANESE STEEL
properties of low-carbon, 20: 13186 (TRG-Report-840)

MANGANESE STRONTIUM LANTHANUM OXIDES
crystal structure, 20: 12865

MANOMETERS
design and fabrication of, using plutonium-240 source, 20: 13045

MARITIME REACTORS
development in France, 20: 14176

MARSHALL ISLANDS
radiation effects on growth of children of, 1954 fallout, 20: 13011

MASERS
measurements using two-cavity, 20: 14227(R) (TID-22419)

MASERS (OPTICAL)
beam effects on nucleation in freon bubble chambers, 20: 13084
effects on plasma resonance in argon and nitrogen, (E/T), 20: 13942
radiation from, Thompson-scattering by particle beams, (E/T), 20: 13925(R) (TID-22419, pp 99-147)
use in interferometric measurement of plasma electron densities, (E), 20: 13923(R) (TID-22419, pp 77-84)

MASS SPECTROMETERS
ion converter detector with gate connections for, 20: 13047
ion source design for, 20: 13051(P)
ion sources for, design of cold-cathode electron-collision, 20: 13053(P)

MATERIALS TESTING
data recording system for in-pile fatigue testing, 20: 14059(R) (IDO-17104)
fracture toughness of metals, double cantilever beam specimen for, 20: 12972 (BNWL-168)
method for measuring hardness of a fast-traveling metallic workpiece, radiation-reflection, 20: 13054(P)
nondestructive methods used at NRTS, 20: 14197
nondestructive, conference on, 20: 14017 (STI/PUB/105(Vol.2))

MATERIALS TESTING REACTOR
fuel element testing for, 20: 14059(R) (IDO-17104)
fuel elements of, ultrasonic water-gap measurements in, 20: 14195

MATHEMATICS
book: *Lectures on Lie Group Theory*, 20: 13169
Minkowski spaces in, relation between isobaric and, 20: 13615
operators in, formalism of multiplicative, 20: 13165 (JINR-E-2542)
series expansion of determinants and solution of secular equation, 20: 13168

MATTER
meson (μ) and (π) absorption and interactions in, (T), 20: 13350
particle and quanta scattering by, transport equation solution for anisotropic multiple, (T), 20: 13968

MEATS
radiation processing of canned chopped ham, effects on viability of spores of *Clostridium botulinum*, 20: 13134 (AD-625252)

MECHANICS
variational principles in classical, generalized, 20: 13351

MEDICAL PERSONNEL
radiation dose to gonads of, from therapy of benign tumors in children, 20: 13013
radiation monitoring of x-ray technicians, 20: 12999 (CEA-R-2746)
radiation protection of, during heart radiography, 20: 12757

MEDICINE
bibliography on nuclear, 20: 12733 (AED-C-10-04)

MEIOSIS
effects on intragenic recombination in maize, 20: 12678
radiation effects on, in mealy bugs, 20: 12715

MELAMINE, TRIETHYLENE-
effects on tumor-bearing mice, effects of radioprotective drugs on, 20: 12719(R) (NP-15668)

MEMBRANES
permeability to chloride and rubidium ions, effects of urea on fruit and leaf cuticular, 20: 14218 (COO-888-44)

MEMORY DEVICES
theory of superconductive, vortex, 20: 13689

MENDELEVIUM ISOTOPES
production in fluorine-19 reactions (F-19,xn) with uranium-238, cross sections for, (E), 20: 13889

MERCAPTO GROUP
radiation effects on, in sea urchin eggs, thermal and uv, 20: 12624

MERCURY
density at 234 to 1733°K, 20: 12825 (NYO-2082-1)
effects on photosensitized decomposition of cyclobutane, 20: 12884(R) (RRL-2310-171)
electric currents in cylinders of, stability of persistent, 20: 13691
electron-beam instability in low-pressure plasma of, counter-streaming, (E), 20: 13951
magnetic field enhancement in superconducting tubes of, empirical formula for, (E/T), 20: 13678
performance in electron-bombardment ion engines, 20: 12975
properties at 234 to 1733°K, volumetric, 20: 12825 (NYO-2082-1)
separation from other inorganic ions by paper chromatography, 20: 12939
technetium electrodeposition in, 20: 12809
thermal capacity at 0.35 to 4.2°K, 20: 13692
volatility of, in radioactive alumina calcine during high-temperature storage, 20: 14207 (IDO-14670)

MERCURY ISOTOPES Hg-199
neutron capture by, analysis of γ-γ cascades from, (E), 20: 13062 (IEA-96)

MERCURY ISOTOPES Hg-200
production in neutron capture by mercury-199, γ-γ cascades from, (E), 20: 13062 (IEA-96)

MESIC MOLECULES
energy levels of d-μ-d and p-μ-p, (T), 20: 13630

MESONS
coupling of pseudoscalar triplet with nucleons, 20: 13611
decay of vector, into lepton pairs, (T), 20: 13476(T)
decay of 1^+, unitary symmetry for radiative, (T), 20: 13541 (JINR-P-2419)
electromagnetic properties of, nonrelativistic quark model for, (T), 20: 13544 (JINR-P-2509)
interactions of pseudoscalar, with baryons, isobar parity in, (T), 20: 13474(T)
interactions of vector, with nucleons, (T), 20: 13479(T)
interactions of vector and scalar, coupling-constant relations for, 20: 13486
interactions of, relativistic Green's functions from strong coupling of, 20: 13557
interactions with nucleons, scattering matrix for, (T), 20: 13448 (JINR-E-2521)
interactions with nucleons at high energies, elementary-particle structure from backward-scattering, 20: 13510
interactions with baryons, models for, 20: 13602
mass formulas in supermultiplet model for, 20: 13583
model of, spinor, 20: 13612
structure of, effects in high-energy interactions, 20: 13514
structure of, SU(3) triplet model for SU(6), 20: 13598
symmetry for, propagator in, (T), 20: 13543 (JINR-P-2474)

MESONS, RESONANCE
production in meson ($\pi^\pm$)-proton interactions at 3.65 and 3.70 Bev/c, (E), 20: 13456 (UCRL-16170)
production in meson (K^-)-proton interactions at 700 to 1400 Mev/c, (T), 20: 13460 (UCRL-16274)
production of K^*, in meson (K^+)-proton interactions at 0.86 to 1.58 Bev/c, (E), 20: 13462 (UCRL-16370)
production of ω_{ABC}, in proton-deuteron reactions, 20: 13528

MESONS (η)
photoproduction on nucleons, (T), 20: 13479(T)
production in meson (π^-)-proton interactions at 592 to 1300 Mev, cross sections for, (E/T), 20: 13457 (UCRL-16195)

MESONS (η')
spin, (E/T), 20: 13522

MESONS (K)
decay of, negative CP-parity of 2π, (T), 20: 13473(T)
interactions with mesons (π), cross section determination for, (T),

20: 13449 (JINR-P-2433)
MESONS (K^-)
interactions in nuclear emulsion, correlations of meson (π) production and decay chains in, (E), 20: 13487
interactions with protons at 700 to 1400 Mev/c, differential cross sections for elastic, (E), 20: 13460 (UCRL-16274)
interactions with protons, research on, (E), 20: 13463(R) (UCRL-16511, pp 1-53)
interactions with protons at 1.15 Bev/c, Y_1^* production in, (E), 20: 13518
interactions with neutrons and protons at 600 to 850 Mev/c, hyperon (Λ)-meson (π) resonances in, (E), 20: 13522
MESONS (K^0)
decay modes of K_2^0, (E), 20: 13450 (JINR-P-2488)
decay of K_2^0, cosmological and gravitational theories for, 20: 13507
decay of, CP invariance in 2π, (E), 20: 13495
decay of, CP violation amplitude from time-dependent interference effects in 2π, (E), 20: 13496
decay of, CP violation in leptonic, (T), 20: 13515
decay of, degenerate SU(4) symmetry for CP violation in 2π, 20: 13625
decay of, modified V-A interaction and CP invariance for 2π, 20: 13597
mass difference of K_1^0 and K_2^0, 20: 13495
MESONS (K^+)
decay chains involving mesons (π), directional correlations in, (E), 20: 13487
decay of, upper limits for spin-1 particle production in, (E), 20: 13497
interactions with protons at 0.86 to 1.58 Bev/c, K* and N* resonance production in, (E), 20: 13462 (UCRL-16370)
MESONS ($K^+_{\mu 3}$)
decay of, axial-vector current in, (T), 20: 13508
MESONS ($K^-_{\mu 3}$)
decay of, meson (μ) energy spectrum and form factors for, (E), 20: 13521
MESONS ($K^+_{\mu 3}$)
decay of, form factors and branching ratios for, (E), 20: 13459 (UCRL-16253)
MESONS ($K^0_{e_3}$)
decay of, modified V-A interaction and CP invariance for, 20: 13597
MESONS (μ)
absorption and interactions in matter, (T), 20: 13350
capture by nuclei, G-parity violation in, (T), 20: 13877
energy from meson ($K^-_{\mu 3}$) decay, (E), 20: 13521
interactions with electrons, cross section for, (T), 20: 13484
mass relative to electrons, calculation using perturbation theory, 20: 13628
polarization in neutrino-induced reactions as test for time reversal violation, (T), 20: 13835
scattering by bromotrifluoromethane and propane, cross sections for, (T), 20: 13480
scattering in nuclear emulsions at 5 Bev/c, inelastic, (E), 20: 13526
MESONS (μ^-)
capture in liquid hydrogen, G-parity in rates of, (T), 20: 13505
interactions with protons, G-parity in rates of capture, (T), 20: 13505
interactions with protons, calculations using six coupling constants, 20: 13519
interactions with deuterons and protons, quantum mechanics of, 20: 13630
MESONS (μ^+)
stopping in solids, depolarization and quenching in, (E), 20: 13498
MESONS (ω)
decay of, current algebras for, (T), 20: 13491
decay of, leptonic, (T), 20: 13476(T)
MESONS (ϕ)
decay of, leptonic, (T), 20: 13476(T)
mass of, calculation of, 20: 13628
MESONS (π)
absorption and interactions in matter, (T), 20: 13350
electromagnetic structure of, (T), 20: 13878
exchange in antiproton-proton interactions at 3.0 to 3.6 Bev/c, (T), 20: 13494
interactions with electrons, cross section for, (T), 20: 13484
interactions with mesons (K) and (π), cross section determination for, (T), 20: 13449 (JINR-P-2433)
interactions with mesons (π), two channel generation of mesons (ρ) in amplitude for, (T), 20: 13483
interactions with nucleons in Bev range, partial-wave analysis of, (T) 20: 13513
interactions with nucleons up to 500 Mev, quasipotential method for, (T), 20: 13467
interactions with nucleons, phase-space volumes for, (T), 20: 13481
interactions with nucleons, scattering matrix for, (T), 20: 13448 (JINR-E-2521)
interactions with protons, energy dependence of real part of amplitude of, (T), 20: 13503
interactions with protons, sum rule for amplitudes of, (T), 20: 13571
interactions with protons, optical model amplitudes for, 20: 13601
interactions with protons at 450 Mev, (E), 20: 13524
phase space integrals for, high-energy behavior of sum of, 20: 13574
photoproduction on nucleons, yup interactios in, (T), 20: 13477(T)
production from meson (K^-) and (K^+) interactions in nuclear emulsions, correlations in, (E), 20: 13487
production in deuteron-proton interactions, cross sections for, (T), 20: 13528
production in meson (π)-proton interactions at 450 Mev, (E), 20: 13524
production in meson (μ) inelastic scattering in nuclear emulsions, (E), 20: 13526
production in meson (π^-)-proton interactions at 350 to 800 Mev, (E), 20: 13527
production in Y_1^* decay, (E), 20: 13518
scattering by bromotrifluoromethane and propane, cross sections for, (T), 20: 13480
scattering on nuclei, electromagnetic form factor from elastic, (T), 20: 13878
MESONS (π^-)
interactions with protons at 3.70 Bev/c, resonance production in, (E), 20: 13456 (UCRL-16170)
interactions with protons at 592 to 1300 Mev, cross sections for, (E/T), 20: 13457 (UCRL-16195)
interactions with protons at 500 to 1300 Mev, charge exchange in, (E), 20: 13458 (UCRL-16209)
interactions with protons at high energies, N* (1920) production in, (T), 20: 13454 (UCRL-14100-T(Rev.1))
interactions with nucleons, phase-shift analysis and spin-flip dispersion relations for, (T), 20: 13492
interactions with protons at 2.01 to 4.95 Bev/c, cross sections and forward dispersion calculations for, (E), 20: 13523
interactions with protons at 1.03 Bev/c, forward differential cross section for elastic, (E), 20: 13525
interactions with protons at 350 to 800 Mev, (E), 20: 13527
interactions with protons, Fubini-Furlan theory for, (T), 20: 13537 (IC/66/8)
mass, (E), 20: 13461 (UCRL-16365)
production in neutron-proton interactions at 600 Mev, (E), 20: 13453 (JINR-P-2511)
reactions (π^-,2N) with nuclei, momentum distribution from, (T), 20: 13874
reactions (π^-,2N) with carbon-12, momentum distribution from, (T), 20: 13874
reactions (π^-,nπ) and (π^-,n) with helium-4, nucleon correlations in, (T), 20: 13884
reactions with emulsion nuclei at 17.2 Bev/c, cross section for, (E), 20: 13893
MESONS (π^0)
photoproduction from hydrogen, polarization of, (E), 20: 13345(R) (NP-15772)
photoproduction on nucleons, (T), 20: 13479(T)
photoproduction on deuterium at 500 to 700 Mev, (E), 20: 13345(R) (NP-15772)
production by electron-proton interactions, (E), 20: 13345(R) (NP-15772)
MESONS (π^+)
decay of, axial-vector current in leptonic, (T), 20: 13508
interactions with protons at 3.65 Bev/c, resonance production in, (E), 20: 13456 (UCRL-16170)
interactions with protons at 4.10 and 4.85 Bev/c, elastic, (E), 20: 13471(T)
interactions with nucleons, phase-shift analysis and spin-flip dispersion relations for, (T), 20: 13492
interactions with protons, Fubini-Furlan theory for, (T), 20: 13537 (IC/66/8)
production in helium-3 (γ,π^+) reactions, cross sections for, (E), 20: 13896
production in neutron-proton interactions at 600 Mev, (E), 20: 13453 (JINR-P-2511)
production in proton-proton interactions at 655 Mev, cross sections for, (T), 20: 13470
MESONS (ρ)
decay of, radiative, (T), 20: 13477(T)
mass of, calculation of, 20: 13628
production by one- and two-particle exchange forces, two-channel, (T), 20: 13483
MESONS (ρ^+)
decay of, leptonic, (T), 20: 13476(T)
METABOLIC DISEASES
radioinduced pituitary ablation for treatment of acromegaly, 20: 12748
therapy of acromegaly, use of radioinduced pituitary ablation in, 20: 12753
METABOLISM

effects on radiosensitivity of rats, 20: 12703
measurement in isopods, comparison of methods for, 20: 12610
METALLIC FILMS
design and performance of thin superconducting cryotron, 20: 13048
superconducting critical fields in thin, angular dependence of upper, (T), 20: 13681
METALLIC FOILS
use as window for electric discharge device, 20: 13052(P)
METALLURGY
research programs in, summaries of USAEC, 20: 13182 (TID-4005(Pt.1, 9th Ed.))
METALS
charged-particle reactions with, transition radiation from relativistic, (E/T), 20: 13788(T) (ORNL-tr-1062)
electron work function for, a-c method for measuring, 20: 13025 (IPP-2/37)
fracture toughness of, double cantilever beam testing method for, 20: 12972 (BNWL-168)
hardness of moving, radiation-reflection method for determination of, 20: 13054(P)
level indicators for liquid, testing ultrasonic, 20: 13031(R) (NYO-2910-13)
research and development programs on, opportunities, roadblocks, and problems in, 20: 13185 (TID-22424)
METASTASES
localization of pelvic, of genital cancers, tracer method for, 20: 12751
METEORITES
age estimation of, by strontium–rubidium method, 20: 12992
lead isotope ratios in, age estimation from, 20: 12991
METEOROLOGY
effects on cesium-137 uptake by Alaskan animals and natives, 20: 12983
METHACRYLIC ACID, METHYL ESTER POLYMERS
electron penetration depths, at 631 kev to 13.8 Mev, LET variations with, 20: 13969
neutron resonance absorption integral of, (E), 20: 14008(R) (ANL-7122, pp 42-69)
METHANE
pyrolysis for carbon deposition on uranium carbide particles, 20: 13215(R) (ORNL-3885, pp 3-86)
separation of normal and deuterated, by gas chromatography, 20: 12930
yields from gas-phase radiolysis of cyclobutane, 20: 12894
METHANE, BROMO-
yields in radioinduced oxidation of isobutane using hydrobromic acid catalyst, 20: 12883 (ORO-634)
METHANE, BROMODIFLUORO-
meson (μ) and (π) scattering cross sections of, (T), 20: 13480
METHANE, CHLORODIFLUORO-
heat transfer and void formation in two-phase flow of, 20: 12962(R) (GEAP-4959)
METHANE, IODO-
nuclear magnetic resonance spin-lattice relaxation times in, deuteron and proton, 20: 12839
METHANOL
nuclear magnetic resonance spin-lattice relaxation times in, deuteron and proton, 20: 12839
synthesis from carbon dioxide and moisture in air using mobile nuclear power system, 20: 12877 (BNL-955)
benzene–methanol, radiation effects on, at 77°K, ESR and tracer studies of x, 20: 12890
METHYL SULFOXIDE
nuclear magnetic resonance spin-lattice relaxation times in, deuteron and proton, 20: 12839
METHYLAMINE
n-hexane–methylamine, vapor pressure of, deuterium isotope effects on, 20: 12879
METROLOGY
apparatus functions for low-accuracy measurements, unfolding of, (T), 20: 13038
resolution corrections in, error propagation in, (T), 20: 13040
response relations in, minimum bias designs for exponential, (T), 20: 13167 (ORNL-3873)
theory for quantum, 20: 13664
MICA
performance of sandwiches of, for fission fragment track registration, 20: 13099
preparation of sandwiches of, for registering fission events, 20: 13099
MICE
effects of radiomimetic substances on tumor-bearing, effects of drugs on, 20: 12717(R) (NP-15666)
effects of radiomimetic agents on tumor-bearing, effects of radioprotective drugs on, 20: 12718(R) (NP-15667)
effects of radiomimetic agents on tumors in, effects of drugs on, 20: 12719(R) (NP-15668)
erythropoiesis and lymphocytopoiesis in, role of splenic reticular cells in, 20: 12681
radiation effects on, protective effects of bone marrow therapy against, 20: 12720(R) (TID-22466)
radiation effects on wound healing time in, x, 20: 12684
radiation effects on etiology of bacteremia in, 20: 12704
radiation effects on cell survival in sarcomas of, effects of oxygen inhalation on x, 20: 12725
radiation effects on antibodies in, gamma, 20: 12631 (CEA-R-2776)
radiation effects on developing embryos of, x, 20: 12650
radiation effects on developing fetuses of, pathological x, 20: 12650
radiation effects on immune reactions to allogenic skin grafts, effects of isogenic grafts on, 20: 12656
radiation effects on chromosomes in Perognathus, chronic-exposure, 20: 12666
radiation effects on spleen in, cytological, x, 20: 12681
radiation effects on developing fetuses of, pathological neutron and x, 20: 12683
radiation effects on, review on recovery from, 20: 12631 (CEA-R-2776)
radiation effects on decarboxylase activity for aromatic amino acids and protein content of liver of, 20: 12782
radiation effects on, role of bone marrow cells in immune reactions in, 20: 12716 (AD-626682)
radioinduced leukemia in, effects of hematopoietic tissue transplants on incidence of, 20: 12647
radioinduced pituitary tumors in, after iodine-131-thyroidectomy, effects of chlorpromazine on, 20: 12657
radiosensitivity of, effects of drug stimulation of central nervous system on x, 20: 12685
radiosensitivity of placenta of, x, 20: 12650
MICROWAVE EQUIPMENT
development for Stanford Linear Accelerator, 20: 13366(R) (SLAC-53)
electromagnetic-wave propagation in waveguides, (E/T), 20: 13370
electron beam interactions with plasma-filled waveguides, 20: 13925(R) (TID-22419, pp 99-147)
use of diaphragmed waveguides, as deflector of h-f separator, 20: 13362 (JINR-P-2503)
MICROWAVE SPECTROSCOPY
research programs on, 20: 14227(R) (TID-22419)
MICROWAVES
emission by plasma at electron cyclotron frequency harmonics, (T), 20: 13903 (CLM-R51)
interactions with plasma, helical instability from, (E/T), 20: 13959
propagation in diaphragmed waveguides, complex constants for, (T), 20: 13363 (JINR-P-2507)
MILK
cesium-137 content in cow and human, 1959 to 1961, 20: 13012
decontamination by electrodialysis, pilot plant study of, 20: 12997 (AD-626210)
strontium-90 content in cow and human, 1959 to 1961, 20: 13012
MINKS
histology of ear of normal and congenitally deaf white, 20: 14214 (BNL-8564)
MITOCHONDRIA
radiation effects on mouse spleen, x, 20: 12681
MITOMYCINS
effects on tumor-bearing mice, effects of radioprotective drugs on, 20: 12719(R) (NP-15668)
MITOSIS
activity in mouse tissue cultures, effects of x-irradiated feeder layers on, 20: 12654
effects of MEA on, in tumor cells, 20: 12680
MOLECULAR BEAMS
scattering of, computer program for calculating classical deflection function for, 20: 13415 (ORNL-3881)
MOLECULAR WEIGHTS
determination in polyglucin, 20: 12722(T) (JPRS-33766)
MOLTEN SALT REACTOR EXPERIMENT
fuel circulation in, pump design for, 20: 14164
MOLTEN SALT REACTORS
fuel cycle for, evaluation of thorium, 20: 14126 (JUL-276-RG)
fuel processing for breeder-type, flowsheet for, 20: 12928(R) (ORNL-3868)
heat transfer and power density in MOSEL, (T), 20: 14128 (JUL-296-RG)
neutron cross sections for MOSEL, tabulations of, 20: 14062 (JUL-214-RG)
neutron spectra in power-breeder, 20: 14127 (JUL-291-RG)
neutron spectra in power-breeder, using beryllium fluoride and sodium fluoride, 20: 14129 (JUL-315-RG)
MOLYBDENUM
argon-ion reactions with, nuclear temperature from, (E), 20: 13885
compatibility with cesium at 550°C, 20: 13203
creep mechanisms in, 20: 13249(R) (GEMP-55A, pp 29-53)

creep rupture at 1600°C, effects of annealing at 1600 to 2400°C on, 20: 13249(R) (GEMP-55A, pp 29-53)
crystallization of, during soldering and welding, 20: 13267(T) (AD-624909)
determination in sodium loop transfer samples, methods for, 20: 12766 (GEAP-4178)
deuteron inelastic scattering at 15 Mev, energy spectra from, (E), 20: 13872
effects on colorimetric determination of vanadium in uranium compounds, 20: 12802
effects on crystal structure of alpha-iron, 20: 13317
electron secondary emission from thin foils of, (E), 20: 13103
etch-pit studies of arc-cast, 20: 13249(R) (GEMP-55A, pp 29-53)
neutron cross sections for, 20: 14062 (JUL-214-RG)
separation from acid solutions by extraction using amine–ether in hydrocarbon diluent, 20: 12941(P)
separation from niobium by solvent extraction using tetra-n-butyl-ammonium bromide, 20: 12933
separation from other inorganic ions by paper chromatography, 20: 12939
solubility in alpha-iron at 600 to 900°C, 20: 13317
vapor pressure of, design of thermobalance for measuring, 20: 13029 (LA-3423)
welding of, effects of purification treatments on, 20: 13251(R) (GEMP-55A, pp 57-82)

MOLYBDENUM ALLOYS
Mo–Re, electric and thermal conductivity of superconducting, critical field measurements from, (E), 20: 13686
Mo–Re–W, fabrication process development, 20: 13251(R) (GEMP-55A, pp 57-82)
Mo–Re–W, phase diagrams for transmutation studies, electron-concentration, 20: 13251(R) (GEMP-55A, pp 57-82)
Mo–Re–W, weld integrity of, effects of carbon and oxygen on, 20: 13251(R) (GEMP-55A, pp 57-82)
Mo–Ti–V, development of refractory, for use in oxygen-contaminated sodium systems, (E), 20: 14007(R) (ANL-7122, pp 1-41)
Mo–Ti–Zr, compatibility of TZM, with niobium–1 zirconium alloy in refluxing potassium at 2000°F, 20: 13192(R) (NASA-CR-54843)
Mo–U, mechanical properties for use in prompt-burst reactor, 20: 13287

MOLYBDENUM FLUORIDES
corrosive effects on nickel and nickel alloys at 500°C, (E), 20: 14008(R) (ANL-7122, pp 42-69)

MOLYBDENUM ISOTOPES Mo-92
alpha reactions (α,n) with, conversion electron spectra from, (E), 20: 13881

MOLYBDENUM ISOTOPES Mo-98
alpha reactions (α,n) with, conversion electron spectra from, (E), 20: 13881

MOLYBDENUM OXIDES
oxidation of, mechanism of, 20: 13198

MOLYBDENUM SILICIDES
oxidation at 1500 to 1800°C, kinetics of, 20: 13195
oxidation kinetics of, in air at 500 to 1000°C, 20: 13198

MOLYBDENUM STEEL
Cr–Mo, properties, 20: 13186 (TRG-Report-840)

MONAZITES
radioactivity of foods grown on Brazilian, 20: 12988

MONTANA
strontium-86 to strontium-87 ratios in carbonate veins and vein-dikes in Rocky Boy Stock, 20: 12980

MONTANA (RAVALLI CO.)
strontium-86 to strontium-87 ratios in carbonate veins and vein-dikes in, 20: 12980

MONTE CARLO METHOD
calculation of neutron reflection from concrete slab, 20: 13742
use in neutron well logging calculations, 20: 12994

MONTMORILLONITES
sorptive properties for cesium, 20: 12873

MOSQUITOES
radiation effects on populations of *Aedes aegypti*, x, 20: 12668

MÖSSBAUER EFFECT
properties of, bibliography on, 20: 13974 (STI/PUB/21/16)

MOTORS
design of pneumatic-nutator, for actuating reactor control drums, (E), 20: 14029 (NASA-CR-54788)

MOUTH
radiotherapy of cancer of, effects on recovery from subsequent surgery of, 20: 12653

MUCOSA
radiation and/or thermal trauma effects on intestinal, in rats, 20: 12630 (BNL-8383)
radiation effects on intestinal, after uterine cancer therapy, gamma, 20: 12700

MULLITES
vaporization of, to 2300°C, 20: 13265(T) (AD-623208)

MULTIPLICATION FACTOR
determination of, modulated and pulsed experiments for, (T), 20: 13723
determination using pulsed neutron source methods, (T), 20: 14075

MUONIUM
formation in solids, from meson (μ^+) stopping, (E/T), 20: 13498

MUSCLES
cesium-137 content in deer, factors affecting, 20: 12984

MUTAGENS
reactions to chemical, 20: 12564

MUTATIONS
radiation effects on, in *D. melanogaster* gonads, 20: 12637 (TID-21466)
radiation effects on frequency of, in inseminated and virgin Drosophila females, x, 20: 12663
radioinduced barley, x, 20: 12714
radioinduced chromosomal, effects of hypothermia in mice on x, 20: 12693
radioinduced eye color, in male progeny of irradiated Dahlbominus females, γ, 20: 12691
radioinduced in male *D. melanogaster* germ cells, effects of age on, 20: 12636 (TID-21459)
radioinduced in maize, x, 20: 12678
radioinduced in *Phaseolus vulgaris*, γ, 20: 12709
radioinduced in *Phaseolus vulgaris*, γ, 20: 12710
radioinduced in Saccharomyces, genetic analysis of, 20: 12655
radioinduced in Ustilago, uv, 20: 12694
radioinduced in wheat, classification of chlorophyll, 20: 12632(R) (EUR-2546.f)
radioinduced silkworm, frequency of β and γ, 20: 12692

N

NAGASAKI
radioinduced aging in, hexosamine-collgen ratio for detecting, 20: 12644

NAPHTHALENE, 1,2,3,4-TETRAHYDRO-
radiolysis of, mass-spectrometric studies of ion-molecule reactions in, 20: 12901

NAPHTHALENE-2,7-DISULFONIC ACID, 4,5-DIHYDROXY-3-[(*p*-SULFOPHENYL)AZO]-
uses for spectrometric determination of rare earths, 20: 12806

NAPHTHOL
effects on radiosensitivity of fruit-spoilage fungi, 20: 13137 (NP-15360)

1-NAPHTHOL, 4-AMINO-
effects on radiosensitivity of fruit-spoilage fungi, 20: 13137 (NP-15360)

2-NAPHTHOL, 1-NITROSO-
analytical use for spectrophotometric determination of ruthenium, 20: 12788

1-NAPHTHYLAMINE
effects on radiosensitivity of fruit-spoilage fungi, 20: 13137 (NP-15360)

NATIONAL REACTOR TESTING STATION
operation of, role of nondestructive testing in, 20: 14197

NAVAL REACTORS
development in France, 20: 14176

NEODYMIUM
determination in glass, emission spectrographic, 20: 12810
solvent properties for tantalum, 20: 13180(R) (IS-RD-4)
spectra of, isotope-displacement effect on arc, (E/T), 20: 13418

NEODYMIUM CHLORIDES
thermal capacity of aqueous solutions of, at 25°C, 20: 12818 (IS-T-52)

NEODYMIUM COMPLEXES
with dilactic, mandelic, and quinic acids, formation and stability constants of, 20: 12817 (IS-1311)

NEODYMIUM ISOTOPES Nd-141
production from neutron reactions (n,2n) with neodymium 142 at 14.7 Mev, 20: 13864

NEODYMIUM ISOTOPES Nd-142
neutron reactions (n,2n) at 14.7 Mev, neodymium-141 production from, (E), 20: 13864
neutron reactions (n,α) and (n,2n) at 14.7 Mev, cross sections for, (E), 20: 13864

NEODYMIUM ISOTOPES Nd-149
decay, 20: 14059(R) (IDO-17104)

NEODYMIUM OXALATES
thermal decomposition in air and carbon dioxide at 30 to 1100°C, 20: 12862

NEODYMIUM OXIDES
crystal lattice transformations at high temperature, (E), 20: 13979
Nd_2O_3–ReO_2, preparation and ferromagnetic properties of phases in, 20: 13260(R) (NP-15852)
Nd_2O_3–ZrO_2, phase studies, 20: 13283

NEON
ionization by fission fragments, plasma production in, (E/T), 20: 13939
spectra of hydrobromic, hydrochloric, and hydriodic acids in, deuterium effects on, 20: 12857
NEON IONS
production and acceleration of beams of, 20: 13804
reactions with titanium, nuclear temperature from, (E), 20: 13885
sputtering on gold at 40 to 100 ev, yields from, (E/T), 20: 13420
NEON ISOTOPES Ne-22
reactions (Ne-22,xn) with uranium-238, cross sections for, (E), 20: 13889
NEON ISOTOPES Ne-23
energy levels of, parity and spin of, (E/T), 20: 13773 (IKF-13)
NEON SYSTEMS
Ar–Ne, plasma production by fission-fragment ionization of, (E/T), 20: 13939
NEPTUNIUM
separation from aluminum alloyed fuels during chemical processing, flowsheets for, 20: 12926 (IDO-14669)
NEPTUNIUM ISOTOPES Np-237
neutron fission rates of, fast, (E), 20: 14202
NERVOUS SYSTEM
radiation effects on human respiratory center, x, 20: 12702
radiosensitivity effects of drug stimulation of, in mice, 20: 12685
NEUTRINOS
emission from stellar plasmas, mechanism of, 20: 13519
interactions of, intermediate vector boson production in, (T), 20: 13464
interactions with neutrons, mass of intermediate bosons from, (T), 20: 13504
reactions (ν,μ^-) with nuclei, test for time reversal violation in, (T), 20: 13835
NEUTRINOS (ν_μ)
mass, (E), 20: 13461 (UCRL-16365)
NEUTRON BEAMS
design of, having sinusoidally modulated intensity, (E), 20: 13704(R) (MIT-2344-4, pp 101-5)
production and analysis of 2.4-Mev, (E), 20: 13088
production of pulsed, design of generator for, 20: 13745(P)
NEUTRON CROSS SECTIONS
calculation from resonance parameters, computer program for, 20: 13786 (ORNL-TM-1396)
calculation of, computer program for, 20: 13751 (AEEW-M-606)
calculation of, computer program for, 20: 13774 (JAERI-1096)
determination of fast, computer system for, 20: 13806
libraries of multigroup, computer program for preparation of, 20: 13706 (NAA-SR-Memo-10884 and Add.)
measurement of total, using silicon detectors, 20: 13101
tabulation for plutonium isotopes at 0.001 to 15 Mev, 20: 13770 (GA-6576)
tabulations for MOSEL reactor materials, 20: 14062 (JUL-214-RG)
NEUTRON MONOCHROMATORS
control systems for three-rotor choppers, (E), 20: 13713
neutron reflection from, by oriented single crystals, (E/T), 20: 13709 (PAEC-IPA(D)PH-652)
NEUTRON SHIELDING
performance of borated-graphite and -iron oxides, 20: 14180 (COO-1430-1)
NEUTRON SOURCES
calibration of beryllium-polonium, 20: 13107
collimators for, development of, 20: 13701 (JUL-294-NP)
design, 20: 13743(P)
design and performance of pulsed, with modulated flux, (E), 20: 13720
design and performance of, with variable pulse frequency and width, 20: 13721
design of pulsed fast reactor, 20: 14096
design of pulsed-beam, 20: 13745(P)
design of, having sinusoidally modulated intensity, (E), 20: 13704(R) (MIT-2344-4, pp 101-5)
design of, with automatic target temperature control, 20: 13744(P)
facility for using, 20: 12954(P)
monitoring of deuterium (d,n), using deuterium (d,p) reaction, 20: 13715
neutron background in laboratory containing, room-scattered, (E/T), 20: 13714
neutron wave excitation by modulated and pulsed, (E/T), 20: 13722
research with pulsed, conference on, 20: 13710 (STI/PUB/104(Vol.1))
research with pulsed, conference on, 20: 13711 (STI/PUB/104(Vol.2))
research with pulsed, review of, 20: 13725
spectrometer design for use with D-D, (E), 20: 13088
use of pulsed, for measurements in heavy water systems, (E), 20: 14076
use of pulsed, for experiments in intermediate and fast critical assemblies, 20: 14083
use of pulsed, for SAPHIR reactivity measurements, (E), 20: 14199
use of pulsed, for subcritical reactivity measurements in IRR-1, (E), 20: 14200
use of pulsed, for measuring spectra in moderators and reactor lattices, (E/T), 20: 13735
uses of pulsed, for kinetics analyses in heavy water lattices, 20: 14066(R) (MIT-2344-4, pp 63-9)
NEUTRON SPECTRA
determination of intermediate, review of activation methods for, 20: 13070 (RCN-40)
measurement in depleted uranium used pulsed sources, (E/T), 20: 14202
measurement in hydrogenous moderators using pulsed sources, (E/T), 20: 13737
measurement in moderators and reactor lattices, use of pulsed sources for, (E/T), 20: 13735
measurement in VERA using fast pulsed sources, (E/T), 20: 14086
NEUTRON SPECTROMETERS
design and performance of gamma-block stilbene, 20: 13063 (JAERI-1092)
design for slow neutrons, 20: 13065 (JUL-295-NP)
design of associated-particle time-of-flight, (E), 20: 13088
design of time-selector for choppers, for two-dimensional analysis, 20: 13075 (UJV-1450/65)
properties of time-of-flight, for slow neutrons, 20: 13061 (IDO-17134)
NEUTRONS
absorption by annular and rod-grid elements in uranyl nitrate critical assemblies, (E), 20: 14091
absorption by materials, resonance integrals for, (E), 20: 14008(R) (ANL-7122, pp 42-69)
capture by nuclei, resonance scattering of gammas from, (E), 20: 13771 (IA-1050)
capture by nuclei, method for analysis of γ-γ cascades from, (E), 20: 13062 (IEA-96)
capture by soils, radioactivity induced in, 20: 12582
capture in boron-bearing slab cores, (E/T), 20: 14063 (KAPL-M-6528)
capture in stars, effects on stellar element abundances, 20: 13410
capture of, two-dimensional gamma spectrometer for analyzing, 20: 13075 (UJV-1450/65)
computer system for control of laboratory for, digital, 20: 13806
detection and measurement of, semiconductor detectors for, 20: 13116(P)
detection and measurement using lithium-6 glass detectors, (E), 20: 13090
detection and measurement of, background gamma discrimination in, 20: 13111
detection by dielectric liquid ionization chambers, 20: 13107
detection in concrete-walled laboratory, room-scattered background for, 20: 13714
detection of, calorimeter performance for, 20: 14170 (EGG-1183-2019)
detection of, counter performance for, 20: 13367 (UCRL-16445(Rev.))
detection of, silicon detectors for, 20: 13101
diffraction by aluminum, magnesium, and vanadium at high pressures, 20: 14059(R) (IDO-17104)
diffraction by manganese oxides, long-range magnetic order from, (E), 20: 13993
diffusion and multiplication in beryllium oxide–natural uranium lattices, (E/T), 20: 14080
diffusion in air-filled aluminum-tube lattices in heavy water, (E/T), 20: 13705(R) (MIT-2344-4, pp 135-44)
diffusion in anisotropic media with no strong distributed absorption or fission, (E/T), 20: 13705(R) (MIT-2344-4, pp 135-44)
diffusion in beryllium oxides and graphite, pulsed, (E), 20: 13727
diffusion in heavy water, pulsed-source technique for measuring, (E), 20: 14076
diffusion in nonmultiplying media, interpretation of pulsed, (T), 20: 13731
diffusion in organic liquids, effects of non–1/v capture on pulsed, (E), 20: 13730
diffusion in reactors, computer program for, 20: 14056 (AWRE-O-99/65)
diffusion parameters organic liquids and water, pulsed, (E), 20: 13729
dosimetry in reactors, pneumatic system for, 20: 13069 (NASA-CR-54468)
dosimetry of, tissue-equivalent proportional counters for, 20: 13060 (CEA-R-2891)
effects on beryllium at 750°C, 20: 14059(R) (IDO-17104)
effects on cobalt complexes, 20: 12897
effects on complexes of cobalt with 3,3-diacetyl-2,4-pentanedione, annealing of chemical recoil damage in, 20: 12896
effects on developing mouse fetuses, effects of dose on, 20: 12683
effects on dimensional changes in raw-coke graphites, 20: 13322 (BNWL-178)
effects on electric conductivity of aluminum, dose dependence of stage II annealing of, 20: 13340
effects on electronic equipment, transient, 20: 13130 (SC-DC-65-1892)
effects on life span of guinea pigs, 20: 12628 (AD-626997)
effects on mechanical properties of beryllium, 20: 13323 (CONF-170, pp 138-59)
effects on mechanical properties of Inconel 600 and X-750, 20: 13333
effects on mechanical properties of austenitic stainless steels, 20: 13333

effects on microstructure of beryllium oxide, 20: 13331
effects on microstructure of uranium carbides, 20: 13332
effects on MOS transistor characteristics, mechanisms for, 20: 13133
effects on NERVA resistance-temperature transducers, 20: 13127 (CONF-651101-61)
effects on oxygen-defect complex formation in silicon, infrared absorption spectra of, (E), 20: 13998
effects on potassium trioxalatoferrates, annealing of, 20: 12903
effects on pressure transducers, 20: 14170 (EGG-1183-2019)
effects on sodium phosphates, 20: 12902
effects on stress-rupture of chromium–nickel–niobium steel, 20: 13328 (ORNL-TM-1359)
effects on tensile properties of iron and iron–titanium alloys, effects on nitrogen content on, 20: 13324(R) (EURAEC-1529)
effects on ternary plutonium–uranium alloys and plutonium-carbide–uranium-carbide fuels, in-pile, (E), 20: 14007(R) (ANL-7122, pp 1-41)
effects on uranium dioxide–lithium fluoride mixtures, 20: 12898
effects on uranium dioxide–zirconium dioxide mixtures, 20: 13330
embrittlement of stainless steel by, effects of grain size on, 20: 13335
emission of secondary, in meson (π^-)-proton interactions, (E), 20: 13525
flux distribution in homogeneous suspension reactors, (E), 20: 14072
flux distribution in Dowtherm A and water, extrapolation distances from pulsed, (E), 20: 13726
flux distribution in matter, dependence on parameters of scattering nuclei, (T), 20: 13734
flux in infinite moderator, grey rod extrapolation distance for, (T), 20: 13712
flux in light water assemblies, ($k\beta/l$) pulsed-source technique for, (E), 20: 14162
flux in reactor deuterium-containing probe for measuring, 20: 13119(P)
flux stability in reactors containing xenon-135, computer program for, 20: 14061 (IDO-17127)
interactions with protons at 600 Mev, meson ($\pi^\pm$) production in, (E), 20: 13453 (JINR-P-2511)
interactions with alpha particles, phase equivalent potentials for elastic, (T), 20: 13482
interactions with protons, soft-core potential for phase-shift energy dependence in elastic, (T), 20: 13489
interactions with protons, real part of forward amplitude of, (T), 20: 13493
interactions with protons at 129 and 150 Mev, cross sections for, (E), 20: 13500
interactions with neutrinos, mass of intermediate bosons from, (T), 20: 13504
interactions with protons, effective ranges in $^1S_0$ states of, (T) 20: 13512
interactions with mesons (K^-) at 600 to 850 Mev/c, hyperon (Λ)-meson (π) resonances in, (E), 20: 13522
kinetics in intermediate and fast critical assemblies, pulsed, 20: 14083
kinetics in reactors, computer program for, 20: 14060 (IDO-17114)
kinetics in reactors, computer program for, 20: 14064 (LA-3427)
mass relative to protons, S-matrix theory for, 20: 13511
moderation in graphite, iron, and lead, pulsed-source measurements of, (E), 20: 13741
moderation of, use of pulsed sources for measuring, (E/T), 20: 13735
momentum distribution from (π^-, 2N) reactions, (T), 20: 13874
production in meson (π)-proton interactions at 450 Mev, (E), 20: 13524
production in meson (π^-)-proton interactions at 350 to 800 Mev, (E), 20: 13527
reactions (n,α) with boron-10 and lithium-6, excitation functions for, (E), 20: 13741
reactions (n,α) and (n,p) with potassium-39 and sodium-23 at 4 to 14 Mev, cross sections for, (E/T), 20: 13773 (IKF-13)
reactions (n,α) and (n,p) with silicon-28 at 13.95 Mev, recoil ionization defects from, (E), 20: 13989
reactions (n,p) with helium-3 and nitrogen-14, excitation functions for, (E), 20: 13741
reactions (n,2n) with neodymium-142 at 14.7 Mev, neodymium-141 production from, (E), 20: 13864
reactions in subcritical lattices, measurement, (E), 20: 14185(R) (MIT-2344-4, pp 70-9)
reactions of reflected, with unit spherical target, (T), 20: 13742
reactions with nuclei, width fluctuation factor for, (T), 20: 13824
reactions with sodium at 1 ev to 40 kev, cross sections for, (T), 20: 13753 (BNL-961)
reactions with uranium isotopes in heavy-water lattices, 20: 14103(R) (MIT-2344-4, pp 48-62)
reactions with uranium-235, cross sections for, 20: 13749 (AEEW-M-502)
reflection by oriented single crystals in neutron monochromators, (E/T), 20: 13709 (PAEC-IPA(D)PH-652)
resonance integrals in MITR, measurement of effective, (E), 20: 14186(R) (MIT-2344-4, pp 145-8)
scattering by A = 208 nuclei at 8 Mev, excitation of 3$^-$ collective state in inelastic, (E/T), 20: 13870
scattering by aluminum, iron, and teflon at 130 to 160 kev, cross sections for, (E), 20: 13716
scattering by boron-11 in orthoboric acid, 20: 12836
scattering by cadmium, indium, and silver at 0.3 to 1.5 Mev, differential cross sections for, (E), 20: 13829
scattering by cobalt indium, gold, silver, and tantalum at 3.5 to 8.5 Mev, level density parameters from, (E), 20: 13827
scattering by helium-4 at 262 kev, polarization in, (E), 20: 13717
scattering by iridium-191, cross sections and spin assignments for resonant, (E), 20: 13796
scattering by nuclei in matter, (T), 20: 13734
scattering from concrete slab, Monte Carlo method for determining, 20: 13742
scattering of, computer program for Legendre coefficients for elastic, 20: 13699 (GA-6690)
scattering of, computer program for angular distributions from elastic, 20: 13697 (AEEW-M-605)
scattering on iron, spin correlations from diffuse magnetic, (E), 20: 13994
slowing down of, computer program for, 20: 13698 (DTMB-1820)
slowing-down and thermalization in graphite, time constants for pulsed, (E), 20: 13728
spectra in heavy water, pulsed-source measurement of time-dependent, (E/T), 20: 13736
thermalization in graphite, wave excitation in, (E/T), 20: 13722
thermalization in paraffin, pulse transfer function for, (E/T), 20: 13724
thermalization in beryllium and graphite, pulsed-source measurements of, (E), 20: 13738
thermalization in water and zirconium hydrides, pulsed-source measurements of, (E), 20: 13739
thermalization in graphite-water systems at large temperature gradients, (E), 20: 13740
transport equations for, adjoint, 20: 14094
transport in inhomogeneous moderators, graphic method for solving, (T), 20: 13732
transport theory for, Bessel and Bickley functions for, (T), 20: 13707 (ORNL-TM-1415)
transport theory for, special functions in, (T), 20: 13708 (ORNL-TM-1417)
use as probe for moisture control in mixtures for agglomeration, 20: 13156

NEUTRONS, COLD

scattering by phosphonium iodides, low-frequency molecular motions and barrier to rotation in, 20: 12859
transport in matter, pulsed, (T), 20: 13733

NEUTRONS, FAST

detection and measurement of, to 50-Mev, device for, 20: 13081
detection of Bev-range, scintillation detector efficiency for, 20: 13109
detection of, performance of dielectric liquid-filled cloud chamber for, 20: 13112
distributions in enriched-uranium heavy-water lattices, computer analysis of, 20: 13703(R) (MIT-2344-4, pp 17-47)
effects on conifer-hardwood, effects of environmental factors on, 20: 12672
effects on defects in aluminum, 20: 13338
effects on dimension of alumina, 20: 13337
effects on hardwood-pine forests, effects of age and dose on recovery from, 20: 12675
effects on molded graphite, effects of pitchbinder on, 20: 13247(R) (GA-6831)
effects on properties and structure of pyrolytic carbons, 20: 13247(R) (GA-6831)
effects on tensile properties of iron–chromium–aluminum–yttrium alloys, 20: 13179(R) (GEMP-55A, pp 13-28)
emission and return fluxes of, in heavy-water reactors, (E), 20: 14070(R) (MIT-2344-4, pp 115-34)
interactions with deuterons at 5.635 and 9.035 Mev, cross sections for elastic, (E), 20: 13520
kinetics in subcritical assemblies, pulsed, (T), 20: 14087
reactions in multiplying media, prompt neutron kinetics from modulated and pulsed, (T), 20: 14088
reactions with neptunium, plutonium, and uranium isotopes, fission rates for, (E), 20: 14202
scattering by uranium at 0.83 Mev, cross sections and polarization from, (E), 20: 13868
spectra in depleted uranium, pulsed-source measurements of, (E/T), 20: 14202
transport in multiplying media, modulated and pulsed experiments on, (T), 20: 13723
transport in nonmultiplying media, pulsed, (E/T), 20: 13719

NEUTRONS, PROMPT

decay in slightly enriched lattices, pulsed-source technique for

measuring, (E), 20: 14076
decay in VERA, pulsed-source measurements of, (E), 20: 14089
kinetics in fast neutron multiplying media, modulated and pulsed experiments for, (T), 20: 14088
lifetime in Swedish reactor FRO, 20: 14178 (AE-207)

NEUTRONS, THERMAL
absorption in natural boron standard, cross sections for, (E), 20: 13807
capture by chlorine-35, electron pair production in, (E), 20: 13762 (CONF-233(Vol.4), pp 700-9)
diffusion lengths in Santowax R poisoned with boron, (E), 20: 13718
distributions around single heavy-water-moderated fuel rods, (T), 20: 14067(R) (MIT-2344-4, pp 80-8)
distributions in enriched-uranium heavy-water lattices, 20: 14065(R) (MIT-2344-4, pp 4-16)
flux in critical assemblies, one-group parameters for, (T), 20: 14073
flux of, boron thermistors for measuring, 20: 13126(P)
intensity distribution from Soller-type collimator, 20: 13702 (LA-DC-7594)
reactions with heated tellurium dioxide to produce iodine-131, 20: 12922(P)
reactions with uranium-233 and -235, zirconium-95 yields from, (E), 20: 13783 (ORNL-TM-1333)
reactions with uranium-235, yields of argon isotopes and cobalt-56 in ternary fission, (E), 20: 13862
scattering by hydrogen molecules, Fadeev equations for, (T), 20: 13417
scattering by liquid and solid argon, inelastic, 20: 14059(R) (IDO-17104)
scattering in reactors, analysis of inelastic, (E/T), 20: 13700 (JAERI-1086)
transport equation for, computer program for Boltzmann, 20: 13698 (DTMB-1820)

NICHROME
heat flux on submerged, during boiling of organic coolants, 20: 12965

NICKEL
corrosion by fluorine and molybdenum and tellurium fluorides at 500°C, (E), 20: 14008(R) (ANL-7122, pp 42-69)
deposition on uranium surfaces, method for electrolytic, 20: 13211 (BNWL-124)
determination in sodium loop transfer samples, methods for, 20: 12766 (GEAP-4178)
electron propagation through vacuum boundary with, relative transition radiation yields from, (E), 20: 13352
electron secondary emission from thin foils of, (E), 20: 13103
neutron absorption and inelastic scattering by, gamma spectra from, 20: 13966 (UNC-5140)
neutron cross sections for, 20: 14062 (JUL-214-RG)
porosity of coating of, on uranium surfaces, x-ray fluorescence determination of, 20: 13211 (BNWL-124)
proton reactions (p,p') at 10.5 Mev, cross sections for, (E), 20: 13897
separation from other inorganic ions by paper chromatography, 20: 12939
sputtering by argon ions, electron diffraction analysis of damage from, (E/T), 20: 13981
use in determination of lead-210 and polonium-210, 20: 12785

NICKEL ALLOYS
corrosion by fluorine and molybdenum and tellurium fluorides at 500°C, (E), 20: 14008(R) (ANL-7122, pp 42-69)
Cr–Fe–Ni, fatigue tests on pressure vessel cladding of, 20: 13255 (KAPL-3108)
Dy–Ni, dysprosium-161 Mössbauer effect in, (E), 20: 13992
Dy–Ni, dysprosium-161 isomer shift in, 20: 13992

NICKEL(II) COMPLEXES
with hexamethylphosphoramide, NMR contact shifts in, 20: 12828 (TID-21587)

NICKEL FLUOBORATES
complexes with pyridine, preparation and properties of, 20: 14225 (TID-21577)

NICKEL IONS
photopolarographic reduction, uv, 20: 12798
spectra of, in nickel glass after reduction, 20: 13260(R) (NP-15852)

NICKEL ISOTOPES Ni-56
decay of, gamma spectra from, (E), 20: 13815

NICKEL ISOTOPES Ni-57
decay of, gamma spectra from, (E), 20: 13815

NICKEL ISOTOPES Ni-58
deuteron reactions (d,p) at 7 Mev, cross sections and nickel-59 levels from, (E), 20: 13858
ion inelastic scattering by, collective level excitation in complex, (T), 20: 13890
proton inelastic scattering at 7 Mev, energy levels and cross sections for, (E), 20: 13858
proton reactions (p,n) at 14.2 Mev, angular distributions, Q values, and spectra from, 20: 13345(R) (NP-15772)

NICKEL ISOTOPES Ni-59
energy levels from deuteron reactions (d,p) with nickel-58 at 7 Mev, (E), 20: 13858

NICKEL ISOTOPES Ni-62
helium-3 reactions (He-3,d), core excitation in, (T), 20: 13816

NICKEL ISOTOPES Ni-63
determination in sea water by liquid scintillation counting, 20: 12779 (USNRDL-TR-924)

NICKEL NITRATES
complexes with pyridine, preparation and properties of, 20: 14225 (TID-21577)

NICKEL OXIDES
Cr_2O_3–NiO–O, phase studies on, 20: 13260(R) (NP-15852)

NICKEL PERCHLORATES
complexes with pyridine, preparation and properties of, 20: 14225 (TID-21577)

NICKEL STEEL
Cr–Ni–Nb, radiation effects on stress-rupture of, 20: 13328 (ORNL-TM-1359)

NICKEL STRONTIUM LANTHANUM OXIDES
crystal structure, 20: 12865

NICKEL SYSTEMS
Al–Mg–Ni–Si, fatigue properties at 250 to 350°C, low-cycle, 20: 13308

NICOTINIC ACID
radiosterilization effects on content of, in strawberries, gamma, 20: 13142(R) (UCD-34P80-3, pp 52-4)

NIOBIUM
compatibility with cesium at 550°C, 20: 13203
crystallization of, during soldering and welding, 20: 13267(T) (AD-624909)
defects in crystals of, stacking-fault, (E/T), 20: 13971 (AD-625834)
deformation behavior of, in transition temperature range, 20: 13253 (IS-T-65)
effects on colorimetric determination of vanadium in uranium compounds, 20: 12802
effects on crystal structure of alpha-iron, 20: 13317
impurity atom relaxation strength in, anisotropy of Snoek, (E), 20: 13980
magnetic field distribution in annealed and plastically deformed type-II-superconducting, (E), 20: 13672
magnetic flux penetration in superconducting, ultrasonic attenuation for determination of, (E), 20: 13684
reactions with carbon and nitrogen at 1150 to 2370°C, 20: 12845
separation from molybdenum by solvent extraction using tetra-n-butylammonium bromide, 20: 12933
solubility in alpha-iron at 600 to 900°C, 20: 13317
solvent properties for nitrogen at 450 to 1000°C, 20: 13303
spectra of, effects of electronic structure on x-ray emission, 20: 12846
superconducting properties of fine wires of, in copper matrix, 20: 13673
thermal capacity below 3.3°K, 20: 13692

NIOBIUM ALLOYS
weld ductility of, comparison of, with weld ductility tantalum-base alloys, 20: 13264(R) (WANL-PR(P)-008)
Al–Ge–Nb–Sn, phase studies, 20: 13275
Al–Nb, phase studies, 20: 13275
Al–Nb–Ti, properties of, mechanical and physical, 20: 13271
Ge–Nb, phase studies, 20: 13275
Nb–Sn, phase studies, 20: 13275
Nb–Sn, superconductivity of Nb_3Sn, 20: 13666 (IPP-4/22)
Nb–Ta–W–Zr, creep behavior in ultrahigh vacuum at 2000 and 2200°F, 20: 13256 (NASA-TN-D-3222)
Nb–Ta–W–Zr, weldability of FS-85, effects of oxygen contamination on, 20: 13264(R) (WANL-PR(P)-008)
Nb–Ti, superconductivity of, 20: 13666 (IPP-4/22)
Nb–V, performance as cladding for plutonium–uranium fuel alloys, (E), 20: 14007(R) (ANL-7122, pp 1-41)
Nb–W–Zr, creep behavior in ultrahigh vacuum at 2000 and 2200°F, 20: 13256 (NASA-TN-D-3222)
Nb–Zr, anomalous critical currents in superconducting noninductive coils of, (E), 20: 13674
Nb–Zr, compatibility with TZM molybdenum alloy in refluxing potassium at 2000°F, 20: 13192(R) (NASA-CR-54843)
Nb–Zr, microstructure, effects of tempering on, 20: 13304
Nb–Zr, performance as cladding for alloy and carbide fuels, (E), 20: 14007(R) (ANL-7122, pp 1-41)
Nb–Zr, rupture properties of, effects of exposure to potassium at 1400°F on stress-, 20: 13191(R) (NASA-CR-54476)
Nb–Zr, superconductivity of, 20: 13666 (IPP-4/22)
Nb–Zr, thermodynamic properties of nitrogen equilibrium solid solutions in, 20: 13263 (ORNL-TM-1355)
Nb–Zr, welding of, nondestructive testing of zones of, 20: 13320

NIOBIUM CARBIDES
reactions with nitrogen at 1150 to 2370°C, 20: 12845
reactions with titanium, 20: 13194
Co–NbC–WC, mechanical properties of, effects of composition on, 20: 13274

NIOBIUM HYDRIDES
chemical bonds in, properties of, 20: 12847
NIOBIUM ISOTOPES Nb-95
beta decay of, gamma spectra from, (E), 20: 13859
diffusion in polycrystalline uranium dioxide at 1100 to 2100°C, 20: 13289
NIOBIUM OXIDES
Al_2O_3–Nb_2O_5, phase studies, 20: 12833
Cr_2O_3–Nb_2O_5, phase studies, 20: 12833
Nb_2O_5–ZrO_2, crystal structure of compounds $ZrO_2 \cdot 5Nb_2O_5$ and $ZrO_2 \cdot 7Nb_2O_5$ in, 20: 13281
NIOBIUM SELENIDES
superconductivity, (E), 20: 13683
NIOBIUM STEEL
Cr–Ni–Nb, radiation effects on stress-rupture of, 20: 13328 (ORNL-TM-1359)
NIOBIUM SULFIDES
superconductivity, (E), 20: 13683
NIOBIUM SYSTEMS
C–Hf–Nb, phase diagrams, 20: 13272
C–Nb–Ti, phase diagrams, 20: 13272
C–Nb–W–Y–Zr, weldability of D-43Y, 20: 13264(R) (WANL-PR(P)-008)
C–Nb–W–Zr, corrosion of D-43, by potassium at 2450°F, stress-, 20: 13191(R) (NASA-CR-54476)
C–Nb–W–Zr, creep behavior in ultrahigh vacuum at 2000 and 2200°F, 20: 13256 (NASA-TN-D-3222)
C–Nb–Zr, phase diagrams, 20: 13272
Nb–N, degasification of solid solutions of, kinetics of, 20: 13202
Nb–N, precipitation from supersaturated, kinetics of, 20: 13303
Nb–N, properties of solid solutions of, effects of nitrogen content on, 20: 13302
NITRATES
volatility of, in radioactive alumina calcine during high-temperature storage, 20: 14207 (IDO-14670)
NITRIC ACID
effects on kerosene in Purex Process, 20: 12934
HNO_3–$K_2Cr_2O_7$, corrosive effects on type 304 stainless steel, effects of reactor irradiation on, 20: 13325(R) (GEAP-4968)
NITROGEN
determination in loop-cover argon by diffusion gasometry, 20: 12767 (GEAP-4833)
effects on fast-neutron effects on tensile properties of iron and iron–titanium alloys, 20: 13324(R) (EURAEC-1529)
effects on gas exchange in irradiated pears, 20: 13140(R) (UCD-34P80-3, pp 27-47)
effects on maize seeds in water at 3 to 45°C, biological, 20: 14216 (BNL-9859)
effects on spectra of hydrochloric acid in argon lattice, 20: 12857
electron paramagnetic resonance of free radicals of, in alkali azides, 20: 13970 (AD-611432, pp 135-47)
pressure of, over beryllium nitride at 1640 to 1950°K, 20: 12830 (UCRL-7802)
radiation and/or thermal trauma effects on content of, in rat intestinal mucosa, 20: 12630 (BNL-8383)
reactions with carbon and niobium or tantalum at 1150 to 2370°C, 20: 12845
reactions with molten uranium–zirconium particles, disintegration properties of, 20: 14169 (AFWL-TDR-64-75)
reactions with niobium and tantalum carbides at 1150 to 2370°C, 20: 12845
reactions with uranium hydrides, 20: 13227
reactions with zirconium droplets, flash heating effects on combustion and explosive, 20: 12826 (SC-RR-65-569)
relaxation strength in niobium, anisotropy of Snoek, (E), 20: 13980
resonance in laser-induced plasma of, optical frequency, (E/T), 20: 13942
solubility in niobium at 450 to 1000°C, 20: 13303
solubility in yttrium, 20: 13180(R) (IS-RD-4)
thermal conductivity at 1000 to 20,000°K, (T), 20: 13644
thermodynamic properties of equilibrium solid solutions of, in niobium–zirconium at 1200 to 1800°C, 20: 13263 (ORNL-TM-1355)
uptake by rice, tracer study of, 20: 12592(R) (NP-15671)
yields in radiolysis of gaseous nitrous oxide, 20: 12884(R) (RRL-2310-171)
NITROGEN IONS
production and acceleration of beams of, 20: 13804
NITROGEN ISOTOPES N-12
energy levels, (E), 20: 13808
NITROGEN ISOTOPES N-14
boron-10 reactions (B-10,3α) at 100 Mev in photoemulsions, mechanism of, (E), 20: 13891
energy levels from carbon-13 proton reactions, (E), 20: 13898
neutron reactions (n,p) with, excitation functions for, (E), 20: 13741
nitrogen-14 reactions (N-14,N-13) with, angular distributions and cross sections for, (T), 20: 13830
NITROGEN ISOTOPES N-15
determination in gases by spectrography, step-filters for, 20: 12807
energy levels from helium-3 reactions (He-3,$p\gamma$) with carbon-13 at 4.95 and 5.25 Mev, (E), 20: 13819
nuclear magnetic moment corrections for, perturbation theory for, 20: 13838
uptake of ammonium sulfate-incorporated, by rice, 20: 12592(R) (NP-15671)
uptake of ammonium sulfate-incorporated, by rice, 20: 12593(R) (NP-15672)
NITROGEN ISOTOPES N-16
content in reactor coolants, power-level determination from, 20: 14019
NITROGEN OXIDES
complexes with iron, kinetics of formation of, 20: 12884(R) (RRL-2310-171)
effects on gas-phase radiolysis of cyclobutane and deuterated cyclobutane, 20: 12894
radiation effects on gaseous nitrous oxide, yields in, 20: 12884(R) (RRL-2310-171)
NITROGEN SYSTEMS
Nb–N, degasification of solid solutions of, kinetics of, 20: 13202
Nb–N, precipitation from supersaturated, kinetics of, 20: 13303
Nb–N, properties of solid solutions of, effects of nitrogen content on, 20: 13302
N–U, phase diagrams, 20: 13286
NOBELIUM ISOTOPES
production in neon-22 reactions (Ne-22,xn) with uranium-238, cross sections for, (E), 20: 13889
NOBELIUM ISOTOPES No-256
half life, (E), 20: 13778 (JINR-P-2525)
production in oxygen-18 reactions with plutonium-242, (E), 20: 13778 (JINR-P-2525)
NOISE
research programs on electron device, 20: 14227(R) (TID-22419)
NUCLEAR EMULSIONS
charged-particle image formation in, exciton mechanism in, (T), 20: 13082
cosmic nucleon interactions in, spectra from, (E), 20: 13345(R) (NP-15772)
meson (K^-) interactions in, correlations of meson (π) production and decay chains in, (E), 20: 13487
meson (μ) inelastic scattering at 5 Bev/c, (E), 20: 13526
meson (π^-) reactions with heavy nuclei at 17.2 Bev/c in, cross sections for, (E), 20: 13893
performance for accelerator monitoring, 20: 13367 (UCRL-16445(Rev.))
testing for use in cyclotrons, 20: 13345(R) (NP-15772)
NUCLEAR ISOMERS
structure of spontaneously fissioning, (T), 20: 13777 (JINR-E-2515)
NUCLEAR MATERIALS MANAGEMENT
analysis of mixed fissionable isotopes, radiometric, 20: 12814(P)
NUCLEAR MODELS
beta transitions in Nilsson model, matrix element of, 20: 13831
nucleon-nucleon and Yukawa potentials in, eigenvalues of Lippmann-Schwinger kernel for, (T), 20: 13836
NUCLEAR MODELS (OPTICAL)
potential and reduction factor for nonlocal wave function in, Perey effect for equivalent local, (T), 20: 13811
NUCLEAR MODELS (SHELL)
calcium-42 energy-level spectrum in, effects of deformed states in, (T), 20: 13839
energy level properties of oxygen-16, ground state, (T), 20: 13785 (ORNL-TM-1374)
energy level transition calculations for even nuclei, E0, 20: 13746 (AD-626681)
theory of, many-body foundations of, 20: 13790
NUCLEAR PHYSICS
developments in, annual report of CEA, 20: 14223(R) (NP-15723)
research, (E/T), 20: 13347(R) (UCRL-16511)
research at Orsay, 20: 13364(R) (LAL-1148)
research on high-energy, summary for university of Tokyo, 20: 13345(R) (NP-15772)
NUCLEAR POWER
economic prospects for, in France, 20: 14151
generating capacities for, listing by country, 20: 14222(R) (NP-15612)
NUCLEAR POWER PLANTS
economics, 20: 14121 (EUR-2453.f)
economics, 20: 14133 (NP-15587)
economics in Germany, 20: 14130 (KFK-366)
feasibility of MHD-reactor, 20: 14132 (LA-3368)
lists of, worldwide, 20: 14222(R) (NP-15612)
steam generator tubes for, nondestructive testing of, 20: 14160
NUCLEAR REACTIONS
core excitation in stripping, (T), 20: 13816

formalism for rearrangement, Born series for symmetric interaction in, 20: 13798
fragment emission in high-energy, mechanism of light, (T), 20: 13880
model for deuteron stripping, angular distribution calculations in, (T), 20: 13851
nucleon knock-out distribution from, excitation energy, nuclear volume, and recoil momentum for, (T), 20: 13892
theory of two-nucleon stripping, DWBA for, 20: 13814
theory of, projection operators in unified, 20: 13850
width fluctuation factor for, correlated multichannel distribution for, (T), 20: 13824

NUCLEAR STRUCTURE
energy levels with high spin, gamma cascade from, (T), 20: 13847

NUCLEAR THEORY
beta transitions in Nilsson model, matrix elements for, 20: 13831
Bethe-Salpeter equation and conservation laws for finite nuclei, 20: 13789
book: *The Theory of Finite Fermi Systems and Properties of Atomic Nuclei*, 20: 13632
energy level coupling schemes in odd-mass nuclei, (T), 20: 13825
forces in, momentum-dependent, 20: 13792
forces in, origin of repulsive core in, (T), 20: 13879
Hartree-Fock field and method of projection in, 20: 13826
many-body problem in, effective interaction in, 20: 13791
nucleon bound states in, Bethe-Salpeter equation for two-body, 20: 13876

NUCLEI
alpha inelastic scattering by deformed, rotational excitation and gamma angular pattern from, (T), 20: 13848
beta decay of, internal bremsstrahlung spectra in, (T), 20: 13761 (CONF-233(Vol.4), pp 656-68)
beta transitions in, Nilsson model for matrix elements of, 20: 13831
beta transitions in $11 \leq A \leq 63$ odd theory of finite Fermi systems for, 20: 13887
binding energy parameters for, from realistic two-nucleon potentials, (T), 20: 13840
book: *The Theory of Finite Fermi Systems and Properties of Atomic Nuclei*, 20: 13632
charged-particle reactions at high energy with heavy, light fragment emission in, (T), 20: 13880
decay of, internal bremsstrahlung spectra from electron-capture, (T), 20: 13760 (CONF-233(Vol.4), pp 637-55)
deuteron stripping reactions with, angular distribution calculations for, (T), 20: 13851
deuteron stripping reactions with odd-n, spectroscopic factors from, (T), 20: 13865
electron and x-ray excitation of, use of low-energy, 20: 13782 (ORNL-P-1927)
electron inelastic scattering by, amplitudes for, (T), 20: 13775 (JINR-P-2490)
electron inelastic scattering by heavy excitation of giant multipole resonances in, (T), 20: 13832
electron scattering by, analysis near 180°, (E), 20: 13089
energy level transitions in even, E0, (T), 20: 13746 (AD-626681)
energy level transitions and octupole vibrations in odd-mass rare-earth region, E1, (T), 20: 13820
energy levels in even, E2 transitions between high-spin rotational, (T), 20: 13801
energy levels in odd-mass, coupling schemes for, (T), 20: 13825
energy levels of even-even spherical, second-vibrational, (T), 20: 13793
fission of heavy, review of chemical studies on low-energy, 20: 12920
fission of heavy, analysis using mica sandwiches, 20: 13099
gamma cascades from high-spin levels in, angular distribution and spectra of, (T), 20: 13847
gamma scattering by, resonance, (E), 20: 13771 (IA-1050)
internal conversion in, correlation of electron polarization in, (T), 20: 13802(T)
ion fission of $176 \leq A \leq 209$, energy and mass distributions from, (E), 20: 13861
ion inelastic scattering by complex, dynamic deformation in heavy, (T), 20: 13794
isomeric states of, spontaneously fissioning, (E), 20: 13777 (JINR-E-2515)
magnetic moment corrections to second order for mirror, perturbation theory for, 20: 13838
meson (μ) capture by, G-parity violation in, (T), 20: 13877
meson (π^-) reactions (π^-,2N) with, momentum distribution from, (T), 20: 13874
meson (π) elastic scattering on, electromagnetic form factor from, (T), 20: 13878
neutrino reactions (ν,μ) with, test for time reversal violation in, (T), 20: 13835
neutron capture by, resonance scattering of gammas from, (E), 20: 13771 (IA-1050)
neutron capture by, method for analysis of γ-γ cascades from, (E), 20: 13062 (IEA-96)
neutron inelastic scattering at 8 Mev by A = 208, excitation of 3⁻ collective state, (E/T), 20: 13870
neutron reactions with, width fluctuation factor for, (T), 20: 13824
neutron scattering by, in matter, (T), 20: 13734
nucleon forces in, origin of repulsive core in, (T), 20: 13879
nucleon reactions with, DWBA for two-body stripping, (T), 20: 13814
photofission of heavy, at 200 to 730 Mev, (E), 20: 13345(R) (NP-15772)
photon reactions with heavy, Levinger-Bethe sum rules for dynamical correlations in, (T), 20: 13873
potential and reduction factor for nonlocal wave function for, Perey effect for equivalent local, (T), 20: 13811
properties of, with momentum-dependent forces, (T), 20: 13792
proton reactions (p,2n) with odd-Z, conversion electrons from, (E/T), 20: 13345(R) (NP-15772)
proton reactions (p,pd) with, momentum distribution from, (T), 20: 13874
radioactivity of, absolute determination of, (T), 20: 13805
scattering of complex, collective level excitation in inelastic, (T), 20: 13890

NUCLEI (CELLS)
radiation effects on mouse spleen, x, 20: 12681

NUCLEONS
binding energy and coupling constant for two-body systems of, Bethe-Salpeter equation for, 20: 13876
distribution from knock-out reactions, excitation energy, nuclear volume, and recoil momentum for, (T), 20: 13892
form factors for, electromagnetic and weak, (T), 20: 13447 (IC/65/95)
form factors of, electromagnetic, (T), 20: 13479(T)
interactions in nuclei, effects on beta decay of strong, (T), 20: 13886
interactions with nucleons, spin structure of, (T), 20: 13455 (UCRL-14240-T)
interactions with mesons, scattering matrix for, (T), 20: 13448 (JINR-E-2521)
interactions with mesons (π) up to 500 Mev, quasipotential method for, (T), 20: 13467
interactions with vector mesons, (T), 20: 13479(T)
interactions with nucleons, phase-space volumes for, (T), 20: 13481
interactions with mesons (π), phase-space volumes for, (T), 20: 13481
interactions with hyperons (Λ), charge-asymmetry effects in, (T), 20: 13485
interactions with mesons (π^-) and (π^+), phase-shift analysis and spin-flip dispersion relations for, (T), 20: 13492
interactions with hyperons (Λ^0), hypernucleus nonmesic decay for, (T), 20: 13501
interactions with mesons at high energies, elementary-particle structure from backward-scattering, 20: 13510
interactions with nucleons at 400 Mev, phase-shift analysis of, (E/T) 20: 13516
interactions with nucleons, cross sections for, (T), 20: 13528
interactions with leptons, permutation symmetry in isospace for weak, 20: 13596
interactions with mesons (π) and nucleons in Bev range, partial-wave analysis of, (T), 20: 13513
interactions with nucleons, momentum-dependent potential for, (T), 20: 13792
interactions with nucleons, eigenvalues of Lippmann-Schwinger kernel for, (T), 20: 13836
interactions with nucleons in nuclei, binding-energy parameters from potentials for realistic two-body, (T), 20: 13840
interactions with nucleons, origin of repulsive core from, (T), 20: 13879
isospin space for fields of, 20: 13611
reactions with carbon-13, fluorine-19, and tin-118, optical-model wave functions for, (T), 20: 13817
reactions with nuclei, DWBA for two-body stripping, (T), 20: 13814

NUCLEOTIDES, PYRIDINE DIPHOSPHATE
effects on phosphate and rubidium uptake by isolated cells of bean seedlings and tobacco leaves, 20: 14217 (COO-888-43)

NUTRIENTS
foliar absorption of, mechanisms for, 20: 14219 (COO-888-47)
permeation through plant foliage, effects of urea on, 20: 14218 (COO-888-44)
radiosensitivity effects on conifer-hardwood forests, fast-neutron, 20: 12672

O

OAK RIDGE
inventory of vascular plants in and around, alphabetic, 20: 12567 (ORNL-TM-1232)

2-OCTANOL
labeling with tritium, Wilzbach method for, 20: 12878

ONTARIO (HALIBURTON CO.)

strontium-86 to strontium-87 ratios in carbonate veins and vein-dikes in, 20: 12980
OÖCYTES
relation of fourth and Y chromosomes in Drosophila, 20: 12690
ORES
analysis for gold, activation, 20: 12769 (IEA-98)
ORGANIC COMPOUNDS
chromatography of, use of integrator in gas, 20: 12777 (UJV-1431/65)
effects on gas-phase radiolysis of cyclobutane and deuterated cyclobutane, 20: 12894
ORGANIC COOLED REACTORS
boiler design for, 20: 14041(P)
design of heavy water-moderated, 20: 14100(P)
ORGANISMS
radiation effects on living, bibliography on, 20: 12629 (AED-C-04-22)
ORGANS
radiation effects on mouse, protective effects of bone marrow therapy against, 20: 12720(R) (TID-22466)
ORNL HIGH FLUX ISOTOPE REACTOR
fuel elements for, fabrication of aluminum–urania dispersion, 20: 13217 (ORNL-TM-1377)
ORNL RELATIVISTIC ISOCHRONOUS CYCLOTRON
experimental facilities of, polarized proton beam, (E), 20: 13375
ORNL RESEARCH REACTOR
fuel burnup testing in, pyrolytic carbon coated oxide, 20: 13215(R) (ORNL-3885, pp 3-86)
fuel element irradiation testing in, 20: 13215(R) (ORNL-3885, pp 3-86)
OSMIUM
spectra of, isotope-displacement effect on arc, (E/T), 20: 13418
OSMIUM ALLOYS
Gd–Os–Y, magnetic and supercooducting ordering in, 20: 13694
Gd–Os–Y, thermal capacity at 0.25 to 20°K, 20: 13694
OXAZOLE, DIPHENYL-
separation from paper chromatograms by acetone elution, 20: 12929
OXAZOLE, 2,2'-*p*-PHENYLENEBIS[5-PHENYL-
separation from paper chromatograms by acetone elution, 20: 12929
OXIDES
properties of sintered metallic, methods for determining, 20: 13319
OXYGEN
determination in sodium by dissolution in ammonia, 20: 12780(T) (ORNL-tr-931)
effects on corrosion of refractory alloys by sodium, (E), 20: 14007(R) (ANL-7122, pp 1-41)
effects on ductility and porosity of welds in tungsten–rhenium–molybdenum alloys, 20: 13251(R) (GEMP-55A, pp 57-82)
effects on effects of chemical sensitizers on radiosensitivity of fruit-spoilage fungi, 20: 13137 (NP-15360)
effects on gas-phase radiolysis of cyclobutane and deuterated cyclobutane, 20: 12894
effects on maize seeds in water at 3 to 45°C, biological, 20: 14216 (BNL-9859)
effects on thermionic emission by tungsten monocrystals, (E), 20: 13432(R) (TID-22419, pp 149-76)
effects on weldability of FS-85 niobium alloy and T-111 and T-222 tantalum alloys, 20: 13264(R) (WANL-PR(P)-008)
neutron inelastic scattering by, gamma spectra from, 20: 13966 (UNC-5140)
radiation effects on evolution of, by chloroplast photoreduction, 20: 12627
radiosensitivity effect on mouse sarcoma cells, x, 20: 12725
radiosensitivity effects on free radical formation in *E. coli*, γ, 20: 12622
reactions with molten uranium–zirconium particles, disintegration properties of, 20: 14169 (AFWL-TDR-64-75)
reactions with uranium carbide, factors affecting, 20: 12925(R) (EURAEC-1446)
reactions with zirconium droplets, flash heating effects on combustion and explosive, 20: 12826 (SC-RR-65-569)
relaxation strength in niobium, anisotropy of Snoek, (E), 20: 13980
thermal conductivity at 1000 to 20,000°K, (T), 20: 13644
uptake by rice, tracer study of, 20: 12592(R) (NP-15671)
yields in radiolysis of carbon dioxide in exchange reactions with oxygen, 20: 12882 (IA-1065)
OXYGEN ISOTOPES O-15
nuclear magnetic moment corrections for, perturbation theory for, 20: 13838
OXYGEN ISOTOPES O-16
energy level transitions of, (E), 20: 13095
energy levels of, shell model calculation for properties of ground state, (T), 20: 13785 (ORNL-TM-1374)
energy levels of, shell model for positive parity, (T), 20: 13844
reactions with nuclei ($176 \leq A \leq 209$), fission fragment energy and mass distributions from, (E), 20: 13861
separation from oxygen-18 by gas chromatography, 20: 12930
OXYGEN ISOTOPES O-17
energy levels from carbon-13 alpha reactions, (E), 20: 13898
nuclear magnetic moment corrections for, perturbation theory for, 20: 13838
OXYGEN ISOTOPES O-18
determination in water, mass spectrometric, 20: 12800
effects on infrared spectra of barium phosphate, 20: 12861
reactions (O-18,xn) with uranium-238, cross sections for, (E), 20: 13889
reactions with plutonium-242, nobelium-256 production in, (E), 20: 13778 (JINR-P-2525)
separation from oxygen-16 by gas chromatography, 20: 12930
OXYGEN SYSTEMS
CdO–Cr_2O_3–O, phase studies on, 20: 13260(R) (NP-15852)
C–O–Pu, phase studies, 20: 13291
Cr_2O_3–MgO–O, phase studies on, 20: 13260(R) (NP-15852)
Cr_2O_3–NiO–O, phase studies on, 20: 13260(R) (NP-15852)
D–O, radiolysis yields in gaseous, 20: 12881 (AD-626609)
O–ThO_2–UO_2, phase studies, 20: 13301
O–V, phase studies on, 20: 13260(R) (NP-15852)
O–W–U, phase studies on, 20: 13235 (BMI-1755)
OZONE
radiation effects on formation of, in flowing and static air, 20: 12885(R) (UCD-34P80-3, pp 59-68)

P

PACIFIC OCEAN
radioactivity from cesium-137, strontium-90, thorium, and thorium-230 off coasts of California and Japan, 20: 13007(T) (NP-tr-1336)
PACKED COLUMNS
design for separating gaseous mixtures, 20: 13161(P)
design for separating gaseous mixtures, 20: 13162(P)
PAINTS
diffusion of tritium from self-luminous, 20: 13153
PALLADIUM
separation from other inorganic ions by paper chromatography, 20: 12939
PANCREAS
radiotherapy of cancer of, using yttrium-90 microspheres, 20: 12738
PARAFFIN
neutron pulse transfer function in, (E/T), 20: 13724
PARTICLE TRACKS
measurement in bubble and spark chambers, systems development for, 20: 13163(R) (ANL-7129)
production by fission fragments in crystals, (E/T), 20: 13984
PEACH BOTTOM POWER REACTOR
fuel conversion ratios and economics for, fission product releasing, 20: 14137(R) (ORNL-3885, pp 236-43)
PEAS
calcium metabolism in *Pisum sativum*, tracer study, 20: 12605
strontium metabolism in *Pisum sativum*, tracer study, 20: 12605
PEBBLE BED REACTOR EXPERIMENT (ORNL)
fluid flow in mockup of, mass transfer and velocity profiles in, 20: 14015 (ORNL-TM-1075)
PEBBLE BED REACTORS
design of Australian HTGCR, 20: 14222(R) (NP-15612)
fluid flow in randomly packed beds of large spheres, mass transfer and velocity profiles in, 20: 14015 (ORNL-TM-1075)
fuel cycle for, evaluation of thorium, 20: 14126 (JUL-276-RG)
PENTANE, 2,2,4-TRIMETHYL-
performance in liquid dielectric ionization chambers for mixed radiation fields, 20: 13107
2,4-PENTANEDIONE, 3,3-DIACETYL-
complexes with cobalt, radiation effects on, annealing of chemical recoil damage in, 20: 12896
PENTANES
performance in liquid dielectric ionization chambers for mixed radiation fields, 20: 13107
radioinduced cracking of, 20: 12908
PERRHENIC ACID
catalytic properties and stability of, 20: 12808
PERSONNEL
hazards to, methods for controlling beryllium, 20: 13016
radiation hazards to, bibliography on, 20: 13002 (JAERI-4034)
radiation monitoring of Japanese, equipment and procedures for, 20: 13003 (JAERI-4035)
PERTECHNETIC ACID
dissociation in solutions, 20: 12808
properties, 20: 12809
PERTURBATION THEORY
formalism for one-particle excitation spectrum in large Bose system, 20: 13559
use in mass difference calculations for elementary particles, 20: 13628
use in weak interactions, limits on, (T), 20: 13622

PETROLEUM
processing of, uses of radioisotopes in, 20: 13155
PHANTOMS
use of body-equivalent water, for dosimetry of x radiation, 20: 12747
PHARMACEUTICALS
purification of iodine-131-labeled, by electrophoresis and chromatography, 20: 12918
PHARYNX
radiotherapy of cancer of, effects on recovery from subsequent surgery of, 20: 12653
PHENOL, AMINO-
effects on radiosensitivity of fruit-spoilage fungi, 20: 13137 (NP-15360)
PHENOLS
labeling with deuterium and tritium by isotopic exchange in alkaline solutions, 20: 12880
PHENOTHIAZINE, 2-CHLORO-10-(3-DIMETHYLAMINOPROPYL)-
effects on morphology of radioinduced pituitary tumors in mice, 20: 12657
PHENYL BORATES
analytical use in reversed-phase chromatography, 20: 12776 (RT/PROT(65)33)
PHENYL ETHER
boiling of, critical heat flux on submerged surfaces during, 20: 12965
biphenyl–phenyl ether, critical heat flux on submerged surfaces during boiling of, 20: 12965
PHONONS
generation of microwave, in dysprosium films, 20: 14003
interactions with electrons in magnetic fields, (E/T), 20: 13925(R) (TID-22419, pp 99-147)
production in electron-magnetic field interactions, (E/T), 20: 13925(R) (TID-22419, pp 99-147)
PHOSPHATE GLASS
performance of silver-activated, for x dosimetry, 20: 13057 (AD-627567)
radiation effects on optical properties of, 20: 13341
PHOSPHATES
effects of dietary, on calcium-45 and strontium-85 retention by rats, 20: 12598(R) (NP-15683)
effects on strontium-85 metabolism by rats, 20: 12606
uptake by cells enzymically isolated from green tobacco leaves, effects of chemicals and temperature on, 20: 14217 (COO-888-43)
PHOSPHINE OXIDE, TRIOCTYL-
analysis and calibration as solvent of, by gas chromatography, 20: 12789
analytical use in reversed-phase chromatographic separations, 20: 12776 (RT/PROT(65)33)
PHOSPHONIC ACID, BUTYL, DIBUTYL ESTER
analysis and calibration as solvent of, by gas chromatography, 20: 12789
PHOSPHONIUM IODIDES
neutron scattering by, low-frequency molecular motions and barrier to rotation in, 20: 12859
PHOSPHORIC ACID
reactions with uranium phosphides, 20: 14008(R) (ANL-7122, pp 42-69)
PHOSPHORIC ACID, BIS(2-ETHYLHEXYL) ESTER
analysis and calibration as solvent of, by gas chromatography, 20: 12789
analytical use in reversed-phase chromatographic separations, 20: 12776 (RT/PROT(65)33)
solvent properties for cerium, 20: 12762 (BNWL-173)
solvent properties for cerium-144 in fission product solutions, 20: 12774 (PG-Report-685)
PHOSPHORIC TRIAMIDE, HEXAMETHYL-
complexes with divalent metals, NMR contact shifts in, 20: 12828 (TID-21587)
PHOSPHORS
preparation of granular coated-particle, incorporating tritium, 20: 12921(P)
separation from paper chromatograms by acetone elution, 20: 12929
use of liquid, for determination of low-energy beta emitters, 20: 12804
PHOSPHORUS
effects of dietary, on calcium-45 and strontium-85 retention by rat skeleton, 20: 12594(R) (NP-15679)
effects of dietary, on calcium-45 and strontium-85 retention by rat skeleton, 20: 12595(R) (NP-15680)
effects of dietary, on calcium-47 and strontium-85 metabolism in rats, 20: 12596(R) (NP-15681)
effects of dietary, on calcium-47 and strontium-85 retention in rat, 20: 12597(R) (NP-15682)
effects of dietary, on strontium-85 retention by rat skeleton labeled *in utero*, 20: 12599(R) (NP-15684)
effects of dietary, on calcium-47 and strontium-85 metabolism and retention by rats, 20: 12600(R) (NP-15685)
effects on photometric determination of uranium in ores using Arsenazo III, 20: 12799
separation from other inorganic ions by paper chromatography, 20: 12939
PHOSPHORUS ISOTOPES P-32
distribution in forest ecosystems after tree inoculation, 20: 12566 (COO-1006-4)
effects on growth of lymph node and thymus cells in culture, 20: 12682
effects on silkworm, frequency of mutagenic, 20: 12692
transport in Douglas-fir forests, 20: 12574
uptake by stomach ulcers, 20: 12742
uptake by stomach cancers, 20: 12742
uptake of superphosphate-incorporated, by rice, 20: 12592(R) (NP-15671)
use for therapy of polycythemia, 20: 12743
PHOTOCHEMISTRY
radiation effects on photoreduction by chloroplasts, 20: 12627
PHOTOELECTRIC EFFECT
cross section calculations for, method for, (T), 20: 13413 (CONF-233 (Vol.4), pp 538-47)
PHOTOGRAPHIC FILM DETECTORS
design of Japanese, 20: 13003 (JAERI-4035)
performance for monitoring medical personnel, 20: 12999 (CEA-R-2746)
performance for x dosimetry, 20: 13057 (AD-627567)
use in Japan for personnel monitoring, 20: 13003 (JAERI-4035)
PHOTOMULTIPLIER TUBES
electron statistics in, models for single, 20: 13096
performance of 56 AVP and XP 1020, for gamma energy determinations, 20: 13100
PHOTONS
detection and measurement using Geiger-Mueller tubes, 20: 13055 (AD-626998)
interactions with protons, meson(π^0) polarization from, (E), 20: 13345(R) (NP-15772)
interactions with carbon, deuteron production in, (E), 20: 13345(R) (NP-15772)
polarization in electron-positron annihilation, covariant formalism for, (T), 20: 13517
reactions with deuterium at 500 to 700 Mev, meson(π^0) production in, (E), 20: 13345(R) (NP-15772)
reactions with heavy nuclei at 200 to 730 Mev, fission fragment spectra from, (E), 20: 13345(R) (NP-15772)
reactions with heavy nuclei, Levinger-Bethe sum rules for dynamical correlations in, (T), 20: 13873
reactions with uranium-238, fission mass-yield curves from, (E), 20: 13345(R) (NP-15772)
scattering by plane slab of matter, transport equation solution for anisotropic multiple, (T), 20: 13968
PHOTOSENSITIVITY
mechanisms in fungal mycelium, 20: 12695
PHTHALIC ACID, OCTYL ESTER
labeling with tritium, Wilzbach method for, 20: 12878
PHYSICAL CONSTANTS TESTING REACTOR
performance of water moderated plutonium fueled, for physics experiments, 20: 14189 (RT/FI(65)43)
PHYSICS
conference on problems in fundamental, 20: 13506
probability in, conditional, 20: 13353
research programs in solid-state, summaries of USAEC, 20: 13182 (TID-4005(Pt.1, 9th Ed.))
temperature averages in statistical, method for calculation of, 20: 13348
PIGMENTS
role in sporogenesis of fungi, 20: 12695
PINCH DEVICES
plasma diagnostics in theta, using double electric probes, (E), 20: 13906 (IPP-1/40)
PIPES
cooldown during liquid hydrogen transport, (E/T), 20: 13668 (LA-3426)
fluid flow in, radiometric determination of spatial concentration of inhomogeneous, (E), 20: 13049
PITUITARY GLAND
radioinduced ablation of, for treatment of acromegaly, 20: 12748
radioinduced ablation of, β, 20: 12753
radioinduced tumors in rat, development histologically of beta, 20: 12652
radioinduced tumors of, after iodine-131-thyroidectomy in mice, 20: 12657
radiotherapy of tumors of, gamma, 20: 12737
PITUITARY HORMONES
determination of thyrotropin content in blood, tracer method for, 20: 12755
labeling with iodine-131, thyrotropin, 20: 12755
radiation effects on production of, 20: 12748
PLACENTA
radiosensitivity of mouse, x, 20: 12650
PLANT CELLS
isolation from bean seedlings and tobacco leaves, enzymic, 20: 14217 (COO-888-43)

uptake of phosphate and rubidium by bean and tobacco, effects of chemicals, light, and temperature on, 20: 14217 (COO-888-43)
PLANT METABOLISM
mechanisms for foliar absorption of nutrients, 20: 14219 (COO-888-47)
PLANT PHYSIOLOGY
tracer study of cambium activity, 20: 12614
PLANTS
aerosol metabolism by, effects on radiation dose to ecosystems, 20: 12607
cambial activity of, tracer study, 20: 12614
carbon-14 contamination of Pacific Proving Ground, 12 years after weapons tests, 20: 12579
cesium-137 content in Colorado forage, 20: 12984
desoxyribonucleic acid synthesis by primary root of *Glycine max*, 20: 14215 (BNL-8643)
fallout uptake by desert, 20: 12572
fallout uptake by Viguiera, in Georgia piedmont, 20: 12985
genetic studies on, applications in breeding programs, 20: 12565
inventory of vascular, in East Tennessee, 20: 12567 (ORNL-TM-1232)
radiation effects on microsporogenesis in sugar beet, x, 20: 12676
radiation effects on chimera stability in, 20: 12632(R) (EUR-2546.f)
radiation effects on populations of *Larrea divaricata*, fission-product, 20: 12670
radiation effects on populations of, review of research on ionizing, 20: 12586
radiation effects on populations of, background, 20: 12587
radioactivity of, growing in areas of high natural radioactivity, 20: 12987
radioinduced tissue softening in, biochemistry and physiology of, 20: 13135 (AD-625483)
radioisotope uptake by, effects of solubility in soils on, 20: 12608
strontium-90 uptake by, effects on food chain contamination, 20: 12607
tritium contamination of Pacific Proving Ground, 12 years after weapons tests, 20: 12579
PLASMA
acceleration by electromagnetic fields, (T), 20: 13911 (JUL-336-PP)
Boltzmann-Vlasov equation for, initial-value problem for, (T), 20: 13910 (JUL-297-MA)
book: *Charged Particle Beam Interactions with Plasma*, 20: 13961
charge carriers in, disintegration and formation of, (E/T), 20: 13952
collision integrals and viscosity of weakly ionized hydrogen–lithium, at 1000 to 10,000°K, (E/T), 20: 13957
containment by dipole magnetic fields, (T), 20: 13928(T) (AD-625070)
current distributions in MHD Hall, (T), 20: 13428 (JAERI-1093)
density variations in Etude, azimuthal, (E), 20: 13915 (MATT-402)
diagnostics of hot, using double electric probes, (E), 20: 13906 (IPP-1/40)
diagnostics of, low-frequency impedance characteristics of Langmuir probe for, (T), 20: 13940
diagnostics of, noncollisional damping in resonances of h-f probe for, (T), 20: 13935
diagnostics of, plane emissive probe for, (E/T), 20: 13934
diagnostics using emission spectra of copper atoms, (E), 20: 13953
diffusion and electric conductivity in strong external magnetic fields, (T), 20: 13938
diffusion and instability of argon, in strong magnetic field, (E), 20: 13943
dispersion diagrams for hot-electron, (E/T), 20: 13925(R) (TID-22419, pp 99-147)
dynamics of, model and numerical technique for, 20: 13960
electric conductivity of argon–potassium oxide, temperature effect on, (E), 20: 13954
electric field modes in Stix coil confined, error in orthogonal assumption for, (T), 20: 13918 (NASA-TN-D-3255)
electromagnetic wave scattering by marginally stable waves of, energy transfer in, (T), 20: 13913 (MATT-317)
electromagnetic wave scattering by ion acoustic waves of, (T), 20: 13914 (MATT-318)
electron densities in, laser interferometer measurement of, 20: 13923(R) (TID-22419, pp 77-84)
electron-beam instability in low-pressure mercury, counter-streaming, (E), 20: 13951
flow velocity optimization in argon–potassium oxide, in MHD generator channel, (T), 20: 13436
gas pressure in magnetic mirror machines, anisotropy of radial neutral, 20: 13907 (IPP-2/42)
heating by electric discharges, magnetic probe measurements in, (E), 20: 13639 (JUL-281-PP)
heating by electron beams in magnetic mirror machines, mirror ratio effect on, (E), 20: 13947(T)
heating by h-f magnetic fields, resonant, (E), 20: 13946(T)
heating by ion cyclotron wave excitation and absorption, (E), 20: 13920(R) (NP-15703, pp 1-51)
heating by ion cyclotron resonance, 20: 13962(P)
heating by stochastic electromagnetic fields, (T), 20: 13948(T)
heating in magnetic mirror machines, (E/T), 20: 13908 (IPP-2/44)
hydromagnetic equations for Vlasov, finite gyro-radius corrections for, (T), 20: 13926 (UCRL-16517)
hydromagnetic oscillations of rotating cylindrical, radial, (T), 20: 13933
ion beam extraction from, current calculations for, (T), 20: 13902 (CEA-R-2898)
kinetics of classical, convergent equation for, (T), 20: 13927 (UCRL-16557)
kinetics of nonequilibrium, balance equations for, (T), 20: 13956
light scattering by, incoherent, (E/T), 20: 13925(R) (TID-22419, pp 99-147)
light scattering by, effect of Coulomb collisions on, (T), 20: 13904 (CLM-R52)
microwave emission at electron cyclotron frequency harmonics, (T), 20: 13903 (CLM-R51)
microwave gyro-interactions in, helical instability from, (E/T), 20: 13959
microwave propagation from slot antennas in, (E/T), 20: 13022(R) (AFCRL-65-859)
neutrino emission from stellar, 20: 13519
oscillations and instabilities in weakly turbulent, (T), 20: 13931(T) (NP-tr-1348)
oscillations in inhomogeneous, operator methods of Vlasov's equation for, (T), 20: 13924(R) (TID-22419, pp 85-98)
oscillations in, Landau damping of longitudinal, (T), 20: 13950
oscillations in, nonlinear mechanics of, (T), 20: 13905 (CONF-651056-1)
production and acceleration of, device for, 20: 13963(P)
production of rare-gas, by fission-fragment ionization, (E/T), 20: 13939
production of, low pressure shock techniques for, (E), 20: 13921(R) (NP-15703, pp 52-63)
properties of alkali–metal, (E), 20: 13432(R) (TID-22419, pp 149-76)
properties of bounded quasistationary, (T), 20: 13912 (LGI-65/21 and App.)
radiation from rotating line charges in, (T), 20: 13958
resonance in laser-induced argon and nitrogen, optical frequency, (E/T), 20: 13942
resonance probes for, susceptance of dipole r-f, (E/T), 20: 13924(R) (TID-22419, pp 85-98)
sheath dynamics, (E/T), 20: 13922(R) (NP-15703, pp 64-81)
shock fronts in electromagnetic tubes, self-luminescence, (E), 20: 13949
shock propagation in argon, microwave reflection technique for, 20: 13936
spectra of argon, at 2500 to 7500 Å, (E), 20: 13955
stability in toroidal discharges, (T), 20: 13929(T) (NP-tr-1340)
stability of cold-cathode discharge, (E/T), 20: 13901 (CEA-R-2822)
stability of helium-discharge, hysteresis effects in helical, (E), 20: 13937
stability of, conservation laws for microscopic, (T), 20: 13909 (IPP-6/40)
striations in positive column of diffuse-mode discharge, in magnetic field, (E/T), 20: 13944
wave production by gap in, interface and surface, (T), 20: 13945
wave propagation along cylindrical column of, magnetic-field effects on resonance of surface, (T), 20: 13941
wave propagation in, properties of hydromagnetic and ion cyclotron, (E/T), 20: 13919(R) (NP-15703)
wave propagation in compressible, effect of boundaries on, (T), 20: 13932
PLASMA JETS
construction of h-f, for growing high-melting crystals, 20: 13189
design, 20: 13963(P)
performance of potassium-seeded, for MHD generators, (E), 20: 13435
production of, design of control device for, 20: 12959(P)
properties of low-density Hall current, (E/T), 20: 13917 (NASA-TN-3250)
PLASTIC COATINGS
radioinduced cross-linking on wires, 20: 12909(P)
PLASTICS
scintillation response of Pilot B to 5- to 1000-kev electrons, (E), 20: 12899
PLATES
stress concentration around cylindrical holes in semi-infinite elastic, (T), 20: 12943 (ANL-7097)
PLATINUM
separation from other inorganic ions by paper chromatography, 20: 12939
sorptive properties for iodine-131 in fission product mixtures, 20: 12772 (ORNL-3840)
PLATINUM ALLOY COUPLES
Pt/Pt–Ru, thermoelectric power to 1600°C, effects of ruthenium content on, 20: 13299
PLATINUM ALLOYS
Pt–Ru, electric conductivity, 20: 13299
Pt–U, phase transformation in, mechanisms of beta-to-alpha, 20: 13307
Pu–U, fabrication of sintered compounds of, 20: 13229(P)
PLATINUM COUPLES

Pt/Pt–Ru, thermoelectric power to 1600°C, effects of ruthenium content on, 20: 13299
PLUTONIUM
criticality effects on center loaded natural uranía fuel rods, (T), 20: 14057 (BNWL-183, Sect.I)
determination in irradiated uranium fuels, isotopic dilution method for, 20: 12811
determination in plutonium tetrafluoride using pyrohydrolysis, 20: 12775 (RFP-601)
determination in solutions, coulometric, 20: 13176(R) (EURAEC-1503)
determination in solutions, methods development for coulometric, 20: 13177(R) (EURAEC-1504)
diffusion in plutonium–uranium alloys at 400 to 550°C, 20: 13313
economics of, as reactor fuels in France, 20: 14105
etching of, electrolytic swab, 20: 13187
fracture of alpha-, effects of temperature on, 20: 13293
ionization around 2000 atm and 5000 to 10,000°K, (T), 20: 14009(R) (ANL-7122, pp 82-90)
microstructure of, effects of pressure and temperature on, 20: 13292
monitoring atmospheric, alarm system for use in, 20: 13122(P)
neutron decay in, pulsed-source measurements of prompt, (E), 20: 14089
neutron kinetics in copper or uranium reflected assemblies of, fast pulsed, (E/T), 20: 14084
processing facility for, criticality control in NUMEC laboratory, 20: 13018
production by electrochemical reduction of plutonium trichloride in molten alkali chlorides, 20: 12816 (BNWL-158)
reactions with graphite crucibles at 1610 to 1650°C, preparation of plutonium monocarbide by, 20: 13208 (ANL-6969)
reactivity in EBWR, (E), 20: 14008(R) (ANL-7122, pp 42-69)
release in nuclear explosions, health hazards from, 20: 13004 (LA-1981 (Rev.))
separation from fission products and uranium in aqueous solutions, process for, 20: 12940(P)
separation from waste solutions, performance of ion exchange resins for, 20: 13177(R) (EURAEC-1504)
x-ray wavelengths of, M, 20: 14059(R) (IDO-17104)
PLUTONIUM ALLOYS
etching of, electrolytic swab, 20: 13187
Al–Pu, analysis for cerium-144 by bis(2-ethylhexyl) phosphate extraction and beta counting, 20: 12774 (PG-Report-685)
Fe–Pu–U, corrosion by air, effects of casting conditions and iron content on, 20: 13200
fissium–Pu–U, radiation effects on, in-pile testing of, (E), 20: 14007(R) (ANL-7122, pp 1-41)
Pu–Th, economics for heavy water reactor fuel cycles, 20: 14117 (BNWL-183, Sect.III)
Pu–Ti–U, phase transformations at 550°C, (E), 20: 14007(R) (ANL-7122, pp 1-41)
Pu–Ti–U, radiation effects on, in-pile testing of, (E), 20: 14007(R) (ANL-7122, pp 1-41)
Pu–U, diffusion of plutonium and uranium in, at 400 to 550°C, 20: 13313
Pu–U, fabrication of fuel rods of, with controlled isotope content, 20: 13214 (EURAEC-1484)
Pu–U–Zr, phase transformations at 550°C, (E), 20: 14007(R) (ANL-7122, pp 1-41)
Pu–U–Zr, radiation effects on, in-pile testing of, (E), 20: 14007(R) (ANL-7122, pp 1-41)
PLUTONIUM CARBIDES
preparation by reaction of plutonium with graphite crucible at 1610 to 1650°C, 20: 13208 (ANL-6969)
PuC–UC, preparation from hydrides, (E), 20: 14008(R) (ANL-7122, pp 42-69)
PuC–UC, radiation effects on fuel elements of, in-pile testing of, (E), 20: 14007(R) (ANL-7122, pp 1-41)
PLUTONIUM(III) CHLORIDES
reduction to plutonium in lithium chloride–potassium chloride eutectic, electrochemical, 20: 12816 (BNWL-158)
PLUTONIUM(IV) FLUORIDES
analysis for fluorine and plutonium using pyrohydrolysis, 20: 12775 (RFP-601)
PLUTONIUM(VI) FLUORIDES
separation from uranium hexafluoride by thermal decomposition to plutonium tetrafluoride, (E), 20: 14008(R) (ANL-7122, pp 42-69)
PLUTONIUM ISOTOPES
determination of fissionable, in presence of thorium and/or uranium, radiometric method for, 20: 12814(P)
PLUTONIUM ISOTOPES Pu-238
processing of, criticality controls for, 20: 14092
PLUTONIUM ISOTOPES Pu-239
criticality-concentration limit for solutions of, effects of boron poisoning on, (T), 20: 13019
energy levels of, parity of ground-state, (E), 20: 13809
fission products of, neutron absorption cross sections for, (E/T), 20: 13748 (AECL-2510)
neutron cross sections at 0.001 to 15 Mev, 20: 13770 (GA-6576)
neutron fission of, fission-fragment yields in, 20: 14059(R) (IDO-17104)
neutron fission rates of, fast, (E), 20: 14202
neutron multiplication factor, 20: 14059(R) (IDO-17104)
photofission at 5.4 to 7.9 Mev, fragment angular distribution anisotropy from, (E), 20: 13809
processing of, criticality controls for, 20: 14092
PLUTONIUM ISOTOPES Pu-240
neutron cross sections at 0.001 to 15 Mev, 20: 13770 (GA-6576)
use in radiometric manometers, 20: 13045
PLUTONIUM ISOTOPES Pu-241
neutron cross sections at 0.001 to 15 Mev, 20: 13770 (GA-6576)
neutron multiplication factor, 20: 14059(R) (IDO-17104)
PLUTONIUM ISOTOPES Pu-242
neutron cross sections at 0.001 to 15 Mev, 20: 13770 (GA-6576)
neutron fission of, yields from, 20: 13752 (ANL-7096)
oxygen-18 reactions with, nobelium-256 production in, (E), 20: 13778 (JINR-P-2525)
PLUTONIUM NITRATES
criticality studies of solutions of, in various container geometries, 20: 14077
PLUTONIUM(IV) NITRATES
criticality concentration limit for solutions of, effects of boron poisoning on, (T), 20: 13019
PLUTONIUM(IV) OXIDES
coating with pyrolytic carbon, deposition parameters for, 20: 13171(R) (BMI-1751)
density and hardness of roasted, effects of moisture content of hydroxide precipitate on, 20: 13177(R) (EURAEC-1504)
density of vibratory compacted pellets of, effects of powder drying and grinding on, 20: 13176(R) (EURAEC-1503)
processing wastes of, performance of Permutit SK resin for, 20: 13176(R) (EURAEC-1503)
reactions with chlorine trifluoride, factors affecting, 20: 12925(R) (EURAEC-1446)
PuO_2–UO_2, density and homogeneity of vibratory-compacted fuel rods of, effects of particle size distribution on, 20: 13177(R) (EURAEC-1504)
PuO_2–UO_2, development as fuel rod, 20: 13176(R) (EURAEC-1503)
PuO_2–UO_2, distribution of plutonia within vibratory compacted pellets of, effects of mixing time on, 20: 13176(R) (EURAEC-1503)
PuO_2–UO_2, equation of state of, 20: 14149(T,R) (ORNL-tr-900)
PuO_2–UO_2, fluorination on fluidized alumina beds, (E), 20: 14008(R) (ANL-7122, pp 42-69)
PuO_2–UO_2, fluorination to hexafluorides, (E), 20: 14008(R) (ANL-7122, pp 42-69)
PuO_2–UO_2, homogeneity of fuel rods of, use of gamma spectrometer for determination of, 20: 13176(R) (EURAEC-1503)
PuO_2–UO_2, oxidation by air, effects of plutonium content and temperature on, 20: 12925(R) (EURAEC-1446)
PuO_2–UO_2, properties of coaxial fuels of, 20: 14102 (BNWL-183, Sect.II)
PuO_2–UO_2, reactivity of water-moderated lattices of, experiments on, 20: 13176(R) (EURAEC-1503)
PuO_2–UO_2, reactivity of water-moderated lattices of, experiments on, 20: 13177(R) (EURAEC-1504)
PuO_2–UO_2, thermal conductivity of vibratory-compacted fuel elements of, effects of filler gas composition and pressure on, 20: 13177(R) (EURAEC-1504)
PuO_2–UO_2–H_2O, criticality studies using pulsed sources, (E), 20: 14078
PLUTONIUM RECYCLE TEST REACTOR
fuel elements for high power density core in, tube power limits for, 20: 14116 (BNWL-177)
PLUTONIUM SUBCRITICAL EXPERIMENT
experimental program for, 20: 14058 (GEAP-4690)
PLUTONIUM SYSTEMS
C–O–Pu, phase studies, 20: 13291
PNEUMATIC SYSTEMS
feasibility for neutron dosimetry in reactors, 20: 13069 (NASA-CR-54468)
PNEUMOCOCCI
radiation effects on genetics in, uv, 20: 12665
POCKET CHAMBERS
design with separate capacitances for charging and integrating currents, 20: 13123(P)
POLARISCOPES
design for double scattering studies, (E), 20: 13899
POLLEN
radiation effects on formation of, in sugar beet plants, effects of ploidy on x, 20: 12676
POLONIUM
photoelectron production cross sections from 0.2 to 2 Mev, (T),

20: 13413 (CONF-233(Vol.4), pp 538-47)
separation from other inorganic ions by paper chromatography, 20: 12939
separation from protactinium by solvent extraction using methyltrioctylammonium chloride, 20: 12937
POLONIUM ISOTOPES Po-210
determination by deposition on nickel and alpha counting, 20: 12785
POLYCYTHEMIA
chemotherapy of, using myleran, 20: 12743
radiotherapy of, using phosphorus-32, 20: 12743
POLYPHENYL SYSTEMS
neutron diffusion length in Santowax R poisoned with boron, thermal, (E), 20: 13718
POLYPHOSPHATES
radioinduced formation of complex, 20: 12902
POLYSACCHARIDES
acid muco-, radiation effects on electrophoretic pattern of, 20: 12756
POPULATIONS
analysis of animal, tracer techniques for, 20: 12583
control of Mediterranean fruit fly, by release of radiosterilized adults, 20: 12633(R) (NP-15348)
control of Mediterranean fruit fly, by release of radiosterilized adults, 20: 12634(R) (NP-15349)
dynamics of *Ambystoma*, 20: 12568(R) (TID-22639)
ecology of *Ambystoma*, 20: 12468(R) (TID-22639)
genetic factors effecting, 20: 12565
radiation effects on human, 20: 12699
radiation effects on chromosomes in Perognathus, chronic-exposure, 20: 12666
radiation effects on *Aedes aegypti*, x, 20: 12668
radiation effects on lizard, chronic-y, 20: 12669
radiation effects on *Larrea divaricata*, fission-product, 20: 12670
radiation effects on animal, 20: 12584
radiation effects on lizard, after gonadal exposure, 20: 12585
radiation effects on plant, review of research on ionizing, 20: 12586
radiation effects on plant, background, 20: 12587
radiation effects on growth of children of Marshall Islands exposed to fallout in 1954, 20: 13011
radioinduced chromosomal polymorphism in Chironomus, background, 20: 12662
PORTLAND CEMENTS
radioactivity determination for low-background counting facilities, 20: 12946 (UCRL-11674)
POSITRON BEAMS
diagnostics in storage rings using synchrotron radiation, 20: 13378
POSITRONIUM
production by positron scattering in teflon, 20: 13468
POSITRONS
annihilation in teflon, effect of crystallinity on angular distributions from, 20: 13468
lifetime in organic compounds, (E), 20: 13499
use for localization of brain tumors after administration of copper-64, 20: 12734 (BNL-9911)
POTASSIUM
corrosion loop development, 20: 13192(R) (NASA-CR-54843)
corrosion loop development, 20: 13193(R) (NASA-CR-54845)
corrosive effects on D-43 niobium alloy at 2450°F, stress-, 20: 13191(R) (NASA-CR-54476)
critical temperature and densities of liquid and vaporous, 20: 12815 (ANL-7025)
determination in sodium loop transfer samples, methods for, 20: 12766 (GEAP-4178)
effects on cesium sorption by montmorillonite, 20: 12873
effects on mass transfer between TZM molybdenum alloy and niobium–1 zirconium alloy at 2000°F, 20: 13192(R) (NASA-CR-54843)
effects on stress-rupture of niobium–1 zirconium at 1400°F, 20: 13191(R) (NASA-CR-54476)
electron band structure of, high-pressure determination of, 20: 14221 (COO-1198-230)
ratio to cesium in animals, effects of age and diet on, 20: 12611
separation from other inorganic ions by paper chromatography, 20: 12939
solvent properties for helium at 704°C, 20: 12827 (TID-21583)
POTASSIUM AZIDES
radioinduced nitrogen free radicals in, EPR spectra of x, 20: 13970 (AD-611432, pp 135-47)
POTASSIUM BROMIDES
radioinduced defects in crystals of, x, (E), 20: 13973(R) (NYO-3033-1)
radioinduced vacancy centers at low temperature, electron- and x-, (E), 20: 13999
$ErBr_3$–KBr, formation in, 20: 12871
POTASSIUM CHLORATES
radiation effects on EPR of, x, 20: 12888
POTASSIUM CHLORIDES
analysis of single crystals of, activation, 20: 12805
color centers in, EPR spectra at 4°K, (E/T), 20: 13975 (TID-21571)
radiation effects on F-center formation in, X, (E), 20: 14000
radioinduced defects in crystals of, x, (E), 20: 13973(R) (NYO-3033-1)
Al–Mg–$MgCl_2$–KCl–NaCl, corrosive effects on steels and tantalum at 500 to 800°C, (E), 20: 14007(R) (ANL-7122, pp 1-41)
Cu–Mg–$MgCl_2$–KCl–NaCl–U, chemical compatibility with vitreous carbon containers at 800°C, (E), 20: 14007(R) (ANL-7122, pp 1-41)
$ErCl_3$–KCl, complex formation in, 20: 12871
POTASSIUM CHROMATES
radiation effects on, from neutron irradiation and chromium-51 labeling, annealing of, 20: 12904
HNO_3–$K_2Cr_2O_7$, corrosive effects on type 304 stainless steel, effects of reactor irradiation on, 20: 13325(R) (GEAP-4968)
POTASSIUM IODIDES
radioinduced luminescence of, at 78°K, effects of thallium doping on, 20: 12891
POTASSIUM ISOTOPES K-39
neutron reactions (n,α) and (n,p) at 4 to 14 Mev, cross sections for, (E/T), 20: 13773 (IKF-13)
nuclear magnetic moment corrections for, perturbation theory for, 20: 13838
POTASSIUM ISOTOPES K-40
determination in water, ultrasensitive system for, 20: 13056 (AD-627000)
uptake by plants in Georgia piedmont, 20: 12985
POTASSIUM ISOTOPES K-42
use for determining action of diuretics in swine, 20: 12613
POTASSIUM ISOTOPES K-43
beta decay of, inhibited, (T), 20: 13837
POTASSIUM ISOTOPES K-45
beta decay of, inhibited, (T), 20: 13837
POTASSIUM OXALATOFERRATES
radiation effects on, effects of water of crystallization on thermal annealing of, 20: 12903
POTASSIUM OXIDES
effects on electric conductivity of argon plasma, (E), 20: 13954
POTASSIUM SILICATE GLASS
preparation and devitrification properties of fuel- and neutron absorbent-bearing, 20: 13209 (ANL-7062)
POTENTIOMETERS
radiation effects on operation of, gamma and neutron, (E), 20: 14170 (EGG-1183-2019)
use in reactor simulators, 20: 14022(P)
POWDER METALLURGY
equipment and methods for, 20: 13230(P)
equipment for loading and compaction of oxide powders in reactor fuel tubes, vibration, 20: 12945 (ORNL-TM-1383)
POWER BREEDER REACTORS
cooling systems for 1000-Mw(e) fast liquid-metal-cooled, stress analysis of piping in, 20: 14120 (COO-1454-1)
development of heavy-water-moderated organic-cooled, using thorium fuel cycle, 20: 14114(R) (BAW-393-2)
development of liquid-metal-cooled, 20: 14149(T,R) (ORNL-tr-900)
neutron spectra in molten-salt, 20: 14127 (JUL-291-RG)
neutron spectra in molten-salt, using beryllium fluoride and sodium fluoride, 20: 14129 (JUL-315-RG)
POWER BURST FACILITY
fuel rod testing in KIWI destructive excursion, 20: 14013(R) (IDO-17123)
POWER PLANTS
economics of conventional, comparison with nuclear power plants, 20: 14133 (NP-15587)
heat exchanger design for MHD, molten-slag, 20: 12971(P)
POWER REACTORS
description and operation of French, 20: 14155
design of Australian HTGCR, 20: 14222(R) (NP-15612)
design of 200-Mw(e) beryllium oxide moderated thorium–uranium fueled, 20: 14122(R) (GA-4451)
development of graphite–gas, in France, 20: 14152
development of, criticality controls for, 20: 14092
economics of heavy-water gas-cooled, 20: 14150
feasibility study of combination desalination-power, for California coast, 20: 14166 (TID-22330(Vol.3))
fuel burnup calculations for sodium-cooled thermal, 20: 14144 (PEL-77)
fuel element testing for superheat, 20: 14125 (GEAP-4898)
fuel elements of British, nondestructive testing of, 20: 14161
temperature transient in loss-of-coolant accidents in, effect of natural convection on, 20: 14147 (UCRL-16394)
POWER SUPPLIES
design of 40- and 400-mamp current generators, 20: 13039
PRASEODYMIUM
determination in glass, emission spectrographic, 20: 12810
separation from other inorganic ions by paper chromatography, 20: 12939
solvent properties for tantalum, 20: 13180(R) (IS-RD-4)
PRASEODYMIUM CHLORIDES

Stark levels of, effects of configuration interaction on, 20: 14005

PRASEODYMIUM COMPLEXES
spectra of, nephelauxetic effect in, 20: 12866
with dilactic, mandelic, and quinic acids, formation and stability constants of, 20: 12817 (IS-1311)

PRASEODYMIUM IONS
energy level interactions in trivalent, 20: 14005

PRASEODYMIUM ISOTOPES Pr-138
decay spectra of, cerium-138 excited states from, (E), 20: 13882

PRASEODYMIUM ISOTOPES Pr-142
decay of, branching ratio for beta and electron-capture, (E), 20: 13797

PRASEODYMIUM OXALATES
thermal decomposition in air and carbon dioxide at 30 to 1100°C, 20: 12862

PRASEODYMIUM OXIDES
preparation by acetic acid leaching, 20: 12874
properties of $PrO_x(1.83 < x < 2.0)$ containing acetate impurity, 20: 12874
$PrO-ZrO_2$, phase studies, 20: 13279

PRECIPITATION, ATMOSPHERIC
cesium-137 content in Colorado, 20: 12984

PRESSURE VESSELS
cladding for, fatigue tests on, 20: 13255 (KAPL-3108)
design of concrete, with liner, 20: 14039(P)
design of prestressed-concrete, 20: 14030
development for reactor containment, 20: 14028 (IITRI-578P22-14)
flange design for, 20: 14049(P)
materials research developments during 1964, summary of, 20: 13184 (TID-11295(Pt.1, 4th Ed.))
stress analysis of cylindrical and spherical, from dynamic and static loadings, 20: 14028 (IITRI-578P22-14)

PRESSURIZED WATER REACTORS
design of heterogeneous self-regulating, heavy water, 20: 14101(P)
fuel cycle cost for, uranium-233–natural uranium, 20: 14117 (BNWL-183, Sect.III)

PROCESS HEAT REACTORS
feasibility study of combination desalination-power, for California coast, 20: 14166 (TID-22330(Vol.3))
use for methanol synthesis in mobile energy depot system, 20: 12877 (BNL-955)
uses of high-temperature, 20: 14165 (ANL-7035)

PROLINE
effects on recovery in x-irradiated Tradescantia, 20: 12728

PROMETHIUM ISOTOPES Pm-147
separation from aqueous solutions by sorption on diatomaceous earth, 20: 12938

PROPANE
meson (μ) and (π) scattering cross sections of, (T), 20: 13480
radioinduced oxidation of, using hydrogen bromide catalyst, yields in gamma, 20: 12883 (ORO-634)

PROPANE, 2-BROMO-2-METHYL-
yields in radioinduced oxidation of isobutane using hydrobromic acid catalyst, 20: 12883 (ORO-634)

PROPANE, 2-METHYL-
radioinduced oxidation of, using hydrogen bromide catalyst, yields in gamma, 20: 12883 (ORO-634)

PROPORTIONAL DETECTORS
performance for accelerator monitoring, 20: 13367 (UCRL-16445(Rev.))
performance of tissue-equivalent, for neutron dosimetry, 20: 13060 (CEA-R-2891)
performance of, coincidence corrections for, (T), 20: 13068 (MLM-1263)
use for neutron detection in concrete-walled laboratory, background determination for, 20: 13714

PROPULSION
ion, development of mercury electron-bombardment and multistrip cesium, 20: 12975

PROSTATE GLAND
zinc uptake by rat, 20: 12601 (TID-22526)

PROTACTINIUM
separation from its decay products by solvent extraction using methyltrioctylammonium chloride, 20: 12937
solvent partition in aqueous and benzene solutions of thenoyltrifluoroacetone, 20: 12832(T) (UCRL-Trans-1244(L))

PROTACTINIUM COMPLEXES
solvent partition in aqueous and benzene solutions of thenoyltrifluoroacetone, 20: 12832(T) (UCRL-Trans-1244(L))

PROTACTINIUM ISOTOPES Pa-231
determination in urine, method for, 20: 12761 (AERE-R-4911)

PROTEINS
radiation effects on DNA crosslinking with, uv, 20: 12621
radiation effects on content of, in mouse liver, automatic determination of, 20: 12782

PROTON BEAMS
effects on majority-carrier density and mobility in n-type germanium, (E), 20: 13977
production of pulsed, ion buncher for, 20: 13379
scattering of polarized, facility for studying at ORIC, (E), 20: 13375

PROTONS
density distribution and energy spectra in inner radiation belt, 20: 13647
distributions in inner Van Allen belts, model for, 20: 13646 (NASA-SP-3024)
emission in compound nuclear reactions, (E), 20: 13897
interactions with mesons (π^-) at high energies, $N^*(1920)$ production in, (T), 20: 13454 (UCRL-14100-T(Rev.1))
interactions with mesons (π^-) at 592 to 1300 Mev, cross sections for, (E/T), 20: 13457 (UCRL-16195)
interactions with mesons (π^-) at 500 to 1300 Mev, charge exchange in, (E), 20: 13458 (UCRL-16209)
interactions with mesons (K^-) at 700 to 1400 Mev/c, differential cross sections for elastic, (E), 20: 13460 (UCRL-16274)
interactions with mesons (K^+) at 0.86 to 1.58 Bev/c, K^* and N^* resonance production in, (E), 20: 13462 (UCRL-16370)
interactions with mesons (K^-), research on, 20: 13463(R) (UCRL-16511, pp 1-53)
interactions with neutrons at 129 and 150 Mev, cross sections for, (E), 20: 13500
interactions with electrons, production of heavy electrons in, (E), 20: 13446 (DESY-65/9)
interactions with neutrons at 600 Mev, meson ($\pi^\pm$) production in, (E), 20: 13453 (JINR-P-2511)
interactions with protons at 655 Mev, meson (π^+) production cross sections for, (T), 20: 13470
interactions with protons, soft-core potential for phase-shift energy dependence in elastic, (T), 20: 13489
interactions with neutrons, soft-core potential for phase-shift energy dependence in elastic, (T), 20: 13489
interactions with neutrons, real part of forward amplitude of, (T), 20: 13493
interactions with antiprotons at 3.0 and 3.6 Bev/c, absorptive model for charge exchange in, (T), 20: 13494
interactions with mesons (π), energy dependence of real part of amplitude of, (T), 20: 13503
interactions with mesons (μ^-), G-parity in rates of capture, (T), 20: 13505
interactions with neutrons and protons, effective ranges in $^1S_0$ states of, (T), 20: 13512
interactions with mesons (K^-) at 1.15 Bev/c, Y_1^* production in, (E), 20: 13518
interactions with mesons (μ^-), calculations using six coupling constants, 20: 13519
interactions with mesons (K^-) at 600 to 850 Mev/c, hyperon (Λ)-meson (π) resonances in, (E), 20: 13522
interactions with mesons (π^-) at 2.01 to 4.95 Bev/c, cross sections and forward dispersion calculations for, (E), 20: 13523
interactions with mesons (π) at 450 Mev, (E), 20: 13524
interactions with mesons (π^-) at 1.03 Bev/c, forward differential cross section for, (E), 20: 13525
interactions with mesons (π^-) at 350 to 800 Mev, (E), 20: 13527
interactions with deuterons, meson (π) production in, (T), 20: 13528
interactions with mesons (π^-) and (π^+), Fubini-Furlan theory for, (T), 20: 13537 (IC/66/8)
interactions with mesons (π), sum rule for amplitudes of, (T), 20: 13571
interactions with mesons (π) and protons, optical model amplitudes for, 20: 13601
interactions with mesons (π^+) at 4.10 and 4.85 Bev/c, elastic, (E), 20: 13471(T)
interactions with meson (μ^-), quantum mechanics of, 20: 13630
interactions with alpha particles and protons in final state of helium-3 (He-3,2p) reaction, (E), 20: 13900
interactions with photons, meson(π^0) polarization from, (E), 20: 13345(R) (NP-15772)
interactions with gamma radiation at 200 to 800 Mev, Compton cross sections for, (E), 20: 13345(R) (NP-15772)
interactions with electrons, meson(π^0) production in, (E), 20: 13345(R) (NP-15772)
mass relative to neutrons, S-matrix theory for, 20: 13511
momentum distribution from (π^-,2N) reactions, (T), 20: 13874
nuclear magnetic resonance spin-lattice relaxation times of, in organic liquids, 20: 12839
production in meson (π)-proton interactions at 450 Mev, (E), 20: 13524
production in meson (μ) inelastic scattering in nuclear emulsions, (E), 20: 13526
reactions (p,γ) with lithium-7 at 0.4 to 2.4 Mev, beryllium-8 single-particle levels from, (E), 20: 13810
reactions (p,γ) with aluminum-27 at 773 kev, silicon-28 internal-pair formation coefficient from, (E), 20: 13843
reactions (p,$\gamma\gamma$) with iron-56 at 1.3 to 1.8 Mev, cobalt-57 levels from, (E),

20: 13857
reactions (p,n) with lithium-6 at 11.6 and 12.6 Mev, beryllium-6 excited states from, (E), 20: 13845
reactions (p,n) with chromium-52 at 14.2 Mev, angular distributions, Q values, and spectra from, (E), 20: 13345(R) (NP-15772)
reactions (p,n) with manganese-55 at 14.2 Mev, angular distributions, Q values, and spectra from, (E), 20: 13345(R) (NP-15772)
reactions (p,n) with iron-56 at 14.2 Mev, angular distributions, Q values and spectra from, (E), 20: 13345(R) (NP-15772)
reactions (p,n) with nickel-58 at 14.2 Mev, angular distributions, Q values, and spectra from, (E), 20: 13345(R) (NP-15772)
reactions (p,n) with selenium-80 at 14.2 Mev, angular distributions, Q values, and spectra from, (E), 20: 13345(R) (NP-15772)
reactions (p,n) with strontium-88 at 14.2 Mev, angular distributions, Q values, and spectra from, (E), 20: 13345(R) (NP-15772)
reactions (p,n) with yttrium-89 at 14.2 Mev, angular distributions, Q values, and spectra from, (E), 20: 13345(R) (NP-15772)
reactions (p,n) with zirconium-90 at 14.2 Mev, angular distributions, Q values, and spectra from, (E), 20: 13345(R) (NP-15772)
reactions (p,n) with zirconium-94 at 14.2 Mev, angular distributions, Q values, and spectra from, (E), 20: 13345(R) (NP-15772)
reactions (p,p') with aluminum-27, cobalt-59, copper-63, nickel, and titanium, (E), 20: 13897
reactions (p,pd) with nuclei, momentum distribution from, (T), 20: 13874
reactions (p,pd) with carbon-12, momentum distribution from, (T), 20: 13874
reactions (p,p'γ) with calcium-40 at 7.5 to 9.6 Mev, energy levels from, (E), 20: 13821
reactions (p,p'γ) with fluorine-19 at 7.5 to 8.5 Mev, spin and M3/E2 mixing ratios for excited levels in, (E), 20: 13822
reactions (p,p'γ) with sulfur-32 at 7.5 to 10.7 Mev, spin and decay modes of excited states from, (E), 20: 13823
reactions (p,pn) with carbon-12 at 50 to 160 Mev, cross sections for, (E), 20: 13833
reactions (p,2n) with odd-Z nuclei at 12 to 14 Mev, conversion electrons from, (E), 20: 13345(R) (NP-15772)
reactions (p,2n) with iodine-127 at 8.7 Mev, conversion electrons from, 20: 13345(R) (NP-15772)
reactions (p,2p) with deuterium at 9.0 and 10.5 Mev, three-nucleon system in, (E/T), 20: 13894
reactions with carbon-13 at 5.0 to 8.1 Mev, nitrogen-14 levels from, (E), 20: 13898
reactions with lithium-7 and tritium at 0.05 to 3.00 Mev, neutron energies from, 20: 13747 (AECD/EP/7)
scattering by aluminum and carbon at 140 Mev, absolute polarization from, (E), 20: 13813
scattering by calcium-40 at 13.065 Mev, energy levels from inelastic, (E), 20: 13821
scattering by carbon-12 at 5.76 to 6.67 Mev, polarization in elastic, (E), 20: 13899
scattering by nickel-58 at 7 Mev, energy levels and cross sections for inelastic, (E), 20: 13858
scattering by zirconium-90 at 18.8 Mev, shell-model analysis of angular distributions from, (E/T), 20: 13866
scattering cross sections for, computer program for calculating, 20: 13774 (JAERI-1096)
sputtering on cadmium and silver at 2 and 300 Mev, (E), 20: 13414 (JUL-304-RW)

PROTOZOA
strontium metabolism in Acantharia, tracer study, 20: 12591(R) (EUR-2475.f)

PSEUDOUREA, 2-(2-AMINOETHYL)-2-THIO-
effects on damages induced in mouse tumors by radiomimetic agents, 20: 12719(R) (NP-15668)
effects on effects of radiomimetic agents in tumor-bearing mice, 20: 12717(R) (NP-15666)
effects on effects of radiomimetic agents in tumor-bearing mice, 20: 12718(R) (NP-15667)
effects on radiation effects on intestinal death in rats, 20: 12721(T) (BNWL-tr-11)
protective effects against radiation damage to bone growth in rats, 20: 12729

PUERTO RICO POWER REACTOR
fuel elements for, inspection of failed, (E), 20: 14141 (ORNL-3910)
startup summary, 20: 14119 (CEND/PRWRA-257)

PULSE ANALYZERS
circuit design for, 20: 13108
design and performance of 100 Mc, 20: 13043
design for γ-γ cascades from neutron capture reactions, 20: 13062 (IEA-96)
design modifications for 512-channel, for time-of-flight analysis, 20: 13097
design of time-selector, for two-dimensional analysis, 20: 13075 (UJV-1450/65)
development for time-of-flight measurements, 20: 13345(R) (NP-15772)
performance with scintillation detectors for particle discrimination, 20: 13110

PULSE COLUMNS
operation of, simulation using analog computer, 20: 14059(R) (IDO-17104)

PULSE GENERATORS (ELECTRONICS)
design of random-time-interval, with repetition rates of 10 to 100,000/sec, (E), 20: 13037
design of 10-Mw, 200-kv, 1- to 2.5-μsec, 20: 13035
development and performance, for coincidence systems adjustment and testing, 20: 13044

PULSE MODIFIERS
design and performance of 100 Mc, 20: 13043
pulse amplitude errors in stretchers, analog-to-digital converter nonlinearity from, 20: 13042

PUMPS (LIQUID METAL)
design and development of high-temperature lithium, 20: 12948

PUPAE
radiation effects on *Aedes aegypti*, x, 20: 12668

PUREX PROCESS
efficiency of, effects of kerosene degradation by nitric acid on, 20: 12934

PYRIDINE
nuclear magnetic resonance spin-lattice relaxation times in, deuteron and proton, 20: 12839

PYRIDINE COMPLEXES
with nickel nitrate, nickel perchlorate, and nickel tetrafluoroborate, properties of, 20: 14225 (TID-21577)

PYRIDOXAL
5-phosphate, protective effects against radiation injuries in dogs, 20: 12645

Q

QUANTUM ELECTRODYNAMICS
field quantities in, geometrical interpretation of, 20: 13662
gauge transformations and inequivalent representations in, 20: 13652
renormalization theory in, using Schwinger equations for Green's functions, 20: 13658

QUANTUM MECHANICS
angular momentum operators in, computer program for calculating, 20: 13648 (ORNL-3877(Rev.))
approximations in, matrix formalism for, 20: 13655
conference on quantum systems with many degrees of freedom, 20: 13649
cosmological foundations of, 20: 13354
Green functions from Lie algebras for systems in, 20: 13661
many-body problem with infinite volume in, 20: 13650
many-body problem in, probability operator in, 20: 13654
many-body systems in, inequivalent representations in field theory for, 20: 13553
measurements in, (T), 20: 13664
Schrödinger equations in complex momentum plane, solutions of, 20: 13653
uncertainty relation between time and energy in, 20: 13657

QUARTZ
energy transformation in, calorimetric measurement of, 20: 13236 (CEA-R-2797)
thermal capacity at 2.15 to 3.8°K, measurement of, 20: 13693
thermal conductivity across interface between copper and, at 1.5 to 4°K, 20: 13693

QUINIC ACID
complexes with lanthanum, rare earths, and yttrium, formation and stability constants of, 20: 12817 (IS-1311)

8-QUINOLINOL
reactions with technetium, 20: 12808

8-QUINOLINOL COMPLEXES
with rhenium and technetium, preparation and properties of, 20: 12808

R

RABBITS
labeling with calcium-45 for population studies, 20: 12583
radioinduced inflammations in, mechanism for x, 20: 12623

RACAH COEFFICIENTS
calculation of, computer program for, 20: 13648 (ORNL-3877(Rev.))

RADIATION
dose to ecosystems, effects of aerosol metabolism by plants on, 20: 12607
dose to plants of, from soils, 20: 12608
dosimetry in Japan, 20: 13003 (JAERI-4035)
effects of background, on Chironomus chromosome, 20: 12662

effects of background, on plant populations, 20: 12587
effects of background, on ecosystems, 20: 12982
effects of ionizing, device for measurement of biological, 20: 13121(P)
effects of reactor, on paraffins, 20: 12908
effects on animals, genetic, 20: 12564
effects on chromosomes in Perognathus, chronic-exposure, 20: 12666
effects on conidia, mycellia, and sclerotia of Botrytis rot on fruits, 20: 13149(R) (UCD-34P80-3, pp 176-89)
effects on cyclobutane and deuterated cyclobutane, 20: 12894
effects on environmental stresses, 20: 12982
effects on gaseous ethylene and nitrous oxide, yields in, 20: 12884(R) (RRL-2310-171)
effects on hexafluoroethane, ESR spectra of fluorinated ethyl radicals during, 20: 12884(R) (RRL-2310-171)
effects on intestinal death in rats, protective effects of AET and cysteamine against, 20: 12721(T) (BNWL-tr-11)
effects on iron perchlorate, transient absorption in, 20: 12884(R) (RRL-2310-171)
effects on liquid argon–ethylene, yields in, 20: 12884(R) (RRL-2310-171)
effects on living organisms and tissues, bibliography on, 20: 12629 (AED-C-04-22)
effects on man, leukemogenic, 20: 12707
effects on man, review on, 20: 12708
effects on mealy-bug cytogenetics, 20: 12715
effects on mice, role of bone marrow cells in immune reactions in, 20: 12716 (AD-626682)
effects on mice, review on recovery from, 20: 12631 (CEA-R-2776)
effects on microörganisms, genetic, 20: 12564
effects on optical properties of glasses, 20: 13341
effects on plant populations, review of research on, 20: 12586
effects on polyethylene, 20: 12905
effects on population ecology in animals, 20: 12584
effects on properties of polyvinyl chloride, 20: 12907
effects on saturated alkanes, scavenging effects of hydriodic acid on, 20: 12884(R) (RRL-2310-171)
effects on stability of carnation chimeras, 20: 12632(R) (EUR-2546.f)
effects on temperature distribution in rotating cylindrical satellite, 20: 13349
effects on testis, pathological, 20: 12686
effects on tumor cells, protective effects of MEA against, 20: 12680
effects on weightless leukocytes, equipment for testing, 20: 12642 (Y-IA-17)
effects on white locus in, Drosophila, mutagenic, 20: 12664
emission by rotating line charge in plasma, (T), 20: 13958
reflection by metals, hardness measurement by, 20: 13054(P)
use in medicine, hazards evaluation for, 20: 12752
uses for density measurements in explosive atmospheres, 20: 13150

RADIATION CHEMISTRY
developments in, annual report of CEA, 20: 14223(R) (NP-15723)

RADIATION DETECTION INSTRUMENTS
alarm system for, 20: 13122(P)
design and performance for fallout monitoring, 20: 12978 (AD-627077)
design for use in radiobiology, 20: 13121(P)
design principles for criticality detection, 20: 13115
development of, 20: 12730

RADIATION DETECTION INSTRUMENTS (COLORIMETRIC)
design using radiochromatic couple suspended in anhydrous translucent matrix, 20: 13125(P)

RADIATION DETECTION INSTRUMENTS (PULSE TYPE)
description of gamma spectrometer with recording instrument, 20: 13086
design and performance of shadow-shielded whole-body, 20: 13074 (SRRC-11/65)
radiation effects on current pulse height in cadmium-sulfide crystal, 20: 13132

RADIATION DETECTORS
apparatus functions for low-accuracy measurements, unfolding of, (T), 20: 13038
performance for accelerator monitoring, 20: 13367 (UCRL-16445(Rev.))
performance for neutrons from 1 to 50 Mev, 20: 13081
performance of mica sandwiches for fission fragment track registration, 20: 13099
response limits of, measurement-time dependence of, (T), 20; 13078

RADIATION INJURIES
pathology of delayed, in mammalian testis, 20: 12686
protection against, using bone marrow grafts in rats, 20: 12651
protection against, using pyridoxal-5-phosphate in dogs, 20: 12645
protection effects of tris(hydroxymethyl) aminomethane against, in cats, 20: 12724
recovery from, effects of biological stress on, 20: 12684
therapy using transplants of hematopoietic tissue, 20: 12731

RADIATION MONITORING
equipment design and performance for, in Japan, 20: 13003 (JAERI-4035)
equipment for alpha, at Saxton plutonium project, 20: 14148(R) (WCAP-3385-5)
equipment for ventilation system, 20: 13006 (ORNL-TM-1384)
equipment for, alarm system for use in, 20: 13122(P)
evaluation of, for medical personnel, 20: 12999 (CEA-R-2746)
instrumentation and methodology for, 20: 12730

RADIATION PROTECTION
bibliography on, in nuclear accidents, 20: 13002 (JAERI-4034)
developments in, annual report of CEA, 20: 14223(R) (NP-15723)
methods and standards in, 20: 13017
methods for patients and personnel, during heart radiography, 20: 12757
methods for, development of, 20: 12730
principles of, review of advanced courses at Harwell on, 20: 12732 (AERE-R-5084)

RADIATION SICKNESS
effects of hydrogen peroxide on, in hypocatalasic guinea pigs, 20: 12643(T) (ANL-Trans-264)

RADIATION SOURCES
activity of, absolute determination of, (T), 20: 13805
electromagnetic momentum from point, complementary moment of, 20: 13576
handling of, design of apparatus for, 20: 12956(P)

RADIATION TARGETS
beta back-scattering by, effects of atomic number on, 20: 13469
design of polarized-proton scattering facility at ORIC, (E), 20: 13375
neutron bombardment of unit spherical, computer program for determining floor-reflected, 20: 13742
scattering from powder-compact, effects of compaction pressure on, 20: 13221
temperature control system for neutron-generator, 20: 13744(P)

RADIO ASTRONOMY
research programs on, 20: 14227(R) (TID-22419)

RADIO WAVES
intensity variations of quasistellar, effect of magnetic bremsstrahlung in variable field on, (T), 20: 13407
propagation of, effects of high-altitude thermonuclear explosions on, 20: 14230(T) (ORNL-tr-972)

RADIOACTIVE MATERIALS
analysis of, equipment for spectrophotometric, 20: 12813(P)
content in atmosphere, effects on health, 20: 13015
distribution of inhaled, review, 20: 12604(T) (JPRS-33958, pp 8-19)
uptake of natural, by plants, 20: 12987

RADIOACTIVITY
decay characteristics of neutron-induced, in soils, 20: 12582
detection limits for, measurement time depeadence of, 20: 13078
monitoring atmospheric, alarm system for, 20: 13122(P)

RADIOBIOLOGY
developments in, annual report of CEA, 20: 14223(R) (NP-15723)
instrument design for, 20: 13121(P)
principles of radiation protection, review of advanced courses at Harwell on, 20: 12732 (AERE-R-5084)
research in ecological, 20: 12570

RADIOCHEMICAL PROCESSING PLANTS
criticality control program in NUMEC Plutonium laboratory, development and administration for, 20: 13018
development of Thorium–Uranium Recycle Facility, 20: 12928(R) (ORNL-3868)
electric conductivity of solutions in, instrument for measuring, 20: 12927 (NP-15756)

RADIOCHEMISTRY
developments in, annual report of CEA, 20: 14223(R) (NP-15723)
research in, using swimming pool reactors, 20: 12914 (IEA-100)

RADIODIAGNOSIS
bibliography on, 20: 12733 (AED-C-10-04)
hazards of, 20: 12752
method for brain tumor, copper-64 positron scanning, 20: 12734 (BNL-9911)
opaque pharmaceuticals for, radiochemical purity control of iodine-131-labeled, 20: 12918

RADIOFREQUENCY GENERATORS
operation in high-Q modes, ion cyclotron resonance in, 20: 13923(R) (TID-22419, pp 77-84)

RADIOGRAPHY
equipment for neutron, Soller-type collimator, 20: 13702 (LA-DC-7594)
gamma, lead screen intensification in, 20: 12974
hazards of diagnostic, 20: 12752
image quality in, effects of screen composition and thickness on, 20: 12973(R) (EURAEC-1519)
methods for inspecting reactor components, 20: 14034
methods for reactor component inspection, 20: 14017 (STI/PUB/105 (Vol.2))
radiation protection of patients and personnel during heart, 20: 12757

RADIOISOTOPES

activity of alpha-emitting, counting methods for determination of, 20: 13066 (JUL-298-PC)
activity of, absolute determination of, (T), 20: 13805
biological importance of soil, factors affecting, 20: 12915
determination of beta-emitting, by scintillation counting in heterogeneous phases with liquid phosphors, 20: 12804
distribution of naturally occurring, in terrestrial ecosystems, 20: 12982
ecological transport of, research in, 20: 12573
environmental contamination by, effects of cosmic spallation on, 20: 12571
gamma scintillation spectroscopy of short-lived, correlation and regression in, (T), 20: 12781
half life of short-lived, proportional counter resolution for determining, (T), 20: 13068 (MLM-1263)
metabolism by plants, effects on radiation dose to ecosystems, 20: 12607
production and use in Australia, 20: 14222(R) (NP-15612)
production of, using swimming pool reactors, 20: 12914 (IEA-100)
uptake by plants of, effects of solubility in soils on, 20: 12608
uses in chemical and petroleum industry, 20: 13155
uses in industry, 20: 14223(R) (NP-15723)

RADIOMETRIC ANALYSIS
method for mixed fissionable nuclides, 20: 12814(P)

RADIOMIMETIC SUBSTANCES
effects of cyclophosphamide and *dl*-sarcolysine on tumor-bearing mice, 20: 12717(R) (NP-15666)
effects on tumor-bearing mice, effects of radioprotective drugs on, 20: 12718(R) (NP-15667)
effects on tumor-bearing mice, effects of radioprotective drugs on, 20: 12719(R) (NP-15668)

RADIOPROTECTIVE COMPOUNDS
effects on damages induced in mouse tumors by radiomimetic agents, 20: 12719(R) (NP-15668)
effects on effects of radiomimetic agents in tumor-bearing mice, 20: 12717(R) (NP-15666)
effects on effects of radiomimetic agents in tumor-bearing mice, 20: 12718(R) (NP-15667)
effects on phage, x, 20: 12617(R) (NP-15863)

RADIOSENSITIVITY
effects of central-nervous-system-stimulating drugs on, in mice, 20: 12685
effects of chemical sensitizers on, of fruit-spoilage fungi, 20: 13137 (NP-15360)
effects of metabolism on, in rats, 20: 12703
effects of pre-irradiation on x, 20: 12701
effects of stress on, in rats, 20: 12703
effects on spermatogenesis in insects, 20: 14224 (TID-21562)

RADIOSTERILIZATION
bibliography on food, 20: 13136 (AED-C-02-06)
effects on appearance, flavor, and texture of cherries, 20: 13141(R) (UCD-34P80-3, pp 48-51)
effects on flavor of peaches exposed when green and ripe, 20: 13147(R) (UCD-34P80-3, pp 92-8)
effects on fruits and vegetables, biochemistry and physiology of tissue-softening, 20: 13135 (AD-625483)
effects on gas exchange in pears, effects of nitrogen atmosphere on, 20: 13140(R) (UCD-34P80, pp 27-47)
effects on incidence of Botrytis rot in strawberries, effects of atmosphere and temperature on, 20: 13139(R) (UCD-34P80-3, pp 9-26)
effects on lemons in nonrefrigerated storage, 20: 13145(R) (UCD-34P80-3, pp 75-83)
effects on manganese content in strawberries, gamma, 20: 13143(R) (UCD-34P80-3, pp 55-7)
effects on niacin and thiamine content in strawberries, gamma, 20: 13142(R) (UCD-34P80-3, pp 52-4)
effects on ripening of bananas, gamma, 20: 13146(R) (UCD-34P80-3, pp 84-91)
effects on shelf life of fruits and vegetables, 20: 13138(R) (UCD-34P80-3)
effects on viability of *Cl. botulinum* spores in canned chopped ham, 20: 13134 (AD-625252)
effects on wholesomeness of prunes, gamma, 20: 13144(R) (UCD-34P80-3, pp 69-74)
effects on wholesomeness of tomatoes, gamma, 20: 13148(R) (UCD-34P80-3, pp 99-175)
use in insect population control, 20: 12633(R) (NP-15348)
use in insect population control, 20: 12634(R) (NP-15349)

RADIOTHERAPY
bibliography on, 20: 12733 (AED-C-10-04)
effects of tumor, on connective tissues, 20: 12756
equipment design for cobalt-60 grid, 20: 13010
hazards of, 20: 12752
hazards of benign tumor, 20: 13013

RADIUM
gamma emissions from, dosimetry of, 20: 13008
separation from protactinium by solvent extraction using methyltrioctylammonium chloride, 20: 12937
uptake by humans living on volcanic intrusions, 20: 12988

RADIUM CHLORIDES
distribution and excretion in rats, 20: 12603(T) (JPRS-33958, pp 1-7)
toxicity in rats, 20: 12603(T) (JPRS-33958, pp 1-7)

RADIUM COMPOUNDS
distribution and excretion in rats, 20: 12603(T) (JPRS-33958, pp 1-7)
toxicity in rats, 20: 12603(T) (JPRS-33958, pp 1-7)

RADIUM ISOTOPES Ra-215
alpha decay, (E), 20: 13779 (JINR-P-2465)

RADIUM ISOTOPES Ra-226
content in foods grown on monazite sands and volcanic intrusions, 20: 12988

RADIUM ISOTOPES Ra-228
content in foods grown on monazite sands and volcanic intrusions, 20: 12988

RADON
separation from protactinium by solvent extraction using methyltrioctylammonium chloride, 20: 12937

RADON ISOTOPES Rn-213
alpha decay, (E), 20: 13779 (JINR-P-2465)

RARE EARTH ALLOYS
phase studies, 20: 13280
properties of, effects of electronic structure on, 20: 13280

RARE EARTH BORATES
crystal structure of vaterite-type, polymorphism in, 20: 12837

RARE EARTH COMPLEXES
spectra of, nephelauxetic effect in, 20: 12866

RARE EARTH IONS
radiation effects on optical centers of trivalent, in crystals of calcium fluoride, 20: 13986(T)

RARE EARTH ISOTOPES
energy levels of, E2 moments for, (T), 20: 13764 (CONF-233(Vol.4), pp 720-2)

RARE EARTH OXIDES
rare earth oxides--ReO_2, preparation and ferromagnetic properties of phases in, 20: 13260(R) (NP-15852)

RARE EARTH SELENIDES
properties of, effects of chemical bond on, 20: 12849

RARE EARTH SULFIDES
properties of, effects of chemical bond on, 20: 12849

RARE EARTH TELLURIDES
properties of, effects of chemical bond on, 20: 12849

RARE EARTHS
determination by spectrometry using 4,5-dihydroxy-3-[(*p*-sulfophenyl)azo]-2,7-naphthalenedisulfonic acid, 20: 12806
determination, effects of atmosphere on emission spectrographic, 20: 12810
energy level transitions in even, E0, (T), 20: 13746 (AD-626681)
separation by reversed-phase chromatography, 20: 12776 (RT/PROT(65)33)
separation from cerium by persulfate oxidation and bis(2-ethylhexyl) phosphate extraction, 20: 12762 (BNWL-173)

RATE METERS
design and performance for fallout monitoring, 20: 12978 (AD-627077)

RATS
cerium-144 deposition in lungs of, effects of carrier on, 20: 12615
effects of chelating agents on toxicity in, 20: 12594(R) (NP-15679)
metabolism and retention of calcium-47 and strontium-85 by, effects of dietary phosphorus on, 20: 12600(R) (NP-15685)
metabolism of calcium-47 and strontium-85 by, effects of dietary phosphorus on, 20: 12596(R) (NP-15681)
physiology of reproductive organs of, 20: 12601 (TID-22526)
radiation effects and/or thermal trauma effects on intestinal mucosa in, 20: 12630 (BNL-8383)
radiation effects on DNA synthesis in liver of, as function of time, 20: 12638 (TID-21474)
radiation effects on reproduction in, following pre- and post-natal exposure, 20: 12640 (TID-22378)
radiation effects on intestinal death in, protective effects of AET and cysteamine against, 20: 12721(T) (BNWL-tr-11)
radiation effects on thermal hemolysis of erythrocytes in, x, 20: 12697
radiation effects on, effects of pre-irradiation on x, 20: 12701
radiation effects on osmotic resistance of leukocytes in, 20: 12705
radiation effects on osmotic resistance of bone marrow cells of, β, 20: 12705
radiation effects on taurine excretion by, γ, 20: 12648
radiation effects on growth of transplanted tumors in, γ, 20: 12651
radiation effects on bone growth in, protective effects of MEG against x, 20: 12729
radiation injuries of tumor-bearing, effects of bone marrow grafts on, 20: 12651
radioinduced tumors in pituitaries of, development histologically of beta,

20: 12652
radiosensitivity of, effects of stress on x, 20: 12703
removal of strontium-85 from, effects of chelating agents on, 20: 12598(R) (NP-15683)
retention of calcium-45 and strontium-85 by skeleton of, effects of phosphorus and strontium in diet on, 20: 12595(R) (NP-15680)
retention of calcium-47 and strontium-85 by, effects of dietary phosphorus on, 20: 12597(R) (NP-15682)
retention of calcium-45 and strontium-85 by, effects of calcium and phosphate in diet on, 20: 12598(R) (NP-15683)
retention of calcium-45 and strontium-85 in skeleton of, effects of dietary phosphorus and strontium on, 20: 12594(R) (NP-15679)
strontium-85 metabolism by, effects of carbonates, magnesium oxide, and phosphates on, 20: 12606
strontium-85 retention by skeleton in female, effects of chelating agents on, 20: 12596(R) (NP-15681)
strontium-85 retention by skeleton labeled *in utero*, effects of dietary calcium and phosphate on, 20: 12599(R) (NP-15684)
terphenyl toxicity in, 20: 12589 (AECL-2507)
zinc uptake by prostate gland of, 20: 12601 (TID-22526)

REACTOR BREEDING BLANKETS
performance of uranium carbide pastes, 20: 14024(R) (APDA-182)

REACTOR BREEDING ELEMENTS
fabrication and testing of depleted uranium slugs for, for EBR-II, 20: 13206 (ANL-6417)

REACTOR COMPONENTS
coolant-temperature monitor for large reactors, testing of, 20: 14025 (DP-944)

REACTOR CONTROL ELEMENTS
actuation of drum, design of pneumatic-nutator motor for, (E), 20: 14029 (NASA-CR-54788)
design for shutdown, 20: 14045(P)
design of floating, for boiling reactors, 20: 14052(P)

REACTOR CONTROL RODS
brake design for, 20: 14043(P)
drive mechanism for, design of pneumatic, 20: 14047
drive winches for EDF-1, 20: 14153
materials for, fabrication and properties of glasses as, 20: 13209 (ANL-7062)
reactivity worth in Saxton criticals, 20: 14148(R) (WCAP-3385-5)
reactivity worth in Swedish reactor FRO, 20: 14178 (AE-207)

REACTOR CONTROL SYSTEMS
electric system for, 20: 14053(P)
motor design for actuating pneumatic nutator in drum-type, (E), 20: 14029 (NASA-CR-54788)
reactivity worths of soluble-boron, 20: 14148(R) (WCAP-3385-5)

REACTOR COOLANTS
bibliography on organic, 20: 14016 (STI/PUB/21/17)
boiling burnout properties of polyphenyl, 20: 14026 (EUR-2299.e)
impurities in sodium, instrumentation development for determining, 20: 14024(R) (APDA-182)
purification at full power, process for, 20: 14051(P)
technology of sodium, 20: 14149(T,R) (ORNL-tr-900)

REACTOR COOLING SYSTEMS
design for swimming pool reactors, 20: 14205(P)
design of emergency, for reactor shields, 20: 14048(P)
flow in, oscillation mechanisms in two-phase, 20: 12962(R) (GEAP-4959)
stress analysis of piping of, in 1000-Mw(e) fast liquid-metal-cooled power breeders, 20: 14120 (COO-1454-1)

REACTOR EXPERIMENTAL FACILITIES
design of pulsed fast reactor, 20: 14096

REACTOR FUEL ELEMENTS
burnup of, gamma spectroscopy for determining, 20: 14158
can design for, finned, 20: 14107(P)
cladding for, eddy current testing of, 20: 14033
cladding materials research developments during 1964, summary of, 20: 13184 (TID-11295(Pt.1, 4th Ed.))
cladding of, economics of nondestructive testing of, 20: 14032
decladding of, fluid-bed fluoride volatility process for, 20: 12923 (ANL-6898)
design of finned pin-cluster, 20: 14108(P)
design of pin-cluster, for improved coolant flow, 20: 14109(P)
design using fuel wedges between concentric tubes, 20: 14112(P)
development for heavy-water-moderated organic-cooled reactor using thorium fuel cycle, 20: 14114(R) (BAW-393-2)
loading arrangement for Saxton tests of, 20: 14148(R) (WCAP-3385-5)
materials for, fabrication and properties of glassy, 20: 13209 (ANL-7062)
preparation and processing, French capacities for, 20: 14105
processing by ion exchange–fluoride volatility, 20: 12940(P)
processing clad uranio, by leach-shear methods, 20: 12928(R) (ORNL-3868)
processing facility for, 20: 14193
production of, costs of uranium losses in, 20: 13212 (CEA-R-2866)
separation of uranium from, fluid-bed fluoride volatility process for, 20: 12924 (ANL-6973)
testing for superheat power reactors, 20: 14125 (GEAP-4898)
testing of boiling, loop design for, 20: 14131 (KR-98)
testing of uranium aluminide, 20: 14059(R) (IDO-17104)
testing of, gamma density gage with amplifier for use in, 20: 13154
testing of, nondestructive methods for, 20: 14017 (STI/PUB/105(Vol.2))
thermal stress distributions in, effect of temperature increment on, 20: 14106
welds of, performance evaluation for, 20: 14196

REACTOR FUEL ELEMENTS (CERAMIC)
burnup of plutonium centered natural urania, (T), 20: 14102 (BNWL-183, Sect.II)
burnup of, nondestructive determination using gamma spectroscopy, 20: 12812
density and homogeneity of plutonia–urania, effects of particle size distribution on, 20: 13177(R) (EURAEC-1504)
design and testing for fast gas-cooled reactors, 20: 14104(R) (ORNL-3885, pp 244-50)
fabrication and properties of thoria–urania, 20: 13207 (ANL-6893)
fabrication of uranium dioxide, by vibratory compaction, 20: 13225
heat transfer properties of, effects of filler gas on, 20: 13176(R) (EURAEC-1503)
performance of Zircaloy-2-clad urania, operated with central melting, 20: 13326 (GEAP-5100C)
reactivity of plutonium center loaded natural urania, (T), 20: 14057 (BNWL-183, Sect.I)
testing of poison-bearing uranium dioxide, 20: 13425(R) (CEND-3107-249)
thermal conductivity of, containing vibratory-compacted powders, effects of filler gas composition and pressure on, 20: 13177(R) (EURAEC-1504)
ultrasonic inspection of uranium, system for, 20: 13318
uranium-235 concentrations in aluminum–uranium, method for determining excess, 20: 14168

REACTOR FUEL ELEMENTS (DISPERSION)
fabrication of plate-type aluminum–urania, for ATR and HFIR, 20: 13217 (ORNL-TM-1377)
testing of aluminum-based plate-type, 20: 14059(R) (IDO-17104)

REACTOR FUEL PINS
corrosion testing of stainless-steel clad EBR-II Mark I, in liquid sodium, (E), 20: 14009(R) (ANL-7122, pp 82-90)
testing of, nondestructive methods for, 20: 14161

REACTOR FUEL PLATES
fabrication of aluminum–urania dispersion, for ATR and HFIR, 20: 13217 (ORNL-TM-1377)

REACTOR FUEL RODS
cans for, mounting end armor on, 20: 14111(P)
criticality parameters of single natural-uranium, in subcritical heavy-water lattices, (T), 20: 14067(R) (MIT-2344-4, pp 80-8)
end cap assembly for sheathed, 20: 14113(P)
end-armor for, method for mounting, 20: 14111(P)
fabrication of, with controlled isotope content, 20: 13214 (EURAEC-1484)
failure of clad uranium dioxide, 20: 14013(R) (IDO-17123)
heat transfer from finned and smooth, boiling, 20: 12961 (GEAP-4786)
radiation effects on pelletized ceramic, 20: 14148(R) (WCAP-3385-5)
testing of PBF, in KIWI destructive excursion, 20: 14013(R) (IDO-17123)

REACTOR FUEL SPHERES
processing of coated graphite, grind-leach method for, 20: 12928(R) (ORNL-3868)

REACTOR FUEL TUBES
loading and compaction of thorium dioxide–uranium dioxide, machine for vibration, 20: 12945 (ORNL-TM-1383)

REACTOR FUELS
analysis of irradiated, for plutonium, 20: 12811
burnup in solid-moderator reactors, compensation of, 20: 14110(P)
burnup of natural uranium, in sodium-cooled thermal power reactors, 20: 14144 (PEL-77)
burnup of uranium, isotopic dilution method for determining, 20: 12811
burnup of, computer program for, 20: 14118 (BNWL-183, Sect.IV)
cycle costs for high temperature gas-cooled reactors, 20: 14137(R) (ORNL-3885, pp 236-43)
cycle development for heavy-water-moderated organic-cooled reactors using thorium, 20: 14114(R) (BAW-393-2)
development for pebble-bed reactors, 20: 14222(R) (NP-15612)
economics in Germany, 20: 14130 (KFK-366)
economics of plutonium–thorium for heavy water reactors, 20: 14117 (BNWL-183, Sect.III)
economics of uranium-233–natural uranium for PWR, 20: 14117 (BNWL-183, Sect.III)
economics of, in France, 20: 14105
fabrication of ceramic, carbon-coated particulate, 20: 13215(R) (ORNL-3885, pp 3-86)

fission gas diffusion from evaporating, 20: 13336
fission product release from pyrolytic carbon coated ceramic, 20: 13261(R) (ORNL-3885, pp 87-149)
fission-product distribution in irradiated, 20: 14059(R) (IDO-17104)
grinding graphite-base, evaluation of ball-milling for, 20: 13218 (ORNL-TM-1412)
materials research developments during 1964, summary of, 20: 13184 (TID-11295(Pt.1, 4th Ed.))
performance of thorium, 20: 14126 (JUL-276-RG)
preparation and processing, French capacities for, 20: 14105
preparation of compacted, using plutonium–uranium alloy powder, 20: 13229(P)
preparation of dense, sintered uranium dioxide, 20: 13228(P)
preparation of particulate carbon-coated, fluidized-bed process for, 20: 12875(P)
processing irradiated, by chlorine trifluoride volatilization, 20: 12925(R) (EURAEC-1446)
processing of irradiated, analysis of organic solvents used in, 20: 12789
processing of, criticality controls for, 20: 14092
production of, costs of uranium losses in, 20: 13212 (CEA-R-2866)
research programs, summaries of USAEC, 20: 13183 (TID-6506(Pt.2, 3rd Ed.))
separation of neptunium and uranium from, flowsheets for, 20: 12926 (IDO-14669)
testing of irradiated, nondestructive methods for dimensional and flaw, 20: 13343

REACTOR MATERIALS
development and testing of refractory, for liquid-metal reactors, (E), 20: 14007(R) (ANL-7122, pp 1-41)
development for pebble-bed reactors, 20: 14222(R) (NP-15612)
research developments during 1964, summary of, 20: 13184 (TID-11295 (Pt.1, 4th Ed.))
research programs, summaries of USAEC, 20: 13183 (TID-6506(Pt.2, 3rd Ed.))

REACTOR MATRICES
cell design for, 20: 14050(P)
experiments on water-moderated, plutonia-enriched urania lattices, 20: 13176(R) (EURAEC-1503)
experiments on water-moderated plutonia-enriched urania lattices, 20: 13177(R) (EURAEC-1504)
neutron capture in boron-bearing slab, (E/T), 20: 14063 (KAPL-M-6528)
neutron diffusion parameters and multiplication constants in beryllium oxide–natural uranium lattices, pulsed, (E/T), 20: 14080
neutron spectra in, use of pulsed sources for measuring, (E/T), 20: 13735
reactivity measurements in aluminum–uranium dioxide–zirconium hydride lattices, pulsed-source, (E), 20: 14082
reactivity of plutonia–urania, effects of boronated water slots on, 20: 14148(R) (WCAP-3385-5)
reactivity of variable-pitch subcritical enriched uranium–water, kinetic and steady-state measurements of, (E/T), 20: 14079

REACTOR MODERATORS
bibliography on organic, 20: 14016 (STI/PUB/21/17)
materials research developments during 1964, summary of, 20: 13184 (TID-11295(Pt.1, 4th Ed.))
neutron spectra in, use of pulsed sources for measuring, (E/T), 20: 13735
support structure for vertically stacked, 20: 14044(P)

REACTOR SAFETY
analysis for Saxton partial-plutonium core II, 20: 14148(R) (WCAP-3385-5)
analysis of maximum credible accident in HWCTR, 20: 14183 (DP-1037)
containment vessels for, design of, 20: 14031
criticality control for, properties of, 20: 13005 (LA-3366)
program for, French, 20: 14018
radioactivity release and deposition from testing of Kiwi B4, 20: 14172 (LA-3397)
studies for sodium-cooled power-breeder reactors, 20: 14149(T,R) (ORNL-tr-900)
system design for electric, 20: 14053(P)
temperature transient in loss-of-coolant accidents, effect of natural convection on, 20: 14147 (UCRL-16394)

REACTOR SAFETY EXPERIMENTS
component displacements in KIWI-TNT, 20: 14171 (LA-3388)
operations of TREAT, (E), 20: 14009(R) (ANL-7122, pp 82-90)
pressure pulses from fuel rod failure in Capsule Driver Core in SPERT IV, 20: 14013(R) (IDO-17123)

REACTOR SHIELDING
cooling system design for, emergency, 20: 14048(P)
design for gas-cooled, graphite-moderated reactors, 20: 14037(P)

REACTOR SIMULATORS
design, 20: 14022(P)
operation, 20: 14222(R) (NP-15612)

REACTOR SLURRIES
performance of uranium carbide, for fast breeder reactors, 20: 14024(R) (APDA-182)

REACTOR TUBES
fabrication of concentrically spaced, method for, 20: 13231(P)
power limits for PRTR high power density core, 20: 14116 (BNWL-177)
testing of thin-walled, eddy current, 20: 14033
testing of, economics of nondestructive, 20: 14032

REACTORS
component inspection of, nondestructive methods for, 20: 14034
containment structures for, design and evaluation of, 20: 14028 (IITRI-578P22-14)
containment vessels for, design of, 20: 14031
control device for, design of shutdown, 20: 14045(P)
control of, time-optimal system for, 20: 14020
coolant-temperature monitor for large, testing of, 20: 14025 (DP-944)
core restraint system for, design of, 20: 14038(P)
core structure design, 20: 14042(P)
criticality control in, properties of, 20: 13005 (LA-3366)
criticality controls for, 20: 14092
development at ANL, 20: 14006(R) (ANL-7122)
gamma flux determination in, isotopic exchange method for, 20: 14012 (IA-1048)
heat exchange processes in, optimal control of, 20: 14020
instrumentation for, incorporation in pressure vessel, 20: 14040(P)
interactions of coupled, infinite-slab calculations of, (T), 20: 14008(R) (ANL-7122, pp 42-69)
kinetics equations for, validity of point, 20: 14013(R) (IDO-17123)
kinetics of computer programs for analysis of, 20: 13163(R) (ANL-7129)
kinetics of large, spatial, 20: 14071(R) (RL-SA-45A and Suppl.)
kinetics of, ARC system for computer analysis of, (E), 20: 14008(R) (ANL-7122, pp 42-69)
kinetics of, computer program for analysis of, 20: 14055 (AEEW-R-445)
loading of, design of transfer system for, 20: 14036(P)
neutron diffusion in inhomogeneous, (E/T), 20: 13705(R) (MIT-2344-4, pp 135-44)
neutron diffusion in, computer program for, 20: 14056 (AWRE-O-99/65)
neutron dosimetry in, using pneumatics, 20: 13069 (NASA-CR-54468)
neutron flux measurements in, instrumentation incorporated in pressure vessel wall for, 20: 14040(P)
neutron flux measurement in, deuterium-containing probe for, 20: 13119(P)
neutron flux stability in zenon-135 containing, computer program for, 20: 14061 (IDO-17127)
neutron kinetics in, computer program for, 20: 14064 (LA-3427)
neutron kinetics of, computer program for, 20: 14060 (IDO-17114)
operation of CEA, outline of, 20: 14223(R) (NP-15723)
reactivity of plutonium-fueled, beryllium oxide–zirconium hydride effects on, 20: 14122(R) (GA-4451)
reactivity of, pulsed neutron source methods for determining, (T), 20: 14075
reactivity period circuit for, design of reciprocal, 20: 14095(P)
seals for, design of fluid-tight, 20: 12949(P)

RECOIL IONS
production in silicon-28 (n,α) and (n,p) reactions, ionization defects from, (E), 20: 13989

REFRACTORY MATERIALS
fabrication of hard dense, hot-pressing method and apparatus for, 20: 13230(P)
growth of high-melting crystals of, using h-f plasma burners, 20: 13189
vapor pressure of, design of thermobalance for measuring, 20: 13029 (LA-3423)

RELATIVITY THEORY
electromagnetic and gravitational fields in, nonlocal, 20: 13663
formulation of general, two-component spinors in Hamiltonian, 20: 13660

REMOTE-CONTROL EQUIPMENT
design for spectrophotometric analysis of radioactive solutions, 20: 12813(P)
design of manipulator arm, 20: 12958(P)
sealing and shielding of hot-cell, 20: 12953(P)

REPTILES
radiation effects on growth in lizard, chronic-γ, 20: 12669
radiation effects on populations of lizard, x, 20: 12585

RESEARCH REACTORS
criticality controls for, 20: 14092
design and use of pulsed, 20: 14191(T) (BNL-tr-60)
experimental facilities for WWR-S, design and operation of corrosion loop, 20: 14190 (UJV-1446/65)
fuel elements of JRR-3, ultrasonic testing of, 20: 14194
fuel elements of JRR-3, performance of end-plug welds of, 20: 14196
gamma flux determination in LRR-1, isotopic exchange method for, 20: 14012 (IA-1048)
neutron effective resonance integrals in MITR, effects of fuel/moderator ratio on, (E), 20: 14186(R) (MIT-2344-4, pp 145-8)
neutron leakage and return fluxes in MIT, (E), 20: 14070(R) (MIT-2344-4, pp 115-34)

performance of PULSTAR, transient characteristics of, 20: 14203
reactivity temperature coefficient measurement for TRIGA, 20: 14188 (RT/FI(65)40)
status of Harmonie, 20: 14149(T,R) (ORNL-tr-900)
RESINS
performance for plutonium recovery from waste solutions by ion exchange, 20: 13177(R) (EURAEC-1504)
RESISTORS
design of boron thermistors for thermal neutron flux measurements, 20: 13126(P)
RESPIRATORY TRACTS
radioactive particle sorption by, review, 20: 12604(T) (JPRS-33958, pp 8-19)
RHENIUM
properties and uses of, review on, 20: 13266(T) (AD-624905)
separation from other inorganic ions by paper chromatography, 20: 12939
RHENIUM ALLOY COUPLES
Re–W/Re–W, emf vs temperature for thermocouples of, 20: 13028 (KAPL-M-6498)
RHENIUM ALLOYS
properties and uses of, review on, 20: 13266(T) (AD-624905)
Mo–Re, electric and thermal conductivity of superconducting, critical field measurements from, (E), 20: 13686
Mo–Re–W, fabrication process development, 20: 13251(R) (GEMP-55A, 20: 13251(R) (GEMP-55A, pp 57-82)
Mo–Re–W, phase diagrams for transmutation studies, electron-concentration, 20: 13251(R) (GEMP-55A, pp 57-82)
Mo–Re–W, weld integrity of, effects of carbon and oxygen on, 20: 13251(R) (GEMP-55A, pp 57-82)
Re–W, age-hardening properties of, 20: 13251(R) (GEMP-55A, pp 57-82)
Re–W, creep rupture properties at 2000°C of arc-cast, 20: 13249(R) (GEMP-55A, pp 29-53)
Re–W, creep rupture properties at 2000°C, effects of annealing at 2400°C on, 20: 13249(R) (GEMP-55A, pp 29-53)
Re–W, powder preparation by hydrogen reduction of volatile fluorides, 20: 13181 (K-L-6076)
Re–W, scrap recovery by fluoride volatility process, economics and technology of, 20: 13181 (K-L-6076)
Re–W, thermocouple insulators for, at 2450°C, properties of calcium oxide as, 20: 13250(R) (GEMP-55A, pp 56-6)
RHENIUM CHLORIDES
with 8-quinolinol, preparation and properties of, 20: 12808
RHENIUM OXIDES
Dy_2O_3–ReO_2, preparation and ferromagnetic properties of phases in, 20: 13260(R) (NP-15852)
Er_2O_3–ReO_2, preparation and ferromagnetic properties of phases in, 20: 13260(R) (NP-15852)
Ho_2O_3–ReO_2, preparation and ferromagnetic properties of phases in, 20: 13260(R) (NP-15852)
Nd_2O_3–ReO_2, preparation and ferromagnetic properties of phases in, 20: 13260(R) (NP-15852)
rare earth oxides–ReO_2, preparation and ferromagnetic properties of phases in, 20: 13260(R) (NP-15852)
ReO_2–Sm_2O_3, preparation and ferromagnetic properties of phases in, 20: 13260(R) (NP-15852)
ReO_2–Y_2O_3, preparation and ferromagnetic properties of phases in, 20: 13260(R) (NP-15852)
RHODIUM
electron secondary emission from thin foils of, (E), 20: 13103
separation from other inorganic ions by paper chromatography, 20: 12939
RIBONUCLEIC ACID
methylases of base-specific t-, effects of uv-induced phage induction on *E. coli* content, 20: 12619
RIBONUCLEIC ACID, DESOXY-
effects of hydroxylamine on phage, 20: 12617(R) (NP-15863)
effects on transforming DNA, inactivating, 20: 12620
enzymatic inactivation of transforming, 20: 12620
radiation effects on synthesis of, in rat liver as function of time, 20: 12638 (TID-21474)
radiation effects on protein crosslinking with, uv, 20: 12621
radioinduced inactivation of transforming, effects of physical properties on uv and x, 20: 12620
sonic inactivation of transforming, 20: 12620
synthesis in primary root of *Glycine max* seedlings, 20: 14215 (BNL-8643)
RICE
nitrogen uptake by, tracer study of fertilizer, 20: 12592(R) (NP-15671)
nitrogen uptake by, effects of amount and time of fertilizer application on, 20: 12593(R) (NP-15672)
phosphorus uptake by, tracer study of fertilizer, 20: 12592(R) (NP-15671)
radionuclide contamination of Po Valley, effects of irrigation on, 20: 12986
ROCKET REACTORS (KIWI)
component displacements in KIWI-TNT, 20: 14171 (LA-3388)
control drum actuation in, design of pneumatic-autator motor for, (E), 20: 14029 (NASA-CR-54788)
radiation effects on resistance-temperature transducers for NERVA, 20: 13127 (CONF-651101-61)
radioactivity release and deposition from testing of B4, 20: 14172 (LA-3397)
ROCKS
lead isotope ratios in, age estimation from, 20: 12991
radioactivity of foods grown on Brazilian volcanic intrusive, 20: 12988
RODS
heat transfer in parallel arrays of, solutions for turbulent flow with, (T), 20: 12967
ROLLING MILLS
thickness measurements using gamma beams in, 20: 13151
ROOTS
desoxyribonucleic acid synthesis in primary, of *Glycine max* seedlings, 20: 14215 (BNL-8643)
tracer techniques for studying, iodine-131, 20: 12581
ROSE BENGAL
purification of iodine-131-labeled, by electrophoresis and chromatography, 20: 12918
separation of iodine-131-labeled, method for chromatographic, 20: 12763 (CNEA-162)
RUBIDIUM
alpha reactions (α,xn) with, yttrium-87 production in, 20: 12917
critical temperature and densities of liquid and vaporous, 20: 12815 (ANL-7025)
electron band structure of, high-pressure determination of, 20: 14221 (COO-1198-230)
heat transfer properties, 20: 13232 (AGN-8162)
permeation through cuticular membranes of fruits and leaves, effects of urea on, 20: 14218 (COO-888-44)
separation from other alkali metals by ion exchange using vanadium ferrocyanide, 20: 12932
separation from other inorganic ions by paper chromatography, 20: 12939
thermophysical properties, 20: 13232 (AGN-8162)
uptake by cells enzymically isolated from bean seedlings, effects of chemicals, light, and temperature on, 20: 14217 (COO-888-43)
uptake by cells enzymically isolated from green tobacco leaves, effects of chemicals, light and temperature on, 20: 14217 (COO-888-43)
RUBIDIUM AZIDES
radioinduced nitrogen free radicals in, EPR spectra of x, 20: 13970 (AD-611432, pp 135-47)
RUBIDIUM CARBONATES
reactions with zirconium dioxide at 870 to 950°C, 20: 12851
RUBIDIUM CHLORIDES
$ErCl_3$–RbCl, complex formation in, 20: 12871
RUBIDIUM ISOTOPES Rb-86
distribution in forest ecosystems after tree inoculation, 20: 12566 (COO-1006-4)
transport in Douglas-fir forests, 20: 12574
RUBIDIUM ISOTOPES Rb-87
content in iron meteorites, 20: 12992
RUBIDIUM SILICATES
reactions with zirconium dioxide at 870 to 950°C, 20: 12851
RUPTURE
mechanics of, for engineering structures, 20: 13248 (GEAP-4678)
RUTHENIUM
determination using 1-nitroso-2-naphthol, spectrophotometric, 20: 12788
thermal capacity of superconducting, at 0.27 to 1.2°K, 20: 13694
RUTHENIUM ALLOY COUPLES
Pt/Pt–Ru, thermoelectric power to 1600°C, effects of ruthenium content on, 20: 13299
RUTHENIUM ALLOYS
Pt–Ru, electric conductivity, 20: 13299
RUTHENIUM ISOTOPES Ru-95
internal conversion electron spectra from (α,n) reactions with molybdenum-92, (E), 20: 13881
RUTHENIUM ISOTOPES Ru-97
decay of isomeric states in, (E), 20: 13881
RUTHENIUM ISOTOPES Ru-101
internal conversion electron spectra from (α,n) reactions with molybdenum-98, (E), 20: 13881
RUTHENIUM ISOTOPES Ru-103
separation from aqueous solutions by sorption on diatomaceous earth, 20: 12938
RUTHENIUM ISOTOPES Ru-106
content in Po Valley rice, effects of crop irrigation on, 20: 12986
separation from aqueous solutions by sorption on diatomaceous earth, 20: 12938
uptake by plants in Georgia piedmont, 20: 12985
volatility of, in radioactive alumina calcine during high-temperature

storage, 20: 14207 (IDO-14670)

S

SALAMANDERS
migratory behavior of *Ambystoma*, 20: 12568(R) (TID-22639)
SALMONELLA
radiation effects on, effects of colicine factor on uv, 20: 12677
SAMARIUM
determination by spectrometry using 4,5-dihydroxy-3-[(*p*-sulfophenyl)azo]-2,7-naphthalenedisulfonic acid, 20: 12806
determination in aqueous solutions, effects of sodium tungstate on spectrofluorometric, 20: 12787
determination in glass, emission spectrographic, 20: 12810
neutron absorption by, gamma spectra from, 20: 13966 (UNC-5140)
reactions with samarium oxide in silica capsules, formation of samarium silicates by, 20: 13260(R) (NP-15852)
separation from other inorganic ions by paper chromatography, 20: 12939
solvent properties for tantalum, 20: 13180(R) (IS-RD-4)
SAMARIUM BORATES
crystal structure of vaterite-type, polymorphism in, 20: 12837
SAMARIUM COMPLEXES
with dilactic, mandelic, and quinic acids, formation and stability constants of, 20: 12817 (IS-1311)
SAMARIUM OXIDES
preparation of divalent, 20: 13260(R) (NP-15852)
reactions with samarium in silica capsules, formation of samarium silicates by, 20: 13260(R) (NP-15852)
$BaO–Sm_2O_3$, optical properties of compounds formed in, 20: 13278
$ReO_2–Sm_2O_3$, preparation and ferromagnetic properties of phases in, 20: 13260(R) (NP-15852)
$Sm_2O_3–SrO$, optical properties of compounds formed in, 20: 13278
SAMPLING
equipment for air, calibration facility for, 20: 13077 (Y-1503)
SAN ONOFRE POWER REACTOR
design features, 20: 14157
SAP (SINTERED ALUMINUM PRODUCTS)
electric conductivity, effects of alumina content on, 20: 13306
phase transformations in, effects of liquid aluminum on alumina, 20: 13296
properties and technology of aluminum–aluminum oxide, 20: 13213 (EUR-2447.f)
properties of, methods for determining, 20: 13319
thermal conductivity, effects of alumina content on, 20: 13306
SARCOMAS
effects of lympho-, on tuberculosis incidence in Hiroshima, 20: 12639 (TID-21517)
radiation effects on cell survival in mouse, effects of oxygen inhalation on x, 20: 12725
SATELLITES
radiation effects on temperature distribution in rotating cylindrical, 20: 13349
SAVANNAH RIVER COMPONENTS TEST REACTOR
safety analysis of maximum credible accident in, 20: 14183 (DP-1037)
SAXTON POWER REACTOR
reactivity tests and zero power experiments with core II of, 20: 14148(R) (WCAP-3385-5)
SCANDIUM
magnetic susceptibility of, pressure effects on, (E), 20: 13312(T)
separation from other inorganic ions by paper chromatography, 20: 12939
SCANDIUM ISOTOPES Sc-41
nuclear magnetic moment corrections for, perturbation theory for, 20: 13838
SCANDIUM ISOTOPES Sc-45
helium-3 reactions (He-3,d) at 24.4 Mev, momentum spectra from, (E), 20: 13345(R) (NP-15772)
SCANDIUM ISOTOPES Sc-47
metabolism and fecal excretion by man after intravenous and oral administration, 20: 12612
SCANDIUM ISOTOPES Sc-49
energy levels from helium-3 reactions (He-3,d) with calcium-48 at 12 Mev, (E), 20: 13854
SCANDIUM OXIDES
$BaO–Sc_2O_3$, optical properties of compounds formed in, 20: 13278
$Sc_2O_3–SrO$, optical properties of compounds formed in, 20: 13278
SCATTERING
amplitudes at high momentum transfers, asymptotic behavior of, (T), 20: 13546 (JINR-P-2519)
amplitudes for many-body, discontinuity equations for, (T), 20: 13531 (IC/65/17)
amplitudes in, axiomatic quantum field theory for, 20: 13565
amplitudes in, impact parameter formalism for, 20: 13610
amplitudes in, optical models for, 20: 13601
amplitudes of, unitarity condition for analytic properties of, 20: 13631
Feynman diagrams in, analytic property of fifth-order, 20: 13593
matrix for nonrelativistic spin-dependent, analytic properties of, 20: 13633
matrix for, inversion of R, (T), 20: 13538 (IDO-17142)
potentials in, approximations of Regge, 20: 13603
potentials in, eigenvalues of Lippmann-Schwinger kernel for Yukawa and nucleon-nucleon, (T), 20: 13836
potentials in, kernels of non-local, (T), 20: 13586
S-matrix for low-energy, threshold poles for, 20: 13588
S-matrix in, conditions of macroscopic causality for, (T), 20: 13539 (JINR-E-2500)
theory for multiparticle, projection operators in unified, 20: 13850
theory for, research on, 20: 13463(R) (UCRL-16511, pp 1-53)
theory of multiple, 20: 13163(R) (ANL-7129)
SCINTILLATION DETECTORS
design and performance of shadow-shielded whole-body, 20: 13074 (SRRC-11/65)
development of ultrasensitive, for ocean monitoring, 20: 13056 (AD-627000)
efficiency for neutrons in Bev range, 20: 13109
efficiency for x-ray counting, (E), 20: 13092
performance in anti-Compton, gamma spectrometers, 20: 13098
performance of large-volume liquid-organic, for gamma radiation, 20: 13079
performance of liquid-organic, for beta particles, effect of added sodium naphthylamine sulfonate on, 20: 13080
performance of lithium-6-glass, for neutron counting, (E), 20: 13090
performance of thallium-activated sodium iodide, for gamma spectroscopy, 20: 13067 (JUL-308-RB)
pulse timing for, optimum filter for, 20: 13104
SEA URCHINS
radiation effects on sulfhydryl groups in eggs of, thermal and uv, 20: 12624
SEA WATER
analysis for nickel-63, liquid scintillation method for, 20: 12779 (USNRDL-TR-924)
desalination of, feasibility of nuclear plant for, 20: 14166 (TID-22330(Vol.3))
radiation processing of, effects on fish, 20: 13152
radioactivity measurements in, detector for, 20: 13056 (AD-627000)
SEALS AND GLANDS
design for hot-cell wall apertures, 20: 12953(P)
design of fluid-tight, for movable parts, 20: 12949(P)
SEED
effects of gases at 3 to 45°C on maize, biological, 20: 14216 (BNL-9859)
radiation effects on germination of conifer, gamma, 20: 12671
SEEDLINGS
desoxyribonucleic acid synthesis by primary root of *Glycine max*, 20: 14215 (BNL-8643)
radiation effects on survival of conifer, gamma, 20: 12671
radiation effects on pine, effects of water stress on γ, 20: 12674
rubidium uptake by isolated cells of bean, effects of chemicals, light, and temperature on, 20: 14217 (COO-888-43)
SELENIUM
neutron resonance absorption integral of, (E), 29: 14008(R) (ANL-7122, pp 42-69)
separation from other inorganic ions by paper chromatography, 20: 12939
SELENIUM ISOTOPES Se-80
proton reactions (p,n) at 14.2 Mev, angular distributions, Q values, and spectra from, 20: 13345(R) (NP-15772)
SEMICONDUCTOR DETECTORS
design and performance of silicon, for charged particle identification, 20: 13076 (UR-875-117)
design of thick-depletion-zone p-n type, for neutrons, 20: 13116(P)
fabrication and performance of thick-surface-barrier, 20: 13093
fabrication of lithium-drifted germanium, 20: 13058 (AD-627930)
fabrication of surface barrier, technique for, 20: 13072 (RT/EL(65)7)
performance of lithium-drift germanium, for gamma rays, 20: 13095
performance of silicon, for neutron total cross section measurements, 20: 13101
use of single crystals of cadmium telluride in gamma spectrometers, 20: 13073(R) (SAN-549-1)
SEMICONDUCTORS
electron band structure of, high-pressure determination of, 20: 14221 (COO-1198-230)
electron work function for, a-c method for measuring, 20: 13025 (IPP-2/37)
meson (μ^+) stopping in, depolarization and quenching in, (E), 20: 13498
performance for gamma spectroscopy, 20: 13067 (JUL-308-RB)
radiation effects on, transient, 20: 13130 (SC-DC-65-1892)
SEPARATION PROCESSES

development for use in activation analysis, 20: 12803
SEX
radiation effects on, of mealy bugs, 20: 12715
SHEEP
metabolism in, tracer studies of, 20: 12609
SHERWOOD PROJECT
status, 20: 13916 (MATT-412)
SHIELDING
bibliography on accelerator and space vehicle, 20: 13965 (ORNL-RSIC-11)
development for Stanford Linear Accelerator, 20: 13366(R) (SLAC-53)
effects of self-, in neutron activation analysis, 20: 12794
SHIELDING MATERIALS
performance of borated-graphite and -iron oxides, for fast neutrons, 20: 14180 (COO-1430-1)
SHOCK TUBES
shock fronts in electromagnetic, self-luminescence, (E), 20: 13949
SHOCK WAVES
effects of low pressure, on plasma ionization, 20: 13921(R) (NP-15703, pp 52-63)
interactions with electromagnetic fields, properties of, (T), 20: 13637 (IPP-3/28)
production of, electromagnetic, (T), 20: 13637 (IPP-3/28)
propagation in argon plasma, microwave reflection technique for, 20: 13936
propagation in magnetic mirrors, effects of, (E), 20: 13921(R) (NP-15703, pp 52-63)
properties of electromagnetic generated, interferometric measurements of, (E), 20: 13636 (IPP-3/24)
SILICON
bremsstrahlung from single-crystal, spectra of, (E), 20: 13345(R) (NP-15772)
design and performance of detectors of, for charged particle identification, 20: 13076 (UR-875-117)
neutron reactions (n,α) and (n,p) in, recoil ionization defects from, (E), 20: 13989
performance of detectors of, for total neutron cross section measurements, 20: 13101
performance of lithium-drifted semiconductors of, for gamma spectroscopy, 20: 13067 (JUL-308-RB)
radiation damage in p-type, transient electron, 20: 13128(R) (NP-15835(Suppl.))
radioinduced oxygen-defect complexes in, infrared absorption spectra of electron and neutron, (E), 20: 13998
SILICON ISOTOPES Si-28
energy level transitions in, internal-pair formation coefficient for 12.33-Mev, (E), 20: 13843
helium-3 reactions (He-3,d) at 24.4 Mev, momentum spectra from, (E), 20: 13345(R) (NP-15772)
neutron reactions (n,α) and (n,p) at 13.95 Mev, recoil ionization defects from, (E), 20: 13989
SILICON OXIDES
analysis for rare earths, emission spectrographic, 20: 12810
moisture control in agglomeration mixtures of, using neutron probe, 20: 13156
use as corrosion inhibitor in high-temperature gas-cooled reactors, 20: 14021(P)
SiO_2–Na_2O–ZrO_2, phase studies, 20: 13284
SILICON SYSTEMS
Al–Mg–Ni–Si, fatigue properties at 250 to 350°C, low-cycle, 20: 13308
Cu–Si, stacking faults in crystals of, (E/T), 20: 13971 (AD-625834)
SILKWORMS
radiation effects on, frequency of mutagenic β and γ, 20: 12692
SILTS
manganese content of deep-sea, activation analysis and thorium-230 dating of, 20: 12976
SILVER
electron secondary emission from thin foils of, (E), 20: 13103
iodine deposition on wires of, properties of, 20: 13261(R) (ORNL-3885, pp 87-149)
neutron inelastic scattering at 3.5 to 8.5 Mev, energy dependence of level density parameters from, (E), 20: 13827
neutron scattering at 0.3 to 1.5 Mev, differential cross sections for, (E), 20: 13829
separation from other inorganic ions by paper chromatography, 20: 12939
sputtering by argon ions at 1 to 7 kev, (E/T), 20: 13414 (JUL-304-RW)
sputtering by protons at 2 and 300 Mev, (E), 20: 13414 (JUL-304-RW)
SILVER ALLOYS
Cd–Ag, crystal structure of, effect of high pressure on, (E), 20: 13316
In–Ag, crystal structure of, effect of high pressure on, (E), 20: 13316
Mg–Ag, crystal structure of, effect of high pressure on, (E), 20: 13316
Sb–Ag, crystal structure of, effect of high pressure on, (E), 20: 13316
SILVER CHLORIDES
chlorine-36 exchange between crystals of, rate of, 20: 12869
SILVER COMPLEXES
yields of, from gamma-irradiated silver salt solutions at 77°K, 20: 12895
SILVER SALTS
radiolysis of, at 77°K, yields of silver complexes from, 20: 12895
SINTERING
effects on materials, methods for determining, 20: 13319
SIOUX FALLS POWER REACTOR
containment leak rate tests, 20: 14143 (PAPP-6401)
SKELETON
retention of calcium-45 and strontium-85 by rat, effects of dietary phosphorus and strontium on, 20: 12594(R) (NP-15679)
retention of calcium-45 and strontium-85 by rat, effects of phosphorus and strontium in diet on, 20: 12595(R) (NP-15680)
retention of calcium-47 and strontium-85 in rat, effects of dietary phosphorus on, 20: 12596(R) (NP-15681)
retention of calcium-47 and strontium-85 by rat, effects of dietary phosphorus on, 20: 12597(R) (NP-15682)
retention of calcium-45 and strontium-85 by rat, effects of calcium and phosphate in diet on, 20: 12598(R) (NP-15683)
strontium-85 retention by female rat, effects of chelating agents on, 20: 12596(R) (NP-15681)
SKIN
radiation effects on guinea pig and rabbit, mechanism for x, 20: 12623
SKIN GRAFTING
radiation effects on response of mice to allogenic, effects of isogenic grafts on, 20: 12656
SLAGS
use of molten, as heat-exchange medium for MHD generator system, 20: 12971(P)
SLURRIES
concentration in pipe lines, radiometric densitometer for measuring spatial, 20: 13049
radioactive, handling and filtration of, 20: 14210
SODIUM
analysis for hydrogen in loop, by diffusion gasometry, 20: 12767 (GEAP-4833)
analysis for impurities in loop transfer, methods for, 20: 12766 (GEAP-4178)
analysis for oxygen by dissolution in ammonia, 20: 12780(T) (ORNL-tr-931)
corrosive effects of oxygen-contaminated, on refractory alloys, (E), 20: 14007(R) (ANL-7122, pp 1-41)
critical temperature and densities of liquid and vaporous, 20: 12815 (ANL-7025)
development and testing of regenerative lead–sodium bimetallic emf cells, (E), 20: 14179(R) (ANL-7122, pp 70-81)
impurities in, instrumentation development for determining, 20: 14024(R) (APDA-182)
neutron cross sections for, 20: 14062 (JUL-214-RG)
neutron reactions at 1 ev to 40 kev, cross sections for, (T), 20: 13753 (BNL-961)
reactions with water, loop development for analyzing, 20: 14024(R) (APDA-182)
reactions with water in steam generators, 20: 14149(T,R) (ORNL-tr-900)
separation from other inorganic ions by paper chromatography, 20: 12939
ultrasonic inspection of, transducer development for, 20: 14024(R) (APDA-182)
uptake by barley seedlings, effects of greasewood forest soil on, 20: 12575
SODIUM AZIDES
effects on phosphate and rubidium uptake by isolated cells of bean seedlings and tobacco leaves, 20: 14217 (COO-888-43)
radioinduced nitrogen free radicals in, EPR spectra of x, 20: 13970 (AD-611432, pp 135-47)
SODIUM BROMIDES
$ErBr_3$–NaBr, complex formation in, 20: 12871
SODIUM CHLORATES
radioinduced color center formation in, thermal bleaching of, 20: 12900
SODIUM CHLORIDES
analysis of single crystals of, activation, 20: 12805
ion association and hydration in aqueous solutions of, x-ray diffraction studies on, 20: 14228 (TID-22527)
radioinduced defects in crystals of, x, (E), 20: 13973(R) (NYO-3033-1)
Al–Mg–$MgCl_2$–KCl–NaCl, corrosive effects on steels and tantalum at 500 to 800°C, (E), 20: 14007(R) (ANL-7122, pp 1-41)
Cu–Mg–$MgCl_2$–KCl–NaCl–U, chemical compatibility with vitreous carbon containers at 800°C, (E), 20: 14007(R) (ANL-7122, pp 1-41)
$ErCl_3$–NaCl, complex formation in, 20: 12871
NaCl–UF_4, uranium production by electrolysis of, 20: 12876(P)
SODIUM FLUORIDES
mechanical properties of single-crystal, effects of uranium additions on, 20: 13277

radioinduced F-center absorption spectra of, effects of temperature on, 20: 12892
sorptive properties for uranium hexafluoride, 20: 12925(R) (EURAEC-1446)
sorptive properties for volatile fission-product halides, 20: 12925(R) (EURAEC-1446)
BeF_2–NaF, use in molten-salt reactor, 20: 14129 (JUL-315-RG)

SODIUM IODIDES
ion association and hydration in aqueous solutions of, x-ray diffraction studies on, 20: 14228 (TID-22527)
performance of thallium-activated, for gamma spectroscopy, 20: 13067 (JUL-308-RB)
performance of thallium activated, in gamma spectrometers, 20: 13098
purification of iodine-131-labeled, by electrophoresis and chromatography, 20: 12918
scintillation response of thallium-doped, to 5- to 1000-kev electrons, (E), 20: 12899

SODIUM IONS
effects of interlayer of, on cesium sorption by montmorillonite, 20: 12873
uptake by cheatgrass in greasewood forests, 20: 12575

SODIUM ISOTOPES Na-23
neutron reactions (n,α) and (n,p) at 4 to 14 Mev, cross sections for, (E/T), 20: 13773 (IKF-13)

SODIUM ISOTOPES Na-24
use for determining action of diuretics in swine, 20: 12613

SODIUM OXIDES
determination in sodium-cooled-reactor cooling systems, (E), 20: 14008(R) (ANL-7122, pp 42-69)
SiO_2–Na_2O–ZrO_2, phase studies, 20: 13284

SODIUM PHOSPHATES
radioinduced formation of complex polyphosphates in, 20: 12902

SODIUM SILICATE GLASS
preparation and devitrification properties of fuel- and neutron absorbent-bearing, 20: 13209 (ANL-7062)

SODIUM TUNGSTATES
effects on spectrofluorometric determination of rare earths, 20: 12787
tungsten-185 exchange in aqueous system of meta- and ortho-, 20: 12822 (IS-T-68)

SODIUM VANADATES
reactions with uranyl nitrate, 20: 12796

SOILS
cesium-137 content in Colorado, 20: 12984
effects of greasewood forest, on sodium uptake by growing plants, 20: 12575
radioactivity in, of EURATOM countries, 1964, 20: 13000(R) (EUR-2520.i)
radioactivity induced in, decay characteristics of neutron, 20: 12582
radioisotope solubility in, effects on plant uptake, 20: 12608
radioisotopes in, factors affecting biological importance of, 20: 12915
radiosensitivity effects on conifer-hardwood forests, fast-neutron, 20: 12672

SOLAR BATTERIES
radiation effects on satellite, from artificial radiation belt, (E), 20: 13131

SOLAR FLARES
radiation from, continuum electromagnetic, 20: 13409

SOLAR RADIATION
properties of, from solar corona and solar flares, 20: 13409

SOLDERING
effects on recrystallization in molybdenum, niobium, tantalum, and tungsten, 20: 13267(T) (AD-624909)

SOLENOIDS
design of superconducting, 20: 13667 (JINR-P-2533)

SOLIDS
analysis for fluorides by automated colorimetry and pyrohydrolysis, 20: 12765 (DP-1004)
atom scattering from, model of, 20: 14227(R) (TID-22419)
beta activity of, detector for low-background, 20: 13102
electron band structure of, high-pressure determination of, 20: 14221 (COO-1198-230)
energy transformations in, method for calorimetric analysis of, 20: 13236 (CEA-R-2797)
meson (μ^+) stopping in, depolarization and quenching in, (E), 20: 13498

SOLUTIONS
analysis for fluorides by automated colorimetry and pyrohydrolysis, 20: 12765 (DP-1004)
electric conductivity in radiochemical processing plants, instrument for measuring, 20: 12927 (NP-15756)

SOLVENT EXTRACTION PROCESSES
contactor for, performance of stacked-clone, 20: 12928(R) (ORNL-3868)
design of amine–ether, for recovery of metal values from aqueous acidic solutions, 20: 12941(P)
development for plutonium determination in irradiated uranium fuels, 20: 12811

SONIC INSPECTION
equipment for MTR fuel elements, 20: 14195
equipment for sodium, development of, 20: 14024(R) (APDA-182)
equipment for uranium fuel elements, 20: 13318
method for JPR-3 uranium fuel elements, 20: 14194
methods for reactor components, 20: 14034
methods for reactor fuel elements, 20: 14161
of reactor components, techniques for, 20: 14017 (STI/PUB/105(Vol.2))
recording equipment for, evaluation of, 20: 12973(R) (EURAEC-1519)

SOUND
effects on transforming DNA, inactivating, 20: 12620

SOUTHWEST EXPERIMENTAL FAST OXIDE REACTOR
core analysis in ZPR-3, (E), 20: 14007(R) (ANL-7122, pp 1-41)

SPACE FLIGHT
effects on human leukocytes, equipment for testing, 20: 12642 (Y-IA-17)
shielding of, bibliography on, 20: 13965 (ORNL-RSIC-11)

SPACE VEHICLES
propulsion of, ion engine development for, 20: 12975
radiation distributions and effects in SNAPSHOT, 20: 14175 (TID-22418)

SPARK CHAMBERS
design and performance of air-shower, 20: 13345(R) (NP-15772)
film scanning systems for, development of, 20: 13163(R) (ANL-7129)
particle track scanning system for, programmed automatic spot, 20: 13106

SPECIFIC HEAT
measurement at low temperatures, method for, 20: 13693

SPECTROMETERS
design of multichannel charged-particle, 20: 13118(P)
pulse-height analyzer for time-of-flight, design of 512-channel, 20: 13097
resolution of magnetic, effects of field inhomogeneities on, (T), 20: 13091

SPECTROPHOTOMETRY
equipment for radioactive-solution, 20: 12813(P)

SPERM
radioinduced mutations in male *D. melanogaster*, effects of age on, 20: 12636 (TID-21459)

SPERMATOGENESIS
maintenance, patterns, and radiosensitivity of, in insects, 20: 14224 (TID-21562)
radiation effects on early stages of, in adult *D. melanogaster* males, 20: 12637 (TID-21466)
radiosensitivity of, 20: 12686

SPHERES
fracture mechanics and stability of, review on, 20: 13248 (GEAP-4678)
material requirements for reinforced Maxwell bodies, (T), 20: 12944

SPINELS
vaporization of, to 2300°C, 20: 13265(T) (AD-623208)

SPLEEN
radiation effects on mouse, cellular x, 20: 12681
reticular cells in mouse, role in erythropoiesis and lymphocytopoiesis, 20: 12681

SPORES
genesis of fungal, reaction mechanisms in, 20: 12695
radiosensitivity of cell stages in Chlamydomonas, effects of repair mechanisms on uv, 20: 12687
radiosensitivity of *Cl. botulinum*, in canned chopped ham, 20: 13134 (AD-625252)

SQUIRRELS
labeling with calcium-45 for population studies, 20: 12583

STAINLESS STEEL
bonding of type 304, to Zircaloy-2, diffusion, 20: 13222
corrosion by chlorine trifluoride–urania reaction-gas mixtures, 20: 12925(R) (EURAEC-1446)
corrosion of type 304 and 405, by aluminum–magnesium–magnesium-chloride–potassium-chloride–sodium-chloride systems at 500 to 800°C, 20: 14007(R) (ANL-7122, pp 1-41)
electron secondary emission from thin foils of, (E), 20: 13103
iodine deposition on wires of, properties of, 20: 13261(R) (ORNL-3885, pp 87-149)
performance as cladding on EBR-II Mark I fuel pins, (E), 20: 14009(R) (ANL-7122, pp 82-90)
performance of type 304, in ultrasonic liquid-metal level indicators, 20: 13031(R) (NYO-2910-13)
performance of type 316, as cladding for plutonium–uranium fuel alloys, (E), 20: 14007(R) (ANL-7122, pp 1-41)
performance of type 304, as cladding for alloy and carbide fuels, (E), 20: 14007(R) (ANL-7122, pp 1-41)
properties of austenitic, 20: 13186 (TRG-Report-840)
radiation effects on corrosion susceptibility and tensile properties of type

304, reactor, 20: 13325(R) (GEAP-4968)
radiation effects on mechanical properties of austenitic, neutron, 20: 13333
radiation embrittlement of, effects of grain size on neutron, 20: 13335
reactions of type 304, with steam at 1400°C, 20: 14009(R) (ANL-7122, pp 82-90)
removal from uranium dioxide, fluid-bed fluoride volatility process for, 20: 12923 (ANL-6898)
testing of fuel claddings of, economics of nondestructive, 20: 14032
testing of fuel cladding of, eddy current, 20: 14033
welding properties of fuel cans of type 304, effects of vibratory-compacting of powders on, 20: 13177(R) (EURAEC-1504)
STANFORD LINEAR ACCELERATOR
development, 20: 13366(R) (SLAC-53)
magnetic field measurements in strong-focusing leases of, (E/T), 20: 13365 (SLAC-39(Rev.))
STARS
element abundances in, effects of beta-decay and neutron capture rates on, 20: 13410
evolution of protostar to quasistatic equilibrium, dynamical and thermal, (T), 20: 13408
neutrino emission from, mechanism of, 20: 13519
radio wave intensity variations of quasars, magnetic bremsstrahlung contributions to, (T), 20: 13407
STATISTICS
apparatus functions for low-accuracy measurements, unfolding of, (T), 20: 13038
apparatus functions for low-accuracy measurements, unfolding of, (T), 20: 13038
error propagation in resolution corrections, (T), 20: 13040
response relations in, minimum bias designs for exponential, (T), 20: 13167 (ORNL-3873)
STEAM
reactions with type 304 stainless steel at 1400°C, 20: 14009(R) (ANL-7122, pp 82-90)
steam–water, boiling burnout in vertical tubes, empirical correlation for, 20: 12968
STEEL
analysis for radioisotopes in mass transfer samples, methods for, 20: 12766 (GEAP-4178)
fatigue tests on pressure vessel, 20: 13255 (KAPL-3108)
heat flux on submerged, during boiling of organic coolants, 20: 12965
neutron absorption by inserts of, in uranyl nitrate critical assemblies, (E), 20: 14091
properties of reactor, summary of, 20: 13186 (TRG-Report-840)
STELLARATORS (A-2)
plasma density variations in, azimuthal, (E), 20: 13915 (MATT-402)
STILBENE
performance in neutron spectrometers, 20: 13063 (JAERI-1092)
STOMACH
radiation effects on carcinostatic properties of tumor extracts from, x, 20: 12625
STRAIN GAGES
design and performance for Project Dribble, 20: 12990 (NVO-1312-1 (Vol.2))
radiation effects on operation of, gamma and neutron, (E), 20: 14170 (EGG-1183-2019)
STRANGE PARTICLES
decay of, spurion model for selection rules in nonleptonic, 20: 13607
decay of, unitary symmetry scheme for leptonic, 20: 13466
properties of, Heisenberg's nonlinear theory for, 20: 13554
STRESS ANALYSIS
of containment structures from internal dynamic and static loading, 20: 14028 (IITRI-578P22-14)
of cylindrical hole in semi-infinite elastic bodies, (T), 20: 12943 (ANL-7097)
STRESS CORROSION
design of potassium refluxing capsule for study of refractory metal, 20: 13191(R) (NASA-CR-54476)
STRONTIUM
effects of dietary, on calcium-45 and strontium-85 retention by rat skeleton, 20: 12594(R) (NP-15679)
effects of dietary, on calcium-45 and strontium-85 retention by rat skeleton, 20: 12595(R) (NP-15680)
metabolism in Acantharia, tracer study, 20: 12591(R) (EUR-2475.f)
metabolism in deer and sheep, tracer study of, 20: 12609
metabolism in *Pisum sativum*, tracer study, 20: 12605
separation from alkali metals by ion exchange using vanadium ferrocyanide, 20: 12932
separation from other inorganic ions by paper chromatography, 20: 12939
STRONTIUM CHROMIUM LANTHANUM OXIDES
crystal structure, 20: 12865
STRONTIUM COBALT LANTHANUM OXIDES
crystal structure, 20: 12865
STRONTIUM COBALT LANTHANUM TITANIUM OXIDES
crystal structure, 20: 12865
STRONTIUM COMPLEXES
with [(1,2-dimethylethylene)dinitrilo]- and (propylenedinitrilo)-tetraacetic acids, stability of, 20: 12594(R) (NP-15679)
with (1,2-cyclopentylenedinitrilo)tetraacetic acid, stability of, 20: 12595(R) (NP-15680)
STRONTIUM GALLIUM LANTHANUM OXIDES
crystal structure, 20: 12865
STRONTIUM IRON LANTHANUM OXIDES
crystal structure, 20: 12865
STRONTIUM ISOTOPES Sr-85
exchange between strontium sulfate crystals, rate of, 20: 12869
excretion by isopods under field and laboratory conditions, 20: 12610
excretion in rat feces and urine, effects of dietary phosphorus on, 20: 12594(R) (NP-15679)
metabolism and retention by rats, effects of dietary phosphorus on, 20: 12600(R) (NP-15685)
metabolism by cows, goats, and hogs, 20: 12588(R) (AD-626320)
metabolism by rats, effects of carbonates, magnesium oxide, and phosphates on, 20: 12606
metabolism in rats, effects of dietary phosphorus on, 20: 12596(R) (NP-15681)
removal from rats, effects of chelating agents on, 20: 12598(R) (NP-15683)
retention by rat skeleton, effects of phosphorus and strontium in diet on, 20: 12595(R) (NP-15680)
retention by rat skeleton labeled *in utero*, effects of dietary calcium and phosphate on, 20: 12599(R) (NP-15684)
retention by rat skeleton, effects of dietary phosphorus and strontium on, 20: 12594(R) (NP-15679)
retention by rat, effects of dietary phosphorus on, 20: 12597(R) (NP-15682)
retention by rats, effects of calcium and phosphate in diet on, 20: 12598(R) (NP-15683)
retention by skeleton in female rats, effects of chelating agents on, 20: 12596(R) (NP-15681)
uptake by barley seedlings, effects of greasewood forest soil on, 20: 12575
use as tracer in metabolism studies in deer and sheep, techniques for, 20: 12609
use in diagnosing bone infections, 20: 12735
STRONTIUM ISOTOPES Sr-86
content in iron meteorites, 20: 12992
content ratio to strontium-87 in carbonate veins and vein-dikes, Idaho, Montana, and Ontario, 20: 12980
STRONTIUM ISOTOPES Sr-87
content in iron meteorites, 20: 12992
content ratio to strontium-86 in carbonate veins and vein-dikes, Idaho, Montana, and Ontario, 20: 12980
production of 2.8-hr isomer of, 20: 12917
STRONTIUM ISOTOPES Sr-88
proton reactions (p,n) at 14.2 Mev, angular distributions, Q values, and spectra from, (E), 20: 13345(R) (NP-15772)
STRONTIUM ISOTOPES Sr-89
distribution in forest ecosystems after tree inoculation, 20: 12566 (COO-1006-4)
separation from aqueous solution by sorption on diatomaceous earth, 20: 12938
uptake by desert shrubs, 20: 12572
STRONTIUM ISOTOPES Sr-90
beta decay of, bremsstrahlung spectra in, (E), 20: 13761 (CONF-233 (Vol.4), pp 656-68)
content in cows' and human milk, 1959 to 1961, 20: 13012
content in Pacific Ocean off coasts of California and Japan, 20: 13007(T) (NP-tr-1336)
content in Po Valley rice, effects of crop irrigation on, 20: 12986
food chain contamination by, effects of plant strontium-90 uptake on, 20: 12607
separation from aqueous solution by sorption on diatomaceous earth, 20: 12938
separation from milk by electrodialysis, pilot plant study of, 20: 12997 (AD-626210)
sorption by clays and sands, 20: 14209 (RT/PHOT(65)29)
uptake by plants in Georgia piedmont, 20: 12985
volatility of, in radioactive alumina calcine during high-temperature storage, 20: 14207 (IDO-14670)
STRONTIUM LANTHANUM RHODIUM OXIDES
crystal structure, 20: 12865
STRONTIUM OXIDES
Dy_2O_3–SrO, optical properties of compounds formed in, 20: 13278
Er_2O_3–SrO, optical properties of compounds formed in, 20: 13278

Eu_2O_3–SrO, optical properties of compounds formed in, 20: 13278
Gd_2O_3–SrO, optical properties of compounds formed in, 20: 13278
Ho_2O_3–SrO, optical properties of compounds formed in, 20: 13278
Lu_2O_3–SrO, optical properties of compounds formed in, 20: 13278
Sc_2O_3–SrO, optical properties of compounds formed in, 20: 13278
Sm_2O_3–SrO, optical properties of compounds formed in, 20: 13278
SrO–Tb_2O_3, optical properties of compounds formed in, 20: 13278
SrO–Tm_2O_3, optical properties of compounds formed in, 20: 13278
SrO–Yb_2O_3, optical properties of compounds formed in, 20: 13278
SrO–Y_2O_3, optical properties of compounds formed in, 20: 13278

STRONTIUM SULFATES
strontium-85 exchange between crystals of, rate of, 20: 12869

STRUCTURAL ENGINEERING
fracture mechanics and stability of materials in, review on, 20: 13248 (GEAP-4678)

STRUCTURES
joints in filament-wound, 20: 14213 (ACF-15)

SUCCINATES
effects on phosphate and rubidium uptake by isolated cells of bean seedlings and tobacco leaves, 20: 14217 (COO-888-43)

SULFATES
effects on iron-59 uptake and transport by bean leaf cells and leaves, 20: 14220 (COO-888-48)

SULFIDE, METHYL PHENYL
spectra of donor sites in Lewis acid adducts of, infrared, 20: 14226 (TID-21586)

SULFUR
determination in copper, activation, 20: 12793
labeling with sulfur-35, 20: 12919

SULFUR ISOTOPES S-32
energy levels of, asymmetric-rotator model for rotational, (T), 20: 13849
proton reactions (p,p' γ) at 7.5 to 10.7 Mev, spin and decay modes of excited states from, (E), 20: 13823

SULFUR ISOTOPES S-35
exchange between barium sulfate crystals, rate of, 20: 12869
incorporation in elemental sulfur and sulfides, 20: 12919

SULFUR ISOTOPES S-36
conversion bremsstrahlung spectra from chlorine-36 decay, (E), 20: 13758 (CONF-233(Vol.4), pp 609-13)

SULFURIC ACID
solvent properties for uranium(IV-VI) oxide in presence of ferric ions, 20: 12863

SUN
corona of, intensity and polarization of light from, 20: 13409
eclipse of, sky brightness during, 20: 13409

SUPERCONDUCTIVITY
effects of structure on eutectic-alloy, 20: 13695
effects of surface, on magnetic hysteresis, (E), 20: 13679
model of, Josephson tunneling and persistent currents in charged Bose gas, 20: 13691
theory for even and odd systems with two kinetic energies, 20: 13669
theory of, eigenstates and spectrum of BCS reduced hamiltonian in, 20: 13688

SUPERCONDUCTORS
critical currents in noninductive coils of niobium–zirconium alloy, anomalous, 20: 13674
critical currents in tin, temperature effects on, 20: 13693
critical fields in thin-films, angular dependence of upper, (T), 20: 13661
critical fields in thin films of, fluxoid quantization and Ginzburg-Landau theory for, 20: 13685
currents in, magnetic hysteresis effects of surface, (E), 20: 13679
design and performance of thin-film cryotron, 20: 13048
electric and thermal conductivity of molybdenum–rhenium alloy, critical field measurements from, (E), 20: 13686
electron tunneling in cylindrical junctions of, d-c Josephson currents and microwave resonances in, (T), 20: 13680
electron tunneling in normal aluminum film laminates with lead, (E), 20: 13687
heating effects on properties of coil, (E/T), 20: 13675
magnetic field distribution in annealed and plastically deformed niobium type-II, (E), 20: 13672
magnetic field enhancement in tubes of, empirical formula for, (E/T), 20: 13678
magnetic flux penetration in niobium, ultrasonic attenuation for determination of, (E), 20: 13684
magnetization of cylindrical tin, by rotation, 20: 13690
model for type-II, Bose gas, (T), 20: 13677
properties of composite, of niobium fine wires in copper matrix, (E), 20: 13673
storage phenomena in thin-film, model for, 20: 13689
testing for magnet coils, 20: 13666 (IPP-4/22)
thermal capacity at low temperatures, (E), 20: 13692
transition temperature of thin film, (T), 20: 13676(T)
transitions in niobium selenide and niobium sulfide, (E), 20: 13683
tunneling in, charged Bose gas model for Josephson, 20: 13691

SUPERFLUIDITY
flow of, relaxation times and vortex rings in, (T), 20: 13671
operators for condensed Bose system, quasi-particle, (T), 20: 13670

SUPERHEATERS (NUCLEAR)
fuel element testing for, 20: 14125 (GEAP-4898)

SURFACE WATERS
radioactive contamination of, effects on Chironomus populations, 20: 12662

SURGERY
radiation effects on recovery from tumor, 20: 12646
radiation effects on recovery from, gamma, 20: 12653

SUSPENSIONS
concentration in pipe lines, radiometric densitometer for measuring spatial, 20: 13049

SWEDEN
cesium-137 content in lichens of, 20: 12578

SWIMMING POOL REACTORS
coolant circulation system for, 20: 14205(P)
design of, to prevent radioactivity diffusion to surface, 20: 14204(P)
loading variable-pitch lattice, device for, 20: 14206(P)
reactivity measurements in IRR-1, pulsed-source technique for subcritical, (E), 20: 14200
reactivity of, modified pulsed-source techniques for measuring, (E), 20: 14199
use for radiochemistry research, 20: 12914 (IEA-100)

SWINE
diuretic action in, tracer study, 20: 12613
metabolism by, cesium-134 and strontium-85, 20: 12588(R) (AD-626320)

SWITCHES
design and performance of thin film superconducting cryotron, 20: 13048
design for high-voltage spark gaps, 20: 13027 (IPP-4/24)

SYNCHROTRONS
beam ejection from CERN proton, design and performance of septum magnets for fast and slow, 20: 13359 (CERN-65-36)
operation summary for Japanese electron, (E), 20: 13345(R) (NP-15772)
radiation monitoring and shielding studies, (E), 20: 13367 (UCRL-16445(Rev.))
radiation monitoring of Japanese, 20: 13345(R) (NP-15772)

SYSTEMS FOR NUCLEAR AUXILIARY POWER
design of SNAPSHOT Agena, 20: 14174 (TID-22417)
radiation effects on instrumentation of, gamma and neutron, 20: 14170 (EGG-1183-2019)
re-entry disintegration of, oxidation properties of uranium–zirconium alloys in, 20: 14169 (AFWL-TDR-64-75)

SYSTEMS FOR NUCLEAR AUXILIARY POWER (SNAP-10)
design and performance of 10A, in SNAPSHOT test, 20: 14177
radiation distributions and effects in SNAPSHOT vehicle, 20: 14175 (TID-22418)
testing of SNAPSHOT vehicle equipment, 20: 14173 (TID-22416)

SYSTEMS FOR NUCLEAR AUXILIARY POWER (SNAP-11)
design and performance, 20: 13158

SZILARD-CHALMERS REACTIONS
recoils from, continuous extraction of, 20: 12897

T

TANTALUM
anodizing electrodes of *a*, pre-, 20: 13204(P)
compatibility with cesium at 550°C, 20: 13203
corrosion by aluminum–magnesium–magnesium-chloride–potassium-chloride–sodium-chloride systems at 500 to 800°C, (E), 20: 14007(R) (ANL-7122, pp 1-41)
corrosion by flowing liquid tin at 800 to 1100°C, 20: 14008(R) (ANL-7122, pp 42-69)
crystallization of, during soldering and welding, 20: 13267(T) (AD-624909)
defects in crystals of, stacking-fault, (E/T), 20: 13971 (AD-625834)
deformation behavior of, in transition temperature range, 20: 13253 (IS-T-65)
effects on crystal structure of alpha-iron, 20: 13317
electron secondary emission from thin foils of, (E), 20: 13103
neutron inelastic scattering at 3.5 to 8.5 Mev, energy dependence of level density parameters from, (E), 20: 13827
reactions with carbon and nitrogen at 1150 to 2370°C, 20: 12845
solubility in alpha-iron at 600 to 900°C, 20: 13317
solubility in liquid rare earth metals, 20: 13180(R) (IS-RD-4)

TANTALUM ALLOYS
weld ductility of, comparison of, with weld ductility niobium-base alloys, 20: 13264(R) (WANL-PR(P)-008)
Hf–Ta–W, creep behavior in ultrahigh vacuum at 2000 and 2200°F, 20: 13256 (NASA-TN-D-3222)

Hf–Ta–W, development of potassium corrosion test loop constructed of T-111, 20: 13193(R) (NASA-CR-54845)
Hf–Ta–W, weldability of T-111, effects of oxygen contamination on, 20: 13264(R) (WANL-PR(P)-008)
Nb–Ta–W–Zr, creep behavior in ultrahigh vacuum at 2000 and 2200°F, 20: 13256 (NASA-TN-D-3222)
Nb–Ta–W–Zr, weldability of FS-85, effects of oxygen contamination on, 20: 13264(R) (WANL-PR(P)-008)
Ta–W, brazing with titanium using diffusion sink method, 20: 13224
Ta–W, creep behavior in ultrahigh vacuum at 2000 and 2200°F, 20: 13256 (NASA-TN-D-3222)
TANTALUM CARBIDES
reactions with nitrogen at 1150 to 2370°C, 20: 12845
TANTALUM HYDRIDES
chemical bonds in, properties of, 20: 12847
TANTALUM ISOTOPES Ta-183
nuclear spectroscopy of, from hafnium-183 beta decay, (E), 20: 13863
TANTALUM ISOTOPES Ta-184
beta decay of, (E), 20: 13767 (CONF-233(Vol.4), pp 730-42)
TANTALUM OXIDES
neutron resonance absorption integral of, (E), 20: 14008(R) (ANL-7122, pp 42-69)
TANTALUM SILICIDES
oxidation at 1400 to 1600°C, kinetics of, 20: 13197
TANTALUM SYSTEMS
C–Hf–Ta, fabrication and properties of sheets of, 20: 13205(R) (AD-626622)
C–Hf–Ta–W, creep behavior in ultrahigh vacuum at 2000 and 2200°F, 20: 13256 (NASA-TN-D-3222)
C–Hf–Ta–W, fabrication and properties of sheets of T-222, 20: 13205(R) (AD-626622)
C–Hf–Ta–W, weldability of T-222, effects of oxygen contamination on, 20: 13264(R) (WANL-PR(P)-008)
TASTE
radiation effects on egg, effects of dose and irradiation temperature on, γ, 20: 12660
TAURINE
content in rats, effects of phosphate on, 20: 12648
radiation effects on excretion of, γ, 20: 12648
TECHNETATES
existence and properties of ionic, 20: 12809
TECHNETIUM
chemical properties, 20: 12809
electrodeposition in mercury, 20: 12809
reactions with 8-quinolinol, 20: 12808
separation from fission products, 20: 12808
separation from fission product mixtures, technique for, 20: 13780 (KFK-358)
TECHNETIUM CHLORIDES
with 8-quinolinol, preparation and properties of, 20: 12808
TECHNETIUM ISOTOPES Tc-99
use as tracer for thyroid function tests, 20: 12749
TECHNETIUM ISOTOPES Tc-103
half life, 20: 13780 (KFK-358)
TECHNETIUM ISOTOPES Tc-104
half life, 20: 13780 (KFK-358)
TECHNETIUM ISOTOPES Tc-105
half life, 20: 13780 (KFK-358)
TECHNETIUM ISOTOPES Tc-106
half life, 20: 13780 (KFK-358)
half life, 20: 13780 (KFK-358)
TECHNETIUM OXIDES
preparation of trivalent, 20: 12809
TELEMETERING SYSTEMS
testing for SNAPSHOT vehicle, 20: 14173 (TID-22416)
TELEVISION EQUIPMENT
x-ray emission by Japanese, 20: 13014
TELLURIC ACID
separation from iodine-131 production waste, 20: 12916
TELLURIUM
deuteron inelastic scattering at 15 Mev, energy spectra from, (E), 20: 13872
separation from other inorganic ions by paper chromatography, 20: 12939
TELLURIUM FLUORIDES
corrosive effects on nickel and nickel alloys at 500°C, (E), 20: 14008(R) (ANL-7122, pp 42-69)
TELLURIUM ISOTOPES Te-134
energy levels of, second-vibrational, (T), 20: 13793
TELLURIUM OXIDES
neutron irradiation to produce iodine-131, thermal, 20: 12922(P)
TEMPERATURE
calculations in statistical physics method for, 20: 13348
effects on critical currents in superconducting tin films, 20: 13693
effects on incidence of Botrytis rot in radiosterilized strawberries, 20: 13139(R) (UCD-34P80-3, pp 9-26)
effects on phosphate and rubidium uptake by isolated cells of bean seedlings and tobacco leaves, 20: 14217 (COO-888-43)
radiosensitivity effects on chromosomal mutations in mice, x, 20: 12693
radiosensitivity effects on whole-egg magna, γ, 20: 12660
radiosensitivity effects on pines, after seed or seedling exposure, gamma, 20: 12673
radiosensitivity effects on ESR in *E. coli*, γ, 20: 12622
TEMPERATURE CONTROL
system for target, in neutron generators, 20: 13744(P)
TENSILE PROPERTIES
measurement of, double cantilever beam specimen for, 20: 12972 (BNWL-168)
TERBIUM
determination in aqueous solutions, effects of sodium tungstate on spectrofluorometric, 20: 12787
separation from other inorganic ions by paper chromatography, 20: 12939
TERBIUM COMPLEXES
with dilactic, mandelic, and quinic acids, formation and stability constants of, 20: 12817 (IS-1311)
TERBIUM ISOTOPES Tb-159
conversion bremsstrahlung spectra from dysprosium-159 decay, (E/T), 20: 13759 (CONF-233(Vol.4), pp 614-24)
TERBIUM OXIDES
$BaO–Tb_2O_3$, optical properties of compounds formed in, 20: 13278
$SrO–Tb_2O_3$, optical properties of compounds formed in, 20: 13278
TEREPHTHALIC ACID, ETHYLENE POLYMER ESTERS
electron propagation through vacuum boundary with, relative transition yields from, (E), 20: 13352
TERPHENYL
boiling burnout properties of, 20: 14026 (EUR-2299.e)
effects in rats, toxic, 20: 12589 (AECL-2507)
benzene–terphenyl, boiling burnout properties of, 20: 14026 (EUR-2299.e)
TETRANEUTRONS
production, (T), 20: 13834
TETRAZOLIUM COMPOUNDS
radiation effects on photoreduction by chloroplasts, gamma, 20: 12627
THALLIUM
effects on crystal structure of alpha-iron, 20: 13317
effects on radioinduced luminescence of potassium iodide, 20: 12891
separation from other inorganic ions by paper chromatography, 20: 12939
solubility in alpha-iron at 600 to 900°C, 20: 13317
thermal capacity at 0.35 to 4.2°K, 20: 13692
THERMAL CAPACITY
measurement at 0.24 to 20°K, apparatus for, 20: 13694
THERMAL CONDUCTIVITY
measurements of, method for calorimetric, 20: 13236 (CEA-R-2797)
THERMAL INSULATION
electron work function for, a-c method for measuring, 20: 13025 (IPP-2/37)
THERMAL RADIATION
effects on sulfhydryl groups in sea urchin eggs, 20: 12624
reflector design for, 20: 14054(P)
THERMAL RADIATION SHIELDING
development for parallel beams, absorbing-particle fluid injection for, (T), 20: 12966
properties of porous bed, (T), 20: 12969
THERMAL RADIATION SOURCES
heat transfer in large radioisotope, 20: 13157 (ORNL-P-1945)
THERMAL REACTORS
economics for uranium conservation, 20: 14011 (BNWL-189, Sect. V)
fuel burnup calculations for sodium-cooled power, 20: 14144 (PEL-77)
fuel burnup in, plutonium centered natural urania, (T), 20: 14102 (BNWL-183, Sect.II)
fuel cycle for, evaluation of thorium, 20: 14126 (JUL-276-RG)
fuel loadings for, optimum plutonium, (T), 20: 14057 (BNWL-183, Sect.I)
fuels for, research on plutonium, 20: 14010 (BNWL-183)
neutron fission yields in, transplutonium, 20: 13752 (ANL-7096)
neutron inelastic scattering in, (E/T), 20: 13700 (JAERI-1086)
THERMAL STRESSES
radiation effects on hemolytic, in rat erythrocytes, x, 20: 12697
THERMIONIC CELLS
design of cesium-vapor, 20: 13441(P)
design of cesium-vapor, 20: 13444(P)
design of internally heated fuel-fired, 20: 13442(P)
development, 20: 13434
THERMOCOUPLES
electromotive force-temperature tables for tungsten-3% rhenium/tungsten-25% rhenium, 20: 13028 (KAPL-M-6498)
THERMODYNAMICS

temperature averages in quantum systems, methods for calculating, 20: 13348
THERMOELECTRIC CELLS
development, 20: 13434
THERMOLUMINESCENT DETECTORS
data read-out system for lithium fluoride finger-tip, design of, 20: 13059 (AEEW-R-411)
THERMONUCLEAR EXPLOSIONS
effects of high-altitude, 20: 14230(T) (ORNL-tr-972)
effects on *Larrea divaricata* populations, 20: 12670
fallout from 1954, effects on growth of Marshall Island children, 20: 13011
THERMONUCLEAR REACTORS
development status, 20: 13916 (MATT-412)
plasma stability in toroidal, (T), 20: 13929(T) (NP-tr-1340)
THICKNESS GAGES
design and performance of gamma or x-ray backscatter, for synthetic fibers, 20: 13050
development of gamma, 20: 13151
THORIUM
content in Pacific Ocean off coasts of California and Japan, 20: 13007(T) (NP-tr-1336)
effects on photometric determination of uranium in ores using Arsenazo III, 20: 12799
neutron cross sections for, 20: 14062 (JUL-214-RG)
performance as reactor fuel, 20: 14126 (JUL-276-RG)
preparation and purification of, process development for, 20: 13180(R) (IS-RD-4)
separation from nitric acid solution by solvent extraction using TBP, 20: 12931
separation from other inorganic ions by paper chromatography, 20: 12939
separation from protactinium by solvent extraction using methyltrioctylammonium chloride, 20: 12937
separation from spent fuels, methods for, 20: 12928(R) (ORNL-3868)
use in heavy-water-moderated organic-cooled power-breeder reactors, 20: 14114(R) (BAW-393-2)
THORIUM ALLOYS
Pu–Th, economics for heavy water reactor fuel cycles, 20: 14117 (BNWL-183, Sect.III)
THORIUM CARBIDES
ThC_2–UC, fission product release from coated particulate, during post-irradiation annealing, 20: 13261(R) (ORNL-3885, pp 87-149)
ThC_2–UC_2, phase diagram, 20: 13215(R) (ORNL-3885, pp 3-86)
ThC_2–UC_2, processing carbon-coated spheres of, by combustion and leaching, 20: 12928(R) (ORNL-3868)
ThC_2–UC_2, radiation effects on carbon coated, 20: 14136(R) (ORNL-3885, pp 150-94)
ThC_2–UC_2, reaction of pyrolytic-carbon-coated, with steam at 1000°C, 20: 13261(R) (ORNL-3885, pp 87-149)
THORIUM COMPLEXES
pentakis(5-isopropyltropolono), preparation, 20: 12853
pentakis(tropolono), preparation, 20: 12853
with carminic acid, preparation and composition of, 20: 12870
THORIUM ISOTOPES
determination of fissionable, in presence of plutonium and/or uranium, radiometric method for, 20: 12814(P)
THORIUM ISOTOPES Th-228
content in foods grown on monazite sands and volcanic intrusions, 20: 12988
THORIUM ISOTOPES Th-230
content in Pacific Ocean off coasts of California and Japan, 20: 13007(T) (NP-tr-1336)
THORIUM NITRATES
analytical use in fluorine determination, 20: 12797
THORIUM(IV) OXIDES
conversion to thorium carbide particles, 20: 13215(R) (ORNL-3885, pp 3-86)
strain in, effects of annealing on, 20: 13295
temperature effects on pyrolytic carbon coated, 20: 13215(R) (ORNL-3885, pp 3-86)
O–ThO_2–UO_2, phase studies, 20: 13301
ThO_2–UO_2, conversion to carbide particles, 20: 13215(R) (ORNL-3885, pp 3-86)
ThO_2–UO_2, fabrication and properties of, 20: 13207 (ANL-6893)
ThO_2–U_3O_8, fabrication and properties of, 20: 13207 (ANL-6893)
ThO_2–UO_2, loading and compaction in reactor fuel tubes by vibration, 20: 12945 (ORNL-TM-1383)
ThO_2–UO_2, radiation effects on, 20: 13207 (ANL-6893)
ThO_2–U_3O_8, radiation effects on, 20: 13207 (ANL-6893)
ThO_2–UO_2, radiation effects on pyrolytic carbon coated, 20: 13215(R) (ORNL-3885, pp 3-86)
THRESHOLD DETECTORS
performance for accelerator monitoring, 20: 13367 (UCRL-16445(Rev.))
THULIUM
crystal structure of, effect of high pressure on, (E), 20: 13316
THULIUM COMPLEXES
with dilactic, mandelic, and quinic acids, formation and stability constants of, 20: 12817 (IS-1311)
THULIUM IONS
energy level interactions in trivalent, 20: 14005
THULIUM ISOTOPES Tm-171
separation from erbium oxide by complexing with HEDTA, 20: 12764 (CONF-660305-8)
THULIUM OXIDES
BaO–Tm_2O_3, optical properties of compounds formed in, 20: 13278
SrO–Tm_2O_3, optical properties of compounds formed in, 20: 13278
THYMUS GLAND
radiation effects on growth of cells of, in tissue culture, β, 20: 12682
THYROID GLAND
diseases of, effects of thyrotropin content of blood on, 20: 12755
function test of, using iodine-132, 20: 12746
function tests of, using technetium-99 as tracer, 20: 12749
radiotherapy of thyrotoxicosis of, using iodine-131, 20: 12744
thyrotoxicosis of, complementation-fixation test for, 20: 12744
THYROXINE
purification of iodine-131-labeled, by electrophoresis and chromatography, 20: 12918
TIMING CIRCUITS
pulse pile-up effects on, amplitude distribution for, 20: 13041
TIN
corrosive effects of liquid, on tantalum at 800 to 1100°C, (E), 20: 14008(R) (ANL-7122, pp 42-69)
critical current density in superconducting switch of, 20: 13048
critical currents in superconducting films of, temperature effects on, 20: 13693
deuteron inelastic scattering at 15 Mev, energy spectra from, (E), 20: 13872
electric currents in cylinders of, stability of persistent, 20: 13691
magnetic field enhancement in superconducting tubes of, empirical formula for, (E/T), 20: 13678
magnetization of superconducting, by rotation, 20: 13690
neutron resonance absorption integral of, (E), 20: 14008(R) (ANL-7122, pp 42-69)
photoelectron production cross sections from 0.2 to 2 Mev, (T), 20: 13413 (CONF-233(Vol.4), pp 538-47)
separation from other inorganic ions by paper chromatography, 20: 12939
TIN ALLOYS
Al–Ge–Nb–Sn, phase studies, 20: 13275
Al–Sn–Ti–Zr, phase studies, 20: 13273
In–Sn, magnetic field enhancement in superconducting tubes of, empirical formula for, (E/T), 20: 13678
In–Sn, superconducting surface current effects on magnetic hysteresis of, (E), 20: 13679
Mg–Sn, crystal structure of, effect of high pressure on, (E), 20: 13316
Mg–Sn, infrared reflectivity of, effects of temperature on, 20: 14227(R) (TID-22419)
Nb–Sn, phase studies, 20: 13275
Nb–Sn, superconductivity of Nb_3Sn, 20: 13666 (IPP-4/22)
TIN ISOTOPES
separation from isotopes of other elements, summary of, 20: 13345(R) (NP-15772)
TIN ISOTOPES Sn-118
ion inelastic scattering by, collective level excitation in complex, (T), 20: 13890
nucleon reactions with, optical-model wave functions for, (T), 20: 13817
TIN ISOTOPES Sn-122
energy levels of, second-vibrational, (T), 20: 13793
TIN ISOTOPES Sn-124
energy levels of, second-vibrational, (T), 20: 13793
TIN ISOTOPES Sn-126
energy levels of, second-vibrational, (T), 20: 13793
TISSUE CULTURES
karyotype of mouse-cell, effects of x-irradiated feeder layers on, 20: 12654
radiation effects on viral-infected HeLa cell, uv, 20: 12711
radiation effects on growth of lymph node and thymus cells in, β, 20: 12682
viability of bone marrow, effects of hemagglutinins on, 20: 12726
TISSUE TRANSPLANTS
effects of hematopoietic, on incidence of radioinduced leukemia in mice, 20: 12647
effects of leukocytic, on survival in γ-irradiated guinea pigs, 20: 12727
immune reactions to, in mice, 20: 12656
radiation effects on immune reactions to, 20: 12645
TISSUES
radiation effects on living, bibliography on, 20: 12629 (AED-C-04-22)

radioinduced softening of plant, biochemistry and physiology of, 20: 13135 (AD-625483)
radium distribution in rat, after radium dye ingestion, 20: 12603(T) (JPRS-33958, pp 1-7)
radium distribution in rat, after radium chloride implantation, 20: 12603(T) (JPRS-33958, pp 1-7)
TITANIUM
argon-ion reactions with, nuclear temperature from, (E), 20: 13885
compatibility with cesium at 550°C, 20: 13203
effects on colorimetric determination of vanadium in uranium compounds, 20: 12802
effects on photometric determination of uranium in ores using Arsenazo III, 20: 12799
electron secondary emission from thin foils of, (E), 20: 13103
neon-ion reactions with, nuclear temperature from, (E), 20: 13885
proton reactions (p,p') at 10.5 Mev, cross sections for, (E), 20: 13897
reactions with niobium carbide, 20: 13194
superconductivity in, 20: 13694
thermal capacity at 0.24 to 4.2°K, 20: 13694
use for brazing tantalum–tungsten alloy by diffusion sink method, 20: 13224
x-ray transition energies in pi mesic atoms of, (E), 20: 13461 (UCRL-16365)
TITANIUM ALLOYS
Al–Nb–Ti, properties of, mechanical and physical, 20: 13271
Al–Sn–Ti–Zr, phase studies, 20: 13273
Fe–Ti, radiation effects on tensile properties of, effects of nitrogen content on fast-neutron, 20: 13324(R) (EURAEC-1529)
Fe–Ti, superconductivity in, 20: 13694
Fe–Ti, thermal capacity at 0.24 to 4.2°K, 20: 13694
Mo–Ti–V, development of refractory, for use in oxygen-contaminated sodium systems, (E), 20: 14007(R) (ANL-7122, pp 1-41)
Mo–Ti–Zr, compatibility of TZM, with niobium–1 zirconium alloy in refluxing potassium at 2000°F, 20: 13192(R) (NASA-CR-54843)
Nb–Ti, superconductivity of, 20: 13666 (IPP-4/22)
Pu–Ti–U, phase transformations at 550°C, (E), 20: 14007(R) (ANL-7122, pp 1-41)
Pu–Ti–U, radiation effects on, in-pile testing of, (E), 20: 14007(R) (ANL-7122, pp 1-41)
Ti–V, development of refractory, for use in oxygen-contaminated sodium systems, (E), 20: 14007(R) (ANL-7122, pp 1-41)
Ti–V, performance as cladding for plutonium–uranium fuel alloys, (E), 20: 14007(R) (ANL-7122, pp 1-41)
TITANIUM HYDRIDES
chemical bonds in, properties of, 20: 12847
TITANIUM ISOTOPES Ti-49
energy level transitions in, multipolarity of, (E), 20: 13803(T)
TITANIUM ISOTOPES Ti-50
energy levels of, second-vibrational, (T), 20: 13793
energy levels of, shell-model description of, (T), 20: 13839
TITANIUM OXIDES
chemical bonds in, properties of, 20: 12848
electric conductivity of, effects of temperature on, 20: 12850
neutron resonance absorption integral of, (E), 20: 14008(R) (ANL-7122, pp 42-69)
TiO_2–UO_2, grain growth at 1450 to 1630°C, 20: 13297
TITANIUM SYSTEMS
C–Nb–Ti, phase diagrams, 20: 13272
TOBACCO
radiation effects on ascorbic acid content of crown-gall tumors on, γ, 20: 12649
uptake of phosphate and rubidium by isolated cells of, effects of chemicals, light, and temperature on, 20: 14217 (COO-888-43)
TOLUENE
neutron diffusion parameters for, pulsed, (E), 20: 13729
separation of normal and deuterated, by gas chromatography, 20: 12930
TOMATOES
radiopreservation effects on wholesomeness of, gamma, 20: 13148(R) (UCD-34P80-3, pp 99-175)
TOXINS
radioinduced in chick embryos, x, 20: 12706
TRACER TECHNIQUES
use in measurement of soldering flux on circuit boards, 20: 13033 (TLW-1110)
TRACER TECHNIQUES (AGRICULTURE)
for fertilizer uptake by rice, nitrogen-15 and phosphorus-32, 20: 12592(R) (NP-15671)
for uptake of nitrogen fertilizer by rice, nitrogen-15, 20: 12593(R) (NP-15672)
TRACER TECHNIQUES (BIOLOGY)
for action of diuretics in swine, potassium-40 and sodium-24, 20: 12613
for biosynthetic measurement, comparison with gravimetric analysis, 20: 12610
for calcium metabolism in mammals, calcium-45, 20: 12609
for cesium metabolism in mammals, cesium-137, 20: 12609
for cesium transport in Liriodendron forest, cesium-137, 20: 12576
for cesium transport in forests, cesium-137, 20: 12577
for fruit fly behavior studies, 20: 12633(R) (NP-15348)
for fruit fly behavior studies, 20: 12634(R) (NP-15349)
for mammalian population studies, calcium-45, 20: 12583
for quantitative autoradiography, 20: 12616
for strontium metabolism in mammals, strontium-85, 20: 12609
TRACER TECHNIQUES (BOTANY)
for cambial activity studies, 20: 12614
for mineral transport in Douglas-fir forests, calcium-45, phosphorus-32, and rubidium-86, 20: 12574
for root systems, iodine-131, 20: 12581
TRACER TECHNIQUES (MEDICINE)
for diagnosing bone infections, calcium-47 and strontium-85, 20: 12735
for diagnosis of brain tumors, 20: 12759
for diagnosis of stomach cancers, 20: 12742
for insulin physiological effects, 20: 12754
for localization of lymph nodes, 20: 12751
for thyroid function test, 20: 12746
for thyroid function tests, 20: 12749
for thyrotropin effects, 20: 12755
TRADESCANTIA
radiation effects on, effects of ATP, histidine, and proline on recovery from x, 20: 12728
TRANSDUCERS
design and performance for Project Dribble, 20: 12990 (NVO-1312-1 (Vol.2))
development for use in high temperature sodium, 20: 14024(R) (APDA-182)
radiation effects on NERVA resistance-temperature, 20: 13127 (CONF-651101-61)
TRANSISTORS
radiation effects on MOS, mechanisms of neutron, 20: 13133
TRANSURANIC ELEMENTS
processing of, equipment and methods for, 20: 12928(R) (ORNL-3868)
production by bombardment of nuclei with heavy ions, 20: 13804
TRAUMA
effects of thermal, with and without x irradiation on intestinal mucosa in rats, 20: 12630 (BNL-8383)
therapy using polyglucin, 20: 12722(T) (JPRS-33766)
TREES
calcium uptake and transport by *Picea excelsa*, during yearly vegetative cycle, tracer study, 20: 12590 (CEA-R-2825)
cesium uptake by Liriodendron, tracer study, 20: 12577
chimeras of fruit, characterization of, 20: 12632(R) (EUR-2546.f)
fallout uptake by juniper, in Georgia piedmont, 20: 12985
radiation effects on seed germination and seedling survival in conifer, gamma, 20: 12671
radiation effects on conifer, effects on environmental factors on fast-neutron, 20: 12672
radiation effects on hardwood, effects of environmental factors on fast-neutron, 20: 12672
radiation effects on pine, after seed or seedling exposure, gamma, 20: 12673
radiation effects on pine, effects of post-irradiation environment on gamma, 20: 12673
radiation effects on pine, effects of water stress on γ, 20: 12674
radioisotope release from litter from forest, 20: 12566 (COO-1006-4)
TRICHLOROAMMINEPLATINATES
hydrolysis of, *trans*-effect in, 20: 12820 (IS-T-57)
TRINEUTRONS
production, (T), 20: 13834
TRIOCTYLAMINE
analytical use in reversed-phase chromatographic separations, 20: 12776 (RT/PROT(65)33)
TRIS(2-ETHYLHEXYL)AMINE
radiosensitivity effects in cats, 20: 12724
TRITIUM
content in Pacific Proving Ground 12 yrs after weapons tests, 20: 12579
determination in heterogeneous phases by liquid scintillators, 20: 12804
deuteron reactions (d,n) at 0.05 to 3.00 Mev, neutron energies from, 20: 13747 (AECD /EP/7)
diffusion from self-luminous paints, 20: 13153
incorporation in cholesteryl arachidonate and linolenate with carbon-14, 20: 12913 (EUR-2446.f)
incorporation in granular coated-particle phosphors, 20: 12921(P)
incorporation in phenols by isotopic exchange in alkaline solutions, 20: 12880
incorporation in 2-octanol and octyl phthalate, Wilzbach method for, 20: 12878
proton reactions (p,n) at 1.50 to 3.00 Mev, neutron energies from,

20: 13747 (AECD/EP/7)
TRITIUM HALIDES
photolysis of, abstraction and scavenging reactions of hydrogen atoms in, 20: 12884(R) (RRL-2310-171)
TRITONS
production in helium-3 (γ,π^+) reactions, cross sections for, (E), 20: 13896
TROPOLONES
complexes with thorium and uranium, preparation of, 20: 12853
TROPONOIDS
structure of, produced by photooxidation of 2-(*p*-chlorophenoxy)-4,5-benztropone, 20: 12819 (IS-T-53)
TUBERCULOSIS
incidence in cases of leukemia, malignant lymphoma, and myelofibrosis in Hiroshima, 20: 12639 (TID-21517)
TUBES
boiling burnout in steam–water mixtures in vertical, empirical correlation for, 20: 12968
fluid flow in, hydrodynamics of two-phase swirling, (E/T), 20: 12960 (EURAEC-1515)
joining of, with different diameters and thermal expansion coefficients, 20: 12951(P)
magnetic field enhancement in superconducting, empirical formula for, (E/T), 20: 13678
testing of steam generator, nondestructive, 20: 14160
TUMORS
effects of radiomimetic agents on mouse, effects of drugs on, 20: 12719(R) (NP-15668)
radiation effects on carcinostatic properties of extracts from gastric, x, 20: 12625
radiation effects on ascorbic acid content of tobacco crown-gall, γ, 20: 12649
radiation effects on growth of transplanted, in rats, γ, 20: 12651
radiation effects on cells of, mechanisms for, 20: 12680
radiodiagnosis of stomach, using macroautoradiography with phosphorus-32, 20: 12742
radioinduced human, review on, 20: 12708
radioinduced pituitary, development histologically in rats of beta, 20: 12652
radioinduced pituitary, after iodine-131-thyroidectomy in mice, 20: 12657
radiotherapy of angiomas, γ and x, 20: 12745
radiotherapy of benign, hazards to medical personnel and patient of, 20: 13013
radiotherapy of cervical, dosimetry in x, 20: 12747
radiotherapy of children's hemangioma, x, 20: 12750
radiotherapy of intraocular, γ and x, 20: 12740
radiotherapy of lung, 20: 12741
radiotherapy of mouth and neck, effects on surgical recovery of gamma, 20: 12653
radiotherapy of pancreatic and liver, using yttrium-90 microspheres, 20: 12738
radiotherapy of pituitary adenoma, x, 20: 12737
radiotherapy of uterine, effects on intestinal mucosa of gamma, 20: 12700
radiotherapy of, surgical complications from, 20: 12646
surgery on head and neck, radiation effects on recovery from, 20: 12646
surgery on mouth and neck, radiation effects on, recovery following, 20: 12653
therapy of breast, use of radioinduced pituitary ablation in, 20: 12753
TUNGSTEN
compatibility with uranium dioxide at 2800°K, 20: 13288
creep rupture properties at 2000°C of arc-cast, 20: 13249(R) (GEMP-55A, pp 29-53)
crystallization of, during soldering and welding, 20: 13267(T) (AD-624909)
effects on crystal structure of alpha-iron, 20: 13317
electron secondary emission from thin foils of, (E), 20: 13103
neutron absorption and inelastic scattering by, gamma spectra from, 20: 13966 (UNC-5140)
performance as cladding for plutonium–uranium fuel alloys, (E), 20: 14007(R) (ANL-7122, pp 1-41)
properties of arc- and electron-beam-melted, mechanical and recrystallization, 20: 13257 (NASA-TN-D-3232)
separation from other inorganic ions by paper chromatography, 20: 12939
solubility in alpha-iron at 600 to 900°C, 20: 13317
spectra of, isotope-displacement effect on arc, (E/T), 20: 13418
surface friction properties of, effects of grain orientation on, 20: 13258 (NASA-TN-D-3238)
thermionic emission from crystalline, effects of oxygen pressure on, (E), 20: 13432(R) (TID-22419, pp 149-76)
TUNGSTEN ALLOY COUPLES
Re–W/Re–W, emf vs temperature for thermocouples of, 20: 13028 (KAPL-M-6498)
TUNGSTEN ALLOYS
Hf–Ta–W, creep behavior in ultrahigh vacuum at 2000 and 2200°F, 20: 13256 (NASA-TN-D-3222)
Hf–Ta–W, development of potassium corrosion test loop constructed of T-111, 20: 13193(R) (NASA-CR-54845)
Hf–Ta–W, weldability of T-111, effects of oxygen contamination on, 20: 13264(R) (WANL-PR(P)-008)
Mo–Re–W, fabrication process development, 20: 13251(R) (GEMP-55A, pp 57-82)
Mo–Re–W, phase diagrams for transmutation studies, electron-concentration, 20: 13251(R) (GEMP-55A, pp 57-82)
Mo–Re–W, weld integrity of, effects of carbon and oxygen on, 20: 13251(R) (GEMP-55A, pp 57-82)
Nb–Ta–W–Zr, creep behavior in ultrahigh vacuum at 2000 and 2200°F, 20: 13256 (NASA-TN-D-3222)
Nb–Ta–W–Zr, weldability of FS-85, effects of oxygen contamination on, 20: 13264(R) (WANL-PR(P)-008)
Nb–W–Zr, creep behavior in ultrahigh vacuum at 2000 and 2200°F, 20: 13256 (NASA-TN-D-3222)
Re–W, age-hardening properties of, 20: 13251(R) (GEMP-55A, pp 57-82)
Re–W, creep rupture properties at 2000°C of arc-cast, 20: 13249(R) (GEMP-55A, pp 29-53)
Re–W, creep rupture properties at 2000°C, effects of annealing at 2400°C on, 20: 13249(R) (GEMP-55A, pp 29-53)
Re–W, powder preparation by hydrogen reduction of volatile fluorides, 20: 13181 (K-L-6076)
Re–W, scrap recovery by fluoride volatility process, economics and technology of, 20: 13181 (K-L-6076)
Re–W, thermocouple insulators for, at 2450°C, properties of calcium oxide as, 20: 13250(R) (GEMP-55A, pp 56-6)
Ta–W, brazing with titanium using diffusion sink method, 20: 13224
Ta–W, creep behavior in ultrahigh vacuum at 2000 and 2200°F, 20: 13256 (NASA-TN-D-3222)
TUNGSTEN BORIDES
preparation, composition, and crystal structure, 20: 12838
TUNGSTEN CARBIDES
grain size of, methods of controlling, 20: 13226
Co–NbC–WC, mechanical properties of, effects of composition on, 20: 13274
WC–Co, tungsten carbide grain size in, methods of controlling, 20: 13226
TUNGSTEN ISOTOPES
neutron absorption by, gamma spectra from, 20: 13966 (UNC-5140)
TUNGSTEN ISOTOPES W-181
decay of, electron-capture ratio and internal bremsstrahlung in, (E), 20: 13869
TUNGSTEN ISOTOPES W-184
energy levels, (E), 20: 13767 (CONF-233(Vol.4), pp 730-42)
TUNGSTEN ISOTOPES W-185
exchange in sodium metatungstate–sodium orthotungstate aqueous system, 20: 12822 (IS-T-68)
TUNGSTEN OXIDES
oxidation of, mechanism of, 20: 13198
TUNGSTEN SILICIDES
oxidation at 1500 to 1800°C, kinetics of, 20: 13196
oxidation kinetics of, in air at 500 to 1000°C, 20: 13198
TUNGSTEN SYSTEMS
C–Hf–Ta–W, creep behavior in ultrahigh vacuum at 2000 and 2200°F, 20: 13256 (NASA-TN-D-3222)
C–Hf–Ta–W, fabrication and properties of sheets of T-222, 20: 13205(R) (AD-626622)
C–Hf–Ta–W, weldability of T-222, effects of oxygen contamination on, 20: 13264(R) (WANL-PR(P)-008)
C–Nb–W–Y–Zr, weldability of D-43Y, 20: 13264(R) (WANL-PR(P)-008)
C–Nb–W–Zr, corrosion of D-43, by potassium at 2450°F, stress-, 20: 13191(R) (NASA-CR-54476)
C–Nb–W–Zr, creep behavior in ultrahigh vacuum at 2000 and 2200°F, 20: 13256 (NASA-TN-D-3222)
O–W–U, phase studies on, 20: 13235 (BMI-1755)
W–UO_2, thermal conductivity at 900 to 2300°C, 20: 13249(R) (GEMP-55A, pp 29-53)
TURBINES
design and testing of closed-cycle gas, 20: 14023 (AD-611432, pp 221-35)

U

ULCERS
radiodiagnosis of stomach, using macroautoradiography with phosphorus-32, 20: 12742
ULTRASONICS
methods for reactor component inspection, 20: 14017 (STI/PUB/105 (Vol.2))
use for fuel cladding tests, economics of, 20: 14032

use for magnetic flux penetration determinations in niobium superconductors, (E), 20: 13684
use for reactor component inspection, 20: 14034
use for reactor fuel element inspection, 20: 14161
use for uranium alloy inspection after heat treatment, 20: 13318
use in molten-metal level indicators, 20: 13031(R) (NYO-2910-13)
welding, bibliography on, 20: 13210 (AWRE/LIB/BIB/13)
ULTRAVIOLET RADIATION
effects on animal cells, morphological, 20: 12635(R) (NYO-2786-1)
effects on bacteriophages, 20: 12617(R) (NP-15863)
effects on cell stages in Chlamydomonas spores, effects of repair mechanisms on, 20: 12687
effects on *E. coli*, effects of nutritional restriction on, 20: 12621
effects on *E. coli* DNA crosslinking with protein, 20: 12621
effects on *Escherichia coli*, inactivating, 20: 12712
effects on *Escherichia coli*, biological, 20: 12713
effects on *Escherichia coli*, lethal, 20: 12677
effects on melezitose locus in Saccharomyces, mutagenic, 20: 12655
effects on phage induction in *E. coli*, effects on base-specific t-RNA methylase levels, 20: 12619
effects on Pneumococcus genetics, 20: 12665
effects on polarographic behavior of cobalt, nickel, and uranium ions, 20: 12798
effects on *Salmonella typhimurium*, lethal, 20: 12677
effects on sporogenesis in fungi, 20: 12695
effects on sulfhydryl groups in sea urchin eggs, 20: 12624
effects on transforming DNA, inactivating, 20: 12620
effects on Ustilago, mutagenic, 20: 12694
effects on viral-infected HeLa cells, 20: 12711
emission from electron-bombarded metal foils, 20: 14004
URACIL, 5-FLUORO-
effects on tumor-bearing mice, effects of radioprotective drugs on, 20: 12719(R) (NP-15668)
URANIUM
analysis of irradiated, isotopic dilution method for plutonium, 20: 12811
burnup in sodium-cooled thermal power reactors, 20: 14144 (PEL-77)
coating with nickel, electrolytic method for, 20: 13211 (BNWL-124)
content in sintered uranium dioxide at grain boundaries, 20: 13294
criticality studies on lattices of enriched, in heavy water, 20: 14065(R) (MIT-2344-4, pp 4-16)
crystal lattice orientation of alpha, inversion of pole figures for, (T), 20: 13983
defects in crystals of, stacking-fault, (E/T), 20: 13971 (AD-625834)
determination in ores by photometry using Arsenazo III, 20: 12799
determination in rocks, gamma-gamma logging method for, 20: 12993
diffusion in plutonium–uranium alloys at 400 to 550°C, 20: 13313
diffusion through iron-base alloy cladding from urania and chromium- or iron-base cermet fuels, 20: 13179(R) (GEMP-55A, pp 13-28)
distribution between copper–magnesium alloy and magnesium chloride, (E), 20: 14007(R) (ANL-7122, pp 1-41)
economics for conservation of, 20: 14011 (BNWL-189, Sect.V)
economics of enriched and natural, as reactor fuels in France, 20: 14105
effects on mechanical properties of sodium fluoride single crystals, 20: 13277
extrusion of fuel elements of, by Dynapak equipment, 20: 13220(R) (BMI-3)
extrusion of Mark V-B tubular, effects of extrusion pressure on grain growth during, 20: 13220(R) (BMI-3)
extrusion of, process development for precision, 20: 13220(R) (BMI-3)
extrusion piercing of Mark V-B billets of, process development for, 20: 13220(R) (BMI-3)
fabrication and testing of depleted blanket slugs of, for EBR-II, 20: 13206 (ANL-6417)
fast neutron distributions in enriched, in heavy-water lattices, 20: 13703(R) (MIT-2344-4, pp 17-47)
gamma reactions (γ,e) at 122 kev, cross sections for, (E), 20: 13755 (CONF-233(Vol.4), pp 548-60)
gamma scattering at 662 kev, cross sections for, (E), 20: 13756 (CONF-233(Vol.4), pp 562-94)
machining of billets of, process development for electrochemical, 20: 13220(R) (BMI-3)
mining and processing of, annual report of CEA on, 20: 14223(R) (NP-15723)
monitoring atmospheric, alarm system for use in, 20: 13122(P)
neutron decay in slightly enriched lattices of, pulsed-source measurements of prompt, (E), 20: 14076
neutron decay in, pulsed-source measurements of prompt, (E), 20: 14089
neutron scattering at 0.83 Mev, cross sections and polarization from, (E), 20: 13868
neutron spectra in depleted, pulsed source measurements of fast, (E/T), 20: 14202
photoelectron production cross sections from 0.2 to 2 Mev, (T), 20: 13413 (CONF-233(Vol.4), pp 538-47)
porosity of nickel plating on, x-ray fluorescence determination of, 20: 13211 (BNWL-124)
preparation by carbon reduction of oxide, 20: 13180(R) (IS-RD-4)
production of solid, by electrolysis in fused salt, 20: 12876(P)
properties of, internal friction measurement for determining, 20: 13321
radiation damage in alpha-phase, krypton-ion, 20: 13334
reactions with carbon, mechanisms of, 20: 13223
reactions with hydrogen and nitrogen to prepare uranium nitride, 20: 13227
reactions with uranium tetrafluoride in molten lithium fluoride, mechanism and rate of, 20: 13170 (BM-RI-6736)
reactivity of plutonium center loaded fuel rods of, 20: 14057 (BNWL-183, Sect.I)
separation from acid solutions by extraction using amine–ether in hydrocarbon diluent, 20: 12941(P)
separation from aluminum alloyed fuels during chemical processing, flowsheets for, 20: 12926 (IDO-14669)
separation from enriched aluminum–uranium and uranium–Zircaloy-2 fuels, fluid-bed fluoride volatility process for, 20: 12924 (ANL-6973)
separation from fission products by solvent extraction using TBP–kerosene, effects of chemical degradation of kerosene on, 20: 12934
separation from fission products and plutonium in aqueous solutions, process for, 20: 12940(P)
separation from nitric acid solution by solvent extraction using TBP, 20: 12931
separation from other inorganic ions by paper chromatography, 20: 12939
separation from spent fuels, methods for, 20: 12928(R) (ORNL-3868)
solvent properties of solid, for iron, 20: 13298
ultrasonic inspection of fuel elements of, system for, 20: 13318
ultrasonic testing of metallic, 20: 14194
URANIUM ALLOYS
Al–U, analysis for cerium-144 by bis(2-ethylhexyl) phosphate extraction and beta counting, 20: 12774 (PG-Report-685)
Al–U, flowsheet for uranium separation from, 20: 12926 (IDO-14669)
Al–U, fluid-bed fluoride volatility process for uranium separation from, 20: 12924 (ANL-6973)
Al–U, testing of reactor fuel elements of UAl_3, 20: 14059(R) (IDO-17104)
Al–U, uranium-235 concentration in, nondestructive method for determining excess, 20: 14168
Fe–Pu–U, corrosion by air, effects of casting conditions and iron content on, 20: 13200
Fe–U, phase studies at 660 to 800°C, 20: 13298
fission–Pu–U, radiation effects on, in-pile testing of, (E), 20: 14007(R) (ANL-7122, pp 1-41)
Mo–U, mechanical properties for use in prompt-burst reactor, 20: 13287
Pt–U, phase transformation in, mechanisms of beta-to-alpha, 20: 13307
Pu–Ti–U, phase transformations at 550°C, (E), 20: 14007(R) (ANL-7122, pp 1-41)
Pu–Ti–U, radiation effects on, in-pile testing of, (E), 20: 14007(R) (ANL-7122, pp 1-41)
Pu–U, diffusion of plutonium and uranium in, at 400 to 550°C, 20: 13313
Pu–U, fabrication of fuel rods of, with controlled isotope content, 20: 13214 (EURAEC-1484)
Pu–U, fabrication of sintered compounds of, 20: 13229(P)
Pu–U–Zr, phase transformations at 550°C, (E), 20: 14007(R) (ANL-7122, pp 1-41)
Pu–U–Zr, radiation effects on, in-pile testing of, (E), 20: 14007(R) (ANL-7122, pp 1-41)
U–Zircaloy-2, fluid-bed fluoride volatility process for uranium separation from, 20: 12924 (ANL-6973)
U–Zr, reactions with air, nitrogen, and oxygen, disintegration properties of, 20: 14169 (AFWL-TDR-64-75)
URANIUM CARBIDE SLURRIES
performance for fast breeder reactors, 20: 14024(R) (APDA-182)
URANIUM CARBIDES
analysis for carbon, combustion method for, 20: 12773 (PEL-80)
coating with pyrolytic carbon from acetylene and methane, properties of, 20: 13215(R) (ORNL-3885, pp 3-86)
diffusion in, relation of defects to self-, 20: 13234 (ANL-7094)
expansion of pellets of, controlled, 20: 13188
fission product release from coated particulate, during postirradiation annealing, 20: 13261(R) (ORNL-3885, pp 87-149)
oxidation by air, oxygen, and water, factors affecting, 20: 12925(R) (EURAEC-1446)
preparation by reaction of carbon and uranium powders, 20: 13223
preparation from hydride, (E), 20: 14008(R) (ANL-7122, pp 42-69)
preparation of powdered mono-, by carbonization of powdered metal, 20: 13190(P)
radioinduced point defect clusters in, formation and properties of neutron, 20: 13332
reaction of pyrolytic-carbon-coated, with steam at 1000°C, 20: 13261(R) (ORNL-3885, pp 87-149)

reactions with hydrofluoric acid, factors affecting, 20: 12925(R) (EURAEC-1446)
thermal expansion, 20: 14008(R) (ANL-7122, pp 42-69)
thermodynamic functions for, 20: 13215(R) (ORNL-3885, pp 3-86)
PuC–UC, preparation for hydrides, (E), 20: 14008(R) (ANL-7122, pp 42-69)
PuC–UC, radiation effects on fuel elements of, in-pile testing of, (E), 20: 14007 (ANL-7122, pp 1-41)
ThC_2–UC, fission product release from coated particulate, during post-irradiation annealing, 20: 13261(R) (ORNL-3885, pp 87-149)
ThC_2–UC_2, phase diagram, 20: 13215(R) (ORNL-3885, pp 3-86)
ThC_2–UC_2, processing carbon-coated spheres of, by combustion and leaching, 20: 12928(R) (ORNL-3868)
ThC_2–UC_2, radiation effects on carbon coated, 20: 14136(R) (ORNL-3885, pp 150-94)
ThC_2–UC_2, reaction of pyrolytic-carbon-coated, with steam at 1000°C, 20: 13261(R) (ORNL-3885, pp 87-149)
UC–ZrC, use as thermionic emitters for cesium-vapor cells, 20: 13444(P)
U–UC, electron and optical microscopy studies on as-cast and heat-treated, 20: 13259 (NLCO-968)
U–UC, phase diagram, 20: 13259 (NLCO-968)

URANIUM COMPLEXES
pentakis(tropolono), preparation, 20: 12853

URANIUM COMPOUNDS
analysis for vanadium, colorimetric, 20: 12802

URANIUM DEPOSITS
thermodynamic state of, (T), 20: 12996 (JEN-155-SIG/I-4)

URANIUM DEPOSITS (FRANCE)
occurrence, 20: 14105

URANIUM(IV) FLUORIDES
conversion to urania in fused salts, 20: 12925(R) (EURAEC-1446)
production from uranium dioxide pellets, development of fluid-bed fluoride volatility process for, 20: 12923 (ANL-6898)
reactions with uranium in molten lithium fluoride, mechanism and rate of, 20: 13170 (BM-RI-6736)
NaCl–UF_4, uranium production by electrolysis of, 20: 12876(P)

URANIUM(VI) FLUORIDES
reduction methods for, 20: 12928(R) (ORNL-3868)
separation from plutonium hexafluoride by thermal decomposition to plutonium tetrafluoride, (E), 20: 14008(R) (ANL-7122, pp 42-69)
sorption by sodium fluoride, 20: 12925(R) (EURAEC-1446)

URANIUM GLASS
preparation and devitrification properties of fuel- and neutron absorbent-bearing, 20: 13209 (ANL-7062)

URANIUM HYDRIDES
reactions with nitrogen, 20: 13227

URANIUM IONS
photopolarographic reduction, uv, 20: 12798
reduction of hexavalent, in sodium carbonate solutions, electrochemical, 20: 12868

URANIUM ISOTOPES
determination of fissionable, in presence of plutonium and/or thorium, radiometric method for, 20: 12814(P)
separation by gaseous diffusion through porous barriers, Breton-Massignoe's theory for, 20: 13160

URANIUM ISOTOPES U-233
boron-10 and -11 reactions with, spontaneously fissionable isomer production in, (E), 20: 13776 (JINR-P-2499)
fission products of, neutron absorption cross sections for, (E/T), 20: 13748 (AECL-2510)
neutron fission cross section at 30 ev to 5 Mev, determination using high-altitude explosion, (E), 20: 13871
neutron fission of, fission-fragment yields in, 20: 14059(R) (IDO-17104)
neutron fission of, zirconium-95 yields from thermal, (E), 20: 13783 (ORNL-TM-1333)
neutron fission rates of, fast, (E), 20: 14202
processing of, criticality controls for, 20: 14092

URANIUM ISOTOPES U-234
neutron fission rates of, fast, (E), 20: 14202

URANIUM ISOTOPES U-235
burnup of, gamma spectroscopy for determining, 20: 14158
burnup of, isotopic dilution method for determining, 20: 12811
content in aluminum–uranium fuel elements, nondestructive method for determining excess, 20: 14168
fission products of, separation of iodine-131 and xenon-133 from, 20: 12772 (ORNL-3840)
fission products of, neutron absorption cross sections for, (E/T), 20: 13748 (AECL-2510)
neutron absorption and inelastic scattering by, gamma spectra from, 20: 13966 (UNC-5140)
neutron cross sections for, tabulations of, 20: 13749 (AEEW-M-502)
neutron fission of, fission-fragment yields in, 20: 14059(R) (IDO-17104)
neutron fission of, zirconium-95 yields from thermal, (E), 20: 13783 (ORNL-TM-1333)
neutron fission rates of, fast, (E), 20: 14202
neutron reactions with, in heavy-water lattices, (E), 20: 14103(R) (MIT-2344-4, pp 48-62)
neutron ternary fission of, yields of argon isotopes and cobalt-56 in thermal, (E), 20: 13862
processing of, criticality controls for, 20: 14092

URANIUM ISOTOPES U-238
fluorine-19 reactions (F-19,xn) with, cross sections for, (E), 20: 13889
helium fission of, mass-yield curves for, (E/T), 20: 13345(R) (NP-15772)
neon-22 reactions (Ne-22,xn) with, cross sections for, (E), 20: 13889
neutron absorption and inelastic scattering by, gamma spectra from, 20: 13966 (UNC-5140)
neutron fission rates of, fast, (E), 20: 14202
neutron reactions with, in heavy-water lattices, (E), 20: 14103(R) (MIT-2344-4, pp 48-62)
oxygen-18 reactions (O-18,xn) with, cross sections for, (E), 20: 13889
photofission at 17.5 Mev, mass yields in, (E), 20: 13860
photofission mass-yield curves for, (E/T), 20: 13345(R) (NP-15772)

URANIUM NITRIDES
diffusion in, relation of defects to self-, 20: 13234 (ANL-7094)
preparation and sintering, 20: 13227
reactions with carbon at 1900°C, 20: 13171(R) (BMI-1751)

URANIUM ORES
analysis for uranium by photometry using Arsenazo III, 20: 12799
mining and prospecting in Australia, 20: 14222(R) (NP-15612)
production of, data on world, 20: 14222(R) (NP-15612)

URANIUM OXIDES
formation of U_4O_9, 20: 13301

URANIUM(IV) OXIDES
analysis for cerium-144 by bis(2-ethylhexyl) phosphate extraction and beta counting, 20: 12774 (PG-Report-685)
analysis for fluorides by automated colorimetry and pyrohydrolysis, 20: 12765 (DP-1004)
compatibility with tungsten at 2800°K, 20: 13288
conversion to uranium carbide particles, 20: 13215(R) (ORNL-3885, pp 3-86)
diffusion in, relation of defects to self-, 20: 13234 (ANL-7094)
diffusion of fission gases from, effects of lattice defects on, 20: 13290
diffusion of niobium-95 in polycrystalline, at 1100 to 2100°C, 20: 13289
fabrication by vibratory compaction, 20: 13225
fission gas release from irradiated carbon coated particulate, 20: 13261(R) (ORNL-3885, pp 87-149)
fission product release from coated particulate, during postirradiation annealing, 20: 13261(R) (ORNL-3885, pp 87-149)
fission products in irradiated fuel elements of, diffusion of gaseous, 20: 13329 (RT/FI(65)46)
fluorination of pellets of, development of fluid-bed fluoride volatility process for, 20: 12923 (ANL-6898)
grain growth at 1450 to 1630°C, 20: 13297
heat of sublimation, 20: 13288
ionization around 2000 atm and 5000 to 10,000°K, (T), 20: 14009(R) (ANL-7122, pp 82-90)
processing Zircaloy-2-clad, leach-shear methods for, 20: 12928(R) (ORNL-3868)
production by electrochemical reduction of uranium(VI) ions in sodium carbonate, 20: 12868
production of dense sintered bodies of, for reactor fuel, 20: 13228(P)
properties of, internal friction measurement for determining, 20: 13321
radiation effects of properties of fuel rods of, operated with central melting, reactor, 20: 13326 (GEAP-5100C)
reactions with aluminum, 20: 14059(R) (IDO-17104)
reactions with chlorine trifluoride, factors affecting, 20: 12925(R) (EURAEC-1446)
separation from fused salts by electrodeposition, 20: 12925(R) (EURAEC-1446)
separation from stainless steel and Zircaloy-2 cladding, fluid-bed fluoride volatility process for, 20: 12923 (ANL-6898)
temperature effects on pyrolytic carbon coated, 20: 13215(R) (ORNL-3885, pp 3-86)
thermal expansion at 20 to 2300°C, 20: 13300
uranium inclusions at grain boundaries in sintered, 20: 13294
vapor pressure at 2200 to 2800°K, 20: 13288
Al–UO_2–ZrH, reactivity measurements in lattices of, near-critical, (E), 20: 14082
B_4C–UO_2, radiation effects on fuel elements of, 20: 13425(R) (CEND-3107-249)
Cr–UO_2, diffusion of uranium through iron-base alloy cladding from fuel of, 20: 13179(R) (GEMP-55A, pp 13-28)
Fe–UO_2, diffusion of uranium through iron-base alloy cladding from fuel of, 20: 13179(R) (GEMP-55A, pp 13-28)
Fe–UO_2, fission product diffusion from cermet fuels of, 20: 13179(R)

(GEMP-55A, pp 13-28)
fission–UO_2, reactions with chlorine trifluoride, 20: 12925(R) (EURAEC-1446)
graphite–UO_2, reactivity of semi-homogeneous systems of, pulsed source measurements of, (E/T), 20: 14081
LiF–UO_2, radiation effects on, xenon fluoride production by neutron, 20: 12898
O–ThO_2–UO_2, phase studies, 20: 13301
PuO_2–UO_2, density and homogeneity of vibratory-compacted fuel rods of, effects of particle size distribution on, 20: 13177(R) (EURAEC-1504)
PuO_2–UO_2, development as fuel rod, 20: 13176(R) (EURAEC-1503)
PuO_2–UO_2, distribution of plutonia within vibratory compacted pellets of, effects of mixing time on, 20: 13176(R) (EURAEC-1503)
PuO_2–UO_2, equation of state of, 20: 14149(T,R) (ORNL-tr-900)
PuO_2–UO_2, fluorination on fluidized alumina beds, (E), 20: 14008(R) (ANL-7122, pp 42-69)
PuO_2–UO_2, fluorination to hexafluorides, (E), 20: 14008(R) (ANL-7122, pp 42-69)
PuO_2–UO_2, homogeneity of fuel rods of, use of gamma spectrometer for determination of, 20: 13176(R) (EURAEC-1503)
PuO_2–UO_2, oxidation by air, effects of plutonium content and temperature on, 20: 12925(R) (EURAEC-1446)
PuO_2–UO_2, properties of coaxial fuels of, 20: 14102 (BNWL-183, Sect.II)
PuO_2–UO_2, reactivity of water-moderated lattices of, experiments on, 20: 13176(R) (EURAEC-1503)
PuO_2–UO_2, reactivity of water-moderated lattices of, experiments on, 20: 13177(R) (EURAEC-1504)
PuO_2–UO_2, thermal conductivity of vibratory-compacted fuel elements of, effects of filler gas composition and pressure on, 20: 13177(R) (EURAEC-1504)
PuO_2–UO_2–H_2O, criticality studies using pulsed sources, (E), 20: 14078
ThO_2–UO_2, conversion to carbide particles, 20: 13215(R) (ORNL-3885, pp 3-86)
ThO_2–UO_2, fabrication and properties of, 20: 13207 (ANL-6893)
ThO_2–UO_2, loading and compaction in reactor fuel tubes by vibration, 20: 12945 (ORNL-TM-1383)
ThO_2–UO_2, radiation effects on, 20: 13207 (ANL-6893)
ThO_2–UO_2, radiation effects on pyrolytic carbon coated, 20: 13215(R) (ORNL-3885, pp 3-86)
TiO_2–UO_2, grain growth at 1450 to 1630°C, 20: 13297
UO_2–H_2O, reactivity of variable-pitch lattices of, kinetic and steady-state measurements of, (E/T), 20: 14079
UO_2–UP, phase studies, 20: 13285
UO_2–UP, weight losses at 2000°C in vacuum, 20: 13285
UO_2–ZrO_2, radioinduced homogenization of two-phase mixtures of, 20: 13330
U–UO_2, phase studies and vapor pressure, 20: 14008(R) (ANL-7122, pp 42-69)
W–UO_2, thermal conductivity at 900 to 2300°C, 20: 13249(R) (GEMP-55A, pp 29-53)

URANIUM(IV-VI) OXIDES
analysis for impurities by carrier distillation, effects of graphite electrodes on, 20: 12771 (NLCO-967)
analysis for vanadium, colorimetric, 20: 12802
reactions with bromine pentafluoride at 250 to 400°C, (E), 20: 14008(R) (ANL-7122, pp 42-69)
solubility in sulfuric acid, effects of ferric ions on, 20: 12863
ThO_2–U_3O_8, fabrication and properties of, 20: 13207 (ANL-6893)
ThO_2–U_3O_8, radiation effects on, 20: 13207 (ANL-6893)

URANIUM(VI) OXIDES
crystal structure of high-pressure modification, 20: 13269

URANIUM PHOSPHIDES
reactions with phosphoric acid, 20: 14008(R) (ANL-7122, pp 42-69)
UO_2–UP, phase studies, 20: 13285
UO_2–UP, weight losses at 2000°C in vacuum, 20: 13285
U–UP, phase studies, 20: 14008(R) (ANL-7122, pp 42-69)

URANIUM(IV) SULFATES
analysis of hydrates of, x-ray-diffraction, 20: 12843
preparation, thermal decomposition, and x-ray spectra of anhydrous, 20: 12843

URANIUM SULFIDES
diffusion in, relation of defects to self-, 20: 13234 (ANL-7094)
preparation of single crystals of, solid-state method for, 20: 12856

URANIUM SYSTEMS
BeO–U, neutron diffusion parameters and multiplication constants of lattices of, pulsed, (E/T), 20: 14080
Cu–Mg–$MgCl_2$–KCl–NaCl–U, chemical compatibility with vitreous carbon containers at 800°C, (E), 20: 14007(R) (ANL-7122, pp 1-41)
N–U, phase diagrams, 20: 13286
O–W–U, phase studies on, 20: 13235 (BMI-1755)
U–UC, electron and optical microscopy studies on as-cast and heat-treated, 20: 13259 (NLCO-968)
U–UC, phase diagram, 20: 13259 (NLCO-968)
U–UO_2, phase studies and vapor pressure, 20: 14008(R) (ANL-7122, pp 42-69)
U–UP, phase studies, 20: 14008(R) (ANL-7122, pp 42-69)

URANYL ACETATES
analysis for vanadium, colorimetric, 20: 12802

URANYL IONS
determination by amperometric titration with sodium vanadate, 20: 12796

URANYL NITRATES
analysis for vanadium, colorimetric, 20: 12802
criticality studies of solutions of, 20: 14077
crystal structure of hexahydrate of, neutron-diffraction study on, 20: 13233 (ANL-6943)
reactions with sodium vanadates, 20: 12796

URANYL VANADATES
preparation and properties, 20: 12796

UREA
effects on iron-59 uptake and transport by bean leaf cells and leaves, 20: 14220 (COO-888-48)

UREA, THIO-
effects on damages induced in mouse tumors by radiomimetic agents, 20: 12719(R) (NP-15668)
effects on effects of radiomimetic agents in tumor-bearing mice, 20: 12717(R) (NP-15666)
effects on effects of radiomimetic agents in tumor-bearing mice, 20: 12718(R) (NP-15667)

UREAS
effects on permeation of chloride and rubidium through cuticular membranes of fruits and leaves, 20: 14218 (COO-888-44)

URINARY TRACT
radiation injuries of, induced by radiotherapy, 20: 12739

URINE
analysis for protactinium-231, method for, 20: 12761 (AERE-R-4911)
excretion of calcium-45 and strontium-85 in rat, effects of dietary phosphorus on, 20: 12596(R) (NP-15681)
excretion of calcium-45 and strontium-85 in rat, effects of dietary phosphorus on, 20: 12594(R) (NP-15679)
radium content in rat, after ingesting radium dyes, 20: 12603(T) (JPRS-33958, pp 1-7)
radium content in rat, after radium chloride implantation, 20: 12603(T) (JPRS-33958, pp 1-7)

UTERUS
radiation effects on cytology of cervical carcinomas in, gamma and x, 20: 12659
radiotherapy of cancer of, effects on intestinal mucosa of gamma, 20: 12700
radiotherapy of cervical carcinomas in, rectal complications from γ, 20: 12696
radiotherapy of cervical cancers in, dosimetry in x, 20: 12747

V

VACUUM GAGES
design of two-chamber ionization, 20: 13026 (IPP-2/39)

VACUUM SYSTEMS
design for particle accelerators, 20: 13396(P)
development for Stanford Linear Accelerator, 20: 13366(R) (SLAC-53)

VALLECITOS SUPERHEAT REACTOR
neutron flux in, ($k\beta/l$) pulsed-source technique for, (E), 20: 14162

VAN ALLEN RADIATION BELTS
effects of artificial, on solar-cell power systems, 20: 13131
electrons and protons in inner, model for, 20: 13646 (NASA-SP-3024)
proton distribution and energy in inner, 20: 13647

VAN DE GRAAFF ACCELERATORS
beam injection system of, 5.5-Mev ion buncher for, 20: 13379
design of tandem, 20: 13401(P)
design of 3-Mev, at Dacca, 20: 13356 (AECD/EP/6)

VANADIUM
determination in uranium compounds, colorimetric, 20: 12802
neutron diffraction at high pressures, 20: 14059(R) (IDO-17104)
performance as cladding for plutonium–uranium fuel alloys, (E), 20: 14007(R) (ANL-7122, pp 1-41)
phase transformation in, effects of hydrogen content on, 20: 13180(R) (IS-RD-4)
separation from acid solutions by extraction using amine–ether in hydrocarbon diluent, 20: 12941(P)
separation from other inorganic ions by paper chromatography, 20: 12939
use as windows in electric discharge devices, 20: 13052(P)

VANADIUM ALLOYS
Al–Cr–V, development of refractory, for use in oxygen-contaminated sodium systems, (E), 20: 14007(R) (ANL-7122, pp 1-41)
Mo–Ti–V, development of refractory, for use in oxygen-contaminated

sodium systems, (E), 20: 14007(R) (ANL-7122, pp 1-41)
Nb–V, performance as cladding for plutonium–uranium fuel alloys, (E), 20: 14007(R) (ANL-7122, pp 1-41)
Ti–V, development of refractory, for use in oxygen-contaminated sodium systems, (E), 20: 14007(R) (ANL-7122, pp 1-41)
Ti–V, performance as cladding for plutonium–uranium fuel alloys, (E), 20: 14007(R) (ANL-7122, pp 1-41)

VANADIUM FERROCYANIDES
properties for use as ion exchange material, 20: 12932

VANADIUM HYDRIDES
chemical bonds in, properties of, 20: 12847

VANADIUM OXIDES
neutron resonance absorption integral of, (E), 20: 14008(R) (ANL-7122, pp 42-69)

VANADIUM SYSTEMS
O–V, phase studies on, 20: 13260(R) (NP-15852)

VEHICLES
fuel for, methanol synthesis using nuclear power in mobile energy depot system, 20: 12877 (BNL-955)

VELA PROJECT
cavity stresses in Project Dribble, (T), 20: 12989 (NVO-1312-1(Vol.1))
instrumentation design and performance for Project Dribble, 20: 12990 (NVO-1312(Vol.2))

VENTILATION
monitoring exhaust from laboratory system for, equipment for, 20: 13006 (ORNL-TM-1384)

VESSELS
design for containment of gaseous fuel reactors, 20: 14054(P)

VIRUSES
radiation effects on HeLa cells infected with adeno-, uv, 20: 12711

VITAMIN B
radiosterilization effects on content of, in strawberries, gamma, 20: 13142(R) (UCD-34P80-3, pp 52-4)

VITAMIN K
effects on radiosensitivity of fruit-spoilage fungi, 20: 13137 (NP-15360)

W

WASTE DISPOSAL
management of, economics of, 20: 14208 (ORNL-P-1926)
radiation protection in, 20: 13017
tank storage of acid and alkaline solutions, economics of, 20: 14208 (ORNL-P-1926)

WASTE PROCESSING
filtration of sludges, two processes for, 20: 14210
fixation in glass, testing rising-level method for, 20: 12928(R) (ORNL-3868)
incinerator for, 20: 14212(P)
sorption, properties of Italian clays for fixation of cesium-137 and strontium-89, 20: 14209 (RT/PHOT(65)29)

WASTE SOLUTIONS
processing methods for, from cobalt-60 and iodine-131 production, 20: 14211

WATER
analysis for chlorine and copper, activation, 20: 12768 (IEA-97)
analysis for oxygen-18, mass spectrometric, 20: 12800
neutron diffusion parameters for, pulsed, (E), 20: 13729
neutron flux distributions in, extrapolation distances from pulsed, (E), 20: 13726
neutron thermalization in, pulsed-source measurements of, (E), 20: 13739
purification by ion exchange, design of fallout treatment kit for, 20: 12942(P)
reactions with sodium, loop development for analyzing, 20: 14024(R) (APDA-182)
reactions with sodium in steam generators, 20: 14149(T,R) (ORNL-tr-900)
thermodynamic and transport properties of, significant-structure theory for, 20: 12858
yields in radioinduced oxidation of isobutane using hydrobromic acid catalyst, 20: 12883 (ORO-634)
air–H_2O, swirl flows in tubes, (E/T), 20: 12960 (EURAEC-1515)
graphite–H_2O, neutron thermalization in, at large temperature gradients, (E), 20: 13740
PuO_2–UO_2–H_2O, criticality studies using pulsed sources, (E), 20: 14078
steam–water, boiling burnout in vertical tubes, empirical correlation for, 20: 12968
UO_2–H_2O, reactivity of variable-pitch lattices of, kinetic and steady-state measurements of, (E/T), 20: 14079

WATER-d_2
air–Al–D_2O, neutron diffusion in air-filled aluminum-tube lattices in heavy water, (E/T), 20: 13705(R) (MIT-2344-4, pp 135-44)
neutron diffusion constant of, pulsed-source technique for measuring, (E), 20: 14076
neutron spectra in, pulsed-source measurement of time-dependent, (E/T), 20: 13736
thermodynamic and transport properties of, significant-structure theory for, 20: 12858
yields in gamma radiolysis of gaseous deuterium–oxygen mixtures, 20: 12881 (AD-626609)

WATER COOLED REACTORS
boiler design for, 20: 14041(P)
control of, use of soluble poison and xenon-135 for, 20: 14099(P)
power level determination from nitrogen-16 activity in coolant, 20: 14019

WATER MODERATED REACTORS
control of, use of soluble poison and xenon-135 for, 20: 14099(P)
fuel burnup in, plutonium centered natural urania, (T), 20: 14102 (BNWL-183, Sect.II)

WATER VAPOR
reactions with pyrolytic-carbon-coated fuel particles at 1000°C, 20: 13261(R) (ORNL-3885, pp 87-149)
reactions with uranium carbide, factors affecting, 20: 12925(R) (EURAEC-1446)

WELDED JOINTS
performance of fuel element end seals, determination of, 20: 14196
testing of niobium–zirconium, nondestructive, 20: 13320

WELDING
effects on recrystallization in molybdenum, niobium, tantalum, and tungsten, 20: 13267(T) (AD-624909)
tube to tubesheet for heat exchanger, automated equipment and process for, 20: 13219 (RL-SEP-710)
ultrasonic, bibliography on, 20: 13210 (AWRE/LIB/BIB/13)

WELDS
flaw detection in, methods development for x-ray, 20: 13177(R) (EURAEC-1504)
inspection of, methods for radiographic and ultrasonic, 20: 12973(R) (EURAEC-1519)
porosity in heat-resisting alloys, causes and effects of, 20: 13264(R) (WANL-PR(P)-008)

WELL LOGGING
method of gamma-gamma, for heavy element concentration in rocks, 20: 12993
neutron calculations in, Monte Carlo method for, 20: 12994

WHEAT
radiation effects on genetic variability in, 20: 12641 (TID-22582)
radioinduced mutations in, classification of, 20: 12632(R) (EUR-2546.f)

WINDOWS
design of vanadium-foil, for electric discharge devices, 20: 13052(P)

WIRES
coating with cross-linked polyvinylidene fluoride polymers using radiation, 20: 12909(P)

WOUNDS
effects of skin, on septicemia in irradiated mice, 20: 12704
radiation effects on healing time of mouse, x, 20: 12684

X

X RADIATION
detection and measurement of, instruments for, (E), 20: 13092
dosimetry of low-level, 20: 12999 (CEA-R-2746)
dosimetry of soft, using G-M counters, 20: 13085
dosimetry of 15-Mev, in cervical cancer therapy, 20: 12747
dosimetry of, circuit arrangement for, 20: 13124(P)
dosimetry of, during benign tumor therapy, 20: 13013
dosimetry of, performance of ionization chambers for, 20: 13113
effects of, review of biological, 20: 12999 (CEA-R-2746)
effects on Aedes populations, 20: 12668
effects on angiomas, effects of age on, 20: 12745
effects on animal cells, morphological, 20: 12635(R) (NYO-2786-1)
effects on anthracene crystals, 20: 12893
effects on barley, genetic, 20: 12714
effects on benign tumors in children, dose to attendant and patient from, 20: 13013
effects on binary mixtures of benzene and alcohols at 77°K, ESR and tracer studies of, 20: 12890
effects on bone growth in rats, protective effects of MEG against, 20: 12729
effects on carbon dioxide in exchange reactions between labeled carbon dioxide and oxygen, 20: 12882 (IA-1065)
effects on carcinostatic properties of gastric cancer extracts, 20: 12625
effects on cell survival in mouse sarcomas, effects of oxygen inhalation on, 20: 12725
effects on cervical carcinomas, cytological, 20: 12659
effects on chick embryos, pathological, 20: 12706
effects on chromosomes in hypothermic mice, mutagenic, 20: 12693

effects on course of bacteremia in mice, 20: 12704
effects on crystals of alkali metal halides, (E), 20: 13973(R) (NYO-3033-1)
effects on decarboxylase activity and protein content of mouse livers, 20: 12782
effects on developing mouse fetuses, effects of dose on, 20: 12683
effects on developing mouse embryos, pathological, 20: 12650
effects on developing mouse fetuses, pathological, 20: 12650
effects on DNA synthesis in rat liver as function of time, 20: 12638 (TID-21474)
effects on dogs, effects of polyglucine on, 20: 12723(T) (JPRS-33766, pp 3-7)
effects on dogs, pathological, 20: 12645
effects on early stages of spermatogenesis of adult *D. melanogaster* males, 20: 12637 (TID-21466)
effects on EPR of potassium chlorate, 20: 12888
effects on F-center formation in potassium chloride crystals, (E), 20: 14000
effects on F-center absorption in sodium fluoride, 20: 12892
effects on feeder layers in mouse tissue cultures, 20: 12654
effects on genetic variability in maize and wheat, 20: 12641 (TID-22582)
effects on hemangiomas in children, 20: 12750
effects on immune reactions to allogenic skin grafts in mice, 20: 12656
effects on inseminated and virgin Drosophila females, mutagenic, 20: 12663
effects on intraocular tumors, therapeutic, 20: 12740
effects on leukocytic chromosomes after abdominal or pelvic therapy, aberrant and ploidy, 20: 12658
effects on lizard populations, gonadal-exposure, 20: 12585
effects on luminescence of potassium iodide, 20: 12891
effects on maize, genetic, 20: 12678
effects on male germ cells of *D. melanogaster*, effects of age on mutagenic, 20: 12636 (TID-21459)
effects on mean viability of Drosophila autosomes, 20: 12661
effects on mice, lethal, 20: 12685
effects on mice, protective effects of bone marrow therapy against, 20: 12720(R) (TID-22466)
effects on microsporogenesis in sugar beet plants, 20: 12676
effects on mouse spleen cells, cytological, 20: 12681
effects on osmotic resistance of rat leukocytes, 20: 12705
effects on phage, recovery from, 20: 12617(R) (NP-15863)
effects on phagocytic activity of leukocytes in preserved blood, 20: 12698
effects on rats, effects of pre-irradiation on, 20: 12701
effects on rats, effects of stress on, 20: 12703
effects on respiratory center of man, 20: 12702
effects on skin of guinea pigs and rabbits, mechanism for, 20: 12623
effects on thermal hemolysis of rat erythrocytes, 20: 12697
effects on Tradescantia, effects of ATP, histidine, and proline on recovery from, 20: 12728
effects on transforming DNA, inactivating, 20: 12620
effects on vacancy center formation in potassium bromides at low temperature, (E), 20: 13999
effects on wound healing time in mice, 20: 12684
effects on wound healing after surgical resection for tumors, 20: 12646
effects on X chromosome in Drosophila females, 20: 12689
effects on X chromosomes in female Drosophila, 20: 12690
effects with and without thermal trauma on intestinal mucosa in rats, 20: 12630 (BNL-8383)
emission from Japanese television equipment, 20: 13014
reactions with alkali azides, EPR study of nitrogen free radicals from, 20: 13970 (AD-611432, pp 135-47)
reactions with nuclei at low energies, excitation in, 20: 13782 (ORNL-P-1927)

X-RAY EQUIPMENT
development of, for reduction of radiation hazards, 20: 12757

X-RAY SOURCES
dose rate and spectra measurements from pulsed, (E), 20: 13057 (AD-627567)

XENON
ionization by fission fragments, plasma production in, (E/T), 20: 13939
spectra of hydrobromic, hydrochloric, and hydriodic acids in, deuterium effects on, 20: 12857

XENON FLUORIDES
crystal structure, 20: 12844
molecular structure of gaseous, 20: 12860
preparation by fission recoil in neutron-irradiated uranium dioxide–lithium fluoride mixtures, 20: 12898

XENON IONS
sputtering on gold at 40 to 100 ev, yields from, (E/T), 20: 13420

XENON ISOTOPES Xe-132
energy level transitions in, internal conversion coefficients for, (E), 20: 13883
reactions with gallium-69, dynamic deformation in inelastic, (T), 20: 13794

XENON ISOTOPES Xe-133
separation from uranium-235 fission products by sorption on charcoal or molecular sieve, 20: 12772 (ORNL-3840)

XENON ISOTOPES Xe-135
buildup in reactor, reactivity control by, 20: 14099(P)

XENON ISOTOPES Xe-136
energy levels of, second-vibrational, (T), 20: 13793

XENON OXIDES
spectra and potential of, analysis of vibrational, 20: 12842

XENON OXYFLUORIDES
Urey-Bradley force constants, 20: 12841

XYLENE
neutron diffusion parameters for, pulsed, (E), 20: 13729

Y

YEASTS
radioinduced mutations at melezitose locus in Saccharomyces, uv, 20: 12655

YTTERBIUM
determination by spectrometry using 4,5-dihydroxy-3-[(*p*-sulfophenyl)azo]-2,7-naphthalenedisulfonic acid, 20: 12806
neutron absorption resonance integrals, 20: 14059(R) (IDO-17104)
preparation of isotopic bulk materials and foils of, from oxide, 20: 13216 (ORNL-P-1899)
separation from other inorganic ions by paper chromatography, 20: 12939
solvent properties for tantalum, 20: 13180(R) (IS-RD-4)

YTTERBIUM ALLOYS
Ca–Yb, phase studies on, by differential thermal analysis, 20: 13254 (IS-T-70)
Pb–Yb, phase studies, 20: 13180(R) (IS-RD-4)

YTTERBIUM BORATES
crystal structure of vaterite-type, polymorphism in, 20: 12837

YTTERBIUM CHLORIDES
thermal capacity of aqueous solutions of, at 25°C, 20: 12818 (IS-T-52)

YTTERBIUM COMPLEXES
with dilactic, mandelic, and quinic acids, formation and stability constants of, 20: 12817 (IS-1311)

YTTERBIUM HYDRIDES
Yb–YbH_2, equilibrium hydrogen dissociation pressure in, 20: 12829 (TID-22502)

YTTERBIUM ISOTOPES
preparation of bulk materials and foils of, from oxide, 20: 13216 (ORNL-P-1899)

YTTERBIUM OXIDES
BaO–Yb_2O_3, optical properties of compounds formed in, 20: 13278
SrO–Yb_2O_3, optical properties of compounds formed in, 20: 13278

YTTERBIUM SYSTEMS
Yb–YbH_2, equilibrium hydrogen dissociation pressure in, 20: 12829 (TID-22502)

YTTRIUM
determination in glass, emission spectrographic, 20: 12810
preparation and purification of, process development for, 20: 13180(R) (IS-RD-4)
separation from other inorganic ions by paper chromatography, 20: 12939
solvent properties for nitrogen, 20: 13180(R) (IS-RD-4)
solvent properties for tantalum, 20: 13180(R) (IS-RD-4)

YTTRIUM ALLOYS
Al–Cr–Fe–Y, diffusion of uranium through cladding of, 20: 13179(R) (GEMP-55A, pp 13-28)
Al–Cr–Fe–Y, impact properties of powder-metallurgy, effects of atomized powders on, 20: 13179(R) (GEMP-55A, pp 13-28)
Al–Cr–Fe–Y, radiation effects on tensile properties of, fast-neutron, 20: 13179(R) (GEMP-55A, pp 13-28)
Gd–Os–Y, magnetic and superconducting ordering in, 20: 13694
Gd–Os–Y, thermal capacity at 0.25 to 20°K, 20: 13694
Pb–Y, phase studies, 20: 13180(R) (IS-RD-4)

YTTRIUM COMPLEXES
with dilactic, mandelic, and quinic acids, formation and stability constants of, 20: 12817 (IS-1311)

YTTRIUM ISOTOPES Y-86
energy level assignments from zirconium-86 decay, (E), 20: 13856

YTTRIUM ISOTOPES Y-87
production by alpha reactions with rubidium at 35 Mev, 20: 12917

YTTRIUM ISOTOPES Y-89
proton reactions (p,n) at 14.2 Mev, angular distributions, Q values, and spectra from, (E), 20: 13345(R) (NP-15772)

YTTRIUM ISOTOPES Y-90
beta decay of, bremsstrahlung spectra in, (E), 20: 13761 (CONF-233 (Vol.4), pp 656-68)

effects on pancreatic and liver cancer, 20: 12738
implantation for pituitary ablation, 20: 12753
use in pituitary gland ablation, 20: 12748
YTTRIUM ISOTOPES Y-91
separation from aqueous solution by sorption on diatomaceous earth, 20: 12938
YTTRIUM ISOTOPES Y-97
half life, (E), 20: 13783 (ORNL-TM-1333)
YTTRIUM OXIDES
performance as crucible for carbon reduction of uranium, 20: 13180(R) (IS-RD-4)
BaO–Y_2O_3, optical properties of compounds formed in, 20: 13278
ReO_2–Y_2O_3, preparation and ferromagnetic properties of phases in, 20: 13260(R) (NP-15852)
SrO–Y_2O_3, optical properties of compounds formed in, 20: 13278
YTTRIUM SYSTEMS
C–Nb–W–Y–Zr, weldability of D-43Y, 20: 13264(R) (WANL-PR(P)-008)
C–Y, phase studies, 20: 13180(R) (IS-RD-4)

Z

ZINC
determination in rocks, gamma-gamma logging method for, 20: 12993
effects on physiology of male reproductive organs of rats, 20: 12601 (TID-22526)
neutron resonance absorption integral of, (E), 20: 14008(R) (ANL-7122, pp 42-69)
separation from other inorganic ions by paper chromatography, 20: 12939
ultraviolet emission from electron-bombarded foils of, 20: 14004
ZINC ALLOYS
Ca–Zn, thermodynamic properties, 20: 13180(R) (IS-RD-4)
Mg–Zn, analysis for ruthenium using 1-nitroso-2-naphthol, spectrophotometric, 20: 12788
ZINC COMPLEXES
with hexamethylphosphoramide, NMR contact shifts in, 20: 12828 (TID-21587)
ZINC OXIDES
neutron resonance absorption integral of, (E), 20: 14008(R) (ANL-7122, pp 42-69)
ZINC SELENIDES
electron band structure of, high-pressure determination of, 20: 14221 (COO-1198-230)
ZINC SULFIDES
electron band structure of, high-pressure determination of, 20: 14221 (COO-1198-230)
radioinduced damage in single crystals of, thermoluminescent trapping states from electron, (E), 20: 13990
use of silver-activated, as intensifier in alpha autoradiography, 20: 12563
ZINC TELLURIDES
electron band structure of, high-pressure determination of, 20: 14221 (COO-1198-230)
ZIRCALOY-2
bonding to type 304 stainless steel, diffusion, 20: 13222
removal from uranium dioxide, fluid-bed fluoride volatility process for, 20: 12923 (ANL-6898)
testing of fuel claddings of, economics of nondestructive, 20: 14032
testing of fuel cladding of, eddy current, 20: 14033
thermal capacity at 50 to 700°C, 20: 13310
U–Zircaloy-2, fluid-bed fluoride volatility process for uranium separation from, 20: 12924 (ANL-6973)
ZIRCALOY-4
testing of fuel claddings of, economics of nondestructive, 20: 14032
testing of fuel cladding of, eddy current, 20: 14033
ZIRCONIUM
combustion and explosion of droplets of, by flash heating, 20: 12826 (SC-RR-65-569)
determination in submicrogram amounts, concentration-dependent distribution methods for, 20: 12778 (UJV-1434/65)
effects on crystal structure of alpha-iron, 20: 13317
mechanical properties at room temperature, effects of prestrain at 77°K on, 20: 13246 (CONF-651017-13)
neutron absorption and inelastic scattering by, gamma spectra from, 20: 13966 (UNC-5140)
separation from other inorganic ions by paper chromatography, 20: 12939
solubility in alpha-iron at 600 to 900°C, 20: 13317
spectra of, effects of electronic structure on x-ray emission, 20: 12846
tensile properties of polycrystalline alpha-, 20: 13245 (CONF-651017-7)
ZIRCONIUM ALLOYS
properties of, internal friction measurement for determining, 20: 13321
Al–Sn–Ti–Zr, phase studies, 20: 13273
Bi–Zr, preparation and phase studies on, 20: 13252 (IS-1269)
Mo–Ti–Zr, compatibility of TZM, with niobium–1 zirconium alloy in refluxing potassium at 2000°F, 20: 13192(R) (NASA-CR-54843)
Nb–Ta–W–Zr, creep behavior in ultrahigh vacuum at 2000 and 2200°F, 20: 13256 (NASA-TN-D-3222)
Nb–Ta–W–Zr, weldability of FS-85, effects of oxygen contamination on, 20: 13264(R) (WANL-PR(P)-008)
Nb–W–Zr, creep behavior in ultrahigh vacuum at 2000 and 2200°F, 20: 13256 (NASA-TN-D-3222)
Nb–Zr, anomalous critical currents in superconducting noninductive coils of, (E), 20: 13674
Nb–Zr, compatibility with TZM molybdenum alloy in refluxing potassium at 2000°F, 20: 13192(R) (NASA-CR-54843)
Nb–Zr, microstructure, effects of tempering on, 20: 13304
Nb–Zr, performance as cladding for alloy and carbide fuels, (E), 20: 14007(R) (ANL-7122, pp 1-41)
Nb–Zr, rupture properties of, effects of exposure to potassium at 1400°F on stress-, 20: 13191(R) (NASA-CR-54476)
Nb–Zr, superconductivity of, 20: 13666 (IPP-4/22)
Nb–Zr, thermodynamic properties of nitrogen equilibrium solid solutions in, 20: 13263 (ORNL-TM-1355)
Nb–Zr, welding of, nondestructive testing of zones of, 20: 13320
Pu–U–Zr, phase transformations at 550°C, (E), 20: 14007(R) (ANL-7122, pp 1-41)
Pu–U–Zr, radiation effects on, in-pile testing of, (E), 20: 14007(R) (ANL-7122, pp 1-41)
U–Zr, reactions with air, nitrogen, and oxygen, disintegration properties of, 20: 14169 (AFWL-TDR-64-75)
ZIRCONIUM BORIDES
Cr–ZrB_2, phase studies, evidence for existence of $CrZrB_2$ in, 20: 13276
ZIRCONIUM CARBIDES
UC–ZrC, use as thermionic emitters for cesium-vapor cells, 20: 13444(P)
ZIRCONIUM HYDRIDES
chemical bonds in, properties of, 20: 12847
neutron spectra in, pulsed-source measurements of, (E/T), 20: 13737
neutron thermalization in, pulsed-source measurements of, (E), 20: 13739
Al–UO_2–ZrH, reactivity measurements in lattices of, near-critical, (E), 20: 14082
BeO–ZrH, reactivity effects on plutonium-fueled reactors, 20: 14122(R) (GA-4451)
ZIRCONIUM ISOTOPES Zr-86
decay of, yttrium-86 levels from, (E), 20: 13856
ZIRCONIUM ISOTOPES Zr-90
alpha inelastic scattering at 65 Mev, nuclear structure analysis from, (E/T), 20: 13784 (ORNL-TM-1336)
alpha reactions (α,He-3) at 65 Mev, nuclear structure analysis from, (E/T), 20: 13784 (ORNL-TM-1336)
proton inelastic scattering by, shell-model form factors for, (T), 20: 13867
proton reactions (p,n) at 14.2 Mev, angular distributions, Q values, and spectra from, (E), 20: 13345(R) (NP-15772)
proton scattering at 18.8 Mev, shell-model analysis of angular distributions from, (E/T), 20: 13866
ZIRCONIUM ISOTOPES Zr-91
alpha inelastic scattering at 65 Mev, nuclear structure analysis from, (E/T), 20: 13784 (ORNL-TM-1336)
alpha reactions (α,He-3) at 65 Mev, nuclear structure analysis from, (E/T), 20: 13784 (ORNL-TM-1336)
ZIRCONIUM ISOTOPES Zr-92
alpha reactions (α,He-3) at 65 Mev, nuclear structure analysis from, (E/T), 20: 13784 (ORNL-TM-1336)
alpha scattering at 65 Mev, nuclear structure analysis from, (E/T), 20: 13784 (ORNL-TM-1336)
ZIRCONIUM ISOTOPES Zr-94
proton reactions (p,n) at 14.2 Mev, angular distributions, Q values, and spectra from, (E), 20: 13345(R) (NP-15772)
ZIRCONIUM ISOTOPES Zr-95
separation from aqueous solution by sorption on diatomaceous earth, 20: 12938
uptake by plants in Georgia piedmont, 20: 12985
yields in thermal-neutron fission of uranium-233 and -235, (E), 20: 13783 (ORNL-TM-1333)
ZIRCONIUM ISOTOPES Zr-97
half life, (E), 20: 13783 (ORNL-TM-1333)
ZIRCONIUM OXIDES
chemical bonds in, properties of, 20: 12848
diffusion of hydrogen in films of, kinetics of, 20: 13201
electric conductivity of, effects of temperature on, 20: 12850
fabrication of hard dense, hot-pressing method and apparatus for, 20: 13230(P)
neutron resonance absorption integral of, (E), 20: 14008(R) (ANL-7122, pp 42-69)
reactions with barium carbonates and barium oxides, 20: 13282
reactions with rubidium carbonates or silicates at 870 to 950°C, 20: 12851

thermal conductivity of powders of, at 100 to 850°C, 20: 12854
thermal conductivity of powders of, at 100 to 850°C, (T), 20: 12855
use as corrosion inhibitor in high-temperature gas-cooled reactors, 20: 14021(P)
vaporization of, to 2300°C, 20: 13265(T) (AD-623208)
Nb_2O_5–ZrO_2, crystal structure of compounds $ZrO_2 \cdot 5Nb_2O_5$ and $ZrO_2 \cdot 7Nb_2O_5$ in, 20: 13281
Nd_2O_3–ZrO_2, phase studies, 20: 13283
PrO–ZrO_2, phase studies, 20: 13279
SiO_2–Na_2O–ZrO_2, phase studies, 20: 13284
UO_2–ZrO_2, radioinduced homogenization of two-phase mixtures of, 20: 13330

ZIRCONIUM SYSTEMS
C–Nb–W–Y–Zr, weldability of D-43Y, 20: 13264(R) (WANL-PR(P)-008)
C–Nb–W–Zr, corrosion of D-43, by potassium at 2450°F, stress-, 20: 13191(R) (NASA-CR-54476)
C–Nb–W–Zr, creep behavior in ultrahigh vacuum at 2000 and 2200°F, 20: 13256 (NASA-TN-D-3222)
C–Nb–Zr, phase diagrams, 20: 13272

REPORT NUMBER INDEX

Reports, conference papers and proceedings, numbered translations, and patents abstracted during the period are included in this index. Each item is listed by report number; this is followed by the abstract number and a brief notation regarding public availability. The index entries show which reports are on file in the depository libraries, which reports have been published in open-literature journals (journal citation given), and which reports can be purchased (source and price). Whenever a report is identified by more than one number, cross references from secondary to primary report numbers are cited.

The report number codes apply to AEC reports unless designated otherwise. Non-AEC reports are identified by parenthetical notes after the report codes; e.g., (non-AEC), (British), (Canadian), (French). The note (Misc.) identifies those codes used for both USAEC and non-AEC reports. Patents are listed under the heading "PATENTS"; the country of origin is included in parentheses.

A comprehensive listing of both AEC and non-AEC report codes is contained in TID-85(5th Rev.), *Report Number Series Used by the Division of Technical Information in Cataloging Reports*. This information is also included in the Cumulative Report Number Index (issued annually).

Public Availability of USAEC Reports

All USAEC reports abstracted in *NSA* are available to the public through one or more of the following sources:

(1) Depository libraries in the United States, in other countries, and in international agencies. A list of these depositories appears on the inside covers of each issue of *NSA*.

(2) Scientific and technical journals or other publications.

(3) Microcard Editions, Inc., in Microcard and micronegative form. Orders and inquiries should be sent to: Accounting and Shipping Department, West Salem, Wisconsin 54669.

(4) Clearinghouse for Federal Scientific and Technical Information, U. S. Department of Commerce, Springfield, Virginia 22151.

(5) Superintendent of Documents, U. S. Government Printing Office, Washington, D. C. 20402.

Public Availability of Non-AEC Reports

U. S. Reports. Many reports of U. S. Government agencies are available to the public from the Clearinghouse for Federal Scientific and Technical Information (CFSTI). This availability is given when known. Such reports should be ordered by AD number or NASA-N number. If availability is not shown, inquiries may be directed to CFSTI. In the case of NP numbers, inquiries should be by title and author.

Non-U. S. Reports. Many reports of atomic energy establishments of other countries are deposited in the libraries listed on the inside covers of each issue of *NSA*.

Additionally, the following have made their reports available as indicated.

AUSTRALIA

Australian Atomic Energy Commission Research Establishment. Available upon request from the Library, Australian Atomic Research Establishment, Private Mail Bag, Sutherland, New South Wales, Australia.

BELGIUM

Centre d'Étude de l'Énergie Nucléaire. Available upon request to individuals and organizations, from the Centre d'Étude de l'Énergie Nucléaire (CEN), 31, Rue Belliard, Bruxelles, Belgium.

CANADA

Atomic Energy of Canada Limited. For sale by the Technical Information Officer, Atomic Energy of Canada Limited, Chalk River, Ontario, Canada. Copies are also deposited in libraries in the United Kingdom.

National Research Council of Canada. Available from the National Research Council of Canada, Ottawa 2, Ontario, Canada.

DENMARK

Atomic Energy Commission Research Establishment, Risø. Available on exchange from the Library, Danish Atomic Energy Commission, Risø, Roskilde, Denmark. Also for sale by Jul. Gjellerup, Booksellers, 87 Sölvgade, København K., Denmark.

Danatom. Available on loan from Research Establishment, Risø, Roskilde, Denmark. Copies are available from Danatom, Aurehøjvej 2, Hellerup, Denmark.

EURATOM

Reports from the Commission of the European Atomic Energy Community are available from: Presses academiques europeennes, 98, chaussee de Charleroi, Brussels 6, Belgium; and Office central de vente des publications des Communautes eurodeennes 2, place de Metz, Luxemburg.

FRANCE

Commissariat à l'Énergie Atomique. Inquiries for reports numbered 1-2199 should be addressed to Commissariat à l'Énergie Atomique, Service Central de Documentation, Centre d'Études Nucléaires de Saclay, Boite Postale No. 2, Gif-sur-Yvette (S. et O.), France. Reports numbered 2200 and above are available from La Documentation Francaise, 16 Rue Lord-Byron, Paris VIII, France.

Service Central de Protection contre les Rayonnements Ionisants. Copies are available from Ministère de la Santé Publique, Service Central de Protection contre les Rayonnements Ionisants, B. P. n° 35–LE VESINET (S. et O.), France.

GERMANY

Deutsches Elektronen-Synchrotron DESY. Copies are available from Deutsches Elektronen-Synchrotron Desy, Dokumentation, 2000 Hamburg-Gr. Flottbek 1, Notkestieg 1, Germany.

Gesellschaft für Kernforschung mbH (KFK). Copies are available from Gesellschaft für Kernforschung mbH, 75 Karlsruhe, Postfach 947, Germany. Copies are also deposited in many national nuclear centers in the world.

Kernforschungsanlage. Copies may be ordered from Zentralbibliothek der Kernforschungsanlage Jülich, Jülich, Bundesrepublik Deutschland.

Hahn-Meitner-Institute für Kernforschung. Available without charge from Hahn-Meitner-Institute für Kernforschung Berlin, Bibliothek, Glienicker Strasse 100, 1 Berlin

39, Germany. Copies are deposited in many national nuclear centers in the world.

Johann-Wolfgang-Goethe Universität, Frankfurt Am Main, Institut für Kernphysik, (IKF). Copies are available from Gmelin Institut, 40-42 Varrentrappstrasse, Frankfurt (Main), West Germany.

ISRAEL

Israel Atomic Energy Commission. Available without charge from Ministry of Defence/Atomic Energy Commission, Soreq Research Establishment, Yavne, Israel. Copies are deposited in libraries in Israel and in other countries.

ITALY

Centro Informazioni Studi Esperienze (CISE). For sale at CISE Press Office, Casella Postale 3986, Milano, Italy. Copies are deposited in libraries in Italy.

Comitato Nazionale per l'Energia Nucleare. Copies are available from Comitato Nazionale per l'Energia Nucleare, Divisione Affari Internazionali e Studi Economici, Ufficio Pubblicazioni, Via Belisario, 15, Roma, Italy.

JAPAN

Japan Atomic Energy Research Institute (JAERI). Available from the Staff Supply Cooperative of Japan Atomic Energy Research Institute (JAERI), 1-1 Tamura-Cho, Shiba, Minato-Ku, Tokyo, Japan. Copies are deposited in depositories in Tokyo, Nagoya, and Osaka.

Nagoya University. Copies are available from Research Information Center, Institute of Plasma Physics, Nagoya University, Nagoya, Japan.

University of Tokyo. Available free of charge from Institute for Nuclear Study, University of Tokyo, Tanashi-Machi, Kitatama-gun, Tokyo, Japan.

NETHERLANDS

Reactor Centrum Nederland. For sale by Reactor Centrum Nederland, 112 Scheveningseweg, 's-Gravenhage, The Netherlands. Copies are deposited in university libraries in Holland and in many national nuclear centers in the world.

NEW ZEALAND

Institute of Nuclear Sciences. Copies are available from Librarian, Institute of Nuclear Sciences, D.S.I.R., Private Bag, Lower Hutt, New Zealand. Copies are deposited in other countries.

NORWAY

Forsvarets Forskningsinstitutt. Copies available from Norwegian Defence Research Establishment, Library, P. O. Box 25, Kjeller, Norway.

Institutt for Atomenergi. "KR" reports are available on an exchange basis from the Library, Institutt for Atomenergi, Box 40, Kjeller, Norway. Other series are not generally available to the public.

Norwegian Reactor School. Copies are available from The Library, Institutt for Atomenergi, P. O. Box 40, Kjeller, Norway.

PAKISTAN

Atomic Energy Center. Copies are available from Atomic Energy Center, P. O. Box 658, Lahore, (West Pakistan).

POLAND

Reports of the Polish nuclear institutes are published by the Nuclear Energy Information Center of the Government Commissioner for Use of Nuclear Energy. Copies are available from Ośrodek Informacji o Energii Jądrowej, Warszawa, PKiN, Poland.

SPAIN

Junta de Energia Nuclear. "JEN" reports are available without charge from Servicio de Documentation, Junta de Energia Nuclear, Ciudad Universitaria, Madrid (3), Spain.

SWEDEN

Aktiebolaget Atomenergi. "AE" reports are for sale from Aktiebolaget Atomenergi, Library Section, Box 43041, Stockholm 43, Sweden. Bibliographies and literature surveys of the VDDIT- series may be obtained from Aktiebolaget Atomenergi, Information Office, Scientific and Technical Information, Box 43041, Stockholm 43, Sweden. Other series are not generally available to the public. Organizations in the atomic energy field may obtain copies from Aktiebolaget Atomenergi. Microcopy of AE reports is available from the International Documentation Centre, Tumba, Sweden.

SWITZERLAND

CERN European Organization for Nuclear Research. Available without charge from CERN European Organization for Nuclear Research, Geneva 23, Switzerland. Copies are deposited in libraries in 13 countries.

Eidgenössisches Institut für Reaktorforschung. "EIR" reports are available from Eidgenössiches Institut für Reaktorforschung, c/o Bibliothek, Würenlingen/Ag, Switzerland.

TURKEY

Turkish Atomic Energy Commission. Copies are available free of charge from T.A.E.C., Çekmece Nuclear Research Center, P. O. Box 1, Airport, Istanbul, Turkey.

UNITED KINGDOM

United Kingdom Atomic Energy Authority. Some reports are for sale in the United States by the British Information Service (BIS), 845 Third Avenue, New York, N. Y. 10022. United Kingdom reports generally may be purchased from Her Majesty's Stationery Office, London. Copies not for sale by Her Majesty's Stationery Office may be purchased in microcopy form from Micro Methods Limited, East Ardsley, Wakefield, Yorks, England. Report copies are deposited in a large number of libraries in England.

Conferences

Published conference proceedings as well as individual unpublished papers from conferences are included in this index. A CONF number is assigned to the conference if published proceedings are received and also if only a single paper is received. The base number used is year-month-sequence. Thus, the number CONF-650101 would indicate that the conference was held in 1965, in January, and that this was the first January 1965 conference so received. This number would be assigned to complete published proceedings, or if individual papers are received, the base number would be extended to include a paper number, i.e., CONF-650101-1. As additional papers are received, they will be assigned consecutive numbers in the series, CONF-650101-1, 2, 3, 4, etc. This numbering system ensures that all papers received from a conference will be associated with that conference in this index.

If published proceedings are received after the receipt of individual papers, the complete proceedings will be abstracted and the abstract number will appear in this index with the base CONF number.

Abbreviations Used in Availability Column

AECL	For sale by Atomic Energy of Canada Ltd., Chalk River, Ontario, Canada.
BIS	For sale by British Information Service, 845 Third Avenue, New York, N. Y. 10022
CFSTI	For sale by the Clearinghouse for Federal Scientific and Technical Information, U. S. Department of Commerce, Spring-

field, Virginia 22151. The symbol "cy" indicates that the format of the item sold may be either a printed document or a photographic reproduction (two-thirds of original size) depending upon the availability of printed stock. The indicated price is for either format. The symbol "mn" is used to indicate that copy is also available in the form of micronegatives (microfiche).

Dep. — AEC reports: Full-size copy is on deposit in the depository libraries both inside and outside the United States. These reports are also for sale by Microcard Editions, Inc., Accounting and Shipping Department, West Salem, Wisconsin 54669.

Non-AEC reports: Full-size copy on deposit in the depository libraries in the United States only.

Dep.(mc) — Same as for Dep., except copy is in Microcard form.

Dep.(mn) — Same as for Dep., except copy is in micronegative (microfiche) form.

DSIR — For sale by the National Lending Library for Science and Technology (D.S.I.R.), Boston Spa, Yorkshire, England.

DTI Extension — Available from the U. S. Atomic Energy Commission, Division of Technical Information Extension, P. O. Box 62, Oak Ridge, Tennessee 37830.

EM — Blueprints and microcopy of AEC engineering drawings are available from Clearinghouse for Federal Scientific and Technical Information, U. S. Department of Commerce, Springfield, Virginia 22151. Current prices of the CAPE- packages may be obtained from this address. TID-4100, available from the Division of Technical Information Extension, P. O. Box 62, Oak Ridge, Tennessee 37831, contains information on all the CAPE- packages for sale.

Gmelin — Available at a nominal charge and under the AED- number shown from Atomic Energy Documentation Center, Gmelin Institute, 40-42 Varrentrappstrasse Frankfurt (Main), West Germany.

GPO — For sale by the Superintendent of Documents, Government Printing Office, Washington, D. C. 20402.

HMSO — Her Majesty's Stationery Office, London.

IAEA — Available from the International Atomic Energy Agency, Vienna, Austria, and from its sales agencies in various countries throughout the world. A list of these agencies is found in each STI/DOC and STI/PUB publication.

JCL — For sale by the Special Libraries Association Translation Center, John Crerar Library, 35 West 33rd Street, Chicago, Illinois 60616.

LC — For sale by the Library of Congress, Photoduplication Service, Washington, D. C. 20540.

NAS — National Academy of Sciences, National Research Council, Washington, D. C. 20418.

NRC — For sale by the National Research Council of Canada, Ottawa, Ontario, Canada.

ORINS — Available on interlibrary loan from the Library, Oak Ridge Associated Universities, Post Office Box 117, Oak Ridge, Tennessee 37830.

OTS — See CFSTI.

UKAEA, London — Available from United Kingdom Atomic Energy Authority, 11 Charles II Street, London, S. W. 1.

UN — United Nations Bookshop, United Nations Headquarters, New York, New York.

USGS — Available free of charge from the U. S. Geological Survey, Washington, D. C. 20242.

[The symbols "ph," "mf," and "fs" are used to designate that copy is available only in photostat, microfilm, or facsimile form. The symbol "mn" is used to designate that copy is available in micronegative (microfiche) form. The symbol "cy" is used to designate full size or photographically enlarged copy (two-thirds of original size).]

Report No.	Abstract No.	Availability
ACF–		
15	20-14213	Dep. mn. CFSTI $3.00 cy, $0.75 mn
412-256	20-14213	See ACF-15
ACNP–	**(Misc.)**	
65522	20-14143	See PAPP 6401
AD–	**(Misc.)**	
476320	20-14175	See TID-22418
476321	20-14173	See TID-22416
476322	20-14174	See TID-22417
607410	20-14169	CFSTI $3.00 cy, $0.75 mn
611432	20-12760	CFSTI $8.25 cy, $2.25 mn
623208	20-13265	CFSTI $1.00 cy, $0.50 mn
624905	20-13266	CFSTI
624909	20-13267	CFSTI
625070	20-13928	CFSTI
625252	20-13134	CFSTI $2.00 cy, $0.50 mn
625483	20-13135	CFSTI $2.00 cy, $0.50 mn
625834	20-13971	CFSTI $1.00 cy, $0.50 mn
626210	20-12997	CFSTI $2.00 cy, $0.50 mn
626320	20-12588	CFSTI $2.00 cy, $0.50 mn
626609	20-12881	CFSTI $1.00 cy, $0.50 mn
626622	20-13205	CFSTI $3.00 cy, $0.75 mn
626681	20-13746	CFSTI $2.00 cy, $0.50 mn
626682	20-12716	CFSTI $1.00 cy, $0.50 mn
626997	20-12628	CFSTI $1.00 cy, $0.50 mn
626998	20-13055	CFSTI $1.00 cy, $0.50 mn
626999	20-13355	CFSTI $2.00 cy, $0.50 mn
627000	20-13056	CFSTI $1.00 cy, $0.50 mn
627077	20-12978	CFSTI $4.00 cy, $0.75 mn
627567	20-13057	CFSTI $1.00 cy, $0.50 mn
627930	20-13058	CFSTI $2.00 cy, $0.50 mn
AE–	**(Non-AEC)**	
207	20-14178	Dep. mn
210	20-13634	Dep. mn
AECD-CH–	**(Pakistani)**	
3	20-12910	Dep. mn
AECD-EP–	**(Pakistani)**	
6	20-13356	Dep. mn
7	20-13747	Dep. mn
AECD/HP–	**(Pakistani)**	
3	20-12911	Dep. mn
AECL–	**(Canadian)**	
2379	20-13797	Can. J. Phys., 44: 409-14(1966)
2381	20-13796	Can. J. Phys., 44: 399-408(1966)
2507	20-12589	Dep. AECL $0.50
2510	20-13748	Dep. AECL $0.50
AED-C–	**(Non-AEC)**	
02-06	20-13136	Dep. mn
04-22	20-12629	Dep. mn
10-04	20-12733	Dep. mn
18-06	20-13357	Dep. mn
AEEW-M–	**(British)**	
502	20-13749	Dep. BIS $1.20. HMSO 6s.
553	20-13750	Dep. BIS $0.50. HMSO 2s. 6d.
604	20-13344	Dep. BIS $0.30. HMSO 1s. 9d.
605	20-13697	Dep. BIS $0.30. HMSO 1s. 9d.
606	20-13751	Dep. BIS $0.50. HMSO 2s. 6d.
AEEW-R–	**(British)**	
411	20-13059	Dep. BIS $1.40. HMSO 7s.
445	20-14055	Dep. BIS $2.20. HMSO 11s.
AERE-NP–	**(British)**	
GEN/40	20-13090	Nucl. Instrum. Methods, 39: 68-76(1966)
AERE-R–	**(British)**	
4287	20-13242	See CONF-170, pp 126-37
4911	20-12761	Dep. BIS $0.80. HMSO 4s.
4923	20-13094	Nucl. Instrum. Methods, 39: 141-9(1966)
4956	20-13332	J. Nucl. Mater., 18: 314-22(1966)
5007	20-13300	J. Nucl. Mater., 18: 305-13(1966)
5059	20-13334	J. Nucl. Mater., 18: 348-56(1966)
5084	20-12732	Dep. BIS $0.70. HMSO 3s. 6d.
AFCRL–	**(Non-AEC)**	
65-859	20-13022	CFSTI $3.00 cy, $0.75 mn
AFWL-TDR–	**(Non-AEC)**	
64-75	20-14169	CFSTI $3.00 cy, $0.75 mn
AGN–	**(Misc.)**	
8162	20-13232	Dep. mn. CFSTI $3.00 cy, $0.75 mn
AN-AGCR–		
958	20-14145	See TID-22595
962	20-14146	See TID-22596
ANL–		
6417	20-13206	Dep. mn. CFSTI $1.00 cy, $0.50 mn
6893	20-13207	Dep. mn. CFSTI $2.00 cy, $0.50 mn
6898	20-12923	Dep. mn. CFSTI $3.00 cy, $0.75 mn
6943	20-13233	Dep. mn. CFSTI $3.00 cy, $0.75 mn
6969	20-13208	Dep. mn. CFSTI $2.00 cy, $0.50 mn
6973	20-12924	Dep. mn. CFSTI $3.00 cy, $0.75 mn
7025	20-12815	Dep. mn. CFSTI $3.00 cy, $0.75 mn
7035	20-14165	Dep. mn. CFSTI $3.00 cy, $0.50 mn
7062	20-13209	Dep. mn. CFSTI $2.00 cy, $0.50 mn
7094	20-13234	Dep. mn. CFSTI $2.00 cy, $0.50 mn
7096	20-13752	Dep. mn. CFSTI $1.00 cy, $0.50 mn
7097	20-12943	Dep. mn. CFSTI $5.00 cy, $1.00 mn
7104	20-12998	Dep. mn. CFSTI $2.00 cy, $0.50 mn
7122	20-14006	Dep. mn; CFSTI $4.00 cy, $0.75 mn
7129	20-13163	Dep. mn. CFSTI $3.00 cy, $0.50 mn
ANL-Trans–		
264	20-12643	Dep. mn. JCL $1.60 fs, $0.80 mf
APDA–	**(Misc.)**	
182	20-14024	Dep. mn. CFSTI $3.00 cy, $0.75 mn
ARL–	**(Non-AEC)**	
63-175(Pt.3)	20-13635	CFSTI $3.00 cy, $0.50 mn
AWRE-Lib–	**(British)**	
BIB/13	20-13210	Dep. mn. BIS $0.80. HMSO 4s. 0d.
AWRE-O–	**(British)**	
9/66	20-13645	Dep. mn. BIS $0.65. HMSO 3s. 3d.
99/65	20-14056	Dep. mn. BIS $1.40. HMSO 7s.
BAW–	**(Misc.)**	
393-2	20-14114	Dep. mn. CFSTI $7.00 cy, $1.75 mn
3576-1	20-14115	Dep. mn. CFSTI $3.00 cy, $0.50 mn
BM-RI–	**(Misc.)**	
6736	20-13170	Bureau of Mines Free
BMI–	**(Misc.)**	
1751	20-13171	Dep. mn. CFSTI $2.00 cy, $0.50 mn
1755	20-13235	Dep. mn. CFSTI $0.50 cy, $0.50 mn
BN–	**(Misc.)**	
432	20-13905	See CONF-651056-1
6503-01	20-13177	See EURAEC-1504
BNL–		
955	20-12877	Dep. mn. CFSTI $1.00 cy, $0.50 mn.
961	20-13753	Dep. mn. CFSTI $2.00 cy, $0.50 mn
8383	20-12630	Dep. mn. CFSTI $1.00 cy, $0.50 mn
8564	20-14214	Dep. mn. CFSTI $1.00 cy, $0.50 mn
8643	20-14215	Dep. mn. CFSTI $1.00 cy, $0.50 mn
8656	20-13011	J. Pediat., 36: 721-31(1965)
8767	20-13529	Dep. mn. CFSTI $1.00 cy, $0.50 mn
9044	20-12678	J. Heredity, 56: 157-62(1965)
9126	20-13168	J. Math. Phys., 7: 27-34(1966)
9152	20-12917	Int. J. Appl. Radiat. Isotop., 17: 9-12(1966)
9403	20-13995	Phys. Rev., 142: 306-17(1966)
9625	20-13862	Phys. Rev., 142: 716-19(1966)
9859	20-14216	Dep. mn. CFSTI $1.00 cy, $0.50 mn
9911	20-12734	Dep. mn. CFSTI $1.00 cy, $0.50 mn
9944	20-13358	Dep. mn. CFSTI $1.00 cy, $0.50 mn
BNL-tr–		
60	20-14191	Dep. mn. CFSTI $2.00 cy, $0.50 mn JCL $3.60 fs, $1.45 mf

Report No.	Abstract No.	Availability
BNWL–		
124	20-13211	Dep. mn. CFSTI $2.00 cy, $0.50 mn
158	20-12816	Dep. mn. CFSTI $1.00 cy, $0.50 mn
168	20-12972	Dep. mn. CFSTI $2.00 cy, $0.50 mn
173	20-12762	Dep. mn. CFSTI $1.00 cy, $0.50 mn
177	20-14116	Dep. mn. CFSTI $1.00 cy, $0.50 mn
178	20-13322	Dep. mn. CFSTI $1.00 cy, $0.50 mn
183	20-14010	Dep. mn. CFSTI $4.00 cy, $1.00 mn
183, Sect.I	20-14057	
183, Sect.II	20-14102	
183, Sect.III	20-14117	
183, Sect.IV	20-14118	
183, Sect.V	20-14011	
BNWL-SA–		
120	20-12571	Health Phys., 11: 1297-1304(1965)
157	20-12575	Health Phys., 11: 1371-4(1965)
222	20-12983	Health Phys., 11: 1401-6(1965)
BNWL-tr–		
11	20-12721	Dep. mn. JCL $1.60 fs, $0.80 mf
BPAD–	(Non-AEC)	
863-16719R	20-14029	See NASA-CR-54788
BRLD–	(Non-AEC)	
2933	20-13069	See NASA-CR-54468
CEA-R–	(French)	
2746	20-12999	Dep. mn
2776	20-12631	Dep. mn
2797	20-13236	Dep. mn
2822	20-13901	Dep. mn
2825	20-12590	Dep. mn
2855	20-13411	Dep. mn
2866	20-13212	Dep. mn
2891	20-13060	Dep. mn
2898	20-13902	Dep. mn
CEND–	(Misc.)	
3107-249	20-13425	Dep. mn. CFSTI $2.00 cy, $0.50 mn
CEND-PRWRA–		
257	20-14119	Dep. mn. CFSTI $9.00 cy, $2.50 mn
CERN–	(European Organization for Nuclear Research)	
65-36	20-13359	Dep. mn
65-41	20-13530	Dep. mn
65-42	20-13360	Dep. mn
CLM–	(British)	
R46	20-13412	Dep. BIS $1.50. HMSO 8s.
R51	20-13903	Dep. BIS $0.80. HMSO 4s.
R52	20-13904	Dep. BIS $0.60. HMSO 3s.
CNEA–	(Argentinian)	
161	20-12912	Dep. mn
162	20-12763	Dep. mn
CONF-170–	20-13172	(Conference on the Physical Metallurgy of Beryllium, Gatlinburg, Tenn., Apr. 30–May 1, 1963) Dep. mn. CFSTI $2.50 cy, 1.25 mn
CONF-233	(Conference on the Role of Atomic Electrons in Nuclear Transformations, Warsaw, Sept. 1963)	
(Vol.4)	20-13754	Dep. ORAU
CONF-241–	(11th International Congress of Genetics, The Hague, Sept. 1963)	
(Vol.2)	20-12564	New York, Pergamon Press, 1965
(Vol.3)	20-12565	New York, Pergamon Press, 1965
CONF-754–	(International Business Machines Medical Symposium, Poughkeepsie and Upton, N. Y., October 9, 1964)	
6	20-12734	See BNL-9911
CONF-758–	(American Physical Society Meeting, New York, Jan. 22–25, 1965)	
14	20-13445	Dep. mn. CFSTI $2.00 cy, $0.50 mn
CONF-631104–	(Meeting on the Utilization of Research Reactors, Sao Paulo, Brazil, Nov. 4–8, 1963)	
8	20-12914	See IEA-100
CONF-640630–	(Army Science Conference, West Point, N. Y., June 17–19, 1964)	
(Vol.1)	20-12760	See AD-611432
CONF-640924–	20-13649	(Symposium on Quantum Theory of Systems with Many Degrees of Freedom, Keszthely, Hungary, Sept. 1964) Acta Phys. Acad. Sci. Hung., 19: 1-363(1965)
CONF-641123–	(11th Argentine Chemical Conference, Bahia Blanca, Argentina, Nov. 1964)	
2	20-12763	See CNEA-162
CONF-641126–	(1st Symposium on Nuclear Medicine, Mendoza, Argentina, Nov. 1964)	
2	20-12912	See CNEA-161
CONF-650410–	(American Physical Society, Washington, D. C., Apr. 26–29, 1965)	
40	20-13768	ORAU
CONF-650504–	(IAEA Symposium on Pulsed Neutron Methods, Karlsruhe, Germany, May 10–14, 1965)	
(Vol.1)	20-13710	See STI/PUB/104(Vol.1)
(Vol.2)	20-13711	See STI/PUB/104(Vol.2)
CONF-650509–	(IAEA Symposium on Nondestructive Testing in Nuclear Technology, Bucharest, May 17–21, 1965)	
(Vol.2)	20-14017	See STI/PUB/105(Vol.2)
CONF-650523–	20-12569	(Symposium on Radiation and Terrestrial Ecosystems, Richland, Wash., May 3–5, 1965) Health Phys., 11: 1255-1675(1965)
4	20-12674	Health Phys., 11: 1653-62(1965)
CONF-650707–	(IEEE Annual Conference on Nuclear and Space Radiation Effects, Ann Arbor, Mich., July 12–15, 1965)	
11	20-13133	ORINS, Gmelin, AED-CONF-65-152-15
CONF-650711–	(AIAA 2nd Annual Meeting and Technical Demonstration, San Francisco, July 26–29, 1965)	
53	20-12975	ORINS
CONF-650804–	(5th Rare Earth Research Conference, Ames, Iowa, Aug. 30–Sept. 1, 1965)	
31	20-13772	See IEA-99
CONF-650827–	(Western Electronics Show and Conference, San Francisco, Aug. 24–27, 1965)	
3	20-13916	See MATT-412
CONF-650928–	(International Conference on Polarization Phenomena of Nucleons, Karlsruhe, Germany, Sept. 6–10, 1965)	
14	20-13455	See UCRL-14240-T
CONF-650945–	(International Conference on Elementary Particles, Oxford, Sept. 19–25, 1965)	
4	20-13462	See UCRL-16370
CONF-650947–	20-13506	(International Conference on Elementary Particles, Kyoto, Sept. 24–30, 1965) [Progr. Theoret. Phys. (Kyoto), 34: Suppl., 1-688(1965)]
CONF-650953–	(Technical Conference on Materials Science and Technology in Integrated Electronics, San Francisco, Sept. 7–9, 1965)	
1	20-13048	ORINS
CONF-651017–	(Electrochemical Society Meeting, Buffalo, Oct. 10–14, 1965)	
7	20-13245	Dep. mn. CFSTI $2.00 cy, $0.50 mn
13	20-13246	Dep. mn. CFSTI $2.00 cy, $0.50 mn
CONF-651023–	(Symposium on Radioisotope Instruments in Industry and Geophysics, Warsaw, Oct. 18–22, 1965)	
22	20-13050	ORINS

Report No.	Abstract No.	Availability
26	20-12993	ORINS
27	20-12994	ORINS
32	20-13049	ORINS
33	20-13156	ORINS
CONF-651025–	**(Symposium on Physical Metallurgy of Refractory Metals, French Lick, Ind., Oct. 3–5, 1965)**	
12	20-13263	See ORNL-TM-1355
CONF-651034–	**(Society of Automotive Engineers, National Aeronautic and Space Engineering and Mfg. Meeting, Los Angeles, Oct. 4–8, 1965)**	
2	20-13158	ORINS
3	20-14177	ORINS
CONF-651055–	**(Preparation and Standardization of Isotopic Targets and Foils Conference, Harwell, England, Oct. 20–21, 1965)**	
1	20-13216	See ORNL-P-1899
CONF-651056–	**(Symposium on the Dynamics of Plasmas and Fluids, College Park, Md., Oct. 6–8, 1965)**	
1	20-13905	Dep. mn. CFSTI $1.00 cy, $0.50 mn
CONF-651101–	**20-3647 20-9102 (American Nuclear Society, Winter Meeting, Washington, D. C., Nov. 15–18, 1965) (Revised 11-8-65)**	
56	20-14057	See BNWL-183, Sect.I
57	20-14102	See BNWL-183, Sect.II
58	20-14117	See BNWL-183, Sect.III
59	20-14118	See BNWL-183, Sect.IV
60	20-14011	See BNWL-183, Sect.V
61	20-13127	Dep. mn. CFSTI $1.00 cy, $0.50 mn
62	20-14071	See RL-SA-45A and Suppl.
CONF-651103–	**(IAEA Symposium on Criticality Control of Fissile Materials, Stockholm, Nov. 1–5, 1965)**	
14	20-13742	ORINS
15	20-14094	ORINS
17	20-14093	ORINS
20	20-13019	ORINS
21	20-13020	ORINS
22	20-13115	ORINS
23	20-14090	ORINS
24	20-13018	ORINS
25	20-14091	ORINS
26	20-14092	ORINS
CONF-651109–	**(1st Symposium on Accelerator Radiation Dosimetry and Experience, Upton, N. Y., Nov. 3–5, 1965)**	
15	20-13367	See UCRL-16445(Rev.)
16	20-13361	See EGG-1183-2066
CONF-651110–	**(American Society of Mechanical Engineers, Annual Winter Meeting, Chicago, Nov. 7–11, 1965)**	
6	20-14164	ORINS
7	20-12948	ORINS
8	20-12967	ORINS
9	20-13696	ORINS
10	20-12966	ORINS
11	20-12969	ORINS
12	20-12968	ORINS
CONF-651118–	**(American Physical Society, Gatlinburg, Tenn., Nov. 11–13, 1965)**	
5	20-13782	See ORNL-P-1927
CONF-651123–	**(Conference on Reactor Physics and Engineering, Budapest, Nov. 1965)**	
19	20-14190	See UJV-1446/65
CONF-660101–	**(1st International Mutation Group Meeting, Vienna, Austria, Jan. 17–21, 1966)**	
1	20-14216	See BNL-9859
CONF-660205–	**(Metallurgical Society of the American Institute of Mining, Metallurgical and Petroleum Engineers, New York, Feb. 1966)**	
2	20-13181	See K-L-6076
CONF-660206–	**(Symposium on Neutron Noise, Waves, and Pulse Propagation, Gainesville, Feb. 14–16, 1966)**	
1	20-13023	Dep. mn. CFSTI $1.00 cy, $0.50 mn
CONF-660207–	**(Radioisotope Applications in Aerospace Symposium, Dayton, Ohio, Feb. 15–17, 1966)**	
3	20-13129	See ORNL-P-1943
CONF-660208–	**(Symposium on Solidification and Long-Term Storage of Highly Radioactive Wastes, Richland, Wash., Feb. 14–18, 1966)**	
1	20-14208	See ORNL-P-1926
CONF-660301–	**(IEEE International Convention, New York, Mar. 21–25, 1966)**	
2	20-13130	See SC-DC-65-1892
CONF-660305–	**(American Nuclear Society, Topical Meeting, Augusta, Ga., Mar. 21–23, 1966)**	
8	20-12764	Dep. mn. CFSTI $1.00 cy, $0.50 mn
9	20-13157	Dep. mn. CFSTI $1.00 cy, $0.50 mn
COO–		
264-261	20-13602	Progr. Theoret. Phys. (Kyoto), 34: Suppl., 108-17(1965)
264-275	20-13486	Nuovo Cimento, (10), 41A: 380-85(1966)
415-1028	20-13164	Dep. mn. CFSTI $3.00 cy, $0.75 mn
888-43	20-14217	Dep. mn. CFSTI $1.00 cy, $0.50 mn
888-44	20-14218	Dep. mn. CFSTI $1.00 cy, $0.50 mn
888-47	20-14219	Dep. mn. CFSTI $1.00 cy, $0.50 mn
888-48	20-14220	Dep. mn. CFSTI $1.00 cy, $0.50 mn
1006-4	20-12566	Dep. mn. CFSTI $4.00 cy, $0.75 mn
1044-18	20-12892	J. Chem. Phys., 44: 1324-6(1966)
1198-230	20-14221	Dep. mn. CFSTI $1.00 cy, $0.50 mn
1198-304	20-13316	Phys. Rev., 142: 392-9(1966)
1400-5	20-12587	Health Phys., 11: 1607-20(1965)
1430-1	20-14180	Dep. mn. CFSTI $2.00 cy, $0.50 mn
1430-2	20-14181	Dep. mn. CFSTI $1.00 cy, $0.50 mn
1430-3	20-14182	Dep. mn. CFSTI $3.00 cy, $0.75 mn
1454-1	20-14120	Dep. mn. CFSTI $3.00 cy, $0.50 mn
CTO–	**(Non-AEC)**	
229	20-13930	For translation see NP-tr-1343
230	20-13929	For translation see NP-tr-1340
237	20-13931	For translation see NP-tr-1348
DASA–	**(Misc.)**	
1688	20-12978	See AD-627077
1703	20-13057	See AD-627567
DESY–	**(German)**	
65/9	20-13446	Dep. mn
DLR-FB–	**(German)**	
64-08	20-13429	See N64-32348
64-11	20-13430	See N64-32349
DOCKET–	**(Misc.)**	
50-130	20-14143	See PAPP-6401
DP–		
944	20-14025	Dep. mn. CFSTI $2.00 cy, $0.50 mn
949	20-13769	Dep. mn. CFSTI $2.00 cy, $0.50 mn
1004	20-12765	Dep. mn. CFSTI $1.00 cy, $0.50 mn
1037	20-14183	Dep. mn. CFSTI $2.00 cy, $0.50 mn
DTMB–	**(Non-AEC)**	
1820	20-13698	
DUBNA REPORTS	**(Russian)**	
See JINR (Russian)		
DVL–	**(German)**	
316	20-13430	See N64-32349
319	20-13429	See N64-32348
EANDC-US–	**(European-American Nuclear Data Committee)**	
82(U)	20-13753	See BNL-961
EFINS–	**(Misc.)**	
65-72	20-13486	See COO-264-275
EGG–		
1183-2019	20-14170	Dep. mn. CFSTI $3.00 cy, $0.75 mn
1183-2066	20-13361	Dep. mn. CFSTI $2.00 cy, $0.50 mn

Report No.	Abstract No.	Availability
ETR–	**(Belgian)**	
175	20-12927	See NP-15756
EUR–	**(European Atomic Energy Community)**	
267.f	20-13324	See EURAEC-1529
2287.d	20-12979	Dep. mn
2299.e	20-14026	Dep. mn
2380	20-12925	See EURAEC-1446
2446.f	20-12913	Dep. mn
2447.f	20-13213	Dep. mn
2453.f	20-14121	Dep. mn
2475.f	20-12591	Dep. mn
2520.f	20-13000	Dep. mn
2544.d	20-13024	Dep. mn
2546.f	20-12632	Dep. mn
2662	20-13177	See EURAEC-1504
2667	20-12960	See EURAEC-1515
2671	20-12973	See EURAEC-1519
EURAEC–		
909	20-14027	Dep. mn. CFSTI $6.00 cy, $0.75 mn
1446	20-12925	Dep. mn; CFSTI $3.00 cy, $0.75 mn
1465	20-14148	See WCAP-3385-5
1484	20-13214	Dep. mn; CFSTI $2.00 cy, $0.50 mn
1503	20-13176	Dep. mn. CFSTI $3.00 cy, $0.75 mn
1504	20-13177	Dep. mn. CFSTI $3.00 cy, $0.75 mn
1515	20-12960	Dep. mn. CFSTI $2.00 cy, $0.50 mn
1519	20-12973	Dep. mn. CFSTI $3.00 cy, $0.50 mn
1526	20-12962	See GEAP-4959
1529	20-13324	Dep. mn; CFSTI $1.00 cy, $0.50 mn
1537	20-13326	See GEAP-5100C
1539	20-13425	See CEND-3107-249
1541	20-13325	See GEAP-4968
1559	20-14058	See GEAP-4690
1560	20-12961	See GEAP-4786
FD–	**(Non-AEC)**	
27	20-13135	See AD-625483
28	20-13134	See AD-625252
FTD-TT–	**(Non-AEC)**	
65-934	20-13265	For translation see AD-623208
65-976	20-13266	For translation see AD-624905
65-1010	20-13267	For translation see AD-624909
65-1168	20-13928	For translation see AD-625070
GA–	**(Misc.)**	
4451	20-14122	Dep. mn. CFSTI $3.00 cy, $0.75 mn
6576	20-13770	Dep. mn. CFSTI $5.00 cy, $1.00 mn
6690	20-13699	Dep. mn. CFSTI $2.00 cy, $0.50 mn
6831	20-13247	Dep. mn. CFSTI $3.00 cy, $0.50 mn
GAMD–	**(Misc.)**	
1561(Rev.)	20-14123	Dep. mn. CFSTI $2.00 cy, $0.50 mn
6859	20-14124	Dep. mn. CFSTI $1.00 cy, $0.50 mn
GAT-T–		
1222	20-13001	Dep. mn. CFSTI $2.00 cy, $0.50 mn
GEAP–	**(Misc.)**	
4178	20-12766	Dep. mn. CFSTI $3.00 cy, $0.50 mn
4678	20-13248	Dep. mn. CFSTI $3.00 cy, $0.50 mn
4690	20-14058	Dep. mn. CFSTI $1.00 cy, $0.50 mn
4786	20-12961	Dep. mn. CFSTI $2.00 cy, $0.50 mn
4833	20-12767	Dep. mn. CFSTI $1.00 cy, $0.50 mn
4898	20-14125	Dep. mn. CFSTI $3.00 cy, $0.75 mn
4959	20-12962	Dep. mn; CFSTI $3.00 cy, $0.50 mn
4968	20-13325	Dep. mn. CFSTI $3.00 cy, $0.75 mn
5100C	20-13326	Dep. mn. CFSTI $5.00 cy, $1.00 mn
GEMP–	**(Misc.)**	
55A	20-13178	Dep. mn. CFSTI $3.00 cy, $0.75 mn
HW–		
70878	20-14167	Dep. mn. CFSTI $2.00 cy, $0.50 mn
IA–	**(Non-AEC)**	
1048	20-14012	Dep. mn
1050	20-13771	Dep. mn
1056	20-13972	Dep. mn
1065	20-12882	Dep. mn
IC–	**(Misc.)**	
65/17	20-13531	Dep. mn
65/95	20-13447	Dep. mn
66/2	20-13532	Dep. mn
66/3	20-13533	Dep. mn
66/5	20-13534	Dep. mn
66/6	20-13535	Dep. mn
66/7	20-13536	Dep. mn
66/8	20-13537	Dep. mn
IDO–		
14669	20-12926	Dep. mn. CFSTI $2.00 cy, $0.50 mn
14670	20-14207	Dep. mn. CFSTI $1.00 cy, $0.50 mn
17104	20-14059	Dep. mn. CFSTI $3.00 cy, $0.75 mn
17114	20-14060	Dep. mn. CFSTI $3.00 cy, $0.75 mn
17123	20-14013	Dep. mn. CFSTI $3.00 cy, $0.75 mn
17127	20-14061	Dep. mn. CFSTI $3.00 cy, $0.75 mn
17134	20-13061	Dep. mn. CFSTI $2.00 cy, $0.50 mn
17142	20-13538	Dep. mn. CFSTI $2.00 cy, $0.50 mn
IEA–	**(Brazilian)**	
96	20-13062	Dep. mn
97	20-12768	Dep. mn
98	20-12769	Dep. mn
99	20-13772	Dep. mn
100	20-12914	Dep. mn
IFA-CO–	**(Rumanian)**	
28	20-12770	Dep. mn
IFK–	**(German)**	
13	20-13773	Dep. mn
IITRI–	**(Misc.)**	
578P22-14	20-14028	Dep. mn. CFSTI $7.00 cy, $1.50 mn
IPP–	**(Non-AEC)**	
1/40	20-13906	Dep. mn
2/37	20-13025	Dep. mn
2/39	20-13026	Dep. mn
2/42	20-13907	Dep. mn
2/44	20-13908	Dep. mn
3/24	20-13636	Dep. mn
3/28	20-13637	Dep. mn
4/22	20-13666	Dep. mn
4/24	20-13027	Dep. mn
6/39	20-13638	Dep. mn
6/40	20-13909	Dep. mn
IS–		
1269	20-13252	Dep. mn. CFSTI $2.00 cy, $0.50 mn
1311	20-12817	Dep. mn. CFSTI $3.00 cy, $0.75 mn
IS-RD–		
4	20-13180	Dep. mn. CFSTI $2.00 cy, $0.50 mn
IS-T–		
52	20-12818	Dep. mn. CFSTI $3.00 cy, $0.75 mn
53	20-12819	Dep. mn. CFSTI $4.00 cy, $0.75 mn
57	20-12820	Dep. mn. CFSTI $3.00 cy, $0.75 mn
62	20-12821	Dep. mn. CFSTI $2.00 cy, $0.50 mn
65	20-13253	Dep. mn. CFSTI $6.00 cy, $1.25 mn
68	20-12822	Dep. mn. CFSTI $3.00 cy, $0.50 mn
70	20-13254	Dep. mn. CFSTI $2.00 cy, $0.50 mn
JAERI–	**(Japanese)**	
1086	20-13700	Dep. mn
1092	20-13063	Dep. mn
1093	20-13428	Dep. mn
1096	20-13774	Dep. mn
4034	20-13002	Dep. mn
4035	20-13003	Dep. mn
JEN–	**(Spanish)**	
155-SIG/1-4	20-12996	Dep. mn
JINR–	**(Russian)**	
E-2494	20-13064	Dep. mn
E-2500	20-13539	Dep. mn
E-2515	20-13777	Dep. mn
E-2521	20-13448	Dep. mn

Report No.	Abstract No.	Availability
E-2542	20-13165	Dep. mn
E-2545	20-13540	Dep. mn
P-2419	20-13541	Dep. mn
P-2433	20-13449	Dep. mn
P-2443	20-13542	Dep. mn
P-2465	20-13779	Dep. mn
P-2474	20-13543	Dep. mn
P-2488	20-13450	Dep. mn
P-2490	20-13775	Dep. mn
P-2499	20-13776	Dep. mn
P-2503	20-13362	Dep. mn
P-2505	20-13451	Dep. mn
P-2507	20-13363	Dep. mn
P-2509	20-13544	Dep. mn
P-2510	20-13452	Dep. mn
P-2511	20-13453	Dep. mn
P-2513	20-13545	Dep. mn
P-2519	20-13546	Dep. mn
P-2523	20-13547	Dep. mn
P-2525	20-13778	Dep. mn
P-2533	20-13667	Dep. mn
JPRS–	**(Non-AEC)**	
33605	20-14229	CFSTI $3.00 cy, $0.75 mn
33766	20-12722	CFSTI $1.00 cy, $0.50 mn
33958	20-12602	CFSTI $2.00 cy, $0.50 mn
JUL–	**(German)**	
214-RG	20-14062	Dep. mn
236-RE	20-14184	Dep. mn
276-RG	20-14126	Dep. mn
281-PP	20-13639	Dep. mn
291-RG	20-14127	Dep. mn
294-NP	20-13701	Dep. mn
295-NP	20-13065	Dep. mn
296-RG	20-14128	Dep. mn
297-MA	20-13910	Dep. mn
298-PC	20-13066	Dep. mn
304-RW	20-13414	Dep. mn
308-RB	20-13067	Dep. mn
315-RG	20-14129	Dep. mn
336-PP	20-13911	Dep. mn
K-L–		
6057	20-12786	Anal. Chem., 38: 198-9(1966)
6076	20-13181	Dep. mn. CFSTI $2.00 cy, $0.50 mn
KAPL–		
3108	20-13255	Dep. mn. CFSTI $3.00 cy, $0.75 mn
KAPL-M–		
6498	20-13028	Dep. mn. CFSTI $1.00 cy, $0.50 mn
6528	20-14063	Dep. mn. CFSTI $3.00 cy, $0.50 mn
KFK–	**(German)**	
358	20-13780	Dep. mn
362	20-13446	See DESY-65/9
366	20-14130	Dep. mn
371	20-13166	Dep. mn
KR–	**(Norwegian)**	
98	20-14131	Dep. mn
LA–		
1981(Rev.)	20-13004	Dep. mn. CFSTI $2.00 cy, $0.50 mn
3366	20-13005	Dep. mn. CFSTI $3.00 cy, $0.50 mn
3368	20-14132	Dep. mn. CFSTI $3.00 cy, $0.50 mn
3388	20-14171	Dep. mn. CFSTI $1.00 cy, $0.50 mn
3391	20-12823	Dep. mn. CFSTI $2.00 cy, $0.50 mn
3397	20-14172	Dep. mn. CFSTI $3.00 cy, $0.75 mn
3423	20-13029	Dep. mn. CFSTI $1.00 cy, $0.50 mn
3426	20-13668	Dep. mn. CFSTI $1.00 cy, $0.50 mn
3427	20-14064	Dep. mn. CFSTI $3.00 cy, $0.75 mn
3443	20-13030	Dep. mn. CFSTI $1.00 cy, $0.50 mn
LA-DC–		
6418	20-13293	J. Nucl. Mater., 17: 336-40(1965)
6703	20-13291	J. Nucl. Mater., 17: 324-9(1965)
6749	20-12824	Dep. mn. CFSTI $1.00 cy, $0.50 mn
7594	20-13702	Dep. mn. CFSTI $3.00 cy, $0.75 mn
LA-tr–		
66-7	20-13550	Dep. mn. CFSTI $1.00 cy, $0.50 mn. JCL $1.10 fs, $0.80 mf
66-8	20-13551	Dep. mn. CFSTI $1.00 cy, $0.50 mn. JCL $1.60 fs, $0.80 mf
LAL–	**(French)**	
1148	20-13364	Dep. mn
LGI–	**(Italian)**	
65/21 and App.	20-13912	Dep. mn
LMSC–	**(Misc.)**	
A763154	20-14173	See TID-22416
A764793	20-14175	See TID-22418
A769348	20-14174	See TID-22417
MATT–		
317	20-13913	Dep. mn; CFSTI $1.00 cy, $0.50 mn
318	20-13914	Dep. mn; CFSTI $1.00 cy, $0.50 mn
402	20-13915	Dep. mn. CFSTI $1.00 cy, $0.50 mn
412	20-13916	Dep. mn. CFSTI $2.00 cy, $0.50 mn
MIT–	**(Misc.)**	
2098-171	20-13858	Phys. Rev., 142: 673-86(1966)
2098-173	20-13853	Phys. Rev., 142: 624-32(1966)
2344-4	20-14014	Dep. mn; CFSTI $5.00 cy, $1.00 mn
MITNE–	**(Misc.)**	
65	20-14014	See MIT-2344-4
MLM–		
1263	20-13068	Dep. mn. CFSTI $2.00 cy, $0.50 mn
1306J	20-12852	J. Amer. Chem. Soc., 88: 179-80(1966)
N–	**(Misc.)**	
64-32348	20-13429	Dep. mn
64-32349	20-13430	Dep. mn
NAA-SR-Memo–		
10884 and Add.	20-13706	Dep. mn. CFSTI $2.00 cy, $0.50 mn
NASA-CR–	**(Misc.)**	
334	20-13781	CFSTI $3.00 cy, $0.75 mn
54468	20-13069	
54476	20-13191	
54723	20-13264	See WANL-PR(P)-008
54788	20-14029	
54794	20-13966	See UNC-5140
54843	20-13192	
54845	20-13193	
NASA-SP–	**(Misc.)**	
3024	20-13646	CFSTI $1.00 cy, $0.75 mn
NASA-TN–	**(Misc.)**	
D-3222	20-13256	CFSTI $1.00 cy, $0.50 mn
D-3232	20-13257	CFSTI $2.00 cy, $0.50 mn
D-3238	20-13258	CFSTI $1.00 cy, $0.50 mn
D-3250	20-13917	CFSTI $3.00 cy, $0.50 mn
D-3255	20-13918	CFSTI $2.00 cy, $0.50 mn
NASA-TT–	**(Non-AEC)**	
F-183	20-13426	CFSTI $6.00 cy, $1.25 mn
NDL-TR–	**(Non-AEC)**	
71	20-12978	See AD-627077
NLCO–		
967	20-12771	Dep. mn. CFSTI $1.00 cy, $0.50 mn
968	20-13259	Dep. mn. CFSTI $2.00 cy, $0.50 mn
NP–	**(AEC File No. for Non-AEC Reports)**	
15348	20-12633	Dep. mn
15349	20-12634	Dep. mn
15360	20-13137	Dep. mn
15587	20-14133	Dep. mn
15612	20-14222	Dep. mn; Australian AEC Free
15666	20-12717	Dep. mn
15667	20-12718	Dep. mn
15668	20-12719	Dep. mn
15671	20-12592	Dep. mn
15672	20-12593	Dep. mn

Report No.	Abstract No.	Availability
15679	20-12594	Dep. mn
15680	20-12595	Dep. mn
15681	20-12596	Dep. mn
15682	20-12597	Dep. mn
15683	20-12598	Dep. mn
15684	20-12599	Dep. mn
15685	20-12600	Dep. mn
15703	20-13919	
15723	20-14223	Dep. mn
15756	20-12927	Dep. mn. CFSTI $1.00 cy, $0.50 mn
15772	20-13345	Dep. mn
15835(Suppl.)	20-13128	CFSTI $1.00 cy, $0.50 mn
15836	20-14187	
15852	20-13260	CFSTI $1.00 cy, $0.50 mn
15863	20-12617	Dep. mn
NP-tr–	**(AEC File No. for Non-AEC Translations)**	
1336	20-13007	Dep. mn. CFSTI $1.00 cy, $0.50 mn. JCL $1.10 fs, $0.80 mf
1340	20-13929	Dep. mn. CFSTI $1.00 cy, $0.50 mn. JCL $1.60 fs, $0.80 mf
1343	20-13930	Dep. mn. CFSTI $2.00 cy, $0.80 mn. JCL $2.60 fs, $1.01 mf
1348	20-13931	Dep. mn. CFSTI $1.00 cy, $0.50 mn. JCL $2.60 fs, $0.89 mf
NTC–		
126	20-14180	See COO-1430-1
127	20-14181	See COO-1430-2
129	20-14182	See COO-1430-3
NYO–		
1312-1(Vol.1)	20-12989	Dep. mn. CFSTI $5.00 cy, $1.00 mn
1312-1(Vol.2)	20-12990	Dep. mn. CFSTI $5.00 cy, $1.00 mn
NYO–		
2082-1	20-12825	Dep. mn. CFSTI $4.00 cy, $1.00 mn
2174-31	20-13102	Nucl. Instrum. Methods, 39: 265-70(1966)
2786-1	20-12635	Dep. mn. CFSTI $1.00 cy, $0.50 mn
2910-13	20-13031	Dep. mn. CFSTI $1.00 cy, $0.50 mn
3033-1	20-13973	Dep. mn. CFSTI $1.00 cy, $0.50 mn
3379-2	20-14134	Dep. mn. CFSTI $7.34 cy, $2.00 mn
OR–	**(Misc.)**	
6891	20-13971	See AD-625834
ORNL–		
3746	20-13964	Dep. mn; CFSTI $2.00 cy, $0.50 mn
3840	20-12772	Dep. mn. CFSTI $1.00 cy, $0.50 mn
3868	20-12928	Dep. mn; CFSTI $4.00 cy, $0.75 mn
3873	20-13167	Dep. mn. CFSTI $5.00 cy, $1.00 mn
3877(Rev.)	20-13648	Dep. mn. CFSTI $1.00 cy, $0.50 mn
3881	20-13415	Dep. mn. CFSTI $3.00 cy, $0.50 mn
3885	20-14135	Dep. mn. CFSTI $7.00 cy, $1.50 mn
3910	20-14141	Dep. mn; CFSTI $5.00 cy, $1.00 mn
ORNL-P–	**(Misc.)**	
793	20-13290	J. Nucl. Mater., 17: 305-12(1965)
933	20-12854	J. Appl. Phys., 37: 40-55(1966)
1044	20-13335	J. Nucl. Mater., 18: 108-18(1966)
1230	20-12672	Health Phys., 11: 1637-42(1965)
1290	20-12580	Health Phys., 11: 1511-19(1965)
1294	20-12834	Acta Crystallogr., 20: 135-8(1966)
1305	20-12573	Health Phys., 11: 1355-61(1965)
1327	20-12576	Health Phys., 11: 1375-84(1965)
1470	20-12577	Health Phys., 11: 1385-92(1965)
1485	20-13375	Nucl. Instrum. Methods, 39: 125-32(1966)
1560	20-12662	Genetics, 53: 131-6(1966)
1641	20-13867	Phys. Rev., 142: 748-57(1966)
1874	20-12844	Inorg. Nucl. Chem. Lett., 1: 145-8(1965)
1899	20-13216	Dep. mn. CFSTI $1.00 cy, $0.50 mn
1926	20-14208	Dep. mn. CFSTI $1.00 cy, $0.50 mn
1927	20-13782	Dep. mn. CFSTI $1.00 cy, $0.50 mn
1943	20-13129	Dep. mn. CFSTI $1.00 cy, $0.50 mn
1945	20-13157	Dep. mn. CFSTI $1.00 cy, $0.50 mn
ORNL-RSIC–		
11	20-13965	Dep. ORNL Free
ORNL-TM–		
1018	20-13289	J. Nucl. Mater., 17: 294-304(1965)

Report No.	Abstract No.	Availability
1075	20-14015	Dep. mn. CFSTI $7.00 cy, $1.50 mn
1232	20-12507	Dep. mn. CFSTI $2.00 cy, $0.50 mn
1333	20-13783	Dep. mn. CFSTI $4.00 cy, $0.75 mn
1336	20-13784	Dep. mn; CFSTI $4.00 cy, $1.00 mn
1352	20-13032	Dep. mn. CFSTI $3.00 cy, $0.75 mn
1354	20-13327	Dep. mn. CFSTI $4.00 cy, $0.75 mn
1355	20-13263	Dep. mn. CFSTI $1.00 cy, $0.50 mn
1359	20-13328	Dep. mn. CFSTI $1.00 cy, $0.50 mn
1374	20-13785	Dep. mn. CFSTI $4.00 cy, $1.00 mn
1377	20-13217	Dep. mn. CFSTI $2.00 cy, $0.50 mn
1378	20-14142	Dep. mn. CFSTI $1.00 cy, $0.50 mn
1383	20-12945	Dep. mn. CFSTI $1.00 cy, $0.50 mn
1384	20-13006	Dep. mn. CFSTI $1.00 cy, $0.50 mn
1396	20-13786	Dep. mn. CFSTI $1.00 cy, $0.50 mn
1412	20-13218	Dep. mn. CFSTI $1.00 cy, $0.50 mn
1415	20-13707	Dep. mn. CFSTI $1.00 cy, $0.50 mn
1417	20-13708	Dep. mn. CFSTI $1.00 cy, $0.50 mn
ORNL-tr–		
900	20-14149	Dep. mn. JCL $9.10 fs, $3.38 mf
931	20-12780	Dep. mn. JCL $1.60 fs, $0.80 mf
972	20-14230	Dep. mn. JCL $2.60 fs, $0.83 mf
1062	20-13788	Dep. mn. CFSTI $1.00 cy, $0.50 mn. JCL $1.60 fs, $0.80 mf
ORO–		
634	20-12883	Dep. mn. CFSTI $2.00 cy, $0.50 mn
PAEC-IPA(D)PH–	**(Phillipines)**	
652	20-13709	Dep. mn
PAPP–	**(Non-AEC)**	
6401	20-14143	Dep. mn. CFSTI $4.00 cy, $1.00 mn
PATENTS	**(British)**	**4s. 6d. each, U. K. Patent Office**
1,013,028	20-13439	
1,013,084	20-14035	
1,013,102	20-14021	
1,013,255	20-14036	
1,013,541	20-14107	
1,013,683	20-12949	
1,013,776	20-13161	
1,013,777	20-13162	
1,013,922	20-14108	
1,013,926	20-14037	
1,014,382	20-13962	
1,014,682	20-13116	
1,014,784	20-14038	
1,014,790	20-14040	
1,014,822	20-14109	
1,014,839	20-13117	
1,014,855	20-12970	
1,014,872	20-14039	
1,015,004	20-13228	
1,015,342	20-12950	
1,015,653	20-12951	
1,015,734	20-12952	
1,015,777	20-12813	
1,015,912	20-14041	
1,016,029	20-12953	
1,016,048	20-14097	
1,016,113	20-14042	
1,016,117	20-13440	
1,016,261	20-14043	
1,016,329	20-12954	
1,016,733	20-12955	
1,016,902	20-12921	
1,017,089	20-12875	
1,017,094	20-13118	
PATENTS	**(Canadian)**	
720,107	20-12876	
723,583	20-13229	
725,279	20-14044	
PATENTS	**(German)**	
1,204,346	20-14045	
1,204,347	20-14110	
1,204,754	20-13385	
1,204,756	20-14046	
1,204,757	20-13119	
1,205,199	20-13120	
1,205,202	20-13386	

Report No.	Abstract No.	Availability
1,205,203	20-14111	
1,205,204	20-14098	
1,205,205	20-14047	
1,205,206	20-14095	
1,205,207	20-13387	
PATENTS	**(Japanese)**	
1964-18483	20-14022	
1964-18487	20-13743	
1964-18489	20-13388	
1964-18491	20-13389	
1964-18492	20-13390	
1964-18495	20-13391	
1964-18496	20-13392	
1964-27165	20-14204	
1964-27170	20-14205	
1964-27174	20-13744	
1964-27175	20-13393	
1964-27176	20-13394	
1964-27178	20-12956	
1964-28699	20-13051	
1964-29018	20-13395	
1964-29019	20-13396	
1964-29020	20-12957	
1964-30364	20-13745	
1964-30365	20-13397	
1964-30366	20-13398	
1964-30367	20-13399	
1964-30368	20-13400	
1964-30369	20-13401	
1964-30375	20-13402	
1964-30376	20-13403	
1964-30377	20-13404	
1964-30378	20-13405	
1964-30380	20-14048	
PATENTS	**(U. S.)**	**$0.25 each, U. S. Patent Office**
25,904	20-12909	
3,217,908	20-12958	
3,218,673	20-13230	
3,218,997	20-14212	
3,219,370	20-14049	
3,220,573	20-14206	
3,220,926	20-14050	
3,220,927	20-14112	
3,221,165	20-13121	
3,221,166	20-13122	
3,221,212	20-13963	
3,222,124	20-12940	
3,222,254	20-14099	
3,222,255	20-14051	
3,222,256	20-14113	
3,222,521	20-12814	
3,222,523	20-13123	
3,222,558	20-13052	
3,222,568	20-12959	
3,222,751	20-13204	
3,222,773	20-13231	
3,223,475	20-13190	
3,223,476	20-12941	
3,223,589	20-14052	
3,223,590	20-14053	
3,223,591	20-14054	
3,223,619	20-12942	
3,223,836	20-13053	
3,223,840	20-13054	
3,223,843	20-13124	
3,223,857	20-13441	
3,223,858	20-13442	
3,223,859	20-13443	
3,223,860	20-12971	
3,226,298	20-12922	
3,226,301	20-14100	
3,226,545	20-13125	
3,226,546	20-12995	
3,226,547	20-13126	
3,226,847	20-13021	
3,227,621	20-14101	
3,227,900	20-13444	
PEL–	**(South African)**	
77	20-14144	Dep. mn
80	20-12773	Dep. mn

Report No.	Abstract No.	Availability
PG-Report–	**(British)**	
685	20-12774	Dep. BIS $0.30. HMSO 1s. 9d.
PUC–		
937-184	20-13837	Phys. Lett., 20: 168-70(1966)
R–	**(Misc.)**	
1788	20-13186	See TRG-Report-840
2347	20-12925	See EURAEC-1446
RCN–	**(Dutch)**	
40	20-13070	Dep. mn
RD–	**(Misc.)**	
65-1084	20-14120	See COO-1454-1
RFP–		
601	20-12775	Dep. mn. CFSTI $2.00 cy, $0.50 mn
RHEL/R–	**(British)**	
111	20-13071	Dep. mn
RL-SA–		
45A and Suppl.	20-14071	Dep. mn. CFSTI $2.00 cy, $0.50 mn
RL-SEP–		
710	20-13219	Dep. mn. CFSTI $1.00 cy, $0.50 mn
RLO–		
1921-3	20-13869	Phys. Rev., 142: 768-74(1966)
RMI–	**(Misc.)**	
3	20-13220	Dep. mn. CFSTI $3.00 cy, $0.75 mn
RRL–		
2310-171	20-12884	Dep. mn. CFSTI $1.00 cy, $0.50 mn
RT-EL–	**(Italian)**	
(65)7	20-13072	Dep. mn
RT-FI–	**(Italian)**	
(65)31	20-13431	Dep. mn
(65)40	20-14188	Dep. mn
(65)43	20-14189	Dep. mn
(65)46	20-13329	Dep. mn
RT-PROT–	**(Italian)**	
(65)29	20-14209	Dep. mn
(65)33	20-12776	Dep. mn
SAN–		
549-1	20-13073	Dep. mn. CFSTI $2.00 cy, $0.50 mn
SC-DC–		
65-1892	20-13130	Dep. mn. CFSTI $2.00 cy, $0.50 mn
SC-RR–		
65-396	20-13346	Dep. mn. CFSTI $3.00 cy, $0.50 mn
65-569	20-12826	Dep. mn. CFSTI $3.00 cy, $0.75 mn
SC-T–		
66-0706	20-12886	Dep. mn. CFSTI $1.00 cy, $0.50 mn. JCL $1.10 fs, $0.80 mf
SLAC–		
39(Rev.)	20-13365	Dep. mn. CFSTI $3.00 cy, $0.75 mn
53	20-13366	Dep. mn. CFSTI $4.00 cy, $0.75 mn
58	20-13548	Dep. mn. CFSTI $1.00 cy, $0.50 mn
SRRC–	**(Scottish)**	
11/65	20-13074	Dep. mn
STI-PUB–	**(International Atomic Energy Agency)**	
21/16	20-13974	IAEA: $3.00; S63,-; 18/-stg; F Fr 12,-; DM 10,50
21/17	20-14016	IAEA: $4.00; S 84,-; £1.4.0; F Fr 16,-; DM 14,-
104(Vol.1)	20-13710	IAEA: $14.00; S 294,-; £4.4.0; F Fr 56,-; DM 49,-
104(Vol.2)	20-13711	IAEA: $18.00; S 378,-; £5.8.0; F Fr 72,-;

Report No.	Abstract No.	Availability
		DM 63,-
105(Vol.2)	20-14017	IAEA: $9.00; S 189,-; £2.14.0; F Fr 36,-; DM 31,50
TID–		
4005(Pt.1, 9th Ed.)	20-13182	Dep. mn. CFSTI $5.00 cy, $2.25 mn
6506(Pt.2, 3rd Ed.)	20-13183	Dep. mn. CFSTI $3.00 cy, $0.75 mn
11295(Pt.1, 4th Ed.)	20-13184	Dep. mn. CFSTI $5.00 cy, $1.00 mn
21459	20-12636	Dep. mn. CFSTI $1.00 cy, $0.50 mn
21466	20-12637	Dep. mn. CFSTI $1.00 cy, $0.50 mn
21474	20-12638	Dep. mn. CFSTI $1.00 cy, $0.50 mn
21517	20-12639	Dep. mn. CFSTI $2.00 cy, $0.50 mn
21562	20-14224	Dep. mn. CFSTI $3.00 cy, $0.75 mn
21571	20-13975	Dep. mn. CFSTI $2.00 cy, $0.50 mn
21577	20-14225	Dep. mn. CFSTI $1.00 cy, $0.50 mn
21583	20-12827	Dep. mn. CFSTI $1.00 cy, $0.50 mn
21586	20-14226	Dep. mn. CFSTI $1.00 cy, $0.50 mn
21587	20-12828	Dep. mn. CFSTI $1.00 cy, $0.50 mn
21883	20-13601	Progr. Theoret. Phys. (Kyoto), 34: Suppl., 104-7(1965)
22105	20-13482	Nucl. Phys., 78: 433-47(1966)
22330(Vol.3)	20-14166	Dep. mn. CFSTI $1.25 cy, $1.25 mn
22378	20-12640	Dep. mn. CFSTI $4.00 cy, $0.75 mn
22399	20-12618	Dep. mn. CFSTI $1.00 cy, $0.50 mn
22416	20-14173	Dep. mn. CFSTI $4.00 cy, $0.75 mn
22417	20-14174	Dep. mn. CFSTI $3.00 cy, $0.75 mn
22418	20-14175	Dep. mn. CFSTI $5.00 cy, $1.00 mn
22419	20-14227	Dep. mn; CFSTI $6.00 cy, $1.50 mn
22424	20-13185	Dep. mn. CFSTI $2.00 cy, $0.50 mn
22466	20-12720	Dep. mn. CFSTI $1.00 cy, $0.50 mn
22502	20-12829	Dep. mn. CFSTI $1.00 cy, $0.50 mn
22526	20-12601	ORAU
22527	20-14228	Dep. mn. CFSTI $4.00 cy, $1.00 mn
22582	20-12641	Dep. mn. CFSTI $2.00 cy, $0.50 mn
22595	20-14145	Dep. mn. CFSTI $6.00 cy, $1.25 mn
22596	20-14146	Dep. mn. CFSTI $3.00 cy, $0.50 mn
22637	20-13787	Dep. mn. CFSTI $3.00 cy, $0.75 mn
22639	20-12568	Dep. mn. CFSTI $1.00 cy, $0.50 mn
TLW–	**(Misc.)**	
1110	20-13033	Dep. mn. CFSTI $4.00 cy, $0.75 mn
TRG-Report–	**(British)**	
840	20-13186	Dep. BIS $7.00. HMSO 35s.
950	20-13320	pp 277-84 of STI/PUB/105(Vol. II)
1031	20-14161	pp 365-83 of STI/PUB/105(Vol. II)
TT–	**(Canadian)**	
66-30049	20-14229	See JPRS-33605
66-30209	20-12722	See JPRS-33766
66-30401	20-12602	See JPRS-33958
UCD–		
34P80-3	20-13138	Dep. mn; CFSTI $5.00 cy, $1.00 mn
UCLA–		
12-545	20-12708	Trans. Amer. Clin. Climatol. Ass., 76: 80-98(1964)
UCDL–	**(Misc.)**	
535-550	20-13866	Phys. Rev., 142: 735-48(1966)
UCRL–		
7802	20-12830	Dep. mn. CFSTI $1.00 cy, $0.50 mn
11674	20-12946	Dep. mn. CFSTI $2.00 cy, $0.50 mn
11954	20-13861	Phys. Rev., 142: 696-715(1966)
12302-T	20-12579	Health Phys., 11: 1445-57(1965)
12397	20-13287	J. Basic Eng., 87: 865-70(1965)
14100-T(Rev.1)	20-13454	Dep. mn. CFSTI $1.00 cy, $0.50 mn
14176-T	20-13871	Phys. Rev., 142: 778-87(1966)
14240-T	20-13455	Dep. mn. CFSTI $2.00 cy, $0.50 mn
14257	20-13717	Phys. Rev., 142: 687-9(1966)
14623	20-13845	Phys. Lett., 20: 190-3(1966)
16101	20-13603	Progr. Theoret. Phys. (Kyoto), 34: Suppl., 118-26(1965)
16170	20-13456	Dep. mn. CFSTI $5.00 cy, $1.00 mn
16195	20-13457	Dep. mn. CFSTI $5.00 cy, $1.00 mn
16209	20-13458	Dep. mn. CFSTI $5.00 cy, $1.00 mn
16210	20-13381	Nucl. Instrum. Methods, 39: 321-4(1966)
16253	20-13459	Dep. mn. CFSTI $3.00 cy, $0.75 mn
16274	20-13460	Dep. mn. CFSTI $3.00 cy, $0.75 mn
16327	20-13855	Phys. Rev., 142: 638-42(1966)
16337	20-13856	Phys. Rev., 142: 657-63(1966)
16341	20-13825	Nucl. Phys., 78: 341-52(1966)
16365	20-13461	Dep. mn. CFSTI $3.00 cy, $0.75 mn
16370	20-13462	Dep. mn. CFSTI $1.00 cy, $0.50 mn
16394	20-14147	Dep. mn. CFSTI $4.00 cy, $0.75 mn
16445(Rev.)	20-13367	Dep. mn. CFSTI $1.00 cy, $0.50 mn
16511	20-13347	Dep. mn. CFSTI $3.00 cy, $0.75 mn
16516	20-12831	Dep. mn. CFSTI $3.00 cy, $0.75 mn
16517	20-13926	Dep. mn. CFSTI $5.00 cy, $1.00 mn
16530	20-13549	Dep. mn. CFSTI $2.00 cy, $0.50 mn
16557	20-13927	Dep. mn. CFSTI $5.00 cy, $1.00 mn
UCRL-Trans–		
1244(L)	20-12832	Dep. mn; JCL $2.60 fs, $1.10 mf
UJV–	**(Czechoslovakian)**	
1431/65	20-12777	Dep. mn
1434/65	20-12778	Dep. mn
1446/65	20-14190	Dep. mn
1450/65	20-13075	Dep. mn
UNC–	**(Misc.)**	
5140	20-13966	
UR–		
875-83	20-13599	Progr. Theoret. Phys. (Kyoto), 34: Suppl., 56-75(1965)
875-117	20-13076	Dep. mn. CFSTI $1.00 cy, $0.50 mn
USNRDL-TR–	**(Misc.)**	
924	20-12779	Dep. mn. CFSTI $1.60 cy, $0.80 mn
926	20-13746	See AD-626681
931	20-12881	See AD-626609
936	20-13355	See AD-626999
937	20-13056	See AD-627000
939	20-13057	See AD-627567
941	20-12628	See AD-626997
944	20-13055	See AD-626998
946	20-12716	See AD-626682
949	20-13058	See AD-627930
WANL-PR–	**(Misc.)**	
M-014	20-13205	See AD-626622
(P)-008	20-13264	
WANL-TME–	**(Misc.)**	
1108	20-12963	Dep. mn. CFSTI $3.00 cy, $0.50 mn
WAPD-T–		
1766	20-13301	J. Nucl. Mater., 18: 77-107(1966)
WCAP–	**(Misc.)**	
3385-5	20-14148	Dep. mn; CFSTI $4.00 cy, $0.75 mn
Y–		
1503	20-13077	Dep. mn. CFSTI $1.00 cy, $0.50 mn
Y-IA–		
17	20-12642	Dep. mn. CFSTI $1.00 cy, $0.50 mn
YALE–		
1807-28	20-13512	[Progr. Theoret. Phys. (Kyoto), 34: Suppl., 449-91(1965)]

DEPOSITORIES OF USAEC REPORTS

In Countries Other than the U.S.

ARGENTINA
Buenos Aires, Comisión Nacional de Energía Atómica
AUSTRALIA
Canberra, Australian National Library
Sutherland, New South Wales, Australian Atomic Energy Commission
AUSTRIA
Vienna, Zentral Bibliothek der Physikalischen Institute der Universität
BELGIUM
Mol-Donk, Centre d'Etude de l'Energie Nucleaire
BOLIVIA
La Paz, Comisión Nacional de Energiá Nuclear
BRAZIL
Rio de Janeiro, Instituto Brasileiro de Bibliografia e Documentacao
São Paulo, Instituto de Energia Atomica, Cidade Universitaria São Paulo
BURMA
Rangoon, Union of Burma Applied Research Institute, Atomic Energy Center Library
CANADA
Hamilton, McMaster University
Ottawa, National Research Council Library
Vancouver, University of British Columbia
CHILE
Santiago, Instituto de Fisica y Matematicas, Universidad de Chile
CHINA
Hsinchu, Taiwan, Free China, National Tsing Hua University
COLOMBIA
Bogota, Instituto De Asuntos Nucleares
COSTA RICA
San Pedro, University of Costa Rica Library
DENMARK
Risö, Danish Atomic Energy Commission
ECUADOR
Quito, Escuela Politécnica Nacional
EL SALVADOR
San Salvador, Universidad de El Salvador, Biblioteca de Energia Nuclear
FINLAND
Helsinki, Teknillisen Korkeakoulun Kirjasto
FRANCE
Gif-sur-Yvette, Centre d'Etudes Nucléaires de Saclay
Paris, Académie des Sciences
GERMANY
Berlin, Hahn-Meitner-Institut für Kernforschung Berlin
Frankfurt/Main, Gmelin-Institut
Munich, Technische Hochschule, Bibliothek
GHANA
Accra, University College of Ghana
GREECE
Athens, Nuclear Research Center "Democritus"
GUATEMALA
Guatemala, Comisión Nacional de Energía Nuclear
INDIA
Bombay, Department of Atomic Energy
IRAN
Tehran, Tehran University Nuclear Centre
IRAQ
Baghdad, Iraqi Atomic Energy Commission
IRELAND
Dublin, University College
ISRAEL
Rehovoth, Israel Atomic Energy Commission
ITALY
Rome, Centro di Studi Nucleari della Casaccia
Rome, Comitato Nazionale per l'Energia Nucleare
JAPAN
Tokyo, National Diet Library
KOREA
Seoul, Office of Atomic Energy
LEBANON
Beirut, Lebanese National Council for Scientific Research
LUXEMBOURG
Luxembourg, Ministry of Transport and Electricity
MALAYSIA
Kuala Lumpur, University of Malaysia
MEXICO
Mexico, D.F., Comisión Nacional de Energía Nuclear
NETHERLANDS
The Hague, Reactor Centrum Nederland
NEW ZEALAND
Lower Hutt, Institute of Nuclear Sciences
NIGERIA
Ibadan, University of Ibadan
NORWAY
Lillestrøm, Institutt för Atomenergi
PAKISTAN
Lahore, West Pakistan, Atomic Energy Centre
PERU
Lima, Junta de Control de Energia Atomica
PHILIPPINE REPUBLIC
Manila, Philippine Atomic Energy Commission
POLAND
Warsaw, Biura Pelnomocnika Rzadu do Spraw Wykorzystania Energii Jadrowej
PORTUGAL
Sacavem, Junta de Energía Nuclear
REPUBLIC OF SOUTH AFRICA
Pretoria, Atomic Energy Board Library
REPUBLIC OF THE CONGO
Leopoldville, Université Lovanium
SPAIN
Madrid, Junta de Energía Nuclear, Biblioteca Documentación y Publicaciones, Ciudad Universitaria
SWEDEN
Nyköping, Aktiebolaget Atomenergi
SWITZERLAND
Zürich, Eidgenössische Technische Hochschule, Bibliothek
THAILAND
Bangkok, Office of the Thai Atomic Energy Commission, Department of Science
TURKEY
Ankara, Turkish Atomic Energy Commission, Atomic Energy Library
UNITED ARAB REPUBLIC
Cairo, Atomic Energy Commission
UNITED KINGDOM
Birmingham, Central Library
Boston Spa, National Lending Library for Science and Technology
Kingston upon Hull, Central Library
Liverpool, Central Library
London, Central Library, Acton
London, National Reference Library
London, Science Museum Library, South Kensington
Manchester, Central Library
Newcastle upon Tyne, Central Library
Nottingham, Central Library
Sheffield, Central Library
URUGUAY
Montevideo, Comision Nacional de Energia Atomica
VENEZUELA
Caracas, Instituto Venezolano de Investigaciones Científicas
VIET-NAM
Saigon, Atomic Energy Office
YUGOSLAVIA
Belgrade, Federal Commission for Nuclear Energy

In International Agencies

AUSTRIA
Vienna, International Atomic Energy Agency
BELGIUM
Brussels, La Bibliotheque EURATOM
FRANCE
Paris, European Nuclear Energy Agency, O.E.C.D.
ITALY
Ispra, EURATOM Research Center
SWITZERLAND
Geneva, United Nations Library

UNITED STATES
GOVERNMENT PRINTING OFFICE
DIVISION OF PUBLIC DOCUMENTS
WASHINGTON, D.C. 20402

OFFICIAL BUSINESS

POSTAGE AND FEES PAID
U.S. GOVERNMENT PRINTING OFFICE

TECHNICAL PROGRESS REVIEWS

The Division of Technical Information, U. S. Atomic Energy Commission, also publishes the Technical Progress Reviews, a series of five quarterly journals on nuclear technology. These journals, compiled by specialists and recognized authorities, summarize, evaluate, and reference the progress of development in five important fields.

Isotopes and Radiation Technology P. S. Baker, A. F. Rupp, and associates, Oak Ridge National Laboratory. Reviews AEC-sponsored projects and related significant worldwide developments in radioisotopes and radiation technology.

Nuclear Safety Wm. B. Cottrell, W. H. Jordan, and associates, Oak Ridge National Laboratory. Covers topics relevant to the analysis and control of hazards associated with nuclear reactors and with operations involving fissionable materials and the products of nuclear fission.

Power Reactor Technology Argonne National Laboratory. Reviews research, development, design practices, and operating experiences associated with power reactors, including aerospace applications.

Reactor Fuel Processing Stephen Lawroski and associates, Argonne National Laboratory. Reviews all aspects of the fuel-processing field, including aqueous and nonaqueous processing and waste disposal.

Reactor Materials R. W. Dayton, E. M. Simons, and associates, Battelle Memorial Institute. Covers the properties, behavior, and fabrication processes of materials used in nuclear reactors and associated equipment.

7886

Availability

SUBSCRIPTION RATE: The Technical Progress Reviews may be purchased from the Superintendent of Documents, U. S. Government Printing Office, Washington, D. C. 20402, at $2.50 per year for each subscription or $0.70 per issue.

POSTAGE: Postpaid within the United States, Canada, Mexico, and all Central and South American countries except Argentina, Brazil, British and French Guiana, Surinam, and British Honduras. For these Central and South American countries and all other countries, add $0.75 per year or $0.20 per single issue.

REMITTANCE: Payment should be by check, money order, or document coupons and MUST accompany order. Remittances from foreign countries should be made by international money order or draft on an American bank payable to the Superintendent of Documents or by UNESCO book coupons.